POWER SYSTEMS DEVELOPMENT FACILITY

TECHNICAL PROGRESS REPORT FOR M.W. KELLOGG TRANSPORT REACTOR TRAIN WITH WESTINGHOUSE PARTICULATE CONTROL DEVICE:

JANUARY 1997 – DECEMBER 1997

DOE Cooperative Agreement Number
DE-FC21-90MC25140

VOLUME II

Prepared by:
Southern Company Services, Inc.
Power Systems Development Facility
P.O. Box 1069
Wilsonville, AL 35186

January 1999

4.0 TRANSPORT REACTOR LOOP OPERATIONS

A few major challenges were left unresolved at the end of commissioning and initial operation of the transport reactor train in 1996. These included the excessive solids carryover from the reactor loop to the PCD and the very low reliability of the reactor start-up burner pilot. Operations in the first half of the 1997 focussed on solving these problem areas. After successfully addressing these challenges the second half of 1997 resulted in a test run in which the basic reactor operations were modified to expose the filter elements in the PCD to higher temperatures.

Section 4.1 provides an operations chronology of various test runs. Analysis of data and reactor performance are discussed in section 4.2. Operational stability of the reactor loop and other major observations are discussed in section 4.3.

4.1 PROGRESS IN OPERATIONS

This section provides a descriptive chronology of combustion test runs that were completed in 1997. In addition to concentrating on reactor loop operation the operation and performance of other systems closely associated with the reactor operation are also discussed. Such systems include the following: coal feed system (FD0210), sorbent feed system (FD0220), start-up burner (BR0201), transport reactor (RX0201), disengager cyclone (CY0207), primary cyclone (CY0201), combustion heat exchanger (HX0203), spent solids screw cooler (FD0206), spent solids conveying system (FD0510), gas analyzer, and pressure letdown valve (PV287). The operational description of the test runs are organized as follows:

Section 4.1.1	Introduction and test objectives for series test runs CCT4
Sections 4.1.1.1 through 4.1.1.4	Characterization test runs CCT4A through CCT4D
Section 4.1.2	Introduction and test objectives for series test runs CCT5
Sections 4.1.2.1 through 4.1.2.2	Characterization test runs CCT5A through CCT5B
Section 4.1.3	Introduction and test objectives for test run CCT6
Section 4.1.3.1	Characterization test run CCT6
Section 4.1.4	Introduction and test objectives for series test runs TC01
Sections 4.1.4.1 through 4.1.4.9	Test campaigns TC01A through TC01I

The CCT series test runs are characterization tests of equipment or the process in the combustion mode of operation. The TC series tests are test campaigns aimed at long-term tests at specified process conditions. Due to commissioning and the unreliability of a few pieces of operation equipment in the process the test run designations (for example, CCT4A, CCT4B, CCT4C, and CCT4D) used in 1997 are based on main process air compressor starts (for test purposes) and stops. Tests ended due to either a forced outage or scheduled shutdowns at the completion of test objectives.

4.1.1 CCT4 Series Test Runs

The CCT4 test run was planned to achieve 150 hours of operation on coal feed at pressures up to 200 psig. The objectives for CCT4 were as follows:

- Evaluate gas/solids separation system performance at various circulation rates. Determine how the cyclone inlet modifications affected the capture efficiency.
- Demonstrate reactor temperature control using the combustor heat exchanger (HX0203) and evaluate the effect, if any, that added nozzles had on the circulating ability of the HX0203.
- Increase the PCD gas inlet temperature by bypassing the primary gas cooler (HX0202) and characterize the effectiveness of the HX0202 gas bypass for temperature control.
- Evaluate the reliability of the coal feed system.
- Evaluate the reactor coal throughput and determine the maximum achievable coal feed rate.
- Evaluate the sulfur capture effectiveness by adding dolomite at a specified calcium-to-sulfur (Ca-to-S) ratio.

Disengager cold flow tests were conducted at General Electric Environmental Services, Inc., (GEESI, the disengager and cyclone vendor) on February 6 and 7, 1997. The performance of the cold flow disengager with sand at GEESI is similar to what was observed during the PSDF disengager tests in December 1996. The data from the November 1996 test strongly suggested that the primary cyclone was not capturing solids since the disengager efficiency seemed to follow the same trend as the cold flow results. During all the 1996 test campaigns at PSDF the cyclone dipleg was not sealed with solids, and it is possible that the gas was bypassing up through the dipleg into the cyclone, causing the cyclone's efficiency to be penalized. It is also possible that a hole (or gap) might have developed in the roof of the cyclone allowing gas and solids to bypass the gas outlet tube. Either of these scenarios would be consistent with the low-cyclone-pressure drop observed during the 1996 PSDF test runs.

The performance of the disengager with fly ash at GEESI is inferior to that with sand. Based on the fly ash and sand data it may be speculated that the actual disengager efficiency with char and transport reactor ash may be significantly lower than the design values of 97.6 and 96.4 percent for combustion and gasification operations, respectively. From these results came the recommendation that the roof of the cyclone be inspected for cracks or a hole that could provide a bypass path, especially around the gas outlet tube. Testing at the PSDF with the cyclone dipleg sealed with solids was also suggested to investigate possible cyclone inefficiency caused by disengager standpipe gas venting up the cyclone dipleg. Such tests would give information on how to improve the overall solids collection efficiency of the transport reactor solid separation system.

Based on tests and recommendations from GEESI, the primary cyclone (CY0201) exit pipe was inspected. There were no apparent holes in the lower metal section. However, some dust was present, so small holes could not be seen. The separation between the refractory above the metal pipe and the metal section was visible.

The inlet to the primary cyclone (CY0201) was modified prior to the start of the CCT4 test runs. A rectangular inlet replaced the circular CY201 inlet, with a 50-percent reduction in flow area in an effort to increase the cyclone collection efficiency. An ultraviolet scanner was installed in the reactor start-up burner (BR0201) through a new penetration in the vessel. The UV scanner would be used for flame detection so that the pilot would need to be operated for short time periods and only when necessary. The original flame-rod-based pilot flame detection system and the pilot tip would, therefore, have a longer operating life. Also, the natural draft pilot was modified to a forced draft pilot and was successfully used to start the burner pilot.

New nozzles were installed to increase aeration to the heat exchanger standpipe. Nozzles were added based on bridging where poor air distribution and poor fluidization was observed in previous test runs and was indicated by the differential pressure measurements. Additions included two nozzles on the HX0203 standpipe, clean-out nozzles for BR0201 J-leg, and the HX0202 gas bypass line. Three additional thermocouples were installed on the upper section of the reactor standpipe.

The start-up procedure was modified to use the Powder River Basin (PRB) coal to preheat the reactor to bituminous coal combustion temperature.

4.1.1.1 Characterization Test Run CCT4A

Test run CCT4A was conducted between March 9 and March 17, 1997. Operating plots are shown in figures 4.1.1.1-1 through -50. The figure number prefix (such as 4.1.1.1- or 4.1.1.2-) does not appear in the text; only the figure number is referenced (such as figures 1 through 50, and the reference will be strictly for figures found in that particular subsection of the document). This convention will be used throughout the document.

<u>CCT4A Test Run Chronology</u>

- On March 7, 1997, the thermal oxidizer (BR0401) air cure was started. The following day all the Clyde systems were tested and the BR0401 burner was started at 16:30.

- On March 9, 1997, at 18:55 the main air compressor (CO0201) was started and the reactor air cure began. The cure out of the thermal oxidizer refractory continued and the steam drum pressure was ramped accordingly. From 12:15 to 18:27 the CO0201 was shutdown due to tuning complications.

- On March 11, 1997, at 03:15 the spent fines screw cooler (FD0502), the spent fines transport system (FD0520), the spent solids screw cooler (FD0206), the spent solids transport (FD0510), and the spent solids feeder system (FD0530) were started up. At 17:10 the start-up burner (BR0201) pilot was lit but tripped at 17:51 (event 1, figure 4).

Several additional attempts were made to relight the pilot but they were unsuccessful. At 19:00 CO0201 was shutdown and the reactor was depressurized to evaluate BR0201. The flame rod response was sluggish and the end of the flame rod was slightly warped, so a new flame rod tip was installed. At 22:15 the CO0201 was started again (event 2, figure 1).

- At 00:12 on March 12, 1997, the BR0201 pilot was lit (event 3, figure 4). At 07:00 the 6-hour, 500°F burner exit temperature hold was completed. The propane pump was started at 07:30 in order to increase pilot propane flow rate and, therefore, lengthen the pilot flame, so as to determine if the UV flame scanner would detect the pilot flame, and to increase the cure out temperature. Attempts to increase the propane flow rate by increasing the differential pressure were unsuccessful. The reactor pressure was decreased to increase the pilot flame length, however, the UV scanner did not detect the pilot flame. Due to physical limitations the UV scanner angle was constrained to detect the flame from the main gun.

- At 08:00 the reactor J-leg aeration and HX0203 aeration flows were adjusted to balance the reactor standpipe, reactor mixing zone, and HX0203 temperatures. Later the UV scanner was removed to determine if the pilot could be visually observed through the sight glass. The flame was not visible from a normal, standing distance and it was barely visible from a closer view. At 10:10 the main burner was lit (event 4, figure 4). When the main burner was lit the flame was easily visible from a distance. However, the UV flame scanner still did not detect the flame. The flame scanner was removed again and successfully bench tested. Later, the problem with the flame scanner was traced to the sight glass, which was replaced. At 10:35 the main burner tripped while the combustion air flow was being adjusted. The BR0201 pilot and main burner were successfully relit (event 5, figure 4).

- On March 13, 1997, the reactor heatup continued. At 10:00 the mixing zone temperatures were decreased to 1,000°F by reducing the BR0201 firing rate (event 6, figures 4 and 6). Also, the process air flows were decreased to lower the riser velocity. At 12:00 the reactor system was ready for sand addition. The mixing zone temperatures were around 950°F (event 7, figure 6). Problems with the programmable logic controller (PLC) gateway caused there to be no distributed control system (DCS) indications for any of the Clyde systems. Operations were put on hold while repairs to the gateway were completed. By 14:30 the gateway repairs were completed and all the indications were functioning (event 8, figures 2, 3, and 19).

- At 15:10, FD0206, FD0510, FD0502, and FD0520 tripped due to a loss of nitrogen supply pressure (event 9, figure 19). A leak around the coal feed system (FD0210) lockhopper spheri shuttle valve was found. This middle spheri valve seal and the shuttle valve were taken out of service for repair. At 16:00 the transport air dryer (DY0210) solenoid valve failed, so DY0210 was taken out of service. The solenoid valves were cleaned and the dryer was put back in service. At 20:00 the gateway problems returned. Even though some DCS indications through the gateway were incorrect the equipment was functioning normally through PLC control. By 22:30 the

FD0210 repairs to the middle spheri valve seal were completed and sand addition was started. At 23:58 the BR0201 tripped and was relit (event 10, figure 4).

- On March 14, 1997, more sand was added to FD0210. At 01:00 and 01:45 the BR0201 tripped due to a high-pressure difference across the burner leg (event 11 and 12, figure 4). At 06:00 the burner firing was increased to continue with heat up. At 10:00 the BR0201 tripped and was relit. At 13:00 Southern Research Institute (SRI) started preparations to take a PCD inlet sample, so conditions were held steady. By 14:10 SRI completed taking the sample. At 14:15 reactor and burner flows were reduced to decrease the riser velocity (event 13, figures 4 and 5).

- At 15:00 the PRB coal was loaded into the sorbent feed system (FD0220). The mixing zone temperatures ranged from 965 to 1,065°F and the riser temperature ranged from 1,096 to 1,067°F (event 14, figure 6). The combustor heat exchanger (HX0203) circulation was unsteady so the HX0203 aeration flows were adjusted to improve the circulation. At 17:00 the BR0201 pilot was lit and the propane flow was reduced to maintain 2,000°F at the burner exit (event 15, figure 4).

- At 18:45 the BR0201 tripped due to a swing in CO0201. At 20:00 the pilot was lit. The main burner was lit immediately and the pilot was shut down. The UV scanner worked well in detecting the main burner flame. At 22:43 there were 3,000 lb of sand added to the reactor from FD0210. The PRB coal was added to FD0210. The remaining PRB coal in FD0220 was fed starting around 23:50 (event 16, figure 3). Due to problems with FD0220 coal feed was switched to FD0210 (event 17, figure 2).

- On March 15, 1997, at 01:37 CO0201 tripped (event 18, figure 26). Within 20 minutes the compressor was back on-line. Bituminous coal feed began at 01:57 (event 19, figures 27, 31 through 34, 37, 39, and 47). At 04:14 the BR0201 firing was reduced and by 05:00 BR0201 was shut down (event 20, figure 29). At 06:25 the HX0203 J-leg flow was reduced and the standpipe J-leg flow was increased to reduce solids circulation through the HX0203 and increase the mixing zone temperature. The coal feed rate was maintained constant while the FD0220 problems were solved.

- At 08:40 the reactor pressure was increased to 100 psig (event 21, figure 37). The HX0203 J-leg flow was increased to increase the solids circulation through HX0203 in order to control the reactor temperature while the burner air flow was reduced to maintain a constant riser velocity. The coal feed rate was also slightly reduced. At this time, the reactor solids inventory was low, so at 10:19 sand addition into the reactor from FD0220 was initiated (event 22, figure 28).

- At 10:40 SRI started sampling at the PCD outlet. At 12:00 the FD0220 dispense lock vessel seal was found to be blown, so sand transfer into the reactor was stopped (event 23, figure 28). At 12:35 all the Clyde systems and FD0502 tripped because of loss of medium pressure seal nitrogen. The nitrogen was back at normal conditions in about 10 minutes. Coal feed was restarted and slowly increased.

- At 13:38 SRI started sampling at the PCD inlet and was completed by 14:30. The reactor pressure was increased at 15:15 (event 24, figure 37). At 17:00 the HX0203 standpipe aeration flows were adjusted to induce more circulation through HX0203. The standpipe pressure differential (PDT259) increased from 120 to 150 inH_20 (event 25, figure 38). At 19:15 the nozzles on the reactor J-leg and the HX0203 J-leg were unplugged. As a result the reactor J-leg flow increased, increasing the carryover to PCD, so the J-leg flows were reduced. At 20:00 the HX0203 J-leg flow was increased to raise the circulation of cold solids so that the coal feed rate could be increased.

- At 23:19 FD0220 was started. At 23:30 it was discovered that FD0220 exit was hot and the material inside was smoldering. The conveying air was swapped to nitrogen via manual block valves and the coal feed was stopped (event 26, figures 27, 31 through 34, 37, 39, and 47). The problem was traced to improper line-up of FD0220 to reactor, causing a reverse flow of hot reactor gases. The FD0220 exit and the feeder motor were disassembled and the system was cleaned and put back in service.

- On March 16, 1997, at 00:40 there were 6,000 lb of sand loaded into FD0210 to replace the lost solids. After sand addition was completed the BR0201 was lit (event 27, figure 29). The reactor J-leg flow was increased to increase the solids circulation through the reactor. At 11:13 SRI sampled the PCD inlet.

- At 11:33 the BR0201 tripped due to a compressor surge. Problems with the compressor continued (event 28, figure 26). Finally at 11:49 the compressor recovered and a considerable amount of solids were carried into the PCD. At 12:12 the BR0201 pilot was lit but tripped after 5 minutes. CO0201 began to have problems again. There was a significant loss of bed material into the PCD caused by depressurizing the reactor below the targeted rate (event 29, figure 37). Several attempts were made to light the burner but they were unsuccessful. The system was shut down to examine the flame rod and the igniter.

- The pilot assembly was removed. The flame rod, igniter, and UV scanner were tested on the bench and found to function correctly. The pilot assembly was reinstalled and CO0201 was started (event 30, figure 26). Several attempts were made to light the burner but none were successful. During one of those attempts, at 12:47, the compressor surged and a temperature spike was noticed in the reactor. Apparently a puff of propane started burning in the riser crossover that caused the bed of coal lying in the riser crossover to ignite, sending hot particles down the standpipe, disengager outlet, cyclone outlet, and cyclone dipleg. Operating temperatures that were higher than desired at that time lasted for about 10 minutes, with 6 minutes above 1,800°F in the secondary crossover and about 2 minutes above 2,000°F.

- At 09:00 on March 17, 1997, the BR0201 pilot assembly and the main gun were inspected and found to be functional. At 09:30 the CO0201 was started up to cool the refractory to permit entry into the PCD vessel and inspect the cyclone. At 10:55 air injection through the reactor loop was stopped and nitrogen flow was started to cool

the reactor for 1 hour. By 12:00 the reactor was cooled so all flows were reduced and the reactor loop was depressurized to atmospheric pressure (event 31, figure 37).

CCT4A Post Test Run Inspections

The FD0220 dispense vessel was taken apart for inspection on March 16, 1997. Part of the agitation (mixing) bar had melted and was replaced. On March 17 the start-up burner's pilot and main burner were pulled and inspected. The pilot was in good shape and there were no burn signs visible on the pilot shroud. There was some rust in the propane lines to the burner. The PCD, cyclone, cyclone dipleg, and secondary crossover were inspected. The lower plenum candles and the FD0502 screw cooler were also inspected and appeared to be in good condition. The cyclone gas outlet pipe, cyclone, and entire vertical portion of the dipleg appeared to be clean. The secondary crossover, visually inspected through a nozzle, was fairly clean and the new refractory that was poured to restrict the cyclone inlet was in fairly good shape.

CCT4A Test Run Observations

The sight glass purchased from Canty and the Purple Peeper did not work well together. The glass (Starphire) would pass UV wavelengths from 320 to 400 nm, however the Purple Peeper only reads in the UV range from 150 to 250 nm. Thus the glass was blocking all readable wavelengths. A quartz sight glass designed for 300 psig and 650°F was installed and it worked well. The only problem with using the quartz sight glass is that it is very delicate. The recommended torque for the sight glass flanges is 5 ft/lb. Also, the torque sequence must be such that the glass is evenly loaded. It is very easily broken. One advantage that the Starphire sight glass had is that the glass was encased in a metal ring and well protected from overtorque. Quartz cannot be encased in a metal ring because the melting point of quartz is higher than the metal.

The UV scanner was successfully used instead of a flame rod for the first time for burner operation. The main burner was operated without the pilot. The forced draft pilot was successfully used for the start-up of the burner pilot. The solids carryover problem continued as in previous test runs. Unlike the previous test runs where a mixture of PRB and cokebreeze was used the use of PRB coal for reactor assist preheat was successful. A total of 24 hours on coal was achieved and 7 tons of coal were fed.

Section 4.1.1.1

Graphs 1 through 25

Test Run CCT 4A
March 11 through March 14, 1997

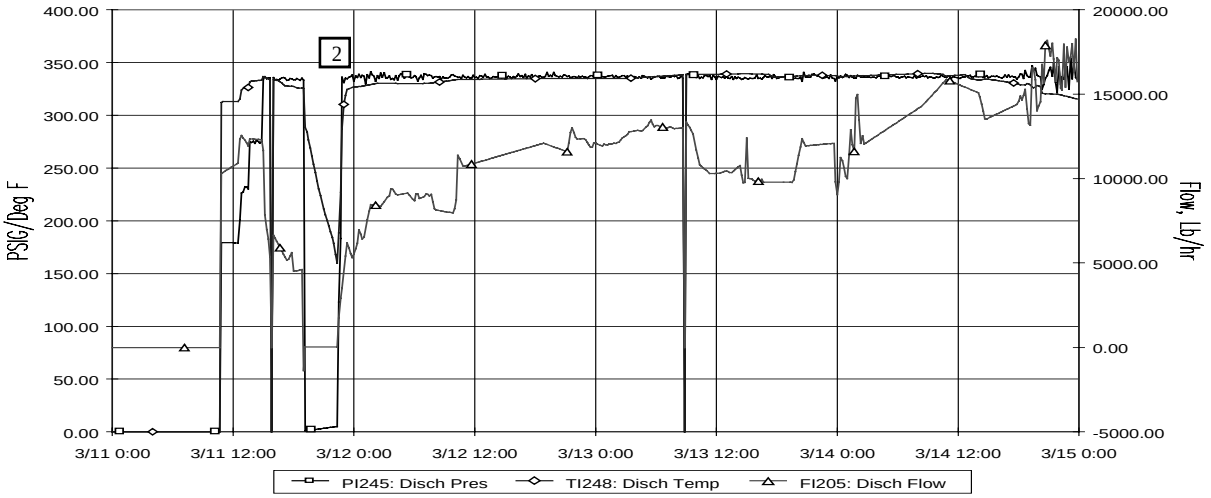

Figure 4.1.1.1-1 CO0201 System Profile

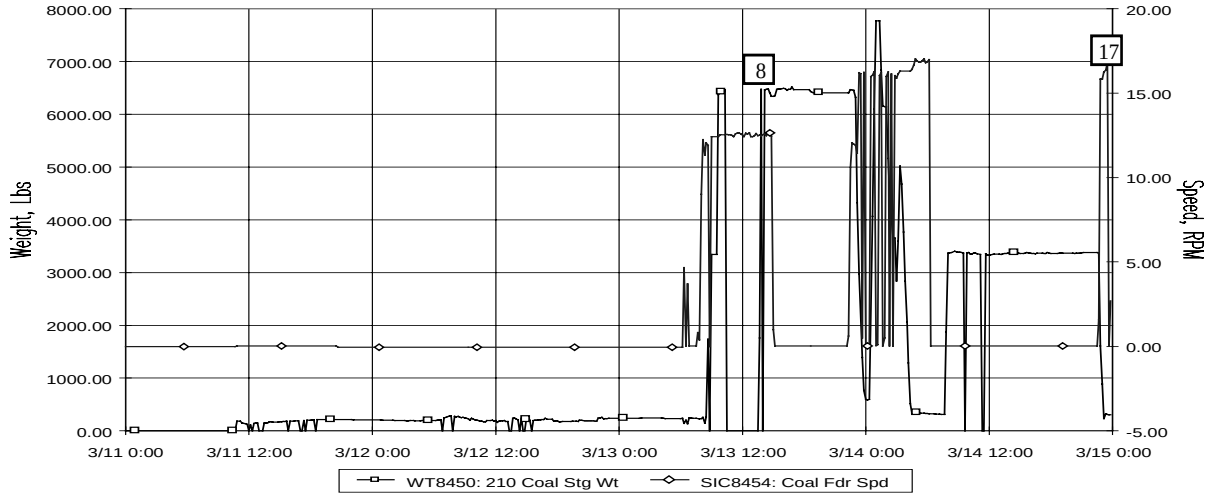

Figure 4.1.1.1-2 Coal Feed System Profile

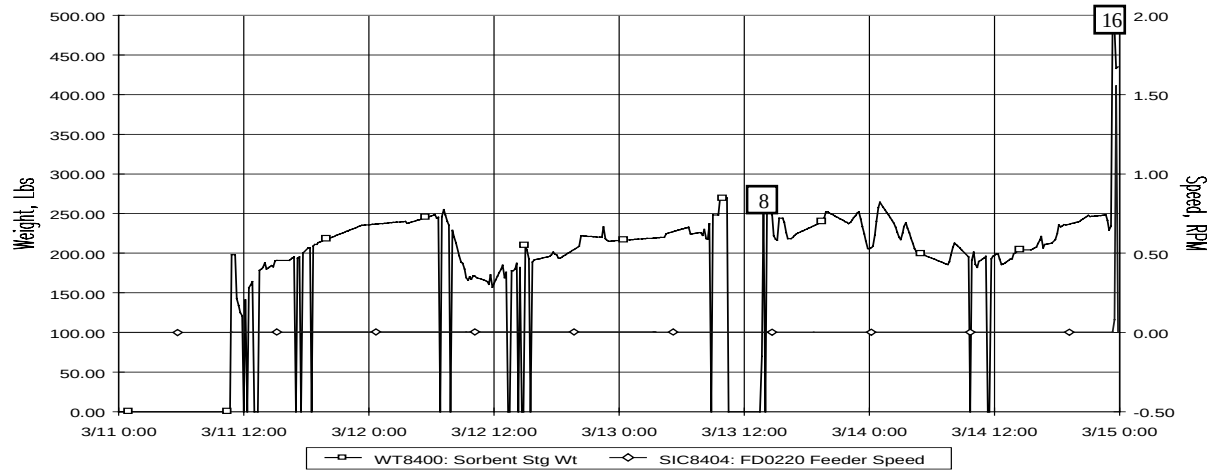

Figure 4.1.1.1-3 Sorbent Feed System Profile

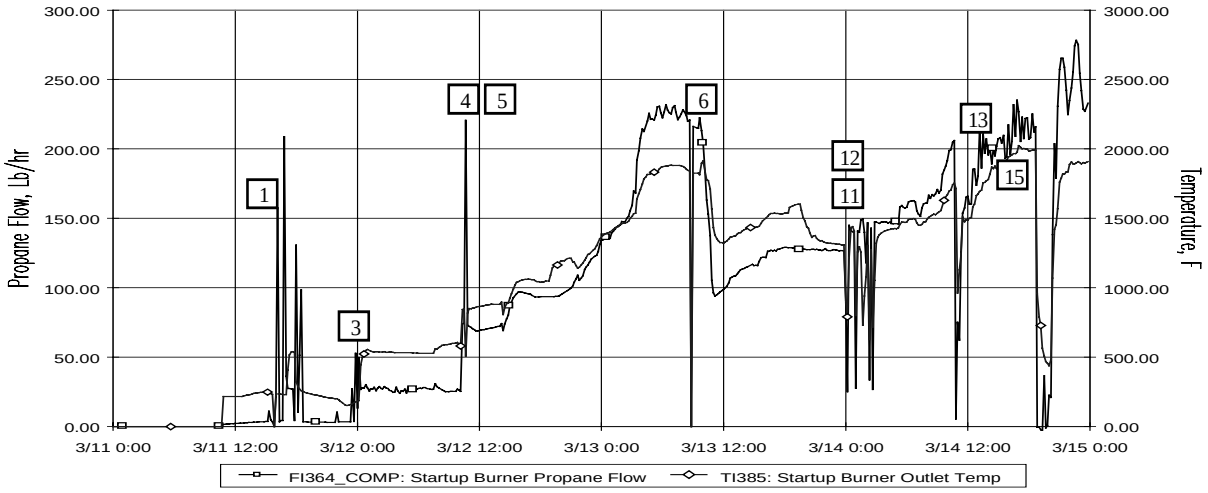

Figure 4.1.1.1-4 Start-Up Burner Flow/Temperature

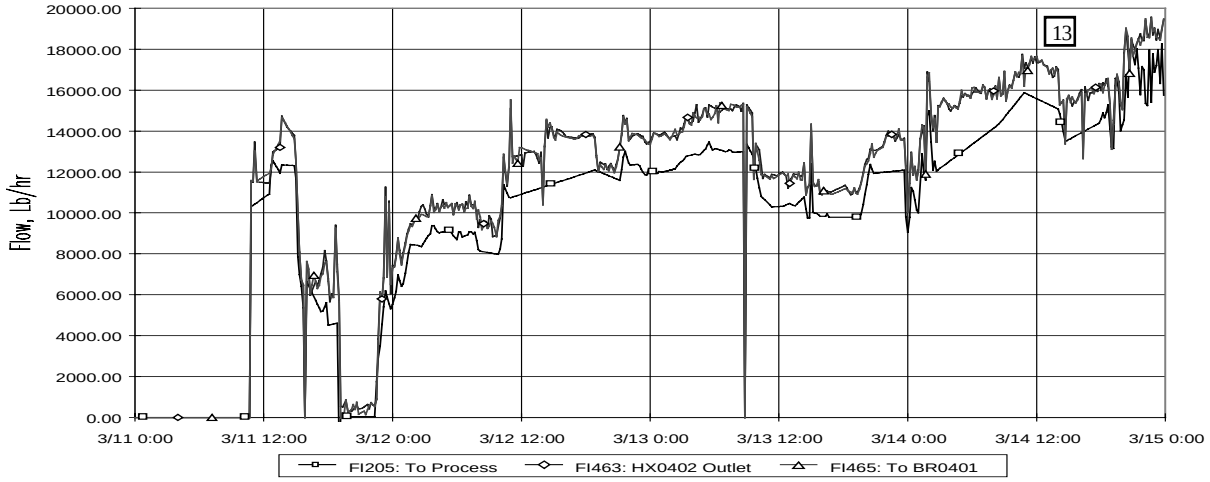

Figure 4.1.1.1-5 Total Gas In/Out Flow Rates

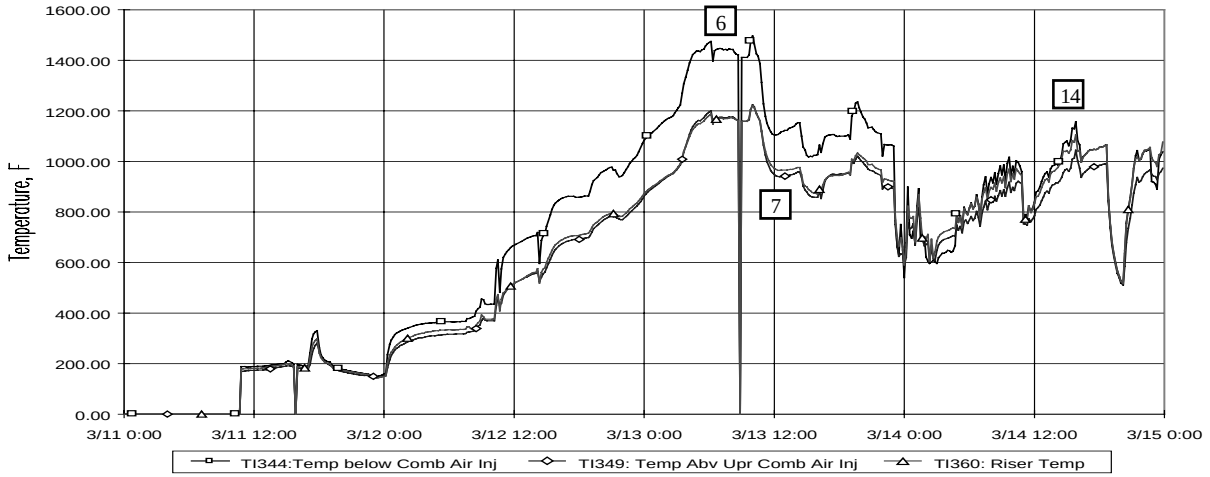

Figure 4.1.1.1-6 Reactor Mixing Zone and Riser Temperatures

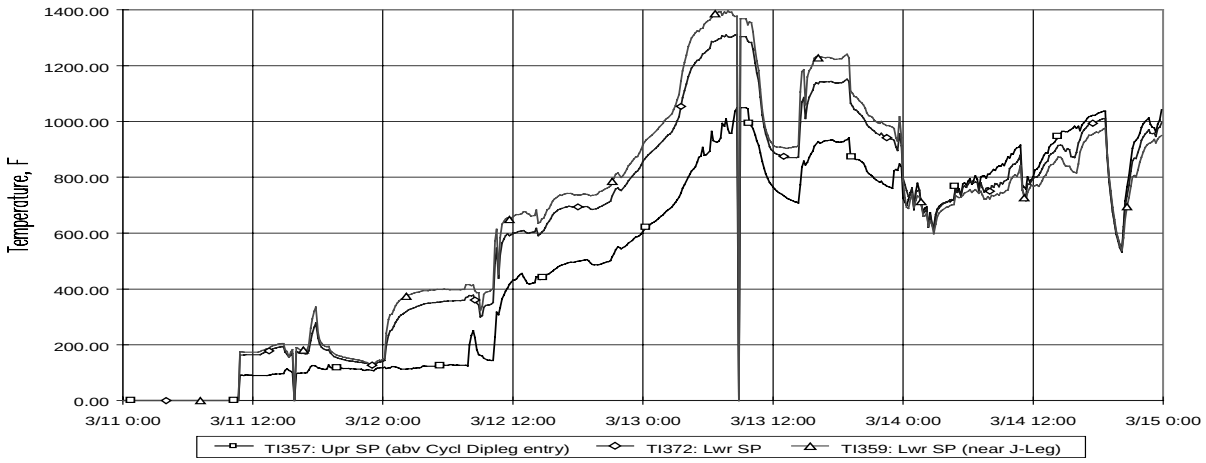

Figure 4.1.1.1-7 Standpipe Temperatures

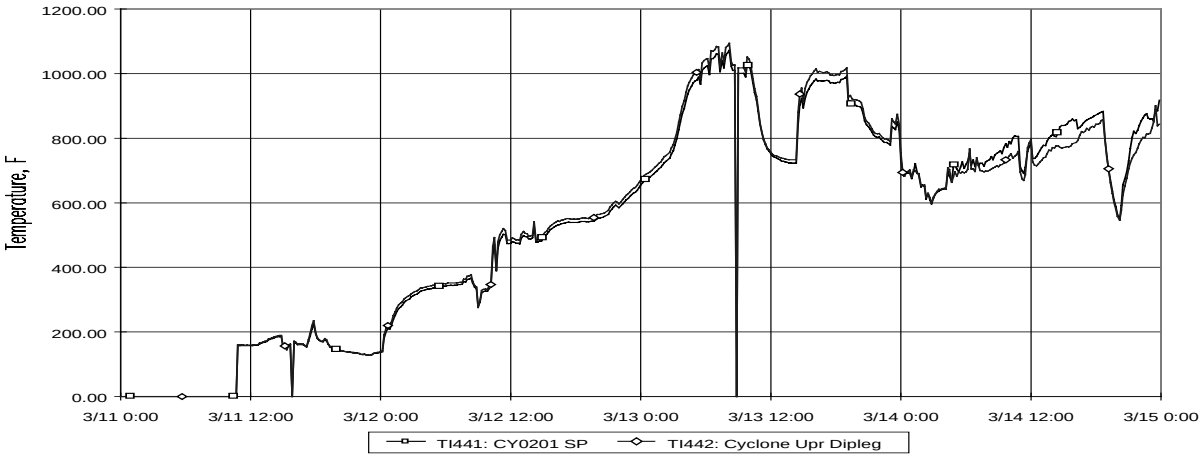

Figure 4.1.1.1-8 Cyclone Dipleg Temperatures

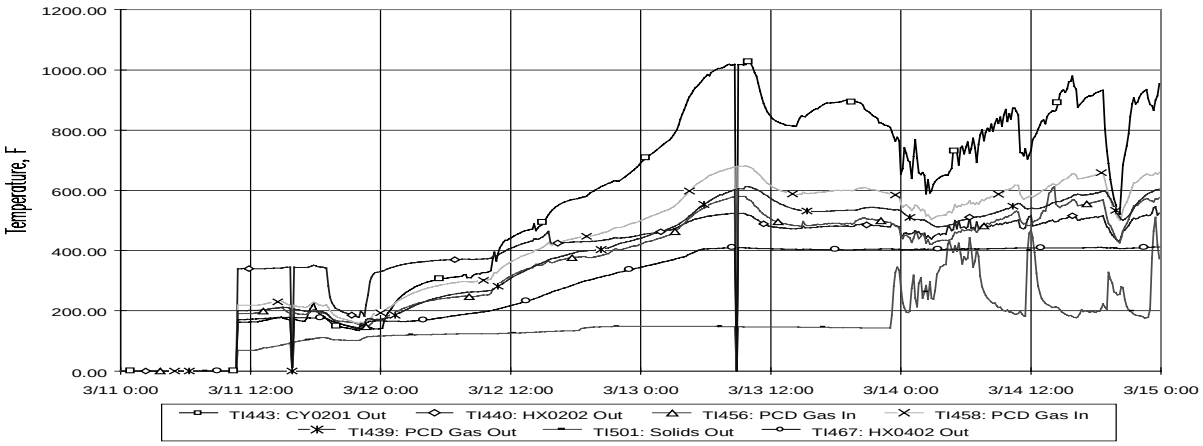

Figure 4.1.1.1-9 Temperature Profile Downstream of Reactor

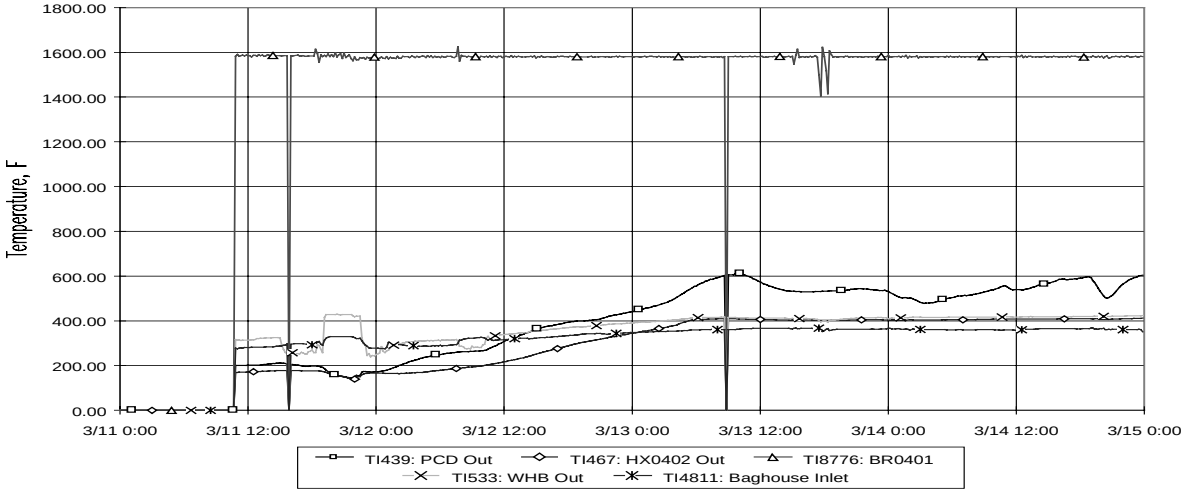

Figure 4.1.1.1-10 System Temperatures Downstream of PCD

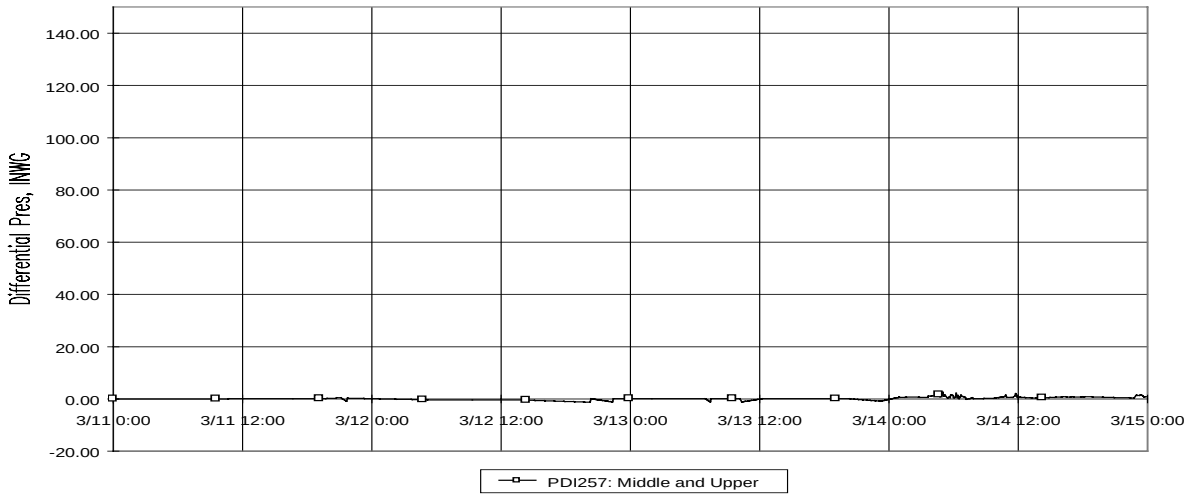

Figure 4.1.1.1-11 Mixing Zone Differential Pressure Profile

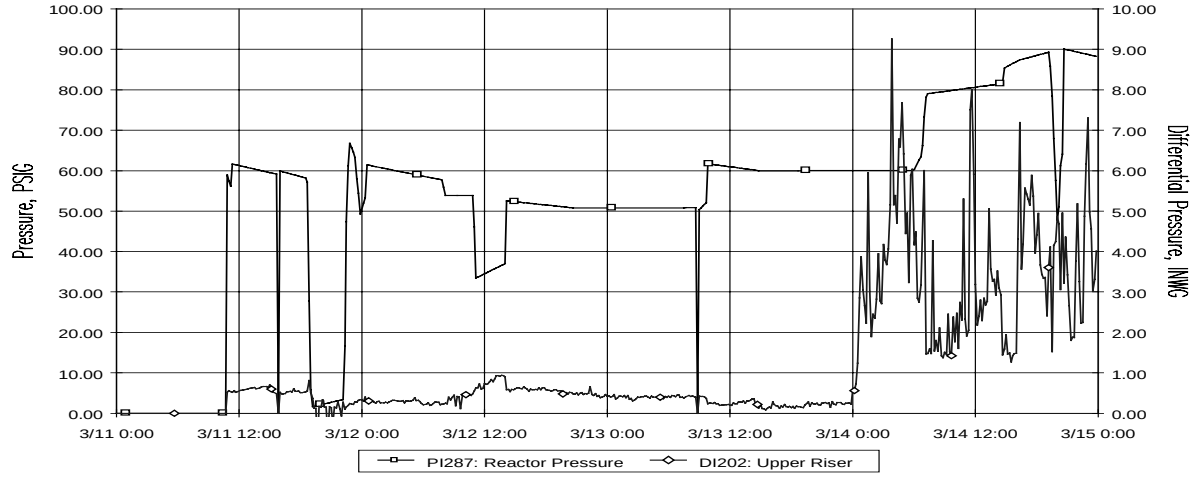

Figure 4.1.1.1-12 Reactor Pressure/Riser Differential Pressure Profiles

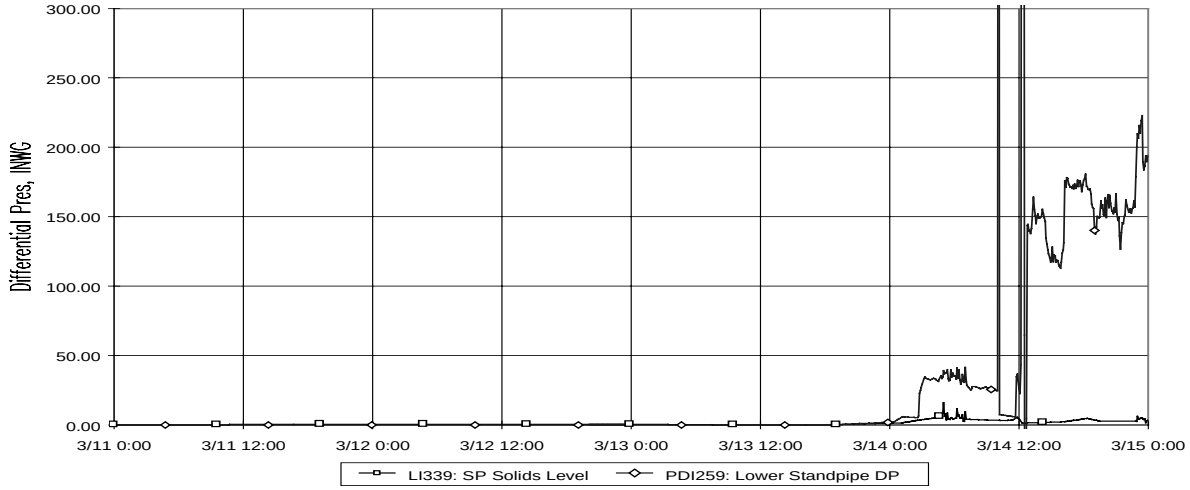

Figure 4.1.1.1-13 Standpipe Differential Pressure Profiles

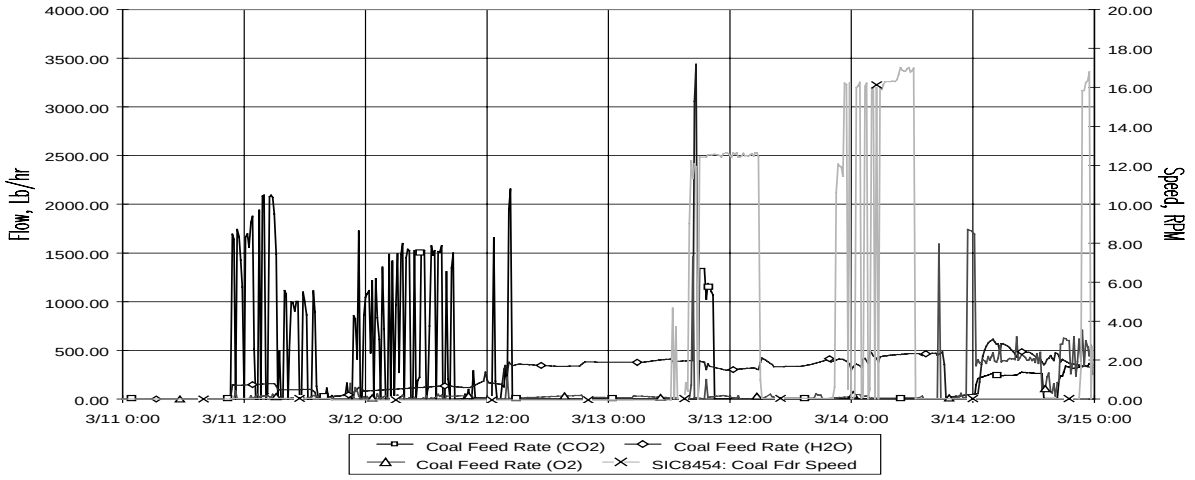

Figure 4.1.1.1-14 Coal Feed Rate Based on Gas Analysis

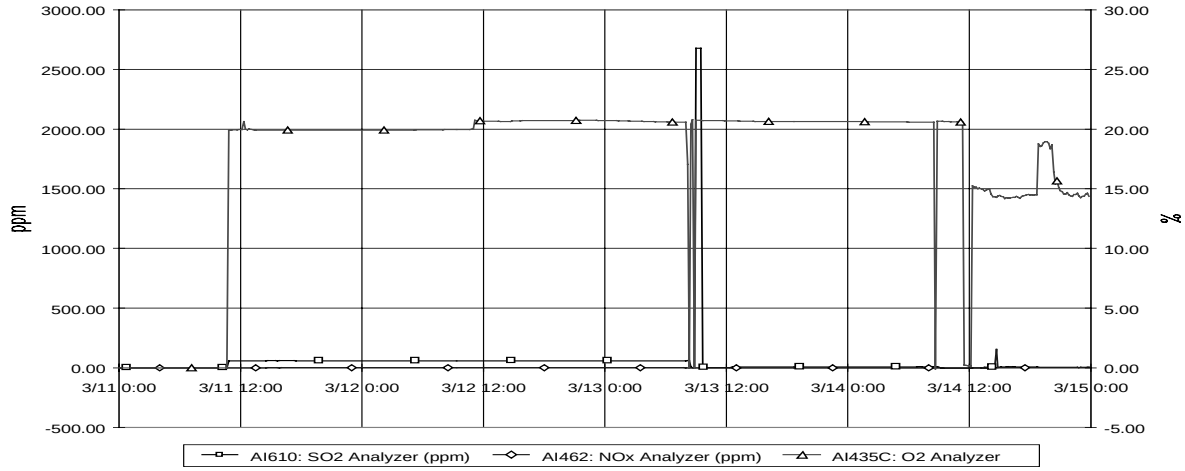

Figure 4.1.1.1-15 O_2, SO_2 and NO_x Analyzers

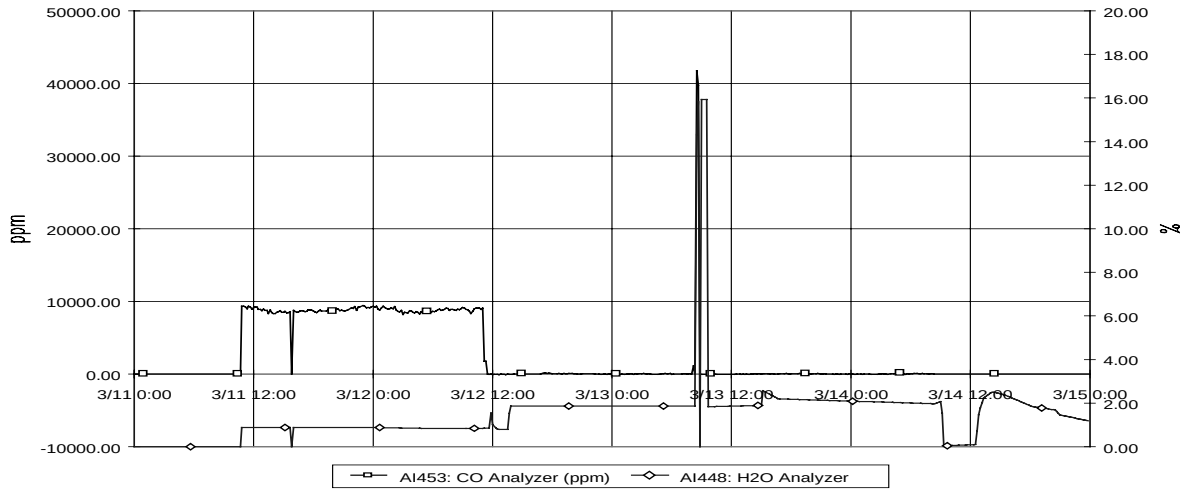

Figure 4.1.1.1-16 CO and H_2O Analyzers

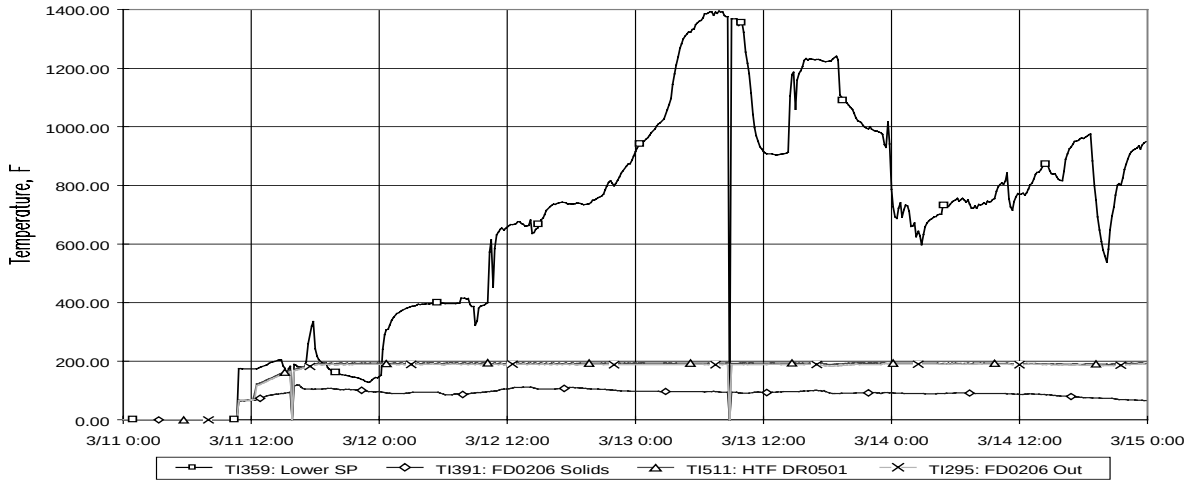

Figure 4.1.1.1-17 FD0510 Temperature Profiles

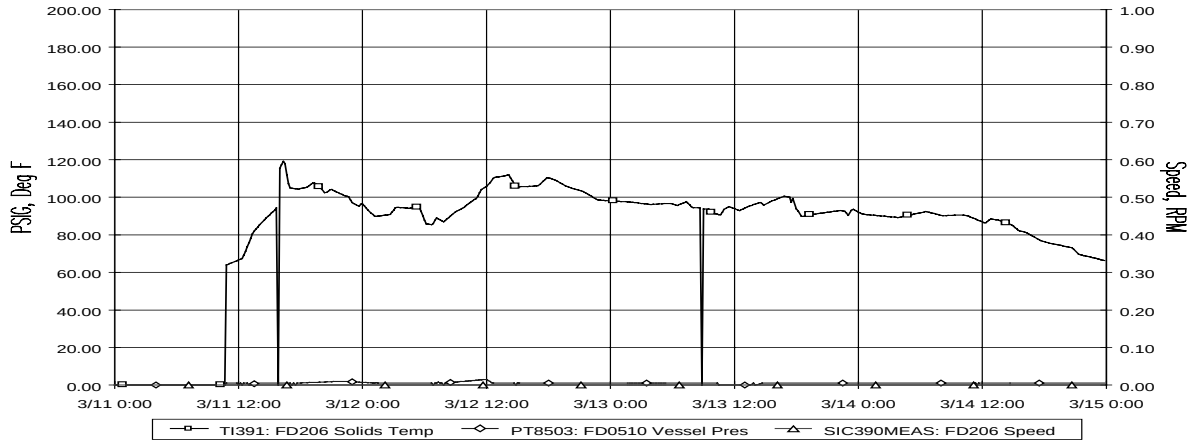

Figure 4.1.1.1-18 FD0206 Profiles

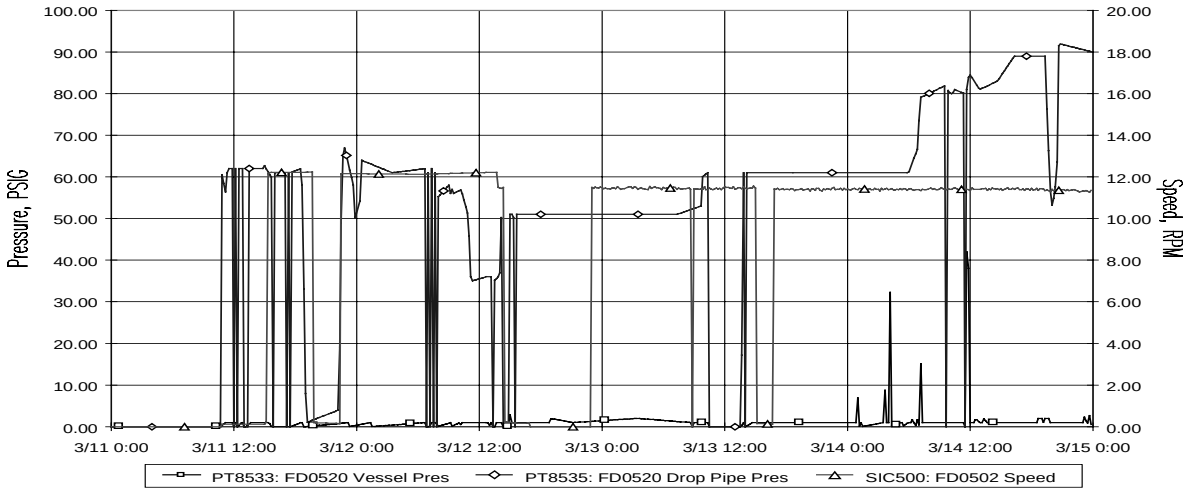

Figure 4.1.1.1-19 FD0520 Pressure Profiles

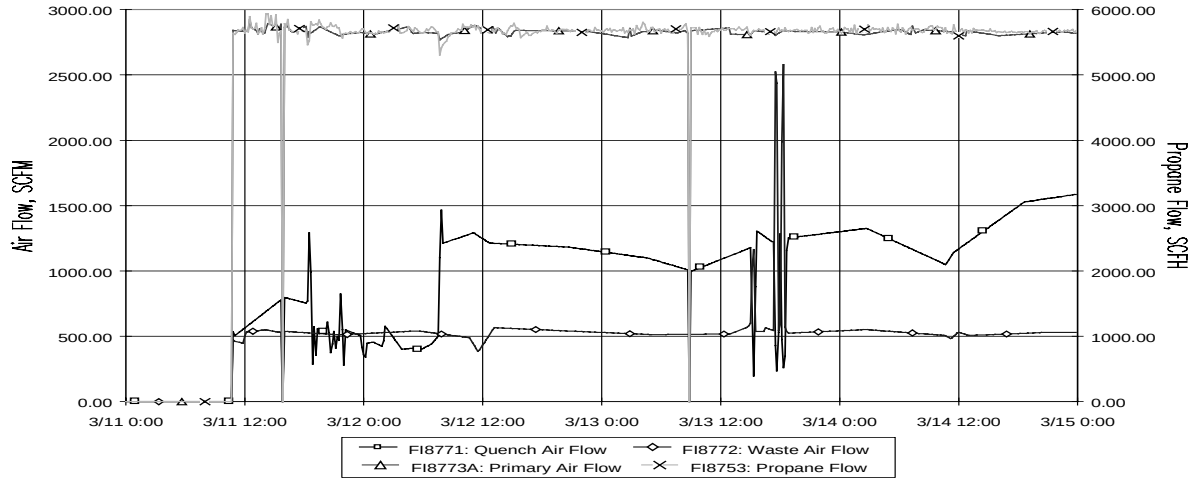

Figure 4.1.1.1-20 Thermal Oxidizer Air/Fuel Flow

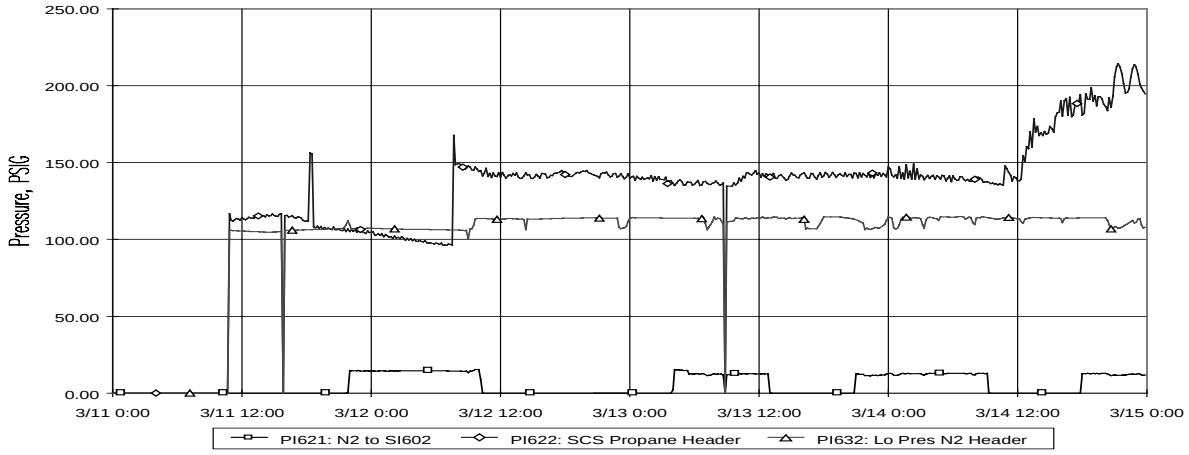

Figure 4.1.1.1-21 Nitrogen/Propane Header Pressure Profiles

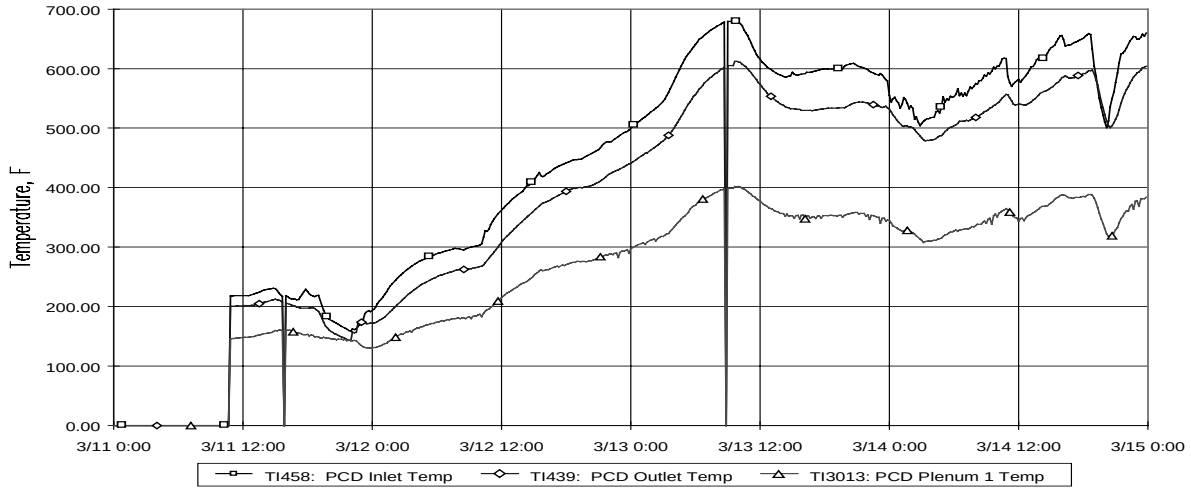

Figure 4.1.1.1- 22 PCD Temperatures

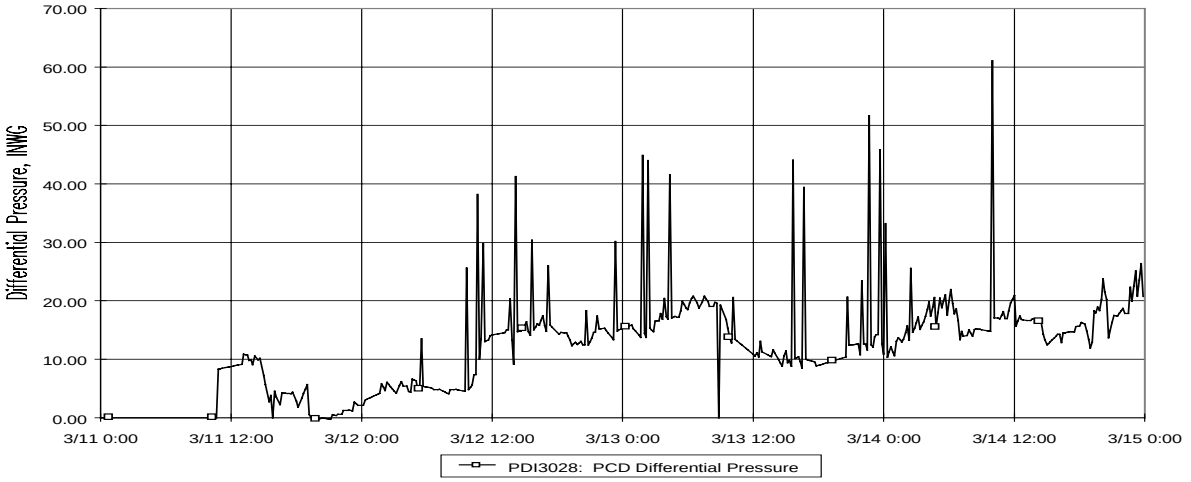

Figure 4.1.1.1-23 PCD Differential Pressure Profile

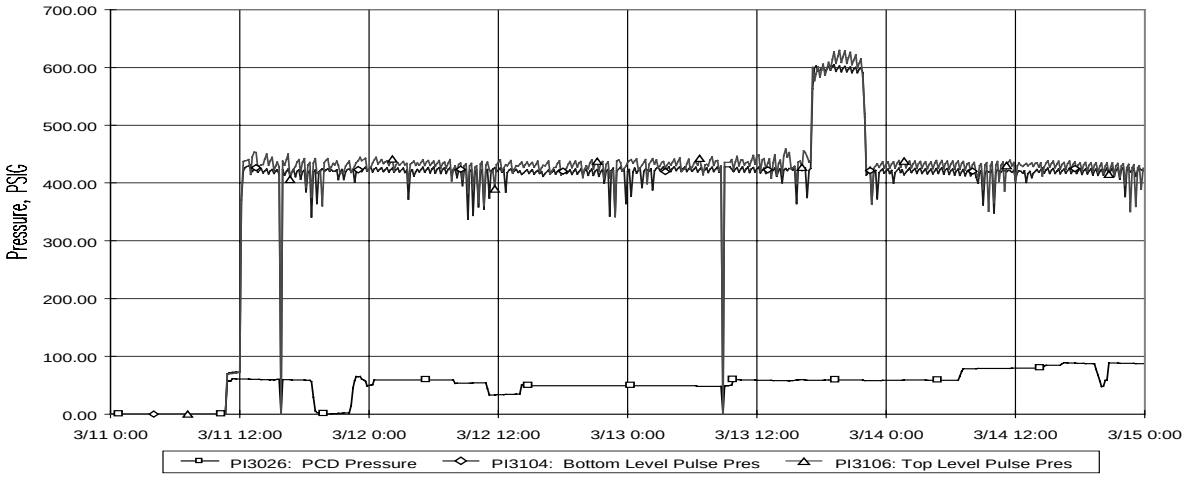

Figure 4.1.1.1-24 PCD Pressure and Pulse Pressure

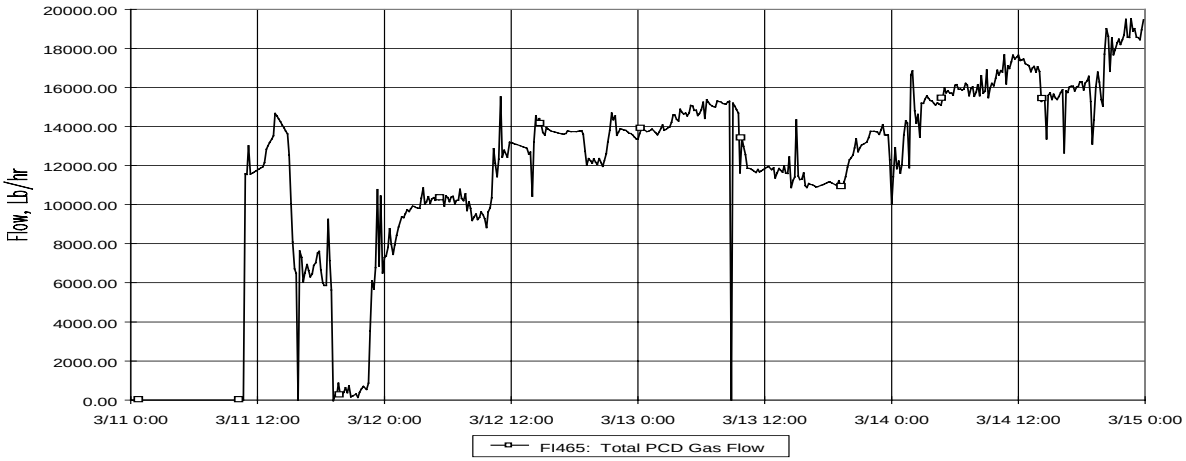

Figure 4.1.1.1-25 Gas Flow Through PCD

Section 4.1.1.1

Graphs 26 through 50

Test Run CCT 4A
March 15 through March 17, 1997

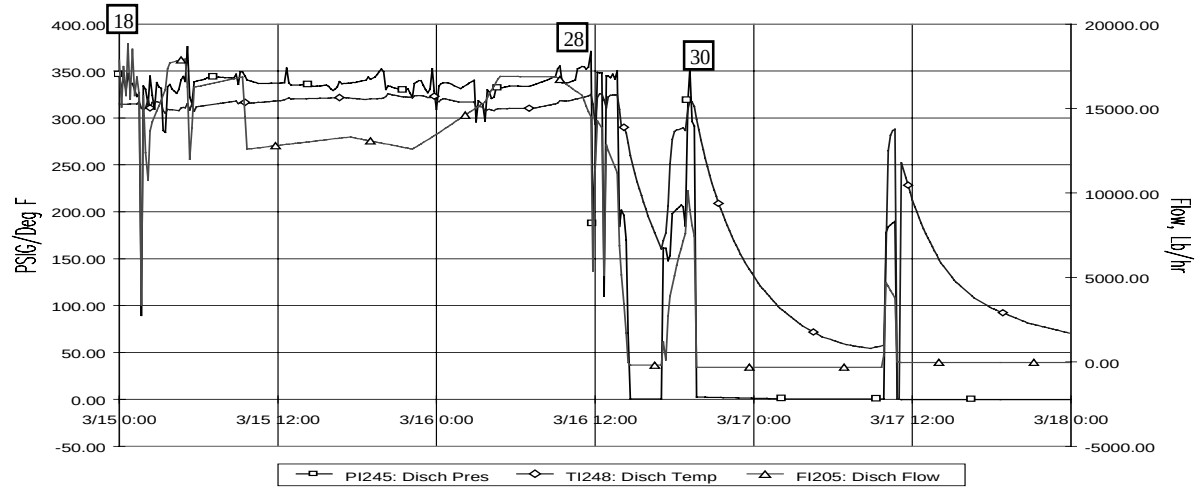

Figure 4.1.1.1-26 CO0201 System Profile

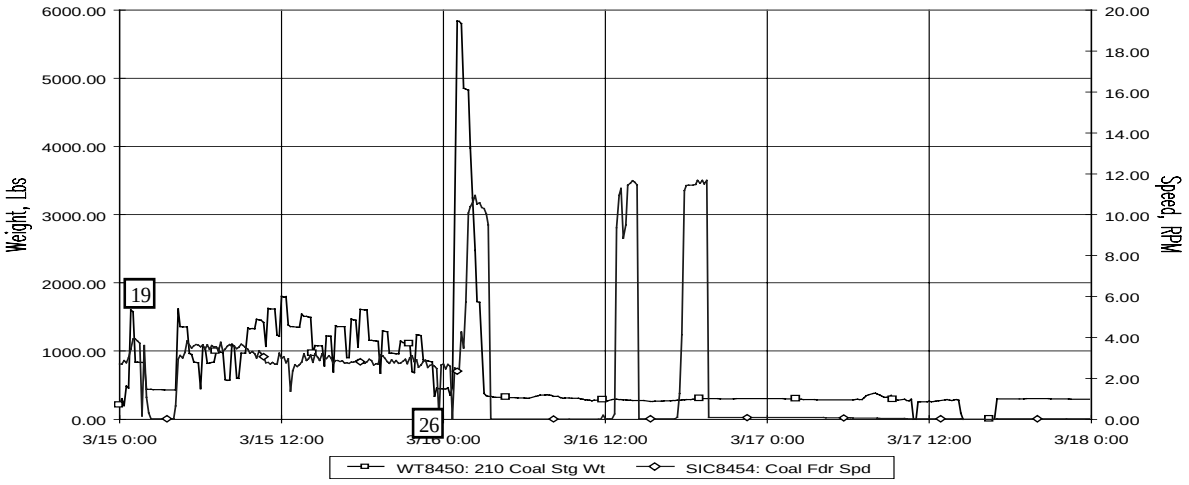

Figure 4.1.1.1-27 Coal Feed System Profile

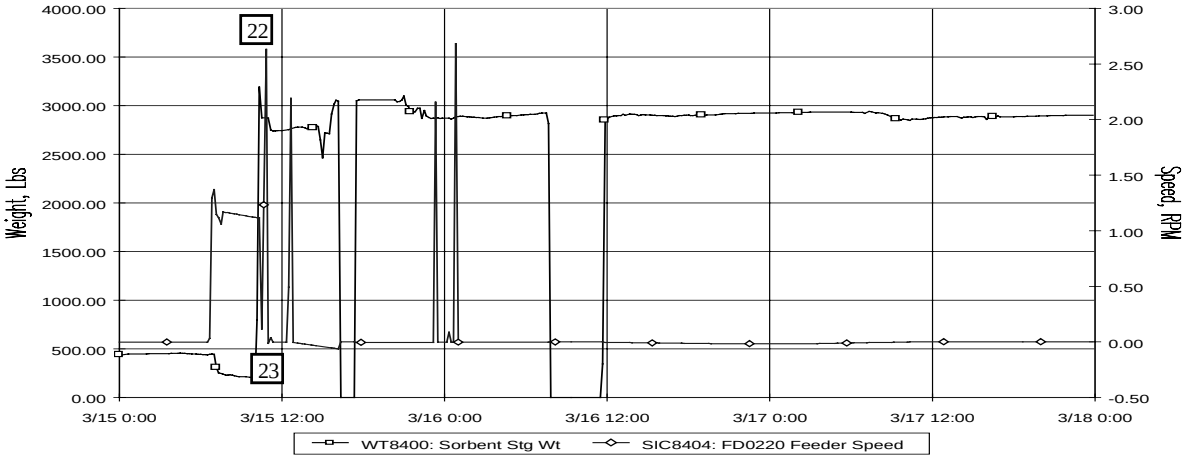

Figure 4.1.1.1-28 Sorbent Feed System Profile

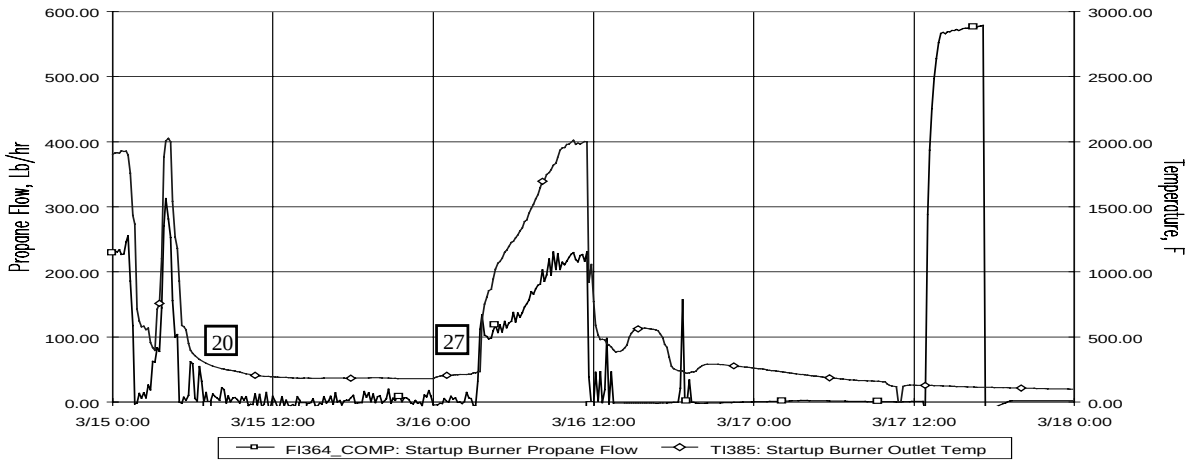

Figure 4.1.1.1-29 Start-Up Burner Flow/Temperature

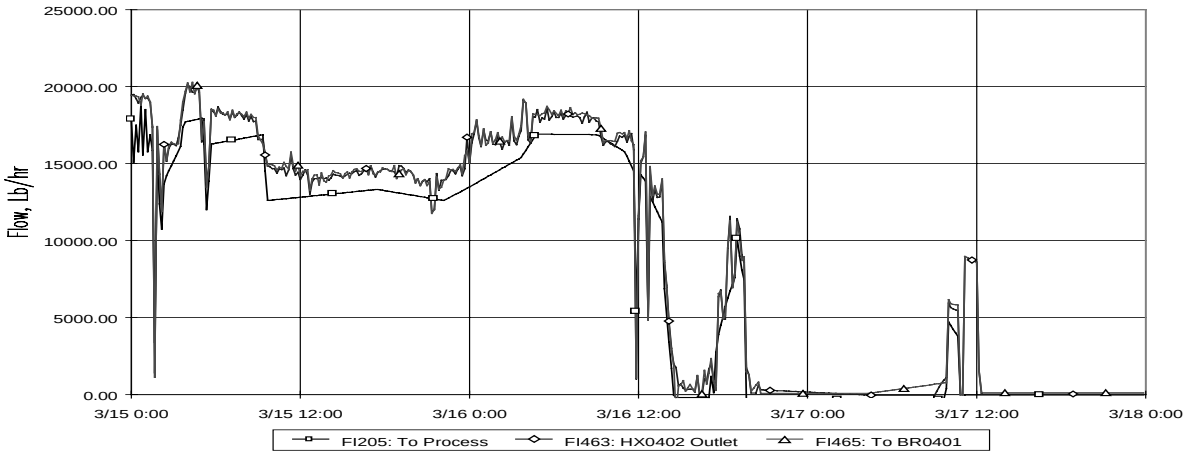

Figure 4.1.1.1-30 Total Gas In/Out Flow Rates

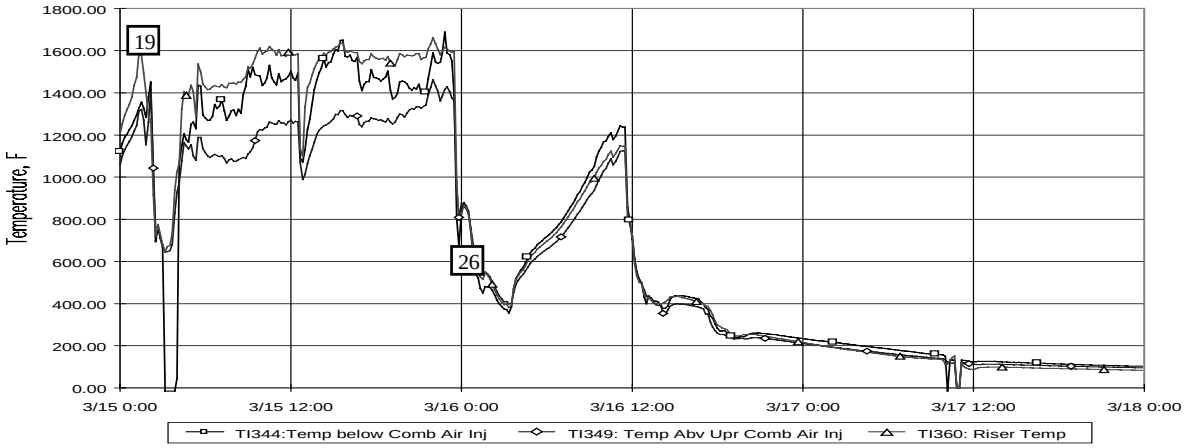

Figure 4.1.1.1-31 Reactor Mixing Zone and Riser Temperatures

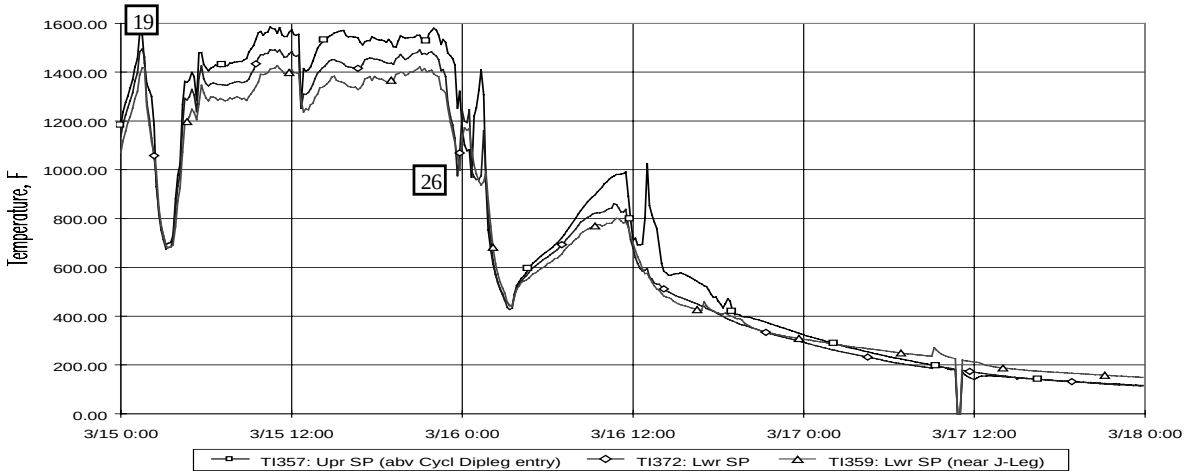

Figure 4.1.1.1-32 Standpipe Temperatures

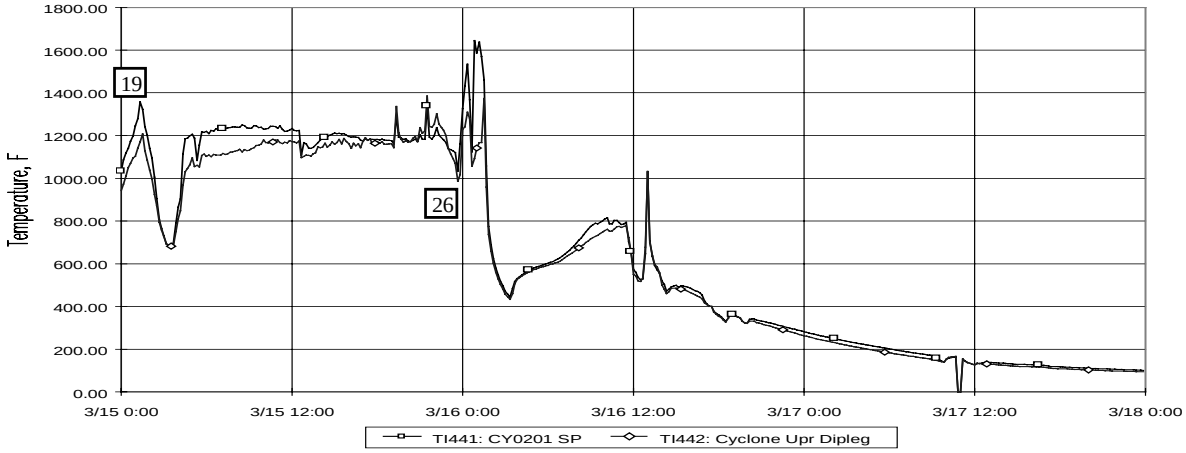

Figure 4.1.1.1-33 Cyclone Dipleg Temperatures

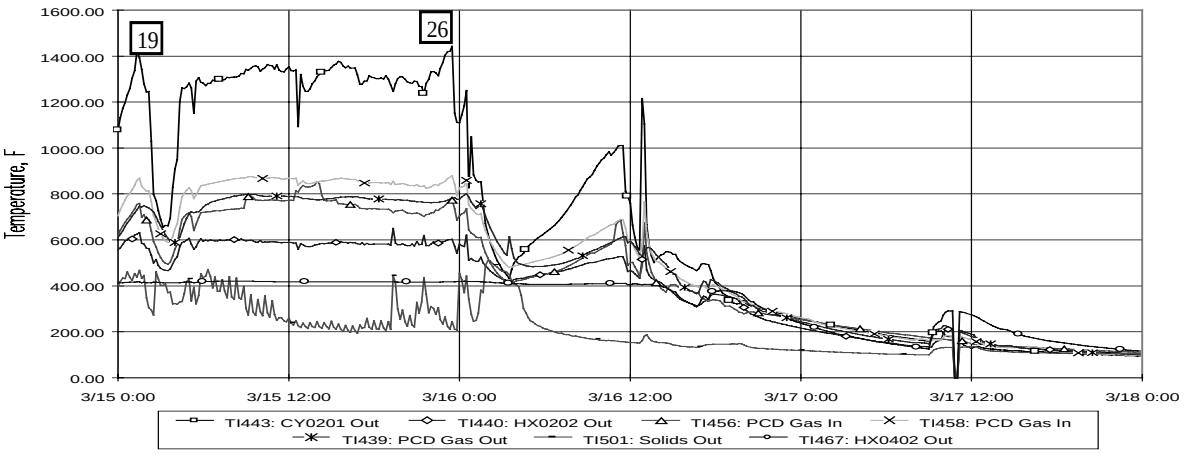

Figure 4.1.1.1-34 Temperature Profile Downstream of Reactor

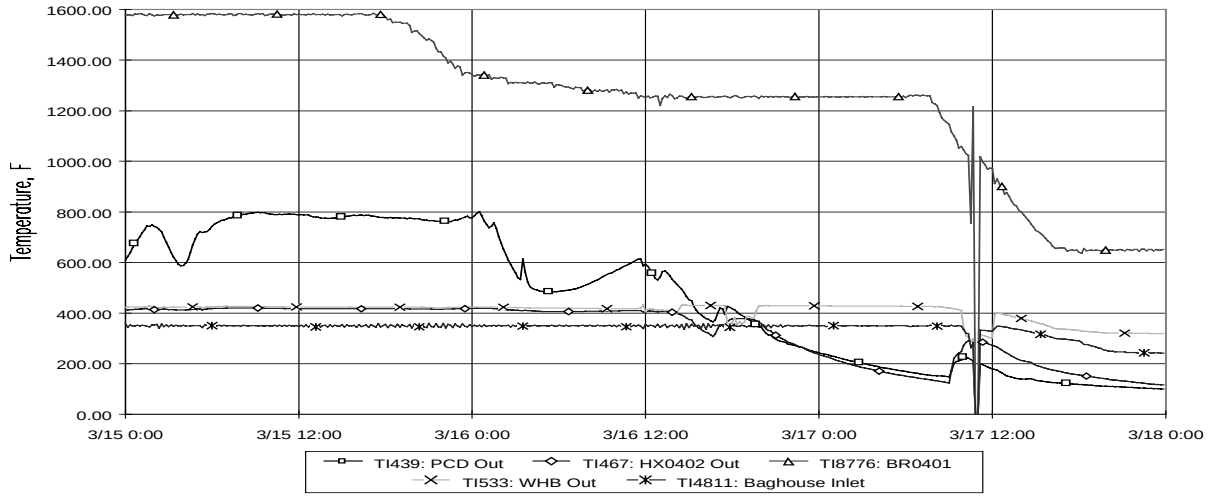

Figure 4.1.1.1-35 System Temperatures Downstream of PCD

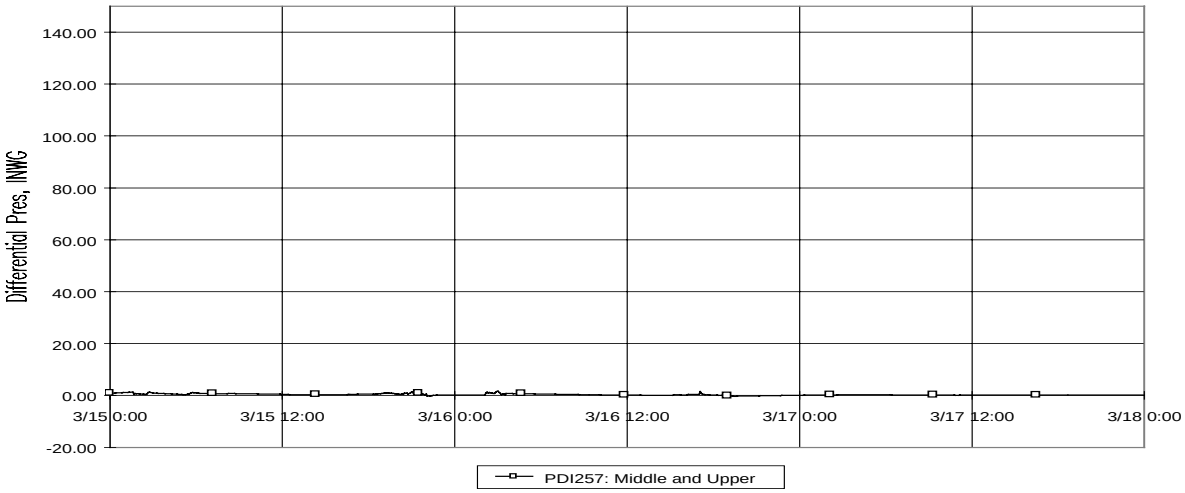

Figure 4.1.1.1-36 Mixing Zone Differential Pressure Profile

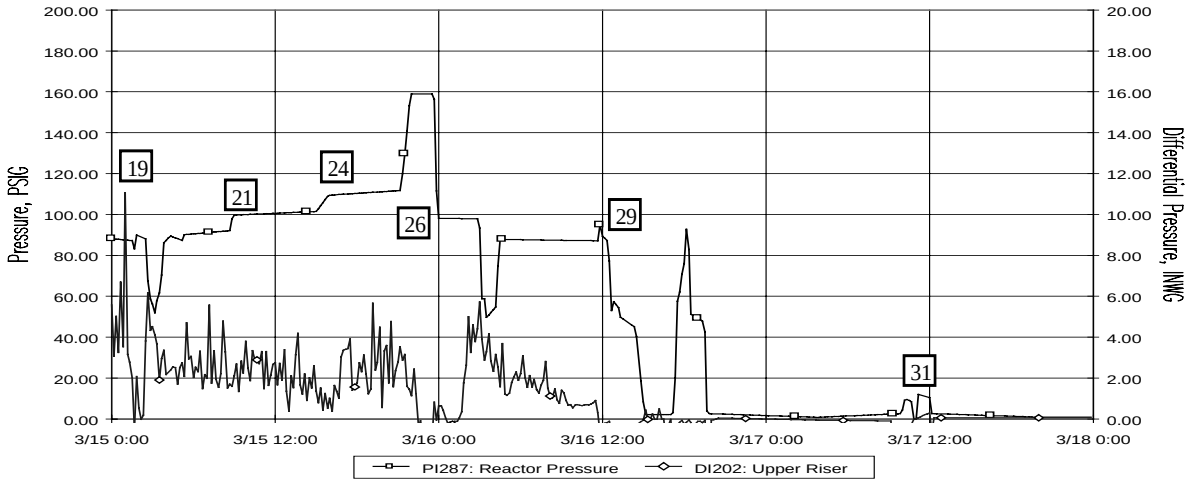

Figure 4.1.1.1-37 Reactor Pressure/Riser Differential Pressure Profiles

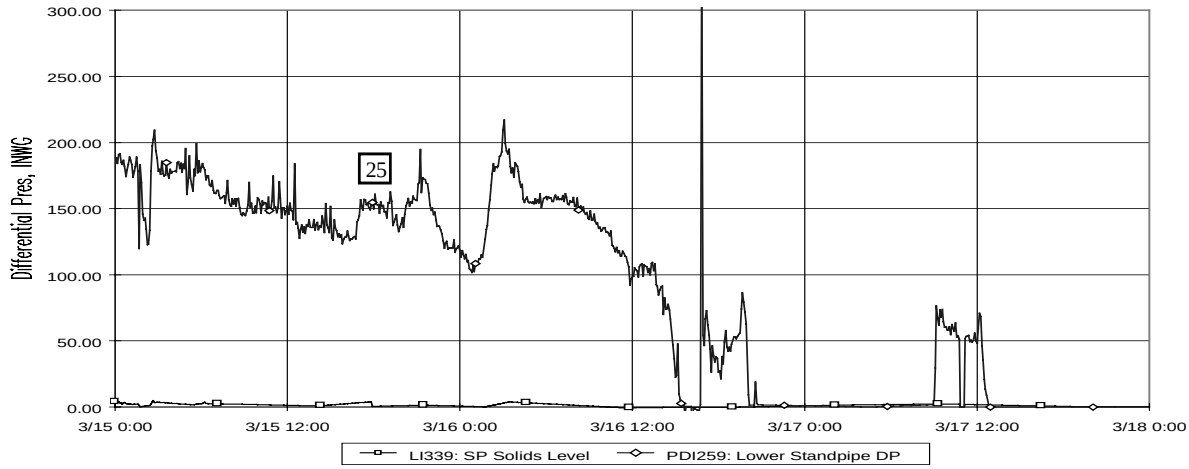

Figure 4.1.1.1-38 Standpipe Differential Pressure Profiles

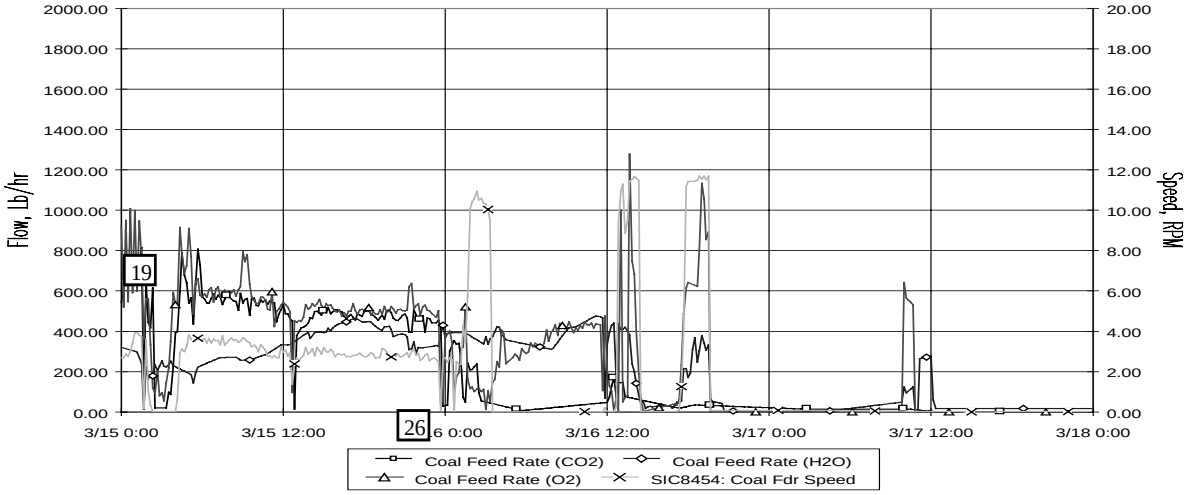

Figure 4.1.1.1-39 Coal Feed Rate Based on Gas Analysis

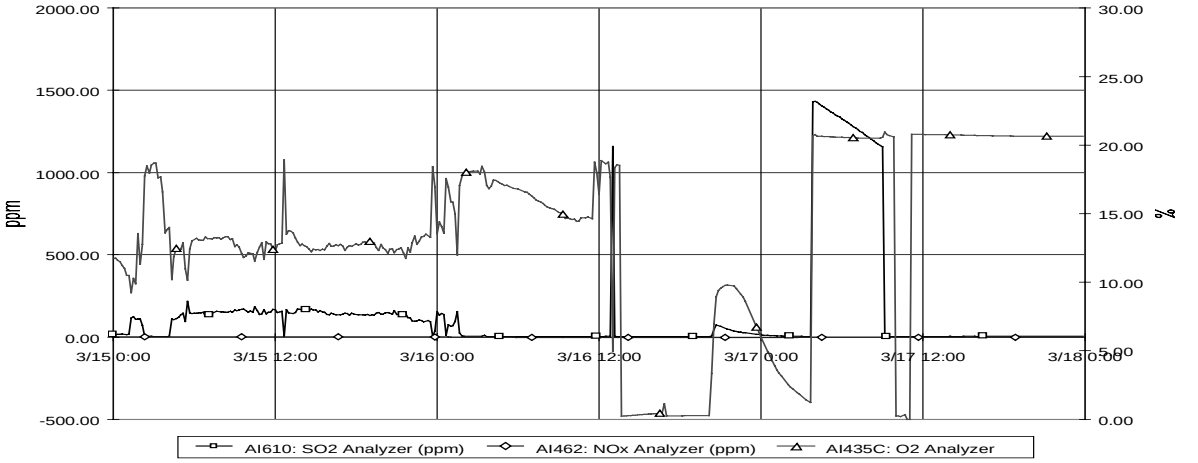

Figure 4.1.1.1-40 O_2, SO_2 and NO_x Analyzers

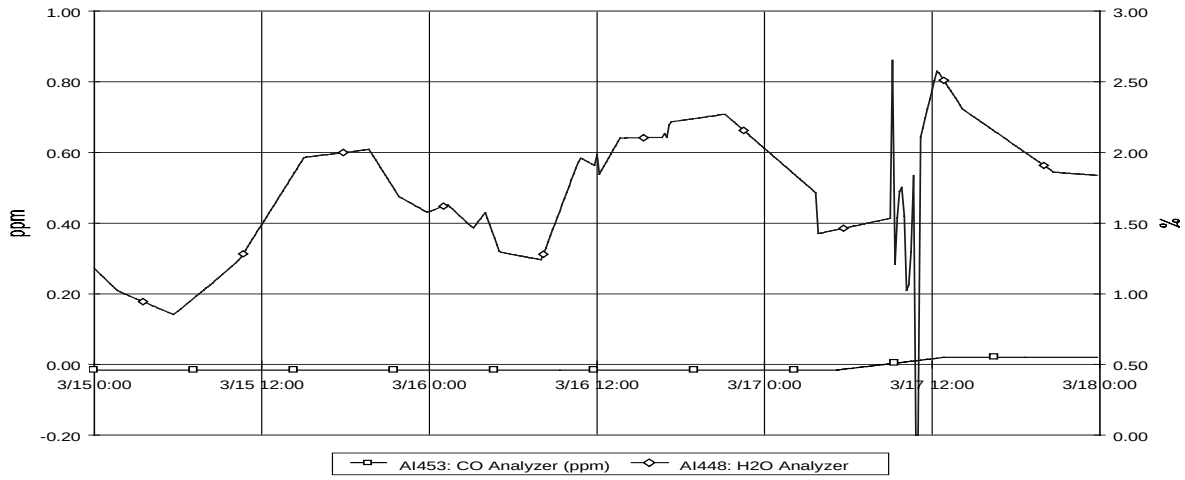

Figure 4.1.1.1-41 CO and H_2O Analyzers

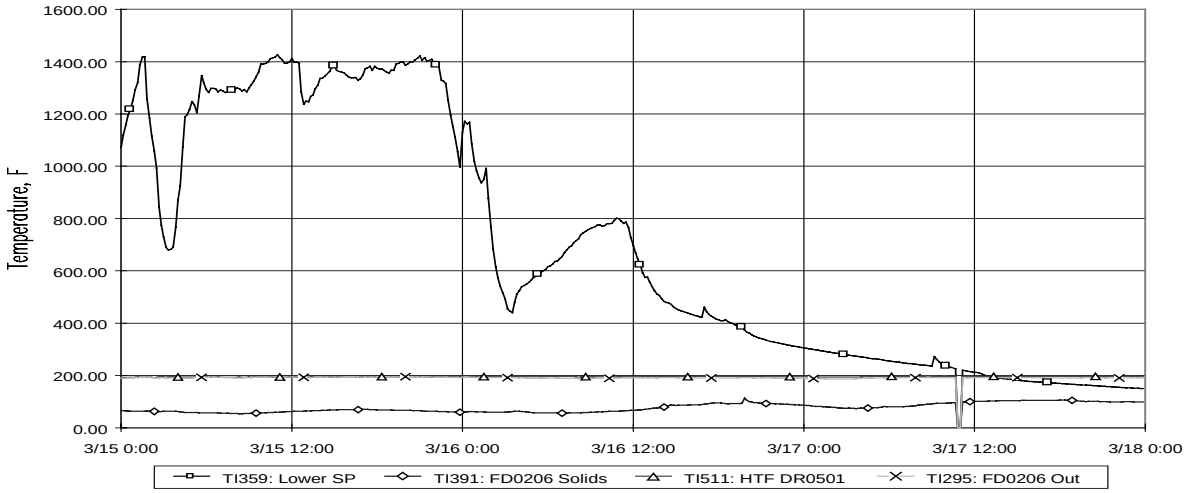

Figure 4.1.1.1-42 FD0510 Temperature Profiles

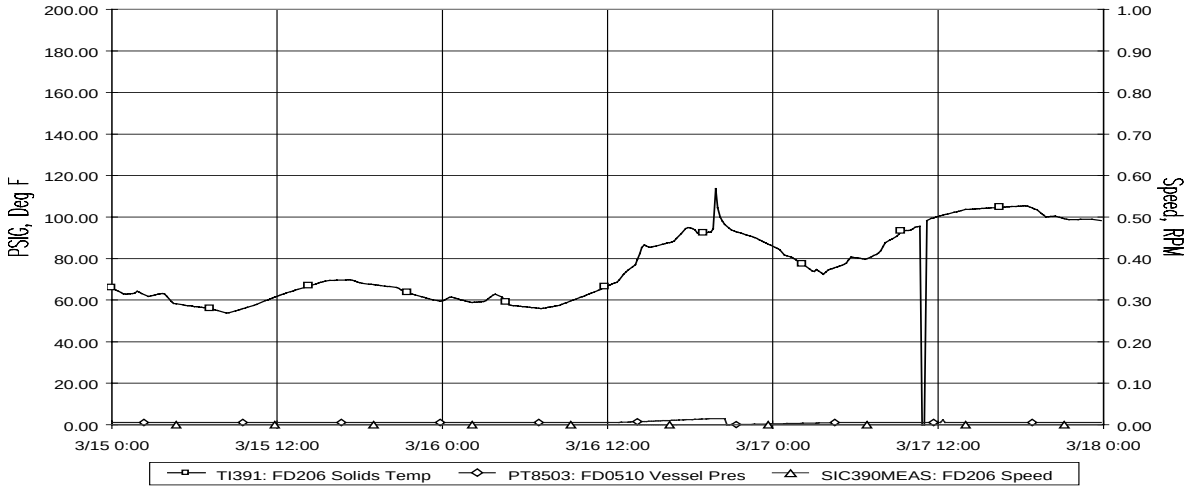

Figure 4.1.1.1-43 FD0206 Profiles

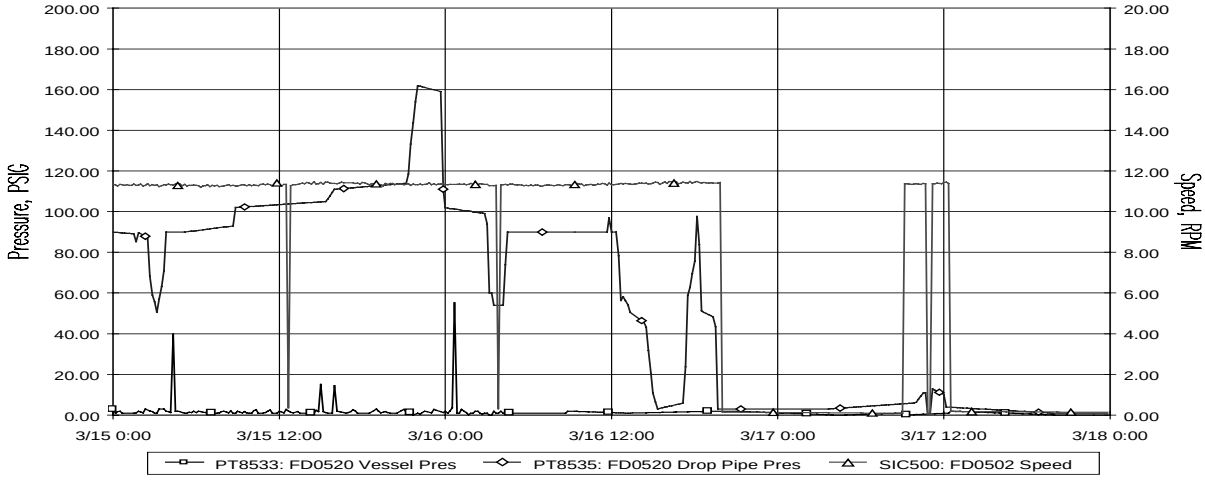

Figure 4.1.1.1-44 FD0520 Pressure Profiles

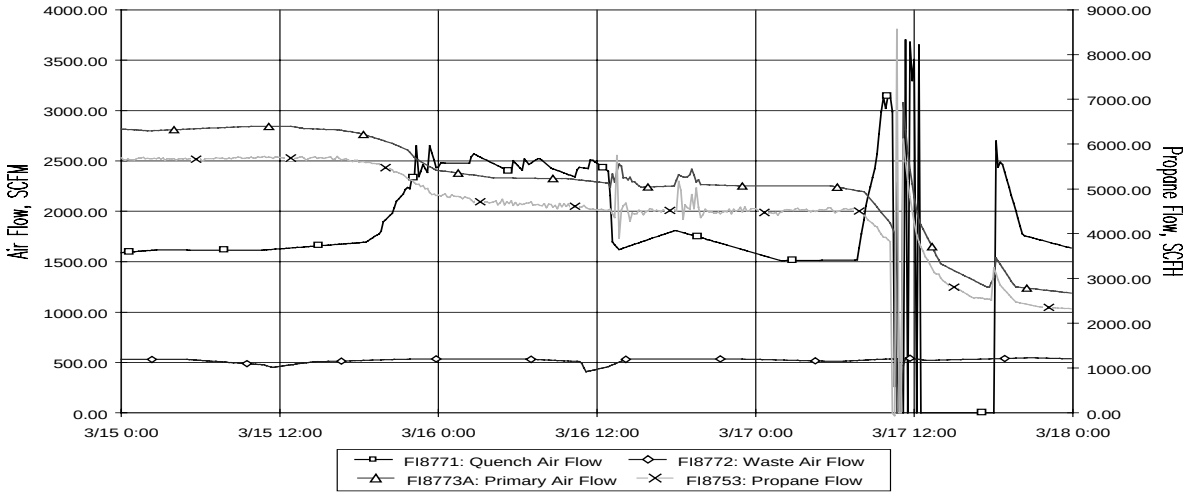

Figure 4.1.1.1-45 Thermal Oxidizer Air/Fuel Flow

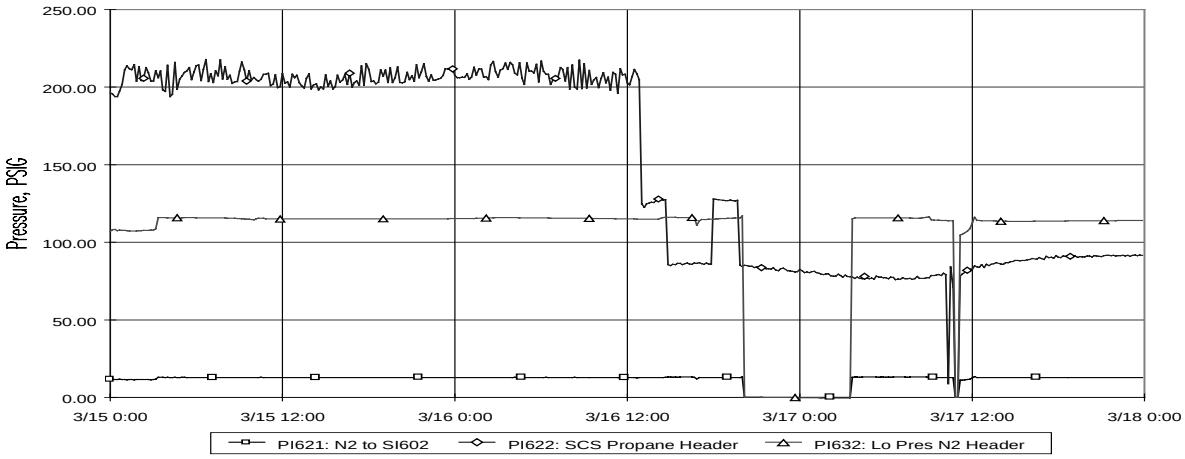

Figure 4.1.1.1-46 Nitrogen/Propane Header Pressure Profiles

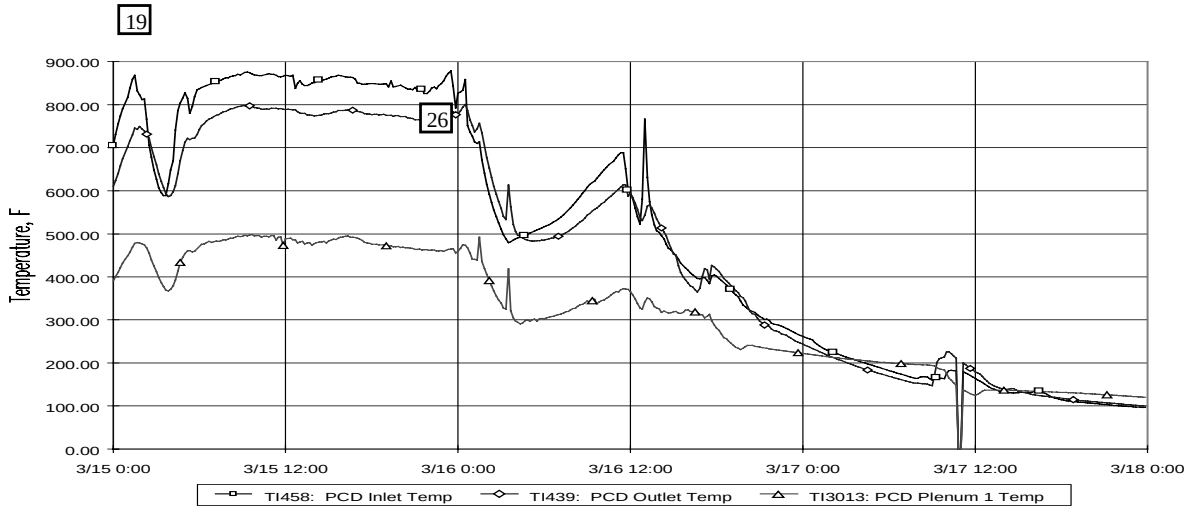

Figure 4.1.1.1-47 PCD Temperatures

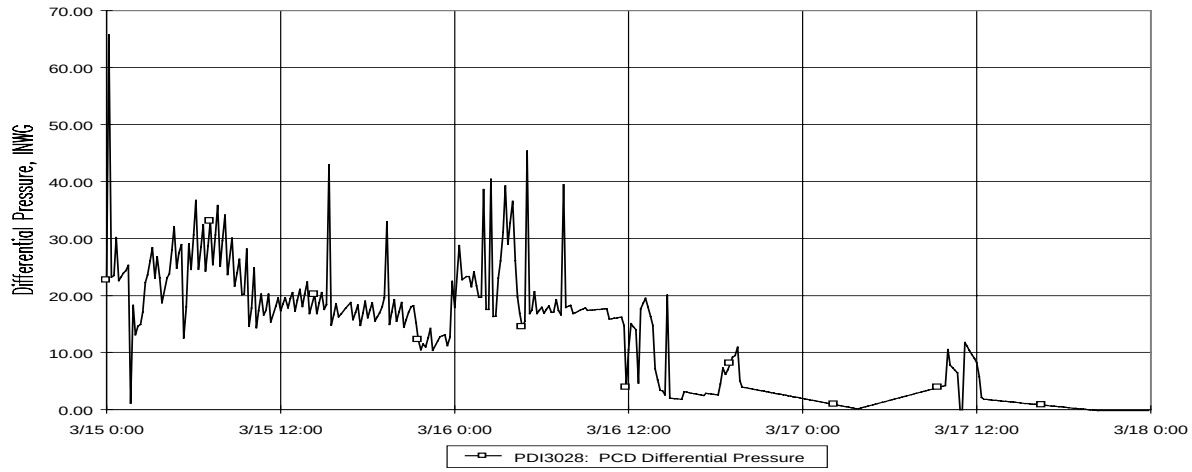

Figure 4.1.1.1-48 PCD Differential Pressure Profile

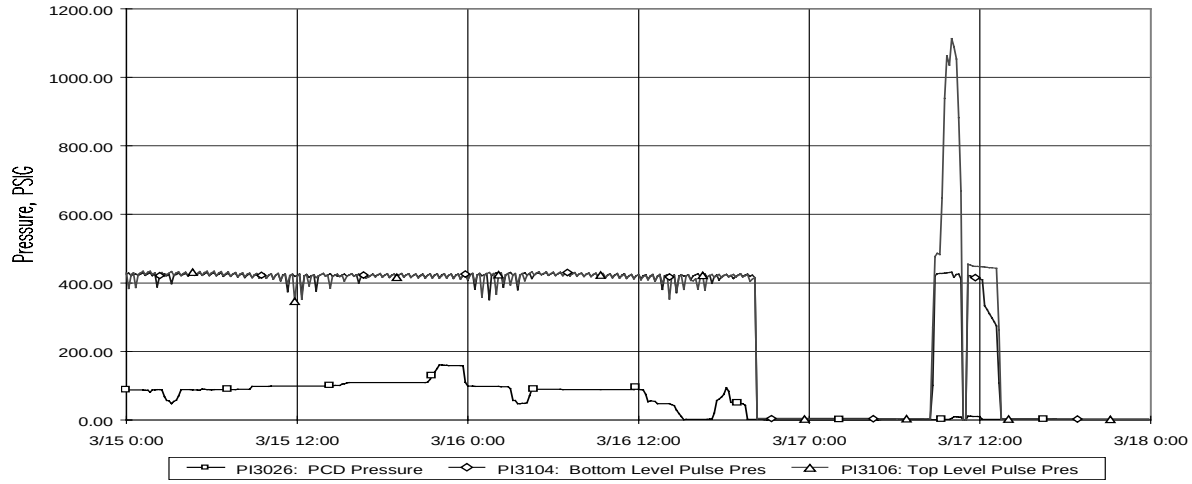

Figure 4.1.1.1-49 PCD Pressure and Pulse Pressure

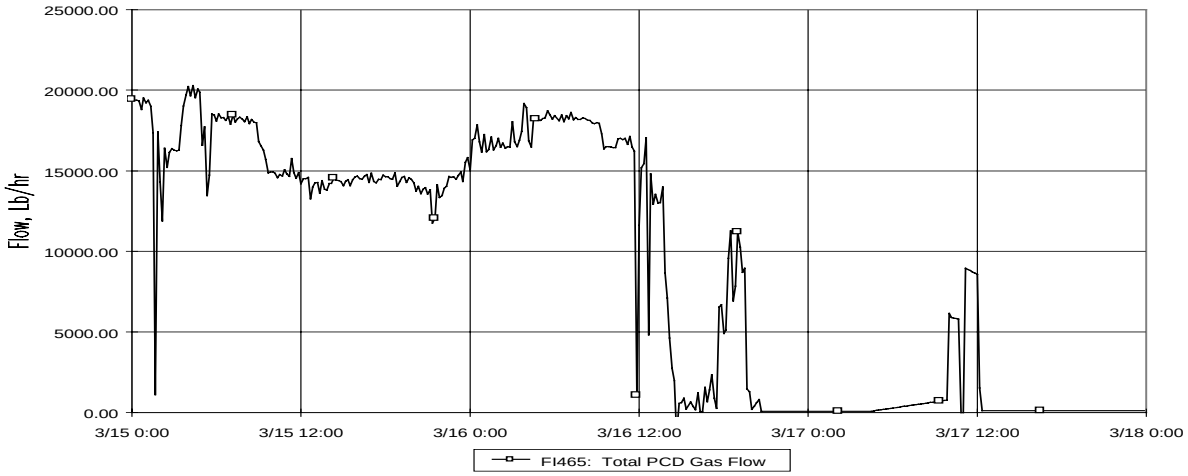

Figure 4.1.1.1-50 Gas Flow Through PCD

4.1.1.2 Characterization Test Run CCT4B

Test run CCT4B was conducted between March 19 and March 22, 1997. Operating plots are shown in figures 4.1.1.2-1 through -25. The silicone gaskets for the Victaulic coupling on the main compressor discharge pipe developed a serious leak and were replaced at the start of CCT4B (event 1, figure 1). Temporary gaskets matching close to vendor specification were installed pending procurement of proper gasket material.

CCT4B Test Run Chronology

- On March 19, 1997, there were 7,400 lb of used sand added to the coal feeder system (FD0210). The repairs to the compressor discharge pipe were completed and the compressor was restarted (event 2, figure 1). Troubleshooting was being conducted on the gas analyzer since it was reading 99.95-percent nitrogen (event 3, figure 17). Unsuccessful attempts were made to light the reactor start-up burner (BR0201) around 06:00. An Atlas Copco service representative tuned CO0201 with the reactor pressure at 21 psig. Most of the trips related to BR0201 in CCT4A were due to problems associated with improper tuning of CO0201.

- At 23:00 the BR0201 was lit after the igniter was replaced (event 4, figure 4). Even though the igniter performed well during the bench tests, it was suspected that under pressure the igniter was arcing internally. At 23:25 CO0201 discharge pressure swung when reactor air flows were adjusted (event 5, figure 1). Sand addition to the reactor from the sorbent feeder system (FD0220) and FD0210 was started around 02:40 (event 6, figures 2 and 3). Around 03:00 on March 20 there was another CO0201 upset which tripped the BR0201 (event 7, figure 4). Within 20 minutes the BR0201 pilot and main gun were restarted. The pilot was then shut down.

- Due to the problems with CO0201 the reactor was shut down so that the service representative (event 8, figure 1) could do additional tuning. The compressor tuning was completed by 15:00. The compressor Victaulic gasket was changed upon vendor recommendation and a new igniter tip was installed on the burner. At 16:53 the BR0201 pilot and main burner were lit (event 9, figure 4). At 17:25 the reactor pressure was increased to 55 psig to maintain the riser velocity within an acceptable range. At 04:00 on March 21, 854 lb of Powder River Basin (PRB) coal were loaded into FD0220. The BR0201 firing was continually increased so the reactor would continue heat up and the reactor pressure was also increased to limit the riser velocity (event 10, figure 4 and event 11, figure 12).

- At 09:23 coal feed was started from FD0220 (event 12, figures 3 and 6 through 10). At 09:35 sand addition was started from FD0210. The reactor temperatures dropped initially and the FD0220 motor speed was increased to maintain the reactor temperature. The reactor temperature stayed steady but then increased rapidly and so FD0220 was shut down (event 13, figures 3 and 6 through 10). It appeared that there was some coal mixed with sand in FD0210. FD0210 and FD0220 were used interchangeably to feed sand and coal, as these feed systems were unreliable. Once

all the sand was fed into the reactor FD0220 was used as a backup to FD0210 to feed coal.

- At 11:09 the reactor pressure was 100 psig and at 11:35 BR0201 was shut down (event 14, figure 12 and event, 15 figure 4). At 12:00 the reactor pressure was increased in 2 psig increments and by 13:40 it was 160 psig (event 16, figure 12). At 14:05 the FD0210 feeder tripped so FD0220 was started (event 17, figures 2 and 3). It appeared that FD0210 tripped due to a low conveying air flow. After adjustments were made to the conveying air valve, FD0210 was restarted. Initially a large amount of coal was added, so there was a corresponding temperature excursion (event 18, figures 2 and 6 through 10). From 09:15 to 14:40 the coal feed rate averaged 700 lb/hr.

- Around 15:00 the combustor heat exchanger (HX0203) circulation increased rapidly causing a considerable amount of solids to be moved from the heat exchanger into the standpipe and causing a significant amount of carryover. The reactor temperature dropped about 200°F when this occurred (event 19, figures 6 through 10). At 15:40 FD0220 was shut down. At 17:10 FD0210 tripped and so FD0220 was started. Two minutes later the FD0210 feeder was restarted. At 17:35 the FD0210 tripped and FD0220 was started. Within 10 minutes FD0210 was back in service and FD0220 was shut down (event 20, figures 2 and 3). At 18:09 FD0210 tripped again due to a seal failure (event 21, figures 2 and 6 through 10). Problems with the transport air system prevented FD0220 from being started. The reactor start-up burner was fired to maintain the reactor temperature.

- By 00:06 on March 22, 1997, the FD0210 middle spheri valve seal was repaired and the shuttle valve was inspected. At 00:47 coal feed from FD0220 was started (event 22, figures 3 and 6 through 10). At 05:30 the BR0201 was shut down (event 23, figure 4). Around 05:00 coal feed from FD0210 was started (event 24, figures 2 and 6 through 10). The average coal feed rate was 700 lb/hr.

- At 09:17 with no changes in any reactor variables the temperature started to rise rapidly to 1,790°F. The coal feed was reduced and the reactor circulation was increased but the temperature continued to climb. The coal feed was stopped. This event happened twice in 10 minutes (event 25, figures 2 and 6 through 10). Either some coal came from HX0203 or coal packed on the FD0220 dispense vessel wall became loose and began to feed into the reactor along with the sand. At 10:27 FD0210 tripped on low instrument air pressure.

- Around 13:30 the HX0203 circulation decreased due to some plugged nozzles causing the standpipe level to slowly decrease. At 14:12 FD0220 was shut down. At 14:30 the reactor riser temperatures dropped quickly and the disengager and crossover temperatures increased. It appeared that the reactor J-leg stopped circulating due to a low-standpipe level. When the heat exchanger J-leg nozzles were unplugged the heat exchanger started circulating transferring solids into the reactor

standpipe. This in turn started the reactor J-leg circulation and improved the reactor temperature distribution.

- At 17:05 FD0220 was started to add more sand to the reactor to increase the inventory levels. The reactor pressure was also increased. The packing on the spent fines screw cooler (FD0502) began to leak with each rotation. The bottom spheri valve in the FD0520 PCD fine ash removal system then failed, which forced a plant shutdown.

CCT4B Post Test Run Inspections

The reactor was inspected after the unit shutdown. The cyclone inlet was borescoped. There was some (small) loss of refractory at the edges of the inlet tapered section but otherwise the narrowed inlet was intact. The cyclone was also inspected from the top where the refractory ends and the vortex pipe starts. All of this section was intact. A light was lowered from the top of the cyclone; only a light scale was present. The refractory-lined orifice plate in the gas bypass line was inspected by borescope and appeared to be in good condition. The riser-to-standpipe crossover was about one-third full of sand. There were some grooves in the top. Small scale was found on the inside of the riser wall when viewed with a light. The standpipe had a small amount of scale. A light was lowered 60 feet into the standpipe from the top; no sand level was detected. The disengager was also borescoped; no accumulation was found.

CCT4B Test Run Observations

Atlas Copco tuned the main air compressor but the control was still very sensitive. The coal feeder (FD0210) tripped several times during the run and as a result FD0220 was used as a backup coal feeder. The unit was shut down because solids could not be removed from the PCD due to failure of a FD0520 bottom spheri valve. A total of 34 hours on coal was achieved and a total of 9 tons of coal were fed.

Section 4.1.1.2

CCT4B

Graphs 1 through 25

March 18 through March 22, 1997

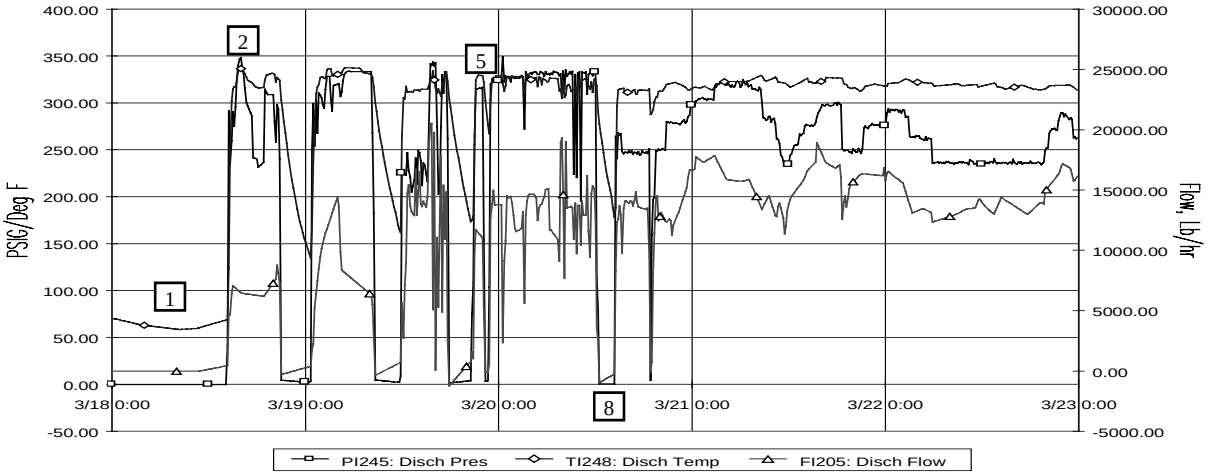

Figure 4.1.1.2-1 CO0201 System Profile

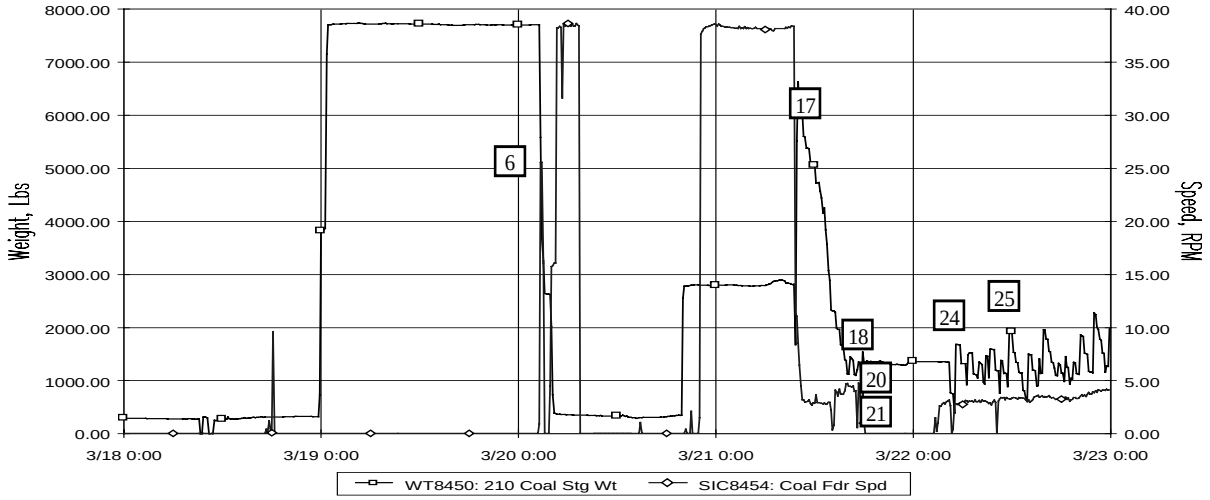

Figure 4.1.1.2-2 Coal Feed System Profile

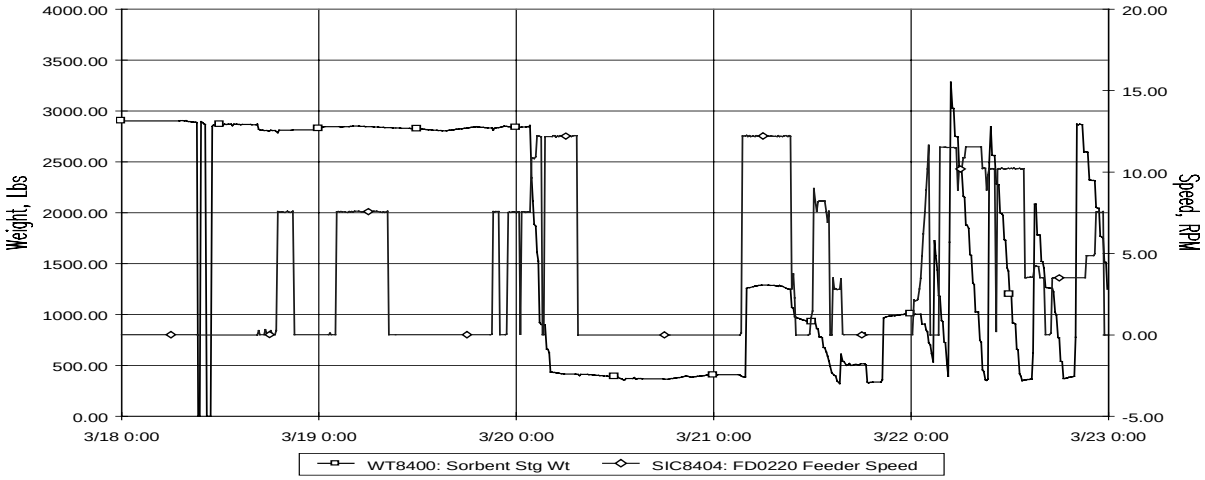

Figure 4.1.1.2-3 Sorbent Feed System Profile

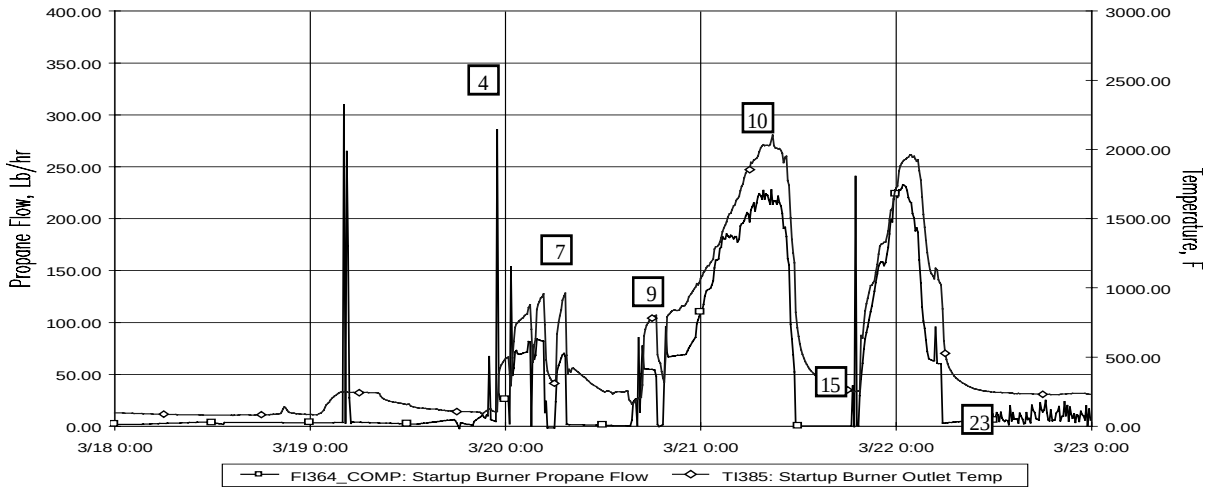

Figure 4.1.1.2-4 Start-Up Burner Flow/Temperature

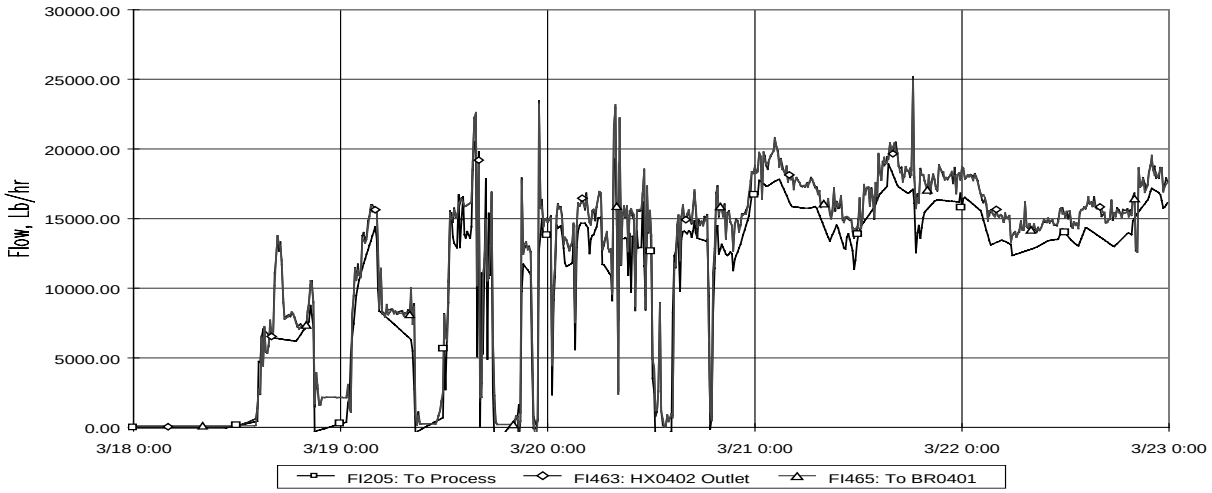

Figure 4.1.1.2-5 Total Gas In/Out Flow Rates

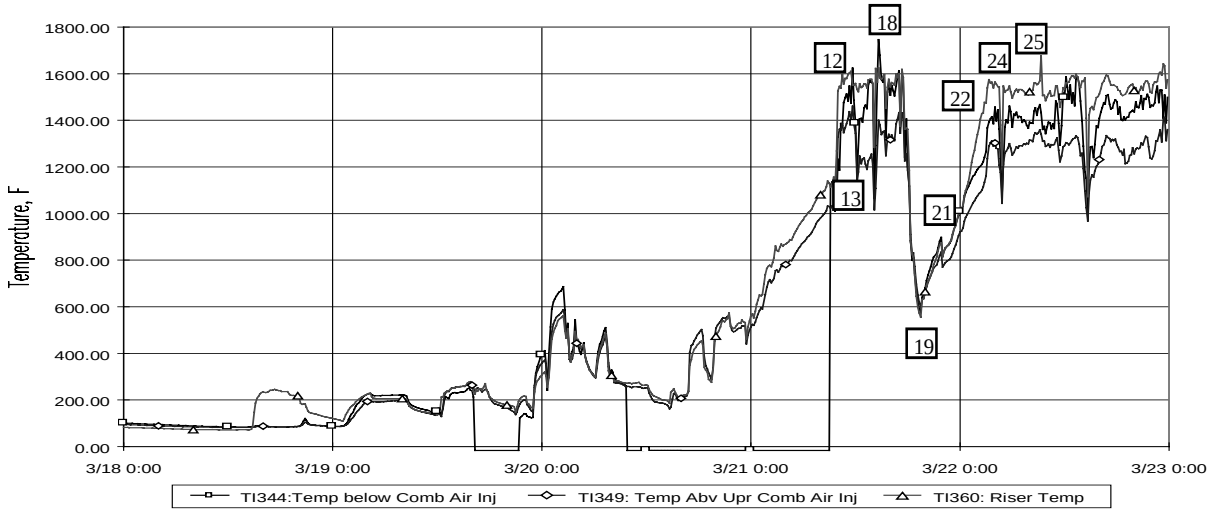

Figure 4.1.1.2-6 Reactor Mixing Zone and Riser Temperatures

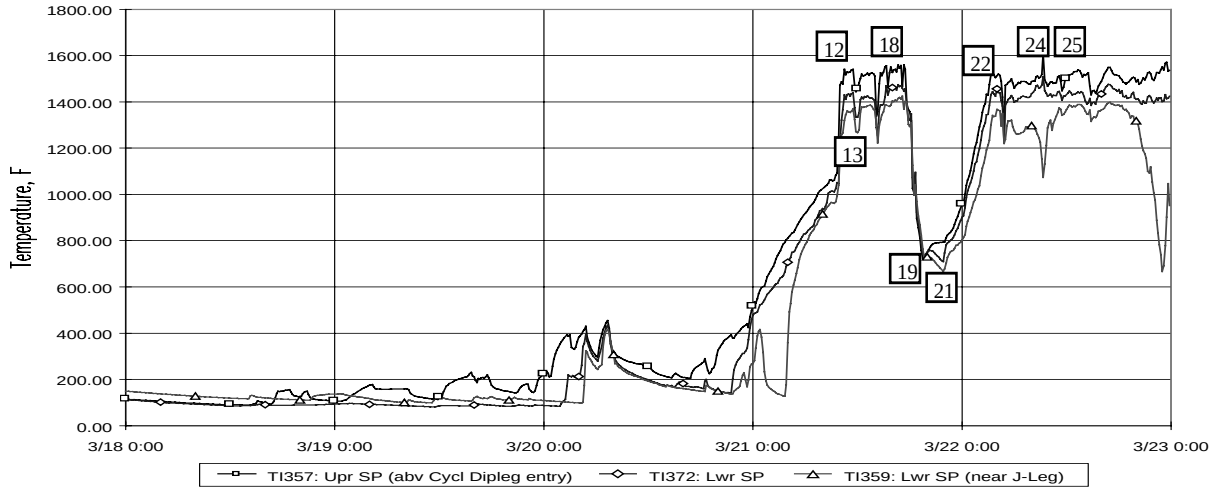

Figure 4.1.1.2-7 Standpipe Temperatures

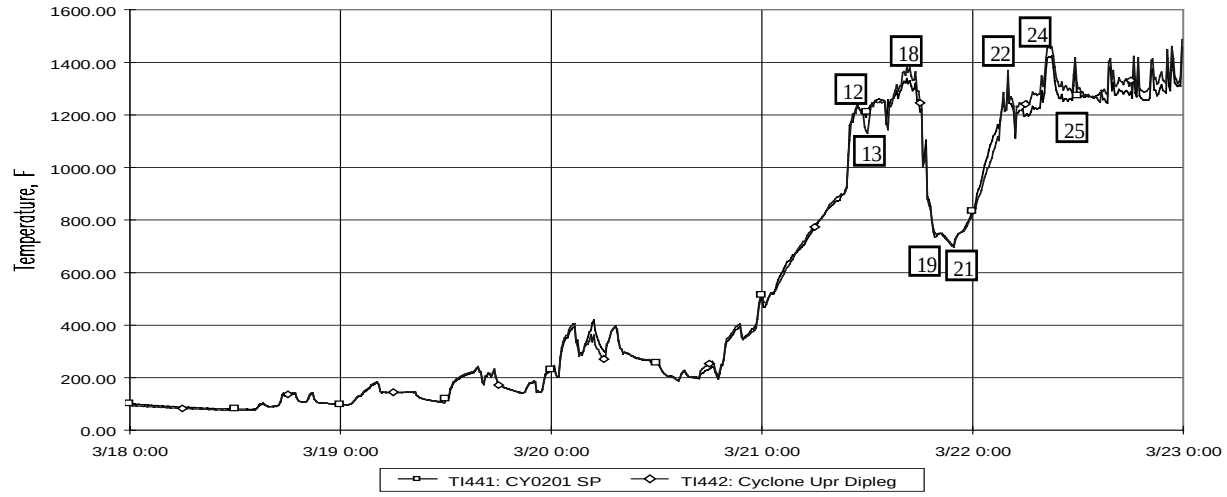

Figure 4.1.1.2-8 Cyclone Dipleg Temperatures

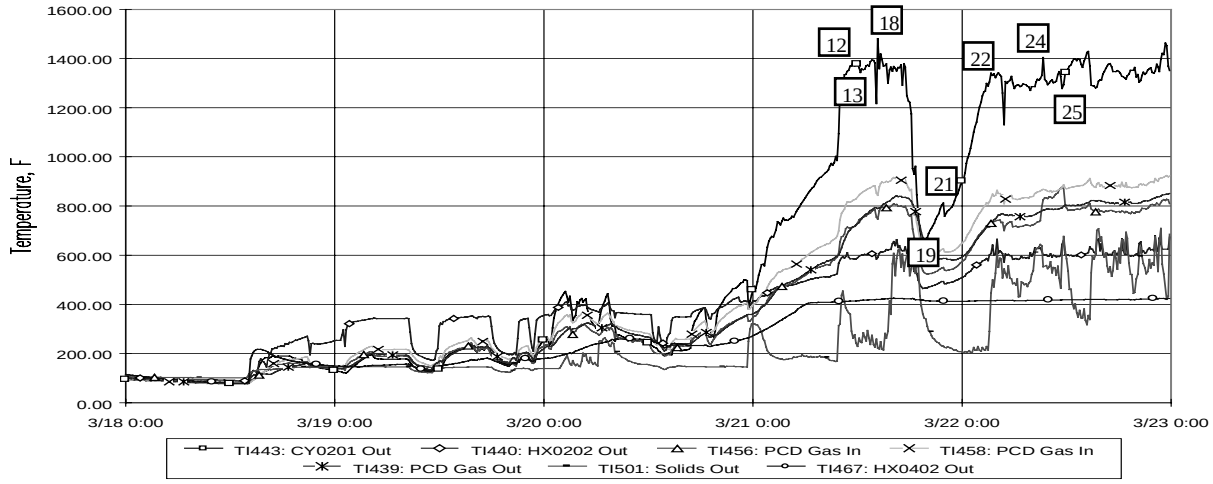

Figure 4.1.1.2-9 Temperature Profile Downstream of Reactor

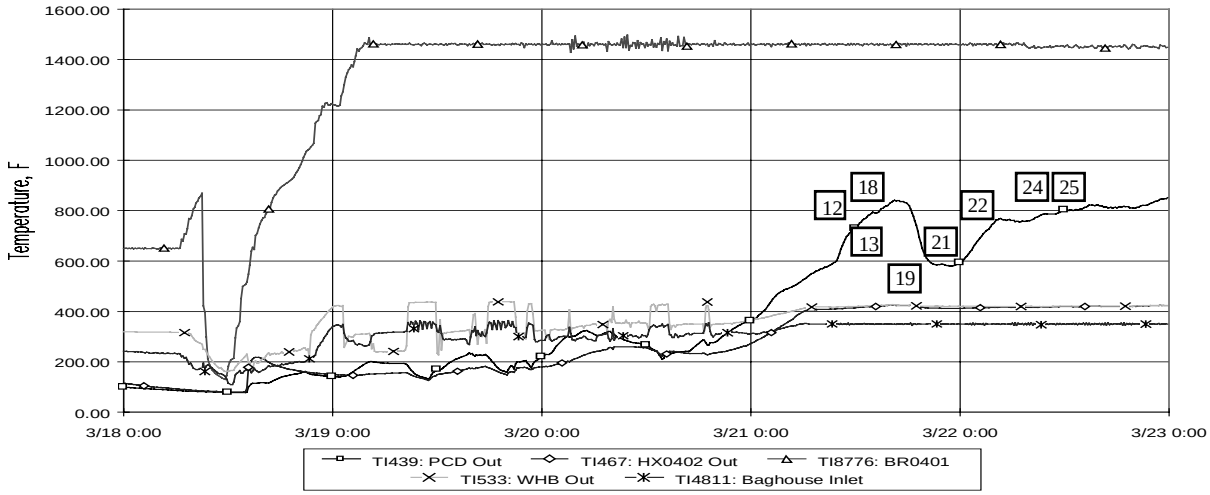

Figure 4.1.1.2-10 System Temperatures Downstream of PCD

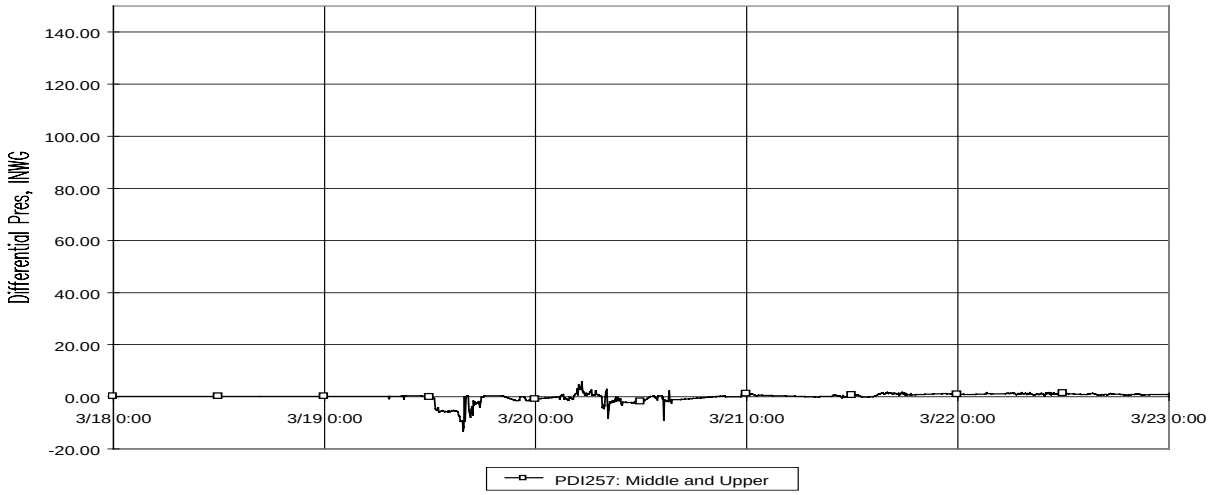

Figure 4.1.1.2-11 Mixing Zone Differential Pressure Profile

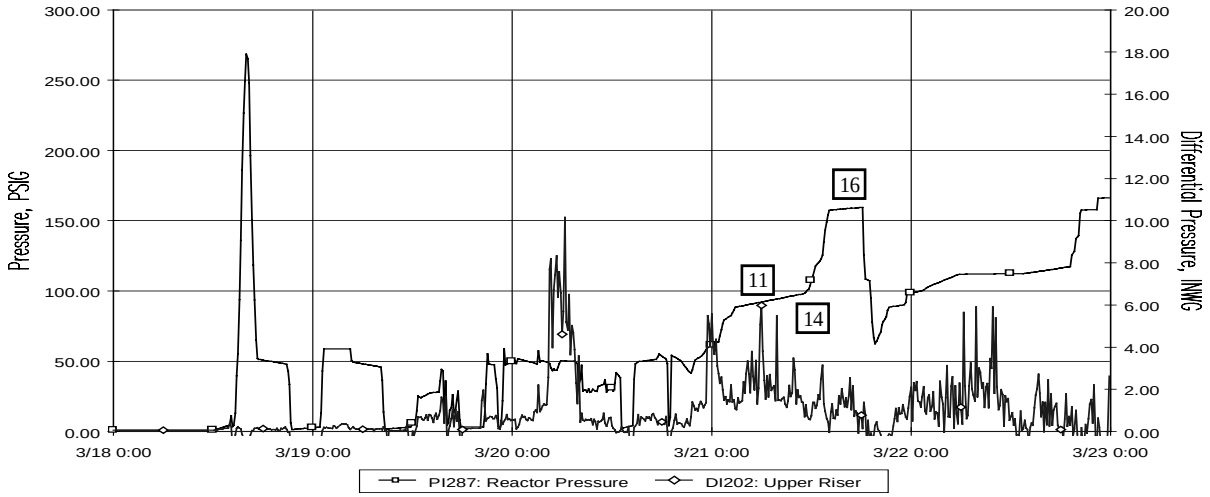

Figure 4.1.1.2-12 Reactor Pressure/Riser Differential Pressure Profiles

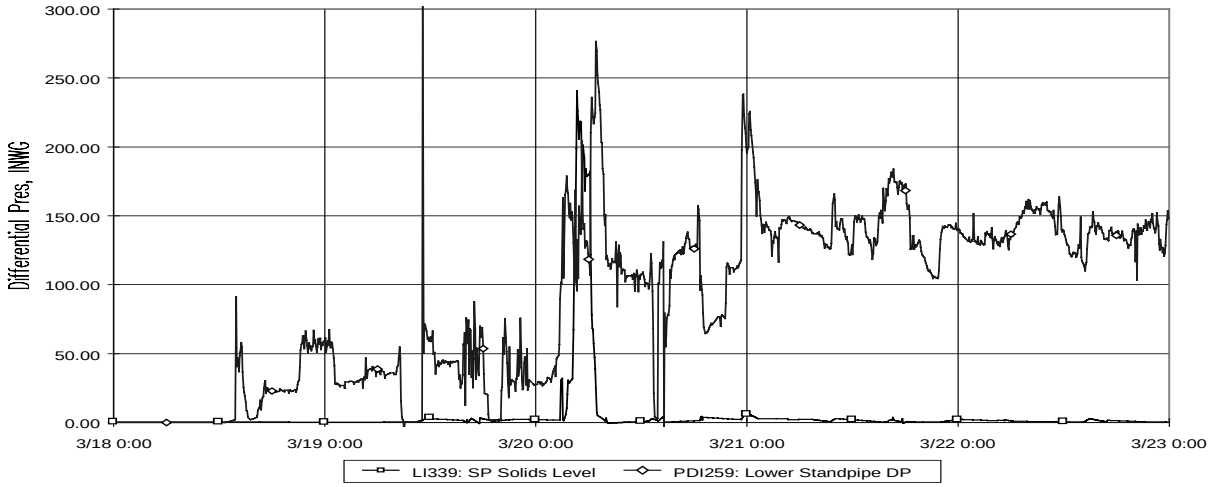

Figure 4.1.1.2-13 Standpipe Differential Pressure Profiles

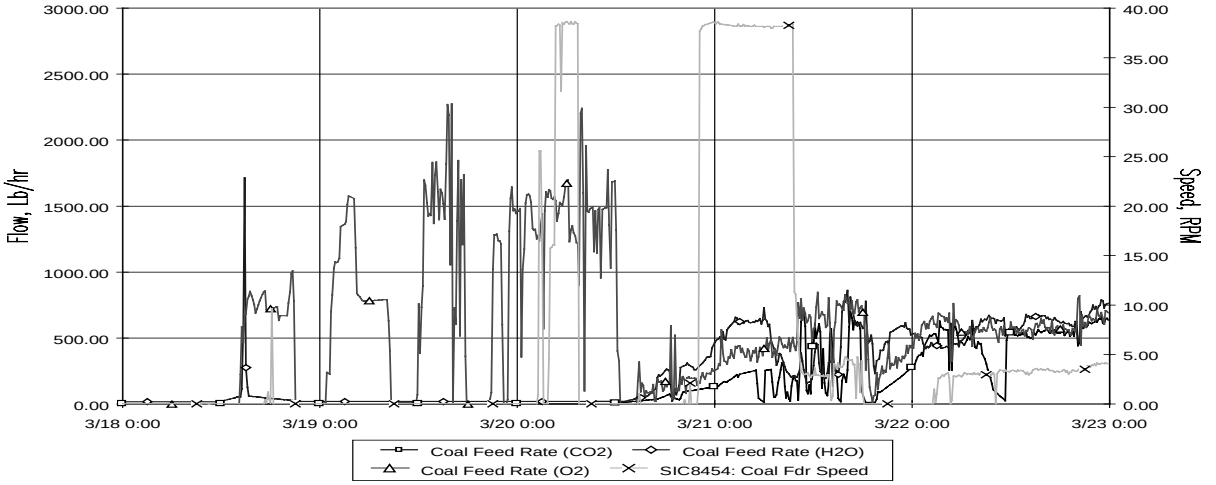

Figure 4.1.1.2-14 Coal Feed Rate Based on Gas Analysis

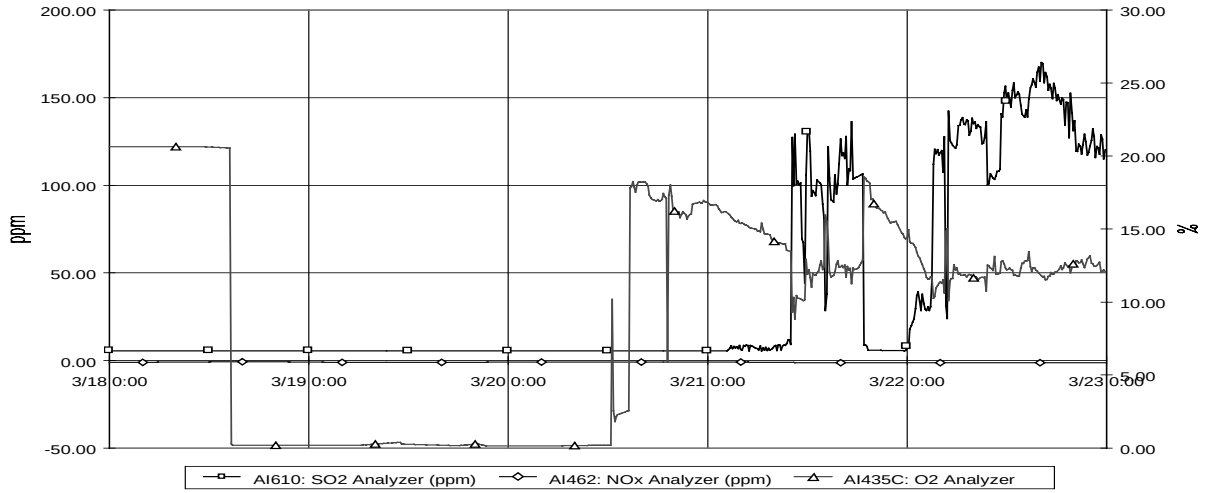

Figure 4.1.1.2-15 O_2, SO_2 and NO_x Analyzers

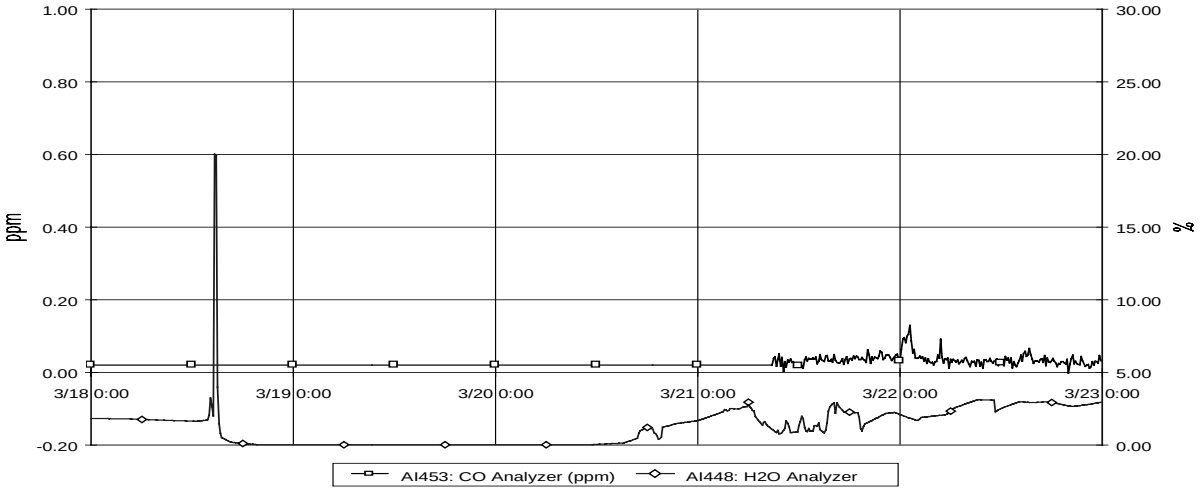

Figure 4.1.1.2-16 CO and H_2O Analyzers

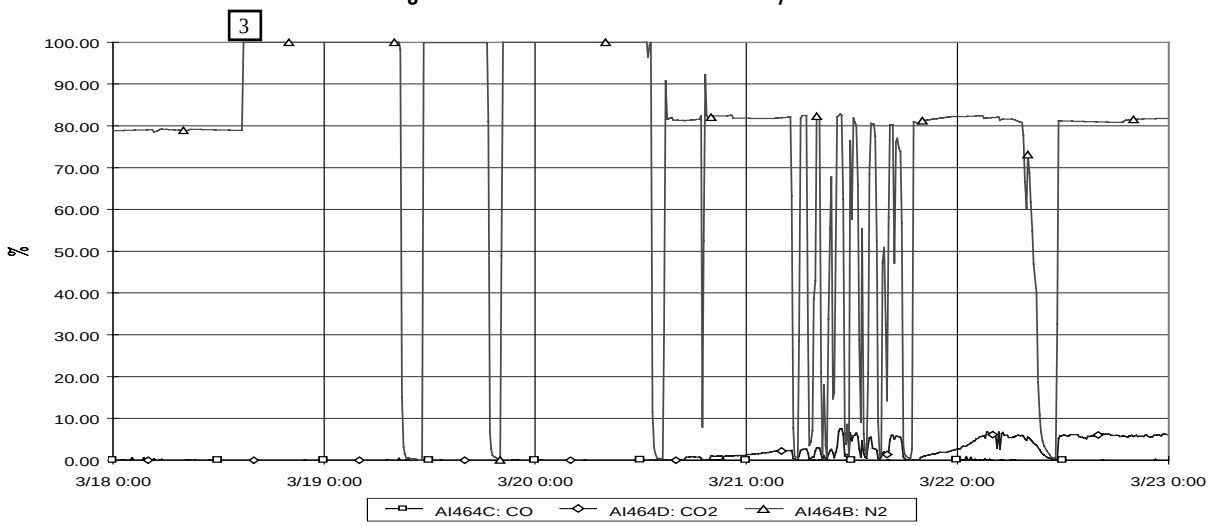

Figure 4.1.1.2-17 GC Analysis

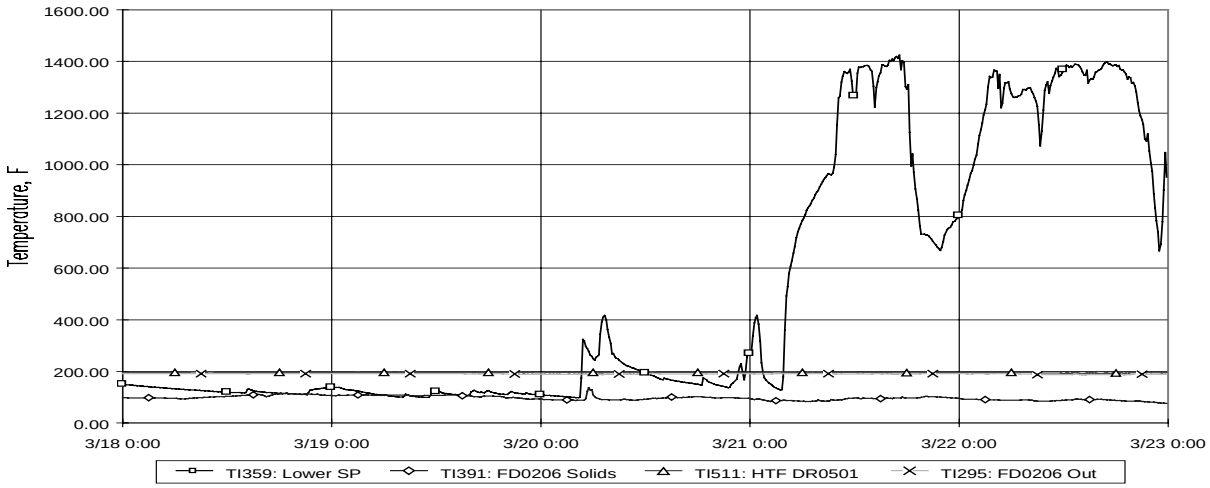

Figure 4.1.1.2-18 FD0510 Temperature Profiles

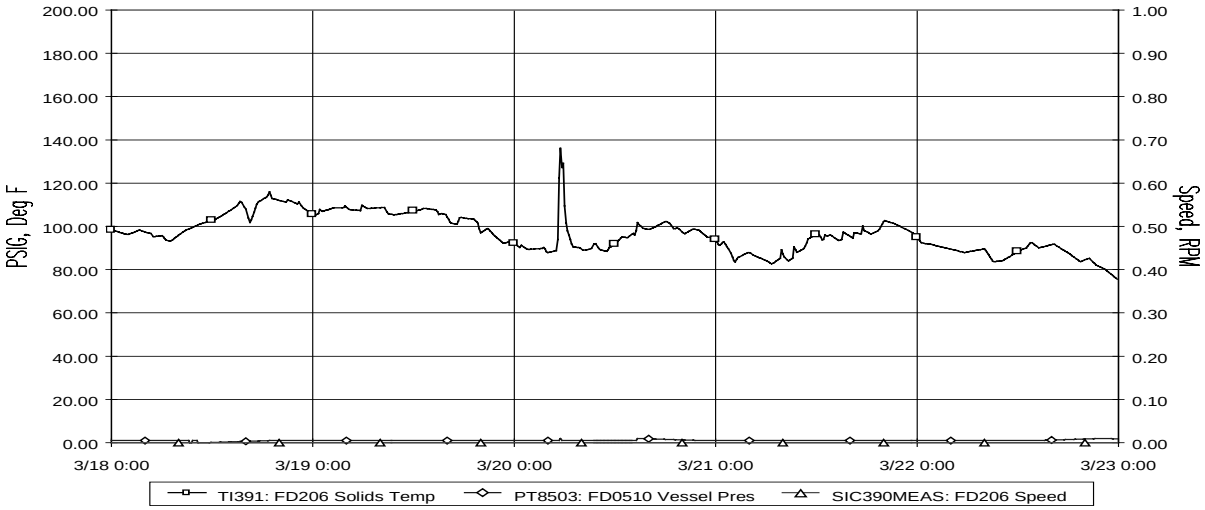

Figure 4.1.1.2-19 FD0206 Pressure Profiles

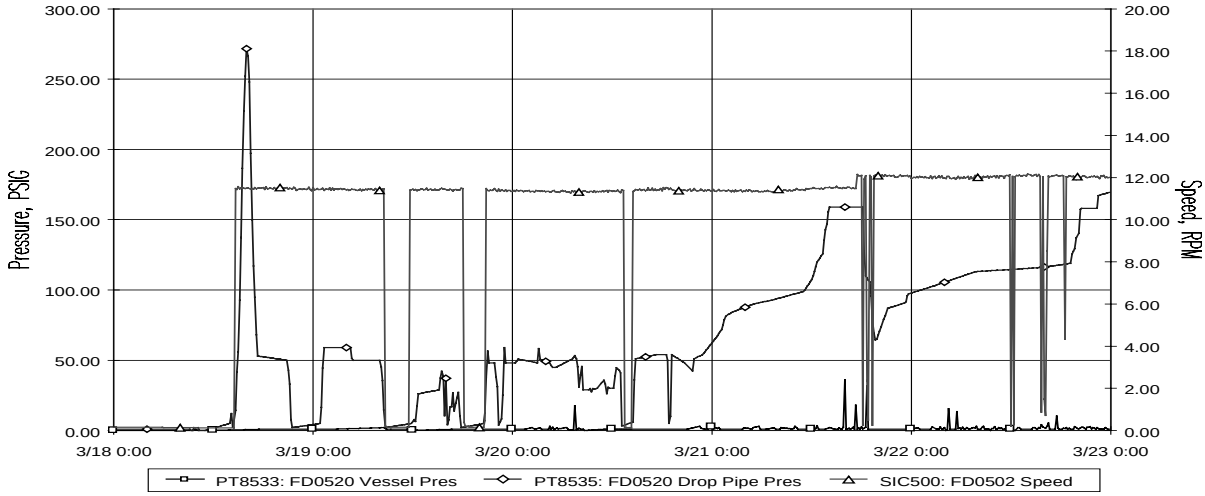

Figure 4.1.1.2-20 FD0520 Pressure Profiles

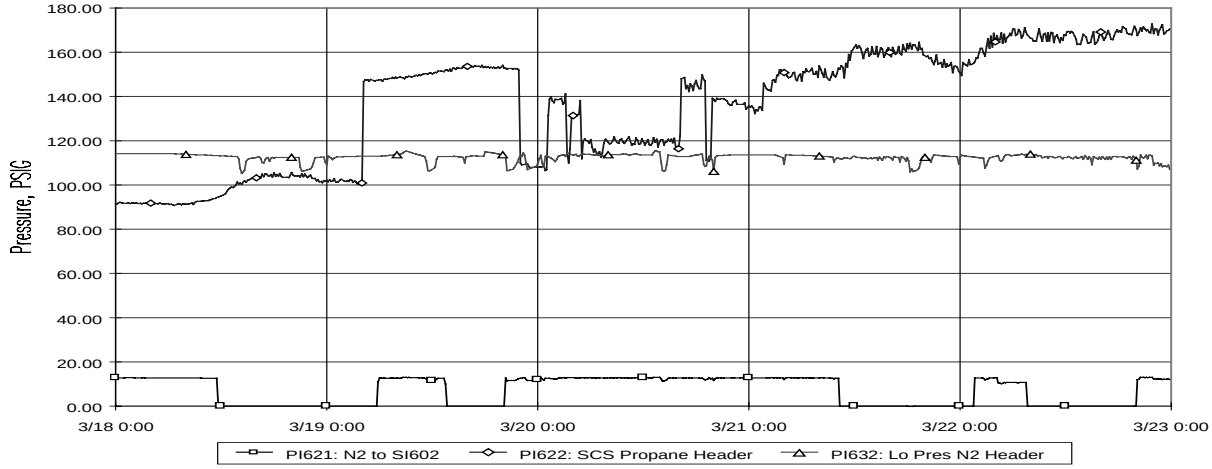

Figure 4.1.1.2-21 Nitrogen/Propane Header Pressure Profiles

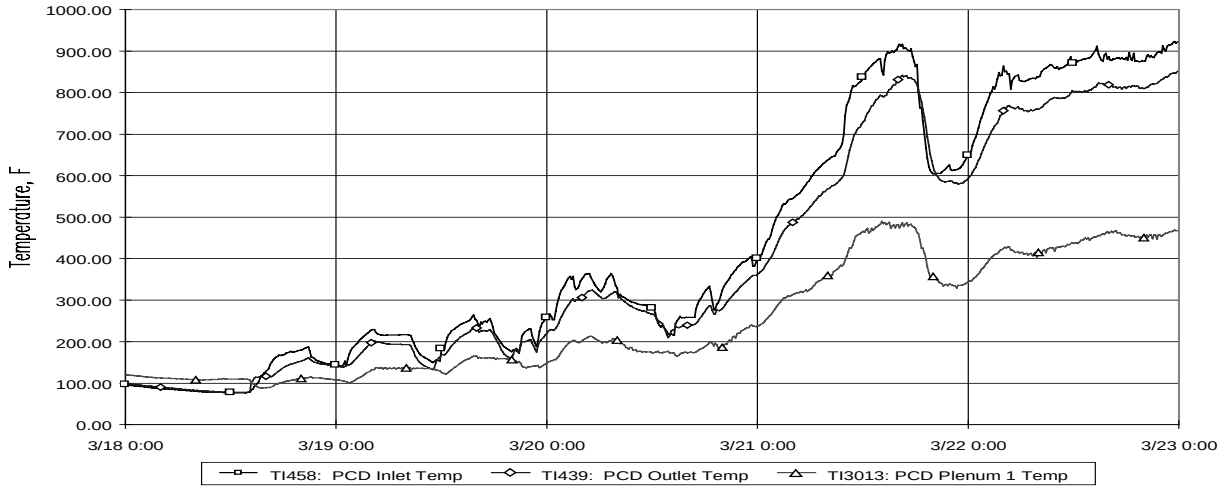

Figure 4.1.1.2-22 PCD Temperatures

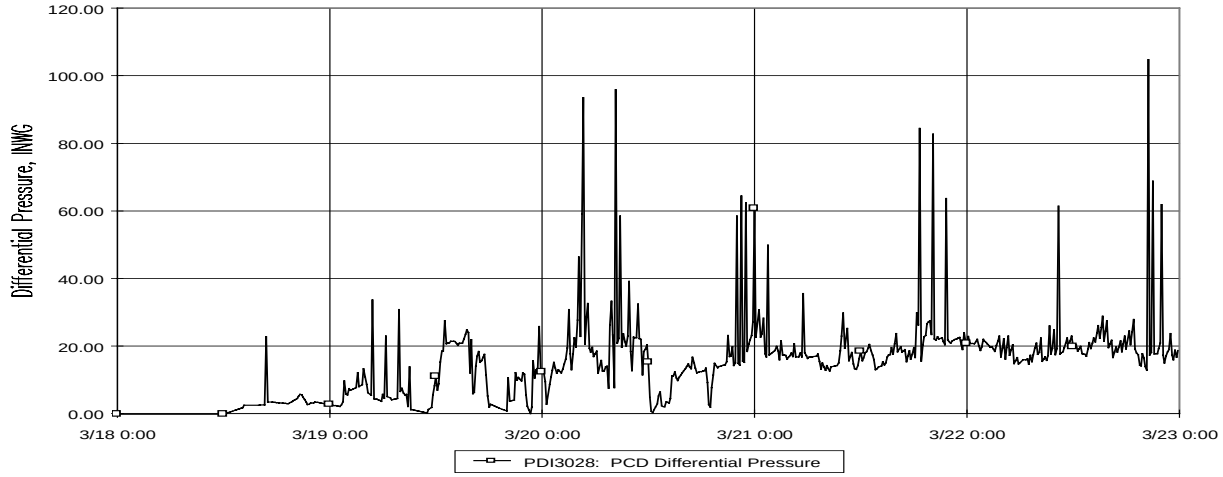

Figure 4.1.1.2-23 PCD Differential Pressure Profile

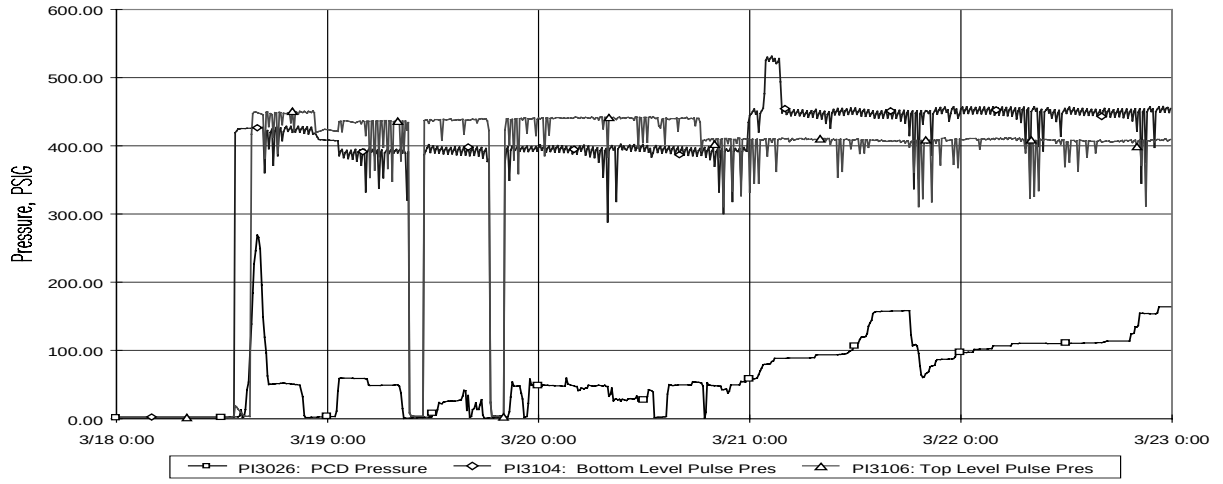

Figure 4.1.1.2-24 PCD Pressure and Pulse Pressure

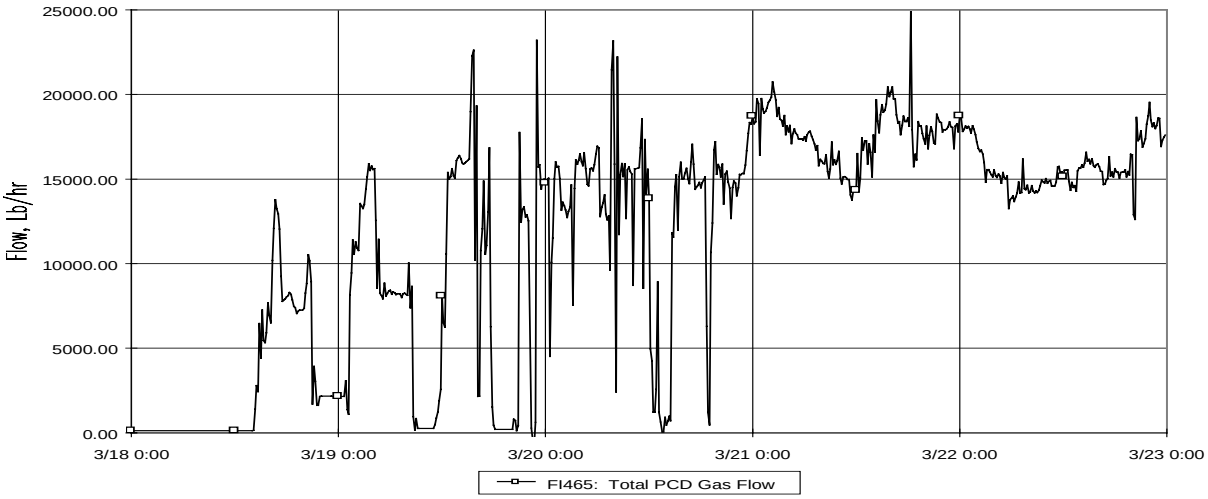

Figure 4.1.1.2-25 Gas Flow Through PCD

4.1.1.3 Characterization Test Run CCT4C

Test run CCT4C was conducted between April 6 and 7, 1997. Operating plots are shown in figures 4.1.1.3-1 through -21. The riser differential pressure indication PDT213 was relocated to measure midriser density and the cyclone differential pressure indication PDT254 was relocated to measure the primary cyclone hopper pressure loss, giving some indication of how solids are draining out of the radish. The FD0520 bottom spheri valve was also repaired.

CCT4C Test Run Chronology

- On April 6, 1997, auxiliary systems were started to begin test run CCT4C. By 21:30 all instrument purges were set. At 21:42 the start-up burner (BR0201) pilot was lit and heat-up of the reactor system began (event 1, figure 3).

- On April 7, 1997, at 07:00 the fluidization flows were adjusted, expanding the reactor standpipe solids and the combustor heat exchanger (HX0203) solids to determine if there were sufficient solids in the reactor. There were insufficient solids in reactor for the tests so it was decided to add sand to the reactor. At 09:20 sand addition into the reactor began using the coal feeder system (FD0210) (event 2, figure 2). The FD0210 tripped many times. Some of the trips were due to the difficulty in turning the feeder motor. Apparently a plug or some extraneous material was binding the star feeder. Due to the frequent feeder trips the feeder speed was temporarily set at a high rate to start the motor. By 09:55 approximately 3,000 lb of sand were fed into reactor after a few FD0210 trips. As the solids level in the standpipe increased solids circulation through the riser also increased (event 3, figure 13). Between 9:30 and 10:00 the oxygen concentration at the exit of the PCD showed a drop (event 4, figure 14). At 10:10 the fines transporter system (FD0520) tripped due to a pluggage in the discharge line (event 5, figure 17). The reactor circulation was reduced to the minimum until the problems with FD0520 could be resolved. At 12:41 the exit line from FD0520 was inspected and broken pieces of ceramic candles were found blocking the exit. The process was shut down to inspect the PCD.

- While the reactor was being shut down, the ash silo was emptied and approximately 1,700 lb of solids were collected. The sample taken from the silo appeared grayish black and contained a high proportion of coal fines. During the reactor shutdown, the oxygen concentration data was retrieved from the data acquisition system and reviewed. The data showed that at approximately 09:51 the oxygen concentration dropped momentarily for approximately 1 to 2 minutes from 17 to 12 percent. There was a second sudden drop in oxygen concentration at 09:55 followed by the third drop at 09:57.

- Further investigation revealed that while sand was being fed into the reactor the PCD exit temperature increased suddenly from approximately 390°F at 09:50 and peaked at approximately 570°F at 10:02, a few minutes after sand addition was completed (event 6, figure 18). It appears that the coal inadvertently left in the dispense vessel was fed into the reactor upon the start of sand addition to the reactor

(done to increase the solids inventory). As the reactor temperatures were low, coal fines ended up in the filter vessel. There was no appreciable increase in reactor temperature. Based on the gas flow rate and the heating value of the coal, the temperature increase observed at the exit of the filter vessel corresponded to combustion of approximately 17 lb of coal fines.

CCT4C Post Test Run Inspections

The FD0210 lockhopper and dispense vessels were inspected to determine if any solids (coal in particular) were stuck to the walls. Except for a small film in a few places the walls on the FD0210 vessels looked clean. The FD0220 lockhopper was also inspected and looked clean, but there was a considerable build-up of solids in the dispense vessel. A hole had formed in the solids directly above the feeder, and once the side of the vessel was struck with a hammer this hole collapsed and the remaining solids fell down to the feeder. The solids appeared to be sand.

CCT4C Test Run Observations

The run was terminated during the reactor preheat phase. Coal inadvertently left in the coal feed system was fed into the reactor along with sand at a high-feed rate when the reactor temperatures were low. Fine coal dust ended up in the PCD vessel where it combusted, causing severe damage to the candles.

Section 4.1.1.3

Graphs 1 through 21

Test Run CCT4C

April 6 and 7, 1997

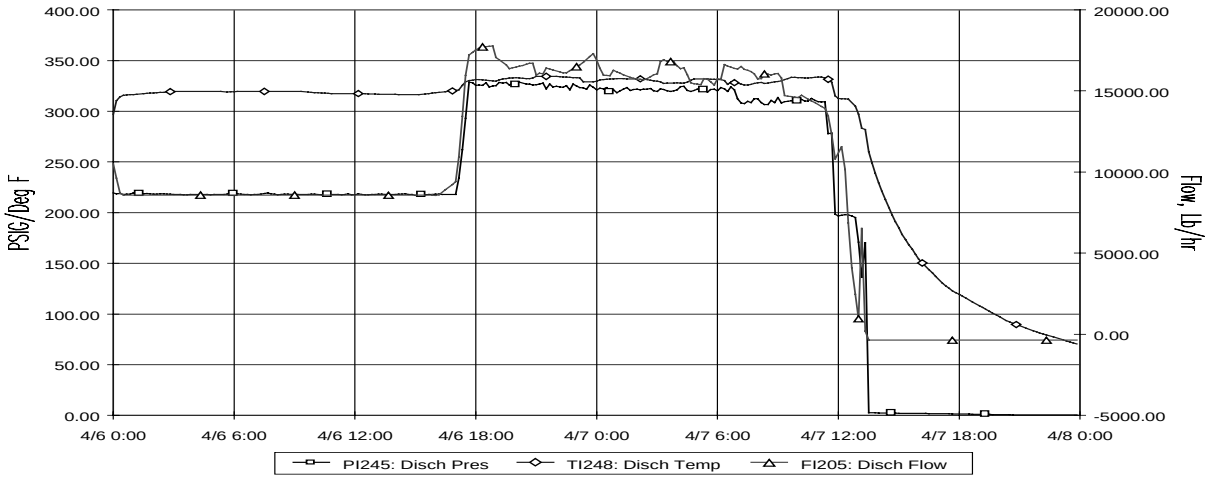

Figure 4.1.1.3-1 CO0201 System Profile

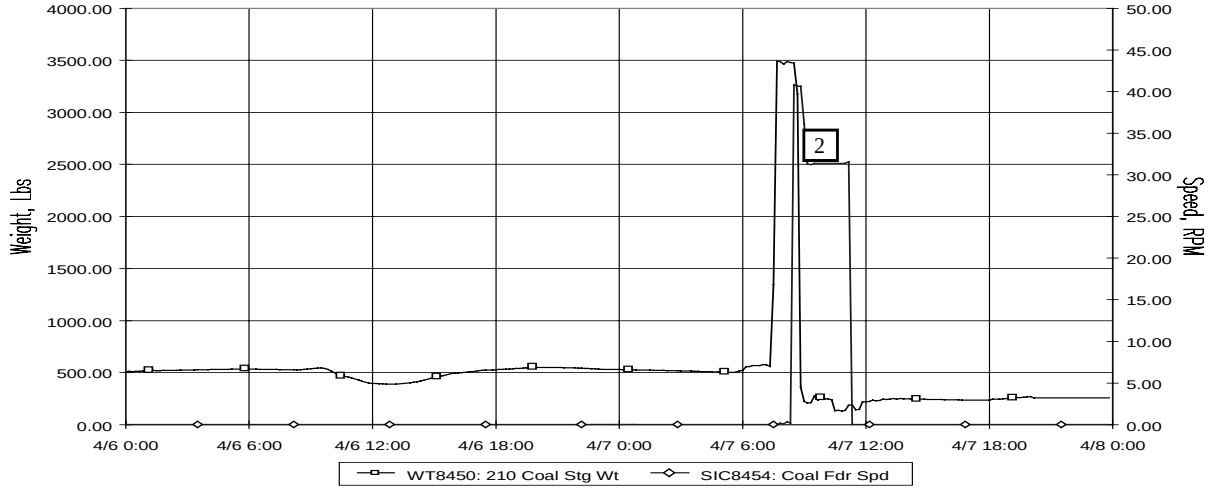

Figure 4.1.1.3-2 Coal Feed System Profile

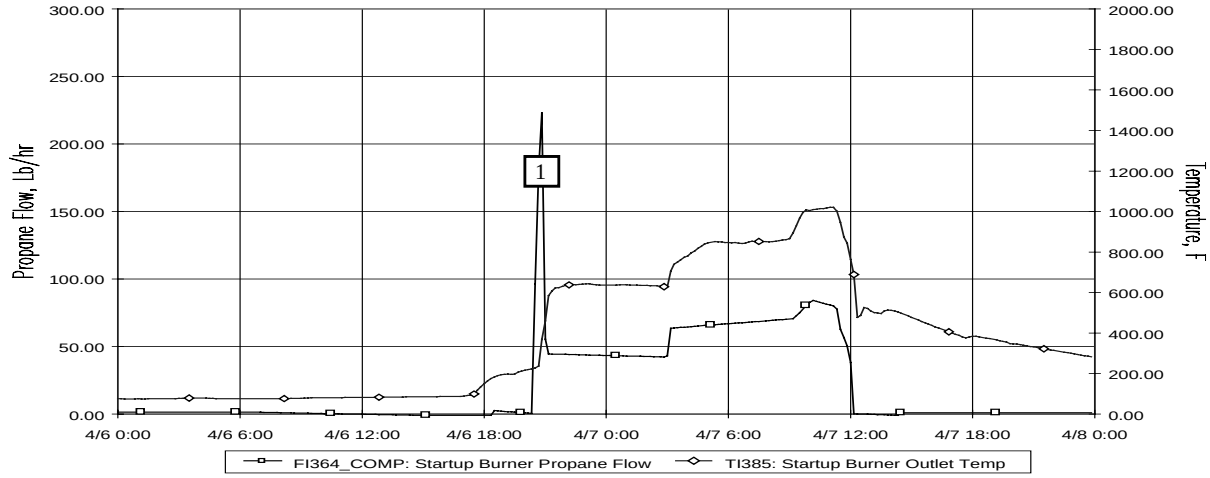

Figure 4.1.1.3-3 Start-Up Burner Flow/Temperature

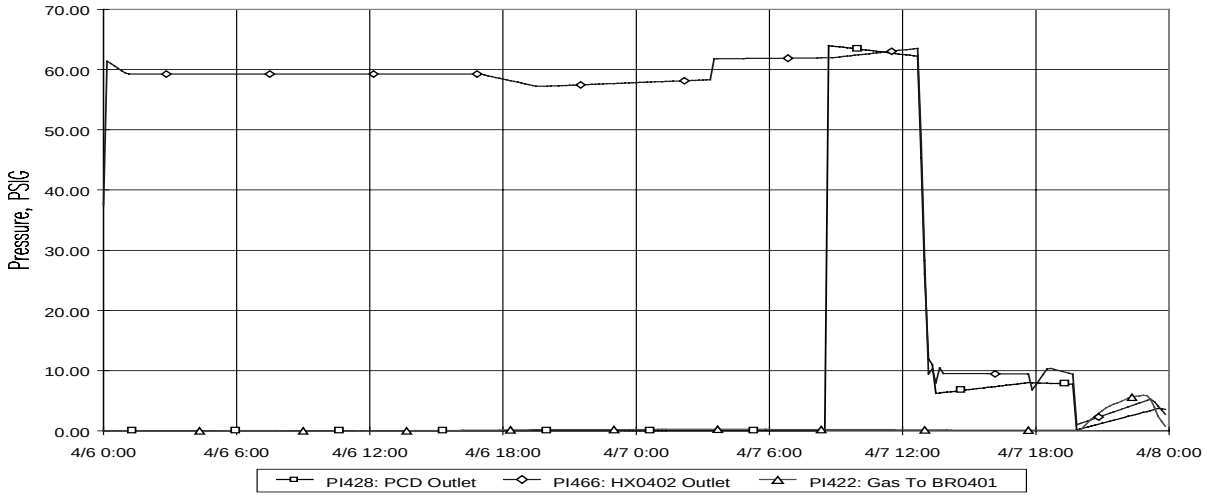

Figure 4.1.1.3-4 System Pressure Downstream of PCD

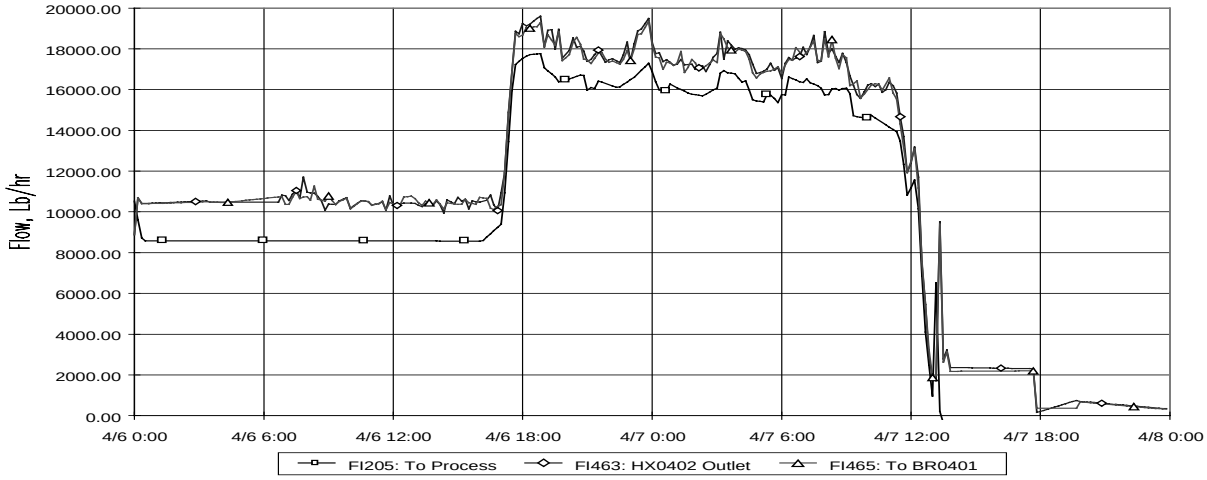

Figure 4.1.1.3-5 Total Gas In/Out Flow Rates

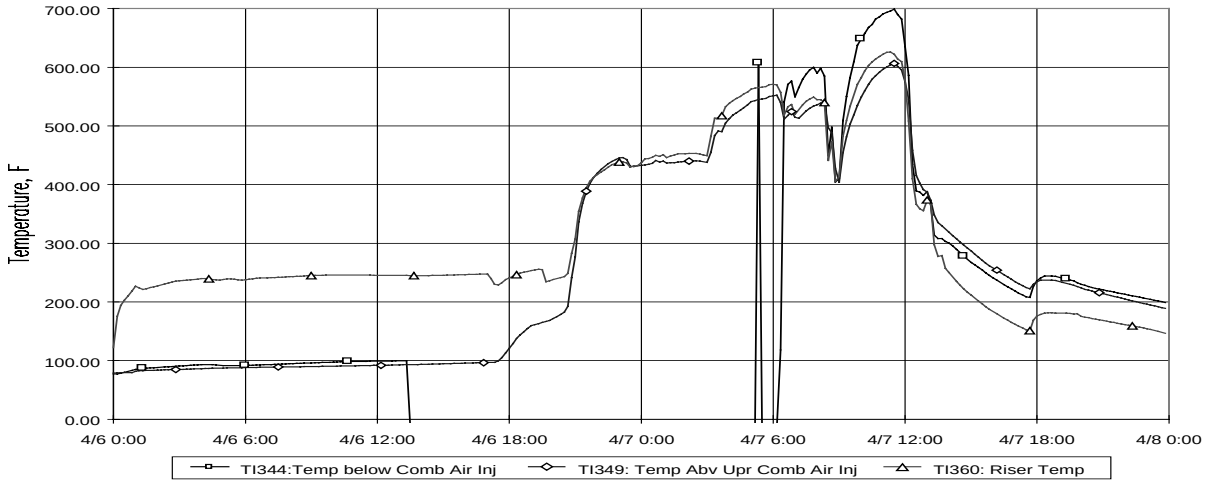

Figure 4.1.1.3-6 Reactor Mixing Zone and Riser Temperatures

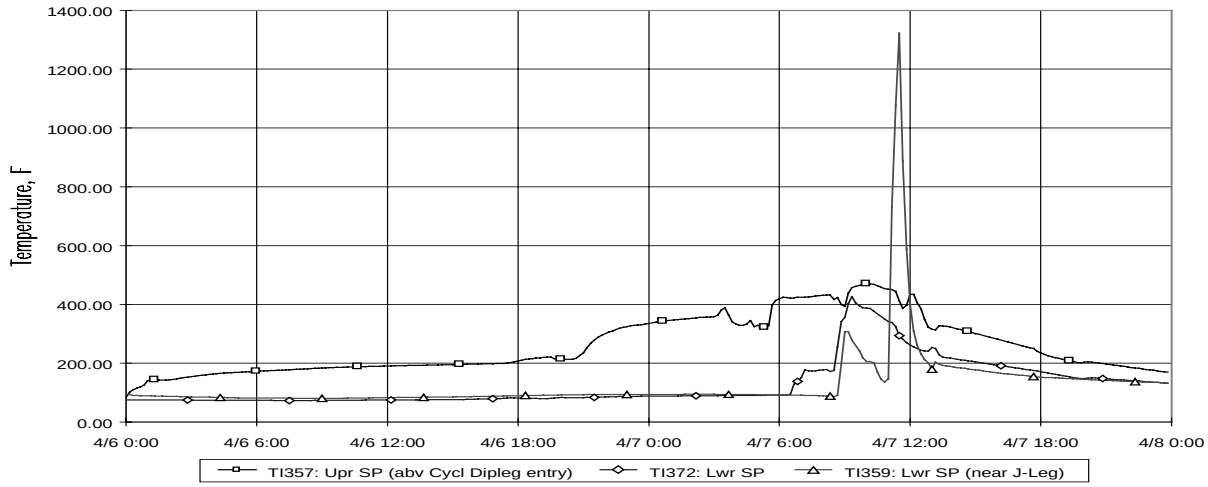

Figure 4.1.1.3-7 Standpipe Temperatures

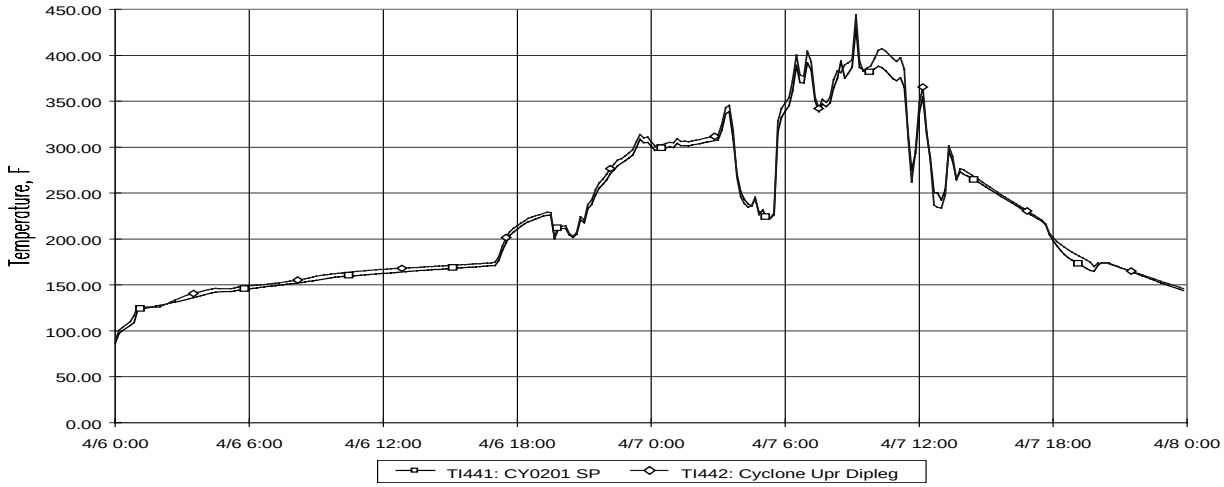

Figure 4.1.1.3-8 Cyclone Dipleg Temperatures

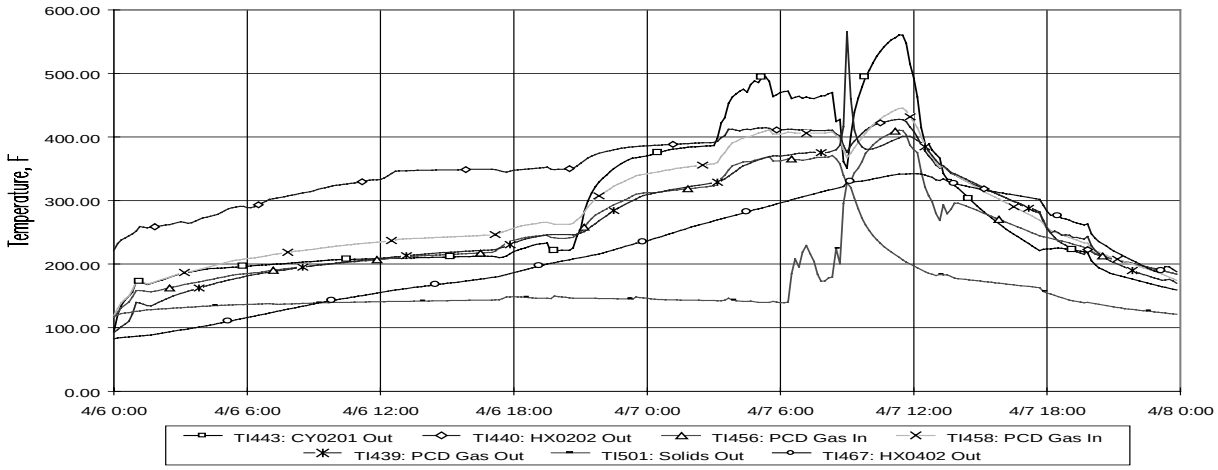

Figure 4.1.1.3-9 Temperature Profile Downstream of Reactor

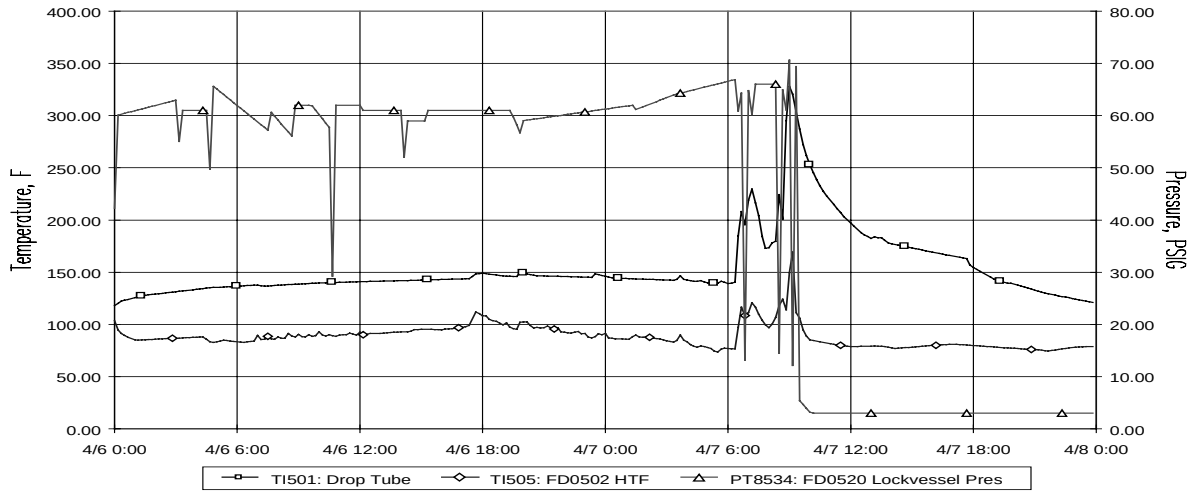

Figure 4.1.1.3-10 PCD Ash Temperatures

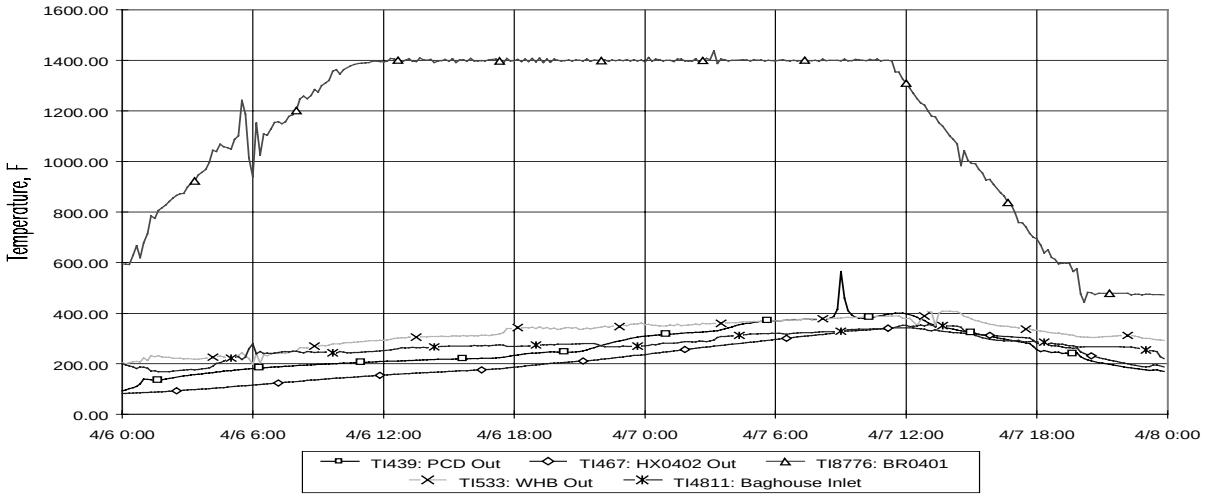

Figure 4.1.1.3-11 System Temperatures Downstream of PCD

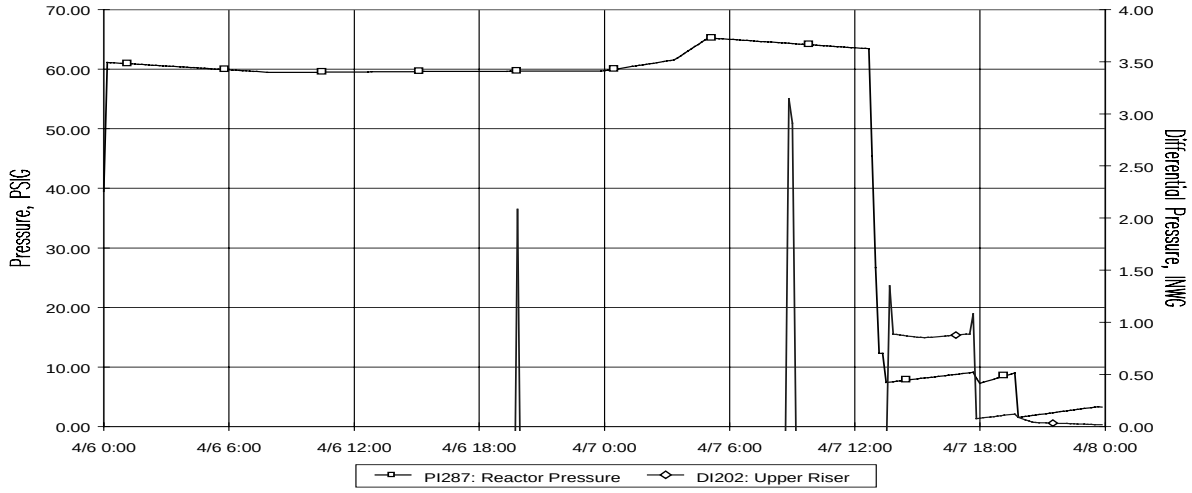

Figure 4.1.1.3-12 Reactor Pressure/Riser Differential Pressure Profiles

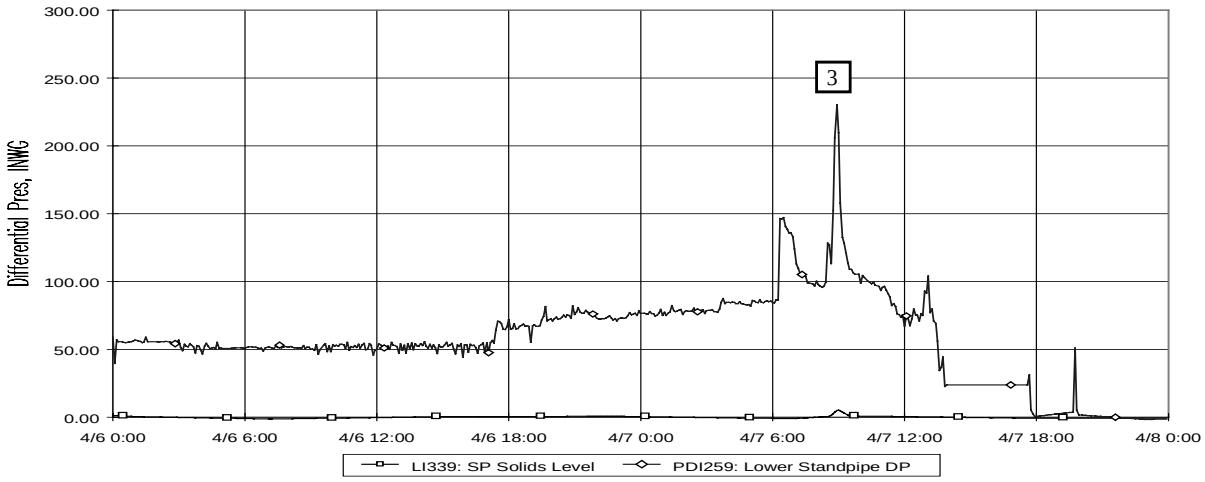

Figure 4.1.1.3-13 Standpipe Differential Pressure Profiles

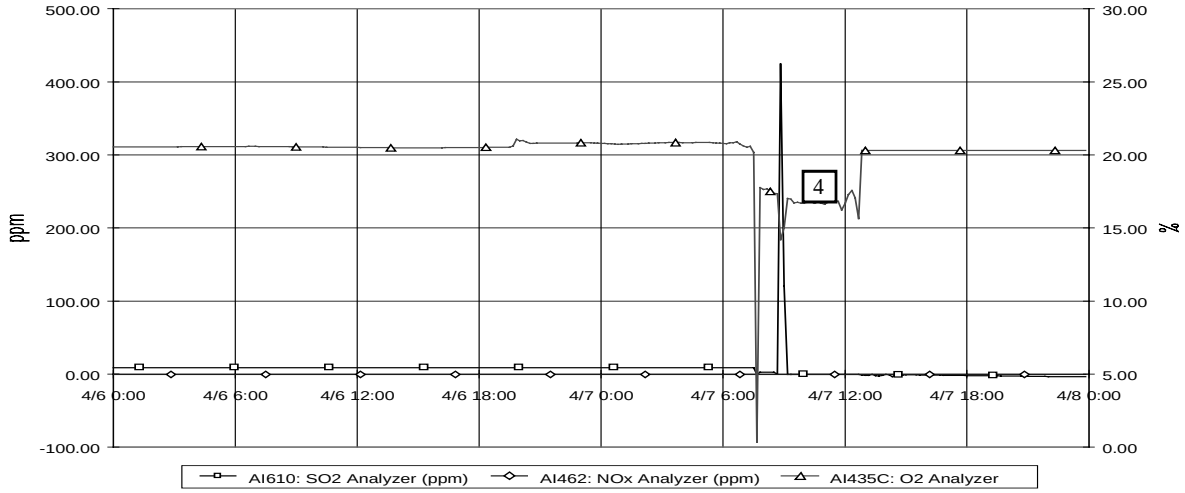

Figure 4.1.1.3-14 O_2, SO_2 and NO_x Analyzers

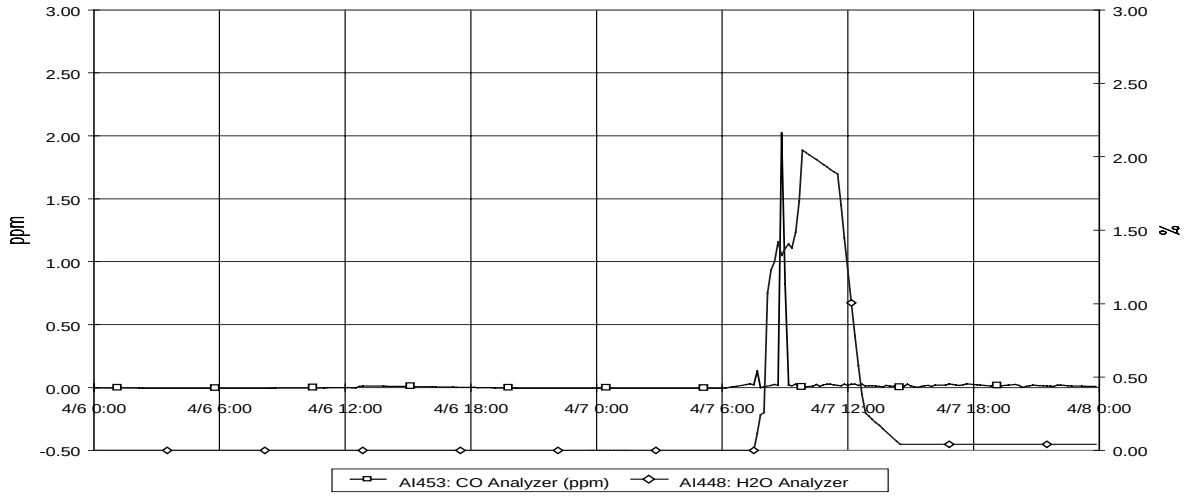

Figure 4.1.1.3-15 CO and H_2O Analyzers

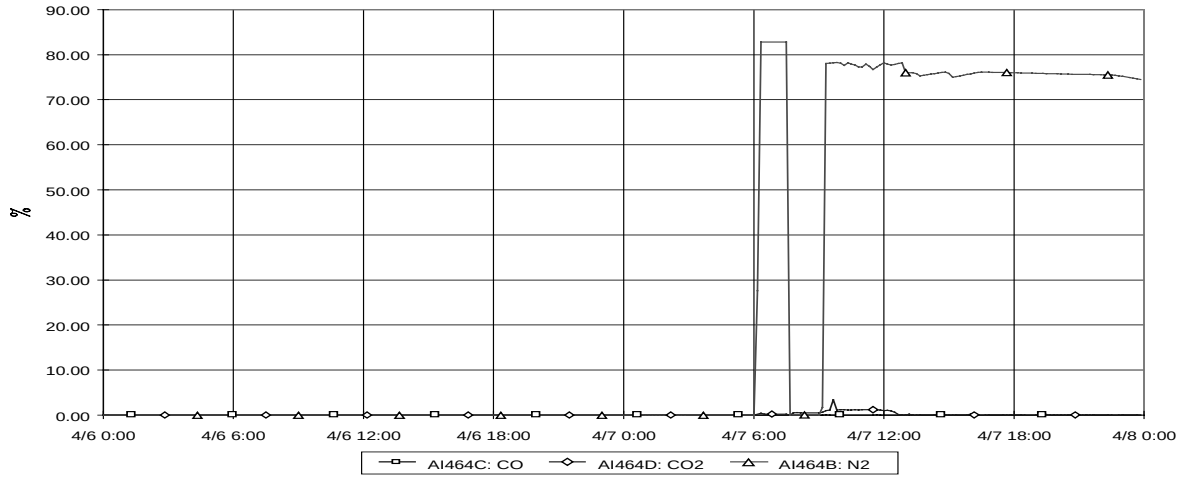

Figure 4.1.1.3-16 GC Analysis

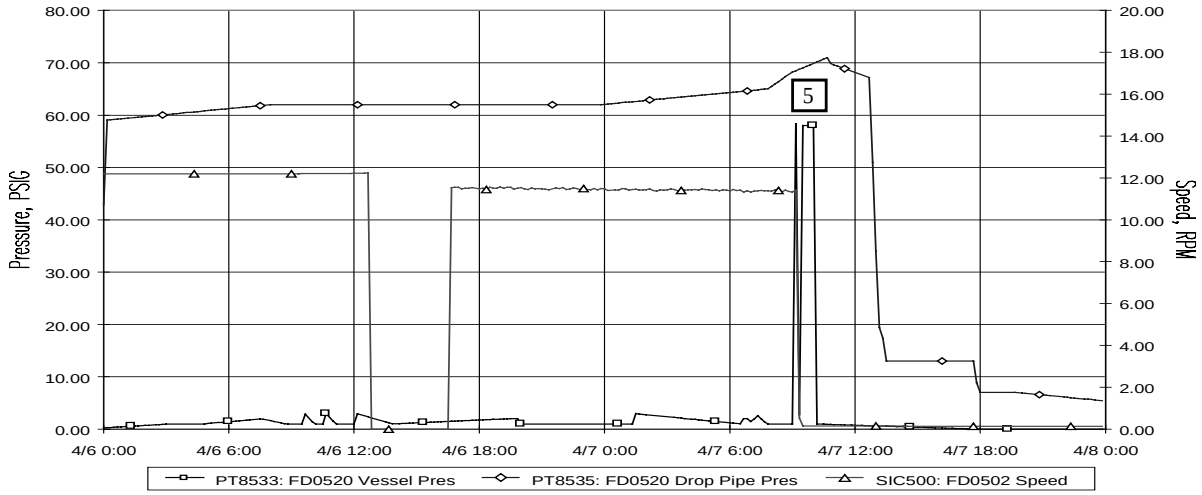

Figure 4.1.1.3-17 FD0520 Pressure Profiles

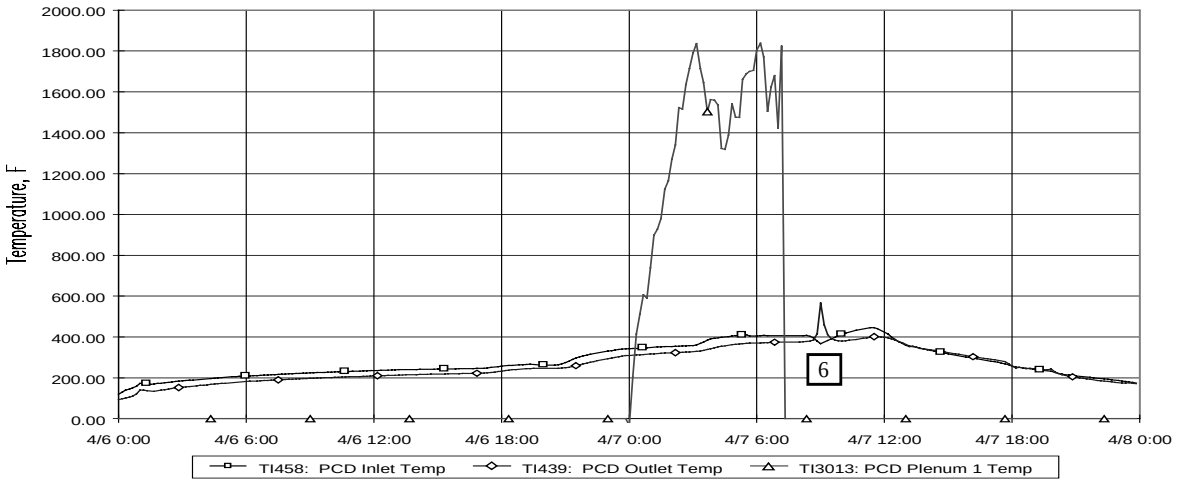

Figure 4.1.1.3-18 PCD Temperatures

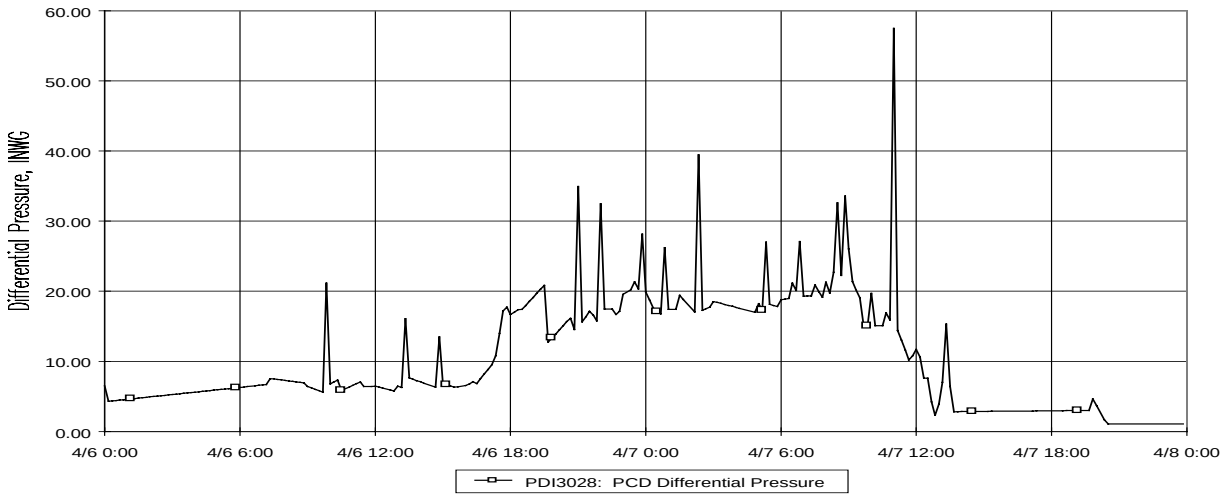

Figure 4.1.1.3-19 PCD Differential Pressure Profiles

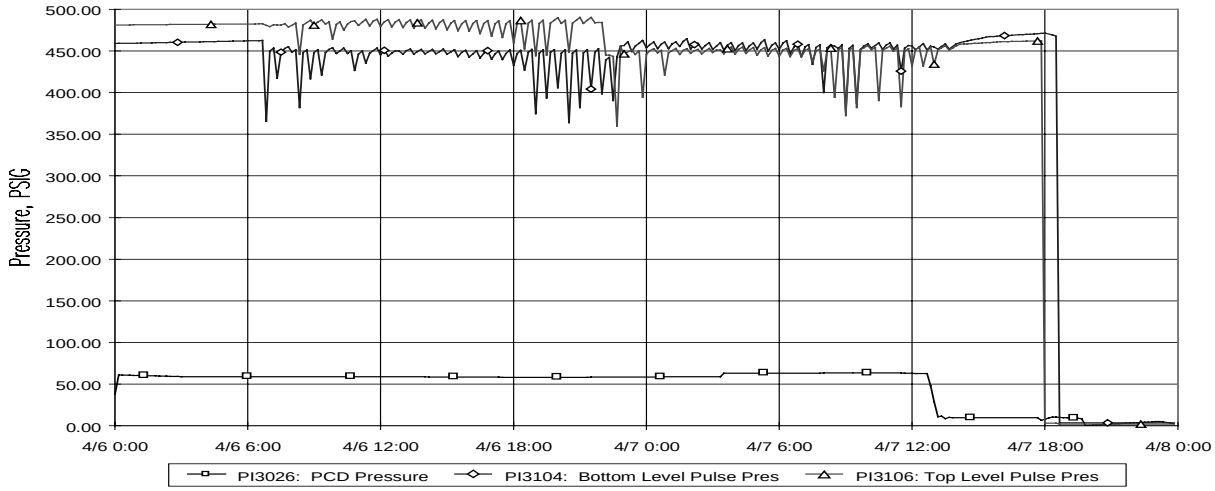

Figure 4.1.1.3-20 PCD Pressure and Pulse Pressure

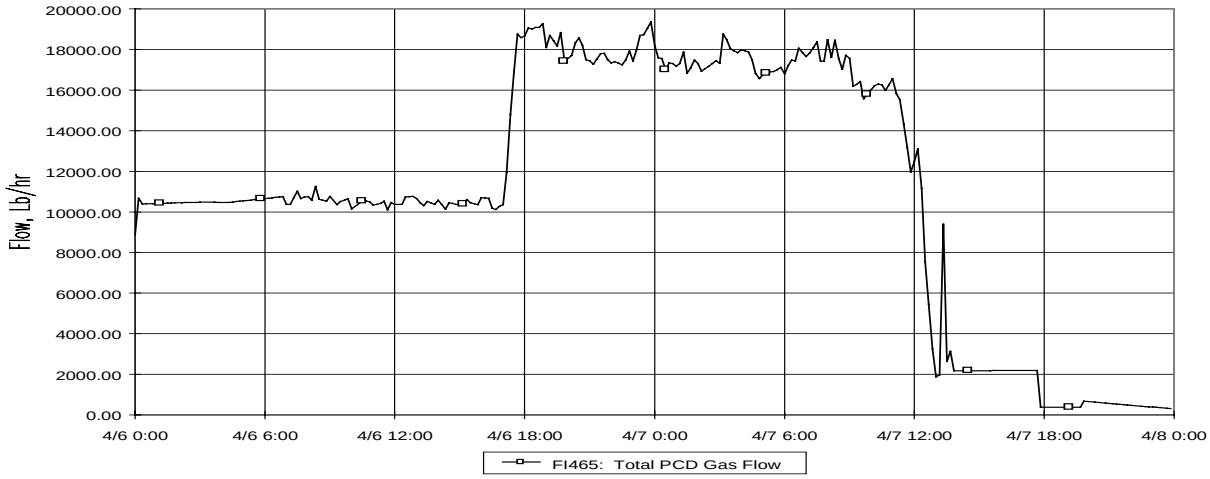

Figure 4.1.1.3-21 Gas Flow Through PCD

4.1.1.4 Characterization Test Run CCT4D

Test run CCT4D was conducted between April 21 and May 3, 1997. Operating plots are shown in figures 4.1.1.1-1 through -104.

Prior to test run CCT4D the bottom four HX0203 aeration nozzles were swapped from air to nitrogen in an attempt to improve the HX0203 circulation. The purge to H4 nozzle on the standpipe in line with the reactor J-leg was also changed to nitrogen due to frequent plugging problems. A DCS manual bypass was added so that the operators would be able to swap from transport air to nitrogen. Modifications were made to the FD0210 and FD0220 feed lines to allow the systems to be isolated from the reactor and back-flushed using nitrogen. This would be helpful to clear the feed lines back into the feeder or to dislodge a plug in the bottom of the feeder. Also, prior to the start of this test run the PCD was recandled and extensive candle studies were initiated.

CCT4D Test Run Chronology

- The leak test was completed on April 15,1997. Atlas Copco once again tuned the main air compressor (CO0201) on April 16 and 17, 1997. After tightening leaking flanges and unions another leak test was performed on April 18, 1997. Following the leak test the flows through the reactor were established and the thermal oxidizer (BR0401) was lit at 22:00 (event 1, figure 21).

- By 07:30 on April 21,1997, the cyclone exit temperature was 175°F and the PCD exit temperature was 225°F. The total flow through the process was reduced from about 20,000 to 5,500 lb/hr to balance selected differential-pressure-indicator bleed flows (event 2, figure 6). After balancing the bleeds the PCD was reheated. The PCD exit temperature (TI439) reached the desired 200°F by 13:00 (event 3, figure 23). The start-up burner (BR0201) pilot was lit at 13:38 (event 4, figure 4) and 1 hour later the main burner was lit and the pilot was shut down. Sand addition into the reactor using the coal feeder system (FD0210) was started around 15:51. Around 17:30 problems with the fines transporter system (FD0520) developed due to plugging.

- On April 22, 1997, BR0201 firing was continually increased to heat the reactor system (event 5, figure 31). Approximately 12,680 lb of solids were added to the reactor consisting of 12,000 lb of sand and 680 lb of dolomite. A flow path test was performed on the combustor heat exchanger (HX0203) to ensure solids circulation through HX0203. Sand addition was started again to replace the sand lost during the HX0203 flow path test.

- Around 14:15 SRI took an inlet solids sample. At 14:45 the reactor pressure was increased from 75 to 95 psig (event 6, figure 39). At 16:00 500 lb of dolomite were fed to the reactor using FD0220 to test draining of solids in the cyclone dipleg. Solids appeared to be draining well and so the feeder speed was reduced. At 17:10 spoiling gas was introduced to determine its effect on the cyclone dipleg operation. The dipleg temperatures increased and the cyclone pressure differential indications

(PDI253 and PDI254) had less fluctuations. At 19:47 with the reactor at 1,000°F bituminous coal feed was started using FD0210 (event 7, figures 30, 33 through 37, and 41).

- Sand addition was started again at 06:00 on April 23, 1997, from FD0220 to maintain the standpipe solids height. From 00:00 to 08:39 on April 23, 1997, the average coal feed rate was 413 lb/hr (event 8, figure 41). At 14:00 the reactor pressure was increased by 5 psi every 30 minutes until the pressure reached 160 psig. The reactor flows were adjusted for the higher operating pressures. Conditions were held constant for the remainder of the day. The gas chromatograph was off-line due to problems with one of the columns. From 09:00 on April 23, 1997, to 08:00 on April 24, 1997, the average coal feed rate was 550 lb/hr.

- The gas chromatograph was fixed and returned to service on April 23, 1997. A PCD outlet sample was taken. From 14:00 to 14:20, while feeding used sand drained from the reactor and HX0203 after test run CCT4C, coal mixed in with sand caused over-temperature in the reactor. The coal feed rate was reduced and in response the HX0203 circulation was increased. The reactor temperatures recovered and operation continued (event 9, figures 33 through 35).

- FD0220 was started but there were problems with the dispense vessel level probe. The conditions at the end of April 24, 1997, were as follows: the reactor pressure was 160 psig; the compressor discharge flow was 16,000 lb/hr; the total reactor outlet gas flow was 20,000 lb/hr; the mixing zone temperatures were between 1,200 and 1,400°F; the riser temperature was between 1,575 and 1,600°F; the standpipe temperature was around 1,500°F; the cyclone exit temperature was 1,400°F; and the PCD gas inlet temperature was around 900°F (event 10, figures 27, and 32 through 35).

- At 02:35 on April 25, 1997, the loss of low-pressure nitrogen tripped the coal feeder. When the low-pressure nitrogen was reestablished coal feed was started again. Due to a low solids levels in the standpipe it appeared from the temperature profile that there was some reverse flow of gases in the reactor. The reactor J-leg flow was increased to stop the reverse flow and the reactor temperatures returned to normal (event 11, figures 33 through 35). At 07:10 FD0210 failed and the reactor temperatures dipped. Coal addition using FD0220 was attempted around 07:30 but the reactor temperatures could not be recovered. The reactor pressure was reduced to 100 psig and at 08:25 BR0201 was lit to increase reactor temperatures (event 12, figures 31 and 33 through 35).

- The burner outlet temperature was ramped to 1,500°F and sand addition into the reactor was started. When the mixing zone and riser temperatures reached 1,000°F, coal was batch fed into the reactor to heat up the solids in the standpipe without having excess combustion at the inlet of the cyclone. The burner firing was continually increased and by 13:15 continuous coal feed to the reactor was achieved (event 13, figures 30 and 33 through 35).

- After BR0201 was shut down around 15:00 the reactor pressure was increased at 20 psig per hour. During this run the spent solids screw cooler (FD0206) was run periodically for short durations to ensure its operability. From 14:00 to 18:00 the reactor riser temperature dropped and temperatures increased at the inlet cyclone and the top of standpipe (event 14, figures 33 through 35). Increasing the reactor J-leg flow recovered the temperatures a few times. There were also some problems with plugging/caking in the FD0210 surge bin. Around 17:30 the same phenomena occurred again. This time the temperatures could not be recovered and the coal feed was stopped (event 15, figures 30 and 33 through 35). BR0201 was started at 19:00 and the firing was gradually increased to 1,700°F.

- Coal addition was tried several times between 22:00 on April 25 and 03:07 on April 26. The reactor pressure was increased to 110 psig but the desired temperature distribution could not be achieved (event 16, figures 59 through 61). Therefore, at 04:37 FD0206 was started in order to drain the standpipe solids and verify that the standpipe was not obstructed. After adjusting various reactor flows the standpipe differential pressure measurement (PDI259) indicated that the standpipe was empty of solids (event 17, figure 66). Flow tests confirmed that the standpipe portion between the HX0203 inlet and the cyclone dipleg was clear. Sand addition into the reactor was started again at 09:20. Coal feed was resumed at 18:33 (event 18, figures 56, 59 through 62, and 67) and BR0201 was shut down at 20:40. After BR0201 was shut down the reactor pressure was increased to 180 psig. The reactor temperature profiles were normal and the reactor loop was operating well.

- The reactor pressure reached 180 psig at 00:11 on April 27, 1997. Conditions were held steady with solids being fed from FD0220 every 4 hours to maintain the standpipe solids level. At this time the average coal feed rate was 790 lb/hr.

- At 09:00 250 pounds of dolomite was added into FD0220. At 09:47 dolomite addition into the reactor began as shown by the SO_2 dropping from 124 to 6 ppm (event 19, figure 68). After FD0220 plugged at 12:00 it was unplugged and restarted. Conditions were then maintained, holding the standpipe level relatively constant by feeding sand (event 20, figure 66).

- At 00:35 on April 28, 1997, problems with the level probe in the FD210 lock vessel developed. Around 03:00 more problems with the coal feeder developed which eventually forced the reactor to be shut down about 1.5 hours later (event 21, figures 56, 59 through 62, and 67). Coal was loaded into FD0220 and fed for a brief period into the reactor. The reactor pressure was reduced to 60 psig and BR0201 was lit. Between 13:00 on April 27, 1997, and 04:00 on April 28, 1997, the average coal feed rate was 860 lb/hr.

- Upon inspection of the coal feeder, five pieces of electrical tape and two large pieces (about 2-inch, diameter) of bin coating (epoxy) material were found in the bend at the exit of the star feeder. The rotofeeder was removed and about 3 ft^3 of cake left

in the dispense vessel collapsed and fell. The cake material was dry and finer than the feed coal. A couple of pieces of about 1-inch spheres of wet cake also came through.

- The burner temperature was ramped to 1,800°F and a slow circulation through the reactor was established. Coal feed was started at 20:55 on April 28 but the feeder tripped at 23:25 (event 22, figures 56, 59 through 62, and 67). The coal feeder problem was addressed and coal feed resumed about an hour later. However, problems with the coal feeder continued and the feeder had to be shut down again.

- At 03:55 on April 29, 1997, coal feed was started again (event 23, figures 56, 59 through 62, and 67). Sand addition continued periodically to maintain the reactor solids inventory. The gas analyzers were calibrated and BR0201 was shut down. Around 11:45 FD0210 started having more problems and was eventually shut down at 14:12 (event 24, figures 56, 59 through 62, and 67). BR0201 was lit to maintain the reactor temperature. All flows were adjusted to their minimum values. During the FD0210 inspection two pieces of epoxy paint and two coal agglomerates were found. Further inspection inside the dispense vessel showed more epoxy coating had peeled off but had not fallen down. All loose coating from the vessel was removed. While attending to the FD0210 problem the reactor continued to be heated up with the start-up burner. The reactor pressure was increased to 110 psig to control riser velocity.

- FD0210 was reassembled and coal feed resumed at 01:25 on April 30,1997 (event 25, figures 82, 85 through 88, and 93). After BR0201 was shut down at 03:40 the reactor pressure was increased to 180 psig (event 26, figure 91). The coal feed rate was gradually increased and SRI took another outlet sample. The FD0210 tripped due to software interlock (loss of pressure on PI244) when the transport air dryer (DY0210) was isolated (event 27, figures 81, 82, 85 through 88, and 93). (Apparently the transport air isolation valve (PV244) did not seal completely and when the dryer was isolated the conveying velocity dropped from 28 to 11 ft/s.) The dryer was then put back in service.

- SRI took an inlet sample in the afternoon. Coal feed once again had to be stopped due to combustion outside the desired zones in the reactor (event 28, figure 82, 85 through 88, and 93). The FD0520 tripped because of the discharge line plugging. The reactor pressure was reduced to 100 psig, and BR0201 was lit. The BR0201 outlet temperature was ramped to 1,800°F. Coal feed was started again at 22:12 and BR0201 was shut down at 22:58. The FD0210 tripped again at 23:30.

- On May 1, 1997, at 01:00 BR0201 was started. FD0520 tripped again due to a pluggage. Coal feed was started again at 04:00 and BR0201 was shut down. Sand was also added to the reactor to build the solids inventory in the reactor. Problems with FD0210 started again when the feeder tripped several times from discharge line plugging (event 29, figures 82, 85 through 88, and 93). The reactor pressure was increased from 150 to 190 psig (event 30, figure 91).

- On May 2,1997, sand was added to increase the solids levels in the reactor. The average coal feed rate on May 2, 1997, was 790 lb/hr. At 10:12 the suction valve to the recycle gas booster compressor (CO0401) was opened (event 31, figure 80). The compressor was started at 10:30 but tripped 5 minutes later due to a low-discharge pressure. The safety relief valve downstream of the compressor lifted at 310 psig so the low-discharge pressure switch could not be made. The switch was jumped out so the compressor could be run at a slightly lower discharge pressure. The CO0401 was started but tripped due to a high cylinder 1 discharge temperature. The compressor was started once more but again cylinder 1 overheated (event 32, figure 80).

- Later in the afternoon dolomite addition into the reactor was started. As scheduled, in preparation for shutting the reactor down, the reactor pressure was decreased from 180 to 100 psig. At 01:06 on May 3, 1997, FD0210 was stopped and the transport reactor was shut down (event 33, figure 82, 85-88, and 93).

CCT4D Post Test Run Inspections

Following test run CCT4D reactor inspections were conducted. The riser was clean, however there was a small refractory crack around the top of the riser. There was a small deposit visible on the riser crossover. Some erosion was evident in the crossover and it appeared to be slightly more than previously observed. The primary cyclone was clean, but the refractory installed at the inlet to the cyclone showed some erosion. The standpipe was also clear and clean. The start-up pilot burner was inspected and was in good condition. The pilot was in much better shape compared to previous inspections. The orifice was cleaned and the burner was reinstalled. The coal feeder was inspected and pieces of bags (from coal silo bags) were found stuck between the rotor and stator of the dispense vessel. The coal feeder was cleaned and the coal silo was deinventoried and cleaned. The PCD was inspected; all candles appeared to be in good condition.

CCT4D Test Run Observations

CCT4D was successfully completed. The main air compressor was retuned by Atlas Copco, which corrected many operational problems. There was a partial bypass of HX0202 that resulted in an increase in PCD temperature. The gas bypass system with the refractory-lined orifice operated well. The recycle gas booster compressor was tested. Cyclone radish aeration tests were performed during operations to evaluate the effect on cyclone operation. Dolomite was also added to determine its effect on cyclone operation. Additional tests were performed to evaluate the effect of the combustor heat exchanger on reactor operation. A total of 173 hours on coal was achieved and a total of 60 tons of coal was fed.

Section 4.1.1.4

Graphs 1 through 26

Test Run CCT4D

April 18 through April 21, 1997

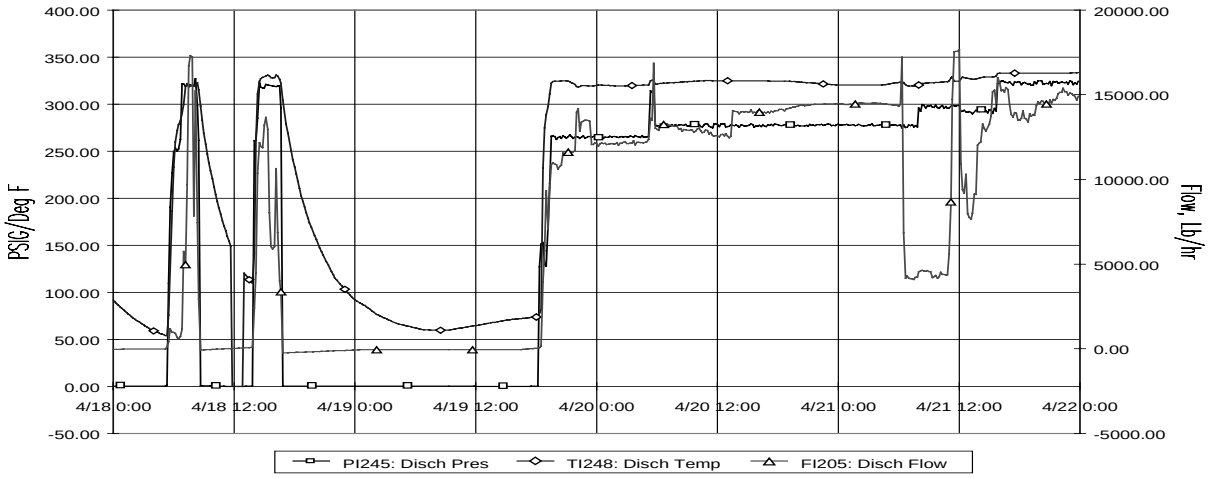

Figure 4.1.1.4-1 CO0201 System Profile

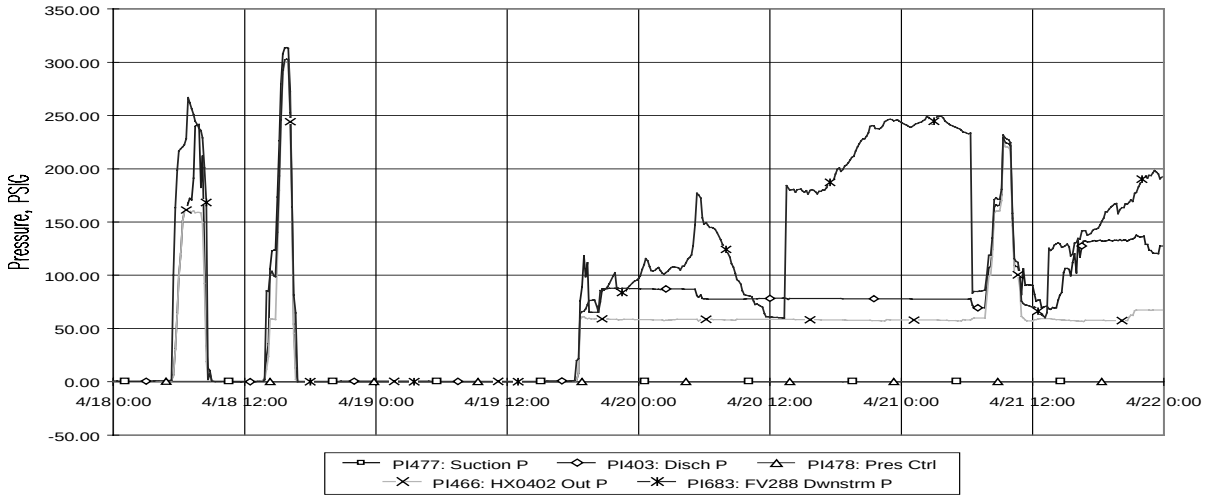

Figure 4.1.1.4-2 Recycle Gas System Pressure Profiles

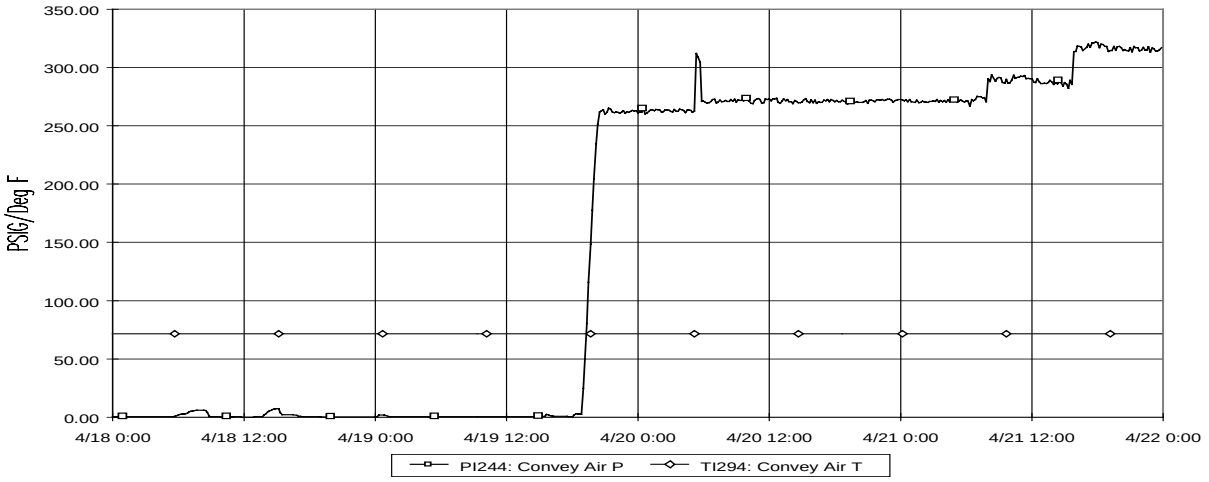

Figure 4.1.1.4-3 Transport Air System Profile

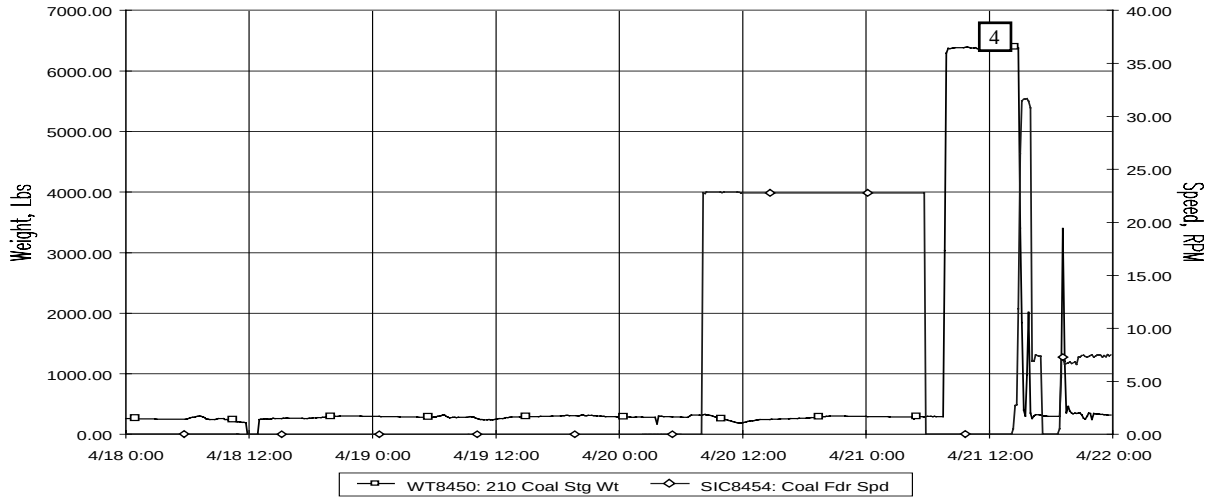

Figure 4.1.1.4-4 Coal Feeder System Profile

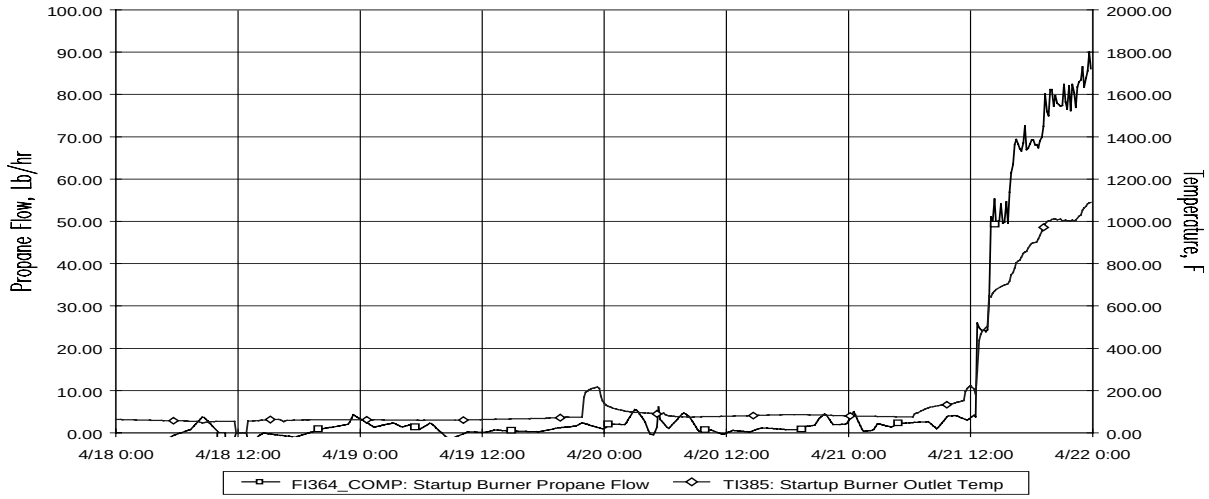

Figure 4.1.1.4-5 Start-Up Burner Flow/Temperature

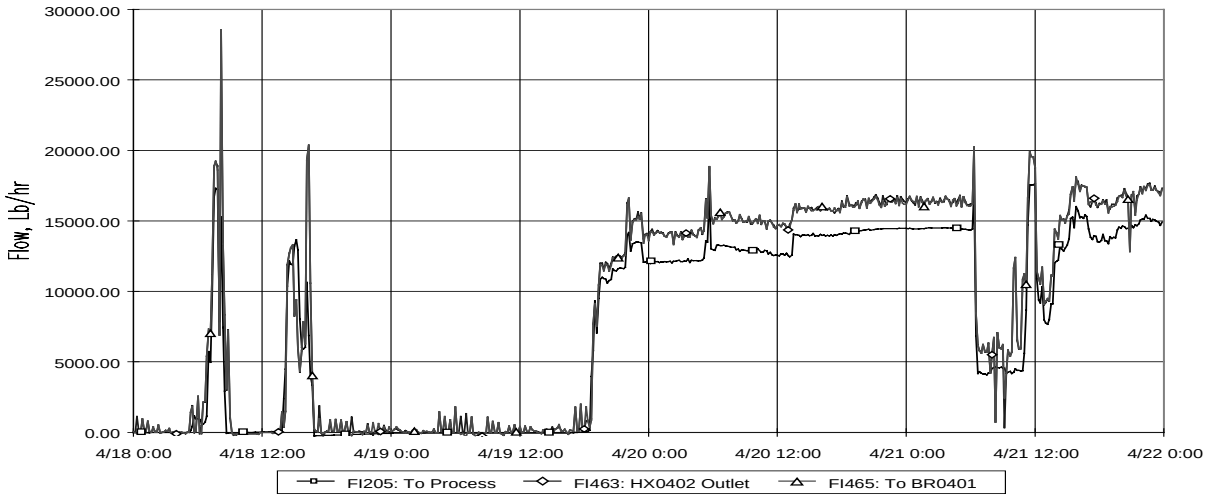

Figure 4.1.1.4-6 Total Gas In/Out Flow Rates

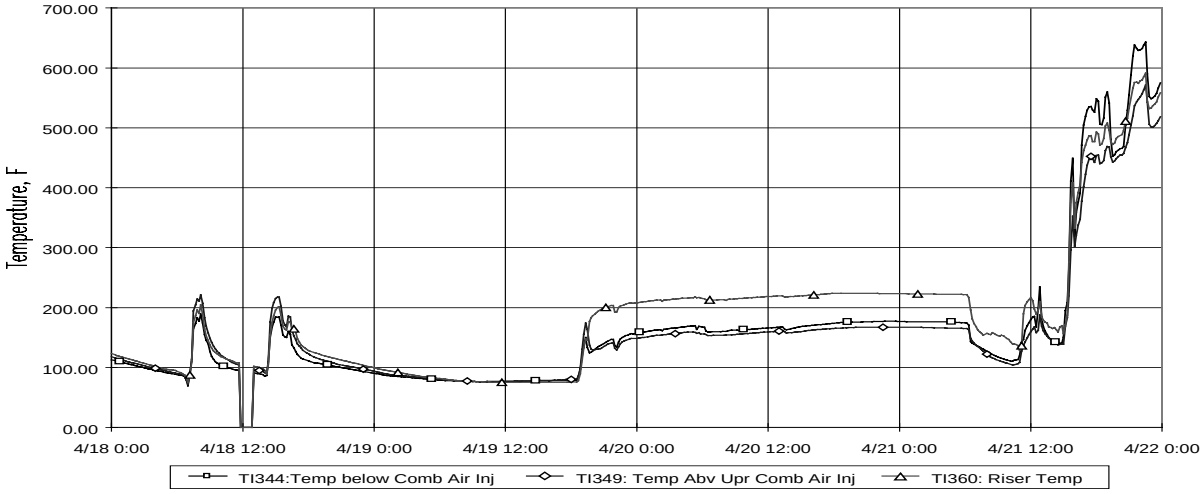

Figure 4.1.1.4-7 Reactor Mixing Zone and Riser Temperatures

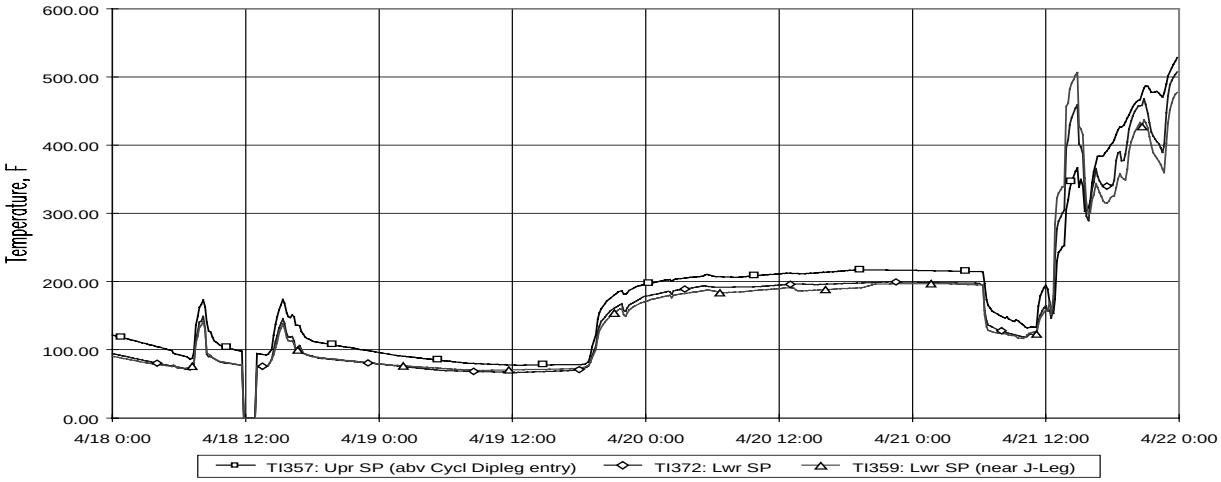

Figure 4.1.1.4-8 Standpipe Temperatures

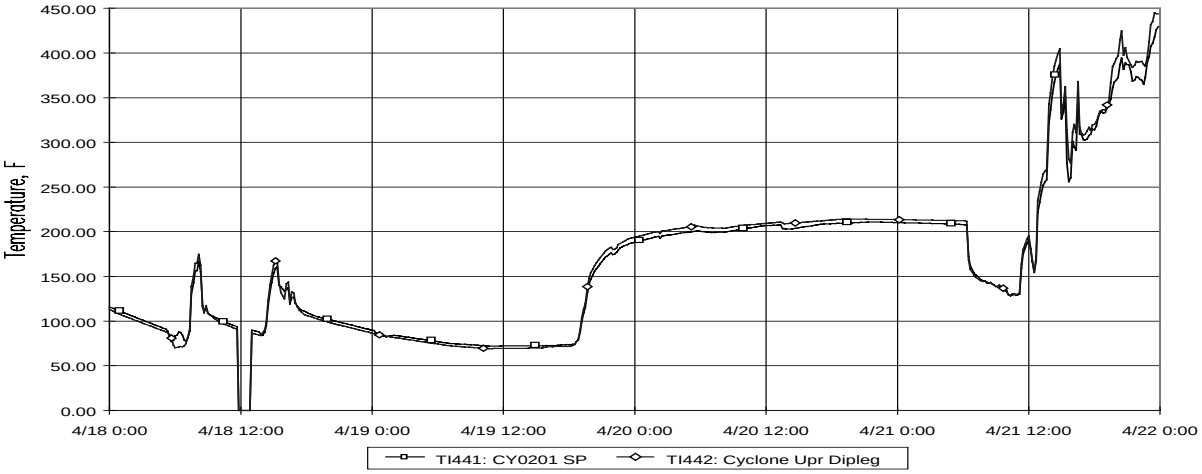

Figure 4.1.1.4-9 Cyclone Dipleg Temperatures

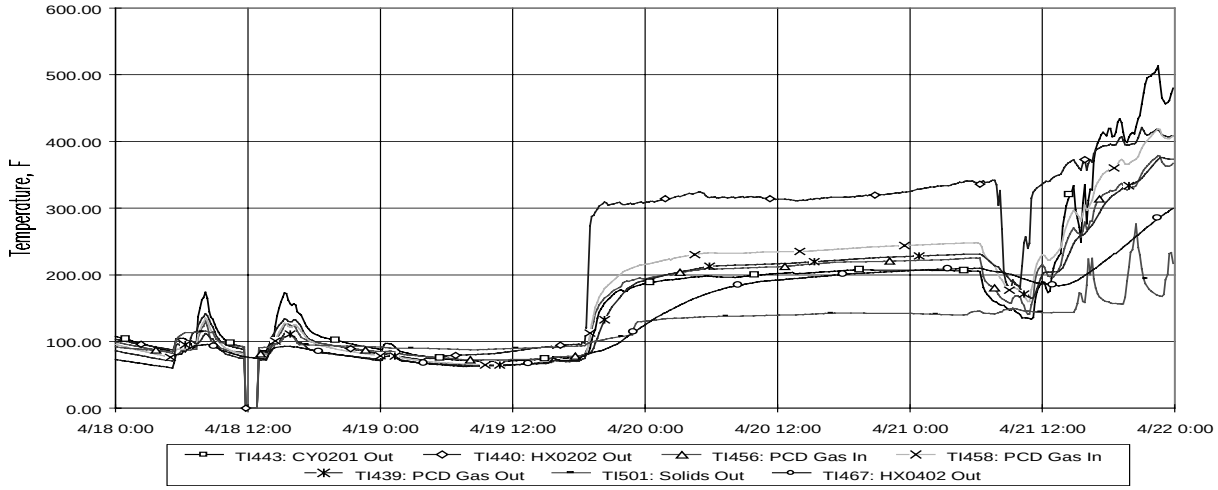

Figure 4.1.1.4-10 Temperature Profile Downstream of Reactor

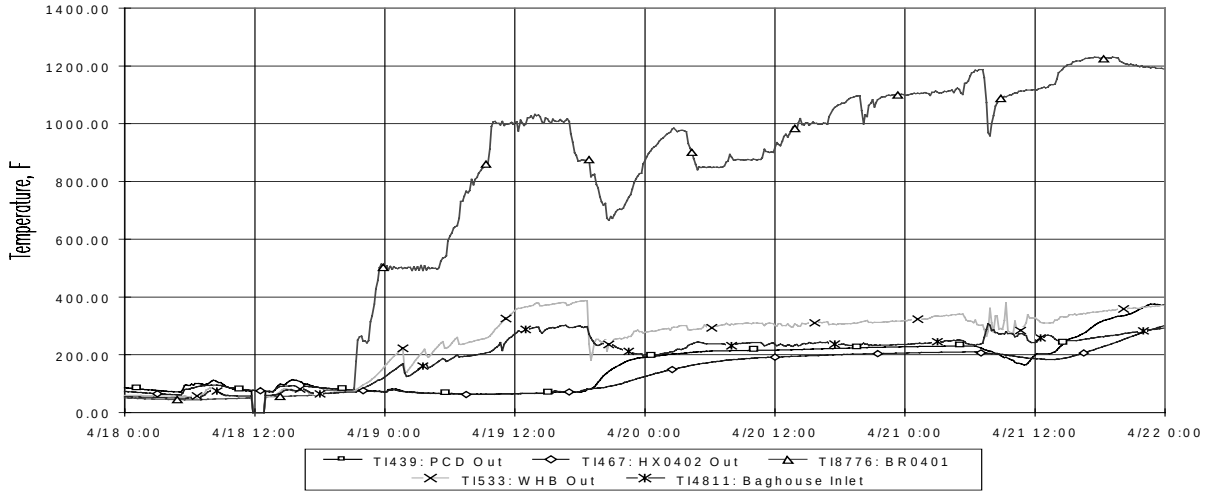

Figure 4.1.1.4-11 System Temperatures Downstream of PCD

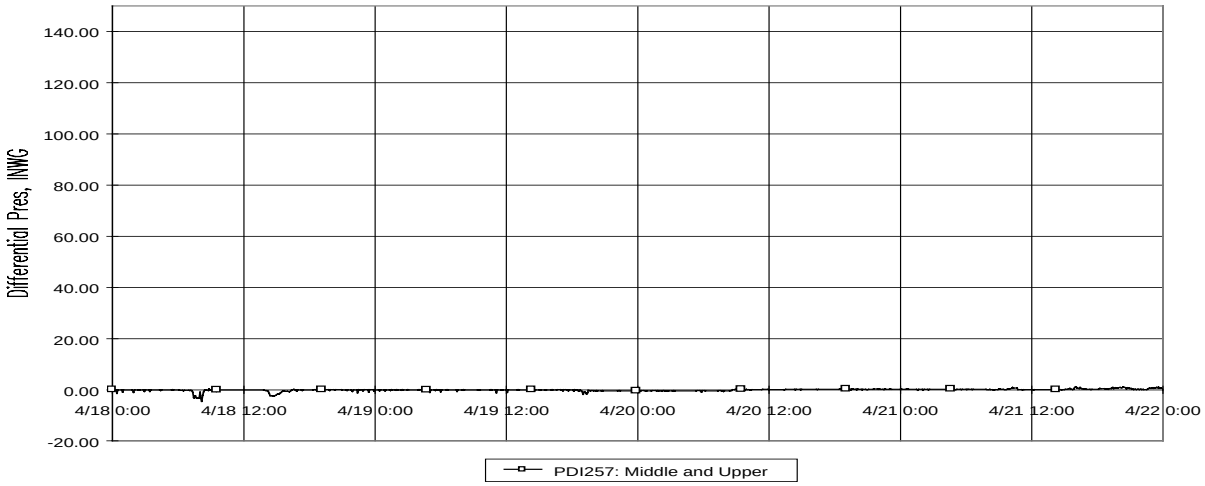

Figure 4.1.1.4-12 Mixing Zone Differential Pressure Profile

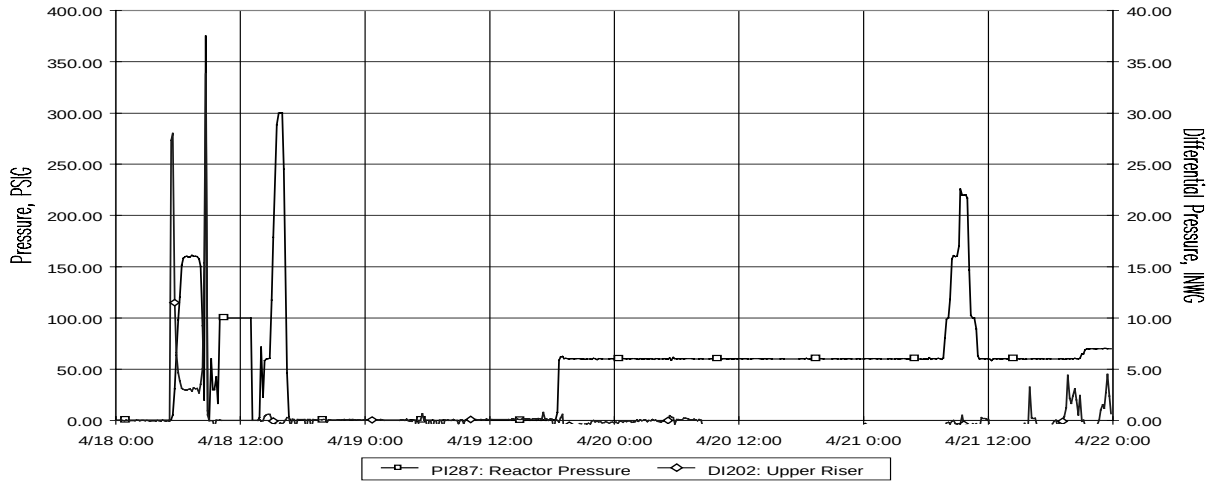

Figure 4.1.1.4-13 Reactor Pressure/Riser Differential Pressure Profiles

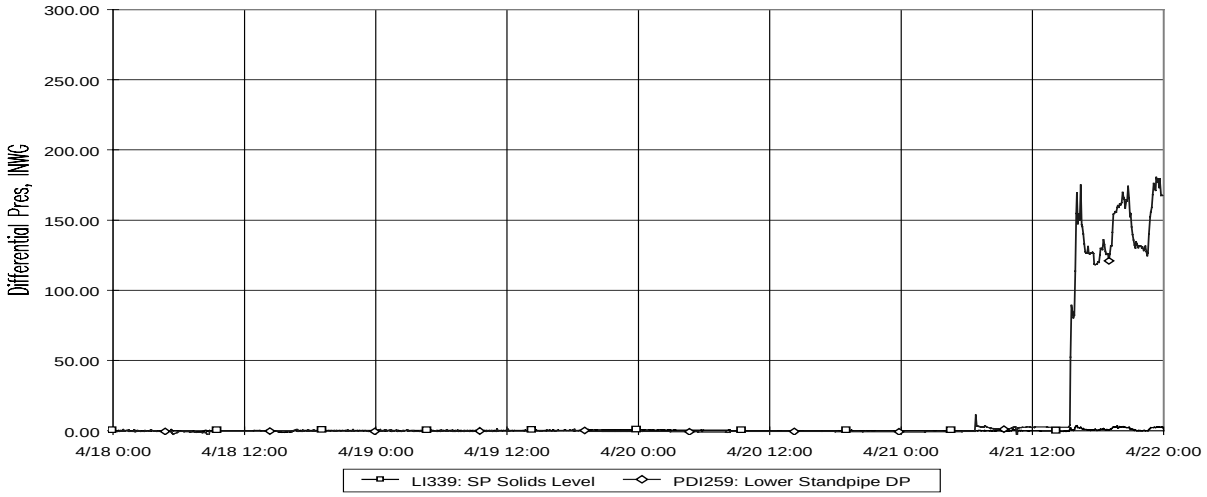

Figure 4.1.1.4-14 Standpipe Differential Pressure Profiles

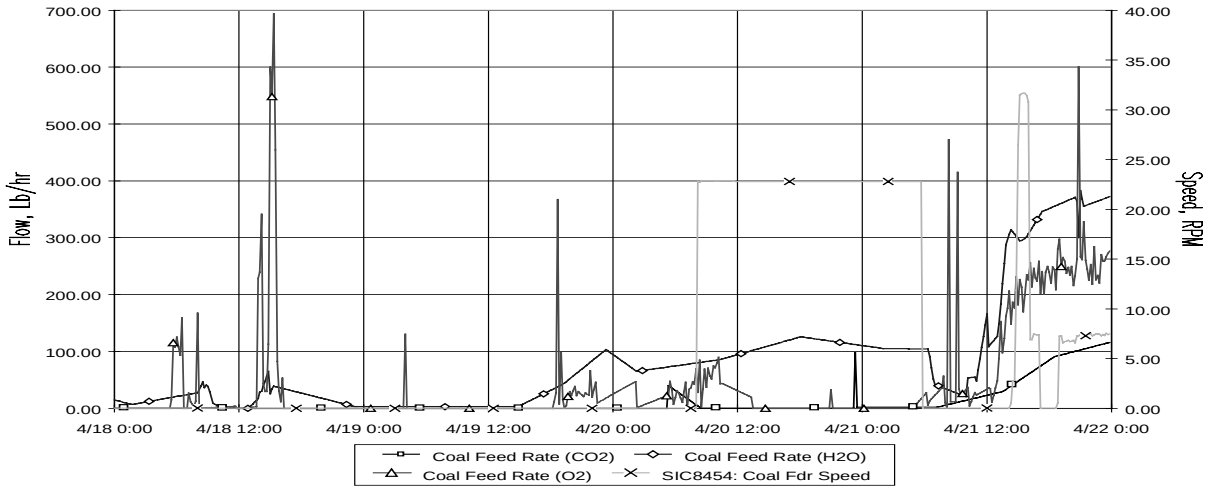

Figure 4.1.1.4-15 Coal Feed Rate Based on Gas Analysis

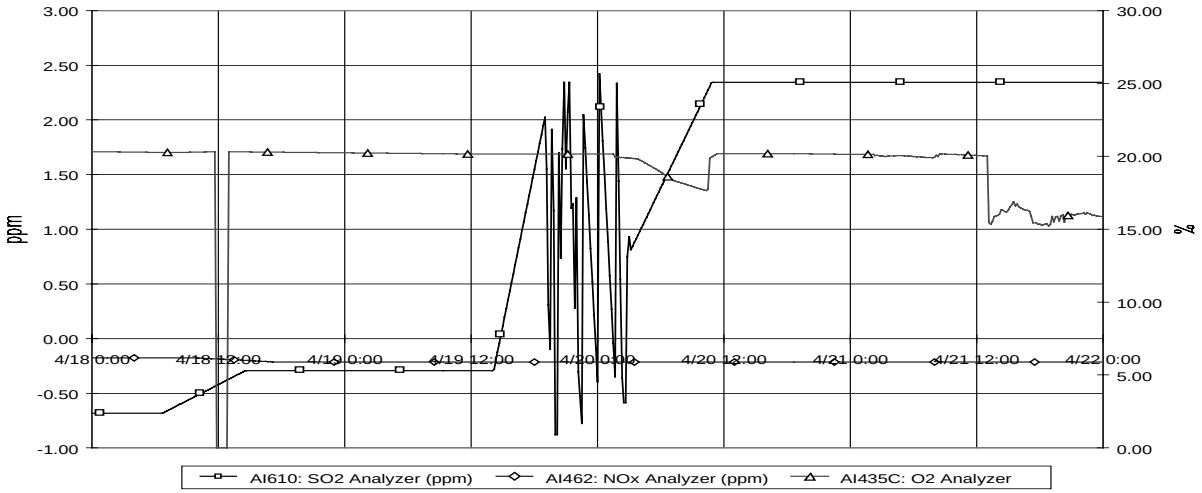

Figure 4.1.1.4-16 O_2, SO_2 and NO_x Analyzers

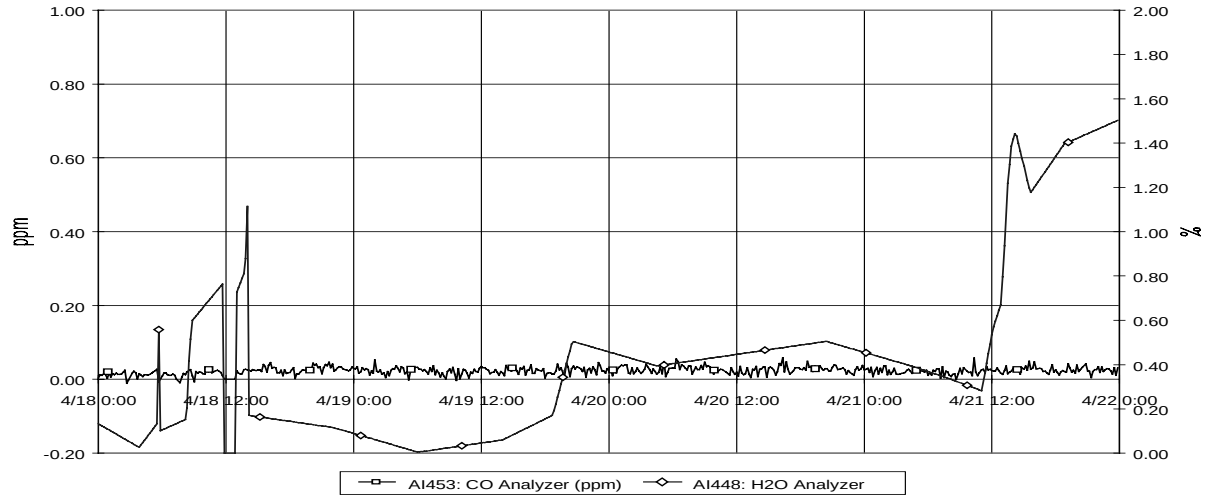

Figure 4.1.1.4-17 CO and H_2O Analyzers

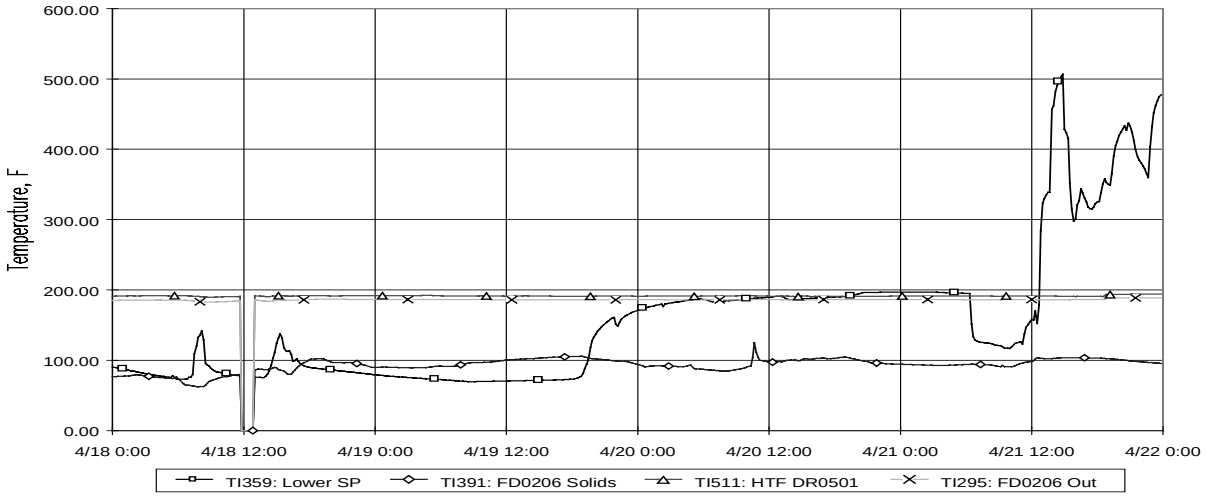

Figure 4.1.1.4-18 FD0510 Temperature Profiles

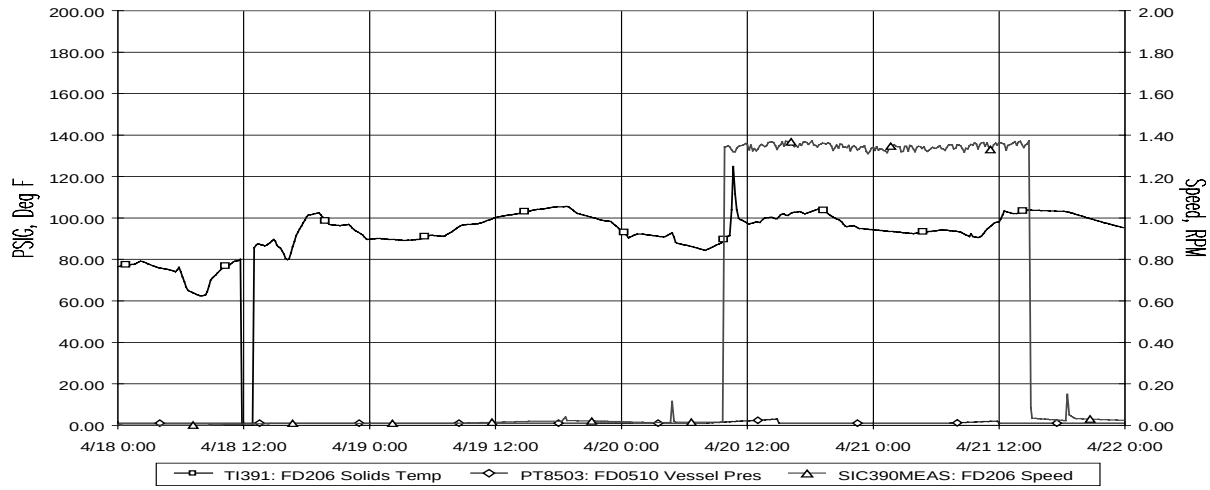

Figure 4.1.1.4-19 FD0206 Profiles

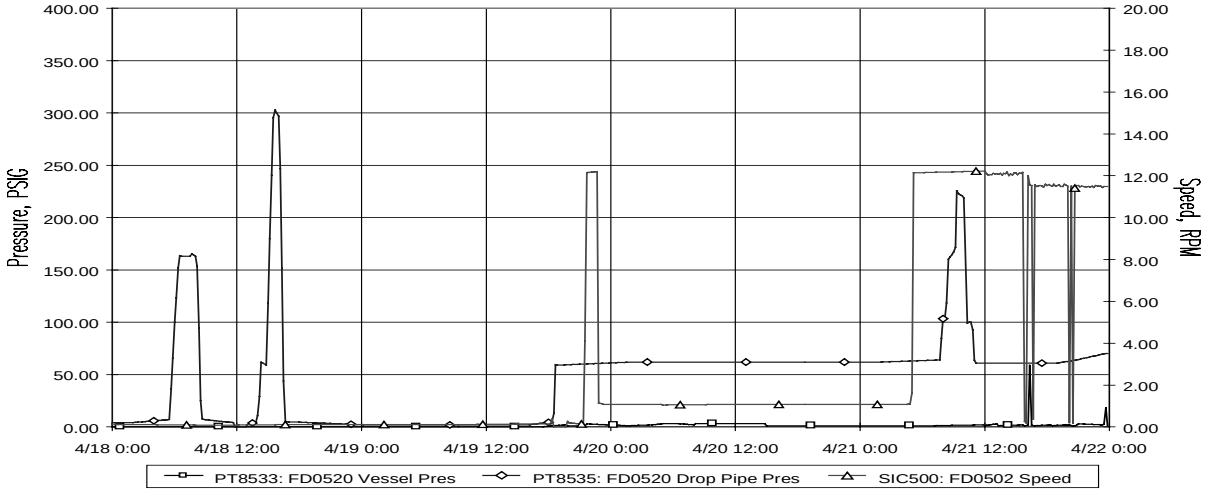

Figure 4.1.1.4-20 FD0520 Pressure Profiles

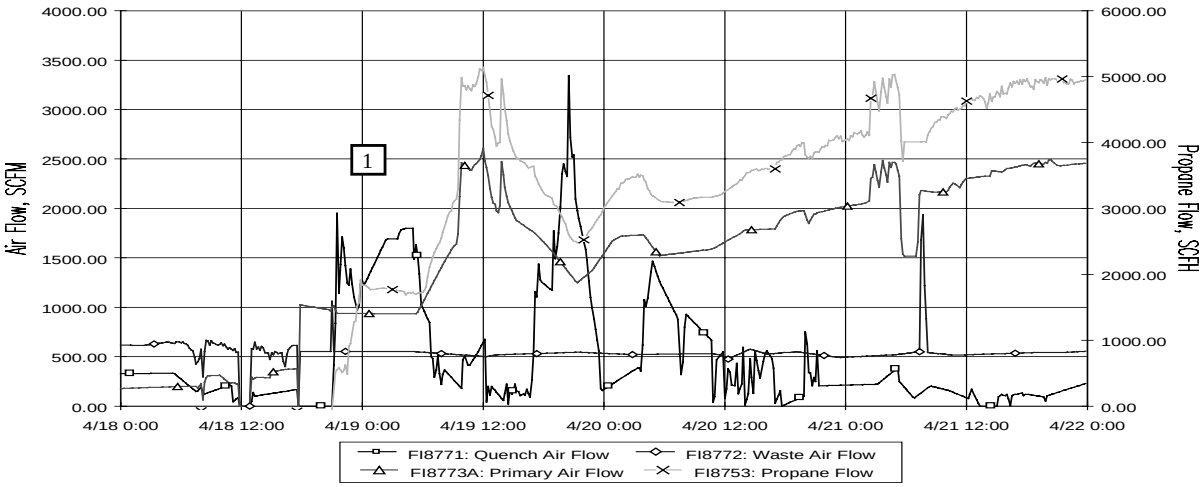

Figure 4.1.1.4-21 Thermal Oxidizer Air/Fuel Flow

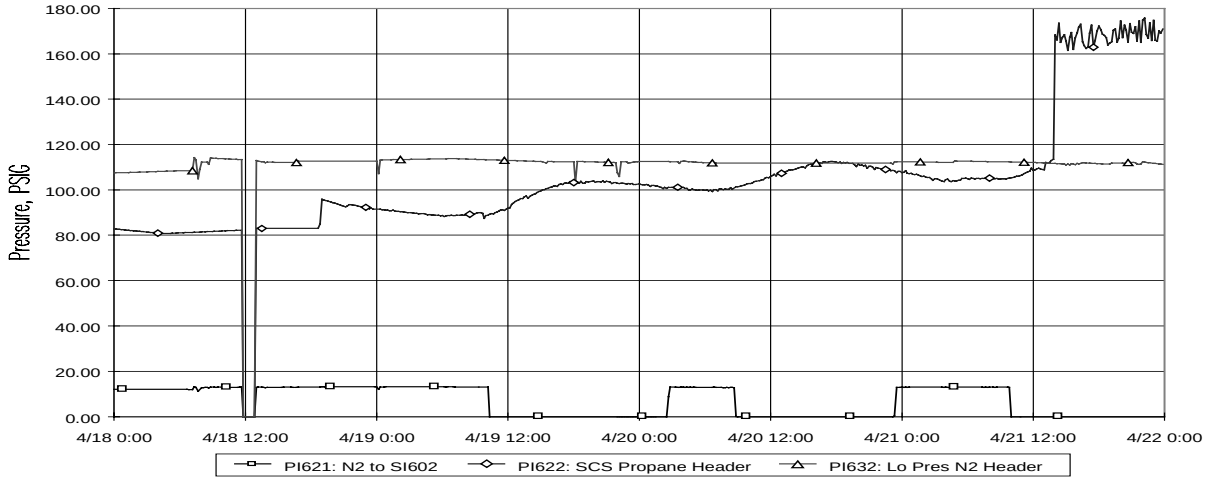

Figure 4.1.1.4-22 Nitrogen/Propane Header Pressure Profiles

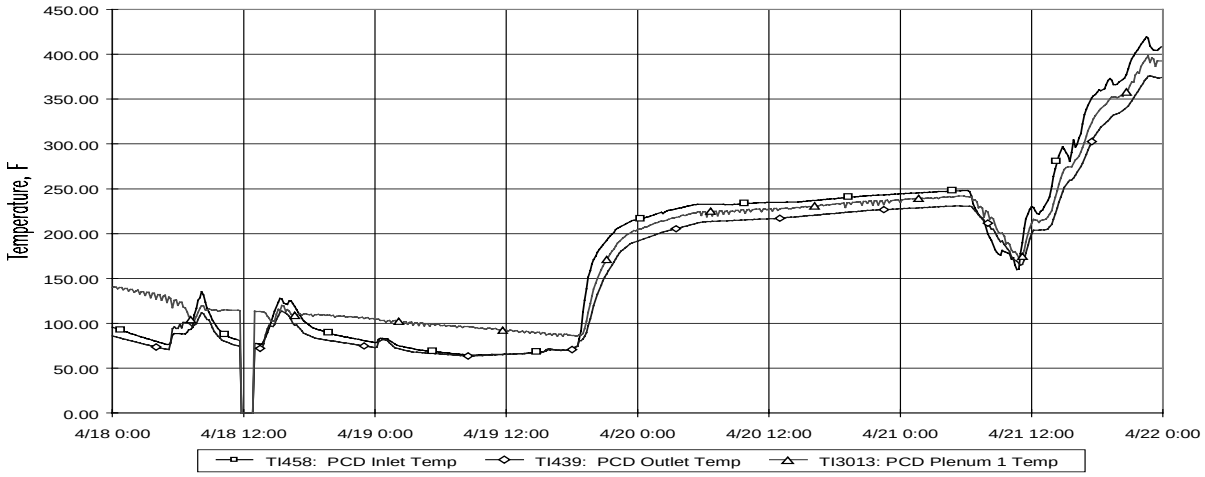

Figure 4.1.1.4-23 PCD Temperatures

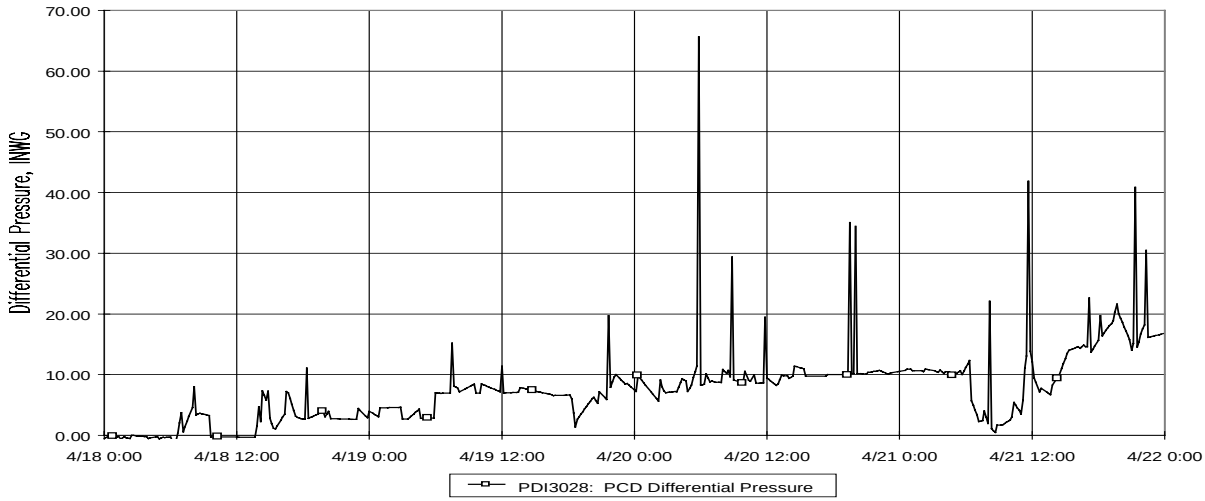

Figure 4.1.1.4-24 PCD Differential Pressure Profile

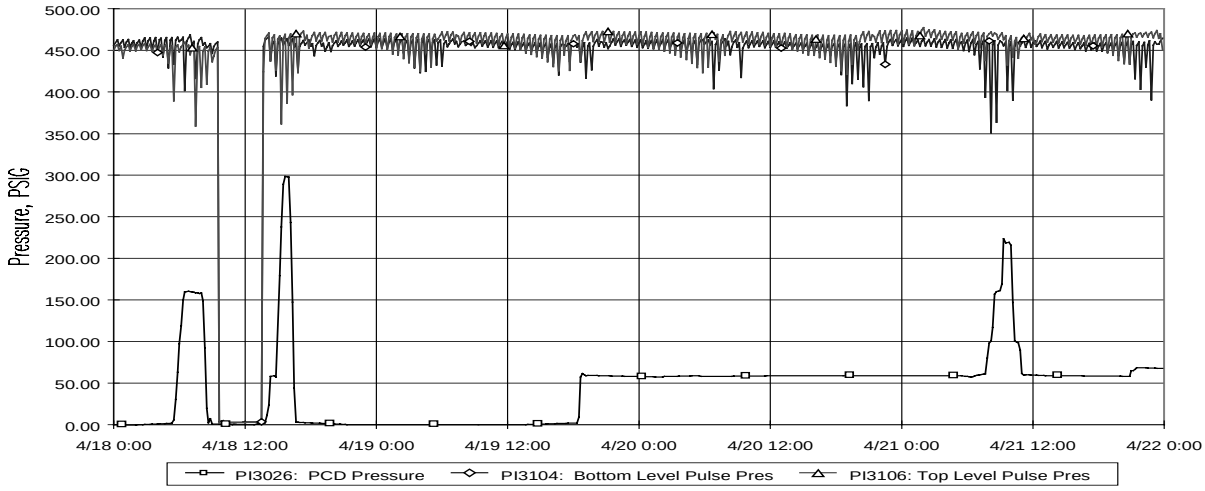

Figure 4.1.1.4-25 PCD Pressure and Pulse Pressure

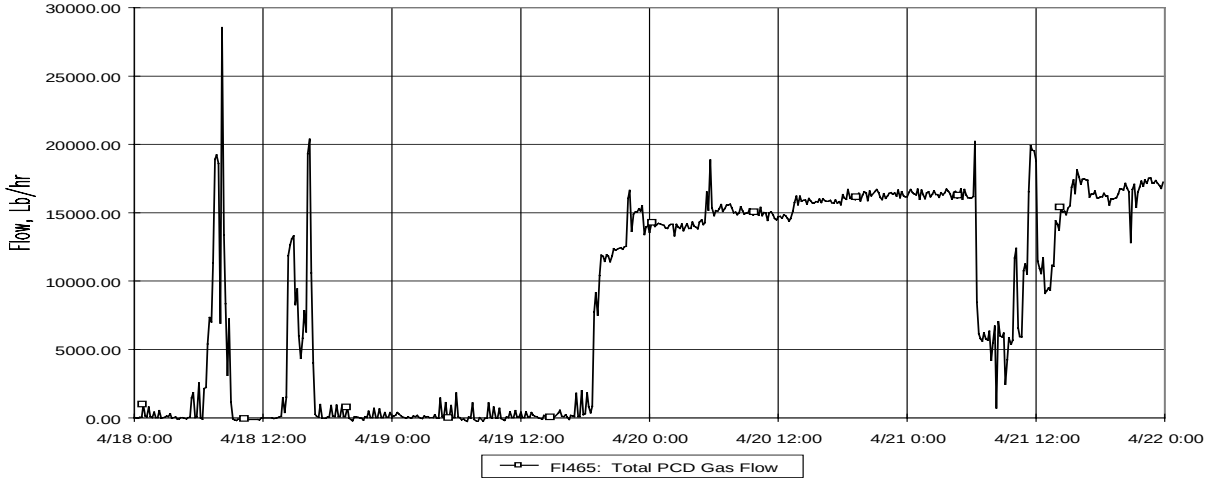

Figure 4.1.1.4-26 Gas Flow Through PCD

Section 4.1.1.4

Graphs 27 through 52

Test Run CCT4D

April 22 through April 25, 1997

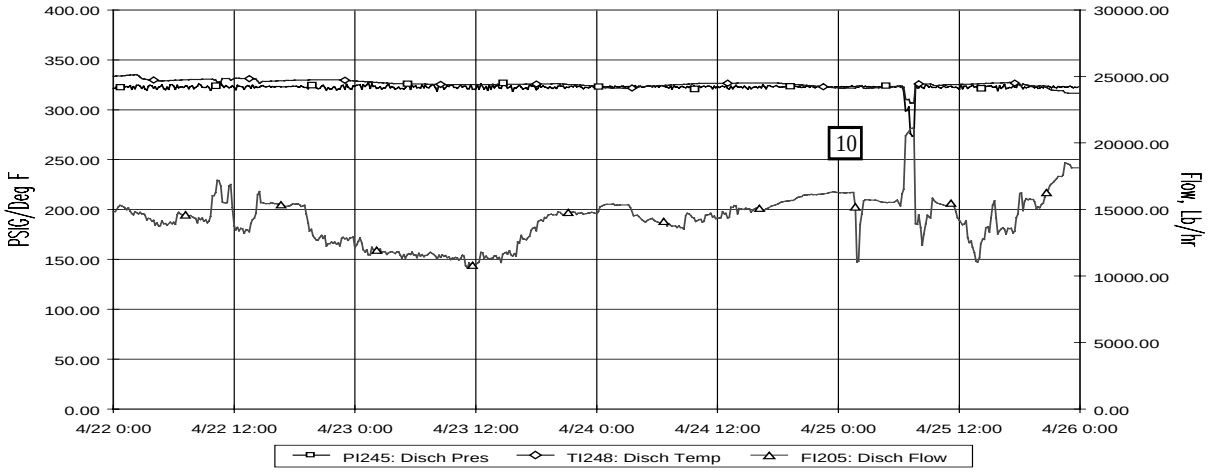

Figure 4.1.1.4-27 CO0201 System Profile

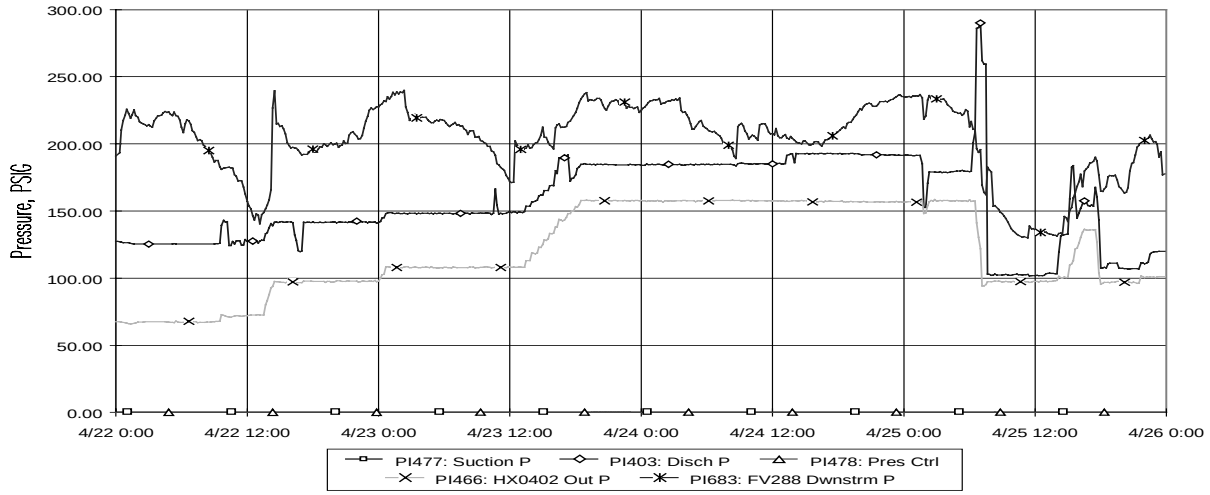

Figure 4.1.1.4-28 Recycle Gas System Pressure Profiles

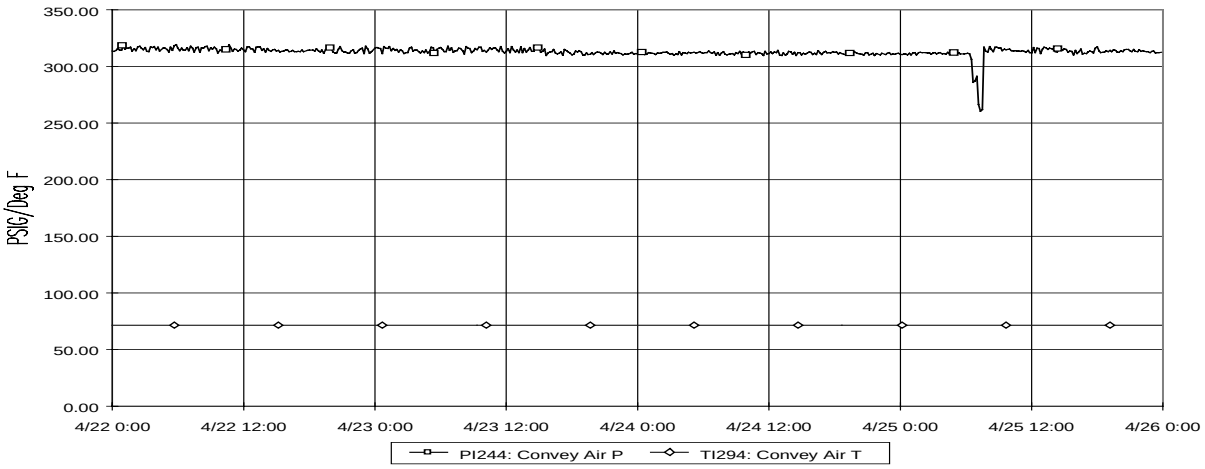

Figure 4.1.1.4-29 Transport Air System Profile

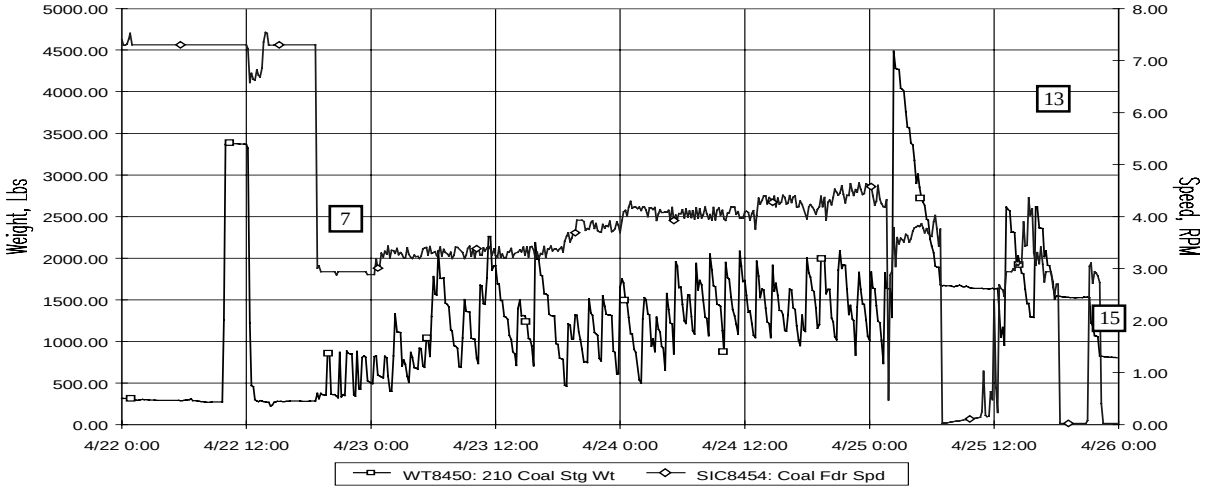

Figure 4.1.1.4-30 Coal Feeder System Profile

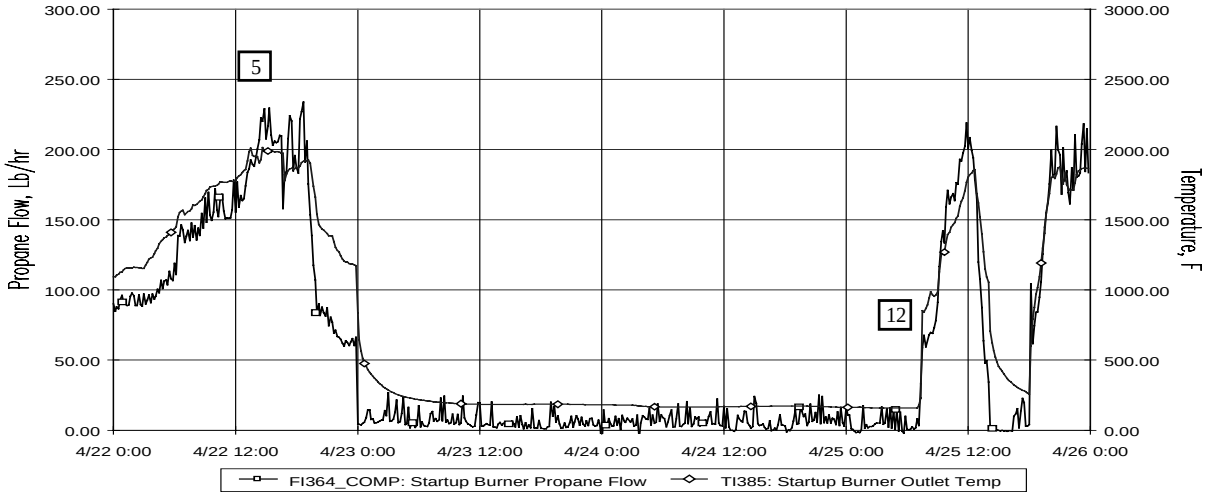

Figure 4.1.1.4-31 Start-Up Burner Flow/Temperature

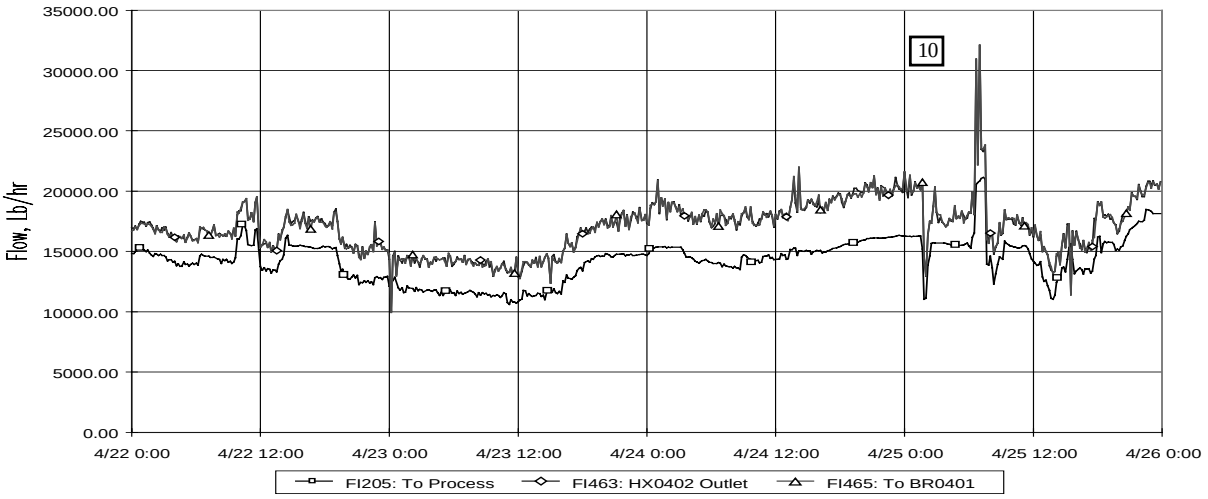

Figure 4.1.1.4-32 Total Gas In/Out Flow Rates

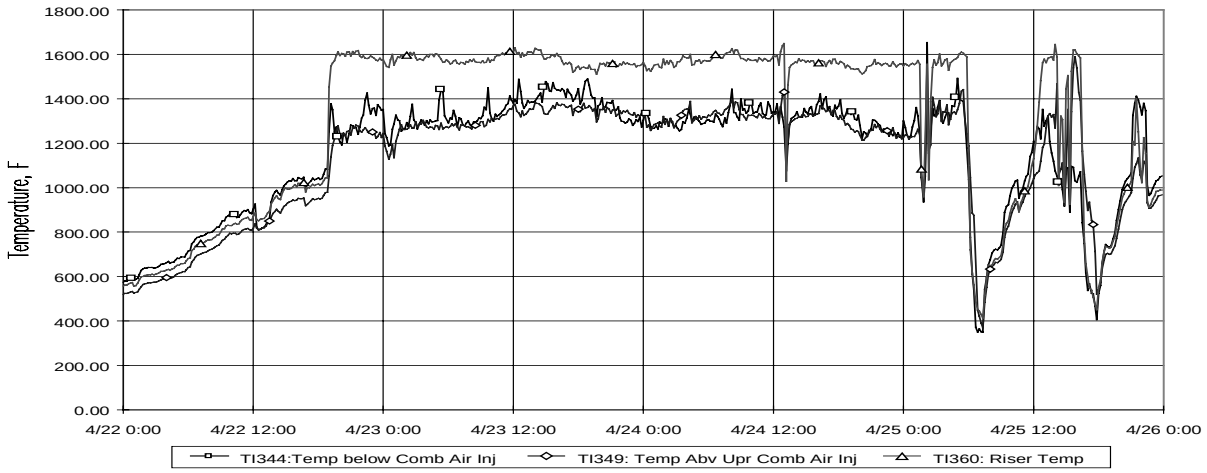

Figure 4.1.1.4-33 Reactor Mixing Zone and Riser Temperatures

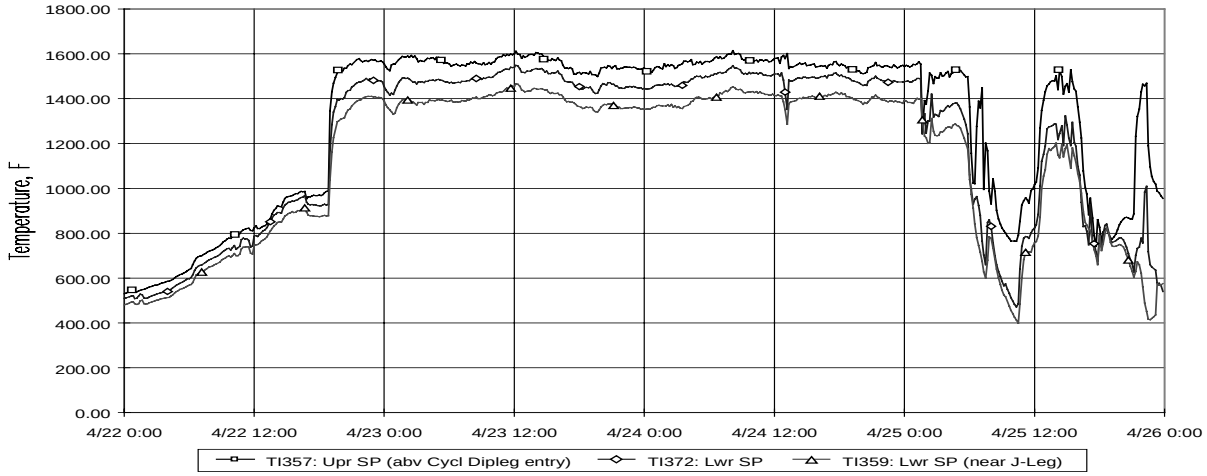

Figure 4.1.1.4-34 Standpipe Temperatures

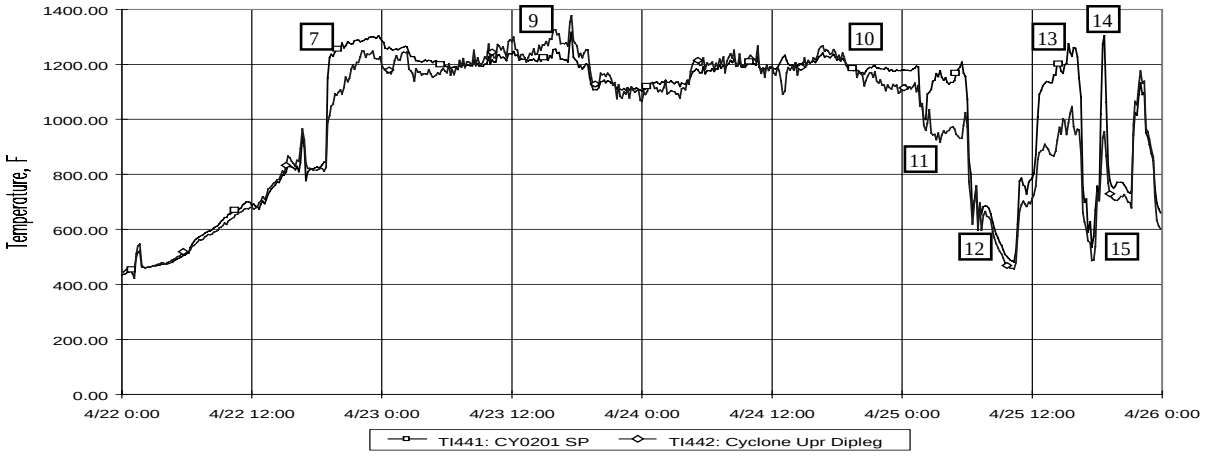

Figure 4.1.1.4-35 Cyclone Dipleg Temperatures

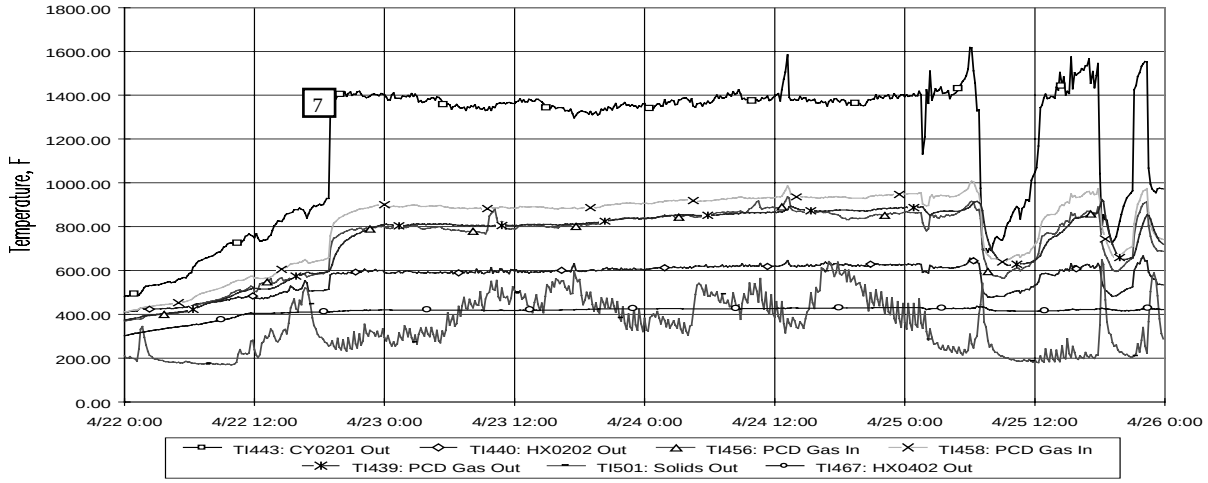

Figure 4.1.1.4-36 Temperature Profile Downstream of Reactor

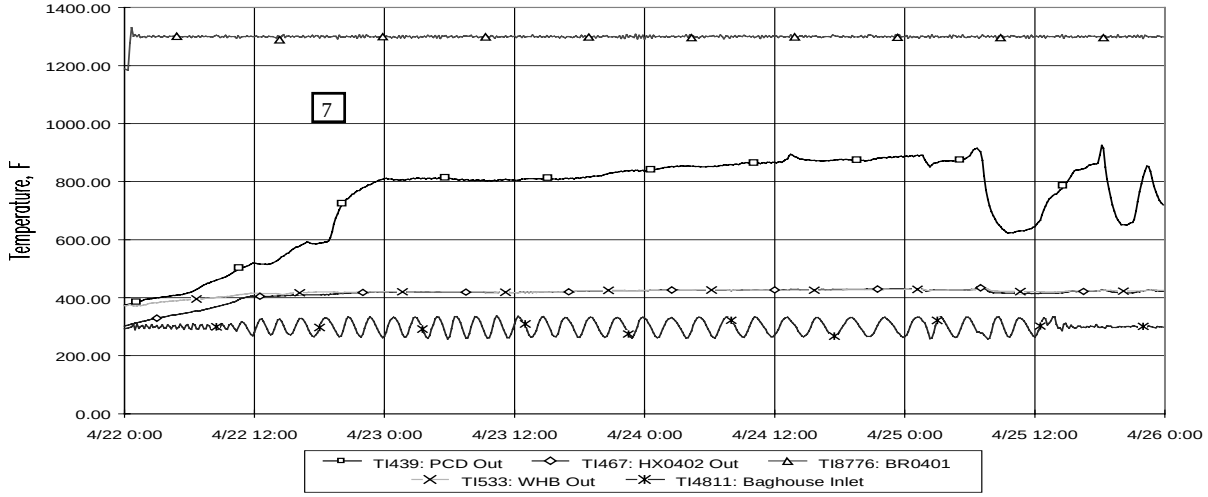

Figure 4.1.1.4-37 System Temperatures Downstream of PCD

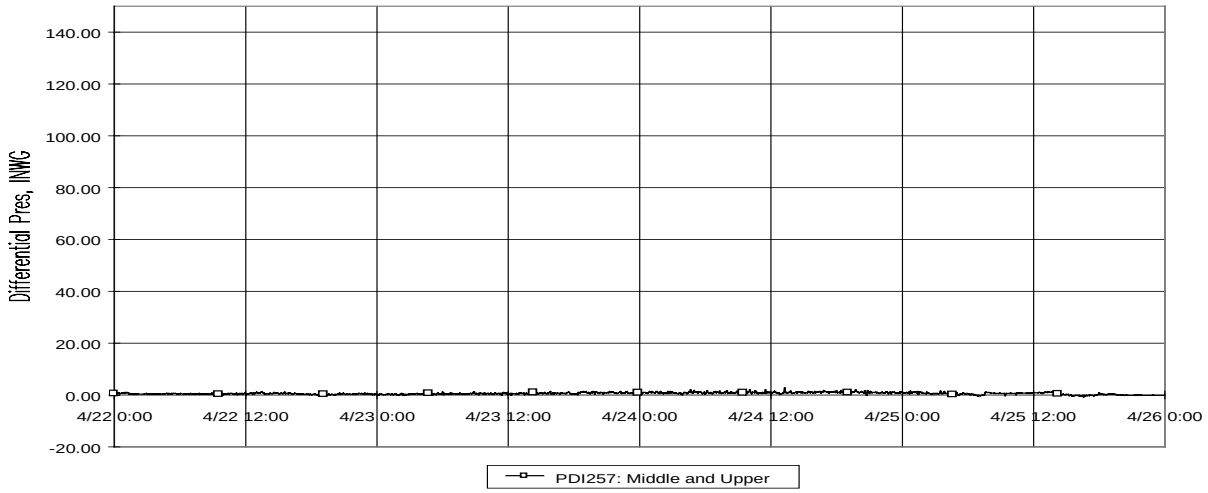

Figure 4.1.1.4-38 Mixing Zone Differential Pressure Profile

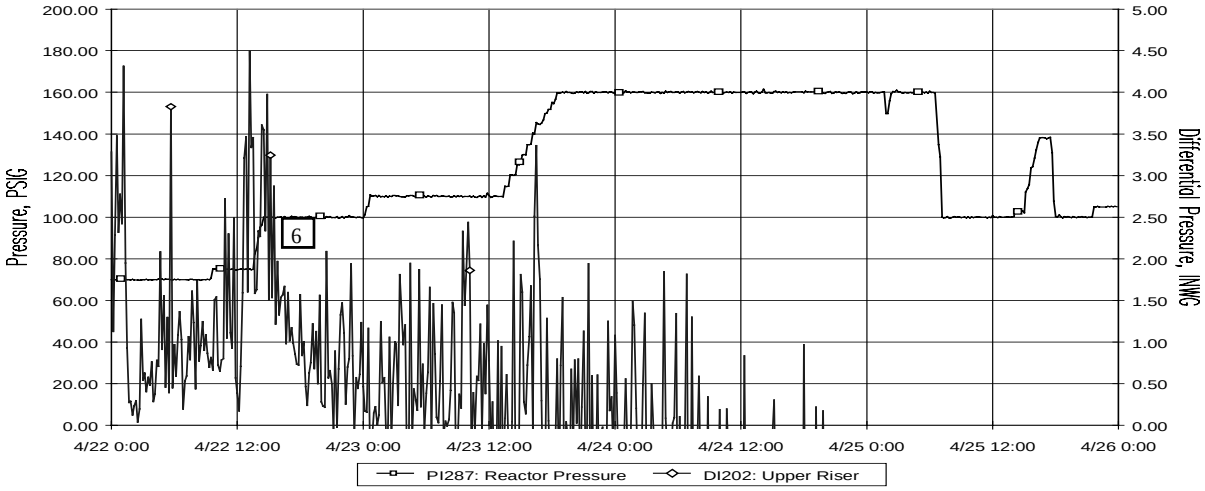

Figure 4.1.1.4-39 Reactor Pressure/Riser Differential Pressure Profiles

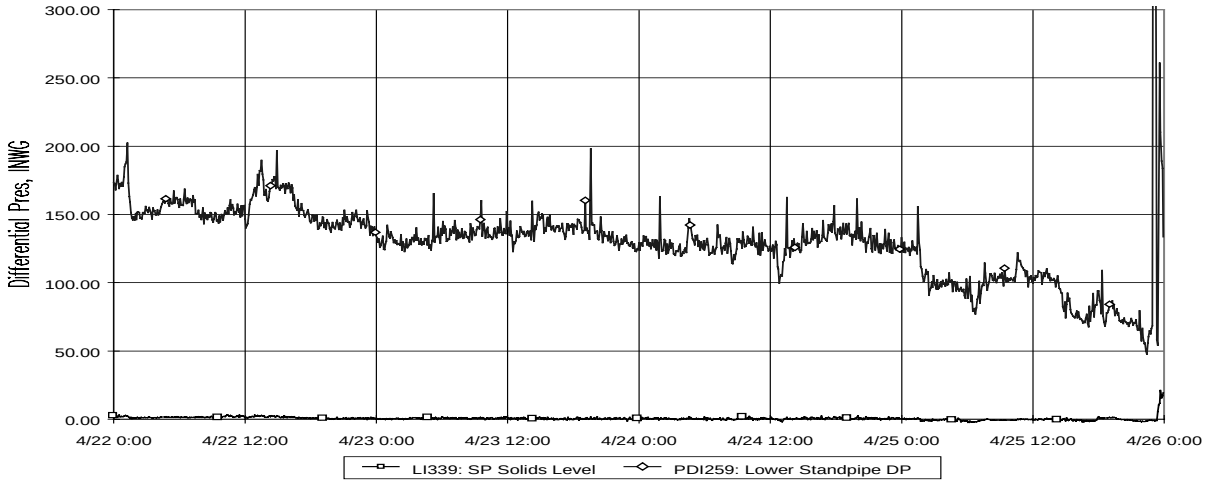

Figure 4.1.1.4-40 Standpipe Differential Pressure Profiles

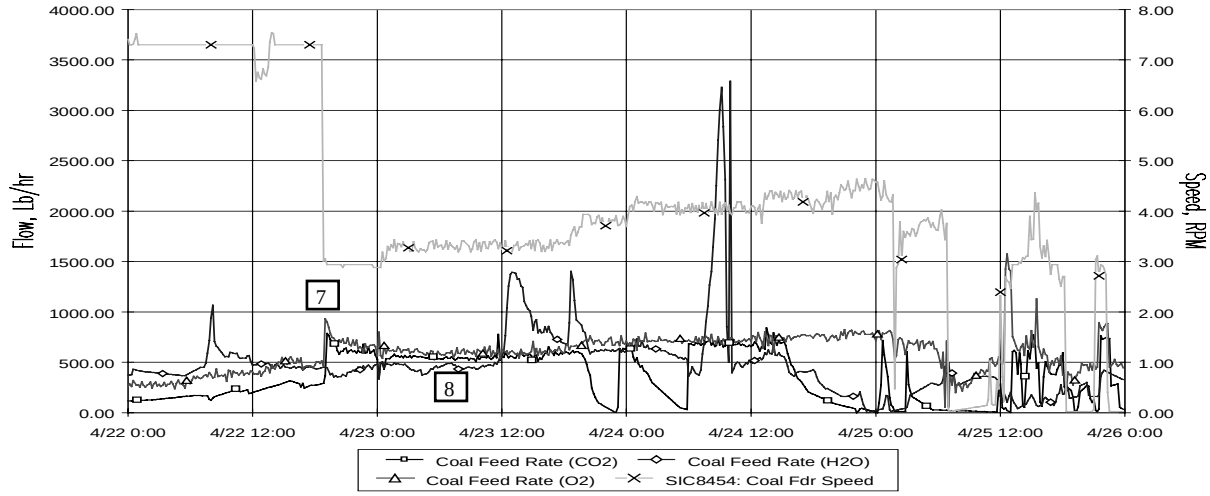

Figure 4.1.1.4-41 Coal Feed Rate Based on Gas Analysis

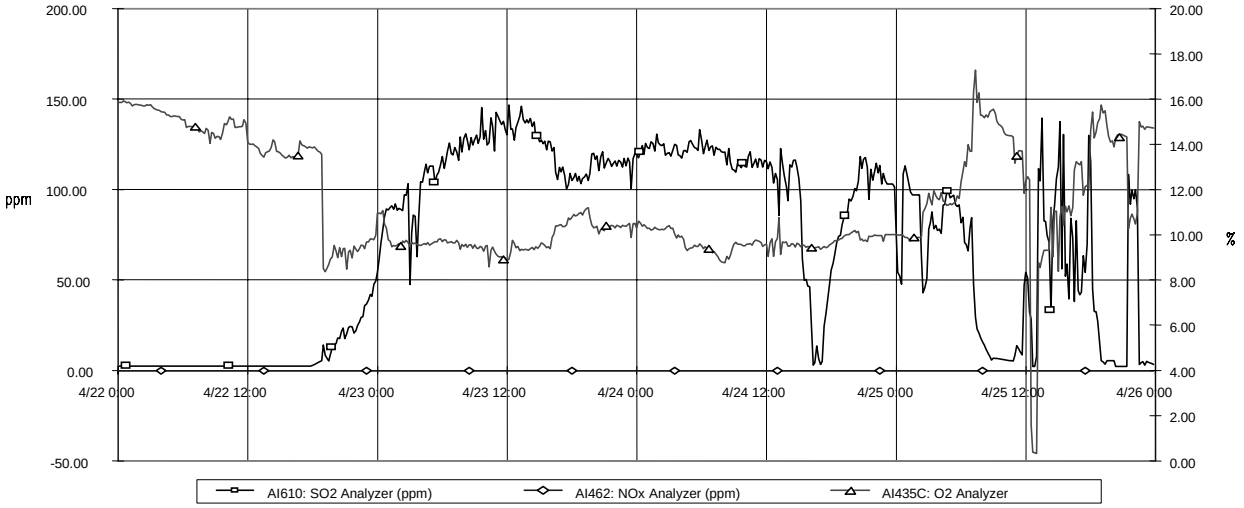

Figure 4.1.1.4-42 O_2, SO_2, and NO_x Analyzers

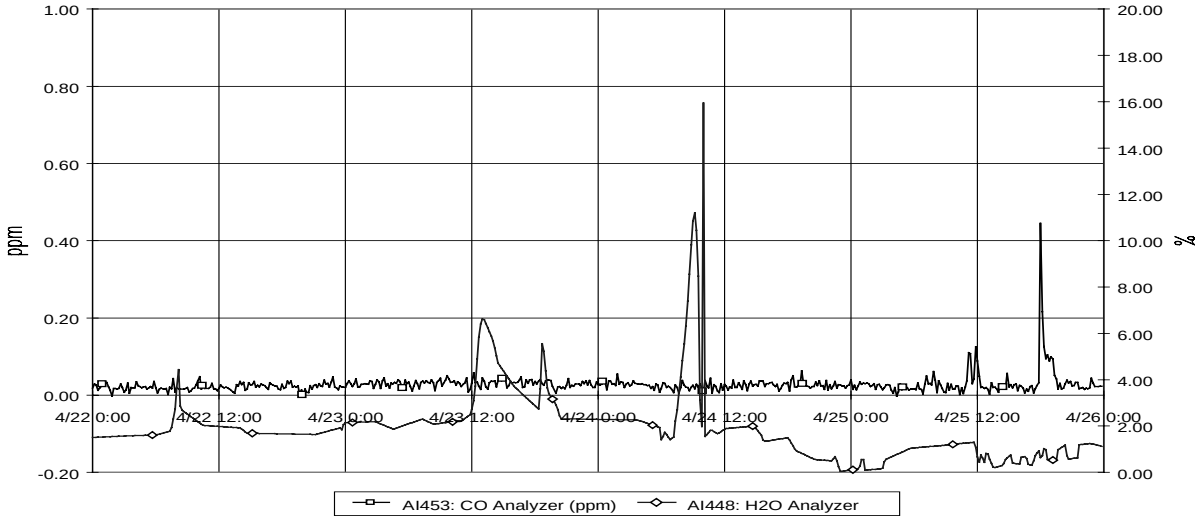

Figure 4.1.1.4-43 CO and H_2O Analyzers

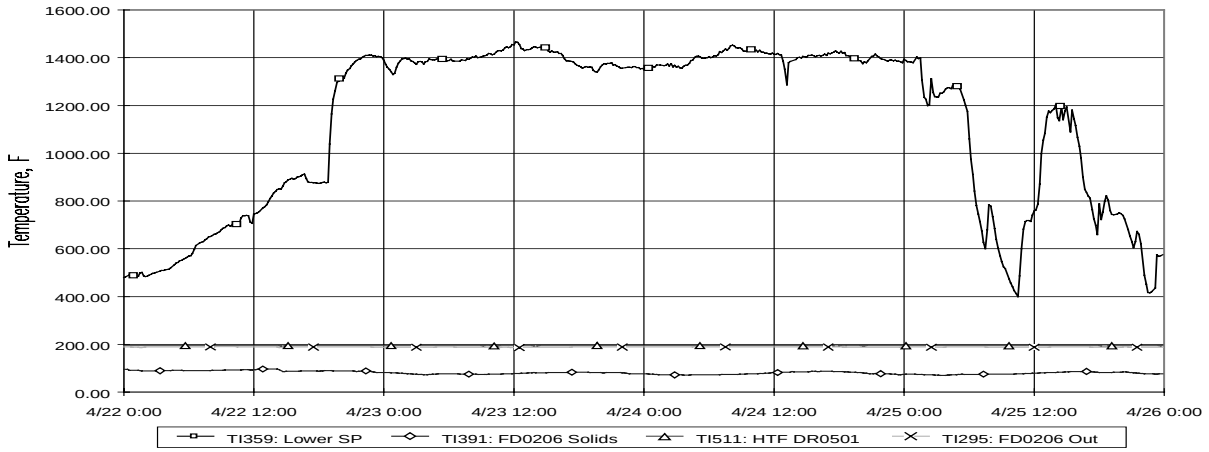

Figure 4.1.1.4-44 FD0510 Temperature Profiles

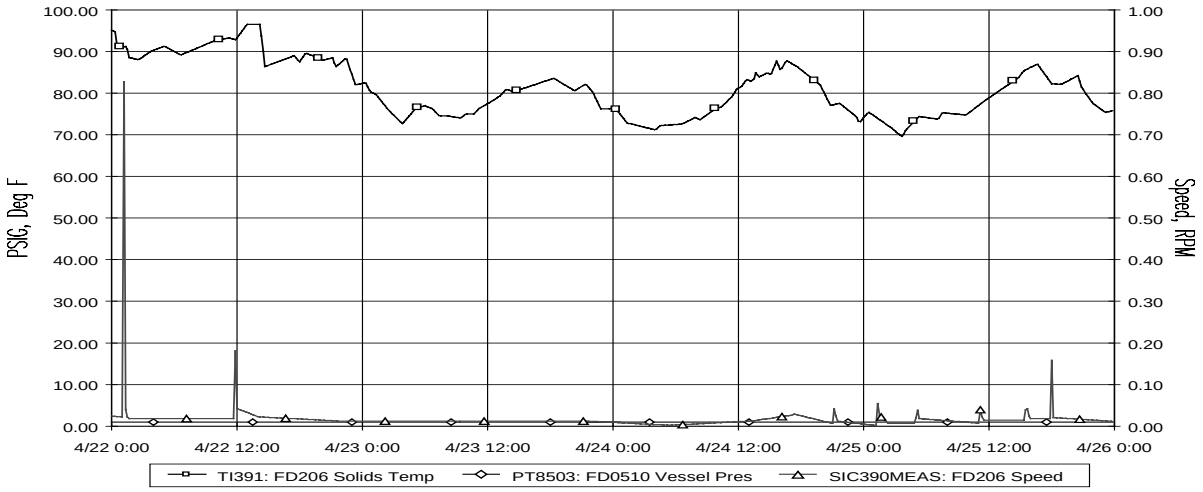

Figure 4.1.1.4-45 FD0206 Profiles

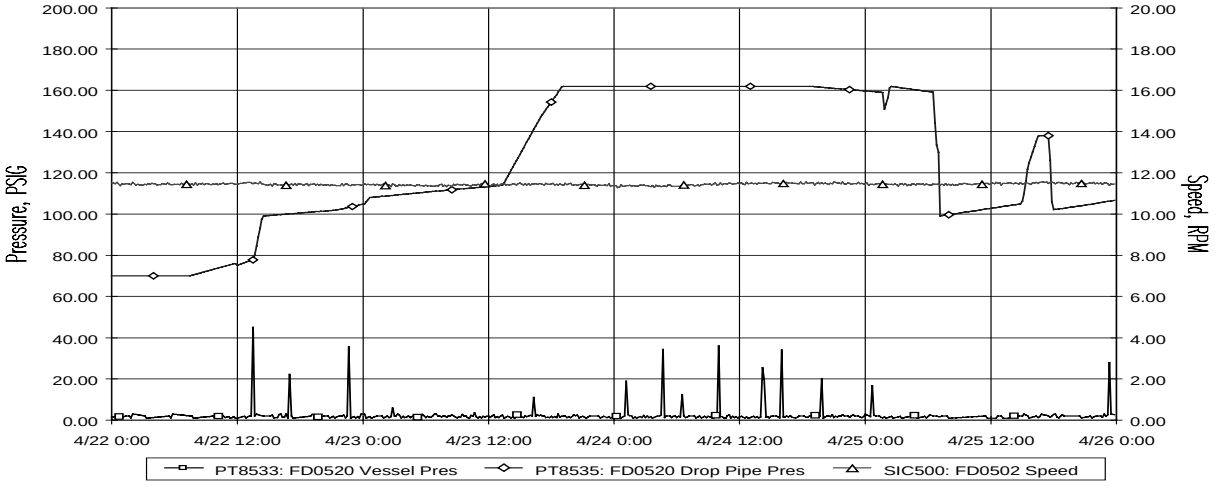

Figure 4.1.1.4-46 FD0520 Pressure Profiles

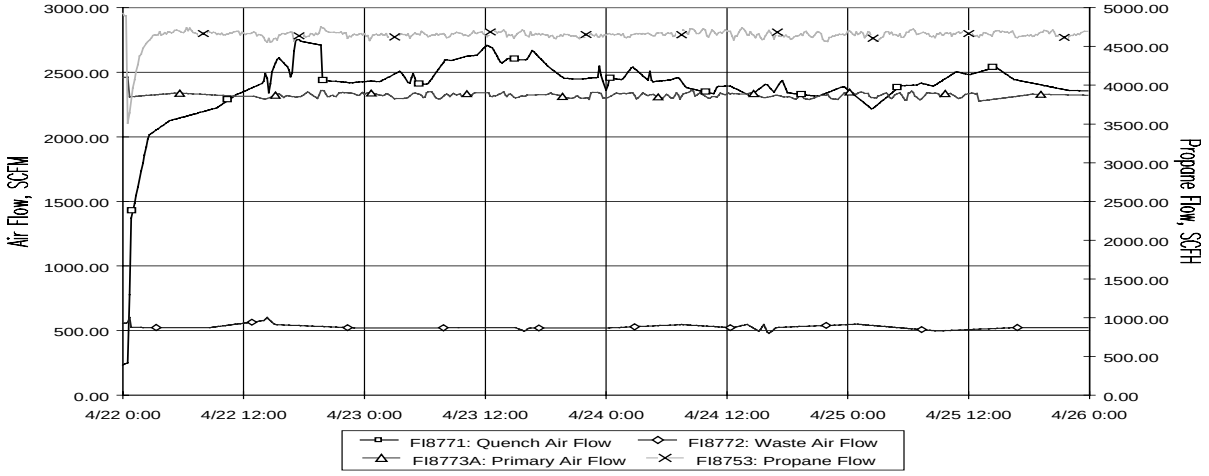

Figure 4.1.1.4-47 Thermal Oxidizer Air/Fuel Flow

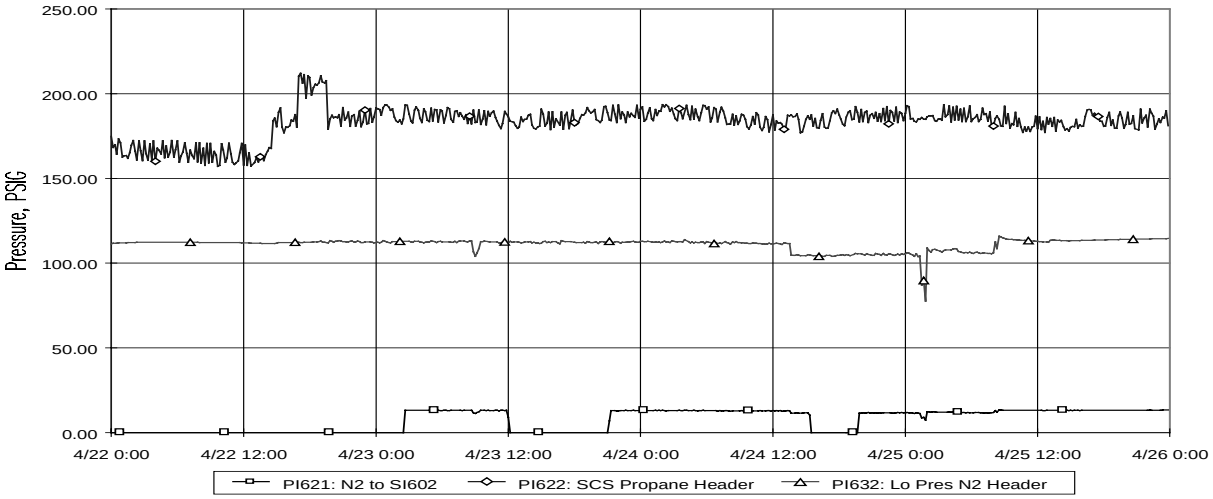

Figure 4.1.1.4-48 Nitrogen/Propane Header Pressure Profiles

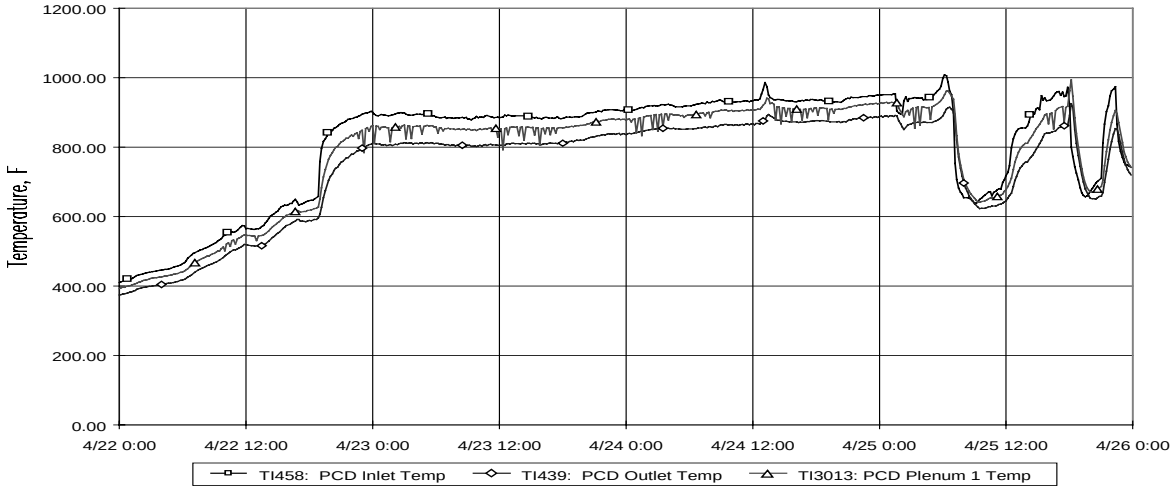

Figure 4.1.1.4-49 PCD Temperatures

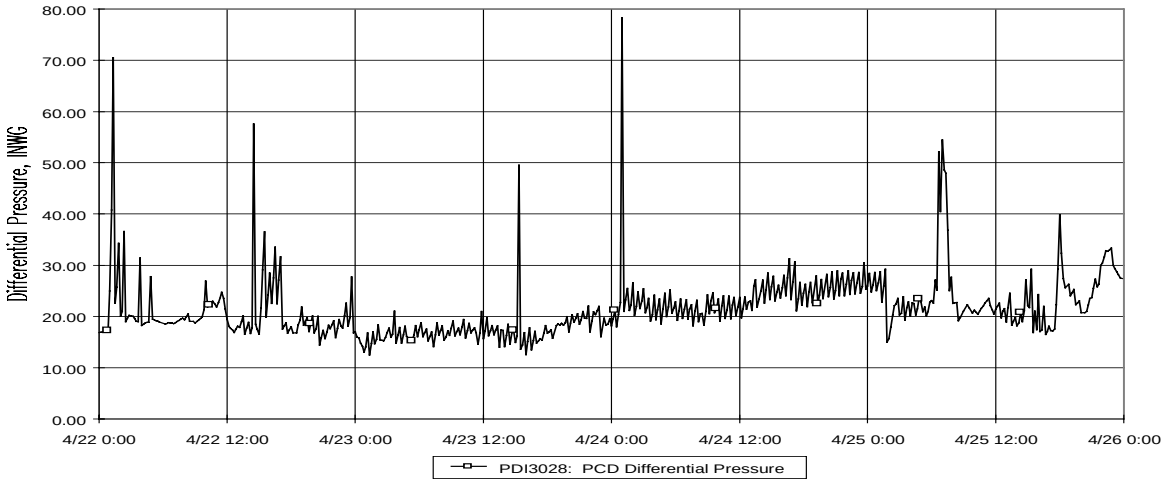

Figure 4.1.1.4-50 PCD Differential Pressure Profile

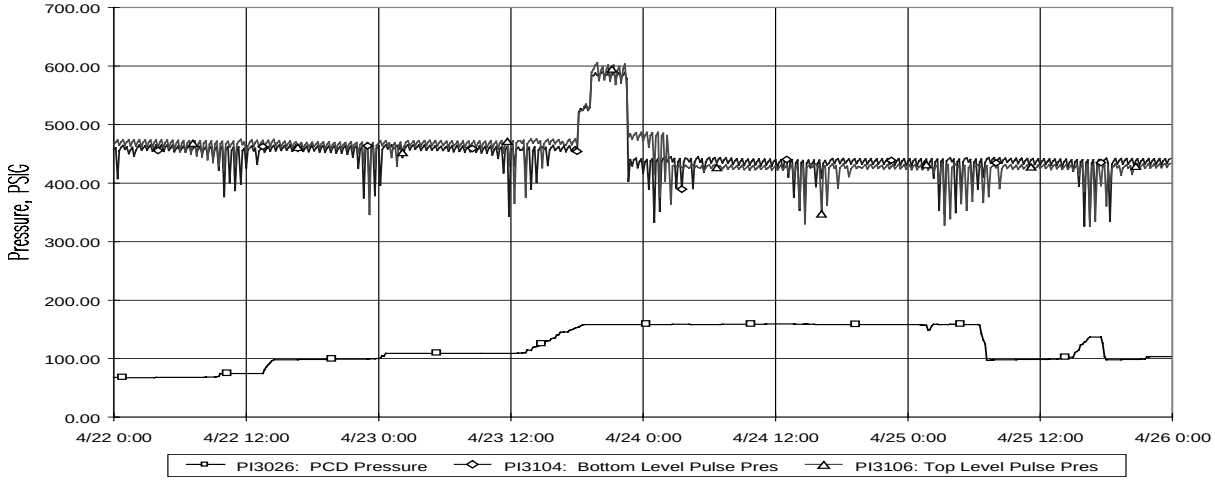

Figure 4.1.1.4-51 PCD Pressure and Pulse Pressure

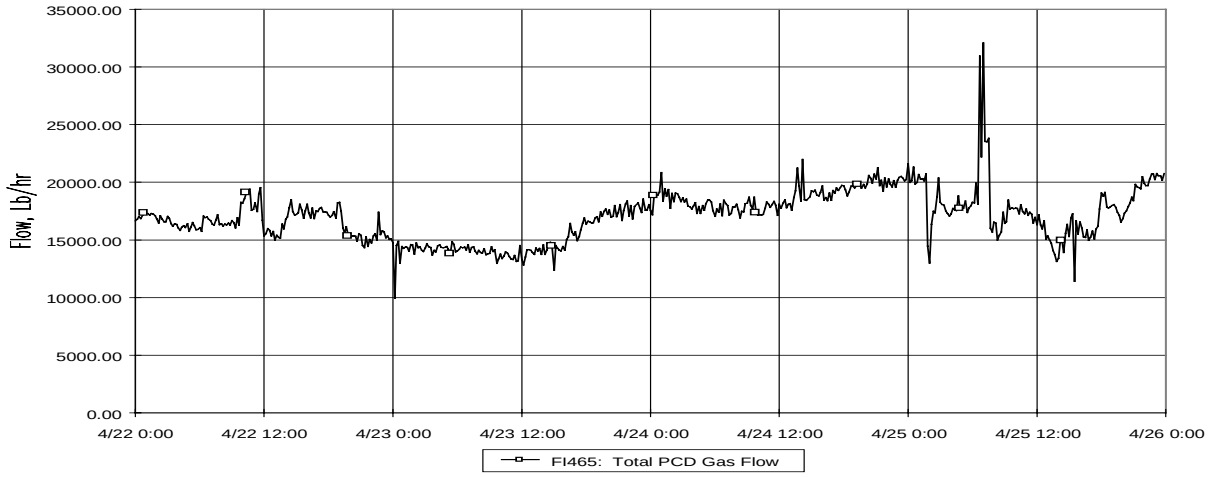

Figure 4.1.1.4-52 Gas Flow through PCD

Section 4.1.1.4

Graphs 53 through 78

Test Run CCT4D

April 26 through April 29, 1997

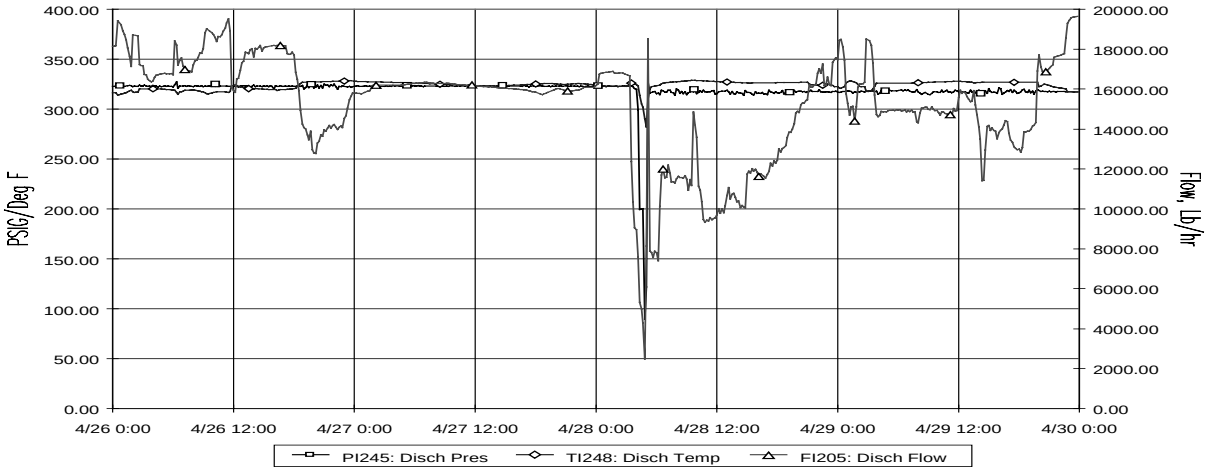

Figure 4.1.1.4-53 CO0201 System Profile

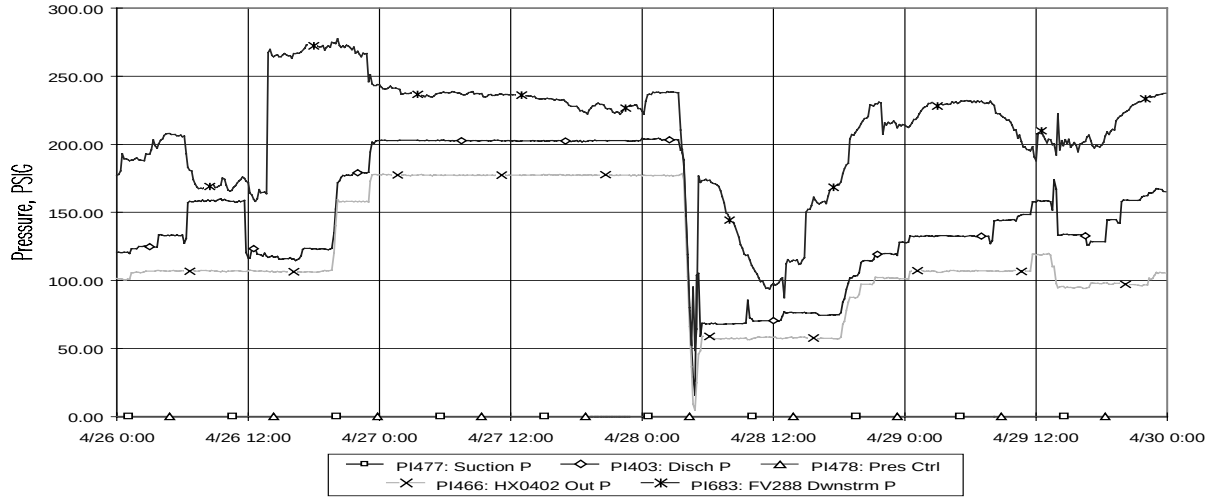

Figure 4.1.1.4-54 Recycle Gas System Pressure Profiles

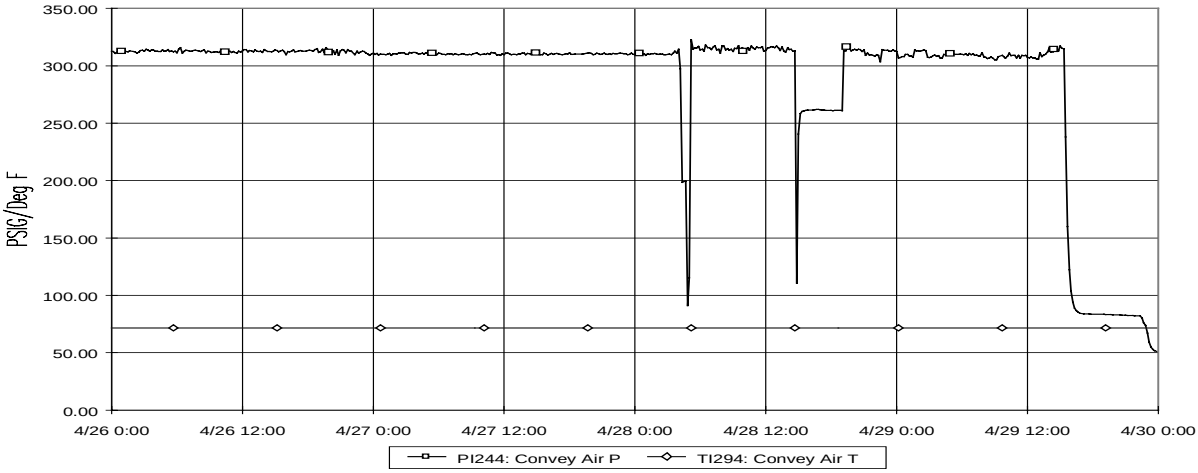

Figure 4.1.1.4-55 Transport Air System Profile

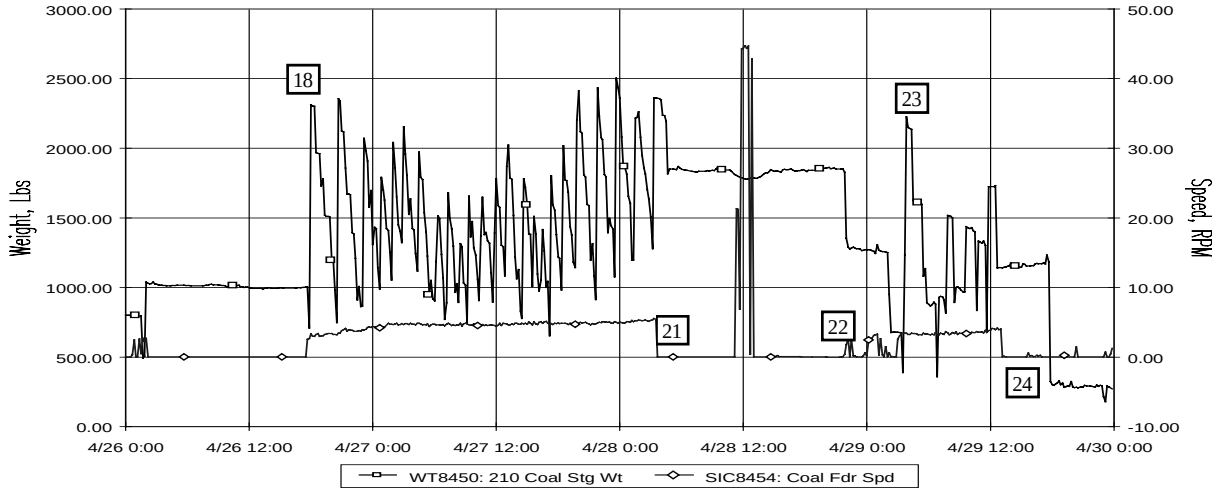

Figure 4.1.1.4-56 Coal Feeder System Profile

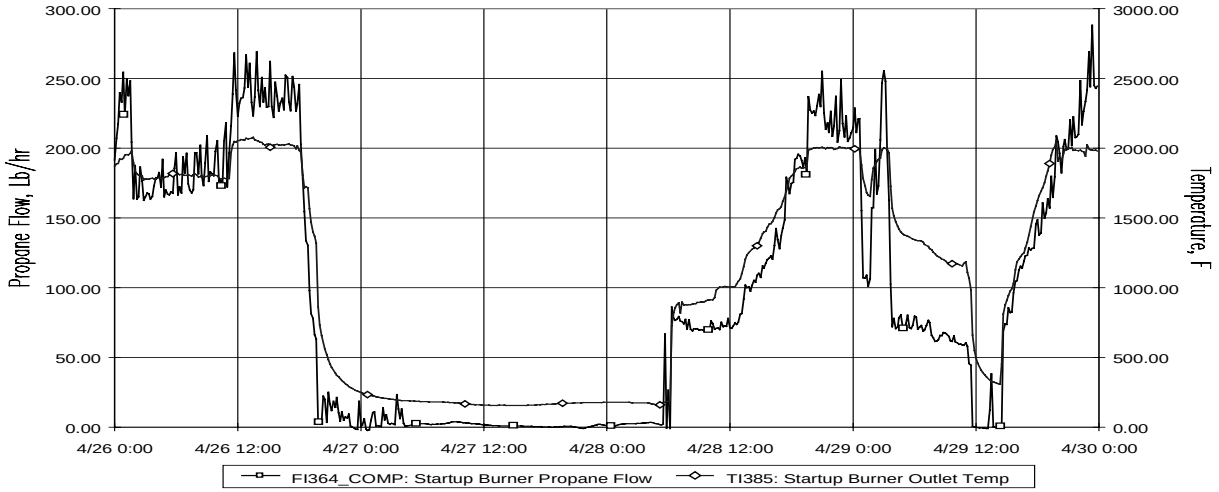

Figure 4.1.1.4-57 Start-Up Burner Flow/Temperature

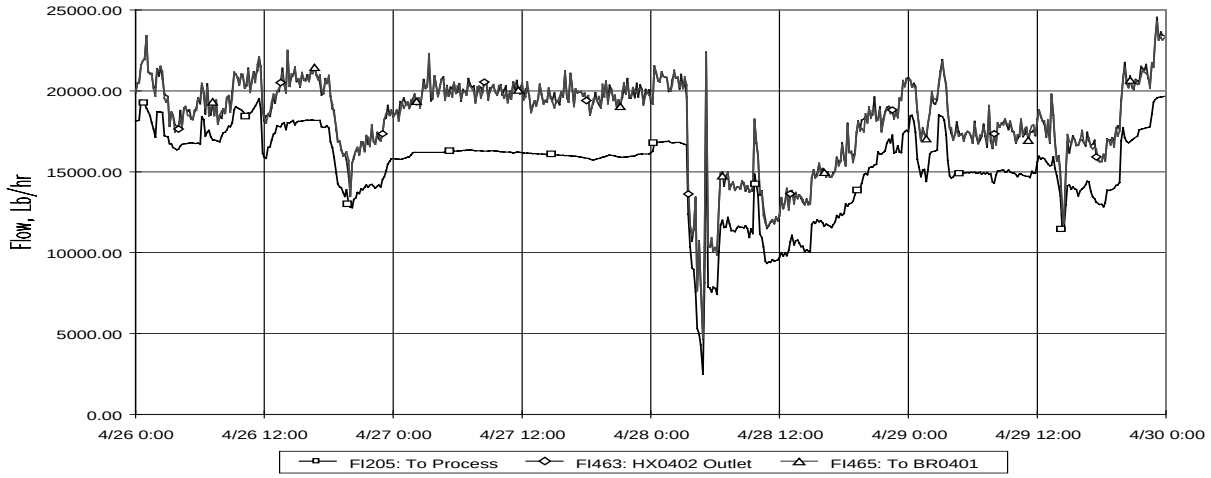

Figure 4.1.1.4-58 Total Gas In/Out Flow Rates

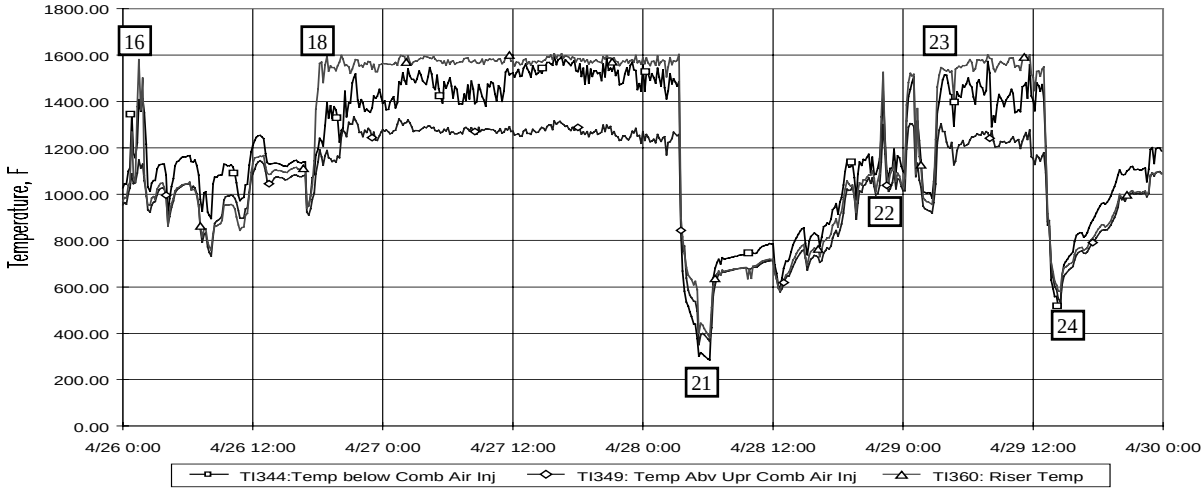

Figure 4.1.1.4-59 Reactor Mixing Zone and Riser Temperatures

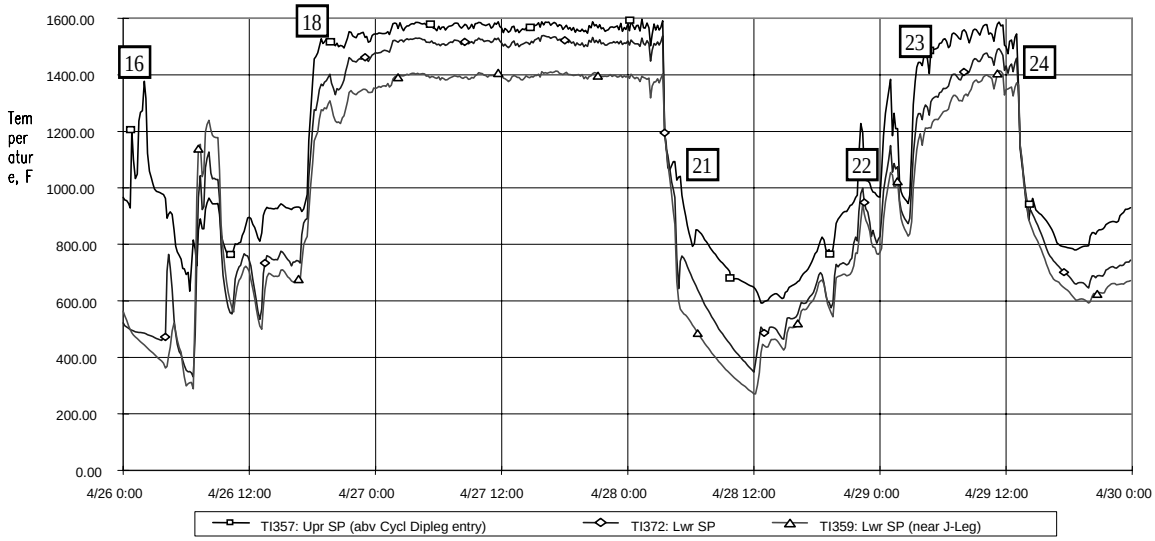

Figure 4.1.1.4-60 Standpipe Temperatures

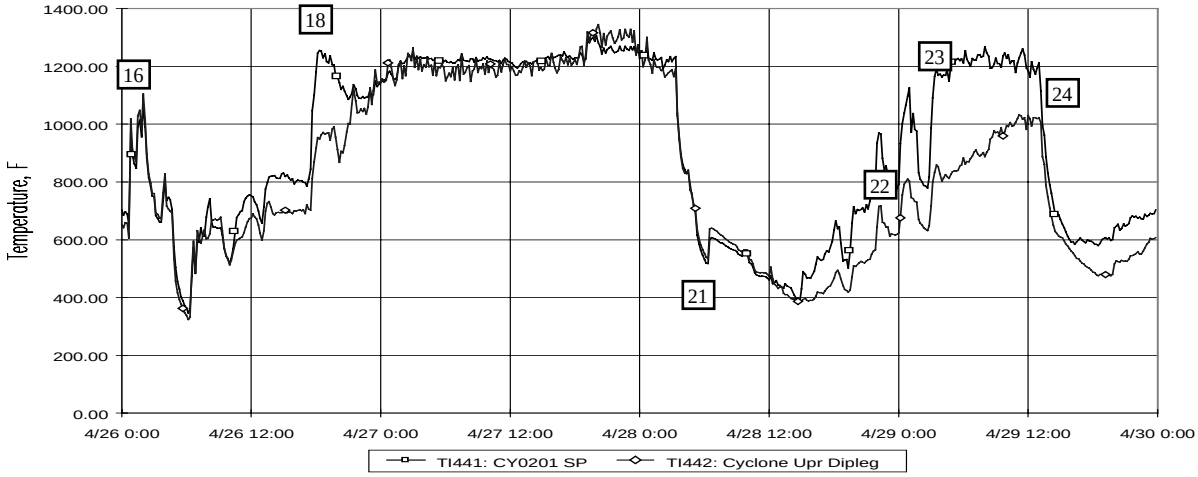

Figure 4.1.1.4-61 Cyclone Dipleg Temperatures

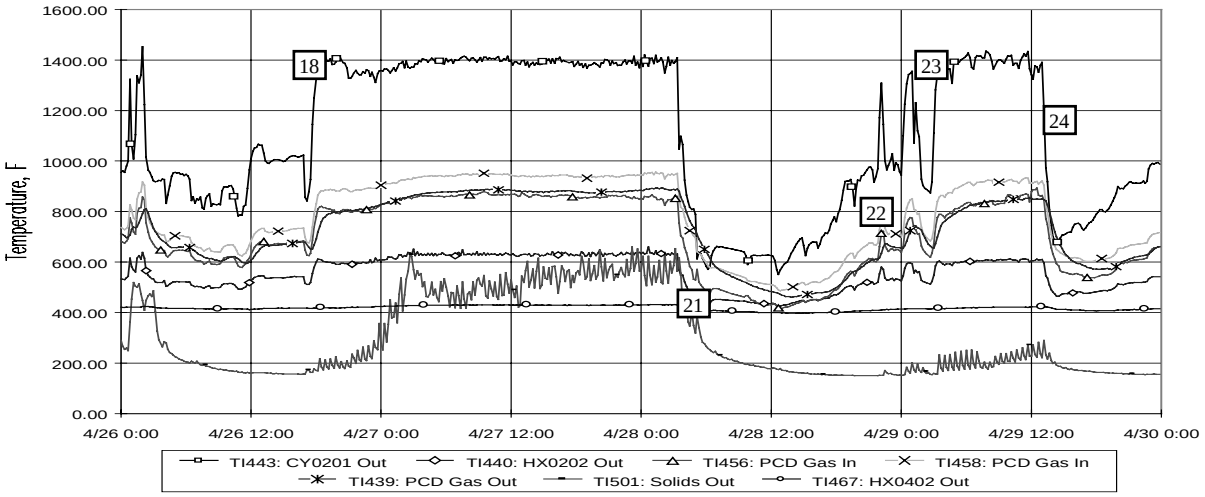

Figure 4.1.1.4-62 Temperature Profile Downstream of Reactor

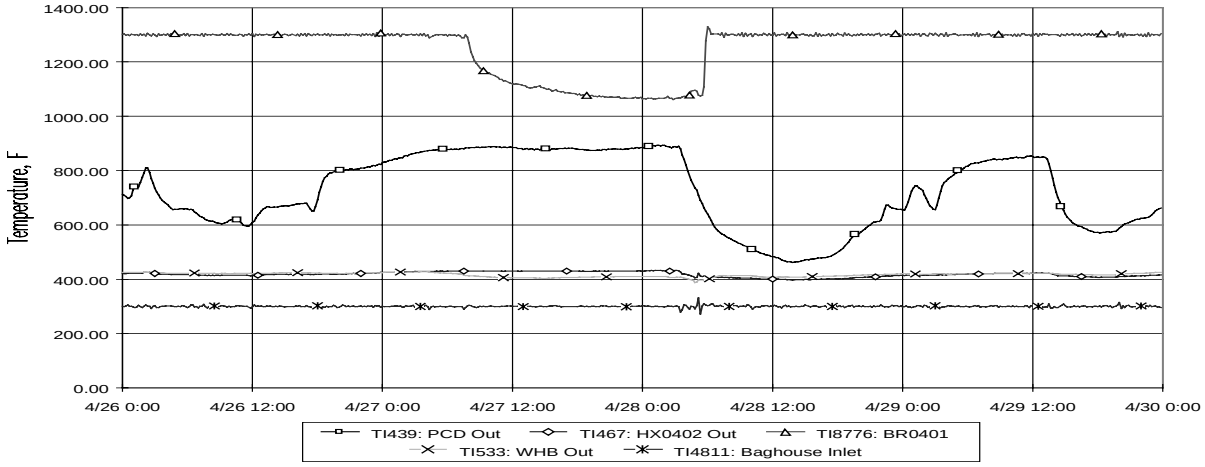

Figure 4.1.1.4-63 System Temperatures Downstream of PCD

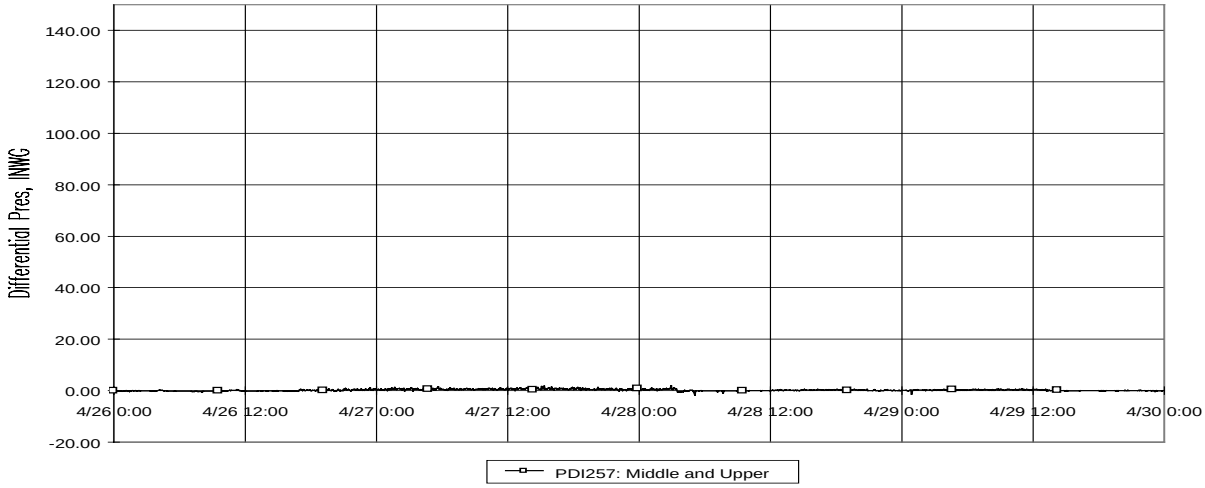

Figure 4.1.1.4-64 Mixing Zone Differential Pressure Profile

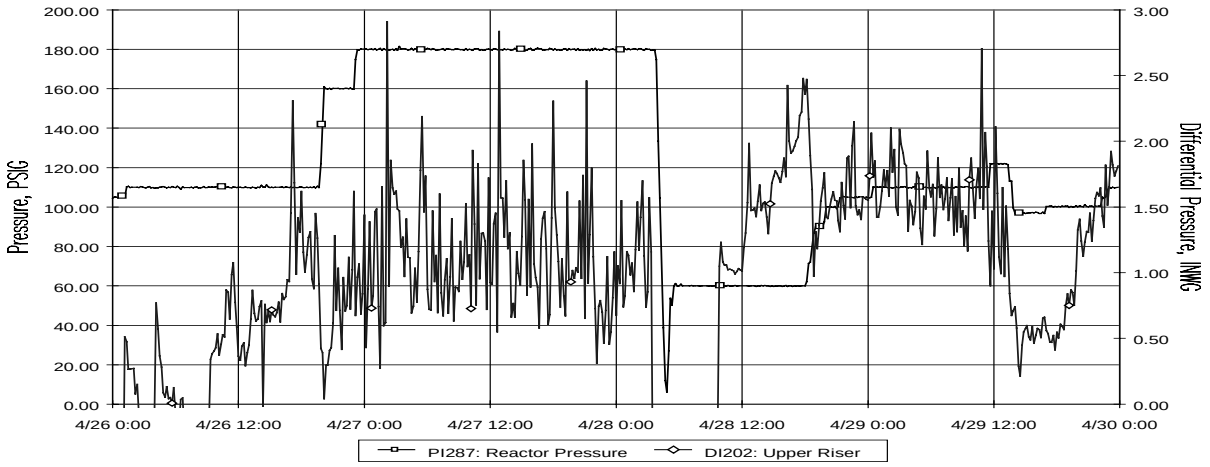

Figure 4.1.1.4-65 Reactor Pressure/Riser Differential Pressure Profiles

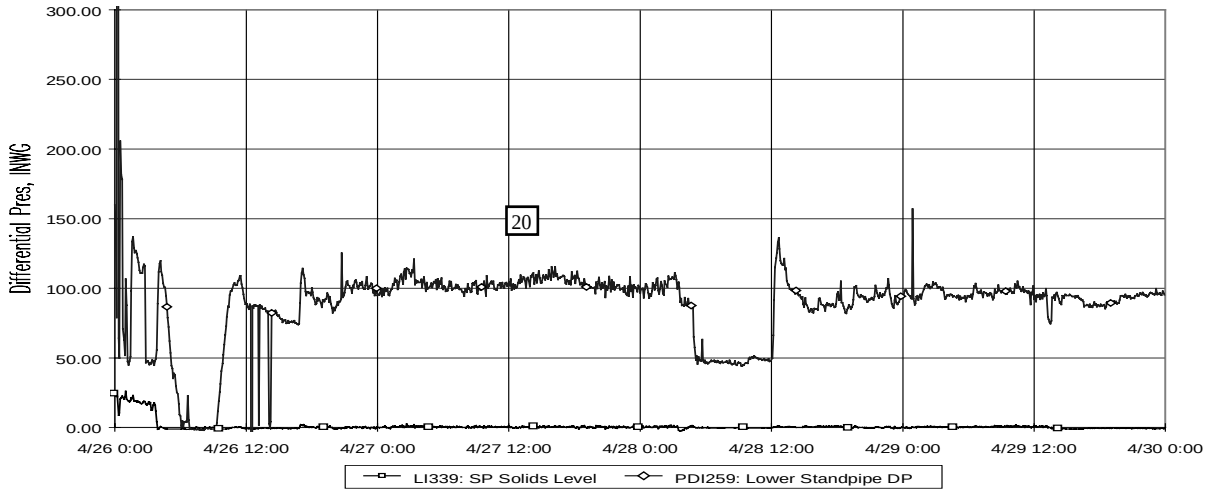

Figure 4.1.1.4-66 Standpipe Differential Pressure Profiles

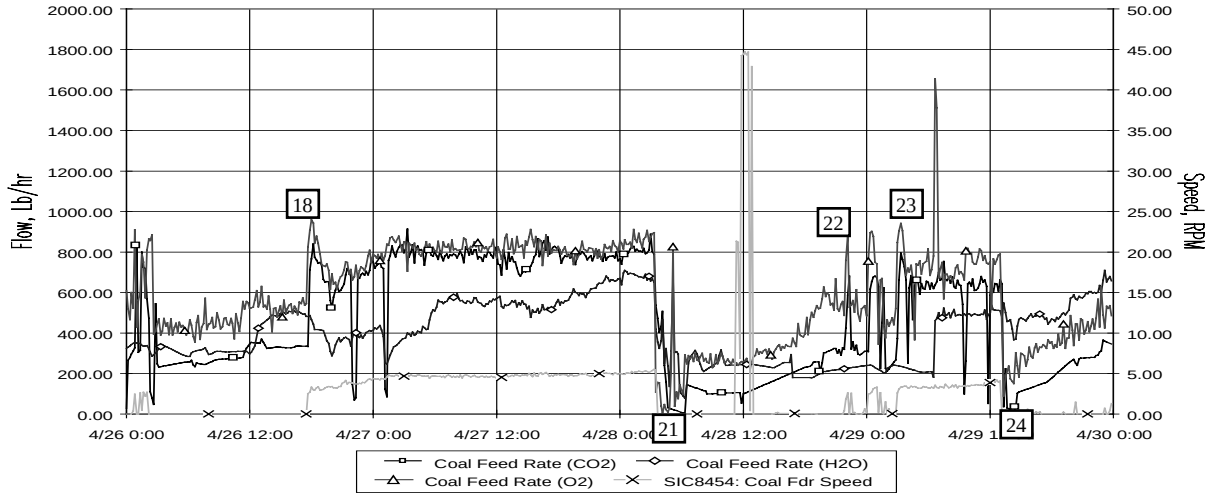

Figure 4.1.1.4-67 Coal Feed Rate Based on Gas Analysis

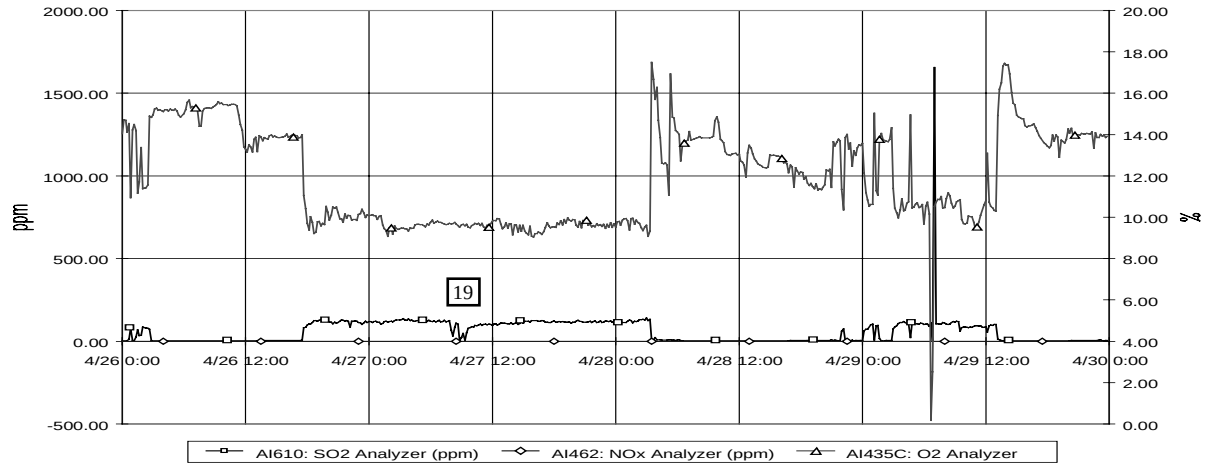

Figure 4.1.1.4-68 O_2, SO_2, and NO_x Analyzers

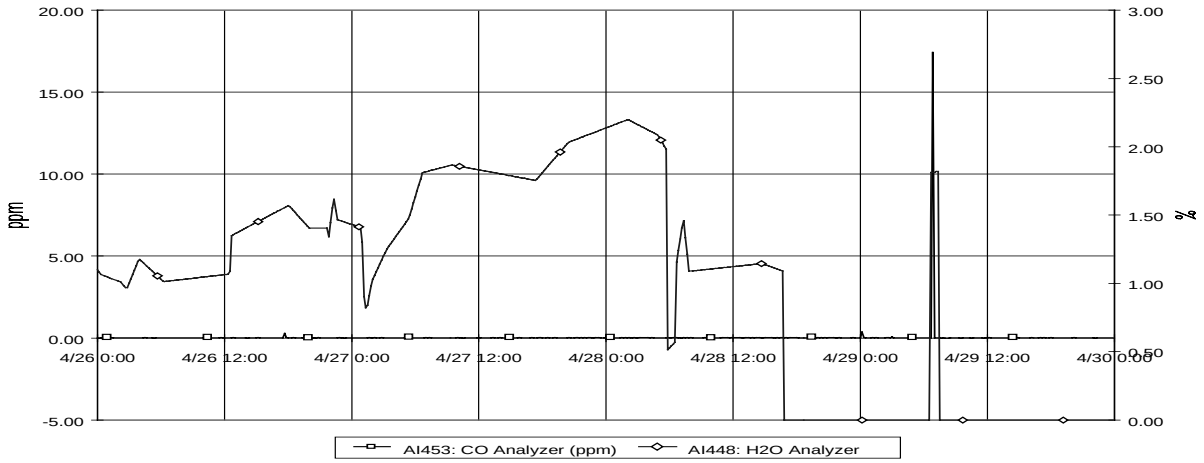

Figure 4.1.1.4-69 CO and H_2O Analyzers

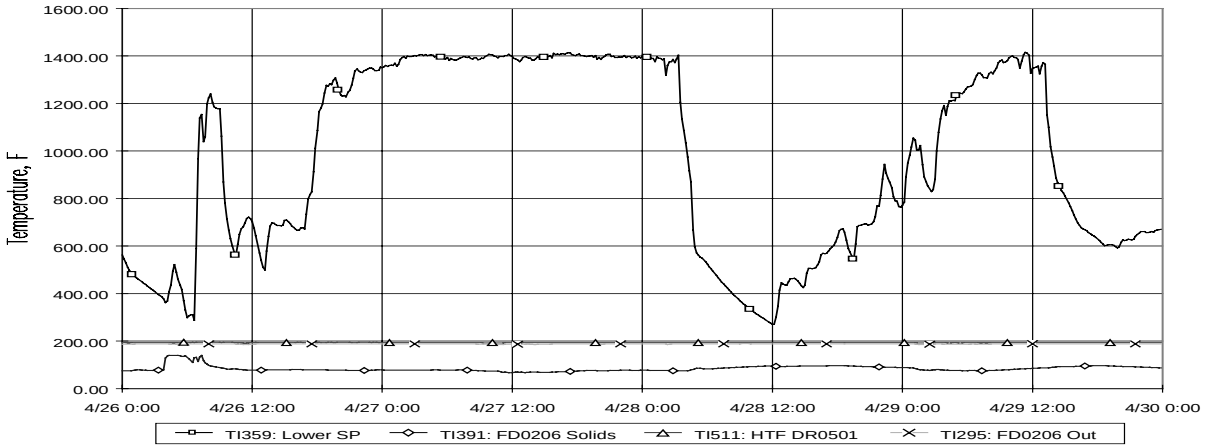

Figure 4.1.1.4-70 FD0510 Temperature Profiles

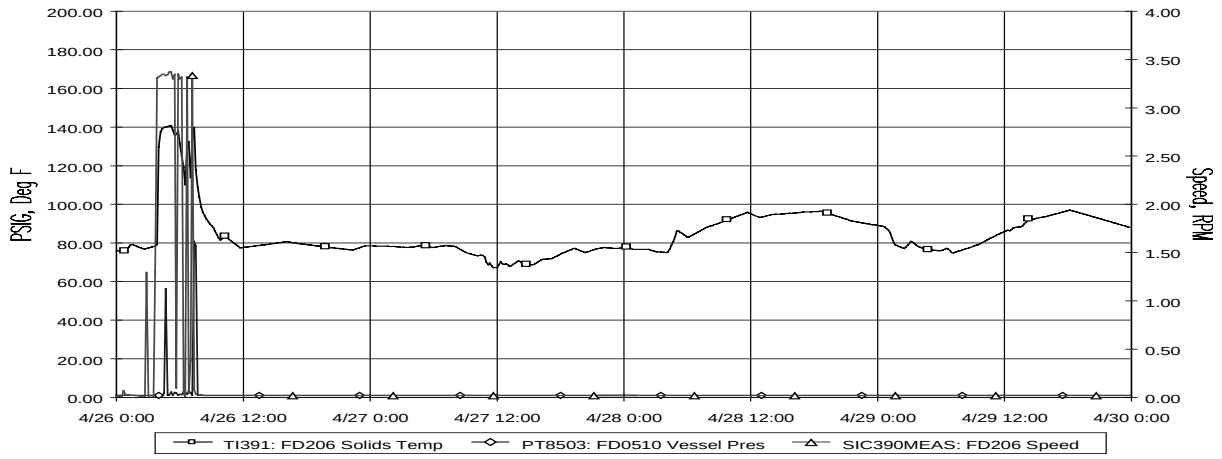

Figure 4.1.1.4-71 FD0206 Profiles

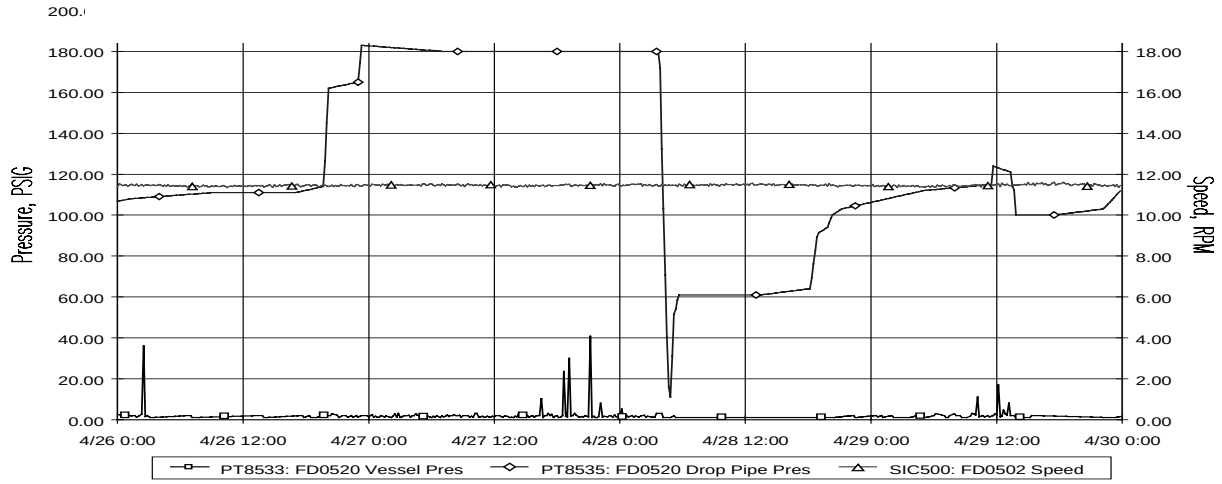

Figure 4.1.1.4-72 FD0520 Pressure Profiles

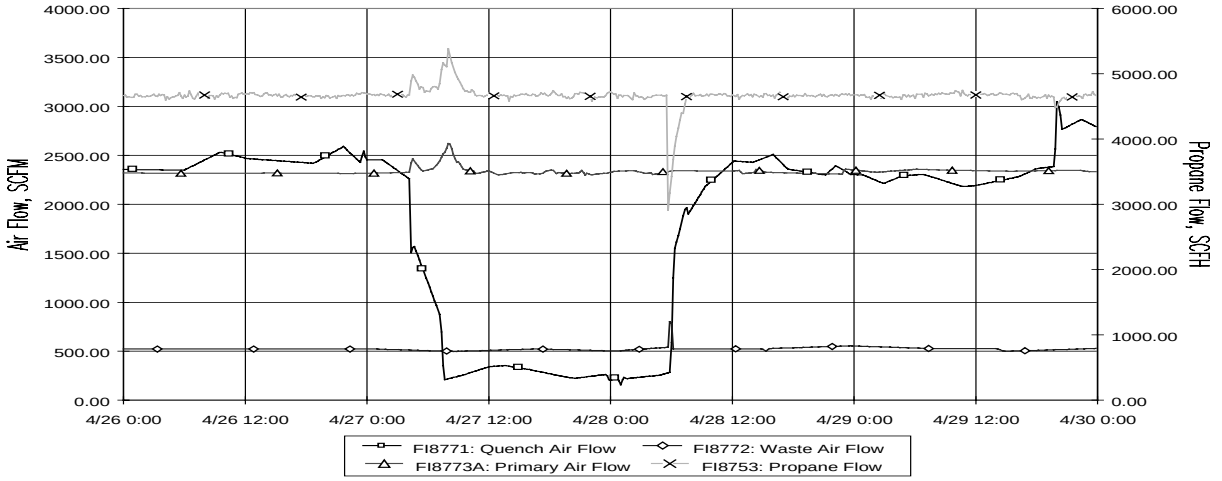

Figure 4.1.1.4-73 Thermal Oxidizer Air/Fuel Flow

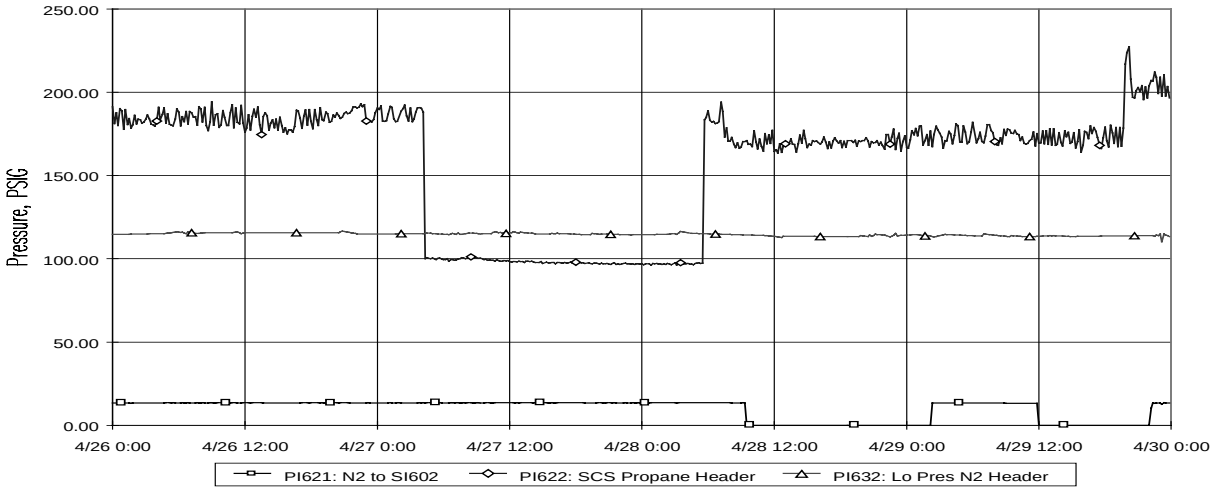

Figure 4.1.1.4-74 Nitrogen/Propane Header Pressure Profiles

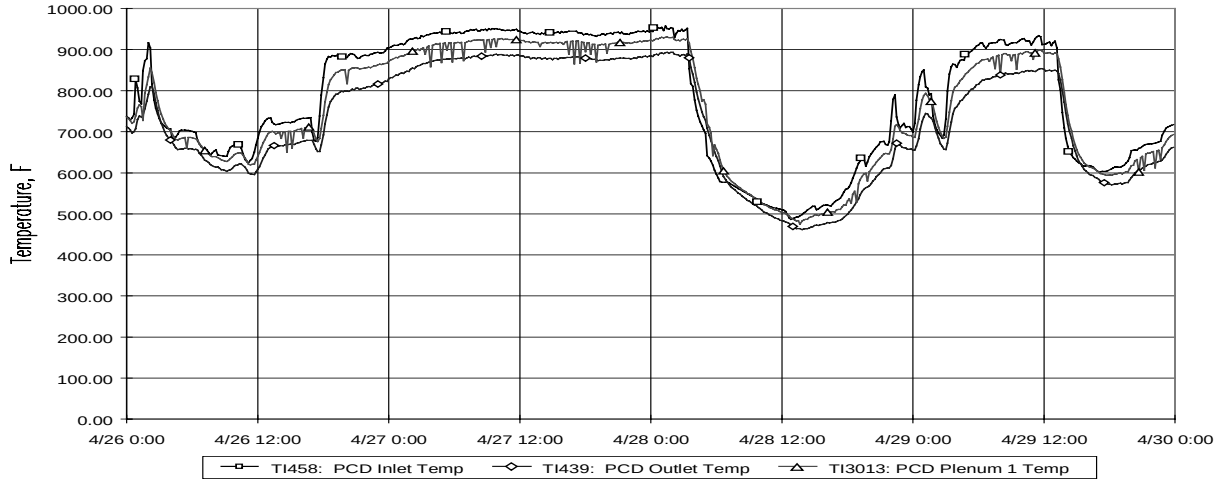

Figure 4.1.1.4-75 PCD Temperatures

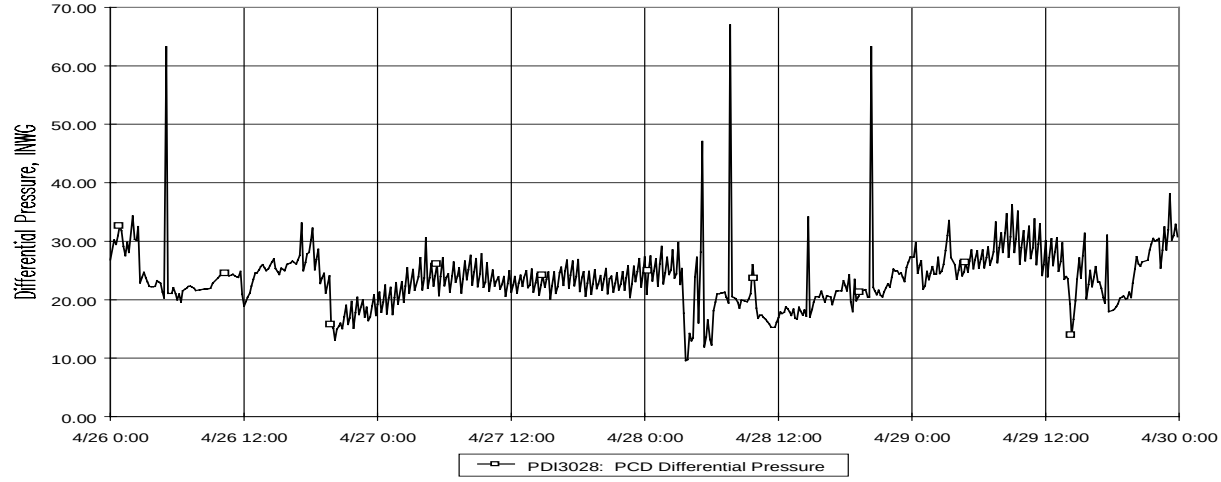

Figure 4.1.1.4-76 PCD Differential Pressure Profile

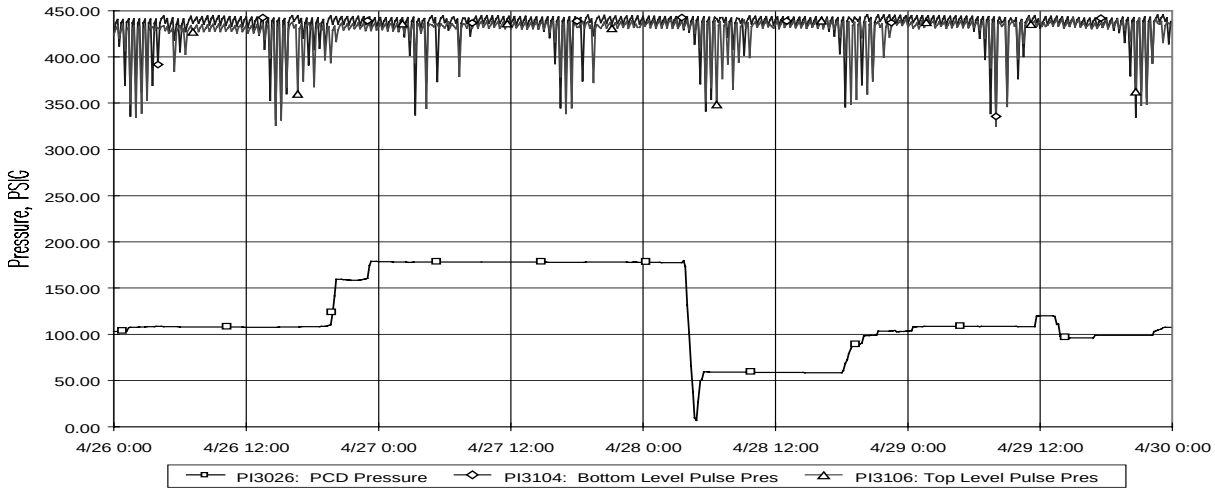

Figure 4.1.1.4-77 PCD Pressure and Pulse Pressure

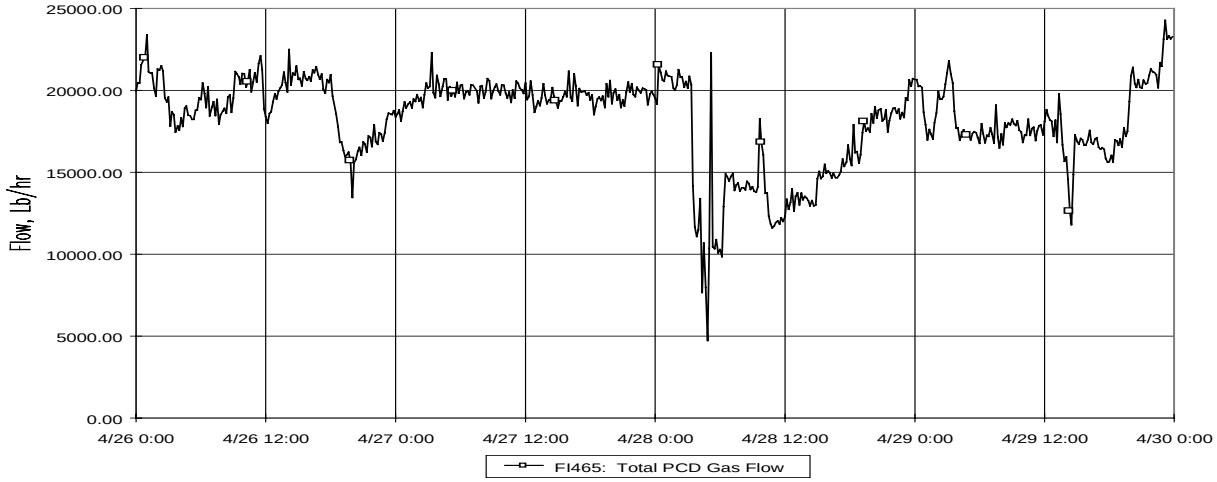

Figure 4.1.1.4-78 Gas Flow Through PCD

Section 4.1.1.4

Graphs 79 through 104

Test Run CCT4D

April 30 through May 3, 1997

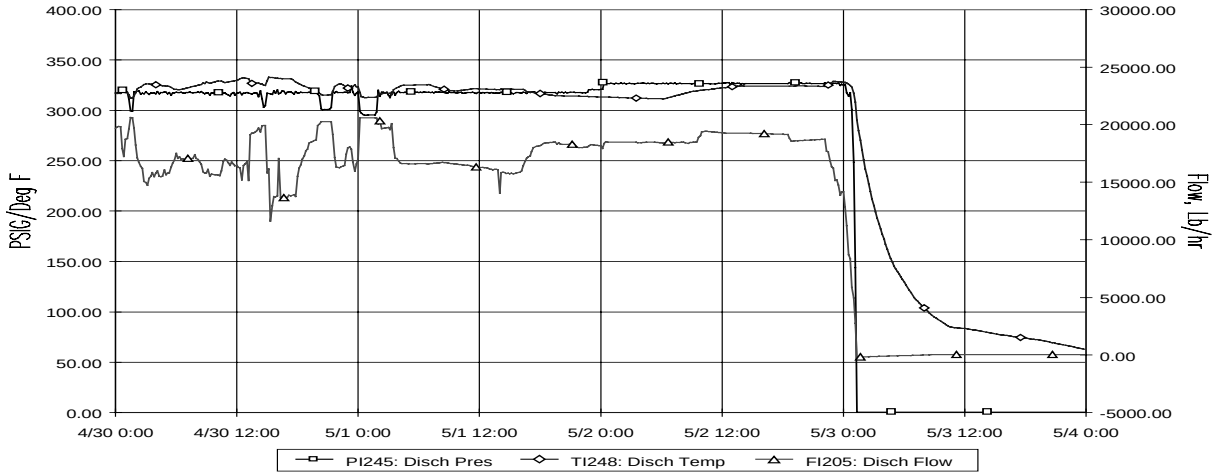

Figure 4.1.1.4-79 CO0201 System Profile

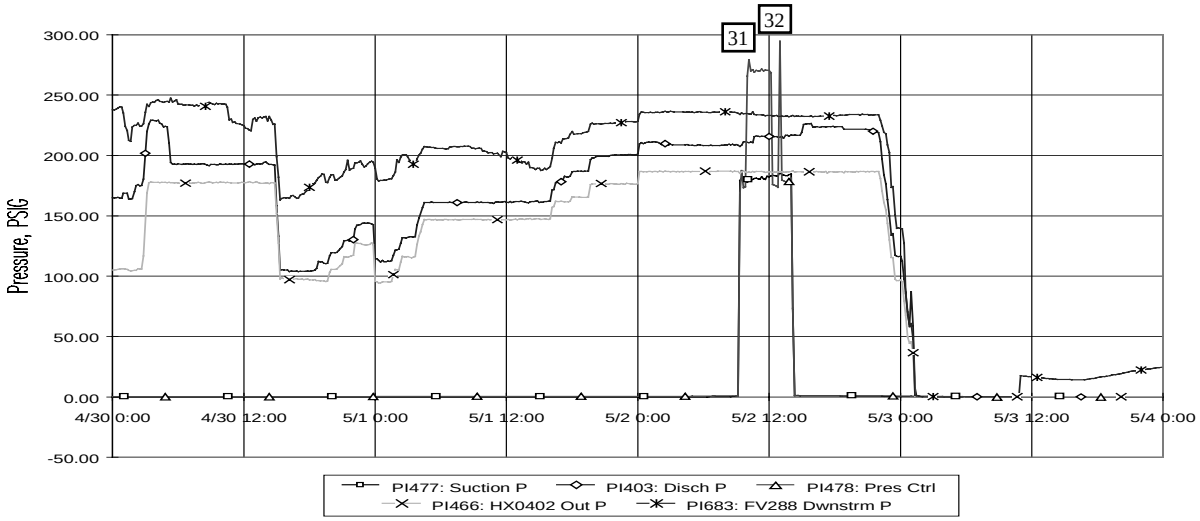

Figure 4.1.1.4-80 Recycle Gas System Pressure Profiles

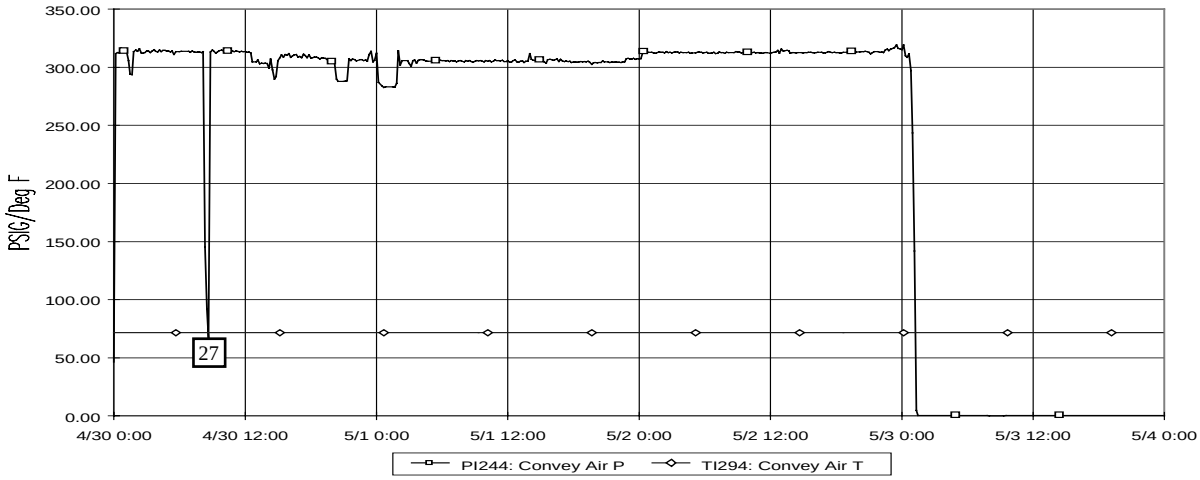

Figure 4.1.1.4-81 Transport Air System Profile

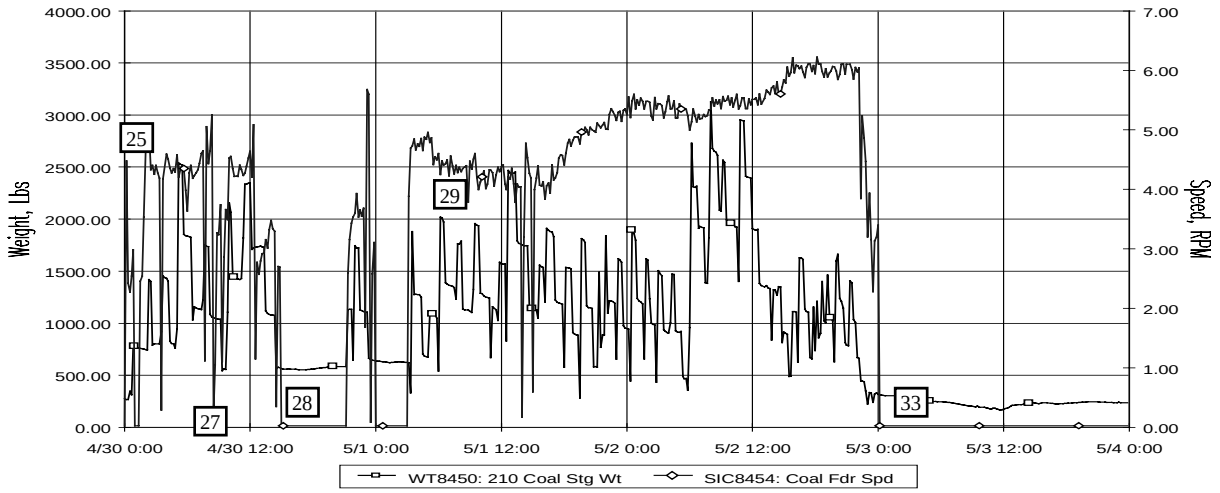

Figure 4.1.1.4-82 Coal Feeder System Profile

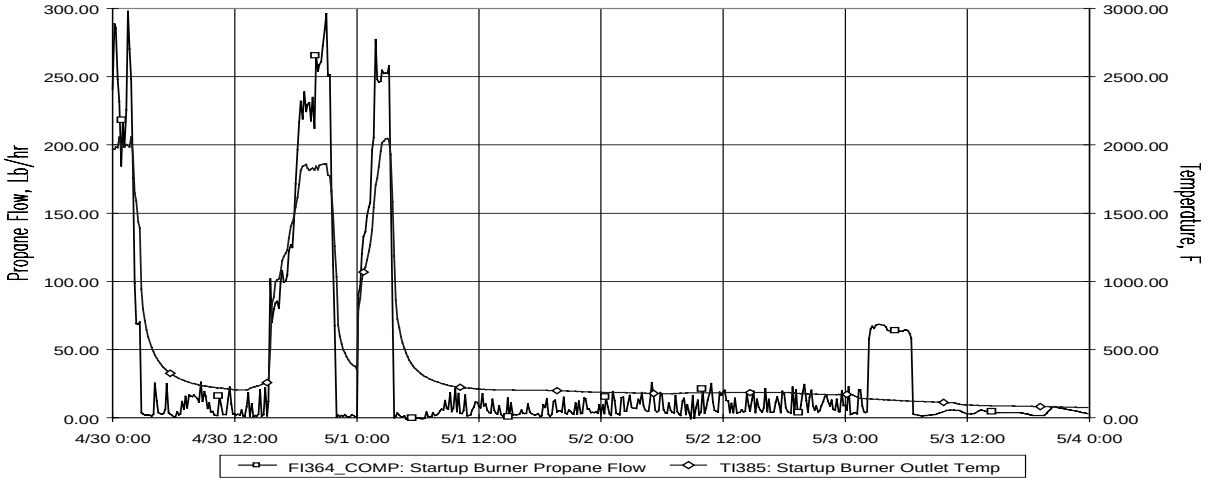

Figure 4.1.1.4-83 Start-Up Burner Flow/Temperature

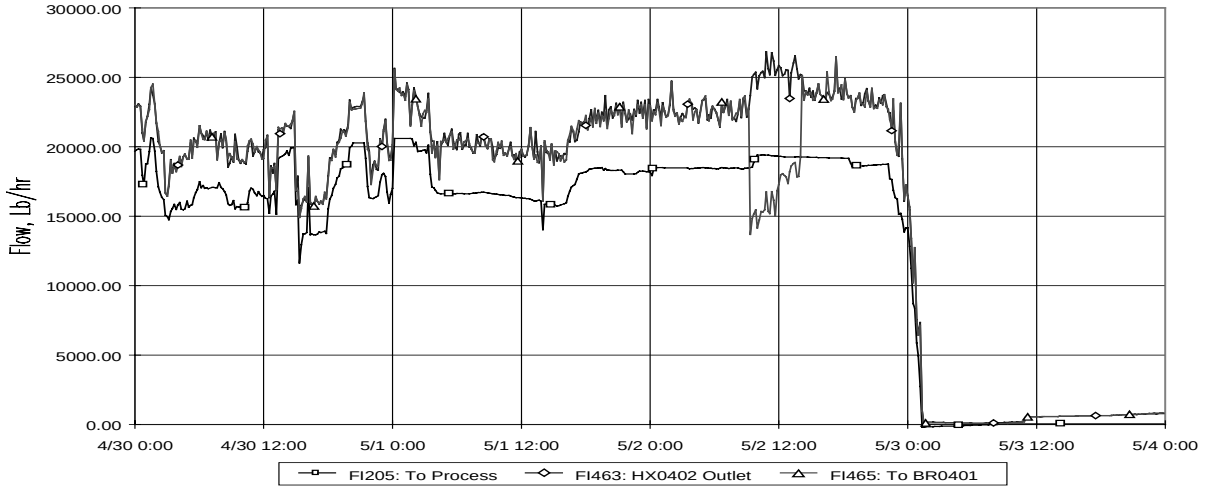

Figure 4.1.1.4-84 Total Gas In/Out Flow Rates

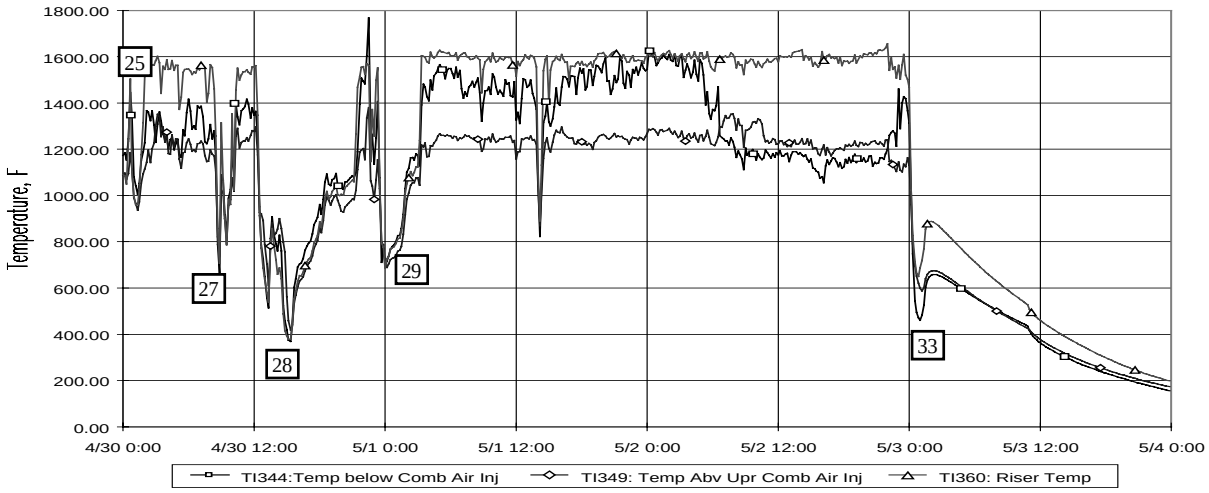

Figure 4.1.1.4-85 Reactor Mixing Zone and Riser Temperatures

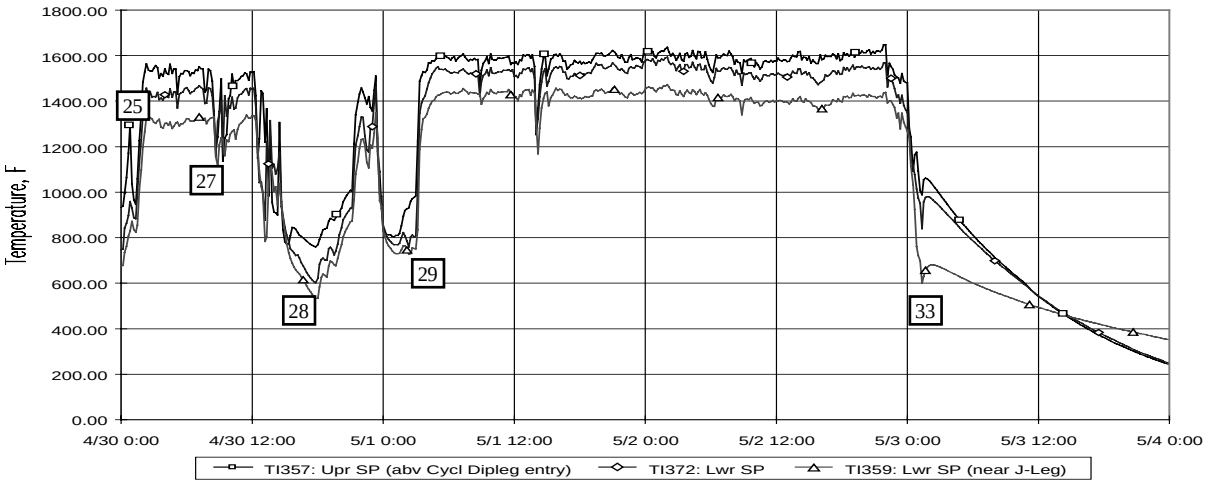

Figure 4.1.1.4-86 Standpipe Temperatures

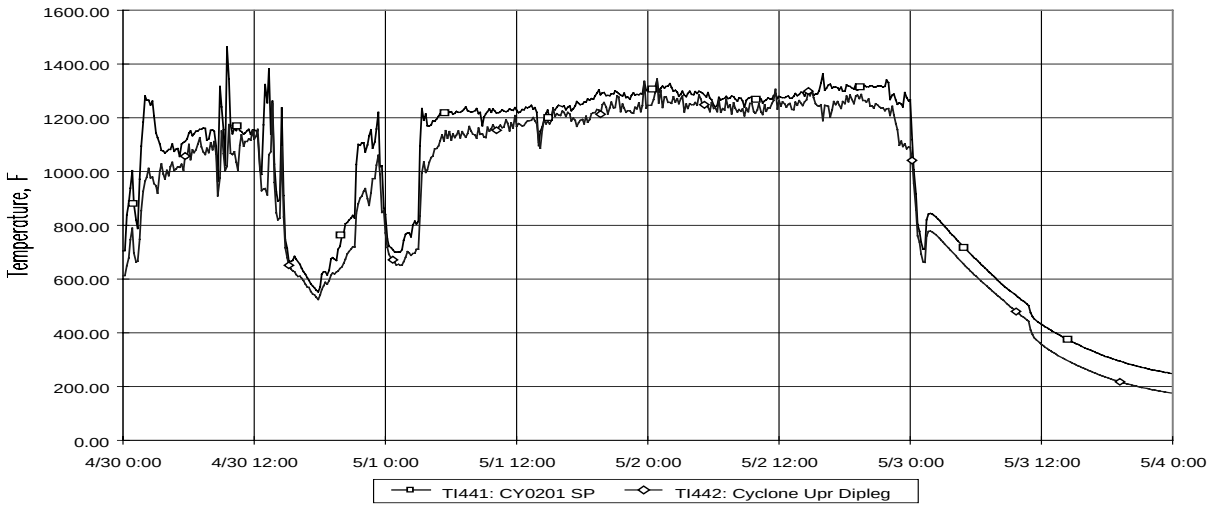

Figure 4.1.1.4-87 Cyclone Dipleg Temperatures

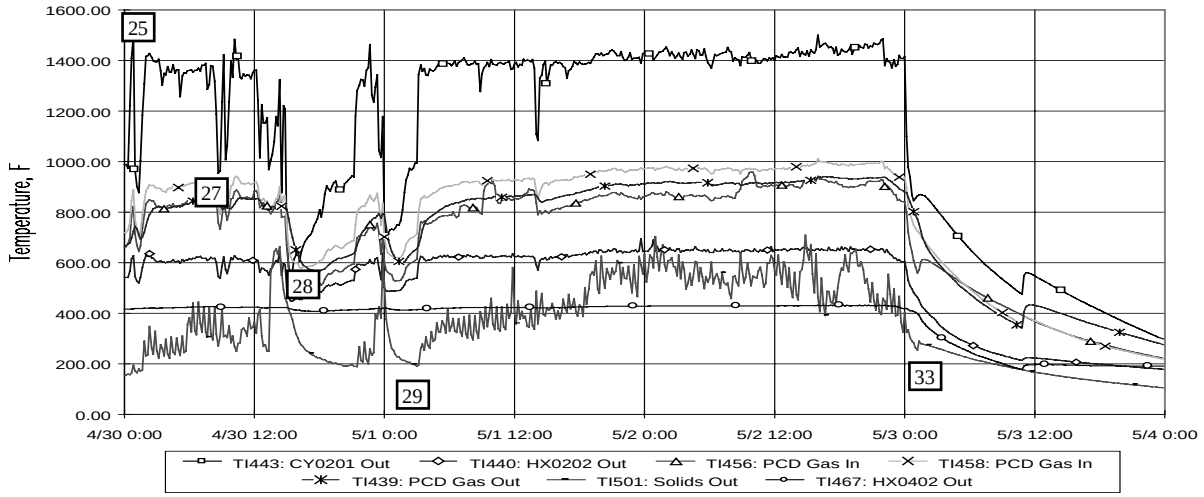

Figure 4.1.1.4-88 Temperature Profile Downstream of Reactor

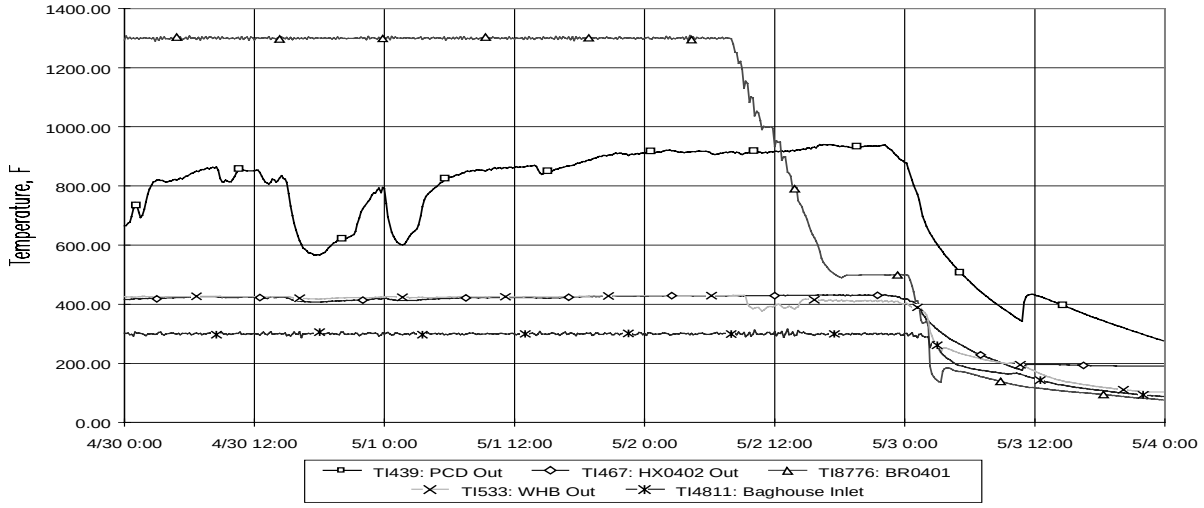

Figure 4.1.1.4-89 System Temperatures Downstream of PCD

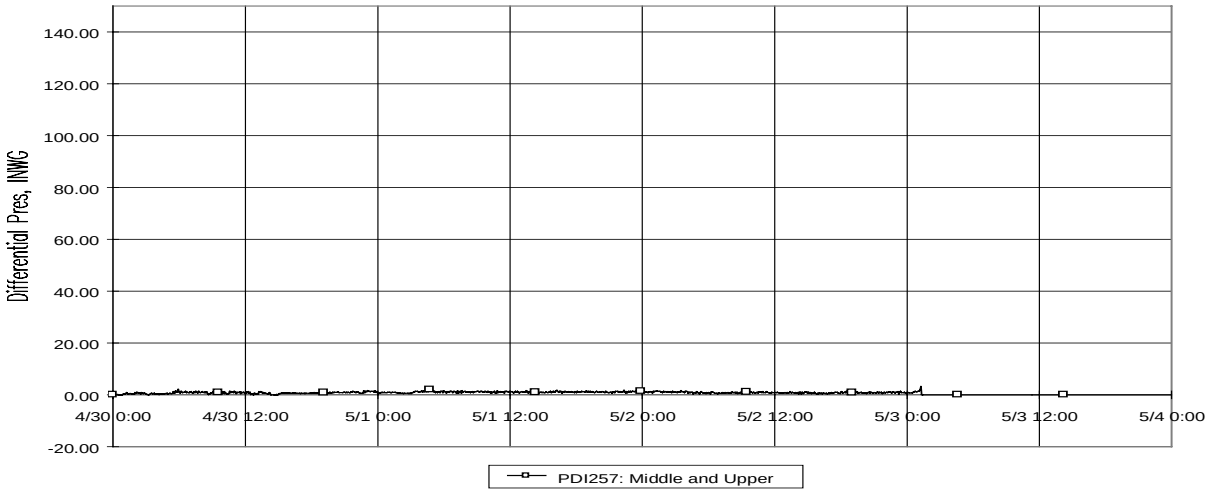

Figure 4.1.1.4-90 Mixing Zone Differential Pressure Profile

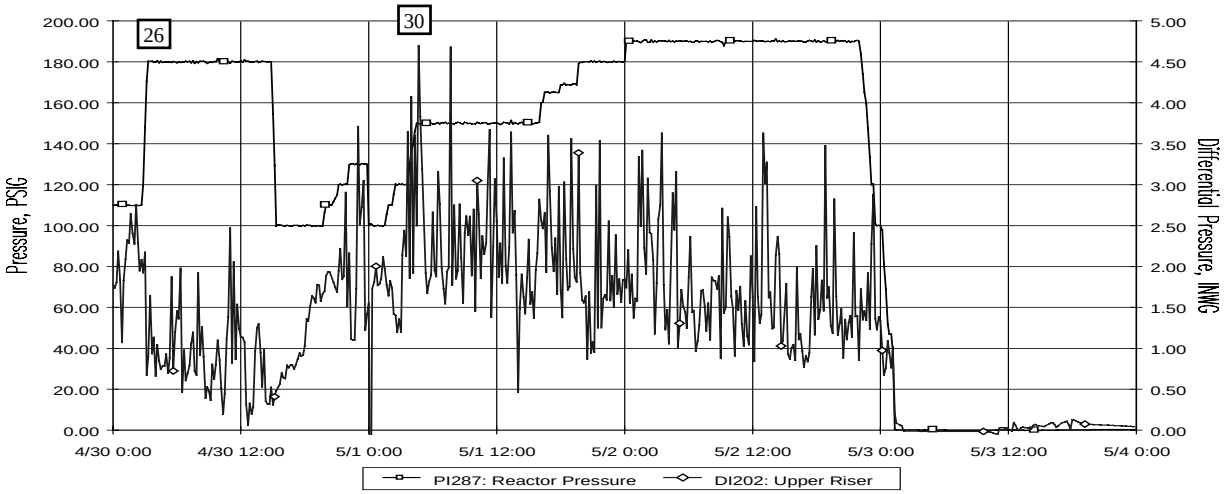

Figure 4.1.1.4-91 Reactor Pressure/Riser Differential Pressure Profiles

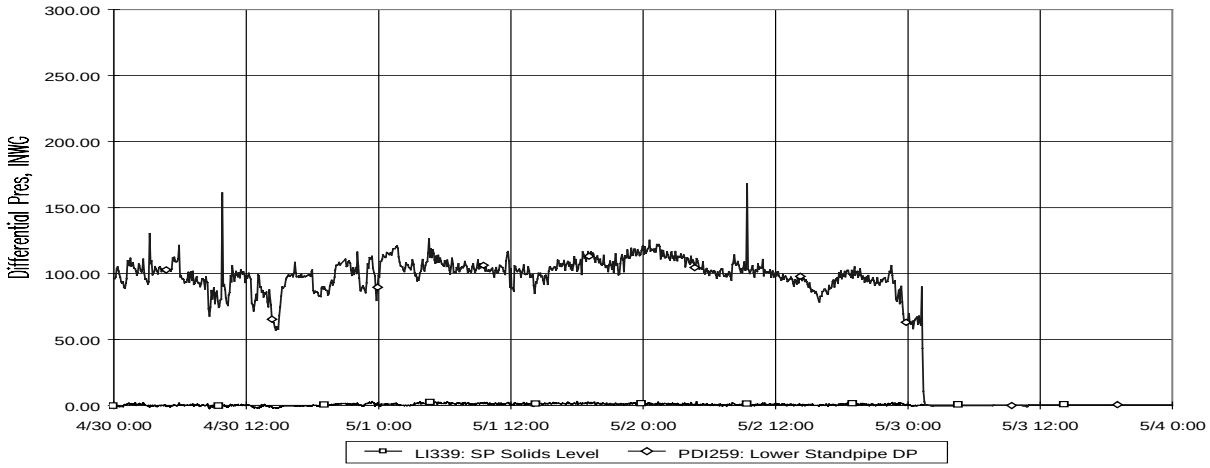

Figure 4.1.1.4-92 Standpipe Differential Pressure Profiles

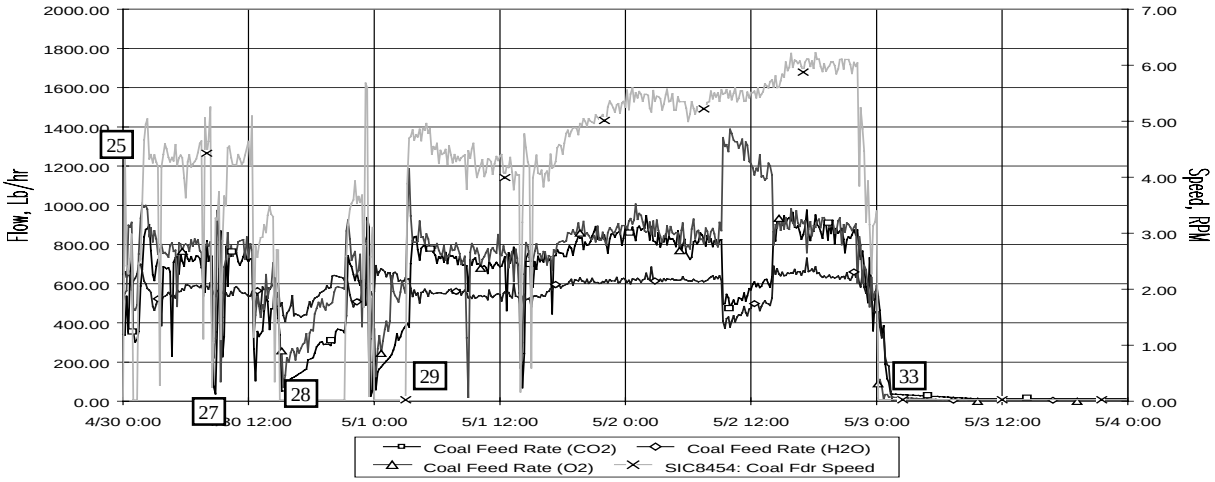

Figure 4.1.1.4-93 Coal Feed Rate Based on Gas Analysis

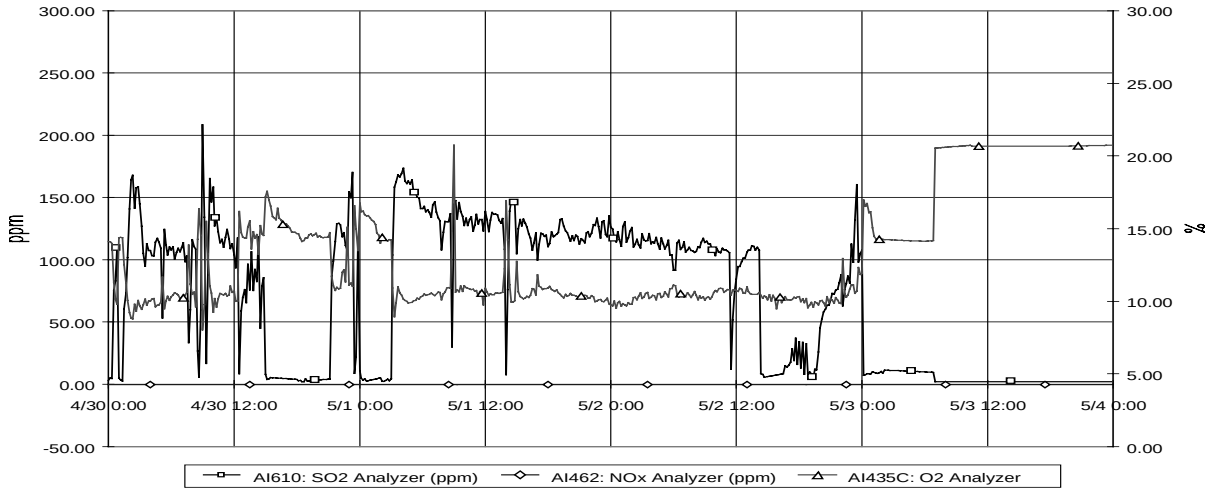

Figure 4.1.1.4-94 O_2, SO_2 and NO_x Analyzers

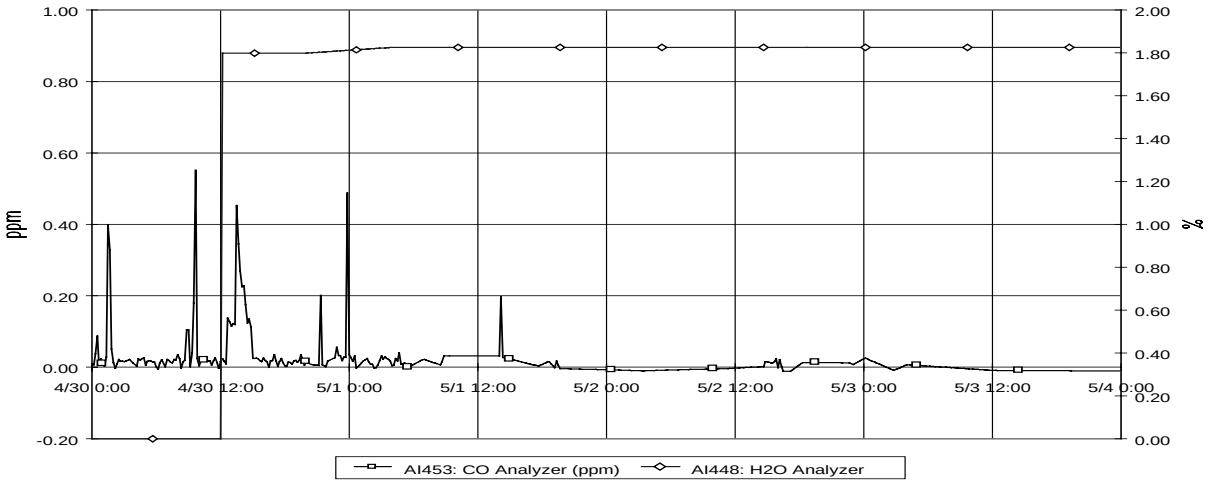

Figure 4.1.1.4-95 CO and H_2O Analyzers

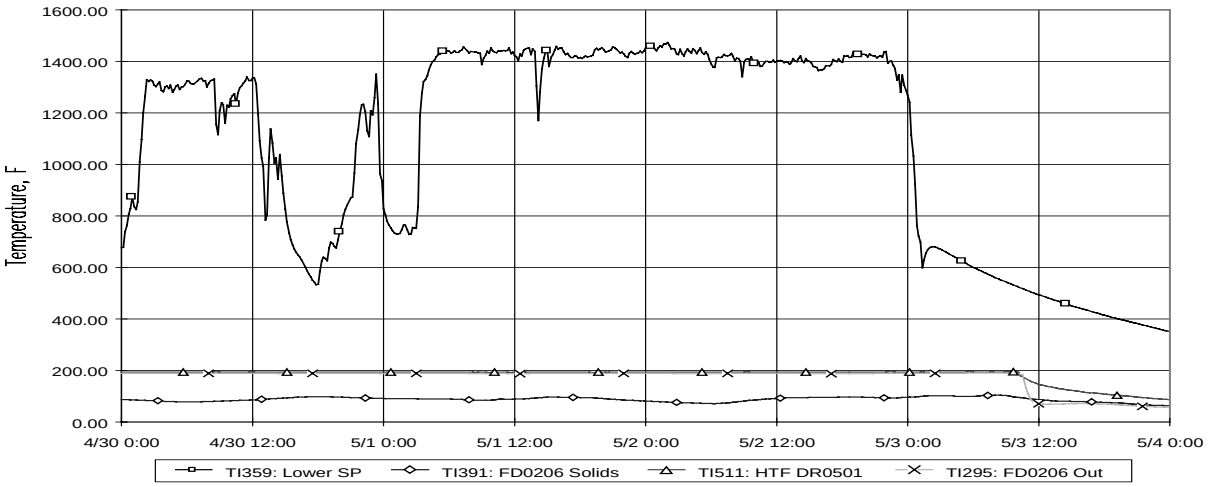

Figure 4.1.1.4-96 FD0510 Temperature Profiles

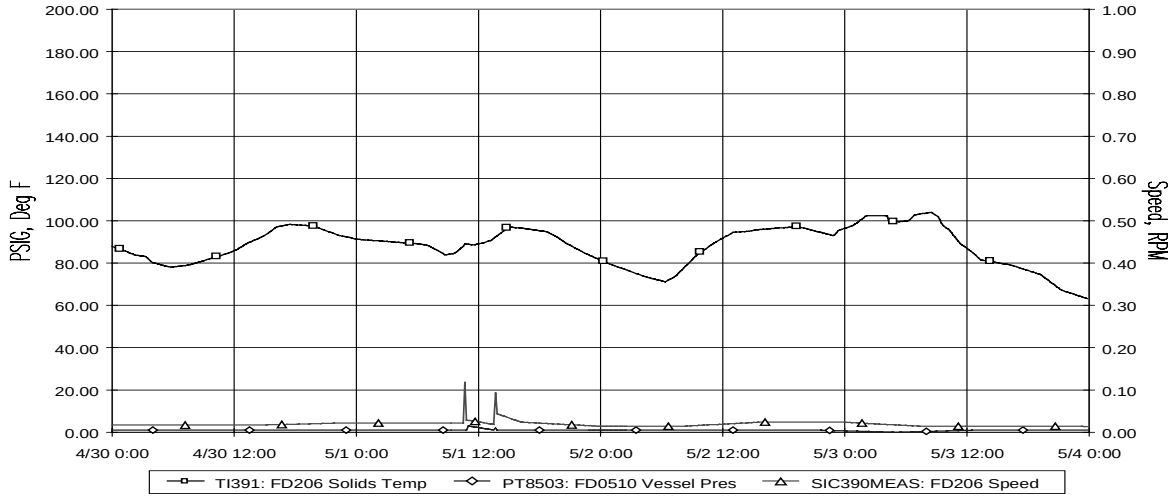

Figure 4.1.1.4-97 FD0206 Profiles

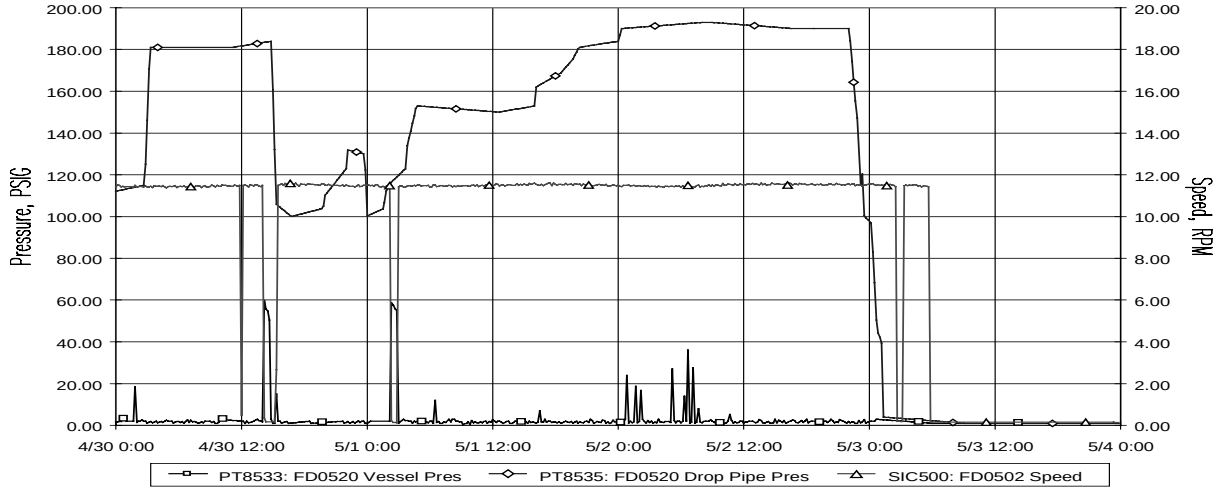

Figure 4.1.1.4-98 FD0520 Pressure Profiles

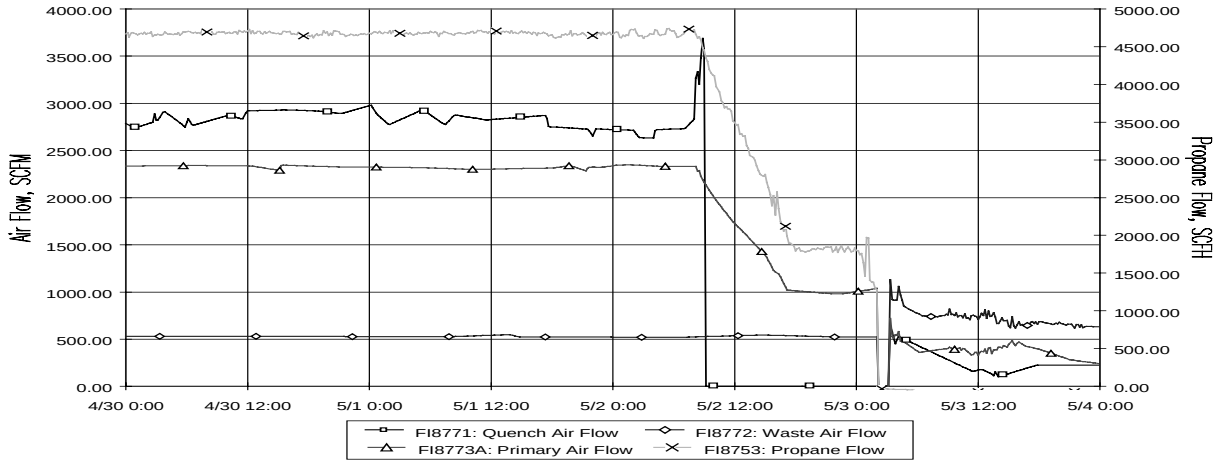

Figure 4.1.1.4-99 Thermal Oxidizer Air/Fuel Flow

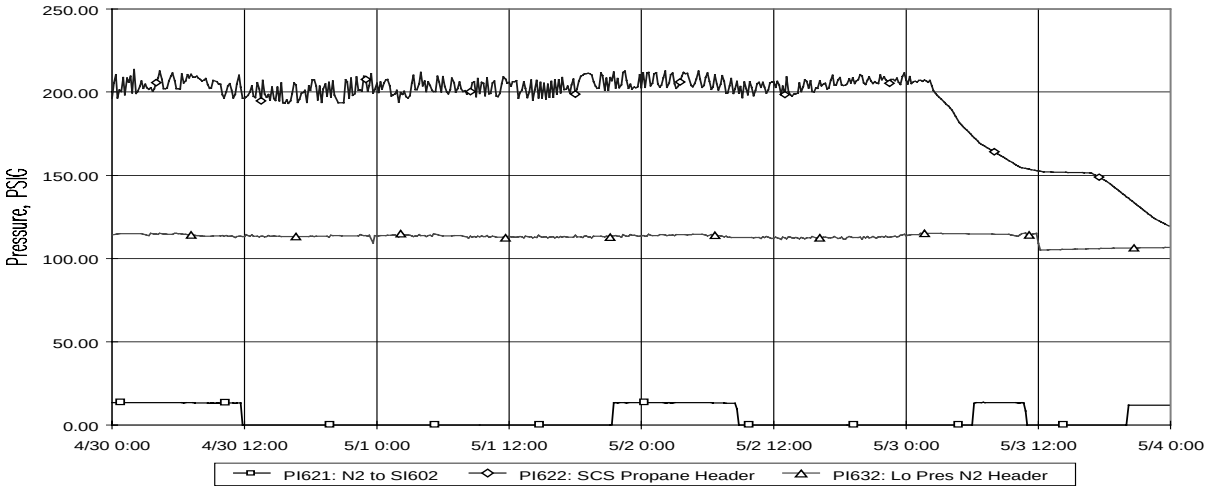

Figure 4.1.1.4-100 Nitrogen/Propane Header Pressure Profiles

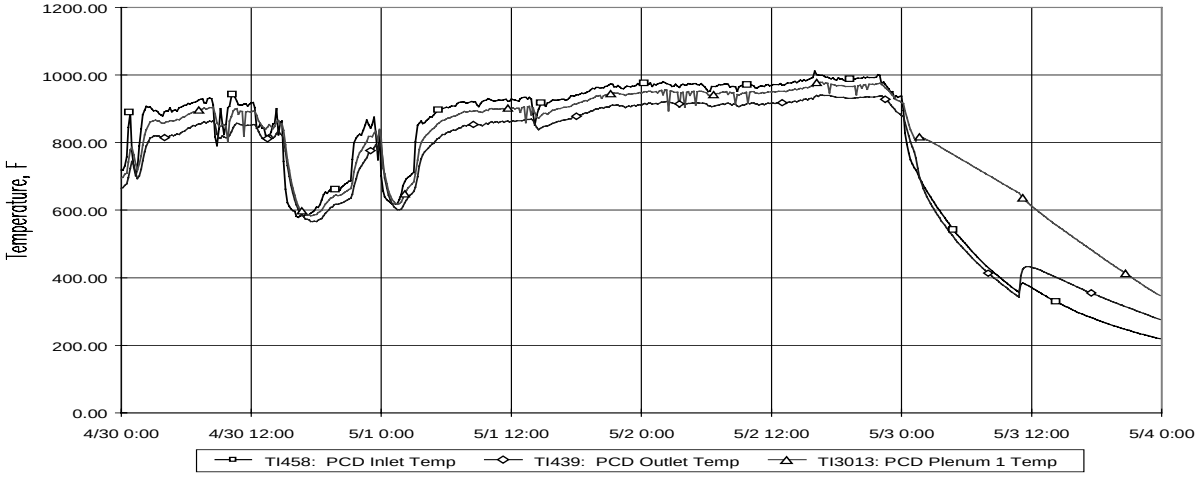

Figure 4.1.1.4-101 PCD Temperatures

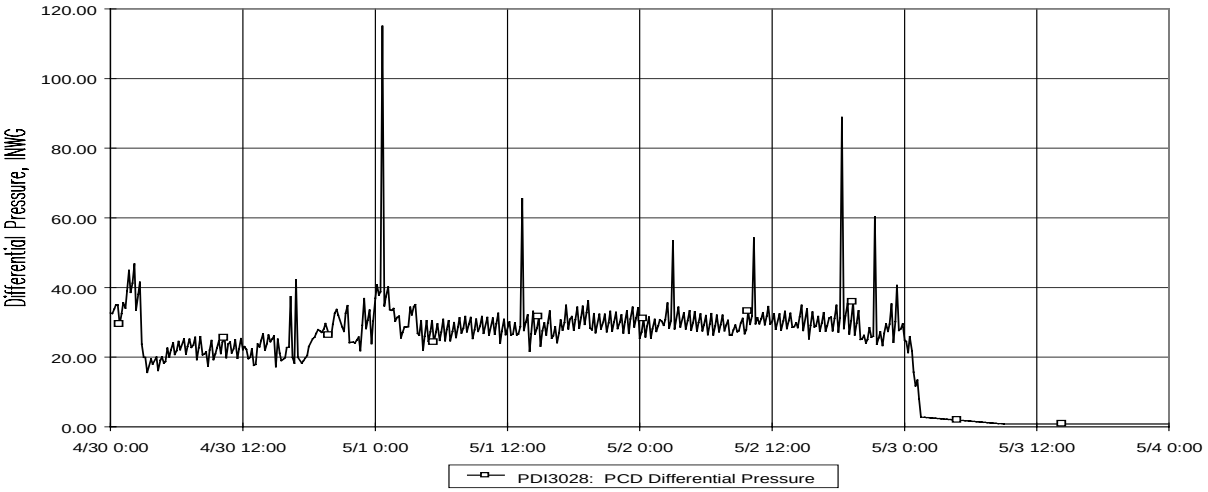

Figure 4.1.1.4-102 PCD Differential Pressure Profile

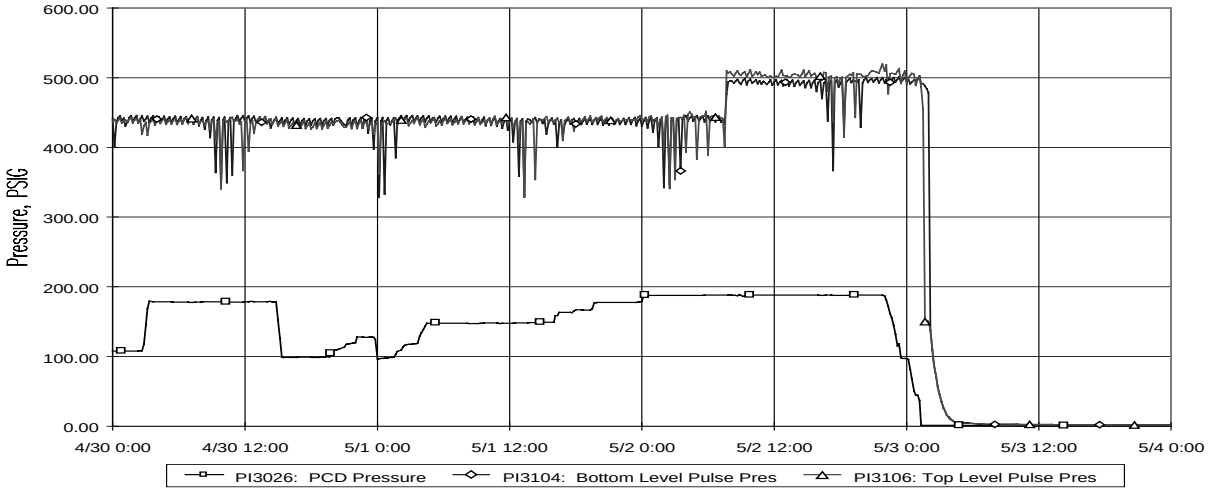

Figure 4.1.1.4-103 PCD Pressure and Pulse Pressure

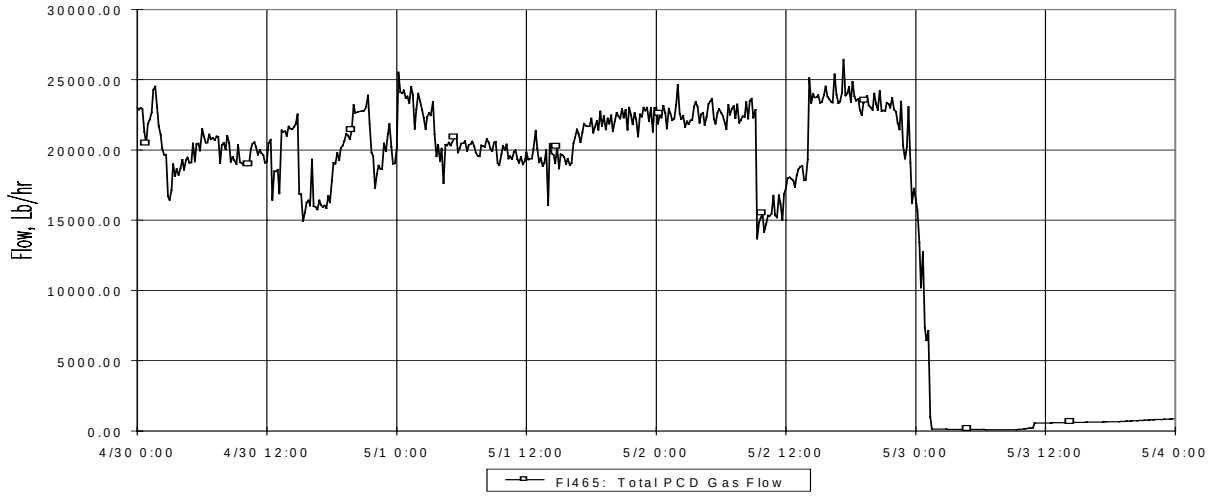

Figure 4.1.1.4-104 Gas Flow Through PCD

4.1.2 CCT5 Series Test Runs

By the end of CCT4D test run the cyclone dipleg was suspected of playing an important role in problems associated with excessive solids carryover from the reactor. To test the cyclone dipleg performance more rigorously a new aeration line was added to augment the exiting aeration in the dipleg. Also, the FD0210/FD0220 DCS logic was modified as follows:

- Logic was changed to unlatch the feeder start command when a permissive is lost. The previous scheme allowed the feeders to restart on their own when the permissives were reset. The new scheme requires the operator to initiate a start command any time a feeder is lost due to loss of one or more of the permissives.

- The conveying air flow permissive for both feeders was previously FSLL309, conveying air flow to FD0210. The new scheme allows FD0210 to operate using FSLL309 as a permissive and FD0220 to operate using FI271 as a permissive. All other reactor protection permissives that will trip both feeders are still in place. The change allows FD0220 to operate independently of FD0210.

In addition to the continuing test objective of understanding and addressing the problem of excessive solids carryover from the reactor the CCT5 series test run objectives included exposing the candles to higher gas temperatures and running the recycle gas compressor. The primary gas cooler was completely bypassed and the refractory-lined orifice spool piece in the gas bypass line was replaced with a straight spool piece.

4.1.2.1 Characterization Test Run CCT5A

Test run CCT5A was conducted between May 12 and May 20, 1997. Operating plots are shown in figures 4.1.2.1-1 through -50. The sulfator burner was set to preheat the PCD.

CCT5A Test Run Chronology

- On May 12, 1997, all auxiliary systems were started in preparation for test run CCT5A. The sulfator burner (BR0602) was used to preheat the PCD for the first time. The PCD was successfully preheated at about 45 psig reactor pressure. After completing the PCD preheat the reactor start-up burner (BR0201) was lit (event 1, figure 5) and BR0602 was shut down. The PCD preheat line was isolated and the reactor pressure was ramped to 60 psig. All instrument purges were then set. Coal feed was started at 22:09, after the reactor loop was heated (event 2, figures 3, 7 through 10, and 15).

- At 00:00 on May 13, 1997, BR0201 was shut down. Conditions were then held steady for several hours. Based on the gas analysis, the calculated coal feed rate was 590 lb/hr (event 3, figure 15). Around 08:20 SRI took an inlet sample. At 10:00 the reactor pressure was increased to 160 psig and the reactor flows and instrument purges were adjusted for the higher operating pressure.

- White plume was noticed coming out of stack around noon. There was a strong sulfur smell near the baghouse. The gas around the top of the baghouse was analyzed and shown to contain 3 ppm SO_2. Also, the sulfur analyzer reading was lower than in previous runs. The baghouse was then bypassed but there was no change in plume intensity. The baghouse screw cooler was run for about 20 minutes, but there were no solids in the baghouse. Dolomite addition into the reactor was started, which decreased the SO_2 from 44 to 12 ppm (event 4, figure 16). Consequently, the plume went away. It appeared that the plume was due to SO_3; SO_2 was getting catalytically oxidized to SO_3 with the accumulated iron from sand that had been deposited on the refractory. Dolomite addition continued at a rate of 120 lb/hr. Sand was added later to build the reactor solids inventory. Around 16:00 cyclone dipleg aeration flows were adjusted.

- Around 04:00 on May 14, 1997, there was gas flow through the spent fines transport system (FD0520) dispense vessel when it was not transferring any solids. The spheri valve dome was suspected to have developed scratches. Conditions were again held steady while SRI took an inlet sample. When SRI finished, sand addition was again started. The gas analyzer was returned to service after the sample line was unplugged. Throughout the day the PCD was manually back-pulsed at various pressures as part of back-pulse valve characterization.

- Around 10:15 the recycle gas booster compressor (CO0401) was started in order to evaluate its performance using process gas. The discharge pressure was 280 psig. The CO0401 was shut down after operating a few hours (event 5, figure 2).

- In the afternoon dolomite was again added to the reactor. The solids circulation was also reduced to lower the solids carryover to the PCD. Cyclone dipleg aeration flows were adjusted to study their effect on the dipleg solids flow. There were also some problems with FD0520. On May 14, 1997, the average coal feed rate was 750 lb/hr.

- Around 06:00 on May 15, 1997, more dolomite was added to the reactor at a high rate and then more sand was added to bring up the reactor solids level. At 08:30 dolomite was fed into the reactor at a very high rate causing an upset in the cyclone dipleg and resulting in a high solids carryover into PCD. The feeder speed was decreased and the cyclone dipleg recovered.

- At 14:00 the gas analyzers were shut down when the chiller failed. The PCD back-pulse also seemed to be upsetting the reactor operation. During the night there were problems with the following solids handling systems: the spent fines screw cooler (FD0502) and the spent solids feeder system (FD0530). The average coal feed rate for the day was 768 lb/hr.

- On May 16, 1997, the PCD back-pulse was substantially disturbing the flow in the dipleg. The pulse pressure was reduced to approximately 400 psig and the reactor pressure was increased to 166 psig. Problems with FD0530 continued but were eventually solved. SRI took two inlet samples during the day. The CO0401 was

started at 12:40 but had to be shut down an hour later for Sanders Engineering to do stack and reactor sampling for internal compliance testing. Sanders Engineering completed the stack and reactor sampling at 16:00. Dolomite addition was started again at an average feed rate of 210 lb/hr. Around 20:00 it was noticed that the pressure letdown valve (PV287) was vibrating, however, the vibrations stopped about 3.5 hours later. The average coal feed rate for May 16, 1997, was 825 lb/hr.

- At 00:20 on May 17, 1997, the plant information (PI) system went down and had to be restarted. At 04:55 a PCD back-pulse upset the cyclone dipleg operation resulting in a large carryover of particles to the PCD (event 6, figures 34 and 40). After sufficient time for the PCD to empty of solids the coal feed rate was increased. At 16:00 the PCD again back-pulsed, greatly disturbing the reactor operations. Due to large carryover of hot solids to the PCD the FD0502 outlet temperature (TI505) increased beyond 400°F, tripping FD0502. Once TI505 dropped to 390°F, FD0502 was started at a low speed, and as TI505 dropped further the FD502 speed was increased. More sand was added to the reactor to replace the solids that were lost during the upset. After the sand was added, more dolomite was added. The back-pulse at 18:25 again caused a reactor upset and about 700 lb of solids were sent to the PCD (event 7, figures 34 and 40). The average coal feed rate for May 17, 1997, was 883 lb/hr.

- Conditions were held steady throughout the morning of May 18, 1997, while the effect of the PCD back-pulse on reactor operations was studied. The dolomite feed rate was reduced to decrease the rate at which the reactor bed level was building and to study its effect on the dipleg operation. The CO0401 was run for about an hour to test its operation. Between 13:27 and 13:29 the dipleg operation was upset but it was not related to a PCD back-pulse. At this time the coal feed rate was approximately 864 lb/hr. The dipleg operated well until the 16:25 back-pulse and operations remained unsteady for about 30 minutes.

- PV287 started vibrating similar to vibrations on May 16, 1997. There were also some minor problems with plugging in the FD0530 system. The reactor pressure was increased to 175 psig to determine if this would stop the PV287 vibrations. The average coal feed rate for May 18, 1997, was 911 lb/hr.

- At 02:15 on May 19, 1997, the pin in the positioner arm on PV287 broke. The reactor pressure increased to 225 psig first, then decreased to 115 psig. The reactor pressure was stabilized and set to 175 psig within 11 minutes (event 8, figure 37). The PV287 vibration returned and the stem started turning. After the nuts on the stem were tightened, the vibration stopped. During the day, various PCD pulse parameters were changed to determine their effect, if any, on the reactor operations. Periodic reactor upsets continued. At 17:00 there was a significant upset which forced a reduction in coal feed and solids circulation rate to allow the PCD to empty of solids (event 9, figures 28, 32 through 34, 37, and 40). The FD0520 vent line plugged but was soon cleared. The FD0530 line also plugged. The average coal feed rate for May 19, 1997, was 870 lb/hr.

- On May 20, 1997, problems with the FD0530 system continued. Excessive solids carryover to the PCD forced the coal feed to be stopped at 11:10 (event 10, figures 28, 32 through 34, and 40). The reactor pressure was ramped down and BR0201 was lit (event 11, figure 30). Coal feed was resumed to bring the reactor temperatures up. But, due to low inventory of solids in the standpipe and low circulation rates, the temperature profile in the reactor loop was such that much of the coal started combusting in the cyclone dipleg. A skin temperature survey revealed a hot spot in the vertical portion of the cyclone dipleg. The combustion in the dipleg led to the formation of clinkers that eventually plugged the dipleg, preventing any solids from flowing down into the standpipe. Attempts to clear the dipleg were unsuccessful. The reactor system was shut down to clear the suspected plugging in the cyclone dipleg (event 12, figures 26 and 31).

CCT5A Post Test Run Inspections

The cyclone dipleg was inspected and found to be plugged by clinkers/agglomerates. Clinkers/agglomerates were also found at the bottom of the cyclone radish, which prevented solids from flowing down into the dipleg. Prior to removing the clinkers the solid level inside the cyclone dipleg was approximately 15 feet from the top of nozzle H2. The solid level in the cyclone was approximately at the bottom of the cyclone barrel. All the clinkers/agglomerates were removed. A couple of small pieces fell into the reactor standpipe. Sand was drained out of the dipleg.

CCT5A Test Run Observations

This test campaign was very successful. A deeper understanding of the operation of the transport reactor was gained. The transport reactor was operated on coal feed for approximately 180 hours. During this time approximately 72 tons of coal were processed. This was the longest of all continuous coal combustion tests. Major observations from the test run include:

- Time requirements for start-up were improved. The period between the start of propane preheat and steady-state on coal was reduced.

- A preliminary understanding of cyclone/cyclone dipleg operation was developed. The cyclone dipleg was sealed with solids through manipulation of dipleg aeration. The PCD back-pulse induced periodic instability in the reactor loop, which at times caused the cyclone dipleg seal (which was not very high) to be lost, resulting in momentary high solids-loss rate.

- Dolomite was fed into the reactor for in situ sulfur capture and to improve solids flowability in cyclone dipleg.

- Because the cyclone dipleg was sealed the transport reactor operation was very stable. For the first time the solids loss rate out of the reactor was less than solids

input rate. This allowed solids level in the reactor to build up, and thus resulted in less sand make-up rate.

- The facility operated at higher solids circulation rate because the solid collection systems and the cyclone dipleg operated more effectively.

- The facility operated at higher coal feed rate because solids circulation through the combustor heat exchanger was smoother.

- The PCD was tested at a higher inlet temperature than previously and the inlet dust loading was lower (at one time close to the design rate).

- The sulfator start-up heater was used for the first time to preheat the PCD.

- Operations started with a low solids bed level and built inventory with coal ash and dolomite.

- The primary gas cooler was bypassed for the first time to obtain higher gas temperature at the PCD inlet. At times the PCD back-pulse affected reactor operations.

Section 4.1.2.1

Graphs 1 through 25

Test Run CCT5A

May 12 through 16, 1997

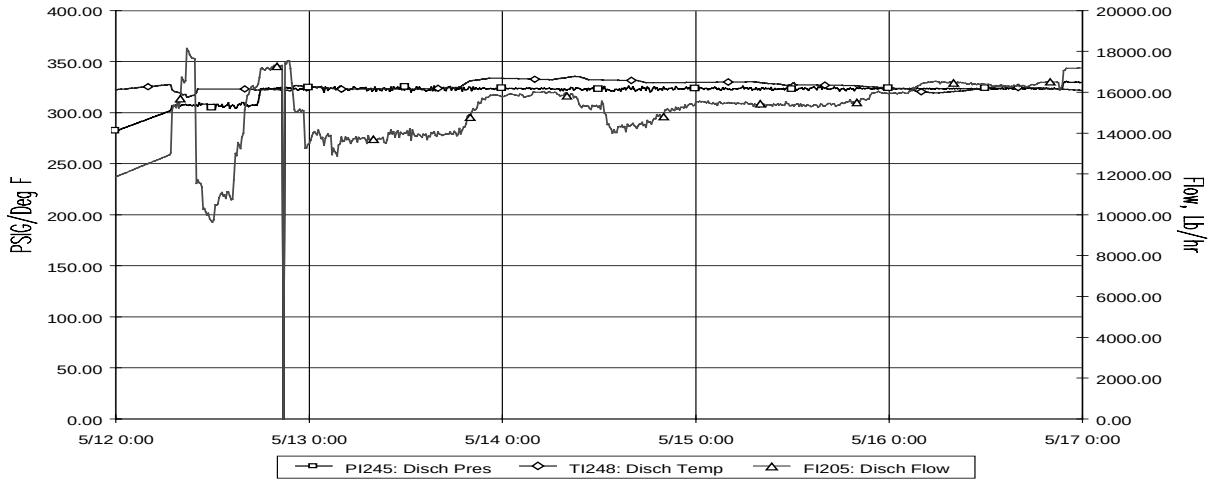

Figure 4.1.2.1-1 CO0201 System Profile

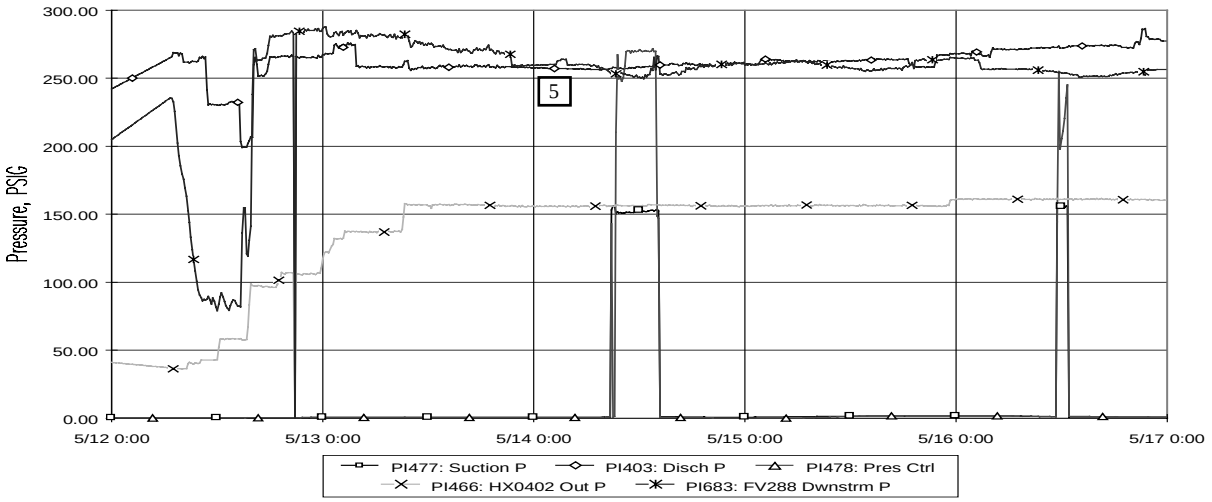

Figure 4.1.2.1-2 Recycle Gas System Pressure

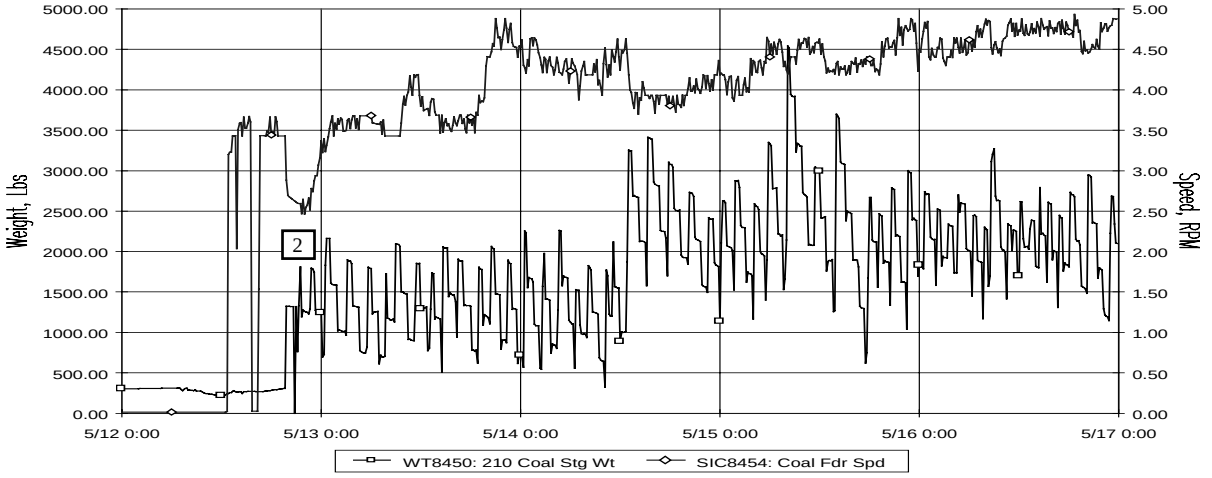

Figure 4.1.2.1-3 Coal Feed System Profile

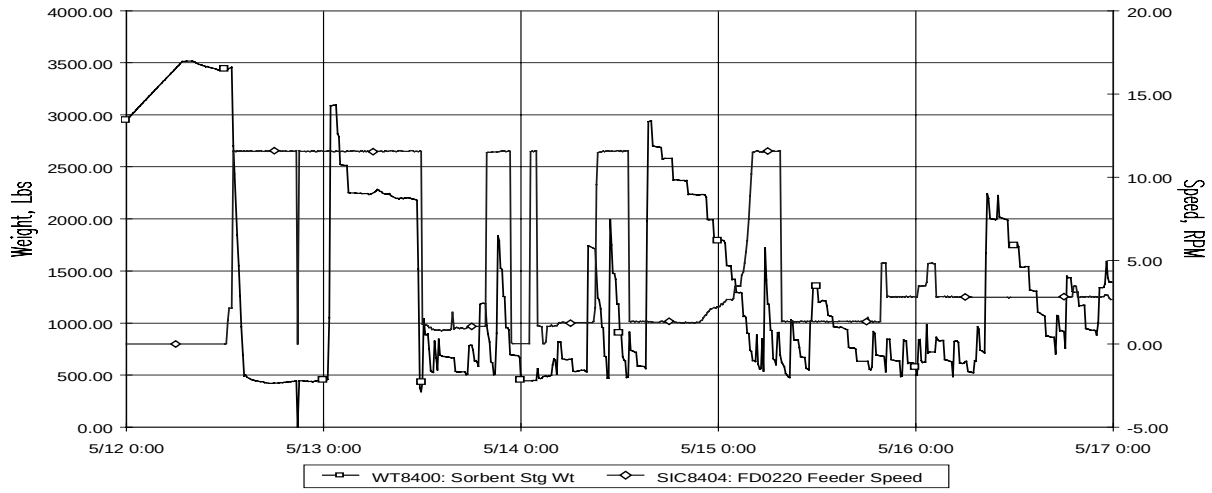

Figure 4.1.2.1-4 Sorbent Feed System Profile

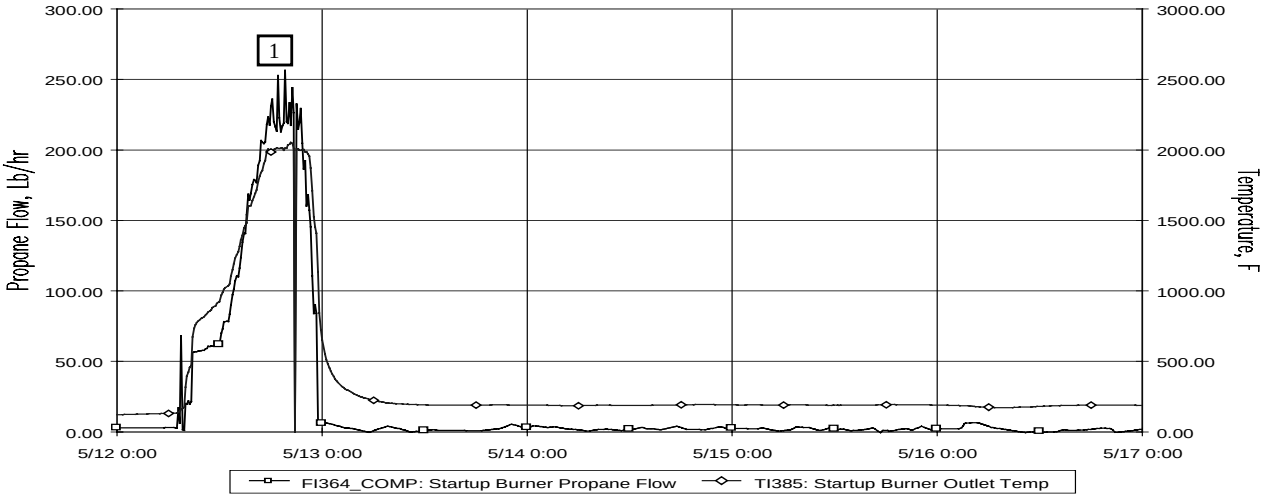

Figure 4.1.2.1-5 Start-Up Burner Flow/Temperature

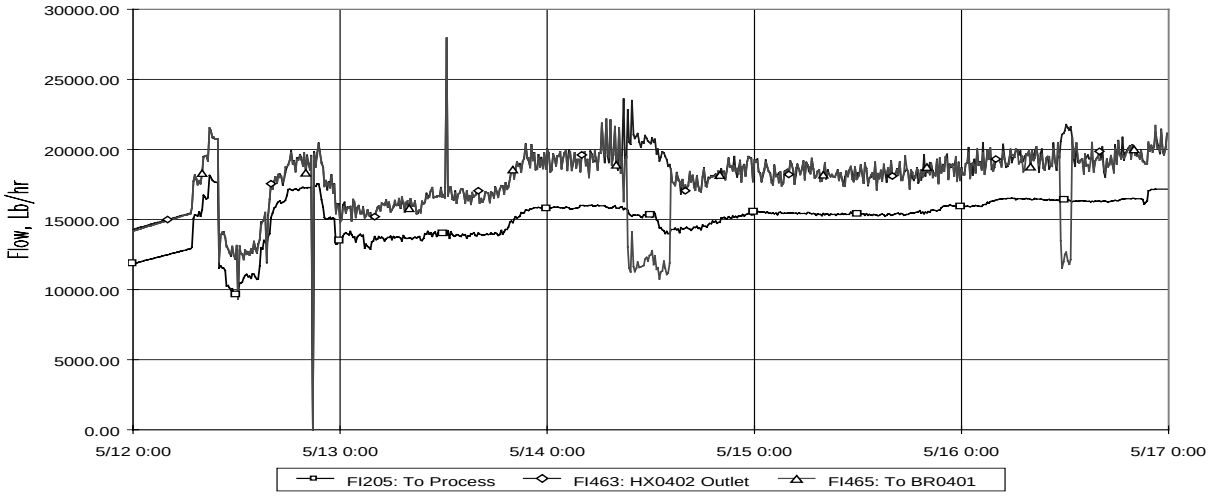

Figure 4.1.2.1-6 Total Gas In/Out Flow Rates

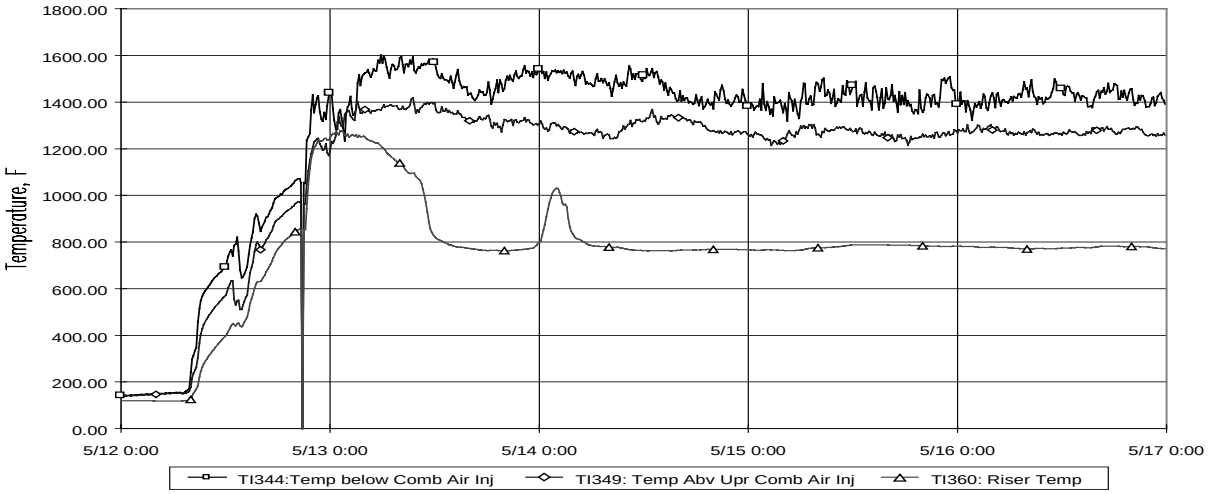

Figure 4.1.2.1-7 Reactor Mixing Zone and Riser Temperatures

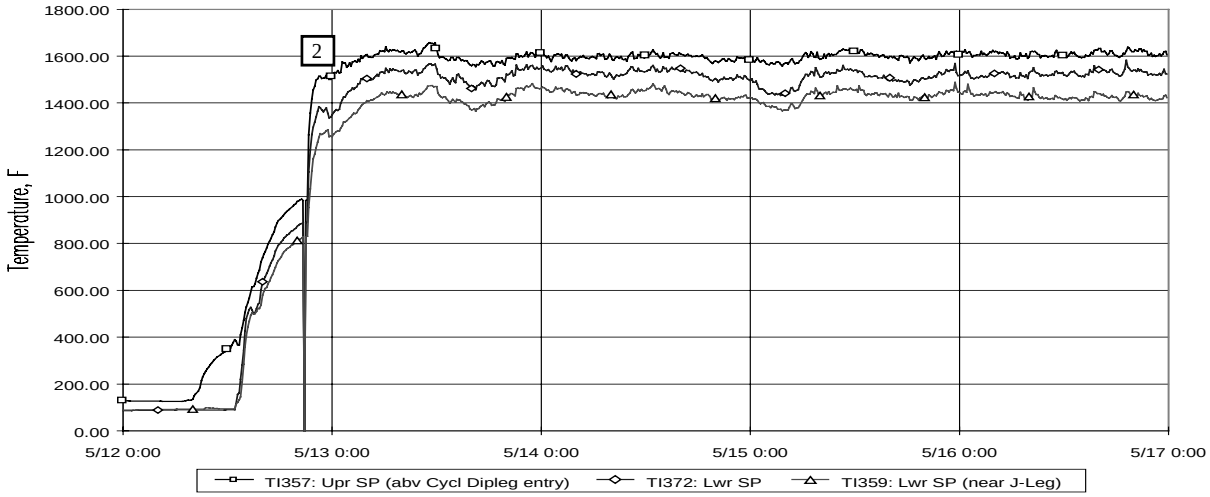

Figure 4.1.2.1-8 Standpipe Temperatures

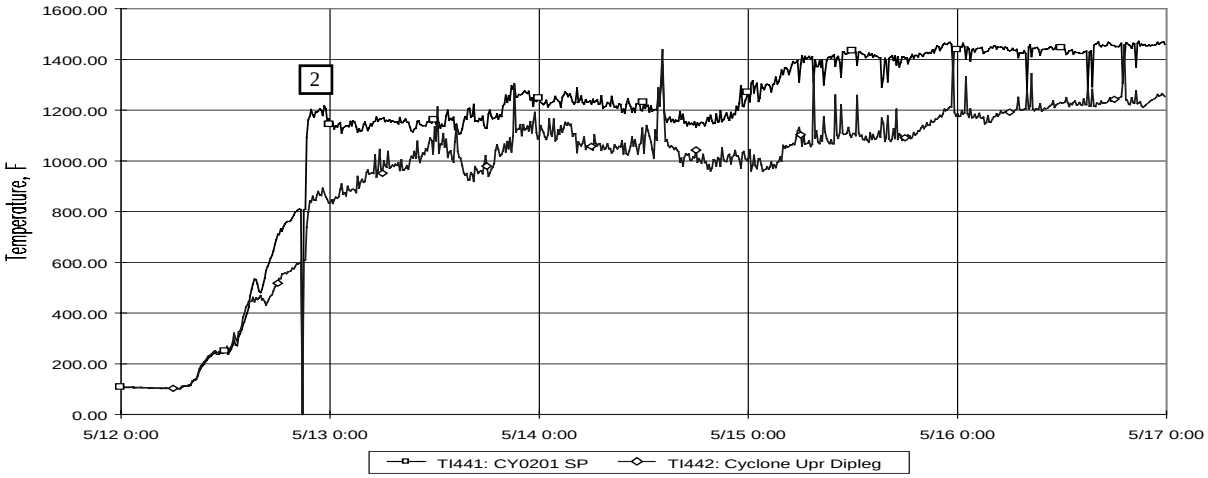

Figure 4.1.2.1-9 Cyclone Dipleg Temperatures

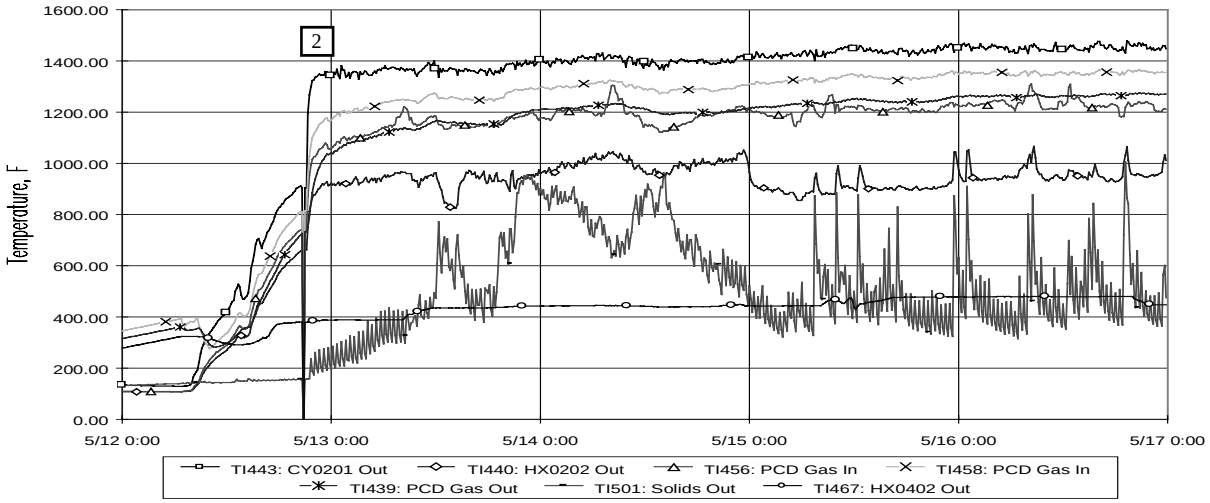

Figure 4.1.2.1-10 Temperature Profile Downstream of Reactor

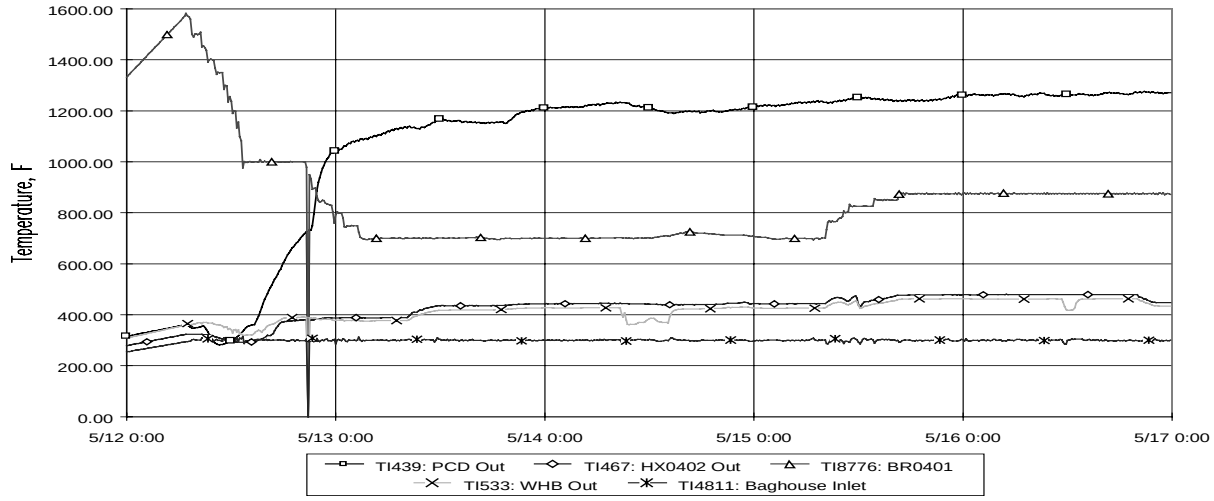

Figure 4.1.2.1-11 System Temperatures Downstream of PCD

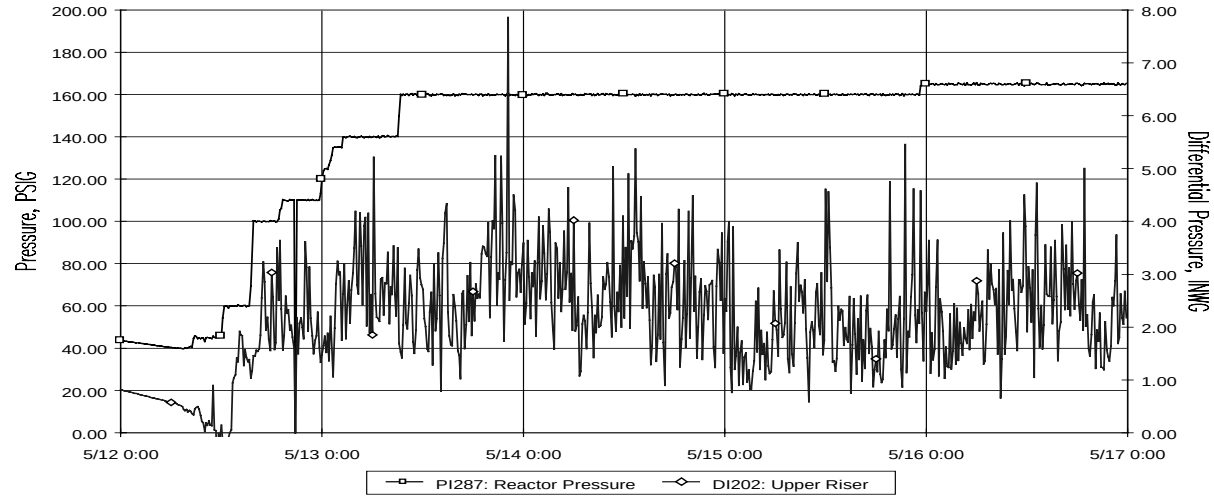

Figure 4.1.2.1-12 Reactor Pressure/Riser Differential Pressure Profiles

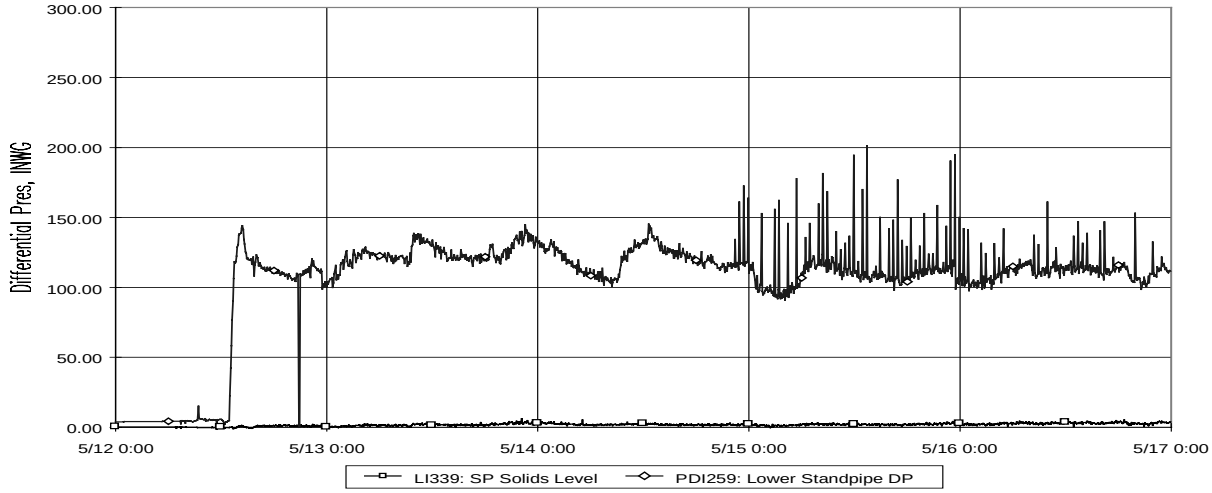

Figure 4.1.2.1-13 Standpipe Differential Pressure Profiles

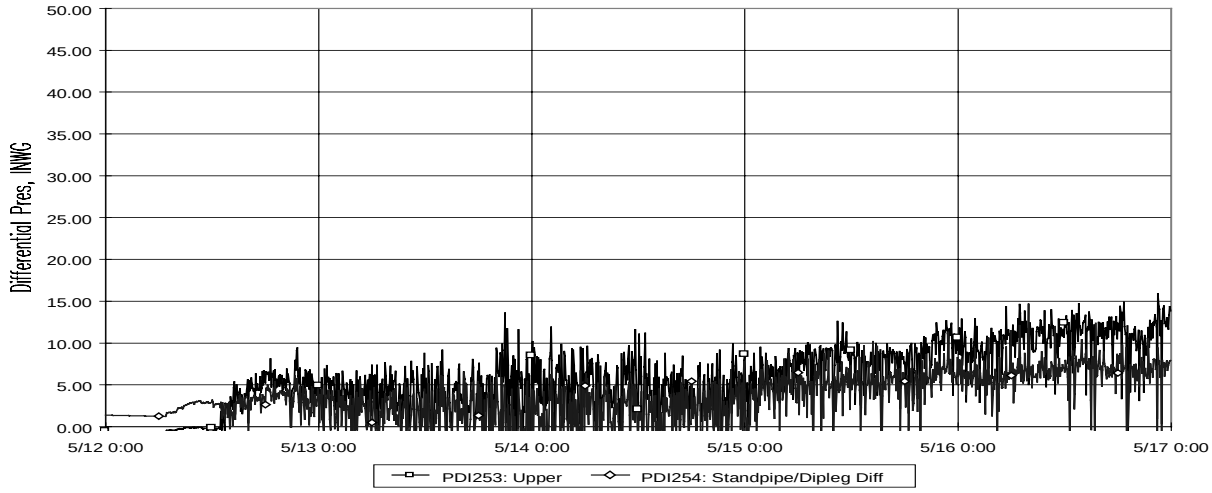

Figure 4.1.2.1-14 CY0201 Dipleg Differential Pressure Profiles

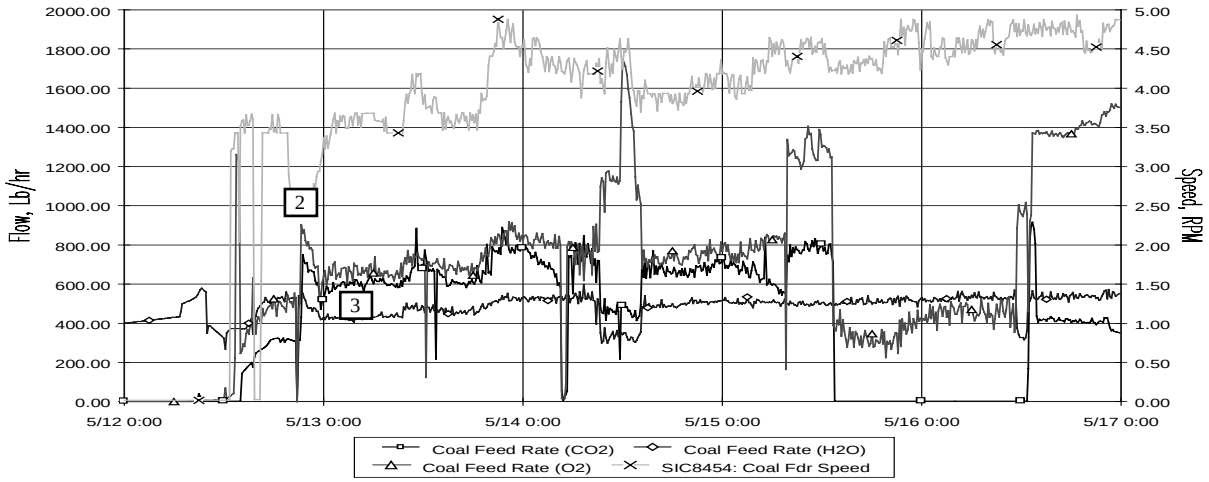

Figure 4.1.2.1-15 Coal Feed Rate Based on Gas Analysis

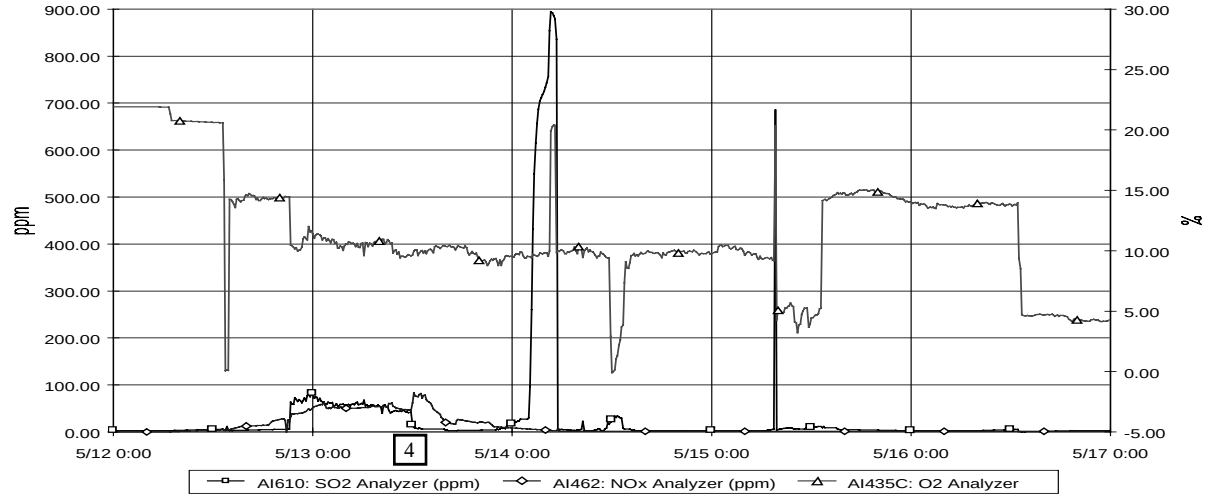

Figure 4.1.2.1-16 O_2, SO_2, and NO_x Analyzers

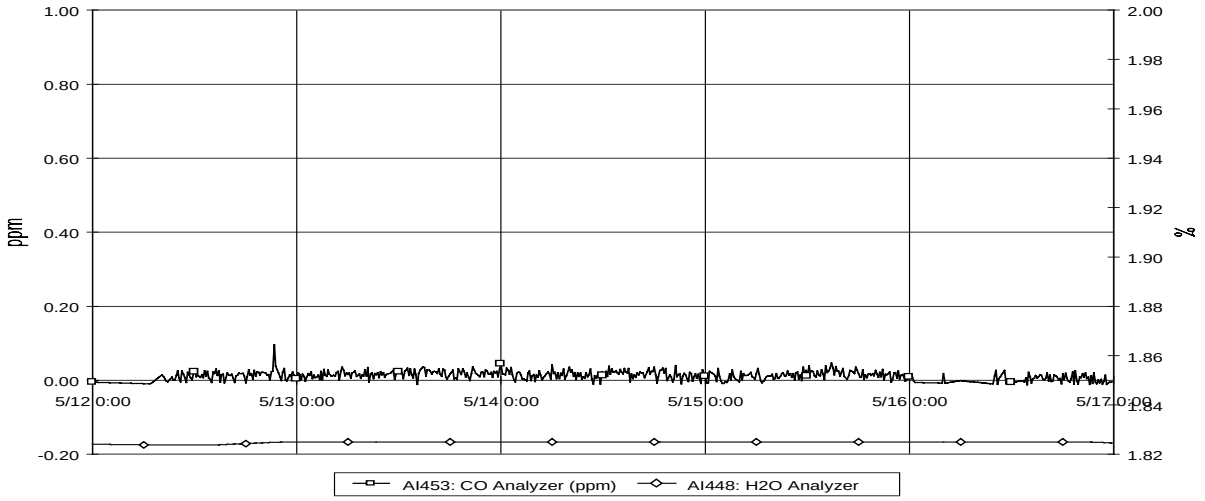

Figure 4.1.2.1-17 CO and H_2O Analyzers

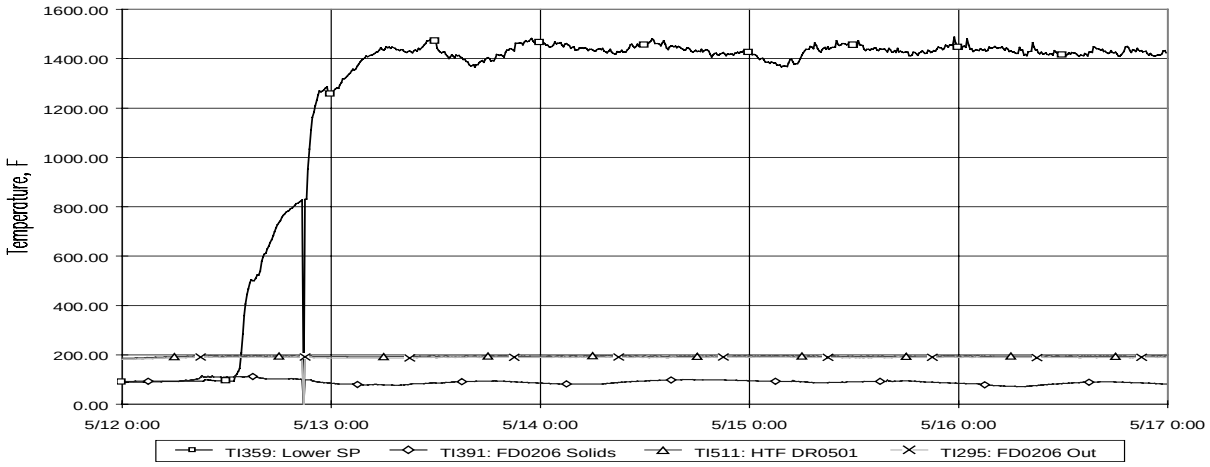

Figure 4.1.2.1-18 FD0510 Temperature Profiles

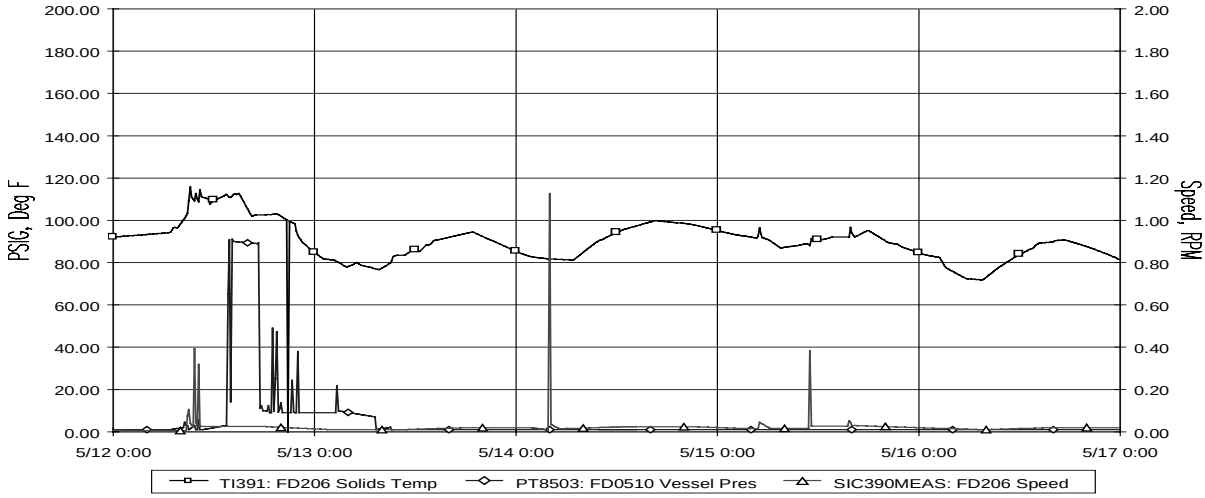

Figure 4.1.2.1-19 FD0206 Profiles

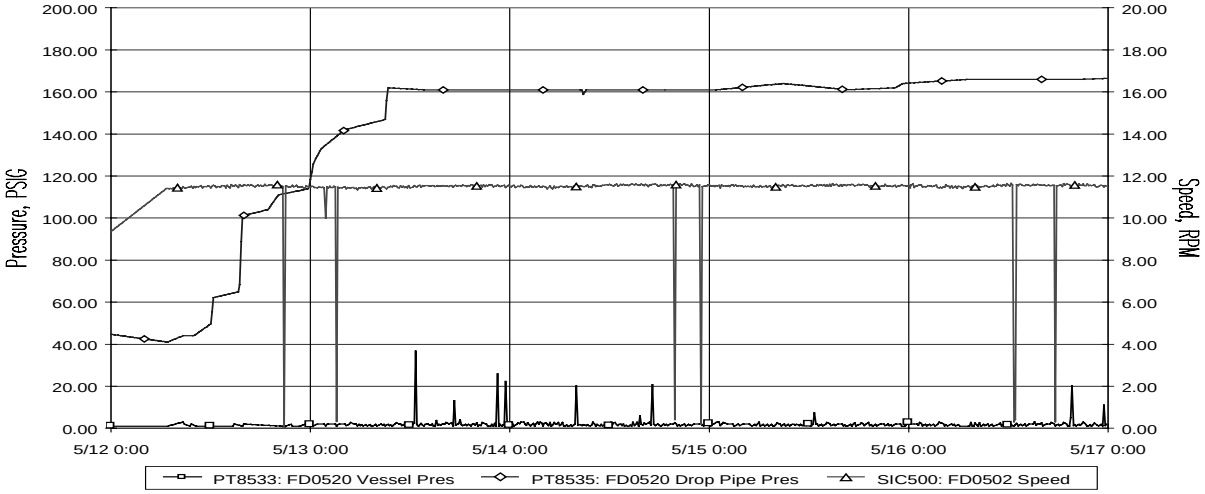

Figure 4.1.2.1-20 FD0520 Pressure Profiles

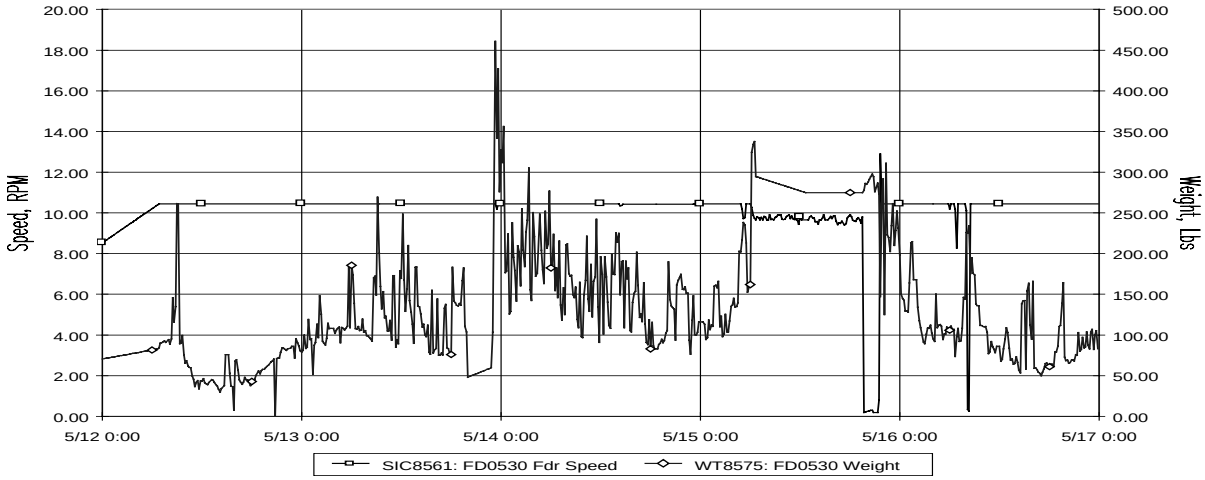

Figure 4.1.2.1-21 FD0530 System Profiles

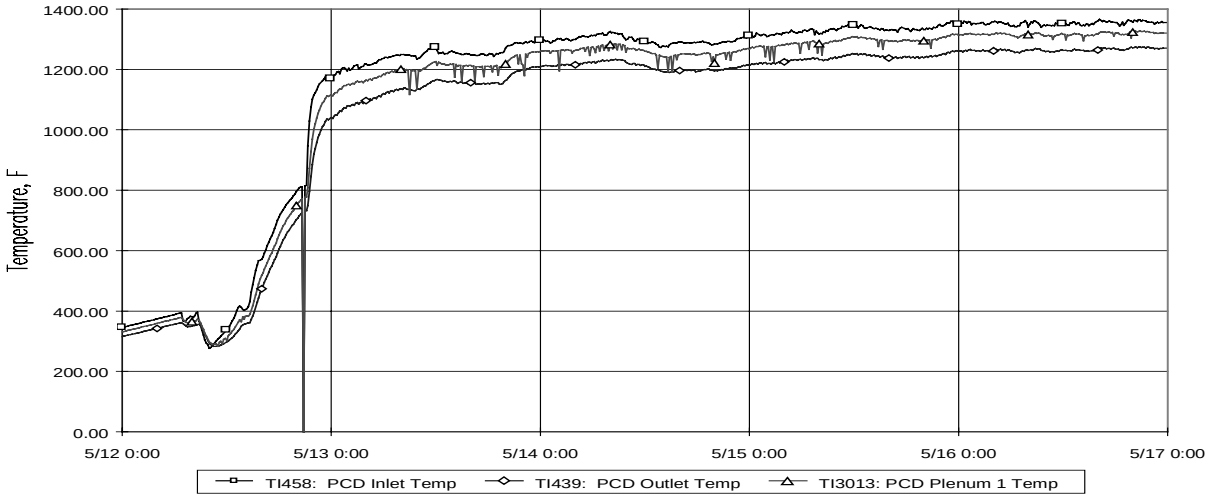

Figure 4.1.2.1-22 PCD Temperatures

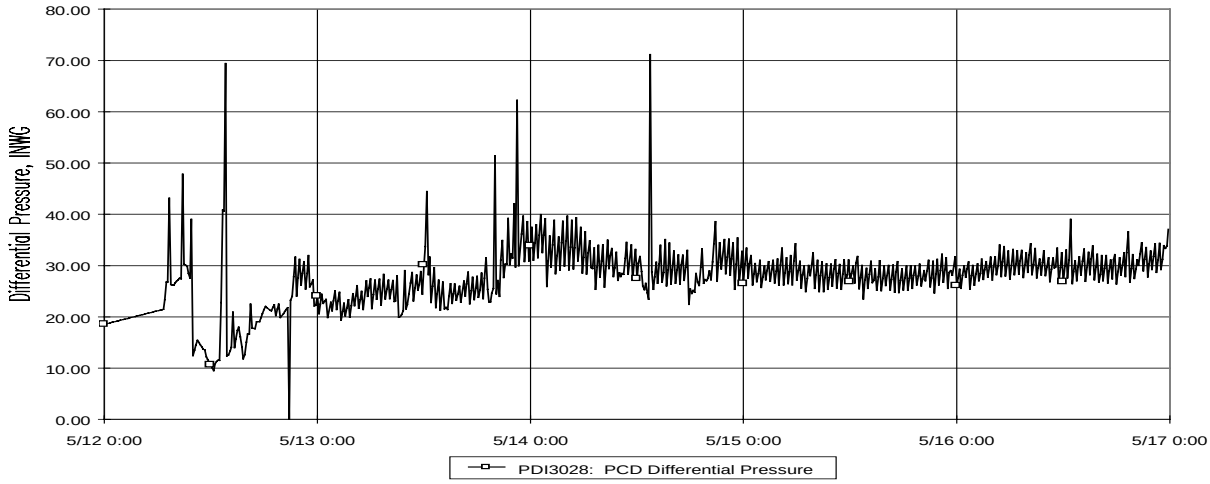

Figure 4.1.2.1-23 PCD Differential Pressure Profile

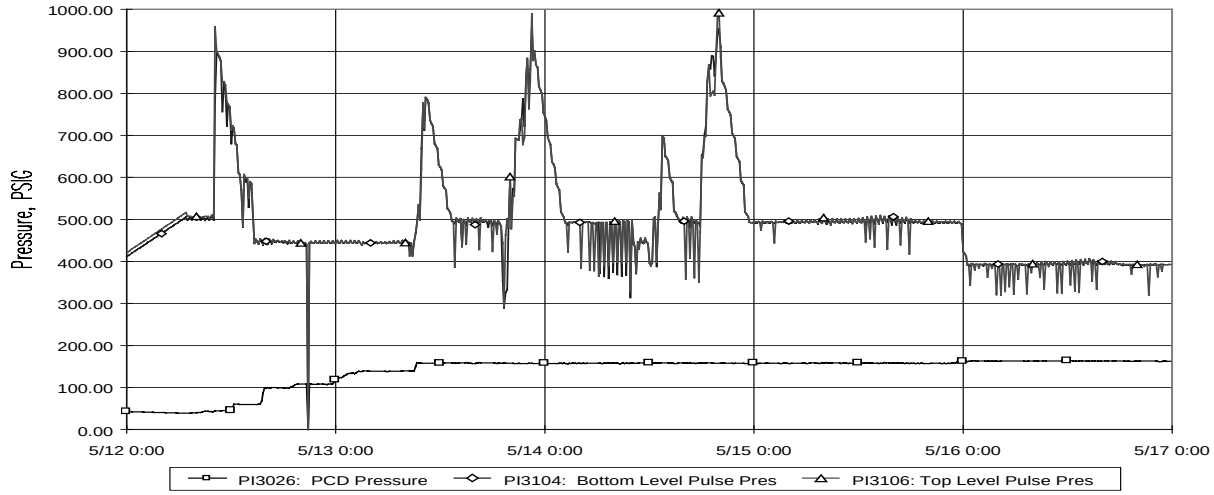

Figure 4.1.2.1-24 PCD Pressure and Pulse Pressure

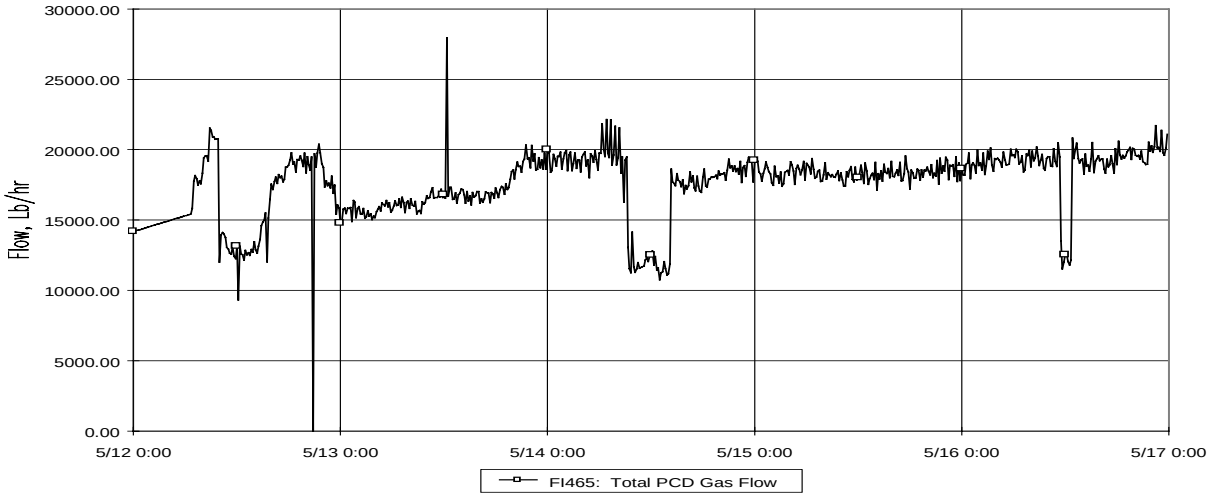

Figure 4.1.2.1-25 Gas Flow through PCD

Section 4.1.2.1

Graphs 26 through 50

Test Run CCT5B

May 17 through 20, 1997

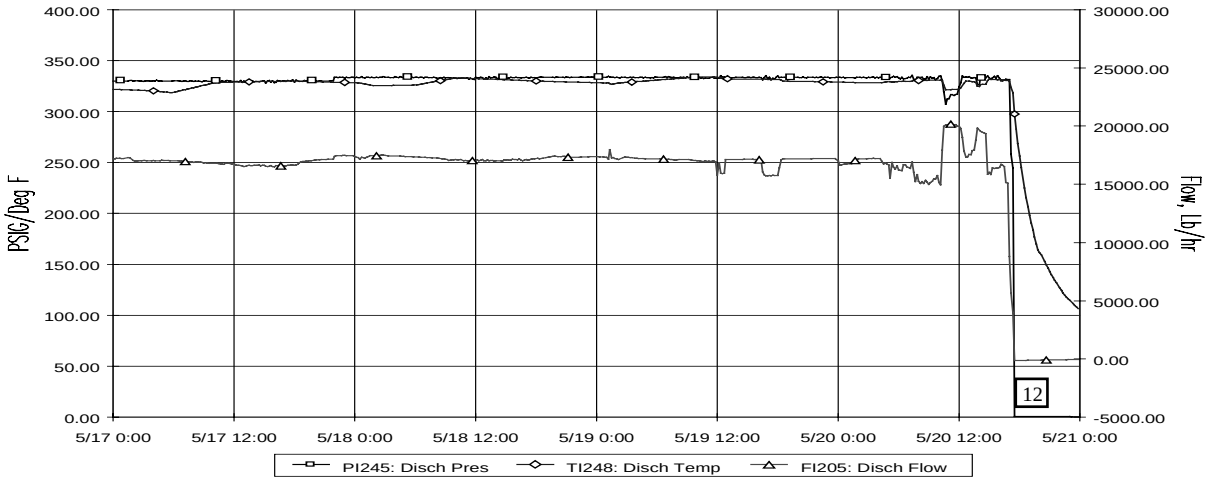

Figure 4.1.2.1-26 CO0201 System Profile

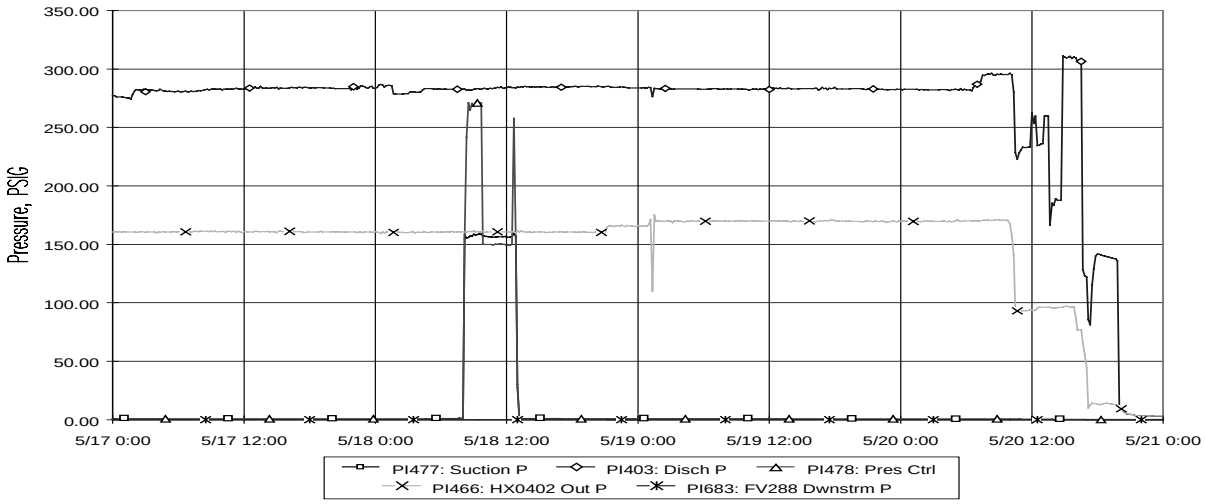

Figure 4.1.2.1-27 Recycle Gas System Pressure

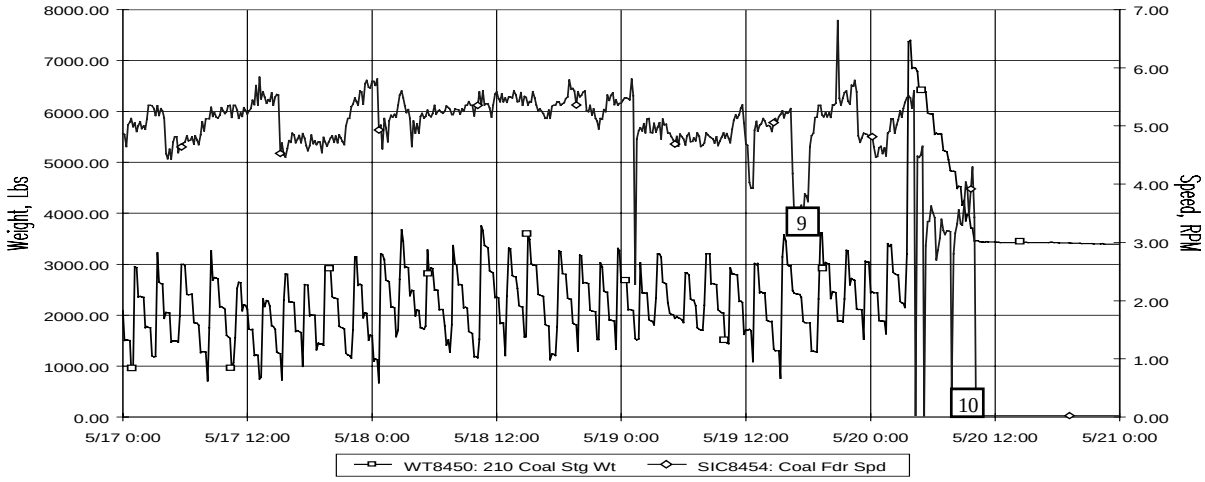

Figure 4.1.2.1-28 Coal Feed System Profile

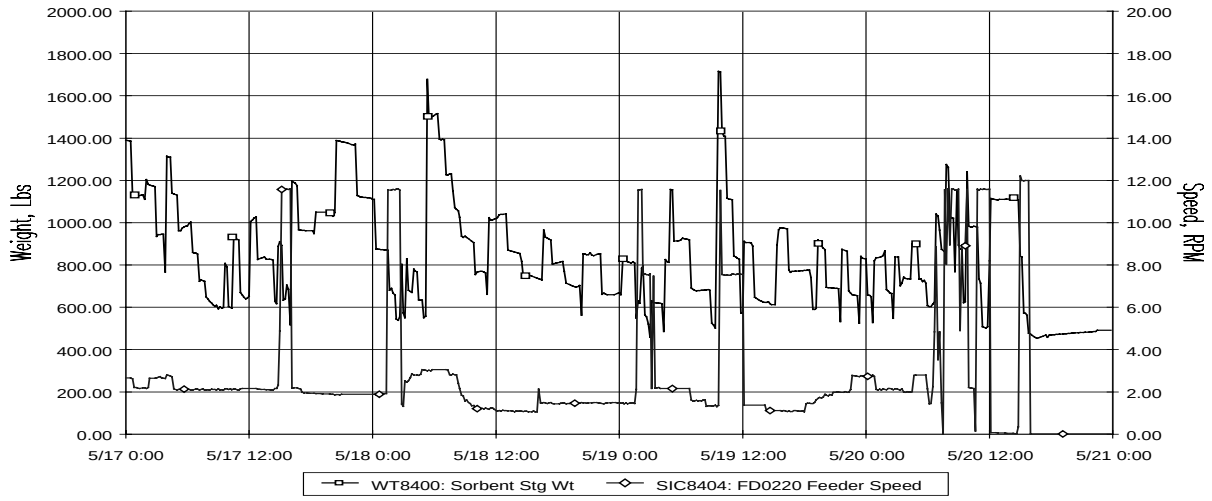

Figure 4.1.2.1-29 Sorbent Feed System Profile

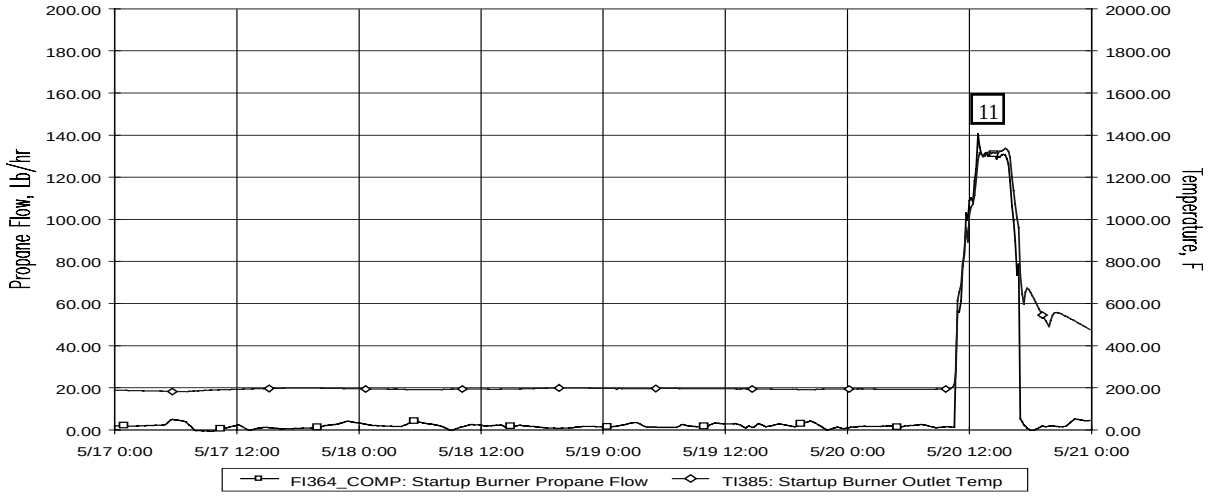

Figure 4.1.2.1-30 Start-Up Burner Flow/Temperature

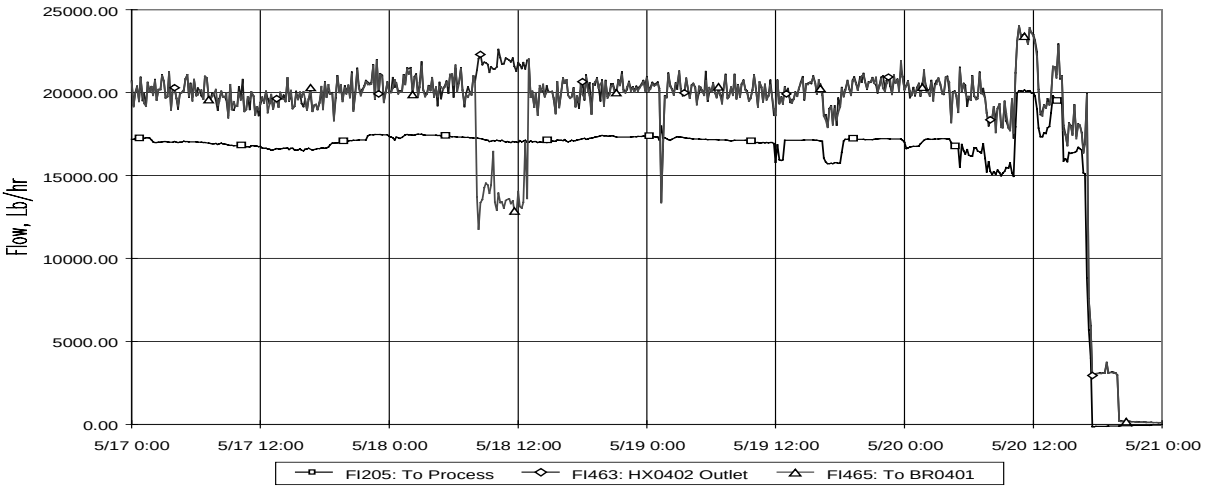

Figure 4.1.2.1-31 Total Gas In/Out Flow Rates

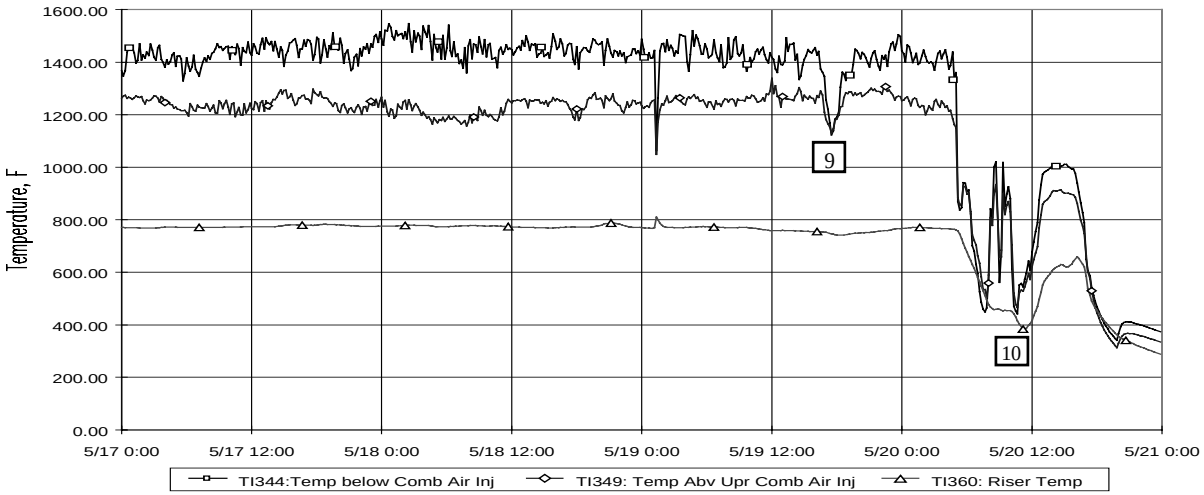

Figure 4.1.2.1-32 Reactor Mixing Zone and Riser Temperatures

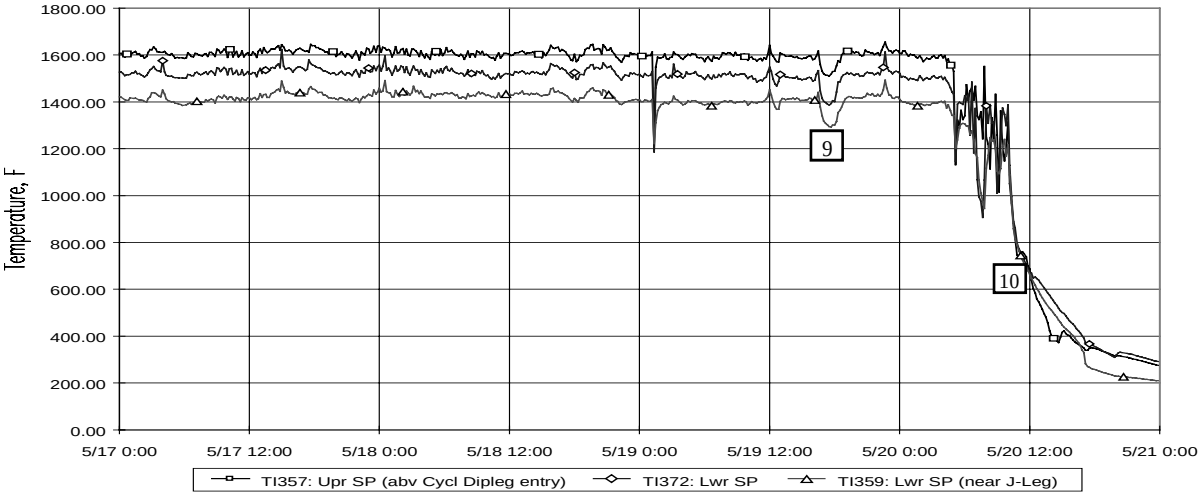

Figure 4.1.2.1-33 Standpipe Temperatures

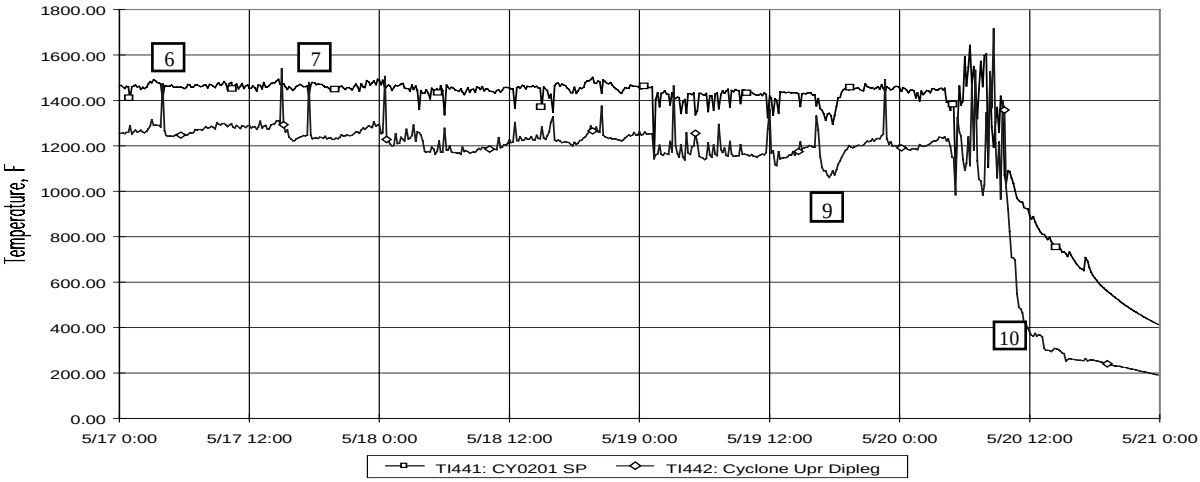

Figure 4.1.2.1-34 Cyclone Dipleg Temperatures

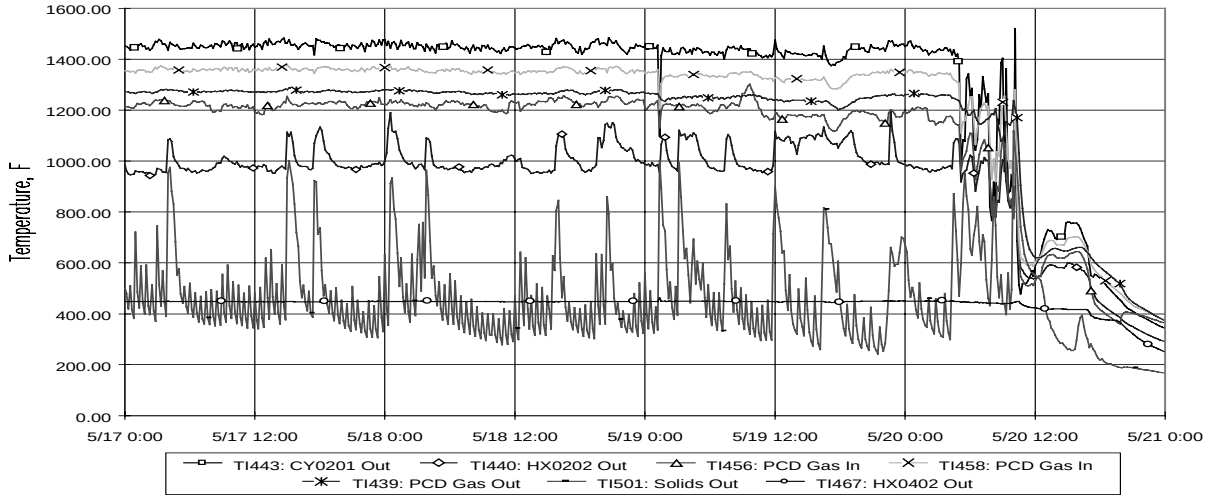

Figure 4.1.2.1-35 Temperature Profile Downstream of Reactor

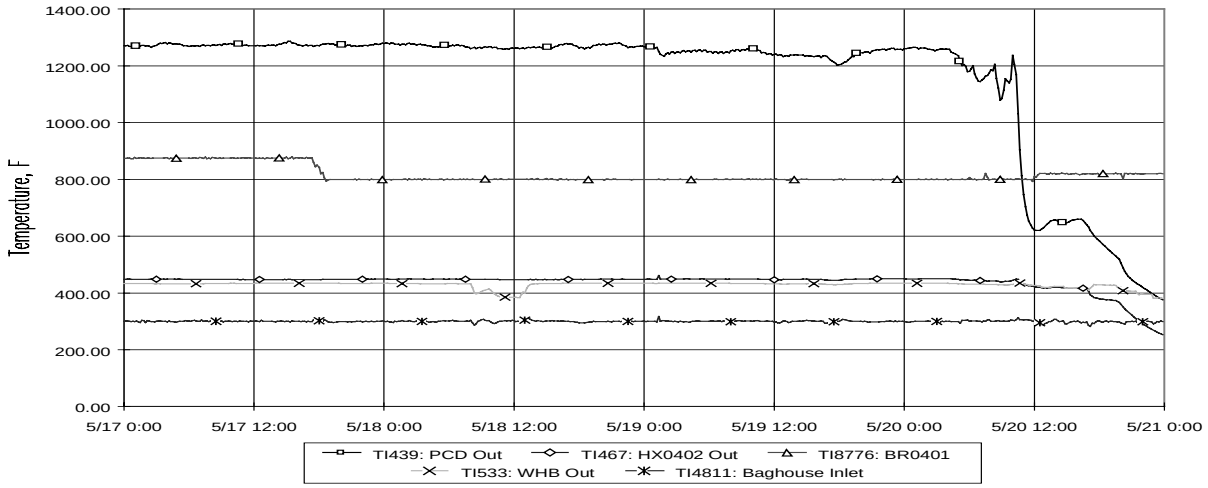

Figure 4.1.2.1-36 System Temperatures Downstream of PCD

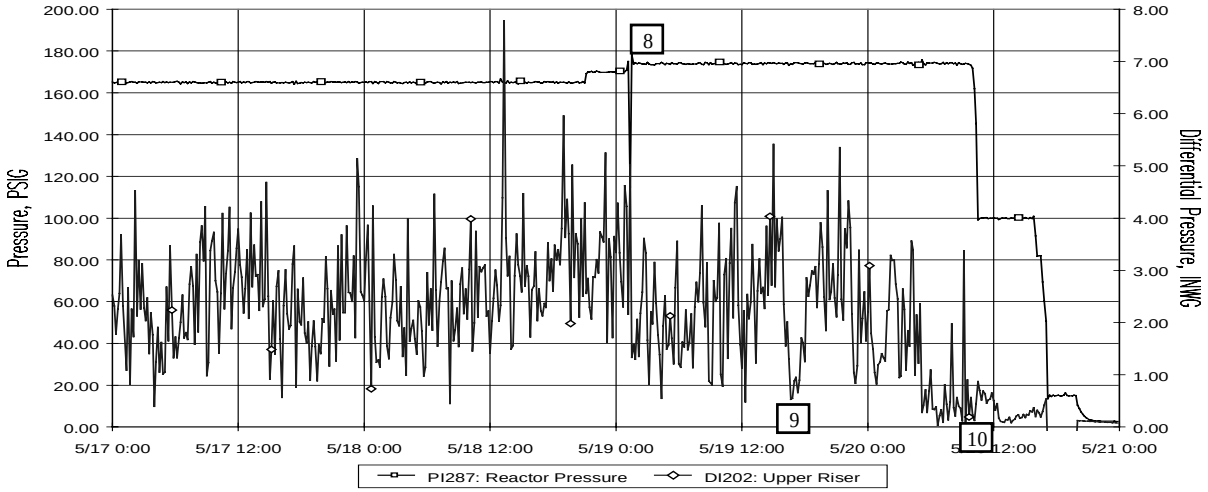

Figure 4.1.2.1-37 Reactor Pressure/Riser Differential Pressure Profiles

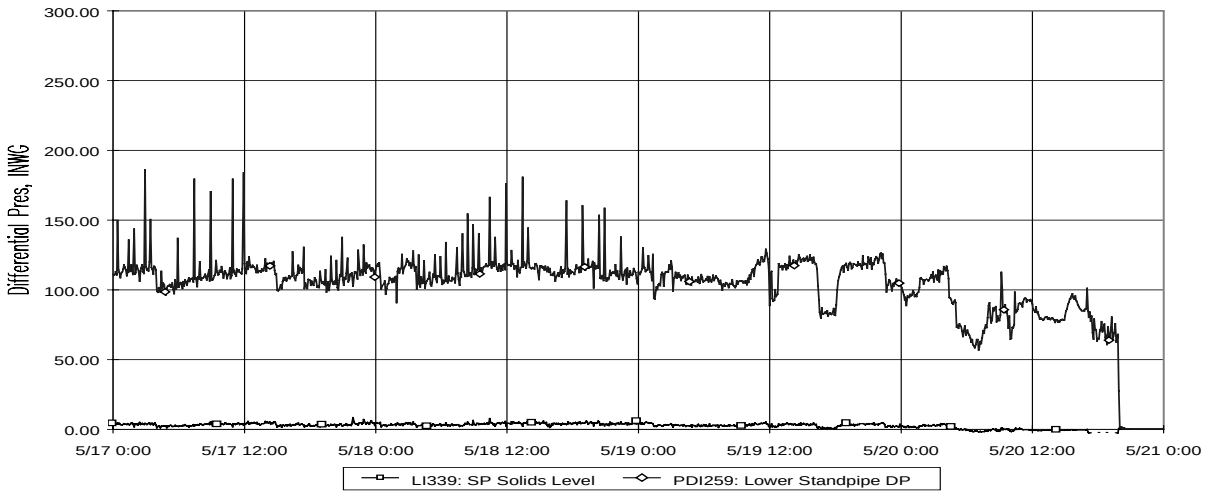

Figure 4.1.2.1-38 Standpipe Differential Pressure Profiles

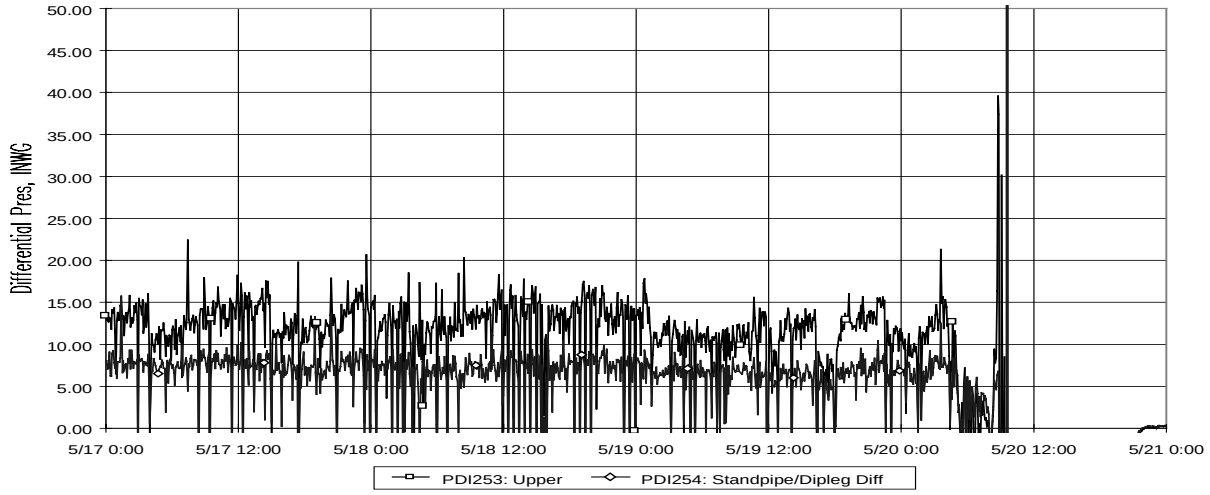

Figure 4.1.2.1-39 Gas Flow Through PCD

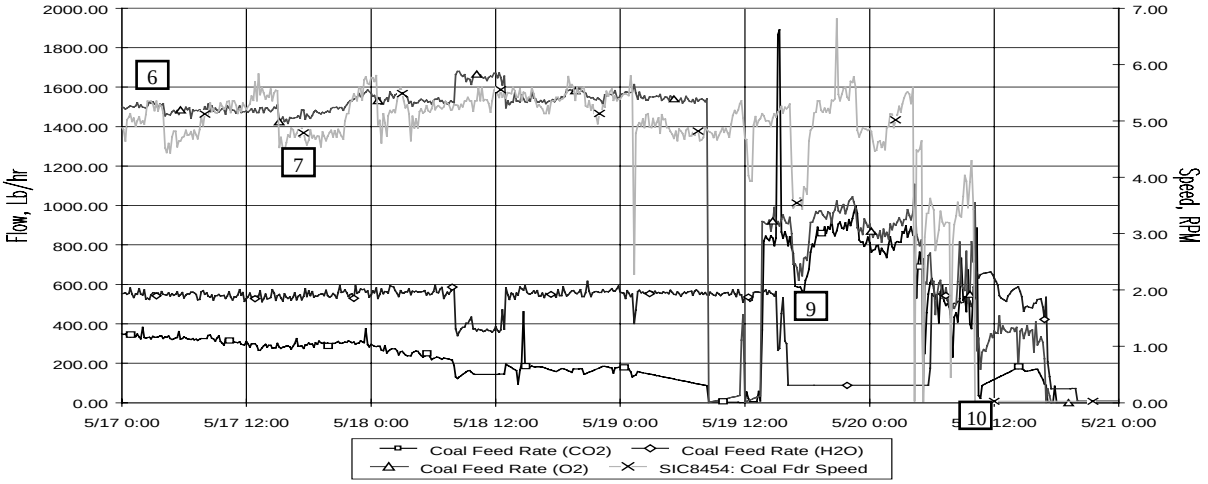

Figure 4.1.2.1-40 Coal Feed Rate Based on Gas Analysis

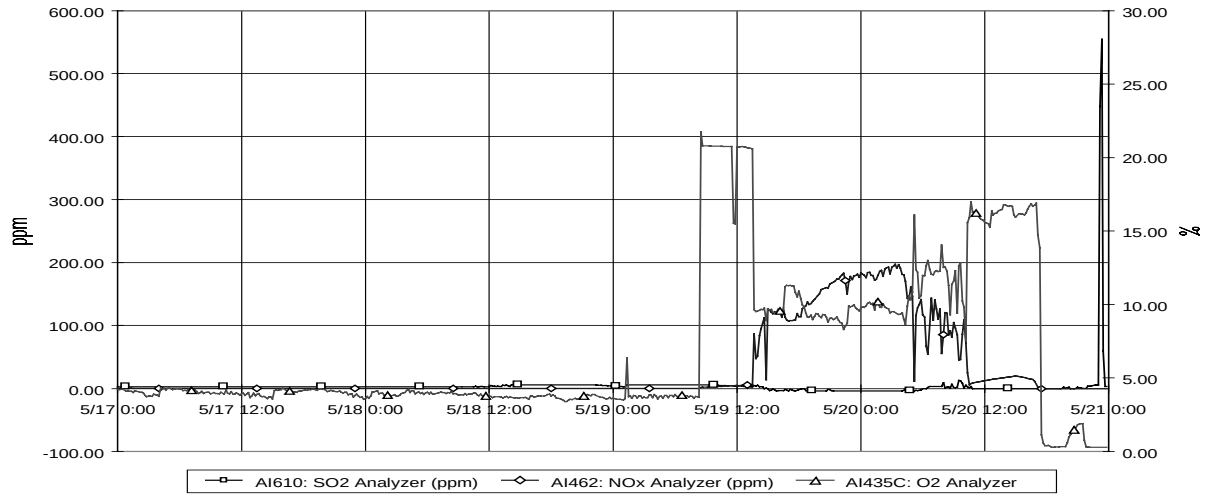

Figure 4.1.2.1-41 O_2, SO_2 and NO_x Analyzers

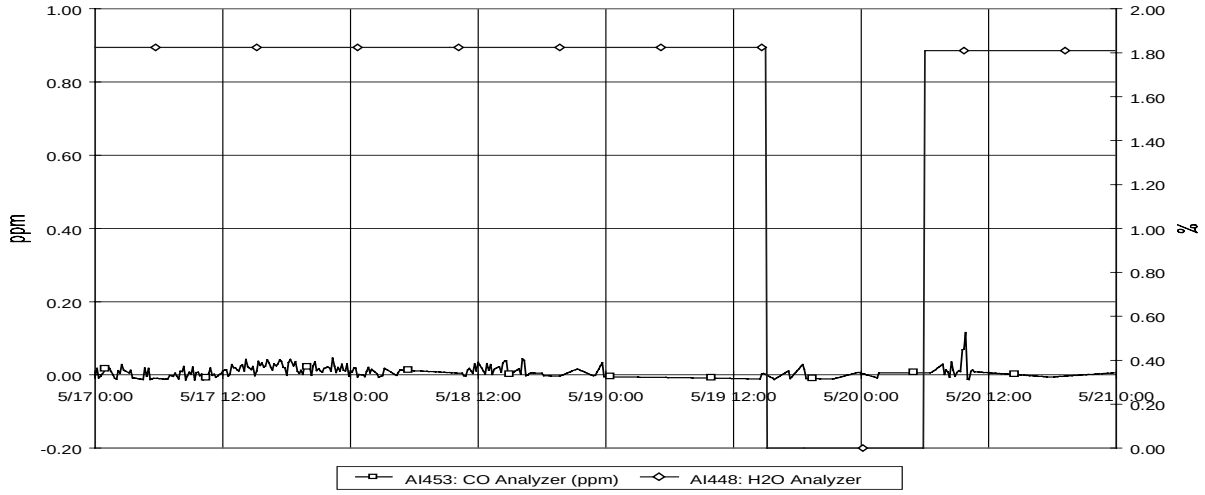

Figure 4.1.2.1-42 CO and H_2O Analyzers

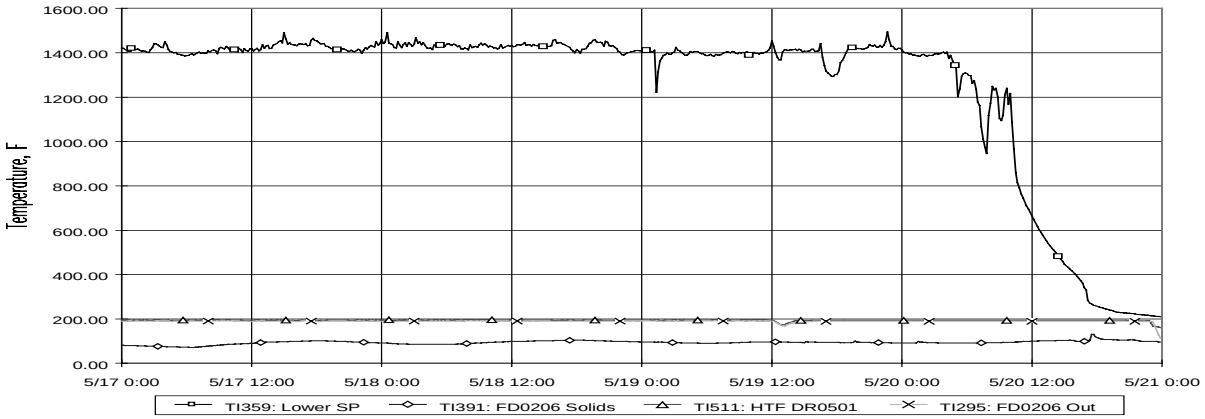

Figure 4.1.2.1-43 FD0510 Temperature Profiles

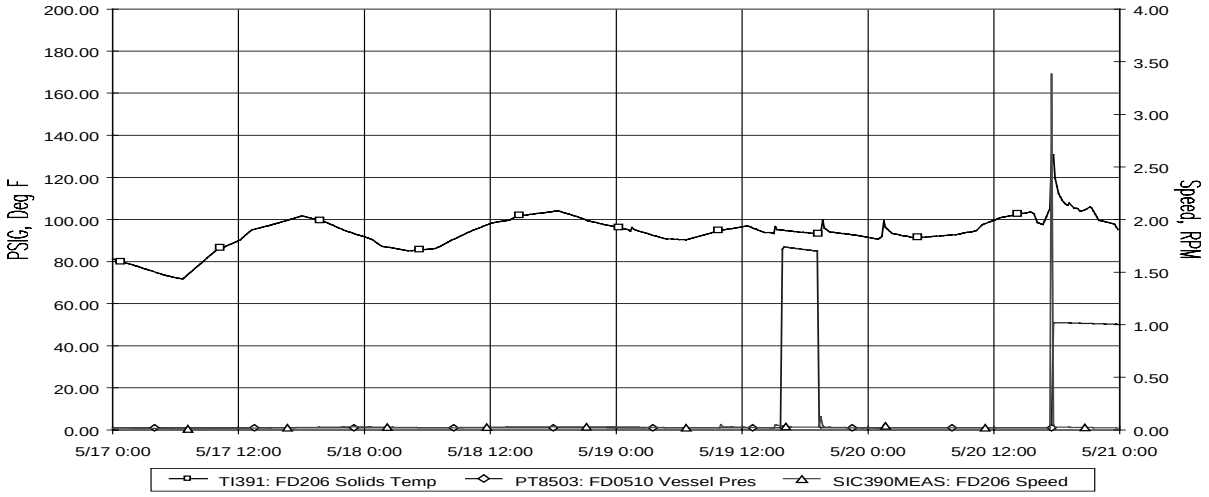

Figure 4.1.2.1-44 FD0206 Profiles

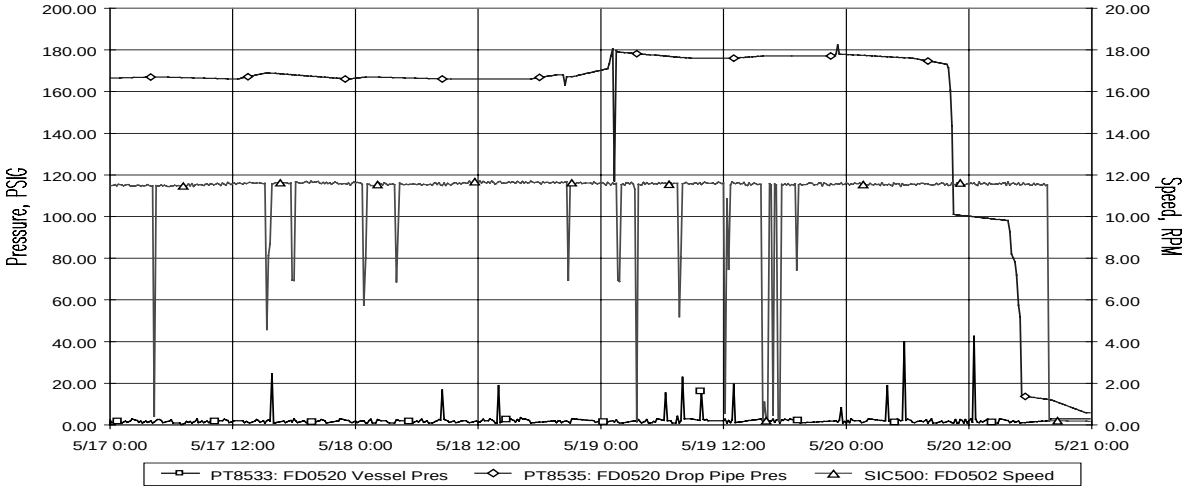

Figure 4.1.2.1-45 FD0520 Pressure Profiles

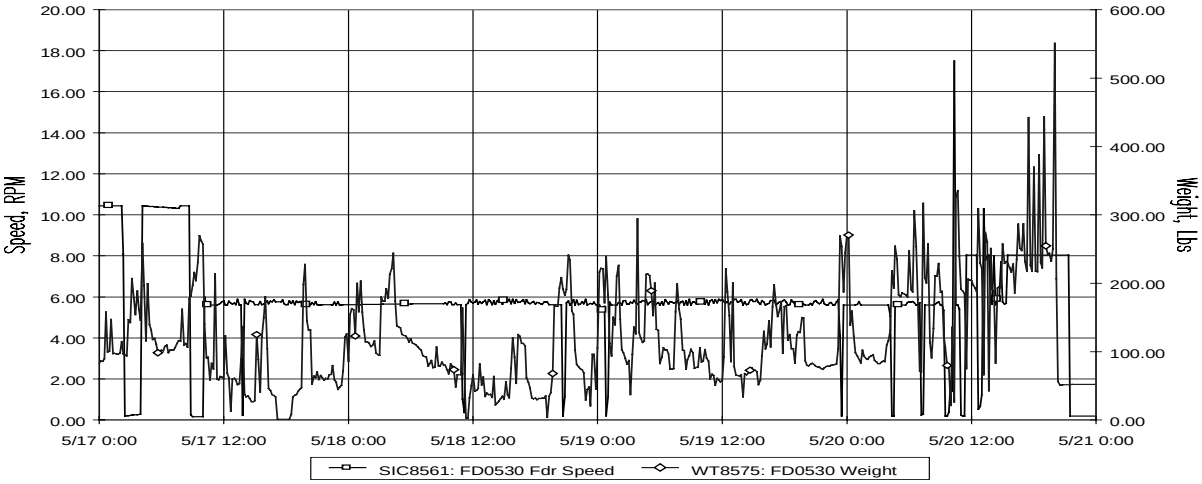

Figure 4.1.2.1-46 FD0530 System Profiles

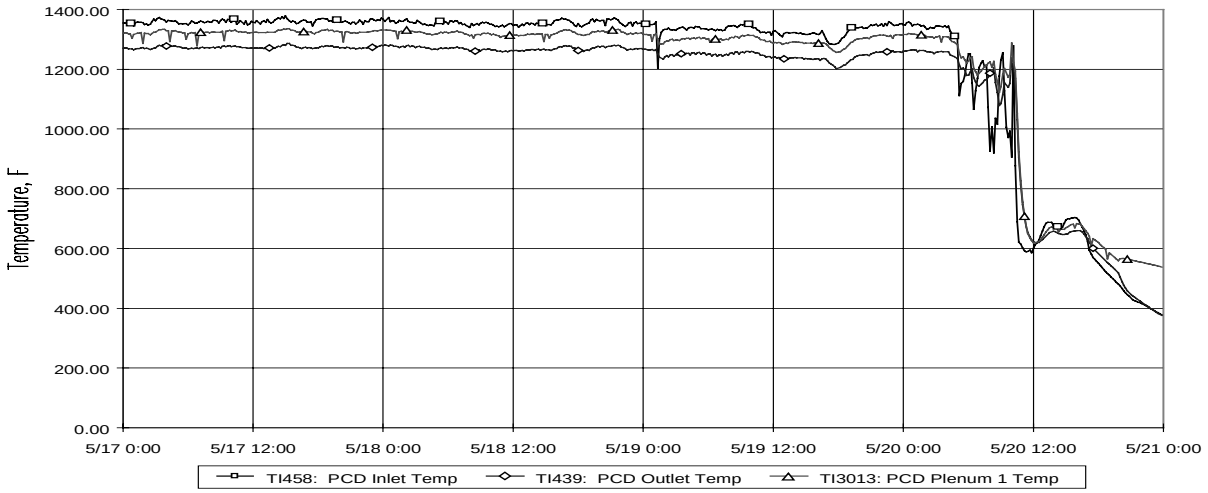

Figure 4.1.2.1-47 PCD Temperatures

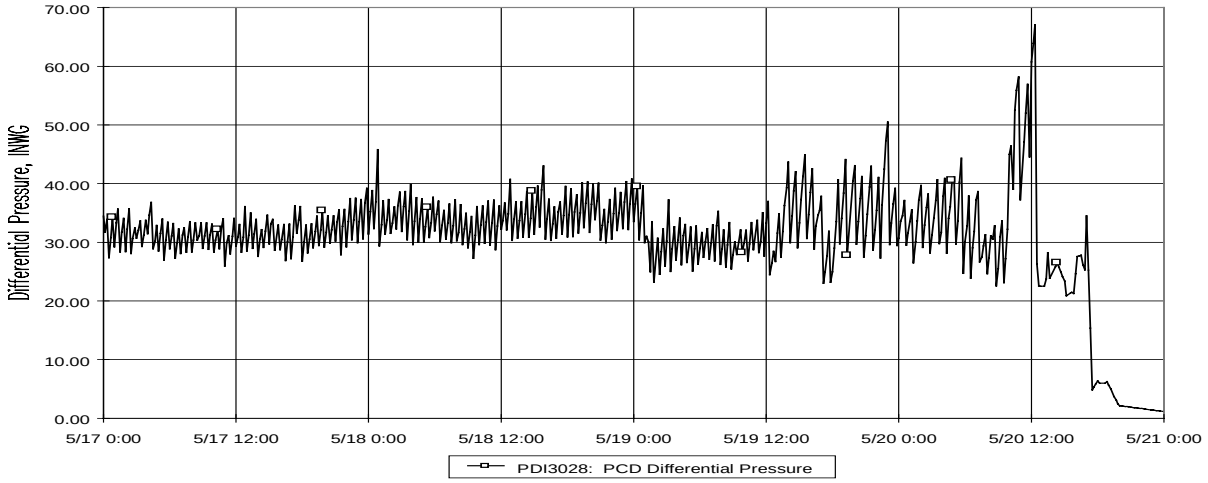

Figure 4.1.2.1-48 PCD Differential Pressure Profile

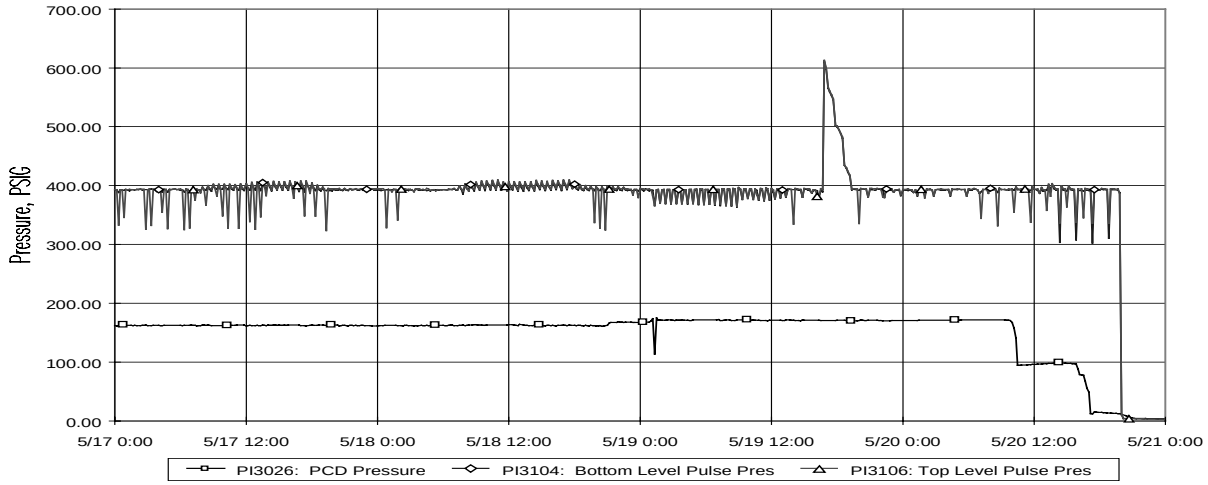

Figure 4.1.2.1-49 PCD Pressure and Pulse Pressure

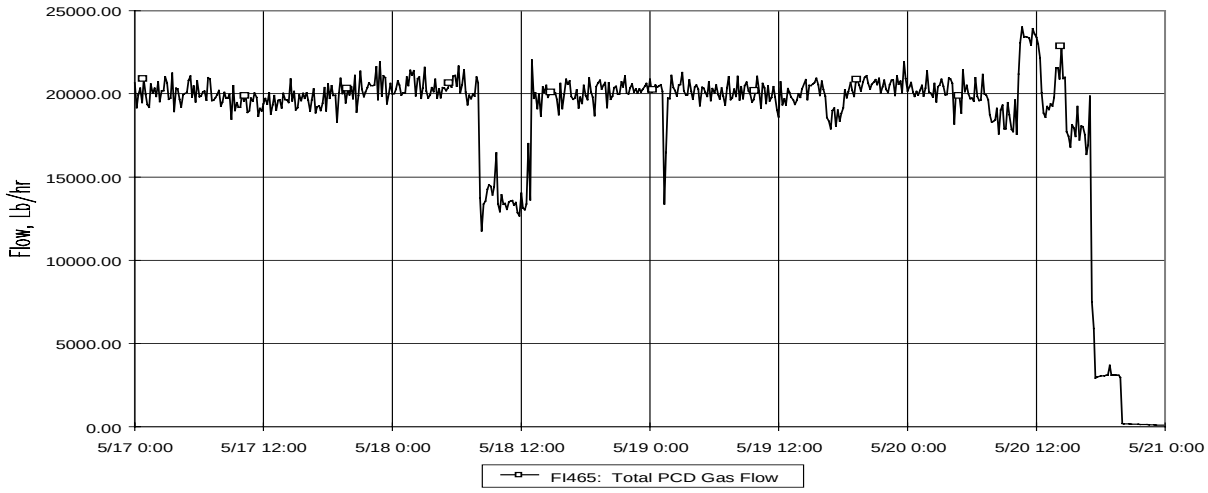

Figure 4.1.2.1-50 Gas Flow Through PCD

4.1.2.2 Characterization Test Run CCT5B

Test run CCT5B was a continuation of CCT5A conducted between May 23 and May 27, 1997. Operating plots are shown in figures 4.1.2.2-1 through -50.

CCT5B Test Run Chronology

- On May 21, 1997, after all reactor inspections were complete and the clinkers were removed from the dipleg the reactor system was started. The following day the leak test was successfully performed and the sulfator burner (BR0602) was lit. The PCD preheat was completed at 07:35 with the PCD exit temperature reading 286°F (event 1, figure 22). Several attempts to light the start-up burner (BR0201) were unsuccessful. The reactor was depressurized to atmospheric pressure and the BR0602 was shut down in preparation for pulling the igniter. A new burner igniter and flamerod were installed but the pilot would not light after numerous trials. The pilot assembly was then pulled and the pilot tip was found missing. A new pilot tip was installed. The BR0602 was lit and shortly thereafter BR0201 was lit without any problems. The BR0602 was ramped down and shutoff at 23:12. The spent solids transport (FD0510) plugged due to large clinkers in the line. The FD0510 was cleared and put back on-line.

- Sand was then added to the reactor and at 04:15 on May 23, 1997, coal feed was started (event 2, figures 2 and 6 through 9). At 06:00 problems with the coal feeder system (FD0210) lockhopper developed. Coal was not being transferred into the dispense vessel. Various measures with the coal feed lockhopper resulted in transfer of coal to the dispense vessel. At 06:40 the gas analyzers were put into service (event 3, figure 16).

- At 06:50 dolomite addition was started and the SO_2 level in the exit gas immediately dropped (event 4, figures 3 and 16). The BR0201 was shutdown at 10:00 and the reactor pressure was increased to 160 psig (event 5, figure 12). All purge and aeration flows were set for the higher operating pressure. Between 06:20 and 16:33 the average dolomite feed rate was 280 lb/hr.

- On May 24, 1997, the spent fines transport system (FD0520) solids samples were collected in drums for testing at DOE/FETC. Early in the morning the dolomite feed rate was decreased. At 06:45 there was slugging in the cyclone dipleg after the PCD back-pulse but it recovered within 3 minutes. At 11:07 solid transfer through the dipleg was upset for 1 minute, but it was not related to a back-pulse. The solid transfer through the dipleg was again upset for 1 minute, 8 minutes after the 12:00 back-pulse. Apparently the brief upsets in the solid transfer through the dipleg are not solely affected by PCD back-pulses.

- At 14:00 FD0210 tripped because the feed line to the reactor was plugged. After 10 minutes the plug was cleared and the temperatures in the reactor recovered (event 6, figures 27, 31 through 34, and 38). The reactor feed line plugged several more times

throughout the day and night. The FD0520 and the spent solids feeder system (FD0530) discharge lines also plugged several times. The plugs were cleared and the systems were put back on-line to continue operations. The average coal feed for May 24, 1997, was 1,000 lb/hr.

- Reactor conditions were held steady throughout May 25, 1997, with only some minor adjustments made to aeration flows as the reactor pressure was increased to 180 psig (event 7, figure 37). The average coal feed rate for the day was 1,030 lb/hr.

- Plugging problems in the discharge line of FD0530 continued on May 26, 1997. Problems with the transport air dryer (DY0210) caused FD0210 to trip twice during the morning. After the FD0210 trip the dipleg operations were unsteady for about 4 minutes. The conveying medium was switched to nitrogen while DY0210 was repaired.

- When the PCD back-pulsed at 09:46 the cyclone dipleg was upset for 7 minutes. The high solids carryover rate induced by the dipleg upset caused the reactor solids level to drop, resulting in a lower circulation rate. The reactor standpipe level dropped from about 125 inH_2O to 103 inH_2O (event 8, figure 38). The coal feeder speed was lowered to maintain the riser temperature at 1,600°F. The DY0210 problems were solved and it was returned to operations. Conveying gas flow was switched back from nitrogen to air. Aeration flows were adjusted and the combustor heat exchanger (HX0203) started circulating very well. The coal feed rate was increased to maintain the reactor temperature. The average coal feed rate for May 26, 1997, was 1,065 lb/hr.

- Problems with FD0210 developed during the morning of May 27, 1997. Again, coal was not dropping from the lockvessel into the dispense vessel. At 06:30 coal feed was lost and the reactor temperatures dropped (event 9, figures 27, and 30 through 34). The reactor pressure was reduced in preparation to light BR0201. At 06:40 control of the pressure letdown valve (PV287) was lost. It failed closed and the reactor pressure increased rapidly to above 250 psig. The main air compressor (CO0201) was tripped to keep the pressure from rising any higher. The control valve was manually opened and the reactor pressure was gradually dropped from over 200 to 43 psig (event 10, figure 37). The CO0201 was restarted and there was an orderly shutdown of the transport reactor (event 11, figure 26).

CCT5B Post Test Run Inspections

The reactor was inspected and no major problems were noticed. There was some powder on the walls of the riser, and the small crack around the top of the riser was about the same size as in previous observations. The riser crossover was borescoped. Erosion was about the same as on the May 5, 1997, inspection. The bottom of the crossover was about one-third full of solids and had more sand than ash. The disengager had some small globules on the wall. The reactor J-leg was totally clear. The disengager-cyclone (secondary) crossover was also borescoped. The feathered leading edge of the new refractory that had been poured to restrict the inlet of the

cyclone still had a gap that appeared large via the borescope, but when measured it was only about 0.1 inch. There was some dust on the walls of the cyclone and there was also a small amount of dust on the top of the inlet part of the slanting portion of the cyclone dipleg line. Otherwise, the line was clean all the way to the standpipe. The cyclone exit was borescoped, but not much could be observed. Start-up burner inspections showed that the pilot tip had again partially burned out.

CCT5B Test Run Observations

This test was terminated due to problems with the pressure letdown valve and the coal feeder system. The coal feeder lock vessel bridged/plugged preventing the transfer of coal into the dispense vessel. While reducing reactor pressure to light the burner, the pressure letdown valve started vibrating causing the position controller to work loose. The control of the valve was lost and the reactor pressure rapidly increased from 180 to 260 psig.

Dolomite was fed for sulfur capture as well as for aiding solids flow in the cyclone dipleg. Smooth operation of the cyclone dipleg and solids circulation through the reactor and HX0203 J-legs enabled operation of the reactor at higher coal feeds for longer periods. Unlike previous test runs, the smooth operation of the cyclone dipleg also resulted in an overall increase in solids inventory in the reactor by about 5,000 lb using coal ash and dolomite. Sand addition for any inventory makeup was minimal. In addition to concentrating on reactor operations the recycle gas compressor was tested with process gas. A total of 99 hours on coal was achieved and a total of 48 tons of coal were fed in this CCT5B test run.

Section 4.1.2.2

Graphs 1 through 25

Test Run CCT5B

May 21 through 23, 1997

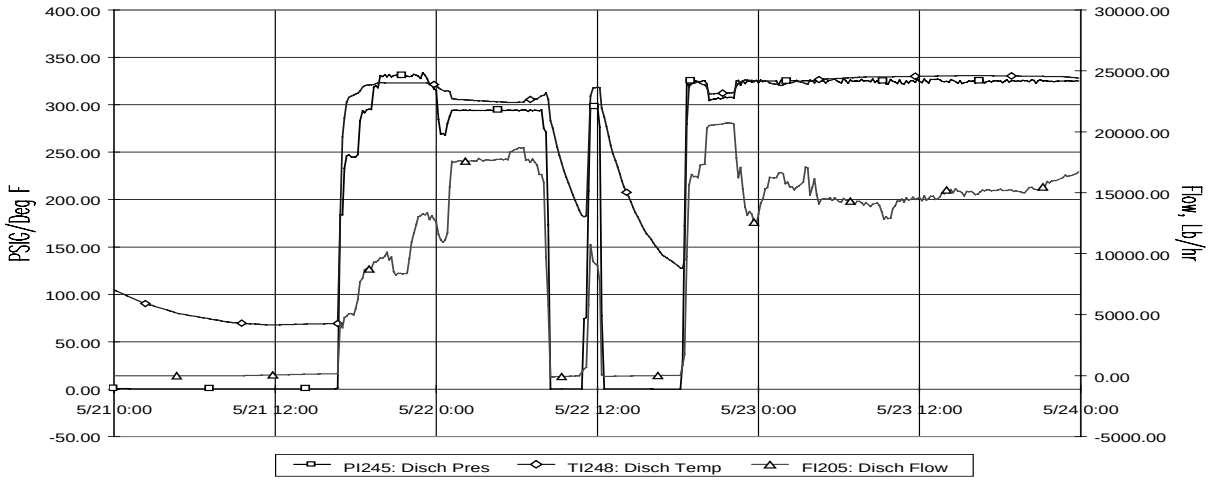

Figure 4.1.2.2-1 CO0201 System Profile

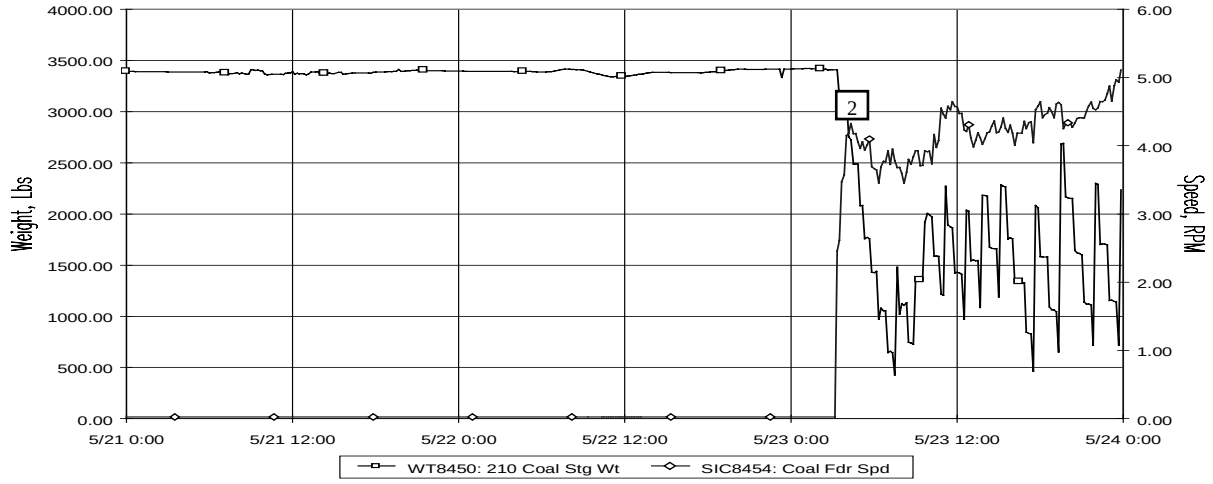

Figure 4.1.2.2-2 Coal Feed System Profile

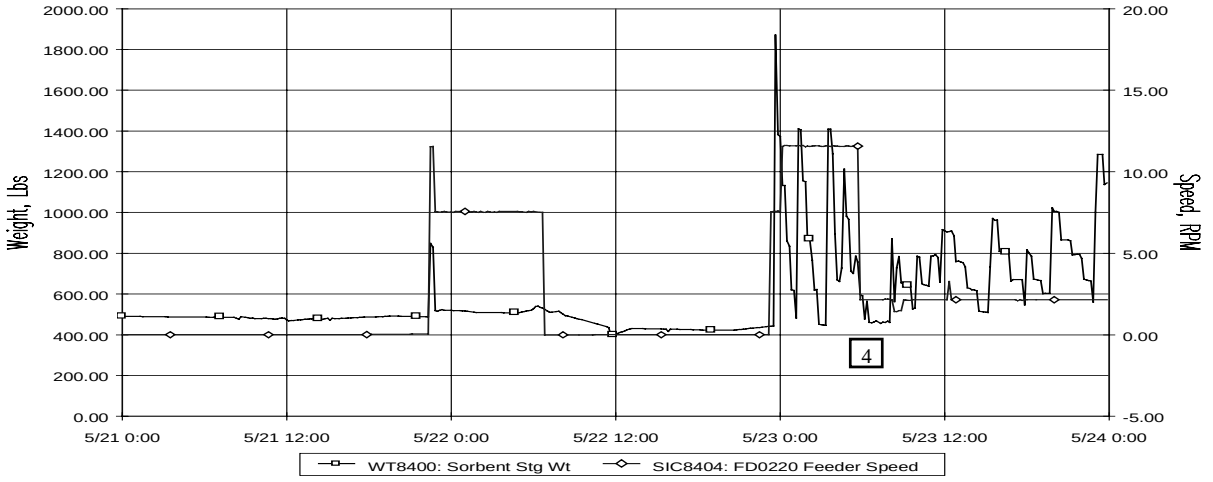

Figure 4.1.2.2-3 Sorbent Feed System Profile

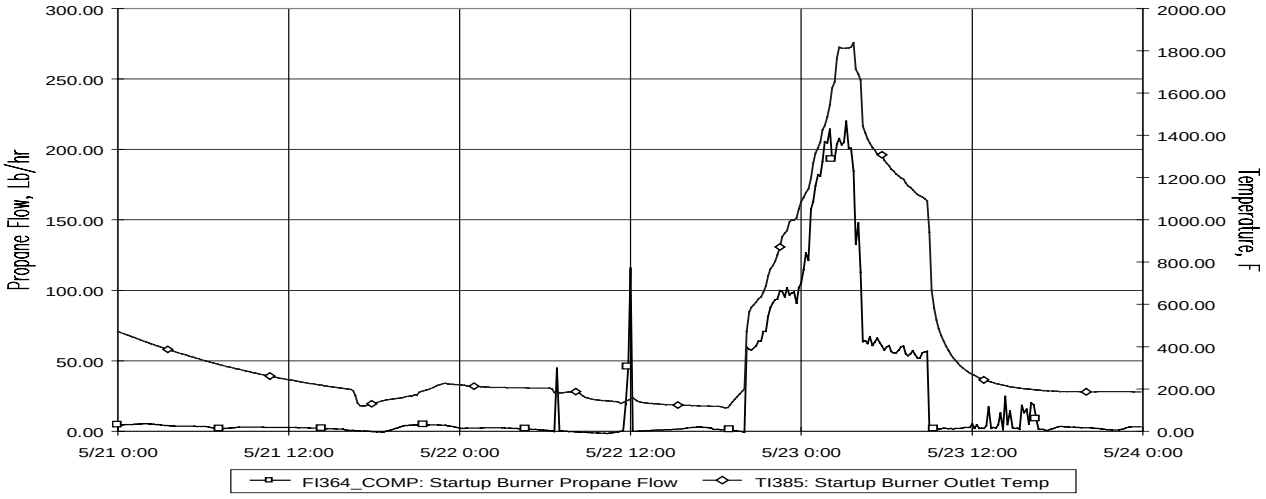

Figure 4.1.2.2-4 Start-Up Burner Flow/Temperature

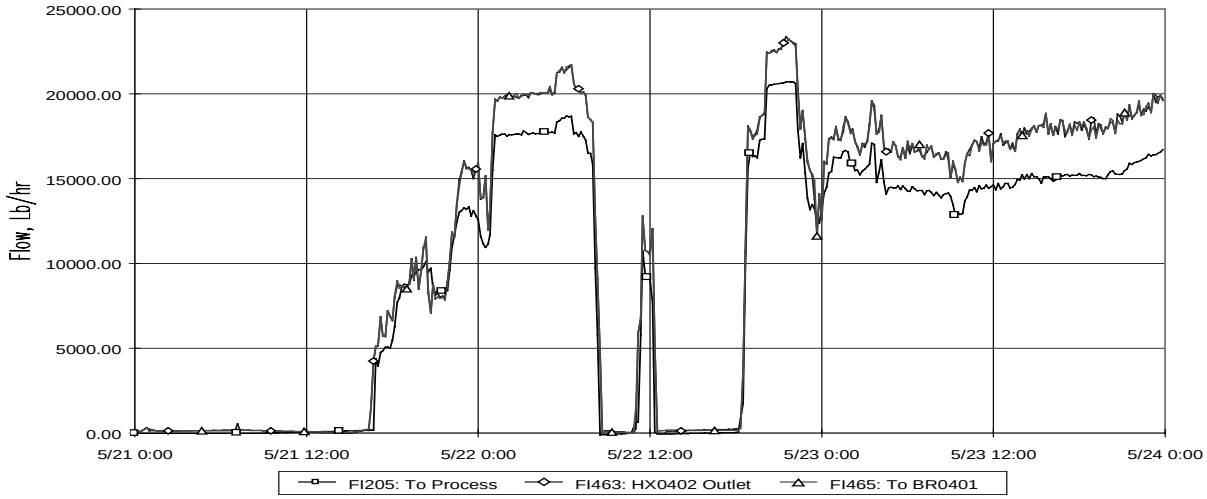

Figure 4.1.2.2-5 Total Gas In/Out Flow Rates

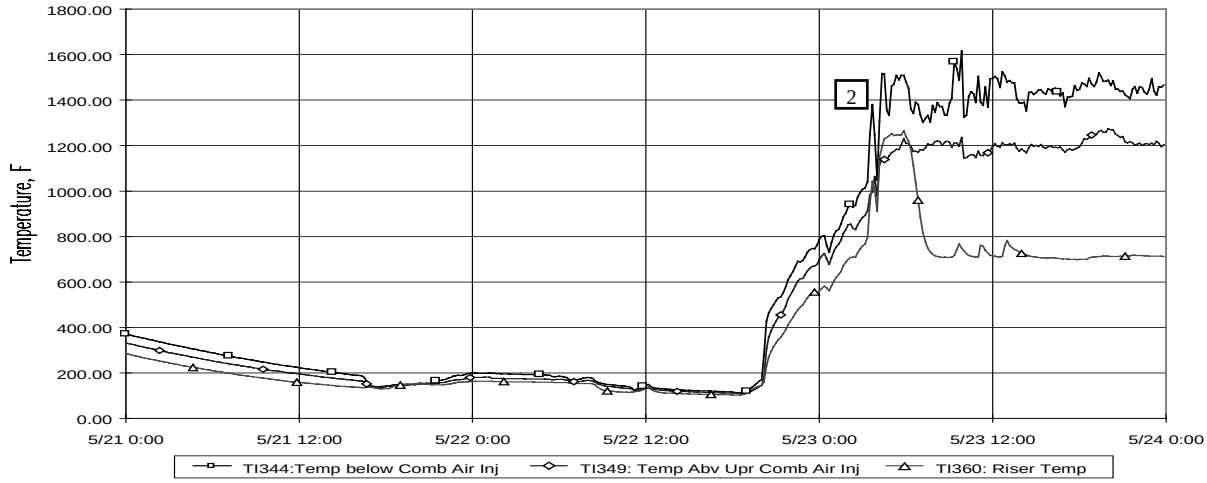

Figure 4.1.2.2-6 Reactor Mixing Zone and Riser Temperatures

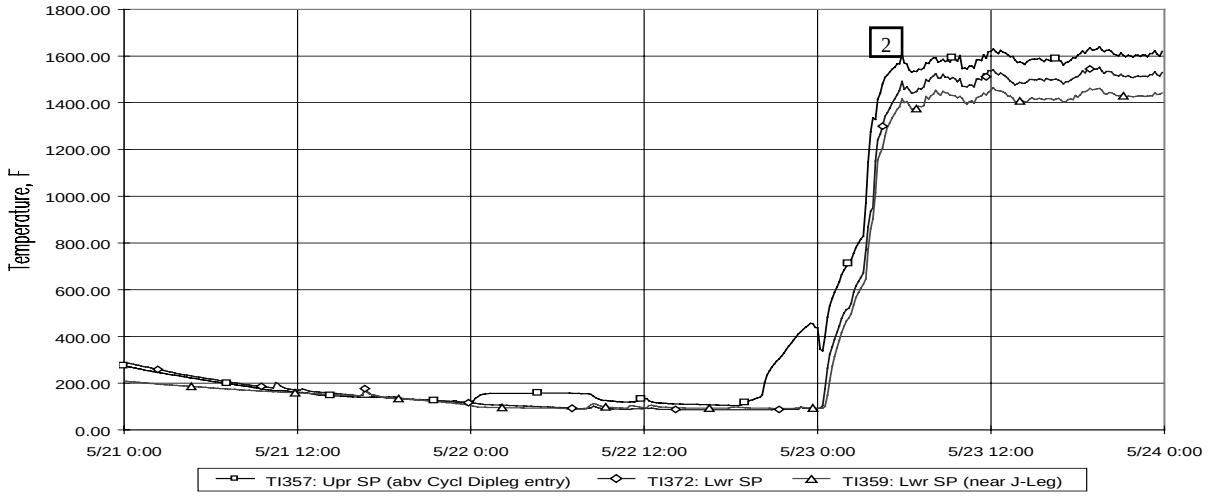

Figure 4.1.2.2-7 Standpipe Temperatures

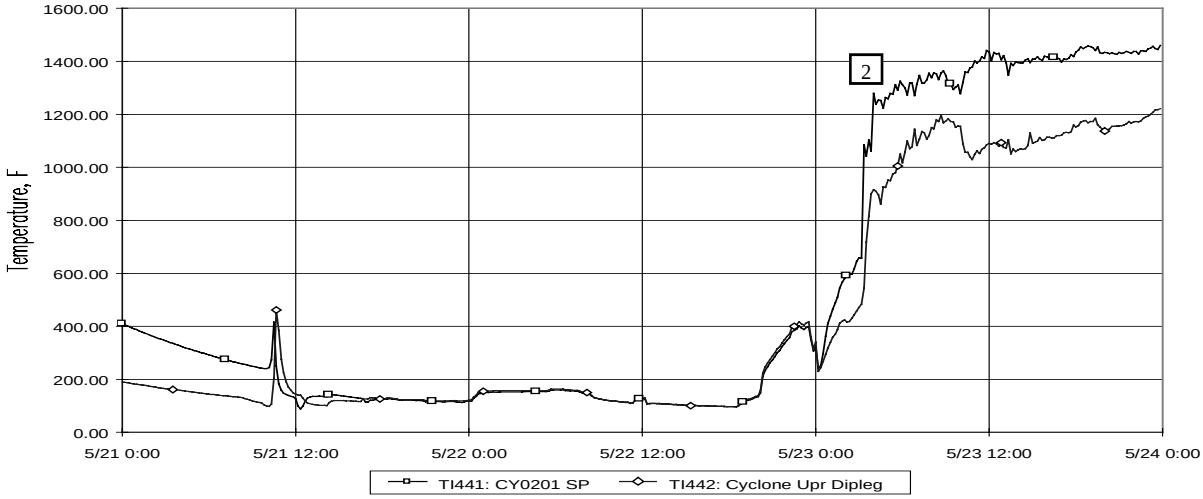

Figure 4.1.2.2-8 Cyclone Dipleg Temperatures

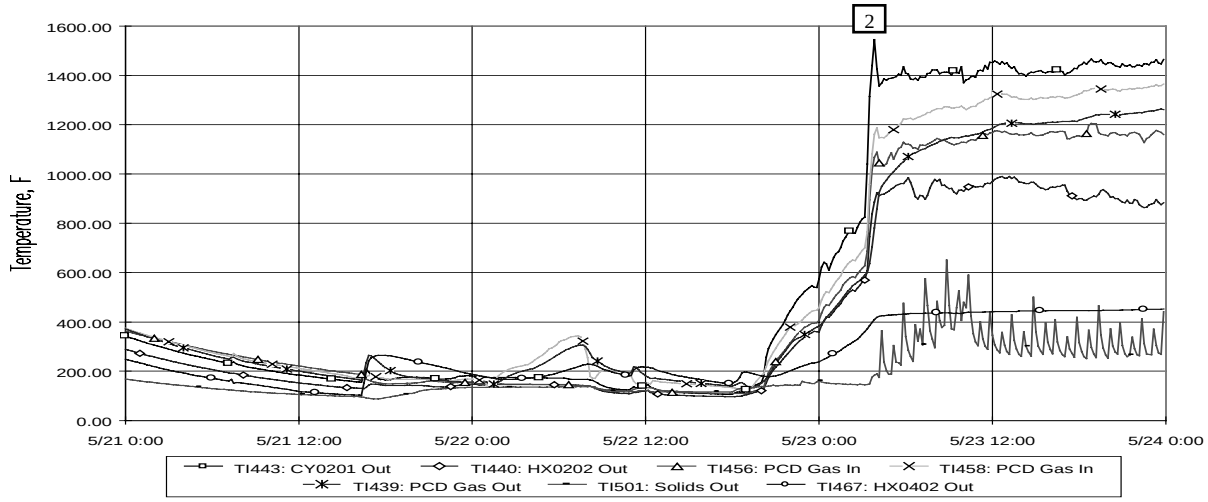

Figure 4.1.2.2-9 Temperature Profile Downstream of Reactor

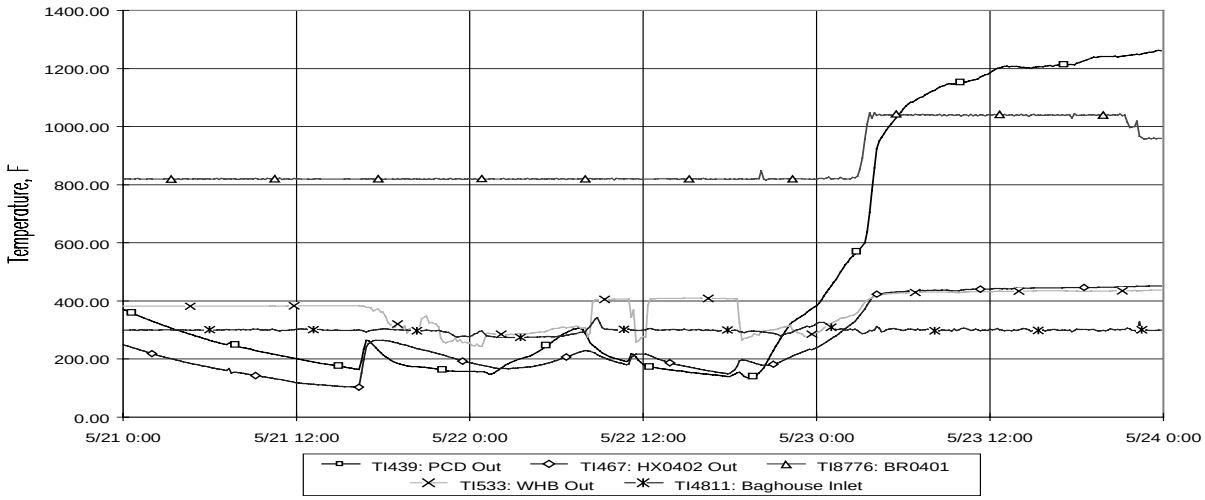

Figure 4.1.2.2-10 System Temperatures Downstream of PCD

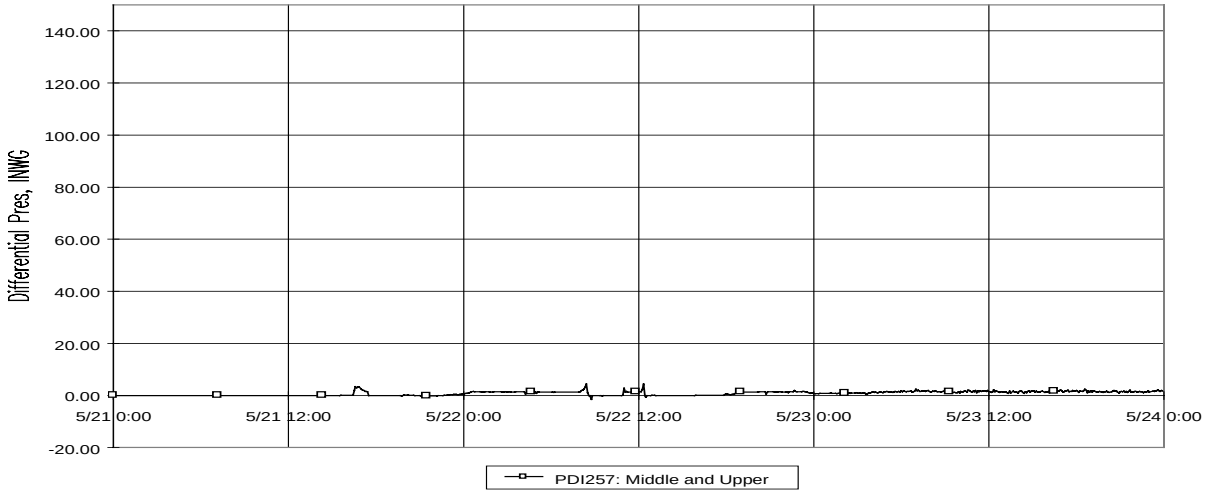

Figure 4.1.2.2-11 Mixing Zone Differential Pressure Profile

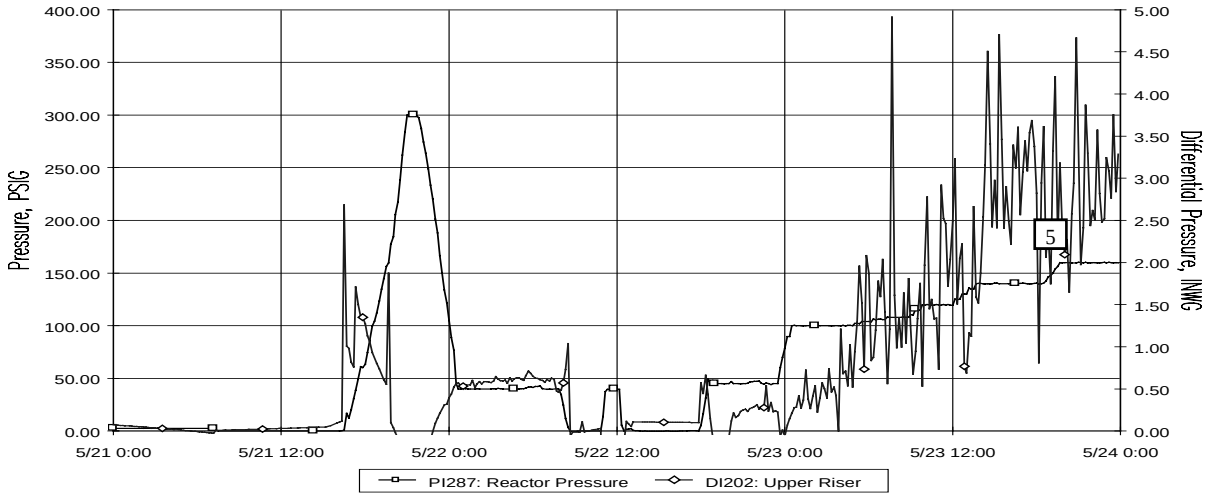

Figure 4.1.2.2-12 Reactor Pressure/Riser Differential Pressure Profiles

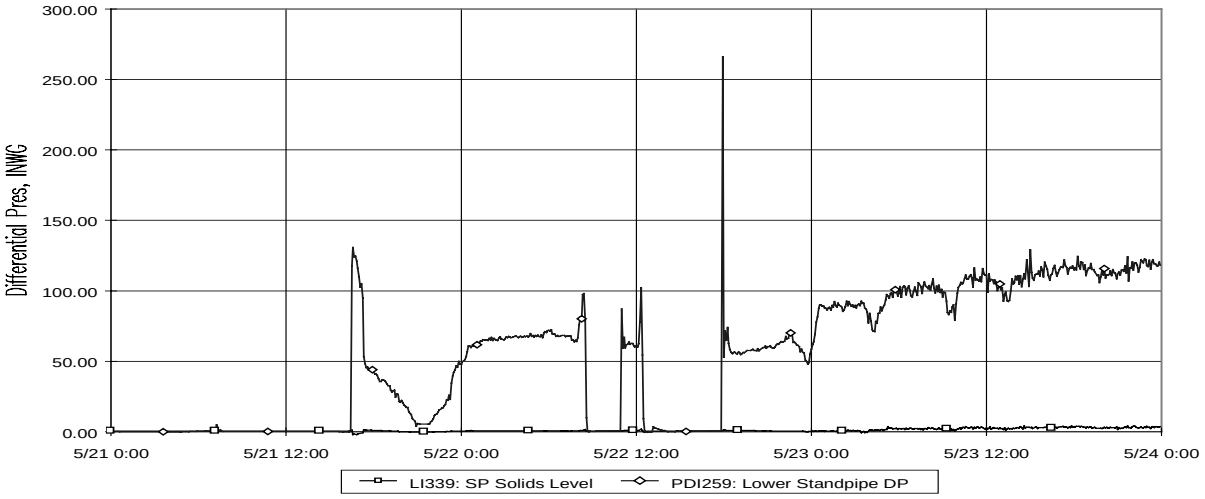

Figure 4.1.2.2-13 Standpipe Differential Pressure Profiles

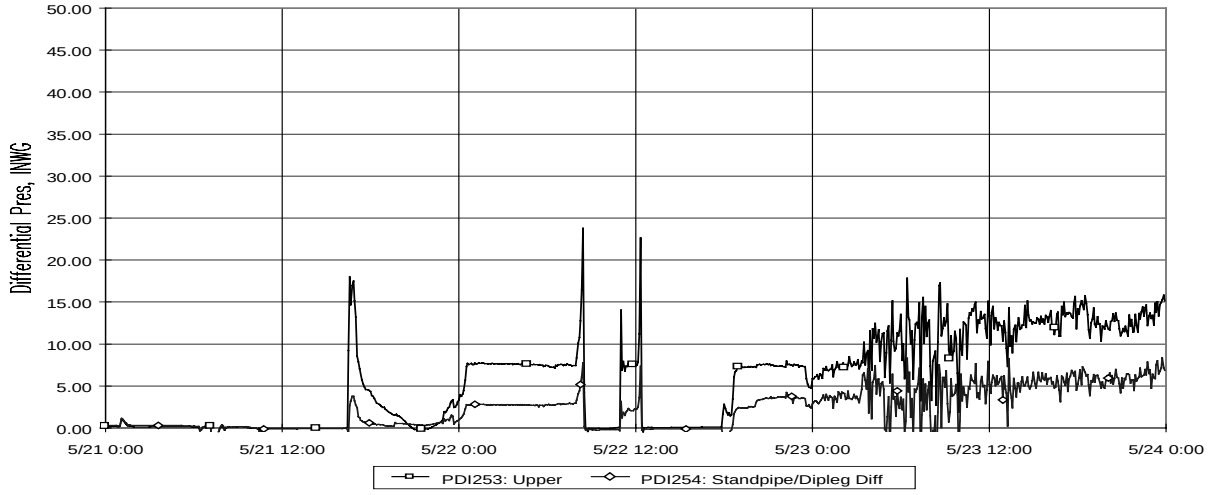

Figure 4.1.2.2-14 CY0201 Dipleg Differential Pressure Profiles

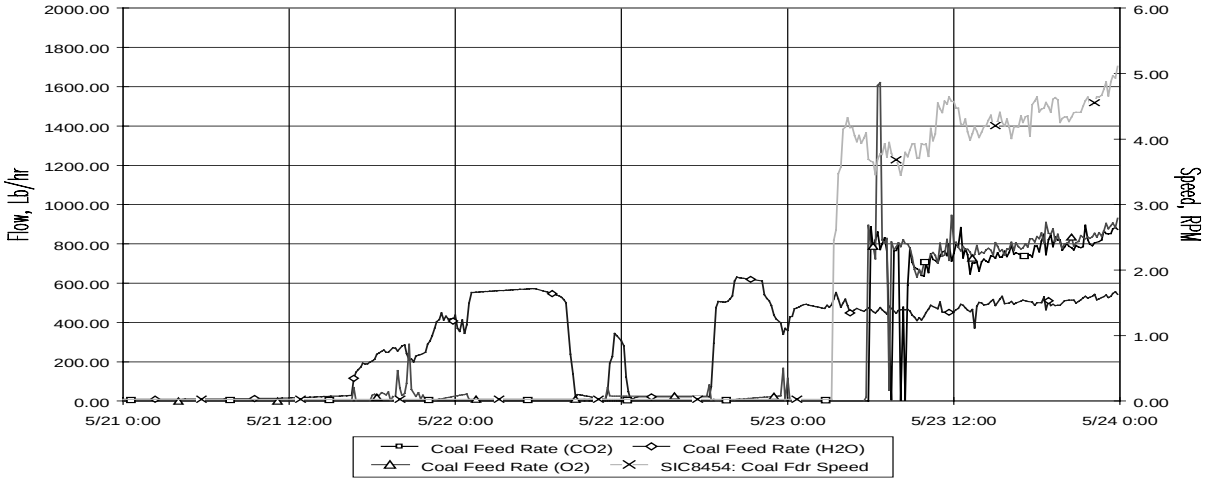

Figure 4.1.2.2-15 Coal Feed Rate Based on Gas Analysis

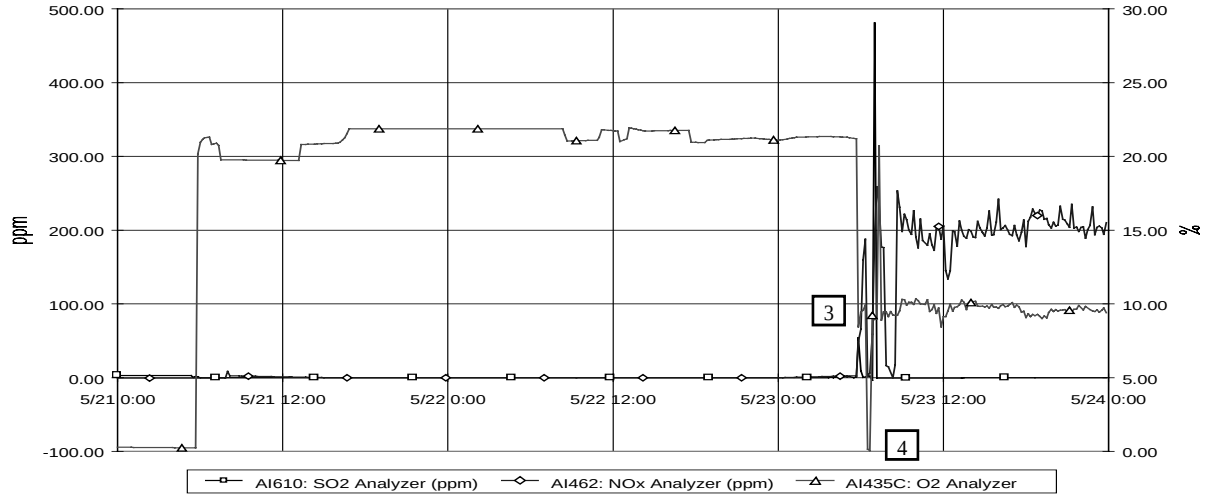

Figure 4.1.2.2-16 O_2, SO_2, and NO_x Analyzers

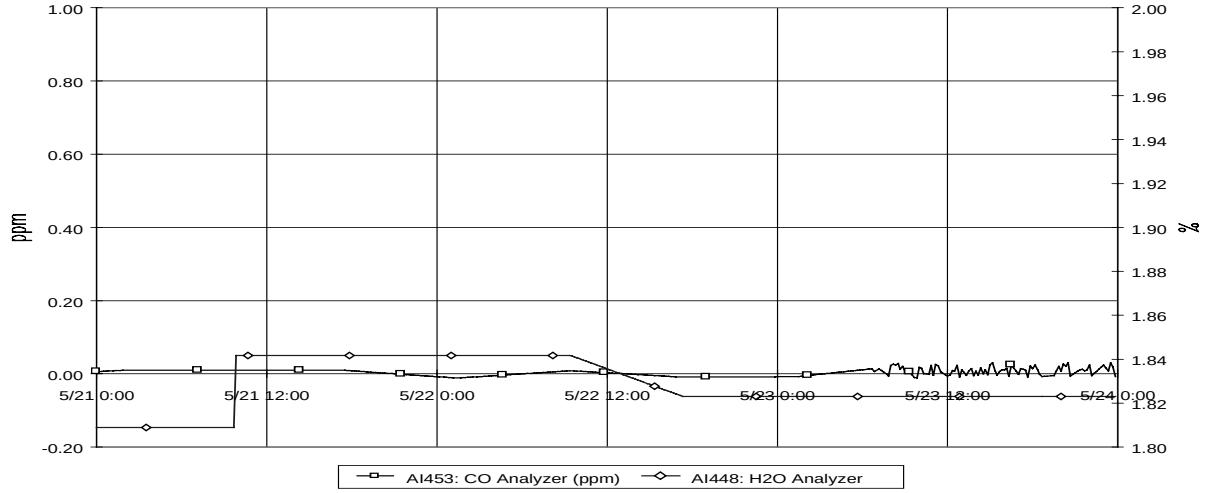

Figure 4.1.2.2-17 CO and H_2O Analyzers

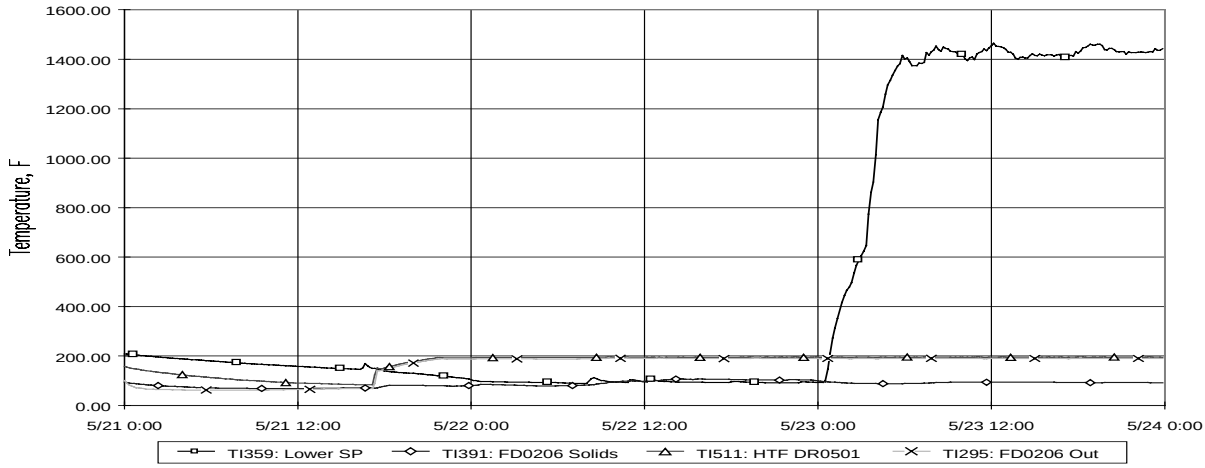

Figure 4.1.2.2-18 FD0510 Temperature Profiles

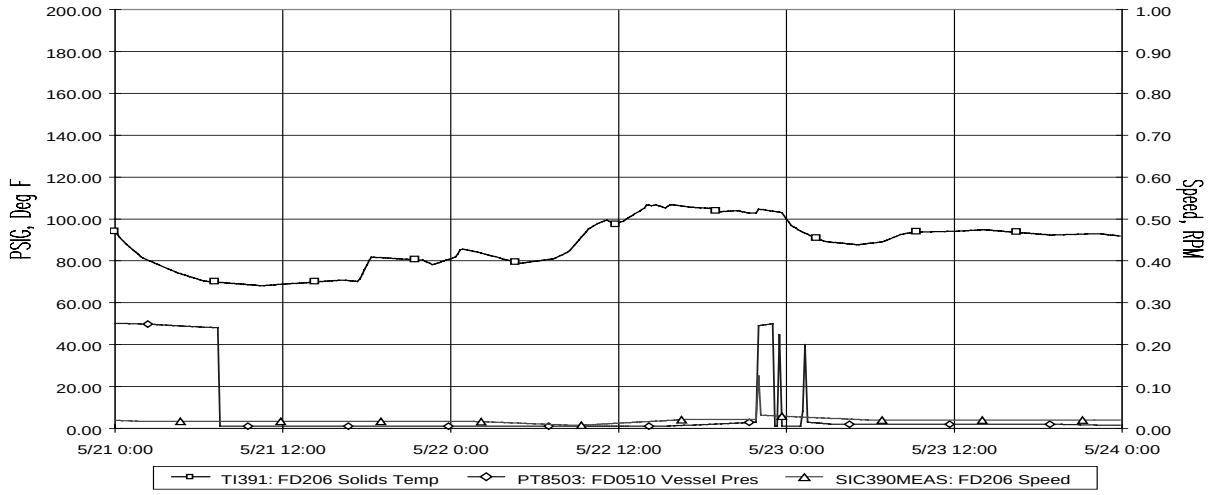

Figure 4.1.2.2-19 FD0206 Pressure Profiles

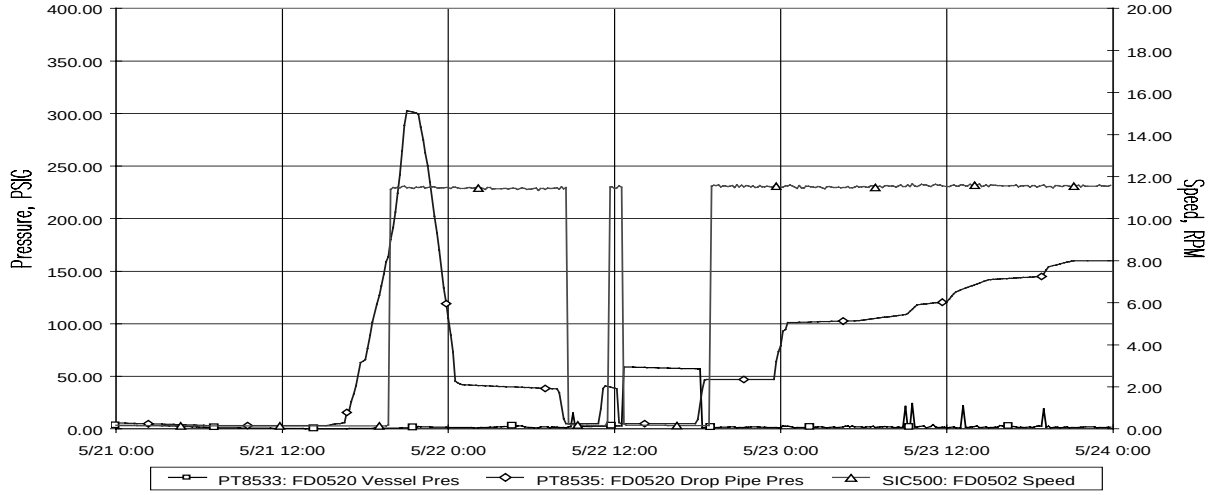

Figure 4.1.2.2-20 FD0520 Pressure Profiles

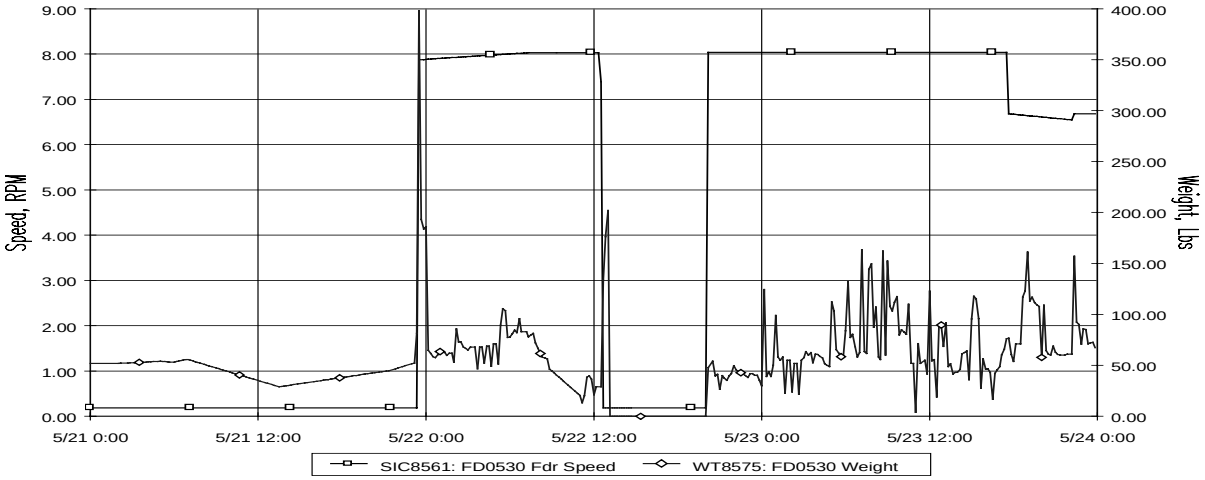

Figure 4.1.2.2-21 FD0530 Feeder Profiles

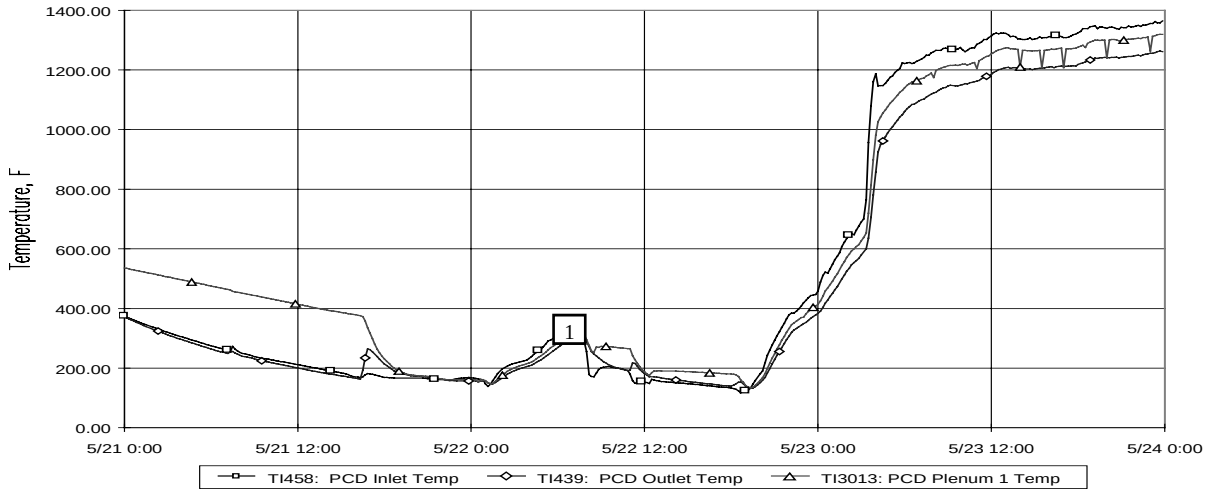

Figure 4.1.2.2-22 PCD Temperatures

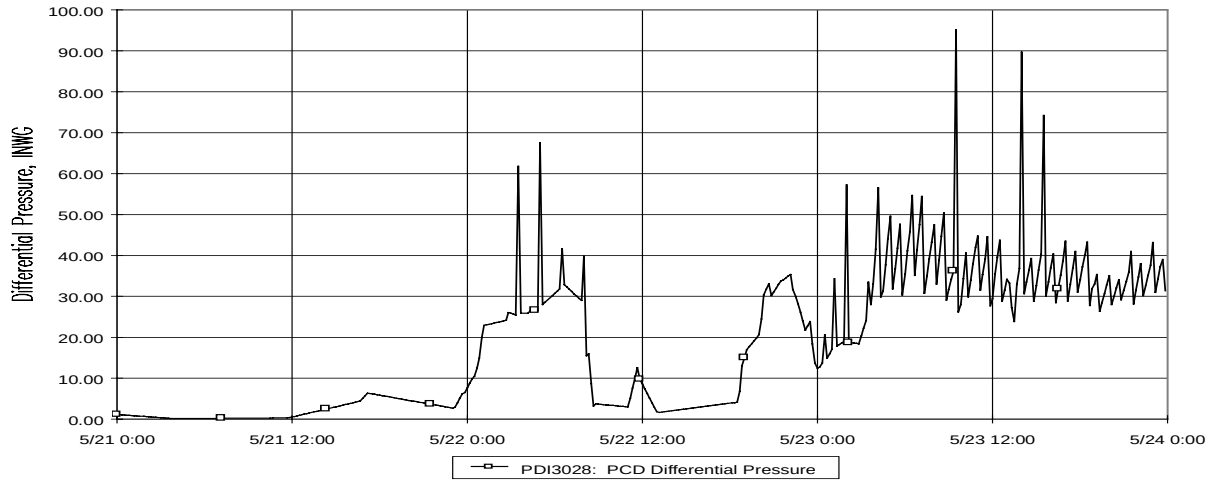

Figure 4.1.2.2-23 PCD Differential Pressure Profile

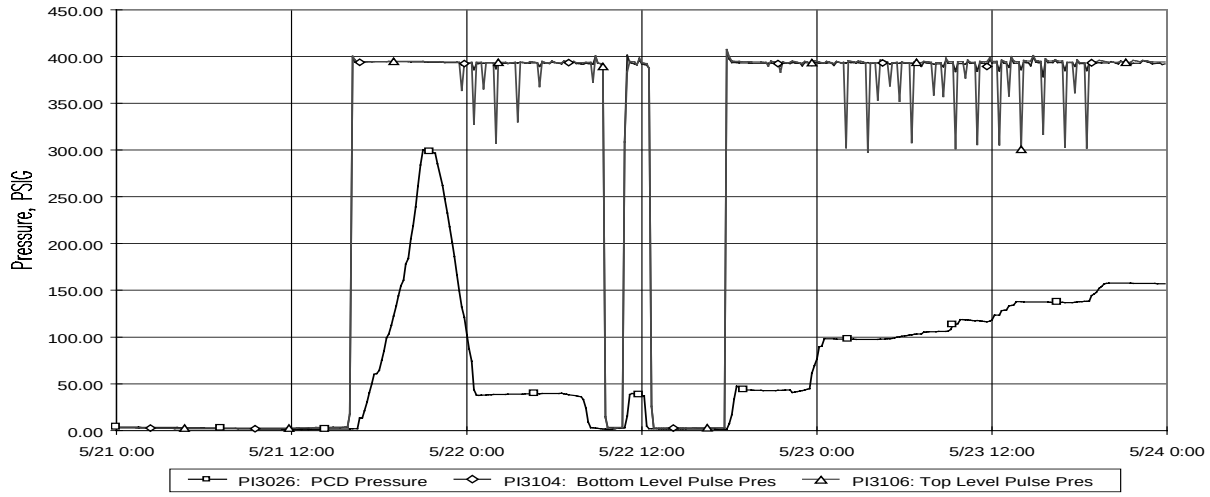

Figure 4.1.2.2-24 PCD Pressure and Pulse Pressure

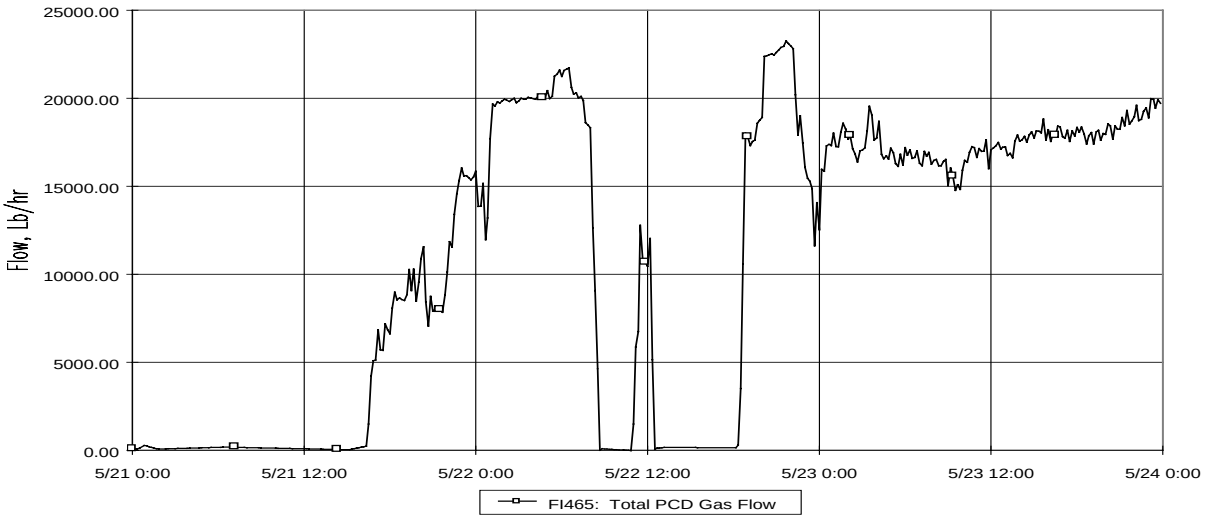

Figure 4.1.2.2-25 Gas Flow Through PCD

Section 4.1.2.2

Graphs 26 through 50

Test Run CCT5B

May 24 through 26, 1997

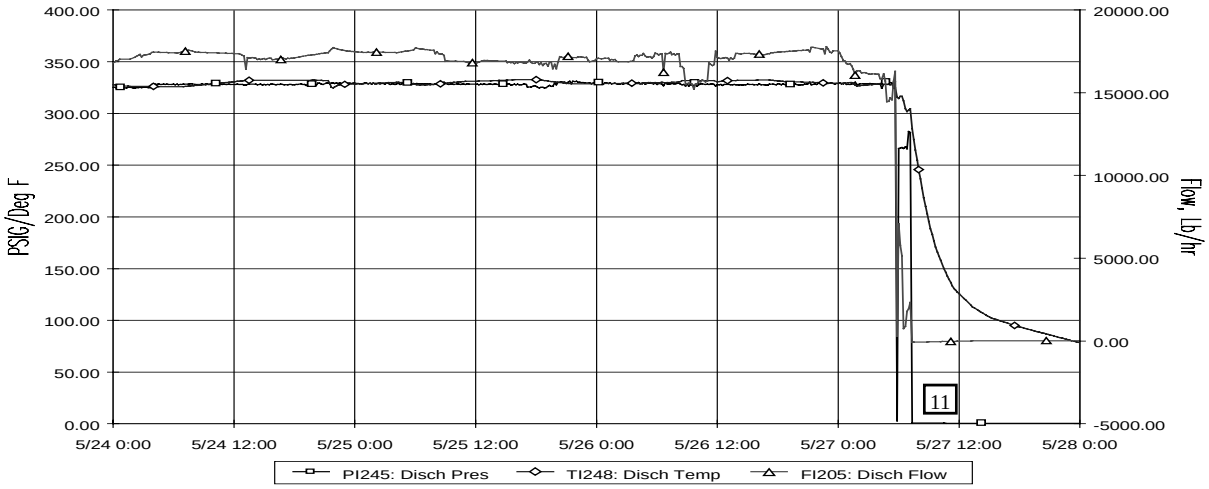

Figure 4.1.2.2-26 CO0201 System Profile

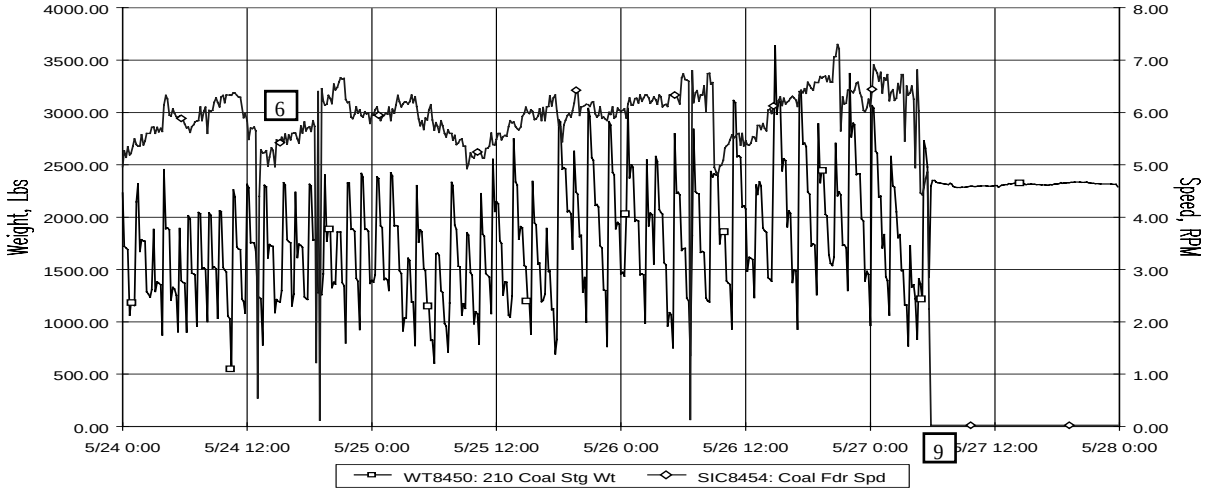

Figure 4.1.2.2-27 Coal Feed System Profile

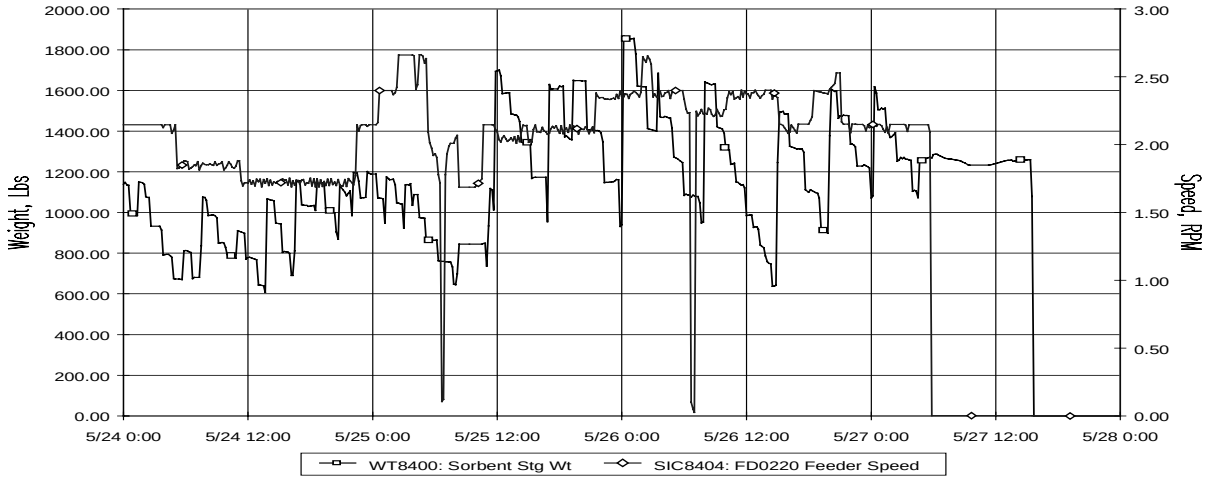

Figure 4.1.2.2-28 Sorbent Feed System Profile

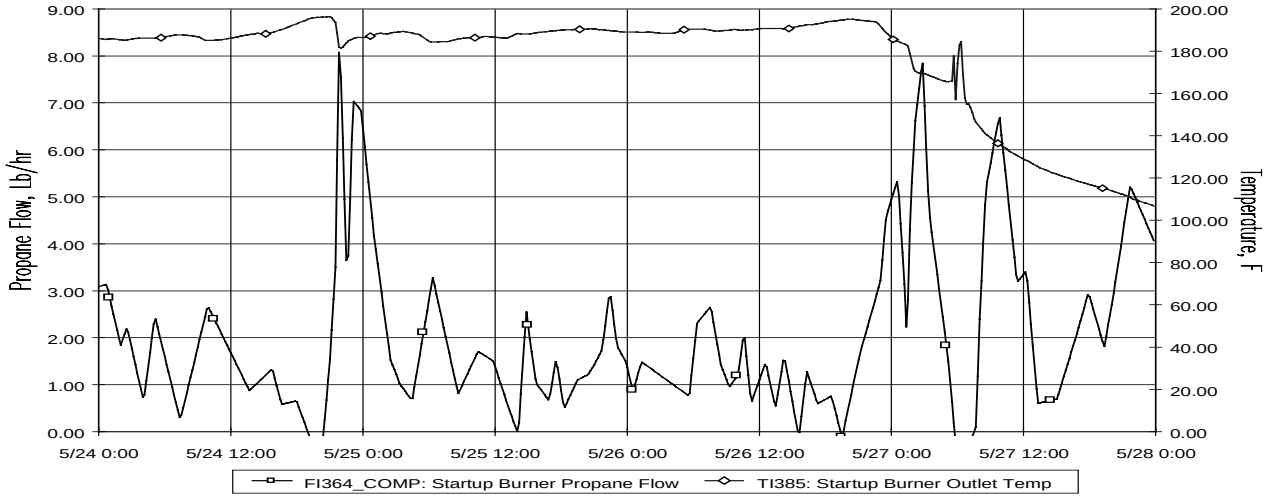

Figure 4.1.2.2-29 Start-Up Burner Flow/Temperature

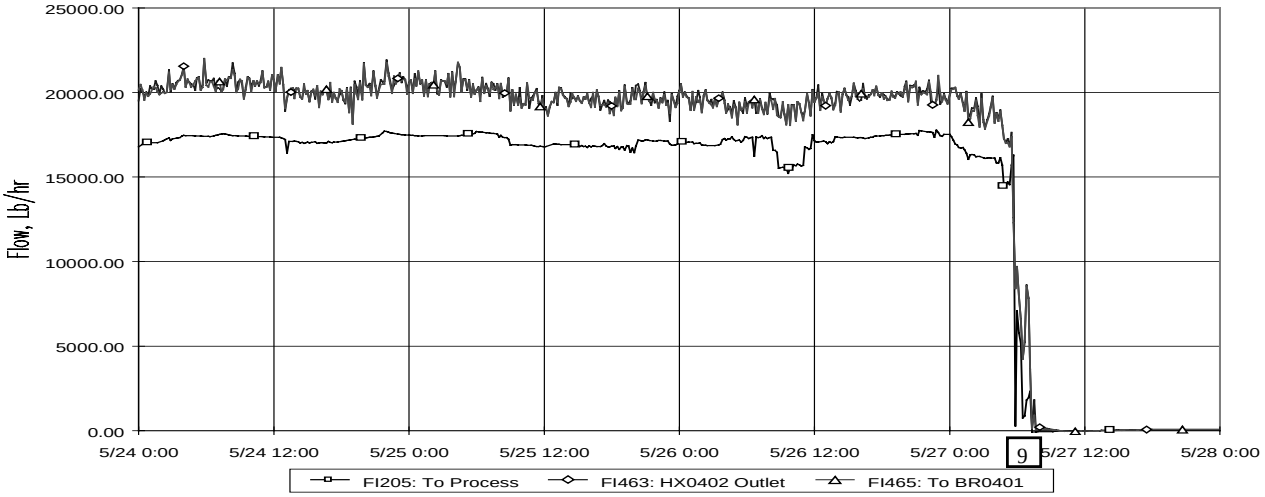

Figure 4.1.2.2-30 Total Gas In/Out Flow Rates

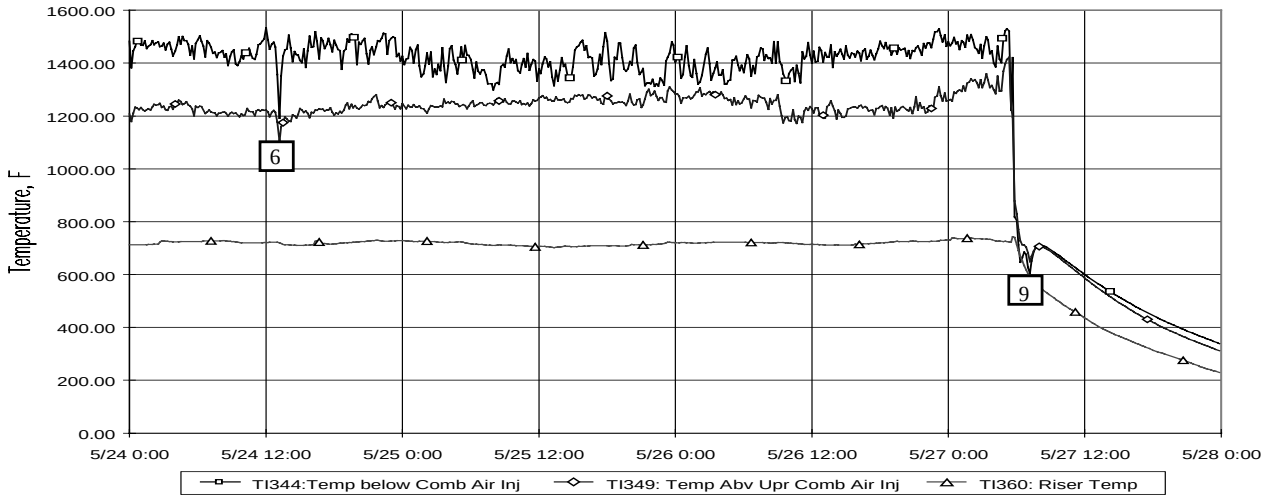

Figure 4.1.2.2-31 Reactor Mixing Zone and Riser Temperatures

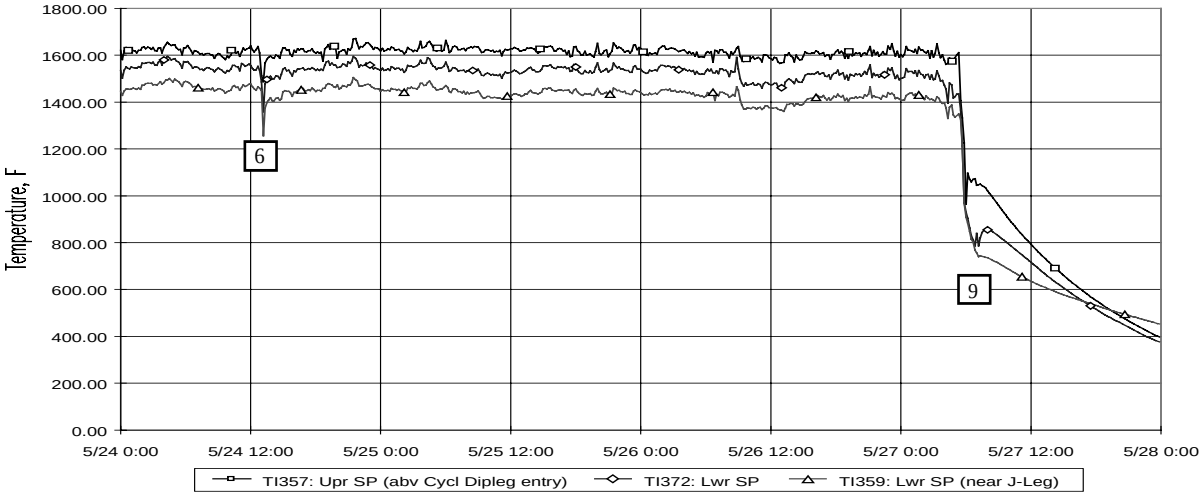

Figure 4.1.2.2-32 Standpipe Temperatures

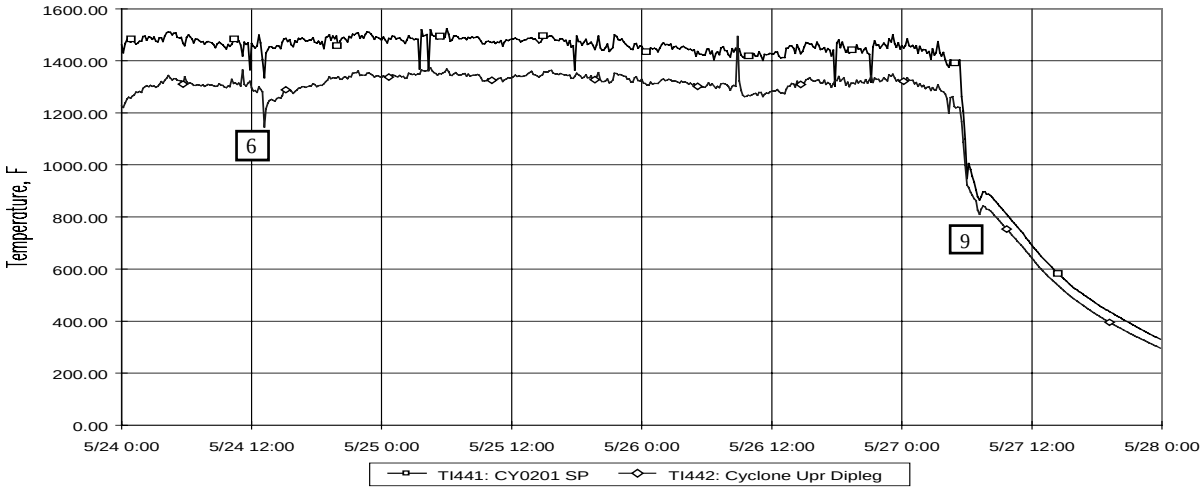

Figure 4.1.2.2-33 Cyclone Dipleg Temperatures

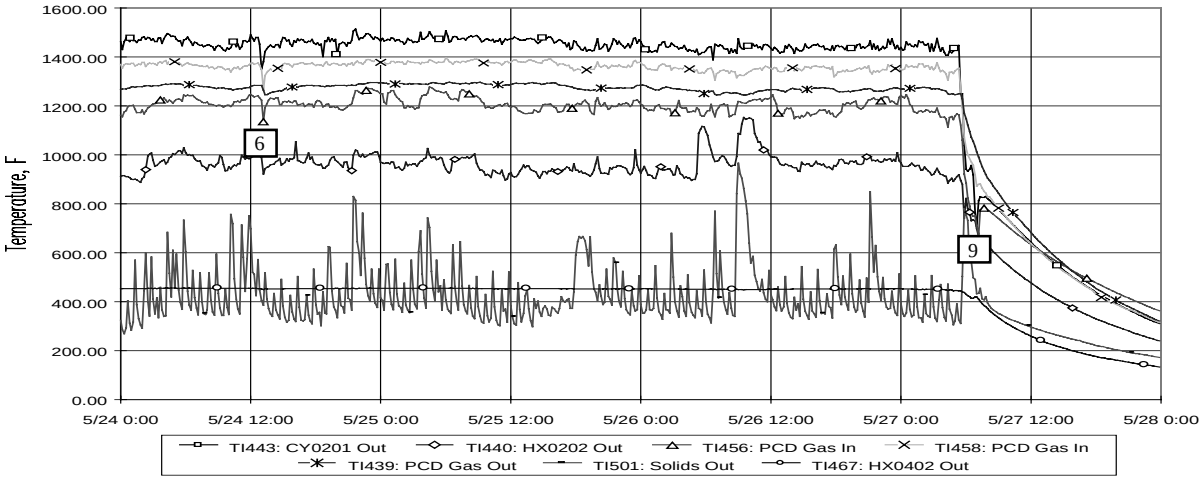

Figure 4.1.2.2-34 Temperature Profile Downstream of Reactor

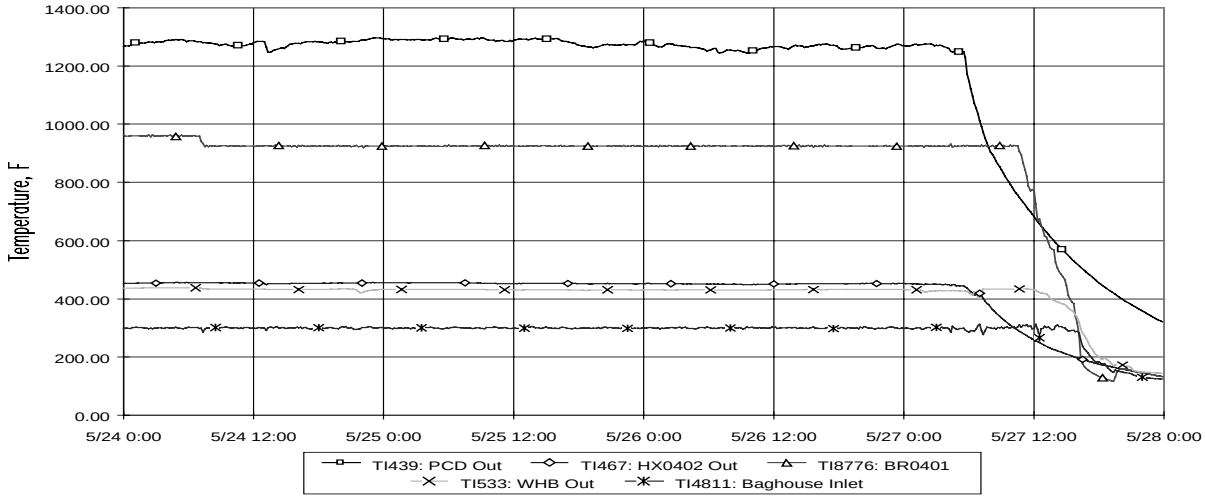

Figure 4.1.2.2-35 System Temperatures Downstream of PCD

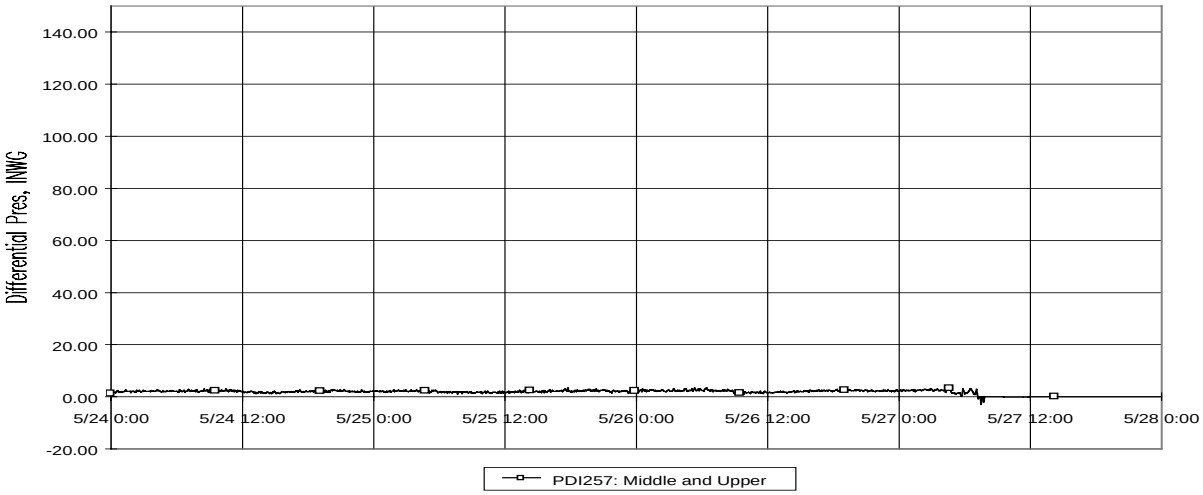

Figure 4.1.2.2-36 Mixing Zone Differential Pressure Profile

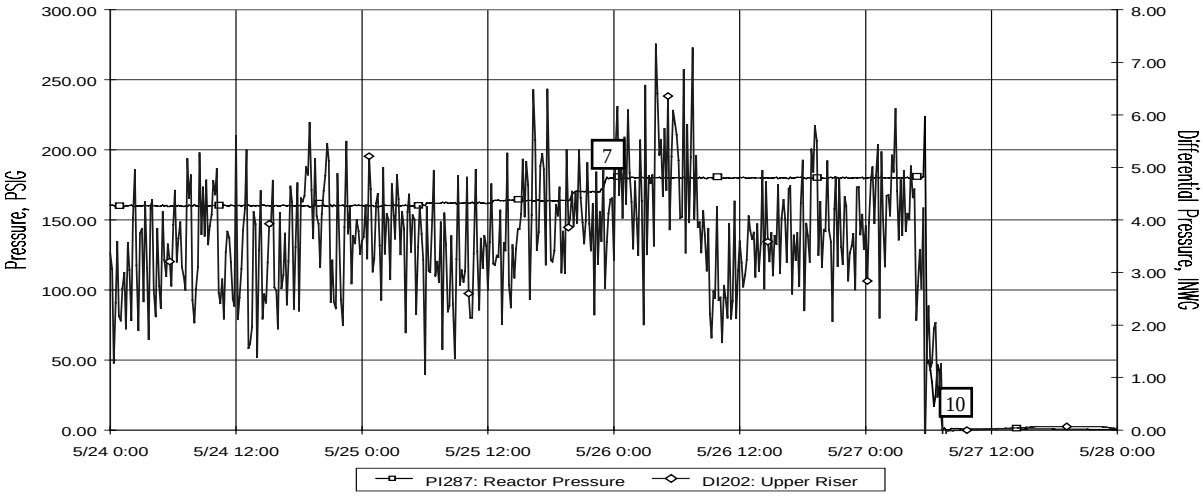

Figure 4.1.2.2-37 Reactor Pressure/Riser Differential Pressure Profiles

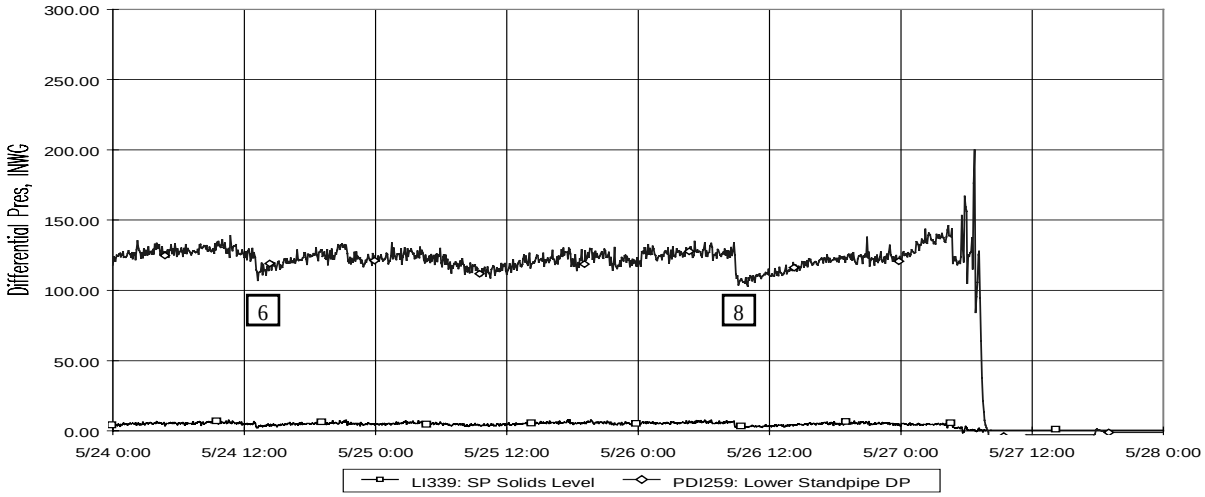

Figure 4.1.2.2-38 Standpipe Differential Pressure Profiles

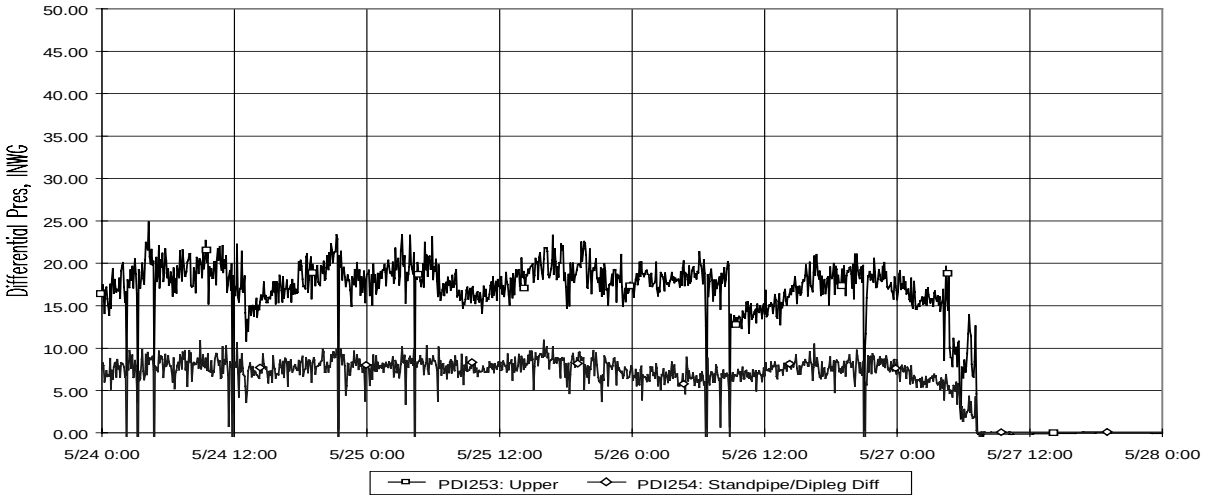

Figure 4.1.2.2-39 CY0201 Dipleg Differential Pressure Profiles

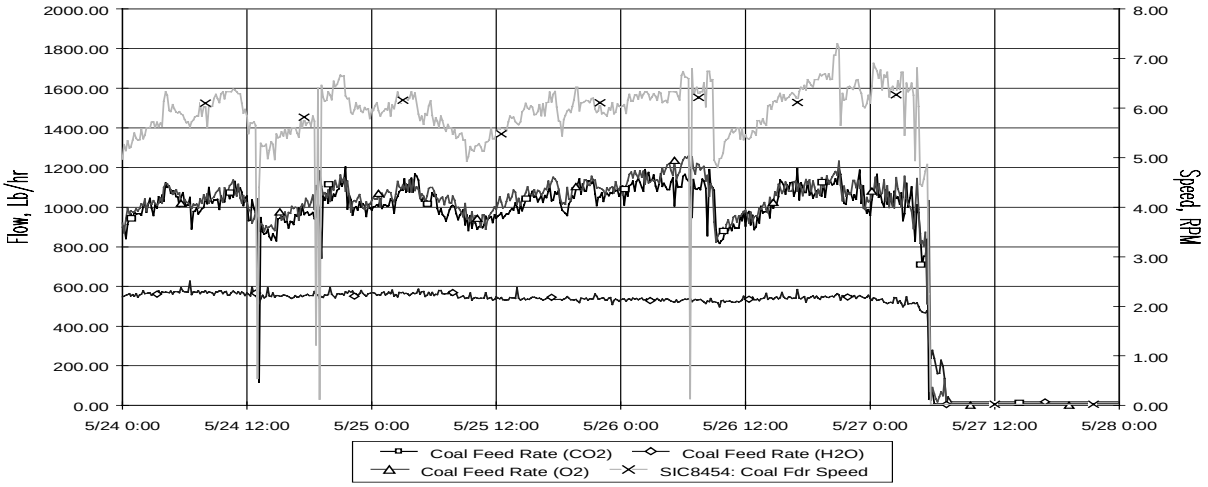

Figure 4.1.2.2-40 Coal Feed Rate Based on Gas Analysis

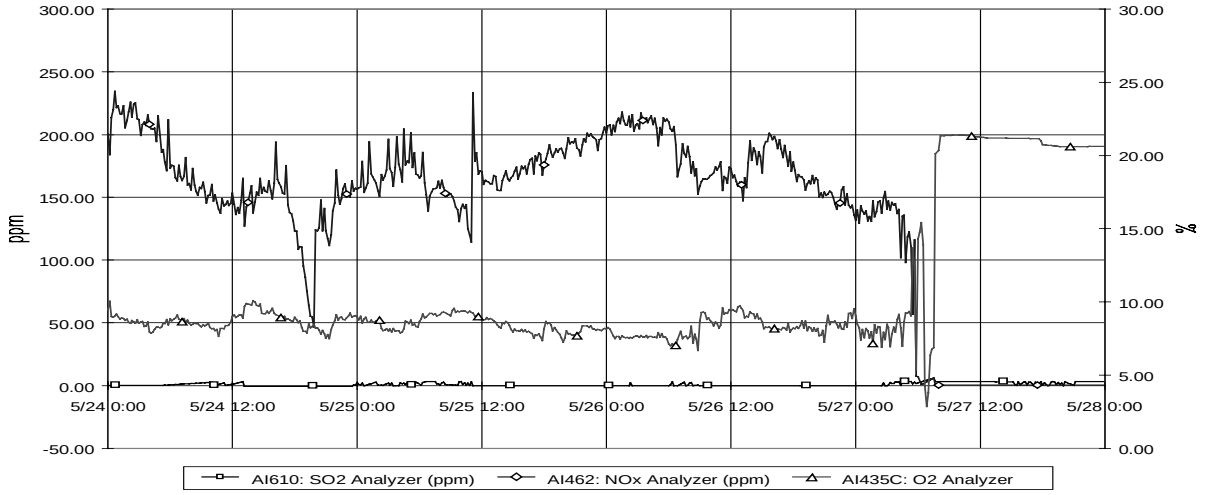

Figure 4.1.2.2-41 O_2, SO_2, and NO_x Analyzers

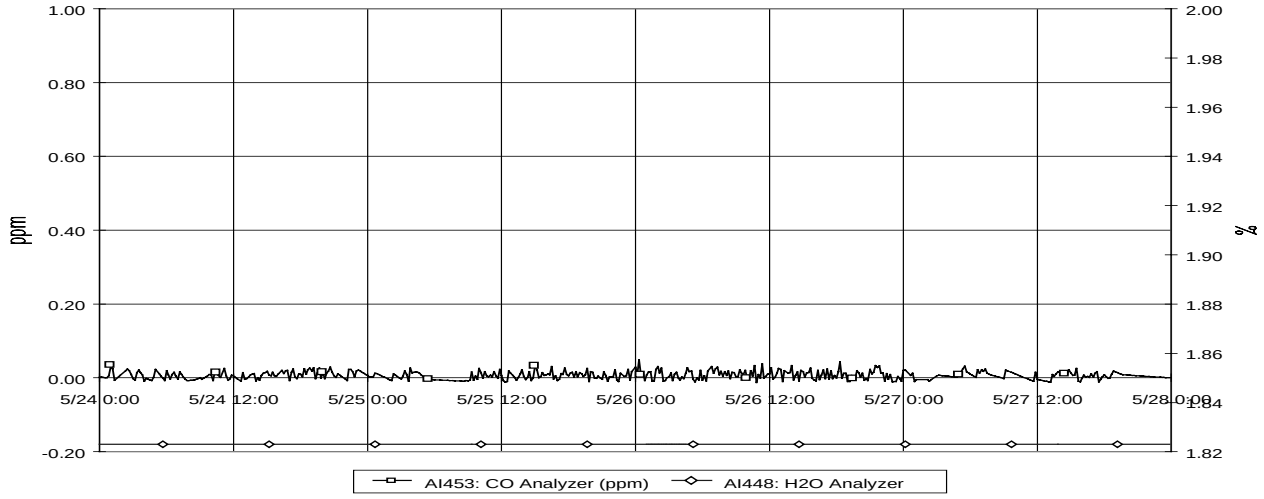

Figure 4.1.2.2-42 CO and H_2O Analyzers

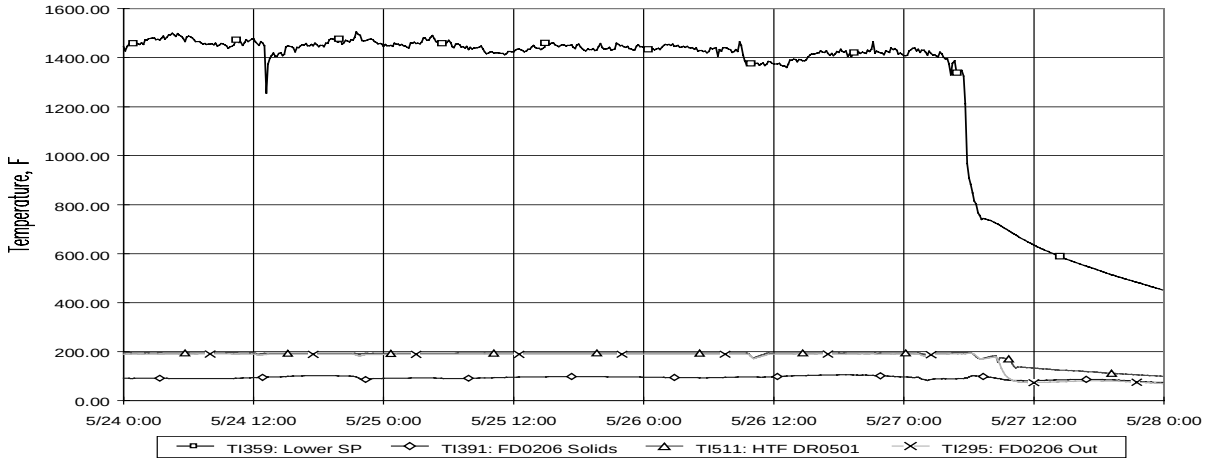

Figure 4.1.2.2-43 FD0510 Temperature Profiles

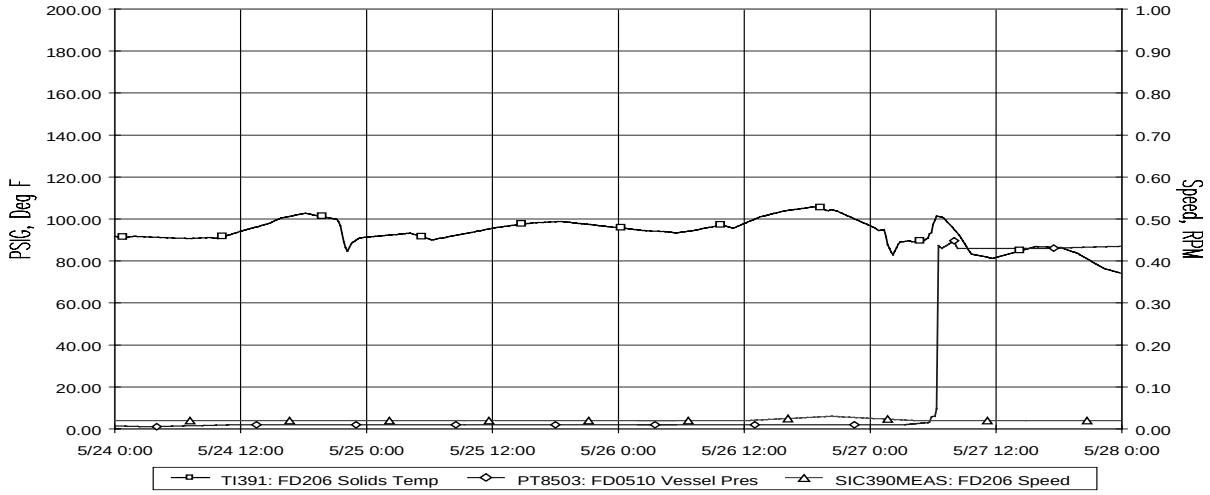

Figure 4.1.2.2-44 FD0206 Pressure Profiles

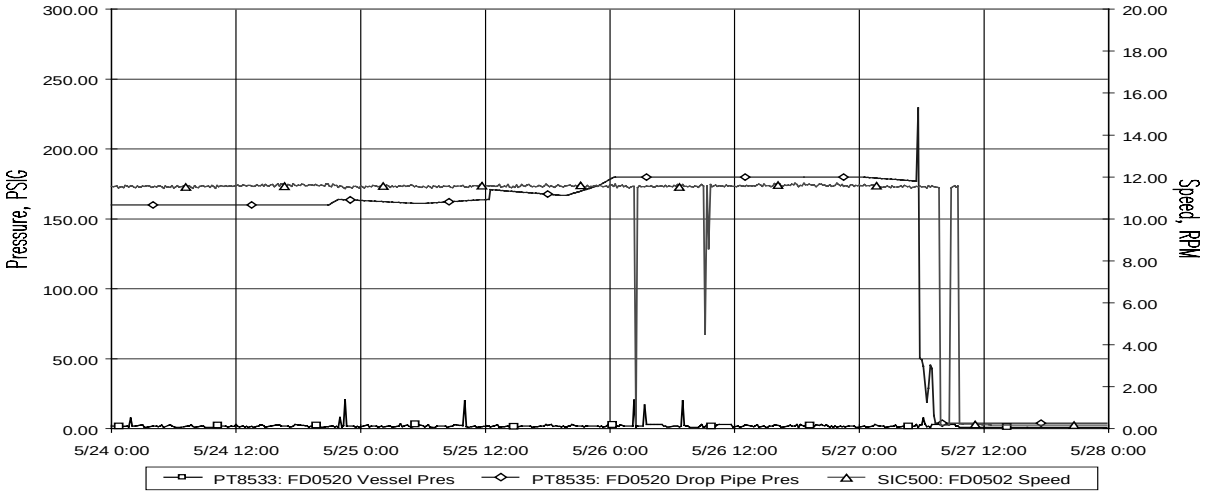

Figure 4.1.2.2-45 FD0520 Pressure Profiles

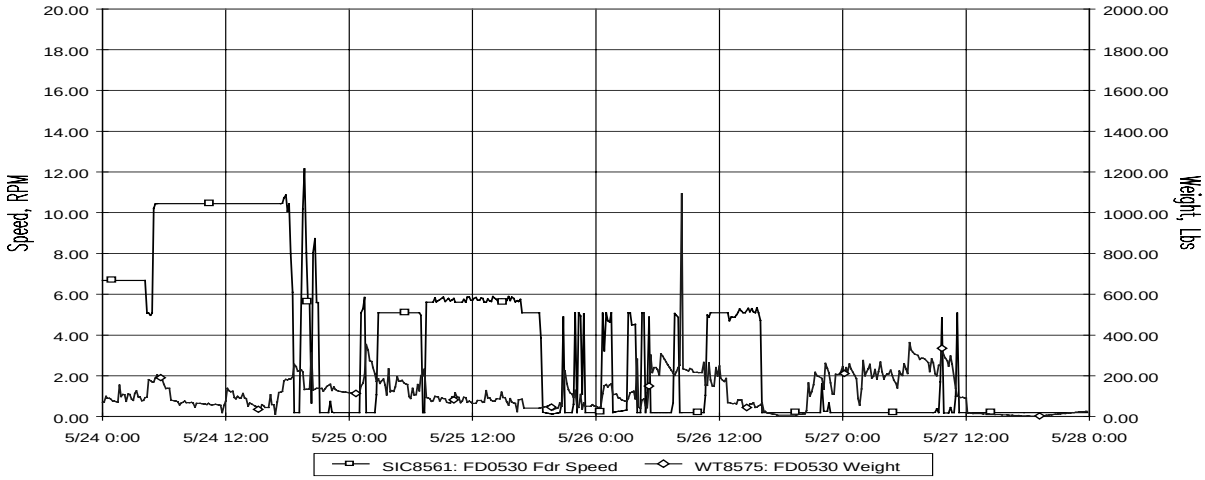

Figure 4.1.2.2-46 FD0530 Feeder Profiles

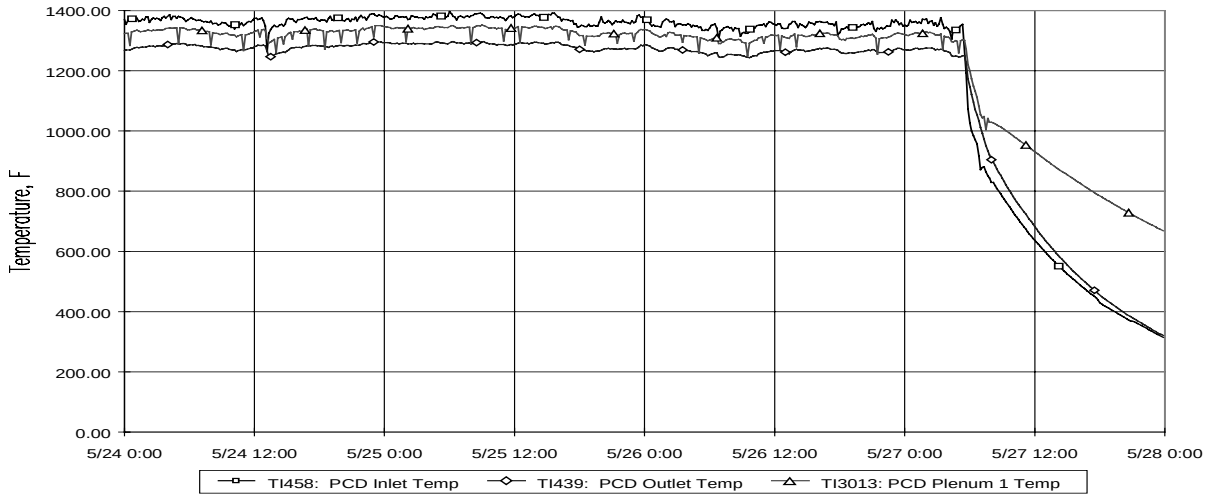

Figure 4.1.2.2-47 PCD Temperatures

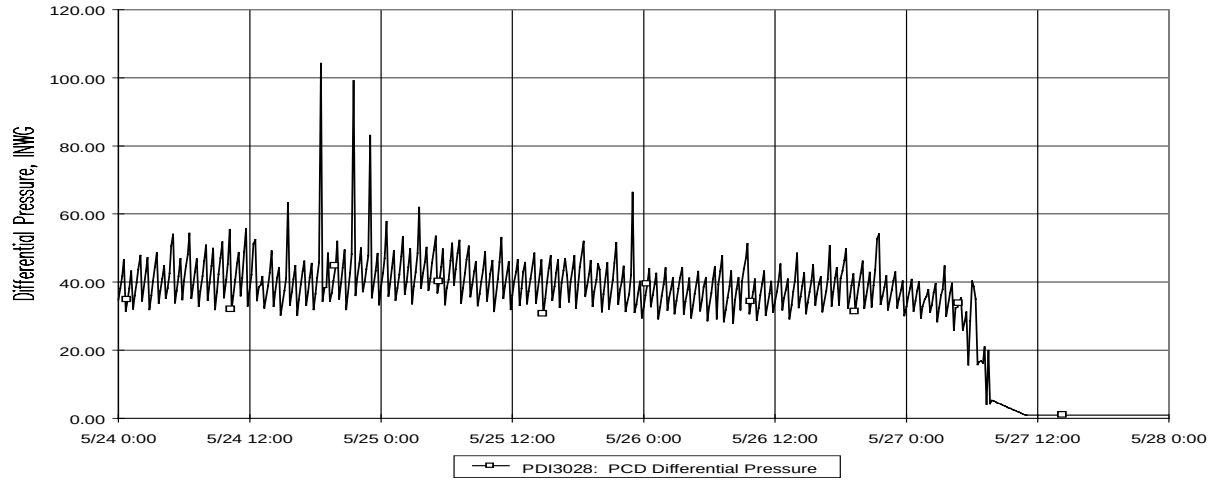

Figure 4.1.2.2-48 PCD Differential Pressure Profile

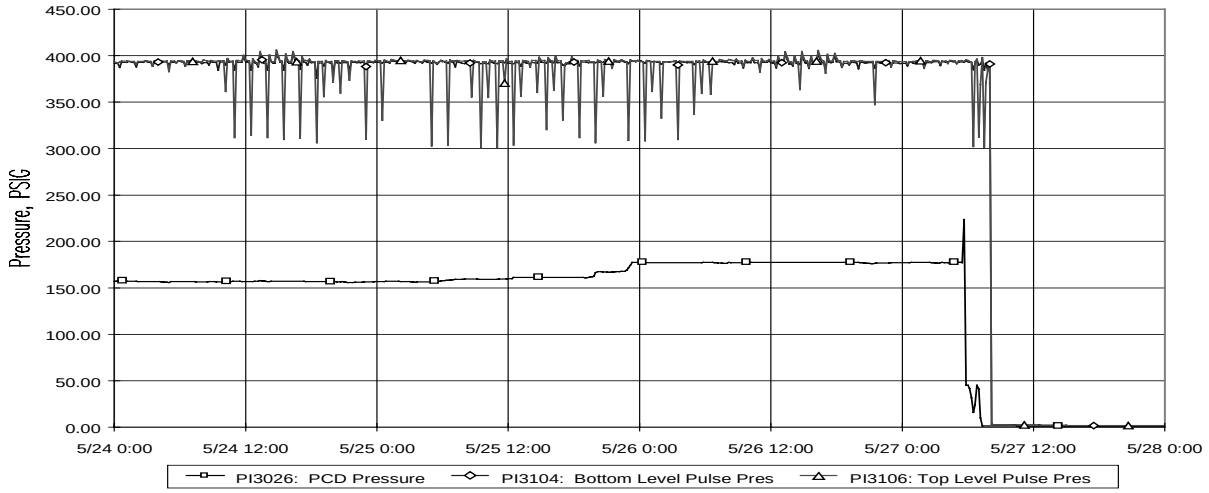

Figure 4.1.2.2-49 PCD Pressure and Pulse Pressure

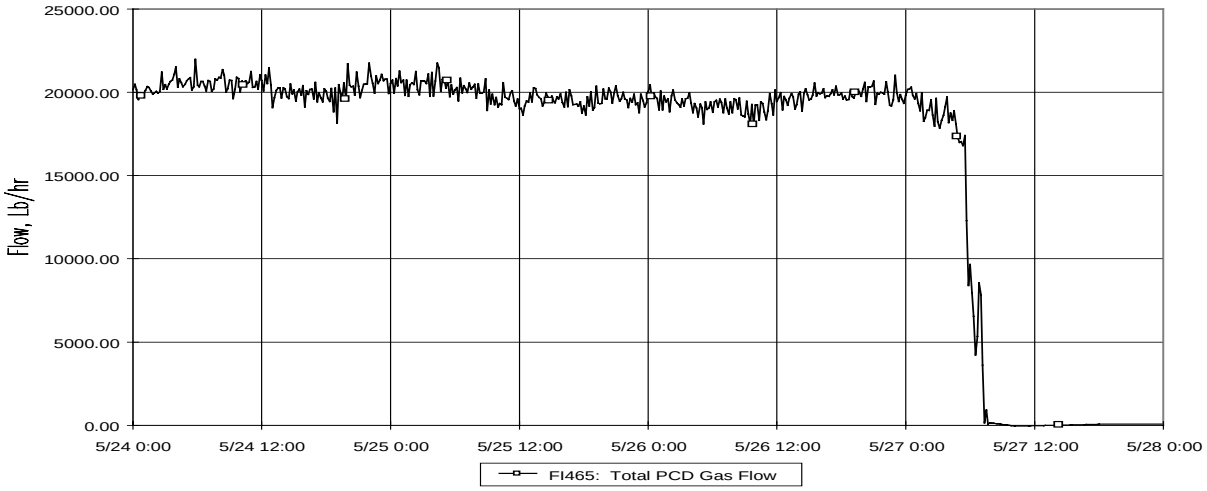

Figure 4.1.2.2-50 Gas Flow Through PCD

4.1.3 CCT6 Series Test Run

Due to a number of modifications and the new perspective gained on the cyclone dipleg operation the reactor loop operations were more stable in the CCT5 series test runs than previous runs. The circulation of cooled solids through the combustion heat exchanger J-leg was much smoother in CCT5 series test runs compared to previous test runs. This greatly improved the ability to operate at higher coal feed rates, capture the heat released in the riser through higher solids circulation rates, and reject the heat in the combustion heat exchanger. Also, the smooth circulation of solids through the combustion heat exchanger J-leg improved the temperature control over reactor loop operations and prevented many upsets in solids flow through the cyclone dipleg due to sudden, uncontrolled perturbations in circulation rates.

Even though operations in CCT5 series test runs were much improved compared to previous test runs the CCT6 test run was undertaken to further the understanding of reactor loop operations. In CCT5 test runs cyclone dipleg operation became sensitive to any small perturbations whenever the solids level in HX0203 reached a certain level. By the time the solids flow through the cyclone dipleg recovered from an upset a large amount of solids was usually lost from the reactor (actually the solids loss is from the HX0203 since it is a large reservoir of reactor solids inventory) in a very short period of time (typically 3 to 7 minutes). The solids lost from the reactor end up in the filter vessel (FL0301) cone and overwhelm the fine ash removal system. If the level in the HX0203 is high the potential for filling the filter vessel cone (and possibly submerging the lower portion of bottom plenum candles) with ash is also high during a dipleg upset.

A better understanding of the dipleg operation was sought by planning various numbers of upsets to the dipleg. To protect the filter vessel from overfilling with ash, the reactor solids inventory needs to be reduced by eliminating the solids circulation through HX0203. Also, by isolating HX0203 or preventing solids circulation through HX0203, the reactor loop can be operated with higher solids level in the standpipe. High solids circulation rates with higher levels in the standpipe require less aeration in the reactor J-leg. The mixing zone density will increase with less aeration from the reactor J-leg and no aeration flow from the HX0203 J-leg due to its isolation. The test objectives for CCT6 were as follows:

- Study operation of disengager, primary cyclone and cyclone dipleg by operating the reactor loop under various scenarios including higher solids level in the standpipe, sufficient to seal the dipleg.

- Investigate the effect of increasing the mixing zone density.

Characterization Test Run CCT6

Prior to the run the combustor heat exchanger (HX0203) was isolated from the solids circulation loop, which minimizes the heat removal and requires a low coal feed rate. High excess air was required to maintain a suitable riser velocity. The sorbent feeder (FD0220) was used to feed coal due to the low coal feed rate. Dolomite and sand were batch fed through FD0210. This setup minimized the solids loss to the PCD in case of a dipleg upset so that the dipleg operations

could be studied over a wide range of operating parameters. Reactor configuration was similar to gasification operation. CCT6 test run was conducted between June 17 and June 26, 1997. Operating plots are shown in figures 4.1.3-1 through -72.

CCT6 Test Run Chronology

- On June 17, 1997, a successful leak test was completed and the thermal oxidizer (BR0401) was started. The following day the pressure differential transmitters were balanced and the sulfator burner (BR0602) was lit to preheat the PCD. The PCD preheat used 6,000 lb/hr of nitrogen flow. The spent fines screw cooler (FD0502) and spent fines transport (FD0520) systems were also started. At 09:00 the data acquisition system was off-line for a brief period of time. The initial attempts to light the start-up burner (BR0201) were unsuccessful, so the reactor was depressurized and the pilot removed. The ignition tip was replaced and the pilot was reassembled. The reactor was pressurized and the BR0201 pilot was then successfully lit. The main burner was lit and the pilot was shut down (event 1, figure 4). The BR0602 was shut down after completing the PCD preheat and the preheat line was isolated. The reactor pressure was then increased to 60 psig and sand addition into the reactor was started.

- Coal feed was started 02:26 on June 19, 1997, from the sorbent feeder system (FD0220) (event 2, figure 3). Soon after the coal feed was started there were periodic problems with discharge line plugging. Since there was frequent loss of coal feed the BR0201 was left at near-minimum firing through the duration of the run. This way the burner firing can be increased rapidly upon loss of coal feed to maintain reactor temperatures. Coal feed was lost for almost an hour at 07:30. Sand addition continued to increase the standpipe solids level.

- Over the course of the subsequent days the dipleg operations were intentionally upset by varying operating conditions so that a better understanding of the dipleg operations could be developed. Sufficient time was given after each upset so that the solids could be emptied out of the PCD cone. Varied conditions included reactor aeration flows, solids level in standpipe, solid circulation rates, solids level in the cyclone dipleg, solids characteristics, and PCD back-pulse parameters.

- At 05:15 on June 20, 1997, the reactor pressure was increased from 105 to 110 psig. The BR0201 firing was reduced to control the reactor temperature. At 10:05 dolomite addition was started. At 16:00 when the PCD back-pulsed the solids flow through the dipleg became unstable for about 5 minutes.

- At 18:40 sand addition into the reactor was initiated. The standpipe differential pressure indication (PDI259) increased from 160 to 185 inH_2O and stabilized around 220 inH_2O (event 3, figure 13). The spent solids screw cooler (FD0206) was run for a few minutes to check its operation and PDI259 decreased from 220 to 206 inH_2O (event 4, figure 13). During previous test runs, the PDI259 (which is an indication of solids level in the standpipe) was typically operated in 120 to 135 inH_2O range. At

20:15 dolomite addition into the reactor was started. From 22:10 to 23:42 coal feed was lost several times. The average coal feed rate for June 20, 1997 was 376 lb/hr.

- Dolomite addition continued on the morning of June 21, 1997, to maintain the solids inventory as changes to PCD back-pulses and other operating parameters were made to induce upsets in the solids flow through the cyclone dipleg. At 15:22 there was a dipleg upset that was not induced by a PCD back-pulse. It was probably due to the high level of solids in the standpipe and the consequent high solids circulation rates. The dipleg upset lasted about 5 minutes, dropping the standpipe level. The dipleg differential pressure also decreased substantially (event 5, figure 38). In the afternoon, sand was added to increase the solids inventory in the reactor.

- On June 22, 1997, coal feed was lost for short times due to plugging in the feeder discharge line (event 6, figures 27 and 30 through 32). On June 23, 1997, dolomite and sand addition continued to make up for solids loss to the PCD. From 12:00 to 15:00 dolomite was added and aeration flows were adjusted to achieve a higher level in the standpipe. During this time there were a few dipleg upsets. At 15:26, when a dipleg aeration flow was adjusted for testing purposes, the dipleg operation was upset and there was a large carryover of solids to the PCD. Problems with the FD0520 system delayed additional tests for some time.

- On June 24, 1997, SRI took two PCD inlet particulate samples. On June 25 and 26, 1997, study of the dipleg operation continued. After completing the test objectives coal feed to the reactor was shutdown at 16:45 on June 26, 1997 (event 7, figures 51 and 54 through 56). The solid circulation rate in the reactor loop was reduced and BR0201 was ramped down. The FD0206 and the spent solids transporter system (FD0510) were started to remove the solids from the reactor. Eventually, the BR0201 was shutdown and the reactor was depressurized (event 8, figures 52 and 60).

CCT6 Test Run Observations

There was frequent loss of coal feed due to plugging at the FD0220 discharge. The FD0220 system is designed to feed sorbent and its discharge pipe id is much smaller than FD0210. The start-up burner was left at near minimum firing through the duration of the run when coal was being fed to the reactor. Upon loss of coal feed, the burner firing was increased rapidly to maintain the reactor temperatures. Since the burner was on during coal feed the flue gas flow through the burner leg was high, precluding the operation of the mixing zone at higher solid densities. A total of 177.5 hours on coal was achieved and a total of 30 tons of coal were fed.

Solid circulation rates, aeration flows, and the solids level in the standpipe were varied to study their effect on the dipleg operation. It was found that the dipleg operations were smoother at lower standpipe levels. With lower levels in the standpipe it appears that the dipleg was sealed with solids in the vertical portion of the dipleg and the slanted portion was empty. With a higher level of solids in the standpipe the slanted portion of the dipleg had some solids and the height of solid column in the vertical portion of the dipleg also increased. This operating point was moderately stable. The effects of PCD back-pulse parameters and solid characteristics in

the reactor on the operation of the dipleg were studied. Dolomite was fed at high rates to study the operation of the reactor and dipleg with a large amount of fine, less-dense solids (similar to gasification operation) in the reactor.

CCT6 Post Test Run Inspections

The transport reactor was inspected following test run CCT6. All pipes were clear. Nozzle H1 was used to inspect the riser down to the mixing zone with a halogen light. The riser walls had the normal layer of ash. The crack at the top of the riser was about the same. The top of the ash did not have any clumps. The riser crossover was clear as observed from nozzle A50 and the wall surface appeared to be less worn than formerly, probably due to the slight layer of white scale. The disengager was observed with the halogen lamp through nozzle A1. The nodule growth on the wall had increased since the last inspection; otherwise, the walls were clean (observed to ~60 feet down). The disengager cyclone crossover was inspected from nozzle A65/SN5 via the borescope. The feathered inlet separation from the wall had slightly increased and there was a small quarter-inch clump lying in the inlet. The cyclone and vertical dipleg walls had the normal scale/dust, as observed from nozzle H2. The start-up burner was inspected through the main gun nozzle via the borescope. The refractory was intact, but there was a small black area on one side of the wall that resembled a coke deposit.

Section 4.1.3

Graphs 1 through 25

Test Run CCT6

June 17 through 20, 1997

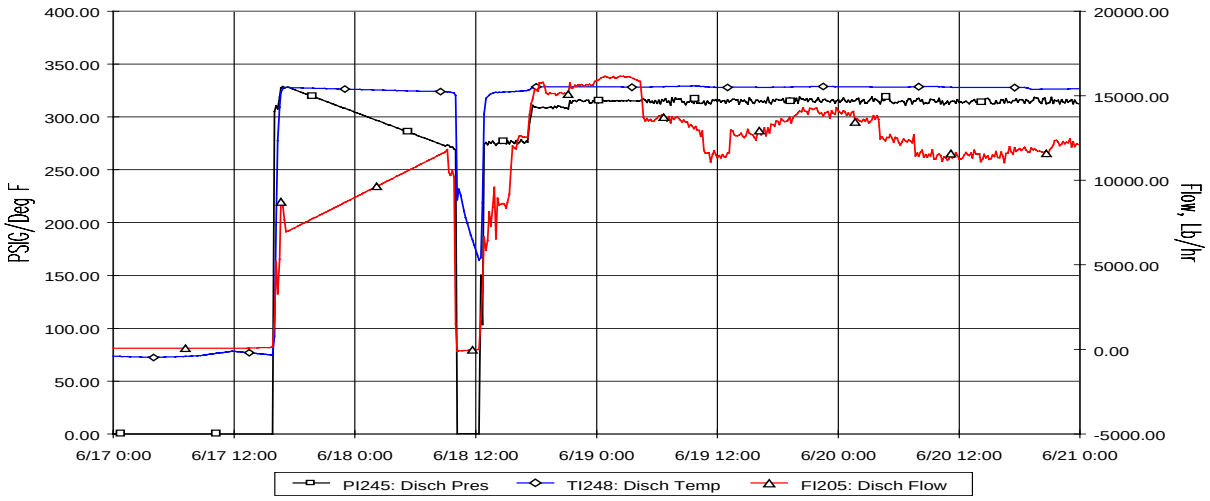

Figure 4.1.3-1 CO0201 System Profile

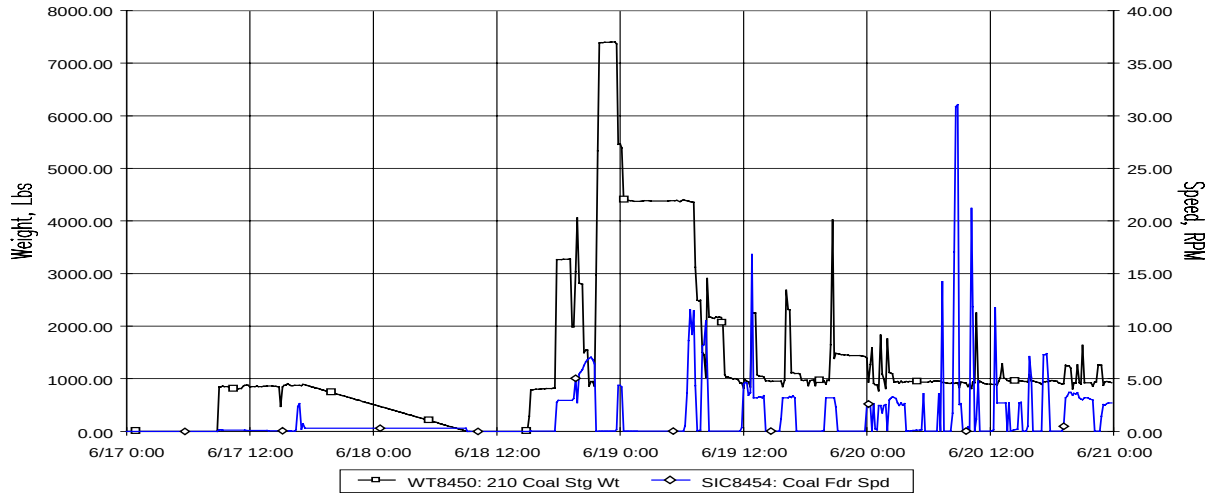

Figure 4.1.3-2 Coal Feed System Profile

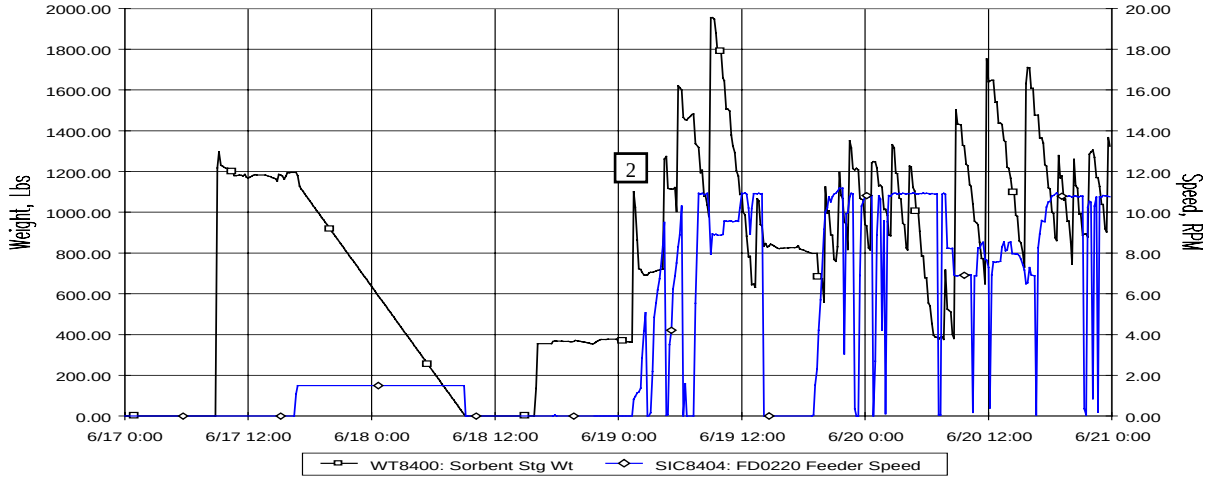

Figure 4.1.3-3 Sorbent Feed System Profile

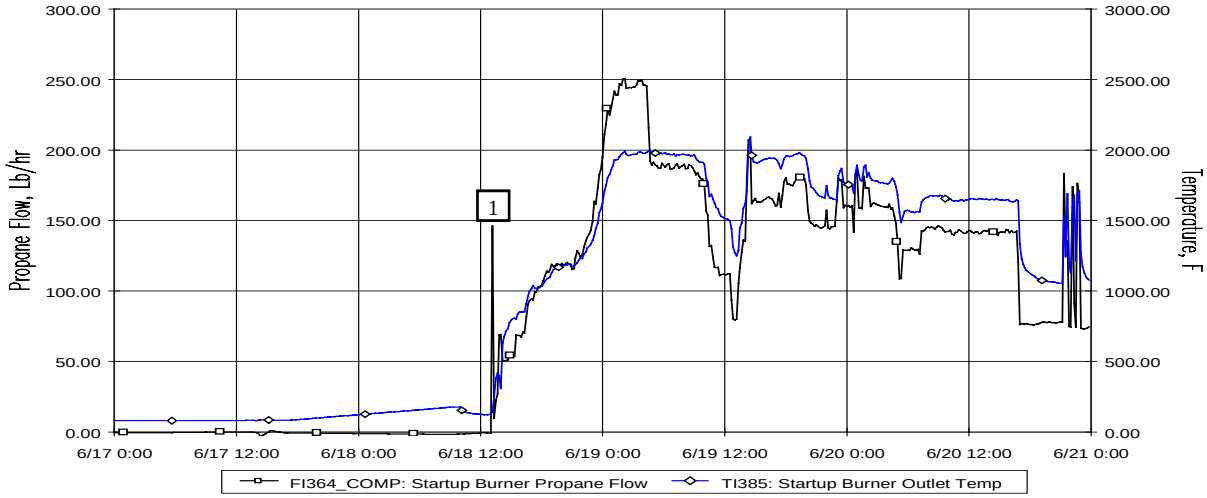

Figure 4.1.3-4 Start-Up Burner Flow/Temperature

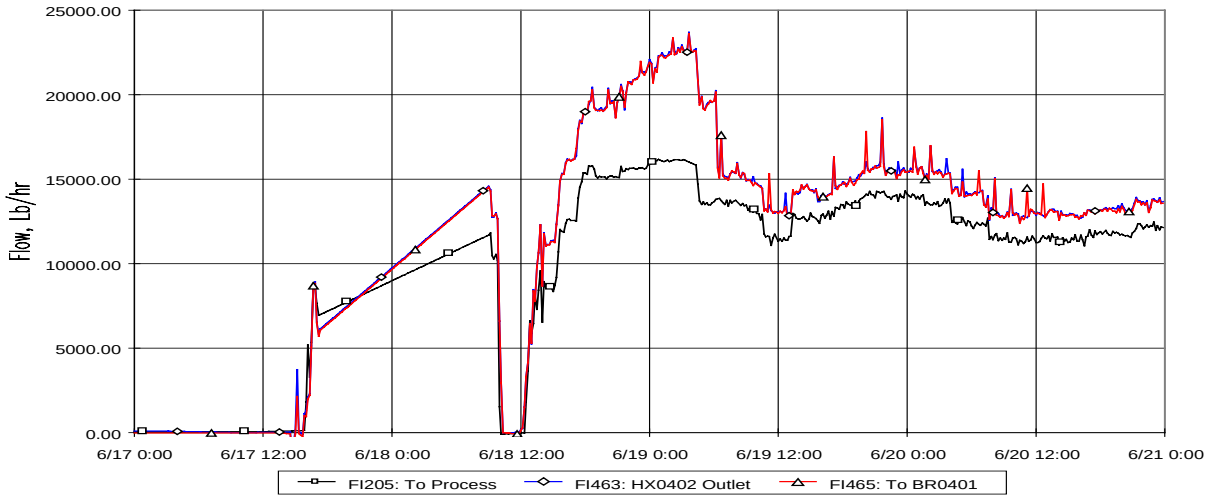

Figure 4.1.3-5 Total Gas In/Out Flow Rates

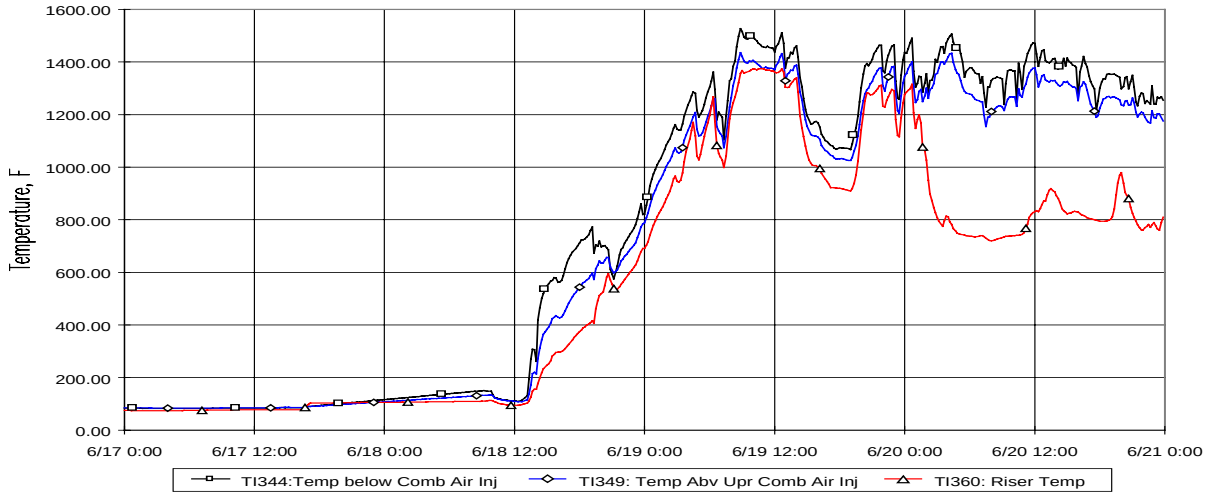

Figure 4.1.3-6 Reactor Mixing Zone and Riser Temperatures

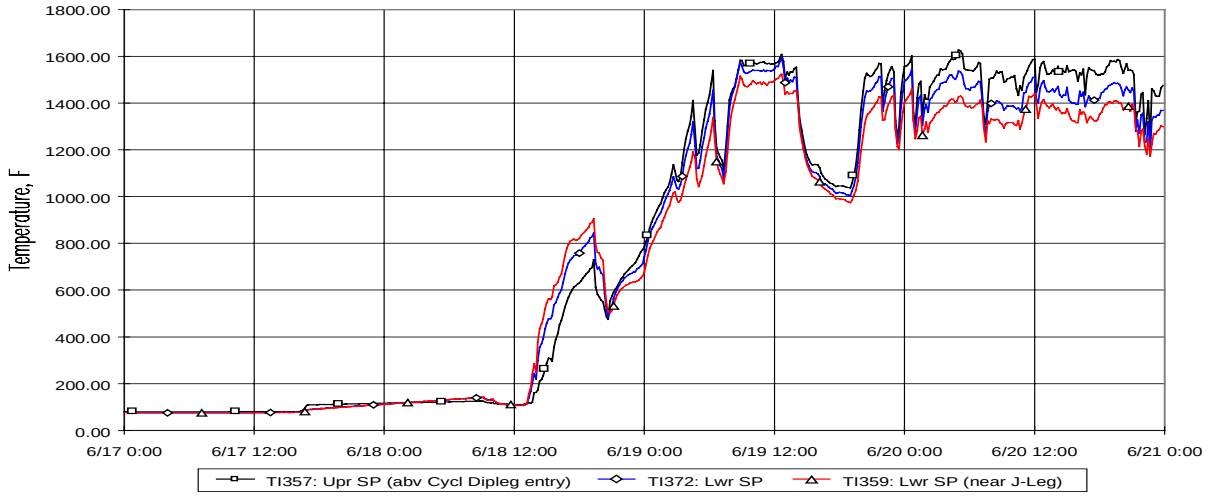

Figure 4.1.3-7 Standpipe Temperatures

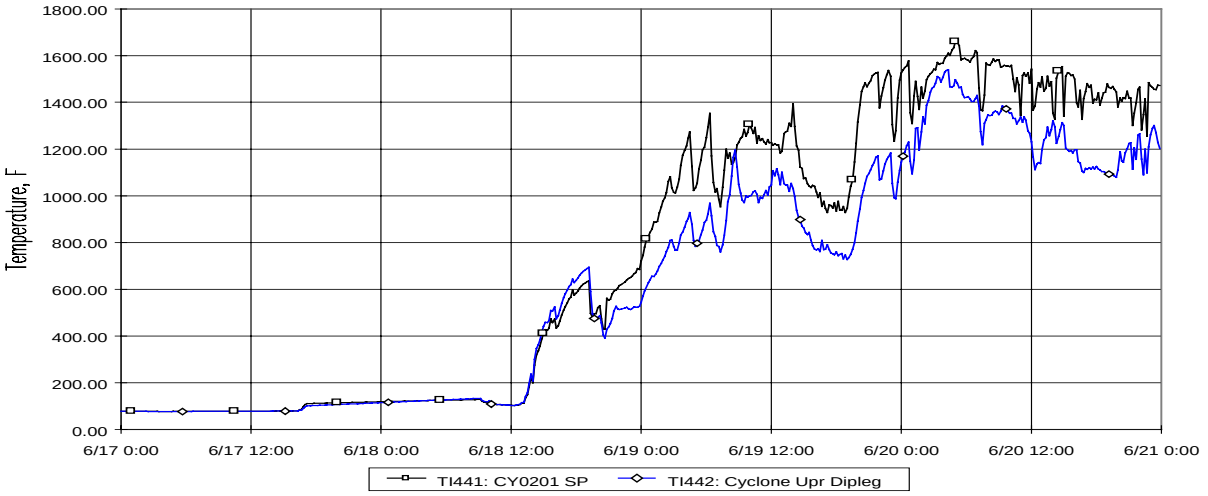

Figure 4.1.3-8 Cyclone Dipleg Temperatures

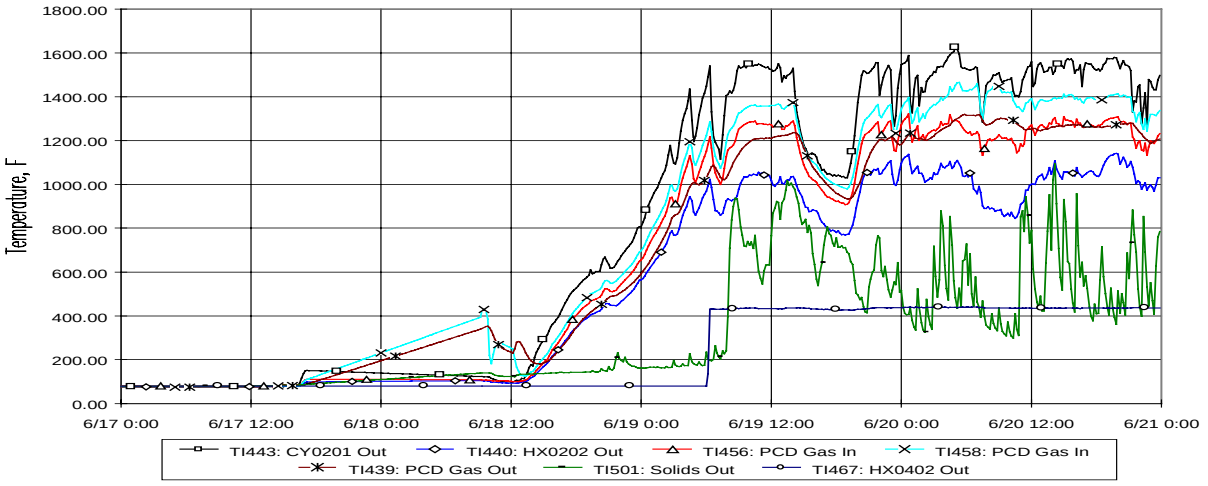

Figure 4.1.3-9 Temperature Profiles Downstream of Reactor

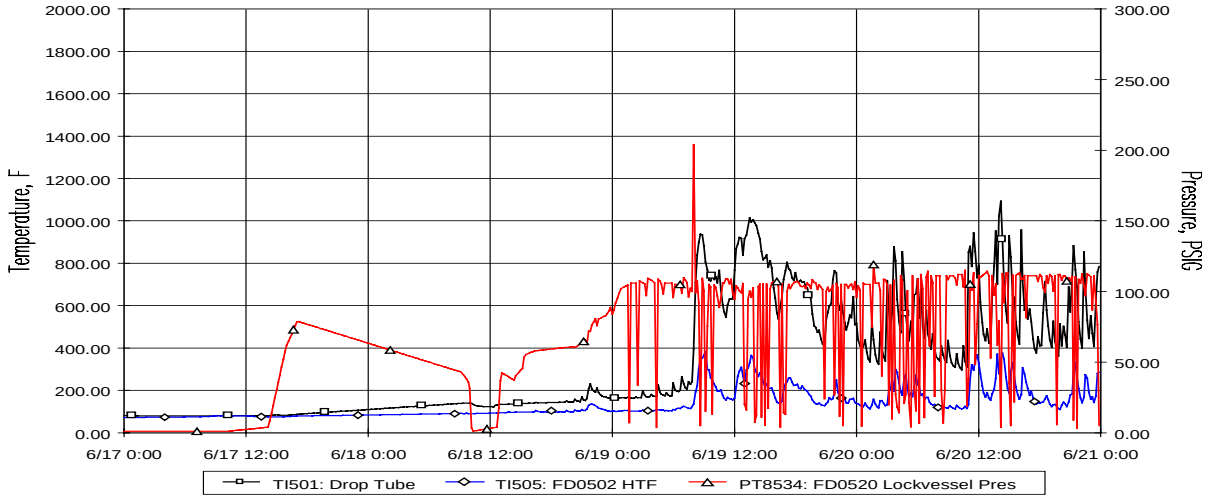

Figure 4.1.3-10 PCD Ash Temperatures

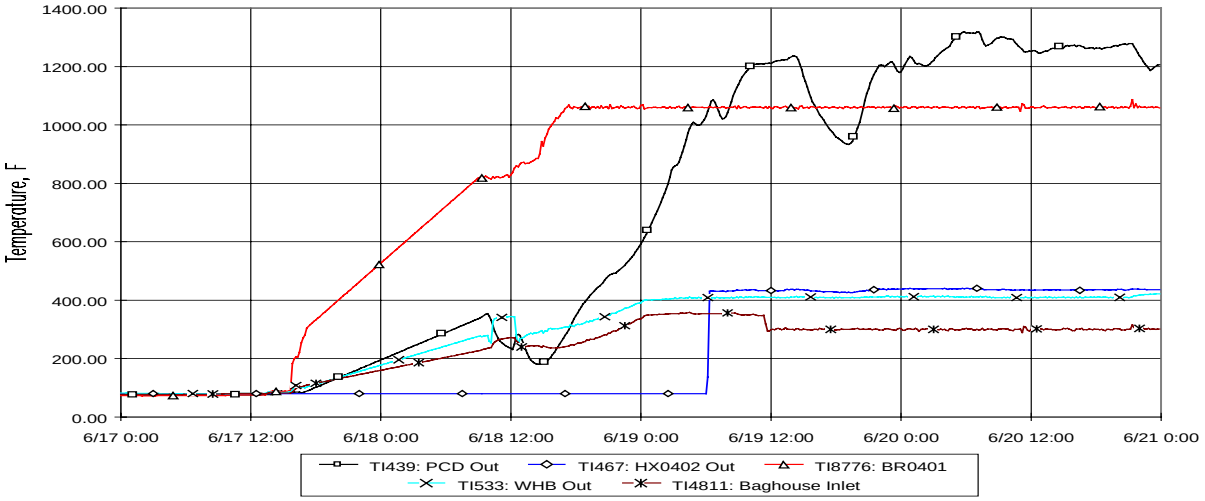

Figure 4.1.3-11 System Temperatures Downstream of PCD

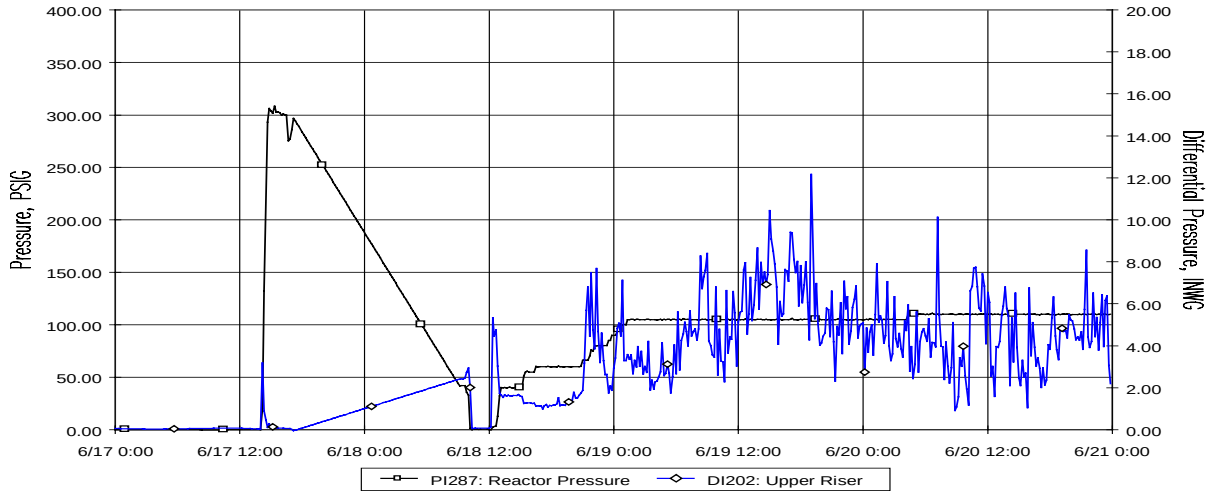

Figure 4.1.3-12 Reactor Pressure/Riser Differential Pressure Profiles

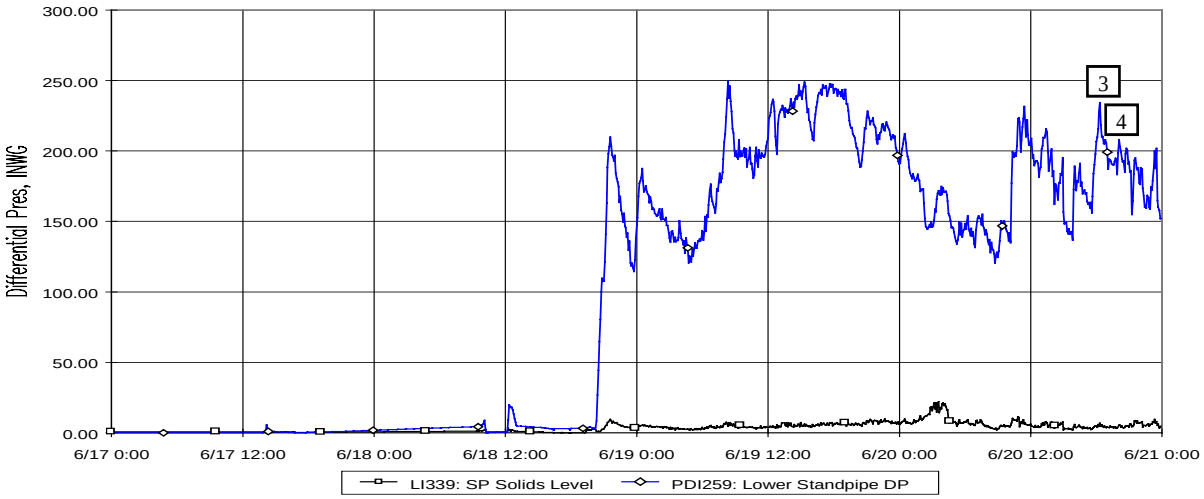

Figure 4.1.3-13 Standpipe Differential Pressure Profiles

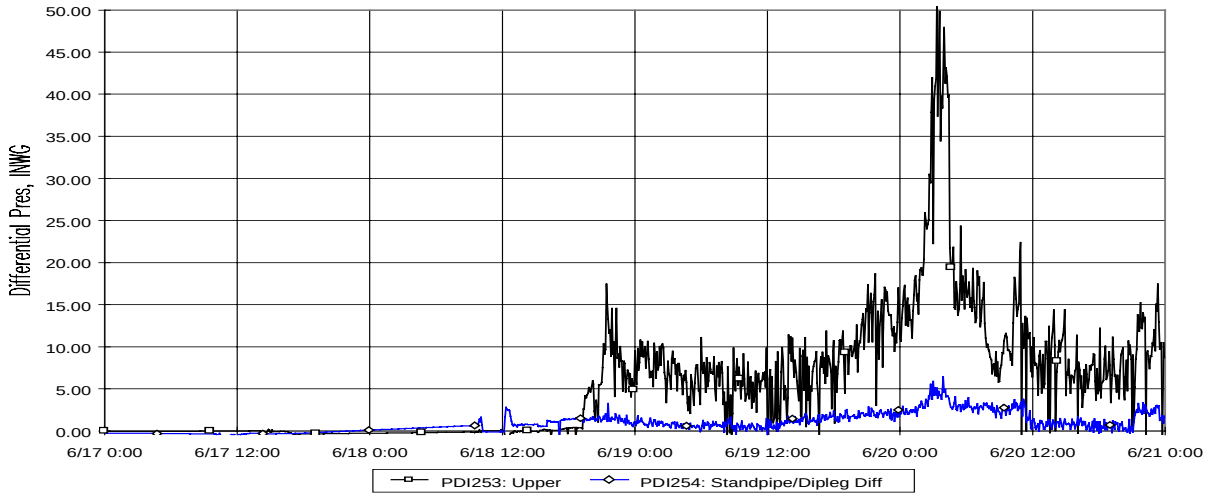

Figure 4.1.3-14 CY0201 Dipleg Differential Pressure Profiles

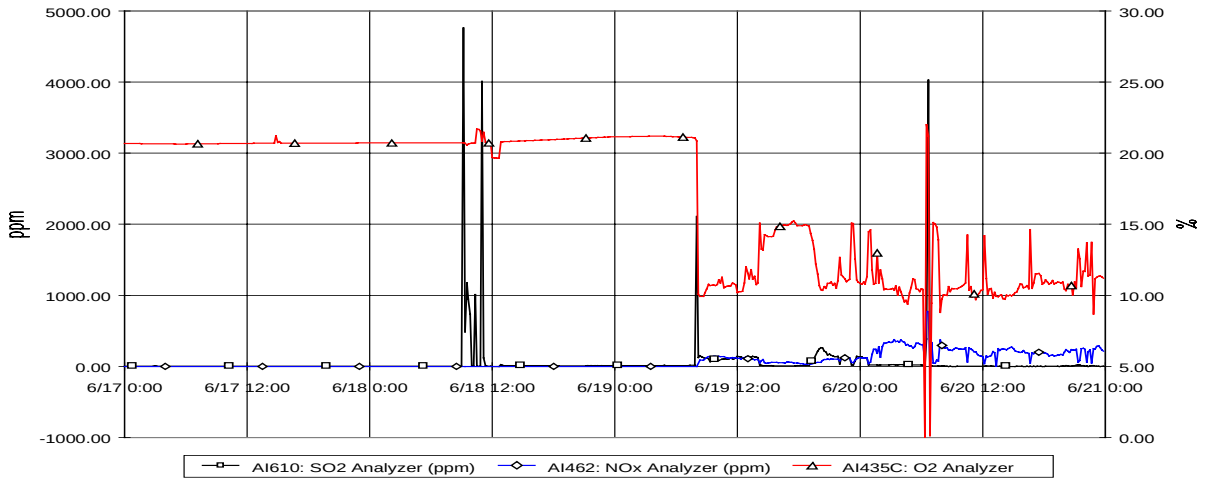

Figure 4.1.3-15 O_2, SO_2, and NO_x Analyzers

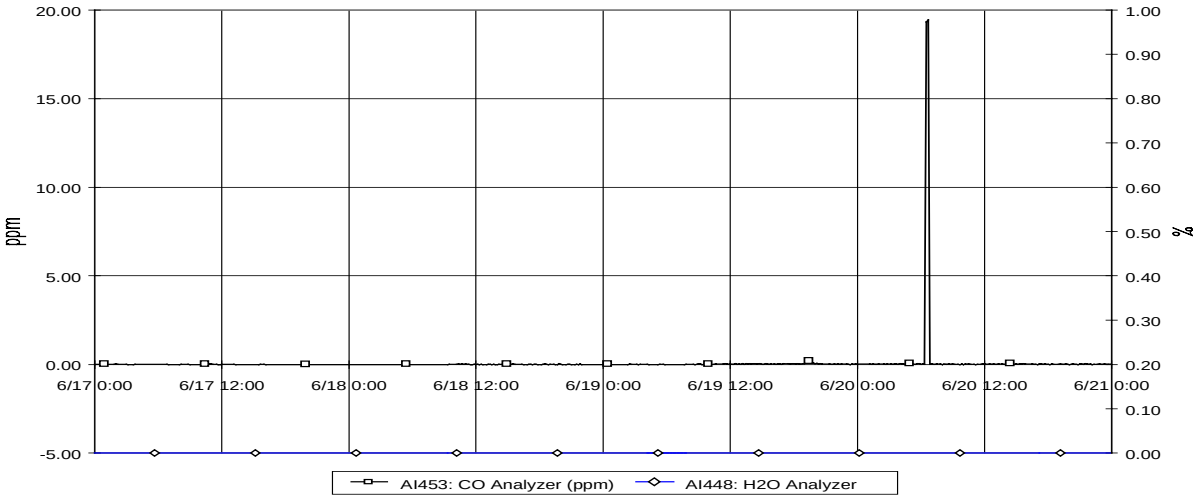

Figure 4.1.3-16 CO and H_2O Analyzers

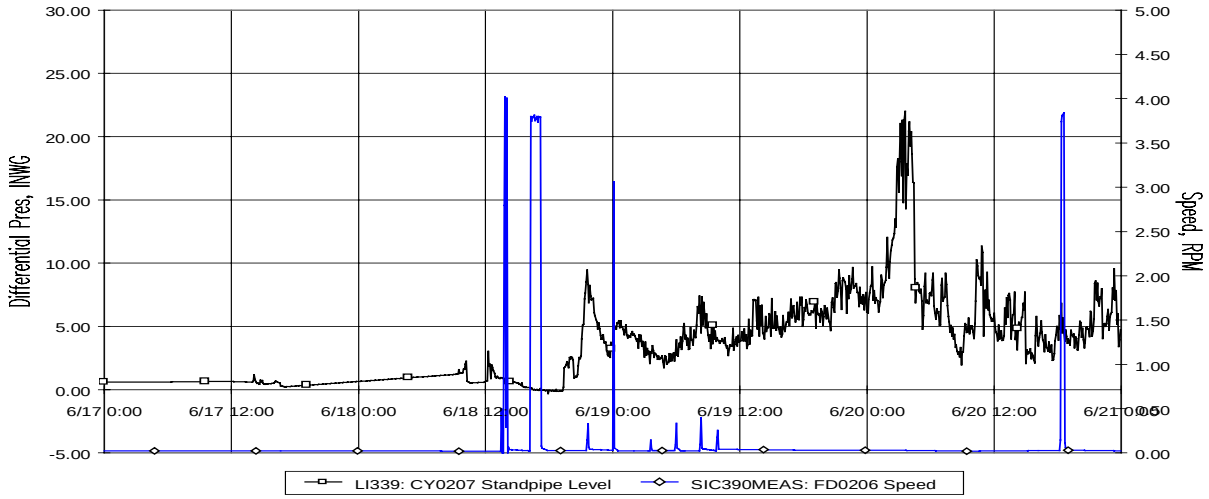

Figure 4.1.3-17 Solids Withdrawal

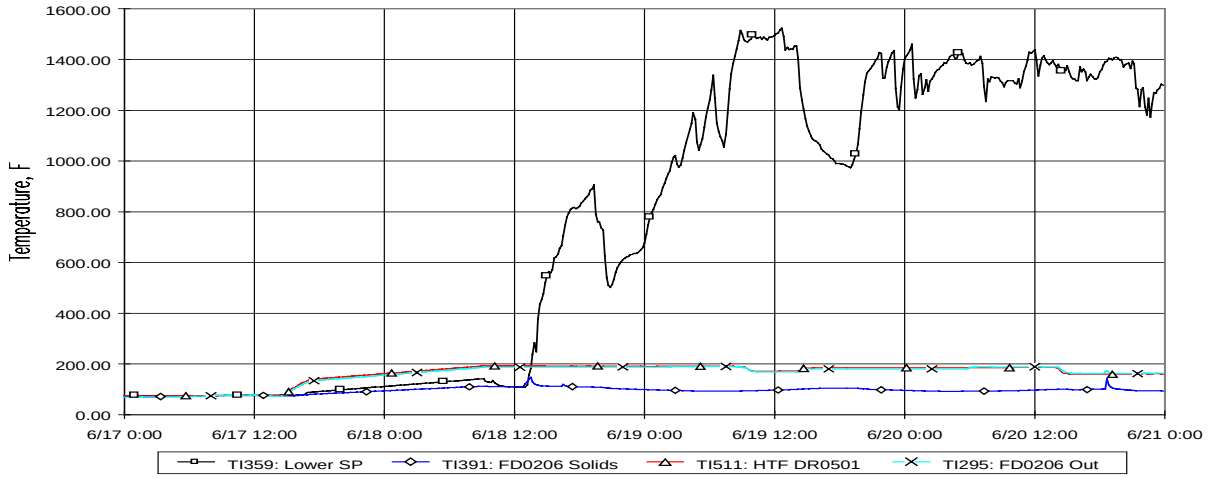

Figure 4.1.3-18 FD0510 Temperature Profiles

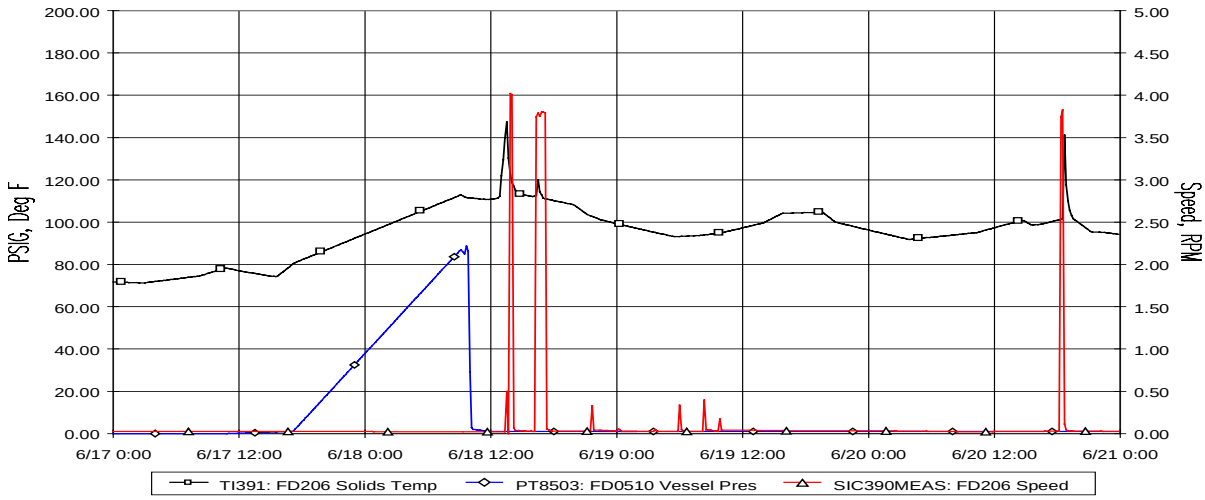

Figure 4.1.3-19 FD0206 Profiles

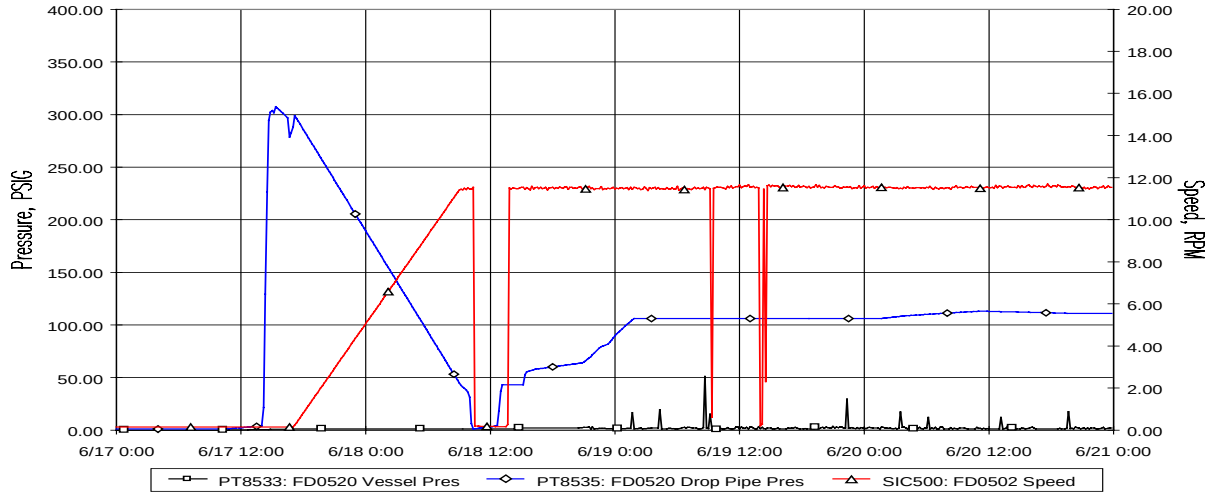

Figure 4.1.3-20 FD0520 Pressure Profiles

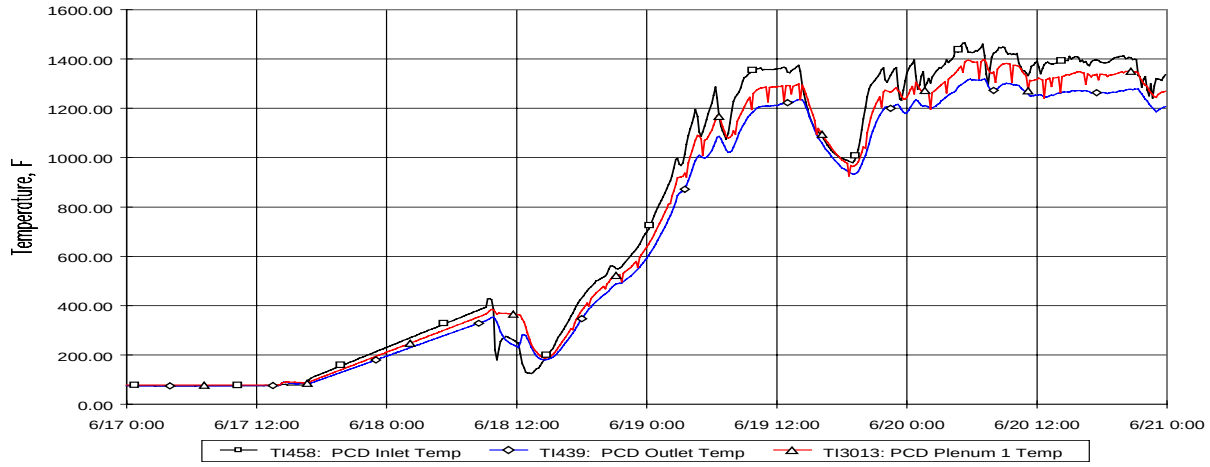

Figure 4.1.3-21 PCD Temperatures

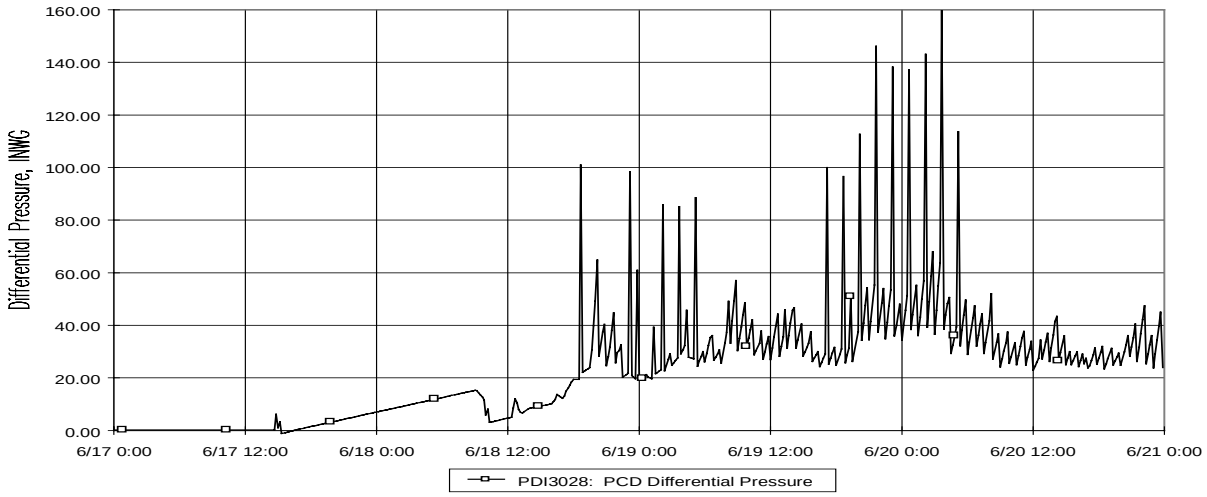

Figure 4.1.3-22 PCD Differential Pressure Profile

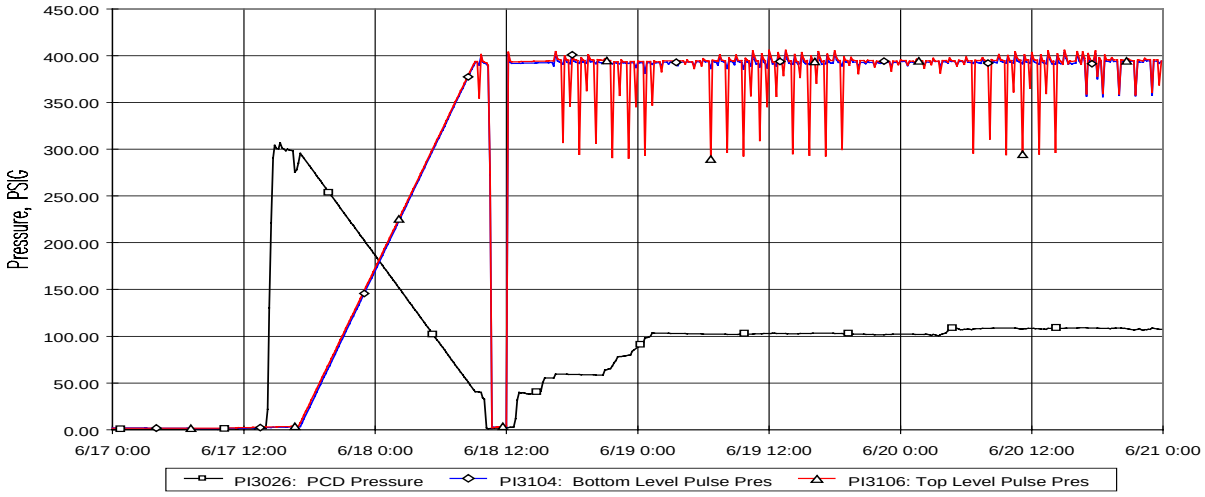

Figure 4.1.3-23 PCD Pressure and Pulse Pressure

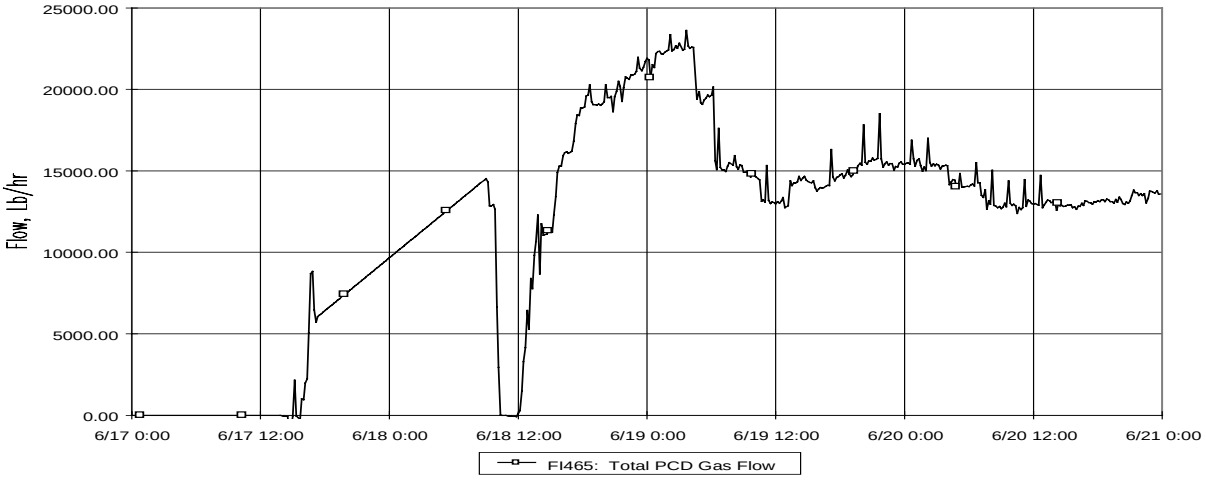

Figure 4.1.3-24 Gas Flow Through PCD

Section 4.1.3

Graphs 25 through 48

Test Run CCT6

June 21 through 23, 1997

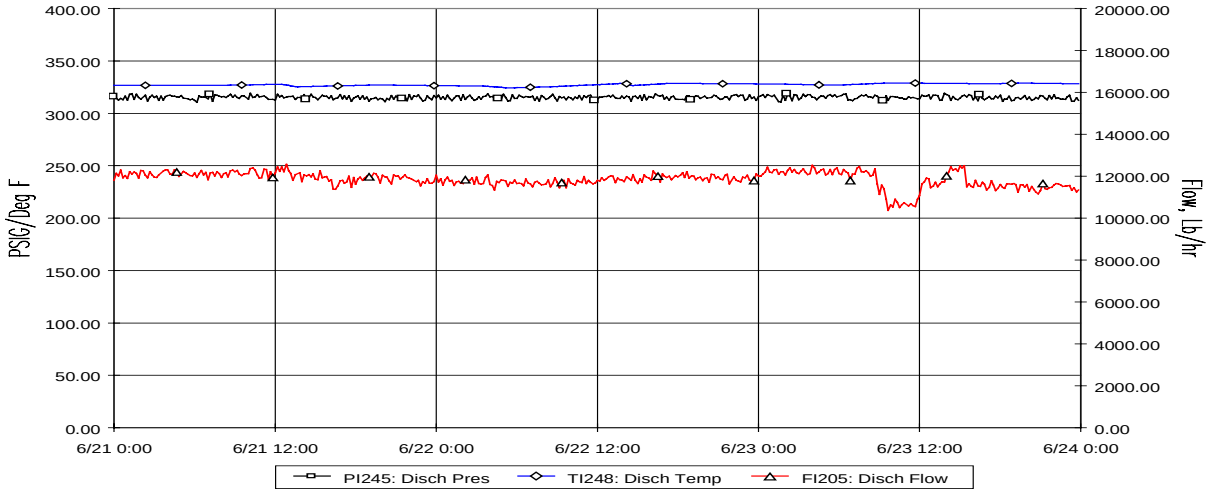

Figure 4.1.3-25 CO0201 System Profile

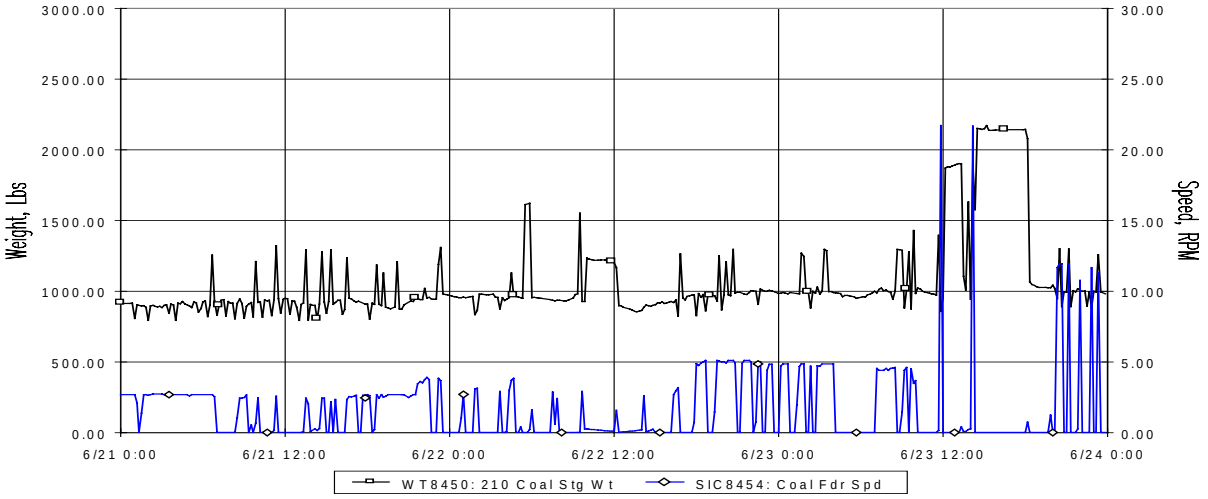

Figure 4.1.3-26 Coal Feed System Profile

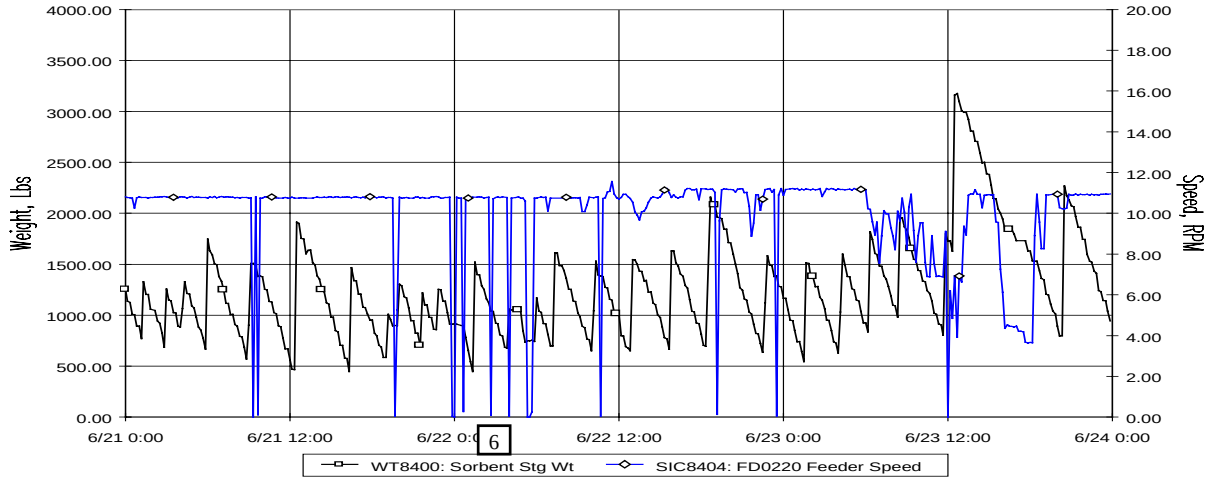

Figure 4.1.3-27 Sorbent Feed System Profile

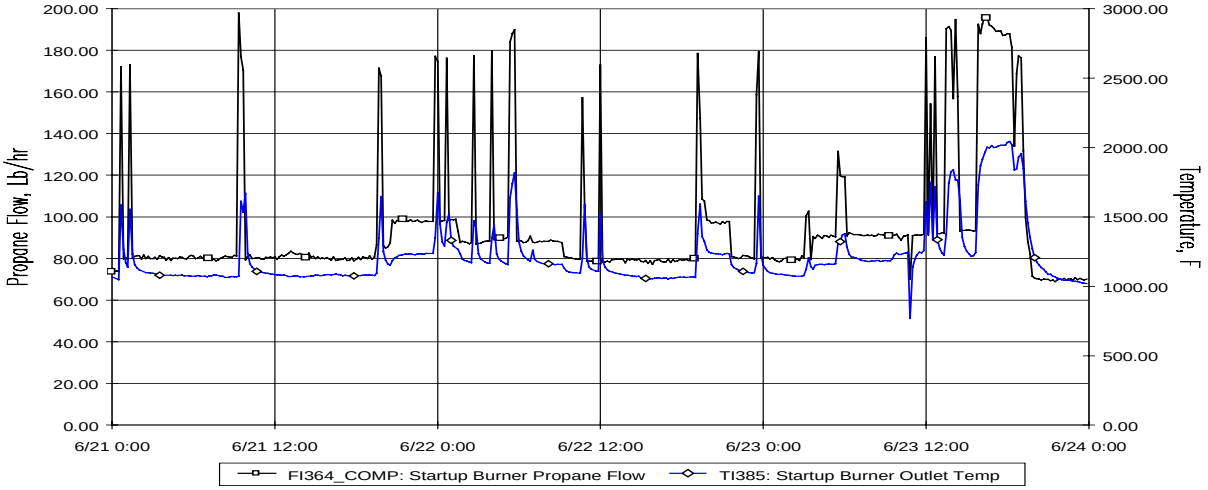

Figure 4.1.3-28 Start-Up Burner Flow/Temperature

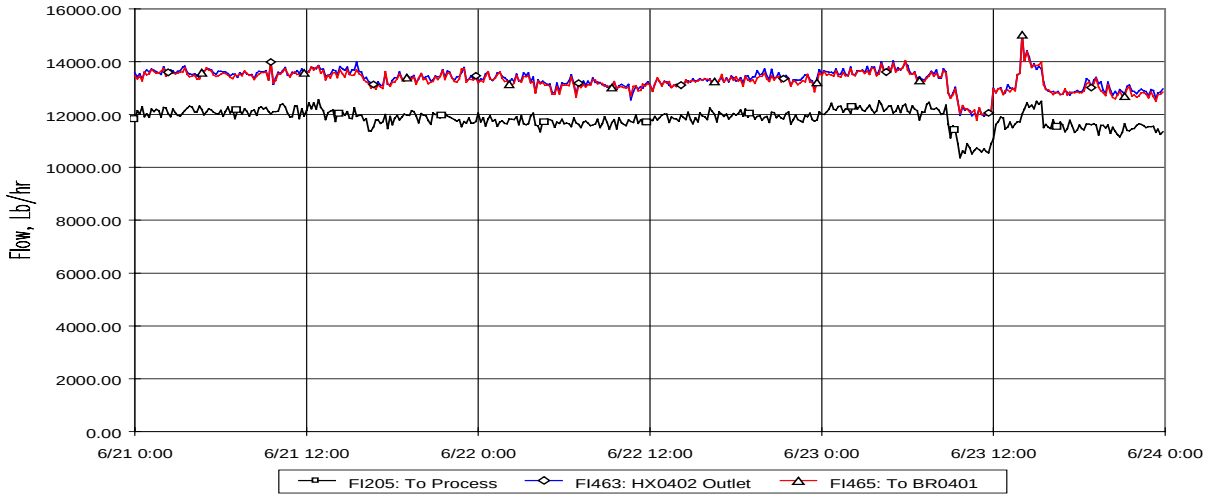

Figure 4.1.3-29 Total Gas In/Out Flow Rates

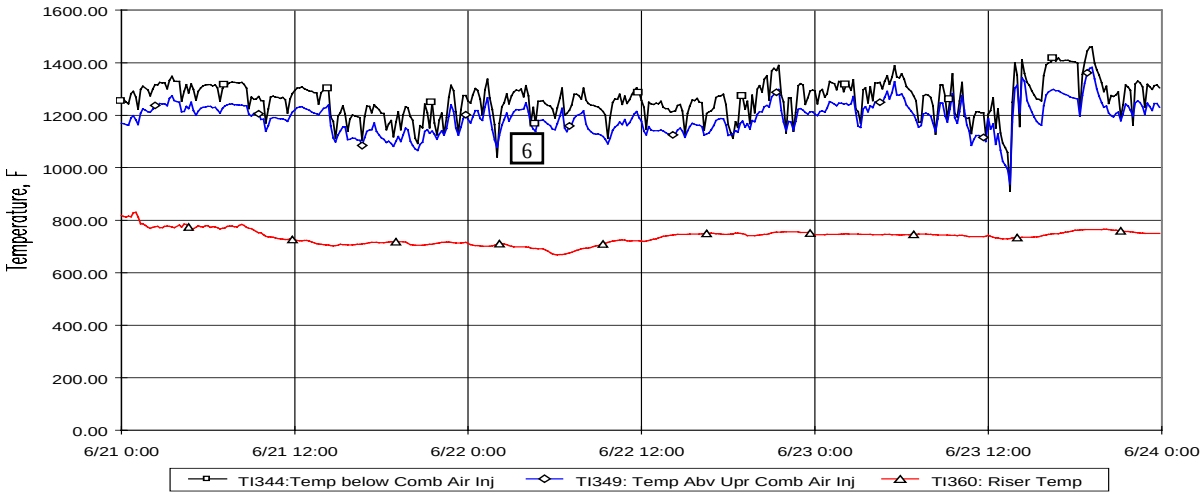

Figure 4.1.3-30 Reactor Mixing Zone and Riser Temperatures

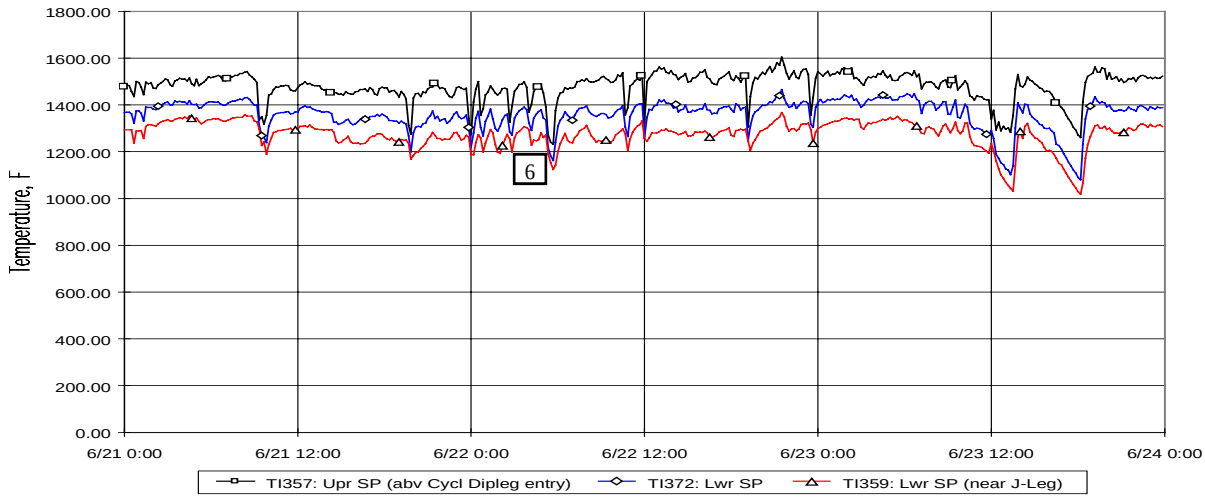

Figure 4.1.3-31 Standpipe Temperatures

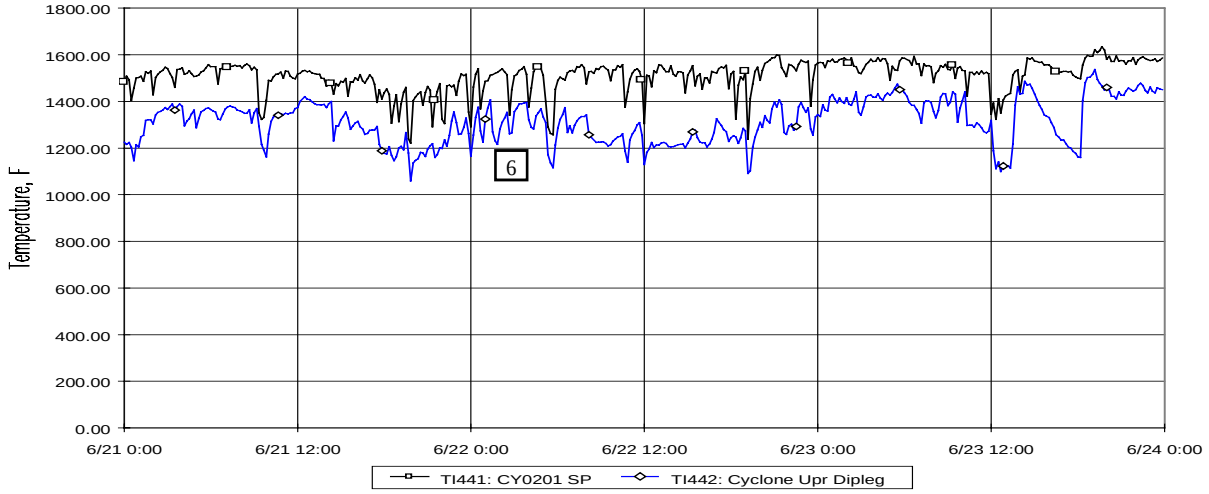

Figure 4.1.3-32 Cyclone Dipleg Temperatures

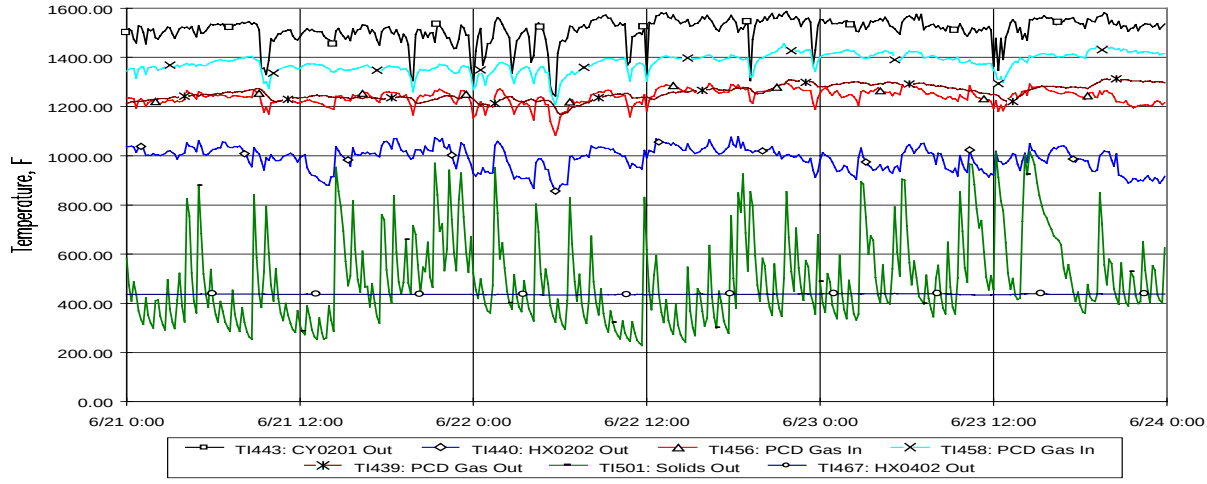

Figure 4.1.3-33 Temperature Profiles Downstream of Reactor

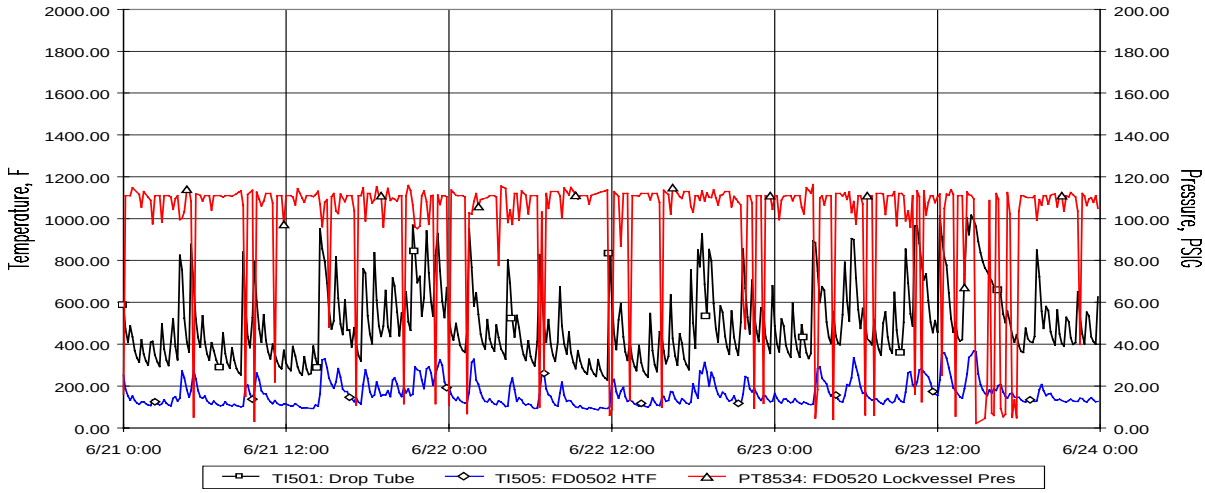

Figure 4.1.3-34 PCD Ash Temperatures

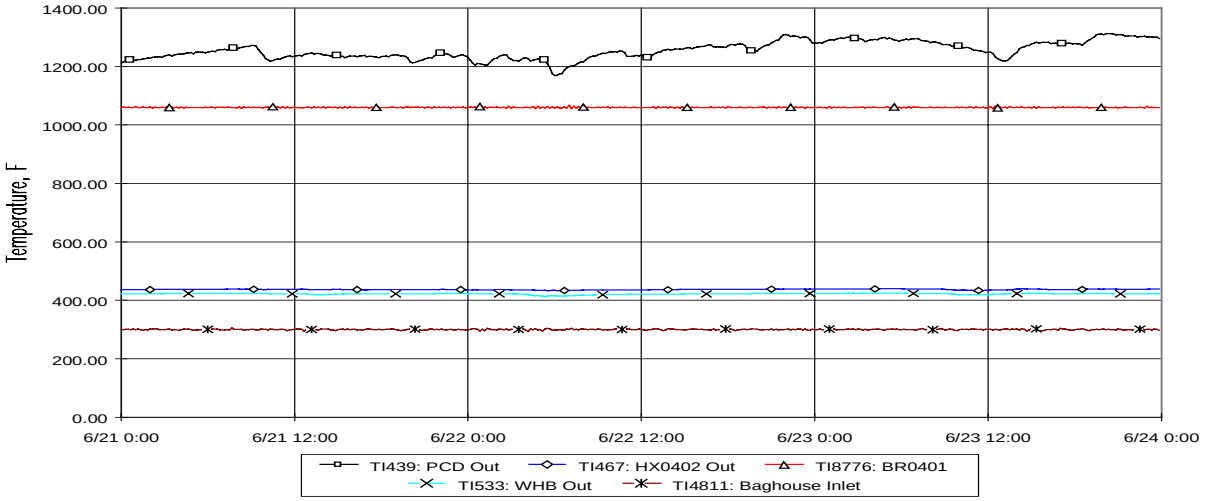

Figure 4.1.3-35 System Temperatures Downstream of PCD

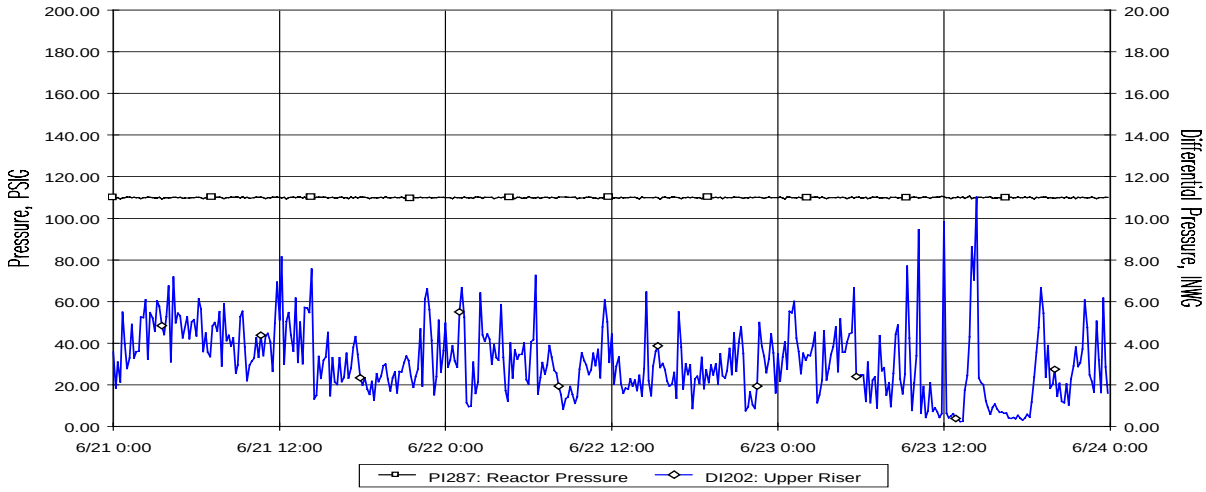

Figure 4.1.3-36 Reactor Pressure/Riser Differential Pressure Profiles

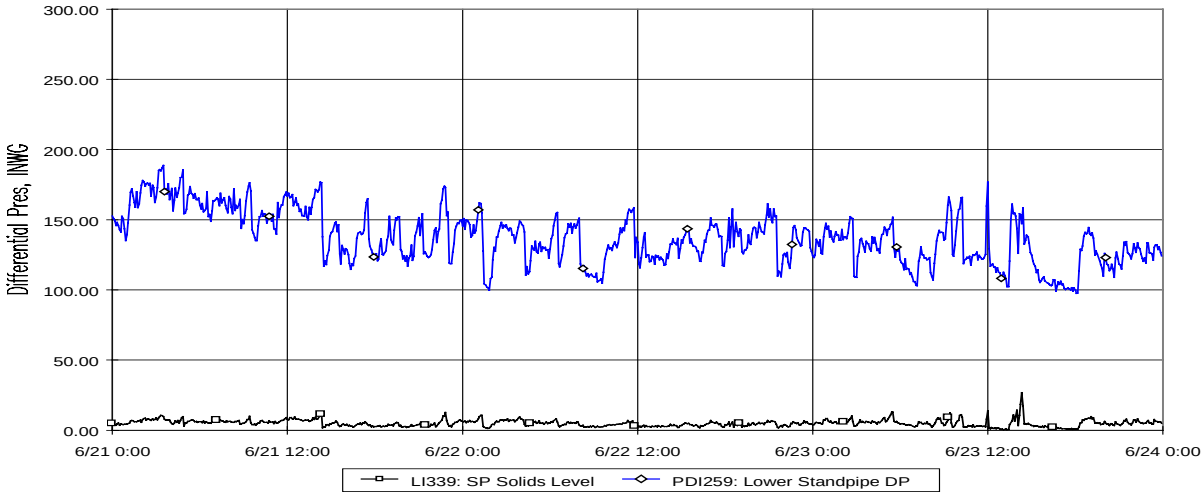

Figure 4.1.3-37 Standpipe Differential Pressure Profiles

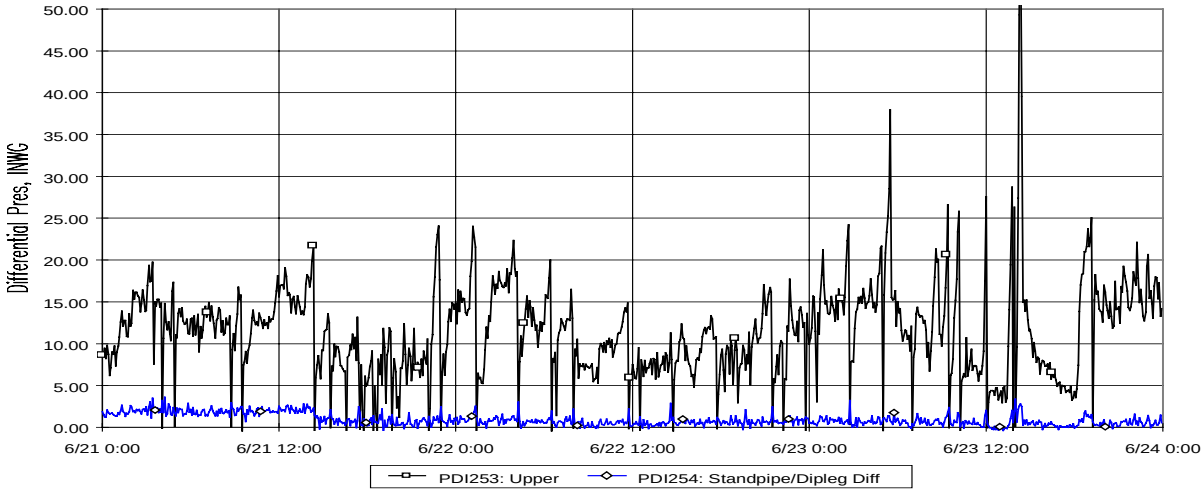

Figure 4.1.3-38 CY0201 Dipleg Differential Pressure Profiles

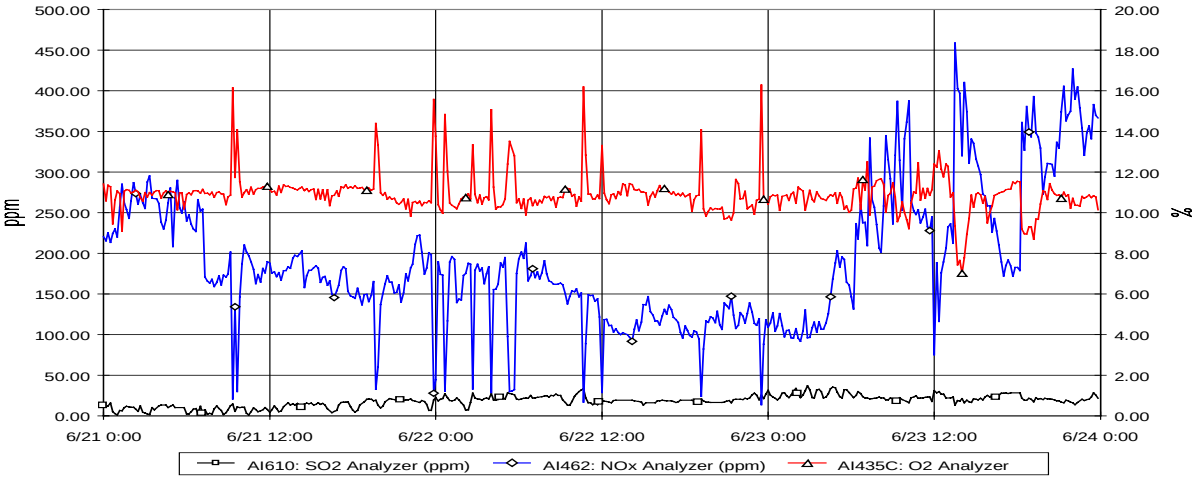

Figure 4.1.3-39 O_2, SO_2, and NO_x Analyzers

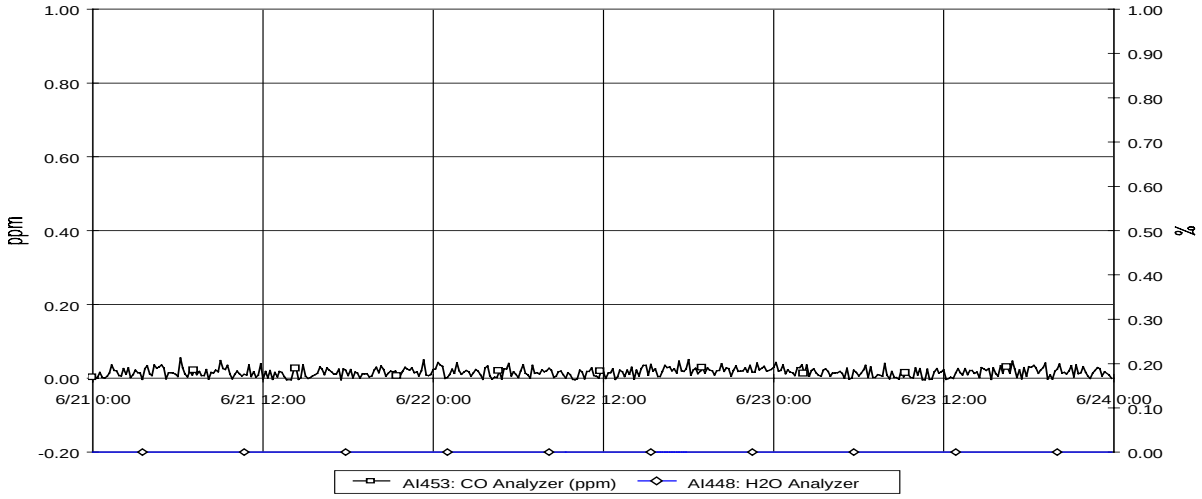

Figure 4.1.3-40 CO and H_2O Analyzers

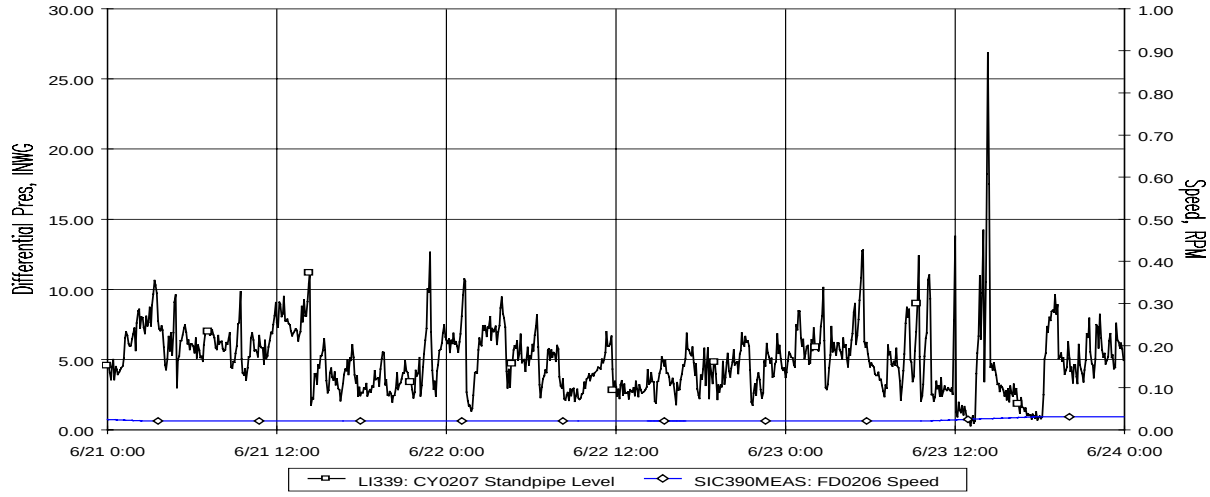

Figure 4.1.3-41 Solids Withdrawal

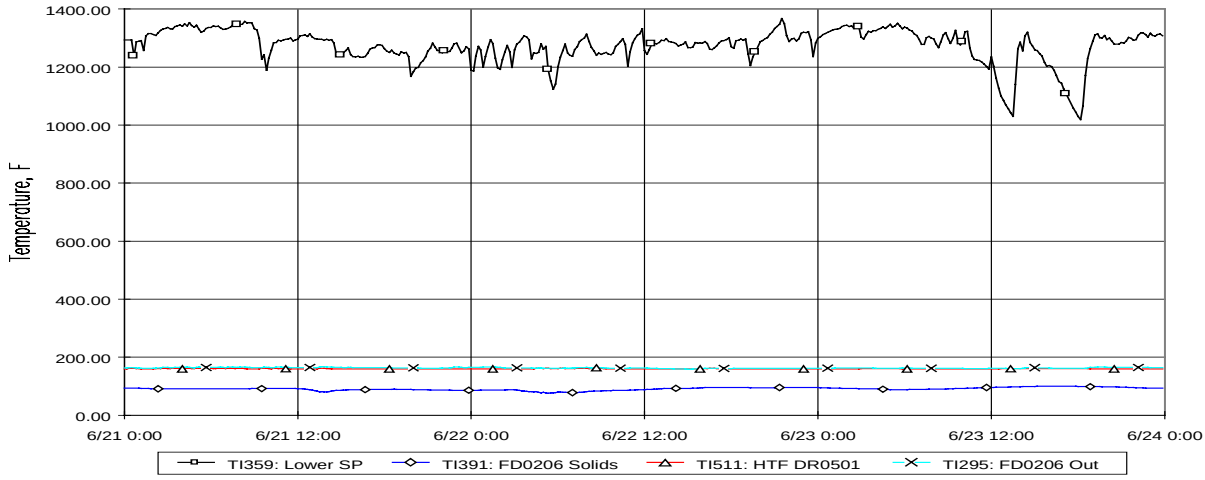

Figure 4.1.3-42 FD0510 Temperature Profiles

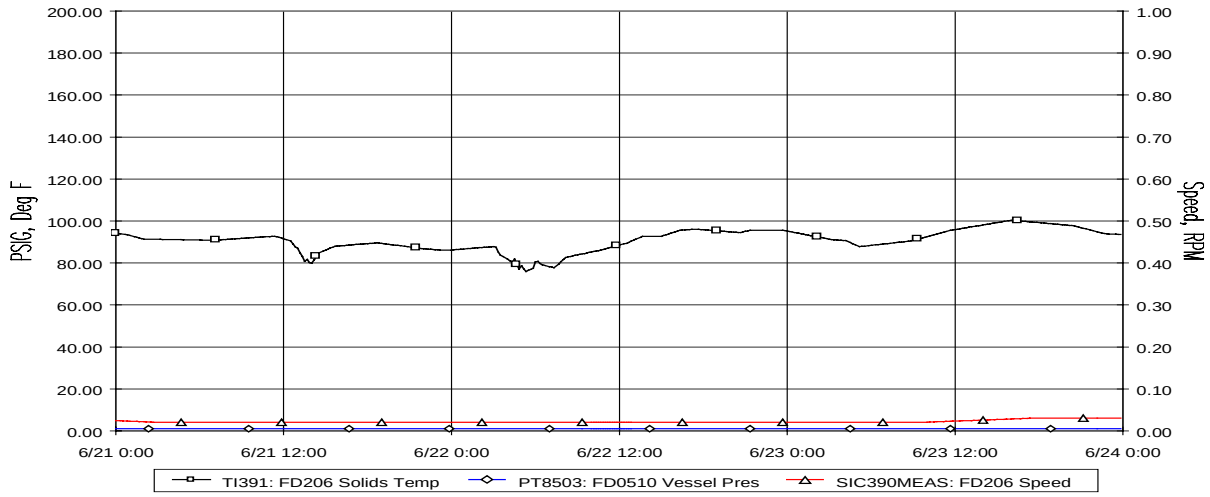

Figure 4.1.3-43 FD0206 Profiles

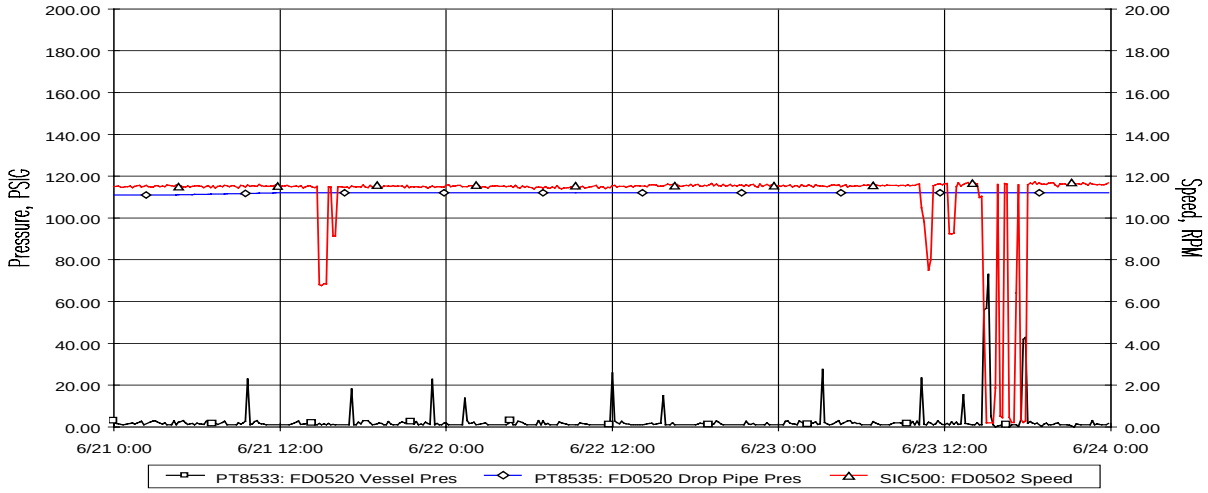

Figure 4.1.3-44 FD0520 Pressure Profiles

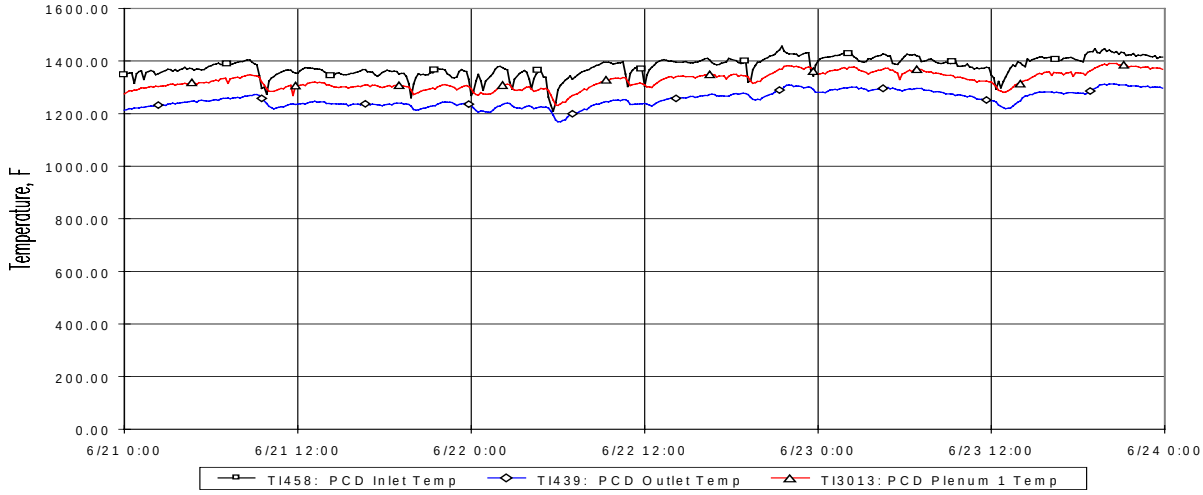

Figure 4.1.3-45 PCD Temperatures

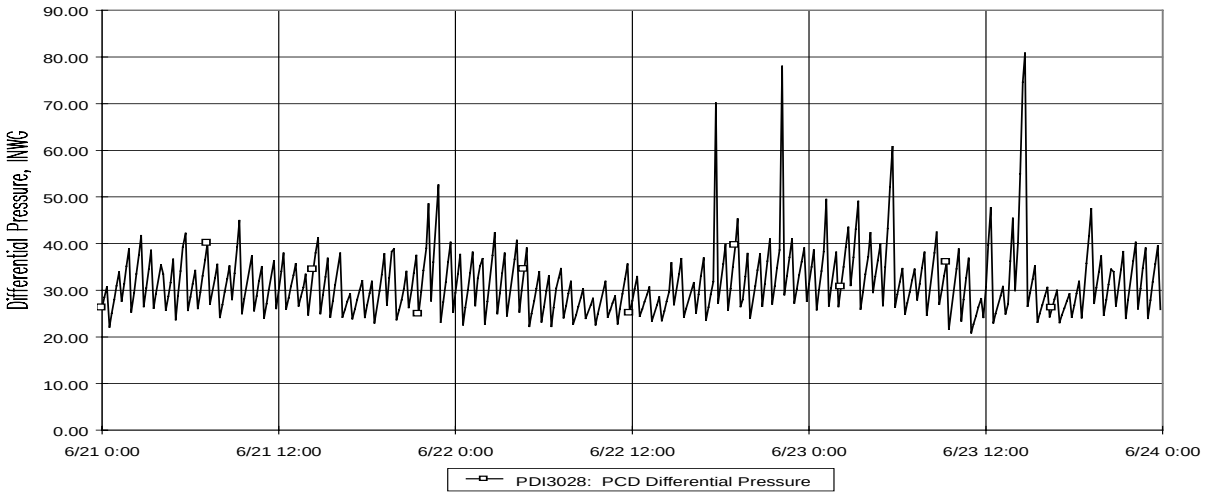

Figure 4.1.3-46 PCD Differential Pressure Profile

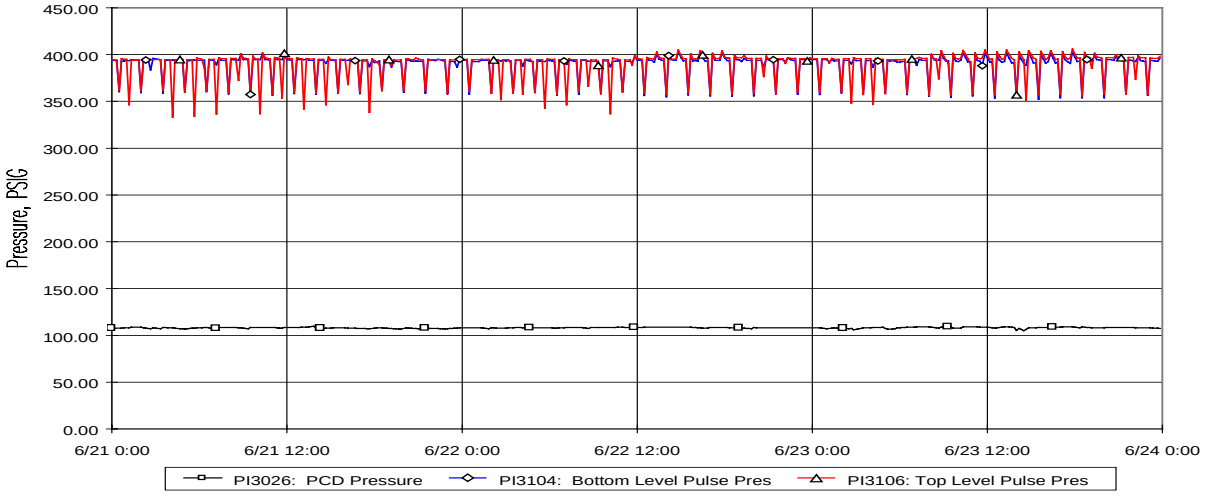

Figure 4.1.3-47 PCD Pressure and Pulse Pressure

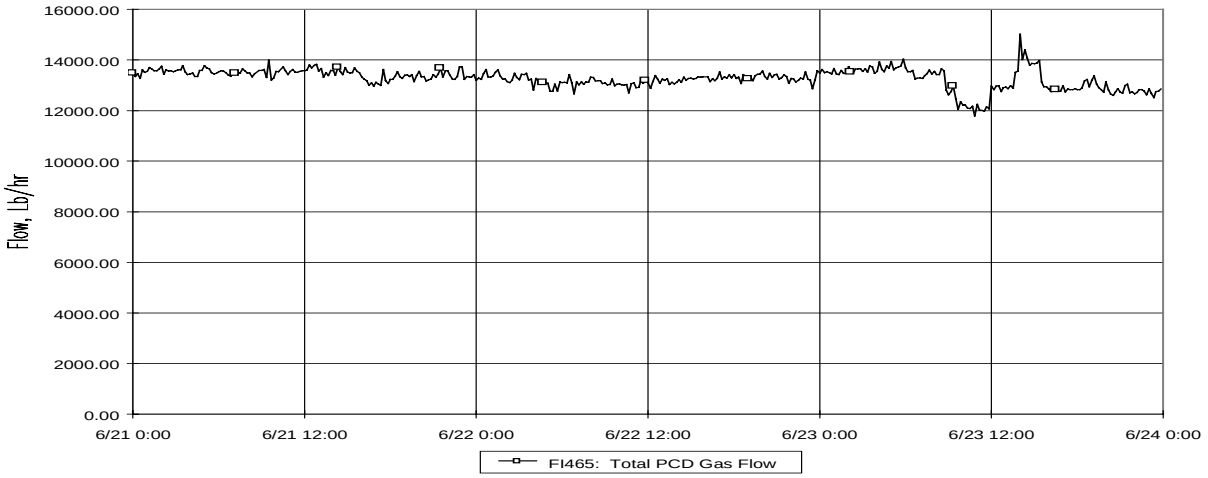

Figure 4.1.3-48 Gas Flow Through PCD

Section 4.1.3

Graphs 49 through 72

Test Run CCT6

June 24 through 26, 1997

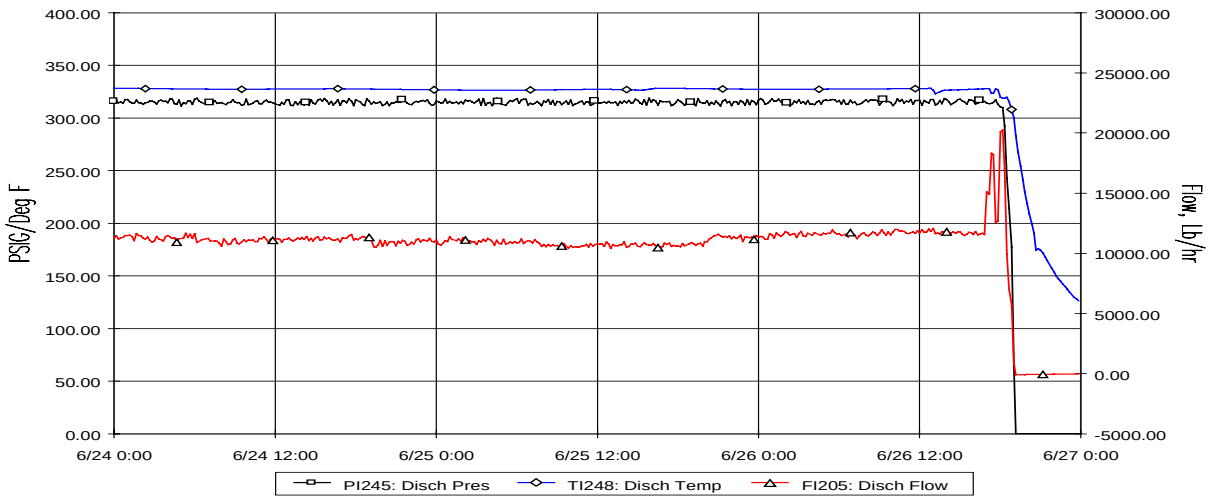

Figure 4.1.3-49 CO0201 System Profile

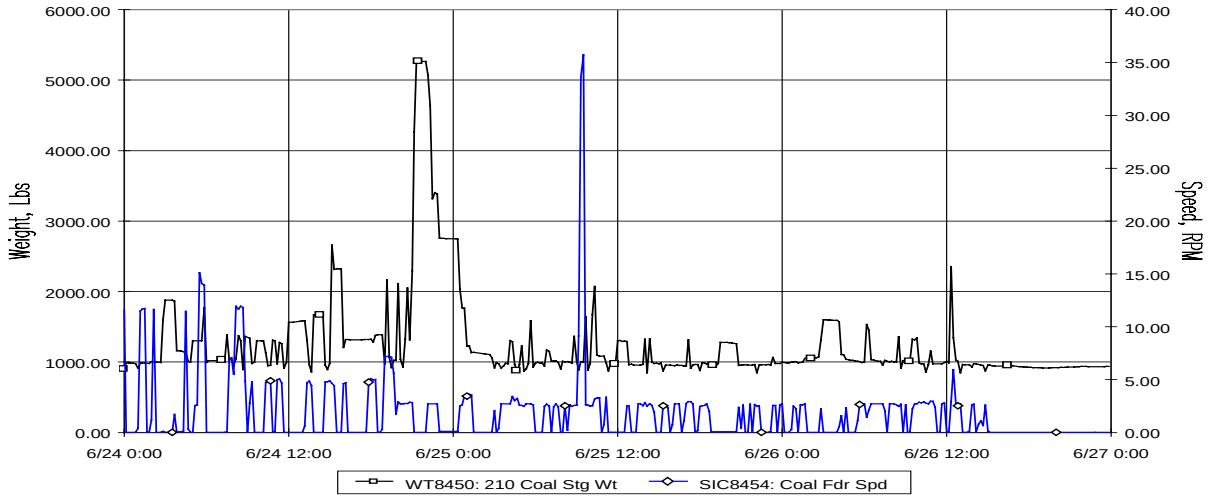

Figure 4.1.3-50 Coal Feed System Profile

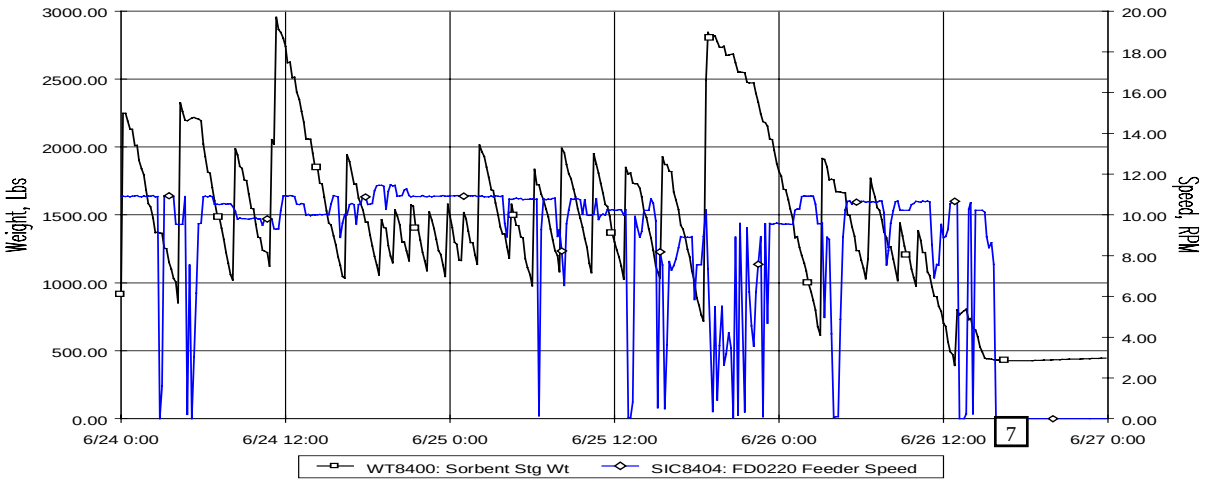

Figure 4.1.3-51 Sorbent Feed System Profile

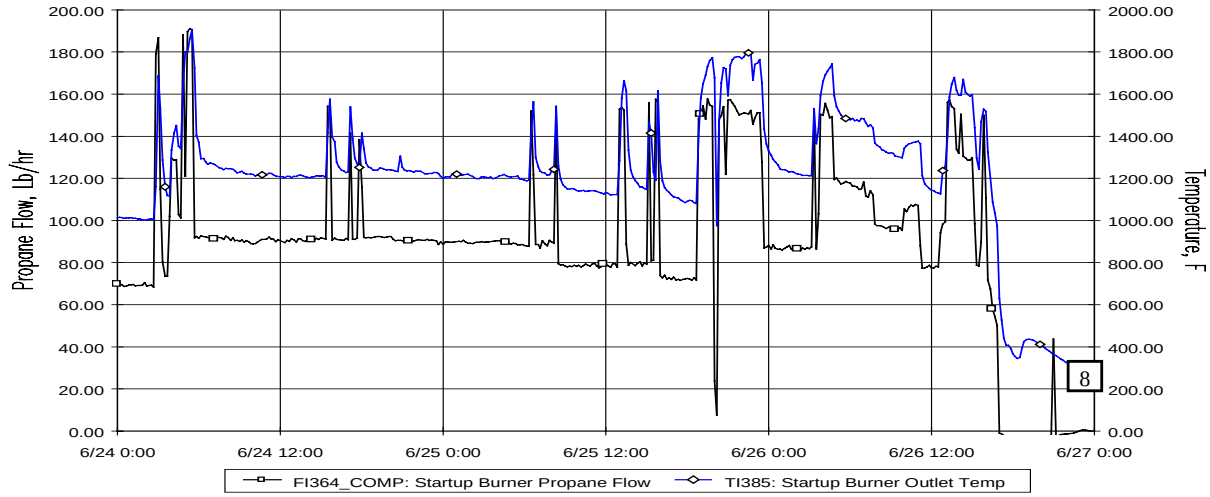

Figure 4.1.3-52 Start-Up Burner Flow/Temperature

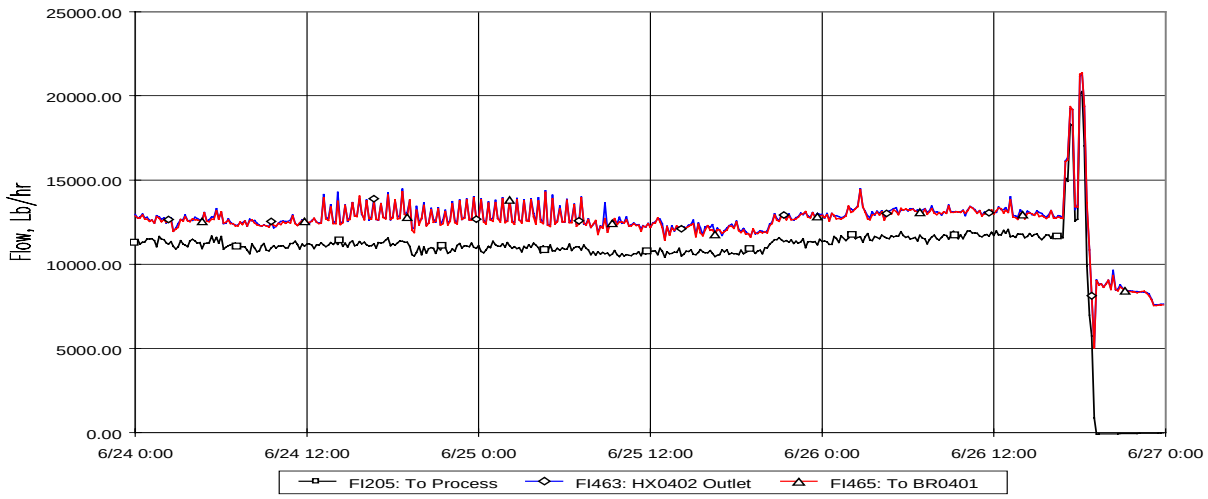

Figure 4.1.3-53 Total Gas In/Out Flow rates

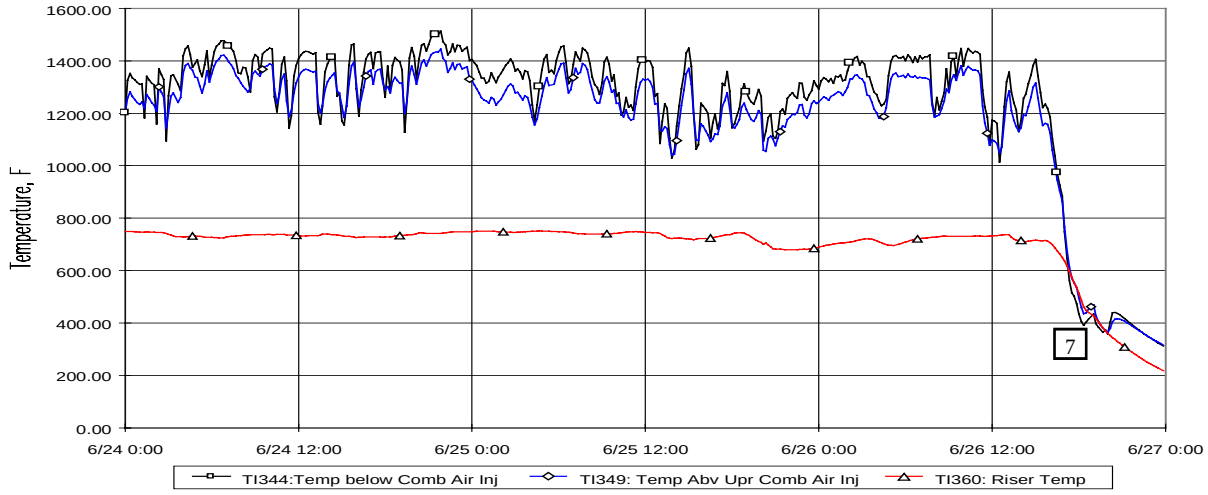

Figure 4.1.3-54 Reactor Mixing Zone and Riser Temperatures

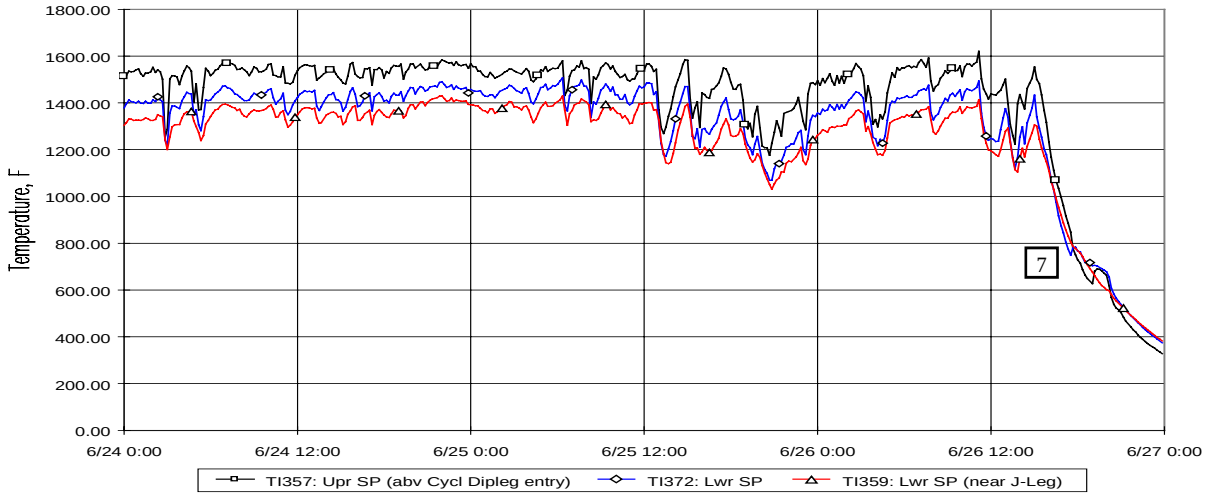

Figure 4.1.3-55 Standpipe Temperatures

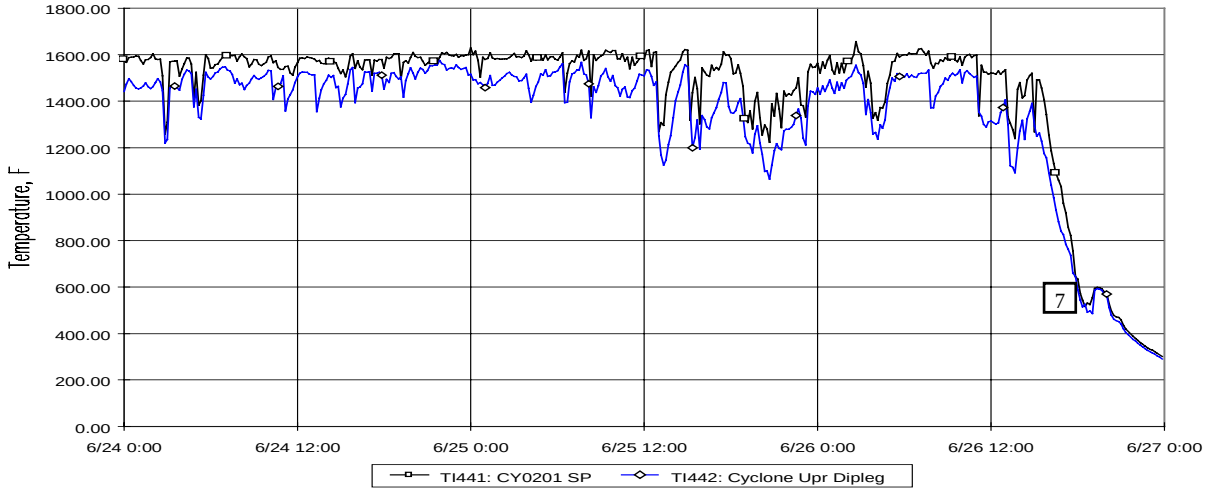

Figure 4.1.3-56 Cyclone Dipleg Temperatures

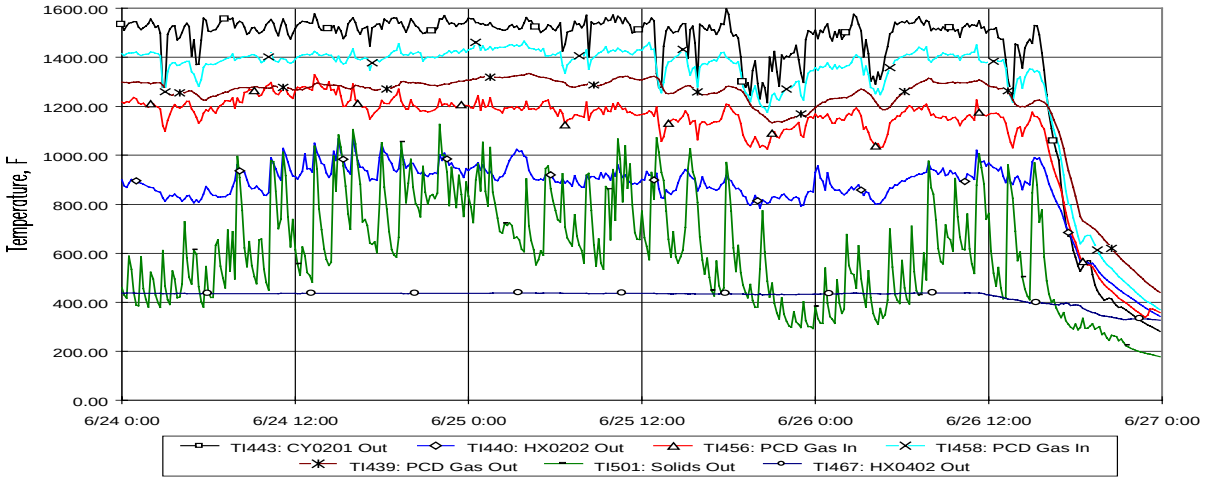

Figure 4.1.3-57 Temperature Profiles Downstream of Reactor

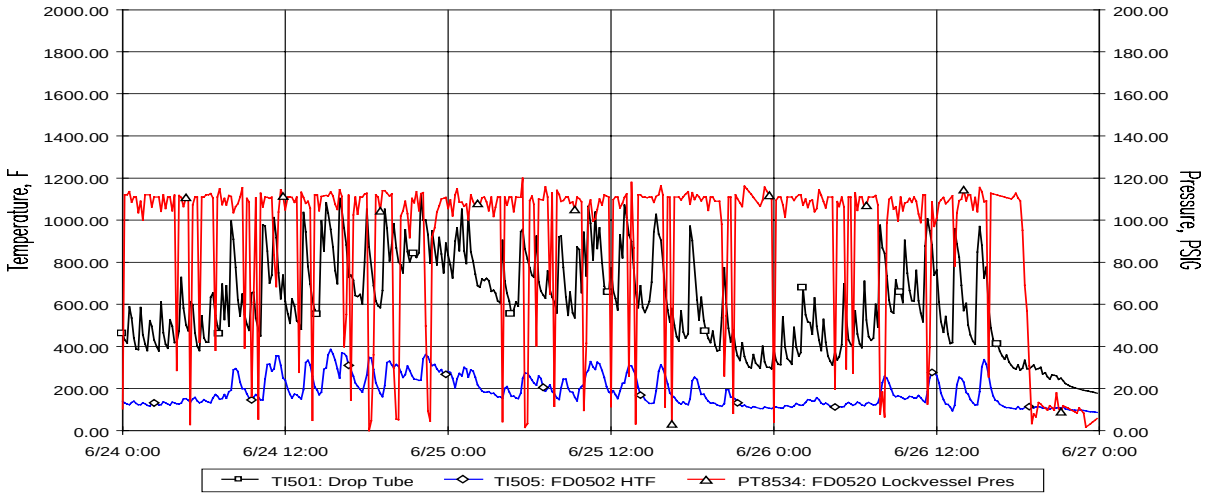

Figure 4.1.3-58 PCD Ash Temperatures

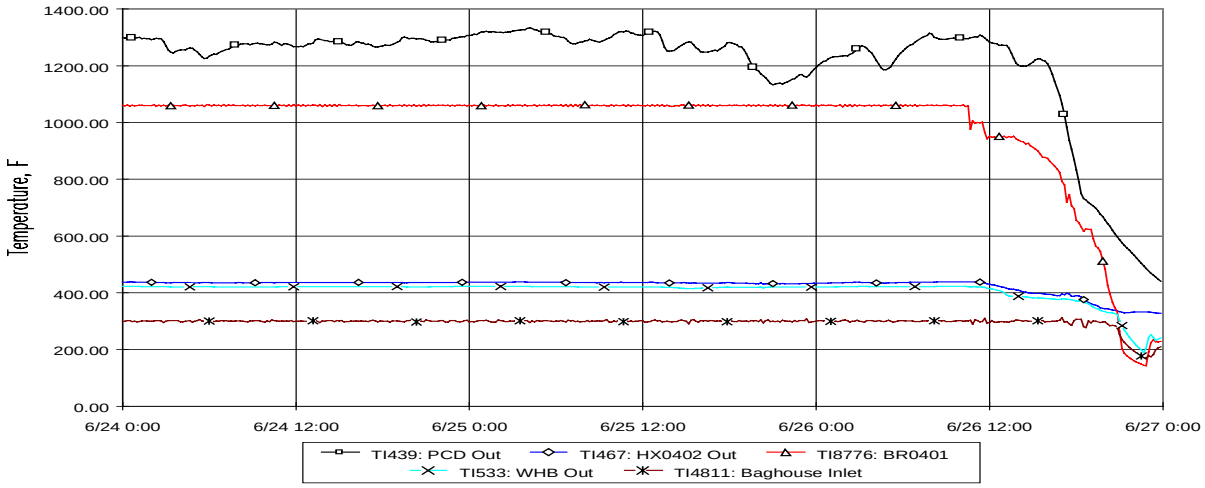

Figure 4.1.3-59 System Temperatures Downstream of PCD

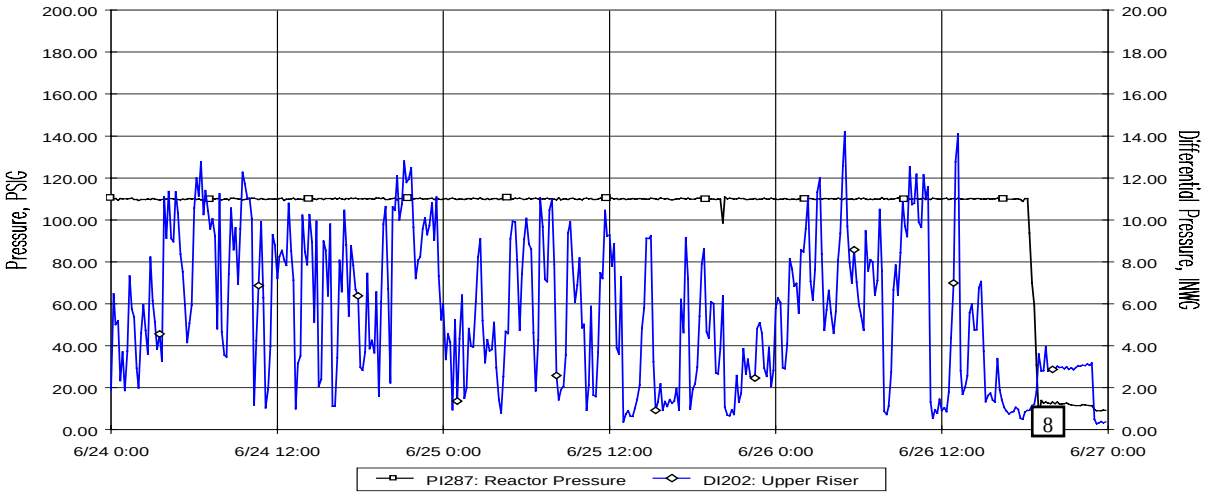

Figure 4.1.3-60 Reactor Pressure/Riser Differential Pressure Profiles

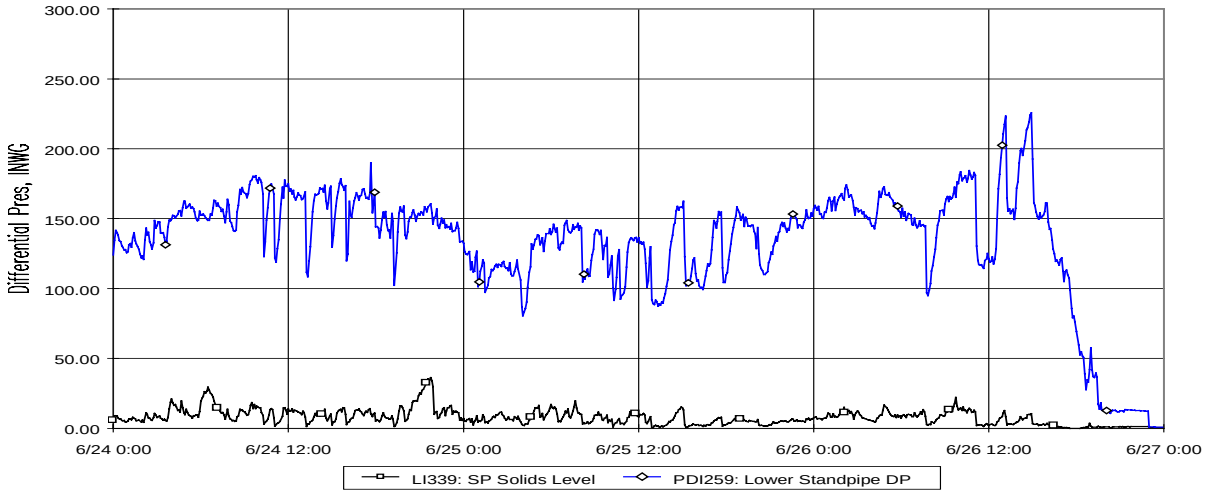

Figure 4.1.3-61 Standpipe Differential Pressure Profiles

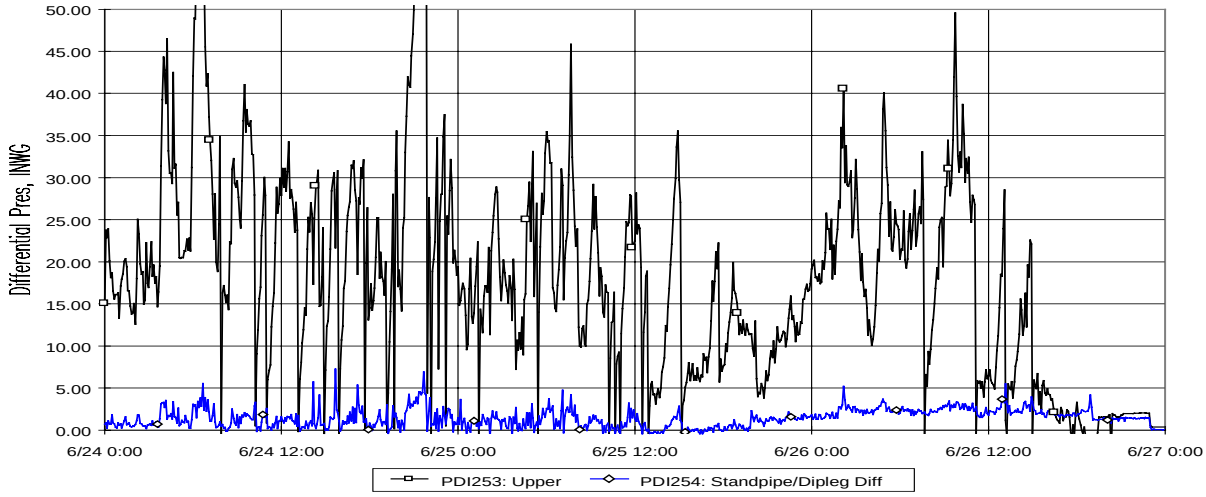

Figure 4.1.3-62 CY0201 Dipleg Differential Pressure Profiles

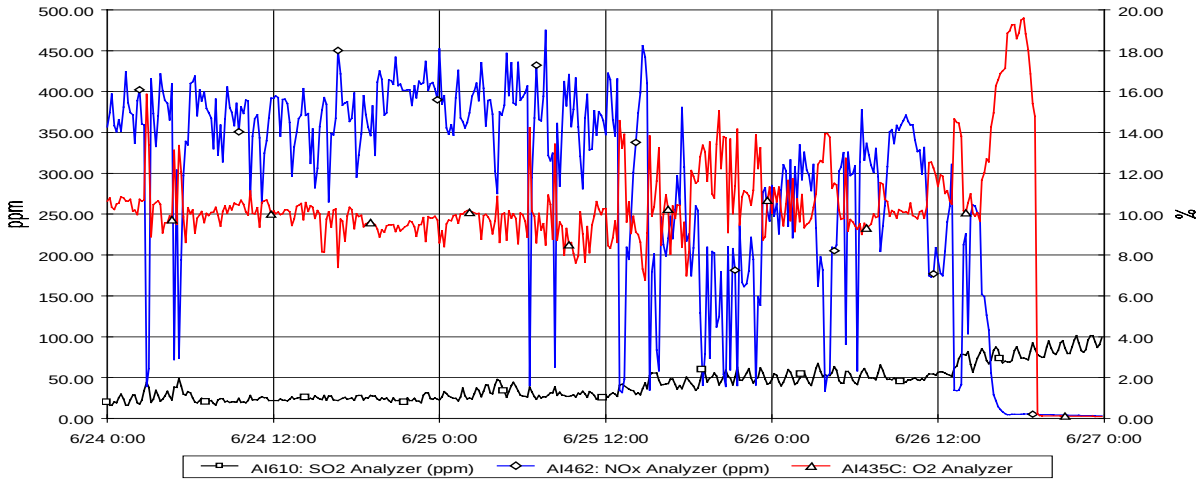

Figure 4.1.3-63 O_2, SO_2, and NO_x Analyzers

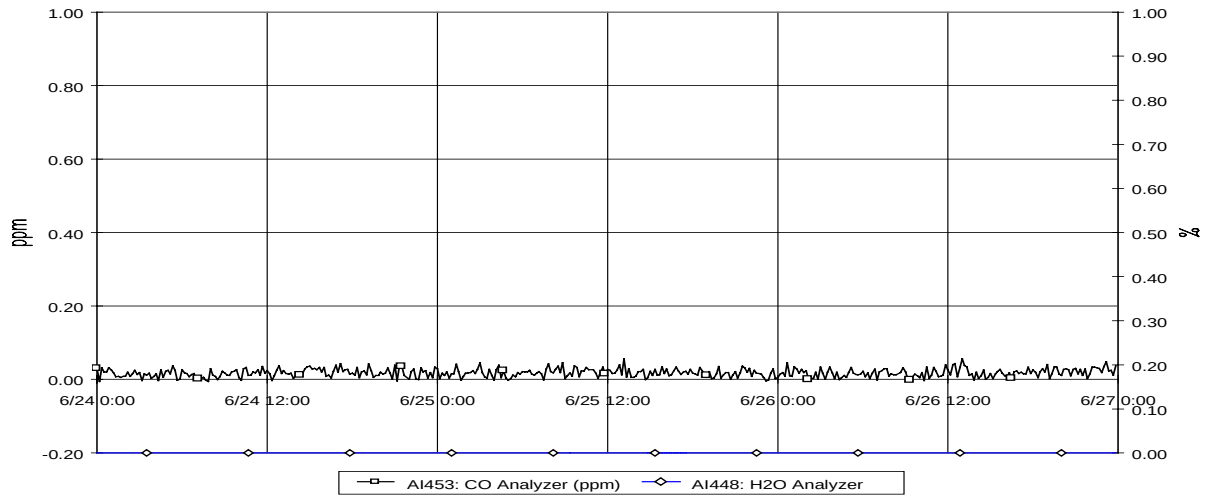

Figure 4.1.3-64 CO and H_2O Analyzers

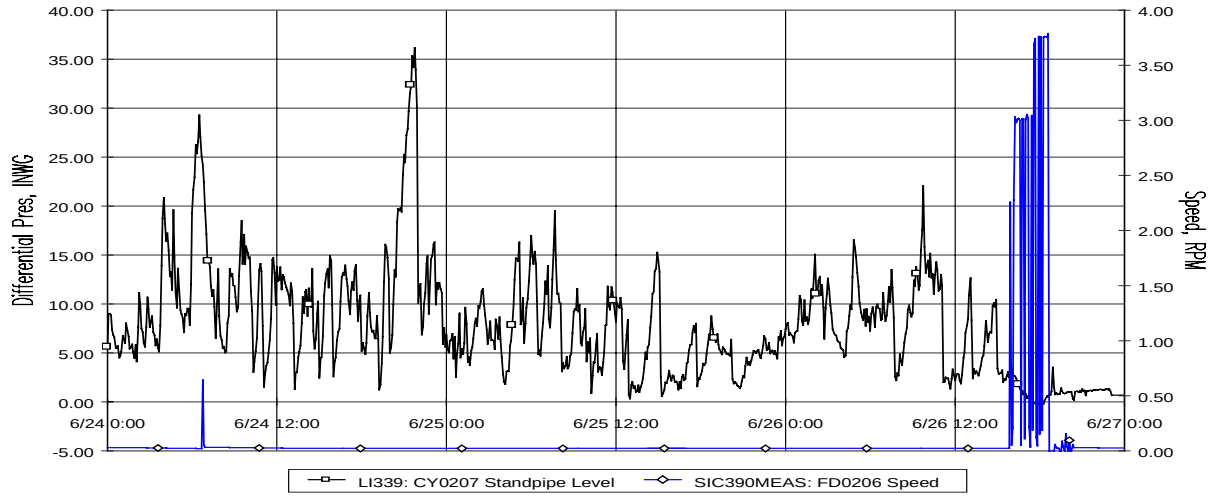

Figure 4.1.3-65 Solids Withdrawal

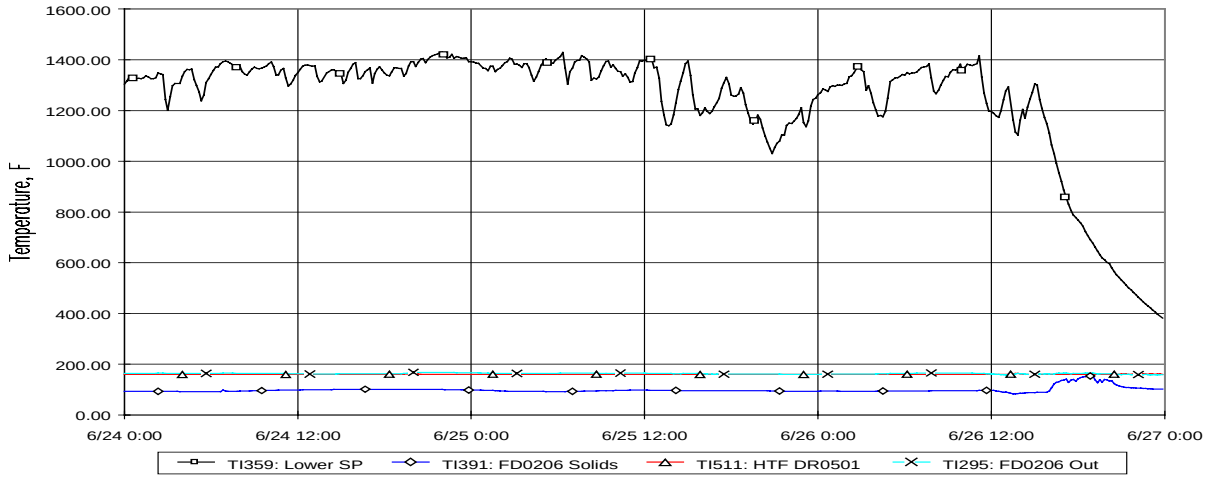

Figure 4.1.3-66 FD0510 Temperature Profiles

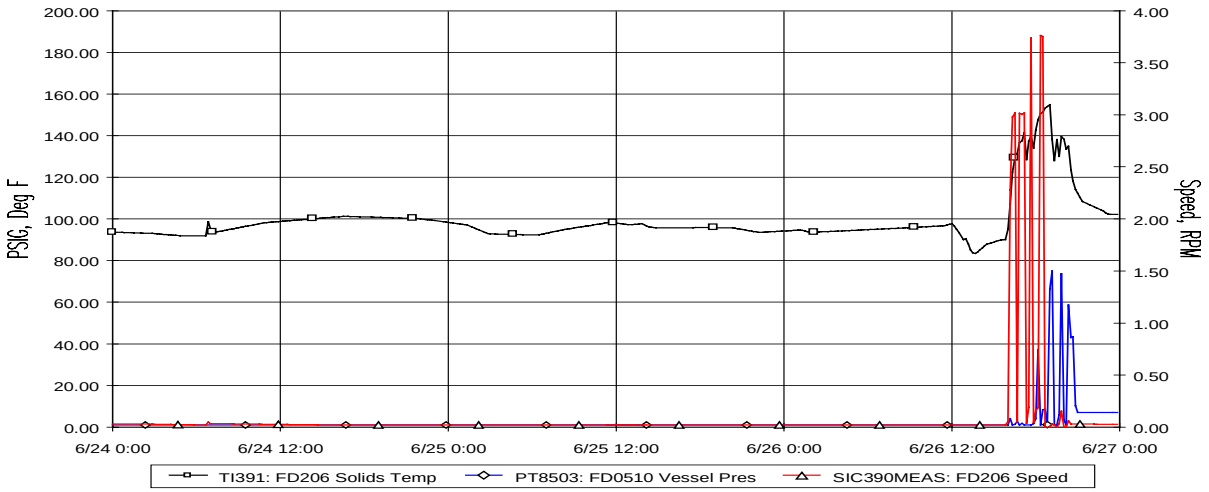

Figure 4.1.3-67 FD0206 Profiles

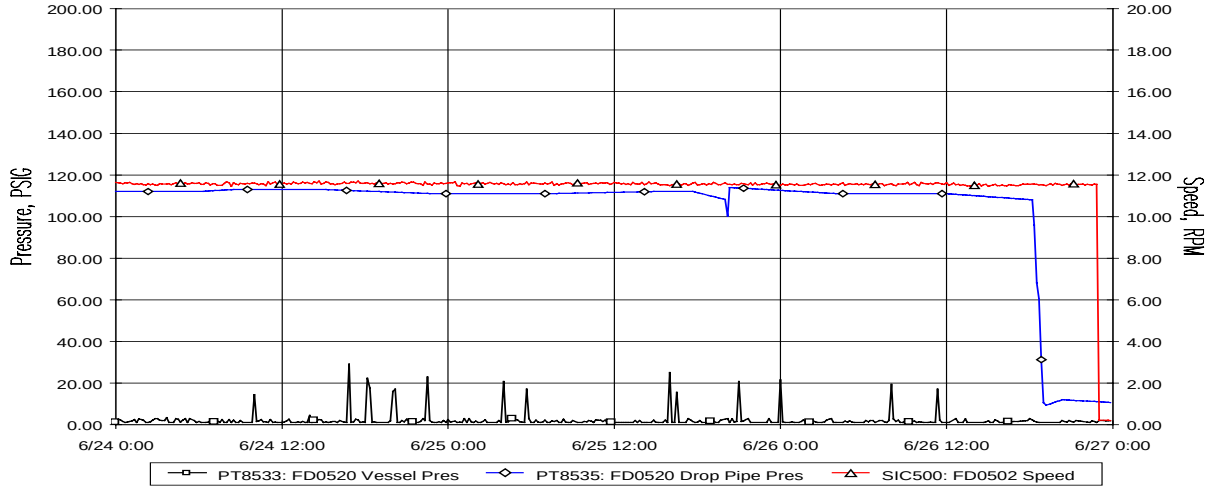

Figure 4.1.3-68 FD0520 Pressure Profiles

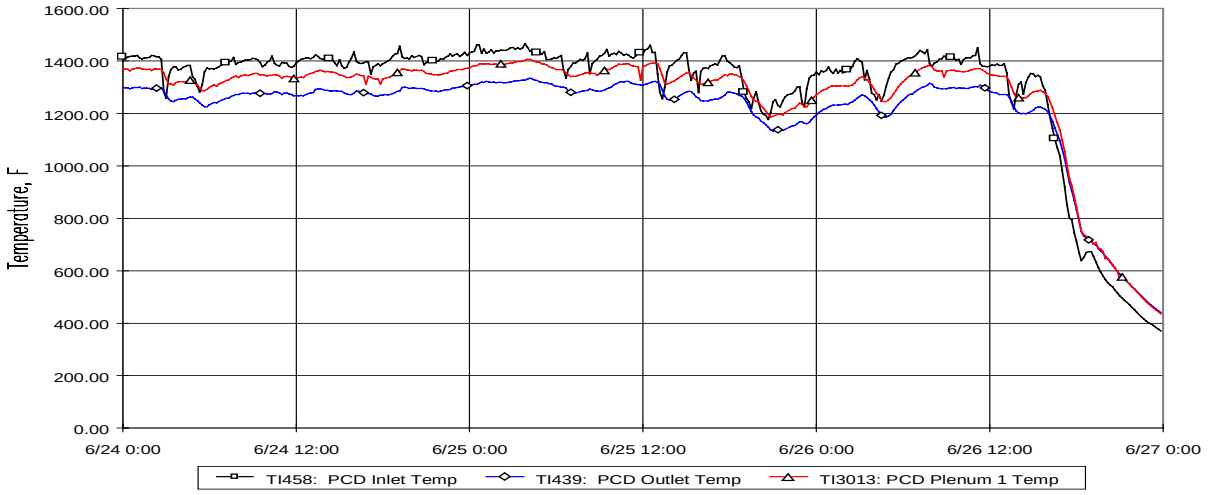

Figure 4.1.3-69 PCD Temperatures

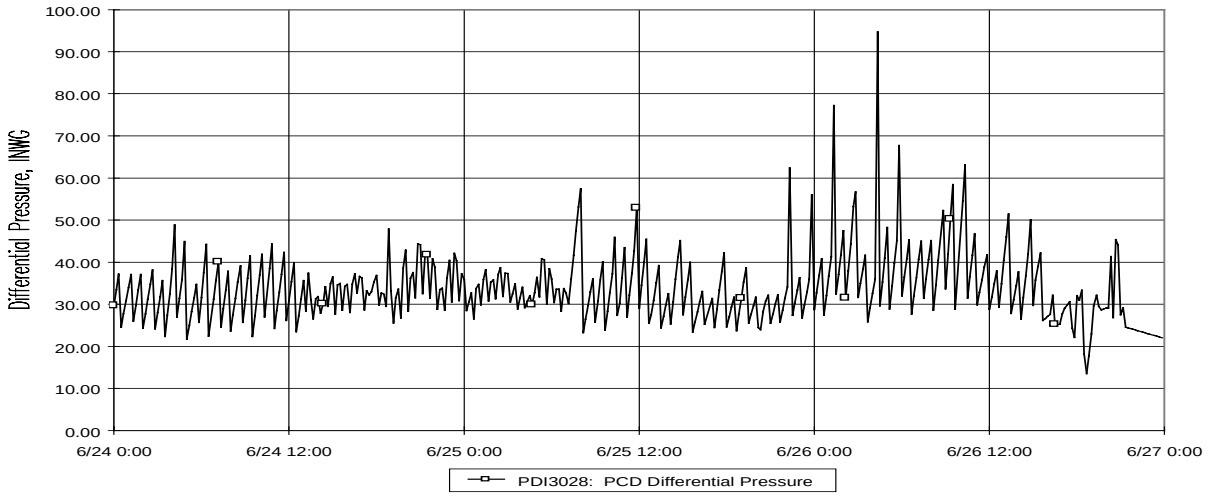

Figure 4.1.3-70 PCD Differential Pressure Profile

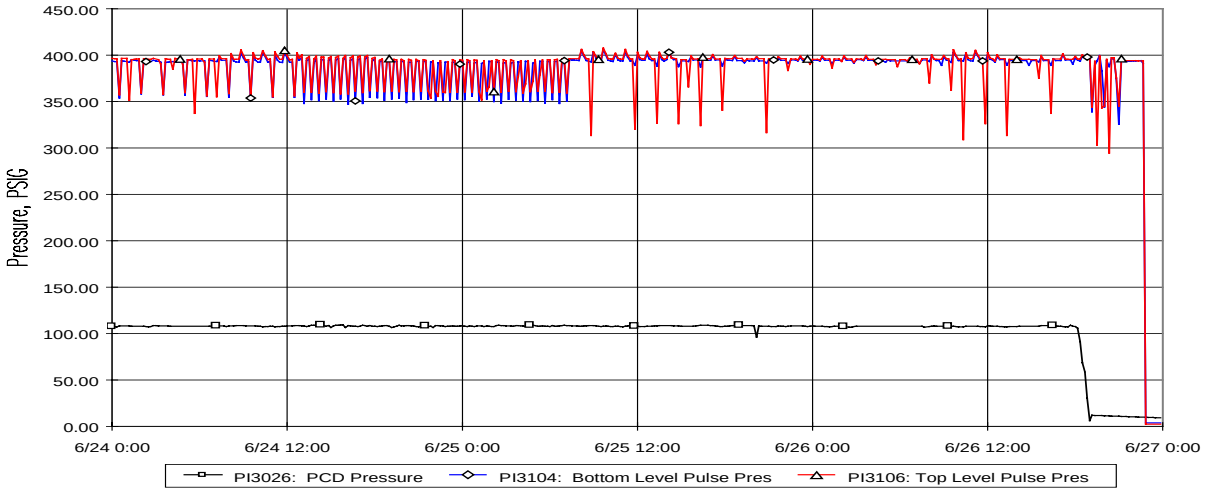

Figure 4.1.3-71 PCD Pressure and Pulse Pressure

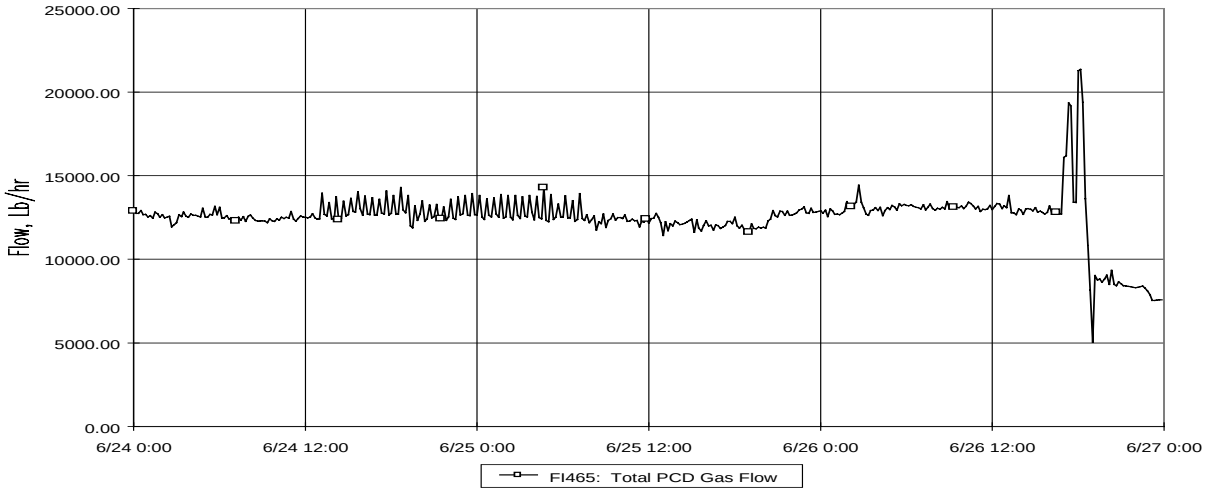

Figure 4.1.3-72 Gas Flow Through PCD

4.1.4 TC01 Series Test Runs

The major outage activities preceding test run TC01 included:

- Aligned the combustion heat exchanger back in the reactor loop for service after completing the CCT6 test run.
- Completed the modification initiated in the previous test runs to recycle the oversized milled coal back to the coal mill instead of the crushed coal silo.
- Added nitrogen bottles (surge capacity) to FD0210, FD0220, FD0510, and FD0520 as a backup to the spheri valve seal nitrogen so that the nitrogen header would not be drained too rapidly in the event of a spheri valve seal failure.
- Added six nozzles around the bottom of the FD0210 lock vessel to dislodge any material remaining on the wall.
- Rewound the FD0210 feeder motor was so that the feeder could be run at a lower speed.

A perforated back-pressure disc was installed downstream of the pressure letdown valve to address the high-frequency vibrations of the plug stem occurring because of flow-induced resonance. Also, the process piping was aligned for all the process gas to flow through the thermal oxidizer to simulate gasification operations.

The objectives of test campaign TC01 were:

- Maintain higher PCD inlet gas temperature (optimize reactor operating conditions to achieve a PCD plenum temperature of at least 1,350°F).
- Demonstrate long-term stable reactor operations (operate the reactor at solid inventory levels and circulation rates that should provide stable reactor operations).
- Prepare for gasification operation (operate the process to allow the entire flow of process gas through the thermal oxidizer and run the recycle gas booster compressor and associated subsystems).

4.1.4.1 TC01A Test Run

Test run TC01A was conducted between August 31 and September 2, 1997. Operating plots are shown in figures 4.1.4.1-1 to -22. (Due to the moisture analyzer not reading correctly the coal feed rate calculated from moisture content is not correct in all TC01 graphs.)

TC01A Test Run Chronology

- A leak test was completed on August 14, 1997, in preparation for test run TC01A. A few minor leaks were detected, which were repaired. The following day a number of sample coupons were installed on the PCD clean side and a leak test was performed on the PCD back-pulse valve.

- On August 23, 1997, the thermal oxidizer blower (BL0401) and the main air compressor (CO0201) were started. The reactor and thermal oxidizer air cure-outs were completed at about 22:00 the following day. The thermal oxidizer (BR0401) and the sulfator burner (BR0601) were lit on August 25, 1997. Startup was delayed for several hours to install two missing hangers on the bypass line of the primary gas cooler (HX0202).

- On August 26, 1997, the coal (FD0210) and sorbent (FD0220) feeder systems were tested. The PCD preheat was stopped to fix the leaks from the FD0530 fluidizing pads and a check valve on the FD0530 surge bin vent line. After these problems were addressed CO0201 was started again. During the restart BR0201 and BR0601 tripped from loss in propane flow due to condensation in the vaporizer explosion proof box.

- On August 27, 1997, the BR0201 pilot and main burner were tested. At 18:30 BR0201 was lit and by 22:15 the reactor pressure was increased to 60 psig.

- At 06:00 on August 28, 1997, the BR0201 exit temperature was 1,200°F. The system was shut down again due to leak problems with the FD0530 fluidizing pads and leaks in the vent line check valve. During the shutdown an isolation valve was installed on the line between FD0530 and the inlet to BR0401. Also, the perforated back-pressure disc was moved from near XV449 to a point immediately after PV287 to prevent the back pressure on FD0530. The new transport air moisture separator was also installed.

- After all maintenance work was completed CO0201 was started on August 30, 1997. The system was again temporarily shut down to reinstall the moisture separator that had been improperly installed. BR0601 was started again to preheat the PCD.

- At about 04:10 on August 31, 1997, 3000 lb of sand was transferred from FD0140 to FD0210. After setting all aeration flows and checking all instrument purges on the reactor the flow through the reactor J-leg was increased. By 11:00 the BR0201 exit temperature was 1,000°F. Around 12:30 sand was fed through FD0210. The FD0210 motor tripped on several occasions (event 1, figure 2). The FD0210 torque curve was reset to correct the problem.

- Sand feed was resumed again at about 16:00 and by 16:30 a total of 8,750 lb of sand was transferred to FD0210. The reactor pressure was set to 100 psig and the instrument purges and the flows were set for this operating pressure. Coal feed was started at about 23:40 (event 2, figures 2 and 4 through 9).

- Just before 01:00 on September 1, 1997, FD0220 was found to be over-pressurizing. A system checkout revealed a missing orifice in the line that purges the vent lines to the dispense vessel, the lock vessel, and a short piece of pipe near the top. At about 02:15 the unit was taken off coal feed because of incessant plugging in FD0520 (event 3, figure 18). The plugging was the result of agglomerated wet ash and small candle pieces. Coal feed started again at about 10:15 (event 4, figures 2 and 4 through 9), but at 11:30 a FD0210 spheri valve seal failure tripped FD0210, FD0502, and FD0520 (event 5, figures 2 and 18).

- Since FD0220 was still over-pressurizing due to the missing orifices on the vent purges, ball valves were installed in both the FD0220 and FD0210 vent line purges. Coal feed was started at about 20:40 (event 6, figures 2 and 4 through 9) and the feeder speed was increased over the next hour. Dolomite feed was started at about 22:40 and about an hour later the FD0520 discharge line plugged with a large number of candle pieces (event 7, figure 18). Between 22:40 and 00:30 several candle pieces were removed through the sampling port. Due to the broken candle pieces coming through the FD0520 system the process was shutdown by 13:30 (event 8, figures 1, 2, 4 through 9, and 13 through 15).

TC01A Post Test Run Inspections

The PCD lower "manway" was opened and the candles were inspected. The PCD tube sheet was pulled; all broken and damaged candles were replaced. Since the pilot was operated for more than 19 hours the pilot and main burner were inspected; the pilot was in good shape but there were a few burn marks on the pilot tip.

TC01A Test Run Observations

The thermal oxidizer ran satisfactorily with full process gas flow. A total of 8 hours on coal was achieved and a total of 1.5 tons of coal were fed.

Section 4.1.4.1

Graphs 1 through 22

Test Run TC01A
August 31 through September 2, 1997

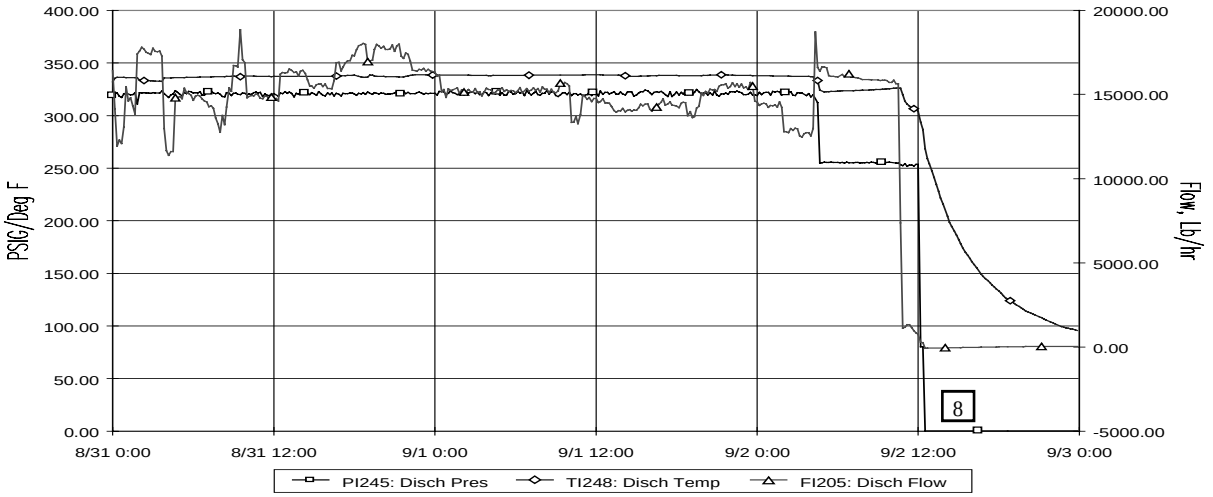

Figure 4.1.4.1-1 CO0201 System Profile

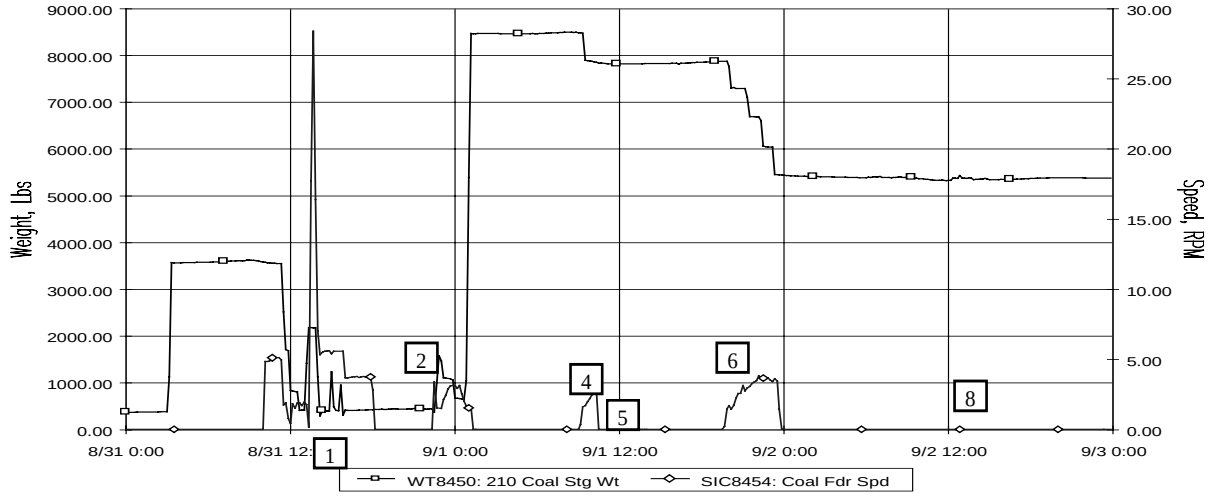

Figure 4.1.4.1-2 Coal Feed System Profile

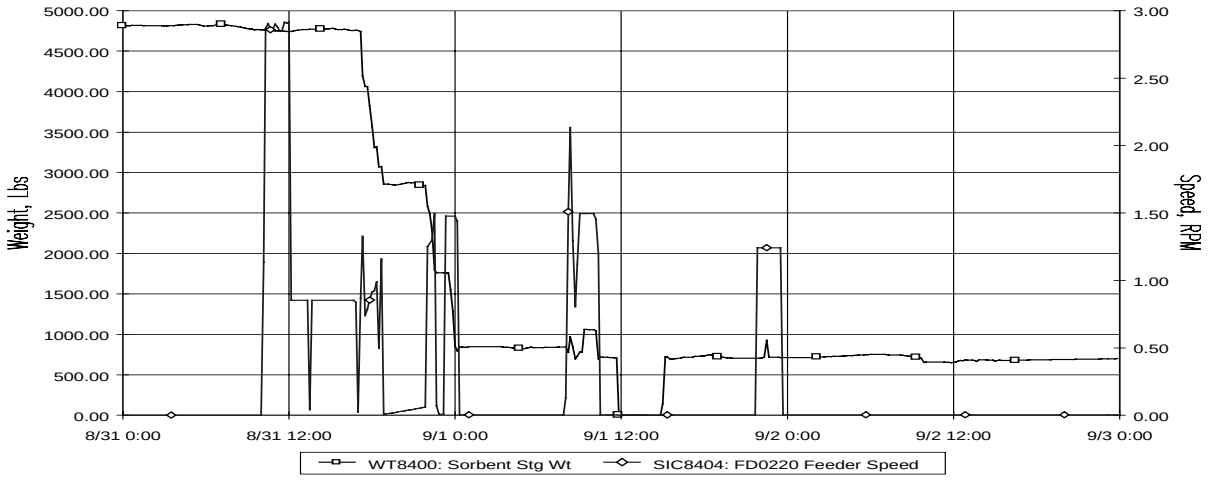

Figure 4.1.4.1-3 Sorbent Feed System Profile

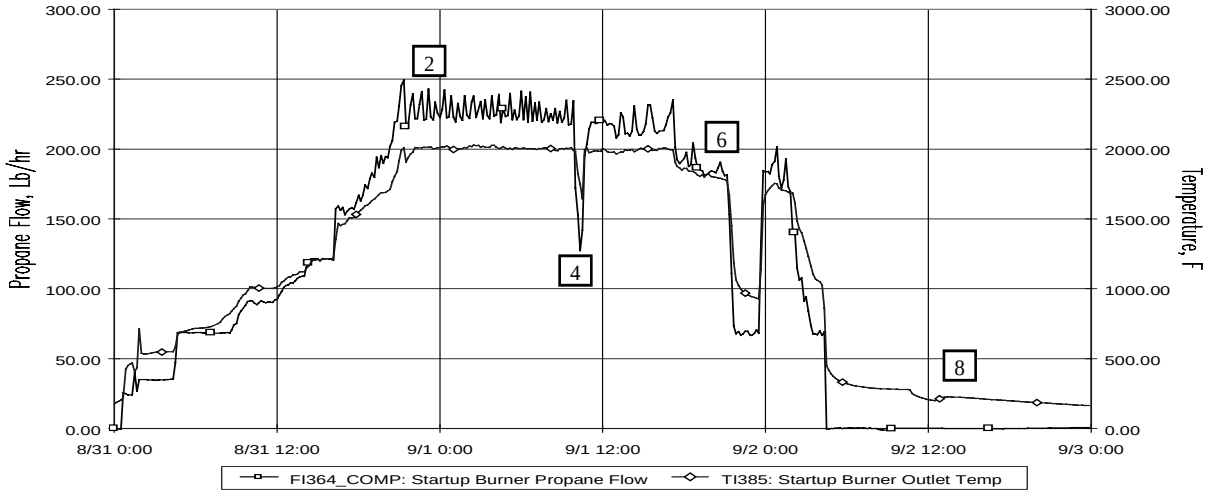

Figure 4.1.4.1-4 Start-Up Burner Flow/Temperature

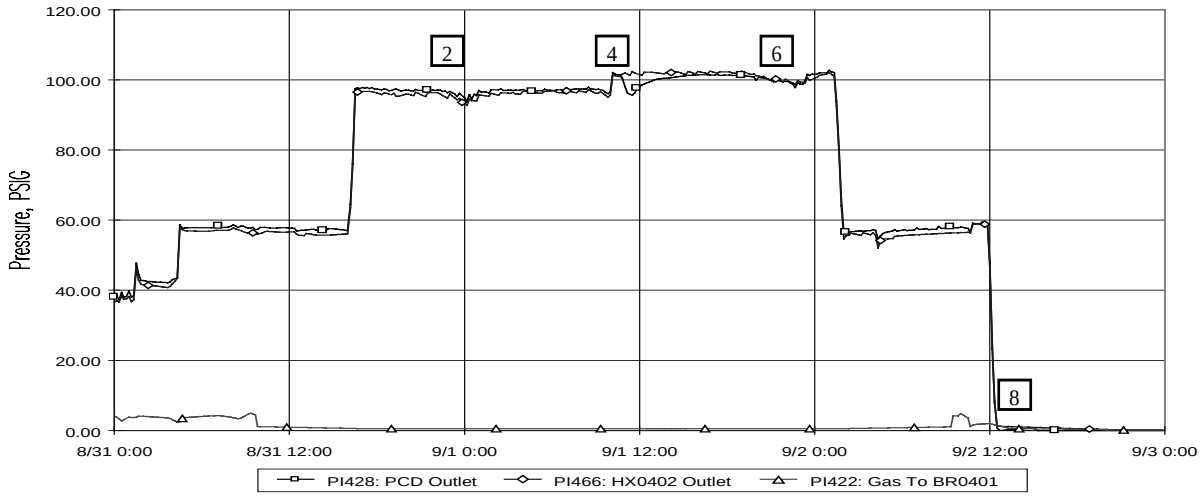

Figure 4.1.4.1-5 System Pressures Downstream of PCD

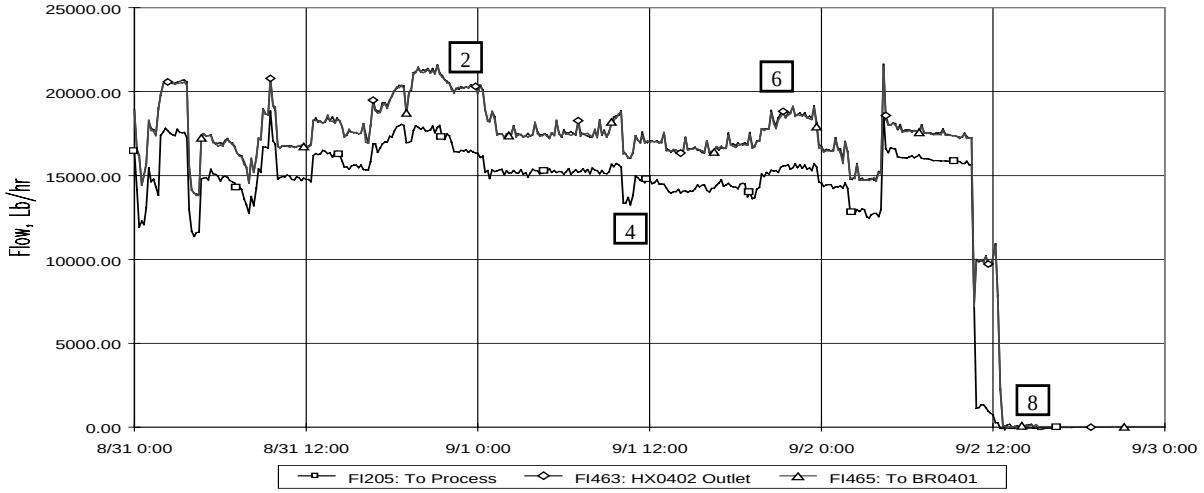

Figure 4.1.4.1-6 Total Gas In/Out Flow Rates

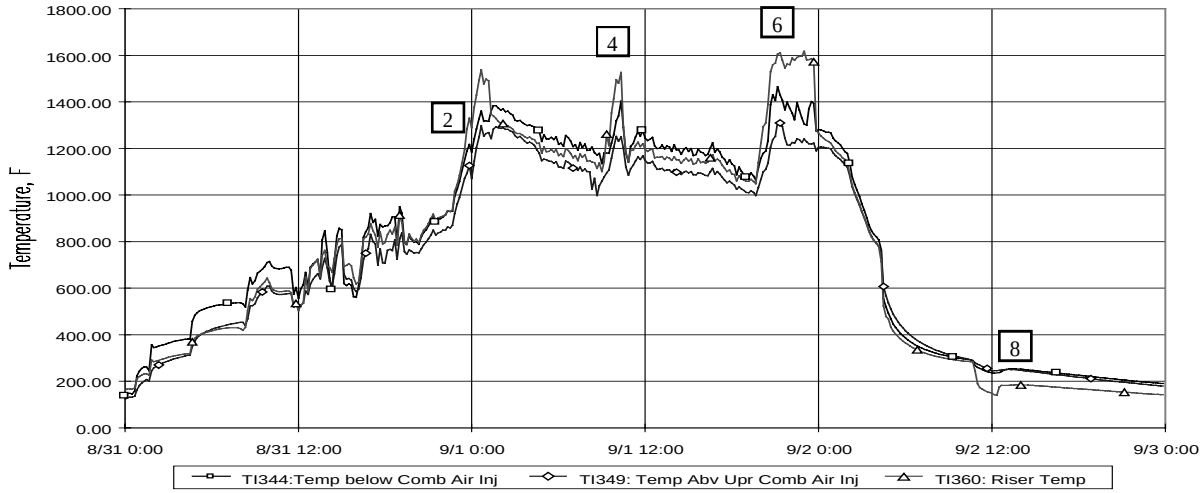

Figure 4.1.4.1-7 Reactor Mixing Zone and Riser Temperatures

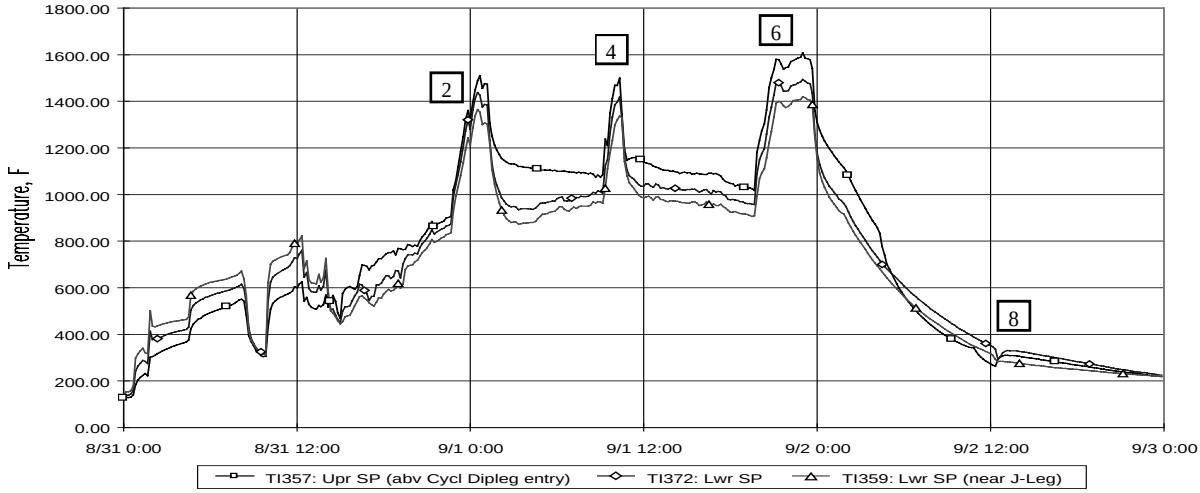

Figure 4.1.4.1-8 Standpipe Temperatures

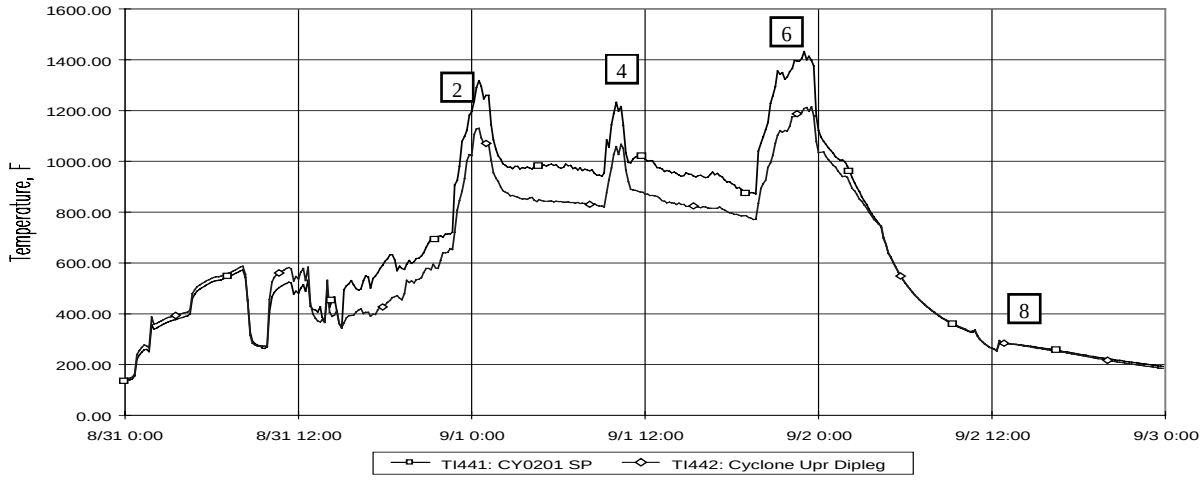

Figure 4.1.4.1-9 Cyclone Dipleg Temperatures

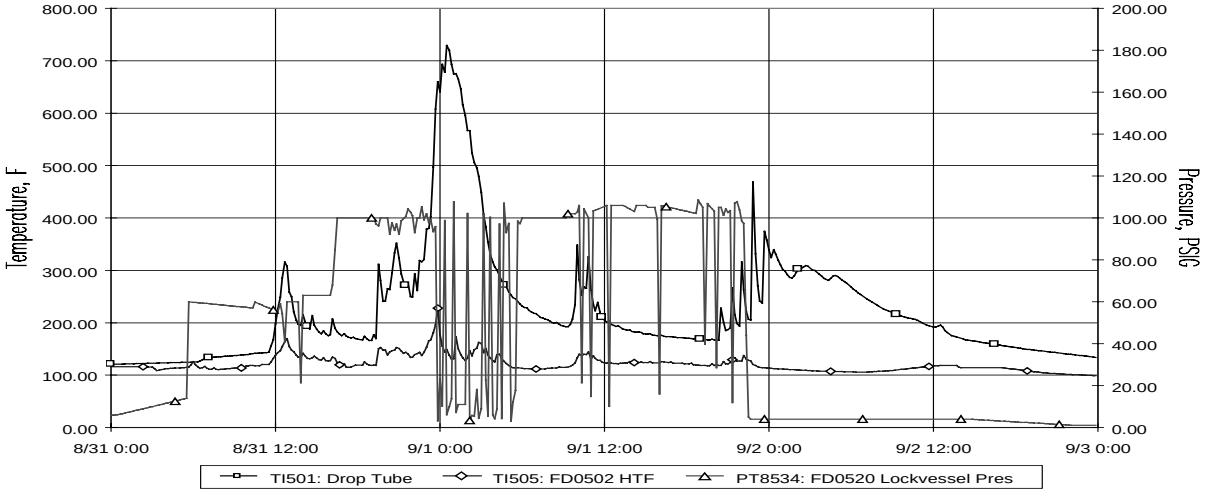

Figure 4.1.4.1-10 PCD Ash Temperatures

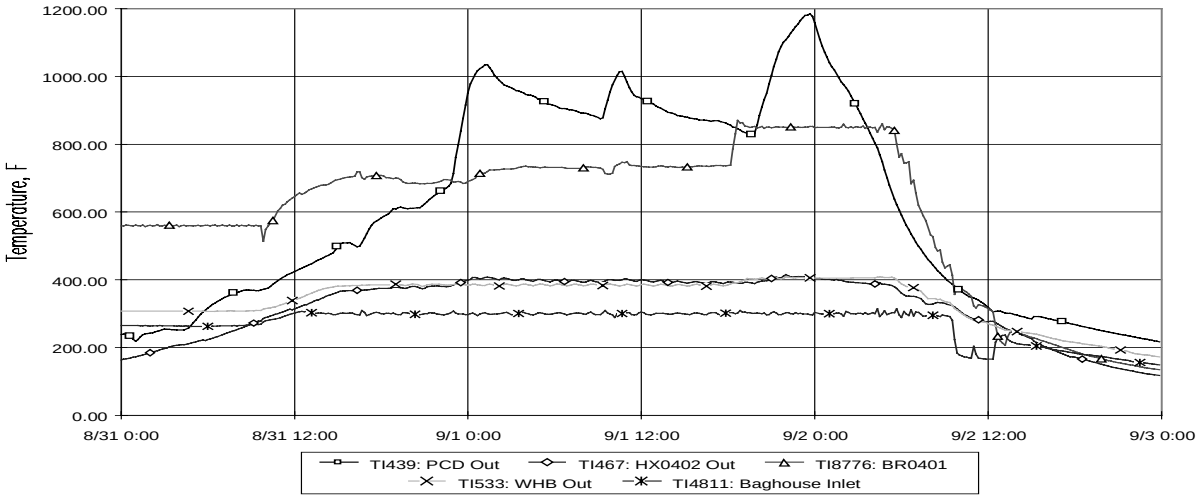

Figure 4.1.4.1-11 System Temperatures Downstream of PCD

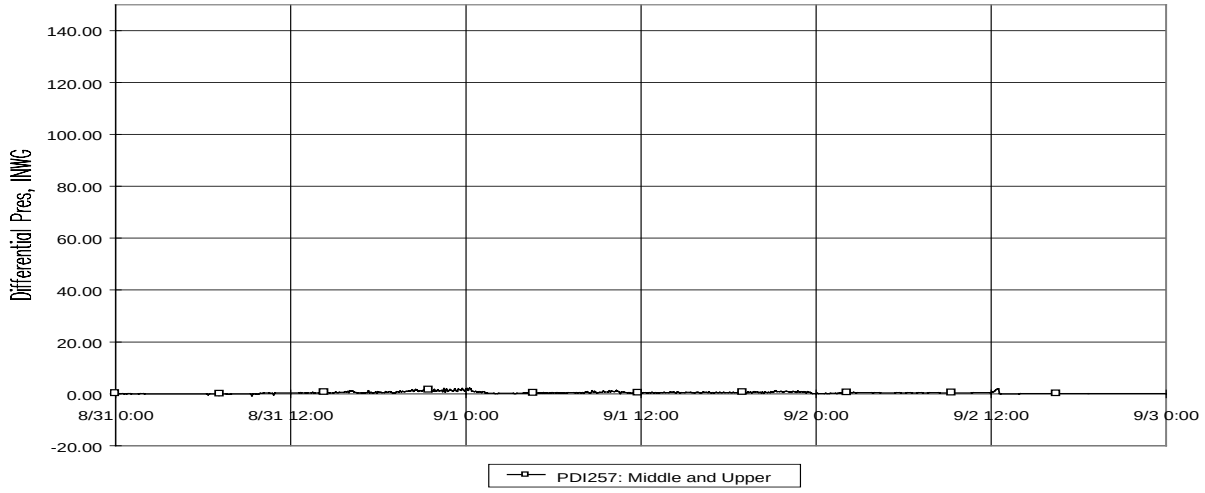

Figure 4.1.4.1-12 Mixing Zone Differential Pressure Profile

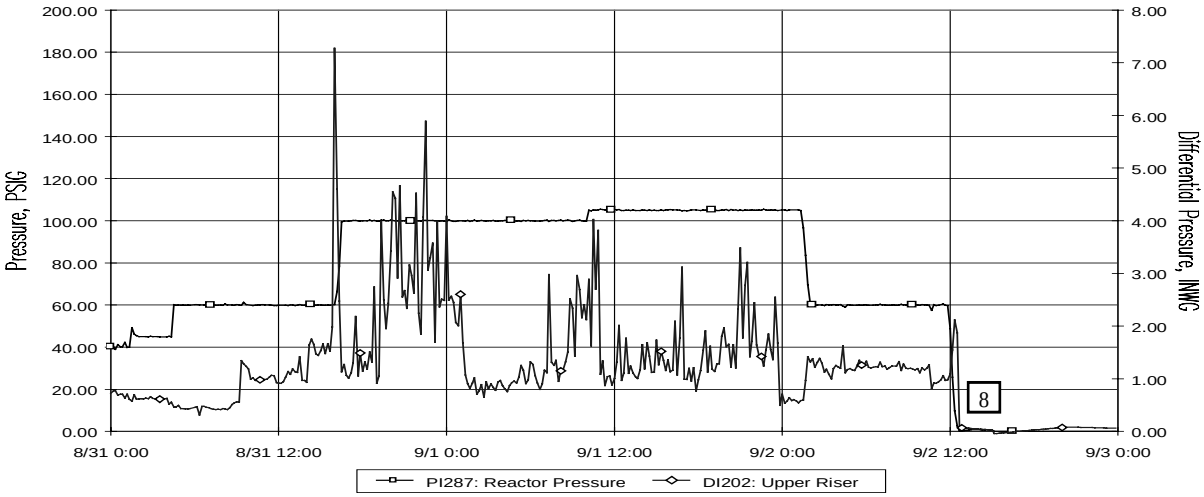

Figure 4.1.4.1-13 Reactor Pressure/Riser Differential Pressure Profiles

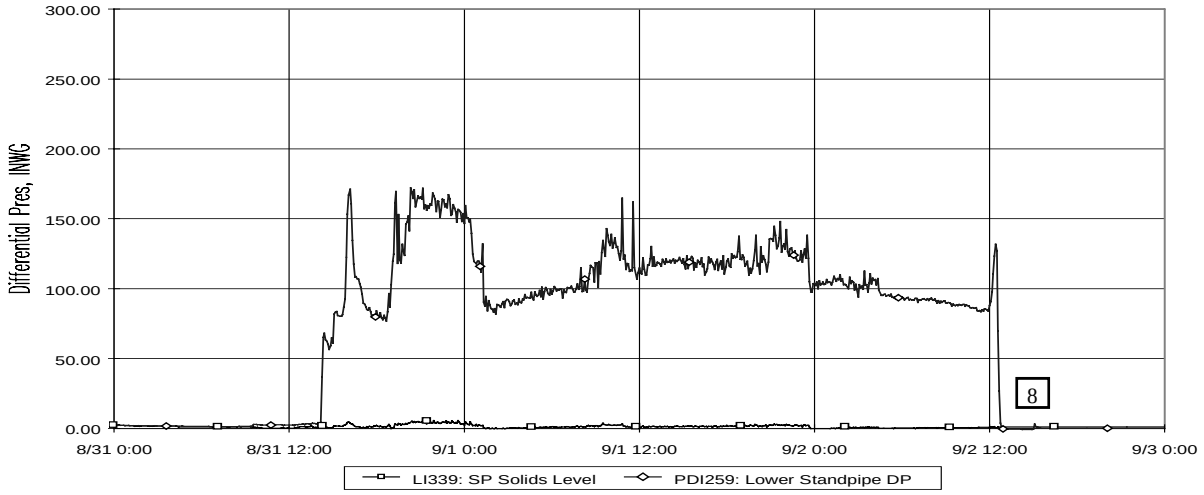

Figure 4.1.4.1-14 Standpipe Differential Pressure Profiles

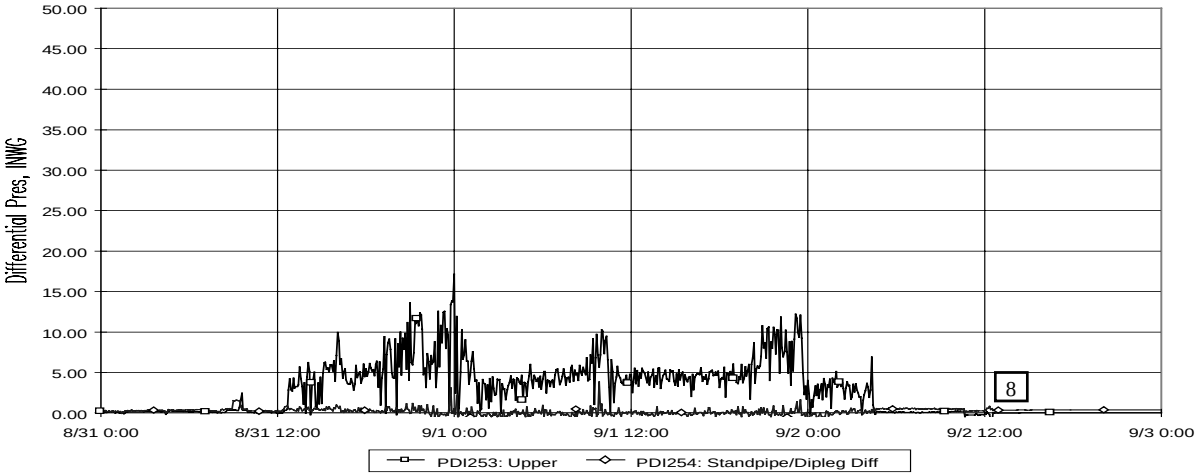

Figure 4.1.4.1-15 CY0201 Dipleg Differential Pressure Profiles

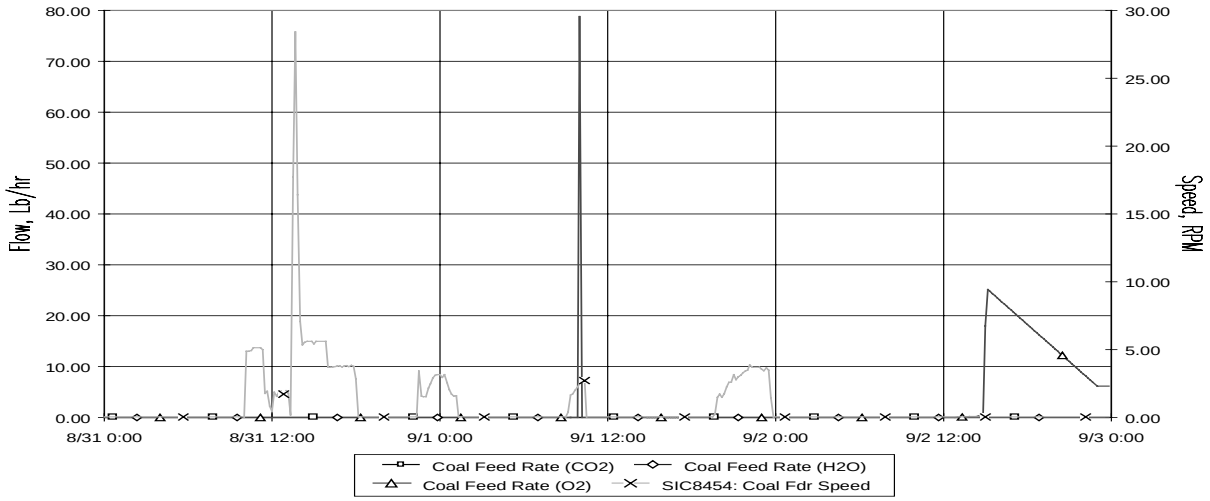

Figure 4.1.4.1-16 Coal Feed Rate Based on Gas Analysis

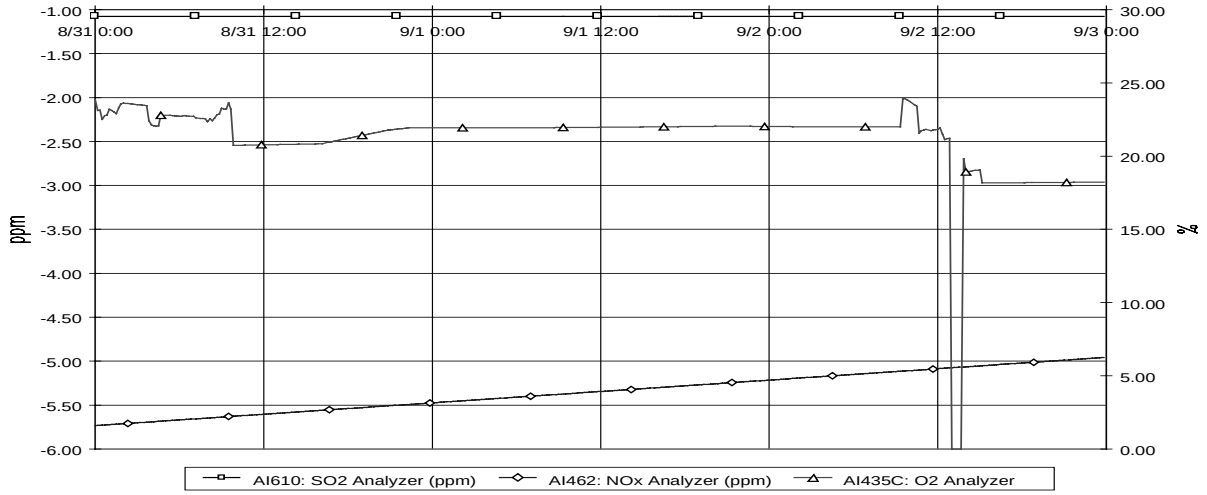

Figure 4.1.4.1-17 O_2, SO_2, and NO_x Analyzers

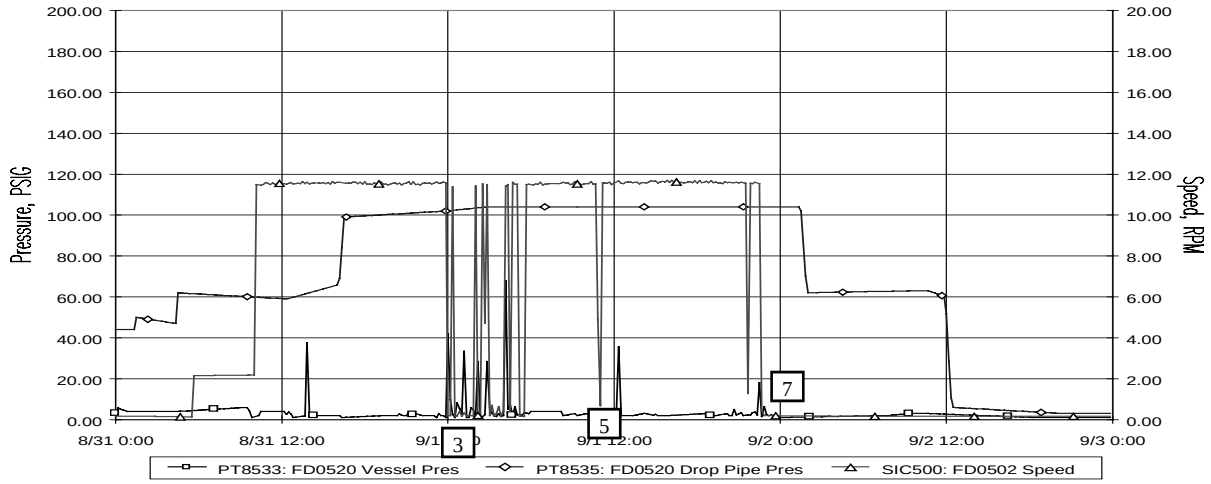

Figure 4.1.4.1-18 FD0520 Pressure Profiles

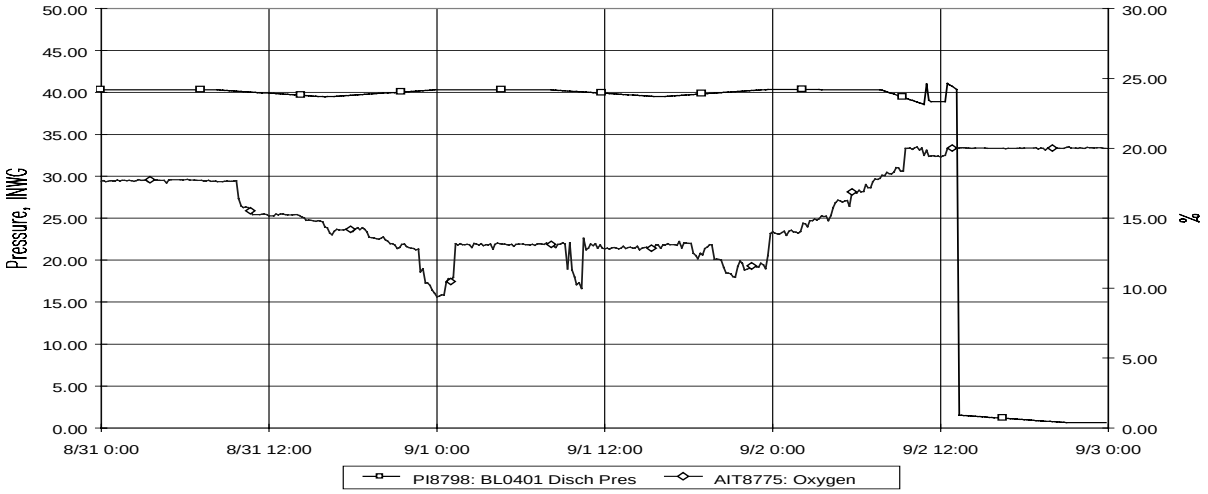

Figure 4.1.4.1-19 Thermal Oxidizer Blower Discharge Pressure

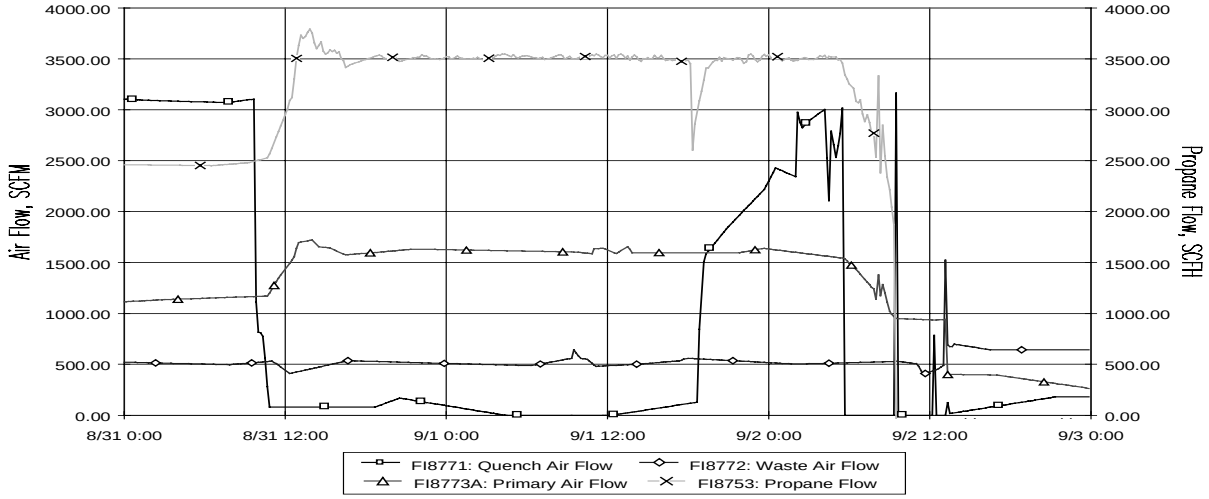

Figure 4.1.4.1-20 Thermal Oxidizer Air/Fuel Flow

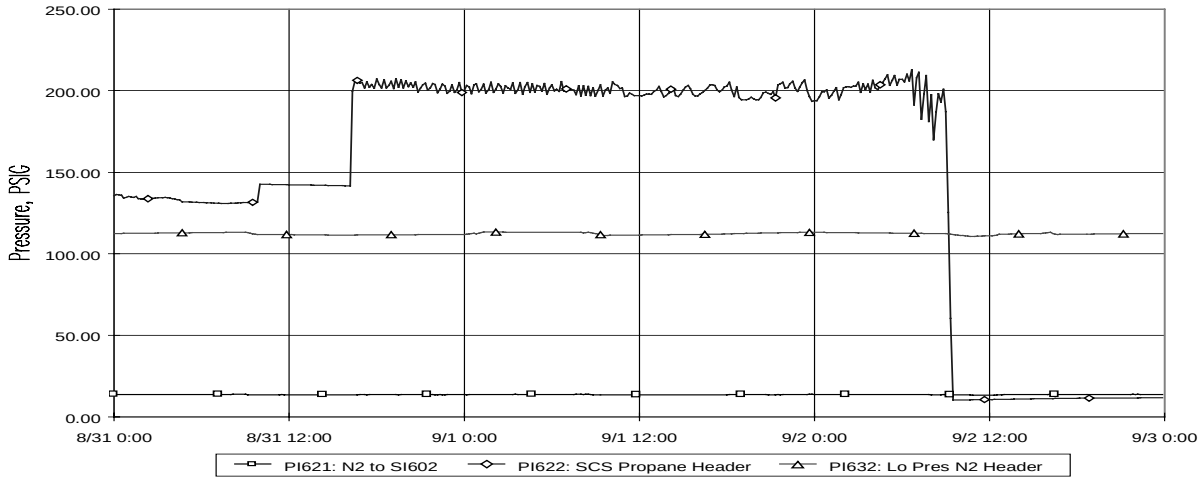

Figure 4.1.4.1-21 Nitrogen/Propane Header Pressure Profiles

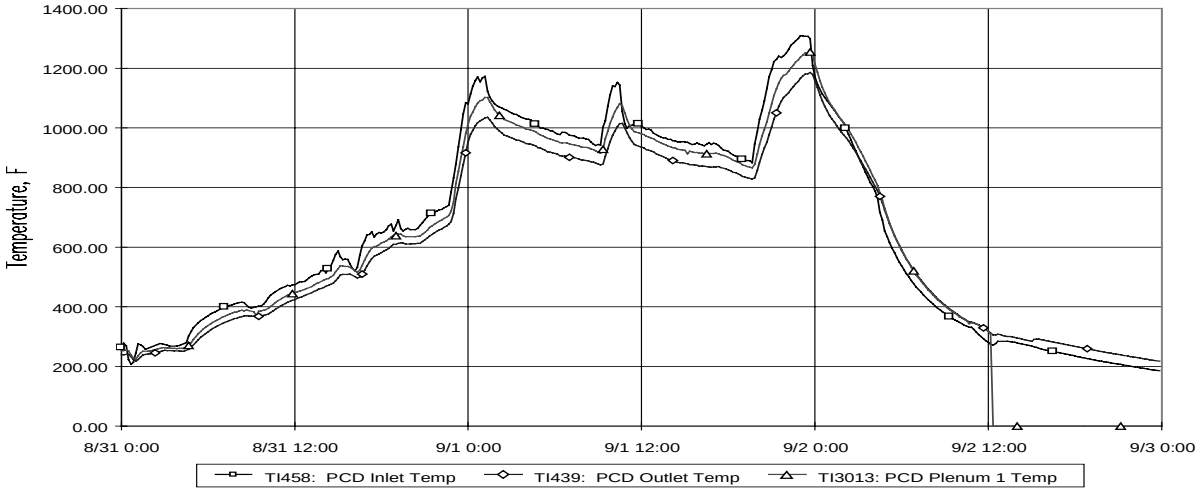

Figure 4.1.4.1-22 PCD Temperatures

4.1.4.2 TC01B Test Run

Test run TC01B was conducted between September 5 and September 22, 1997. Operating plots are shown in figures 4.1.4.2-1 through -96.

TC01B Test Run Chronology

- Leak tests began at about 19:00 on September 5, 1997, but were temporarily shut down due to a leak in the main air compressor (CO0201) line. The leak tests were completed by the end of the day.

- On September 6, 1997, the thermal oxidizer (BR0401) was started around 00:15 (event 1, figure 20); CO0201 was started around 03:35 (event 2, figure 1); and the sulfator heater (BR0602) was lit at 03:50. The PCD preheat was completed at 08:10 (event 3, figure 21). After establishing flows through the reactor the start-up burner (BR0201) was lit at 15:05 (event 4, figure 4). Solids circulation through the reactor was started at 18:30 (event 5, figures 12 through 14). The reactor pressure was gradually increased starting at 20:00 (event 6, figure 12) and by 22:20 it was 70 psig. The start-up burner (BR0201) tripped at about 22:30 (event 7, figure 4) and was relit.

- On September 7, 1997, the reactor pressure was increased to 100 psig. Coal feed was started at about 03:50 (event 8, figures 2 and 7 through 10) but was stopped at about 04:35 (event 9, figures 2 and 7 through 10) when the spent fines transport system (FD0520) tripped. The FD0520 tripped due to broken candle pieces plugging the discharge line. FD0520 was restarted after removing the broken candles and coal feed resumed at about 10:50 (event 10, figures 2 and 7 through 10). Over the next several hours coal feed was intermittent to control the temperature rise in the PCD.

- Propane flow through BR0201 was gradually reduced as the coal feed rate was increased. At about 14:10 there was an increase in air flow through the solids conveying line that resulted in an increase in coal feed rate. The increase in coal feed led to a sharp rise in reactor temperature. Consequently, the circulation through the combustion heat exchanger (HX0203) was increased to control the reactor temperature. FD0210 plugged at 17:15 but it was unplugged in less than 5 minutes. The spent solids screw cooler (FD0502) later tripped on several occasions because the dispense vessel on FD0520 was not depressurizing within the allowed time. The BR0201 was shut down just before 23:00.

- On September 8, 1997, the reactor pressure was increased to 160 psig. The FD0520 plugged again at 01:15 (event 11, figure 19) due to candle pieces, so FD0210 and FD0220 were stopped. Coal feed could not be reestablished due to poor circulation and reactor temperatures that were too low. The reactor pressure was reduced and BR0201 was lit at about 02:10. Coal feed resumed at 09:15 and the BR0201 was subsequently shut down at about 16:30 (event 12, figures 2, 4, and 7 through 10).

- The FD0520 had a few problems during the day mainly because the dispense vessel spheri valve was not closing within the time allowed. The problem was fixed by spraying some lubricant on the shaft and by tapping on the shuttle valve a few times to close. By 22:10 the reactor pressure was increased to 160 psig.

- On September 9, 1997, there were problems with start-up due to low solids inventory. Later, bridging in the lower portion of coal silo prevented coal flow into the surge bin. The reactor was taken off coal feed and BR0201 was lit (event 13, figures 2, 4, and 7 through 10). Wet cakes bridged the line between FD0104 (this system transfers coal from the silo to FD0210 surge bin) and FD0210. Blowing into the silo broke the bridge and cleaned the transfer line. Propane flow to BR0201 tripped in the evening but was restored. Coal feed was started at about 20:00 and by the end of the day the reactor pressure had reached 100 psig (event 14, figure 12).

- BR0201 was shut down on September 10, 1997, and afterwards the reactor pressure was increased to 180 psig. FD0206 was run for about 4 hours in order to control the solids level in the reactor. At the end of the day a plastic plug on the instrument air line to BR0401 developed a leak.

- The BR0401 tripped while the plastic plug was being replaced on September 11, 1997, but it was relit. SRI took a PCD inlet sample. There continued to be problems transferring solids from FD0520 due to broken candle pieces intermittently plugging the discharge line.

- SRI took samples at the PCD on September 12, 1997. At about 05:20 problems developed with the FD0510 level probe and FD0206 was stopped. By 07:30 the solids level in HX0203 was increasing at 6 inches per hour and FD0206 was started to control the level. The FD0510 system was manually cycled by forcing LS8501 on (level probe uncovered) to decrease the level in the standpipe. The FD0220 was increased to achieve a Ca/S ratio of 1.5 (event 15, figure 27). The FD0206 and FD0510 systems were stopped at about 08:40 to work on the level probe. The FD0502 and FD0520 were also stopped later in order to replace the safety on the dispense vessel.

- At about midday the PV287 control configuration was modified so that PV287 would open prior to both (upper and lower plenum) PCD back-pulses. Prior to this it was opening only before the first back-pulse. This new change affected the dipleg operation on the second back-pulse, so further adjustments were made to the PIC287 feed-forward logic to improve the dipleg operation.

- There were 30 drums of reactor and PCD fines dash collected for DOE on September 13, 1997. The dolomite feed rate was decreased to reduce the solids carryover to the PCD and to conserve dolomite since the dolomite inventory was low. The HX0203 circulation was also lowered to reduce carryover to the PCD. By 16:45 the FD0220 was emptied. Solids recycled from the May run were added in order to maintain the solids level in the reactor until more dolomite was transferred to

FD0220. The FD0220 was subsequently restarted at about 17:30. Problems with the coal feeder forced a coal feed stop at about 21:30 (event 16, figures 26 and 31 through 34). The lock vessel level probe was checked and the lock vessel was cleaned.

- Coal feed resumed at 00:05 on September 14, 1997, (event 17, figures 26 and 31 through 34) but was stopped 40 minutes later (event 18, figures 26 and 31 through 34) because the reactor temperatures were too low. The reactor pressure was decreased to 100 psig and BR0201 was lit at about 02:15 (event 19, figure 28). Coal feed was attempted at 14:00 (event 20, figures 26 and 31 through 34) but there were problems with the feeder motor binding. Coal feed resumed at 15:25 after addressing the problems.

- The dipleg started to slug at about 18:25 and coal feed was stopped at 19:00 to allow it to stabilize (event 21, figures 26 and 31 through 34). Coal and dolomite feed started again at 19:20 but the coal feed was stopped again 40 minutes later because the PCD back-pulses upset the dipleg stability. The burner firing and the HX0203 circulation were increased (event 22, figure 28). After increasing the solids level in the standpipe by adding sand, coal feed was restarted at 21:00 (event 23, figures 26 and 31 through 34).

- The BR0201 was shut down at 04:10 (event 24, figure 52) on September 15, 1997. Coal feed was stopped around 05:15 (event 25, figures 50 and 55 through 58) because the solids level in the reactor was low. The BR0201 was then lit (event 26, figure 52). The cyclone dipleg aeration was reset at 07:15 and adjusted again around 11:05. About 5,400 lb of recycled solids were added to increase the reactor solids inventory.

- Coal feed started at 17:10 (event 27, figures 50 and 55 through 58) and was intermittent for the next hour to control the temperature rise in the PCD to a ramp rate equivalent of 200°F/hour or less. It was suspected that the high-temperature ramp rates experienced during the transition from propane fire to coal fire might have adversely affected some candles. Aeration rates were adjusted since the dipleg operations had become unsteady. The burner firing was reduced at 19:10 and it was shut down at 21:07 (event 28, figure 52). After shutting down BR0201 the reactor pressure was steadily increased (event 29, figure 60).

- The FD0206 was stopped at 01:10 (on September 16, 1997) due to problems with the FD0510 dispense vessel spheri valve. About 8 pieces of refractory and slag chunks were pulled out of FD0510 exit. The FD0206 and FD0510 were restarted at 14:15. The FD0210 system tripped for a short time (event 30, figures 50 and 55 through 58) and resulted in the PCD temperature falling below 1,350°F for about 30 minutes. Plugging in the exit line caused FD0210 to trip again at 18:00 (event 31, figures 50, 55 through 58, and 60 through 63). The line was unplugged and the feeder restarted at about 18:15.

- The FD0210 lock vessel was fluffed several times on September 17, 1997, to prevent bridging. The reactor operation was steady until CO0201 tripped around 05:20 (event

32, figure 49). It was restarted without disrupting the reactor operations too severely. The HX0203 aeration was increased to raise the level of solids in the standpipe because the standpipe differential pressure (PDI259) had dropped from 130 to 110 inH_2O at 05:30 (event 33, figure 61). The reactor pressure was increased to 190 psig (event 34, figure 60) and the staged air through the riser was redistributed around 13:25. The BR0401 tripped at 18:55 (event 35, figure 68) but was restarted 40 minutes later. The aeration at the bottom of the HX0203 was adjusted around 21:00 to counteract the fluctuating pressure difference across the heat exchanger standpipe, experienced since CO201 tripped earlier that morning.

- At 05:30 on September 18, 1997, the aeration through the HX0203 J-leg was reduced to lower the circulation rate. The PCD back-pulse pressure was increased from 500 to 550 psig at 05:30 (event 36, figure 71). At 06:15, the following changes were made for the PCD back-pulse: 1) the filter differential pressure trigger was raised from 100 to 125 inH_2O; 2) the time trigger was reduced from 45 to 40 min; and 3) the valve-open time was increased from 0.3 to 0.4 sec. Ever since the changes made to the feed-forward logic on September 12 the reactor pressure indicator (PI287) had read higher than normal during back-pulse. The bias on the measured PI287 value was therefore increased from 12 to 15 psi.

- A back-pulse at 10:05 destabilized the dipleg causing a high-solids carryover to the PCD. Consequently, the reactor solid levels dropped and the FD0206 speed was reduced. Since the solids level in HX0203 was still falling the aeration rate on the J-leg was increased to maintain a constant circulation rate, and the speed of FD0206 was further reduced (event 37, figures 60 and 66). Finally, FD0206 was shut down at 12:45 (event 38, figure 66) to maintain the reactor levels at the desired setting. The bias on the feed-forward logic was decreased from 20 to 15 psig at 13:05 since the first pulse was upsetting the dipleg operation. This had little effect on the dipleg, so the bias was further reduced to 12 psig. The aeration on HX0203 J-leg was increased to raise the solids level in the standpipe. The FD0206 was started again as the levels started increasing.

- As part of the PCD back-pulse valve characterization the back-pulse pressure was increased from 500 to 550 psig at 09:20 (event 39, figure 95) on September 19, 1997. The back-pulse pressure was increased by 50 psi after every back-pulse up to 750 psig at 14:50 before it was decreased to 600 psig at about 15:40 (event 40, figure 95). The Jonas acoustic probe at the PCD outlet had a leak around the packing at about 10:10. The leak caused an increase in the skin temperature from ambient to 550°F, so the probe was isolated.

- The process gas was checked for SO_2 at 14:45 but the analyzer did not detect any. Plugging of the FD0520 system exit led to accumulation of ash in the PCD cone. Consequently, coal feed and combustion air flows to the reactor were reduced at about 19:25 (event 41, figures 74 and 78). Dolomite and coal feeds were stopped at 21:00 and 21:10, respectively, because the plugging problems continued (event 42,

figures 74, 75, and 79 through 82). FD0520 was unplugged and small pieces of ceramic candles were found.

- The reactor pressure was reduced at about 00:10 on September 20, 1997, and BR0201 was lit around 01:55 (event 43, figure 76). Coal feed was started at 12:25 (event 44, figures 79 and 84 through 87). The start-up burner was shut down at 16:30 (event 45, figures 74 and 79 through 82), and the reactor pressure was increased. The FD0520 continued to have problems with the exit line plugging. At 08:45 (on September 21, 1997) ceramic candle pieces were again pulled from the FD0520 exit. Between 11:50 and 16:00 more candle pieces were removed from the FD0520 discharge line.

- At 01:50 on September 22, 1997, it was discovered that coal was not dropping from the FD0210 surge bin into the lock vessel. The reactor circulation rate and coal feed were reduced while the problem was investigated (event 46, figures 74 and 84). CO0201 tripped at 02:25 (event 47, figure 73) and was immediately restarted. At about 03:35 the FD0520 system plugged (event 48, figure 91) again. Inspection revealed more candle pieces in the discharge line. The FD0520 system tripped on several occasions. Consequently, coal feed and solid circulation rates were reduced to minimize the solids carryover to PCD (event 49, figures 74 and 79 through 82). Also, FD0220 was shut down (event 50, figures 74 and 79 through 82) until the PCD cone was clear of accumulated ash.

- The FD0520 system was restarted (event 51, figure 91) after all broken candle pieces were removed. Coal feed was increased (event 52, figures 74 and 79 through 82) and the reactor was brought back to previous operating conditions. The FD0220 was also restarted at about 14:20. There was a major steam leak at 19:20 on the HX0203 differential pressure impulse line on the riser. Coal feed was stopped at 19:30 (event 53, figures 74 and 79 through 82) and shutdown of the process was initiated. The CO0201 was stopped at about 23:15 (event 54, figure 73).

TC01B Test Run Observations

A total of 311 hours on coal was achieved and a total of 179 tons of coal were fed. An attempt was made to maintain the PCD temperature rise below 200°F/hr during any given small-time interval when transitioning from propane fire to coal. The insert and the flowmeter feeding PT301 impulse line were removed so that nitrogen could be used through the PT301 and FI902 (disengager and cyclone bypass) to moderate the temperature rise in the PCD during the first hour of coal feed. About 1,500 lb/hr of nitrogen flow could be obtained through the FI902 and PT301 nozzles. During the initial coal feed this flow was used but had no apparent effect on PCD inlet temperature. During initial coal feed the PCD ramp temperature was effectively controlled at a rate less than 200°F/hr by interrupting coal feed often and by effectively using the combustion heat exchanger.

Apparently, the configuration changes made to the feed forward logic of the pressure letdown valve lessened the effect of back-pulse on dipleg operations. The FD0206 screw cooler was run often for the first time and was able to achieve and maintain steady solid levels in the reactor and

HX0203. Problems with low-coal-transfer amounts during a FD0210 cycle forced one reactor shutdown. Feeding coal was stopped a few times from the FD0520 plugging due to broken candle pieces. By adjusting aeration, stable dipleg operations were achieved under various operating conditions. The recovery (solid circulation and reactor temperatures) from two main air compressor trips was smooth. The cause of the two momentary compressor trips was not clearly established. The PCD back-pulse valves were characterized for the effect of pressure on gas flow. Frequently during the second and third FD0510 cycles after the startup of coal feed the exit plugged with small refractory, slag, and agglomerated char pieces. The process was shut down due to a steam leak on the HX0203 differential pressure gauge PDI694 impulse line.

Section 4.1.4.2

Graphs 1 through 24

Test Run TC01B
September 5 through September 9, 1997

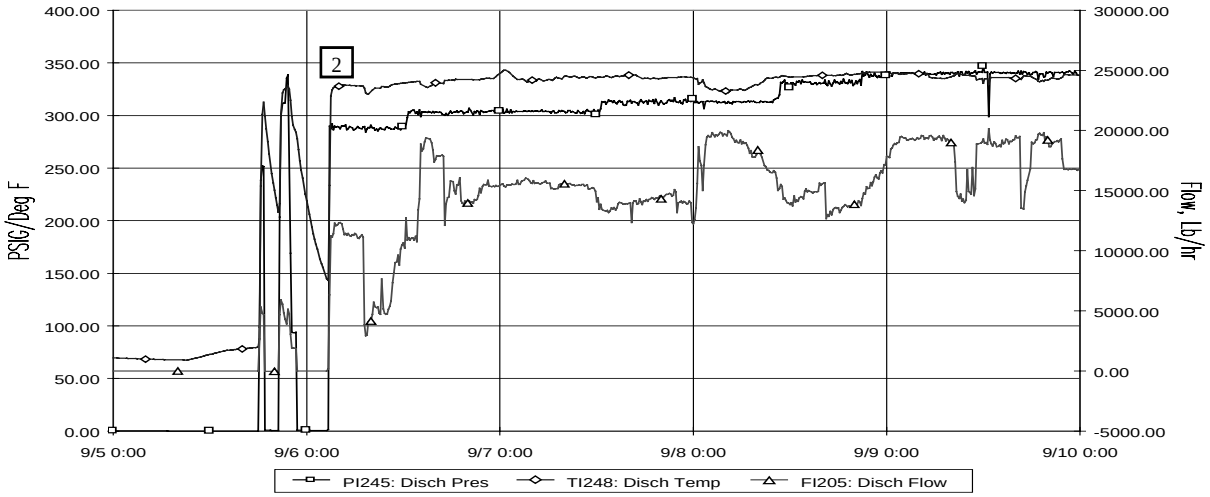

Figure 4.1.4.2-1 CO0201 System Profile

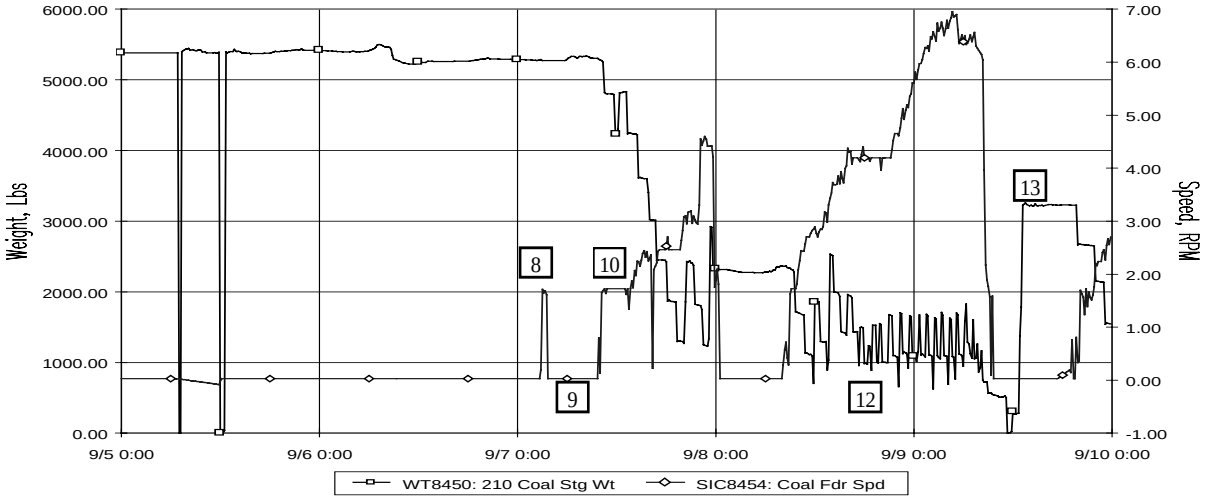

Figure 4.1.4.2-2 Coal Feed System Profile

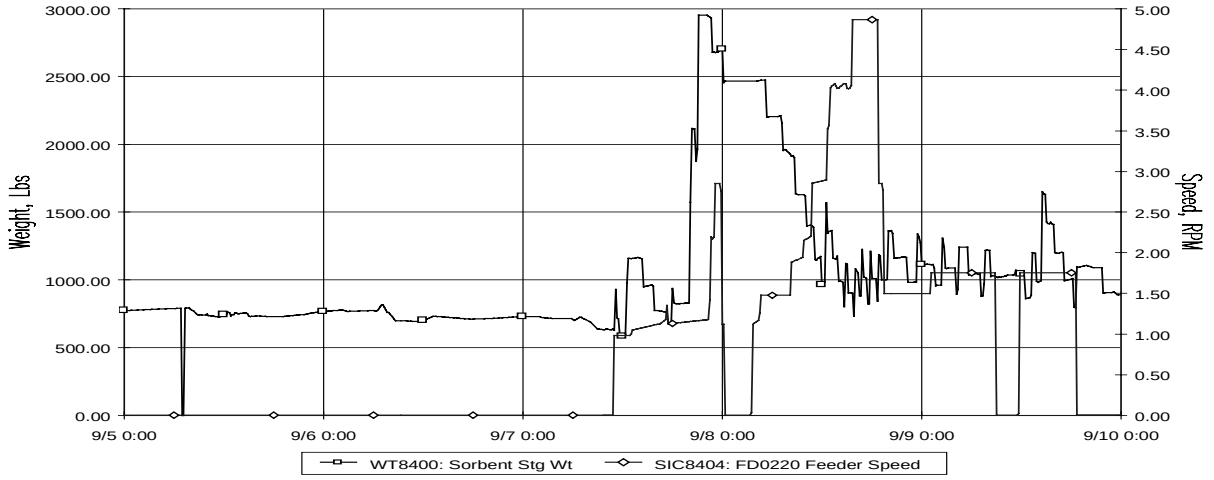

Figure 4.1.4.2-3 Sorbent Feed System Profile

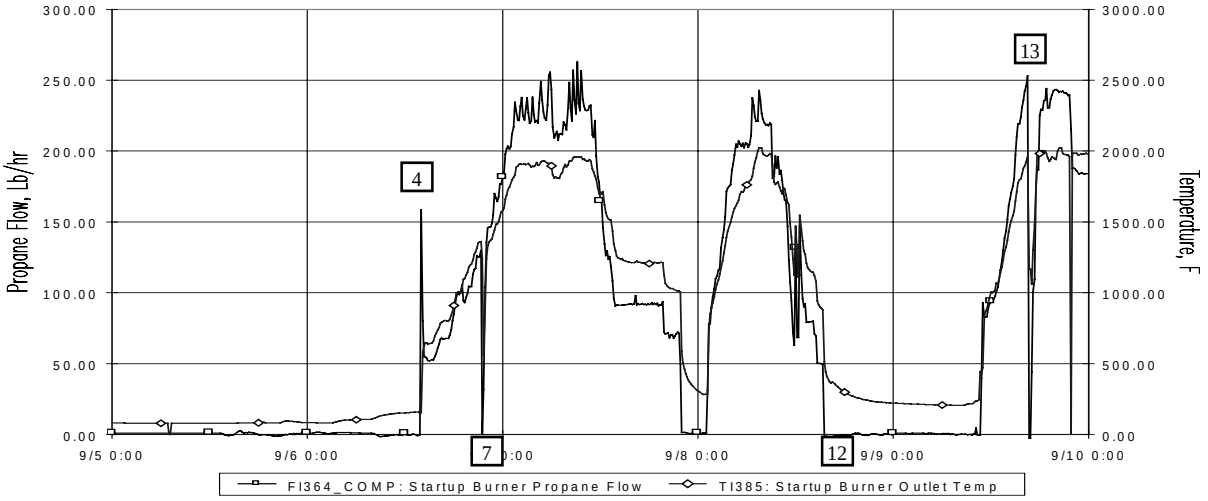

Figure 4.1.4.2-4 Start-Up Burner Flow/Temperature

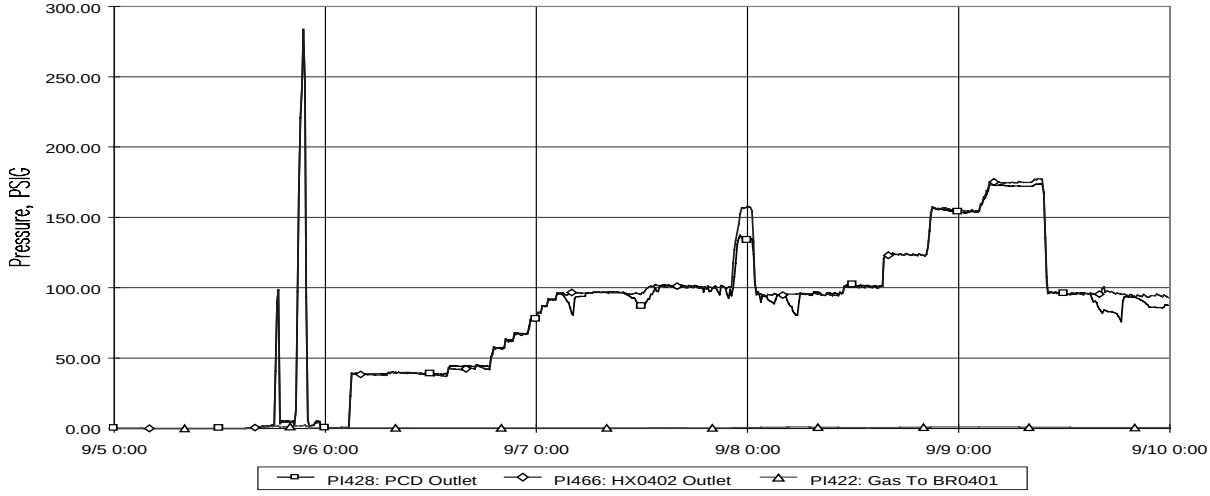

Figure 4.1.4.2-5 System Pressures Downstream of PCD

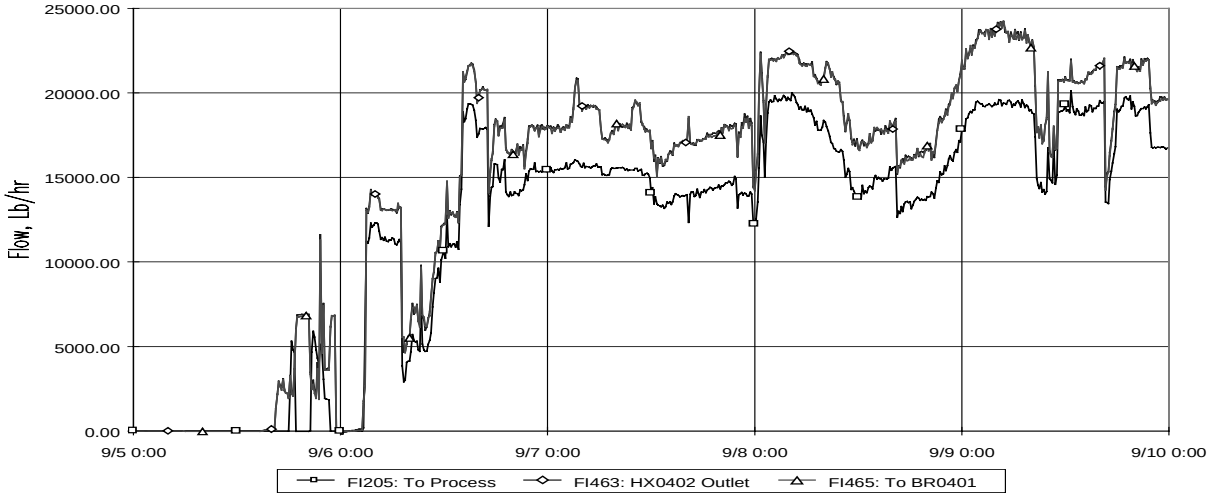

Figure 4.1.4.2-6 Total Gas In/Out Flow Rates

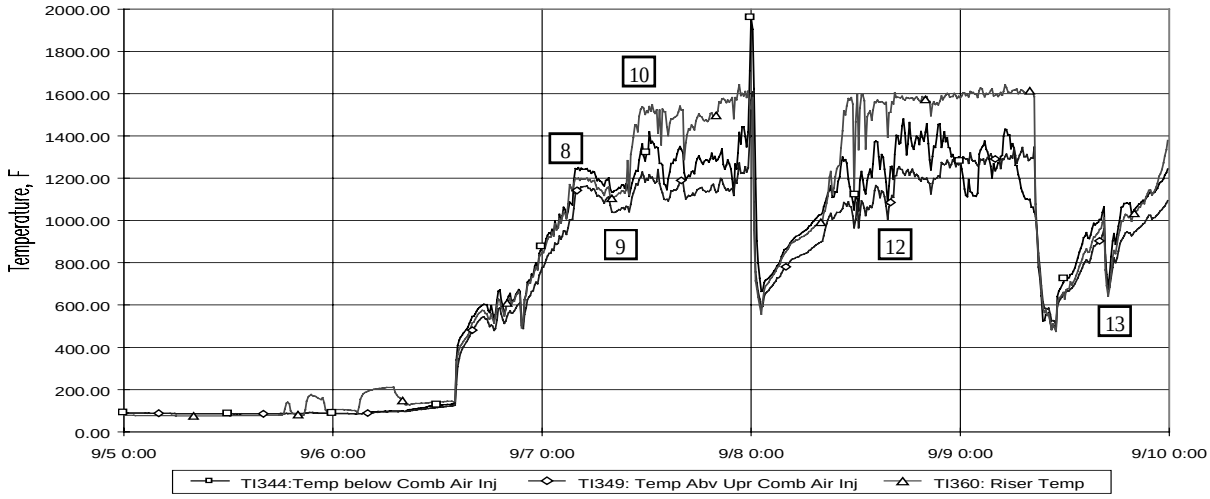

Figure 4.1.4.2-7 Reactor Mixing Zone and Riser Temperatures

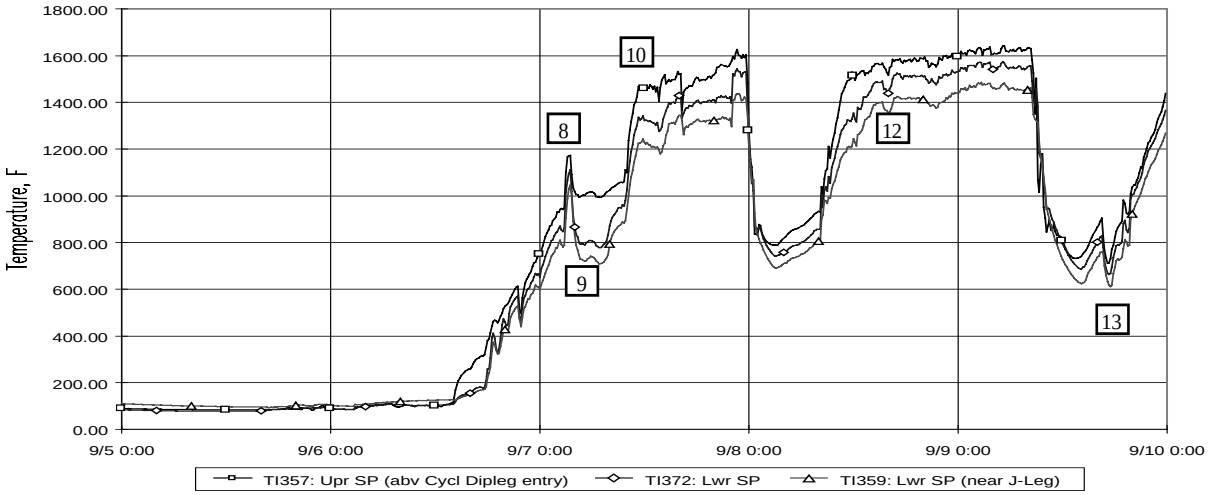

Figure 4.1.4.2-8 Standpipe Temperatures

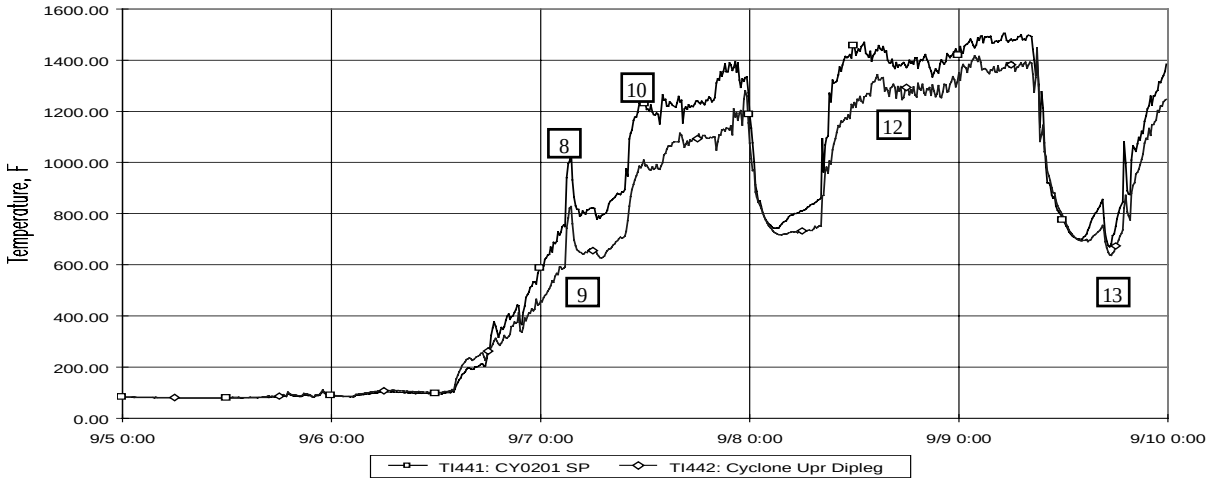

Figure 4.1.4.2-9 Cyclone Dipleg Temperatures

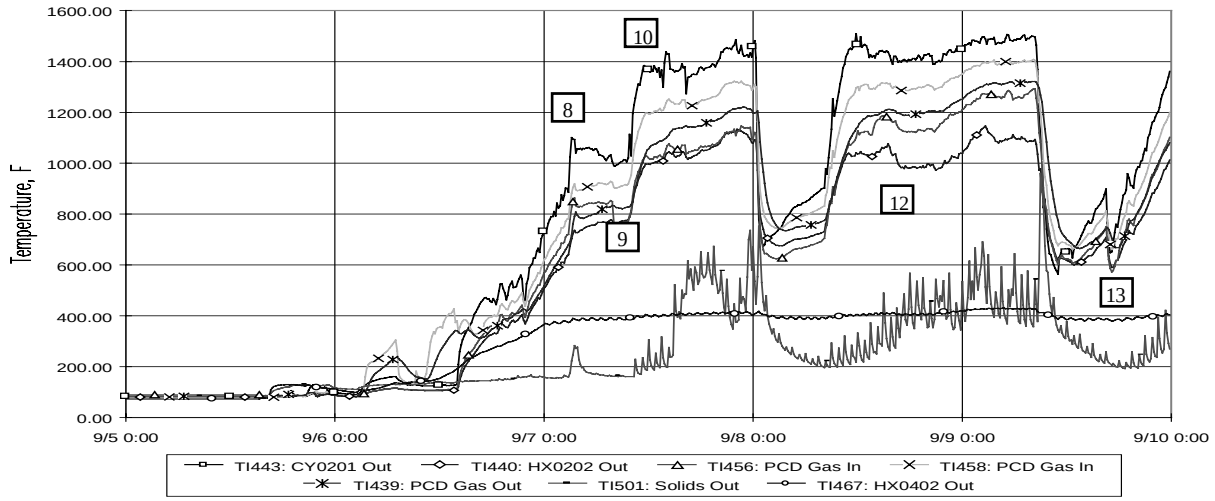

Figure 4.1.4.2-10 Temperature Profiles Downstream of Reactor

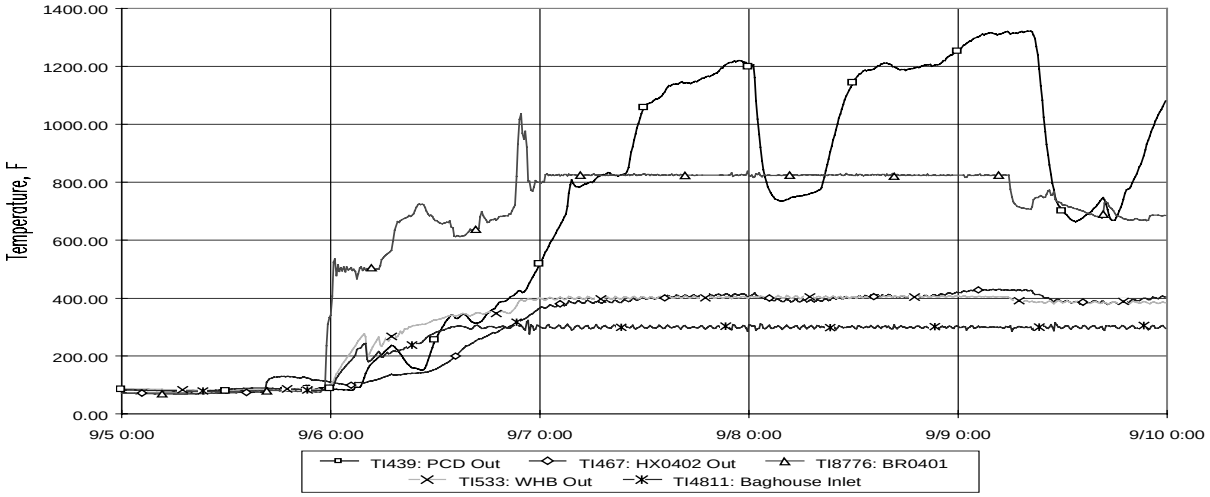

Figure 4.1.4.2-11 System Temperatures Downstream of PCD

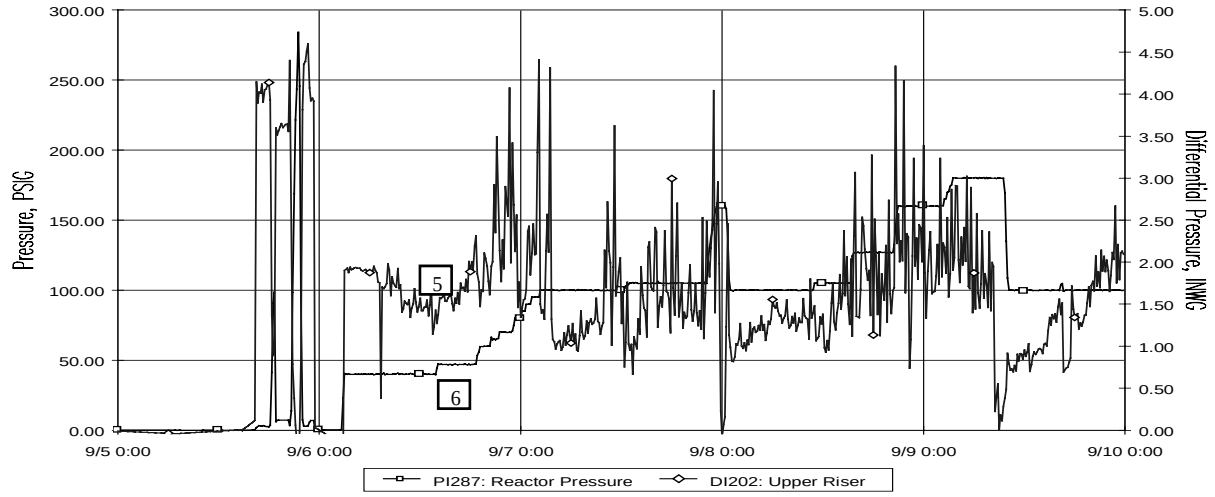

Figure 4.1.4.2-12 Reactor Pressure/Riser Differential Pressure Profiles

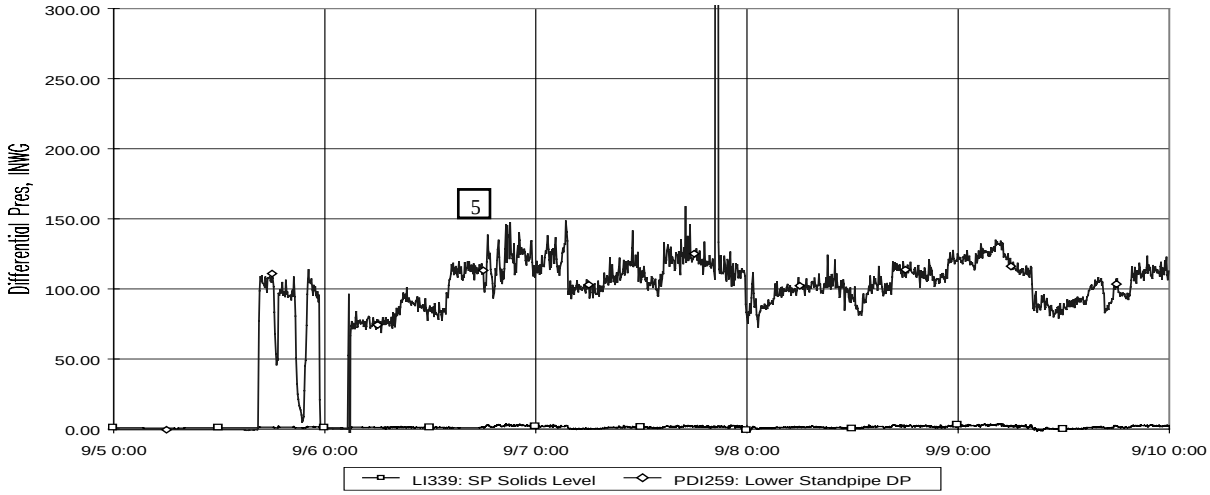

Figure 4.1.4.2-13 Standpipe Differential Pressure Profiles

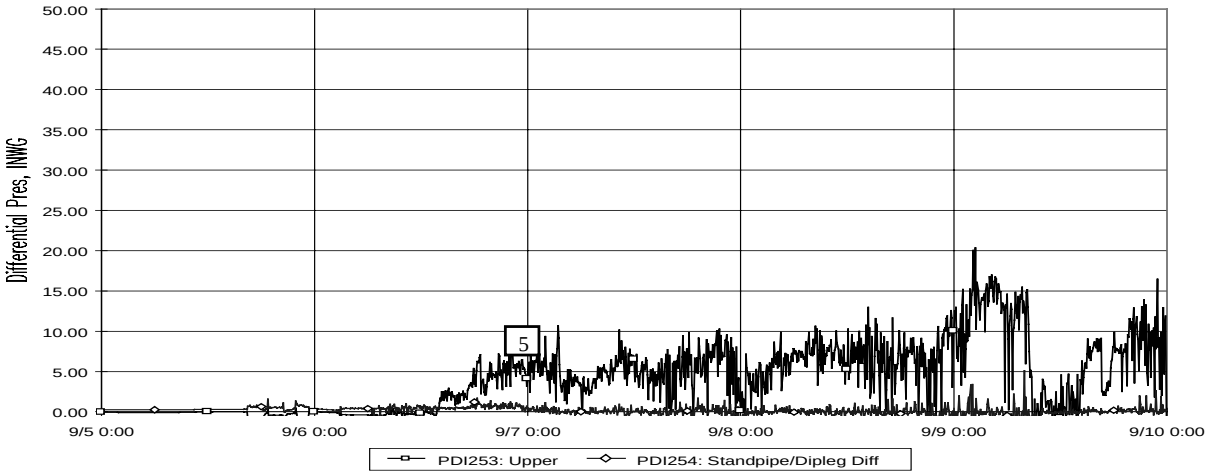

Figure 4.1.4.2-14 CY0201 Dipleg Differential Pressure Profiles

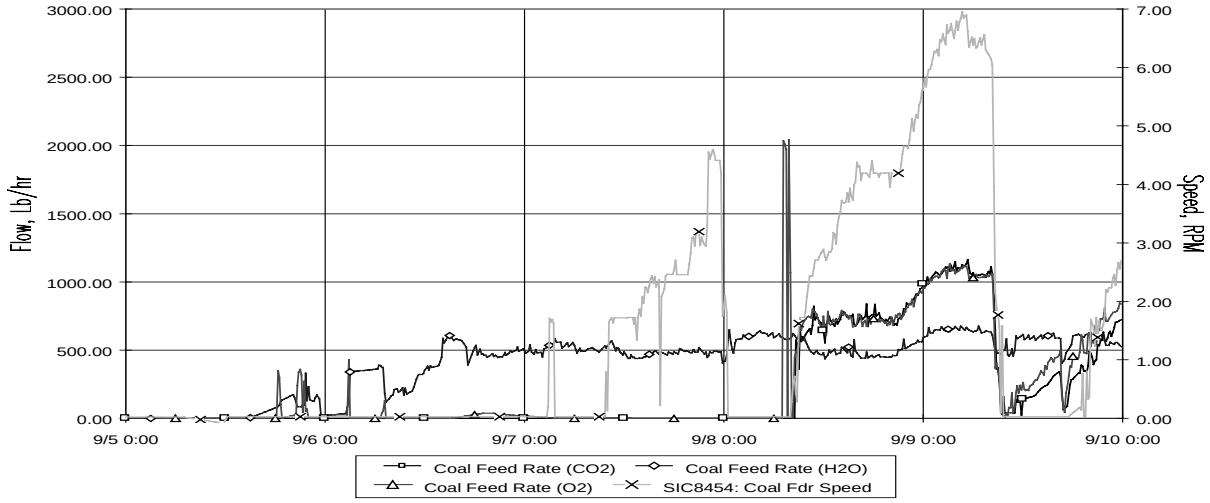

Figure 4.1.4.2-15 Coal Feed Rate Based on Gas Analysis

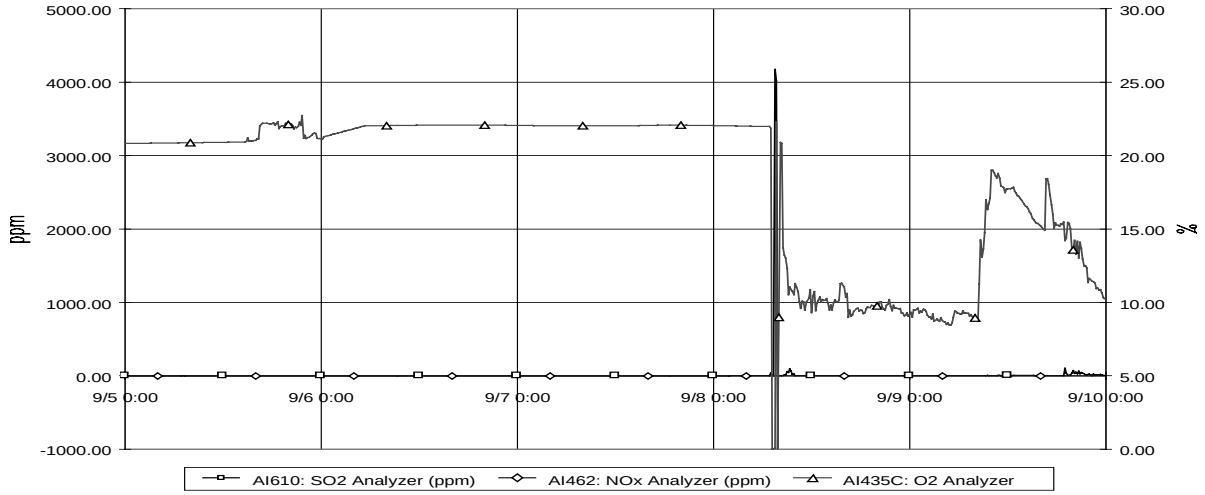

Figure 4.1.4.2-16 O_2, SO_2, and NO_x Analyzers

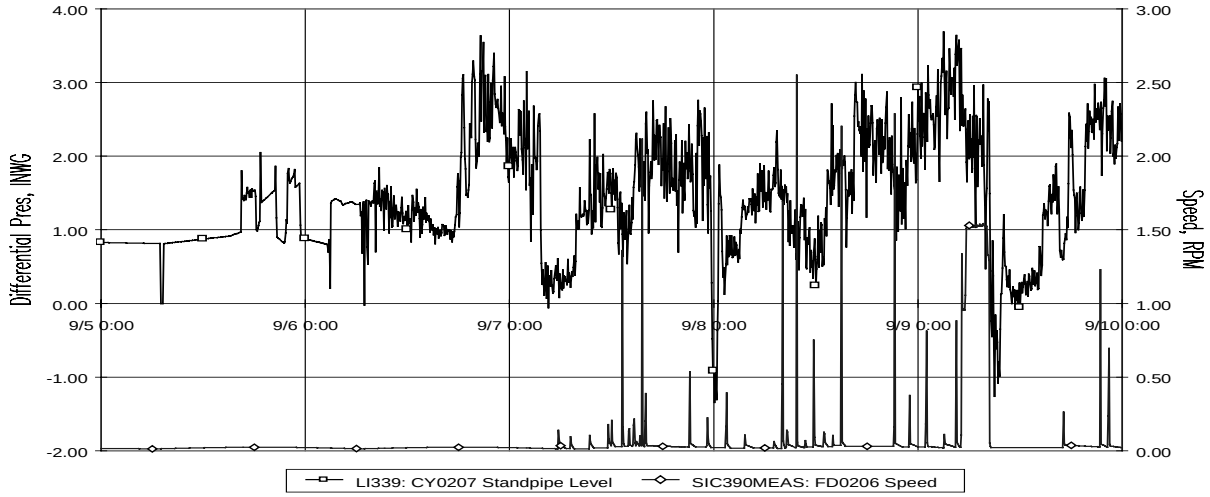

Figure 4.1.4.2-17 Solids Withdrawal

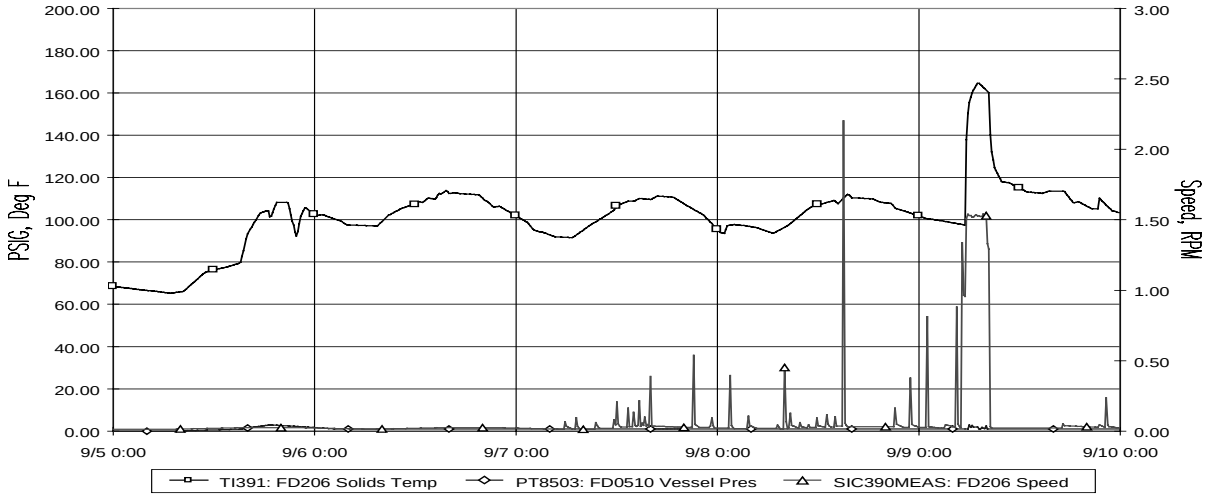

Figure 4.1.4.2-18 FD0206 Profiles

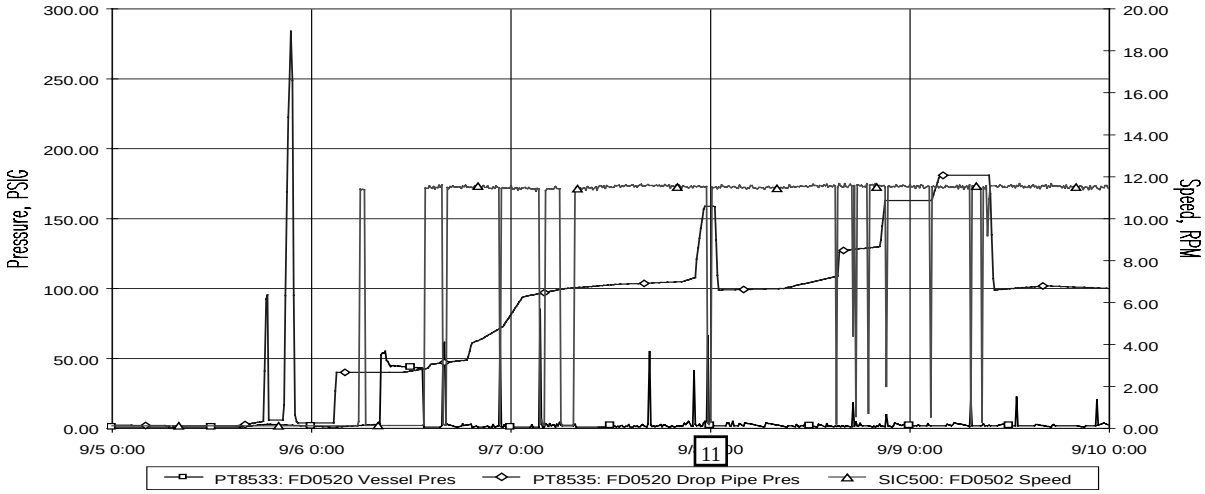

Figure 4.1.4.2-19 FD0520 Pressure Profiles

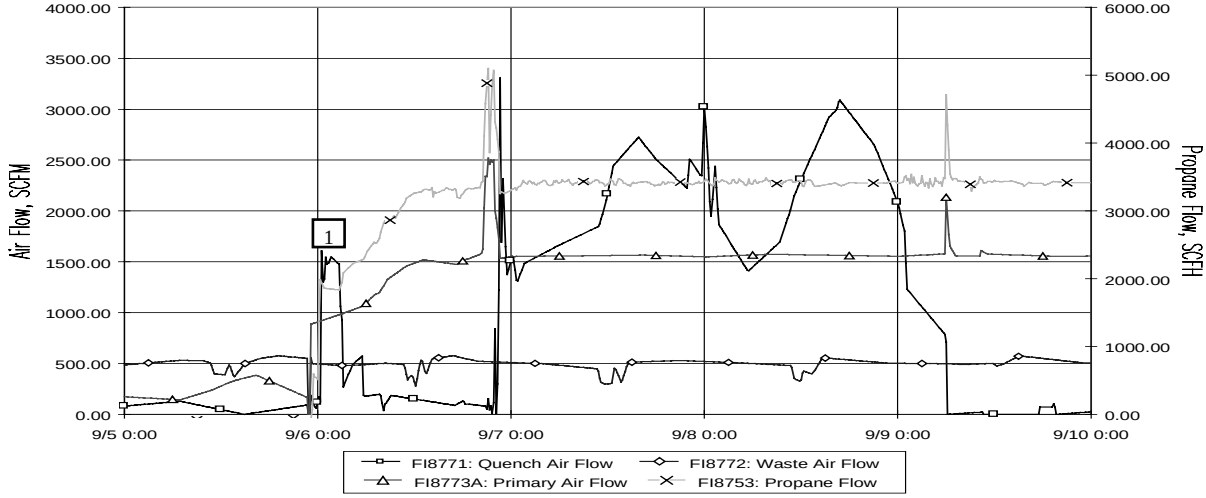

Figure 4.1.4.2-20 Thermal Oxidizer Air/Fuel Flow

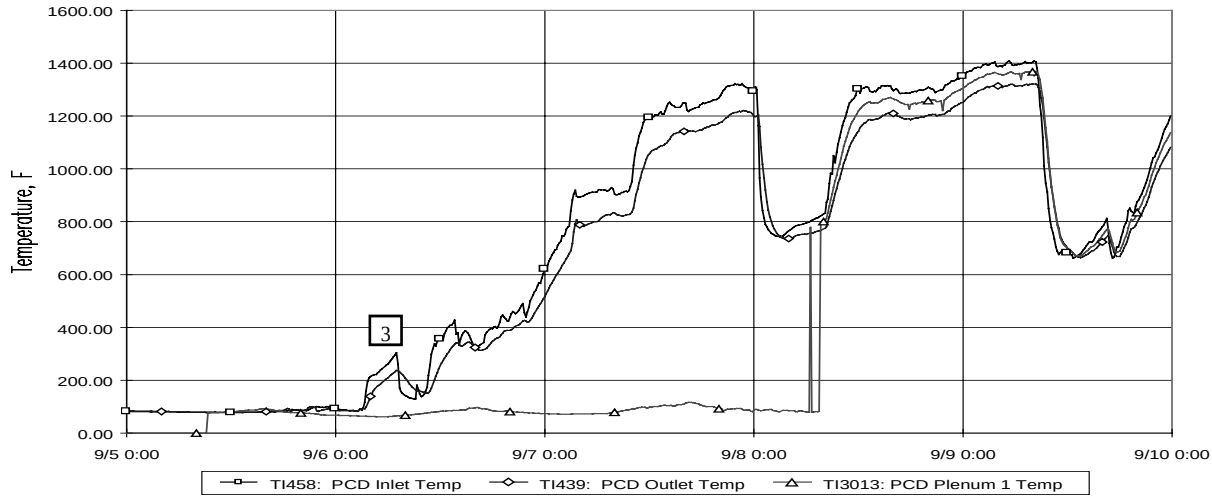

Figure 4.1.4.2-21 PCD Temperatures

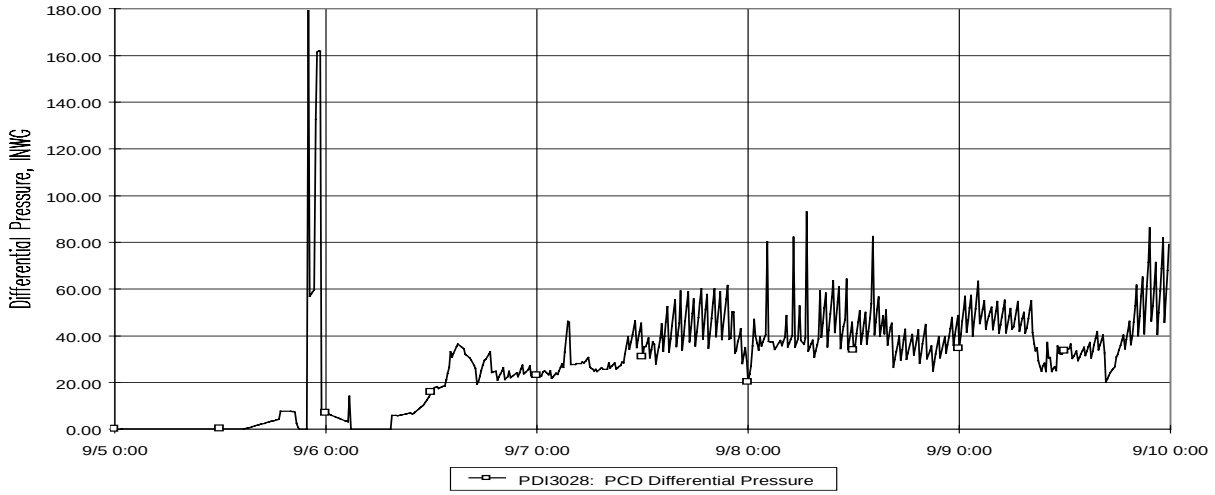

Figure 4.1.4.2-22 PCD Differential Pressure Profile

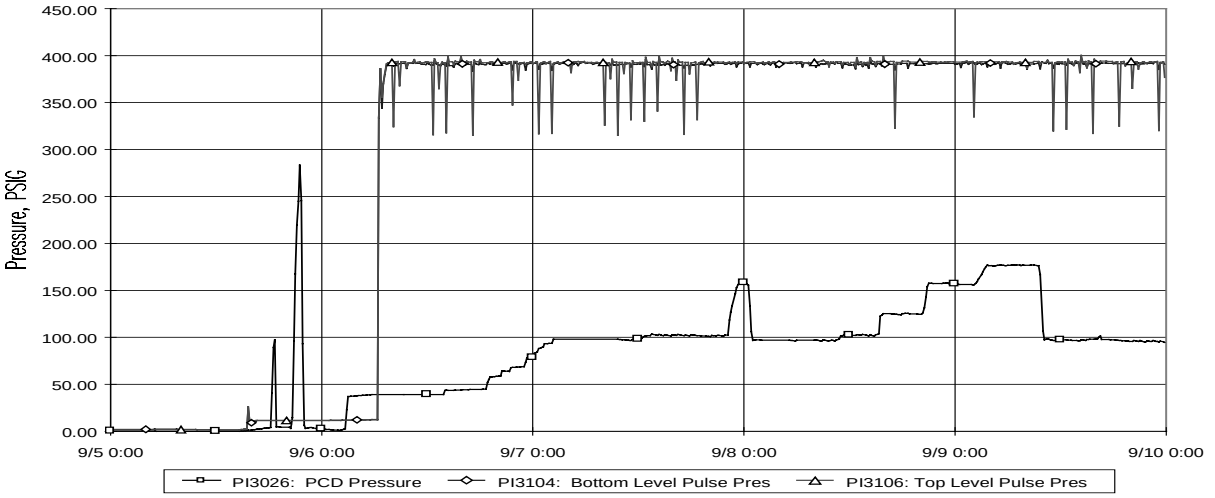

Figure 4.1.4.2-23 PCD Pressure and Pulse Pressure

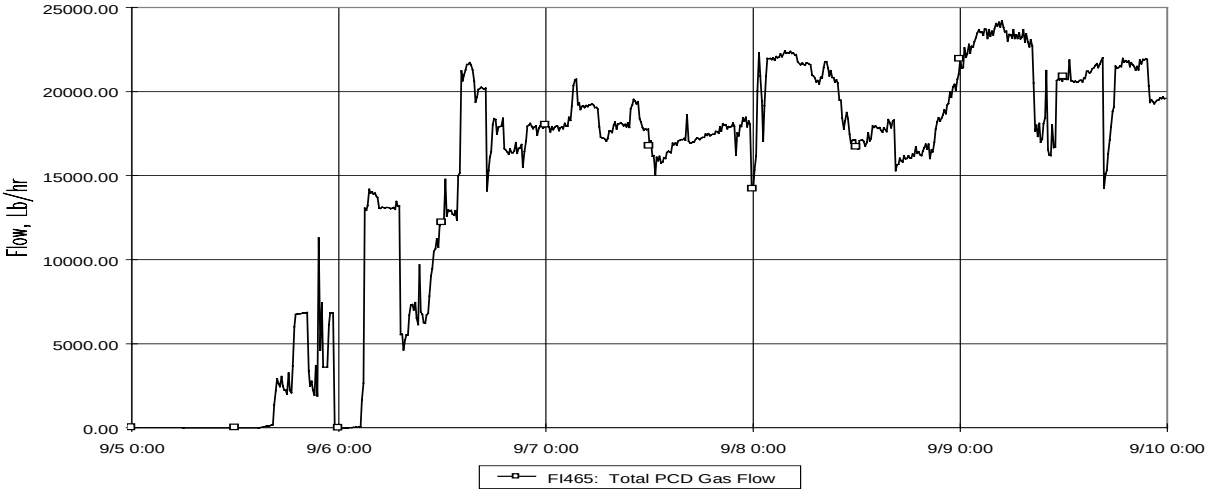

Figure 4.1.4.2-24 Gas Flow Through PCD

Section 4.1.4.2

Graphs 25 through 48

Test Run TC01B
September 10 through September 14, 1997

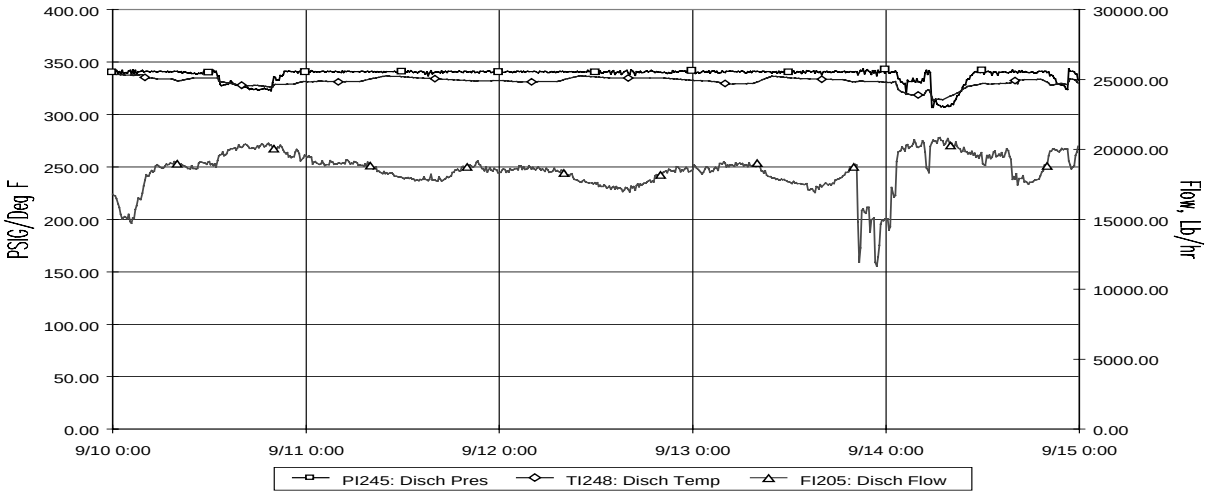

Figure 4.1.4.2-25 CO0201 System Profile

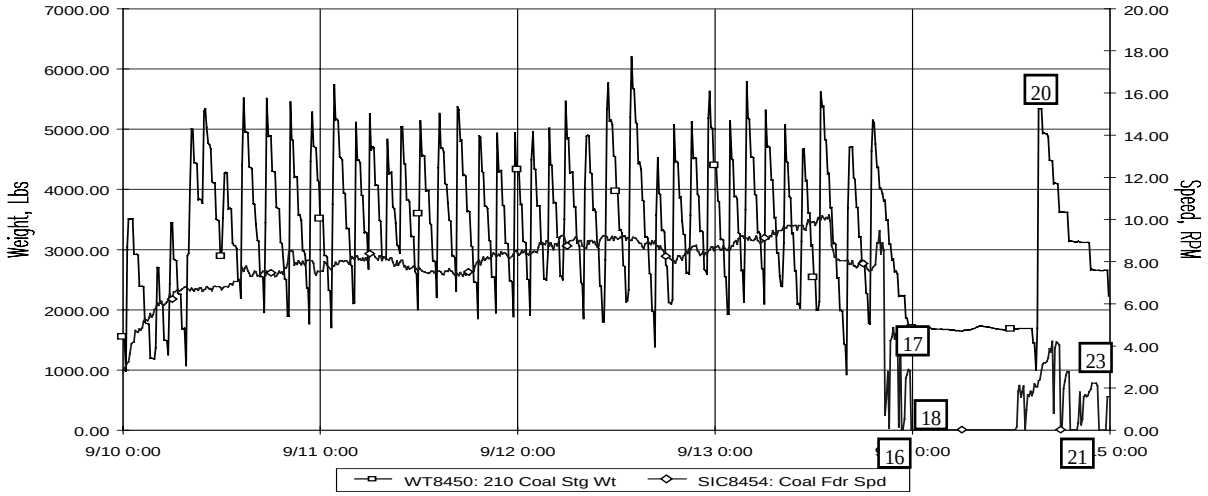

Figure 4.1.4.2-26 Coal Feed System Profile

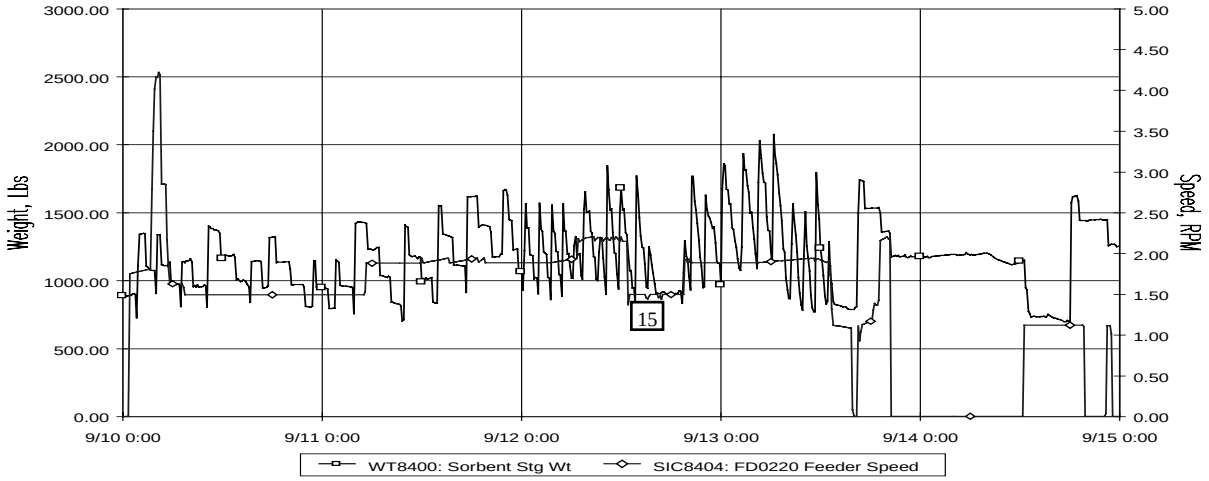

Figure 4.1.4.2-27 Sorbent Feed System Profile

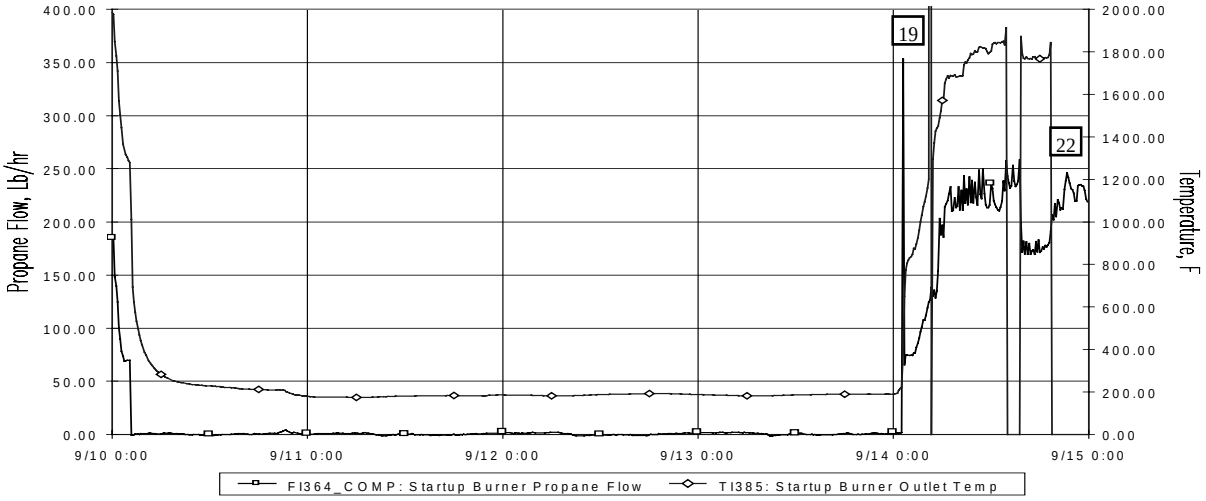

Figure 4.1.4.2-28 Start-Up Burner Flow/Temperature

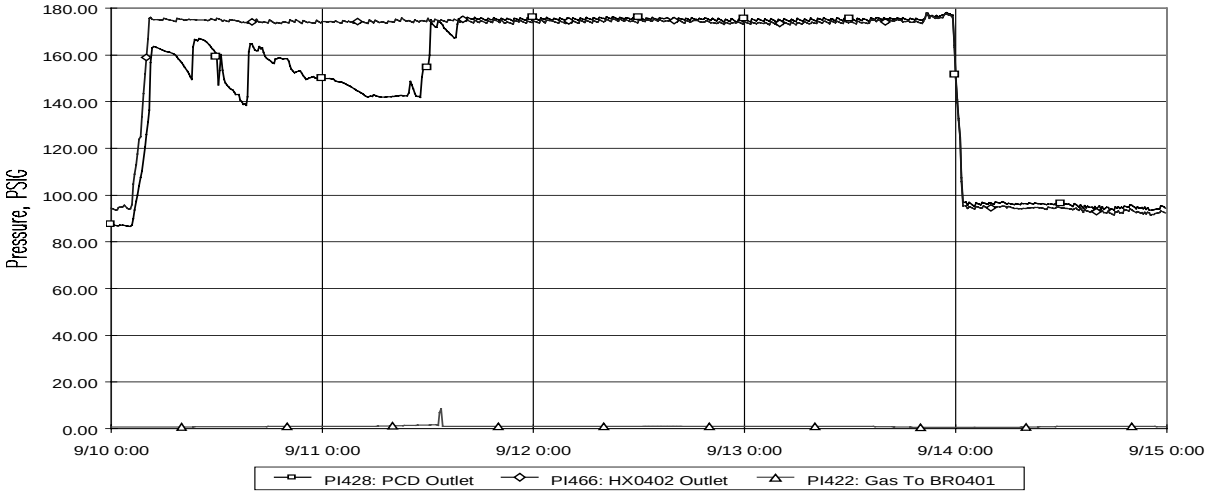

Figure 4.1.4.2-29 System Pressures Downstream of PCD

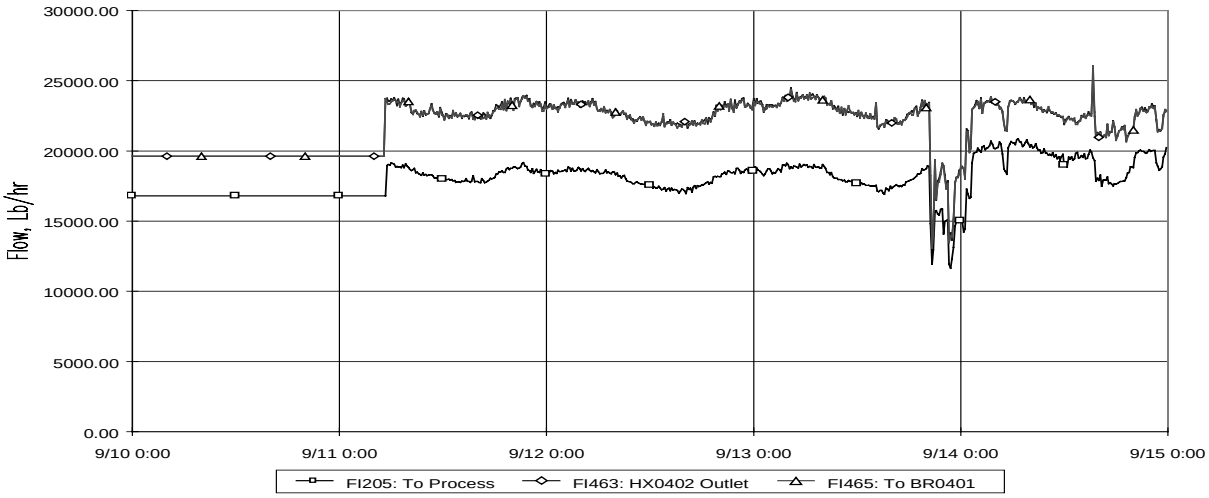

Figure 4.1.4.2-30 Total Gas In/Out Flow Rates

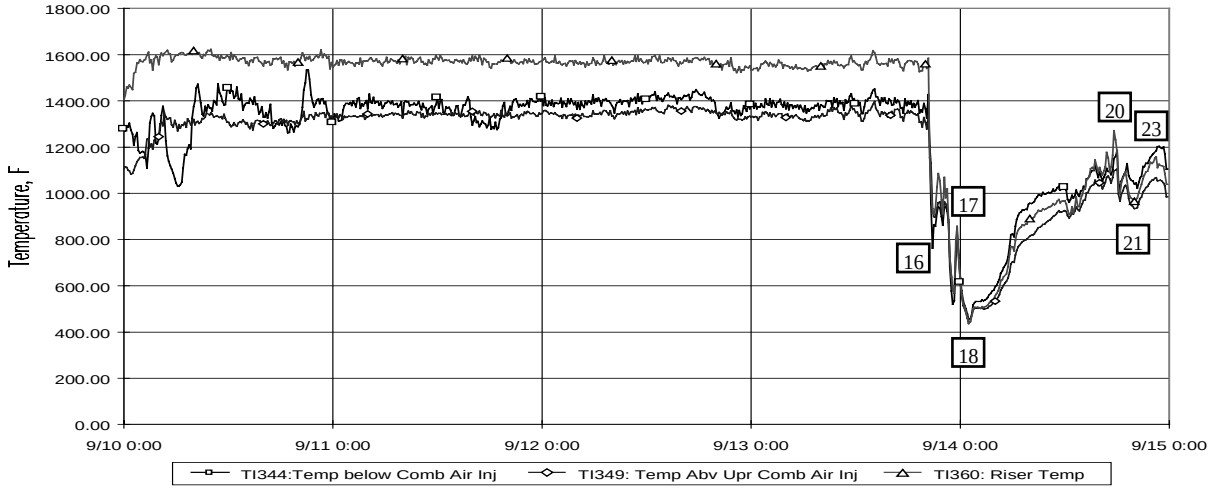

Figure 4.1.4.2-31 Reactor Mixing Zone and Riser Temperatures

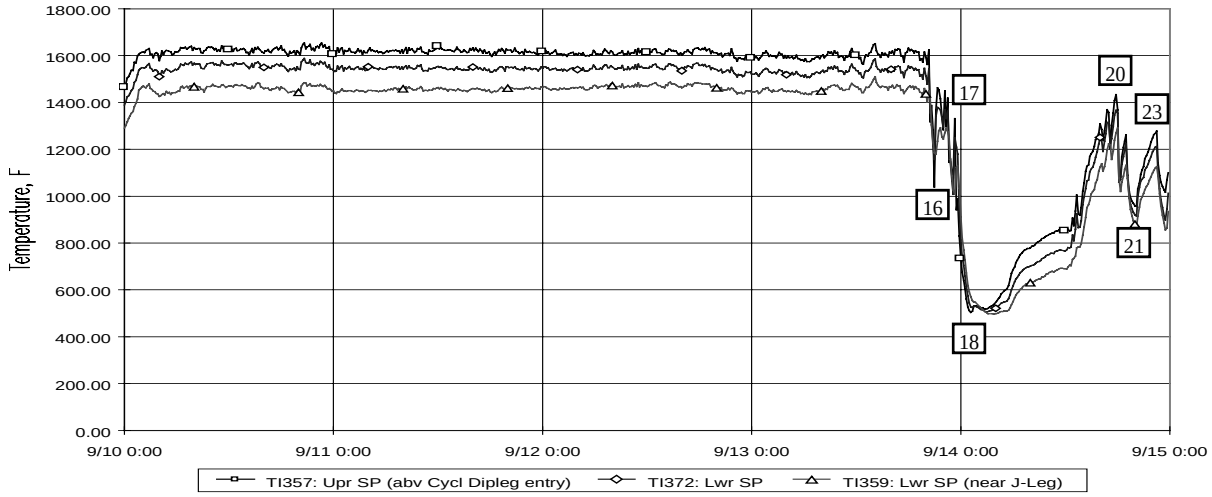

Figure 4.1.4.2-32 Standpipe Temperatures

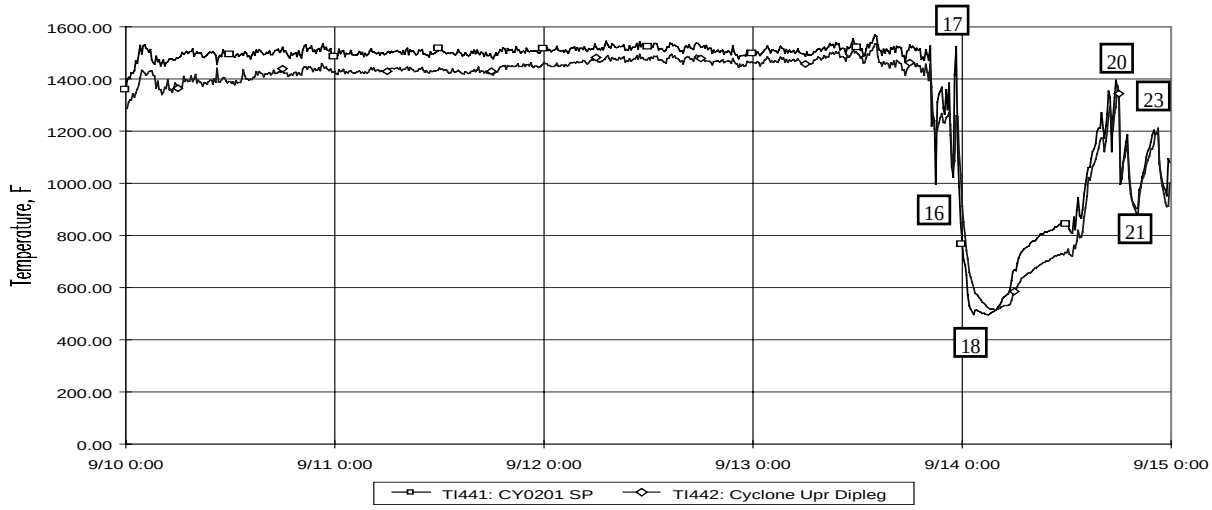

Figure 4.1.4.2-33 Cyclone Dipleg Temperatures

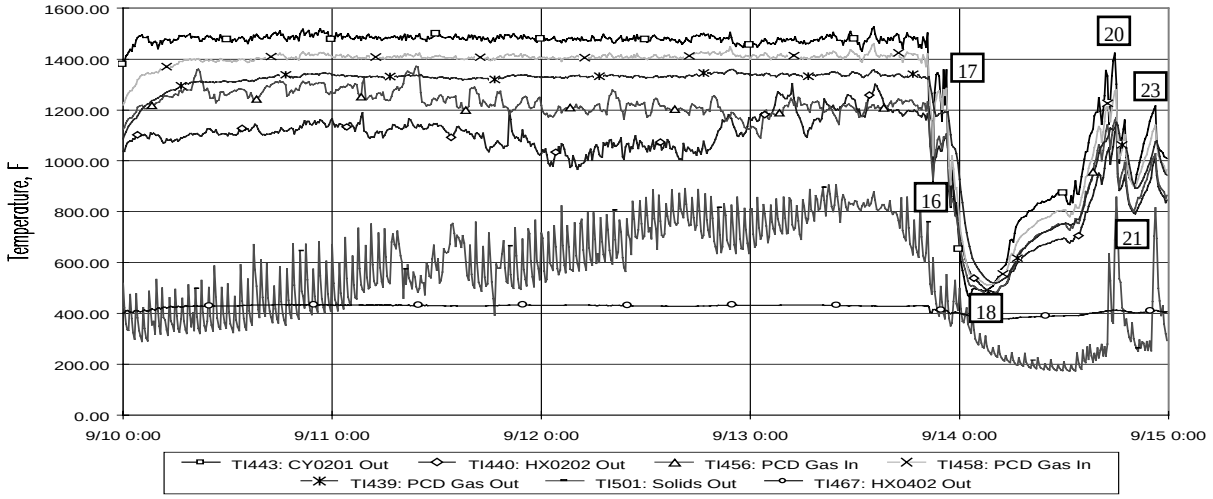

Figure 4.1.4.2-34 Temperature Profiles Downstream of Reactor

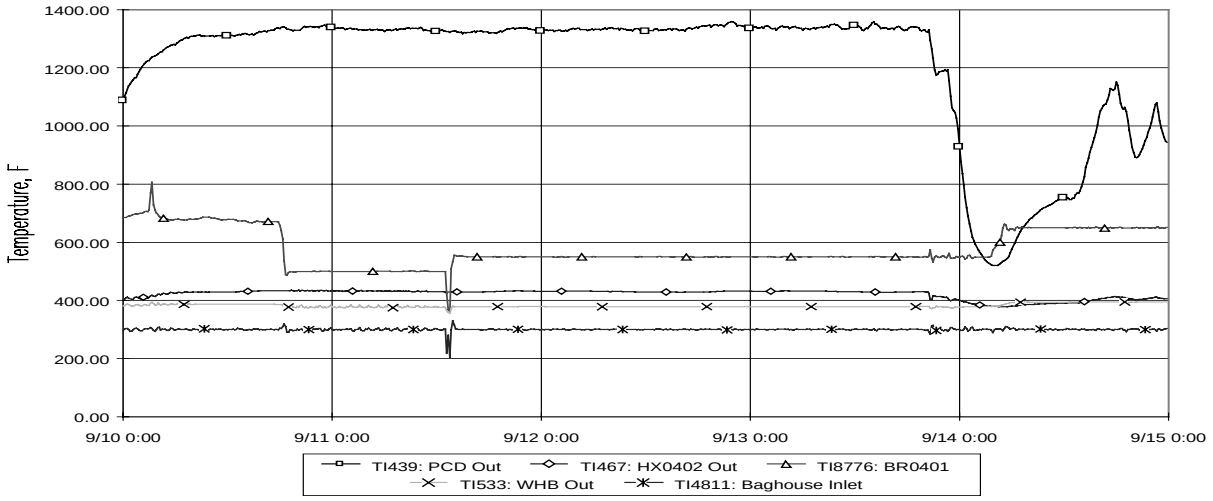

Figure 4.1.4.2-35 System Temperatures Downstream of PCD

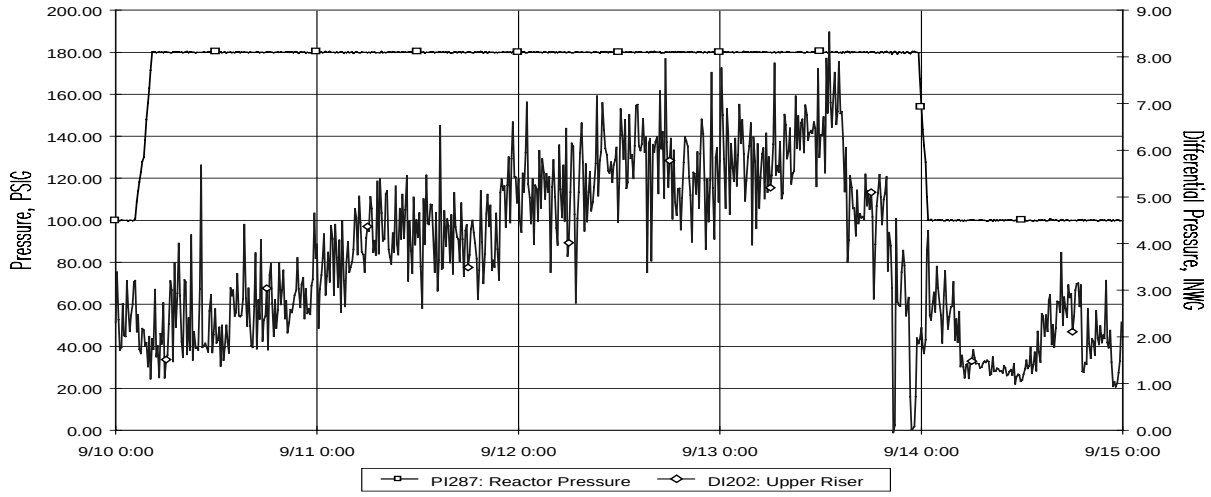

Figure 4.1.4.2-36 Reactor Pressure/Riser Differential Pressure Profiles

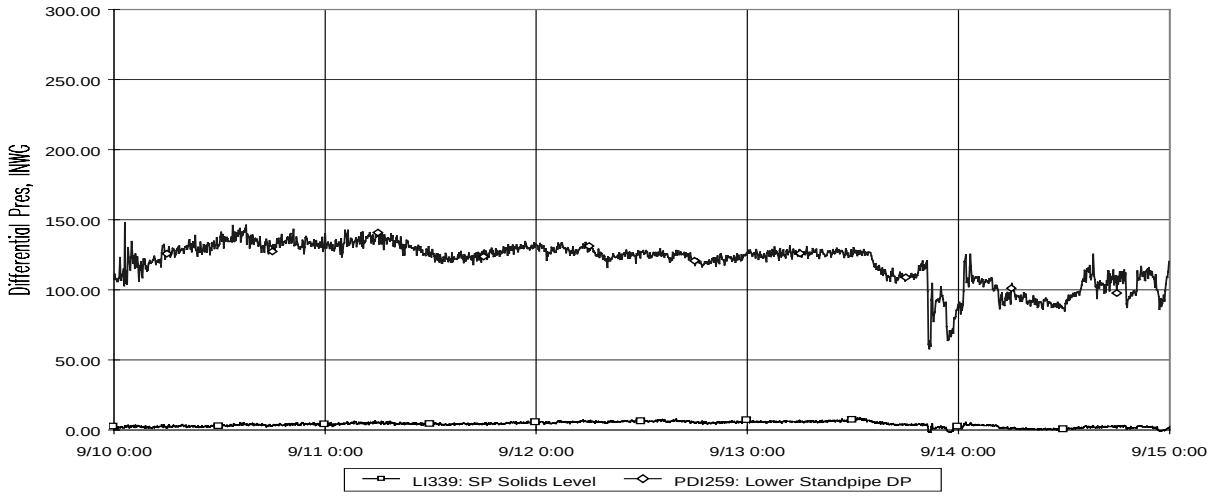

Figure 4.1.4.2-37 Standpipe Differential Pressure Profiles

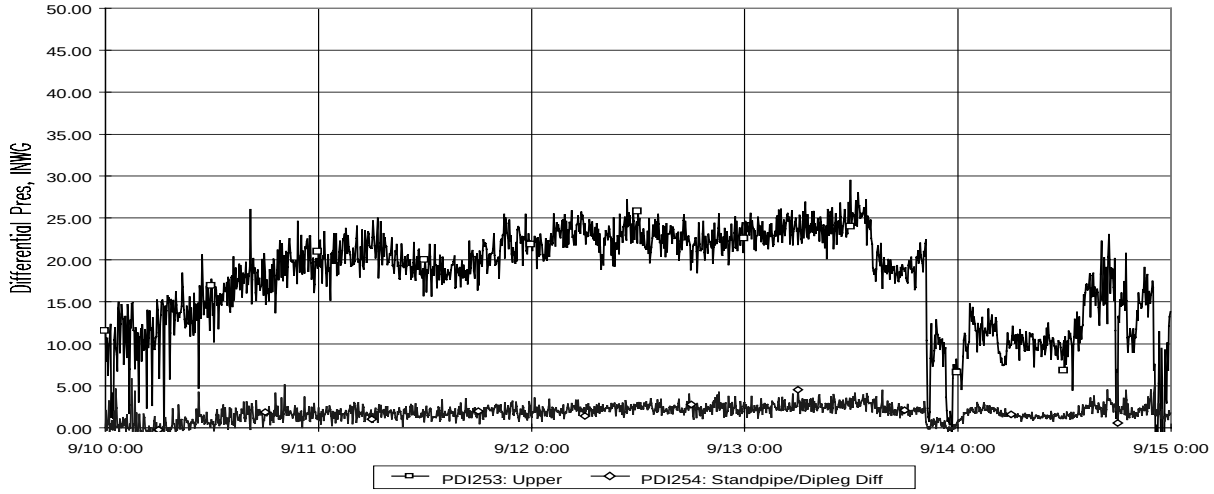

Figure 4.1.4.2-38 CY0201 Dipleg Differential Pressure Profiles

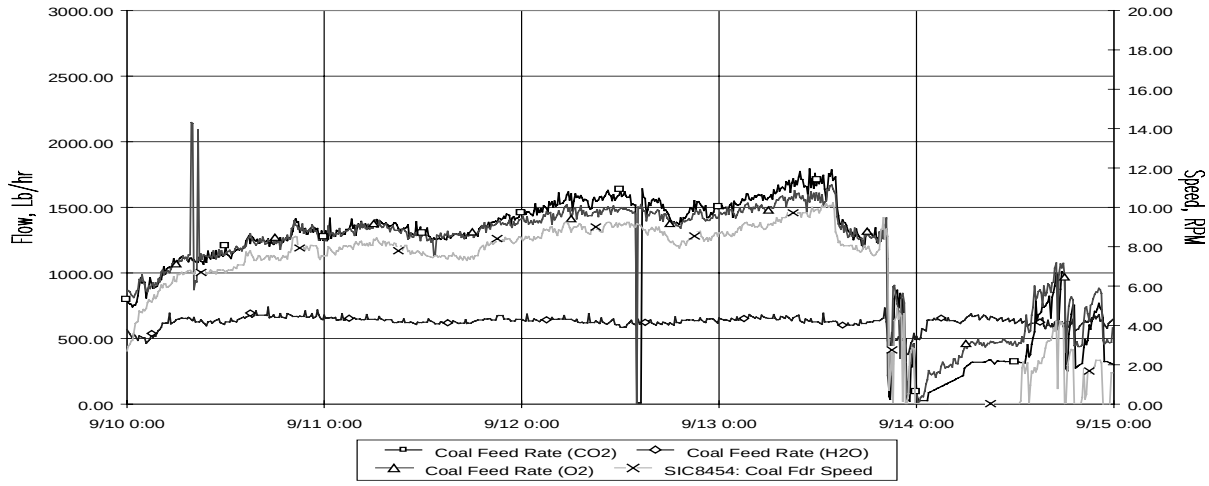

Figure 4.1.4.2-39 Coal Feed Rate Based on Gas Analysis

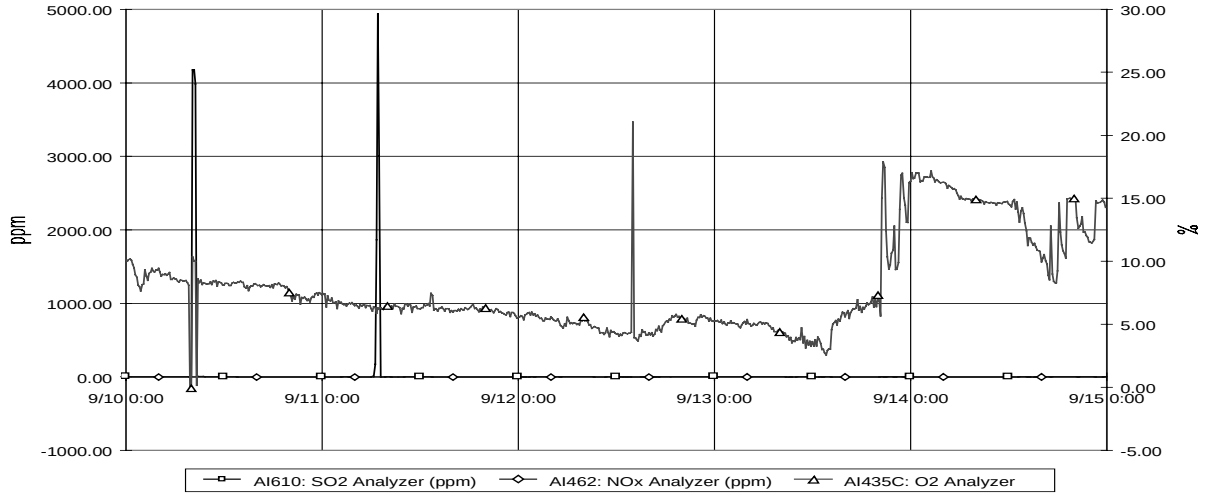

Figure 4.1.4.2-40 O_2, SO_2, and NO_x Analyzers

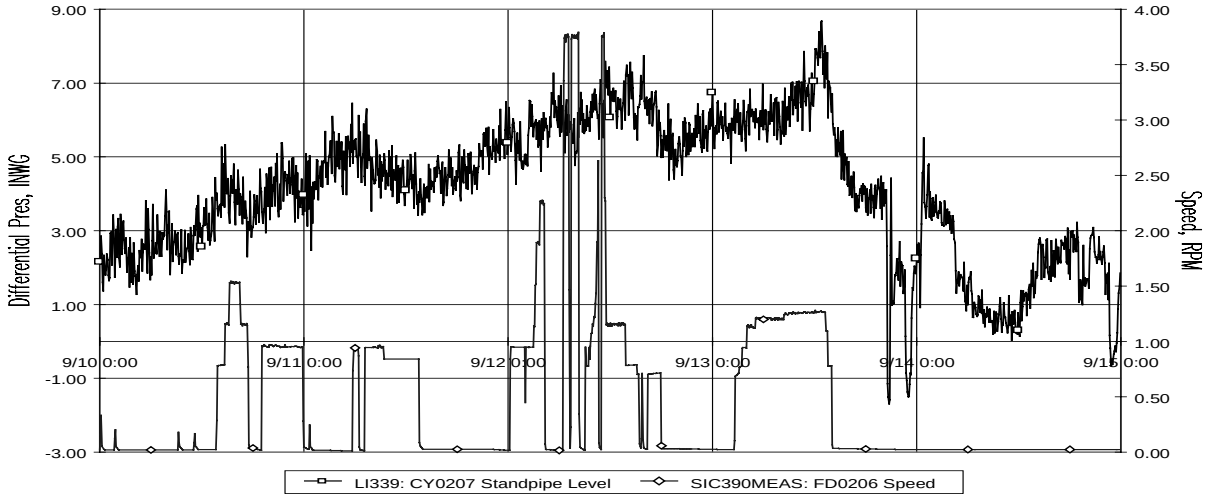

Figure 4.1.4.2-41 Solids Withdrawal

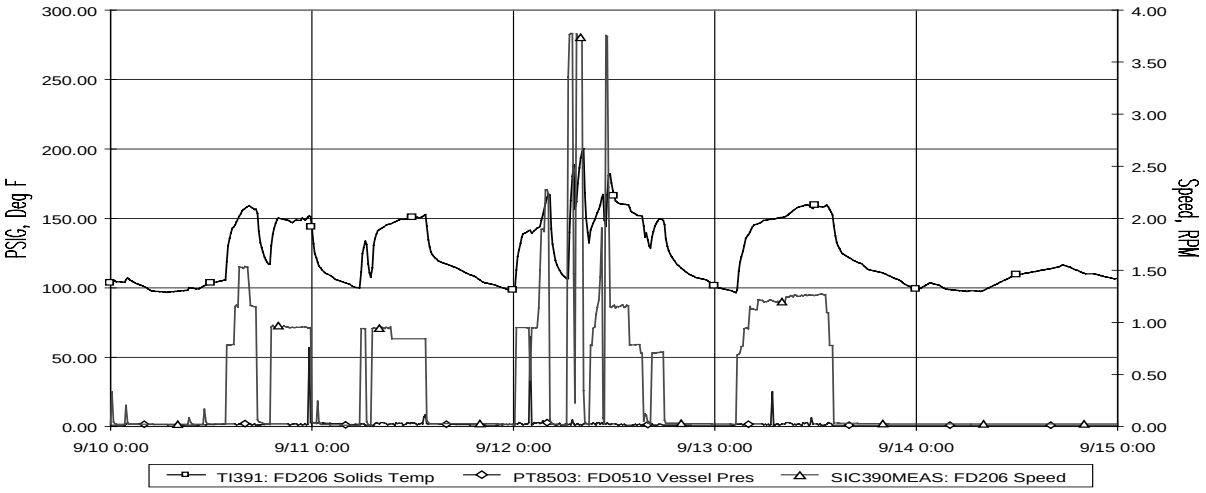

Figure 4.1.4.2-42 FD0206 Profiles

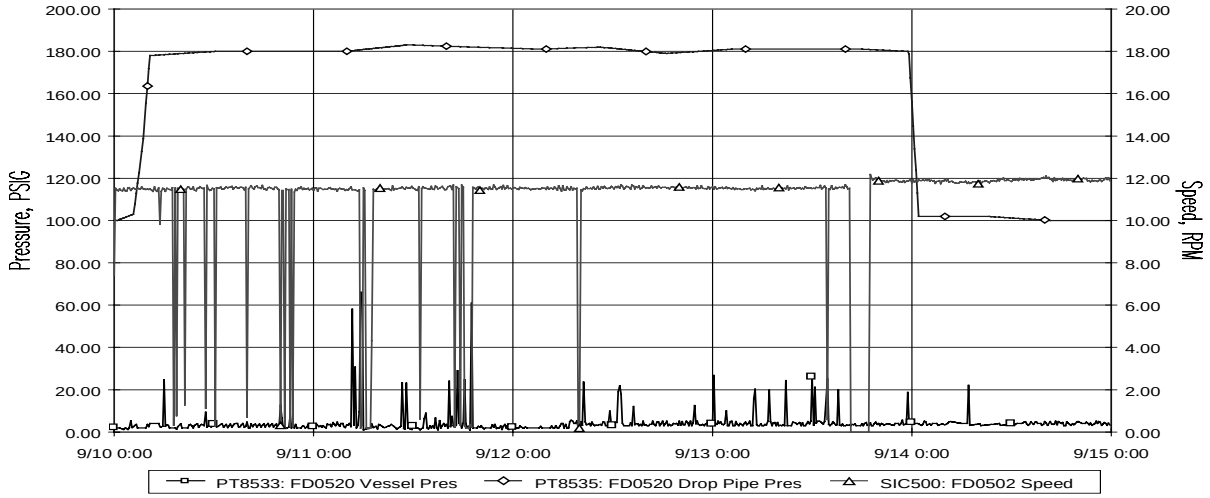

Figure 4.1.4.2-43 FD0520 Pressure Profiles

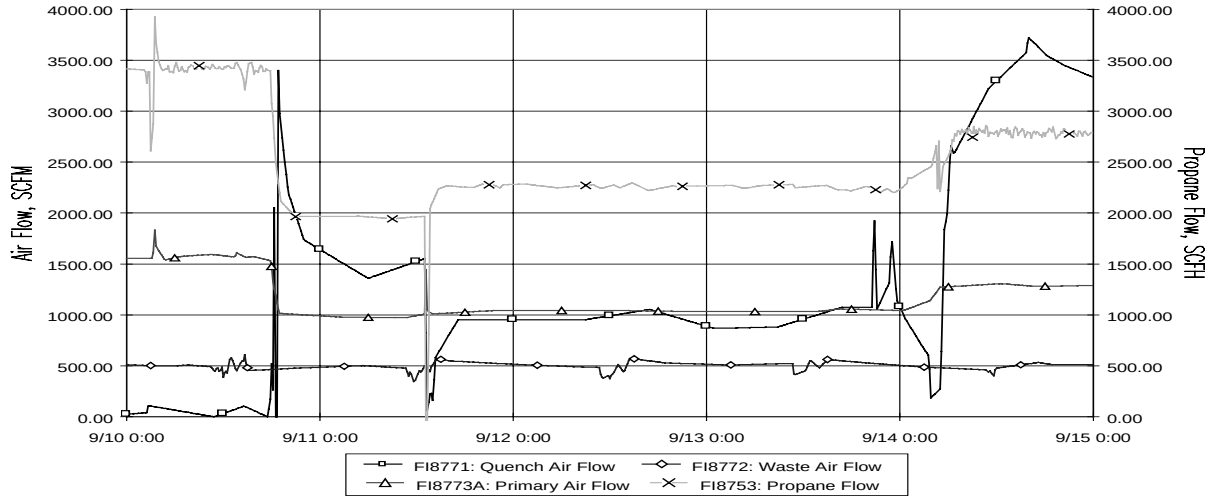

Figure 4.1.4.2-44 Thermal Oxidizer Air/Fuel Flow

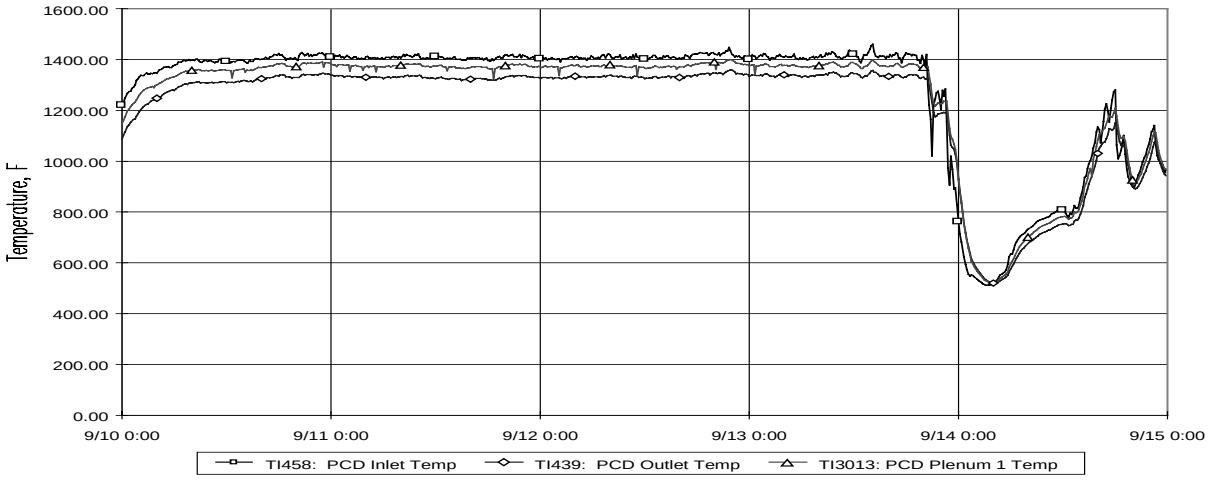

Figure 4.1.4.2-45 PCD Temperatures

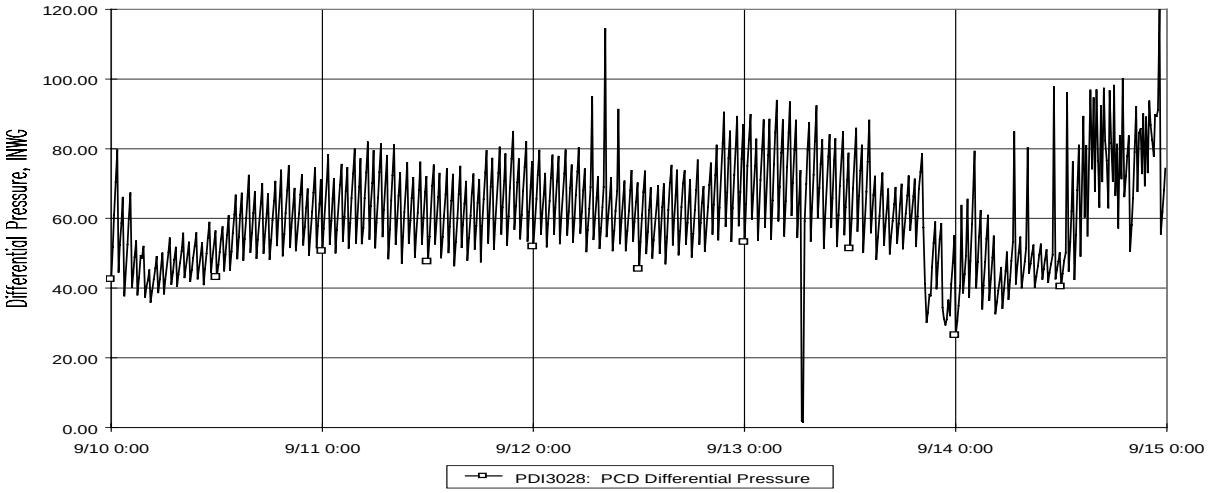

Figure 4.1.4.2-46 PCD Differential Pressure Profile

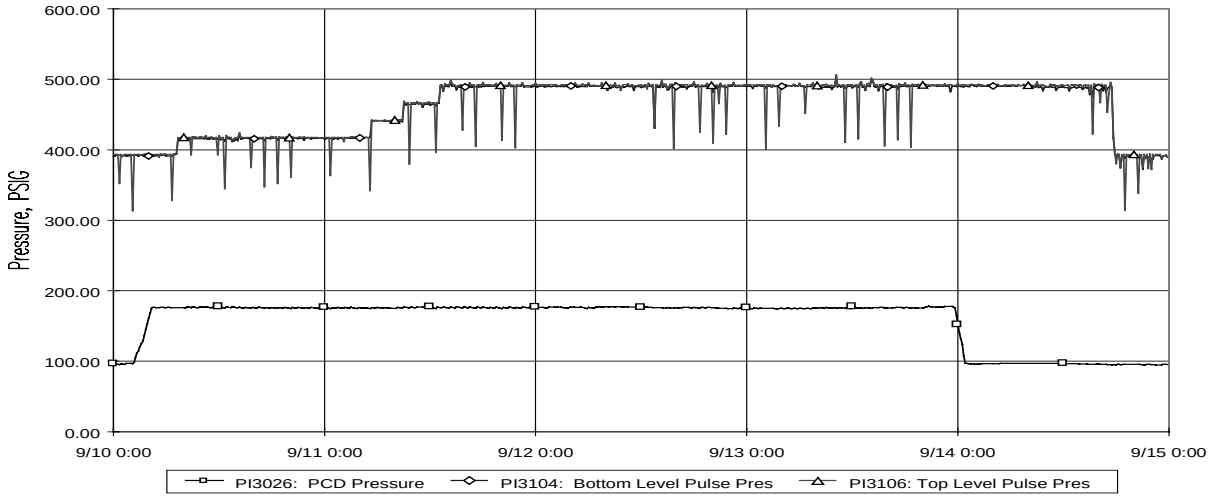

Figure 4.1.4.2-47 PCD Pressure and Pulse Pressure

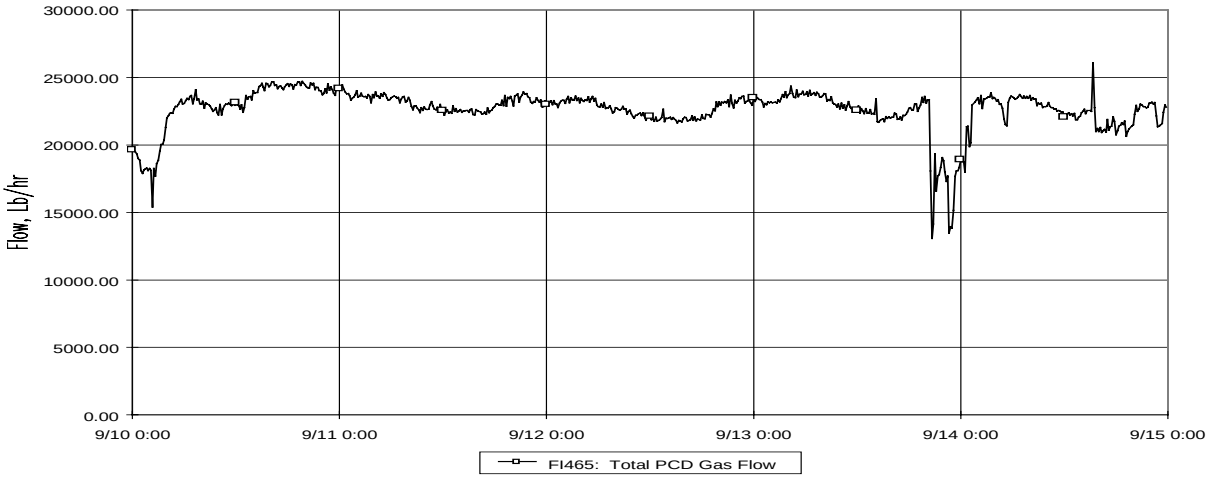

Figure 4.1.4.2-48 Gas Flow Through PCD

Section 4.1.4.2

Graphs 49 through 72

Test Run TC01B
September 15 through September 18, 1997

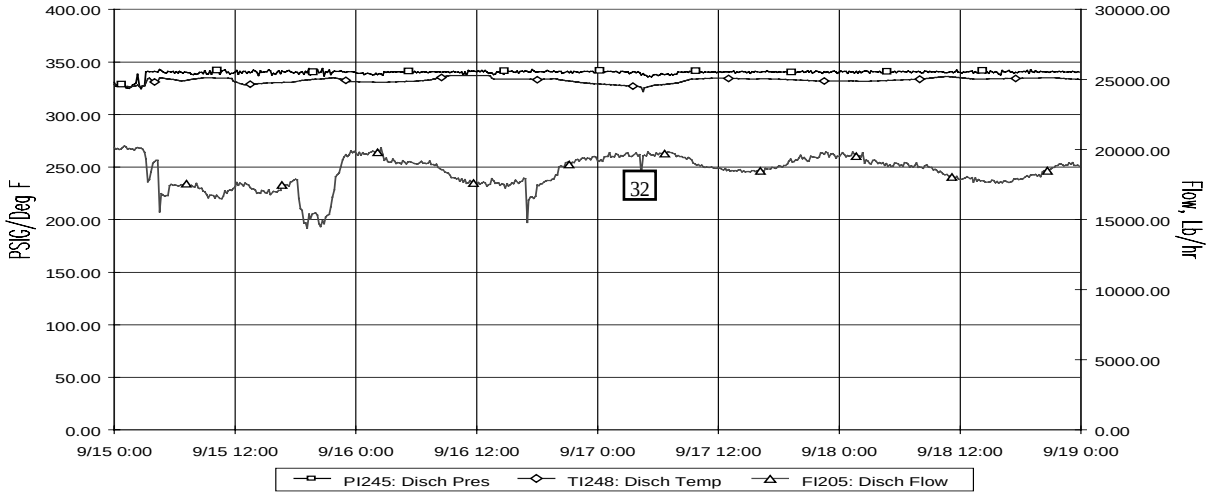

Figure 4.1.4.2-49 CO0201 System Profile

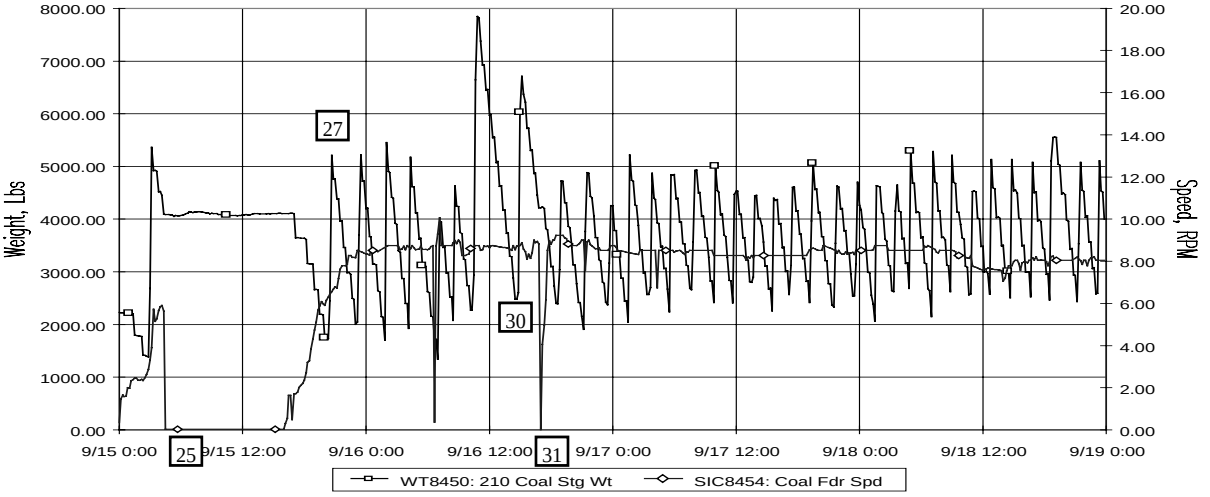

Figure 4.1.4.2-50 Coal Feed System Profile

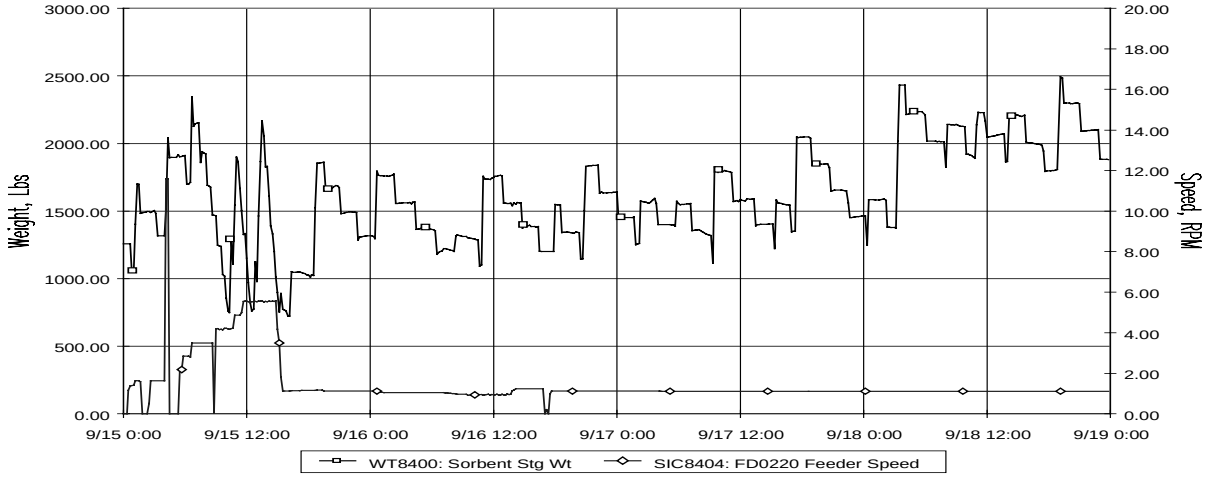

Figure 4.1.4.2-51 Sorbent Feed System Profile

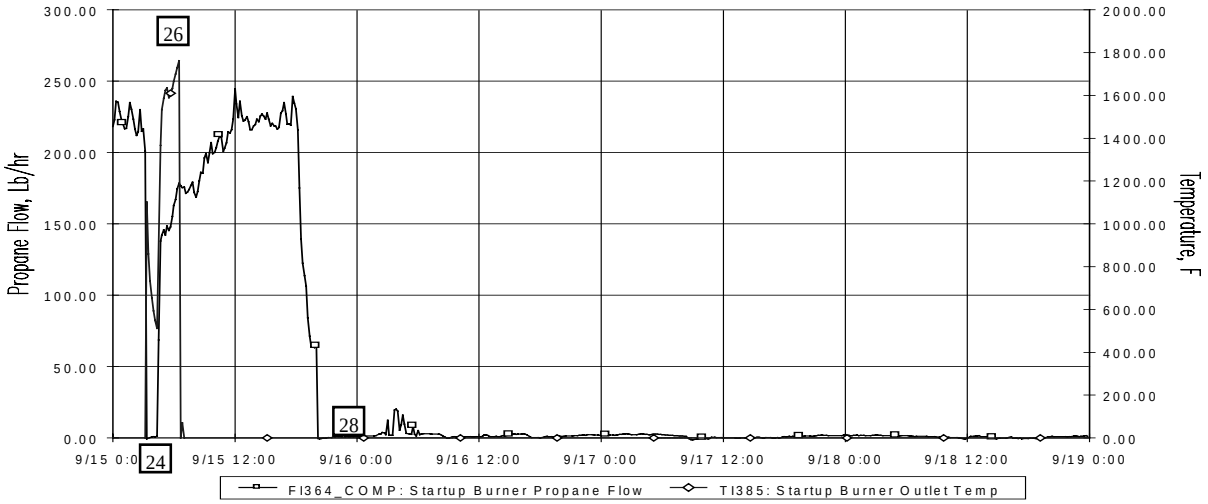

Figure 4.1.4.2-52 Start-Up Burner Flow/Temperature

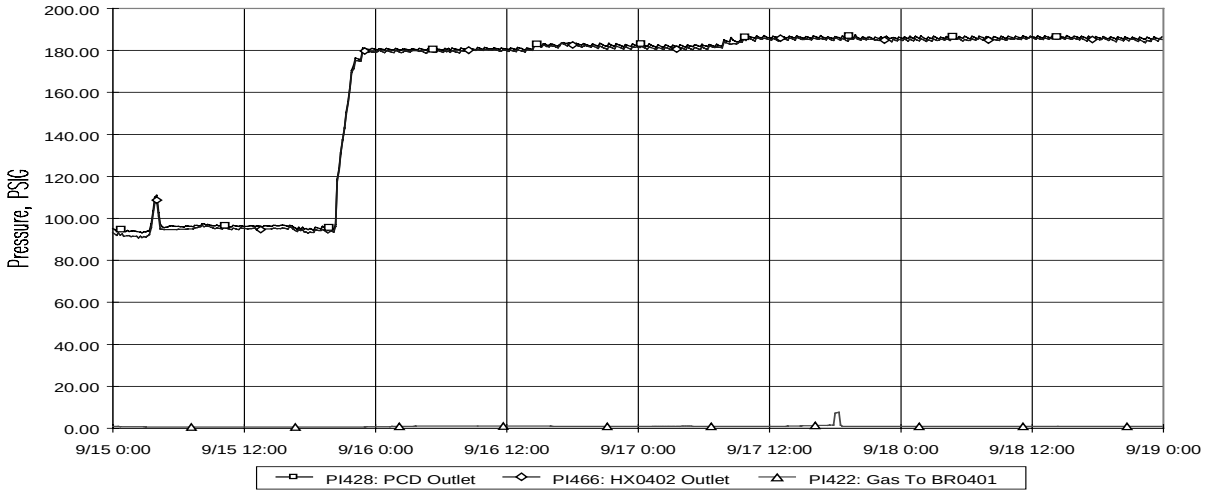

Figure 4.1.4.2-53 System Pressures Downstream of PCD

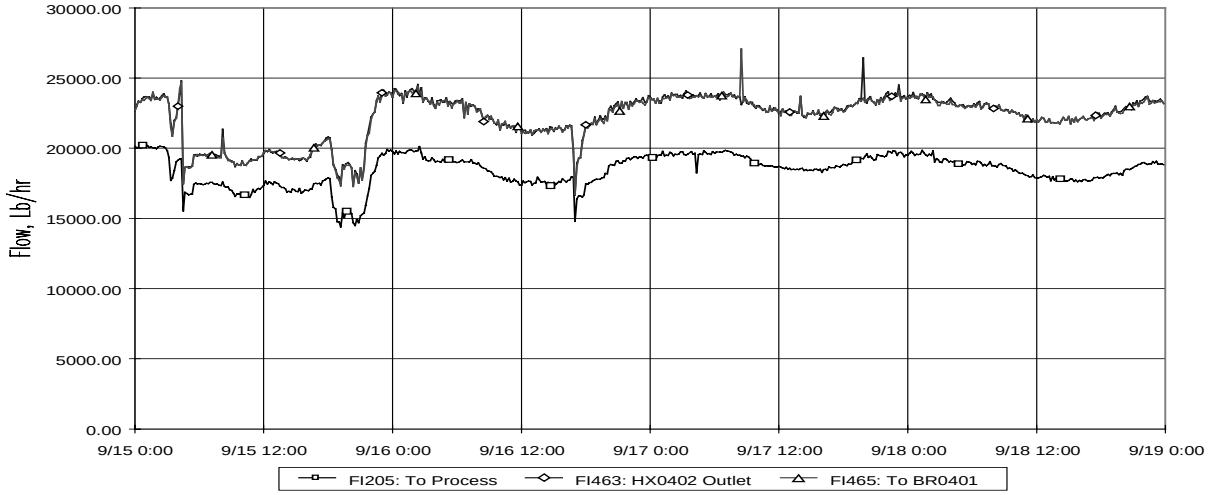

Figure 4.1.4.2-54 Total Gas In/Out Flow Rates

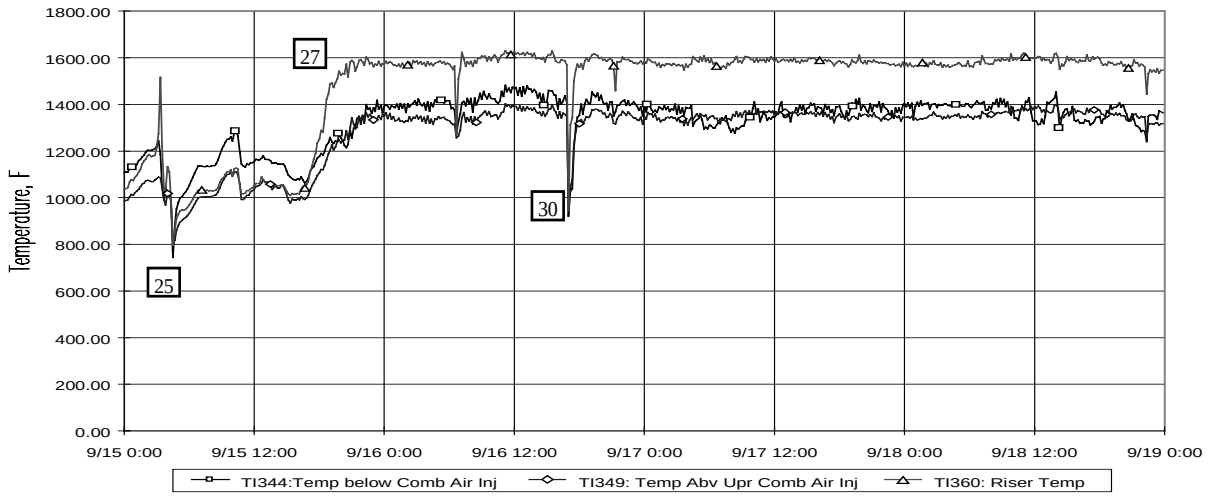

Figure 4.1.4.2-55 Reactor Mixing Zone and Riser Temperatures

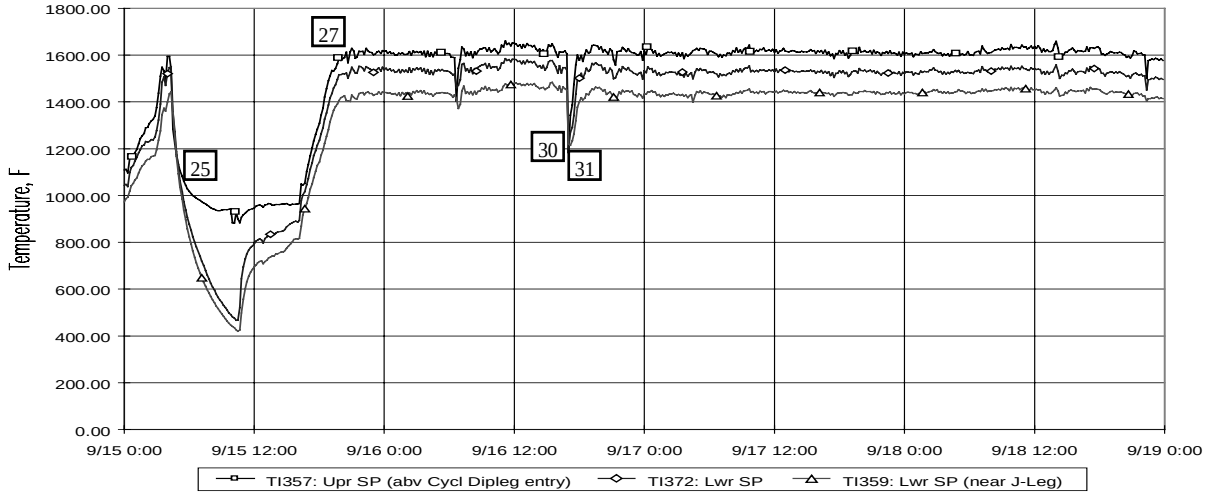

Figure 4.1.4.2-56 Standpipe Temperatures

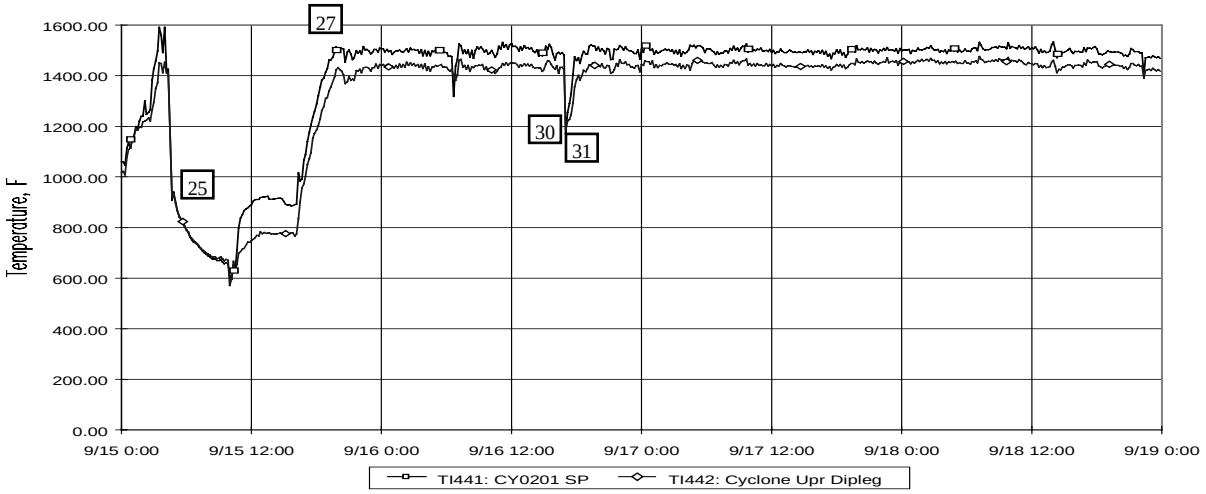

Figure 4.1.4.2-57 Cyclone Dipleg Temperatures

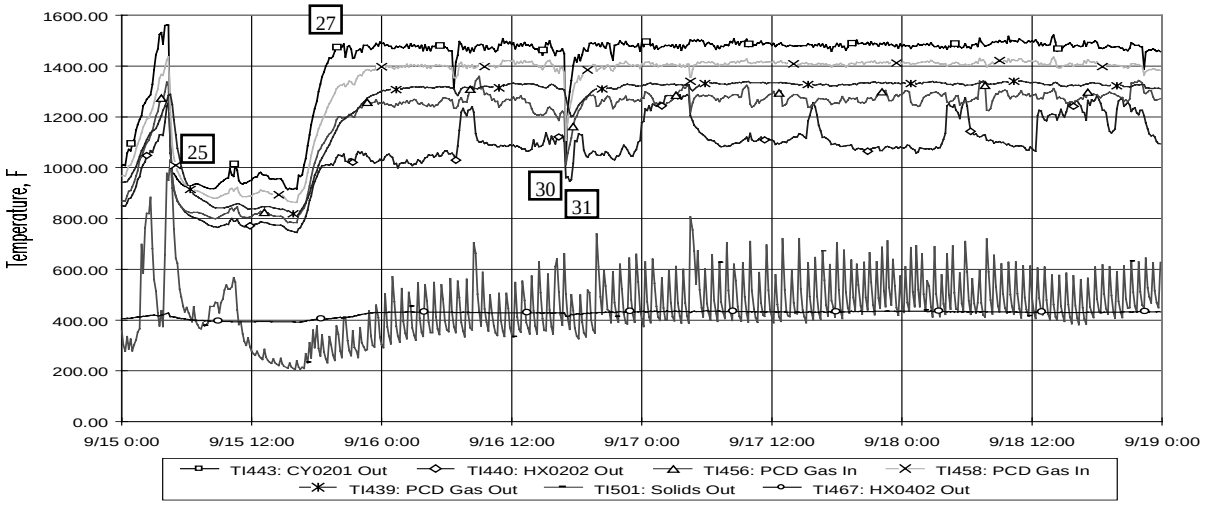

Figure 4.1.4.2-58 Temperature Profiles Downstream of Reactor

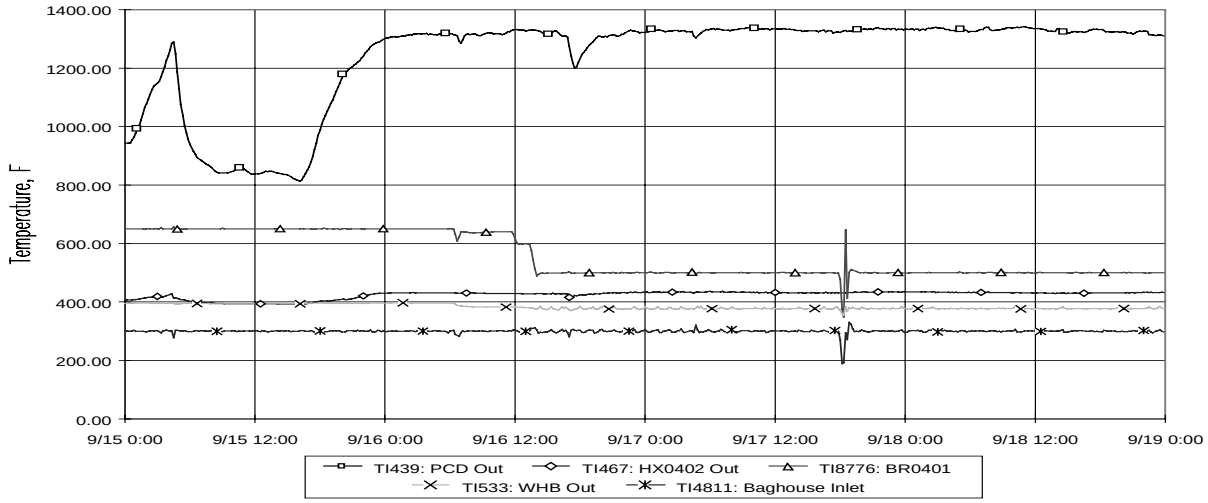

Figure 4.1.4.2-59 System Temperatures Downstream of PCD

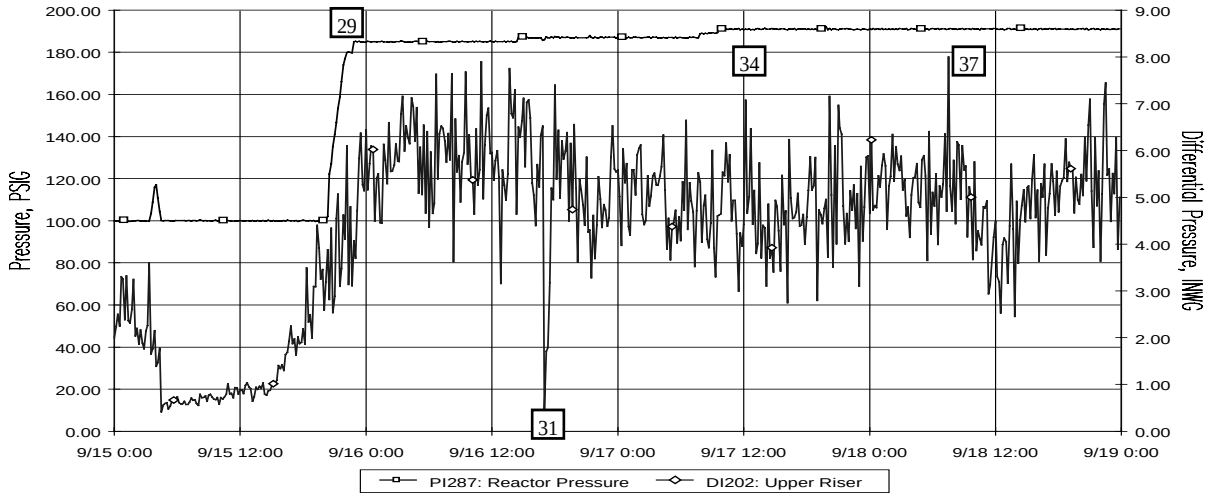

Figure 4.1.4.2-60 Reactor Pressure/Riser Differential Pressure Profiles

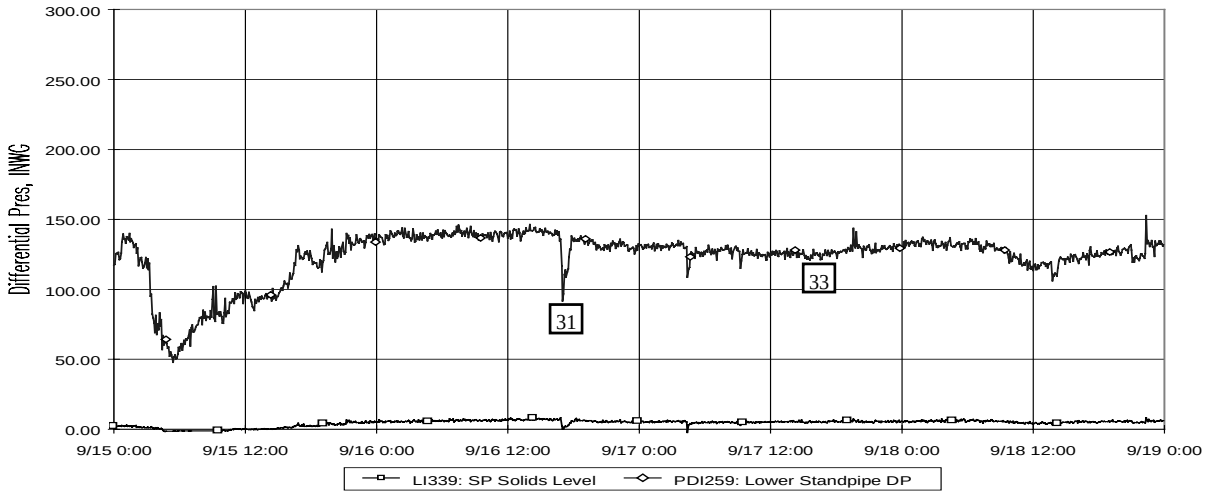

Figure 4.1.4.2-61 Standpipe Differential Pressure Profiles

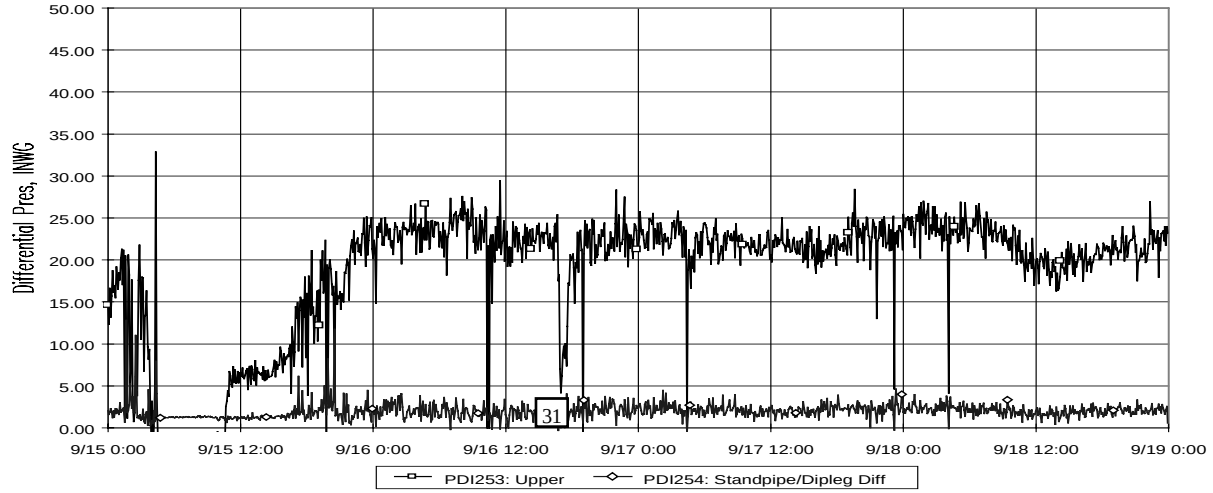

Figure 4.1.4.2-62 CY0201 Dipleg Differential Pressure Profiles

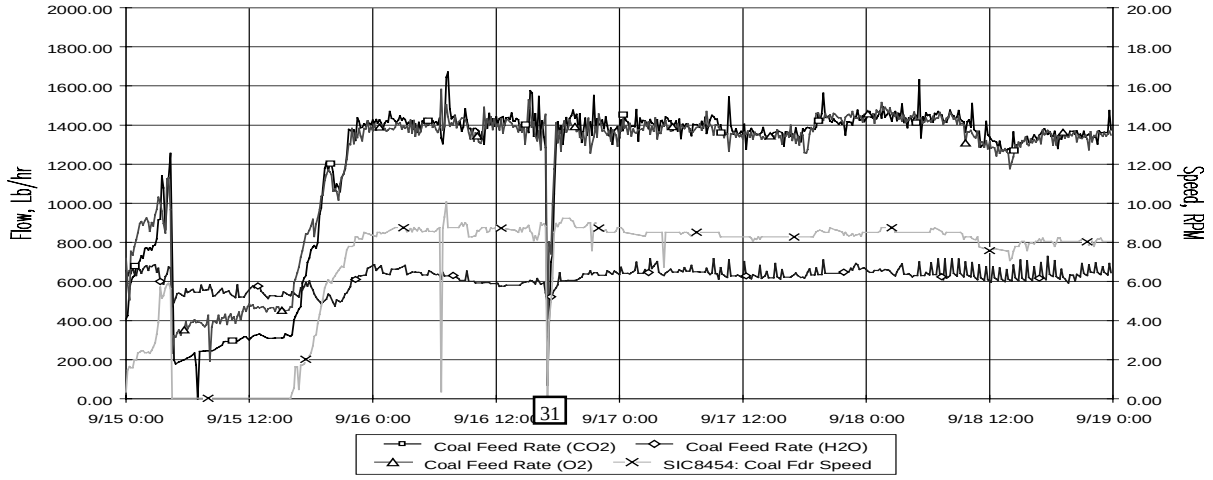

Figure 4.1.4.2-63 Coal Feed Rate Based on Gas Analysis

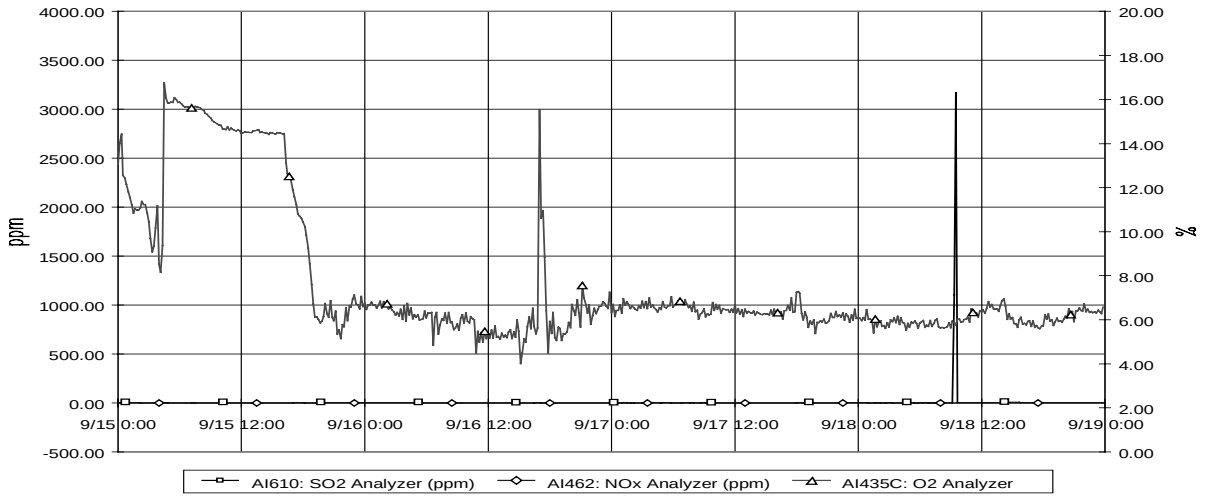

Figure 4.1.4.2-64 O_2, SO_2, and NO_x Analyzers

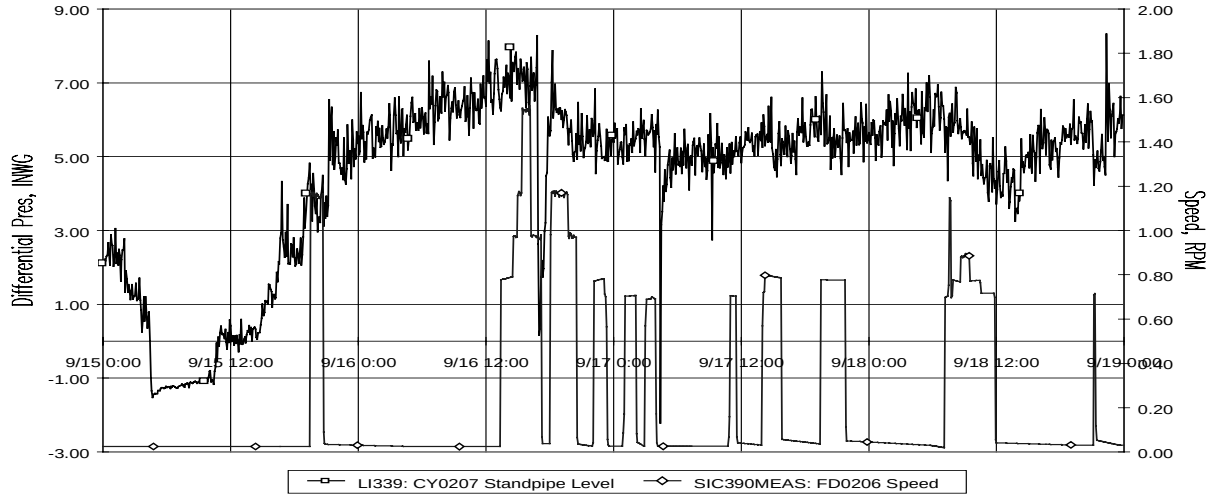

Figure 4.1.4.2-65 Solids Withdrawal

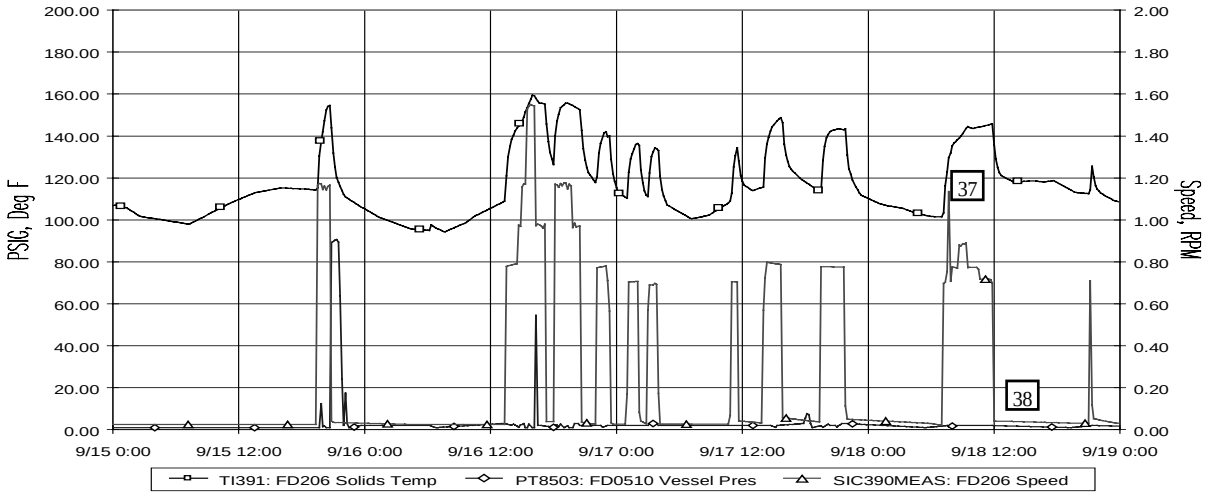

Figure 4.1.4.2-66 FD0206 Profiles

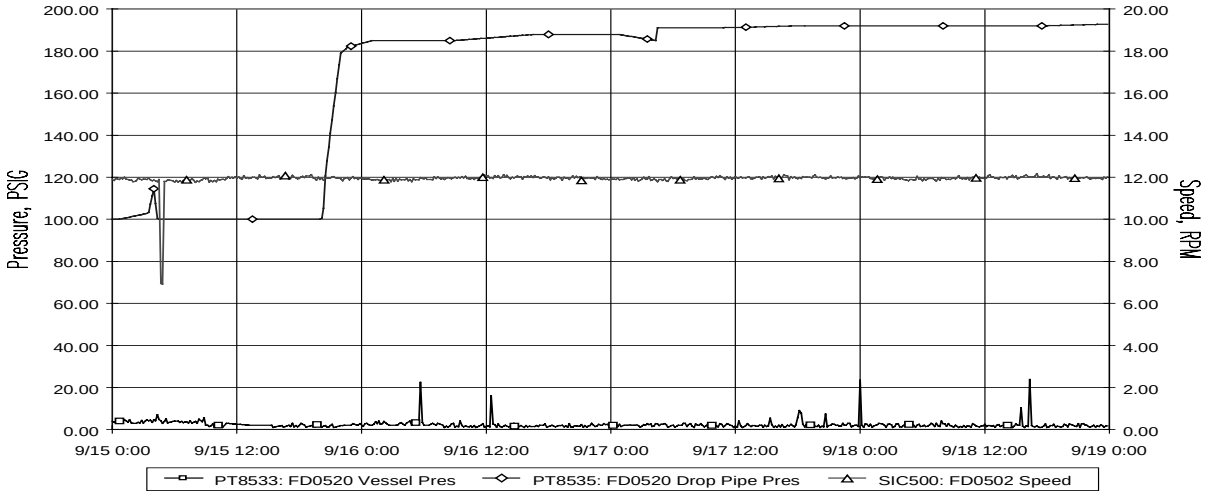

Figure 4.1.4.2-67 FD0520 Pressure Profiles

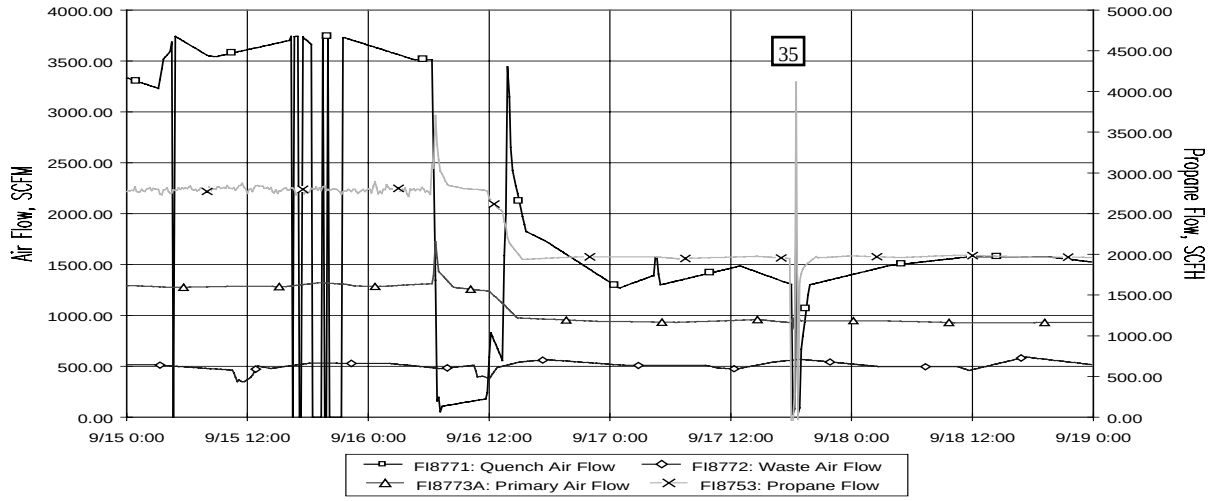

Figure 4.1.4.2-68 Thermal Oxidizer Air/Fuel Flow

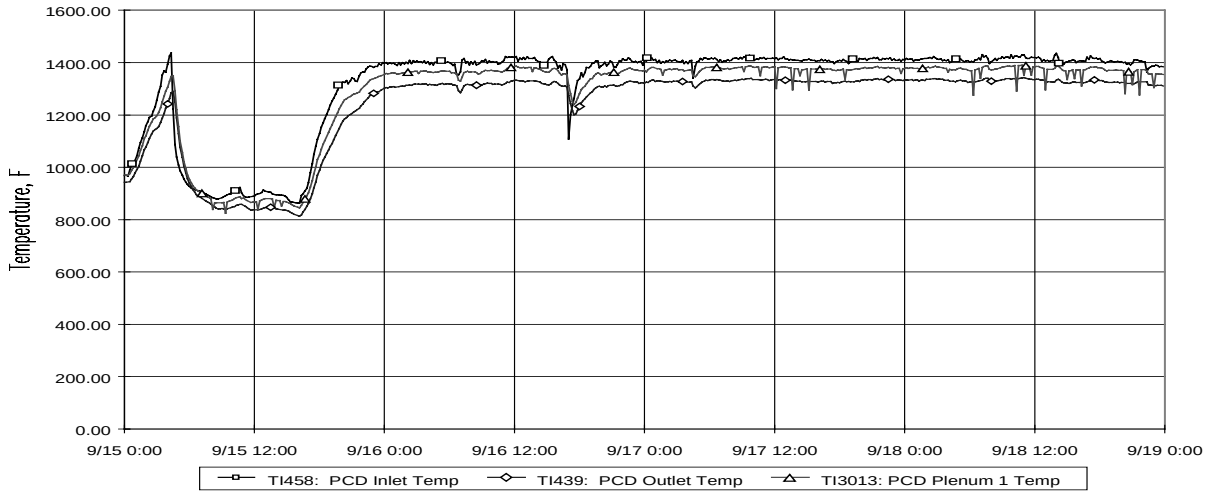

Figure 4.1.4.2-69 PCD Temperatures

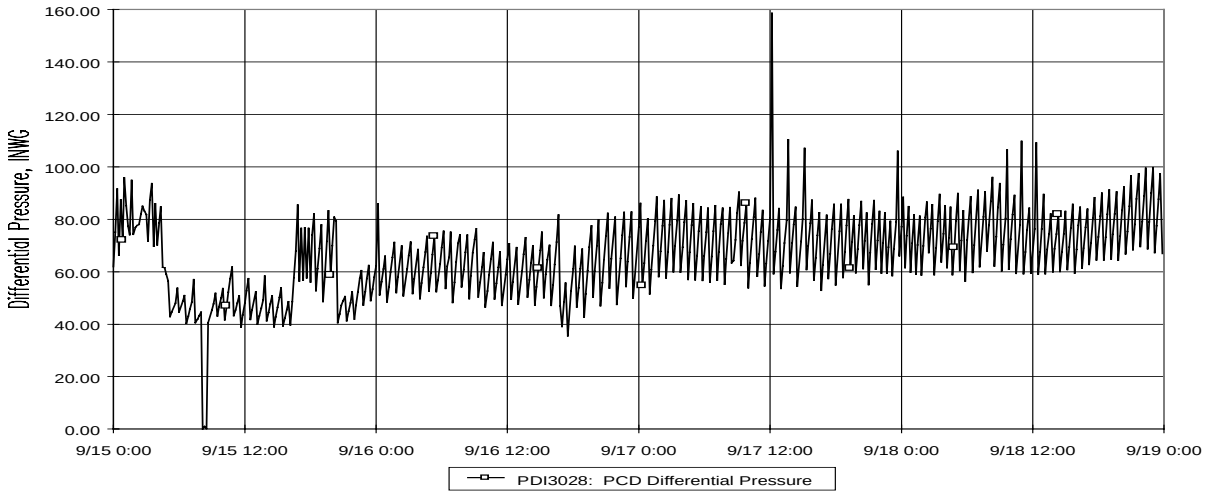

Figure 4.1.4.2-70 PCD Differential Pressure Profile

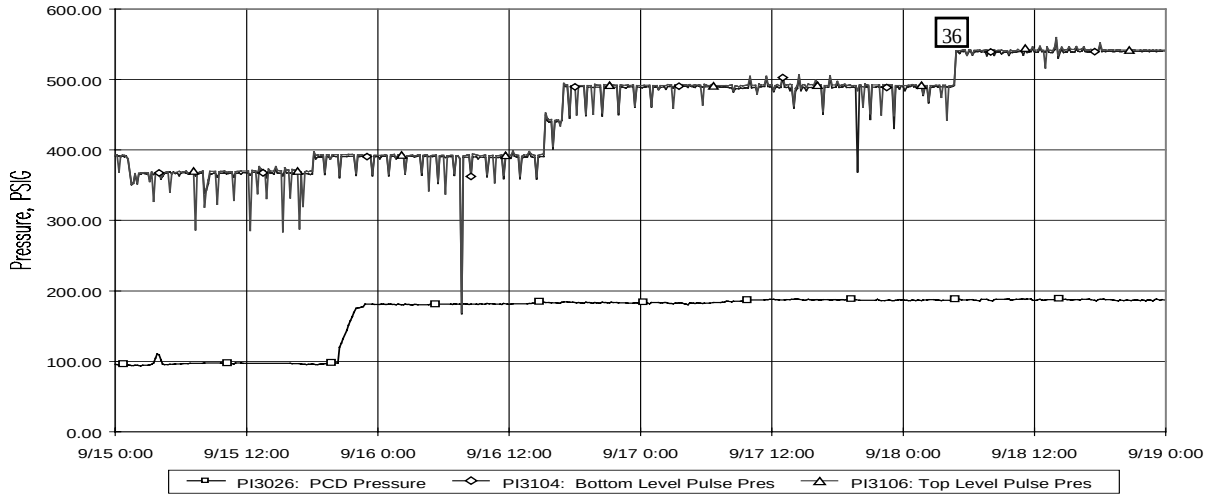

Figure 4.1.4.2-71 PCD Pressure and Pulse Pressure

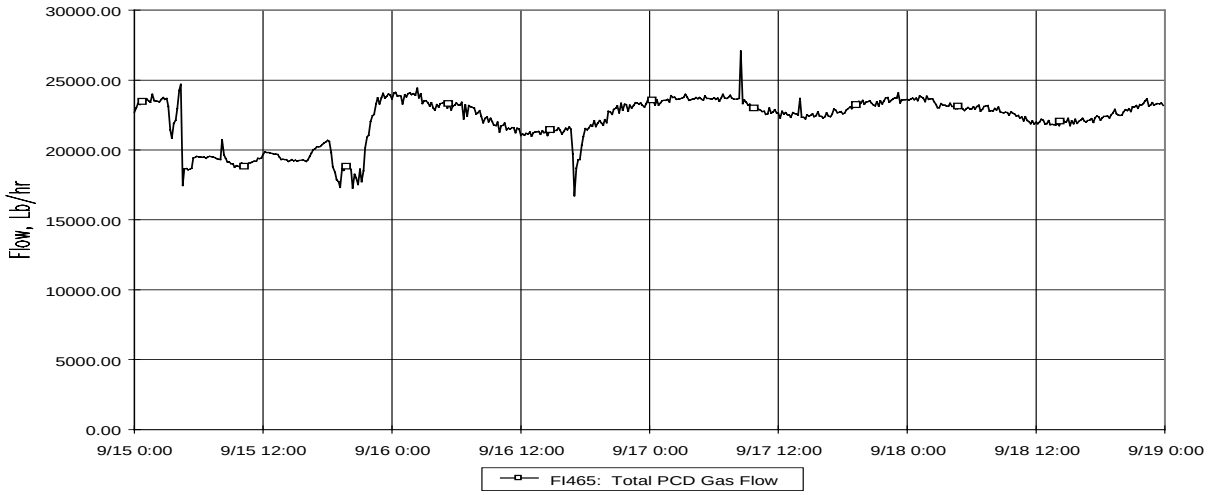

Figure 4.1.4.2-72 Gas Flow Through PCD

Section 4.1.4.2

Graphs 73 through 96

Test Run TC01B
September 19 through September 22, 1997

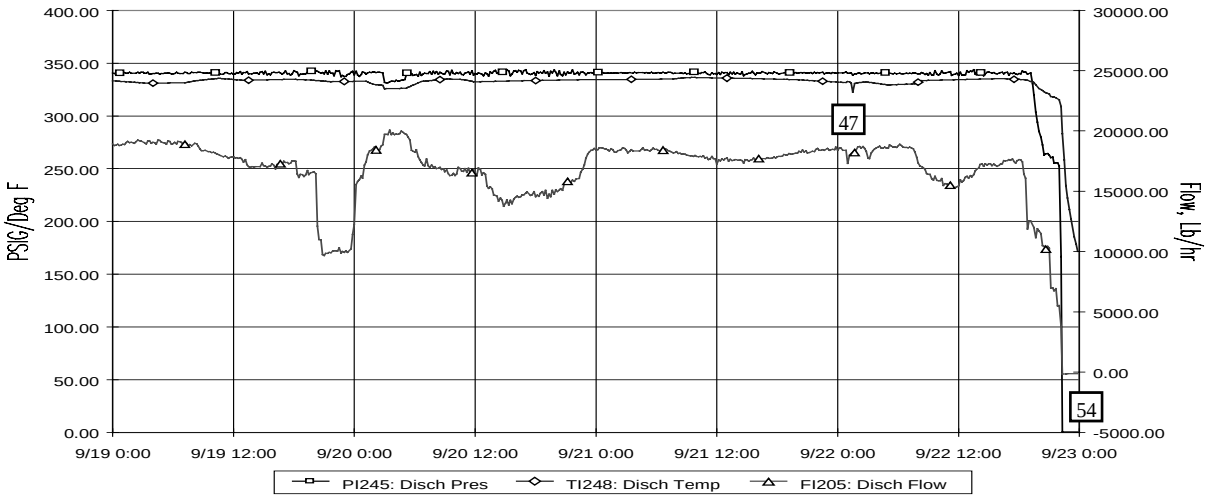

Figure 4.1.4.2-73 CO0201 System Profile

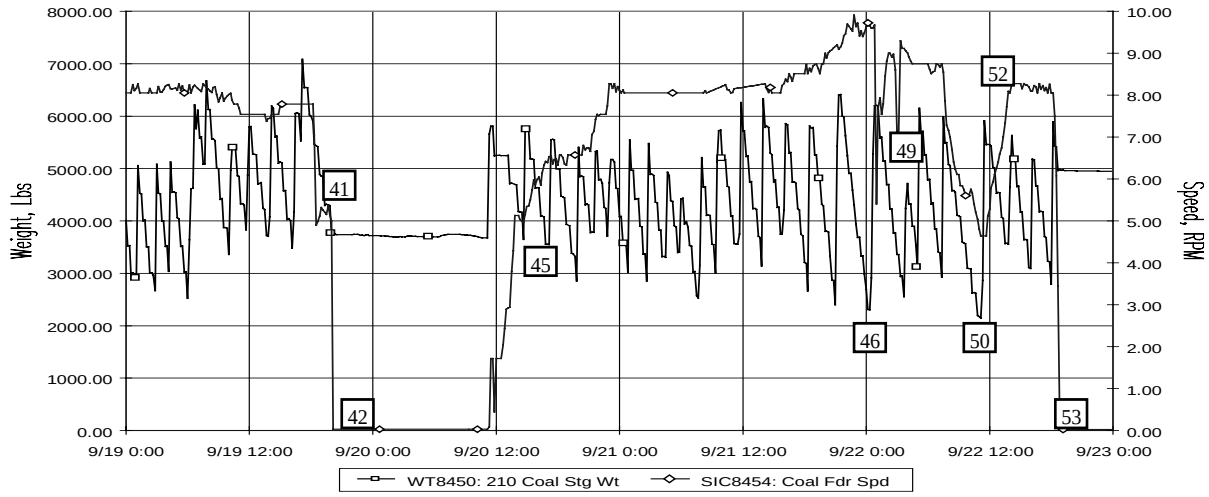

Figure 4.1.4.2-74 Coal Feed System Profile

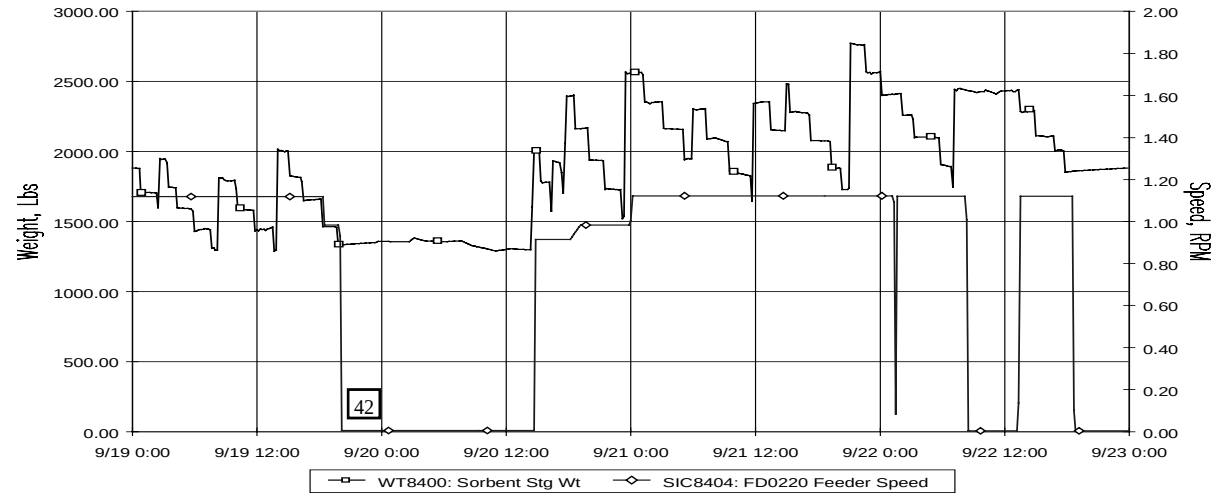

Figure 4.1.4.2-75 Sorbent Feed System Profile

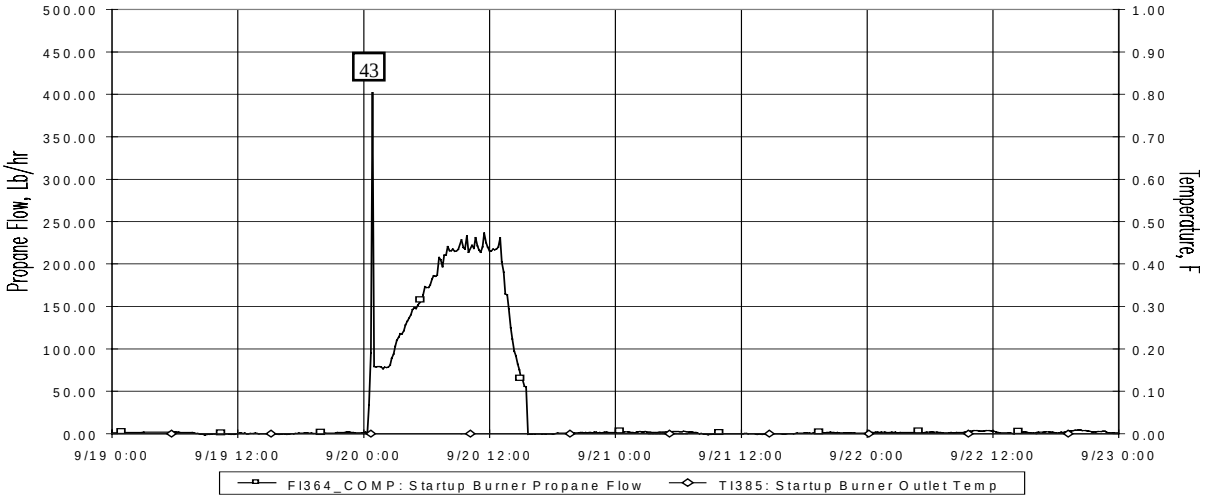

Figure 4.1.4.2-76 Start-Up Burner Flow/Temperature

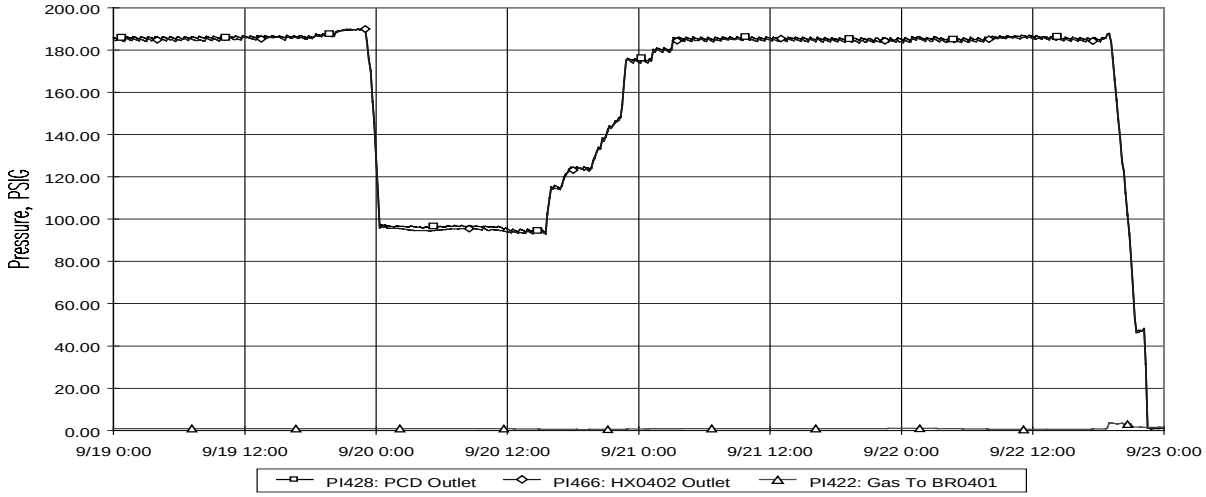

Figure 4.1.4.2-77 System Pressures Downstream of PCD

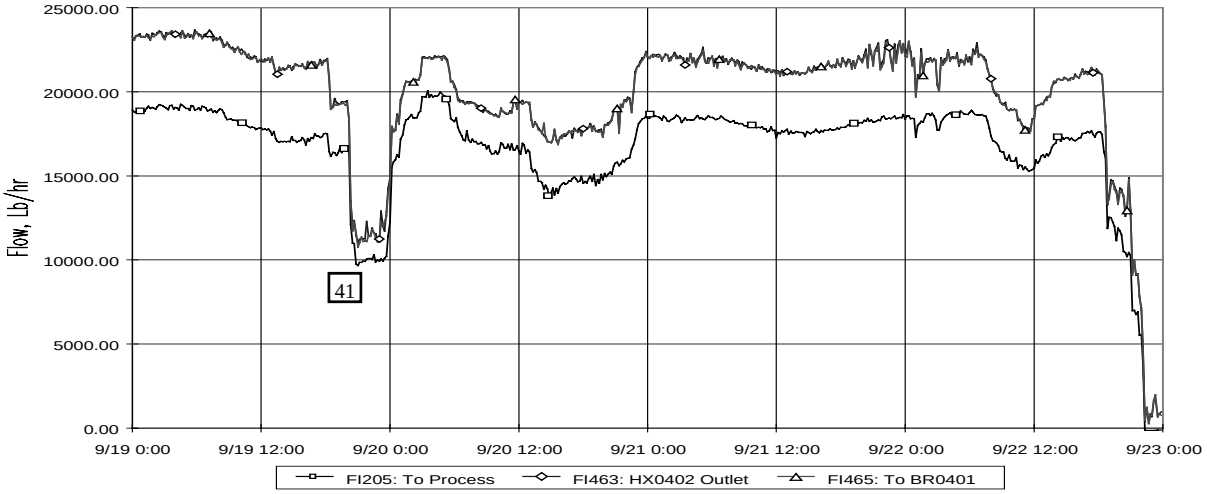

Figure 4.1.4.2-78 Total Gas In/Out Flow Rates

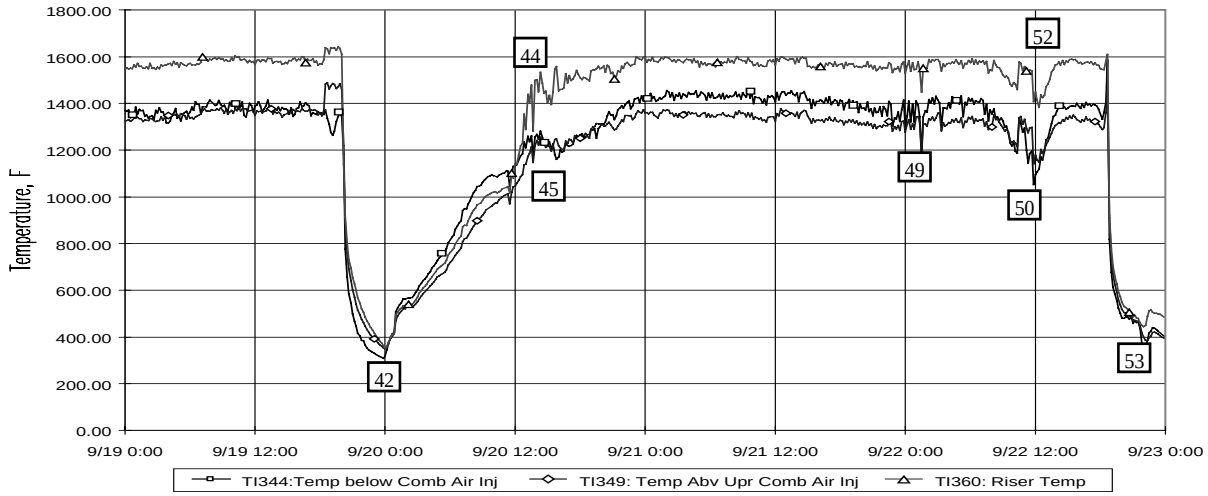

Figure 4.1.4.2-79 Reactor Mixing Zone and Riser Temperatures

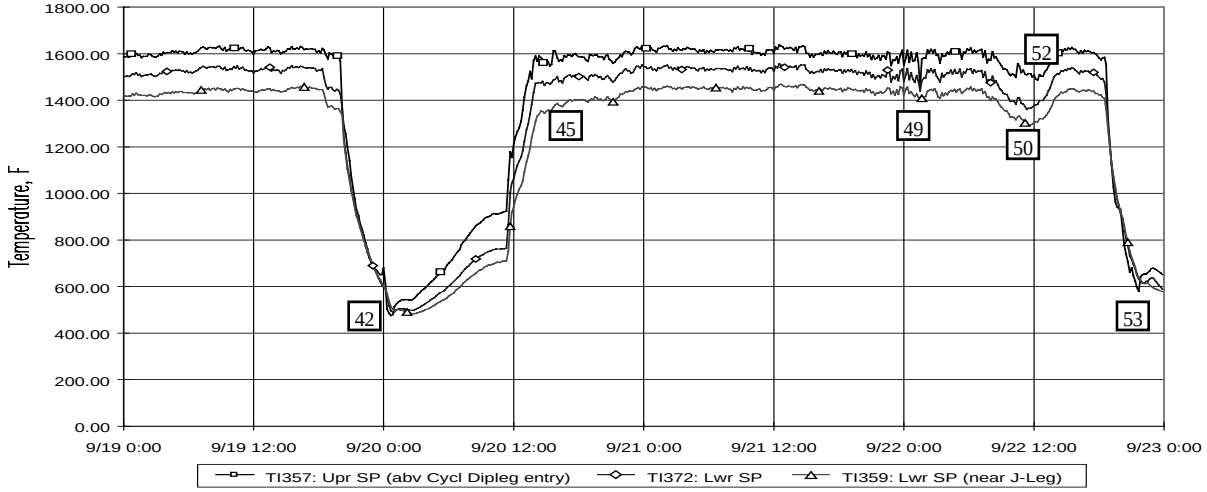

Figure 4.1.4.2-80 Standpipe Temperatures

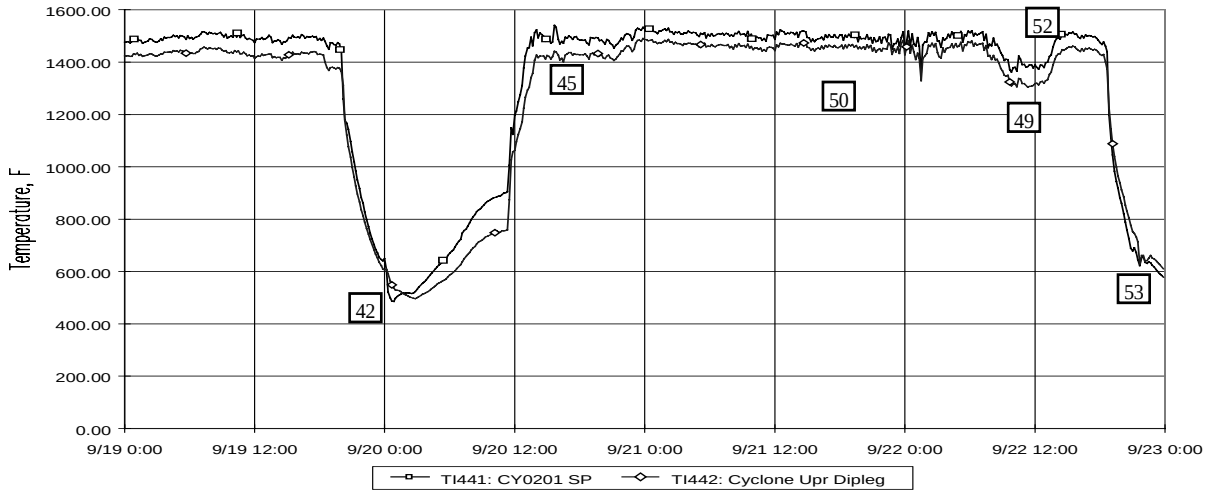

Figure 4.1.4.2-81 Cyclone Dipleg Temperatures

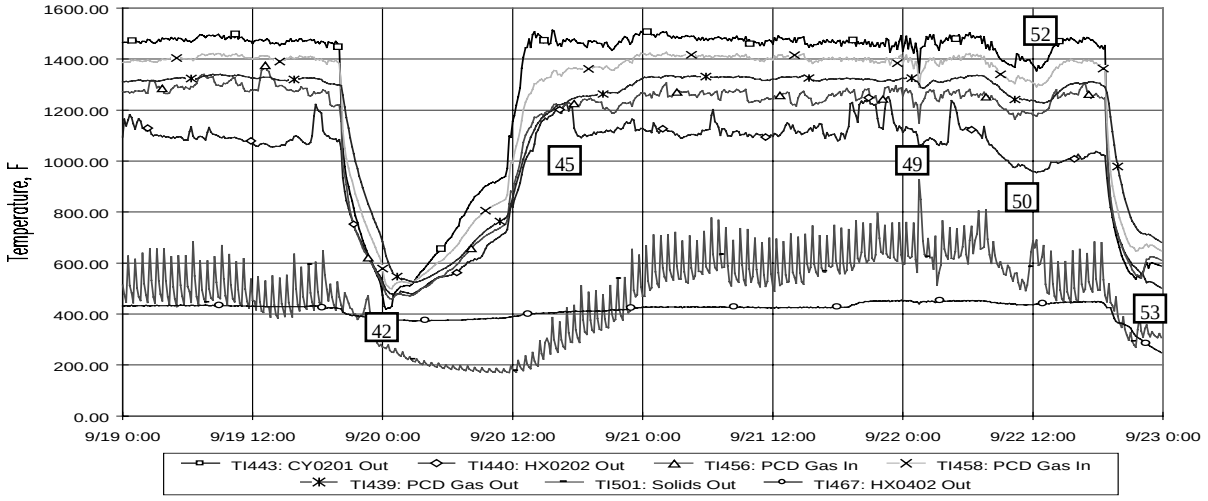

Figure 4.1.4.2-82 Temperature Profiles Downstream of Reactor

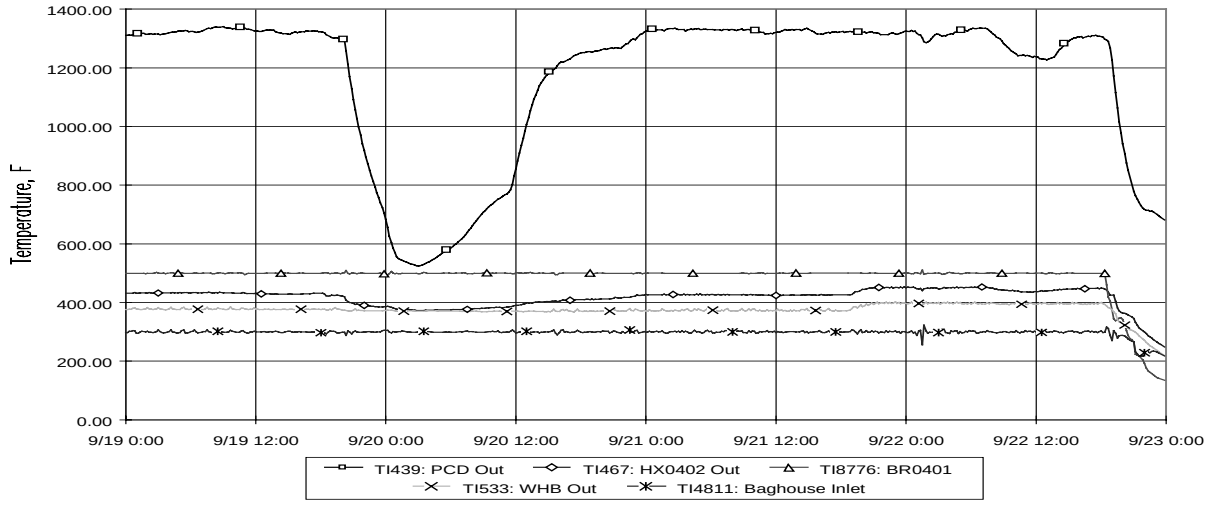

Figure 4.1.4.2-83 System Temperatures Downstream of PCD

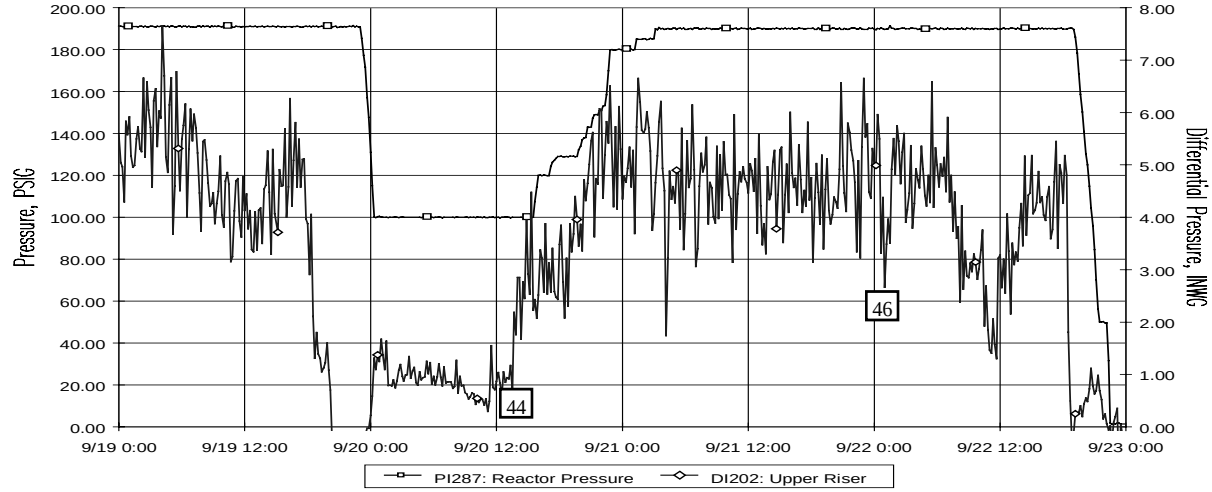

Figure 4.1.4.2-84 Reactor Pressure/Riser Differential Pressure Profiles

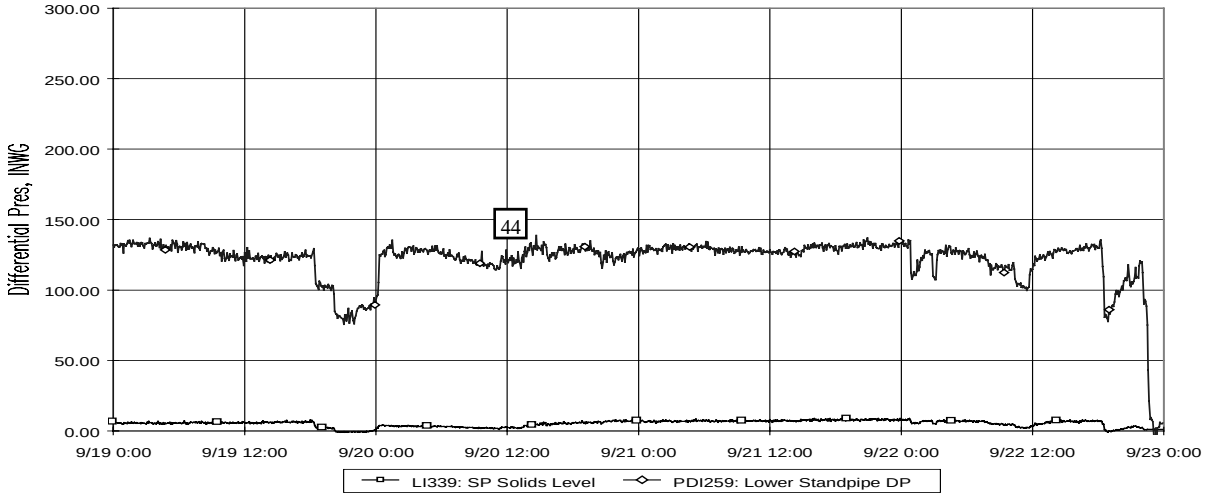

Figure 4.1.4.2-85 Standpipe Differential Pressure Profiles

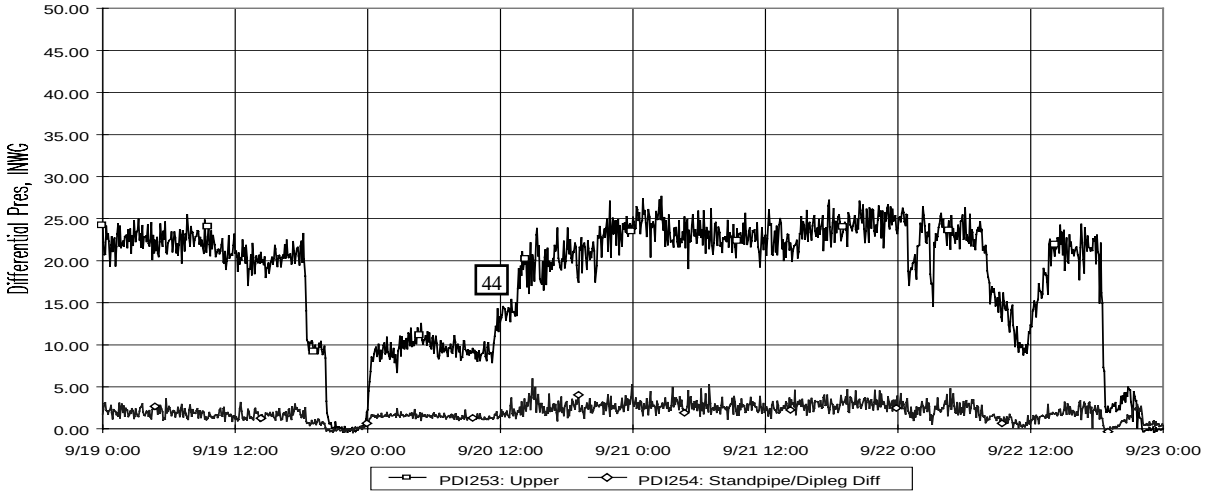

Figure 4.1.4.2-86 CY0201 Dipleg Differential Pressure Profiles

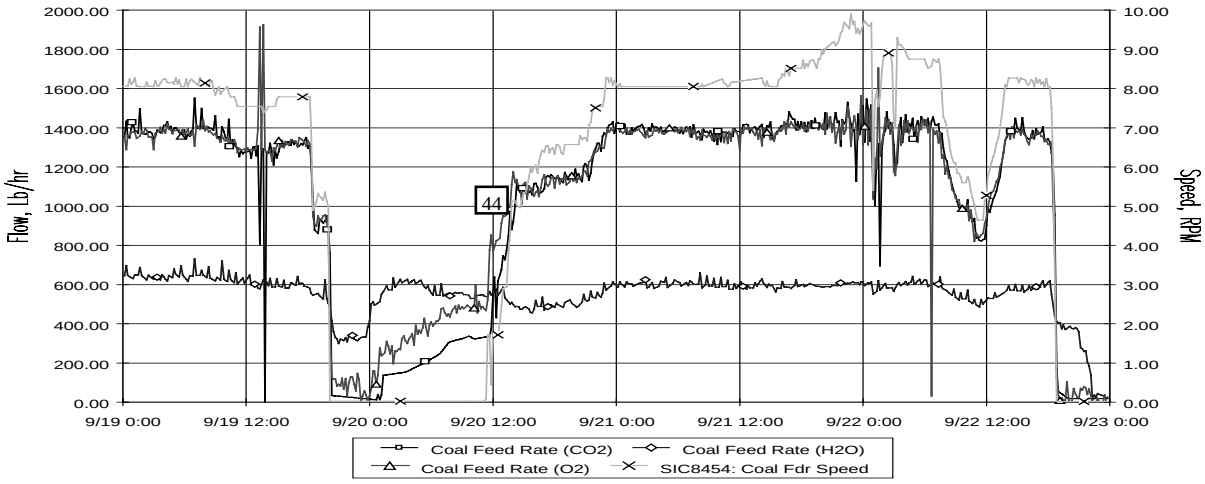

Figure 4.1.4.2-87 Coal Feed Rate Based on Gas Analysis

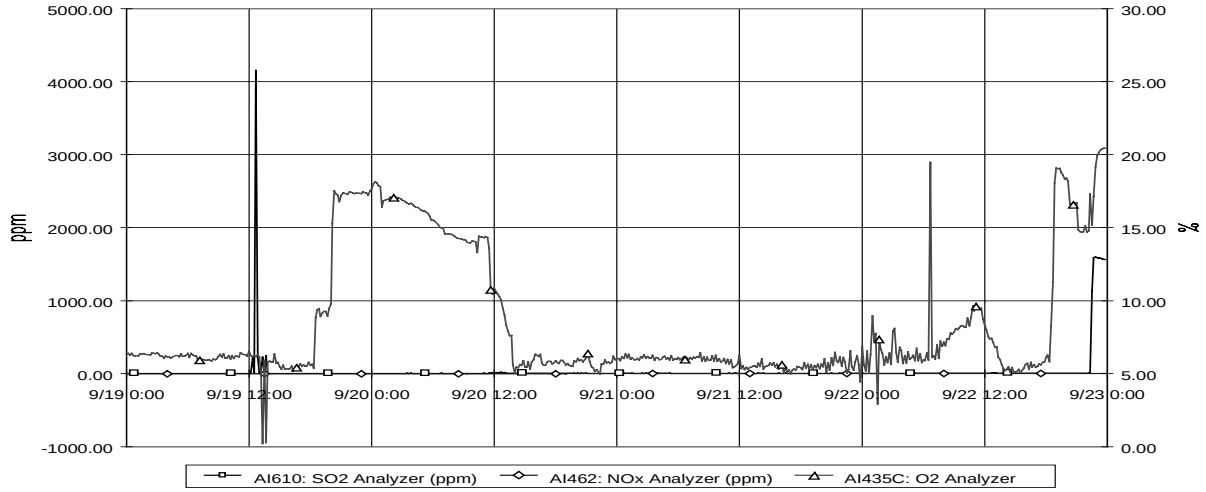

Figure 4.1.4.2-88 O_2, SO_2, and NO_x Analyzers

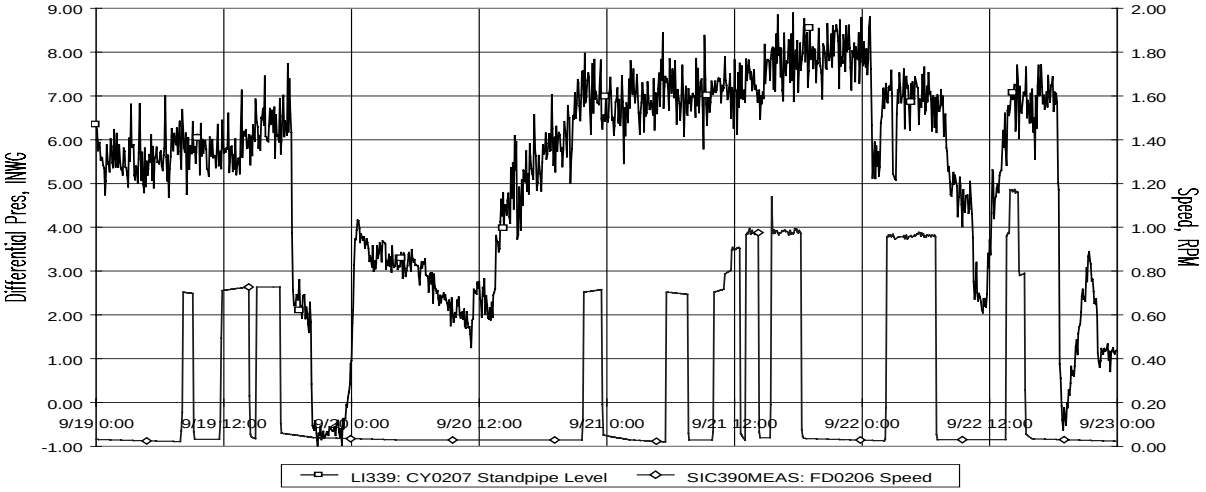

Figure 4.1.4.2-89 Solids Withdrawal

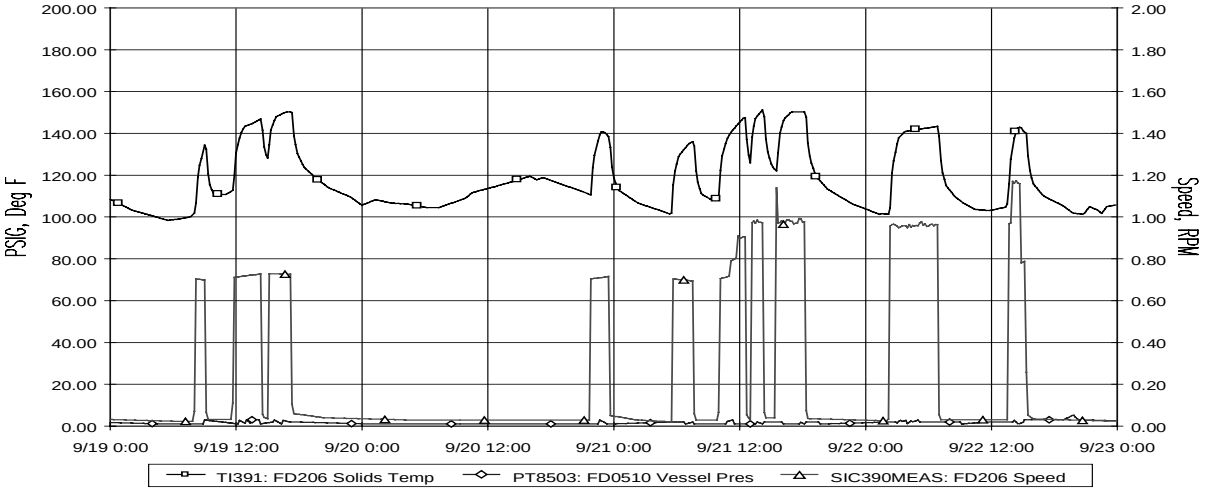

Figure 4.1.4.2-90 FD0206 Profiles

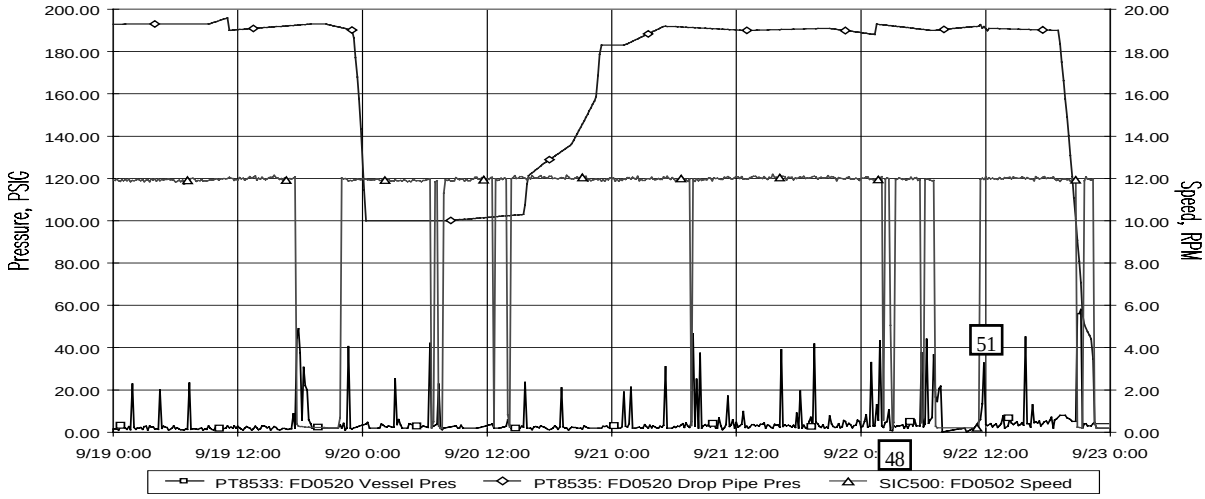

Figure 4.1.4.2-91 FD0520 Pressure Profiles

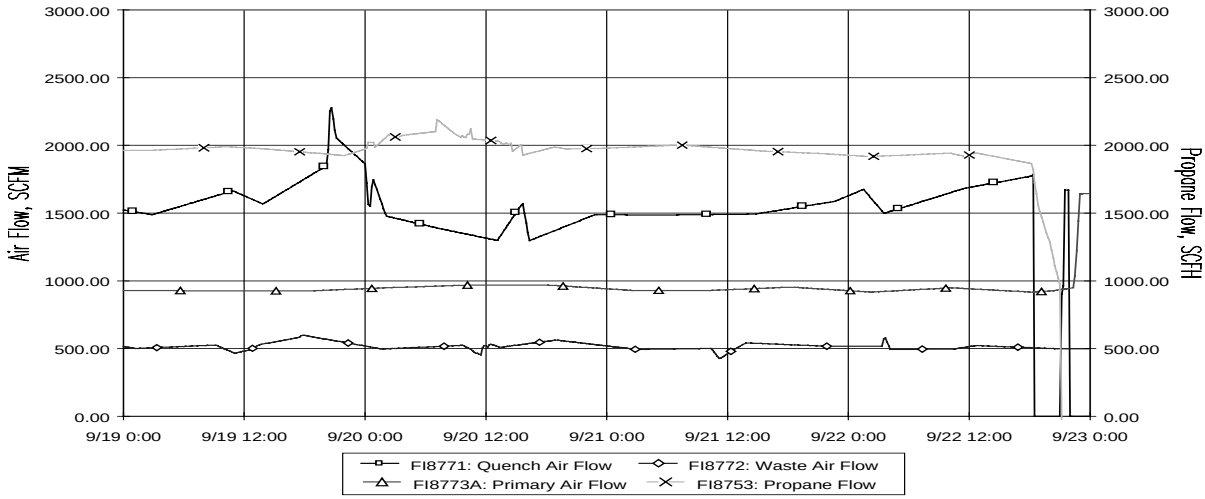

Figure 4.1.4.2-92 Thermal Oxidizer Air/Fuel Flow

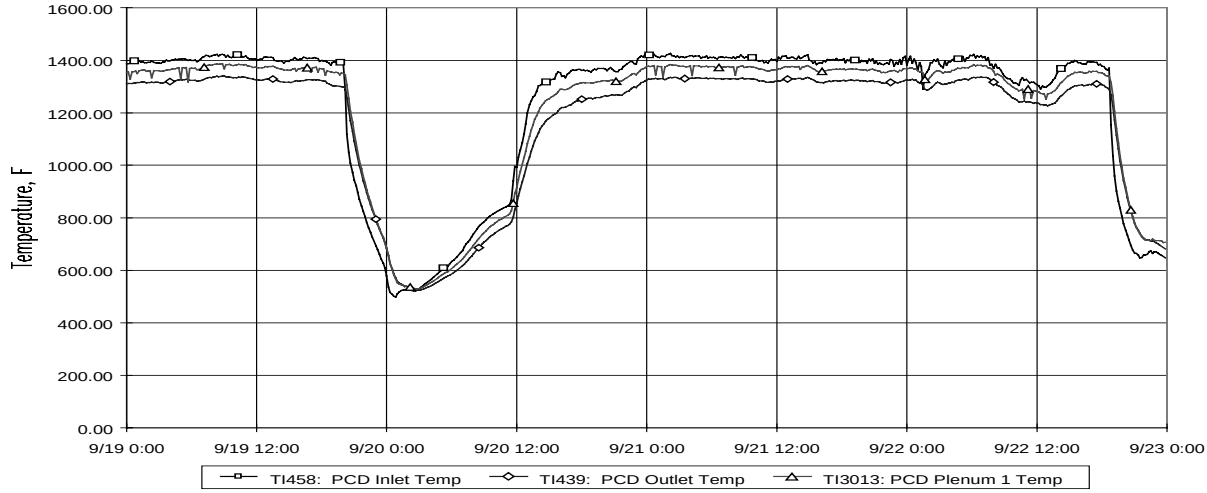

Figure 4.1.4.2-93 PCD Temperatures

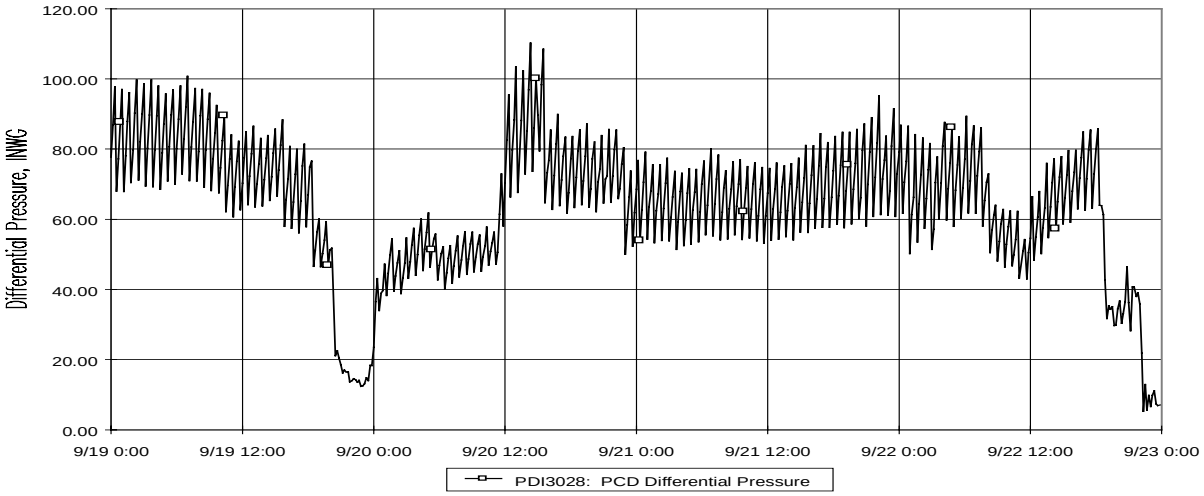

Figure 4.1.4.2-94 PCD Differential Pressure Profile

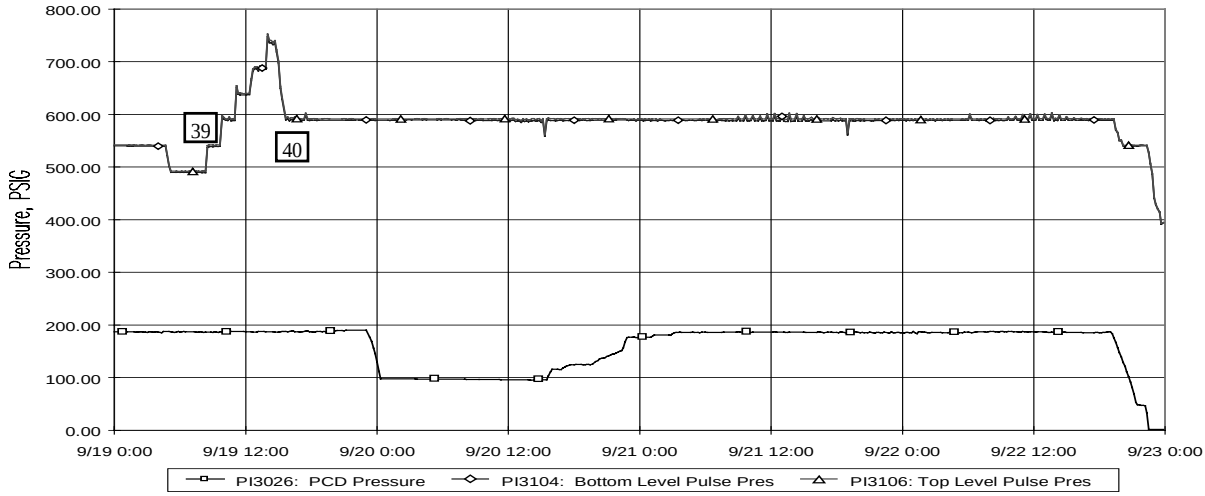

Figure 4.1.4.2-95 PCD Pressure and Pulse Pressure

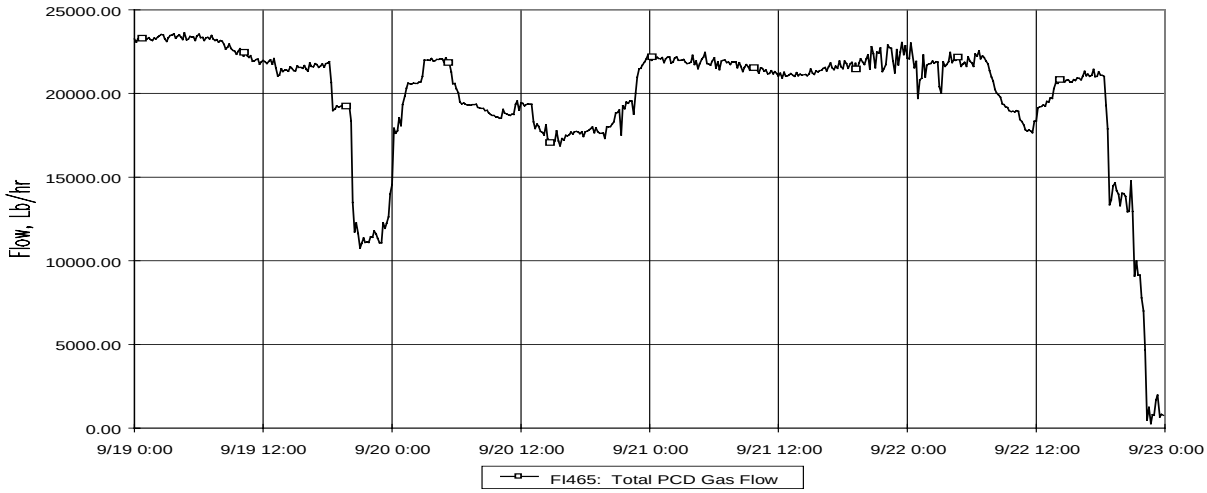

Figure 4.1.4.2-96 Gas Flow Through PCD

4.1.4.3 TC01C Test Run

Test run TC01C was conducted between September 23 and 28, 1997. Operating plots are shown in figures 4.1.4.3-1 through -46. During the outage preceding test run TC01C the following work was completed:

- The strainer on the circulating water line was cleaned.
- The PCD outlet acoustic detector probe was pulled and the nozzle blinded.
- The spent fines transport system (FD0520) exit valve seal was replaced.
- The fines screw cooler (FD0502) was repacked.

TC01C Test Run Chronology

- On September 23, 1997, the main air compressor (CO0201), the thermal oxidizer (BR0401), and the start-up burner (BR0201) were started (event 1, figure 1; event 2, figure 4). The blocking valves on the reactor were opened around 17:15 (event 3, figure 12) and at 20:15 the aeration on the reactor J-leg was increased. The reactor pressure was increased and by 20:35 it was 100 psig (event 4, figure 13).

- On September 24, 1997, coal feed was started at 00:55 (event 5, figures 2 and 7 through 10). The combustion heat exchanger (HX0203) circulation was increased to control the reactor temperatures, and consequently, the temperature ramp in the PCD. At 05:55 the burner firing was decreased and coal feed was increased (event 6, figures 2 and 4). As coal feed was increased the HX0203 circulation was further increased to control reactor temperatures. Dolomite feed was started at 09:45 (event 7, figure 3). The BR0201 was shut down at 11:50 (event 8, figure 4) and by 12:10 the PCD plenum temperature was above 1,350°F (event 9, figure 20). At 12:40 the reactor pressure was increased at 1 to 2 psig/minute (event 10, figure 13) and the aeration was set to maintain the desired circulation rate.

- Around 15:00 the pressure letdown valve (PV287) plug stem began to vibrate at high frequency. The stem vibrations were suspected to be due to flow-induced resonance. The pressure was decreased and then increased (event 11, figure 13) rapidly to stop the vibration and noise. The sudden movement of the actuator stopped the stem vibrations. At 16:20 a PCD back-pulse upset the cyclone dipleg for about 30 seconds. When the PCD was manually back-pulsed around 18:45 the first back-pulse did not have much effect on the dipleg but the second caused an upset for about 15 seconds. The vent valve on FD0520 lock vessel started leaking at about 22:40. An hour later the reactor pressure was increased to 200 psig to further stabilize the reactor operations (event 12, figure 13).

- On September 25, 1997, at 01:10, the dolomite feed rate was increased to achieve a Ca/S ratio of about 2.0 (event 13, figure 3). The FD0206 was started around 02:10 and the

speed was increased during the next 2 hours to control the solids level in the reactor and HX0203. The solids level was lost for a few seconds when the PCD back-pulsed at 02:15. At about 04:05 the FD0510 system exit plugged. The exit was unplugged and the system was put back on-line. At 08:30 FD0220 was shut down (event 14, figure 3). CO0201 tripped momentarily at 10:00 (event 15, figures 1, 2, and 6 through 10). The FD0220 system was restarted around 11:50 (event 16, figure 3). Small pieces of refractory plugged FD0510 system again causing it to be shut down at 12:31 for cleaning.

- At 14:30 the HX0203 riser line started vibrating due to hammering, so the steam drum pressure was increased by 50 psig, which didn't seem to make any difference. As in previous test runs the two riser lines from the secondary gas cooler (HX0402) continued to vibrate due to hammering around bends. Around 17:30 the SO_2 analyzer reading jumped from 4 to over 1,000 ppm due to an analyzer malfunction (event 17, figure 17).

- On September 26, 1997, the FD0510 and FD0206 systems were operated intermittently to keep solid levels within the desired limits in the reactor and HX0203. At 07:00 the PV287 stem started shaking again so the reactor pressure was reduced. By 07:15 there was no control of PV287, resulting in a rapid rise in the reactor pressure (event 18, figure 36). The CO0201 discharge pressure was reduced to slow down the rise in reactor pressure. The FD0502 tripped at about 07:20 (event 19, figure 42) due to high-PCD-exit temperature. The PV287 settled around 07:30 but started rattling again after 30 minutes. Coal feed was stopped at 09:15 (event 20, figures 25 and 30 through 33) and circulation as well as reactor pressure were reduced. A leak was detected in the FD0210 system, so the process and CO0201 were shut down at 11:00 (event 21, figure 24).

- During the brief shutdown the FD0520 dispense vessel spheri valve seal was changed. The Jonas acoustic probe on the PCD inlet was pulled and a blind flange was installed. The CO0201 was restarted at 19:30 (event 22, figure 24). After a leak test BR0201 was lit at about 23:55 (event 23, figure 27) and the firing was increased.

- Aeration on the reactor J-leg was increased to raise temperatures in the lower standpipe and also to reduce the effect of burner gas flows impinging on solids from the J-leg. The coal feed was started around 10:20 on September 27, 1997 (event 24, figures 25 and 30 through 33). The dipleg was slugging; the dipleg aeration was adjusted to stabilize this. The BR0201 was shut down at 15:50 (event 25, figure 27) and the reactor pressure was gradually increased over the next several hours. The PCD temperature reached 1,350°F around 18:50; the PCD back-pulse pressure was increased to 550 psig at 18:55 (event 26, figure 45).

- On September 28, 1997, the FD0520 top and bottom spheri valve seals failed. Consequently, circulation and coal feed were reduced and process shutdown was initiated (event 27, figures 24, 25, 30 through 33, and 36).

TC01C Test Run Observations

A total of 70.2 hours on coal was achieved and a total of 43.6 tons of coal were fed. During TC01B the transition from propane fire to coal with a limit on the PCD temperature ramp rate could be achieved only by interrupting the coal feed. In this run the transition was achieved with continuous coal feed and by controlling the temperature ramp using HX0203 circulation and propane firing. The maximum PCD temperature ramp rate was below 250°F/hour. The main air compressor tripped a few times yet coal feed was restarted without any problems. There were some minor problems with plugging in the FD0206/FD0510 system. Pieces of refractory and fused char were found during clean out. The reactor operations were smooth and stable at 200 psig.

Section 4.1.4.3

Graphs 1 through 23

Test Run TC01C
September 23 through September 25, 1997

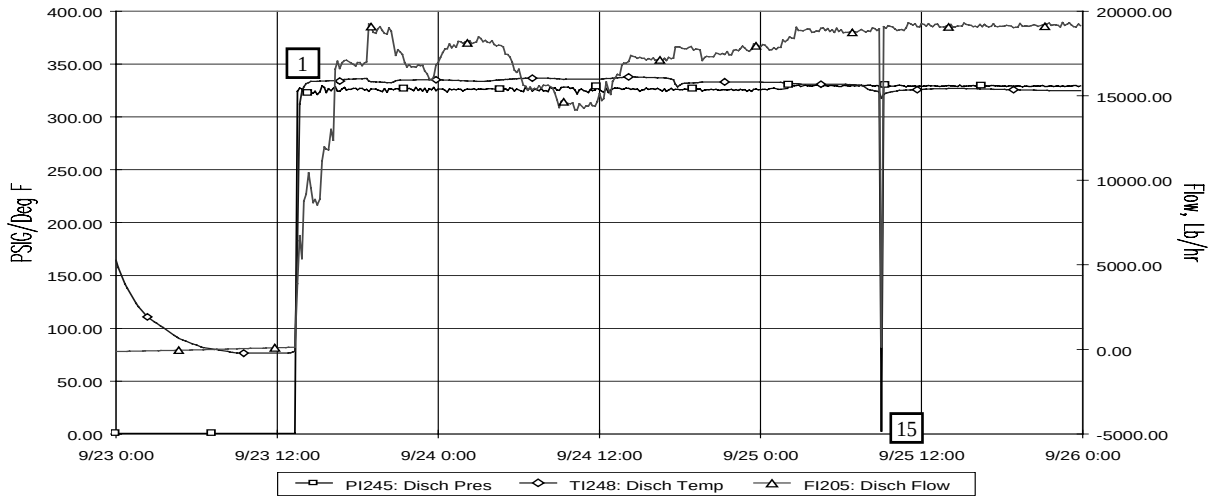

Figure 4.1.4.3-1 CO0201 System Profile

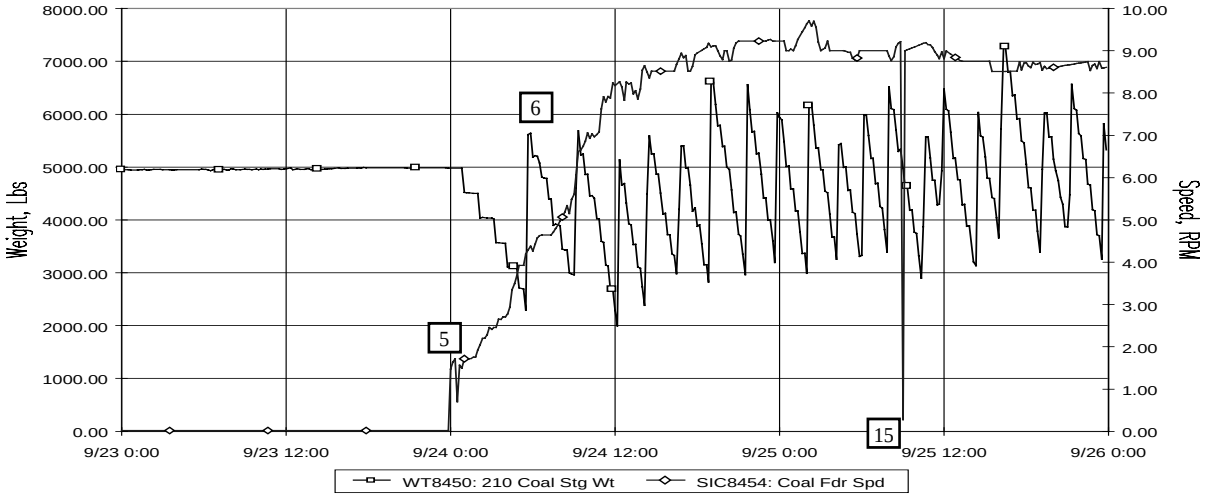

Figure 4.1.4.3-2 Coal Feed System Profile

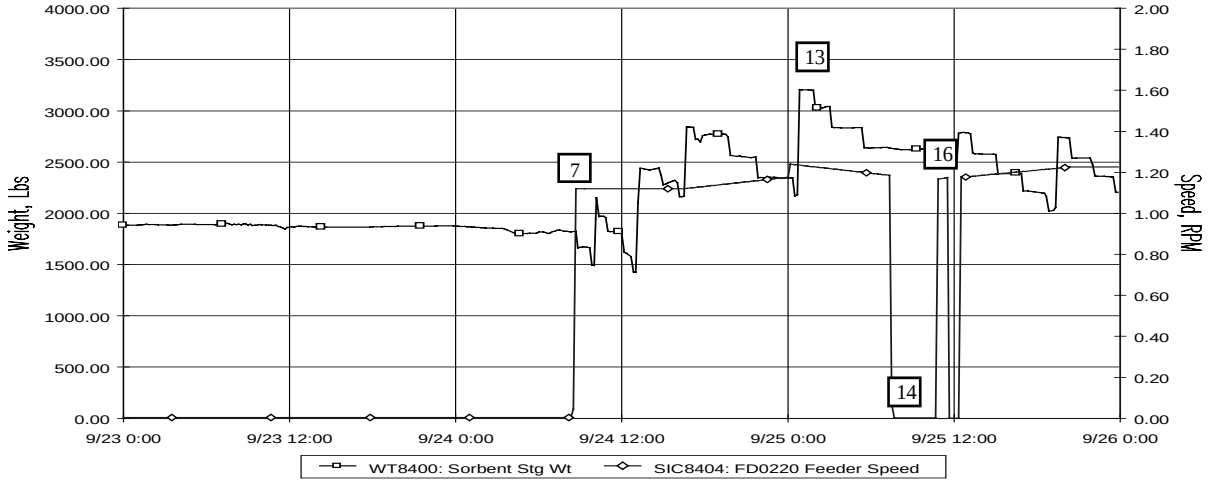

Figure 4.1.4.3-3 Sorbent Feed System Profile

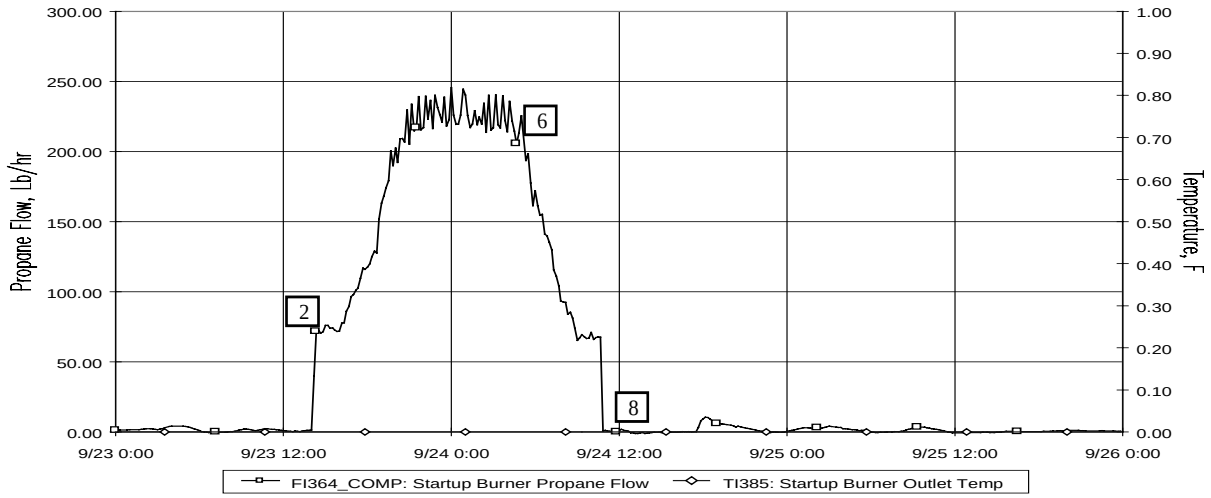

Figure 4.1.4.3-4 Start-Up Burner Flow/Temperature

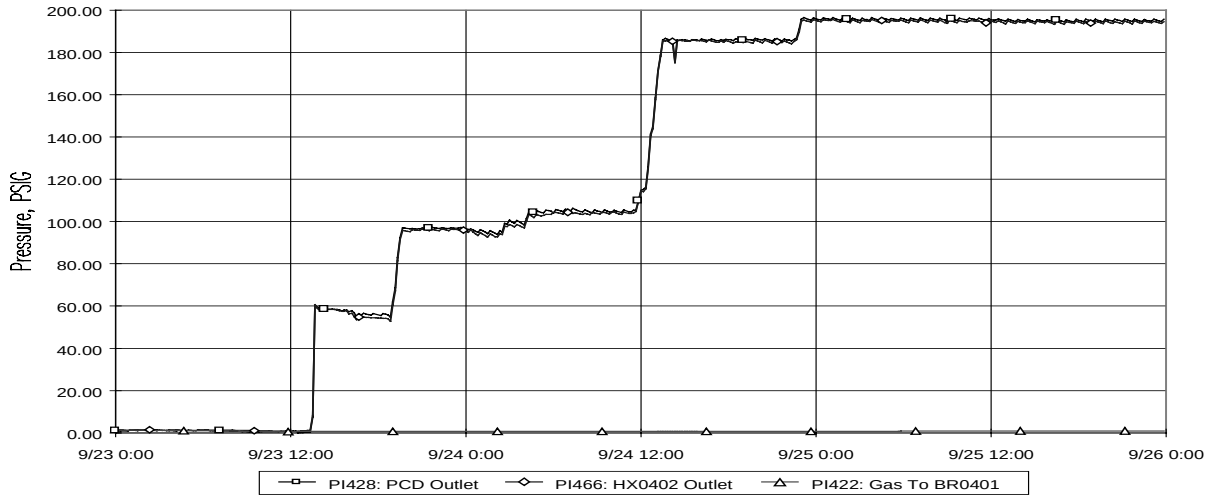

Figure 4.1.4.3-5 System Pressures Downstream of PCD

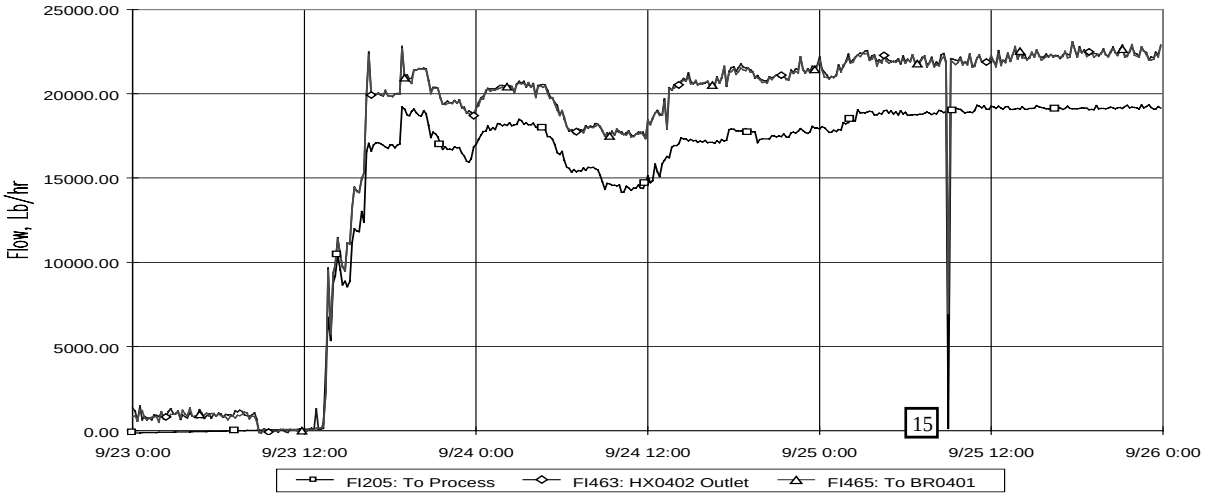

Figure 4.1.4.3-6 Total Gas In/Out Flow Rates

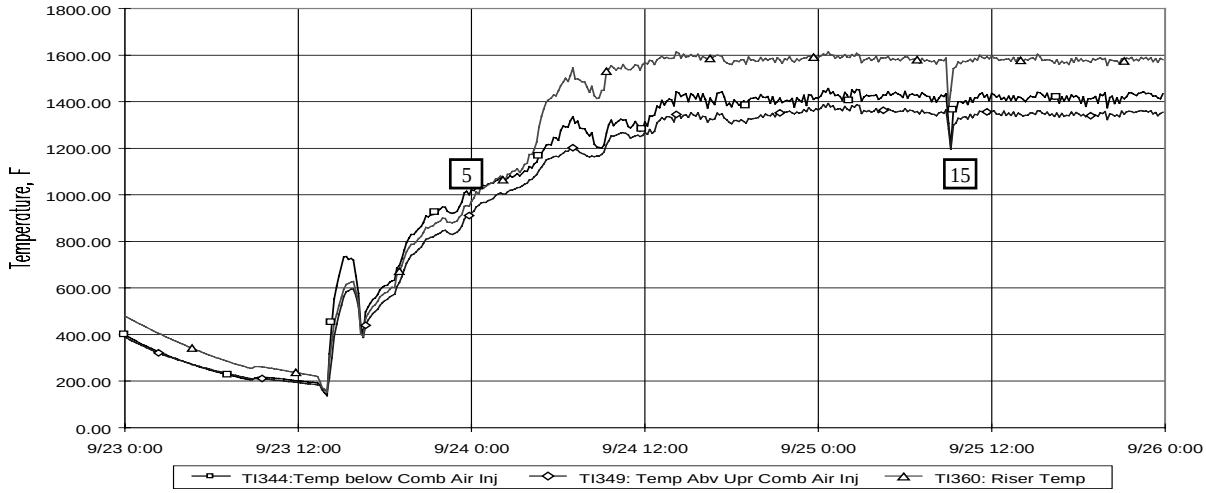

Figure 4.1.4.3-7 Reactor Mixing Zone and Riser Temperatures

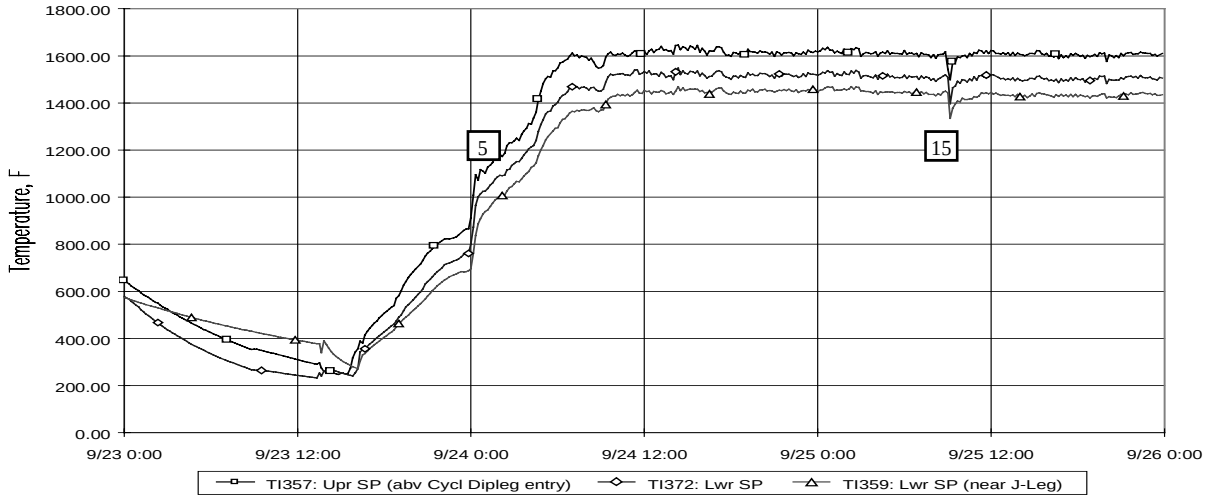

Figure 4.1.4.3-8 Standpipe Temperatures

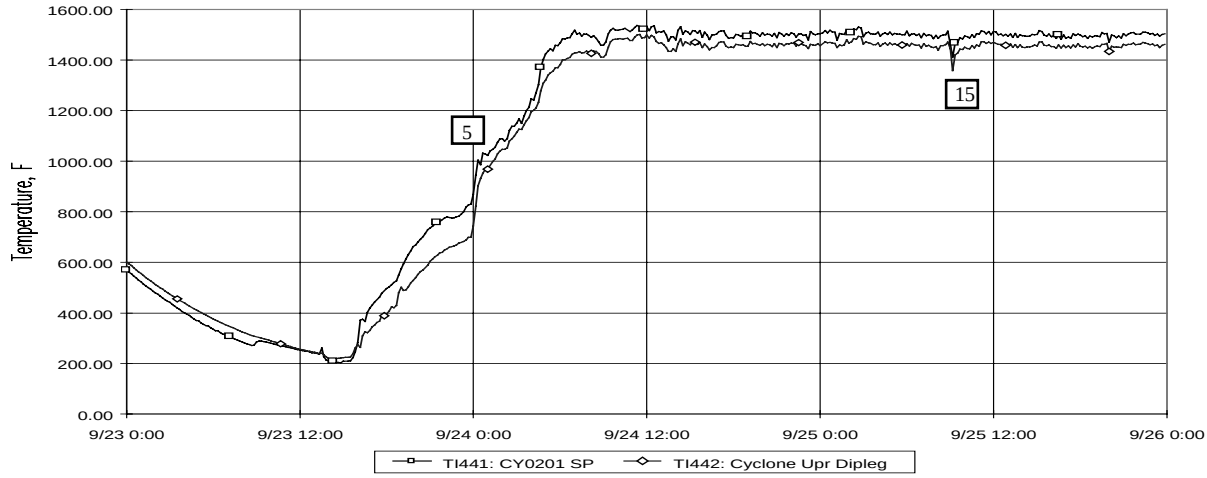

Figure 4.1.4.3-9 Cyclone Dipleg Temperatures

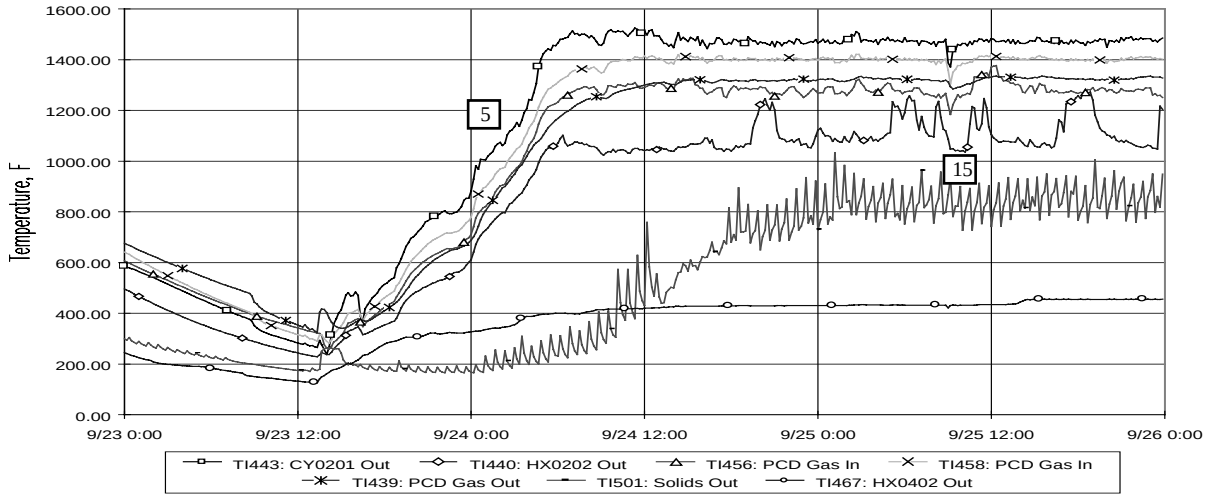

Figure 4.1.4.3-10 Temperature Profile Downstream of Reactor

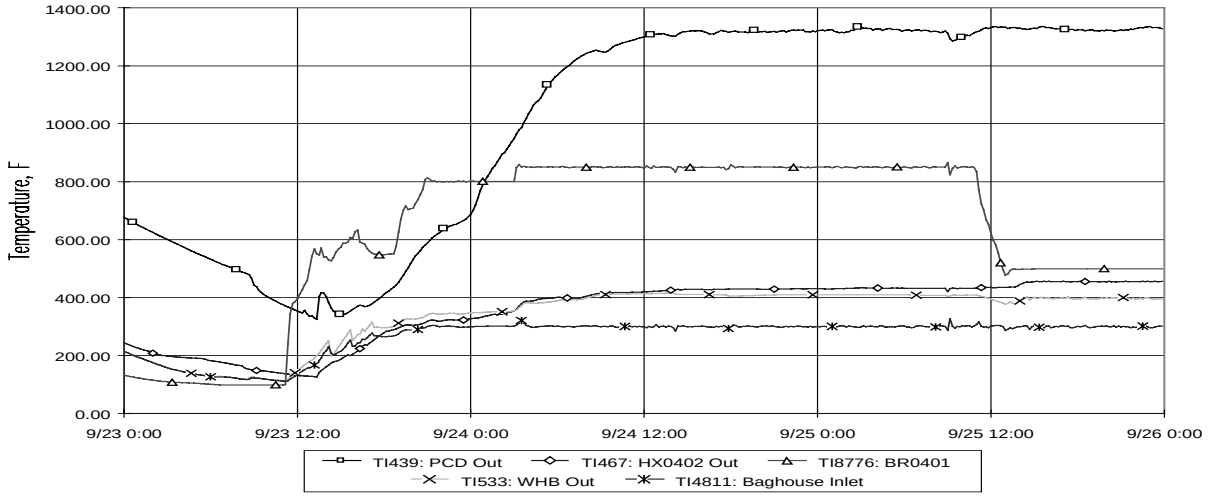

Figure 4.1.4.3-11 System Temperatures Downstream of PCD

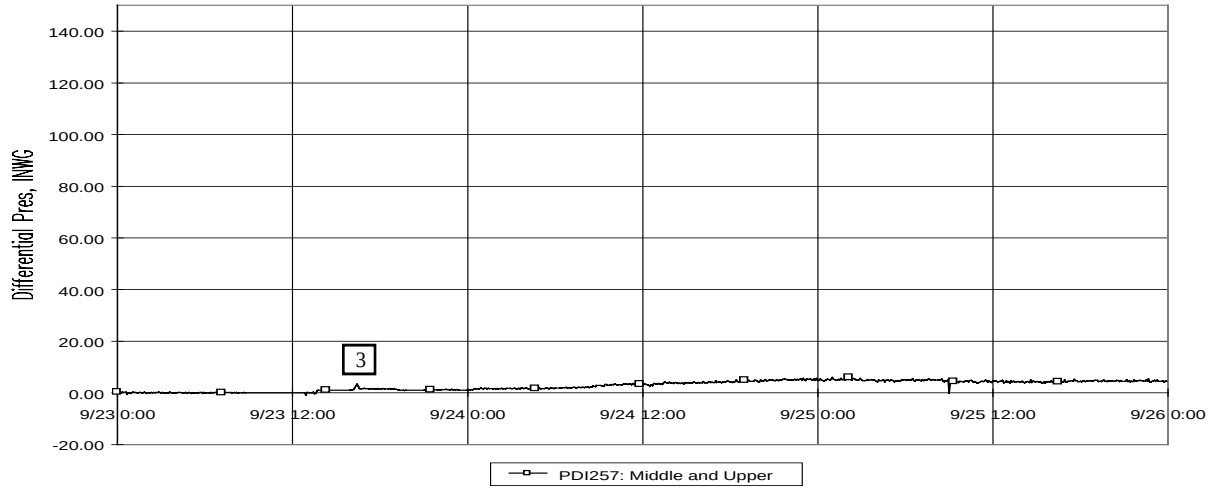

Figure 4.1.4.3-12 Mixing Zone Differential Pressure Profile

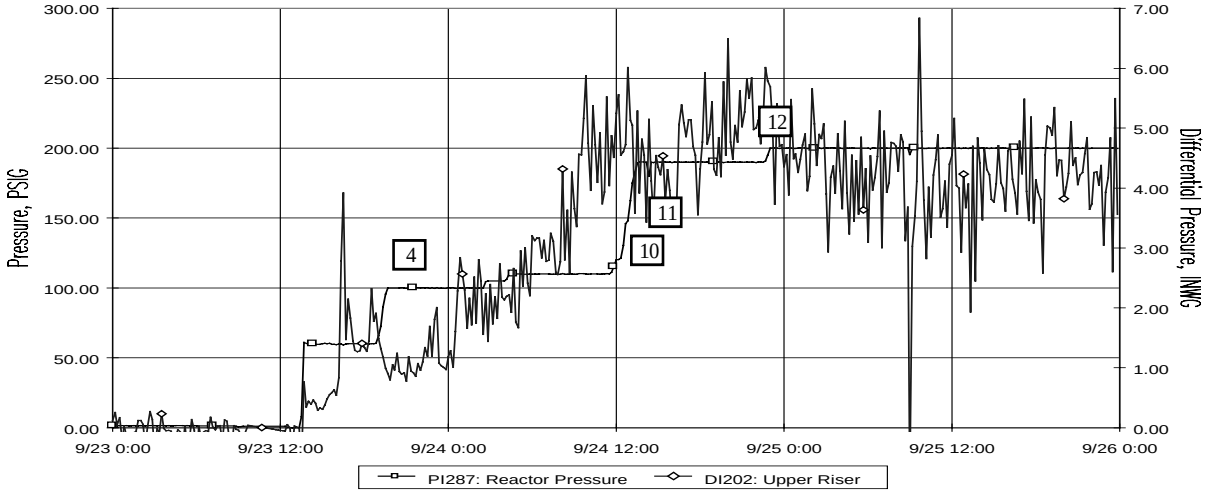

Figure 4.1.4.3-13 Reactor Pressure/Riser Differential Pressure Profiles

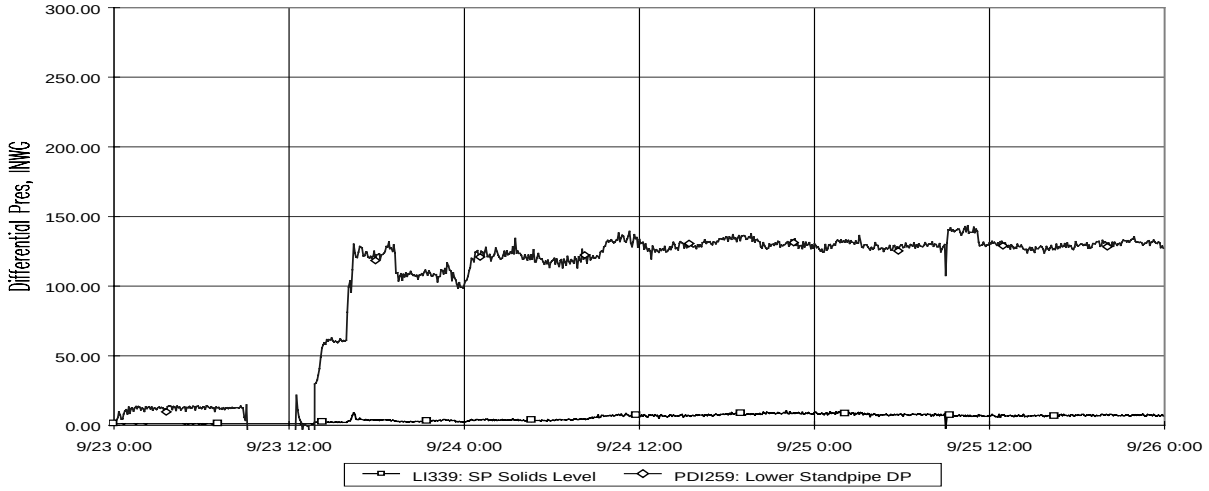

Figure 4.1.4.3-14 Standpipe Differential Pressure Profiles

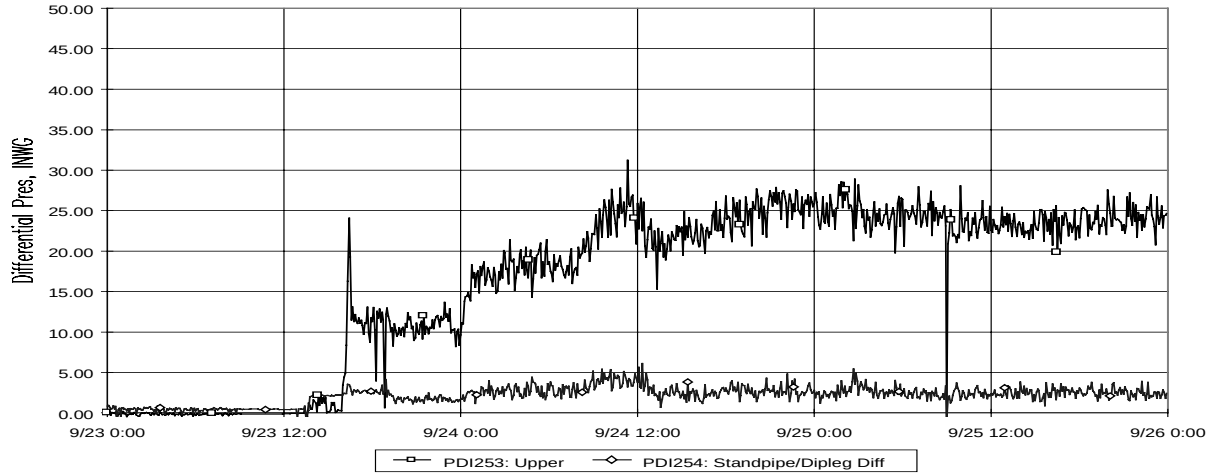

Figure 4.1.4.3-15 CY0201 Dipleg Differential Pressure Profiles

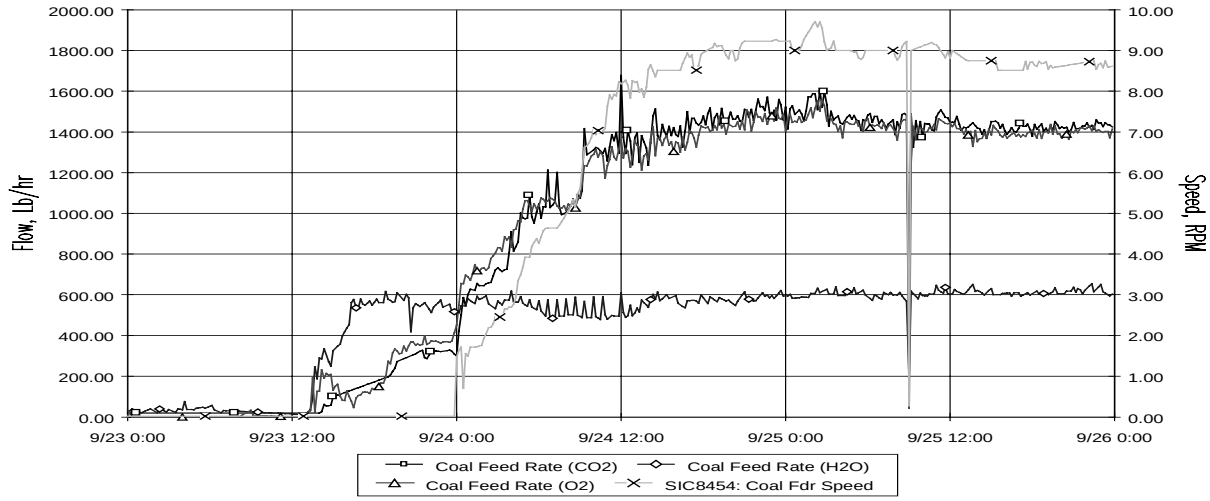

Figure 4.1.4.3-16 Coal Feed Rate Based on Gas Analysis

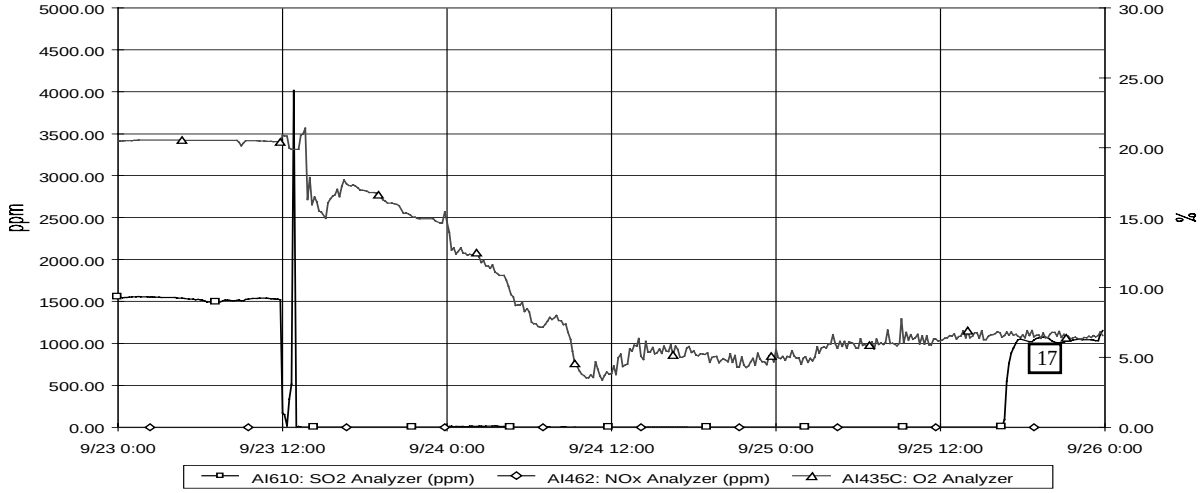

Figure 4.1.4.3-17 O_2, SO_2, and NO_x Analyzers

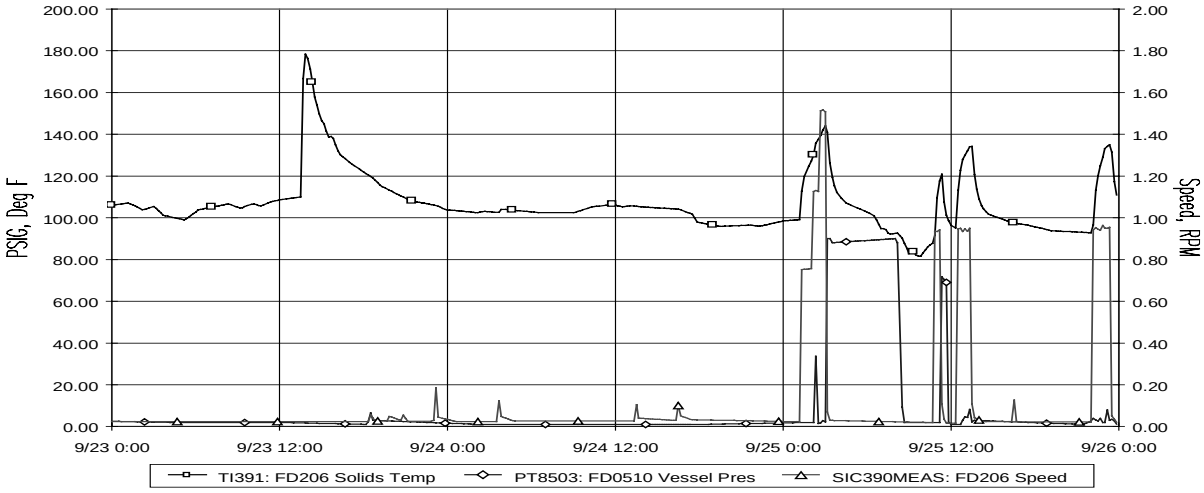

Figure 4.1.4.3-18 FD0206 Profiles

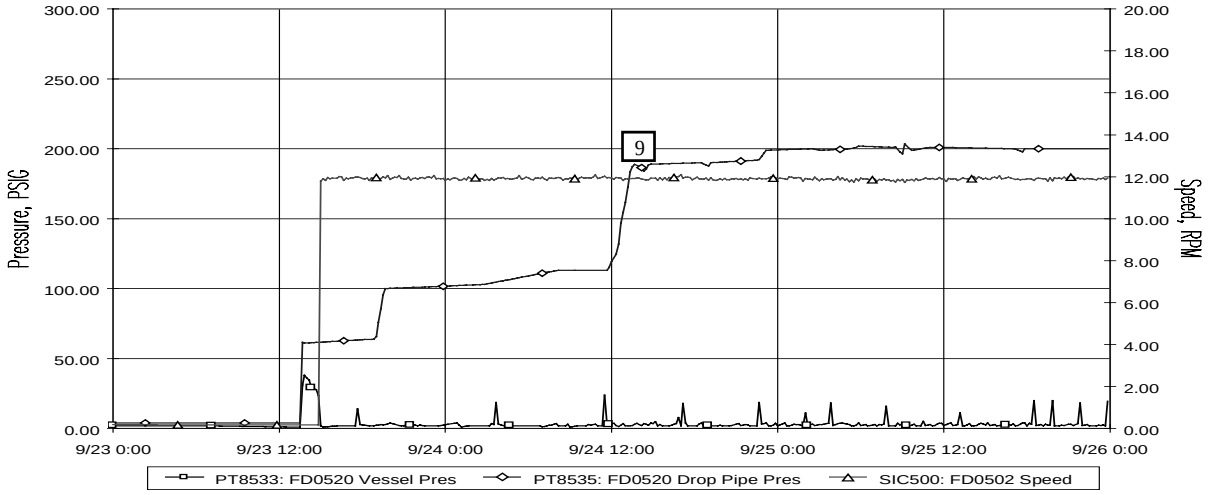

Figure 4.1.4.3-19 FD0520 Pressure Profiles

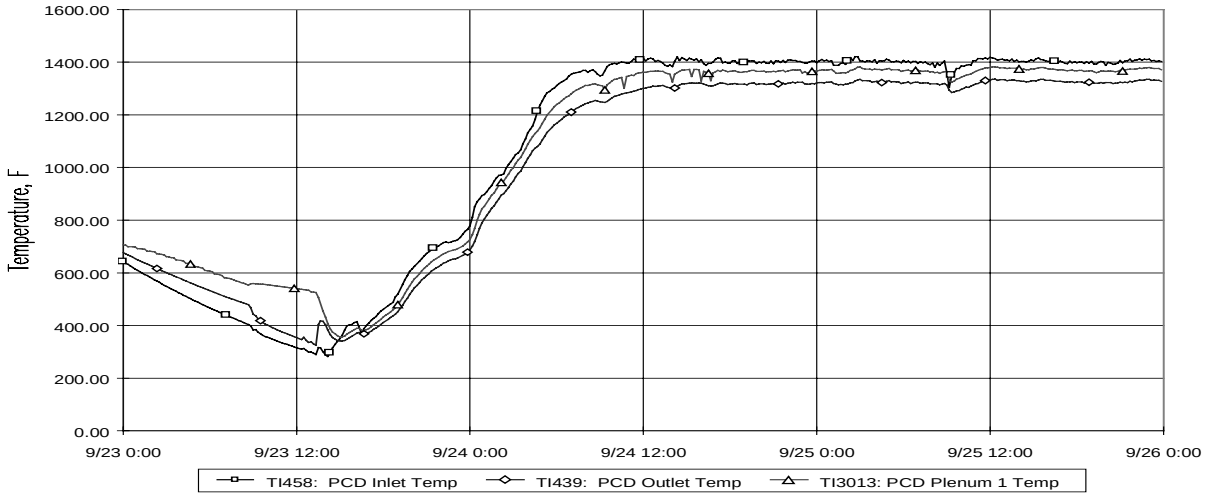

Figure 4.1.4.3-20 PCD Temperatures

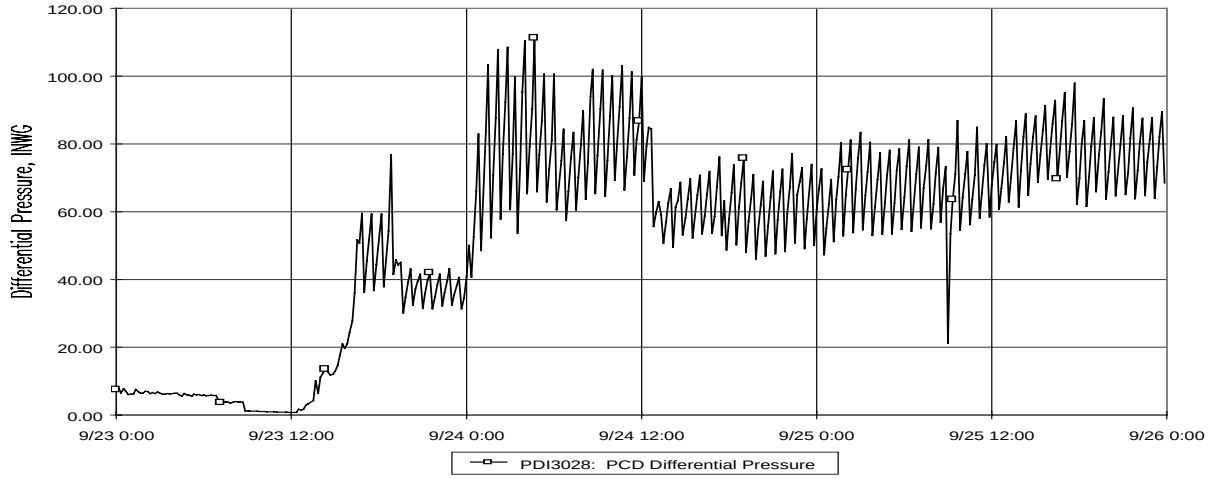

Figure 4.1.4.3-21 PCD Differential Pressure Profile

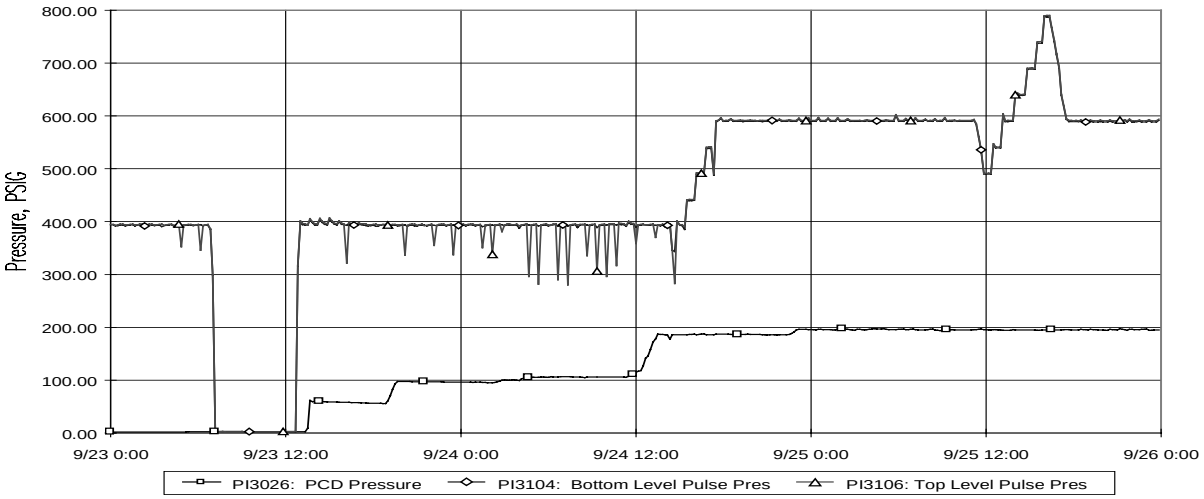

Figure 4.1.4.3-22 PCD Pressure and Pulse Pressure

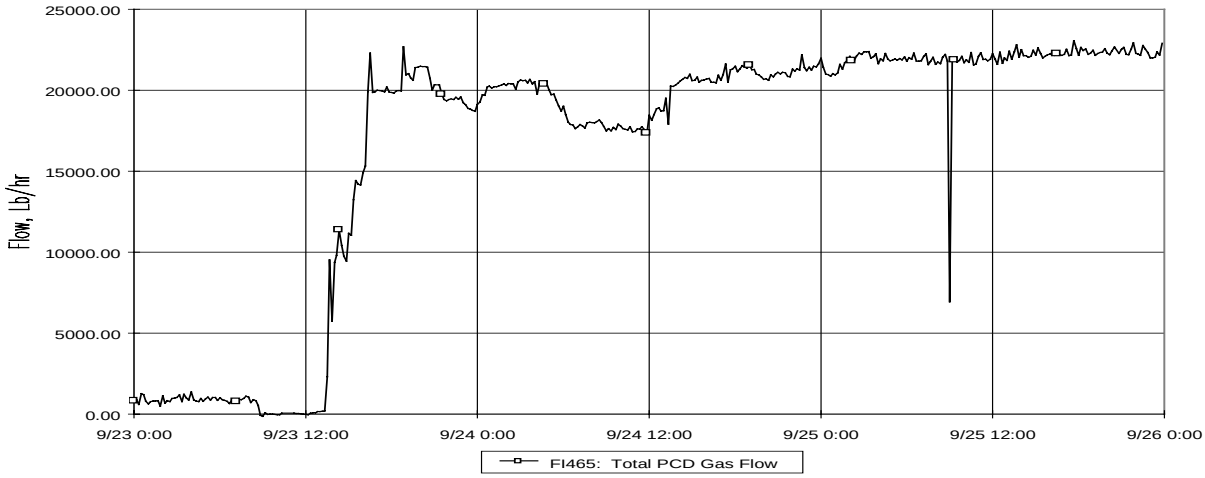

Figure 4.1.4.3-23 Gas Flow Through PCD

Section 4.1.4.3

Graphs 24 through 46

Test Run TC01C
September 26 through September 28, 1997

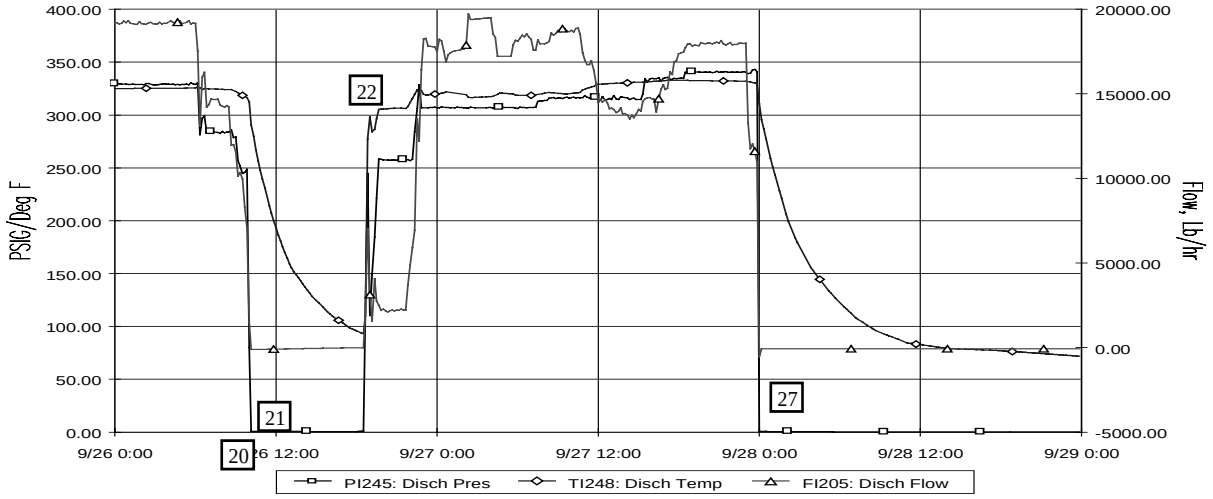

Figure 4.1.4.3-24 CO0201 System Profile

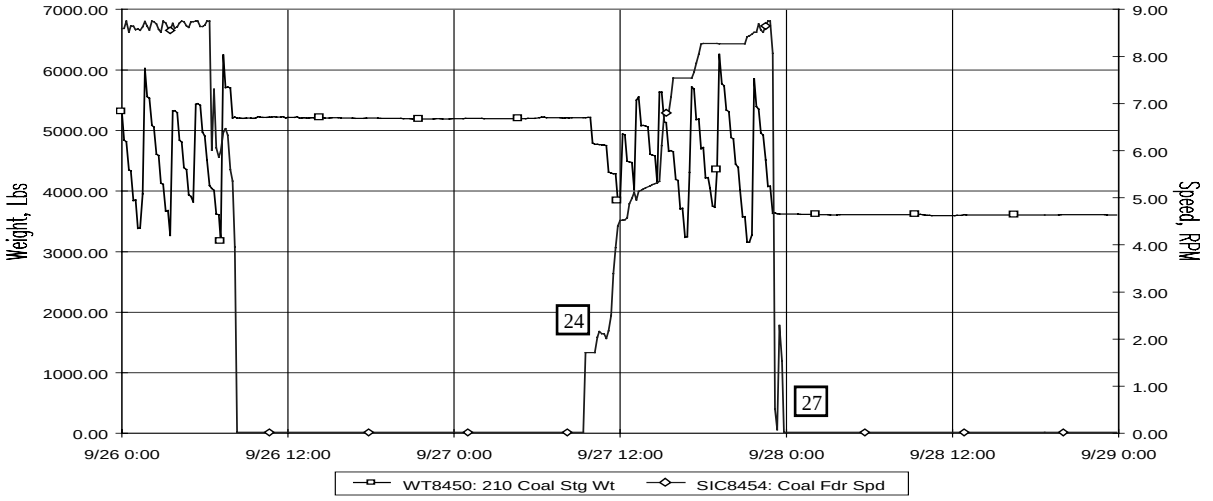

Figure 4.1.4.3-25 Coal Feed System Profile

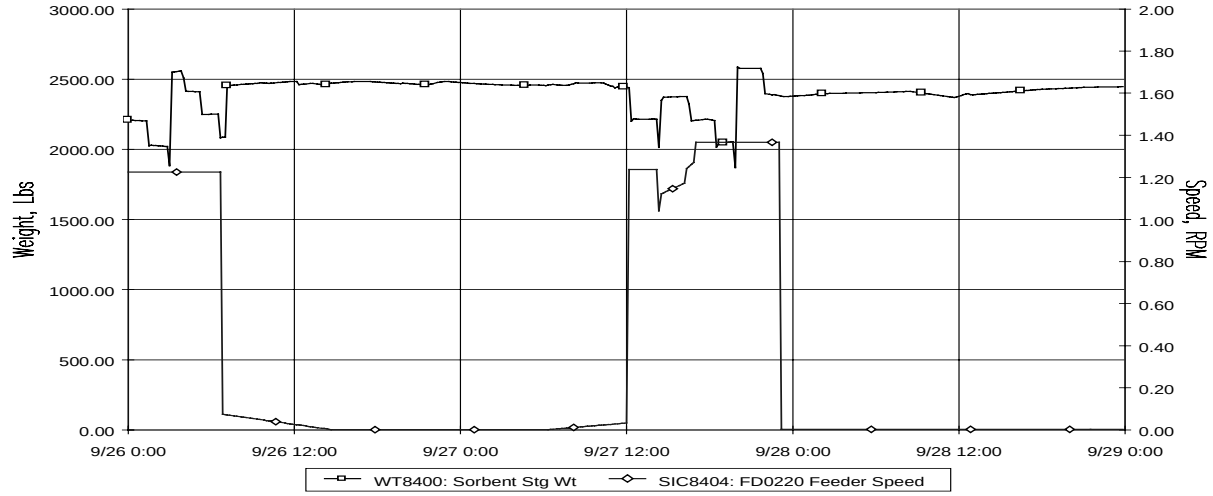

Figure 4.1.4.3-26 Sorbent Feed System Profile

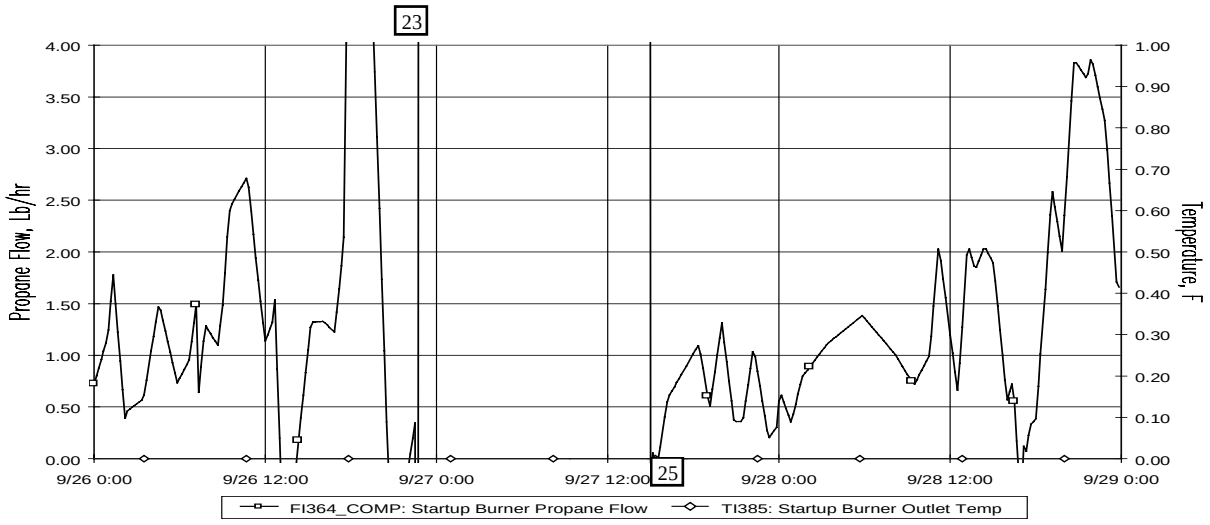

Figure 4.1.4.3-27 Start-Up Burner Flow/Temperature

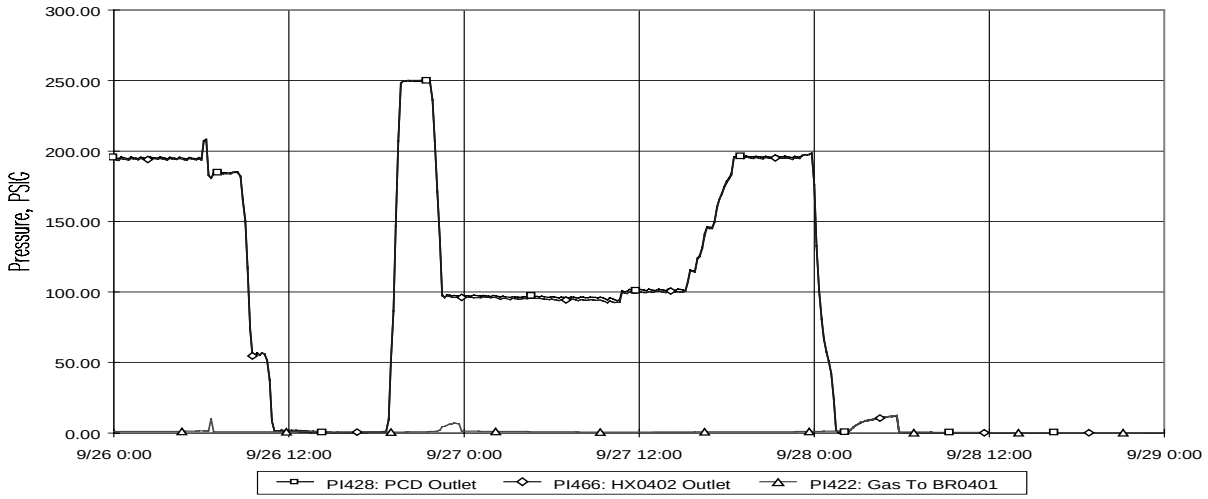

Figure 4.1.4.3-28 System Pressures Downstream of PCD

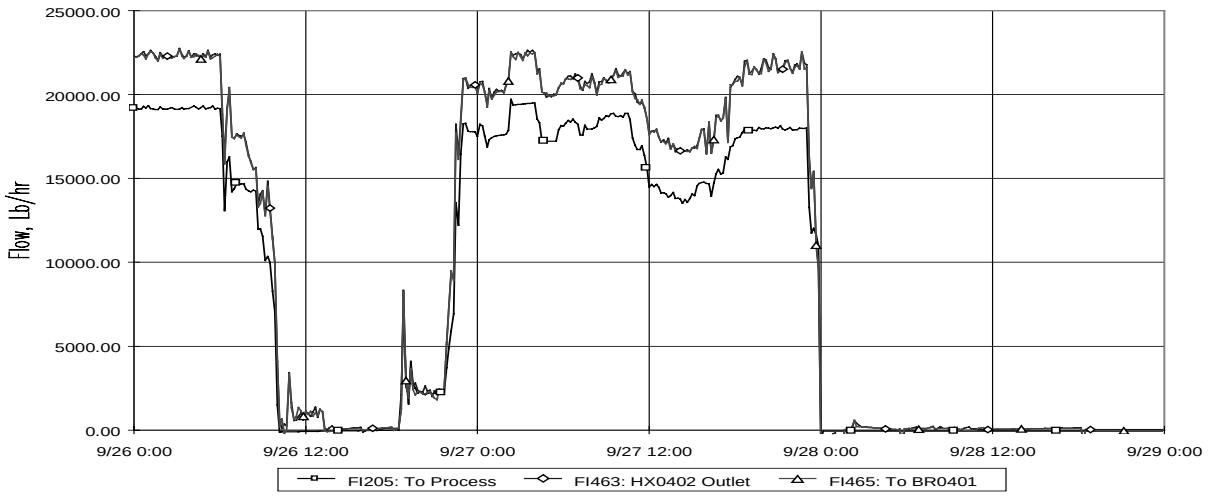

Figure 4.1.4.3-29 Total Gas In/Out Flow Rates

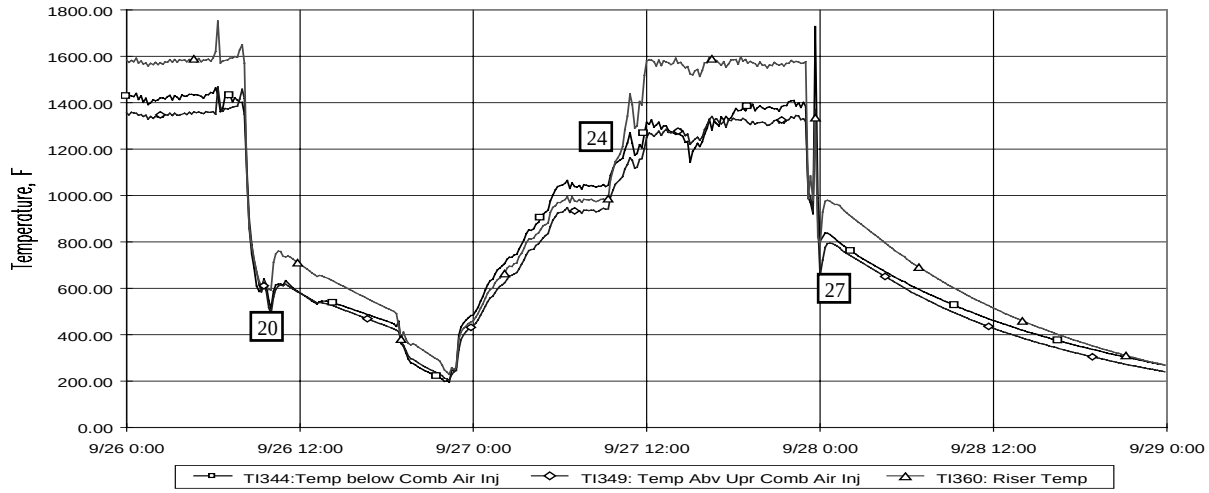

Figure 4.1.4.3-30 Reactor Mixing Zone and Riser Temperatures

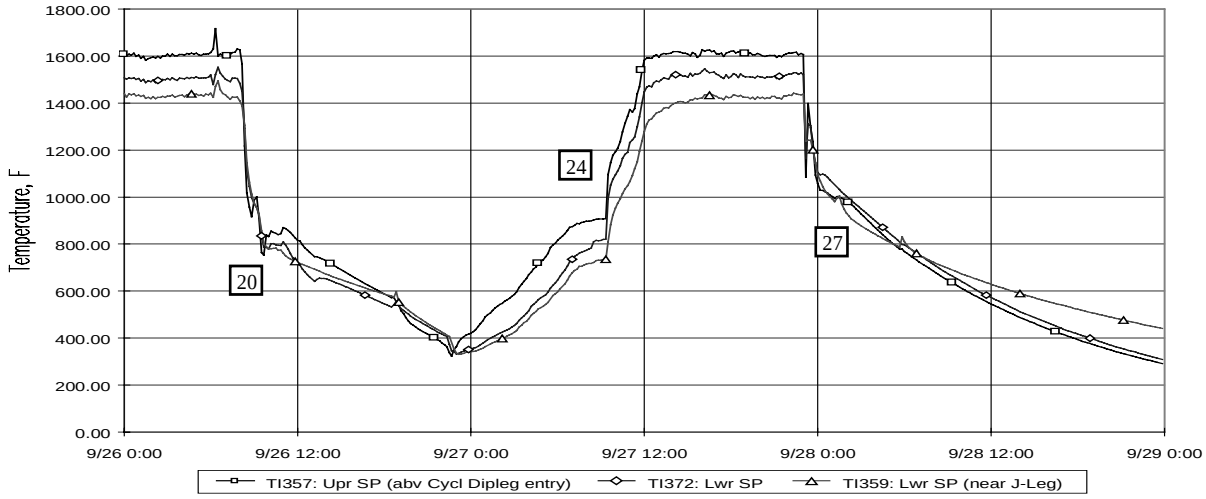

Figure 4.1.4.3-31 Standpipe Temperatures

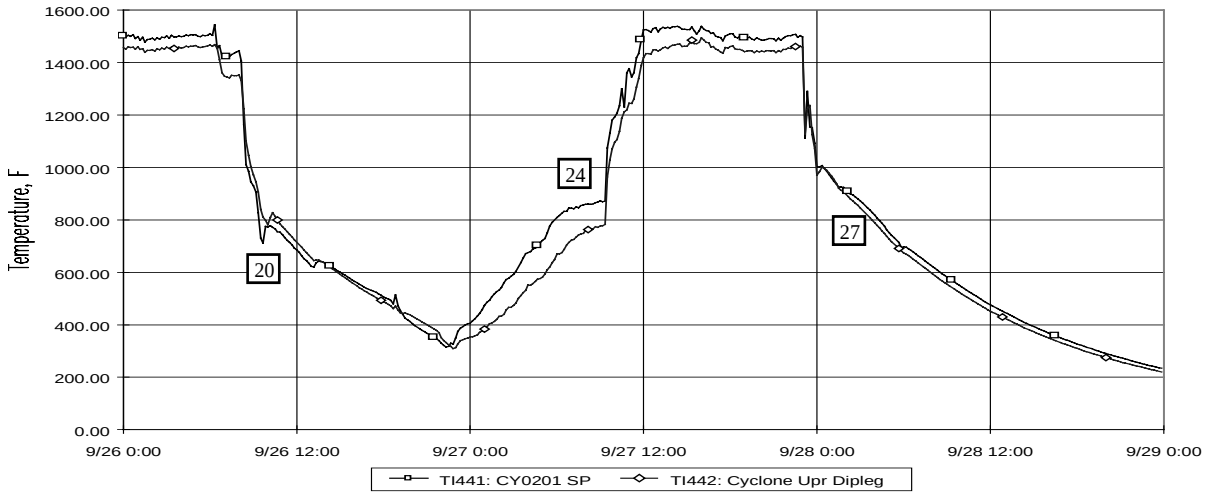

Figure 4.1.4.3-32 Cyclone Dipleg Temperatures

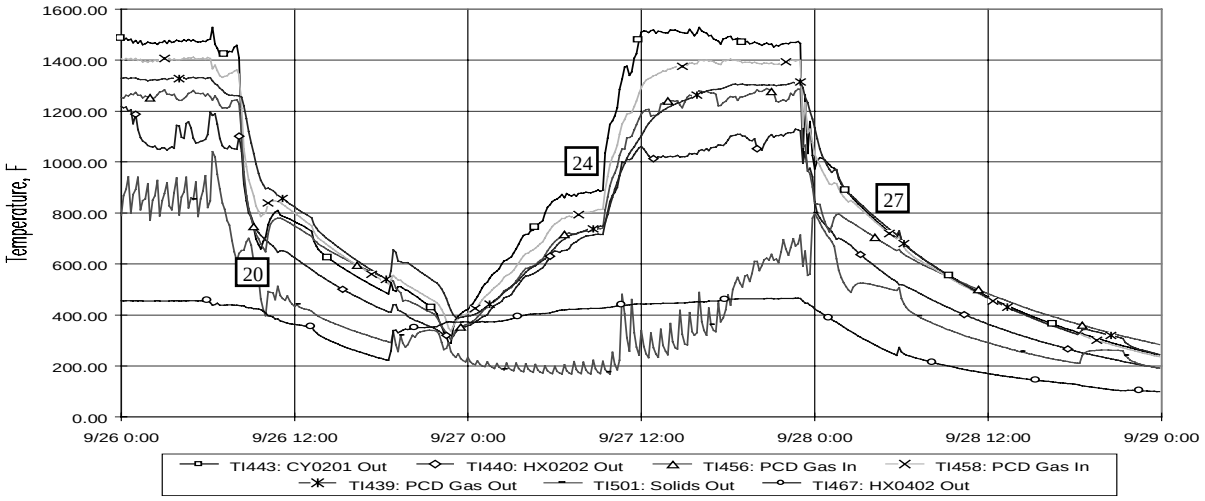

Figure 4.1.4.3-33 Temperature Profile Downstream of Reactor

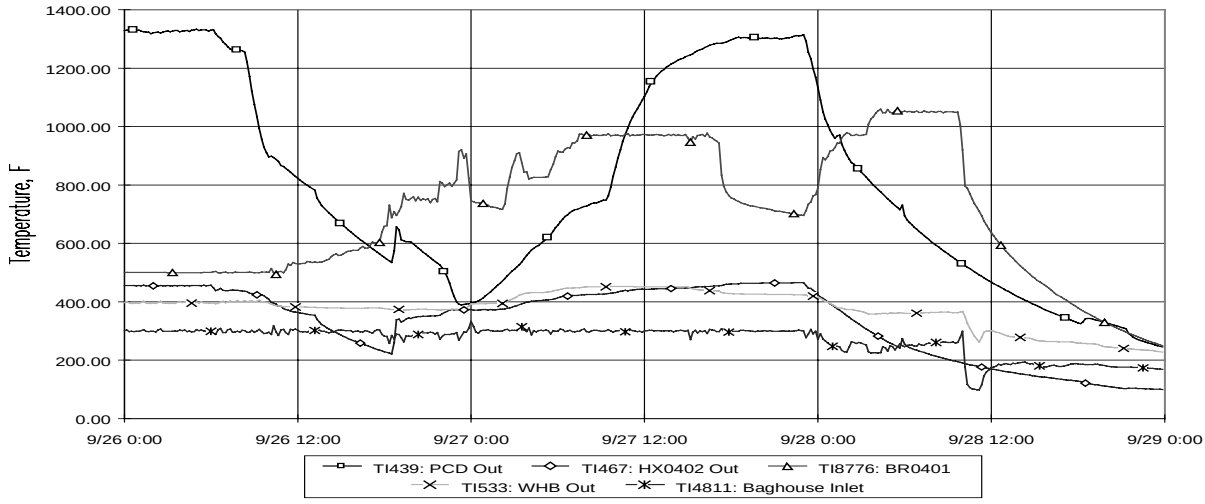

Figure 4.1.4.3-34 System Temperatures Downstream of PCD

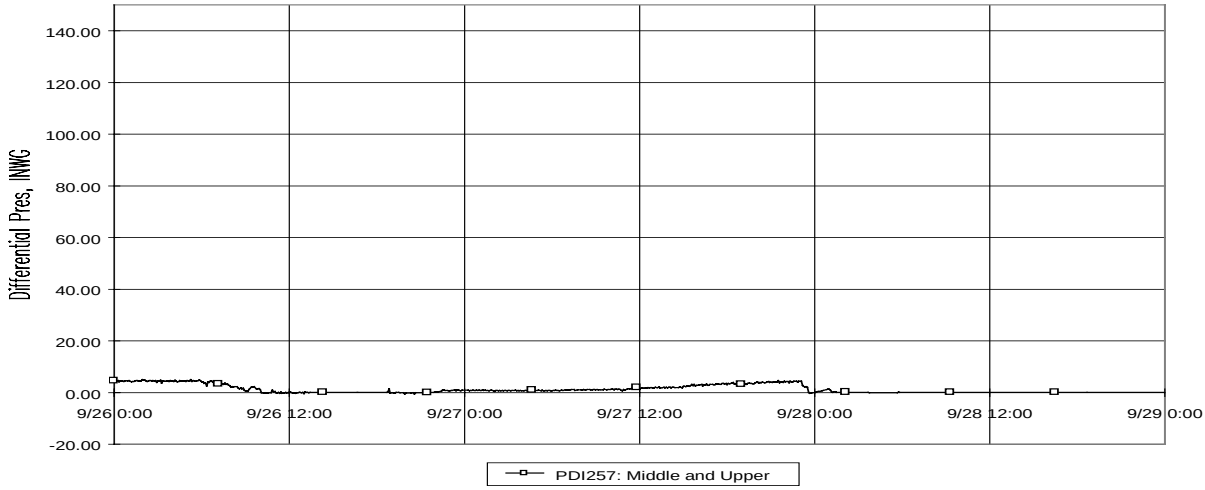

Figure 4.1.4.3-35 Mixing Zone Differential Pressure Profile

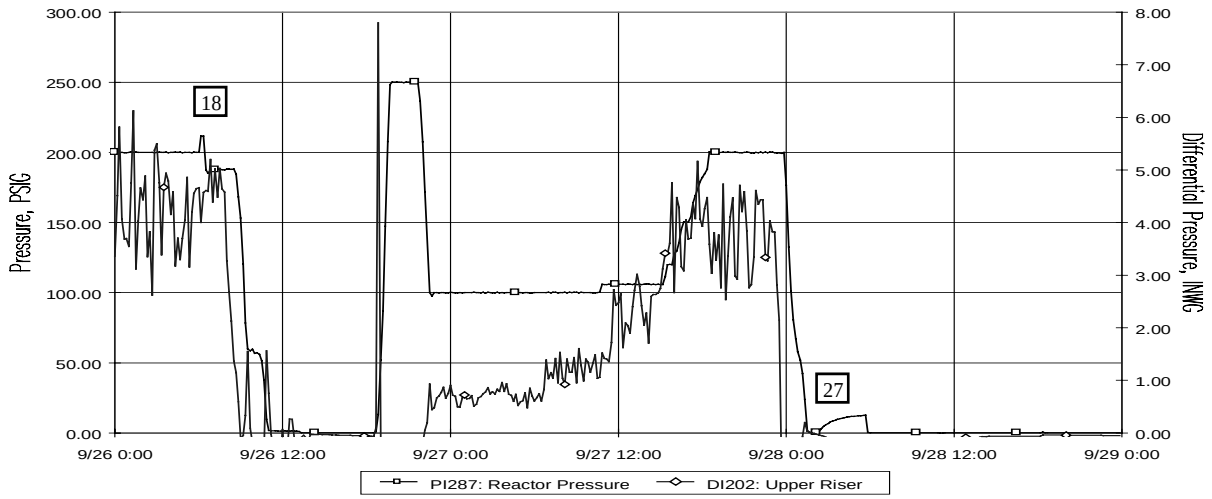

Figure 4.1.4.3-36 Reactor Pressure/Riser Differential Pressure Profiles

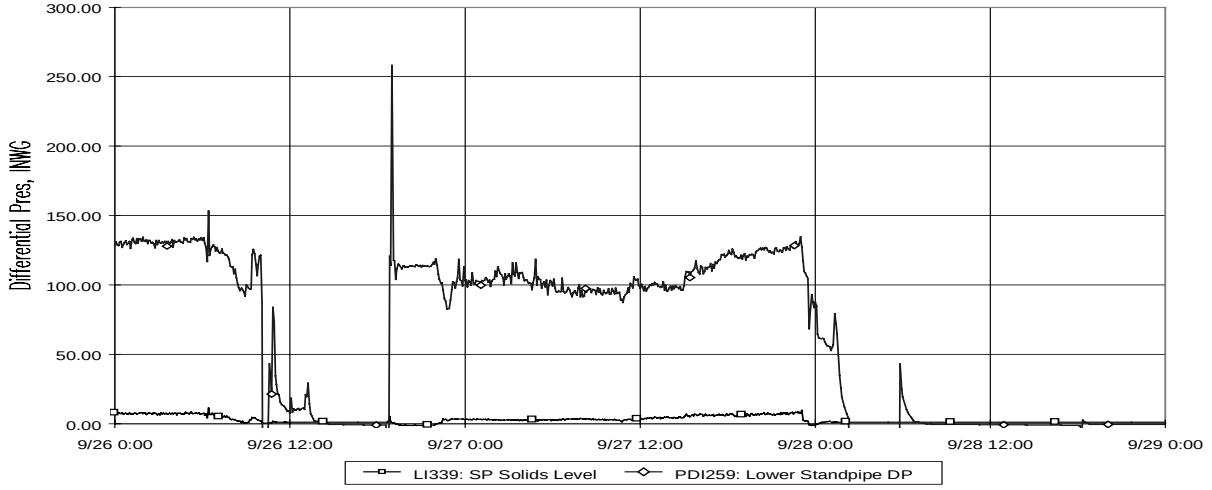

Figure 4.1.4.3-37 Standpipe Differential Pressure Profiles

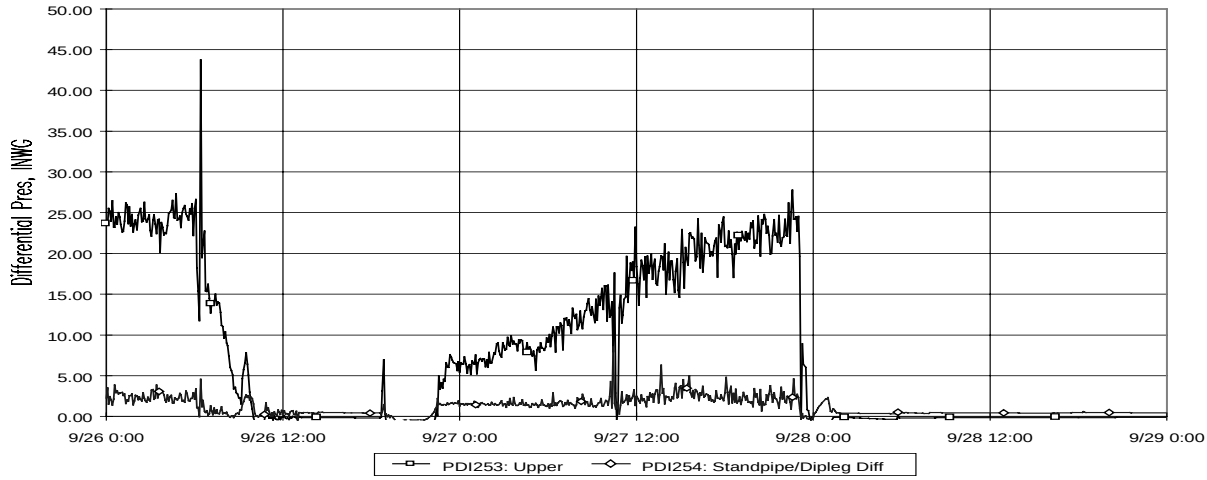

Figure 4.1.4.3-38 CY0201 Dipleg Differential Pressure Profiles

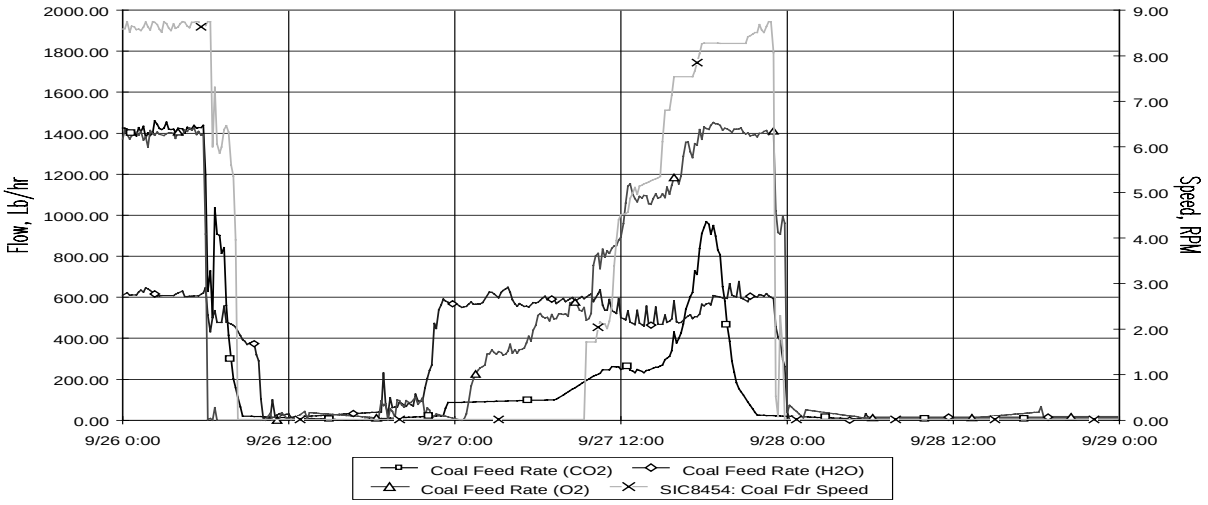

Figure 4.1.4.3-39 Coal Feed Rate Based on Gas Analysis

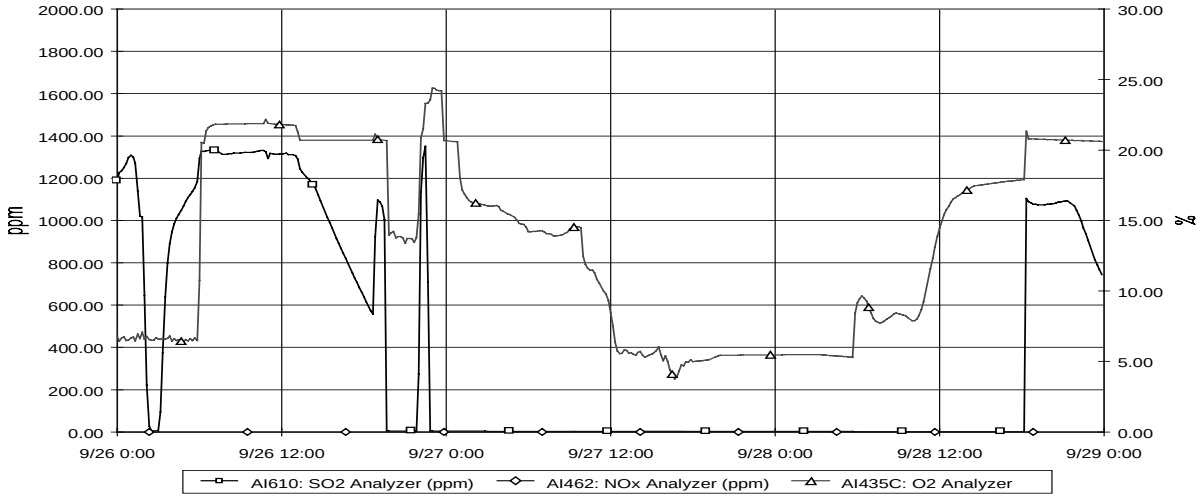

Figure 4.1.4.3-40 O_2, SO_2, and NO_x Analyzers

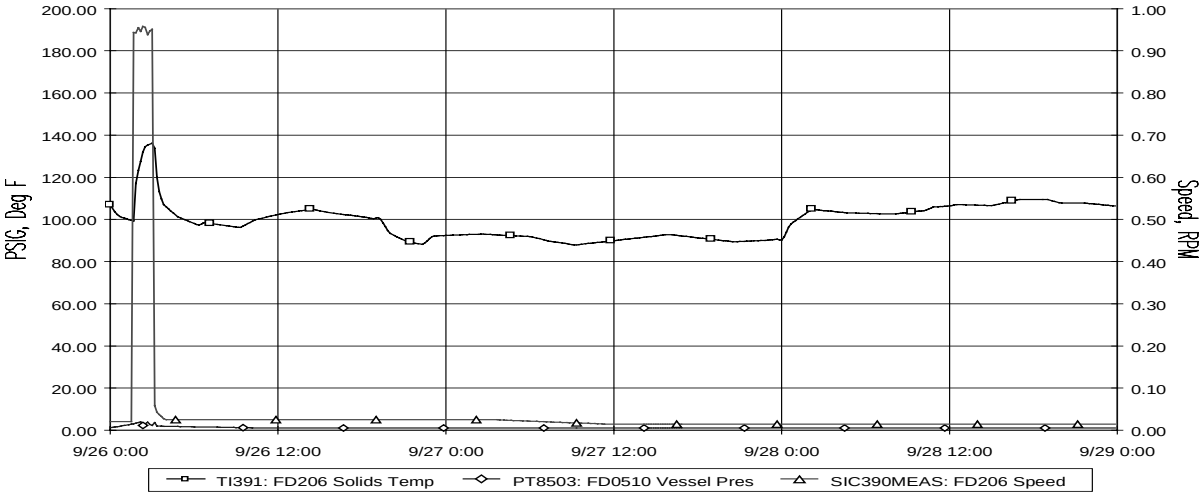

Figure 4.1.4.3-41 FD0206 Profiles

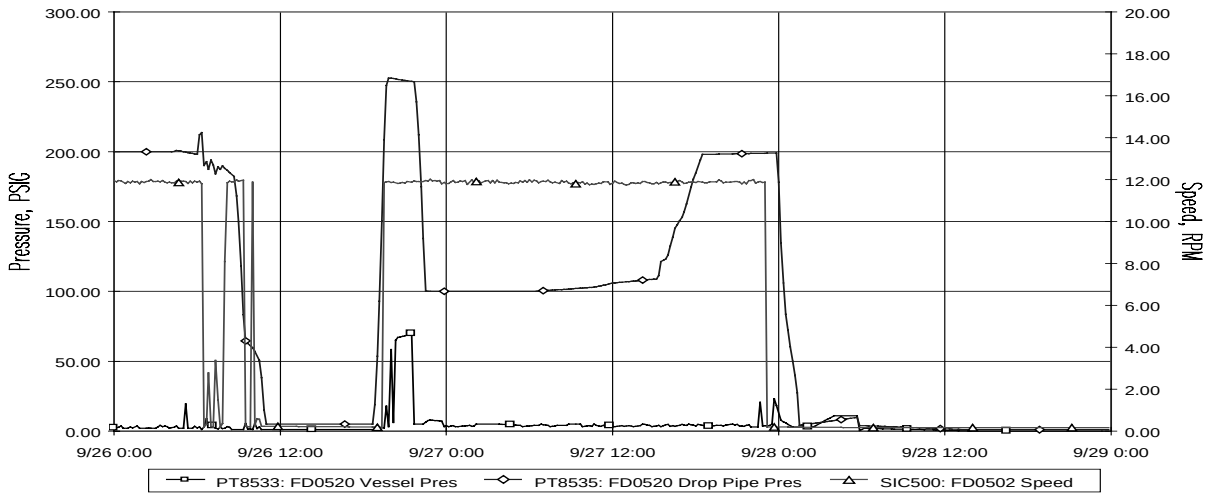

Figure 4.1.4.3-42 FD0520 Pressure Profiles

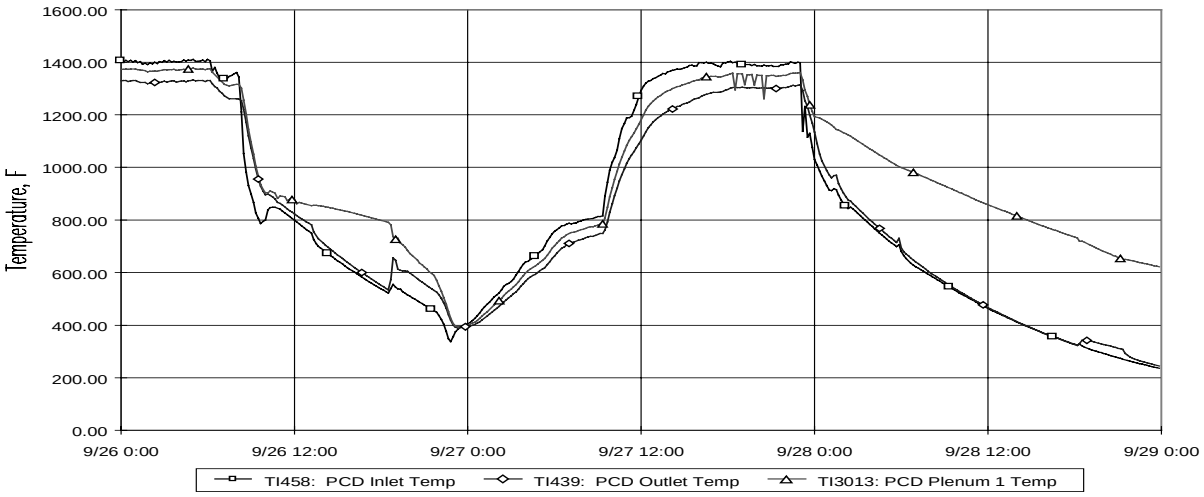

Figure 4.1.4.3-43 PCD Temperatures

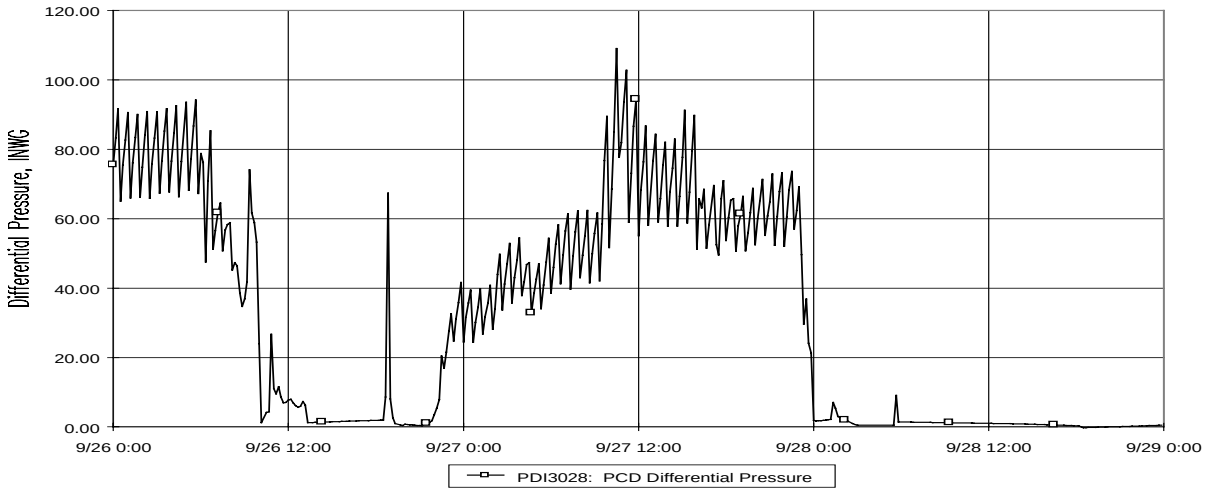

Figure 4.1.4.3-44 PCD Differential Pressure Profile

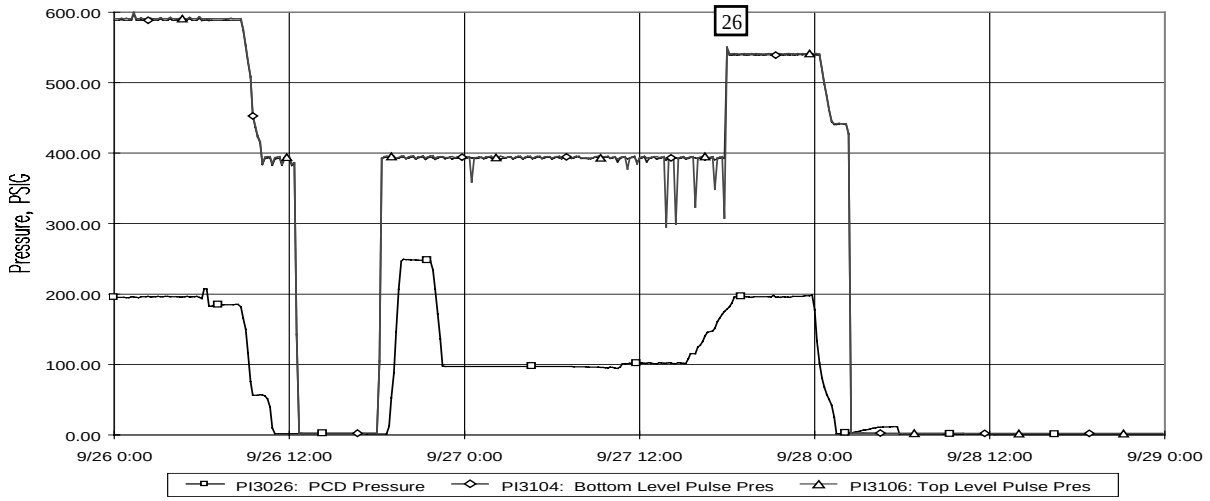

Figure 4.1.4.3-45 PCD Pressure and Pulse Pressure

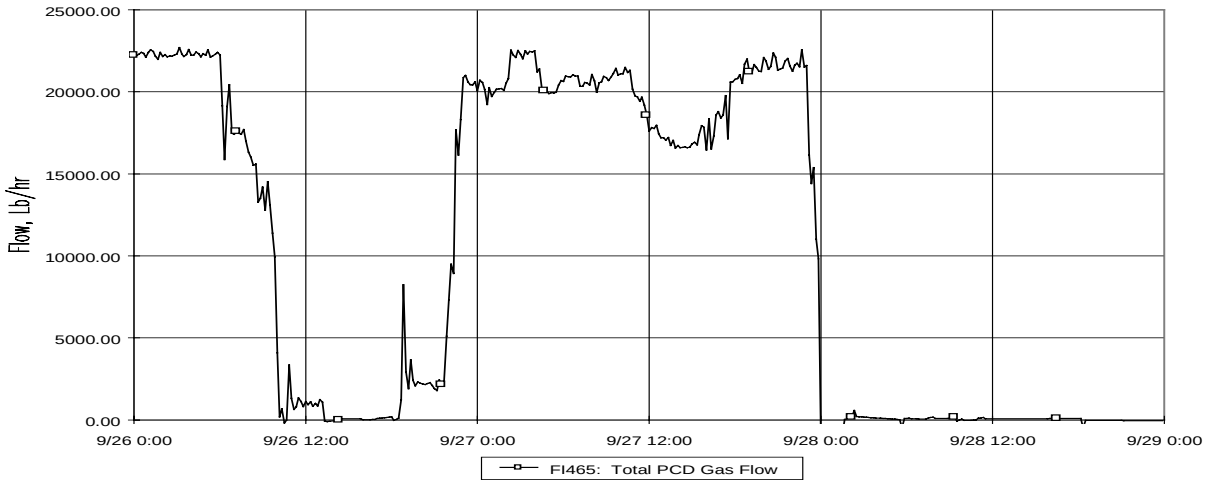

Figure 4.1.4.3-46 Gas Flow Through PCD

4.1.4.4 TC01D Test Run

Test run TC01D was conducted between September 29 and October 5, 1997. Operating plots are shown in figures 4.1.4.4-1 through -40.

TC01D Test Run Chronology

- On September 29, 1997, the top and bottom spheri valve seals were replaced on the fines transporter system (FD0520). In preparation for the test run the main air compressor (CO0201) was started at 21:35 (event 1, figure 1).

- On September 30, 1997, the sulfator heater (BR0602) was lit to preheat the PCD. The preheat was completed at about 04:00 (event 2, figure 17), the reactor start-up burner (BR0201) was lit at about 06:20 (event 3, figure 4), and about an hour later BR0602 was shut down. The reactor pressure was gradually increased to 100 psig by 10:00. Between 11:30 and 15:00 back-pulsing tests were performed at various valve-open times, valve actuation pressures, and pulse pressures. The coal feed was started at 13:40 (event 4, figures 2 and 6 through 9). The reactor pressure was slightly increased around 14:45 to reduce the inlet cyclone velocity and thereby stabilize the dipleg operation.

- At 16:30 coal feed was momentarily lost because the FD0210 dispense vessel fill cycle was left disabled. The BR0201 was shut down at 17:10 (event 5, figure 4). Over the next several hours the reactor pressure was increased and the reactor aerations were adjusted. By 21:00 the reactor pressure was 190 psig and the PCD temperature was 1,350°F (event 6, figure 17).

- Around 06:10 on October 1, 1997, the reactor pressure was increased to 195 psig (event 7, figure 12). At 07:30 there was a considerable increase in N_2 required to pressurize the spheri valve seals when FD0210 cycled. At about 13:10 the FD0210 middle spheri valve seal failed (event 8, figures 2 and 6 through 9). The system was slowly depressurized and BR0201 was lit at 14:35 (event 9, figure 4). The FD0210 middle spheri valve seal between the surge bin and lock vessel was replaced and FD0210 was lined up at 22:00.

- Coal feed started at 02:50 on October 2, 1997 (event 10, figures 2 and 6 through 9). During the first FD0210 cycle, around 03:15, the lock vessel vent line plugged because the gate valve was not set properly, causing the lock vessel to overfill. The two shuttle valves and the poppet valve associated with the middle spheri were pulled and cleaned.

- Coal feed resumed just before 13:00 (event 11, figures 2 and 6 through 9). The BR0201 was shut down at about 16:45 (event 12, figure 4) and the reactor pressure was gradually increased to 200 psig around 17:35 (event 13, figure 12). The back-pulse pressure was increased to 550 psig and adjustments to the aeration rate on the

combustion heat exchanger (HX0203) were made. By 20:40 the PCD was above 1,350°F (event 14, figure 17).

- SRI took samples on October 3, 1997. A leak in the FD0502 packing was repaired by tightening the packing. The process ran smoothly throughout the day except for a temporary plug in the coal silo (FD0104).

- On October 4, 1997, FD0502 tripped momentarily due to the failure of the bottom spheri valve to close before the timer timed out. The reactor pressure was increased in steps until the pressure reached 210 psig. Staged air (through the riser) was redistributed to evaluate its effect on the reactor temperature profile. There was no apparent effect on the temperature profile. Fluctuations in the coal feeder speed resulted in unsteady temperatures in the reactor and PCD. The FD0510 was shut down for about 1 hour to fix a crack in its exit elbow.

- On October 5, 1997, the FD0210 discharge line plugged, resulting in a decrease in reactor temperatures that forced the coal and dolomite feed to be stopped (event 15, figures 22 and 25 through 29). The reactor pressure was reduced to 100 psig and BR0201 was lit at 09:20 (event 16, figure 32). Coal feed was attempted at 11:50 but failed because the discharge vessel was bridged. After completing maintenance work on the FD0210 coal feed was started at 16:30 (event 17, figures 22, 25, and 29) but the feeder tripped several times during the next 3 hours. The FD0520 bottom spheri valve seal failed at about 19:45 forcing a shutdown of the process (event 18, figures 21, 22, 25 through 29, and 32).

TC01D Test Run Observations

A total of 97.2 hours on coal was achieved, a total of 58.8 tons of coal were fed, and 86 hours with PCD plenum temperature above 1,350°F was accumulated. There were three temporary coal feed shutdowns during this run due to problems with the coal feed system.

1. The FD0210 system middle spheri valve seal failed.

2. The lock vessel vent line plugged due to improper installation of an orifice plate and vent valve in the line.

3. The amount of coal transferred per cycle to the lock hopper and dispense vessel decreased considerably, indicating bridging in these vessels.

The coal feeder discharge line also plugged. All of these problems were addressed as they occurred and the coal feed system was put back on-line. The FD0210 and FD0220 lock vessels were inspected and cleaned during the outage. There was little buildup in either vessel. The final process shutdown was caused by a combination of problems with the coal feeder system and the blown spheri valve seal on the fines transport system.

Section 4.1.4.4

Graphs 1 through 20

Test Run TC01D
September 29 through October 2, 1997

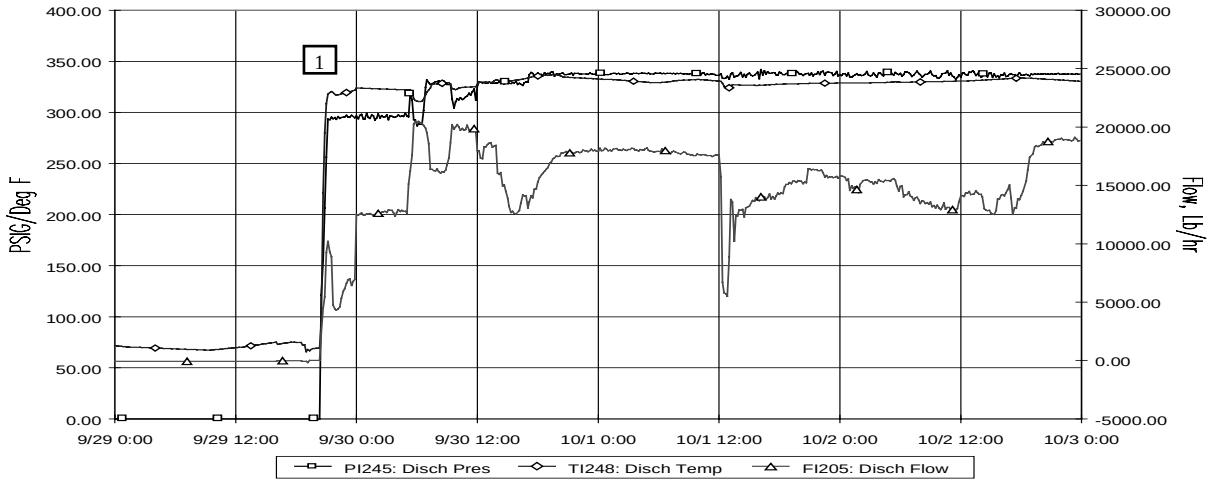

Figure 4.1.4.4-1 CO0201 System Profile

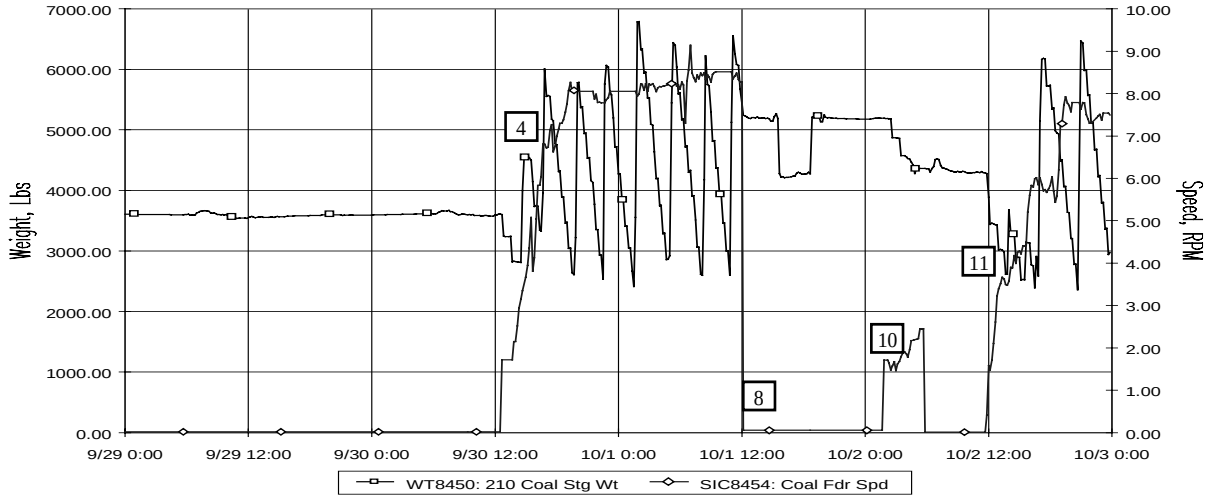

Figure 4.1.4.4-2 Coal Feed System Profile

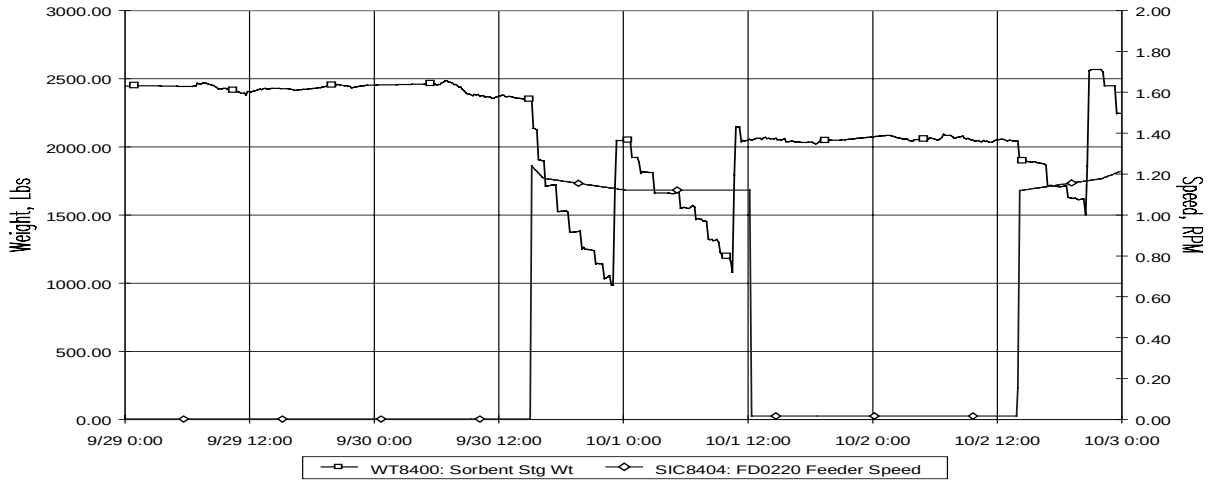

Figure 4.1.4.4-3 Sorbent Feed System Profile

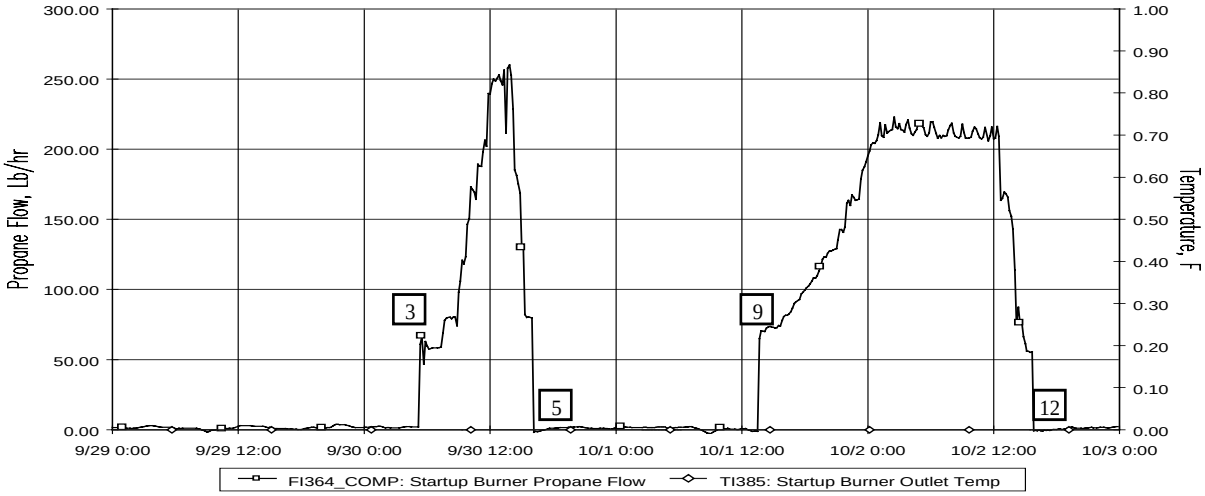

Figure 4.1.4.4-4 Start-Up Burner Flow/Temperature

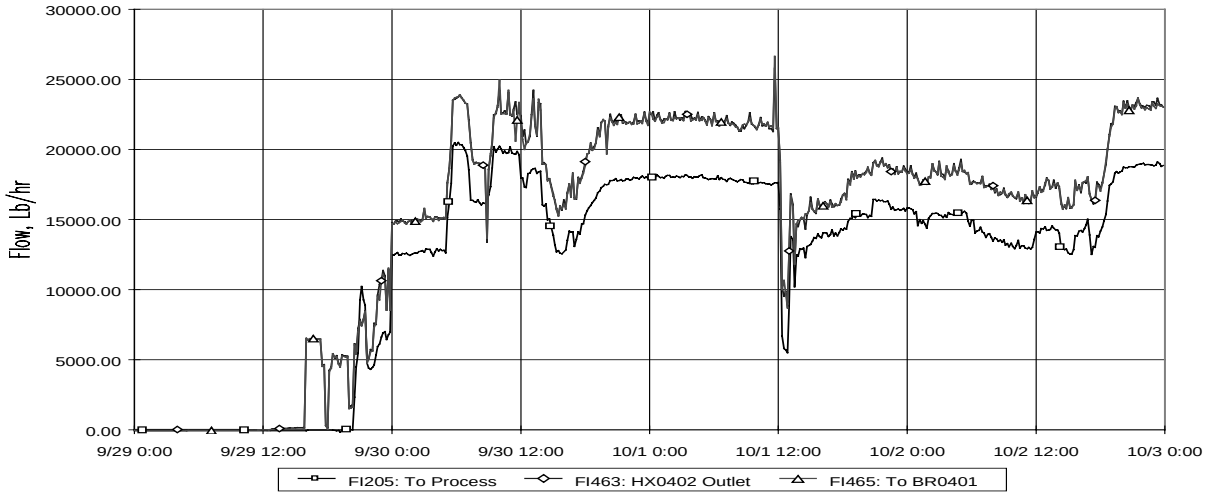

Figure 4.1.4.4-5 Total Gas In/Out Flow Rates

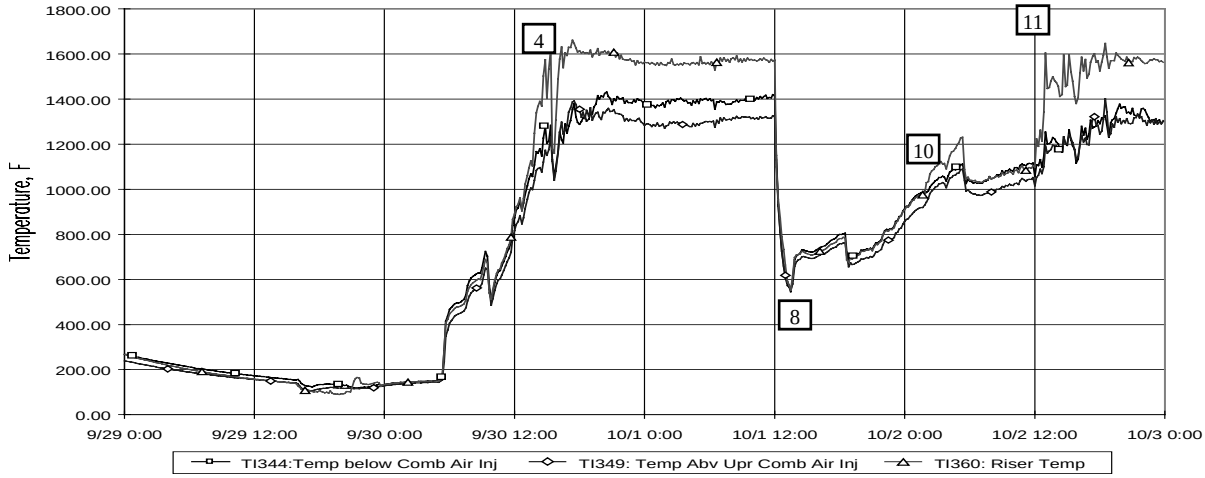

Figure 4.1.4.4-6 Reactor Mixing Zone and Riser Temperatures

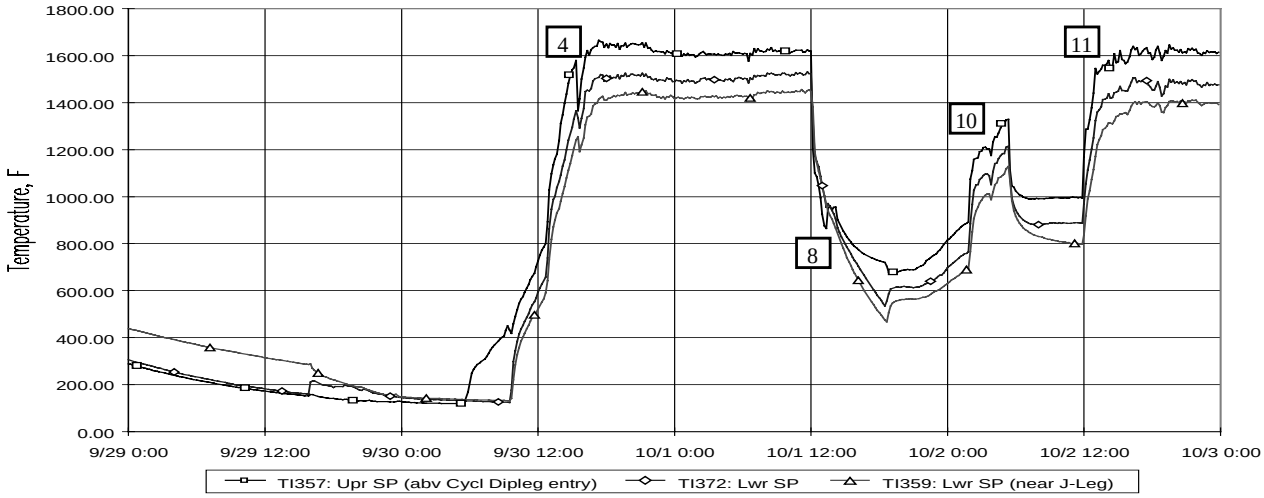

Figure 4.1.4.4-7 Standpipe Temperatures

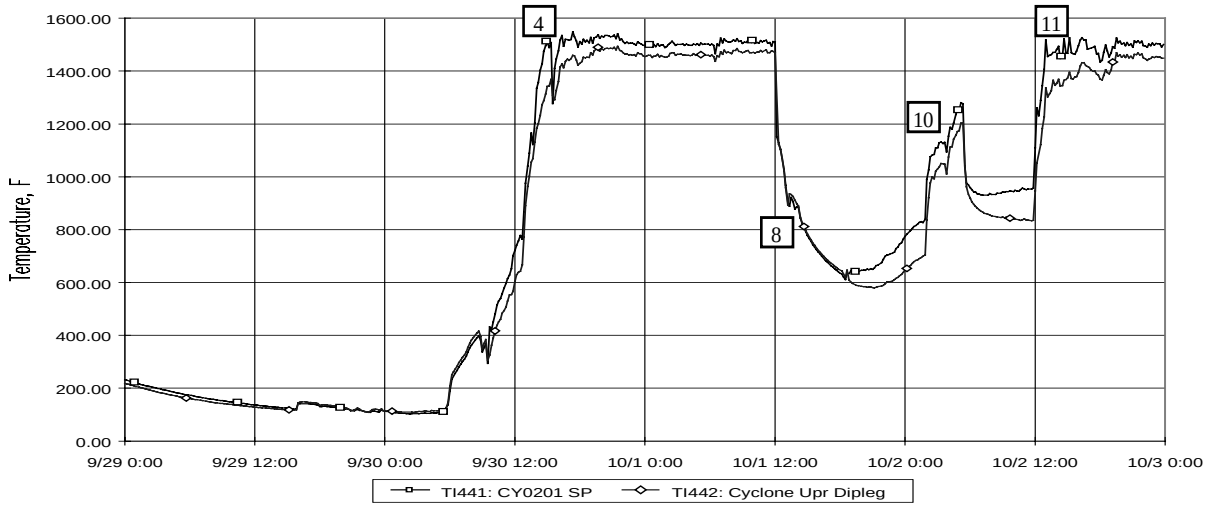

Figure 4.1.4.4-8 Cyclone Dipleg Temperatures

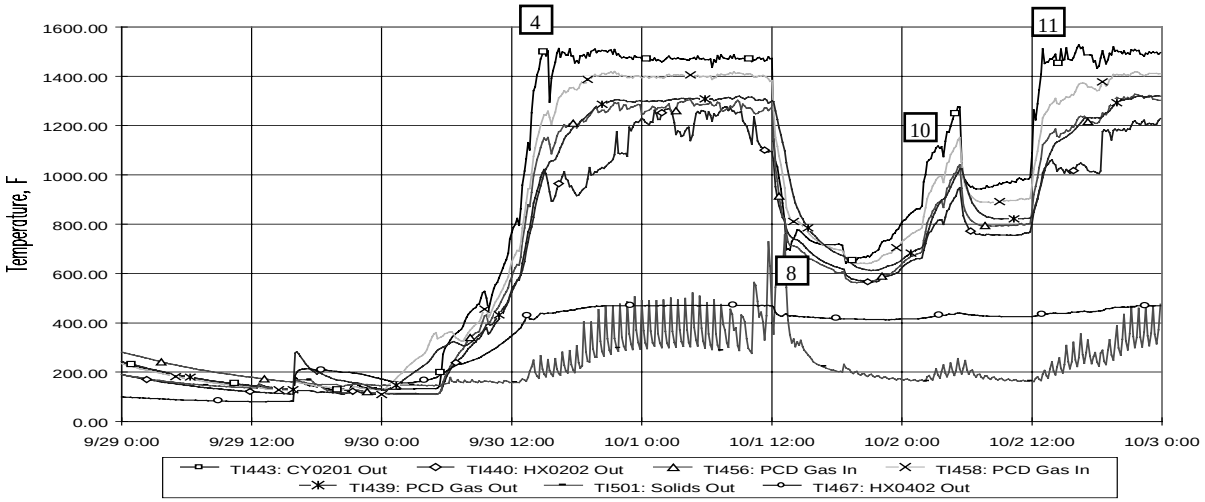

Figure 4.1.4.4-9 Temperature Profile Downstream of Reactor

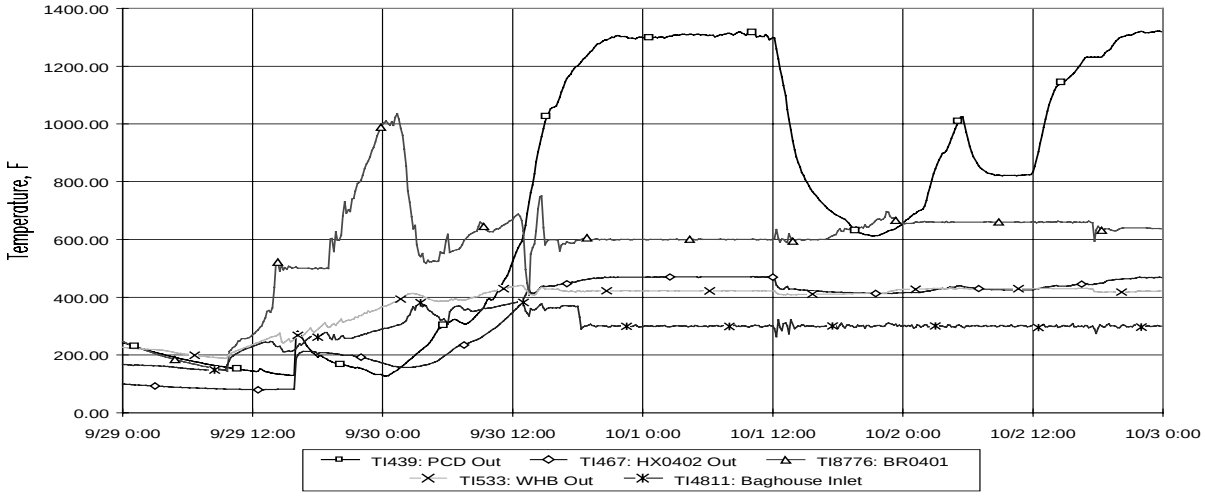

Figure 4.1.4.4-10 System Temperatures Downstream of PCD

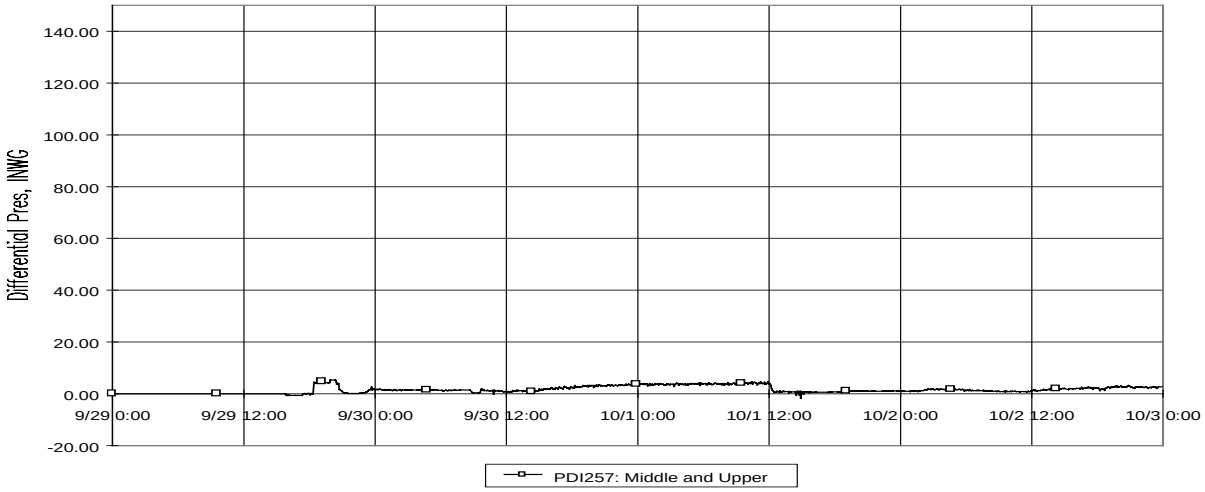

Figure 4.1.4.4-11 Mixing Zone Differential Pressure Profile

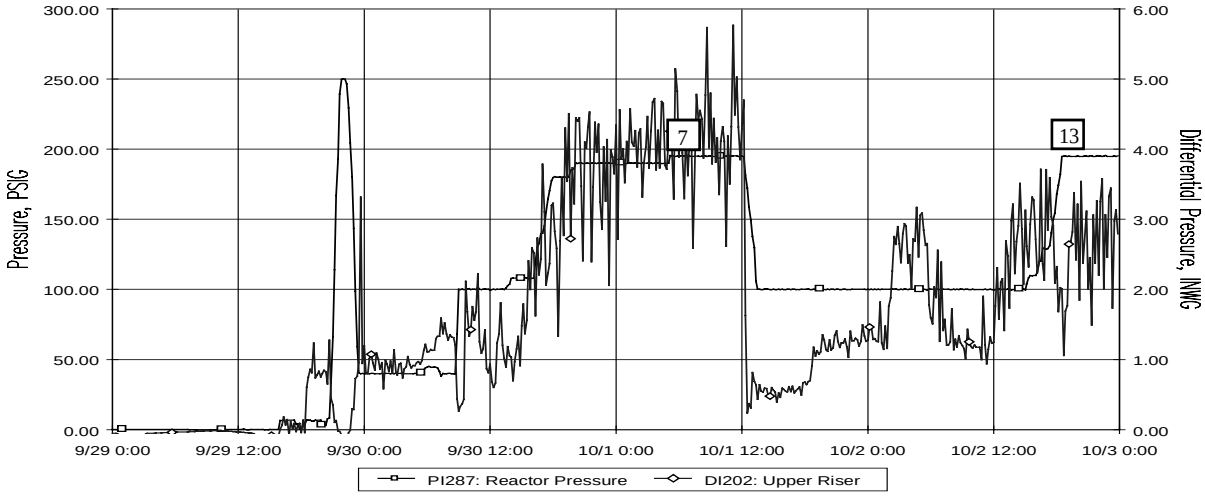

Figure 4.1.4.4-12 Reactor Pressure/Riser Differential Pressure Profile

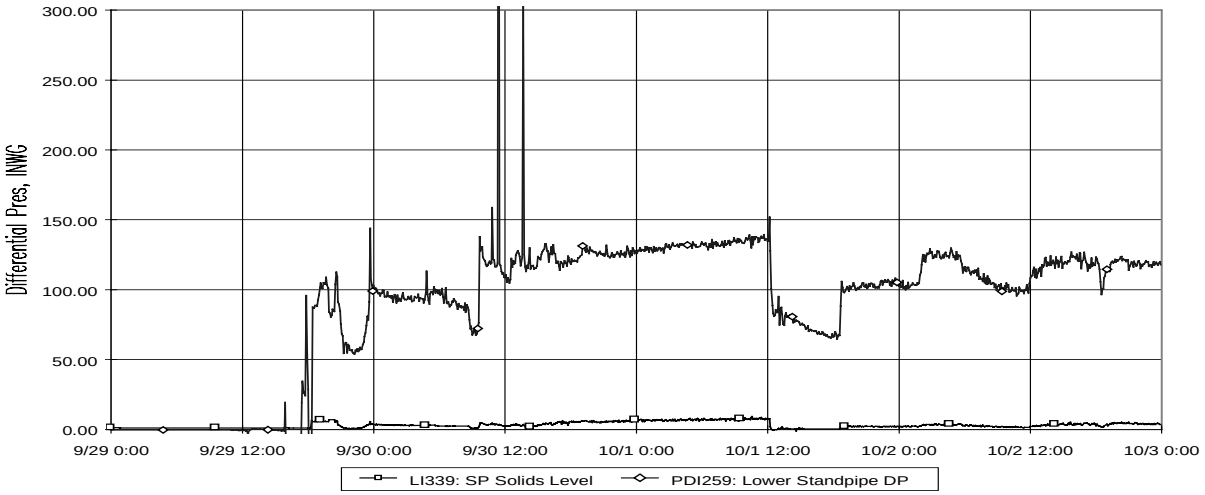

Figure 4.1.4.4-13 Standpipe Differential Pressure Profiles

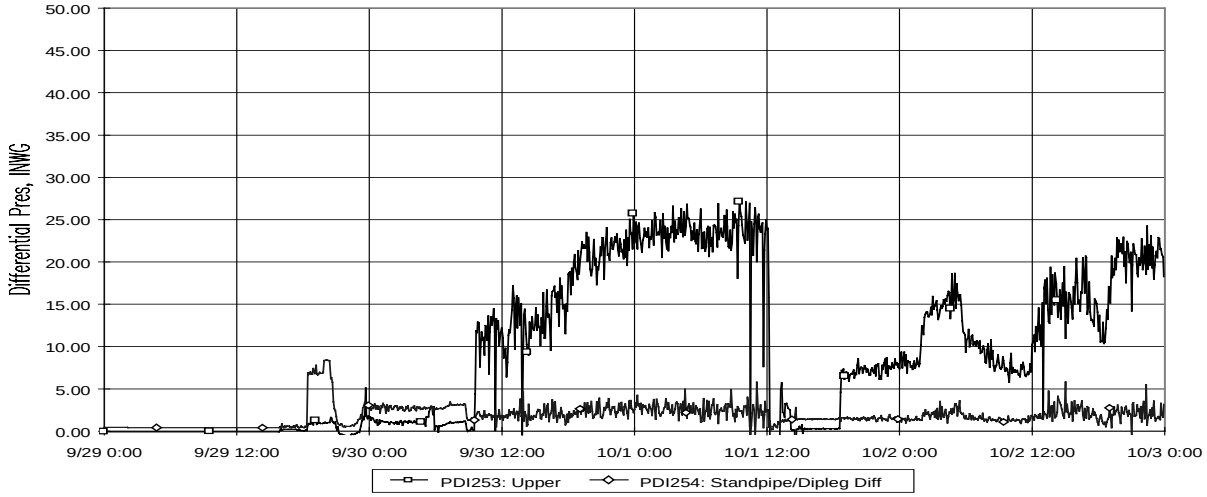

Figure 4.1.4.4-14 CY0201 Dipleg Differential Pressure Profiles

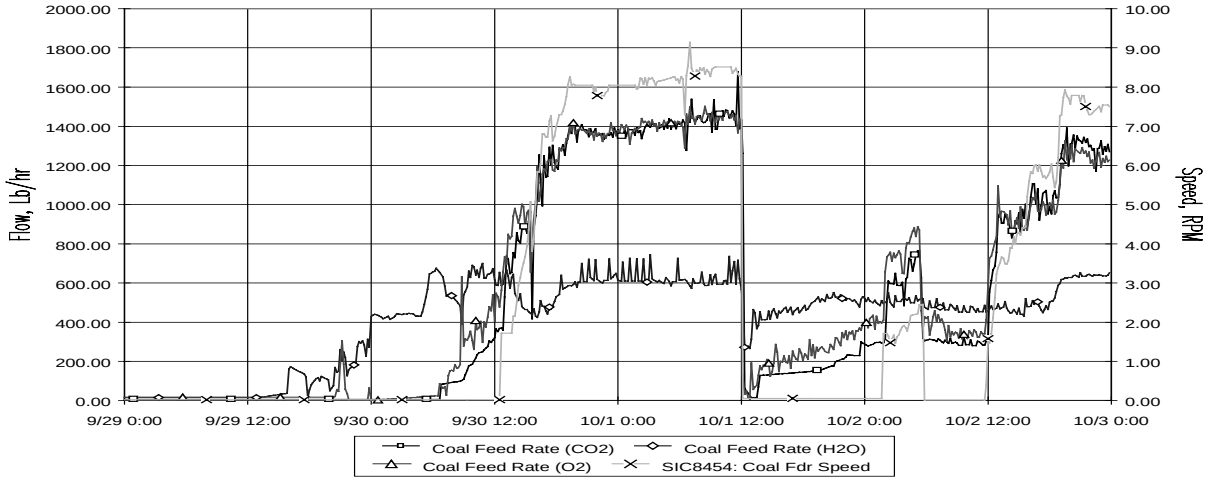

Figure 4.1.4.4-15 Coal Feed Rate Based on Gas Analysis

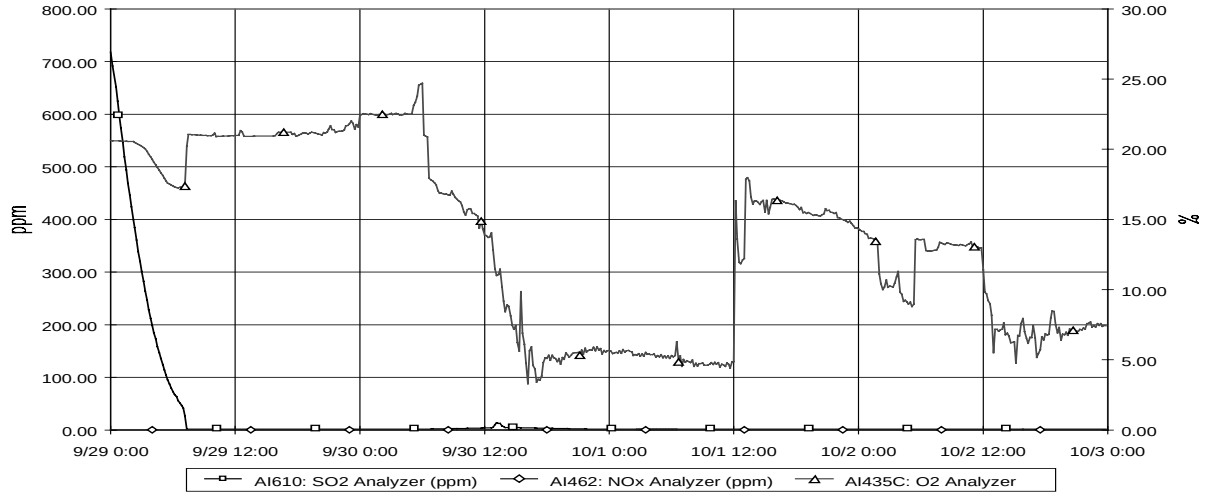

Figure 4.1.4.4-16 O_2, SO_2, and NO_x Analyzers

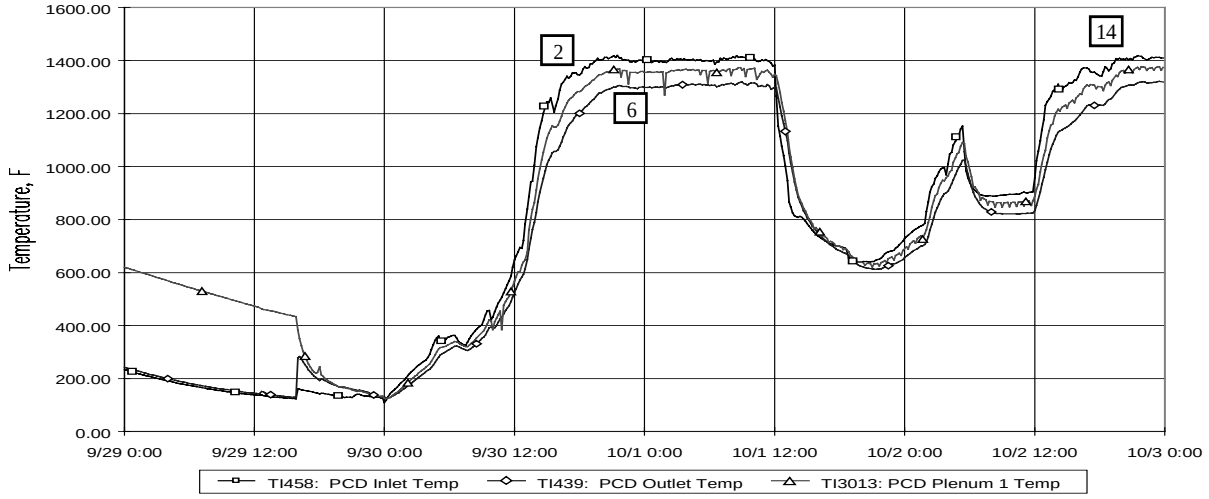

Figure 4.1.4.4-17 PCD Temperatures

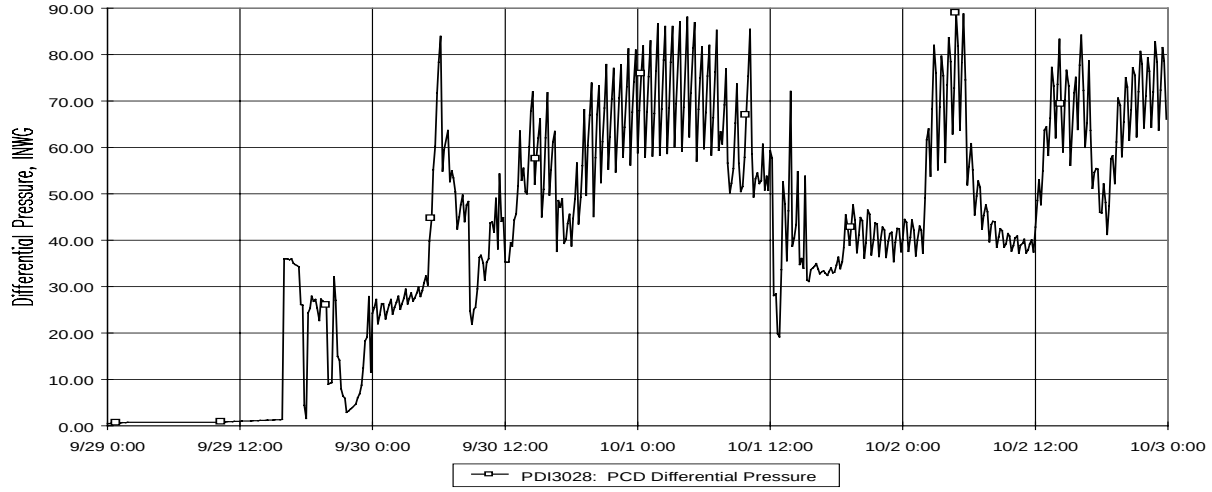

Figure 4.1.4.4-18 PCD Differential Pressure Profile

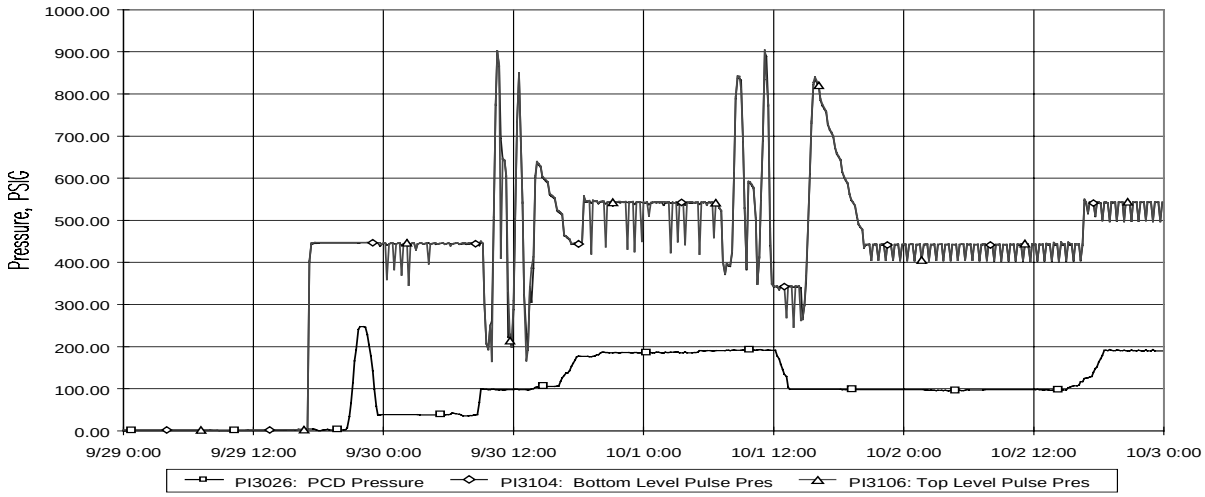

Figure 4.1.4.4-19 PCD Pressure and Pulse Pressure

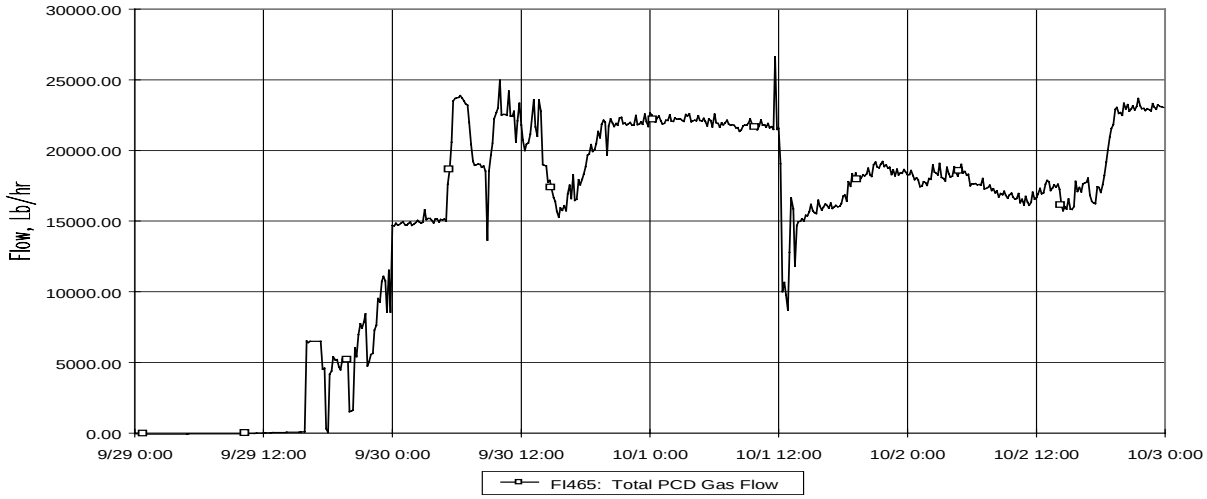

Figure 4.1.4.4-20 Gas Flow Through PCD

Section 4.1.4.4

Graphs 21 through 40

Test Run TC01D
October 3 through October 5, 1997

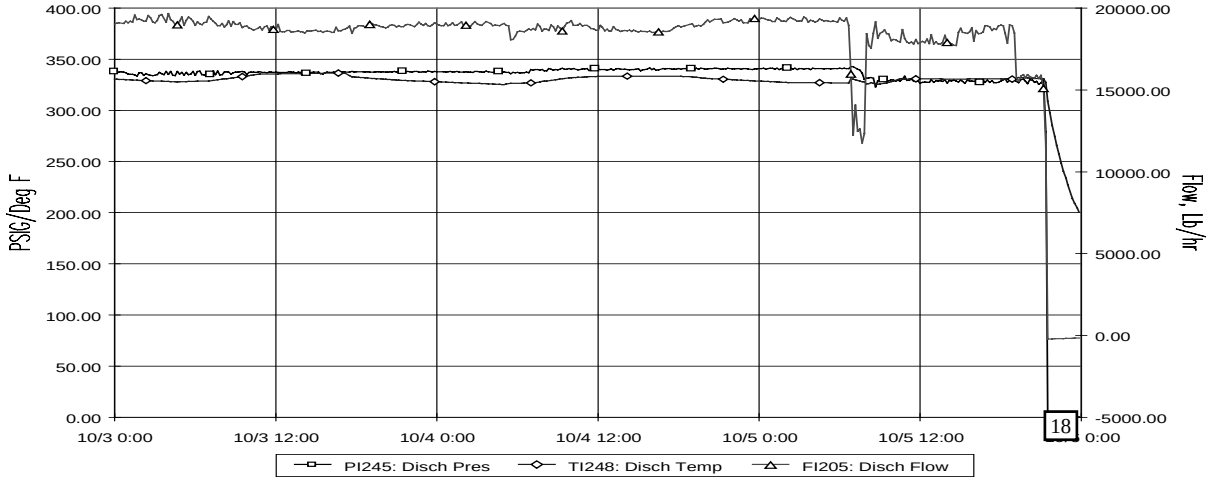

Figure 4.1.4.4-21 CO0201 System Profile

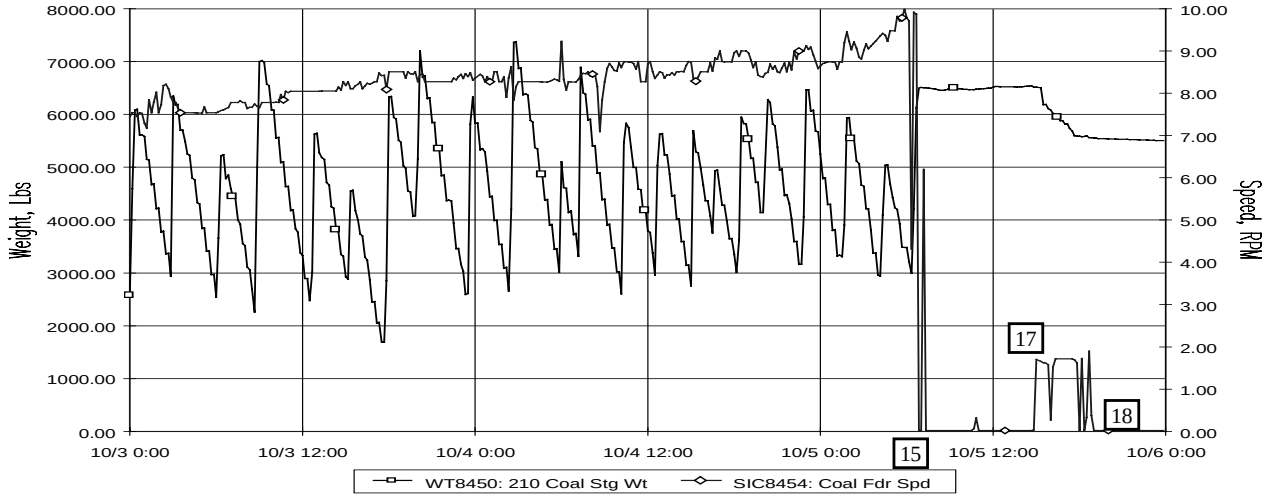

Figure 4.1.4.4-22 Coal Feed System Profile

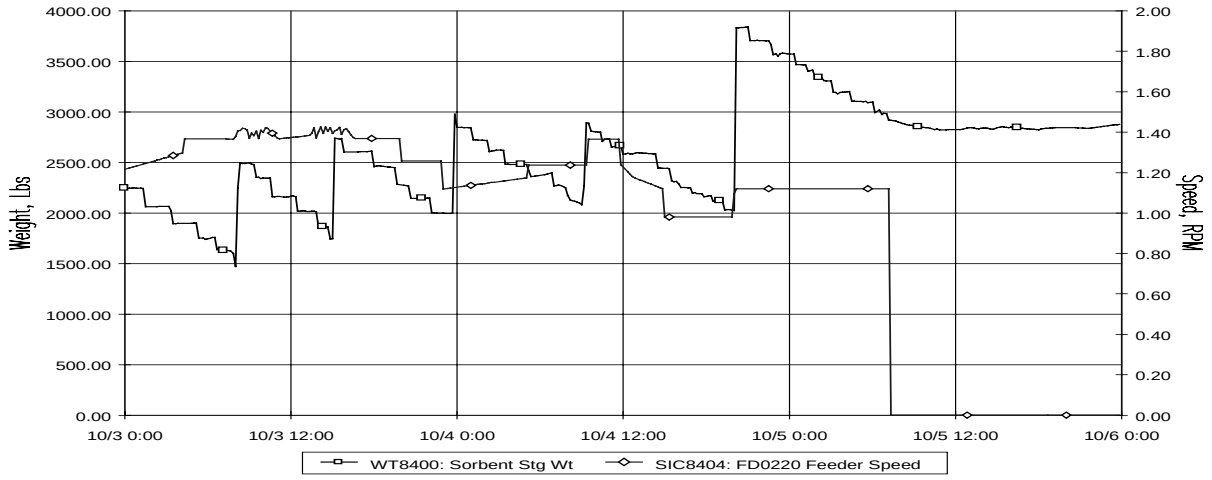

Figure 4.1.4.4-23 Sorbent Feed System Profile

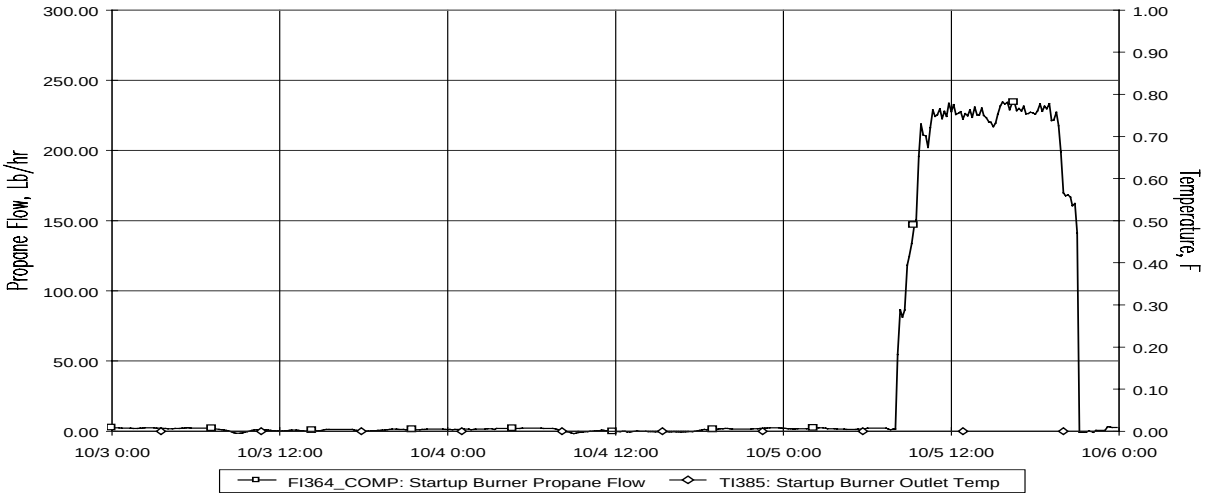

Figure 4.1.4.4-24 Start-Up Burner Flow/Temperature

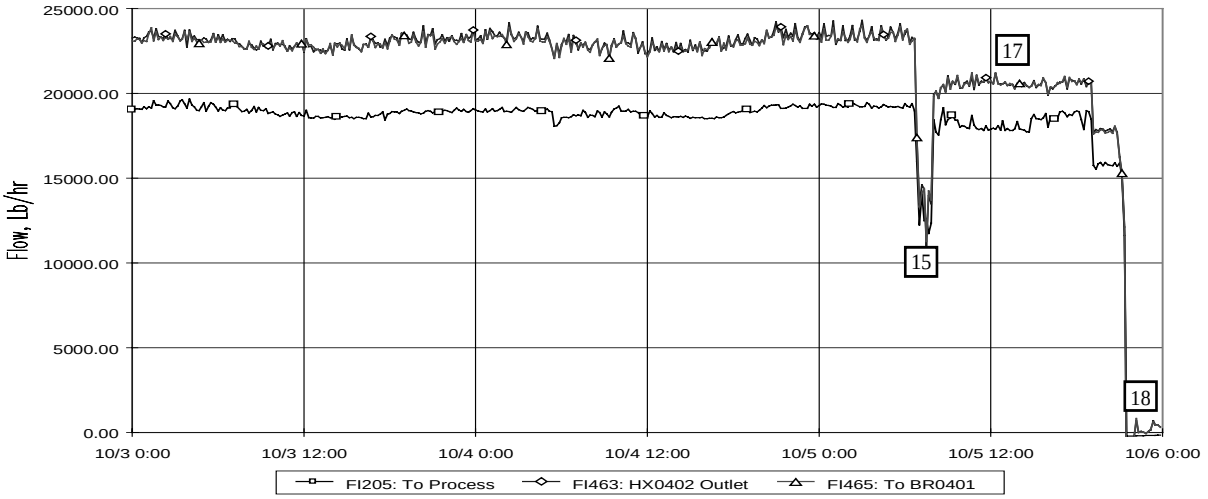

Figure 4.1.4.4-25 Total Gas In/Out Flow Rates

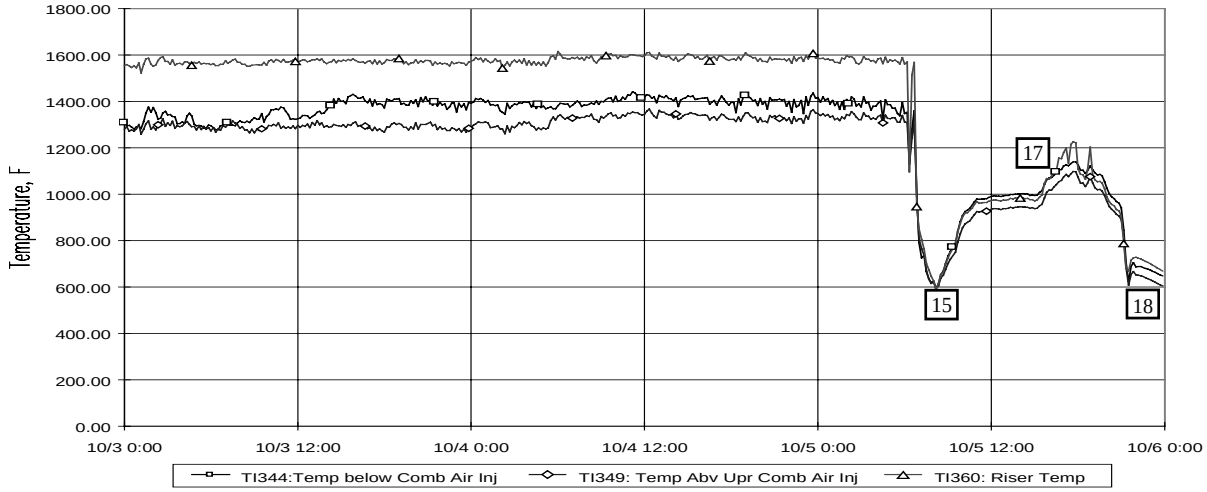

Figure 4.1.4.4-26 Reactor Mixing Zone and Riser Temperatures

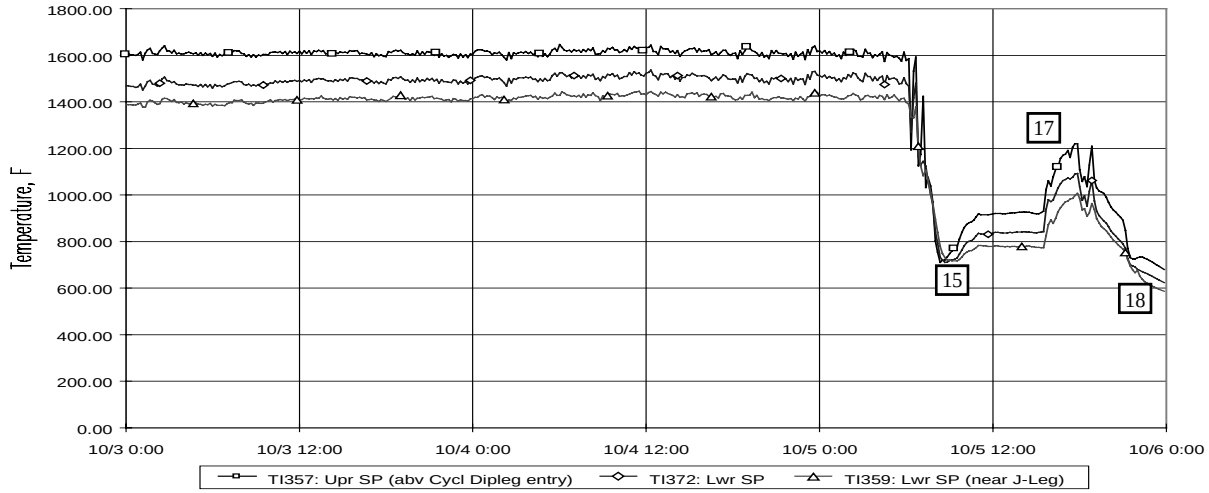

Figure 4.1.4.4-27 Standpipe Temperatures

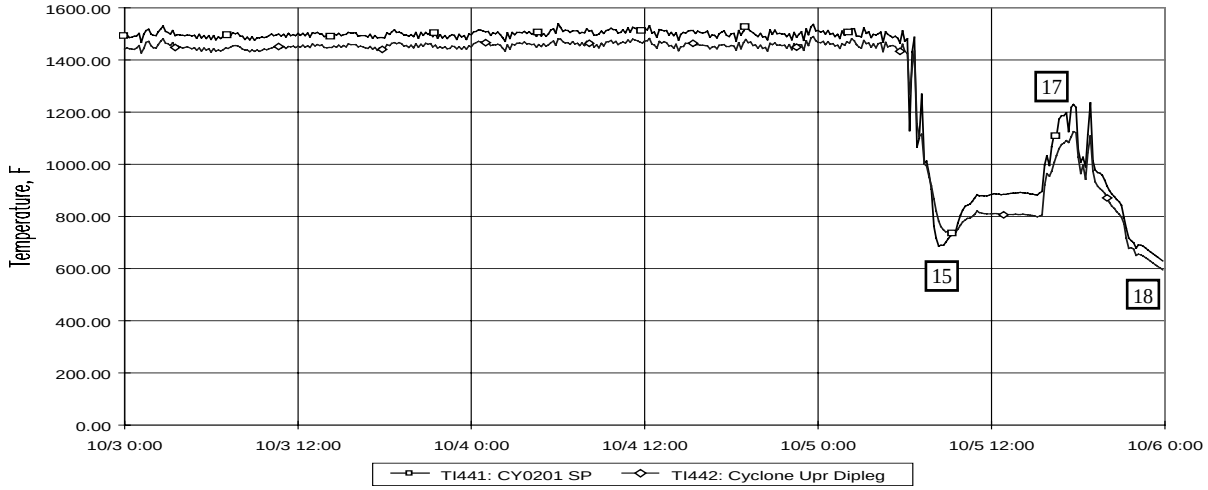

Figure 4.1.4.4-28 Cyclone Dipleg Temperatures

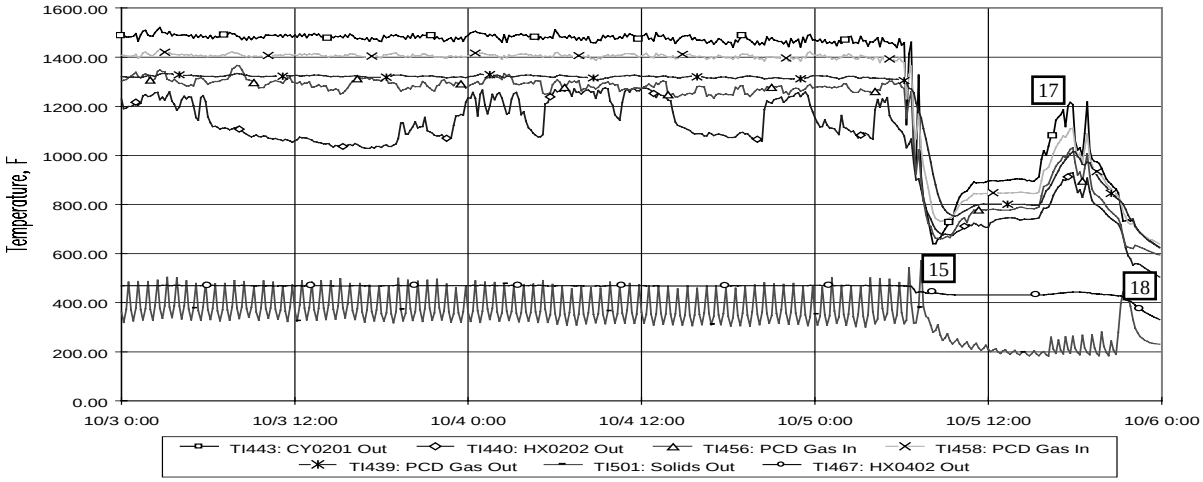

Figure 4.1.4.4-29 Temperature Profile Downstream of Reactor

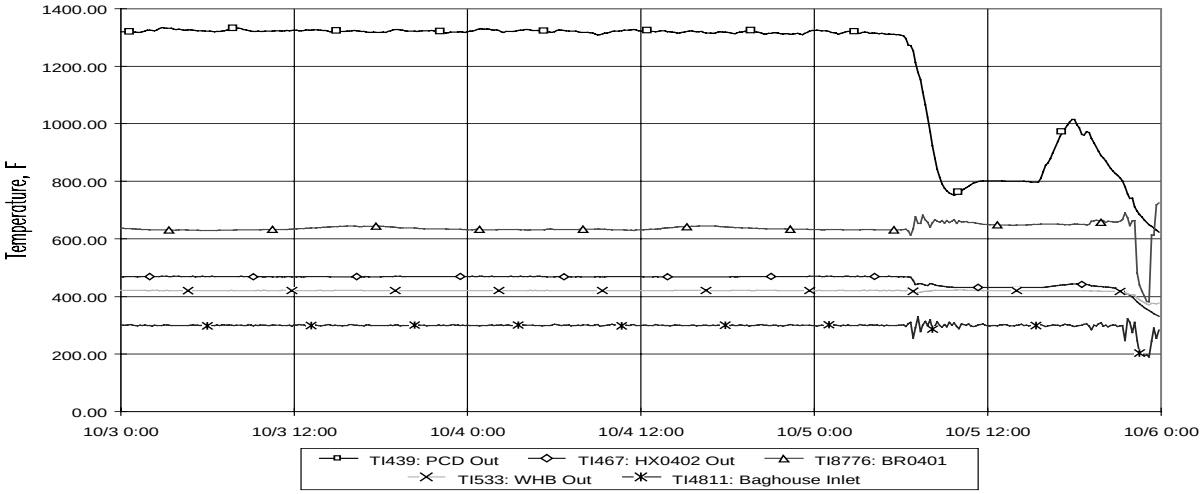

Figure 4.1.4.4-30 System Temperatures Downstream of PCD

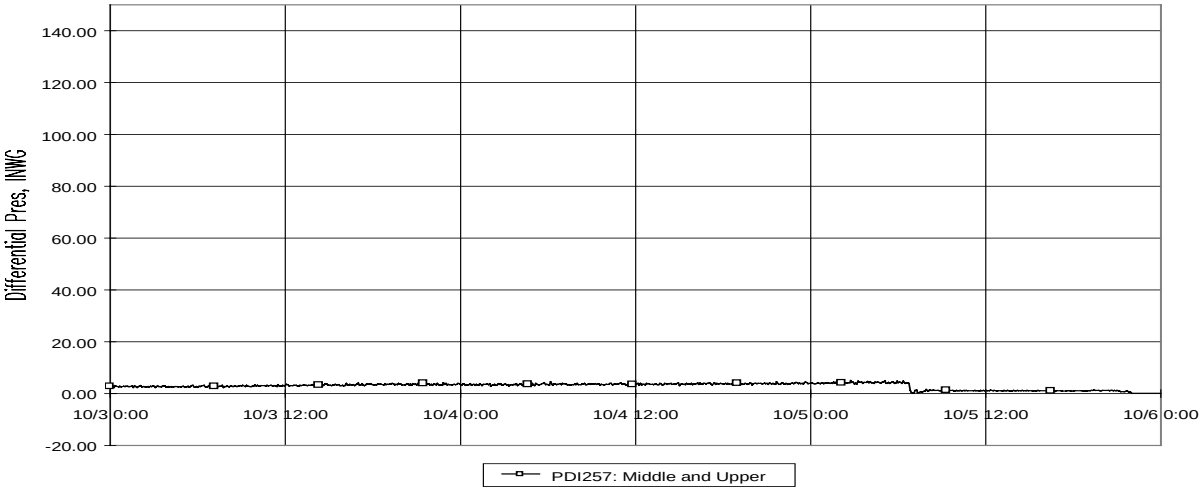

Figure 4.1.4.4-31 Mixing Zone Differential Pressure Profile

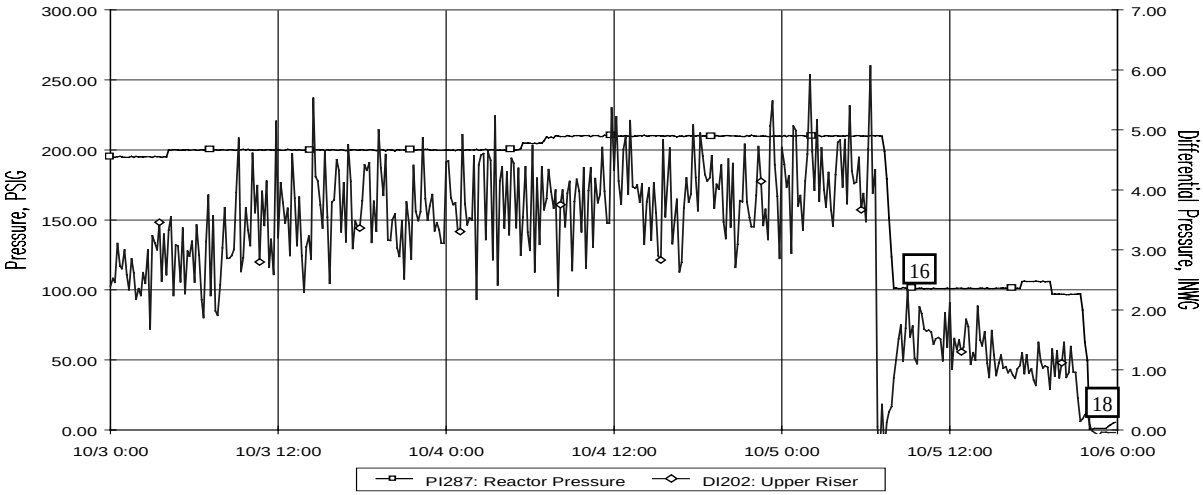

Figure 4.1.4.4-32 Reactor Pressure/Riser Differential Pressure Profiles

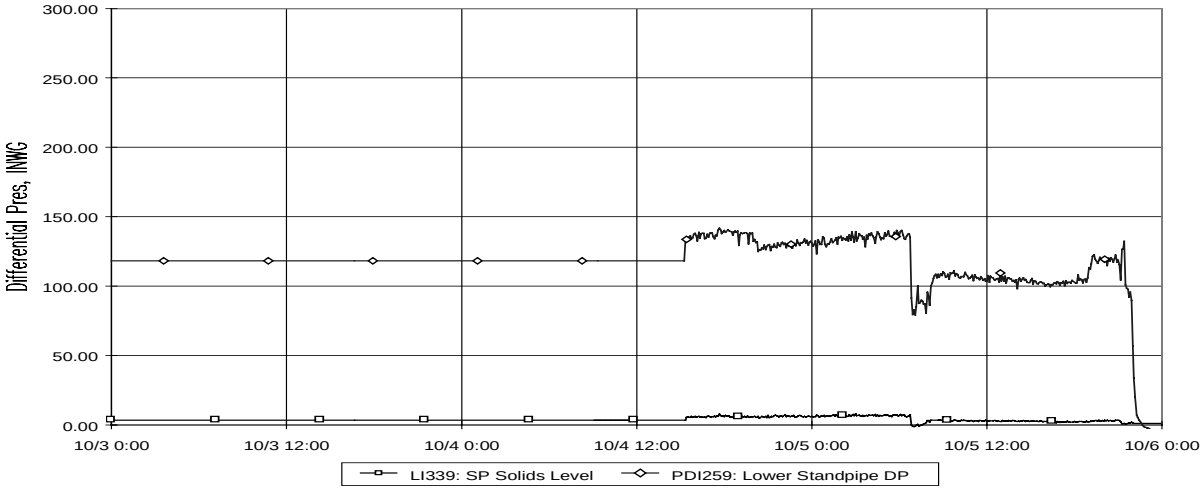

Figure 4.1.4.4-33 Standpipe Differential Pressure Profiles

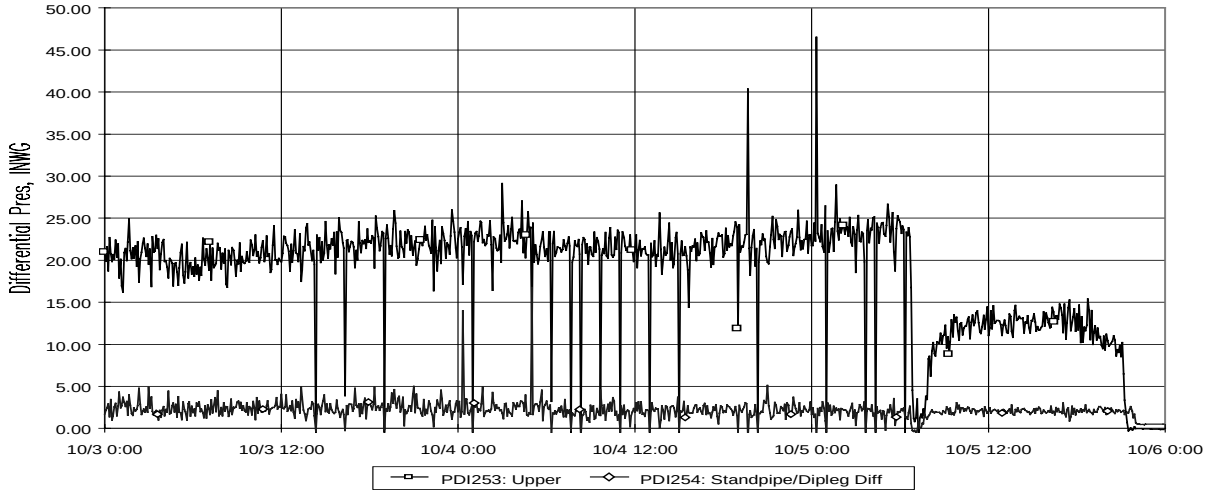

Figure 4.1.4.4-34 CY0201 Dipleg Differential Pressure Profiles

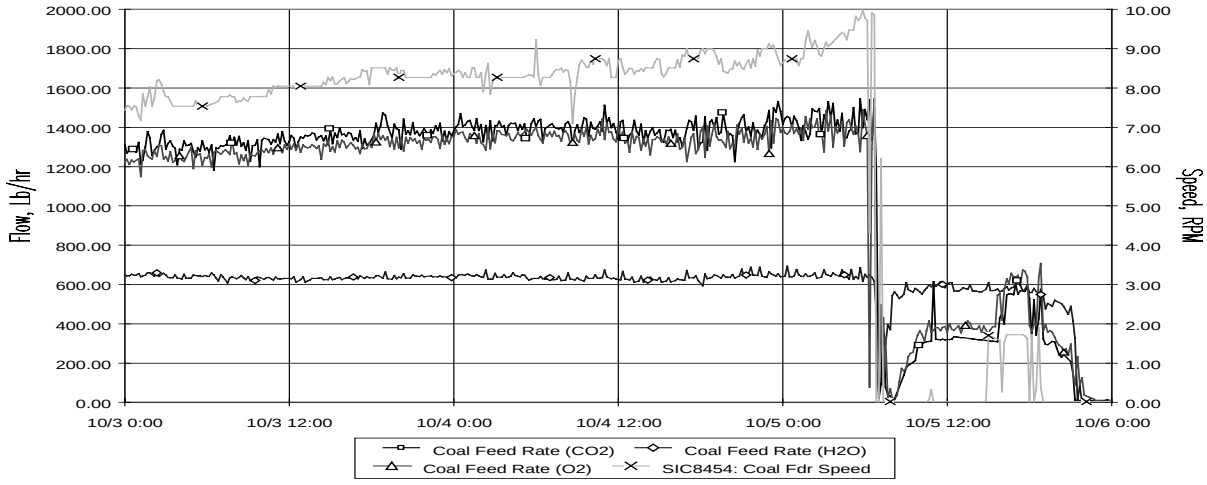

Figure 4.1.4.4-35 Coal Feed Rate Based on Gas Analysis

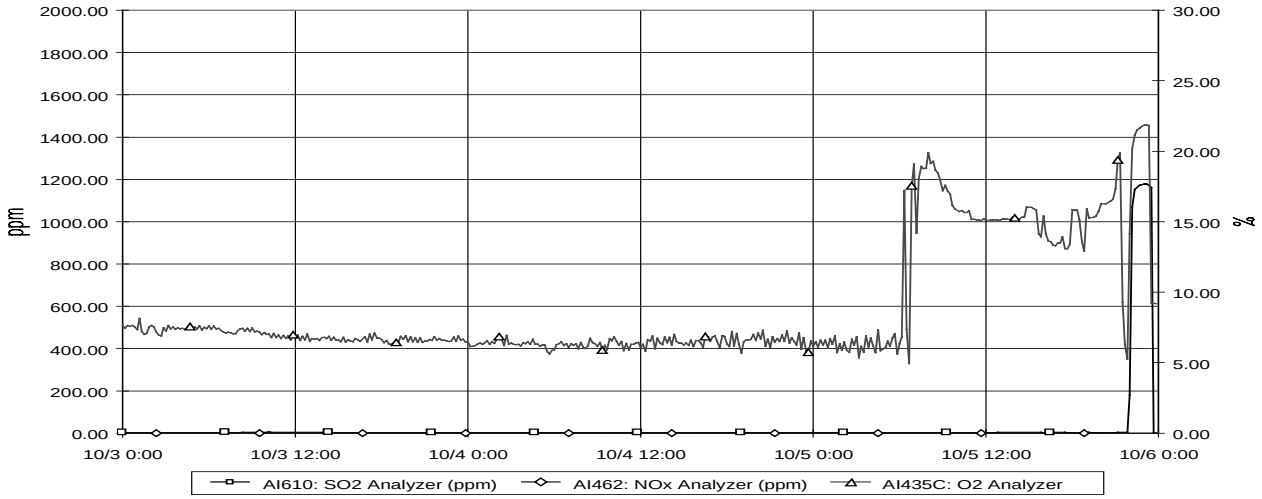

Figure 4.1.4.4-36 O_2, SO_2, and NO_x Analyzers

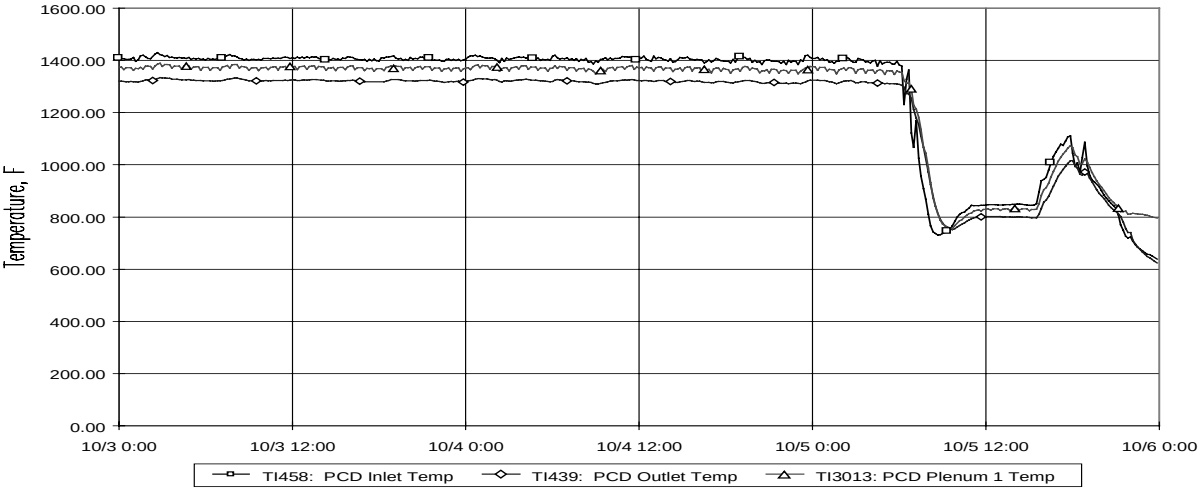

Figure 4.1.4.4-37 PCD Temperatures

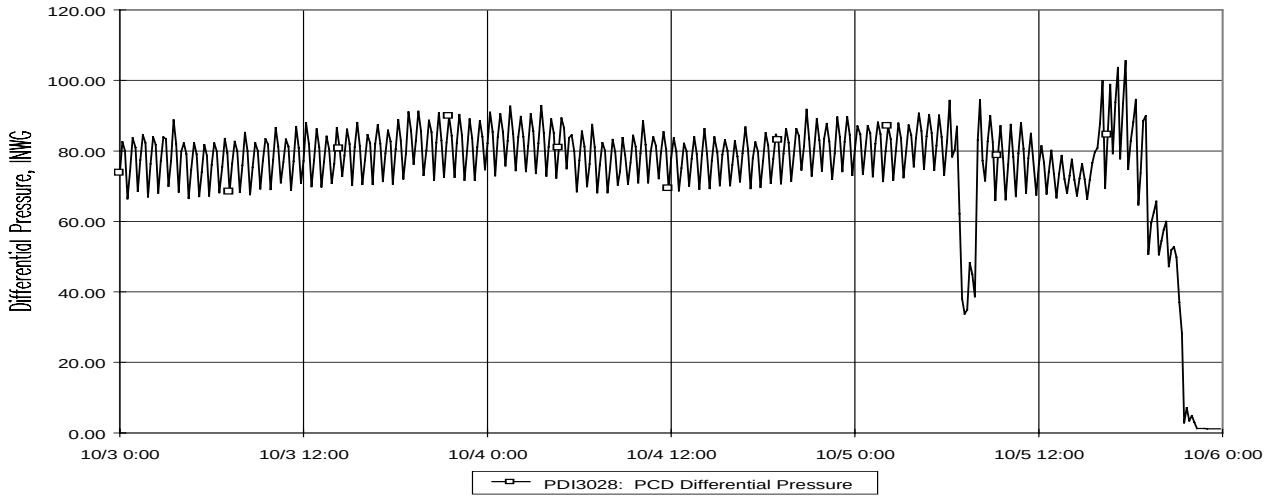

Figure 4.1.4.4-38 PCD Differential Pressure Profile

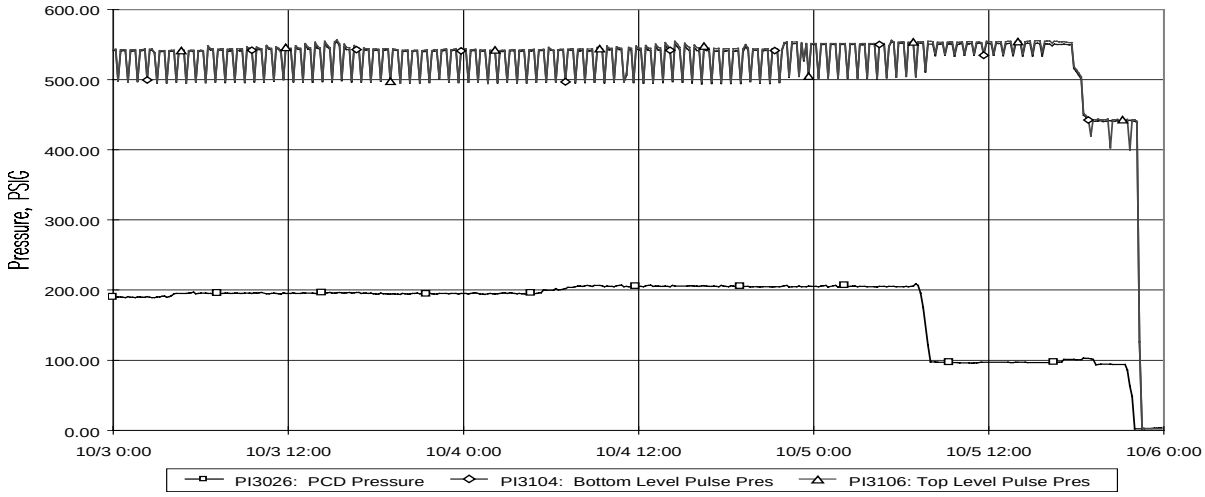

Figure 4.1.4.4-39 PCD Pressure and Pulse Pressure

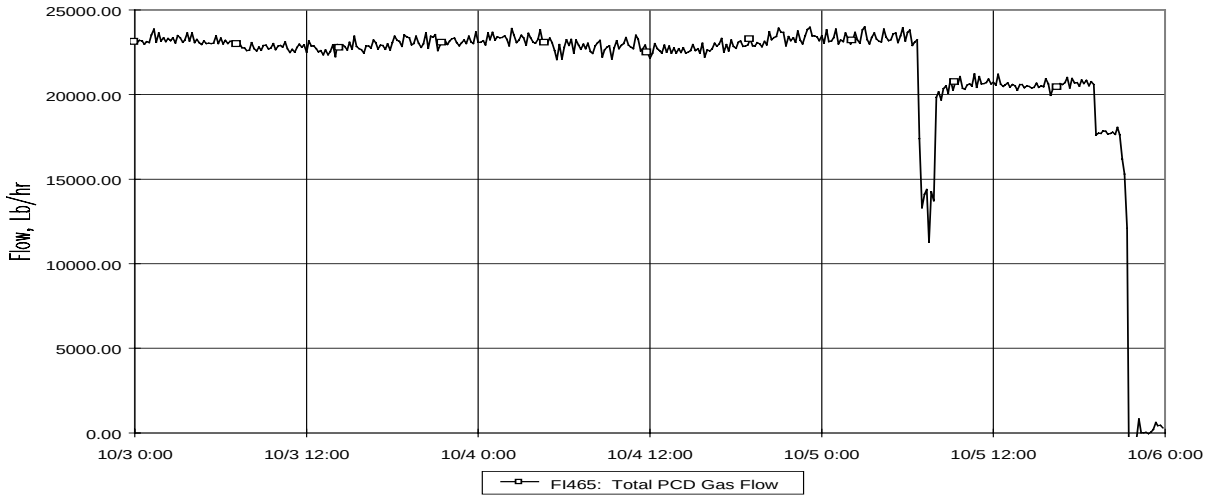

Figure 4.1.4.4-40 Gas Flow Through PCD

4.1.4.5 TC01E Test Run

Test run TC01E was conducted between October 8 and October 16, 1997. Operating plots are shown in figures 4.1.4.5-1 through -44.

During the outage from October 6 to 8, 1997, the following maintenance work was performed:

- The operation of the fines transport system (FD0520) bottom spheri valve was subjected to various tests in the maintenance shop for troubleshooting purposes. The contact switch was adjusted to ensure that the valve closes before the seal is inflated and the damaged seal was replaced. The FD0520 shuttle valves (XV8536 and XV8540) and the mechanical valve (ZV8531) were cleaned to improve their operation.

- The leaking tube bundle in the condensate subcooler (HX2004) was replaced.

- Mechanical work on the installation of the coal rejects recycle circuit was completed. The rejects will be directly sent into the coal mill instead of the crushed coal silo to improve the coal grind consistency.

- The start-up burner main gun was pulled and cleaned.

- The insert and the flow indicator for the PT301 pressure transmitter were reinstalled.

- The six orifices in the FD0210 and FD0220 vent purge lines were reinstalled and the throttling valve was removed.

- An additional strand of packing was added to the FD0502 packing.

TC01E Test Run Chronology

- The leak test was conducted on October 8 and 9, 1997. Leaks were found and repaired around tubing fittings on both the top and bottom FD0520 spheri valves. Start-up was delayed when the safety valve on the propane vaporizer lifted due to a swing in the pressure and would not reseat. After replacing the safety valve the thermal oxidizer was lit at about 01:45 on October 10, 1997.

- The main air compressor (CO0201) was started about 2 hours later and the start-up burner was lit at 04:20 (event 1, figure 4). The addition of recycled solids from CCT6 started at 09:20 from FD0220. The data acquisition system was off-line for about 1 hour (event 2, figures 1 through 10). The cyclone dipleg differential pressure reading (PDT253) had dropped from 5.0 to 0.5 in H_2O. At 12:15 PDT253 still read 0.5 in H_2O (event 3, figure 14). The riser differential pressure was also low and the bottom standpipe temperatures were dropping, indicating that there was little or no solids circulation through the reactor J-leg. Skin temperatures were taken to make sure that the mixing zone and lower standpipe temperature difference did not exceed

130°F. Since the solids circulation in the reactor was low it was not sufficient to prime the cyclone dipleg. The standpipe and dipleg aerations were adjusted and the burner flows were also adjusted in an attempt to increase circulation and solids flow through the dipleg. There were no immediate improvements in the operation but as sand was added the standpipe level started increasing, which in turn increased the circulation. PDI253 started fluctuating between zero and 5.0 in H_2O before stabilizing at about 13:45. At almost the same time solid circulation started through the standpipe and continued to increase (event 4, figures 12 through 14).

- Coal feed was started around 16:45 (event 5, figures 2 and 5 through 10) but the FD0210 system soon started having problems. The middle spheri valve failed to open during the transfer cycle due to a loose electrical plug in the cabinet. Coal feed started again after the problem was corrected at about 20:05, but problems with the coal feeder continued. The system would cycle yet very little coal was transferred into the dispense vessel, forcing shutdown of the system at 04:15 on October 11, 1997 (event 6, figures 2 and 5 through 10). Several things were done to address the coal feeder problems but none were successful. Fines had apparently accumulated in the transfer system during test run TC01D and were bridging at the top of the dispense vessel or at the bottom of the lock vessel. Once all the fine coal was fed by repeated purging, venting, and blowing through the system the feeder returned to normal operation. The BR0201 was shut down at 18:00 (event 7, figure 4). By 20:15 the reactor pressure was 200 psig (event 8, figure 12) and by 22:00 the PCD plenum temperature reached 1,350°F (event 9, figure 18).

- On October 12, 1997, the spent solids screw cooler (FD0206) was run periodically to control the solids level in the reactor. The FD0510 plugged on a few occasions but this did not affect the process stability. The plugging was cleared each time and the system was put back on-line.

- On October 13, 1997, SRI sampled the PCD inlet/outlet between 8:45 and 11:25. At about 09:30 the PV287 stem started vibrating when the PCD back-pulsed. The reactor pressure was decreased from 210 to 205 psig and then increased to 216 psig. The increase in pressure decreased the temperature at the HX0402 outlet by about 5°F (TI467), which made the vibration stop; however, the PV287 vibration caused a leak around the stem. Later, the FD0520 bottom spheri valve failed to close within the acceptable time limit so the torque on the torque arm was increased and the cycle initiation to seal the pressurization timer was increased; however, this did not correct the problems. Therefore, FD0520 was isolated for maintenance. The FD0520 was returned to service at about 16:10. The coal feeder tripped at 23:00 (event 10, figures 24 and 28 through 30) but was restarted without any problems.

- Since the SO_2 analyzer was reading low throughout the test run other methods of sampling and analysis were attempted to confirm the readings. On October 14, 1997, at 09:15, a bomb sample of process gas was taken at the HX0402 outlet for SO_2 analysis. Another process gas sample was analyzed with a portable zero-to-5-ppm "draeger" tube but SO_2 was not detected. At 09:30 the FD0520 exit line

plugged, causing ash to build up in the PCD (event 11, figure 39). Consequently, dolomite feed and reactor solid circulation were reduced. The FD0520 line was unplugged around 13:00 and the FD0520 was placed back in service.

- At about 15:00 a high-frequency vibration developed in the PV287 stem. For the next 2 hours a number of variables on the reactor were changed to eliminate the vibration. Finally, the instrument air to the PV-287 diaphragm was instantaneously closed and the air was bled off the regulator. This caused the valve to quickly close and reopen and the vibration stopped.

- At 18:00 circulation through the reactor and reactor temperatures were increased (event 12, figures 28, 30, and 34). The purpose was to increase carryover to PCD so that changes to the screw cooler (FD0502) HTF flows could be evaluated. The HTF flows were reduced in an attempt to maintain a higher solids-exit temperature to prevent condensation from occurring. The theory was that the FD0520 exit line was plugging due to wet solids. Coal was lost briefly at about 20:35 (event 13, figures 28 through 30). Throughout the night the FD0520 bottom spheri was manually closed and the system also plugged several times. The HTF system cooling fans were turned off and the temperature of the HTF system was set to 240°F to increase the ash temperature at the FD0502 exit.

- On October 15, 1997, from 09:15 to 13:20, SRI sampled the PCD loading. A gas bomb sample was taken at the PCD inlet probe to detect the presence of SO_2 since the online gas analysis system was not detecting any. The data acquisition system was lost at 15:30 for about 10 minutes. At about 21:15 the PV287 stem began to vibrate again. As before, reactor conditions were varied in an attempt to stop the vibrations. The induced pressure swings to stop the PV287 stem vibrations caused a carryover of solids to the PCD. The FD0520 bottom spheri valve seal failed at 22:50, so a shutdown of the process was initiated (event 14, figures 23, 24, and 27 through 30).

TC01E Test Run Observations

Before the start of TC01E the FD0520 bottom spheri valve assembly was subjected to a number of tests in the maintenance shop to determine the modes of seal failure. The rejects recycle line was redirected to the mill (instead of to the crushed coal silo) in the coal grinding circuit, which improved the grind consistency.

During this test period coal feed was lost once due to low and eventually no transfer of coal into the FD0210 dispense vessel. Repeated purging, venting, and blowing through the lock and dispense vessels finally restored the coal feed system to its normal operation. Apparently, a batch of fine coal through the FD0210 system caused the problems. Once this batch of fine coal was either drained or fed into the reactor the coal feed system operated without any problems.

There were periodic problems with the pressure letdown valve plug stem vibrating at high frequencies. Initially the vibrations were stopped by rapidly moving the actuator, but this technique did not work at all times. The vibrations were the result of flow-induced resonance.

At the suggestion of valve manufacturer a back pressure of 10 psig on the pressure letdown valve was created by inserting a preforated disk on the downstream side of the valve. This did not solve the problem; the manufacturer suspected that the valve was incorrectly sized for the operation.

Since the SO_2 levels detected by the online analyzer were so very low, bomb samples were collected at the PCD inlet and at HX0402 outlet to confirm the observed SO_2 measurements. (See section 4.2.4 for more details.)

The process was shut down due to a failure of the fines transporter system bottom spheri valve seal. There were periodic problems with this valve failing to close before the seal gave up. A total of 118.75 hours on coal was achieved and 61.7 tons of coal were fed.

Section 4.1.4.5

Graphs 1 through 22

Test Run TC01E
October 8 through October 12, 1997

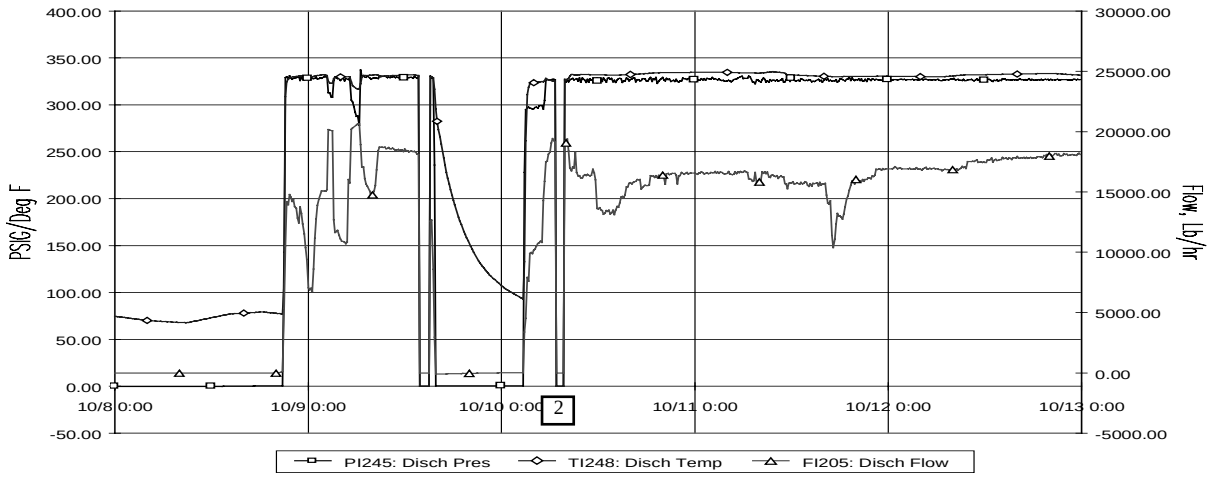

Figure 4.1.4.5-1 CO0201 System Profile

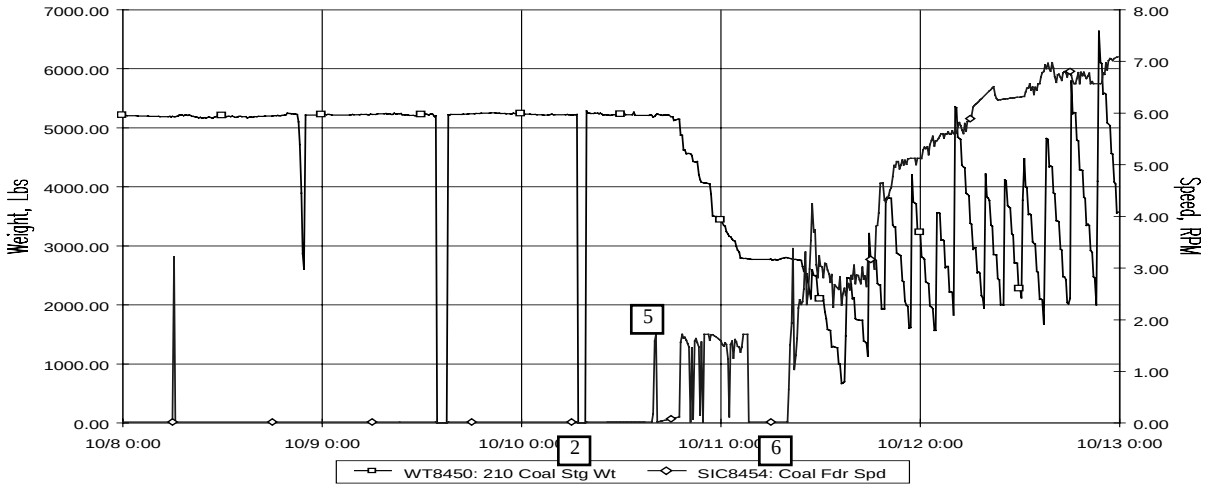

Figure 4.1.4.5-2 Coal Feed System Profile

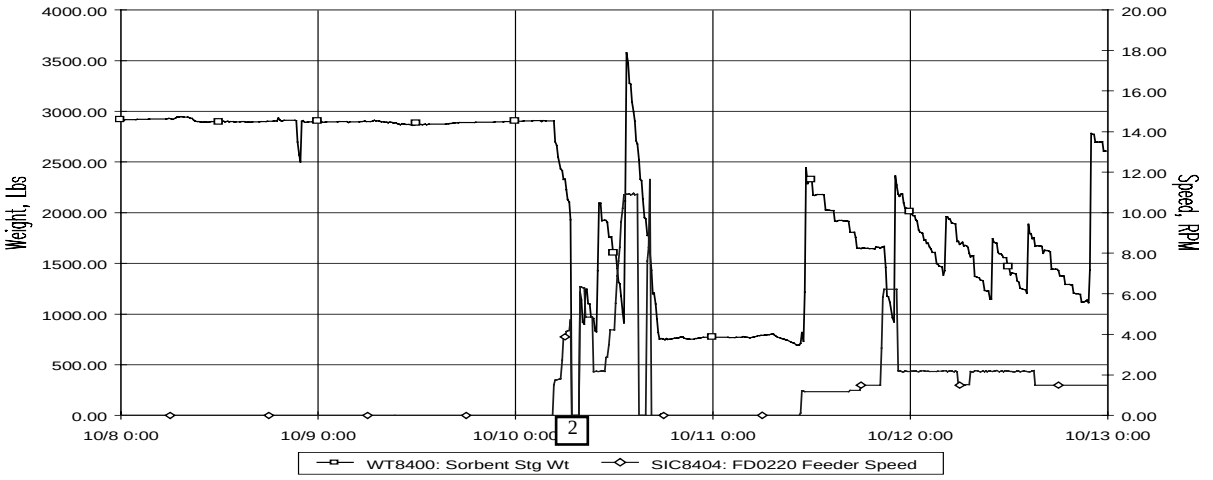

Figure 4.1.4.5-3 Sorbent Feed System Profile

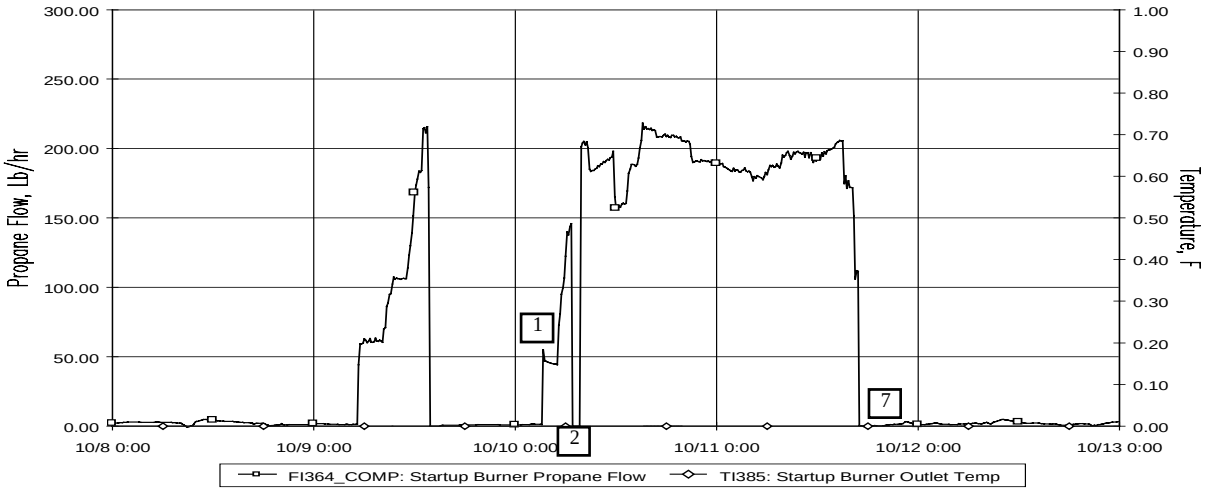

Figure 4.1.4.5-4 Start-Up Burner Flow/Temperature

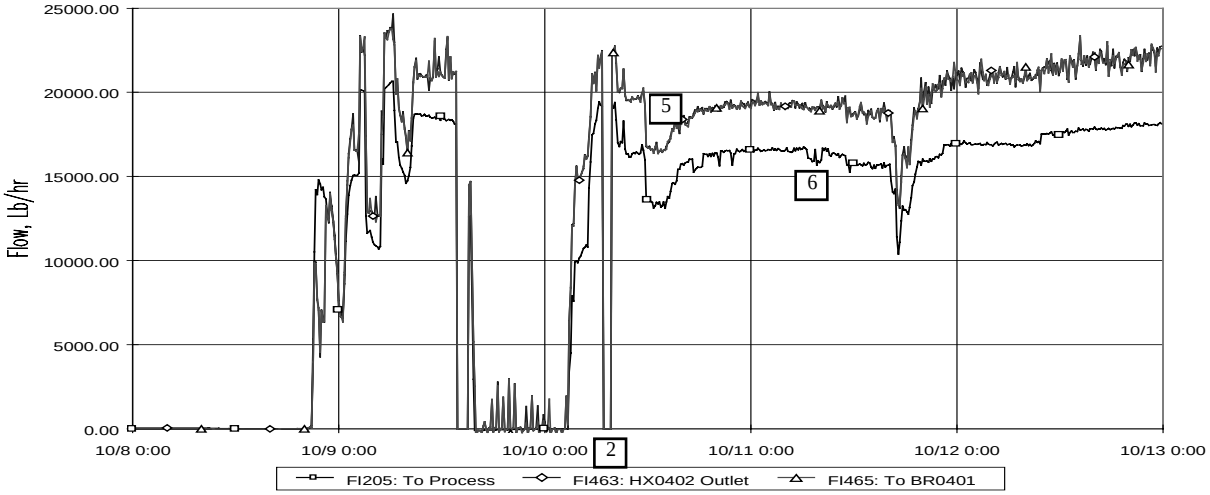

Figure 4.1.4.5-5 Total Gas In/Out Flow Rates

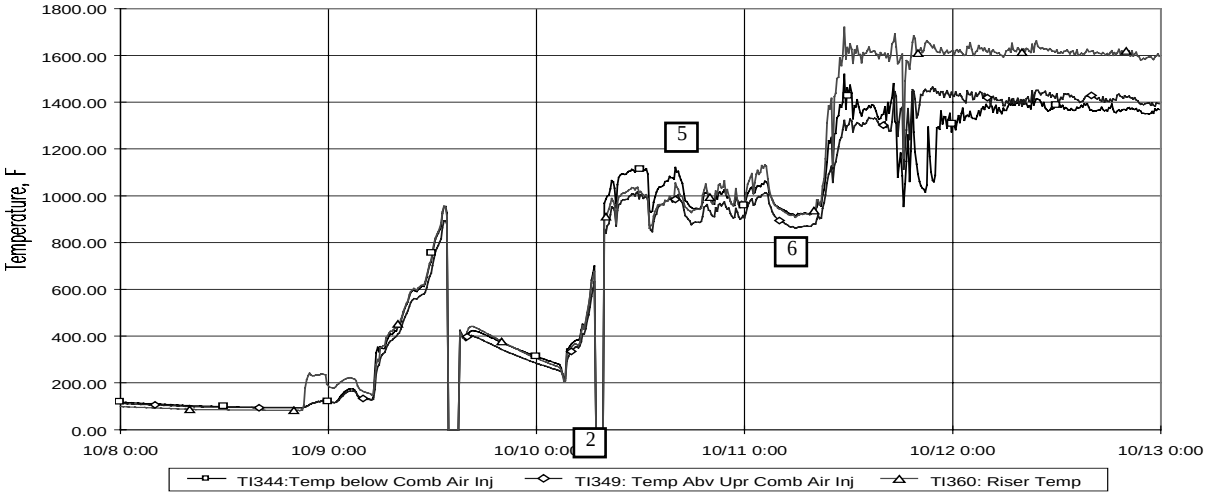

Figure 4.1.4.5-6 Reactor Mixing Zone and Riser Temperatures

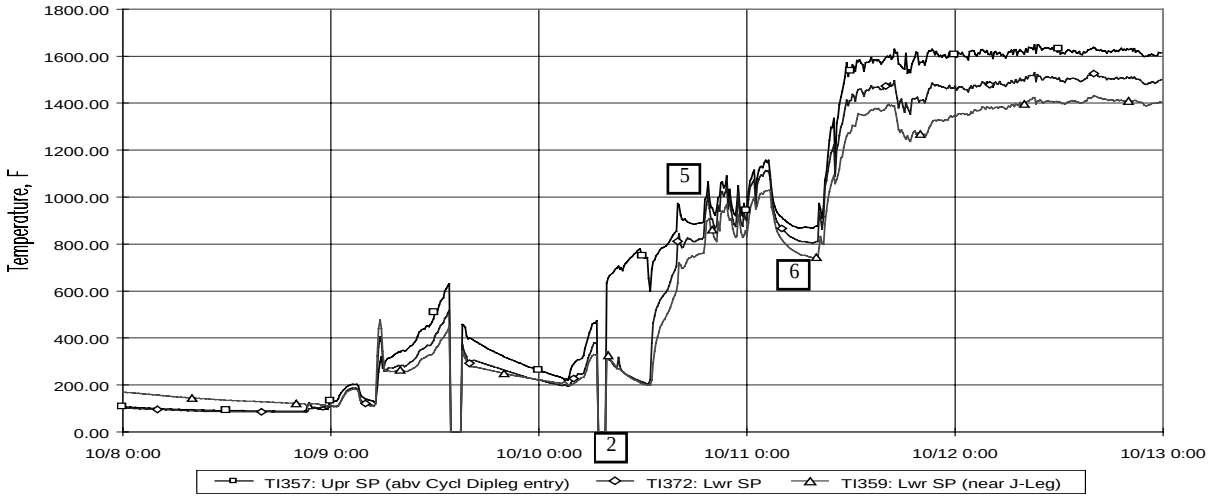

Figure 4.1.4.5-7 Standpipe Temperatures

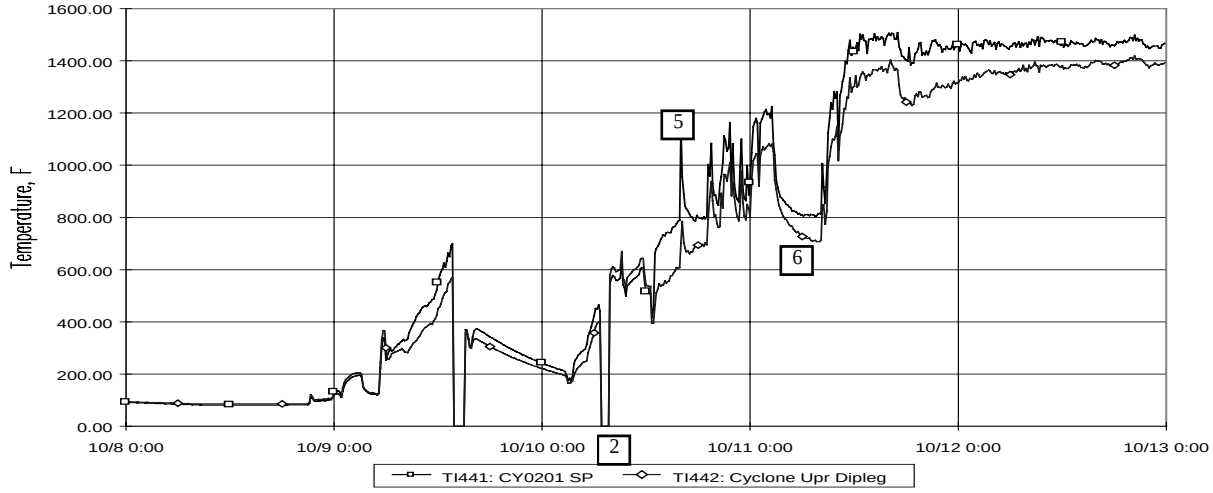

Figure 4.1.4.5-8 Cyclone Dipleg Temperatures

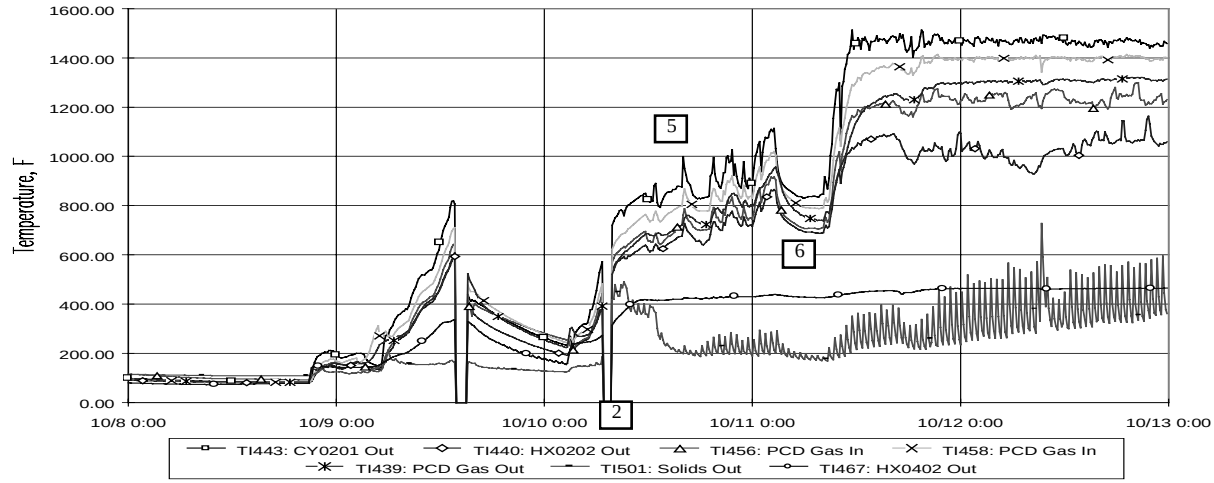

Figure 4.1.4.5-9 Temperature Profile Downstream of Reactor

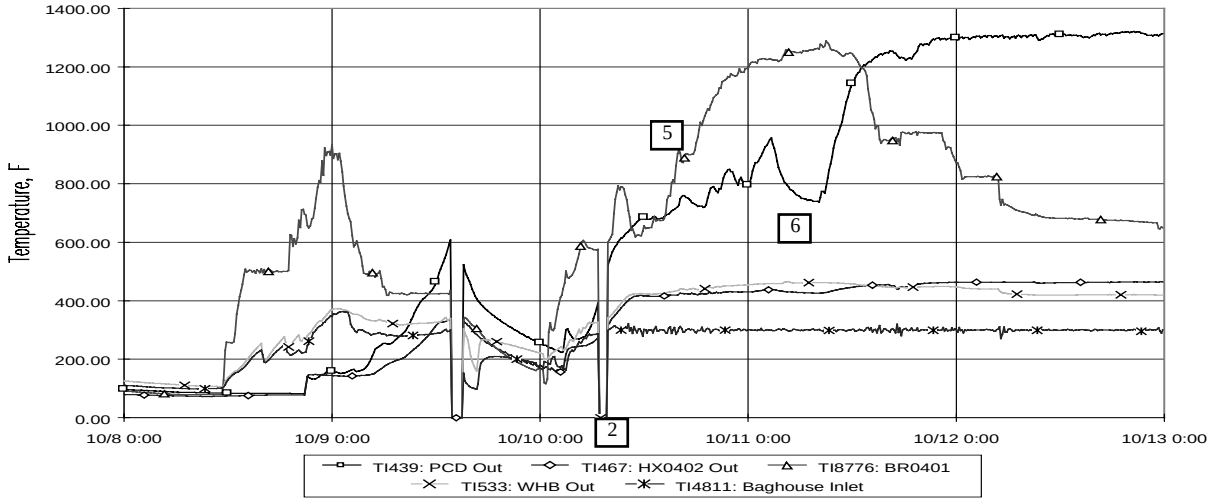

Figure 4.1.4.5-10 System Temperatures Downstream of PCD

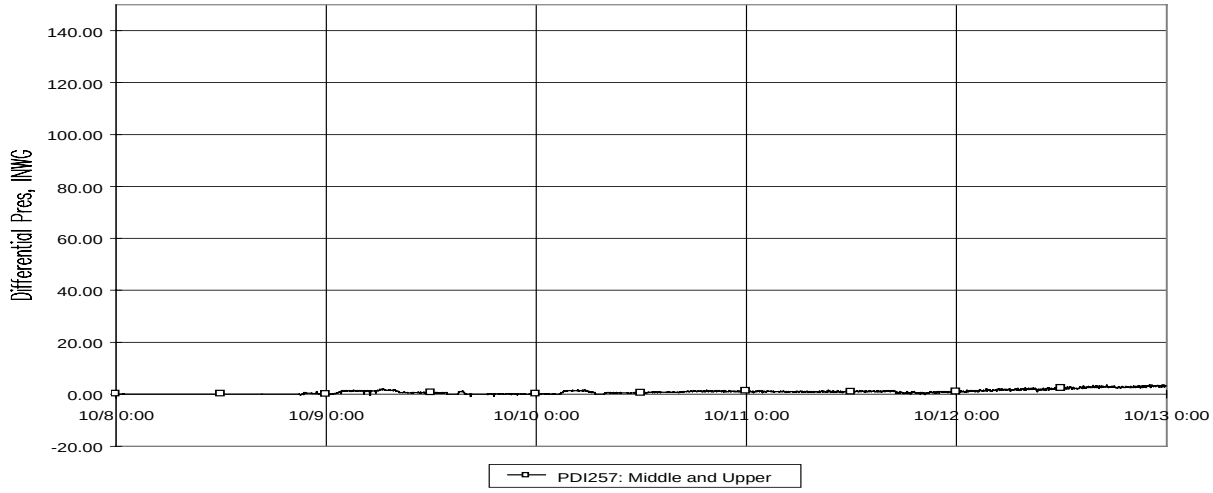

Figure 4.1.4.5-11 Mixing Zone Differential Pressure Profile

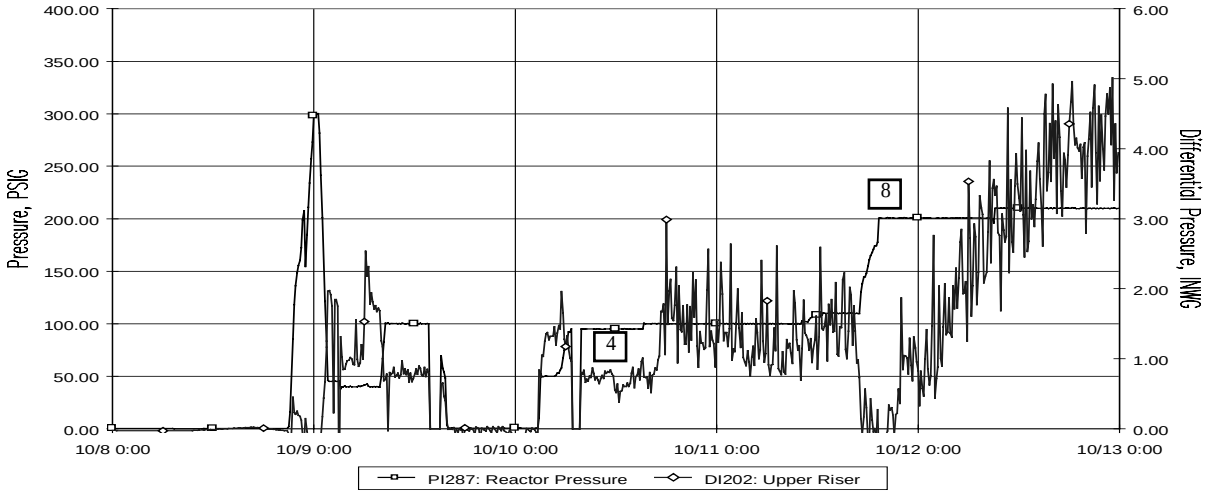

Figure 4.1.4.5-12 Reactor Pressure/Riser Differential Pressure Profiles

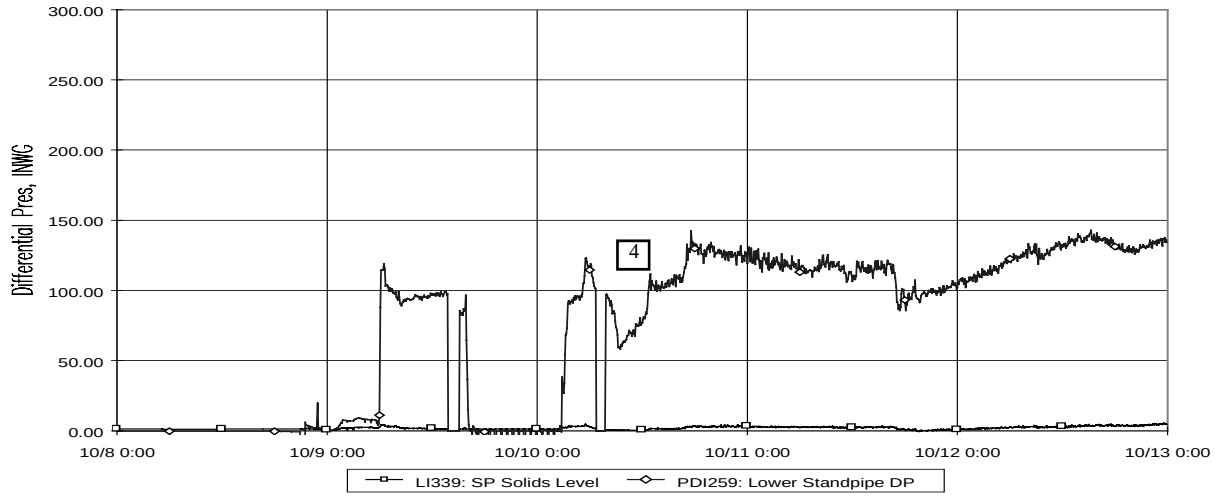

Figure 4.1.4.5-13 Standpipe Differential Pressure Profiles

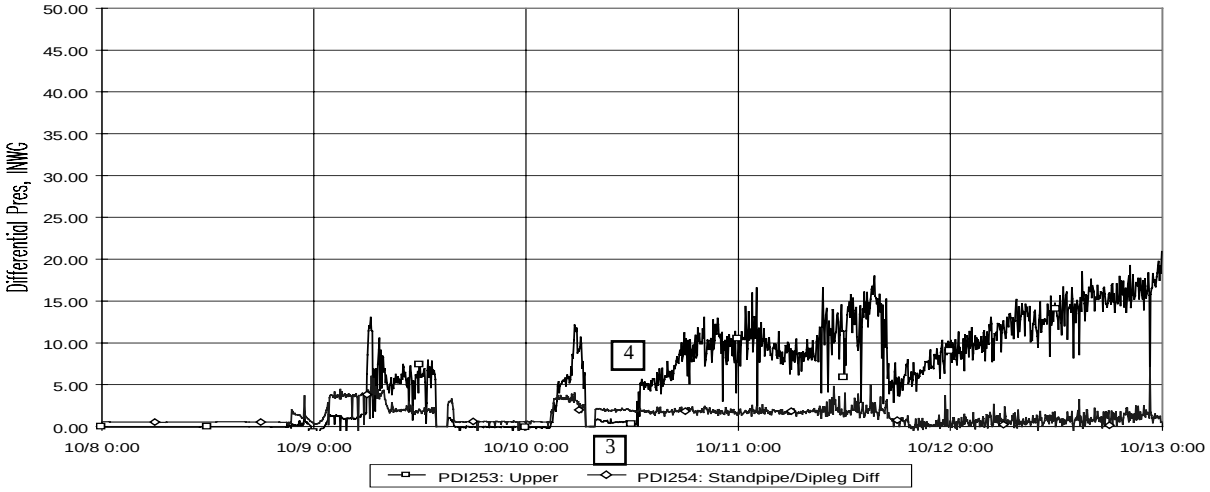

Figure 4.1.4.5-14 Cyclone Dipleg Differential Pressure Profiles

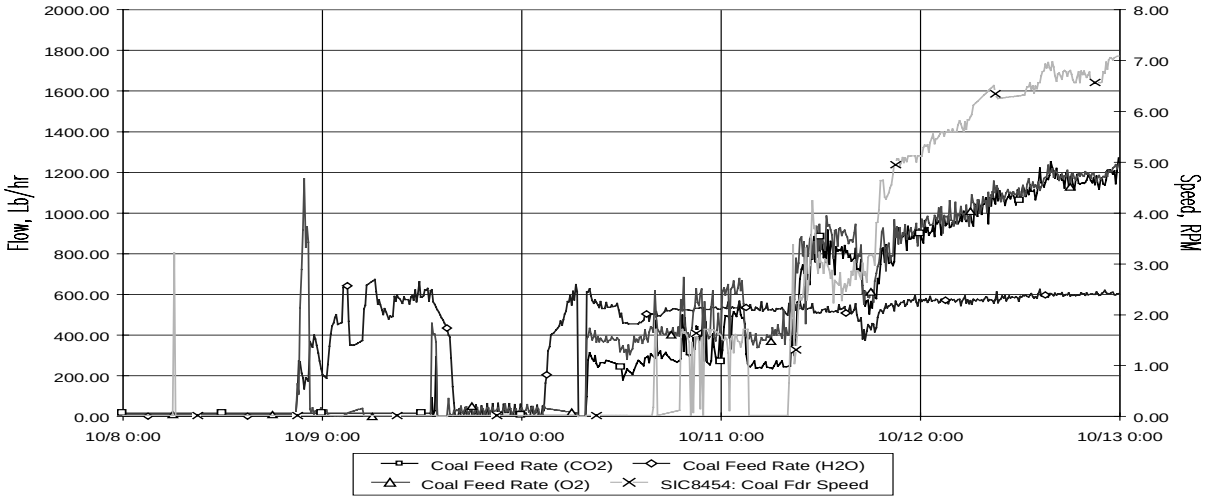

Figure 4.1.4.5-15 Coal Feed Rate Based on Gas Analysis

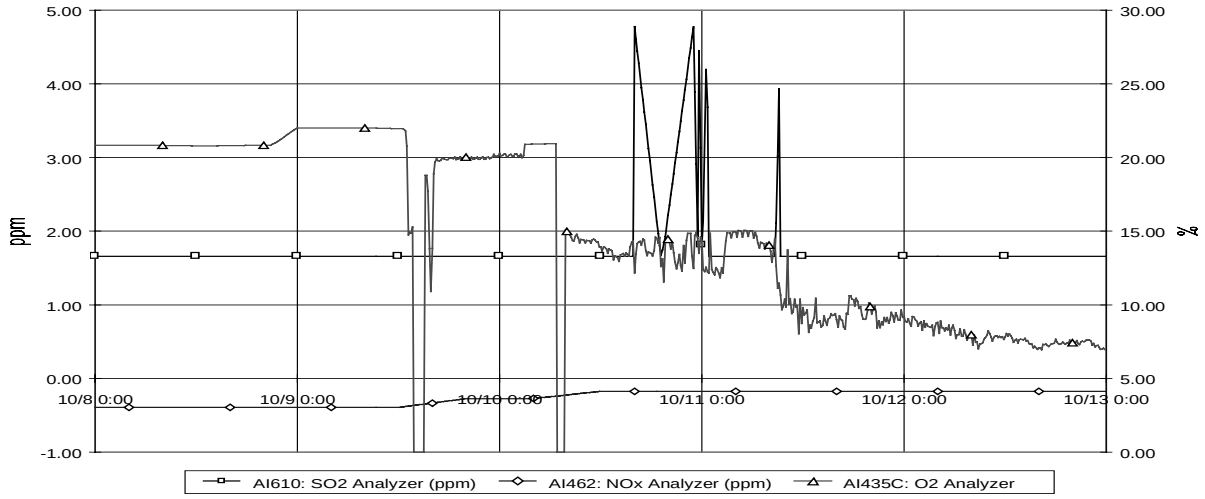

Figure 4.1.4.5-16 O_2, SO_2, and NO_x Analyzers

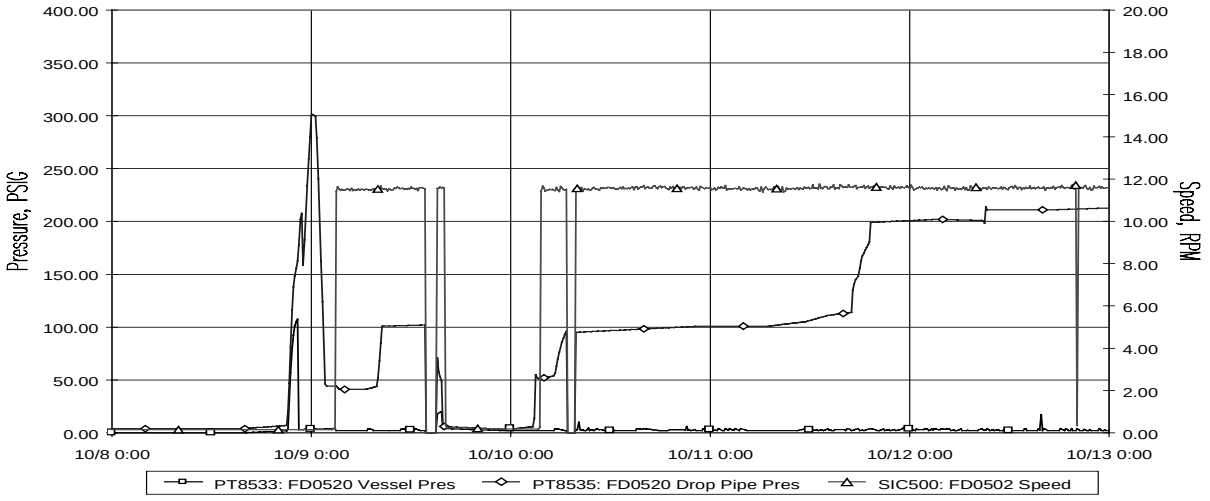

Figure 4.1.4.5-17 FD0520 Pressure Profiles

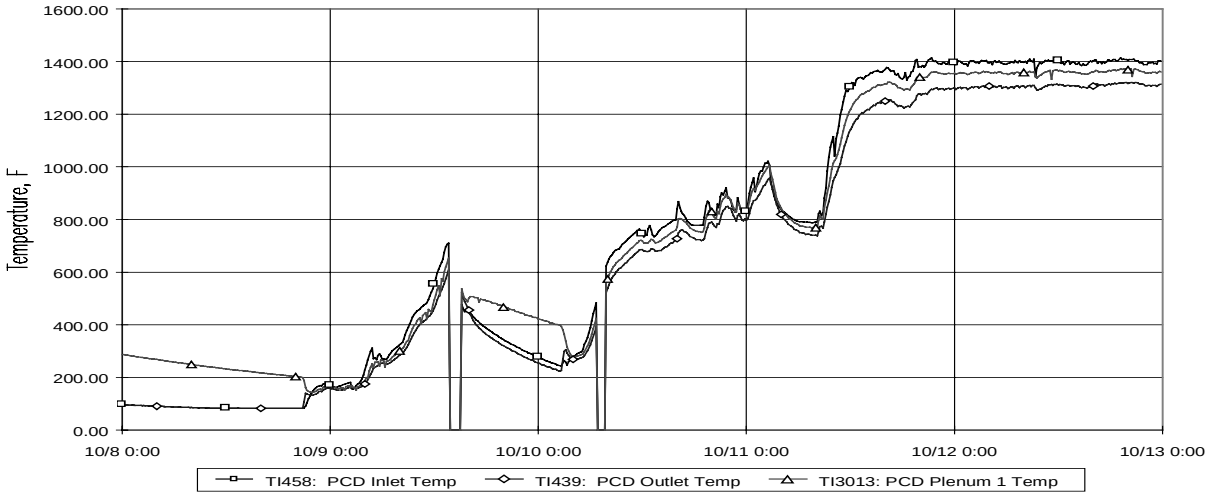

Figure 4.1.4.5-18 PCD Temperatures

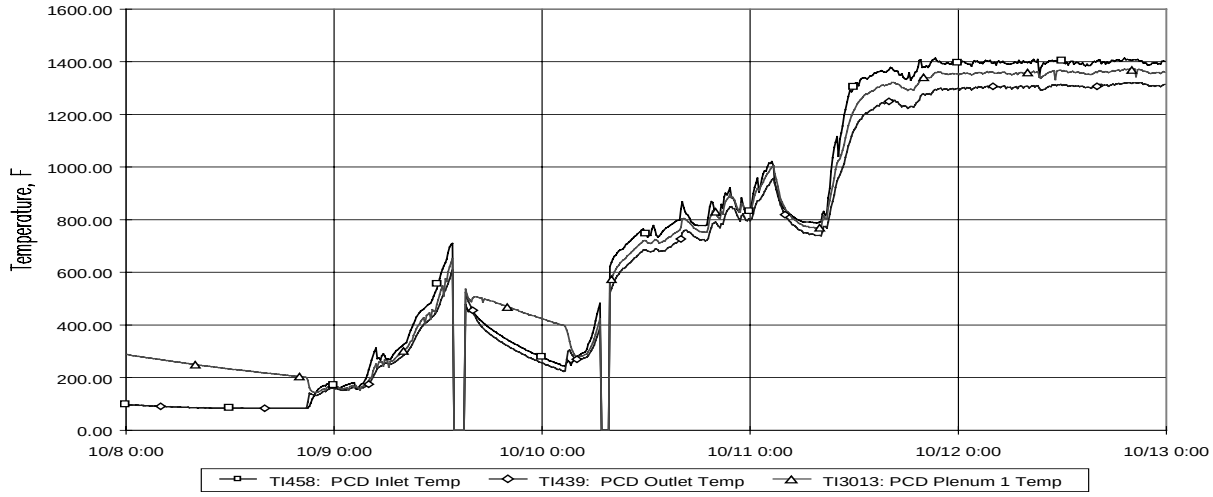

Figure 4.1.4.5-19 PCD Temperatures

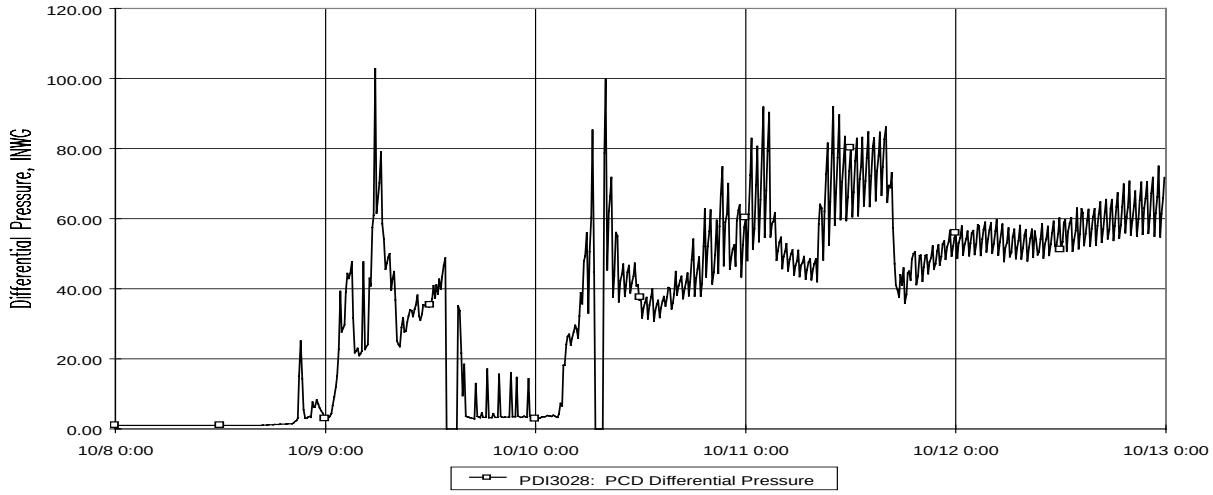

Figure 4.1.4.5-20 PCD Differential Pressure Profile

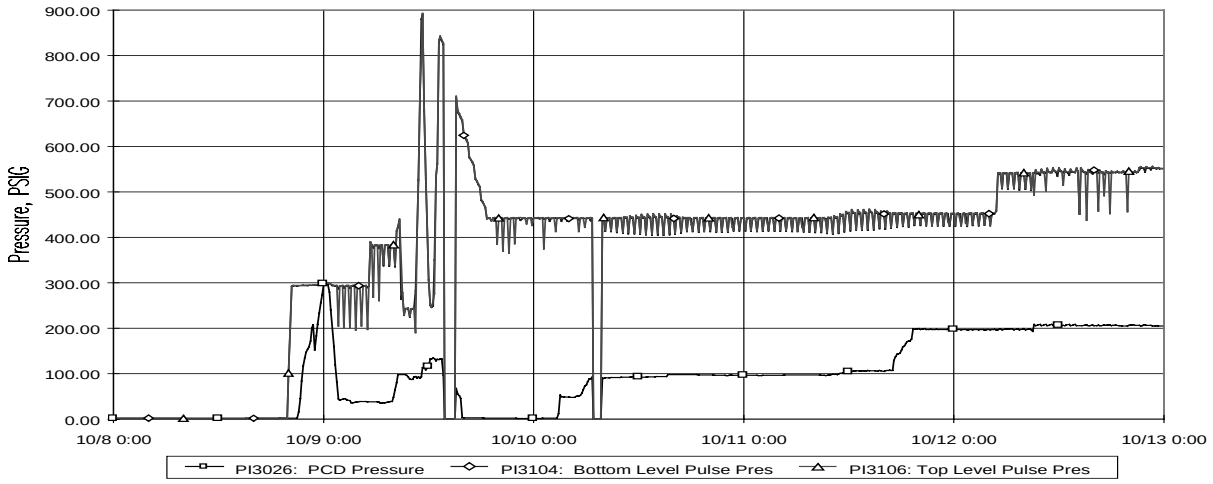

Figure 4.1.4.5-21 PCD Pressure and Pulse Pressure

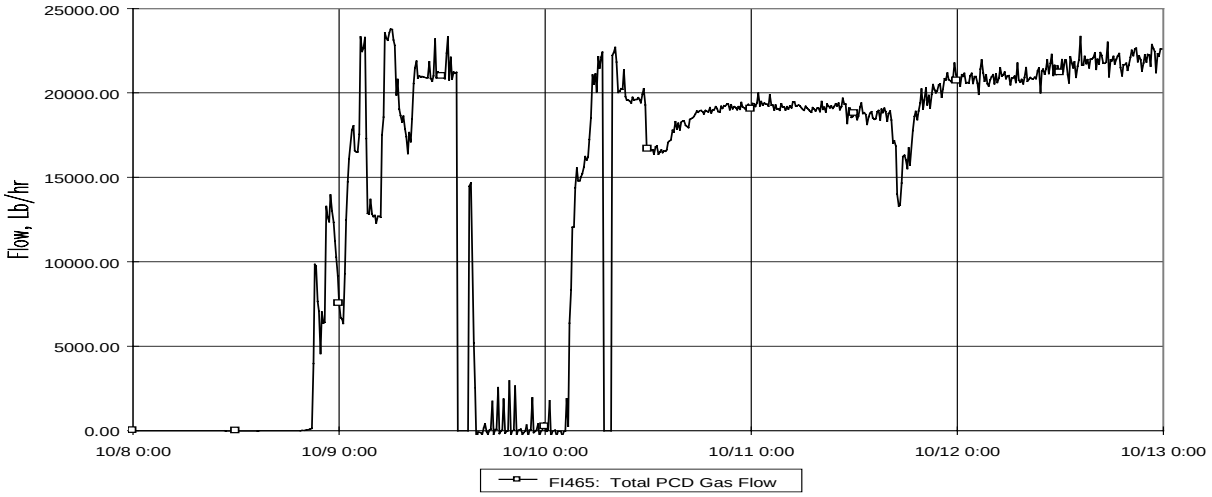

Figure 4.1.4.5-22 Gas Flow Through PCD

Section 4.1.4.5

Graphs 23 through 44

Test Run TC01E
October 13 through October 16, 1997

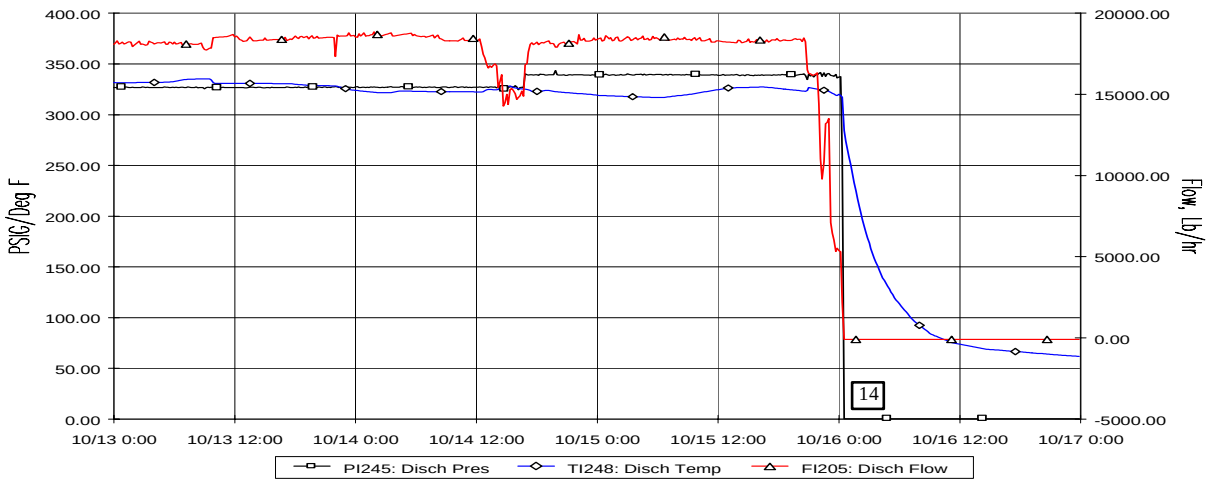

Figure 4.1.4.5-23 CO0201 System Profile

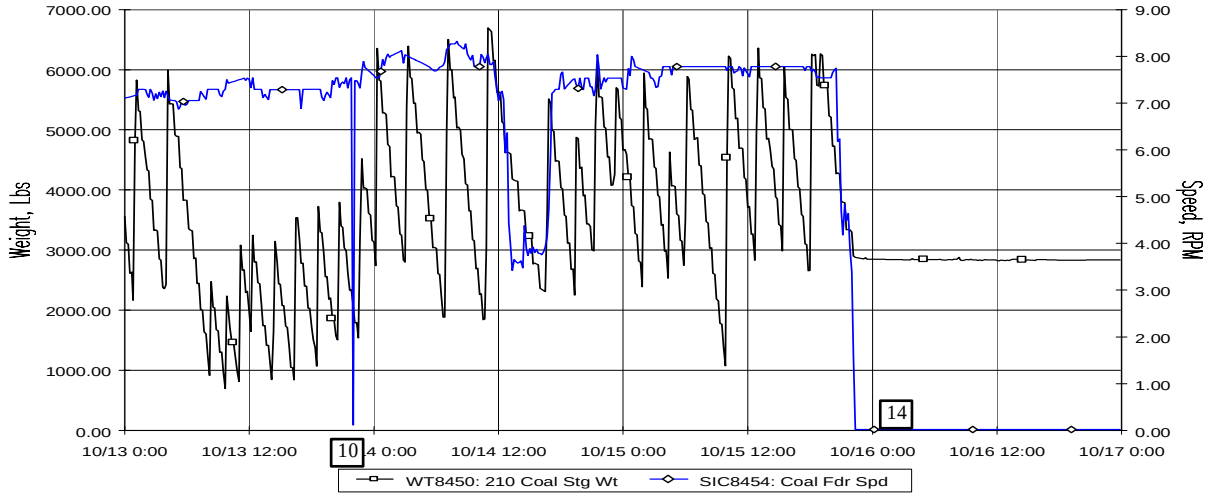

Figure 4.1.4.5-24 Coal Feed System Profile

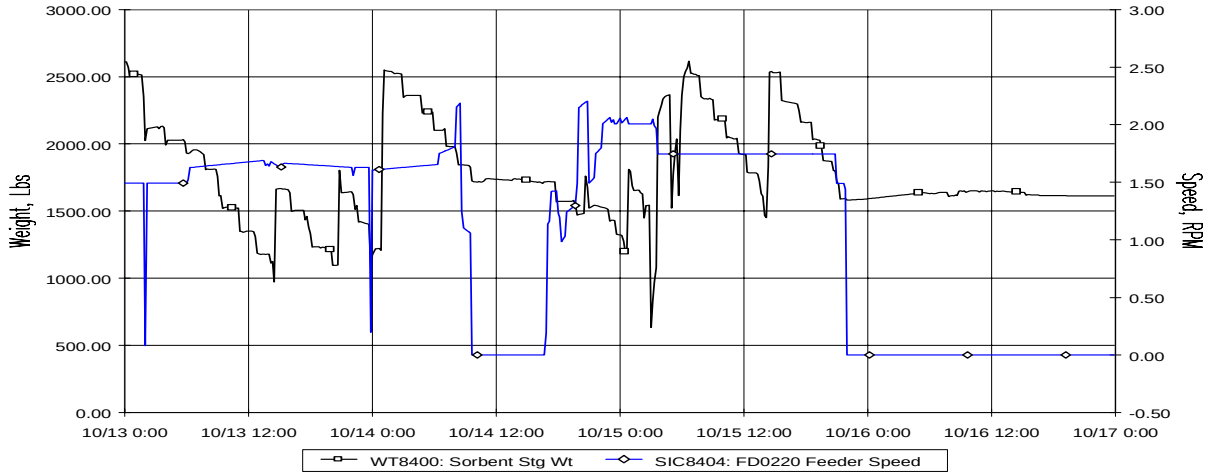

Figure 4.1.4.5-25 Sorbent Feed System Profile

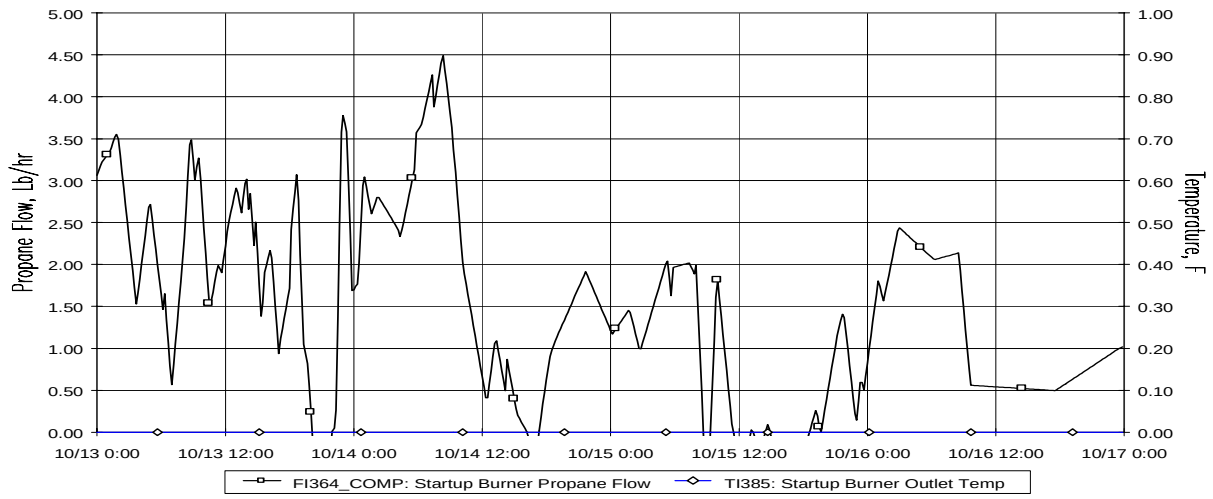

Figure 4.1.4.5-26 Start-Up Burner Flow/Temperature

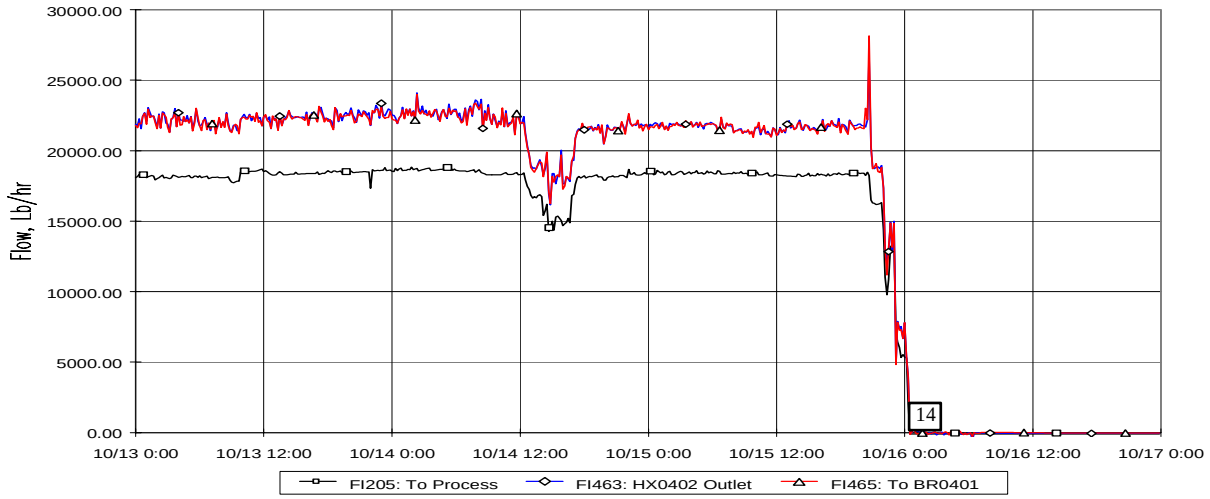

Figure 4.1.4.5-27 Total Gas In/Out Flow Rates

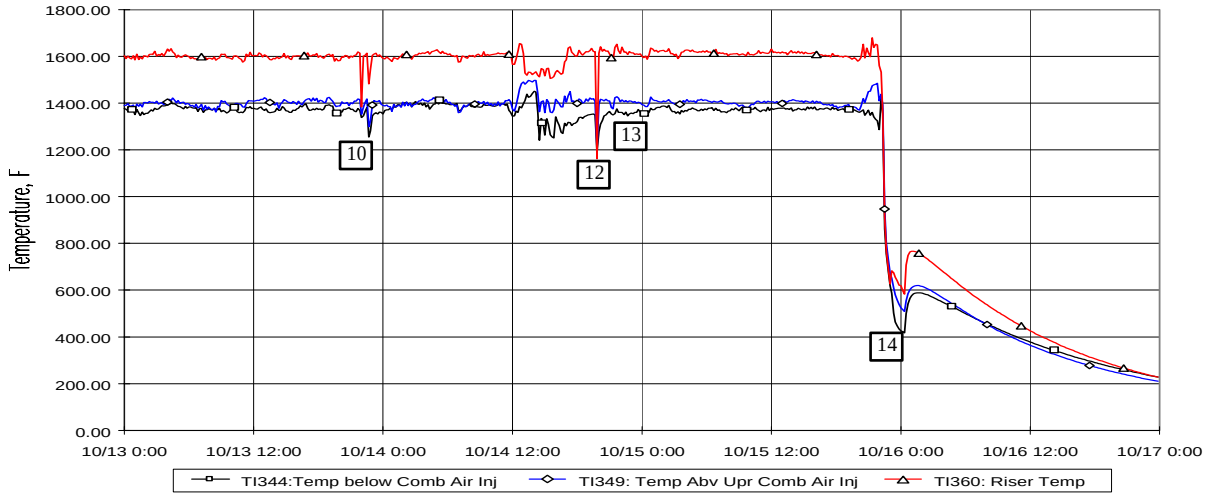

Figure 4.1.4.5-28 Reactor Mixing Zone and Riser Temperatures

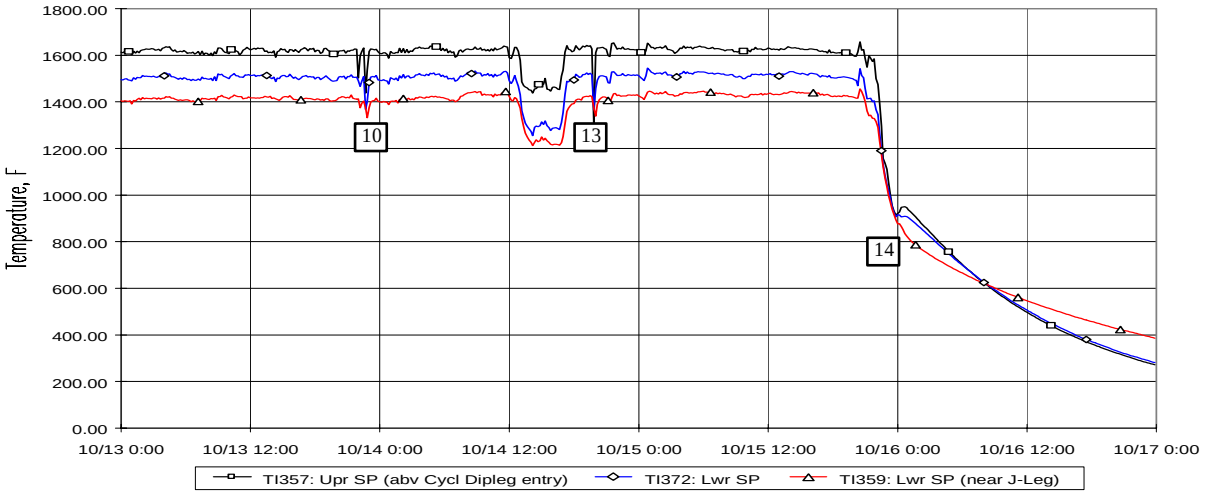

Figure 4.1.4.5-29 Standpipe Temperatures

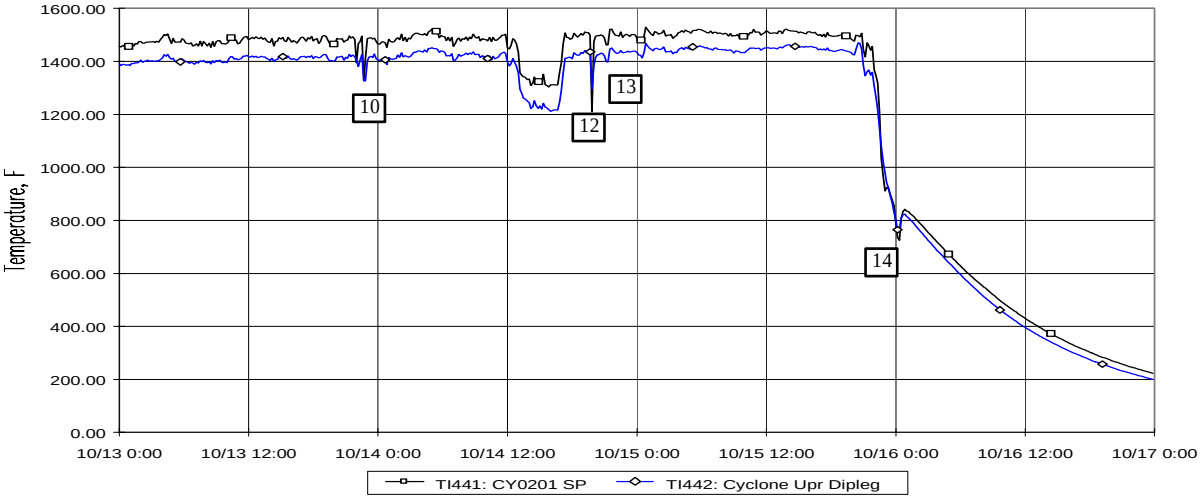

Figure 4.1.4.5-30 Cyclone Dipleg Temperatures

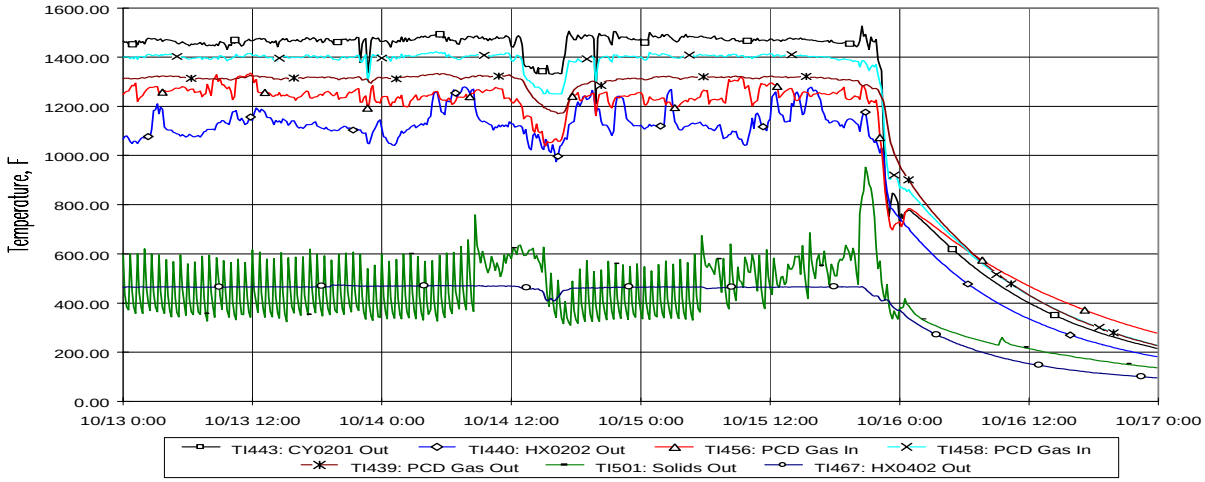

Figure 4.1.4.5-31 Temperature Profile Downstream of Reactor

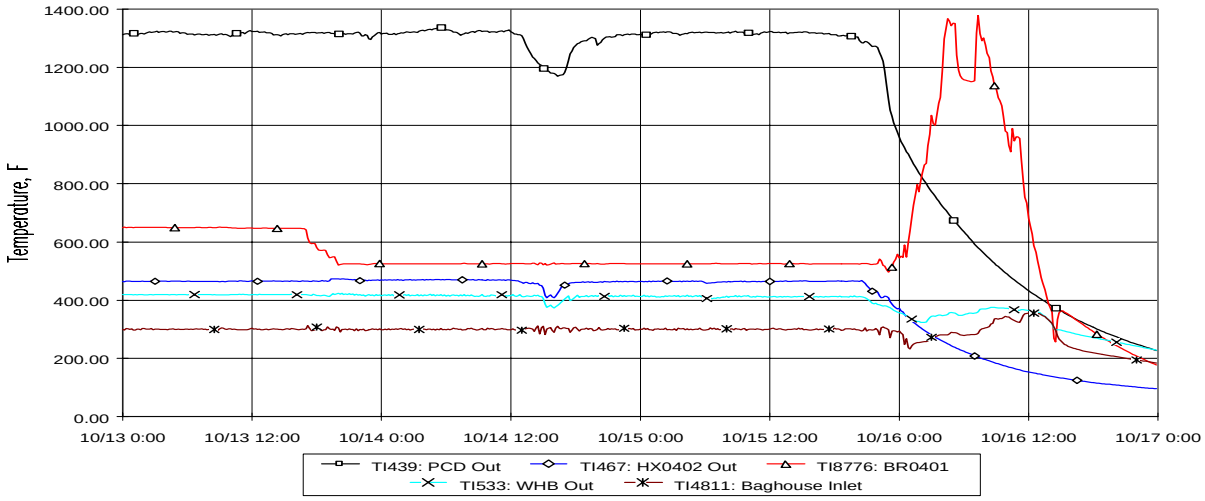

Figure 4.1.4.5-32 System Temperatures Downstream of PCD

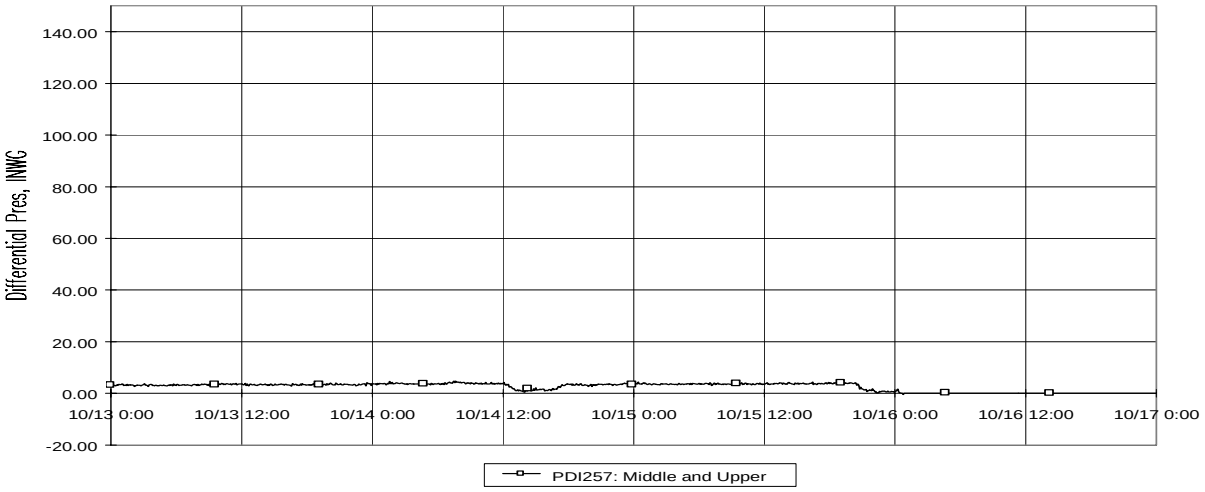

Figure 4.1.4.5-33 Mixing Zone Differential Pressure Profile

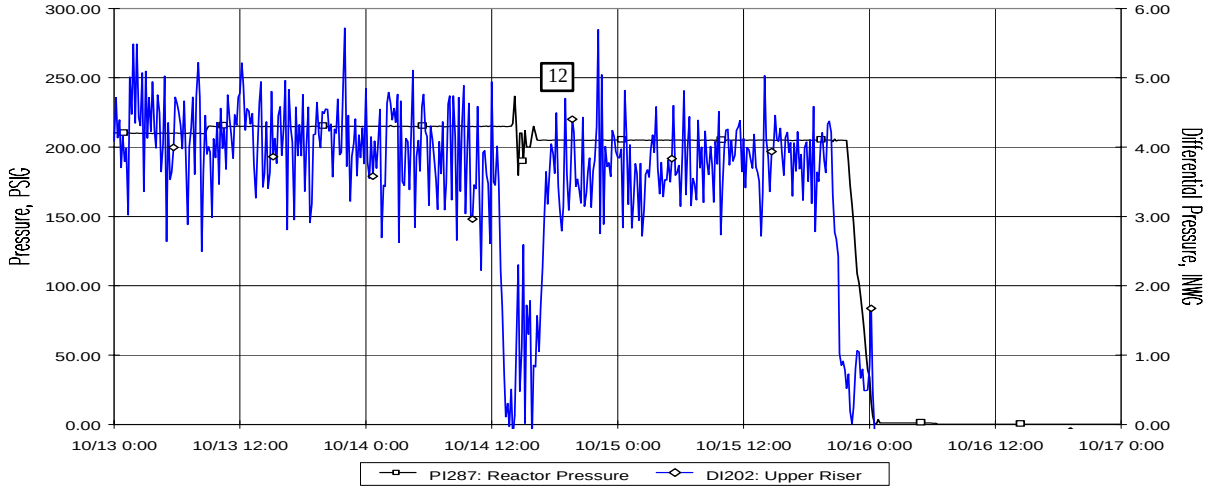

Figure 4.1.4.5-34 Reactor Pressure/Riser Differential Pressure Profiles

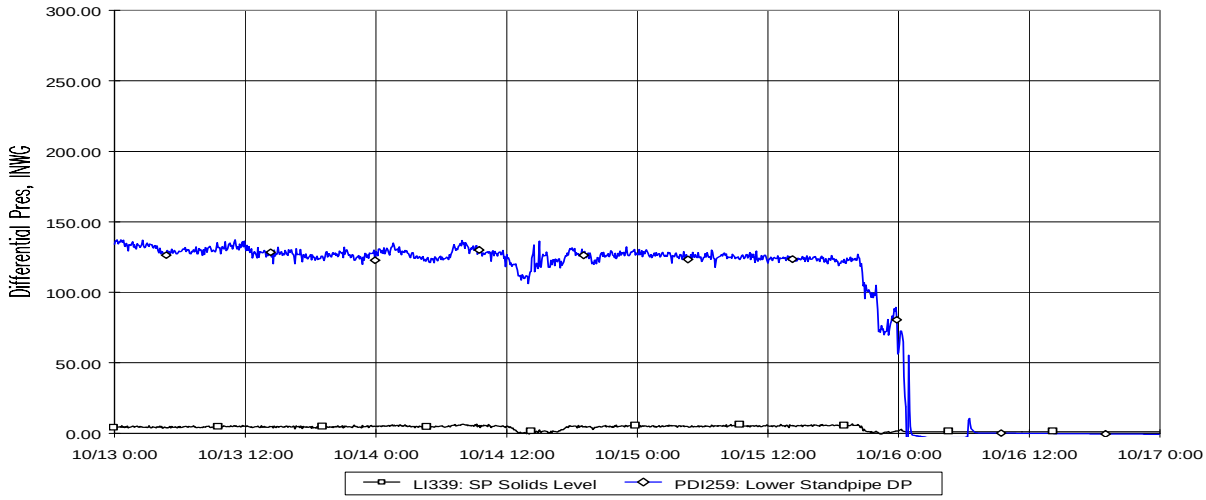

Figure 4.1.4.5-35 Standpipe Differential Pressure Profiles

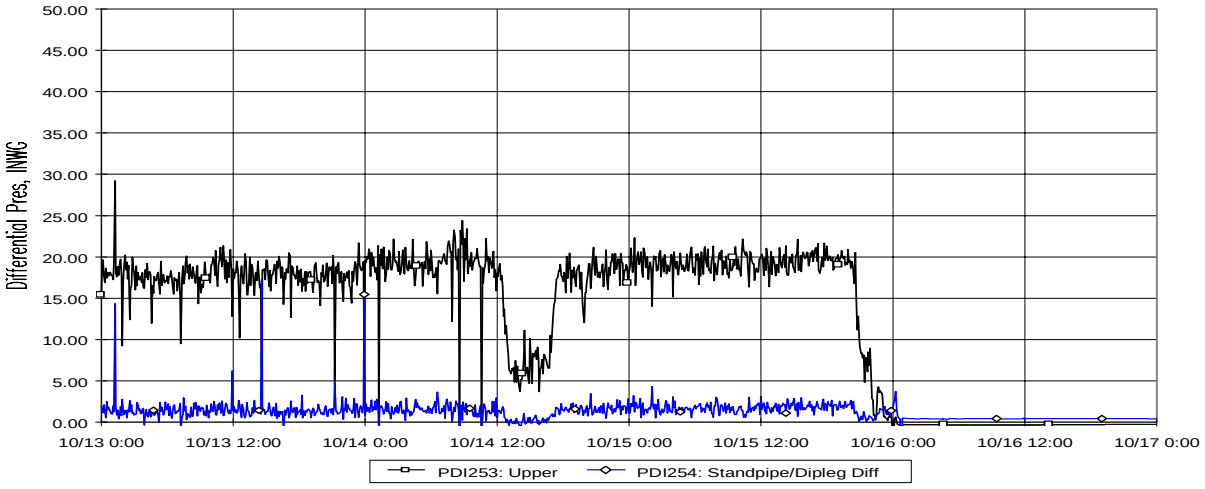

Figure 4.1.4.5-36 Cyclone Dipleg Differential Pressure Profiles

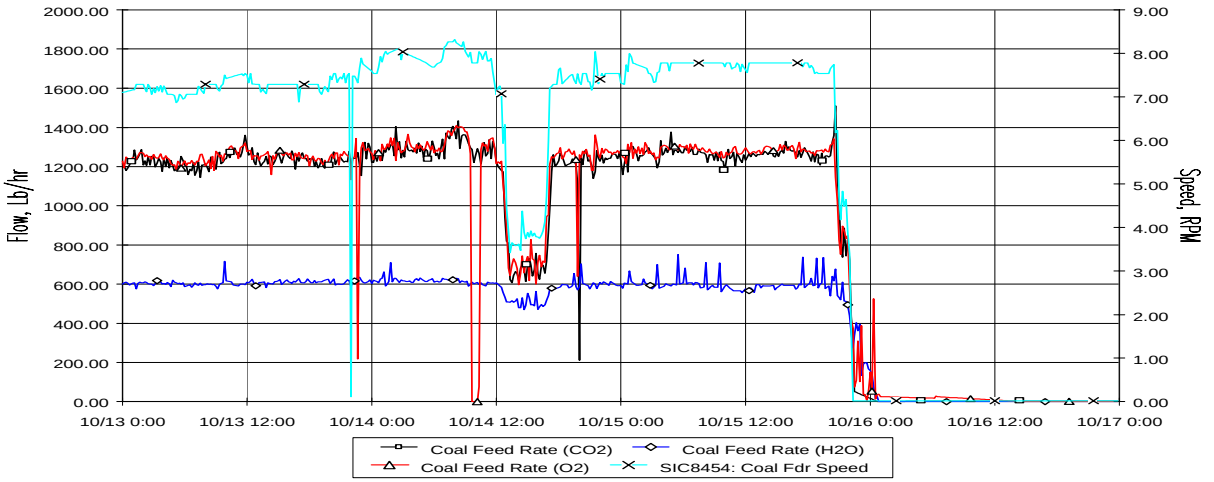

Figure 4.1.4.5-37 Coal Feed Rate Based on Gas Analysis

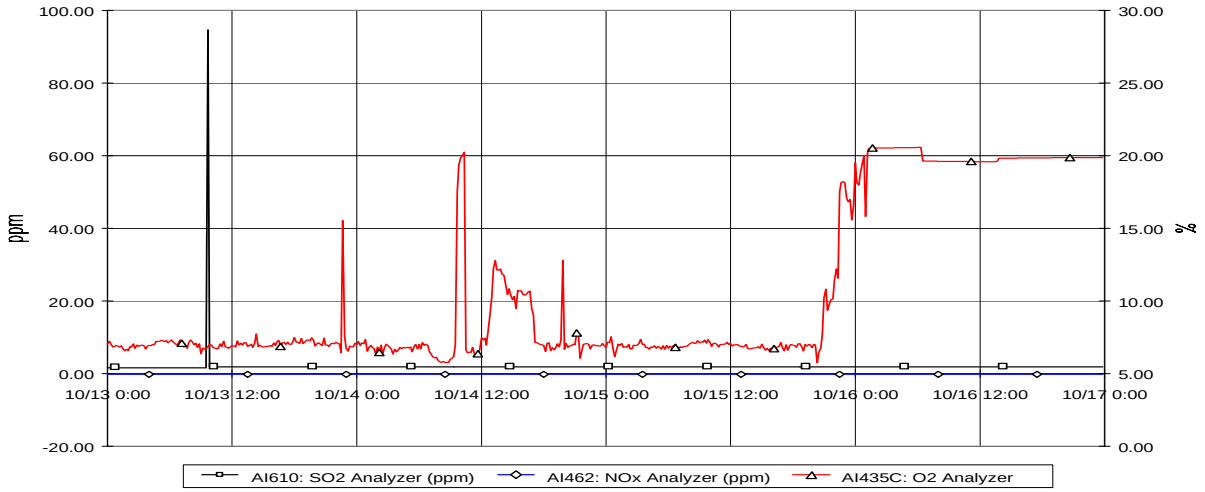

Figure 4.1.4.5-38 O_2, SO_2, and NO_x Analyzers

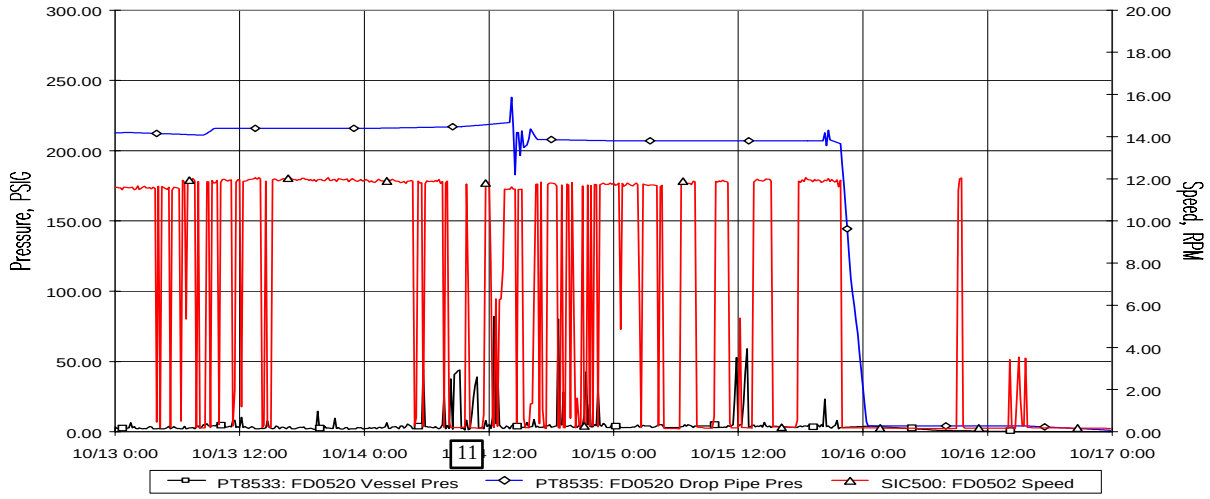

Figure 4.1.4.5-39 FD0520 Pressure Profiles

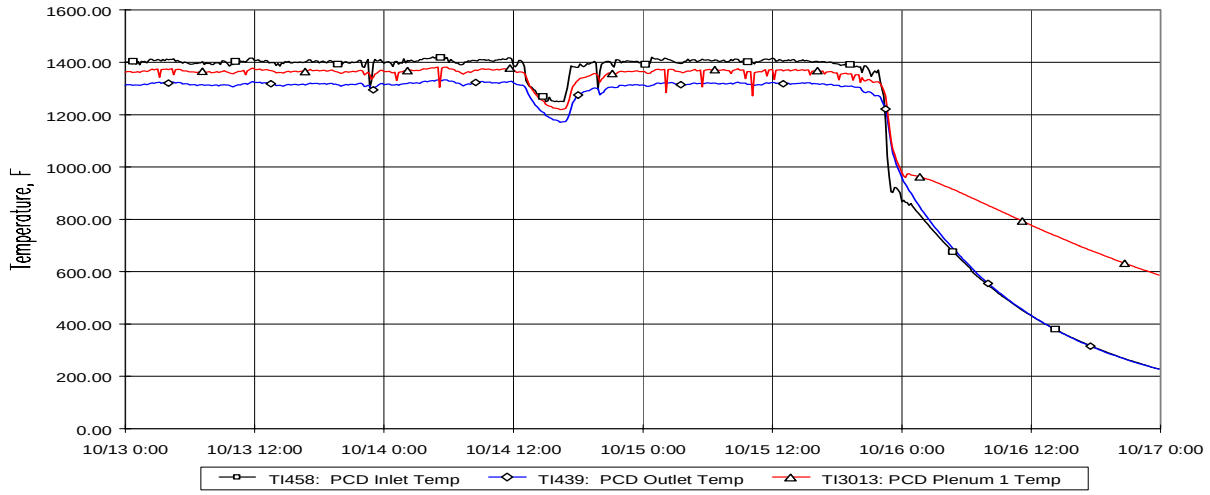

Figure 4.1.4.5-40 PCD Temperatures

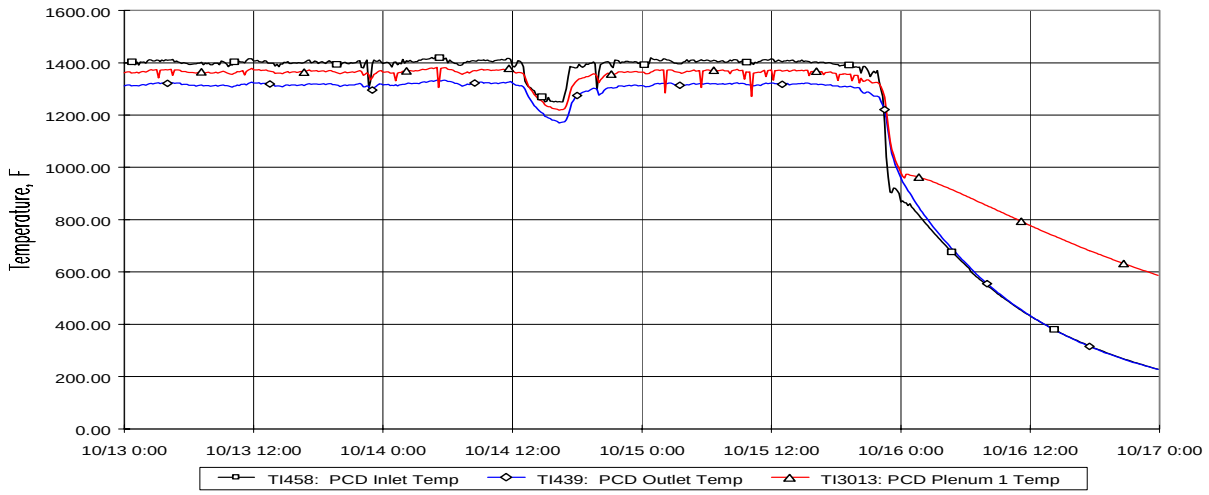

Figure 4.1.4.5-41 PCD Temperatures

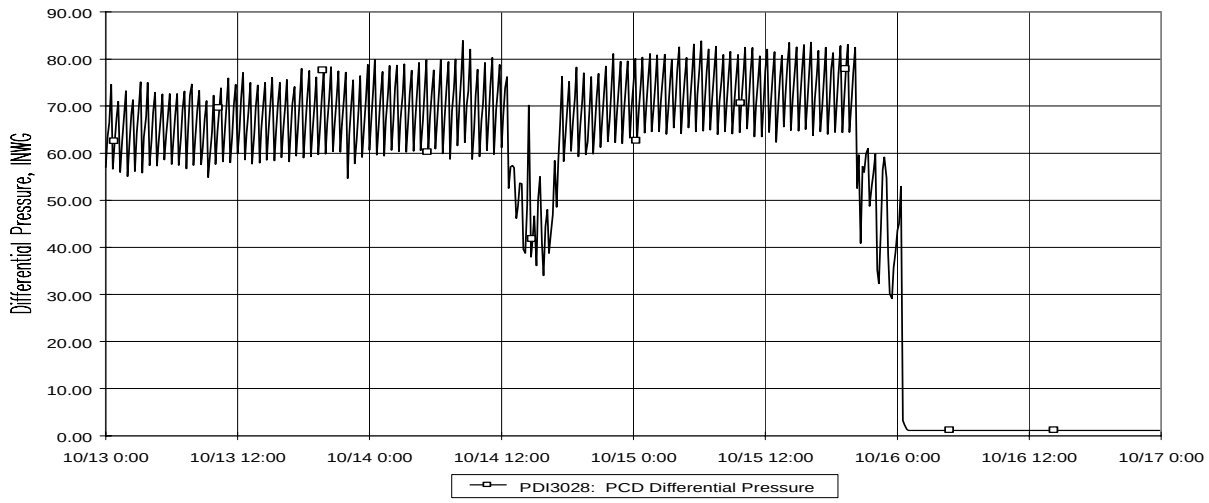

Figure 4.1.4.5-42 PCD Differential Pressure Profile

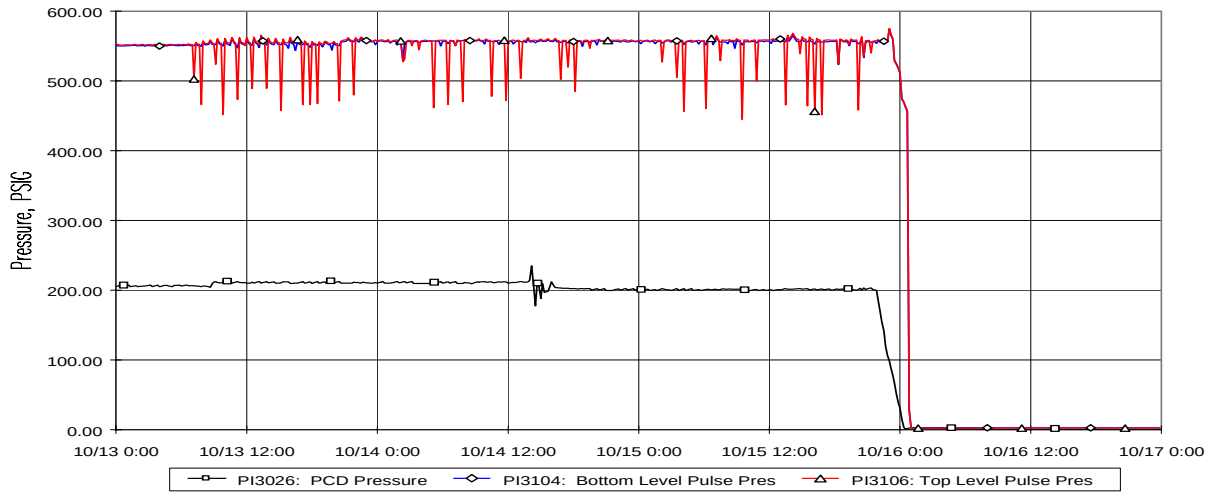

Figure 4.1.4.5-43 PCD Pressure and Pulse Pressure

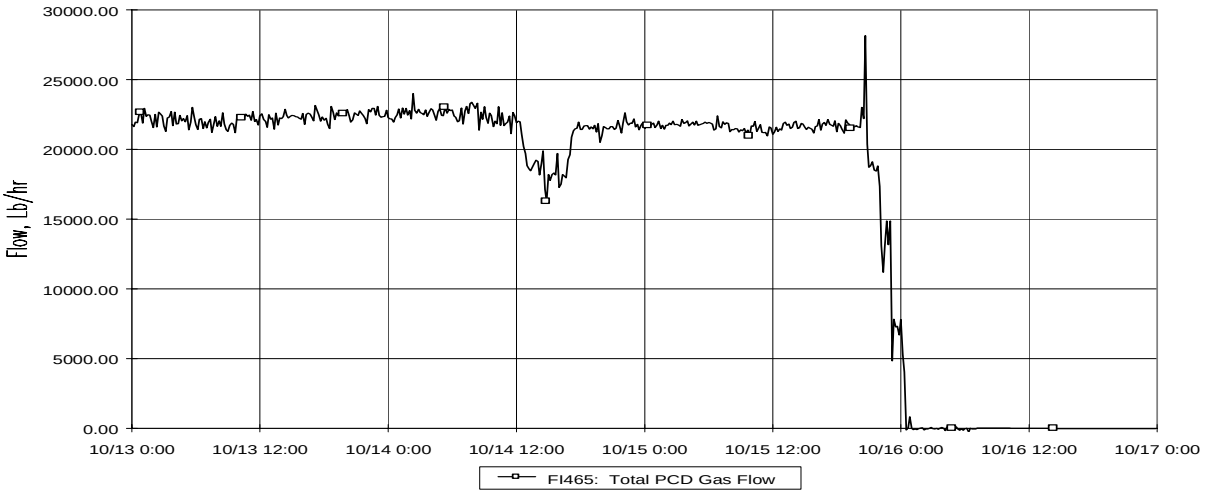

Figure 4.1.4.5-44 Gas Flow Through PCD

4.1.4.6 TC01F Test Run

Test run TC01F was conducted between October 18 and 24, 1997. Operating plots are shown in figures 4.1.4.6-1 through -38. The following maintenance work was completed during the October 16 to October 18, 1997, outage:

- The top and bottom spheri valve seals were replaced on the spent fines transport system (FD0520). A pressure switch with a solenoid valve was added to the bottom spheri valve so that the bottom spheri valve would open only when the pressure switch is made.

- A leaking safety valve on the propane vaporizer was replaced.

- Isolation valves were installed where the seal nitrogen splits to spheri valves on FD0520 and the spent solids transport (FD0510), coal (FD0210), and dolomite (FD0220) feeder systems so that seal nitrogen to each spheri valve can be isolated separately.

- The heat transfer fluid leak on the spent solids screw cooler (FD0206) was repaired.

- The packing on FD0502 was replaced.

- A new 100-psig safety valve on FD0520 discharge vessel was installed so that when a line plugs the safety valve does not needlessly lift. The line and vessel are designed to take 100-psig pressure.

- The strainer on the circulating water line was cleaned.

- In PV287 the whisper trim was replaced with an equal-percentage trim. The internals were changed and the actuator was rebuilt.

TC01F Test Run Chronology

- The main air compressor (CO0201) was started at 21:50 on October 18, 1997. Preheat of the PCD by the sulfator start-up burner began the following day. The PCD preheat was completed at about 04:40 on October 19 (event 1, figure 16), the start-up burner (BR0201) was lit around 06:15 (event 2, figure 3), and the reactor pressure was set to 100 psig (event 3, figure 11). Coal feed started at 16:30 (event 4, figures 2 and 4 through 8) but for the next 2 1/2 hours slugging in the standpipe caused the standpipe differential pressures and riser temperatures to oscillate. After the reactor operations stabilized the start-up burner (BR0201) was shut down at 20:30 (event 5, figure 3). The reactor pressure was increased starting at about 20:45 (event 6, figure 11) and by 22:15 the pressure was 190 psig (event 7, figure 11).

- By the start of October 20, 1997, the temperature in the PCD was above 1,350°F (event 8, figure 16). A heat transfer fluid (HTF) leak at the end of drive FD0502 (event 9, figure 15) caused the cooler to be shut down at 08:45. The leaking collar was replaced and the cooler was restarted. Plugging of the instrument air filter on FD0530 caused the system to short cycle without any transfer of solids for about 3 hours. The filter was replaced and the system put back online. A cracked Teflon O-ring seal caused a nitrogen seal to leak from the bottom spheri valve in the FD0520 system around 16:00. Efforts made to close the leak were unsuccessful. The aeration on the combustion heat exchanger (HX0203) J-leg was therefore lowered to reduce circulation and, therefore, solids carryover to the PCD.

- On October 21, 1997, SRI took samples between 08:55 and 10:15. The FD0206 was operated intermittently to maintain the solids level in the standpipe and HX0203 within preset limits. The FD0210 feeder tripped at 21:45 (event 10, figures 2 and 4 through 8) because the tubing to the piston actuator that closes the top spheri valve became loose. The tubing was put back in place and the top spheri valve operated properly. However, the loss of coal feed caused a drop in reactor temperature, so BR0201 was lit at about 22:30 (event 11, figure 3).

- Coal feed resumed at 04:55 on October 22, 1997 (event 12, figure 21 and 23 through 27). The BR0201 was shut down at 09:45 (event 13, figure 22); an hour later the reactor pressure was 190 psig (event 14, figure 30) and by midday the PCD plenum temperature had reached 1,350°F (event 15, figure 35). At 17:45 the medium-pressure nitrogen controller PV490 went 100-percent open, indicating that there was a spheri valve seal leak. The FD0520 system was isolated and the lower spheri valve seal was found to be leaking. The FD0520 system was restarted to remove the ash from the PCD during the shutdown period. However, after the system had cycled three times the PV490 controller returned to its previous position, indicating that the seal was no longer badly leaking. After several additional cycles PY490 still remained at the same position so it was decided to continue on with coal feed. Around 18:05 the coal feed rate was increased (event 16, figures 21 and 23 through 27). The PCD temperature reached 1,350°F by 19:15 (event 17, figure 35). However, the problem with the FD0520 bottom spheri valve seal continued to affect the operation of the FD0520 system throughout the rest of the day.

- On October 23, 1997, SRI took samples at the PCD inlet and outlet. Problems with the FD0510 system began around 12:30 due to a plug at the exit. A few small refractory pieces were found during clean out. At 21:45 PY490 again went 100-percent open and the FD0520 bottom spheri valve seal was found to be leaking. As a result of the FD0520 bottom spheri valve seal leak a controlled shutdown of the unit was begun at 23:30. The coal feed was stopped 15 minutes later (event 18, figures 21 and 23 through 27).

TC01F Test Run Observations

A total of 97.25 hours on coal was achieved and 62.7 tons of coal were fed. The PCD plenum temperature was above 1,350°F for 79 hours. The recycle gas booster compressor was successfully run for about 2.5 hours before a leak on the compressor feed cooler forced a compressor shutdown. More bomb samples were taken at the PCD inlet and HX0402 outlet for SO_2 analysis during the test run. Unlike the plug stem vibration problems experienced in the previous test run the pressure letdown valve operated smoothly with the equal percentage trim.

Section 4.1.4.6

Graphs 1 through 19

Test Run TC01F
October 18 through 21, 1997

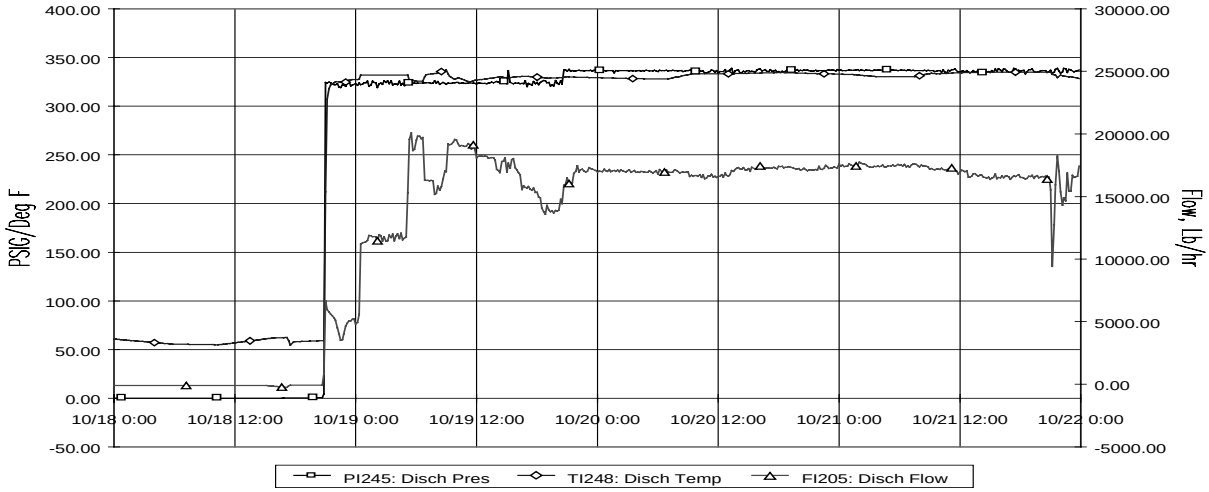

Figure 4.1.4.6-1 CO0201 System Profile

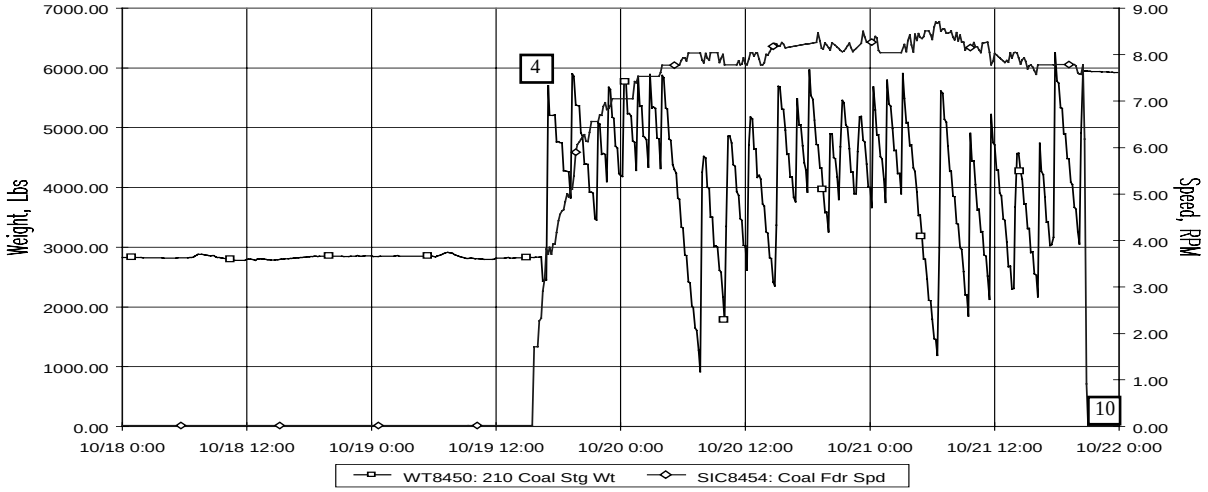

Figure 4.1.4.6-2 Coal Feed System Profile

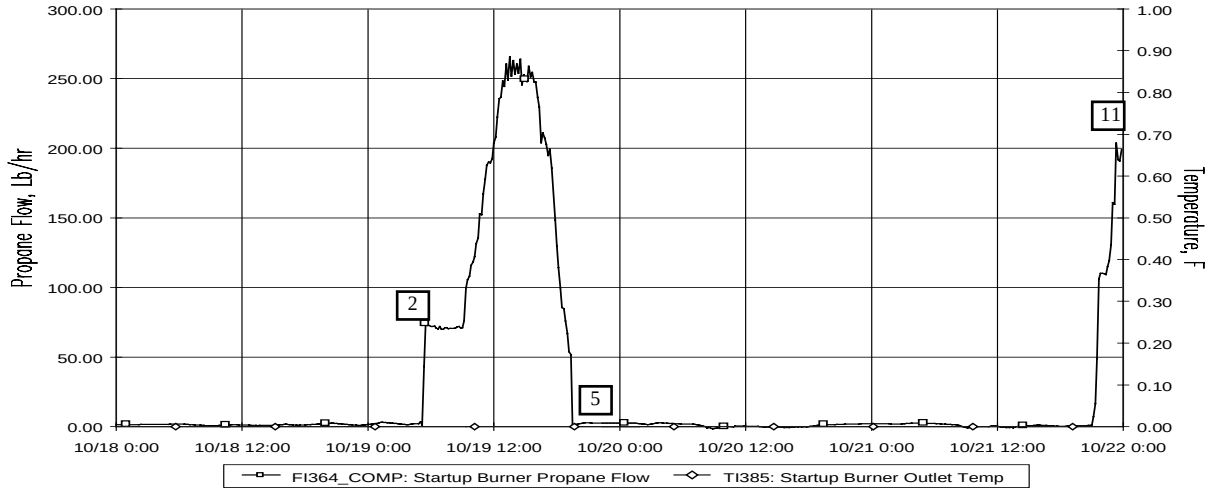

Figure 4.1.4.6-3 Start-Up Burner Flow/Temperature

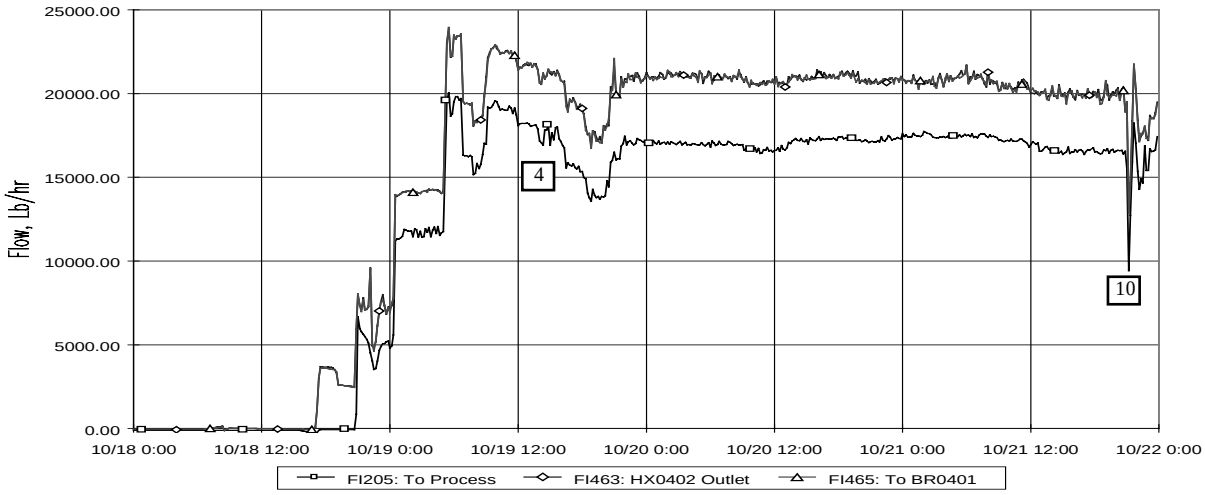

Figure 4.1.4.6-4 Total Gas In/Out Flow Rates

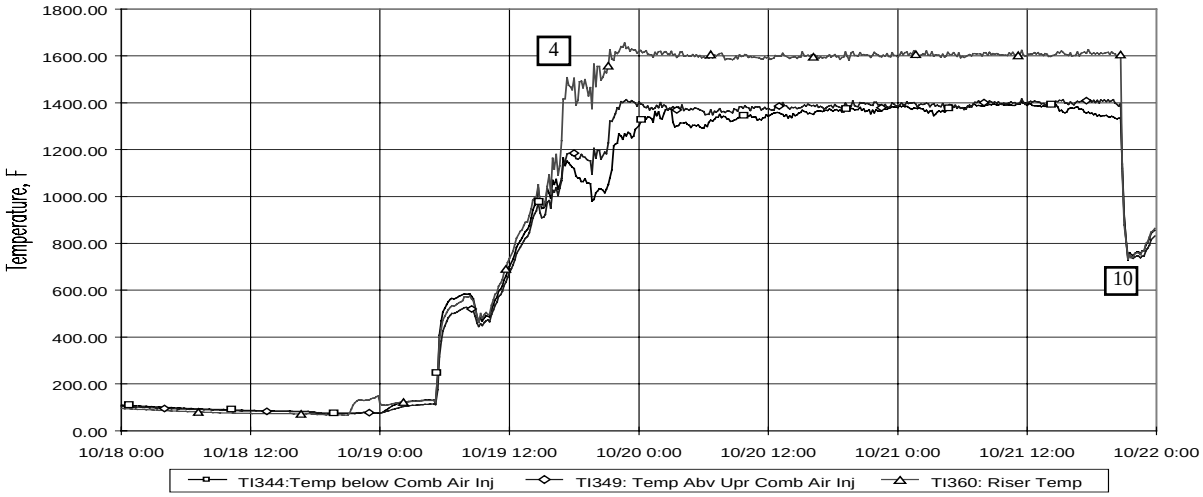

Figure 4.1.4.6-5 Reactor Mixing Zone and Riser Temperatures

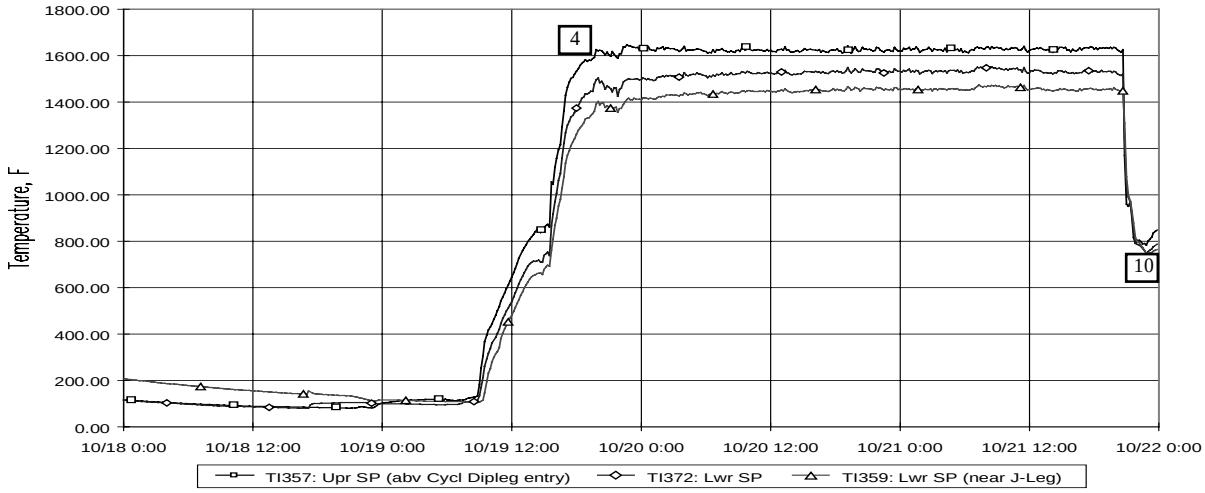

Figure 4.1.4.6-6 Standpipe Temperatures

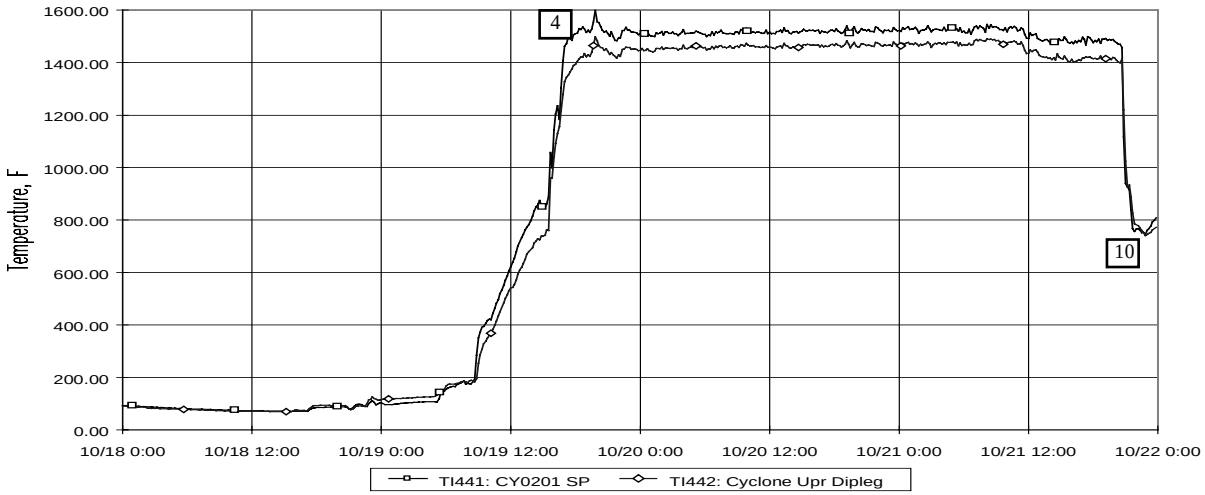

Figure 4.1.4.6-7 Cyclone Dipleg Temperatures

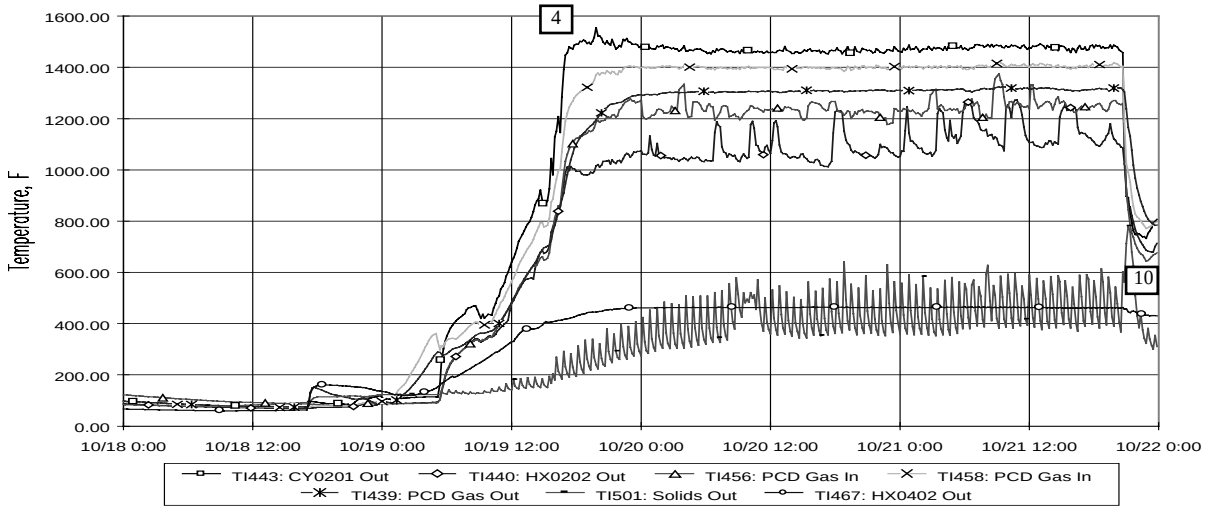

Figure 4.1.4.6-8 Temperature Profile Downstream of Reactor

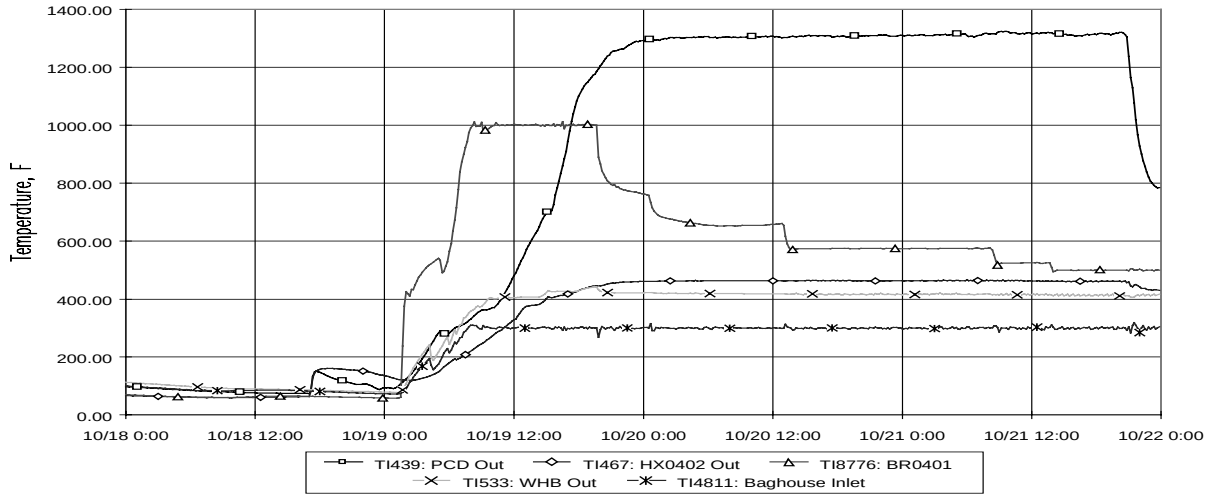

Figure 4.1.4.6-9 System Temperatures Downstream of PCD

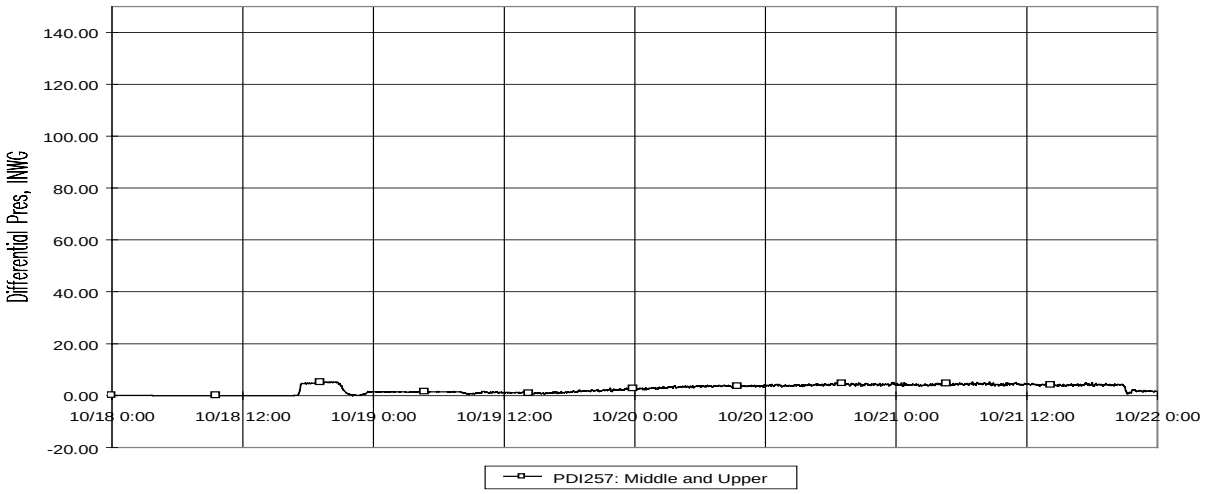

Figure 4.1.4.6-10 Mixing Zone Differential Pressure Profile

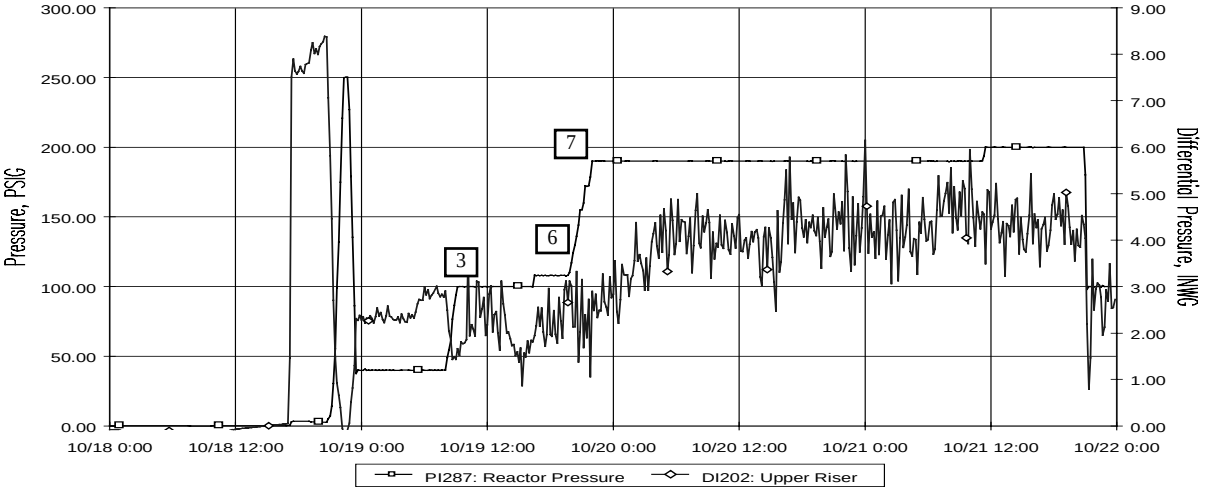

Figure 4.1.4.6-11 Reactor Pressure/Riser Differential Pressure Profiles

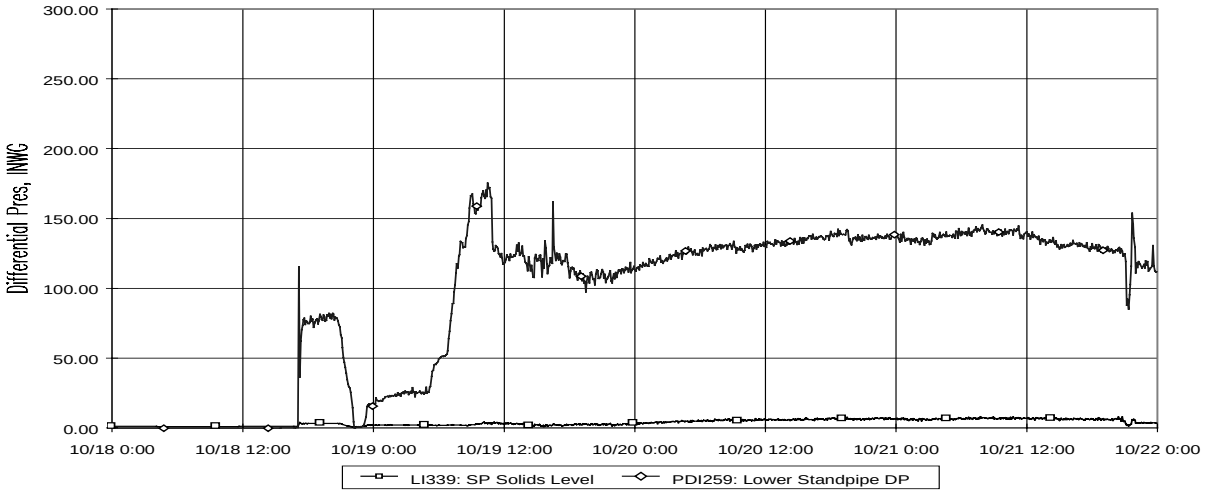

Figure 4.1.4.6-12 Standpipe Differential Pressure Profiles

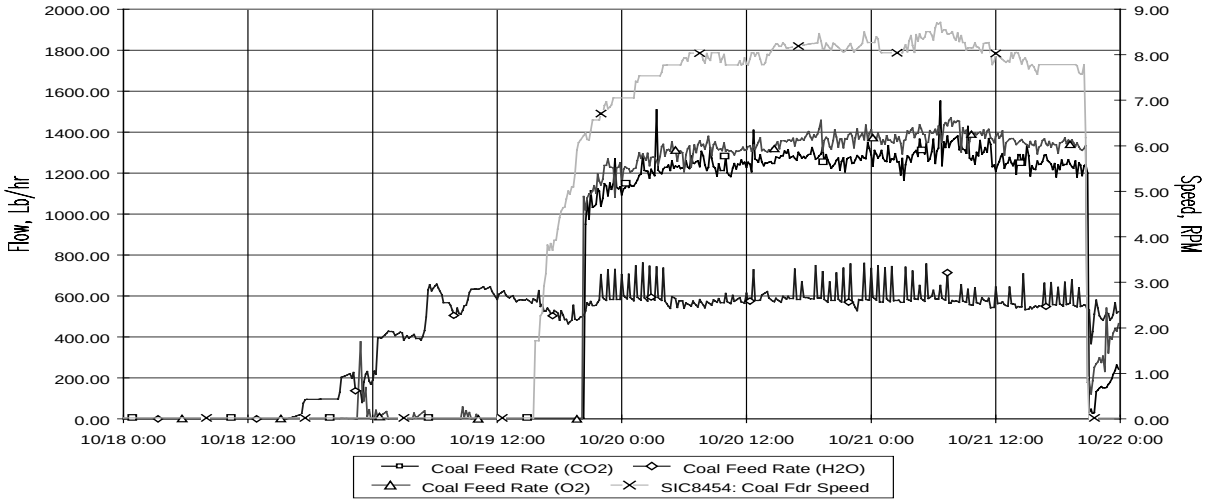

Figure 4.1.4.6-13 Coal Feed Rate Based on Gas Analysis

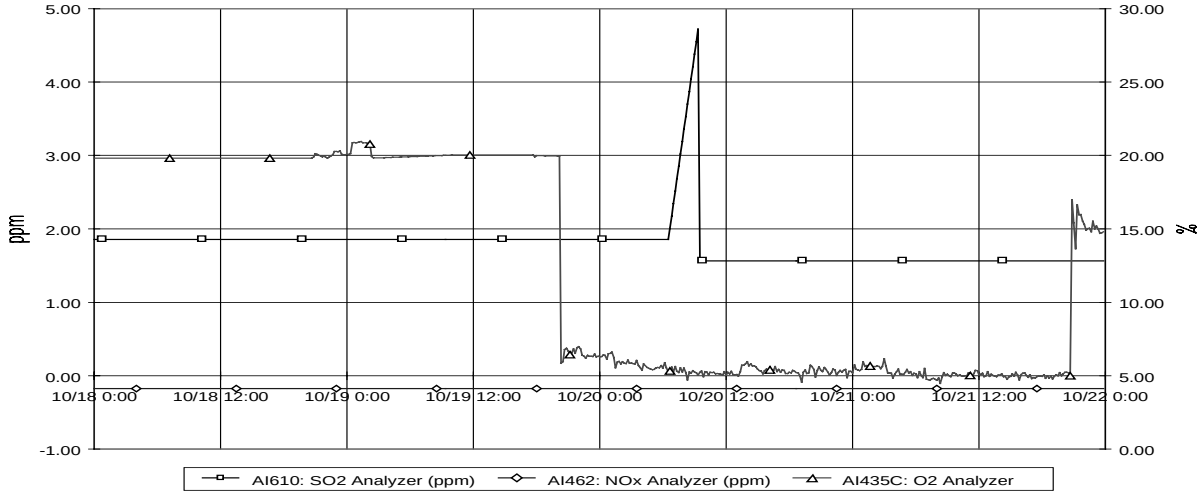

Figure 4.1.4.6-14 O_2, SO_2, and NO_x Analyzers

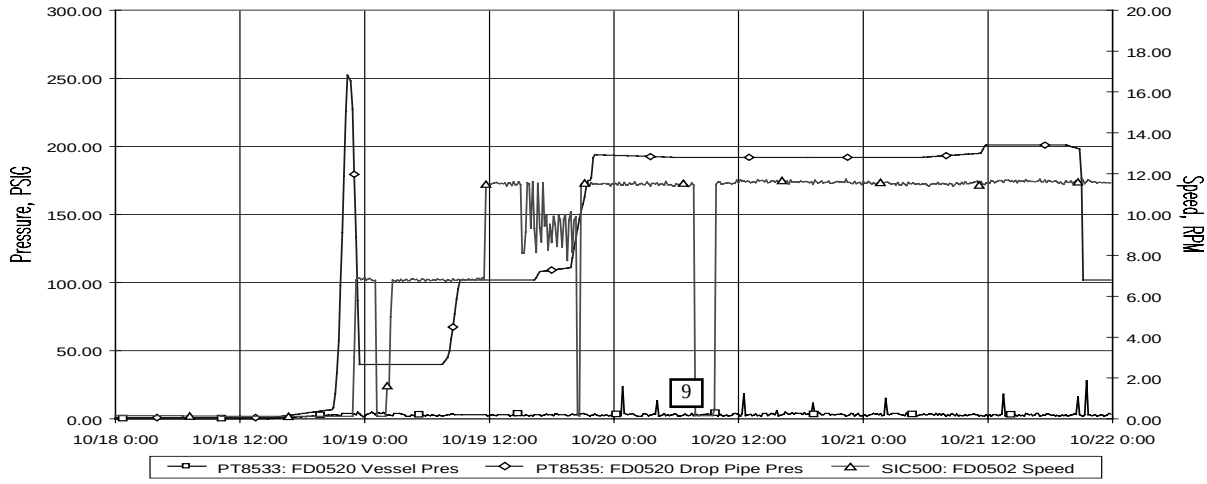

Figure 4.1.4.6-15 FD0520 Pressure Profiles

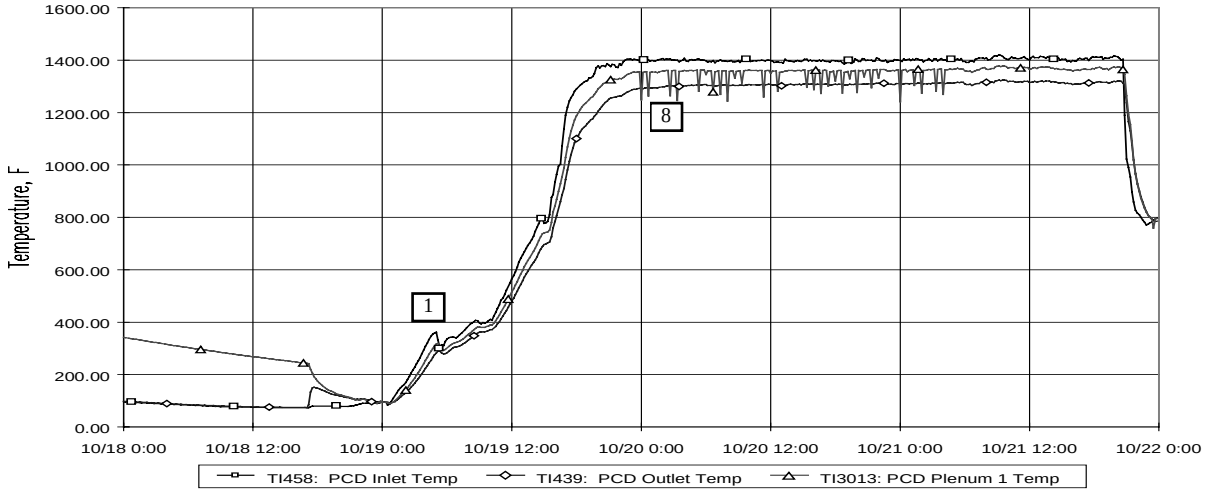

Figure 4.1.4.6-16 PCD Temperatures

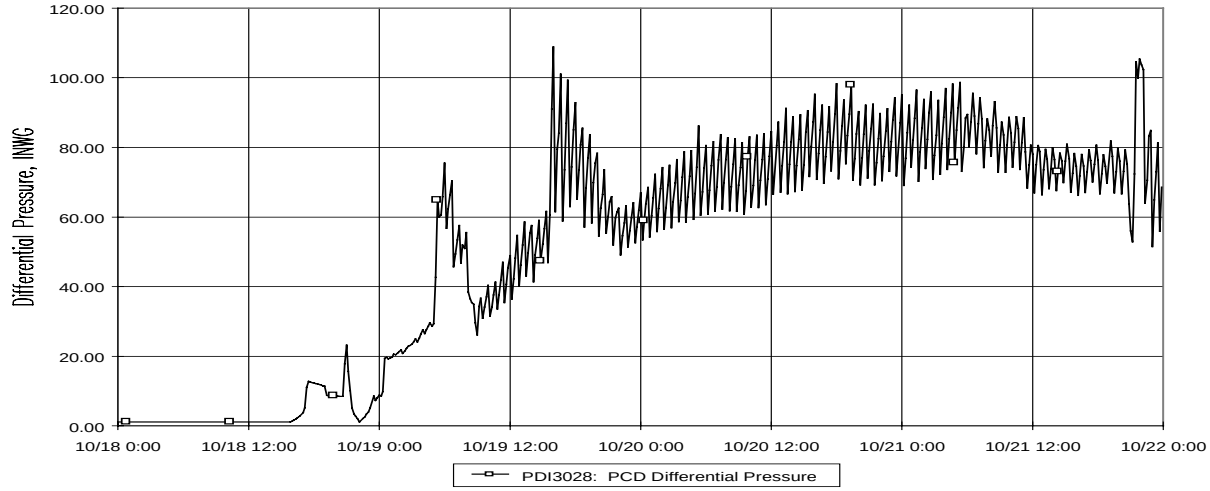

Figure 4.1.4.6-17 PCD Differential Pressure Profile

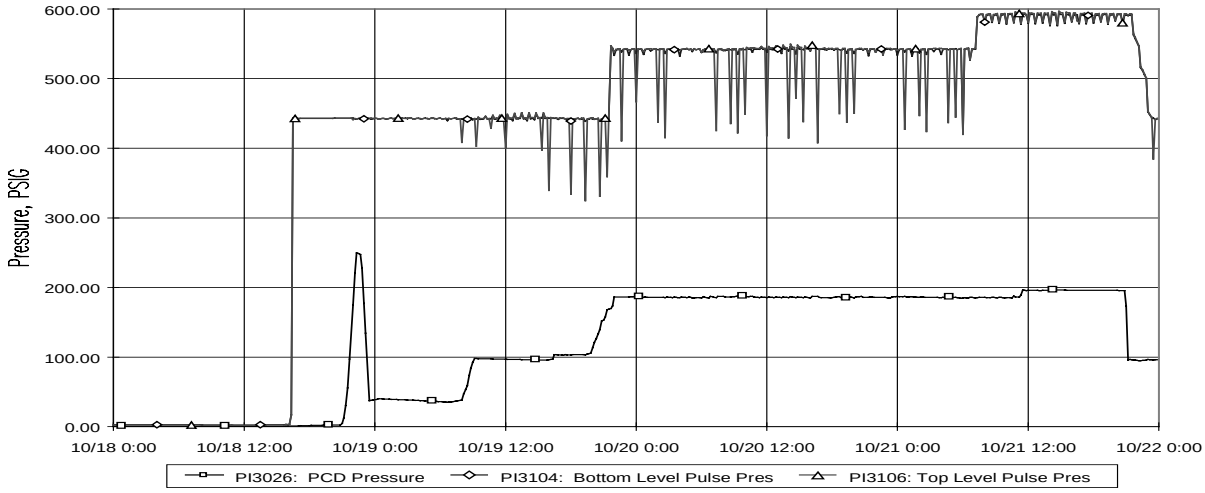

Figure 4.1.4.6-18 PCD Pressure and Pulse Pressure

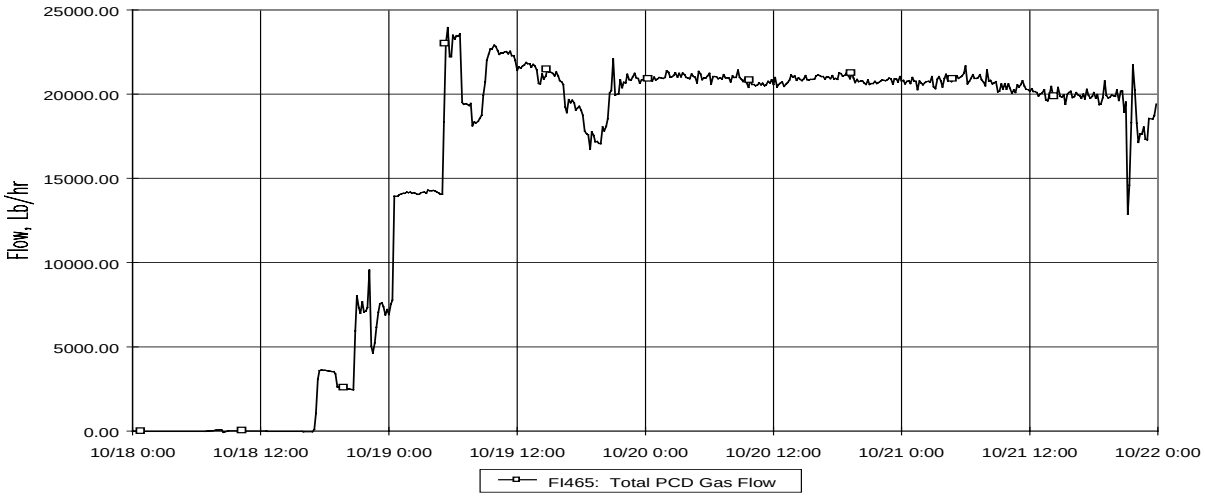

Figure 4.1.4.6-19 Gas Flow Through PCD

Section 4.1.4.6

Graphs 20 through 38

Test Run TC01F
October 22 through 24, 1997

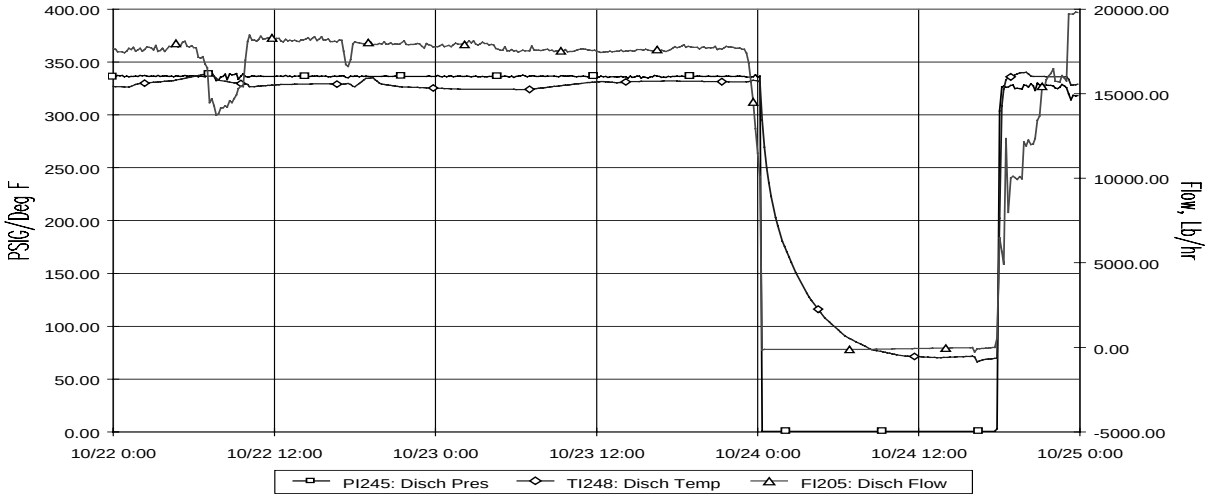

Figure 4.1.4.6-20 CO0201 System Profile

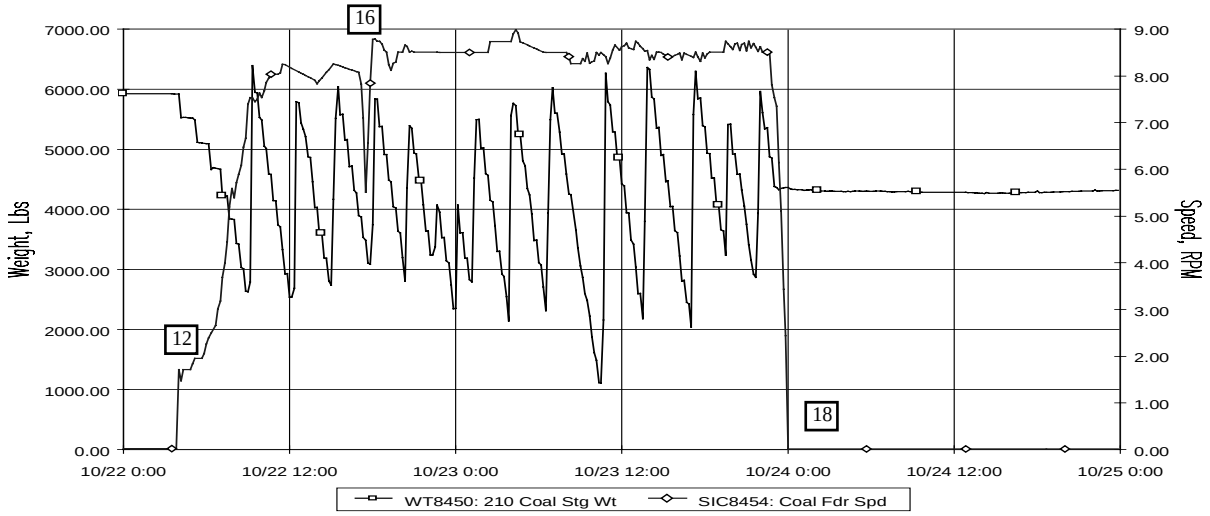

Figure 4.1.4.6-21 Coal Feed System Profile

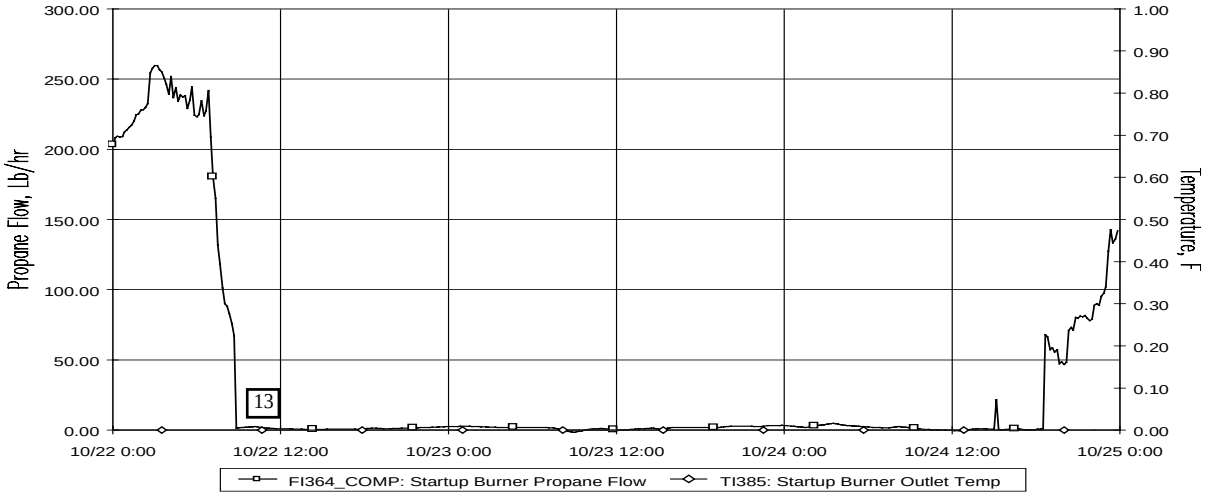

Figure 4.1.4.6-22 Start-Up Burner Flow/Temperature

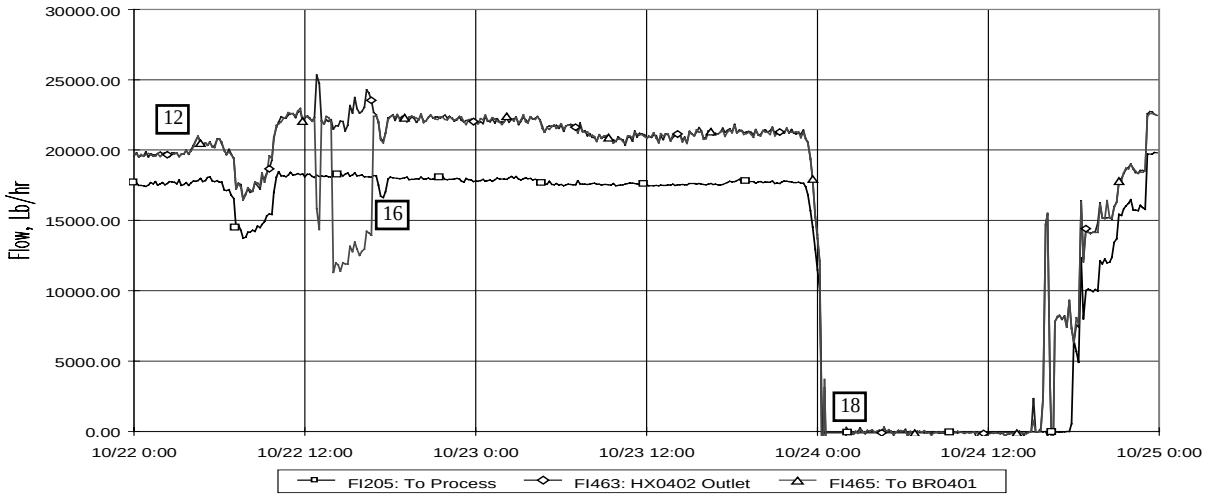

Figure 4.1.4.6-23 Total Gas In/Out Flow Rates

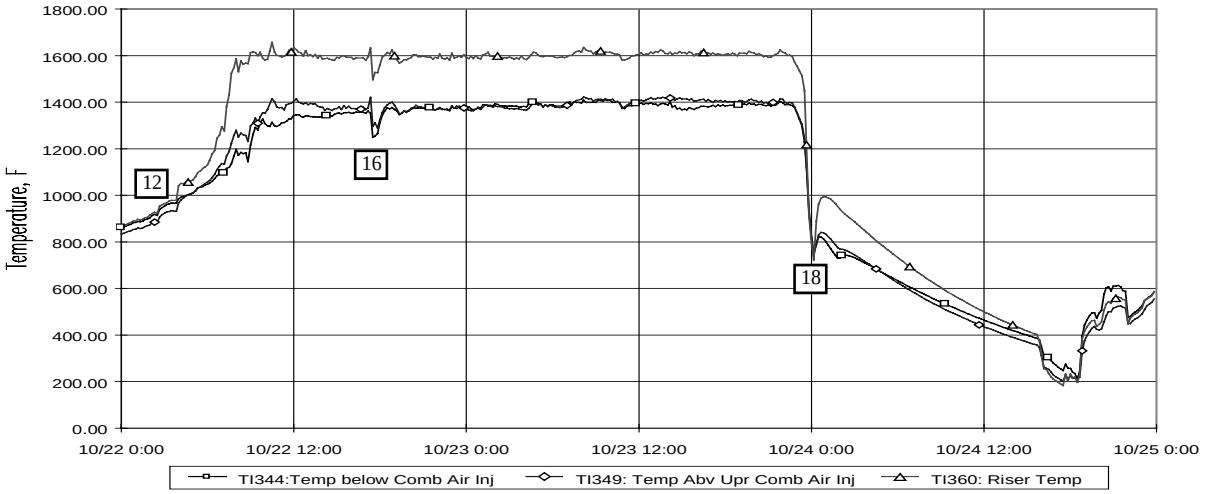

Figure 4.1.4.6-24 Reactor Mixing Zone and Riser Temperatures

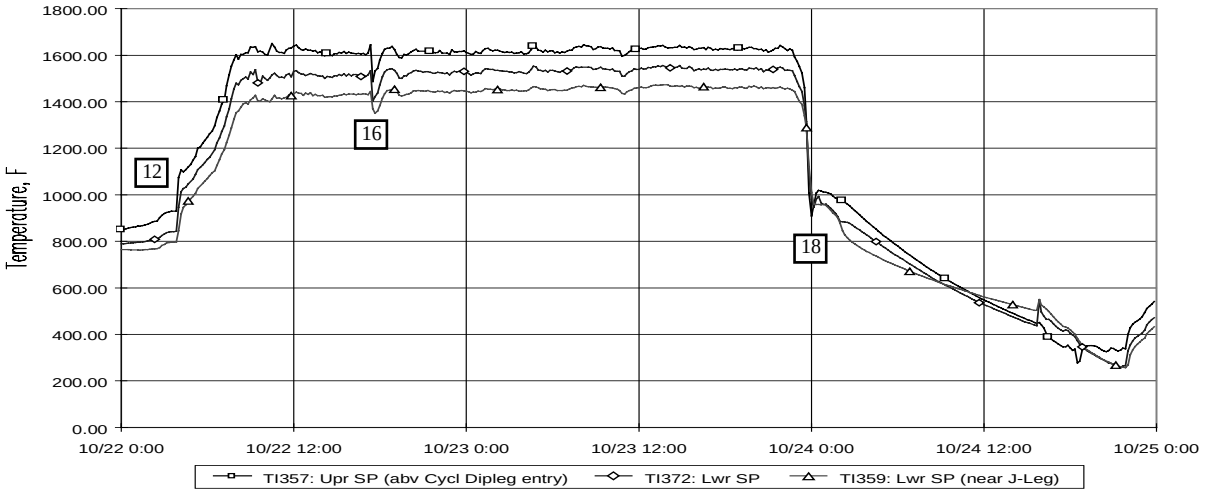

Figure 4.1.4.6-25 Standpipe Temperatures

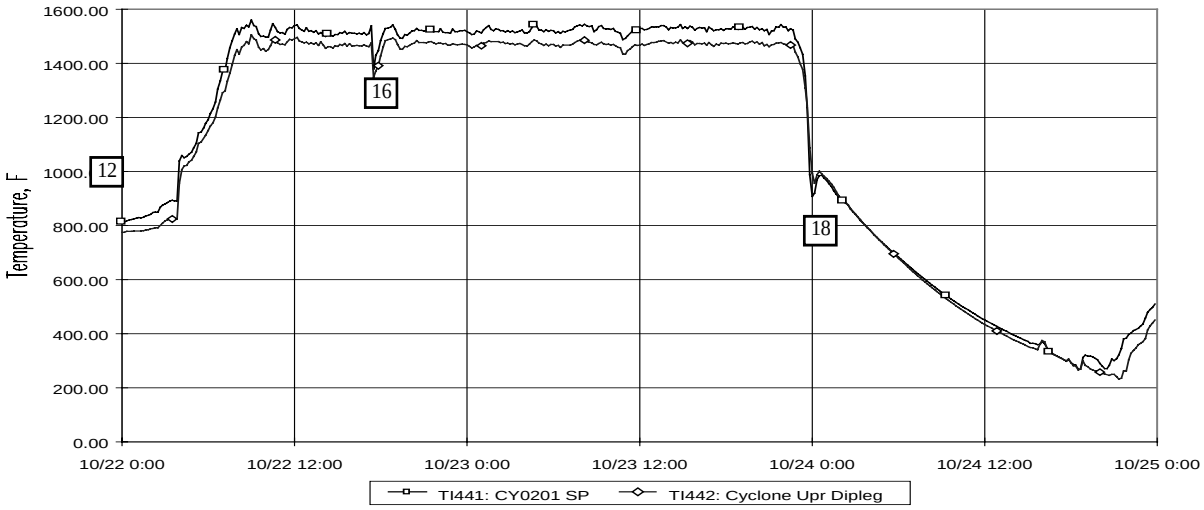

Figure 4.1.4.6-26 Cyclone Dipleg Temperatures

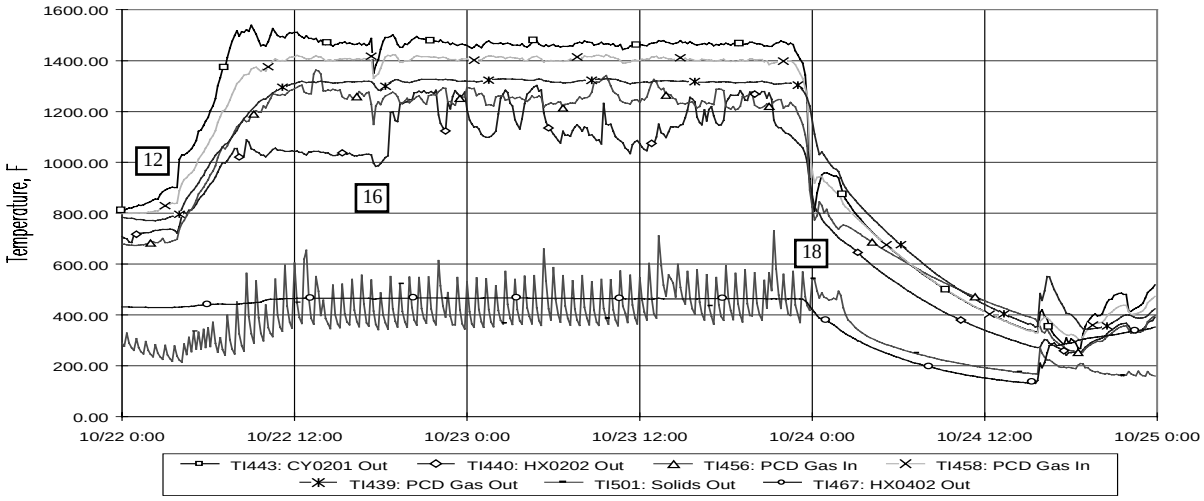

Figure 4.1.4.6-27 Temperature Profile Downstream of Reactor

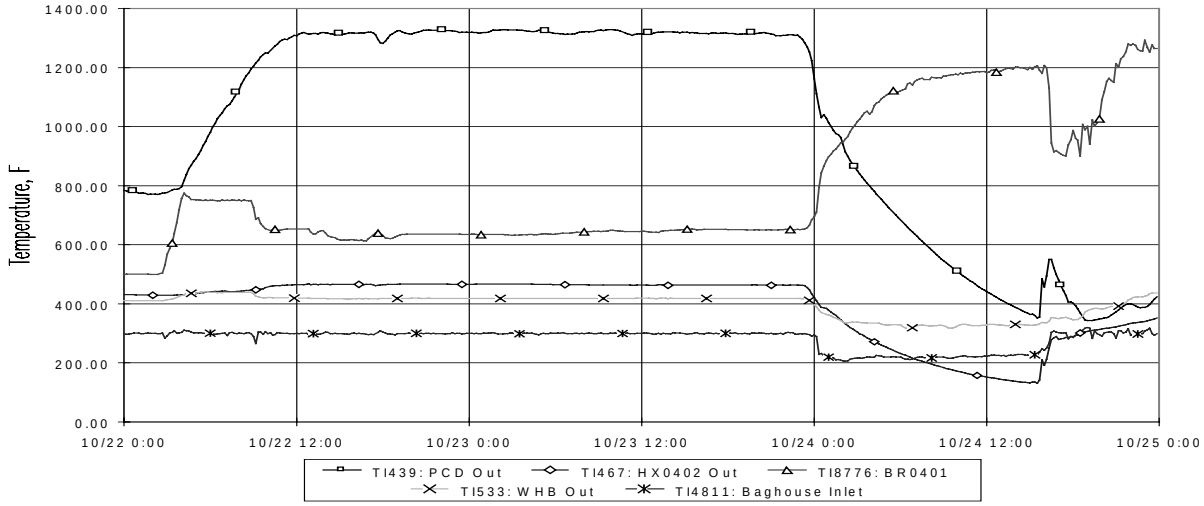

Figure 4.1.4.6-28 System Temperatures Downstream of PCD

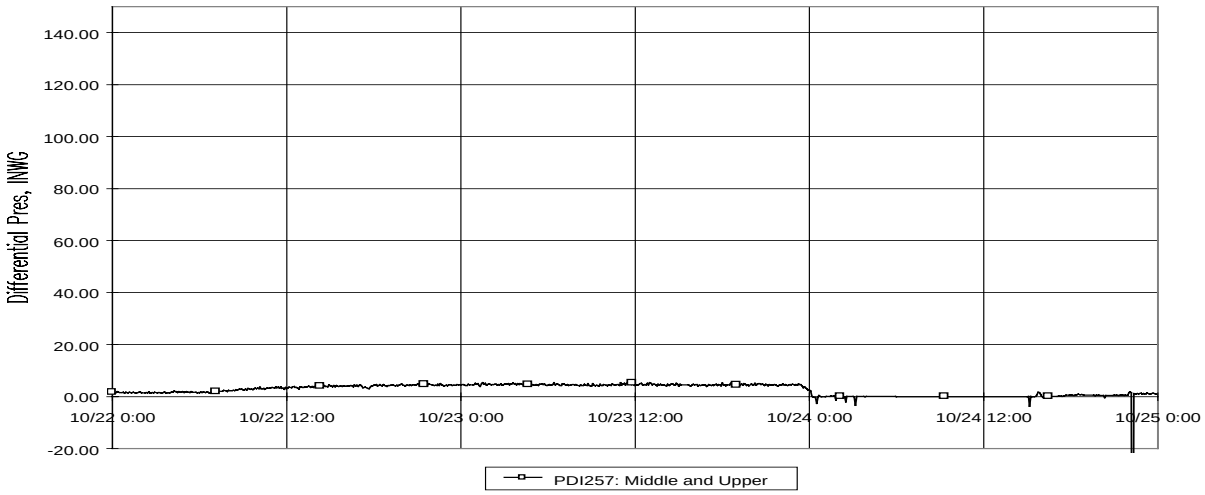

Figure 4.1.4.6-29 Mixing Zone Differential Pressure Profile

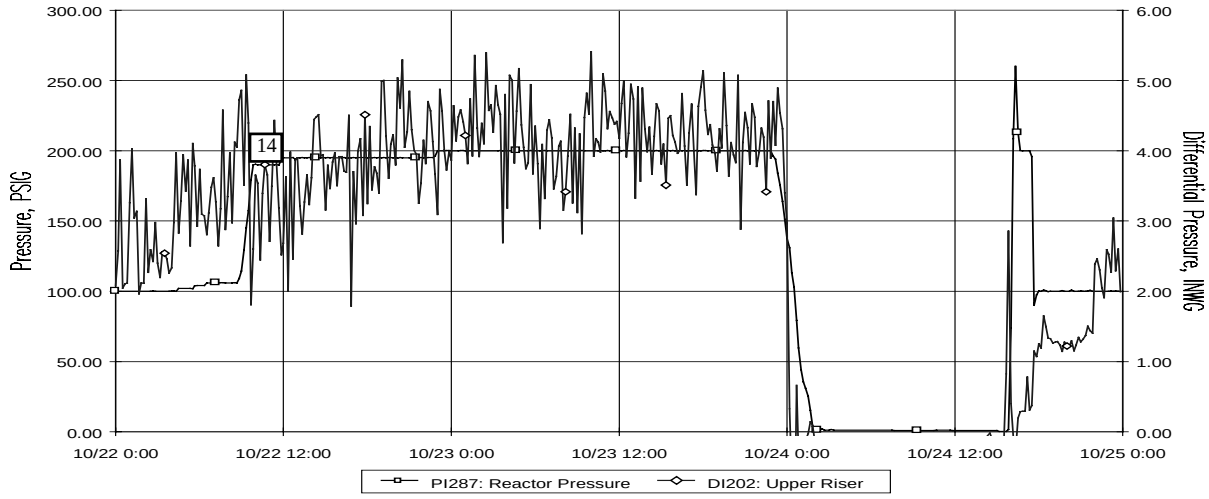

Figure 4.1.4.6-30 Reactor Pressure/Riser Differential Pressure Profiles

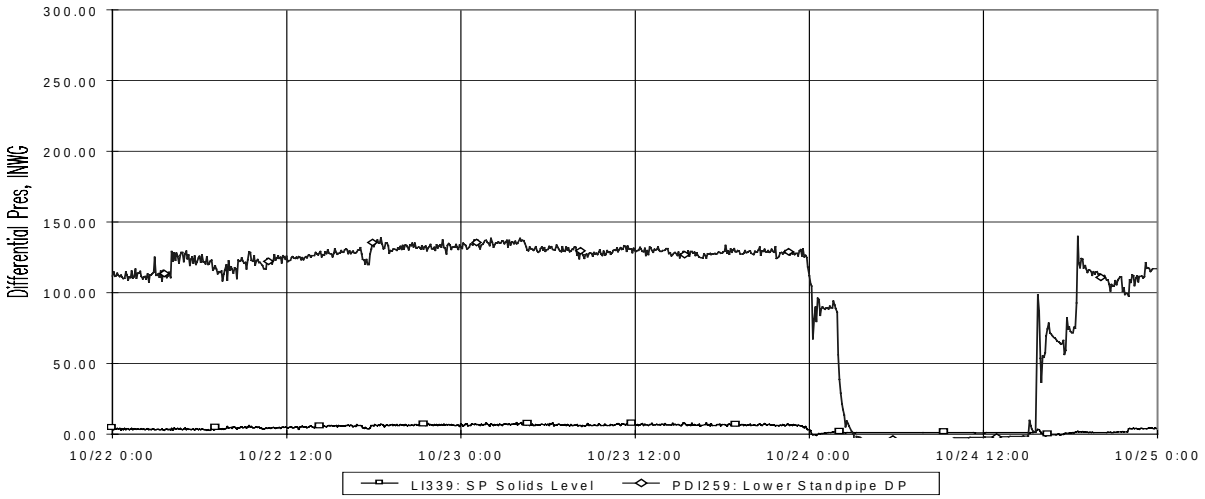

Figure 4.1.4.6-31 Standpipe Differential Pressure Profiles

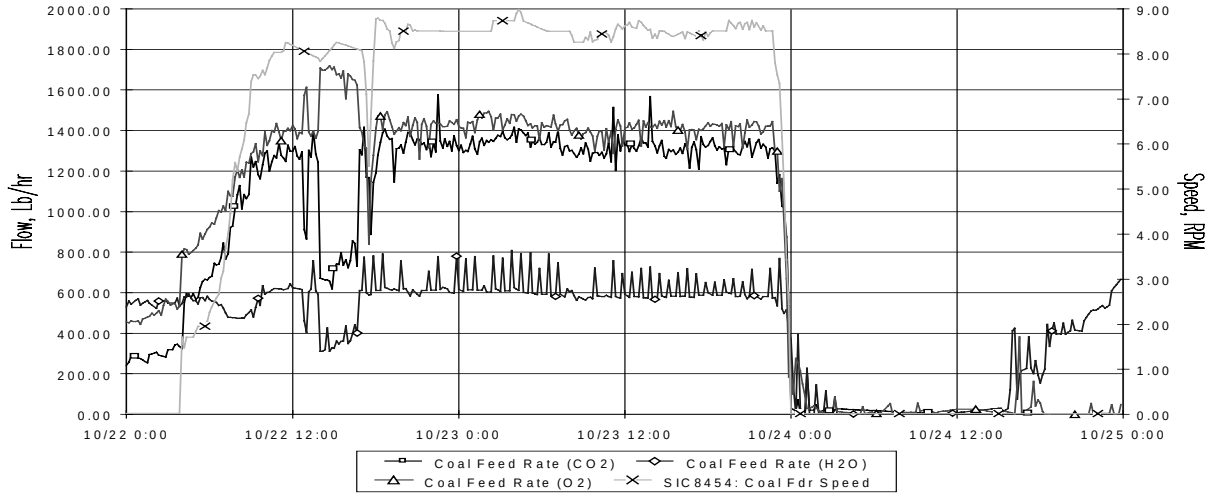

Figure 4.1.4.6-32 Coal Feed Rate Based on Gas Analysis

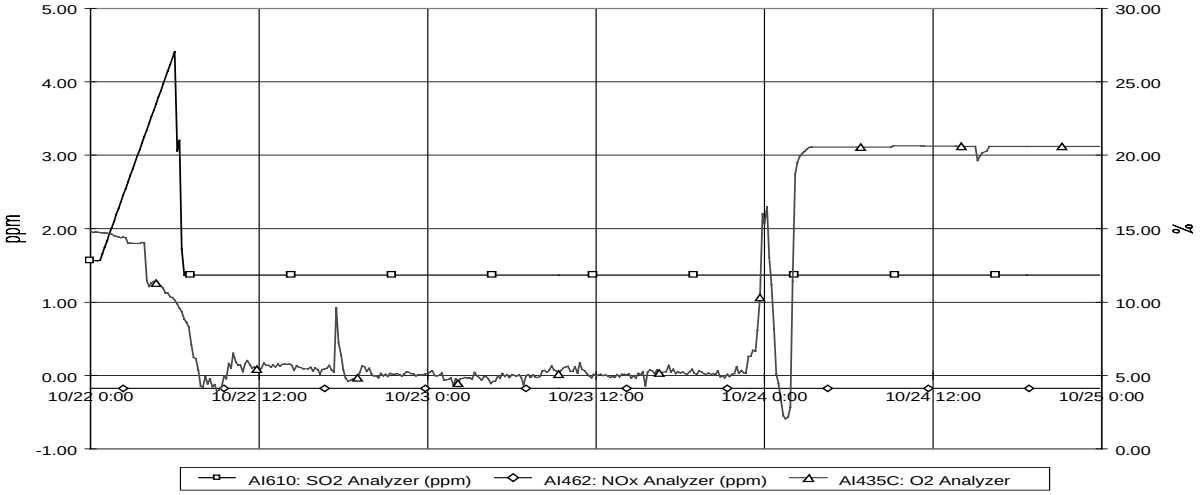

Figure 4.1.4.6-33 O_2, SO_2, and NO_x Analyzers

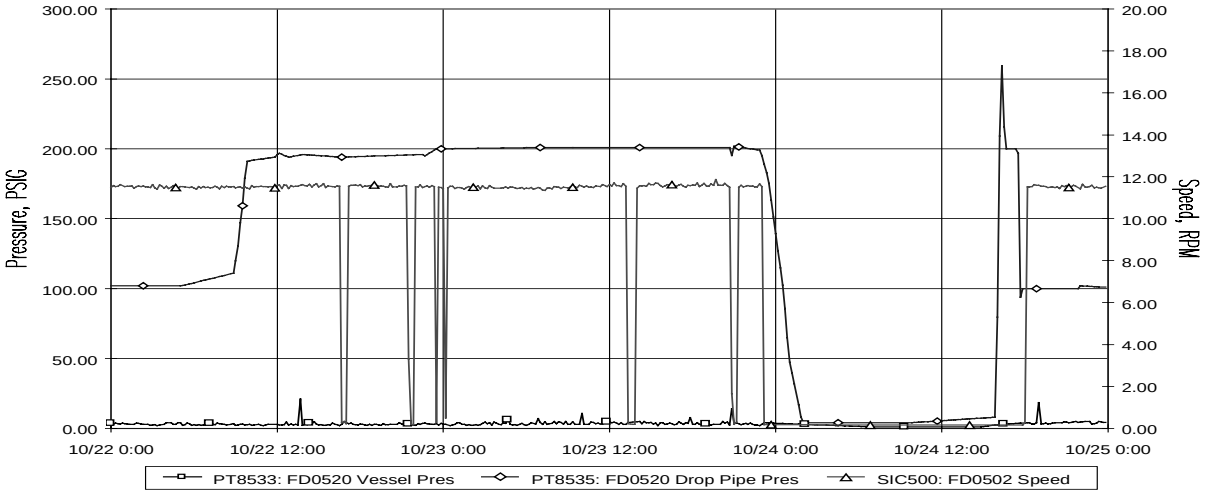

Figure 4.1.4.6-34 FD0520 Pressure Profiles

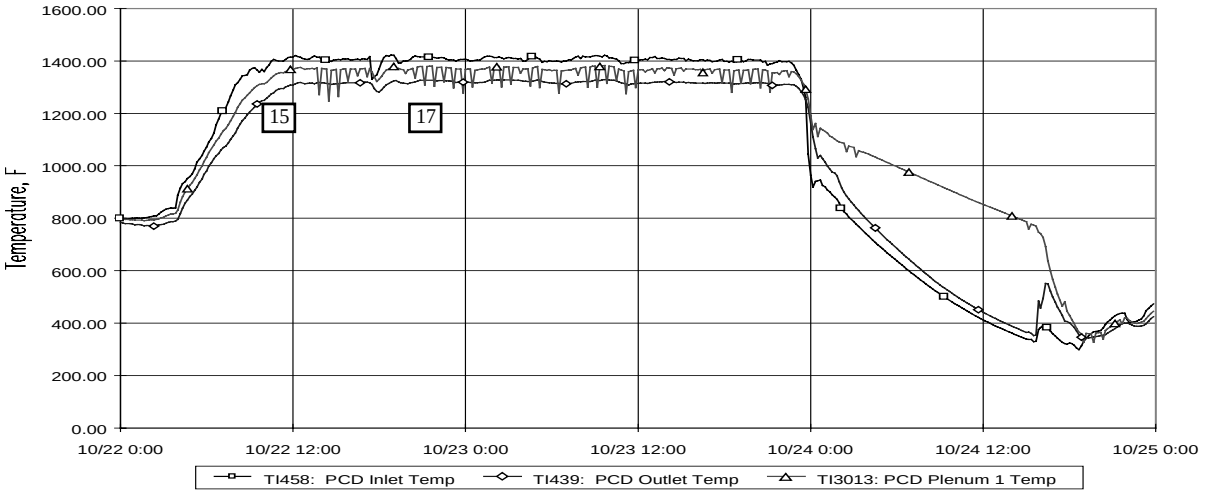

Figure 4.1.4.6-35 PCD Temperatures

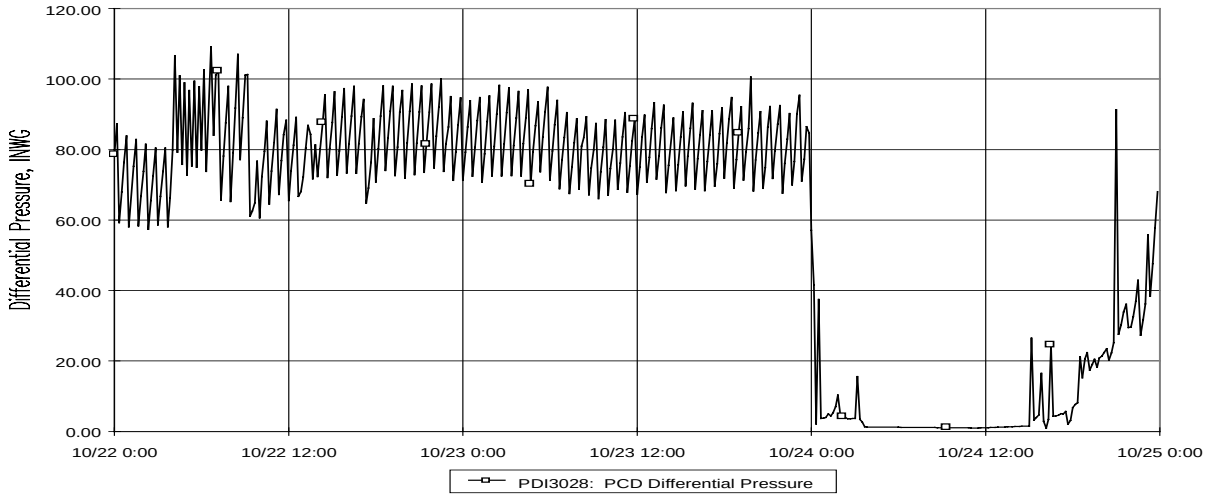

Figure 4.1.4.6-36 PCD Differential Pressure Profile

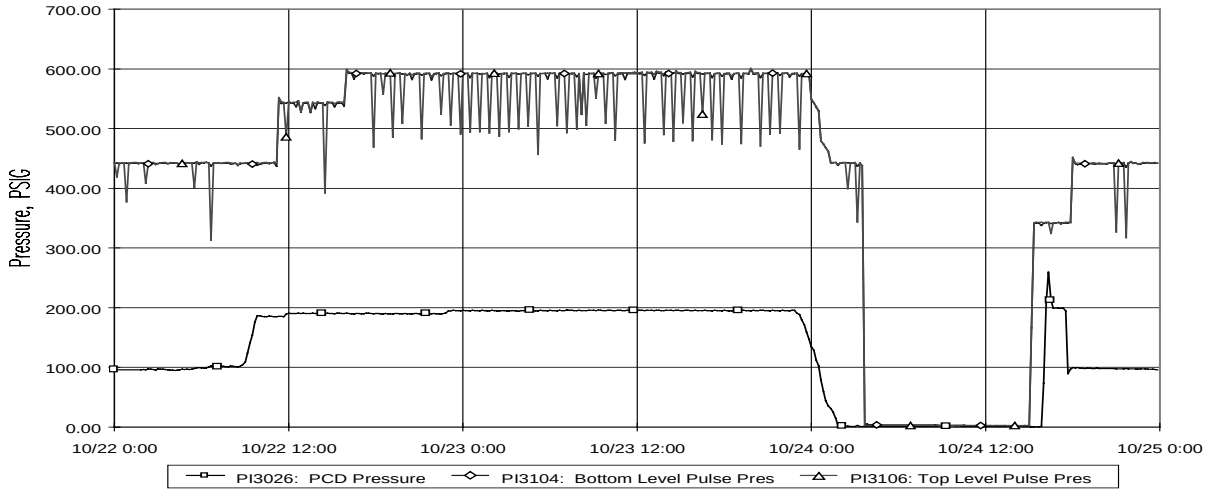

Figure 4.1.4.6-37 PCD Pressure and Pulse Pressure

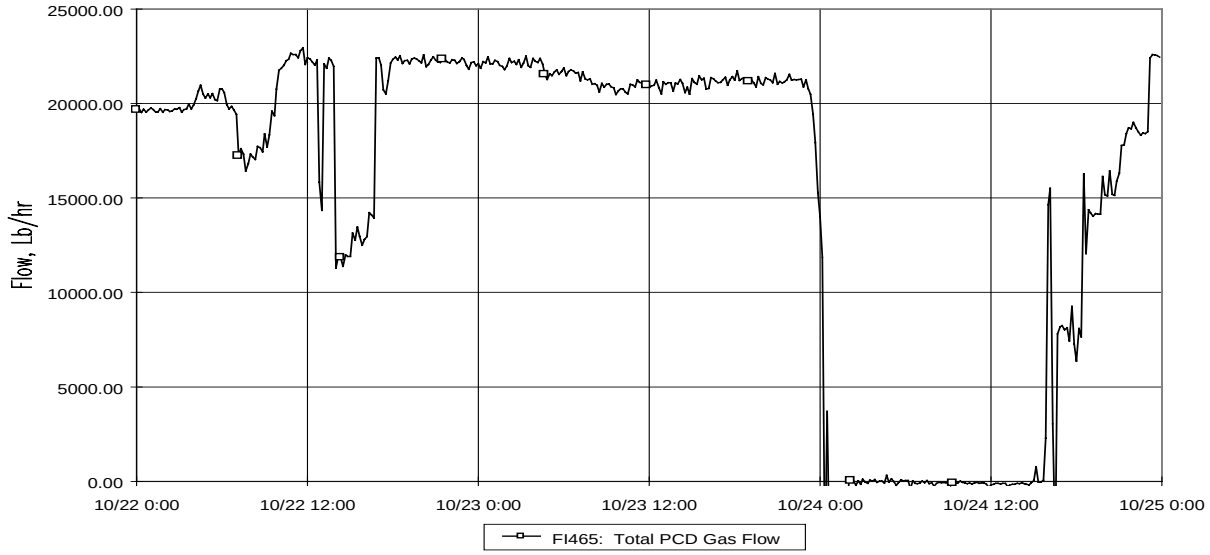

Figure 4.1.4.6-38 Gas Flow Through PCD

4.1.4.7 TC01G Test Run

Test run TC01G was conducted between October 25 and November 2, 1997. Operating plots are shown in figures 4.1.4.7-1 through -42. The following maintenance work was completed during the October 24, 1997, outage:

- The repressurization line of the transport air dryer (DY0210) was rerouted so that the source air comes off the line downstream of the afterfilter. This was done to prevent desiccant carryover from interfering with the repressurization solenoid valve operation.

- Based on recommendations from Clyde, the seal pressure was reduced to the eight high-pressure spheri valves on the coal feeder (FD0210), sorbent feeder (FD0220), spent solids (FD0510), and the spent fines (FD0520) transport systems. During bench tests it was observed that the clearance between the seal and dome dramatically decreases after just a few cycles. By pressurizing to a lower pressure the decrease in clearance should be lessened.

- Also based on recommendations from Clyde, the seal material in the lower spheri valve on the FD0520 system was changed to address the seal extrusion problems.

- The O-ring causing the seal nitrogen leak was replaced on the lower spheri valve on the FD0520 system.

- The trip pressure for the baghouses for the FD0210, FD0220, and FD0530 systems was changed from 10 to 5 inH_2O since the FD0210 bags were found to have a sufficiently thick layer of fine dust.

TC01G Test Run Chronology

- Following the completion of the leak test the main air compressor (CO0201) was started at 18:50 on October 24, 1997. The start-up burner (BR0201) was lit at about 19:35 and after a 1-hour hold at 500°F the exit temperature was steadily increased.

- On October 25, 1997, plugging in BR0201 main gun obstructed the flow of propane, decreasing the reactor pressure from 100 to 90 psig and causing an increase in the pressure difference across the burner tip that dislodged the clog. At 05:15 the coal and sorbent feed systems were aligned for service. It was noticed that the reactor temperatures increased by about 50°F when the coal feeder was aligned, indicating that coal dust had blown into the reactor. At 05:27 coal feed was started (event 1, figures 2 and 5 through 9). At 09:15 the reactor temperatures were oscillating, so the HX0203 aeration was adjusted to smooth the circulation through the heat exchanger and, therefore, reduce the fluctuation in reactor temperatures. After stabilizing the reactor temperatures BR0201 was shut down at about 10:45 and the reactor pressure was increased. By 12:00 the reactor pressure was increased to 190 psig (event 2, figure 12).

- As with all other test runs the coal feed lockhopper and the PCD were periodically fluffed to prevent any bridging. At 14:00 FD0502 started making an unusual noise, which suggested that the shaft of the screw could have been warped. By 16:15 the PCD plenum temperature had reached 1,350°F (event 3, figure 18). The aeration on the combustion heat exchanger (HX0203) was adjusted around 16:20 to stabilize the circulation through the heat exchanger J-leg. A timer in FD0520 PLC was adjusted because there had been multiple cycles where the level probe was not becoming uncovered when the bottom spheri valve opened.

- The data acquisition system failed to capture data for about 40 minutes beginning about 02:00 on October 26, 1997, (event 4, figures 1 through 3 and 6 through 10) due to a DCS problem with the change from daylight savings time. There were problems with the FD0220 weigh cell that were related to the lock vessel pressure not venting down to below 5 psig due to leaks in the vent. Also, the pressure equalization valve (XV8407) on FD0220 was leaking badly. As a result of the leak FD0220 would not cycle and had to be manually vented.

- Coal feed was lost at 14:00 (event 5, figures 2 and 5 through 9) as a result of a problem with FD0210. Circulation was reduced to conserve reactor temperatures while several attempts were made to fix the problem. Since the coal feeder problems could not be resolved the reductions in reactor pressure began at 21:20 (event 6, figure 12) and BR0201 was lit at about 22:55 (event 7, figure 4). Additional trouble-shooting with FD0210 was done throughout the night in preparation for starting coal feed the next morning.

- Coal feed resumed at 06:30 on October 27, 1997 (event 8, figures 2 and 5 through 9), but was stopped at 09:00 (event 9, figures 2 and 5 through 9) due to continued problems with FD0210. The FD0210 system was isolated to investigate the cause of the coal feed problems. The upper breaker arm on the star feeder was found bent by about 120 degrees and was close to the horizontal. It was supposed to be about 30 degrees to the vertical and about 1.0 inch from the cone surface. A thick cake had built up in the cone section of the dispense vessel but there was no cake present in the barrel section of the dispense vessel. At the top of the cone the cake thickness was about 10 inches. The tunnel hole in the middle was clear to the spheri valve. The likely cause of the problem appeared to be bridging at the bottom of the lock vessel.

- A noise in the FD0502 system that started on October 25, 1997, was traced to a loose bolt at the bottom of the drive chain cover. The screw cooler shaft was shifting slightly from side to side indicating the shaft might be warped. Coal feed started again at 16:25 (event 10, figures 2 and 5 through 9) but there was difficulty transferring coal from the lockhopper to the dispense vessel due to the presence of excess fines in the coal. After hours of continuously working with the FD0210 system in the field the system began operating normally around 22:10. At 22:15 the FD0220 system was stopped to replace the leaking XV8407 pressure equalization

valve. The BR0201 was shutdown at about 22:55 and the reactor pressure was increased (event 11, figure 12). The FD0220 was restarted at 23:15.

- The PCD plenum temperature reached 1,350°F by 05:00 on October 28, 1997 (event 12, figure 18). The FD0206 was run periodically to control the solids levels in the reactor and HX0203. The HX0203 solid level was at its highest for this test run. It was covering the solids inlet to HX0203. SRI took PCD inlet and outlet dust samples. Overall, the process conditions were stable with only minor adjustments to increase the circulation rate.

- Other than some minor problems with plugging at the FD0510 system exit around 01:45 the process and all equipment ran well on October 29, 1997.

- The FD0220 system was stopped at 08:25 (event 13, figure 24) on October 30, 1997, for a gas bomb sample to be taken from the secondary crossover for SO_2 analysis. The purpose was to ascertain the accuracy of the gas analysis system since it previously had not detected any SO_2. After the sampling was completed FD0220 was restarted at 08:55. The FD0502 was momentarily stopped at about 09:00 (event 14, figure 38) for maintenance.

- At 10:15 the reactor pressure was gradually increased to 205 psig (event 15, figure 33). The gas analysis system was taken out of service due to few leaks and a broken flow indicator. The back-pulse pressure was increased to 600 psig around 16:55 (event 16, figure 41) because the PCD showed a gradual decrease in permeability.

- On October 31, 1997, SRI took samples for about 2 hours and the gas analysis system was put back in service. Around 15:00 a gas leak from FD0502 packing was found. The packing was tightened to minimize the leak.

- Throughout November 1, 1997, FD0206 was periodically run to maintain the solids level in HX0203 within acceptable limits. The FD0502 packing was again tightened to reduce the leak that began on October 31, 1997. The baghouse screw started squealing around 11:00. Since the probe in FD0820 appeared to produce inaccurate results the baghouse screw was shut down. The FD0820 timer was reset at 13:30 so that it cycled only every half-hour. The aeration on HX0203 J-leg was reduced at 18:30 due to a high solids level in HX0203 and a high-circulation rate.

- At 06:00 on November 2, 1997, BR0201 was lit after problems with the coal feeder system developed. The problems with the coal feed system started at about 22:00 on November 1, 1997. The usual steps were taken to resolve the problem but with no success. Reactor heat up continued throughout the morning. The feeder motor was pulled on the morning of November 2, 1997, to inspect the coal feed system. After the maintenance items were completed on the coal feeder system it was aligned for service. With the reactor temperatures ranging from 900 to 950°F coal feed to the reactor was initiated at around 13:00 (event 17, figures 23 and 26 through 30). The motor was started but the dispense vessel/conveying line differential pressure was

high (~20 psid), which caused the motor to stop (event 18, figure 23). The high differential pressure was an indication of a plug at the exit of the coal feeder or at the bottom of the dispense vessel. The coal feeder motor was restarted. However, the differential pressure continued to oscillate from zero to 20 psig, causing the motor to stop. The motor was restarted and it tripped several more times during the next 5 minutes. During this 5-minute period some coal was fed into the reactor, as shown by the small increases in reactor temperature at the rate of approximately 20 deg/min (event 19, figures 23 and 26 through 30). The feeder motor was disabled at 13:06 due to the continued high differential pressure.

- Approximately 1.5 minutes later the dispense vessel/conveying line differential pressure started to swing from zero to 20 psid and the conveying line pressure also started to swing from 105 to 155 psig, indicating that coal was blowing into the reactor. The reactor temperature increased 200°F in about 1.25 minutes causing the PCD inlet temperature to increase 80°F in about the same time period and the PCD upper plenum temperature to increase 50°F in about 1 minute. The oxygen content in the reactor dropped from about 12 to 4 percent during this time (~13:10) (event 20, figure 37). Before the isolation valve to the reactor was closed the differential pressure again went high, as did the conveying line pressure, at around 13:13. At 13:15, as the bridge/plug broke loose, the conveying line pressure decreased and started swinging. It was estimated that about 100 lb of coal was blown into the reactor in about 1 minute. Again, the reactor temperatures increased rapidly (in 1 minute): the riser temperature from 1,000 to 1,215°F; the PCD inlet temperature from 900 to 1,045°F; and the PCD upper plenum temperature from 870 to 960°F. The oxygen dropped from 12.8 to 1.8 percent. At 13:17 the manual isolation valve was closed to the reactor, preventing any additional coal from being blown into the reactor. At 13:30 the fines transporter system tripped due to a high conveying line pressure (event 21, figure 38).

- As in the past, and with the other three Clyde systems, the swing in the dispense vessel/conveying line differential pressure and increases in conveying line pressure in FD0210 occurred whenever the exit elbow plugged, the exit line plugged, or problems existed inside the discharge vessel.

TC01G Post Test Run Inspections

On November 3, 1997, the coal feeder motor was again removed to inspect the coal feed system. The dispense vessel was clean. Coal was packed in the pockets of the star feeder. The exit elbow and part of the exit line were all packed with coal. The line from the isolation valve to reactor was clear. There were no deposits in the line at the reactor entry.

There were many pinhole-size openings in the gas line to the analyzer house and in the process gas tubing in the SRI probes. These holes were later confirmed as being caused by chloride- and fluoride-related corrosion.

TC01G Test Run Observations

A total of 174.75 hours on coal was achieved and 113.2 tons of coal were fed. About 133 hours of PCD plenum temperature above 1,350°F was accumulated. Process gas bomb samples were taken from secondary crossover, PCD inlet and HX0402 exit for SO_2 analysis, and there was no trace of SO_2. Pin holes were detected in gas sampling tubes and in SRI gas treatment tubes. Analysis showed that these pin holes were caused by chloride- and fluoride-corrosion.

This test run was plagued by intermittent problems with the coal feeder system. Coal feed was interrupted two times before the last interruption and eventual shutdown of the process. The change in the seal material for the FD0520 bottom spheri valve seal appears to have eliminated the problems associated with blown seals that had plagued previous test runs. The change to equal-percentage trim in the pressure letdown valve eliminated the plug stem vibration problems experienced in previous test runs.

Section 4.1.4.7

Graphs 1 through 21

Test Run TC01G
October 25 through 29, 1997

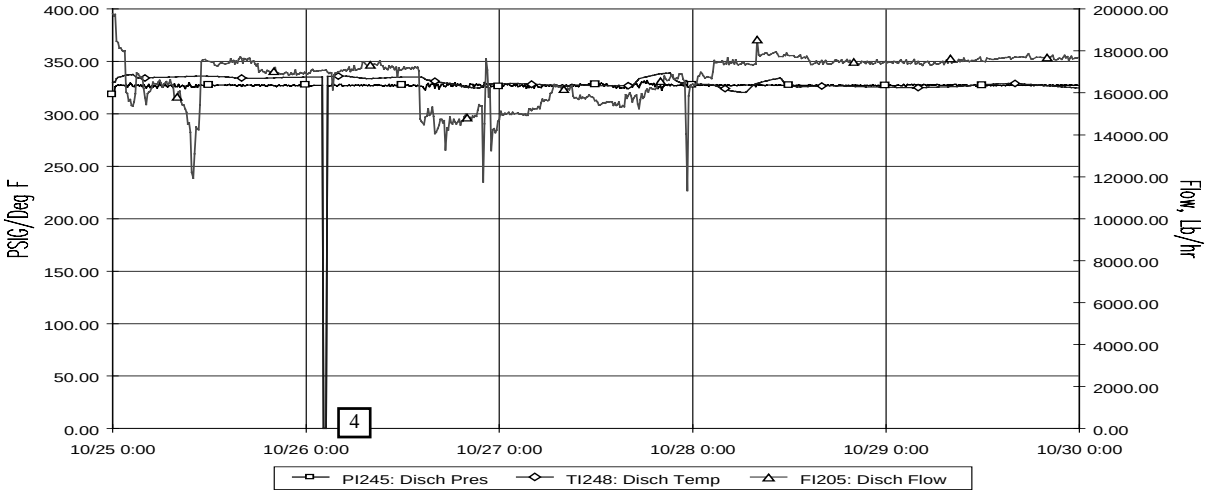

Figure 4.1.4.7-1 CO0201 System Profile

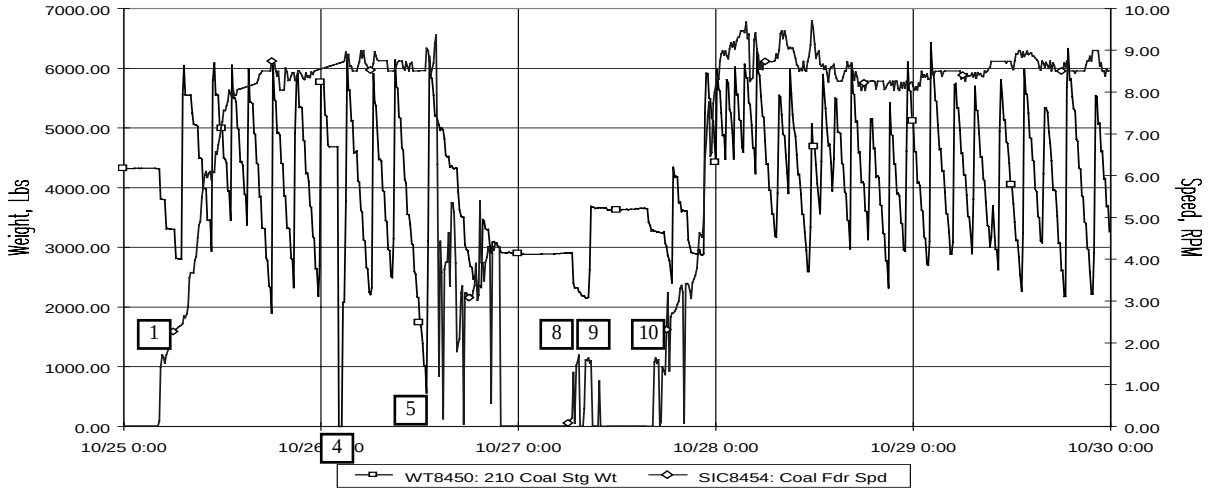

Figure 4.1.4.7-2 Coal Feed System Profile

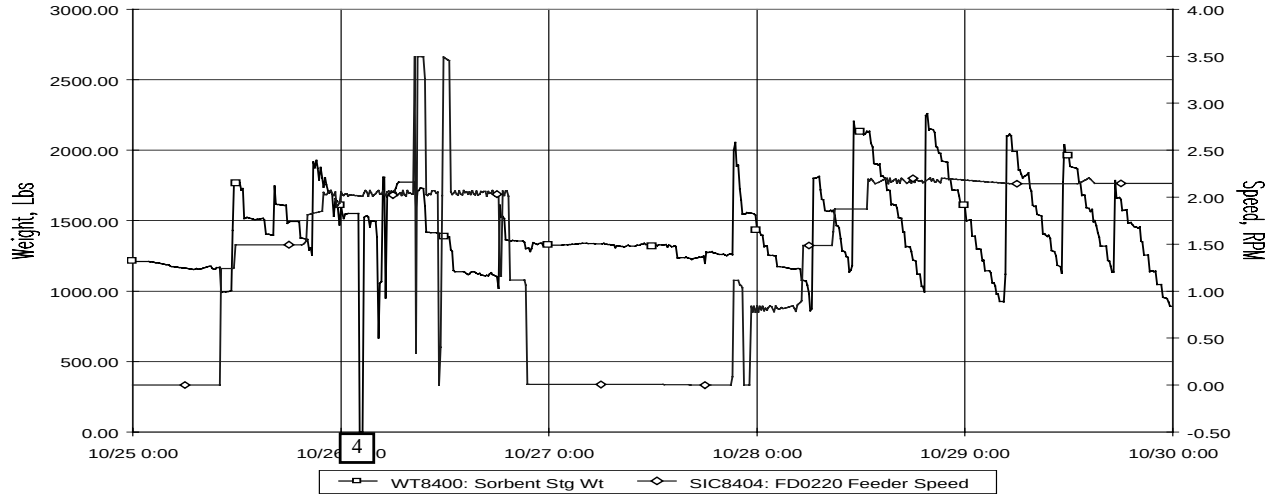

Figure 4.1.4.7-3 Sorbent Feed System Profile

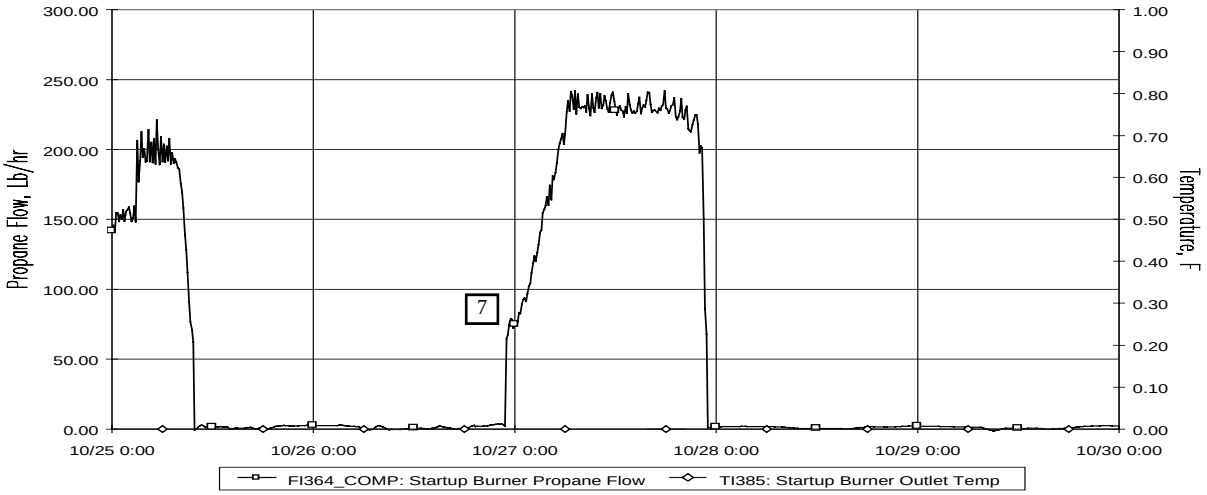

Figure 4.1.4.7-4 Start-Up Burner Flow/Temperature

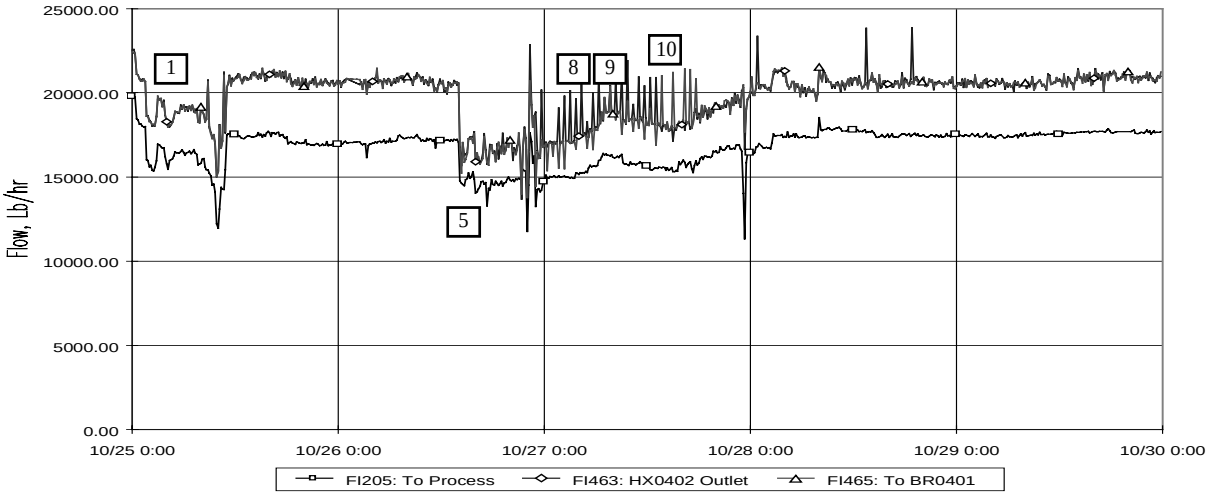

Figure 4.1.4.7-5 Total Gas In/Out Flow Rates

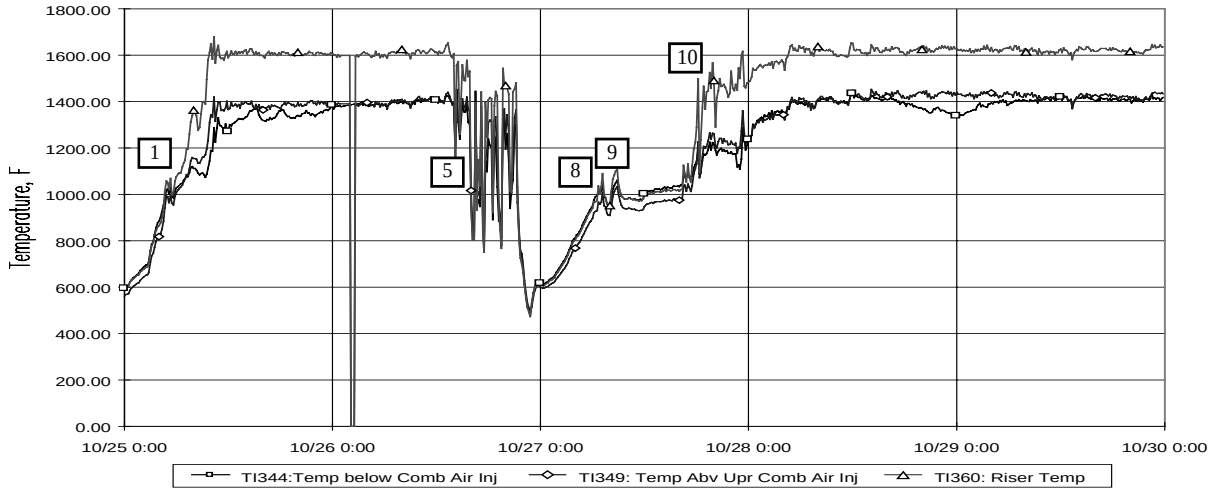

Figure 4.1.4.7-6 Reactor Mixing Zone and Riser Temperatures

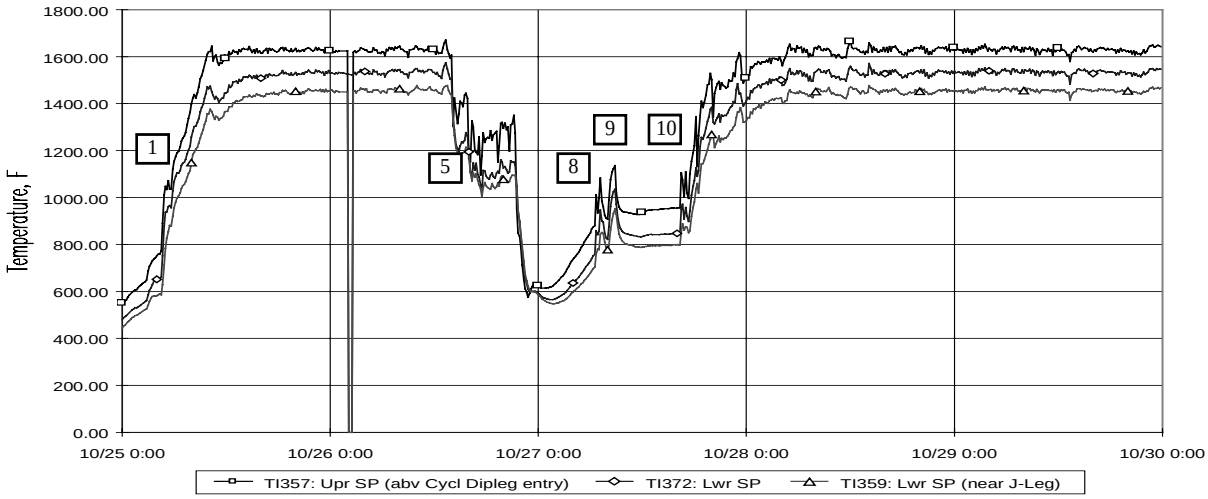

Figure 4.1.4.7-7 Standpipe Temperatures

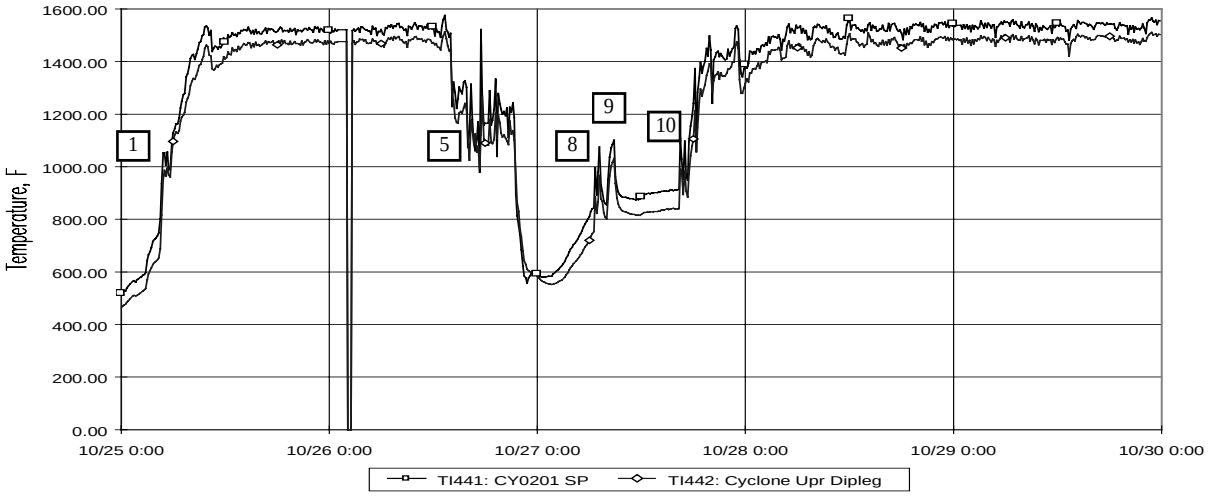

Figure 4.1.4.7-8 Cyclone Dipleg Temperatures

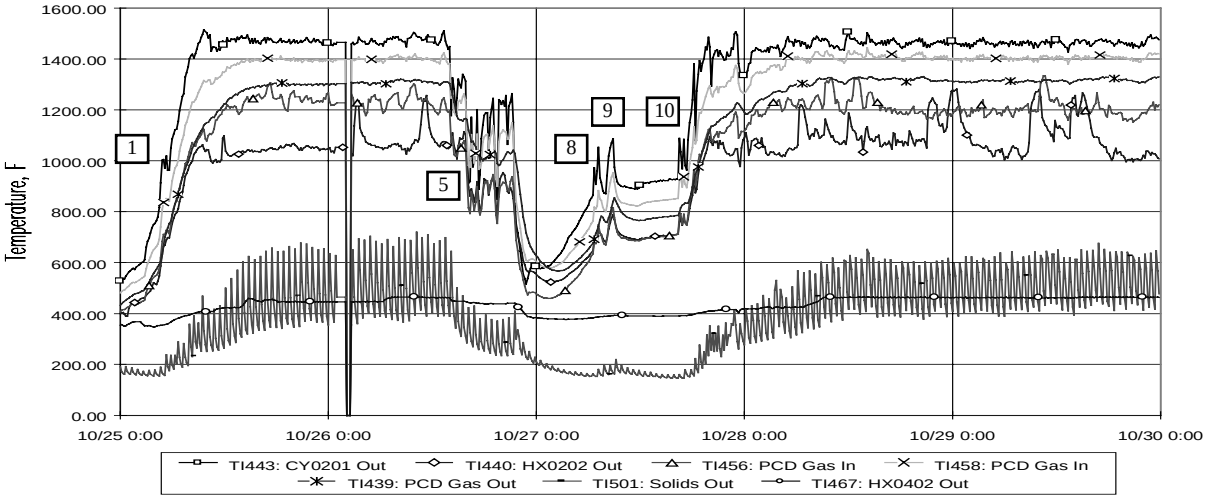

Figure 4.1.4.7-9 Temperature Profile Downstream of Reactor

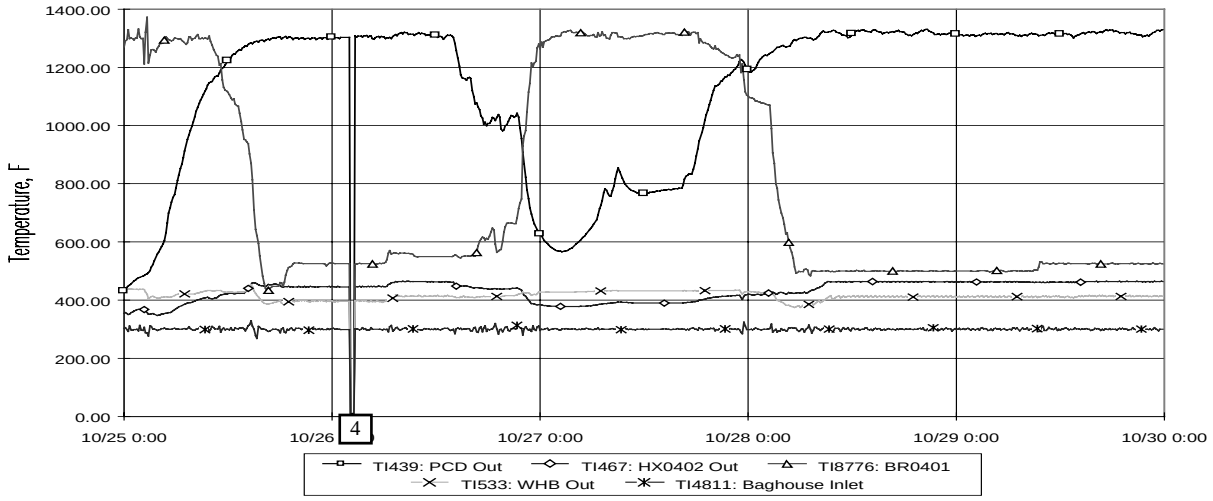

Figure 4.1.4.7-10 System Temperatures Downstream of PCD

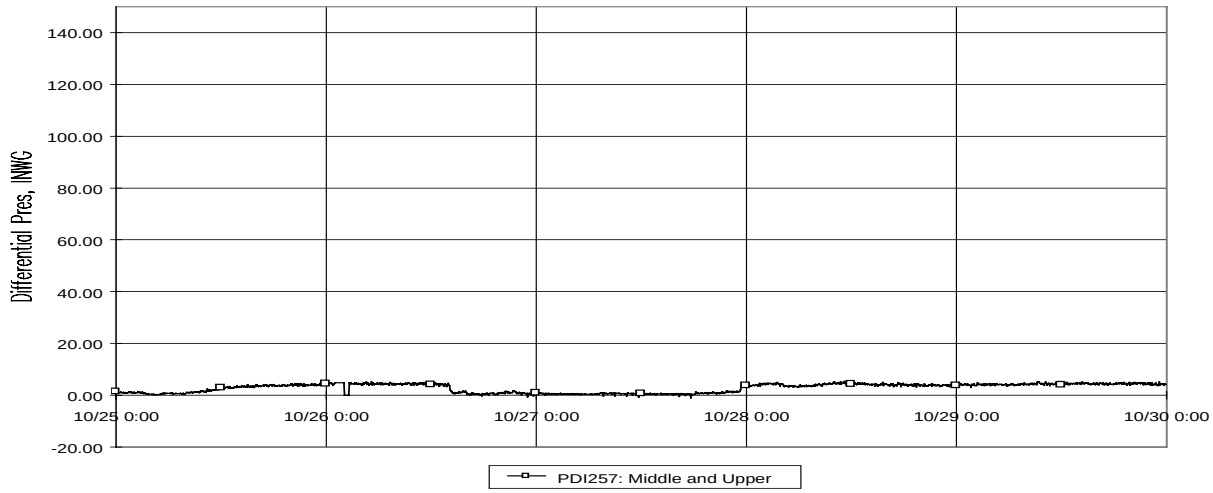

Figure 4.1.4.7-11 Mixing Zone Differential Pressure Profile

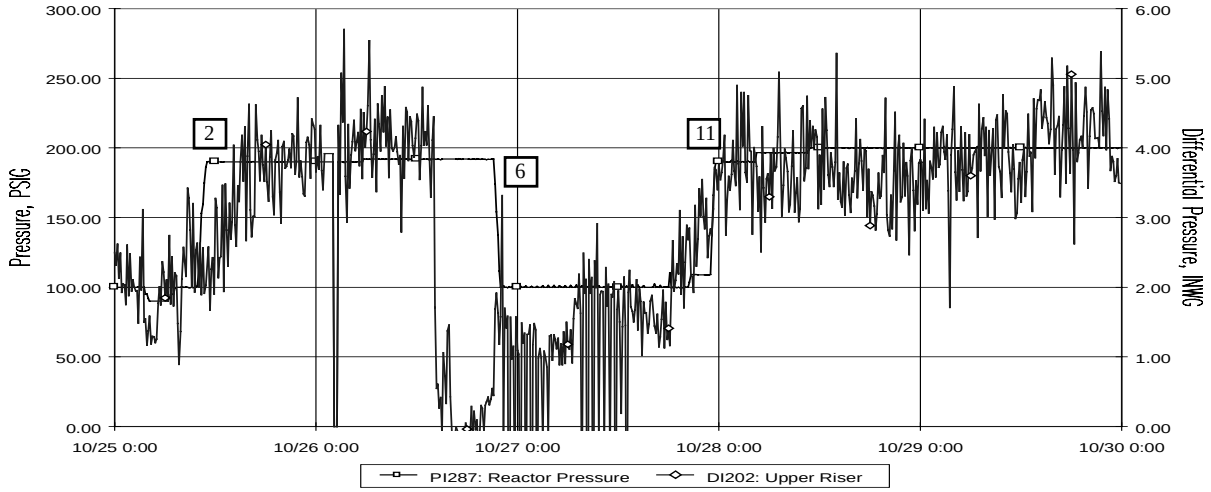

Figure 4.1.4.7-12 Reactor Pressure/Riser Differential Pressure Profiles

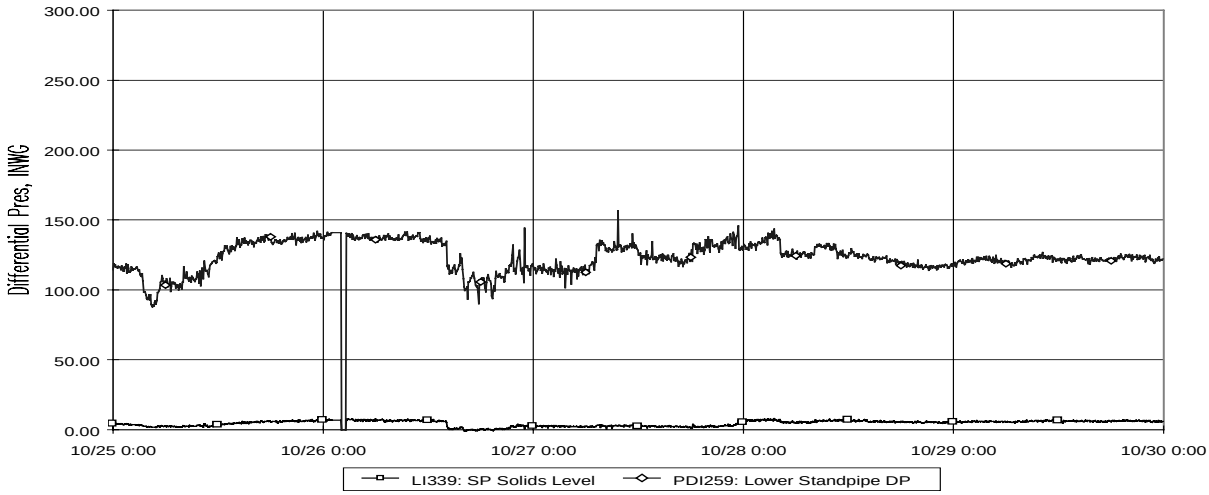

Figure 4.1.4.7-13 Standpipe Differential Pressure Profiles

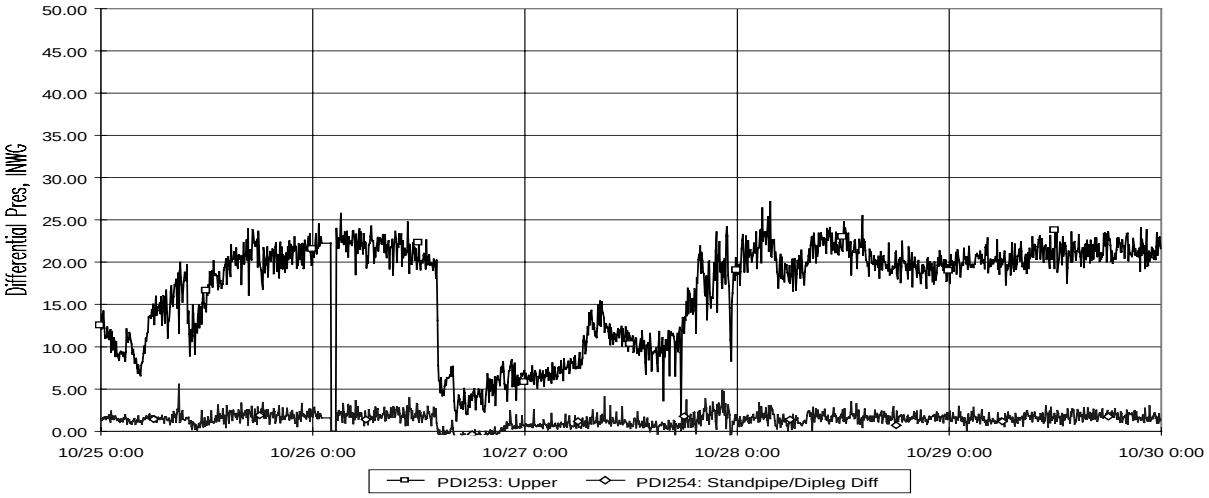

Figure 4.1.4.7-14 CY0201 Dipleg Differential Pressure Profiles

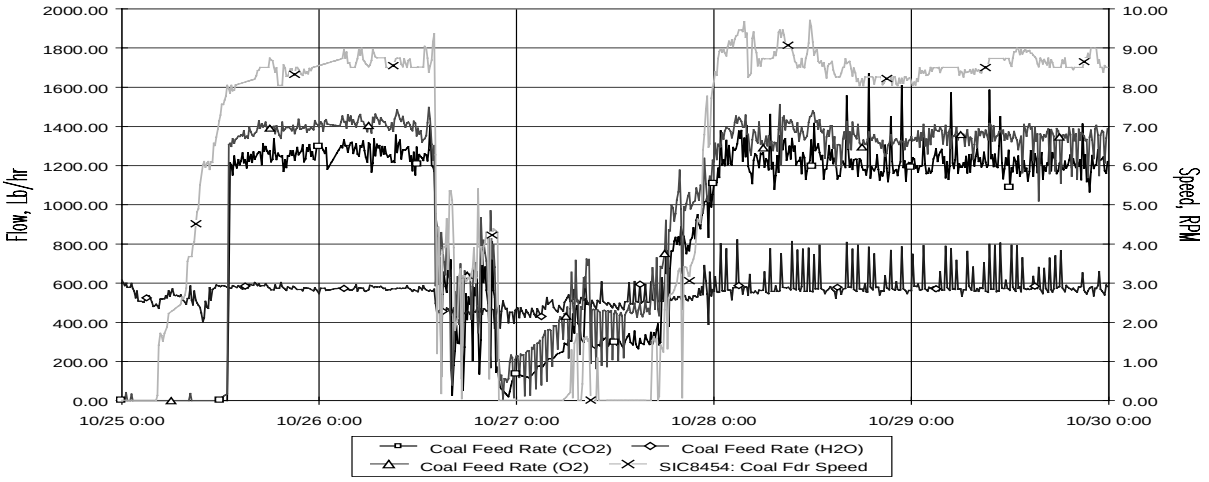

Figure 4.1.4.7-15 Coal Feed Rate Based on Gas Analysis

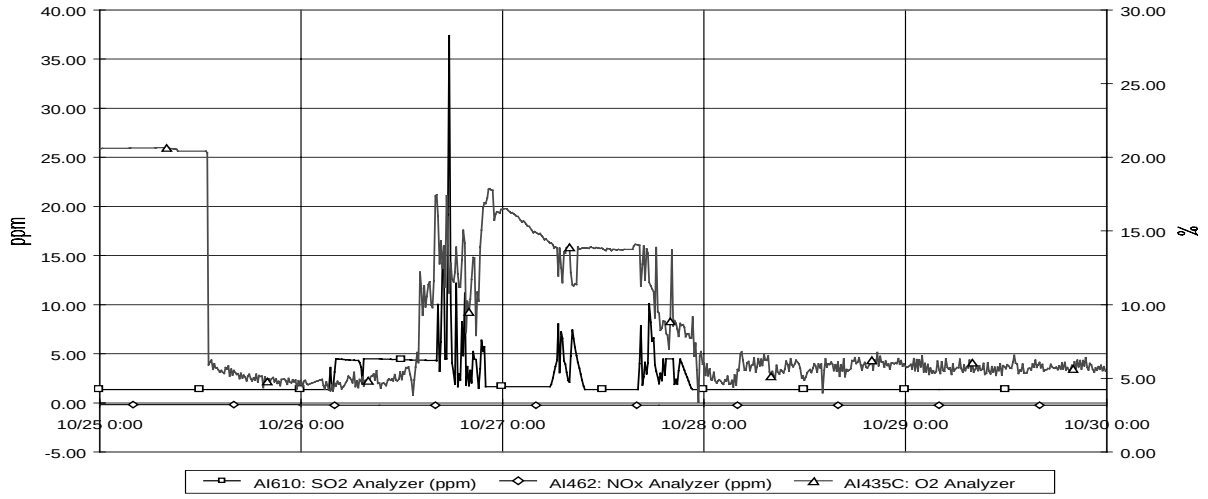

Figure 4.1.4.7-16 O_2, SO_2, and NO_x Analyzers

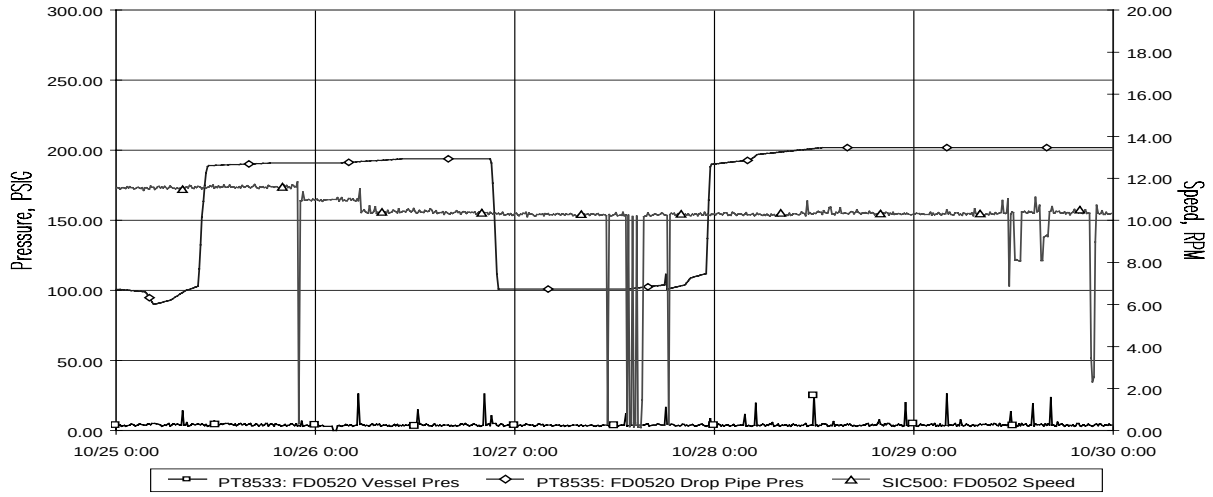

Figure 4.1.4.7-17 FD0520 Pressure Profiles

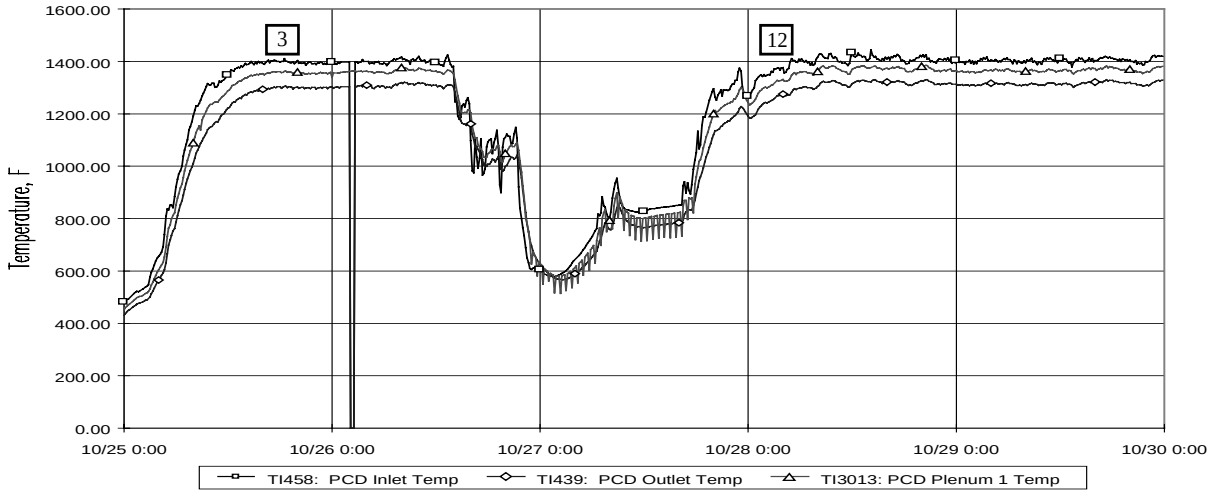

Figure 4.1.4.1-18 PCD Temperatures

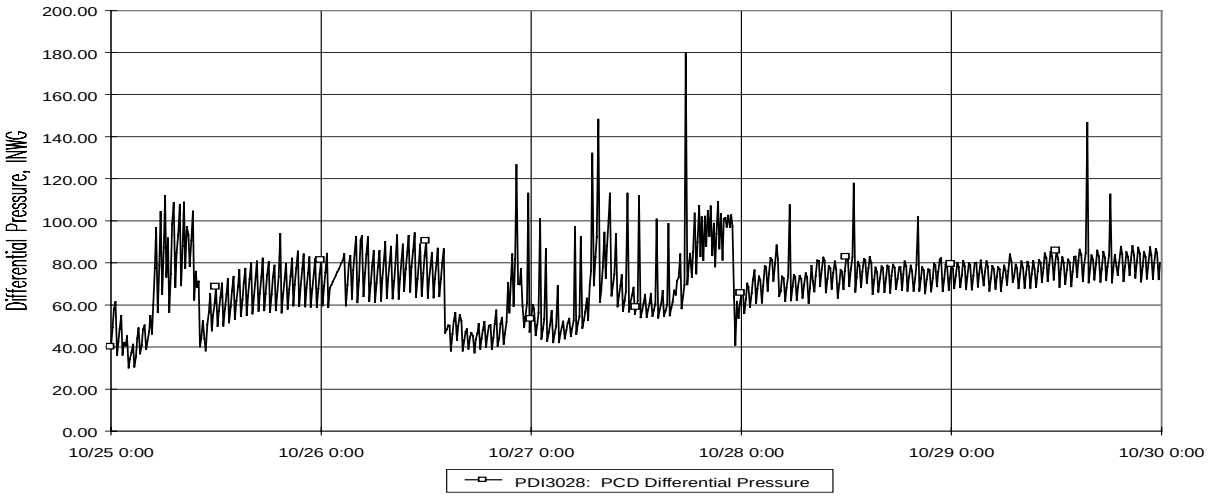

Figure 4.1.4.7-19 PCD Differential Pressure Profile

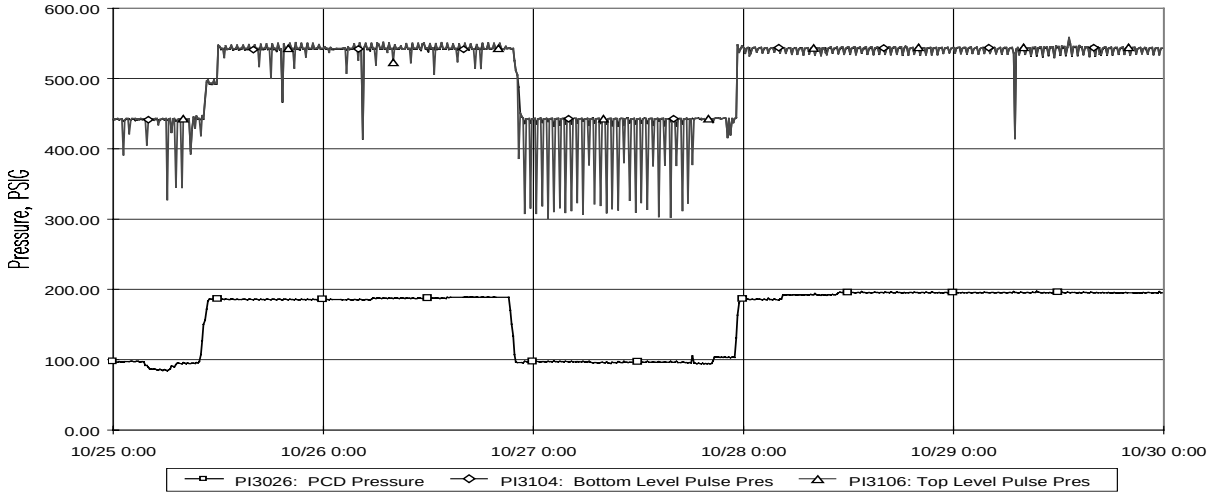

Figure 4.1.4.7-20 PCD Pressure and Pulse Pressure

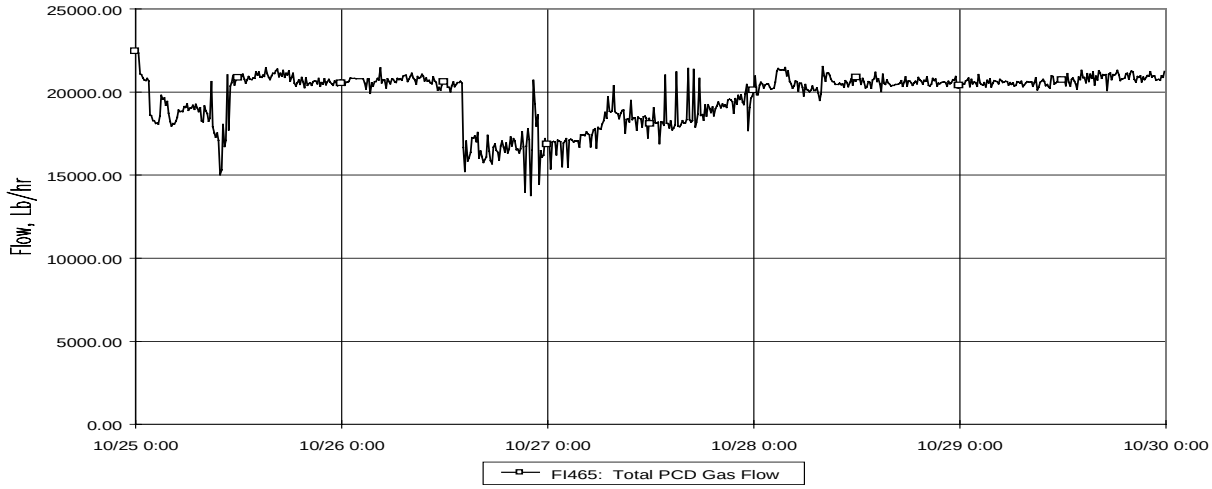

Figure 4.1.4.7-21 Gas Flow Through PCD

Section 4.1.4.7

Graphs 22 through 42

Test Run TC01G
October 30 through November 2, 1997

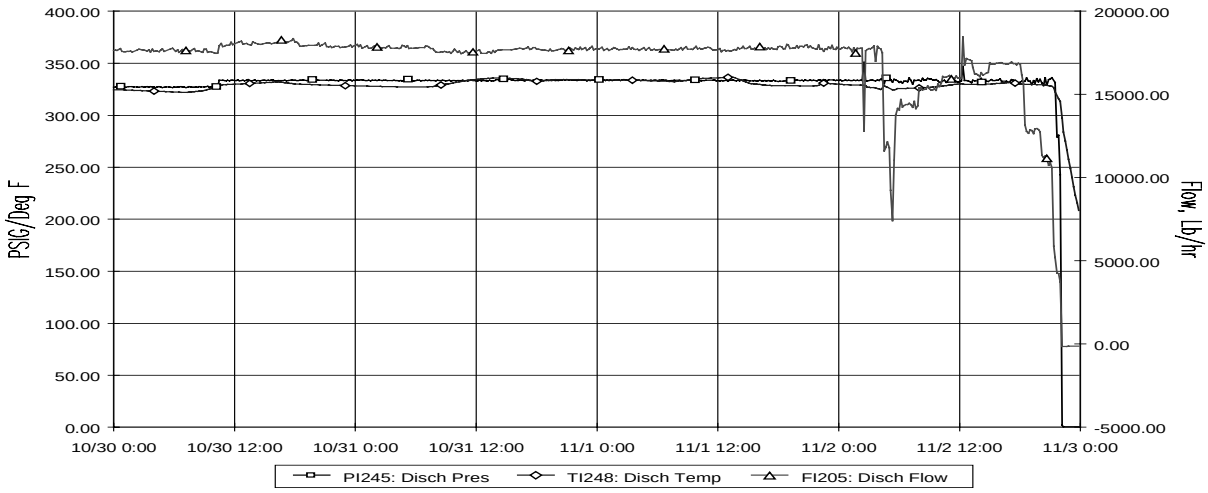

Figure 4.1.4.7-22 CO0201 System Profile

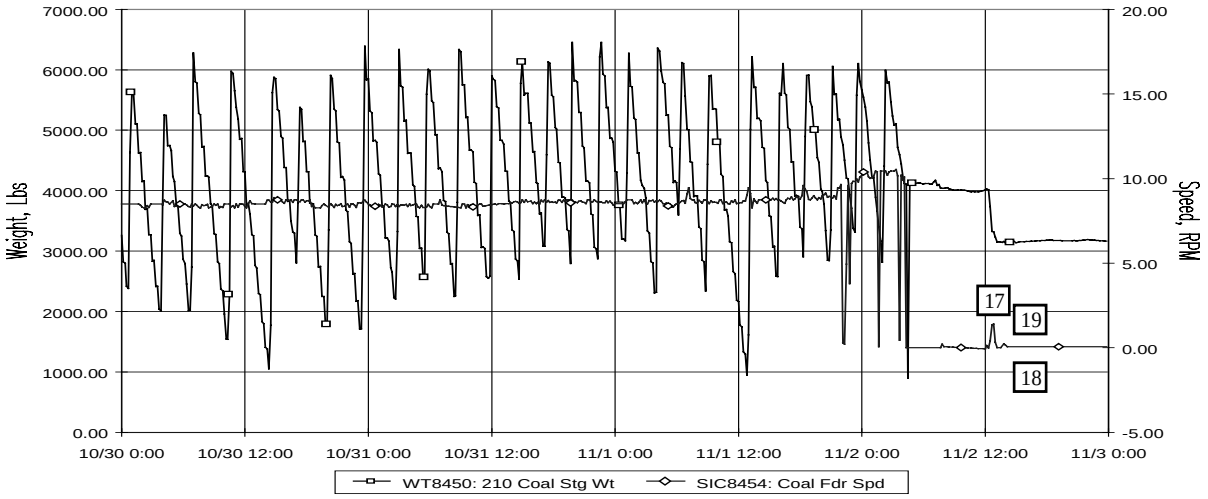

Figure 4.1.4.7-23 Coal Feed System Profile

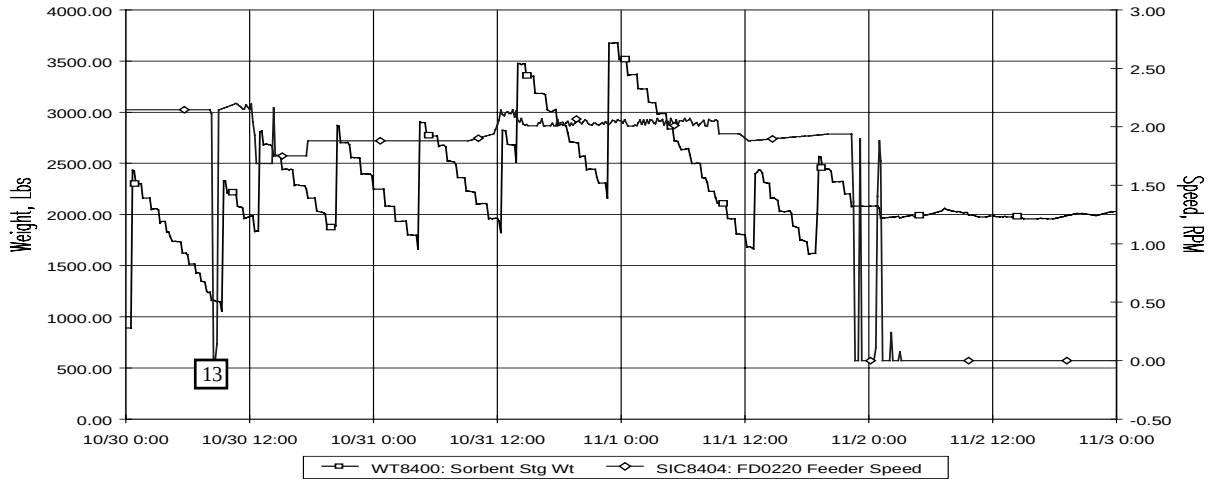

Figure 4.1.4.7-24 Sorbent Feed System Profile

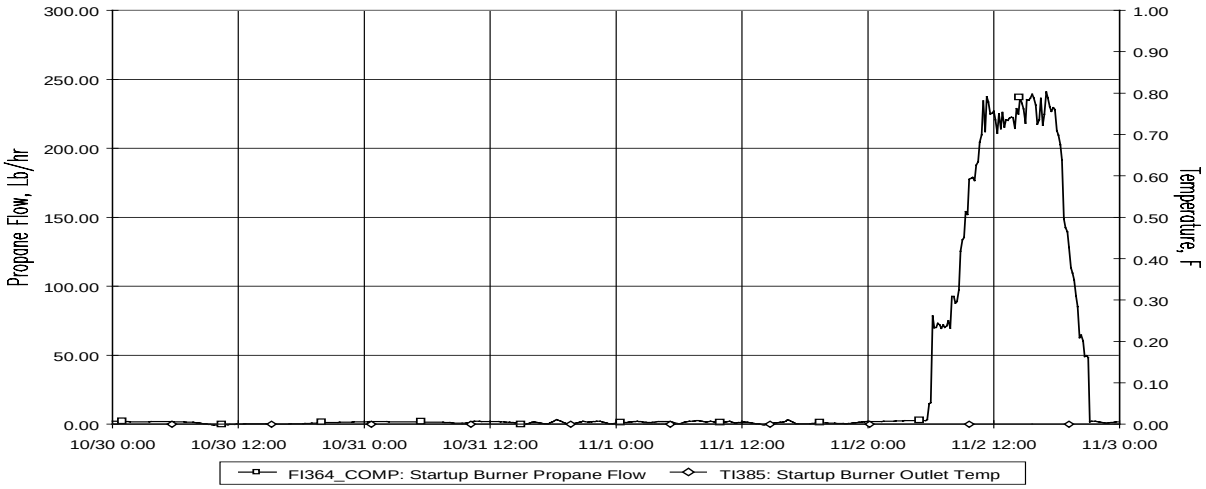

Figure 4.1.4.7-25 Start-Up Burner Flow/Temperature

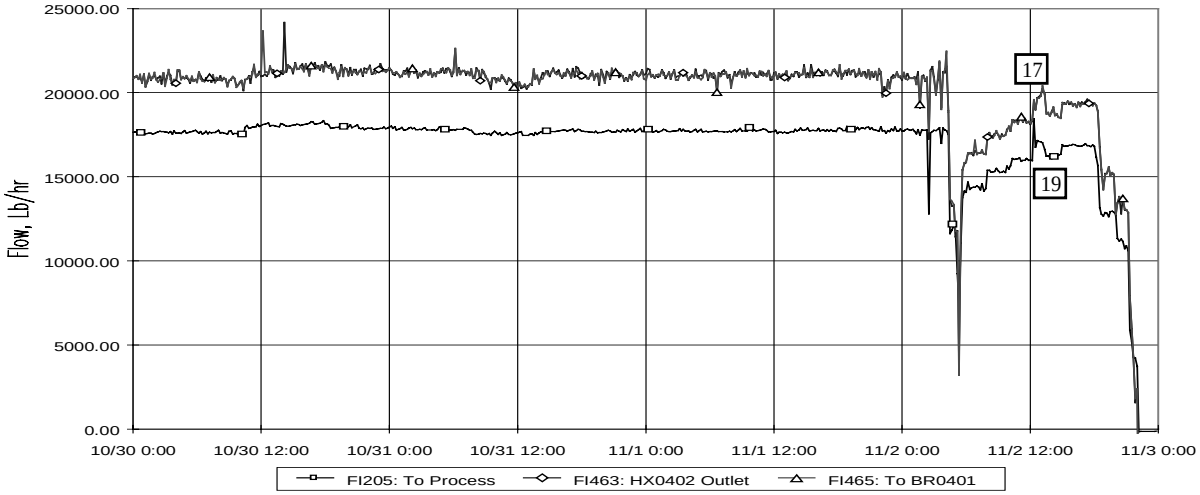

Figure 4.1.4.7-26 Total Gas In/Out Flow Rates

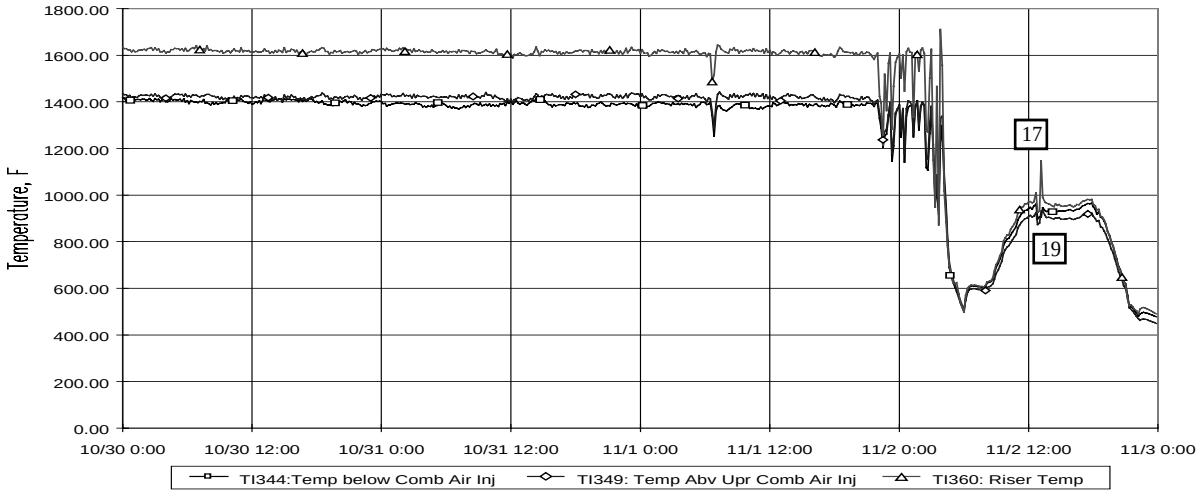

Figure 4.1.4.7-27 Reactor Mixing Zone and Riser Temperatures

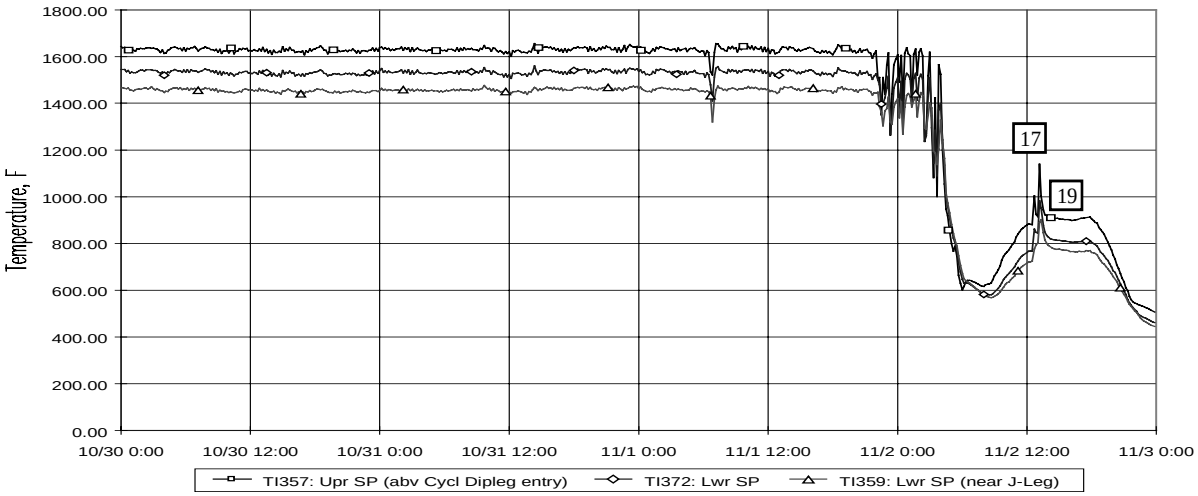

Figure 4.1.4.7-28 Standpipe Temperatures

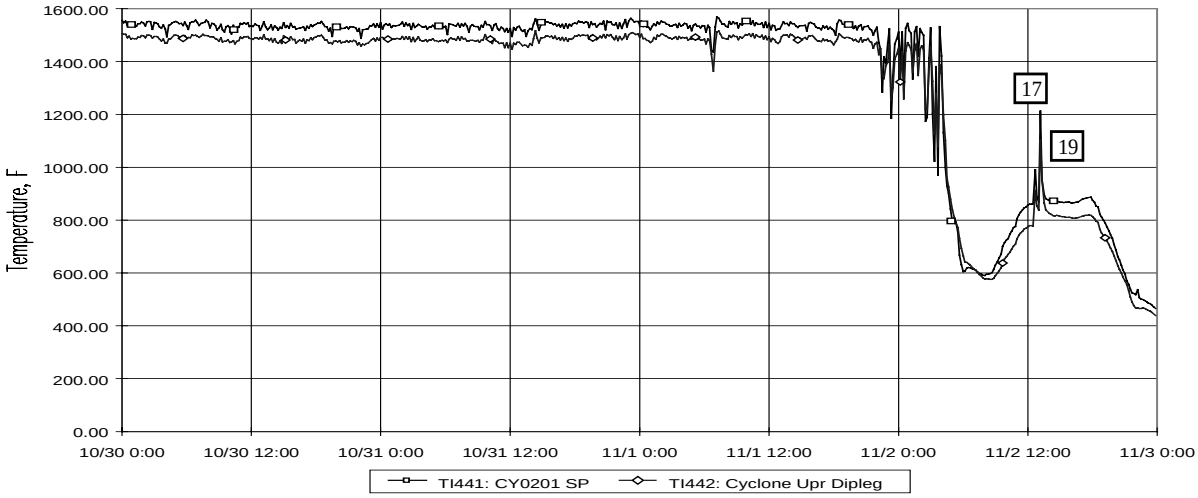

Figure 4.1.4.7-29 Cyclone Dipleg Temperatures

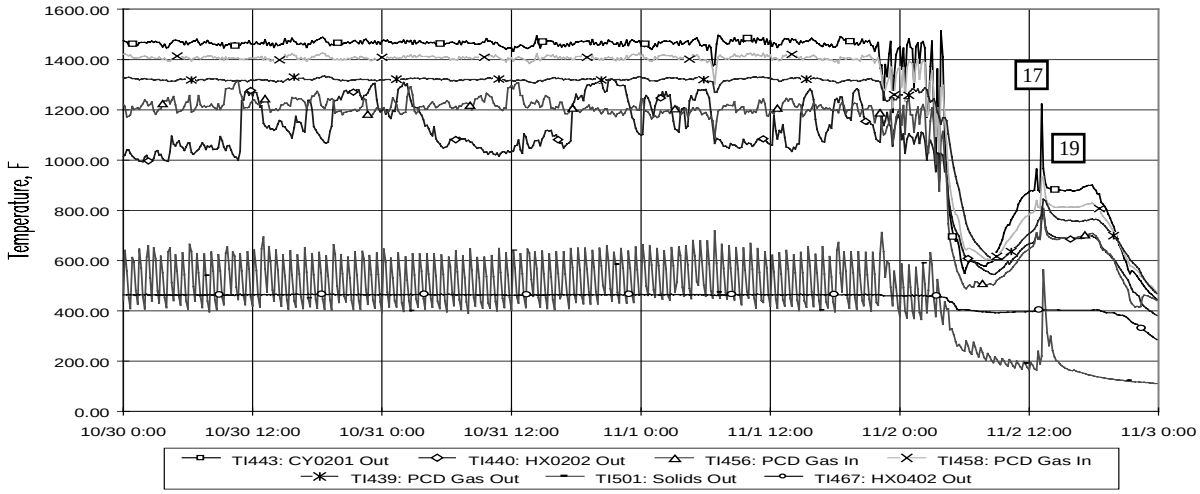

Figure 4.1.4.7-30 Temperature Profile Downstream of Reactor

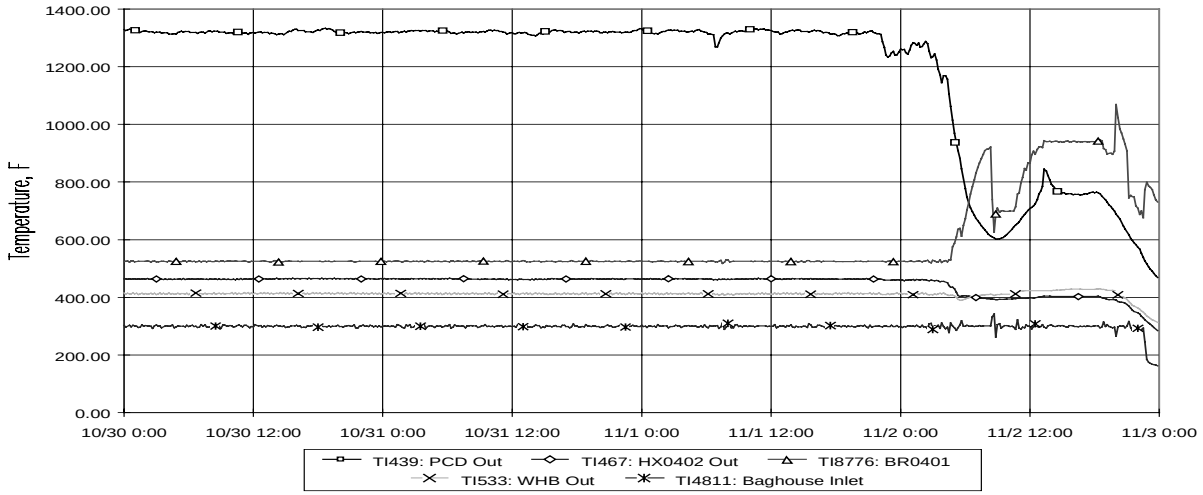

Figure 4.1.4.7-31 System Temperatures Downstream of PCD

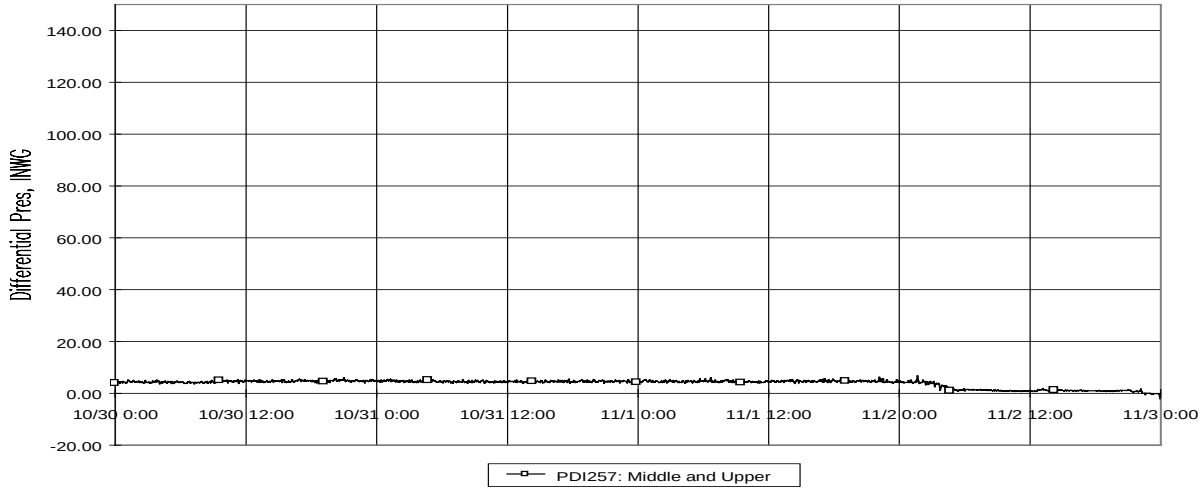

Figure 4.1.4.7-32 Mixing Zone Differential Pressure Profile

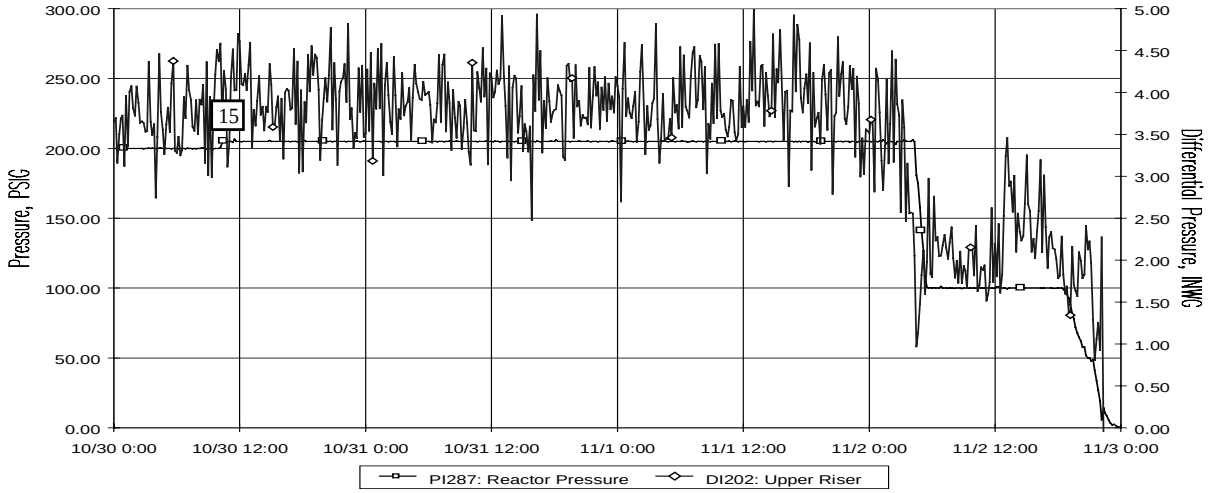

Figure 4.1.4.7-33 Reactor Pressure/Riser Differential Pressure Profiles

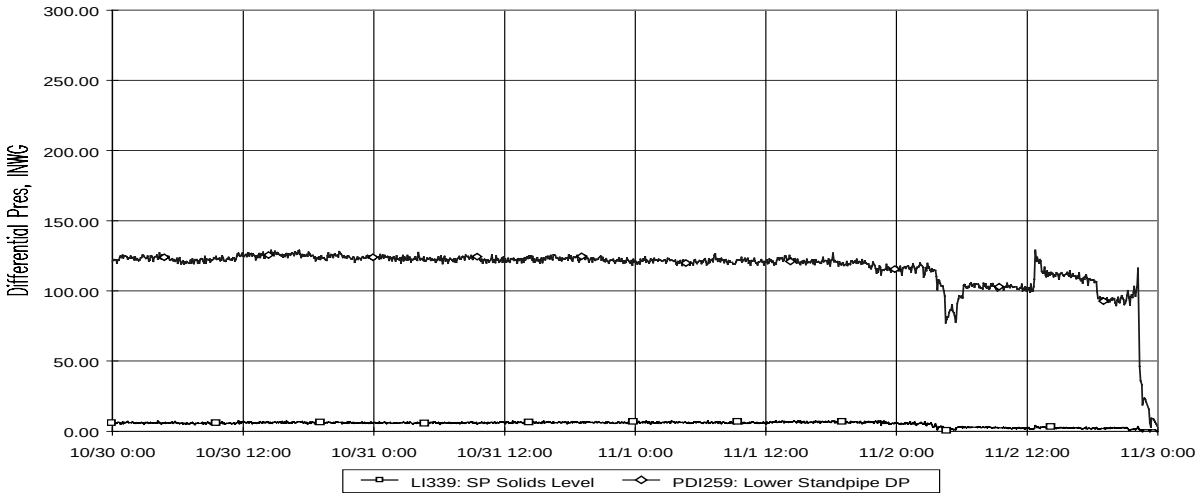

Figure 4.1.4.7-34 Standpipe Differential Pressure Profiles

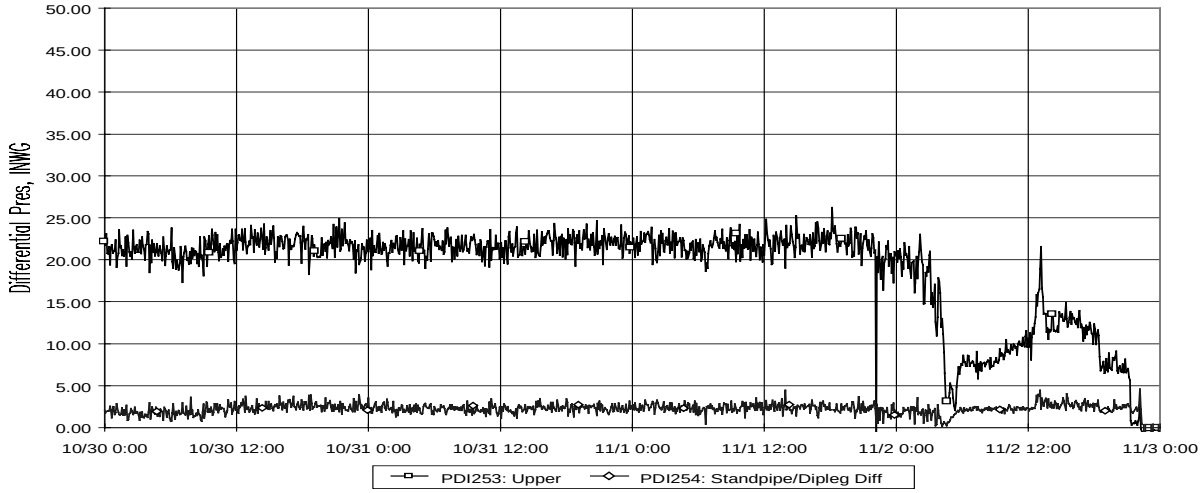

Figure 4.1.4.7-35 CY0201 Dipleg Differential Pressure Profiles

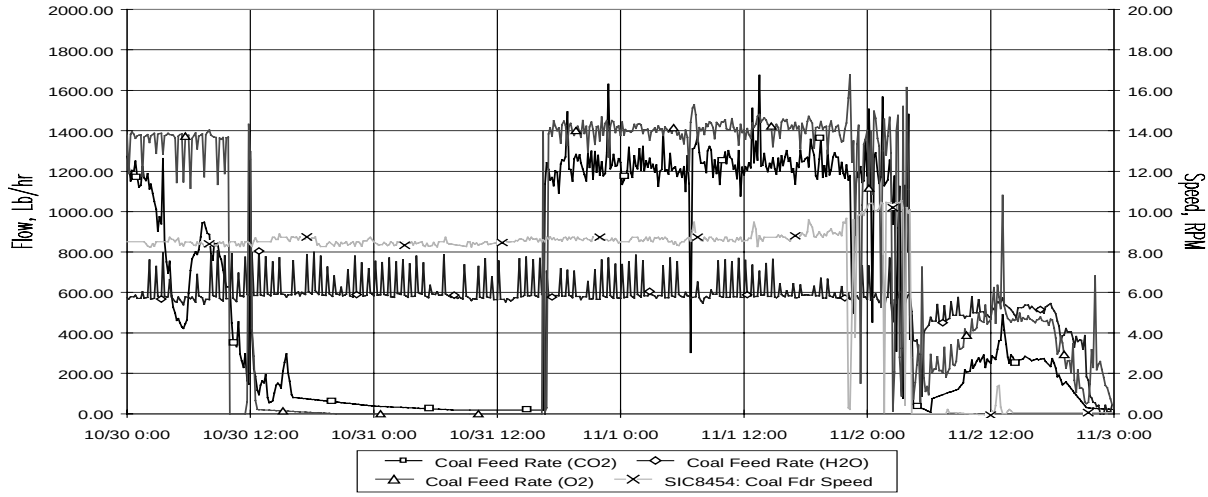

Figure 4.1.4.7-36 Coal Feed Rate Based on Gas Analysis

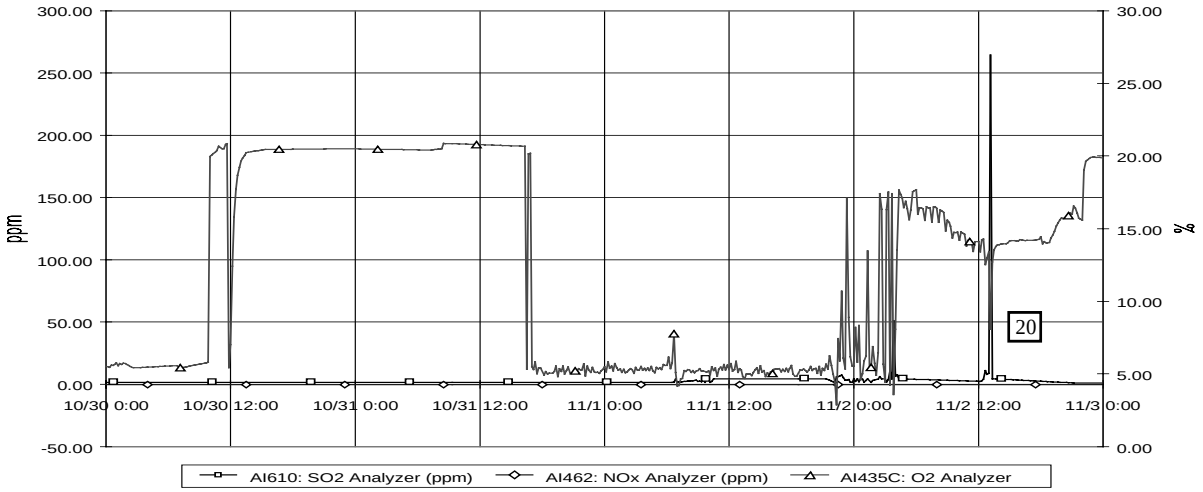

Figure 4.1.4.7-37 O_2, SO_2, and NO_x Analyzers

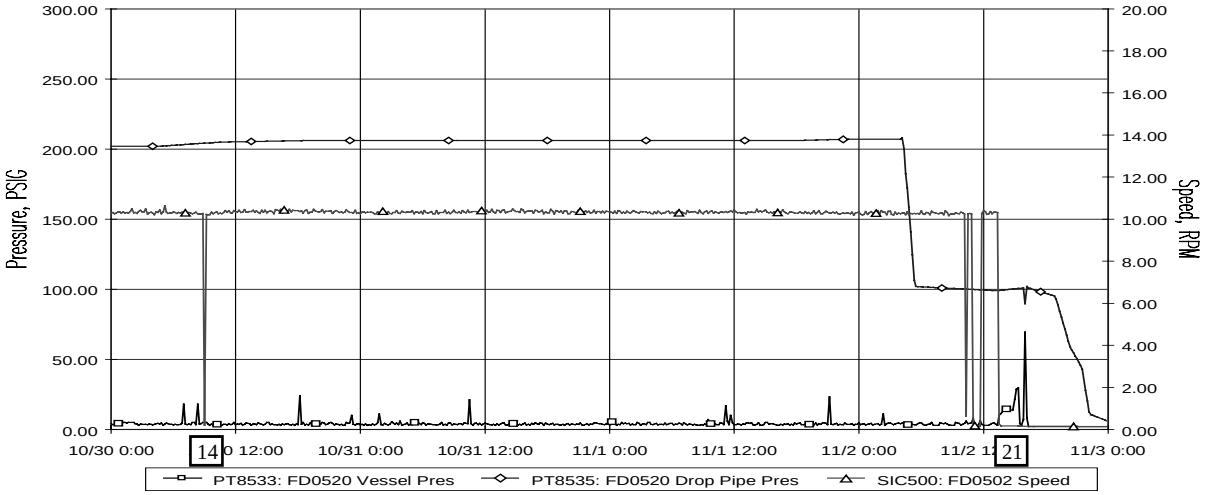

Figure 4.1.4.7-38 FD0520 Pressure Profiles

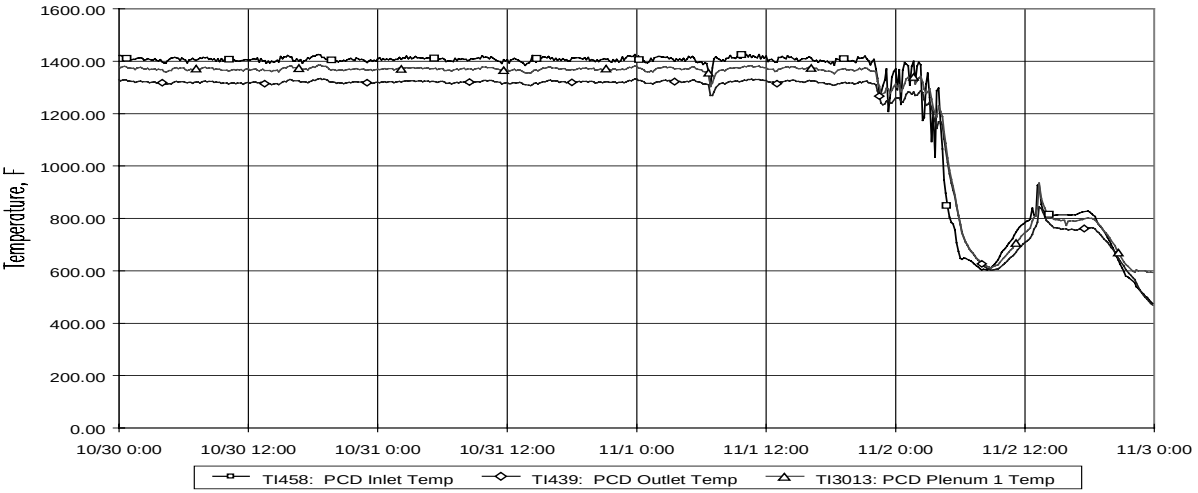

Figure 4.1.4.1-39 PCD Temperatures

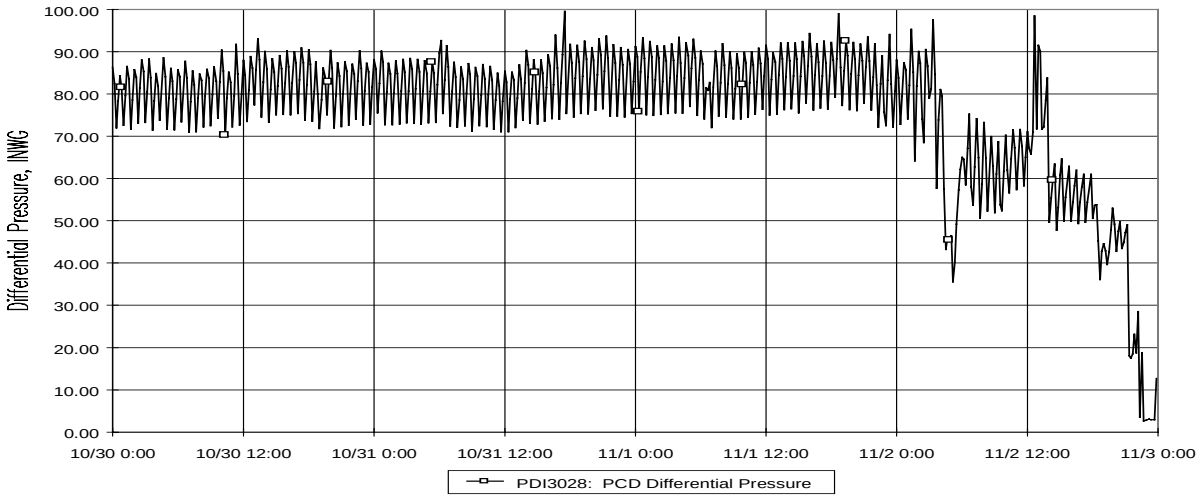

Figure 4.1.4.7-40 PCD Differential Pressure Profile

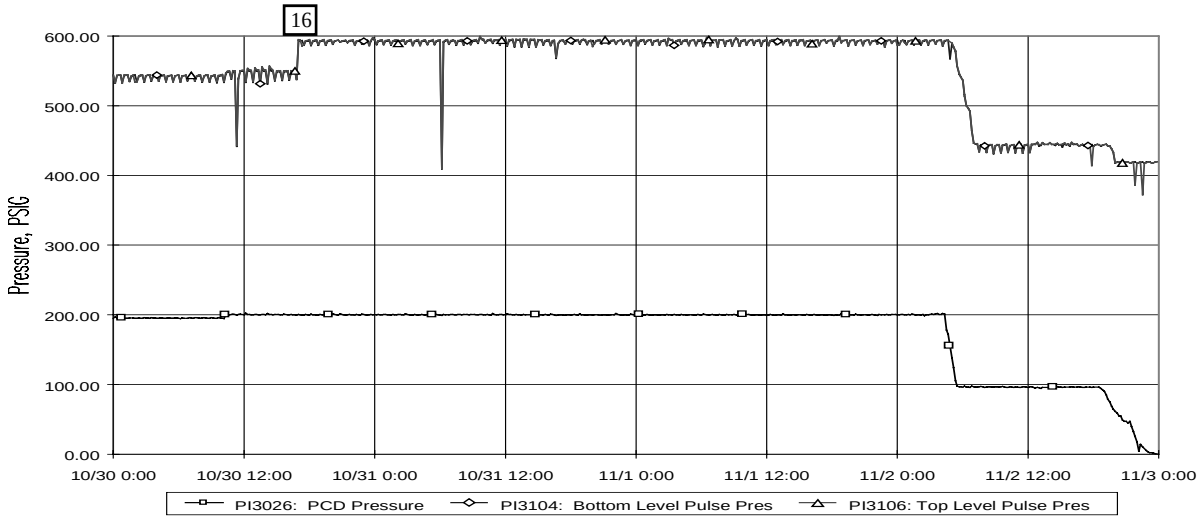

Figure 4.1.4.7-41 PCD Pressure and Pulse Pressure

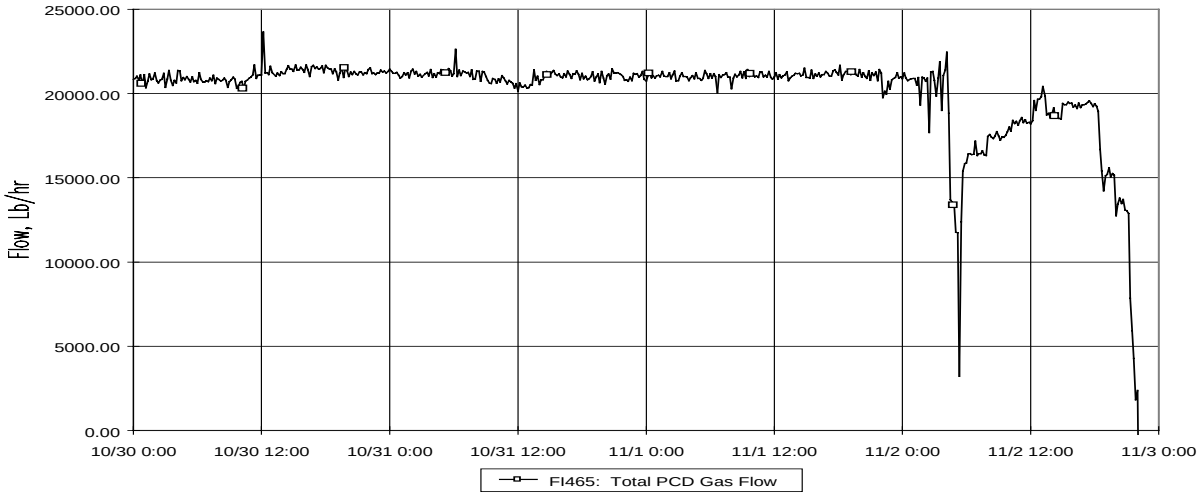

Figure 4.1.4.7-42 Gas Flow Through PCD

4.1.4.8 TC01H Test Run

Test run TC01H was conducted between November 16 and 23, 1997. Operating plots are shown in figures 4.1.4.8-1 through -45. The following maintenance work was performed during the outage from November 3 to 14, 1997:

- The spent fines screw cooler (FD0502) shaft was straightened because the shaft end under the PCD was warped. A worn ceramic bushing was replaced and the shaft on the motor end was rebuilt to its original size. The tightening of packing made deep gouges on the shaft.

- Broken PCD candles were replaced.

- The spacing between the spent fines transport system (FD0520) bottom seal and the dome was changed to prevent brushing of the uninflated seal and the dome. A new seal was also installed.

- A leaking upper ring valve on the sorbent feeder (FD0220) was replaced.

- A rubber boot was installed in the line from FD0154 to FD0220 to prevent interference of the line (near the FD0220 surge bin) with weigh cell readings.

- Snubbers were installed on both the secondary gas cooler (HX0402) riser lines and the combustion heat exchanger (HX0203) riser line to minimize vibrations in these lines caused by water hammering.

- The coal feed line from FD0210 to the reactor was cleaned.

- A manual ball valve was added to bypass the vent valves and orifices (XV8453 and XV8454) on the FD0210 vent line to allow more flow when fluffing the FD0210 lock vessel.

- A new Rosemount NO_X analyzer was installed.

- The PLC logic on FD0210 and FD0220 was changed to limit vessel over pressurization in the event of plugging in the exit line.

- An automatic shutoff valve was added onto the coal feed line to the reactor to prevent undesirable coal from being blown into the reactor.

TC01H Test Run Chronology

- On November 15, 1997, the main air compressor (CO0201) was started at about 21:10 for the leak test but it was stopped at about 21:45 due to leaks in several cyclone dipleg and at HX0203 standpipe flow indicators. The system was depressurized and

these flow indicators were replaced with blank pipes, as these flow meters could not be repaired and the replacements were on order. At about 22:45 the thermal oxidizer (BR0401) was lit.

- At about 11:55 on November 16, 1997, CO0201 was started again (event 1, figure 1). The reactor (RX0201) was leak tested and the pressure was set to 45 psig. The sulfator heater (BR0602) was lit at 15:00 and the FD0520 and FD0530 systems were started at 15:40. There was plugging in FD0520 around 18:15 and broken ceramic candles were pulled out of its exit. The PCD preheat was completed around 19:00 (event 2, figure 18), the aeration flow indicators were set at 23:00, and the start-up burner (BR0201) was lit at about 23:35 (event 3, figure 3).

- At 01:35 on November 17, 1997, BR0602 was shut down and by 05:05 the BR0201 exit temperature was 1,000°F. The PCD was manually back-pulsed at 07:55 due to malfunctioning of SV3104B and the pulse solenoid. Around 10:00 the PI system was shut down for a short period (event 4, figures 1 through 10). At 11:30 the FD0210 motor had problems due to a bad thermistor in the motor. Coal feed started at about 12:20 (event 5, figures 2 and 5 through 8) but problems soon developed with the low transfer weights from the FD0210 surge bin to the lock vessel. The transfer weights were only ranging from 15 to 300 lb. Some adjustments were made to increase the amount of material transferred each cycle. At 17:00 Electrical and Instrumentation (E&I) personnel adjusted the FD0520 lock vessel level probe sensitivity because FD0520 was cycling continuously. By 20:25 the PCD plenum temperature was above 1,350°F (event 6, figure 18). At about 23:05 BR0201 was shut down (event 7, figure 3) and the RX0201 pressure was gradually increased to 160 psig.

- On November 18, 1997, a screw that held the solenoid for an isolation ball valve for the bottom PCD plenum became loose at 02:30 and resulted in malfunctioning of the solenoid. When the back-pulse system was put on manual it led to a continuous back-pulse, which caused the reactor operations to become unstable. The solids flow through the cyclone dipleg was upset (event 8, figure 13), resulting in a large solids carryover to the PCD. Coal feed was stopped at 02:40 (event 9, figures 2 and 5 through 8) to drain the solids from the PCD cone and to fix the problems with the back-pulse system. The continuous back-pulse stopped when the back-pulse system was put back on automatic. Action was initiated to correct a flaw in the back-pulse logic. The BR0201 was lit at about 04:15 (event 10, figure 3).

- Solids removal from the PCD cone was slow due to the temperature limits imposed by the new FD0520 seal material on the bottom spheri valve. At 16:10 the HX0203 circulation became unsteady, so its aeration was adjusted to smooth out the operation. Coal feed was started and BR0201 was shut down at 18:45 (event 11, figure 3) and at about 18:50 the reactor pressure was increased from 108 to 120 psig (event 12, figure 11).

- On November 19, 1997, the aeration in the reactor mixing zone and in HX0203 as well as the staged air through the reactor riser were increased in increments throughout the day. The reactor pressure was increased to 160 psig around 08:15 (event 13, figure 11) and the back-pulse pressure was increased to 500 psig at 08:20 (event 14, figure 20). Except for a 45-second cyclone dipleg upset at 17:20 the reactor operation was smooth.

- At 04:10 on November 20, 1997, the FD0210 system began to experience problems with the conveying line plugging (event 15, figures 23 and 25 through 28). This resulted in the PCD plenum temperature falling below 1,350°F on several occasions. Between 06:00 and 08:45 the FD0210 lock vessel was fluffed to improve the operation. At about 08:45 the FD0210 system tripped (event 16, figures 23 and 25 through 28) due to plugging in the conveying line. After unplugging the conveying line FD0210 was put back on-line and by 09:05 (event 17, figures 23 and 25 through 28) the PCD plenum temperature was above 1,350°F. Operations continued to be smooth except for partial plugging of the FD0520 lock vessel vent valve.

- The FD0206 was started at about 00:10 on November 21, 1997, and was run continuously until 09:50 to maintain the solids levels in the reactor standpipe and HX0203. The reactor pressure was increased from 171 to 180 psig (event 18, figure 32) around 06:15. At 13:15 a fast-dump valve connected to the bottom spheri valve failed and resulted in a seal nitrogen leak, which lowered the seal nitrogen pressure. This rendered all spheri valves inoperable. Since the initial reaction with the loss of seal pressure nitrogen was a blown seal, coal feed was cut off at 13:20 (event 19, figures 23 and 25 through 28) and the solids circulation rate in the reactor was reduced. After the seal pressure nitrogen was back to 265 psig, coal feed was restarted at 13:25 (event 20, figures 23 and 25 through 28) and the solids circulation rate was gradually increased. The FD0206 was started again at 15:20. The process then ran at steady conditions for the remainder of the day.

- On November 22, 1997, a leak developed in the FD0502 system at 08:30. There were also some problems with the FD0502 shaft rotation. The FD0210 system tripped a few times between 16:15 and 19:50 and the problem with low transfer weights also returned.

- The problems with FD0210 continued until early November 23, 1997, which caused the reactor temperatures to decrease. Starting at 02:40 the reactor pressure was reduced. By 04:00 the reactor pressure was 100 psig (event 21, figure 32), but there was difficulty lighting BR0201. At 07:15 the FD0210 system was isolated for maintenance. Since BR0201 would still not light shutdown of the process started at about 09:10. The CO0201 was tripped at 09:55 (event 22, figure 22).

- The FD0502 leak was addressed and the burner pilot assembly was replaced. The bridge at the bottom of the FD0210 surge bin was also dislodged. The CO0201 was started again at 16:30 (event 23, figure 22) and by 17:20 the reactor pressure was 225

psig. After several additional attempts to light BR0201 had failed CO0201 was shut down at 22:30 (event 24, figure 22).

TC01H Test Run Observations

HX0203 J-leg circulation was uneven due to a number of plugged nozzles in the HX0203 standpipe. Also, the lower nozzles on the HX0203 J-leg were plugged. The recycle gas booster compressor feed cooler (HX0405) insulation was removed and a number of pinhole-size openings were found. The new dispense vessel vent line was tested for the first time and operated well, providing a path for continuous fluidization in the dispense vessel. A total of 122.3 hours on coal was achieved and 75 tons of coal were fed.

Section 4.1.4.8

Graphs 1 through 21

Test Run TC01H
November 16 through 19, 1997

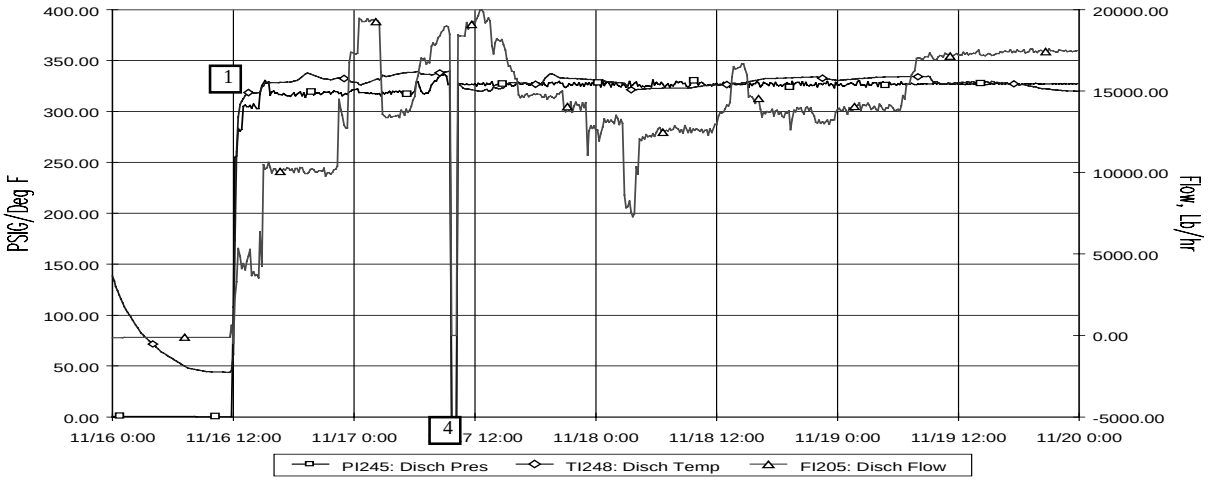

Figure 4.1.4.8-1 CO0201 System Profile

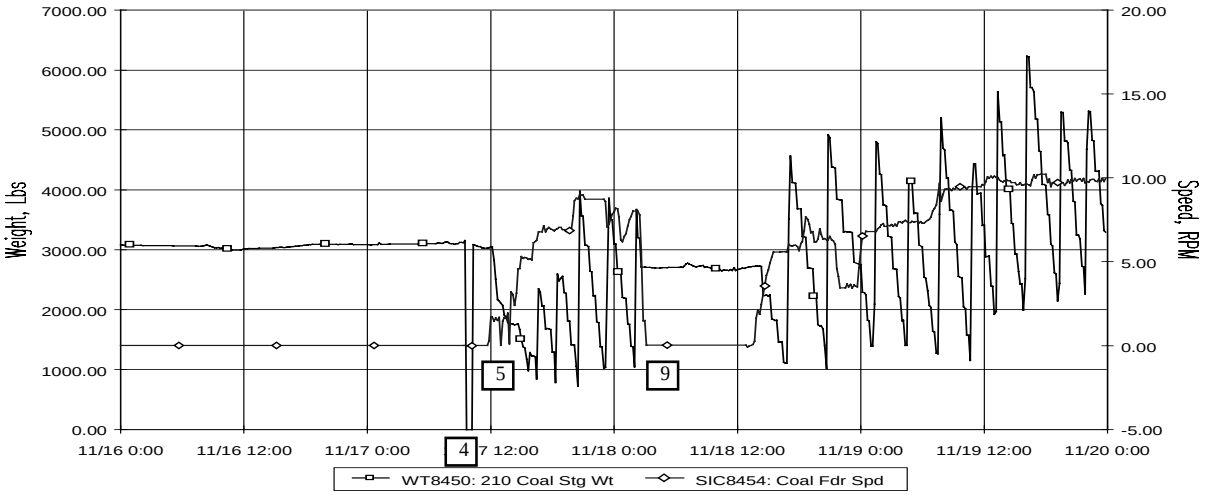

Figure 4.1.4.8-2 Coal Feed System Profile

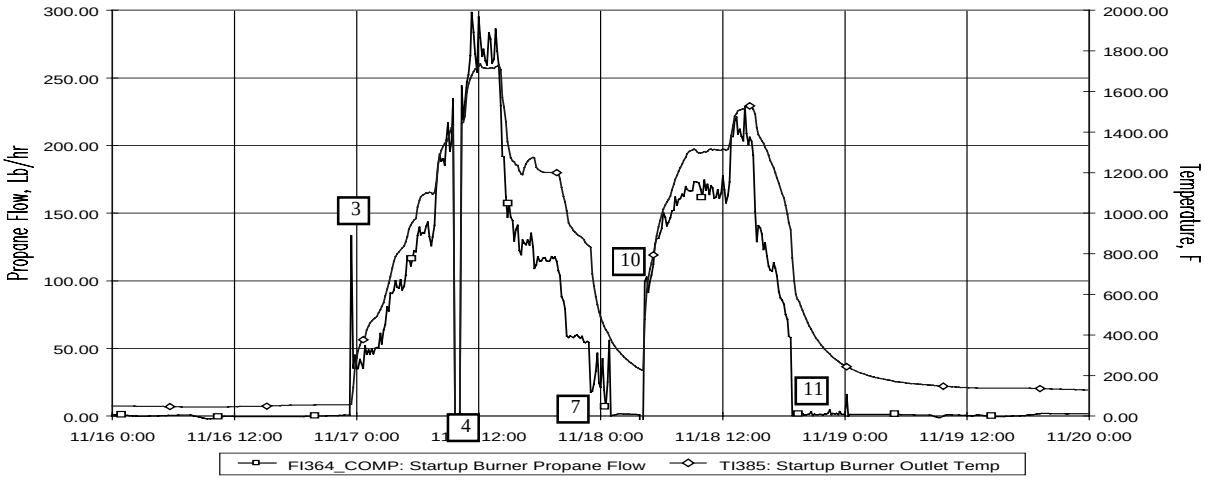

Figure 4.1.4.8-3 Start-Up Burner Flow/Temperature

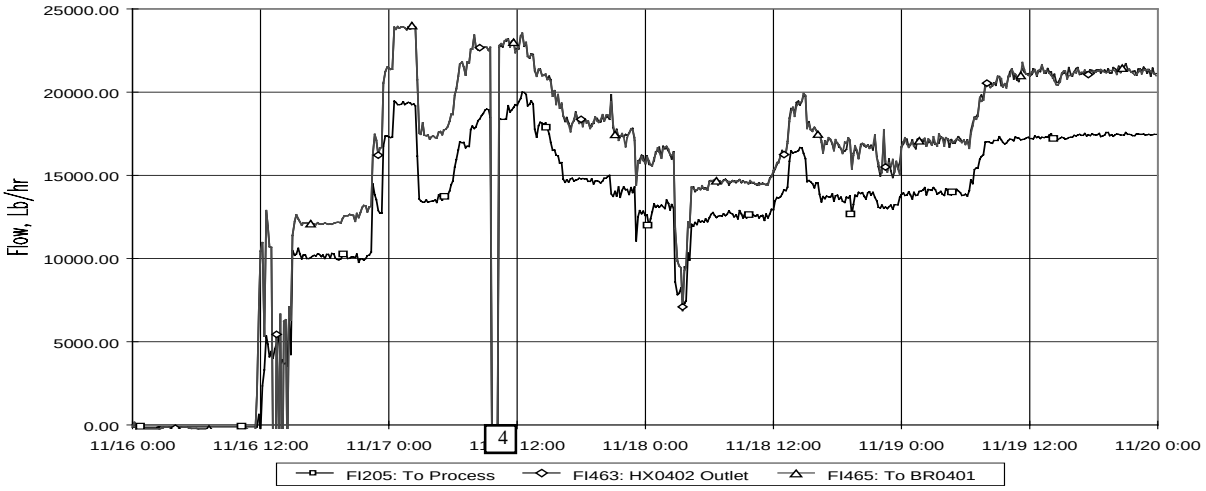

Figure 4.1.4.8-4 Total Gas In/Out Flow Rates

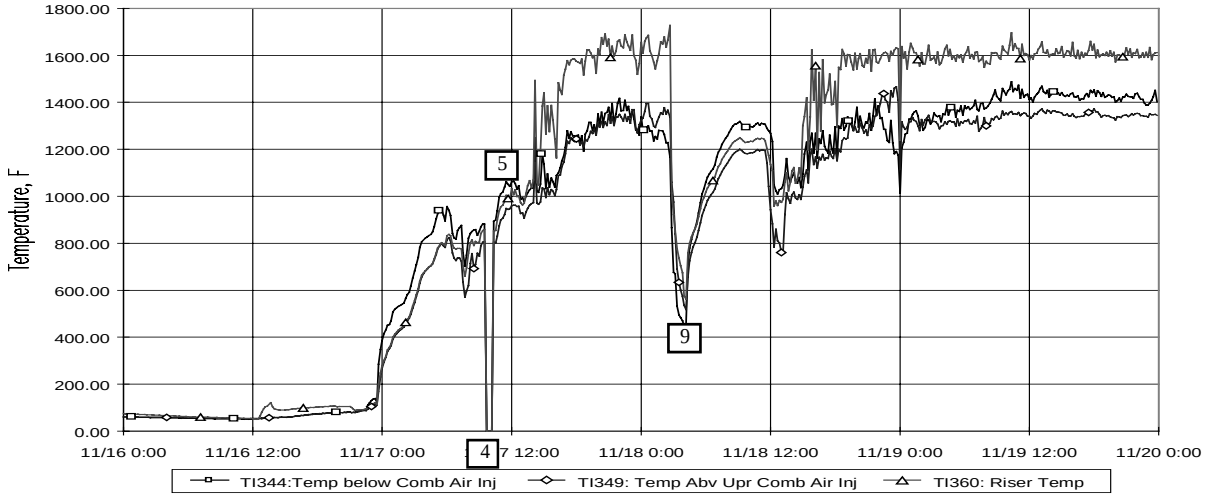

Figure 4.1.4.8-5 Reactor Mixing Zone and Riser Temperatures

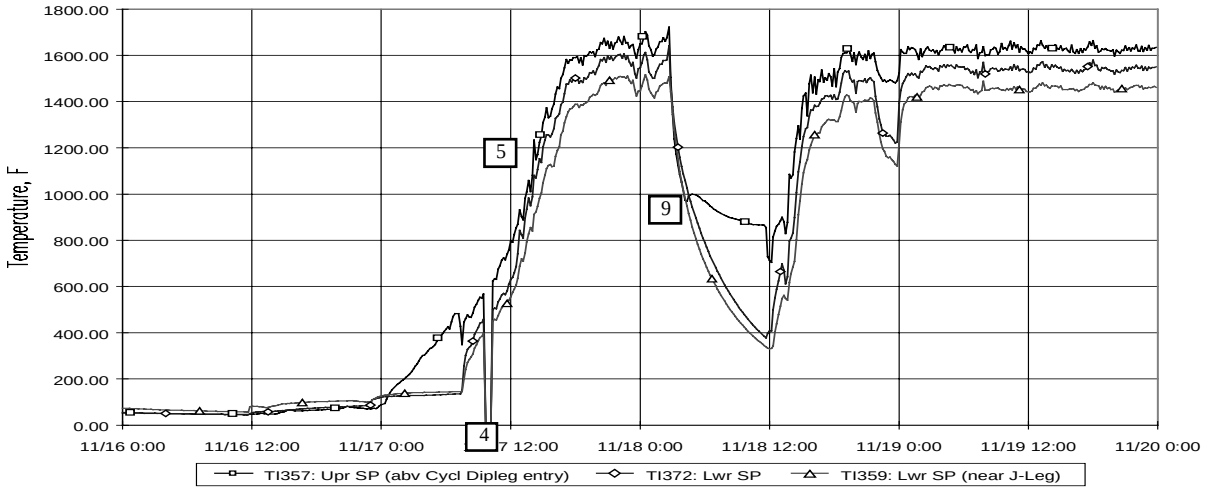

Figure 4.1.4.8-6 Standpipe Temperatures

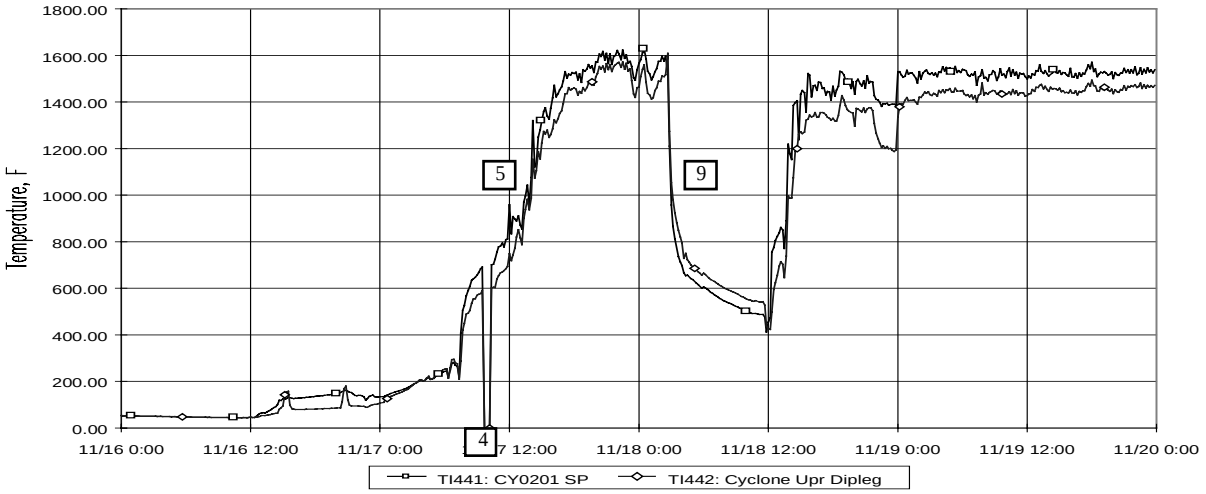

Figure 4.1.4.8-7 Cyclone Dipleg Temperatures

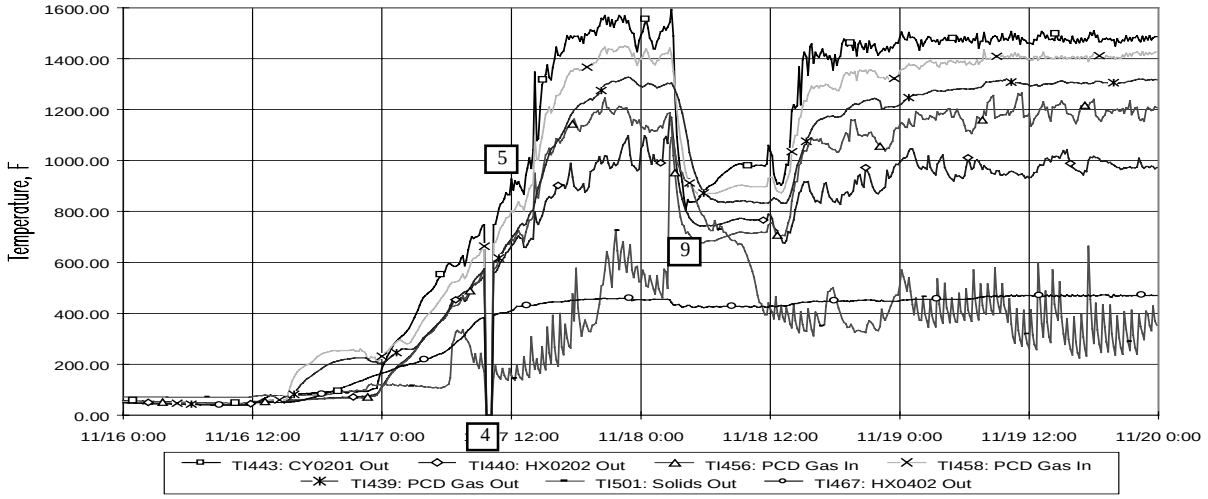

Figure 4.1.4.8-8 Temperature Profile Downstream of Reactor

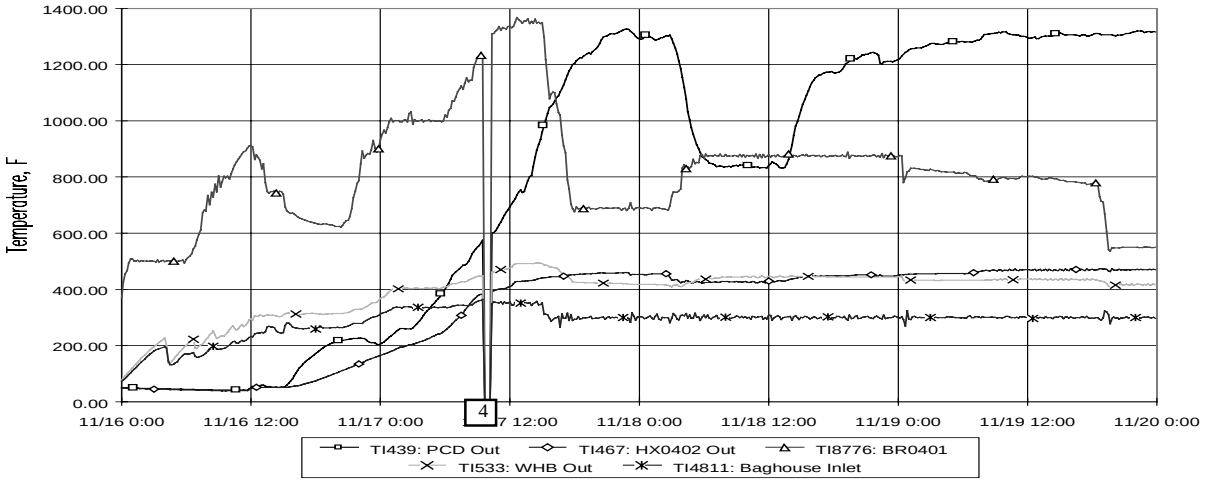

Figure 4.1.4.8-9 System Temperatures Downstream of PCD

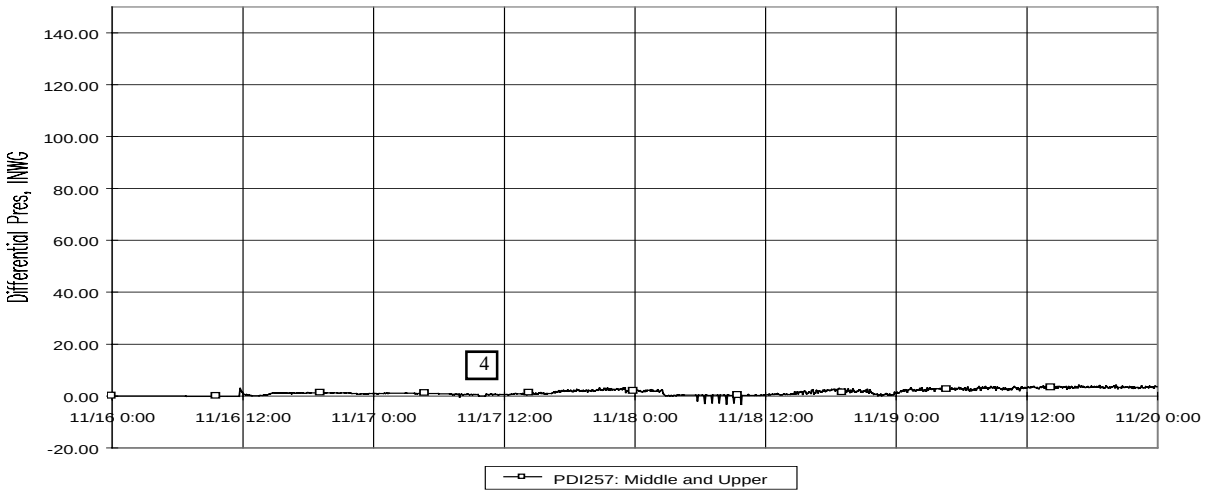

Figure 4.1.4.8-10 Mixing Zone Differential Pressure Profile

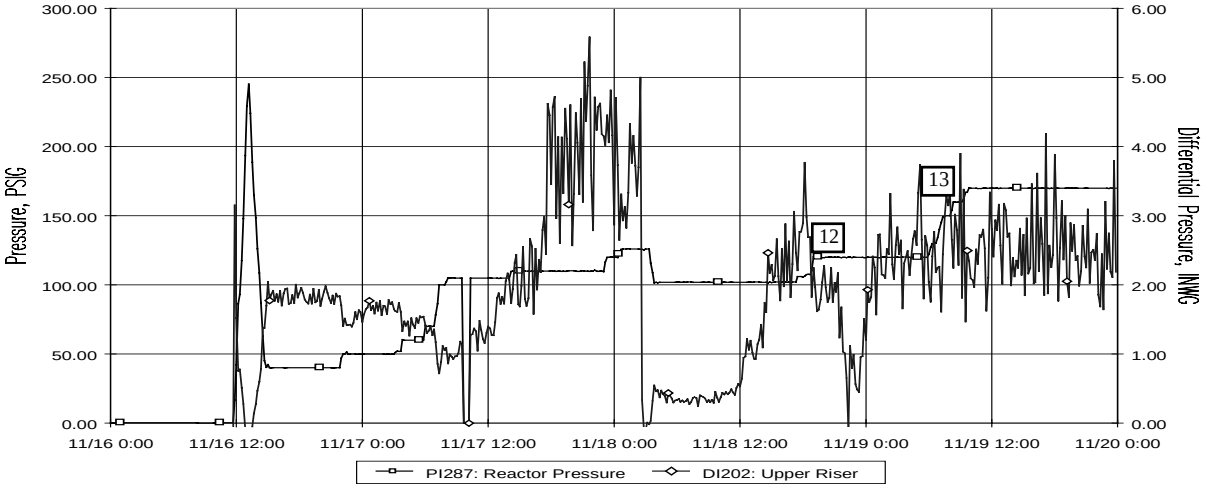

Figure 4.1.4.8-11 Reactor Pressure/Riser Differential Pressure Profiles

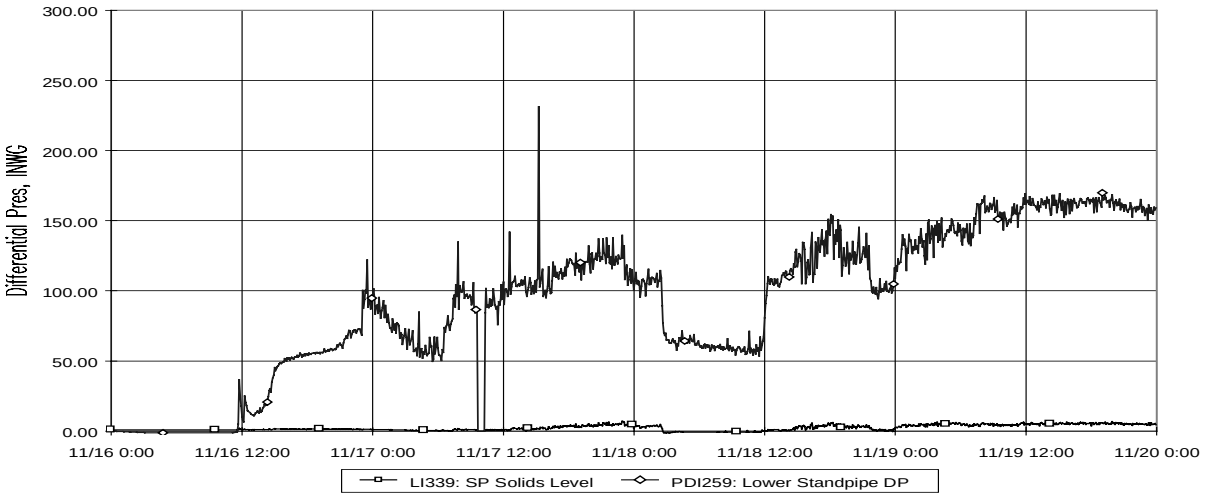

Figure 4.1.4.8-12 Standpipe Differential Pressure Profiles

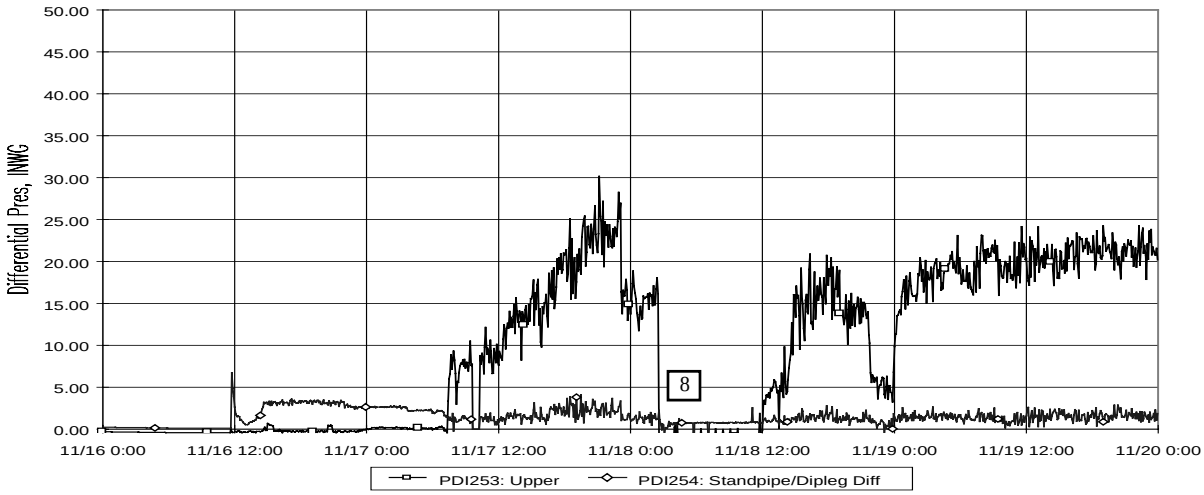

Figure 4.1.4.8-13 CY0201 Dipleg Differential Pressure Profiles

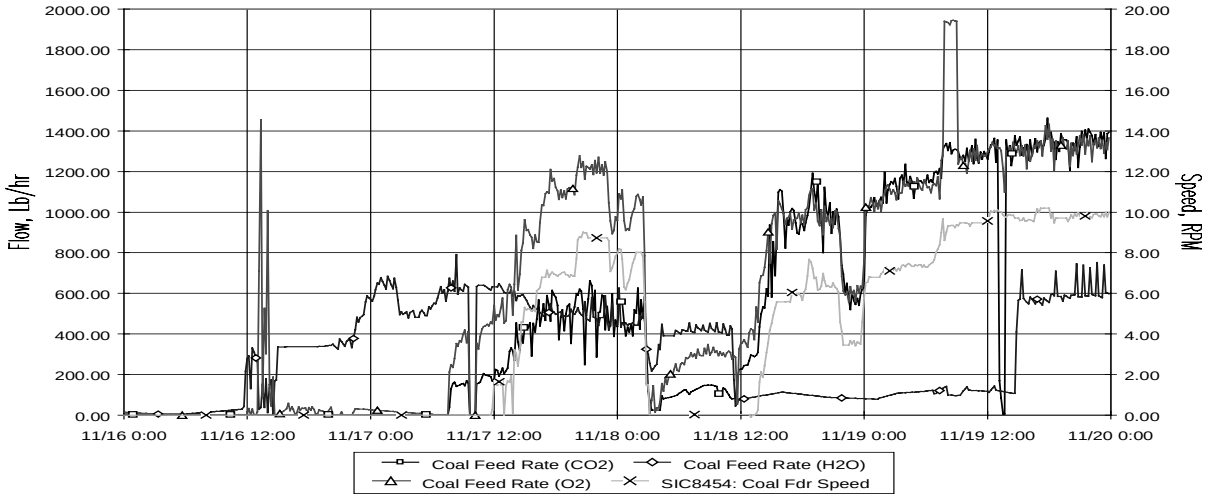

Figure 4.1.4.8-14 Coal Feed Rate Based on Gas Analysis

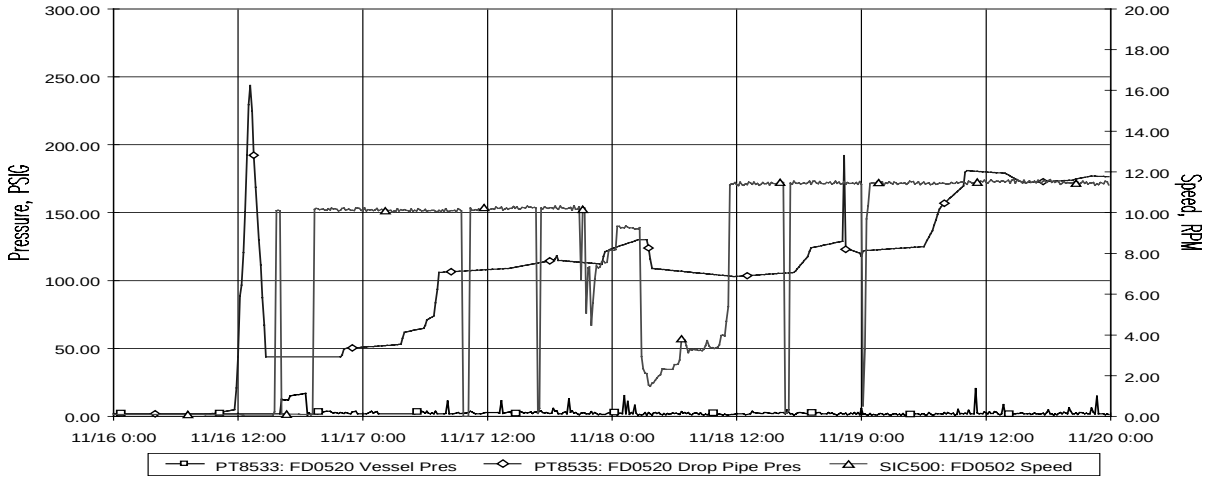

Figure 4.1.4.8-15 FD0520 Pressure Profiles

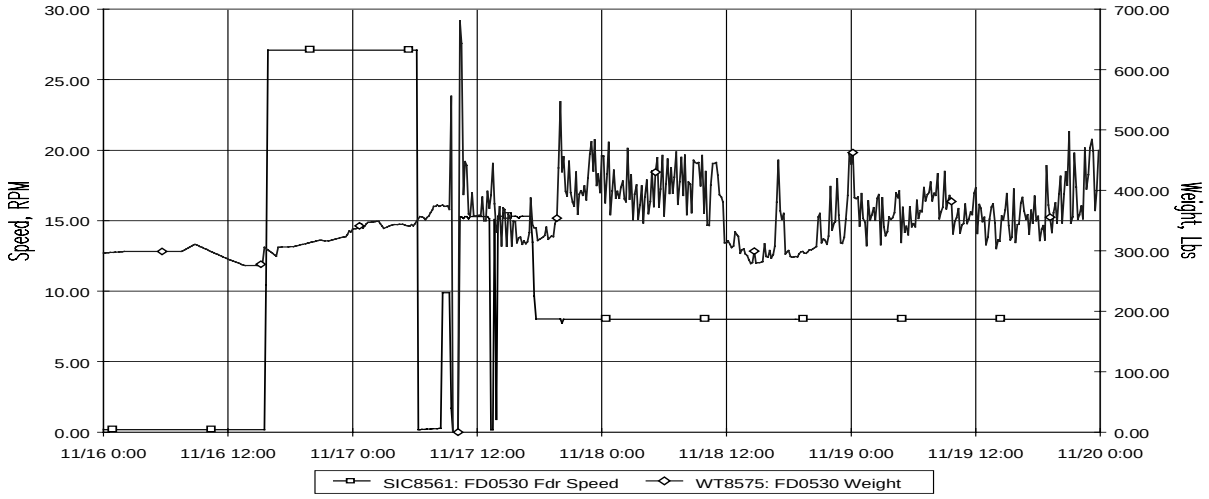

Figure 4.1.4.8-16 FD0530 Feeder Profile

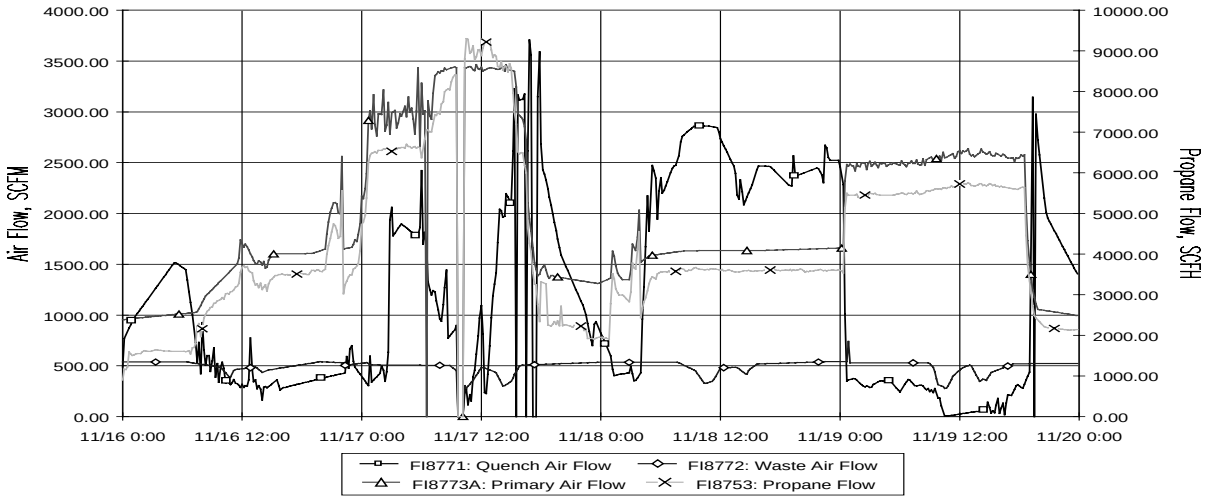

Figure 4.1.4.8-17 Thermal Oxidizer Air/Fuel Flow

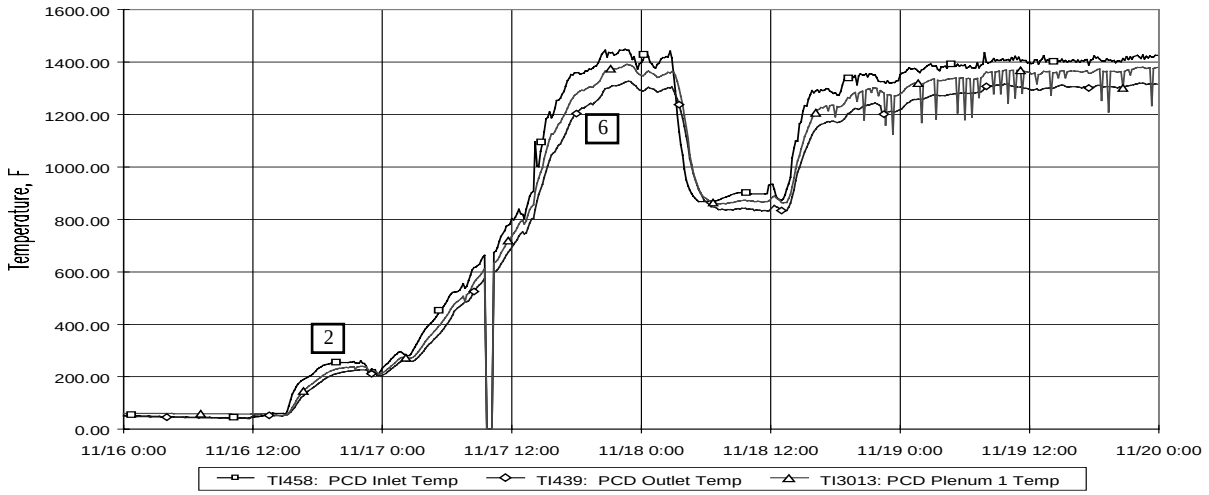

Figure 4.1.4.8-18 PCD Temperatures

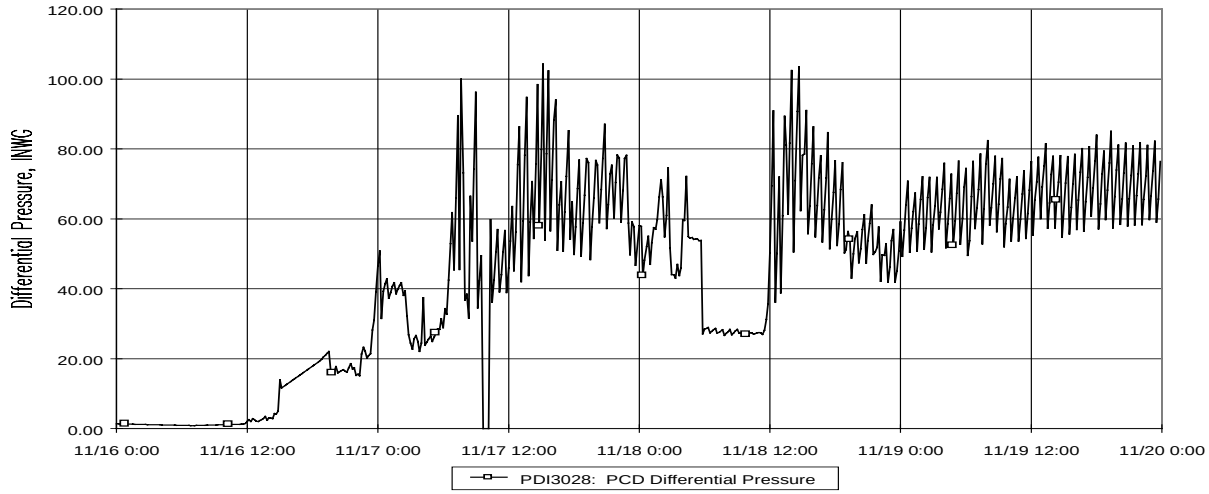

Figure 4.1.4.8-19 PCD Differential Pressure Profile

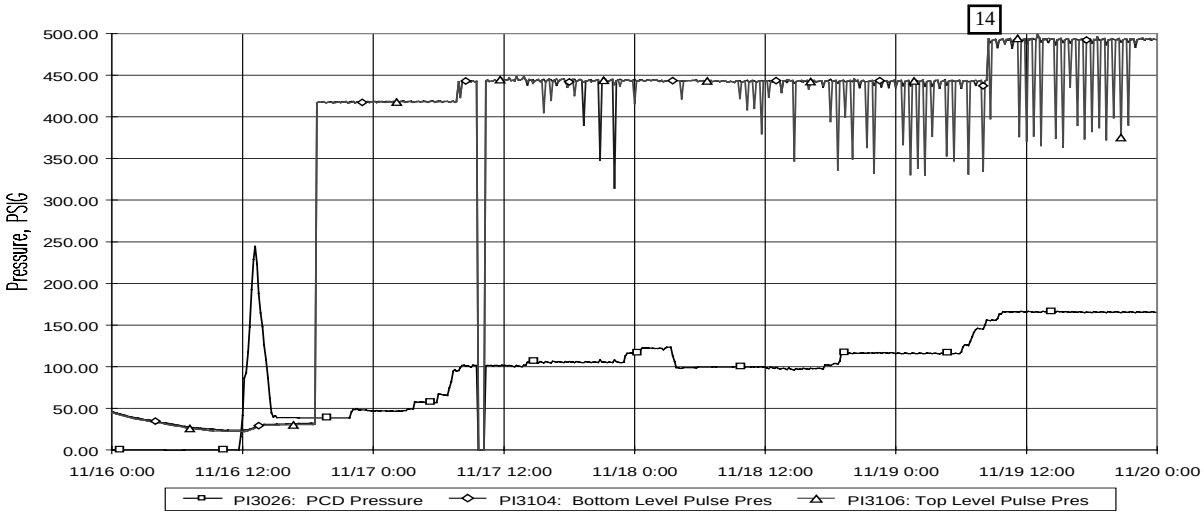

Figure 4.1.4.8-20 PCD Pressure and Pulse Pressure

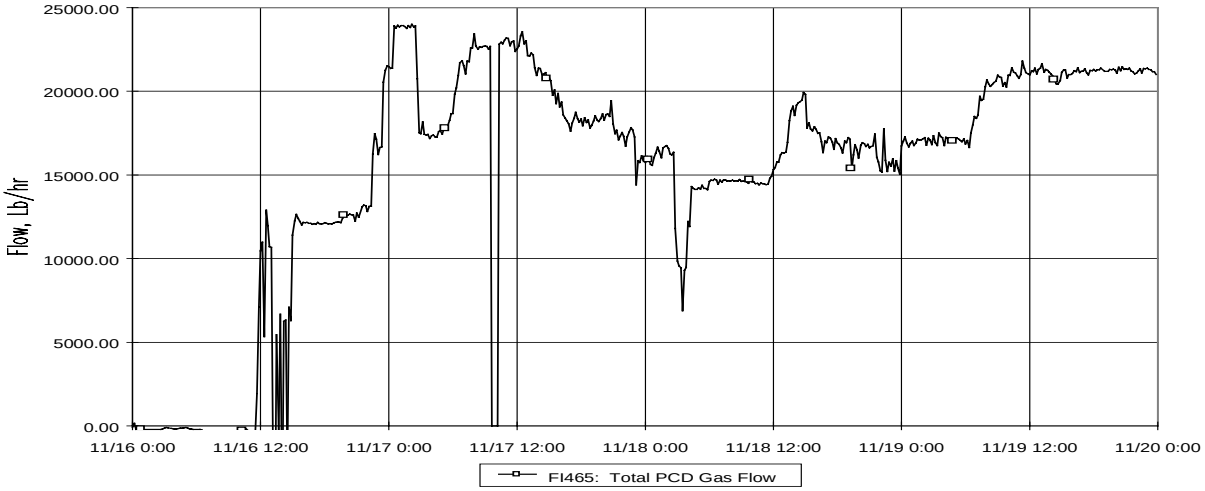

Figure 4.1.4.8-21 Gas Flow Through PCD

Section 4.1.4.8

Graphs 22 through 42

Test Run TC01H
November 20 through 23, 1997

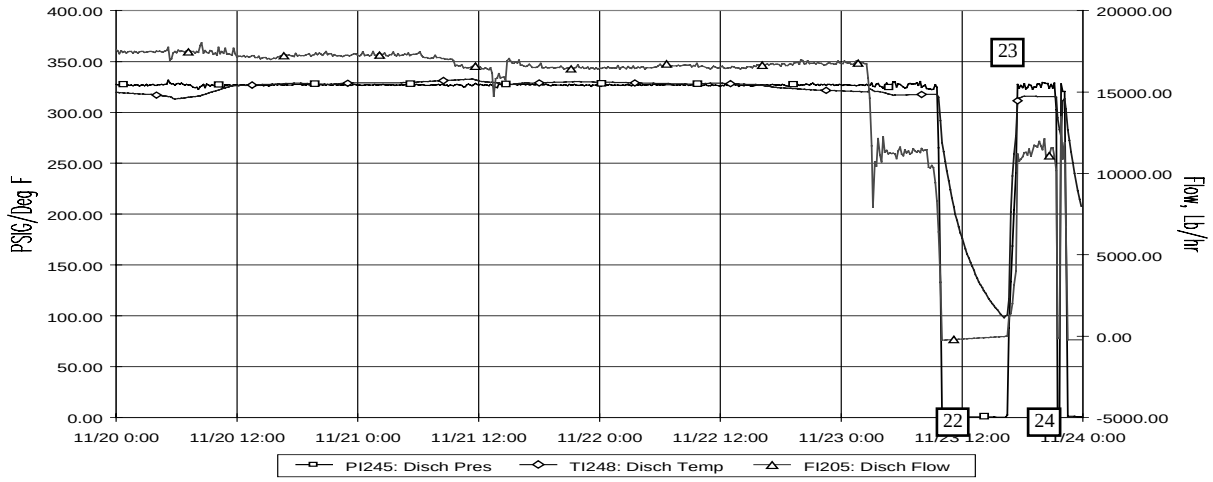

Figure 4.1.4.8-22 CO0201 System Profile

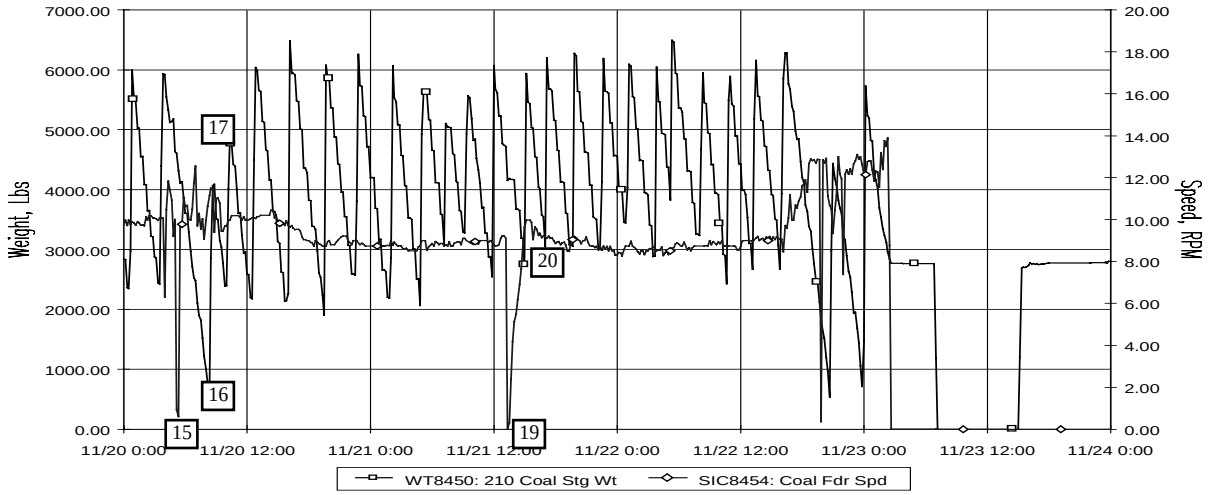

Figure 4.1.4.8-23 Coal Feed System Profile

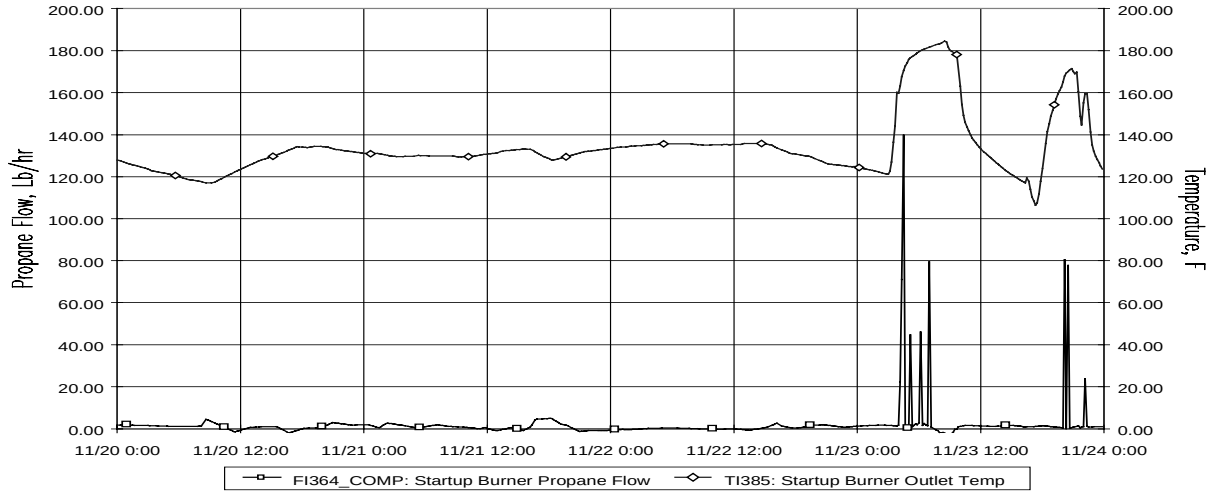

Figure 4.1.4.8-24 Start-Up Burner Flow/Temperature

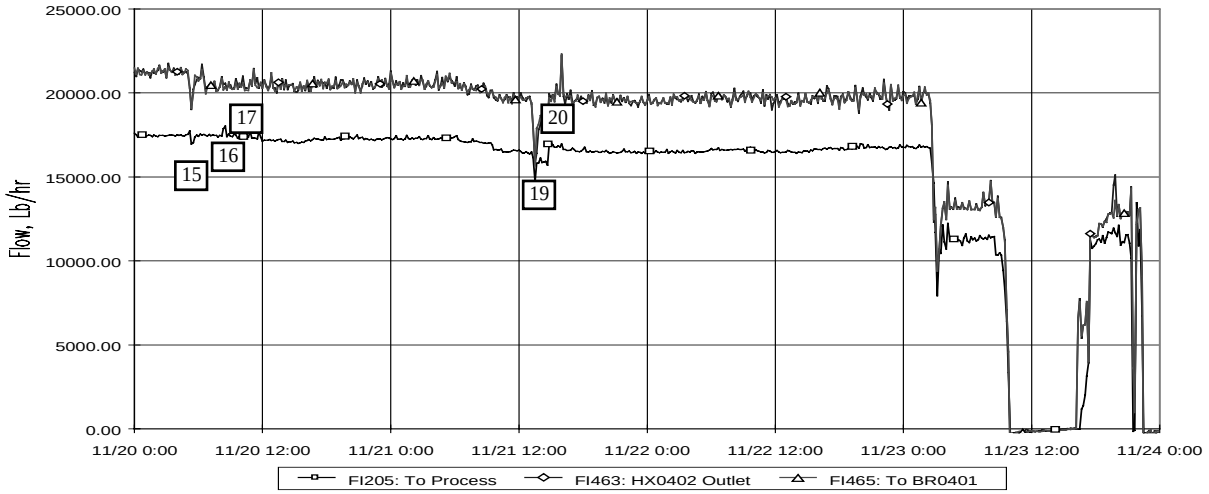

Figure 4.1.4.8-25 Total Gas In/Out Flow Rates

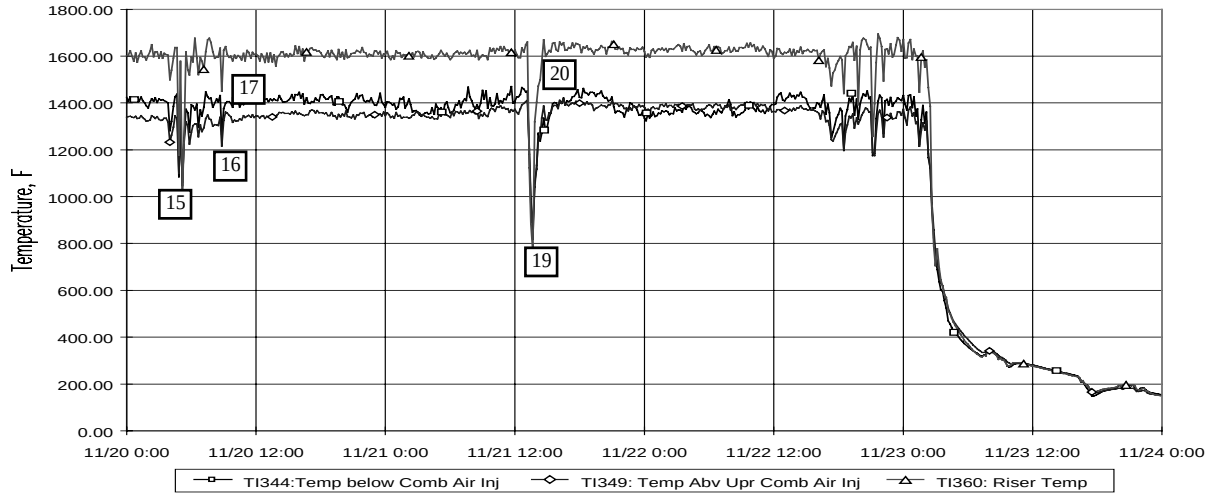

Figure 4.1.4.8-26 Reactor Mixing Zone and Riser Temperatures

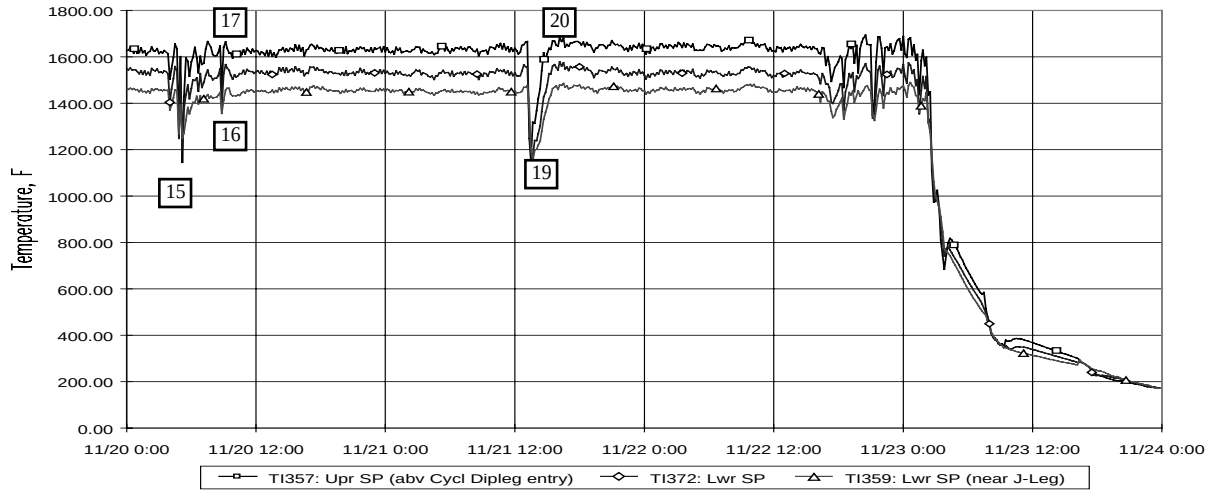

Figure 4.1.4.8-27 Standpipe Temperatures

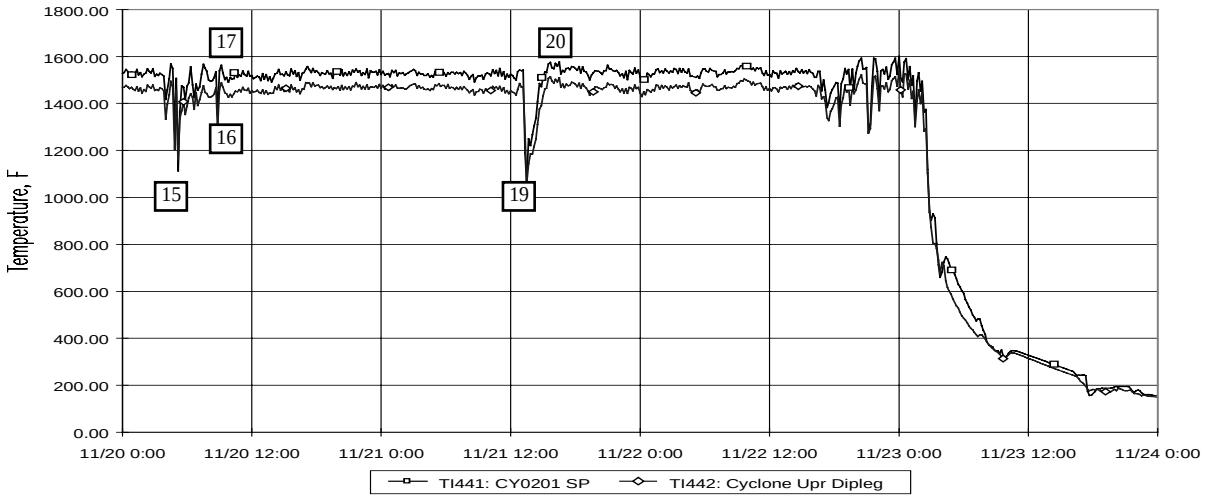

Figure 4.1.4.8-28 Cyclone Dipleg Temperatures

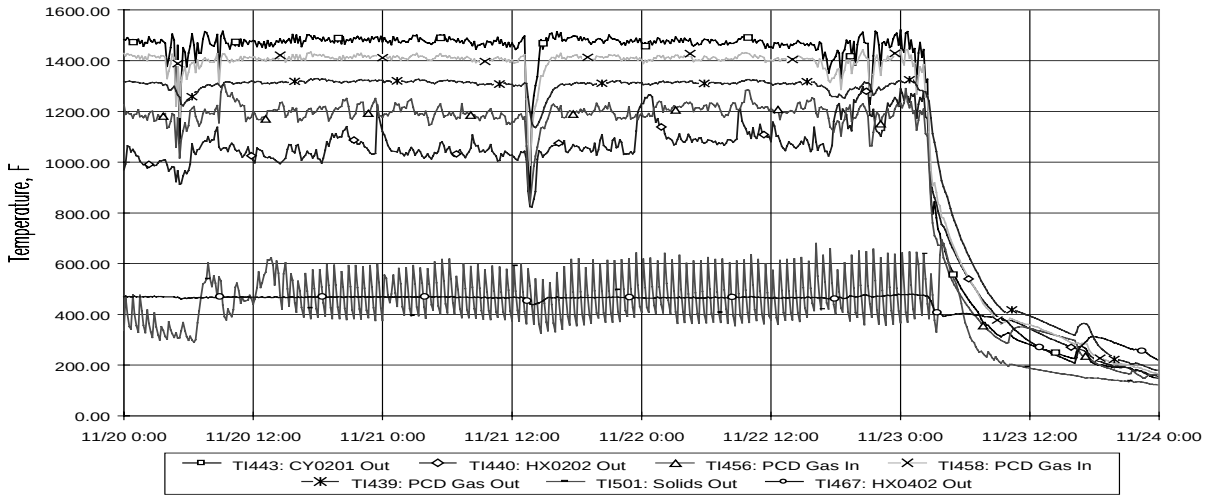

Figure 4.1.4.8-29 Temperature Profile Downstream of Reactor

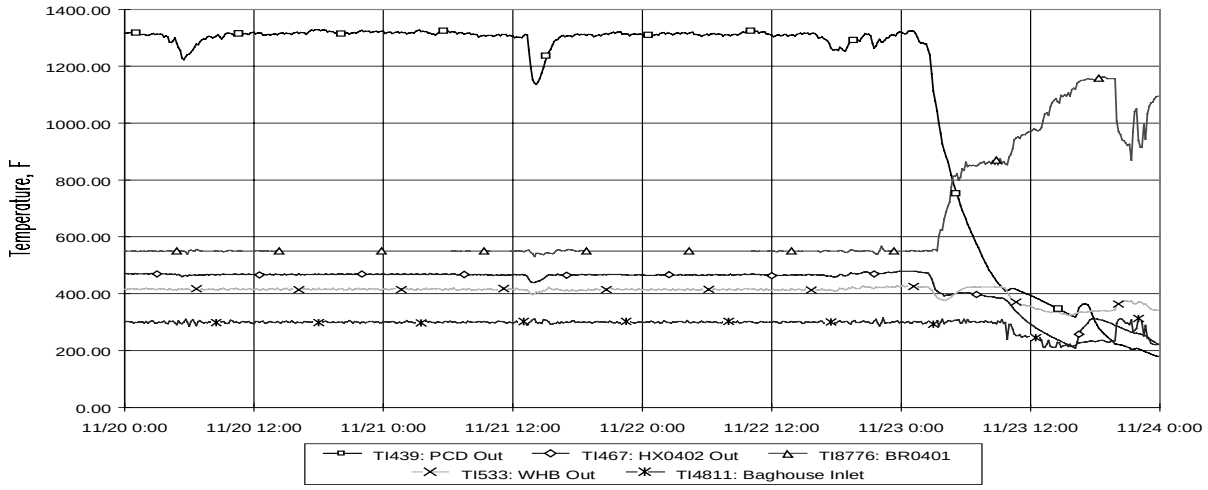

Figure 4.1.4.8-30 System Temperatures Downstream of PCD

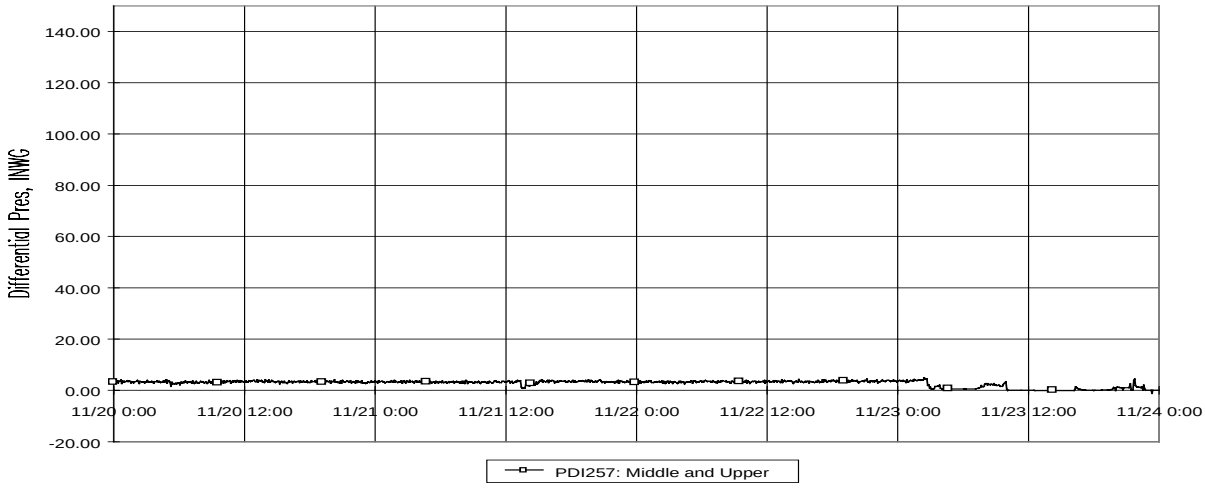

Figure 4.1.4.8-31 Mixing Zone Differential Pressure Profile

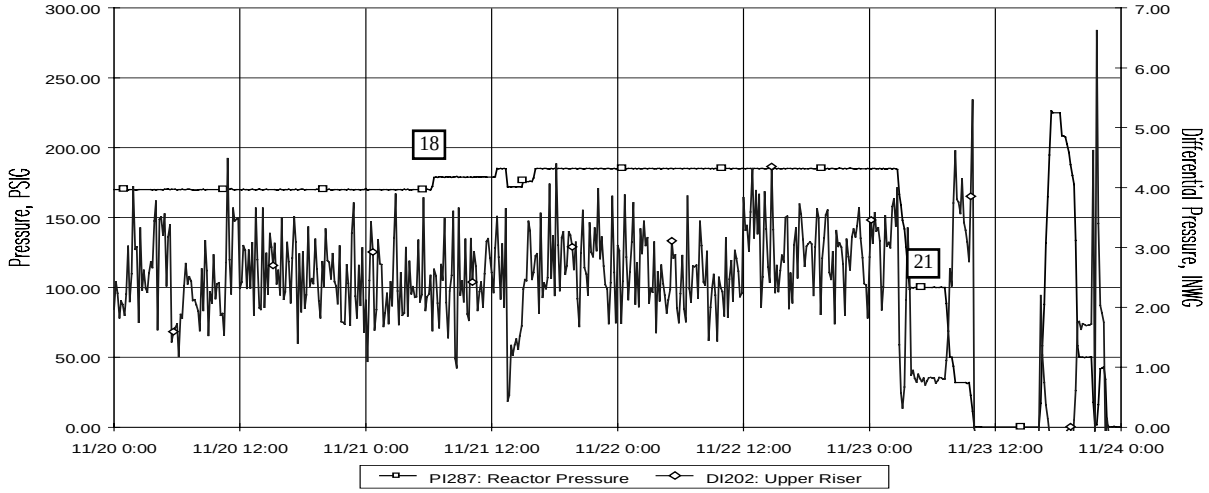

Figure 4.1.4.8-32 Reactor Pressure/Riser Differential Pressure Profiles

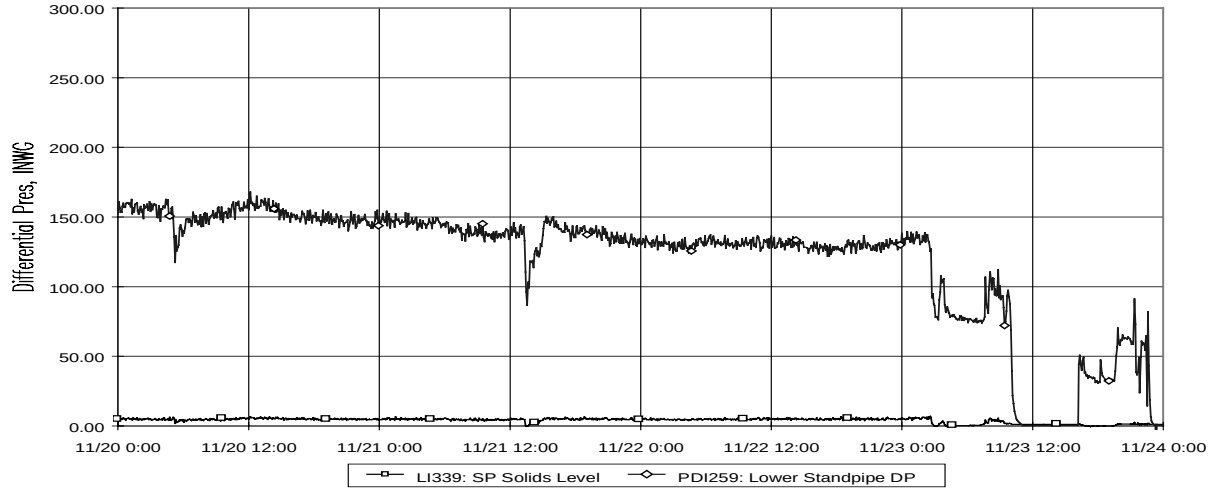

Figure 4.1.4.8-33 Standpipe Differential Pressure Profiles

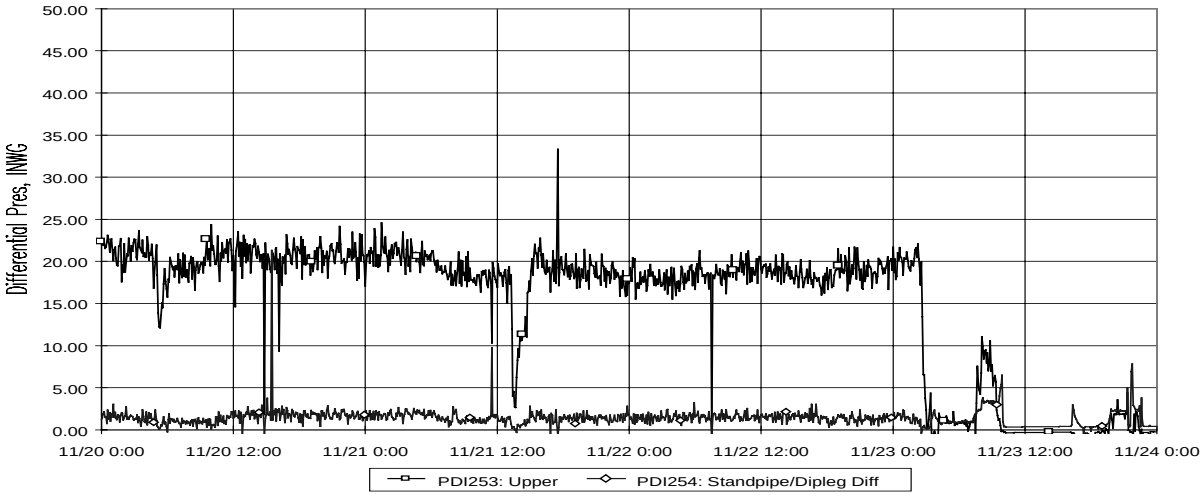

Figure 4.1.4.8-34 CY0201 Dipleg Differential Pressure Profiles

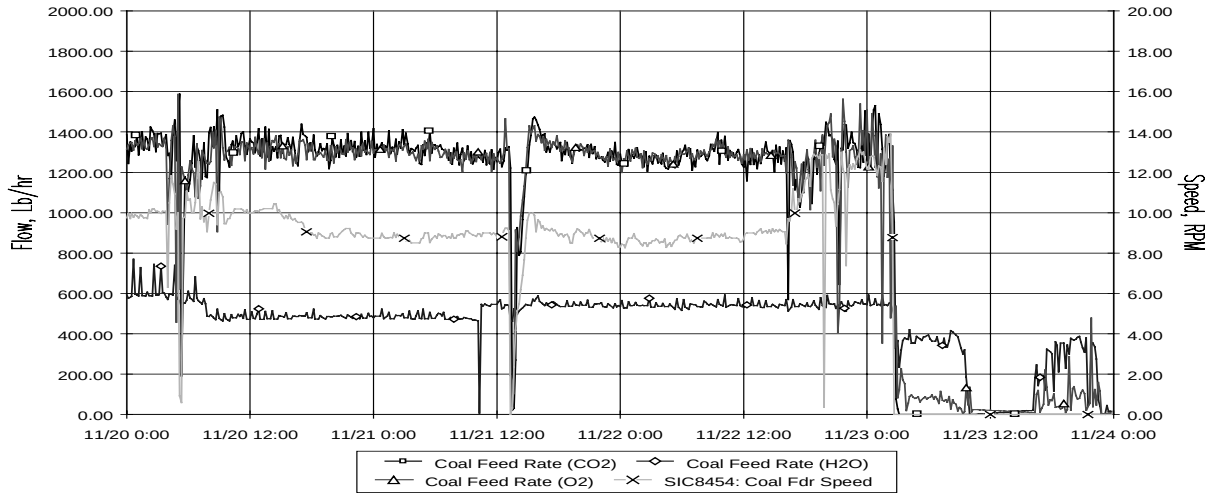

Figure 4.1.4.8-35 Coal Feed Rate Based on Gas Analysis

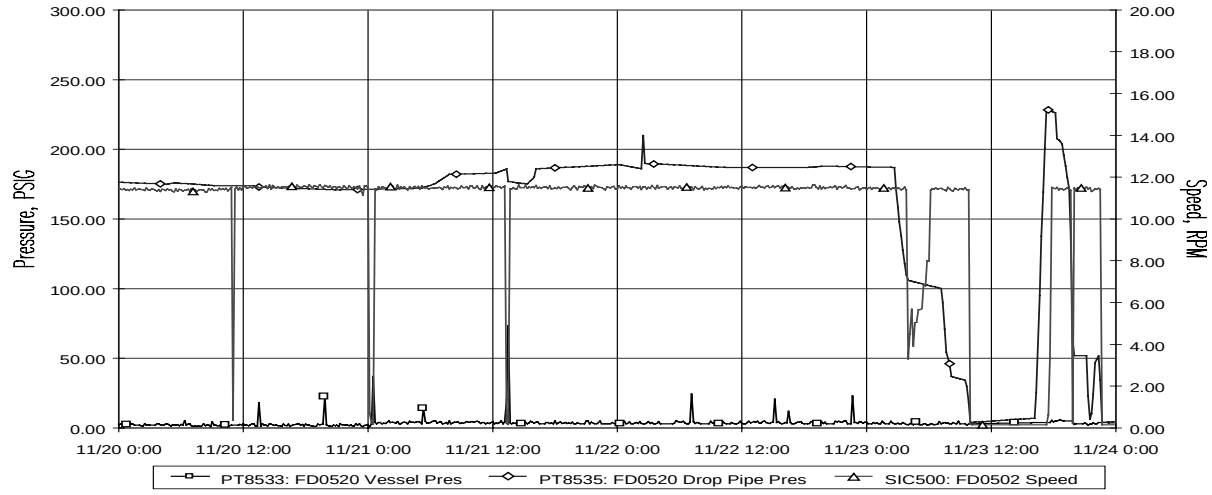

Figure 4.1.4.8-36 FD0520 Pressure Profiles

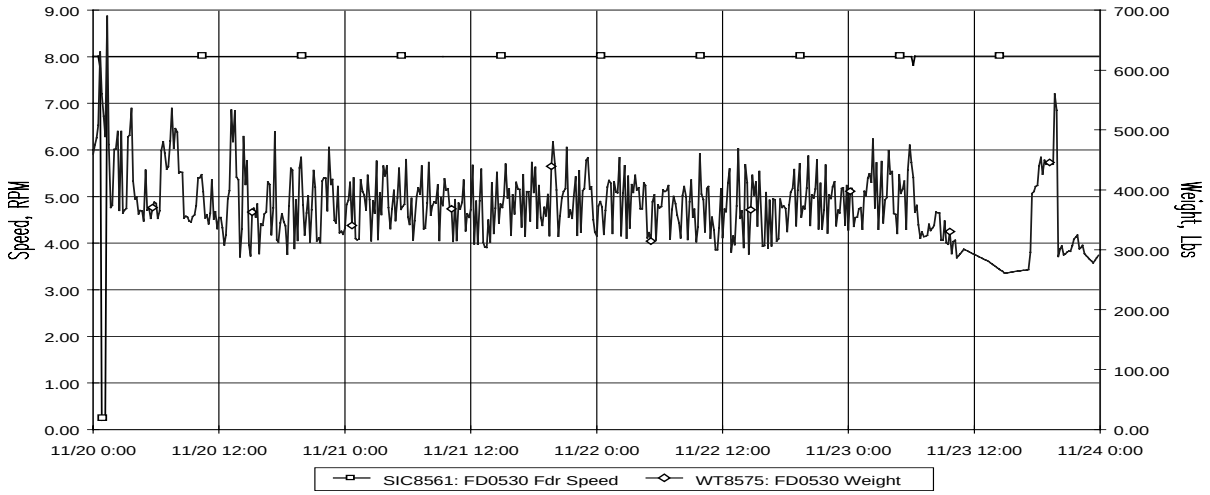

Figure 4.1.4.8-37 FD0530 Feeder Profile

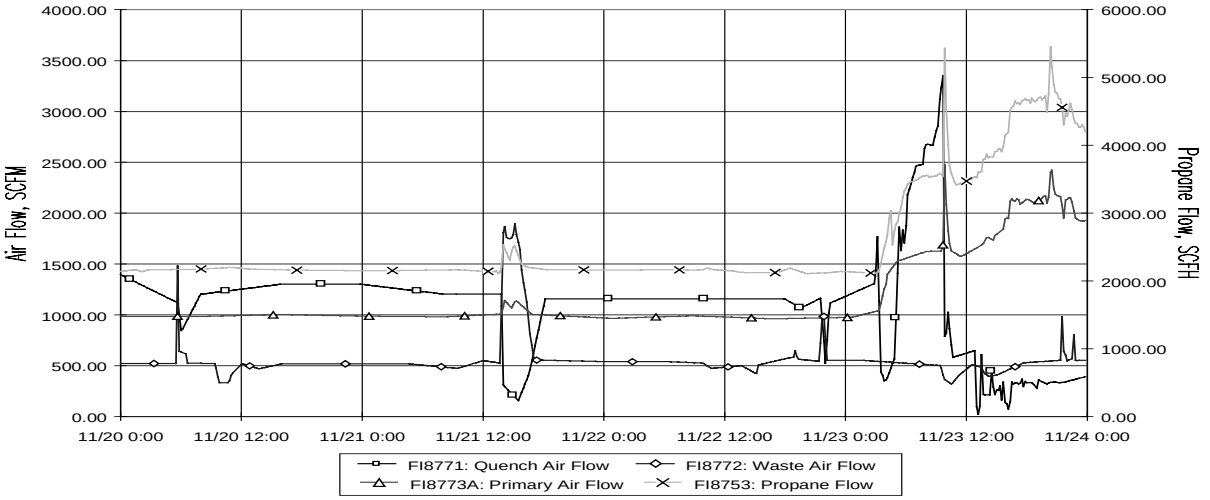

Figure 4.1.4.8-38 Thermal Oxidizer Air/Fuel Flow

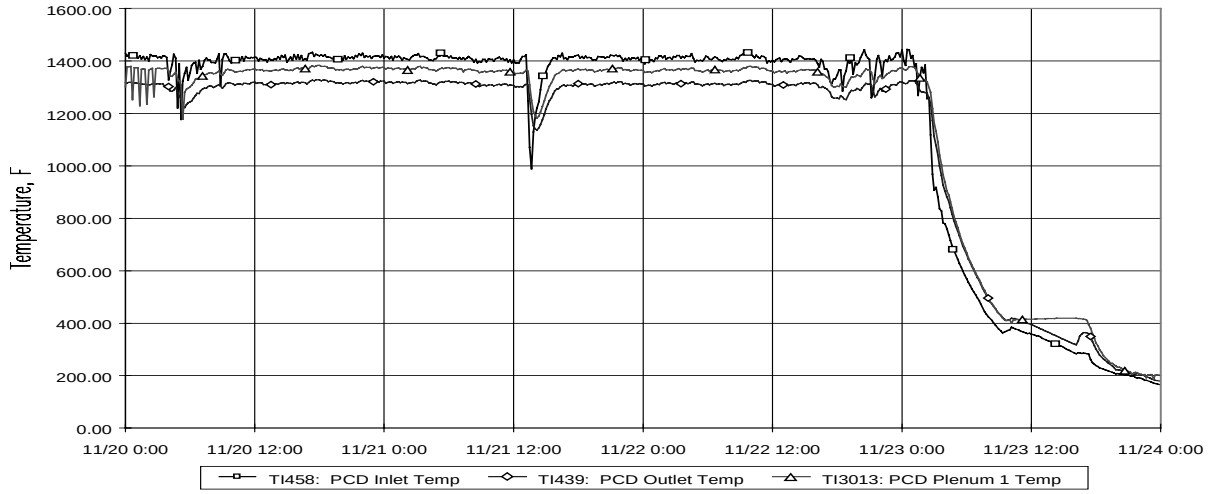

Figure 4.1.4.8-39 PCD Temperatures

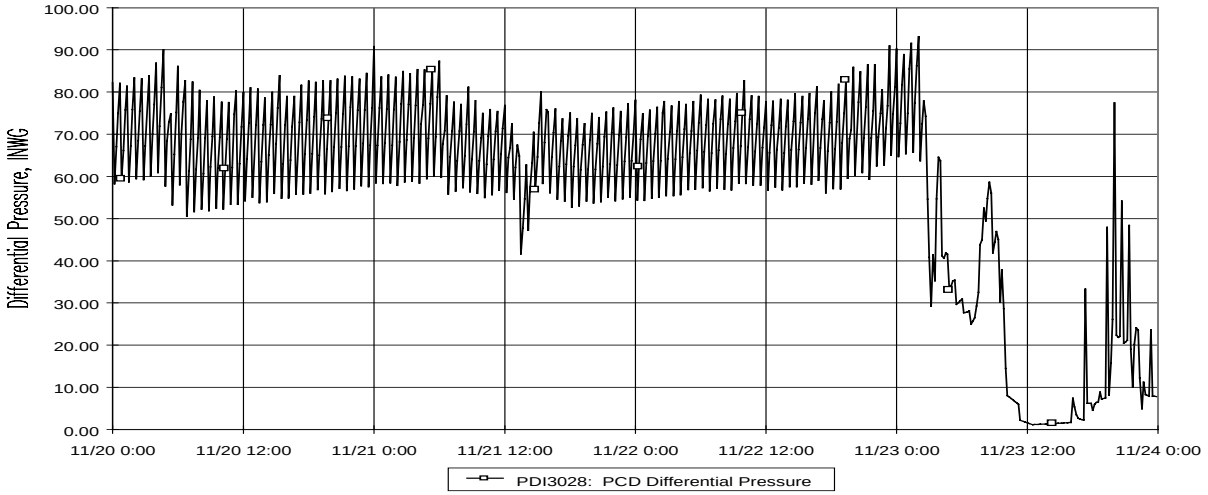

Figure 4.1.4.8-40 PCD Differential Pressure Profile

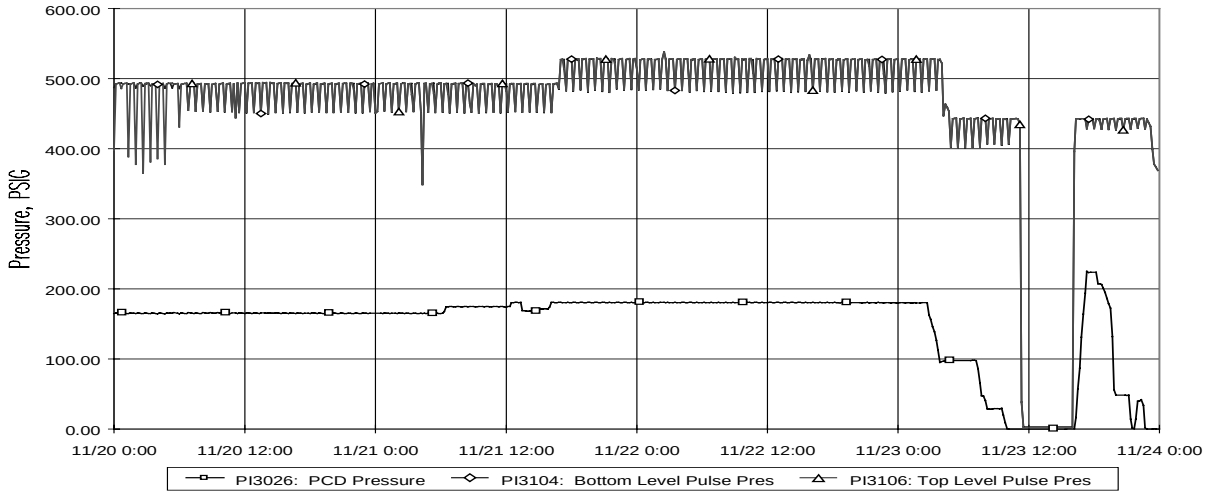

Figure 4.1.4.8-41 PCD Pressure and Pulse Pressure

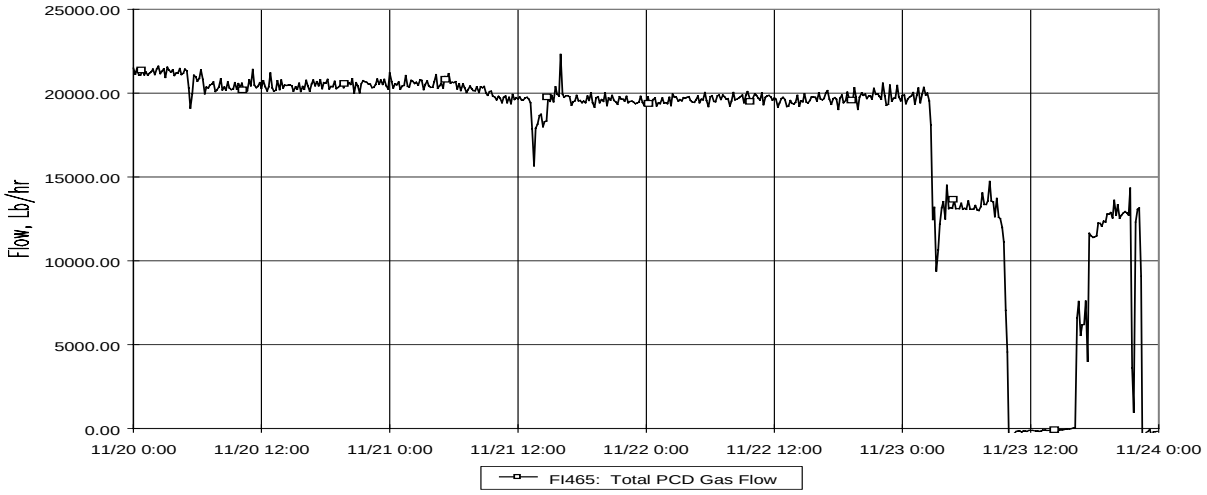

Figure 4.1.4.8-42 Gas Flow Through PCD

4.1.4.9 TC01I Test Run

Test run TC01I was conducted between November 24 and December 9, 1997. Operating plots are shown in figures 4.1.4.9-1 through -88. The following maintenance work was performed during the outage on November 23 and 24, 1997.

- The start-up burner (BR0201) pilot assembly and igniter were replaced. A hole was also cut in the shroud near the igniter to improve combustion by allowing closer contact between propane and the igniter.

- The FI838 line was cut and drilled to remove material that plugged the line at various places between the check valve and the reactor nozzle.

- The spent fines screw cooler (FD0502) seal was repacked.

TC01I Test Run Chronology

- The main air compressor (CO0201) was started at 16:30 on November 24, 1997. The sulfator heater (BR0602) was lit at about 17:30 and the PCD preheat was completed at 19:30. BR0201 was lit at 20:30 and BR0602 was shut down at 21:40. At about 23:35 the reactor pressure was increased to 60 psig.

- By 06:35 on November 25, 1997, the reactor pressure was 100 psig (event 1, figure 12). The coal feeder (FD0210) was lined up at 08:45 and coal feed was started around 9:30 (event 2, figures 2 and 5 through 9). At about 13:55 all Clyde systems were shut down (event 3, figures 2, 3, 17, and 18) due to a problem with the FD0210 PLC logic associated with limit on coal transfer from surge bin to the lock vessel. After correcting the problem all Clyde systems were restarted at 14:05 (event 4, figures 2, 3, 17, and 18) and coal feed was resumed at 14:10 (event 5, figures 2 and 5 through 9). BR0201 was shut down at 15:05 (event 6, figure 4), the reactor pressure was increased to 125 psig at 15:25 (event 7, figure 12) and by 16:15 the PCD plenum temperature was above 1,350°F (event 8, figure 19). Aeration through the combustion heat exchanger (HX0203) J-leg was increased and the reactor pressure was gradually increased to 150 and 180 psig at 16:25 and 17:55, respectively.

- On November 26, 1997, the back-pulse pressure was increased to 535 psig around 01:10 (event 9, figure 21). The top spheri valve seal in the spent fines transporter (FD0520) failed around 07:00 (event 10, figure 17) and at 07:15 FD0210 tripped (event 11, figures 2 and 5 through 9) due to lack of seal pressure. In addition to losing coal feed a back-pulse at 07:17 led to a dipleg upset (event 12, figure 14). The upset lasted 11 minutes and caused about 2,000 lb of solids carryover to the PCD. Coal feed was reestablished around 07:20 (event 13, figures 2 and 5 through 9).

- Failure of the FD0520 bottom spheri seal, coupled with ash accumulation in the PCD cone, prompted a temporary shutdown of the unit to address the problems.

The CO0201 was therefore stopped at 11:30 (event 14, figure 1). After work was completed on the FD0520 bottom spheri seal CO0201 was started again at 17:35 (event 15, figure 1) and BR0201 was lit around 19:30 (event 16, figure 4). Sand was added to the reactor to make up for the low-solids level in the reactor (due to the solids carryover to the PCD).

- Coal feed resumed at 05:20 (event 17, figures 2 and 5 and 10) on November 27, 1997, and BR0201 was shut down at 08:45 (event 18, figure 4). There were dipleg upsets at 09:25 and 09:30 but after resetting the aeration on the dipleg operation became normal. By 14:20 the PCD plenum temperature was above 1,350°F (event 19, figure 19).

- The FD0210 low-transfer weight problem started around 21:00 on November 27. At 03:00 on November 28, 1997, adjustments were made to FD0210 to increase the transfer weight to lock vessel. Between 08:25 and 12:15 the reactor pressure was increased in steps to 200 psig. The FD0210 system tripped momentarily at 12:50 (event 20, figures 5 and 6). Plugging in the HX0203 standpipe aeration lines led to poor circulation in the reactor, resulting in lower PCD cone temperatures (than in previous runs). The FD0510 system was plugged at 22:45 but the line was cleared and the system restarted.

- On November 29, 1997, the FD0510 system plugged at 01:25 and 02:35. Upon inspection a few refractory pieces were recovered from the sample line. The plugged HX0203 standpipe aeration lines continued to pose circulation problems in the unit which resulted in uneven solid buildup in the HX0203. The solids buildup on one side of the vessel gave rise to nonuniform HX0203 skin temperatures that varied by as much as 100°F. Several attempts were made to improve circulation through HX0203, and at 20:15 the circulation through the HX0203 J-leg improved.

- The solids screw cooler (FD0206) was run intermittently throughout November 30, 1997. There was bridging in the FD0210 lock vessel and surge bin at 08:00. Two of the plugged HX0203 standpipe aeration lines were unplugged. At 05:00 and 21:00 there were problems with the transfer of solids from the PCD cone to FD0520. All these problems were addressed and the unit continued on coal feed. Apart from these problems the process ran well.

- On December 1, 1997, there was a leak in the weld at the attachment of the transport air line to the bottom of FD0210, but it was manageable and operation continued. Otherwise, the process ran well.

- A nuclear density vendor took density readings on the standpipe and cyclone dipleg on December 2, 1997. At 09:20 the PLC control computer was inadvertently put in test mode during backup, tripping all of the Clyde systems (event 21, figures 46, 47, 49 through 53, 56 through 59, 61, and 62). The PCD temperature consequently fell below 1,350°F at 09:30. After putting the PLC control computer in run mode all

Clyde systems were restarted and coal feed was resumed at about 9:40 (event 22, figures 46, 47, 49 through 53, 56 through 59, 61, and 62).

- SRI took PCD inlet and outlet samples on December 3, 1997. The process ran well on December 3 and 4, 1997. On December 4, 1997, FD0206 was run throughout the day in order to control the HX0203 solids level.

- On December 5, 1997, failure of the MWK cooling water pump caused CO0201 to trip at 05:05 (event 23, figures 45 through 47, 49 through 53, and 56 through 59) and coal feed was stopped. After switching to an alternative cooling water pump CO0201 was restarted and coal feed resumed at 05:40. The FD0520 vent line was plugged at 14:40 but was unplugged by 15:10. The quick-dump valve on FD0520 started leaking nitrogen at 16:00 and was replaced. The FD0520 line to FD0530 plugged a couple of times.

- On December 6, 1997, ash that had collected on one side of the FD0502 screw cooler drop tube began to restrict solids flow to FD0520. Consequently, there was ash back-up in the PCD cone. Tapping on the drop tube dislodged the ash build-up. Otherwise, the process ran well.

- On December 7, 1997, the FD0510 lock vessel top spheri valve failed at about 02:15 (event 24, figures 79, 80, and 82). The solids level in HX0203 dropped as a result of solids being blown through the lock vessel. The problem was corrected and FD0510 was restarted at 02:45. The rest of the process ran well.

- On December 8, 1997, the FD0210 system tripped several times due to loss of seal nitrogen pressure (event 25, figures 68 and 72 through 75). About 3 minutes after each trip the seal nitrogen pressure was restored and the system restarted. At 04:40 the line between FD0520 and FD0530 plugged (event 26, figures 83 and 84). Ash was drummed out of the sample port because the line could not be unplugged. FD0520 tripped at 07:30 (event 27, figure 83) due to plugging and was restarted at 08:50 after the line was cleared. At 14:15 FD0210 tripped (event 28, figures 68 and 71 through 75) due to plugging in the coal conveying line. The plugging was cleared and coal feed was restored at 16:30. Coal feed continued to be erratic throughout the day due to plugging in this line. FD0530 tripped at about 18:50 (event 29, figure 84) due to a foreign material binding the star feeder that caused ash accumulation in FD0530.

- On December 9, 1997, the goal of TC01 test run was achieved. By 02:35 there was a total of 1,000 hrs during which the PCD plenum temperature was above 1,350°F. Coal feed was lost at 06:20 (event 30, figures 68 and 71 through 75) due to plugging in the FD0210 exit line. Shutdown of the process was initiated at 06:30 (event 31, figures 67 and 78). The process ran for 1,003 hr, 10 minutes with the PCD temperature above 1,350°F.

TC01I Post Test Run Inspections

The transport reactor was inspected January 28 and 29, 1998, with the borescope and through visual inspection using a halogen lamp. The following observations were made:

- Riser. The riser was inspected through nozzle H1 at the top of the riser. Riser was clear. A crack previously observed at top of riser was not getting worse. Some small nodules were observed at the top of riser.

- Standpipe. The disengager/standpipe was inspected through nozzle A1 above disengager. There was some loose and agglomerated sand deposit on the lip of the refractory leading to nozzle A52. There were many small nodules on the disengager walls and on the upper sections of the standpipe. Below this the standpipe was clear. The bottom of the standpipe was inspected by placing the borescope into nozzle TN6 with the halogen light in TE359. There was a small area approximately 1/4-inch wide and several inches long where refractory was missing in the cone section of the transition piece; it caused no problems with operations.

- Crossover. The riser crossover was inspected through nozzles A50 and A52. A52 was completely full of loose and agglomerated sand. The shelf of the refractory beyond A52 was also covered in solids. The walls of the crossover appeared to be covered in solids and there was a large blockage (deposit) at the south end (riser end) of the crossover. The deposit was at the bottom of the crossover just as the gas/solids turn into the crossover from the riser. The deposit covered about half of the diameter of the riser, extended perhaps 0.5 feet in length, and was hard.

- Dipleg. The cyclone and the dipleg were inspected through nozzle H2. A small crack in refractory just above the radish was noticed. The vertical and slant portions of the cyclone dipleg looked clear.

- Cyclones. A borescope was inserted through nozzle A65. The disengager looked good. Some small cracks were visible. The cyclone also looked good with only a few small cracks in the refractory. Some very small separation was evident in the modified cyclone inlet refractory versus the original refractory. Also, a 1/4-inch crack was noticed just upstream of where the feathering is located.

- Burner. BR0201 was inspected from where the flame rod was removed. Some black marks (possibly coke) were on the walls. Small cracks were visible looking back at the top of the burner with the boroscope.

- Mixing Zone. The mixing zone and the reactor J-leg looked clear through TE18 (TI376) when inspected with the borescope. Attempts to look at the burner J-leg were unsuccessful.

- HX0203. The manway on HX0203 was removed for inspection. The tubes looked good with only a thin, loose layer of dust. Walls were clear and had no major cracks. The bottom of the heat exchanger was inspected with the borescope and nothing unusual was seen.

TC01I Test Run Observations

A total of 313.5 hours on coal was achieved and 75 tons of coal were fed. The desired 1,000 hours of candle exposure time at between 1,350 through 1,400°F was also achieved. Test run TC01I had been the longest continuous test run up to this point, with 289 hours on continuous coal feed. With the coal feed system operating well the reactor system operating parameters could be set to achieve very stable reactor operations and the desired PCD inlet temperature. During this test run the coal feed rate was maintained at high rates (1,400 through 1,600 lb/hr) for several days in a row. Additional experience showed that nonuniform dipleg aeration stabilized the dipleg operations. With the change in trim in test run TC01F the pressure letdown valve continued to operate well in test run TC01I and did not experience any high-frequency flow-induced resonance vibrations as in earlier test runs. The FD0210 system reliability was increased by using a constant nitrogen purge under the lock vessel dispersion pad.

Section 4.1.4.9

Graphs 1 through 22

Test Run TC01I
November 24 through 27, 1997

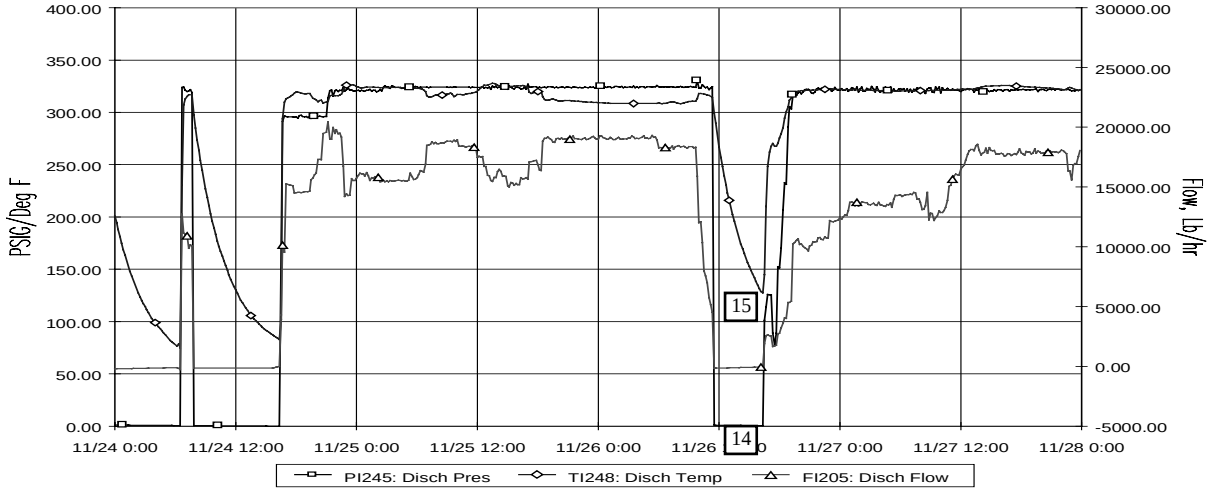

Figure 4.1.4.9-1 CO0201 System Profile

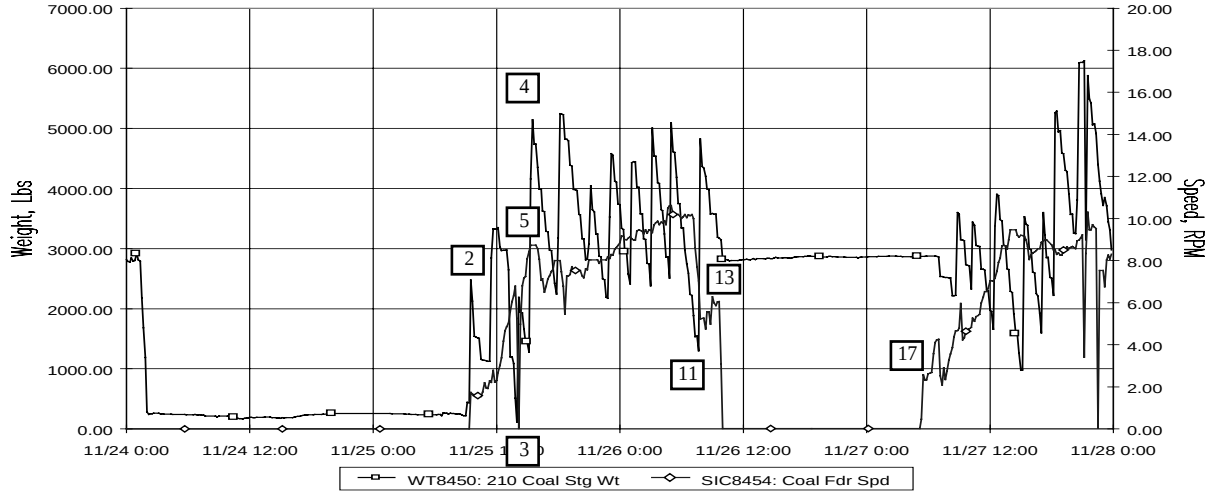

Figure 4.1.4.9-2 Coal Feed System Profile

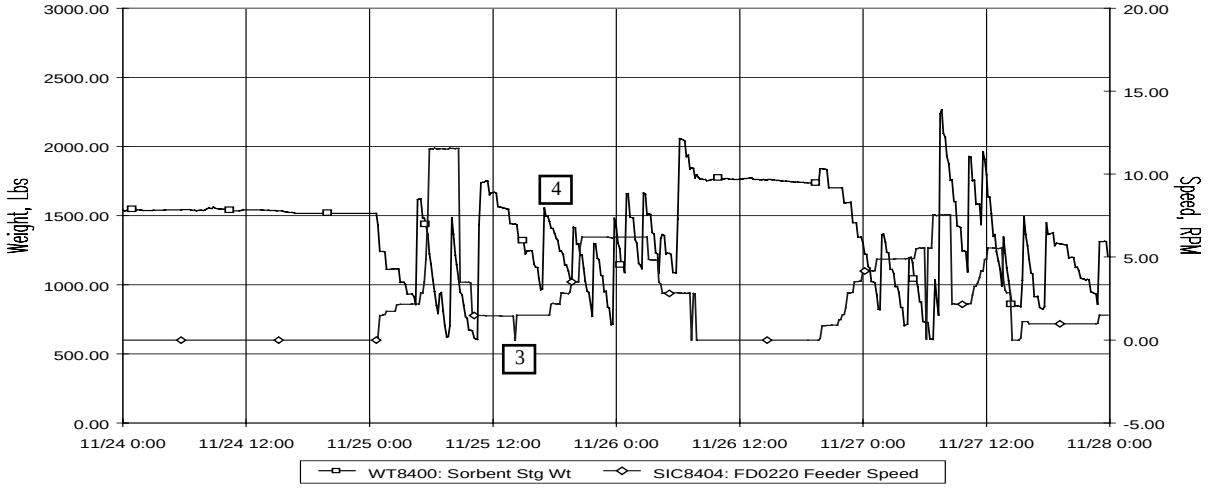

Figure 4.1.4.9-3 Sorbent Feed System Profile

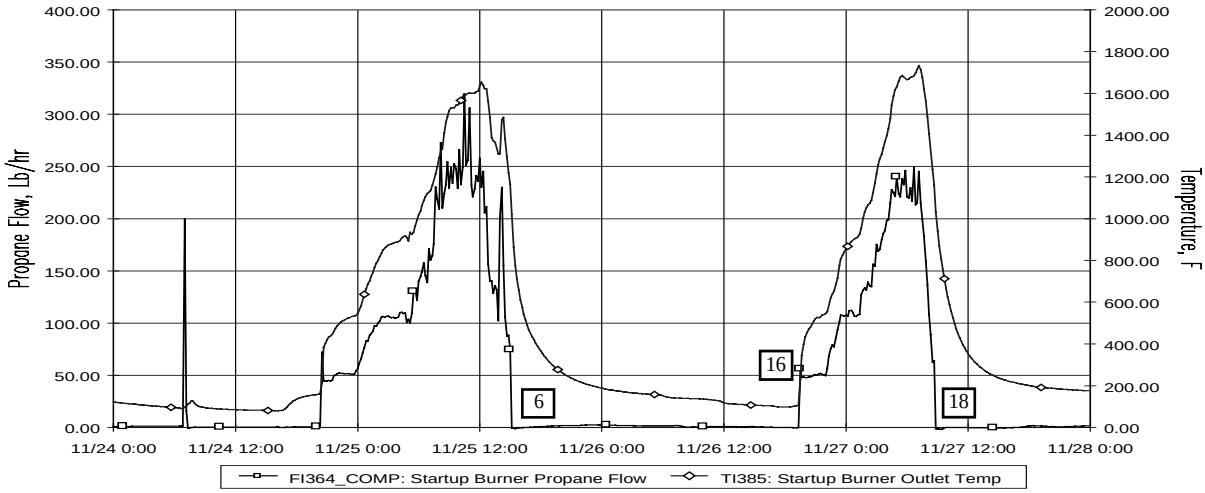

Figure 4.1.4.9-4 Start-Up Burner Flow/Temperature

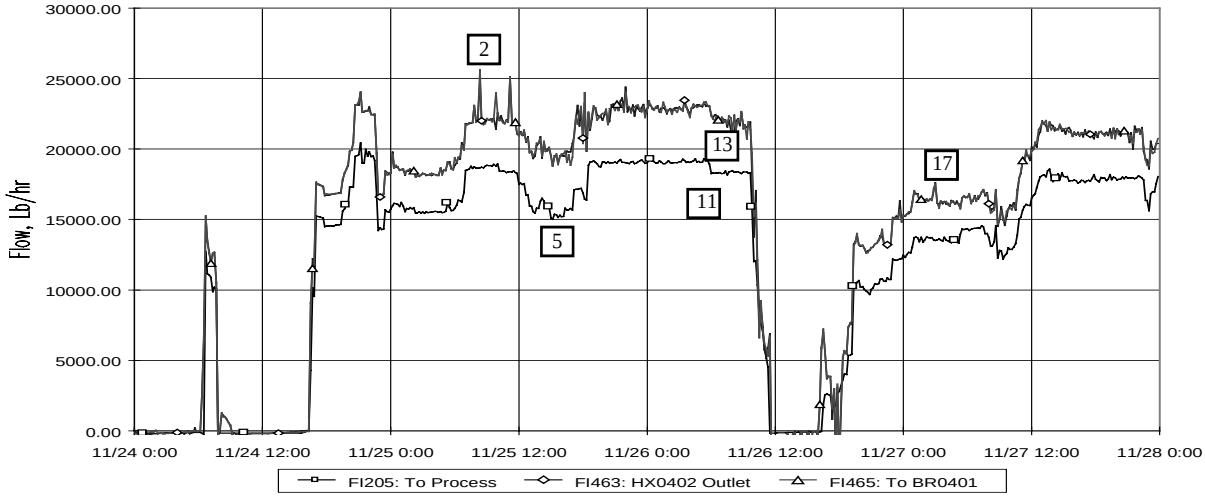

Figure 4.1.4.9-5 Total Gas In/Out Flow Rates

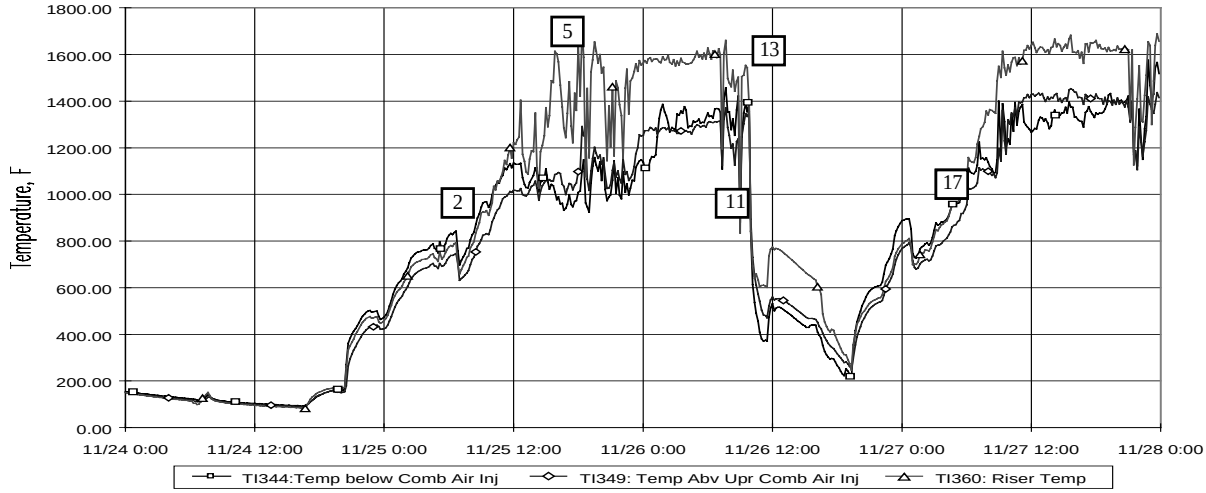

Figure 4.1.4.9-6 Reactor Mixing Zone and Riser Temperatures

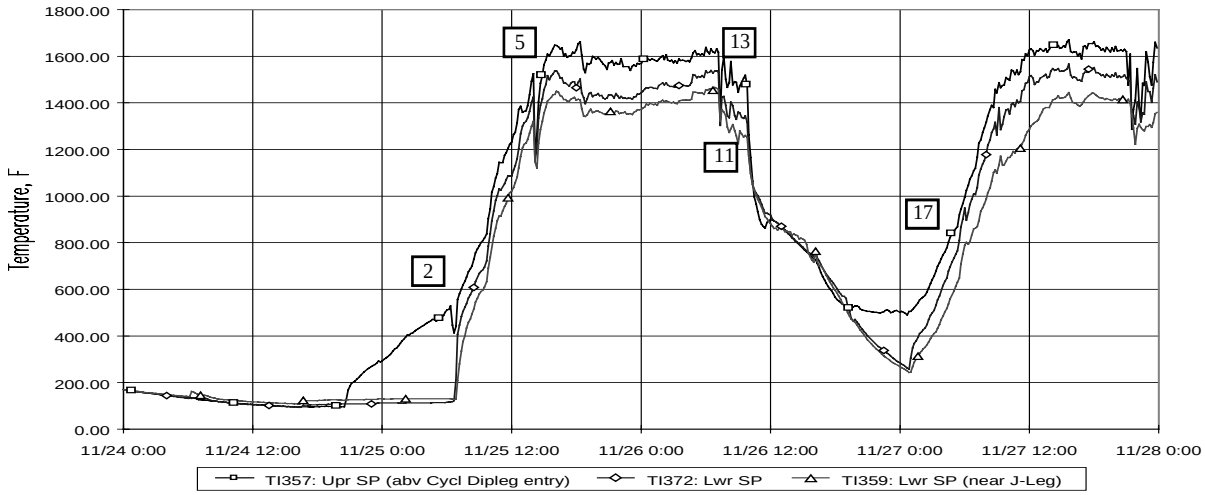

Figure 4.1.4.9-7 Standpipe Temperatures

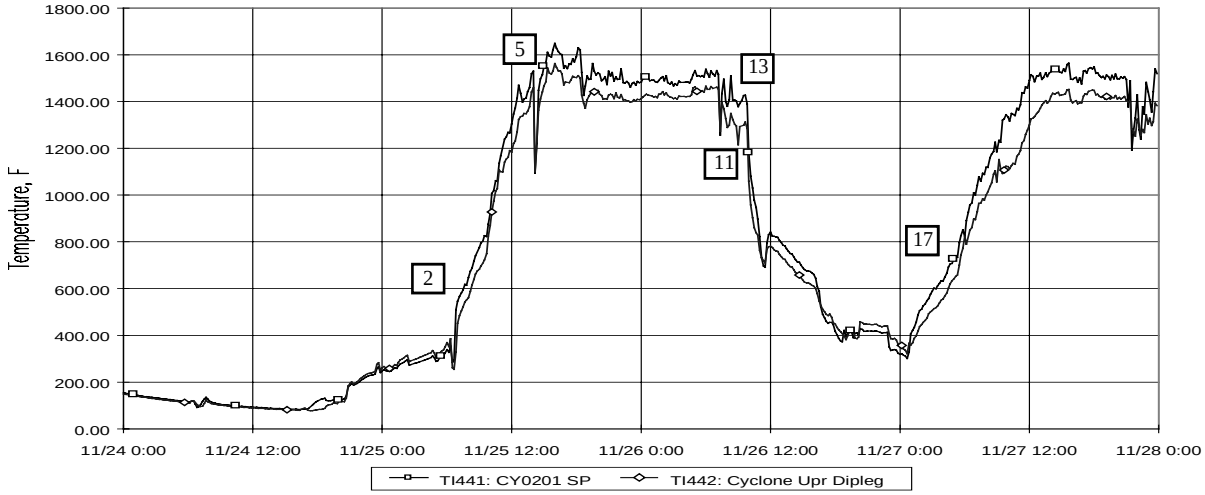

Figure 4.1.4.9-8 Cyclone Dipleg Temperatures

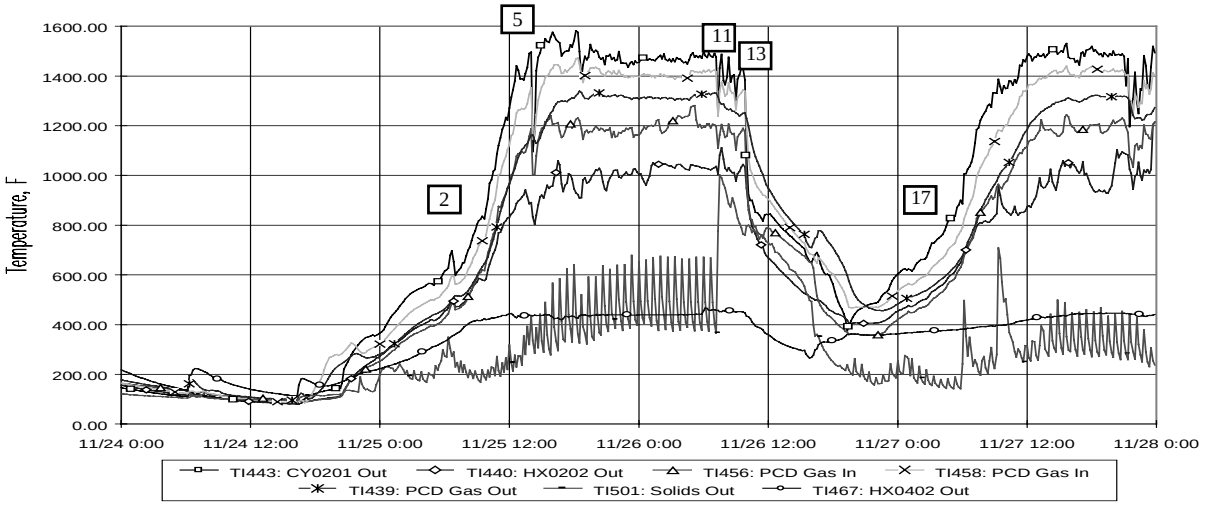

Figure 4.1.4.9-9 Temperature Profile Downstream of Reactor

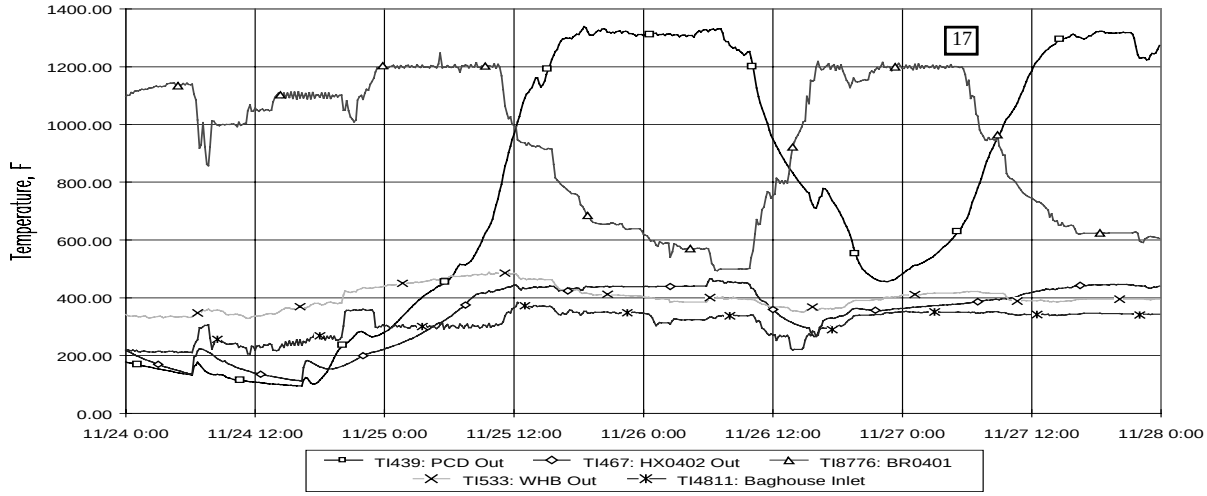

Figure 4.1.4.9-10 System Temperatures Downstream of PCD

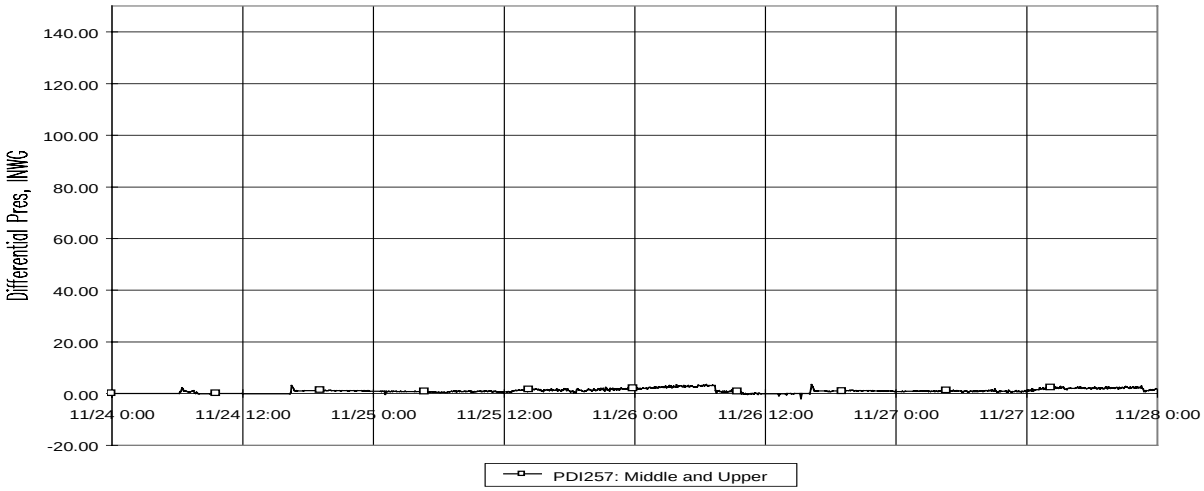

Figure 4.1.4.9-11 Mixing Zone Differential Pressure Profile

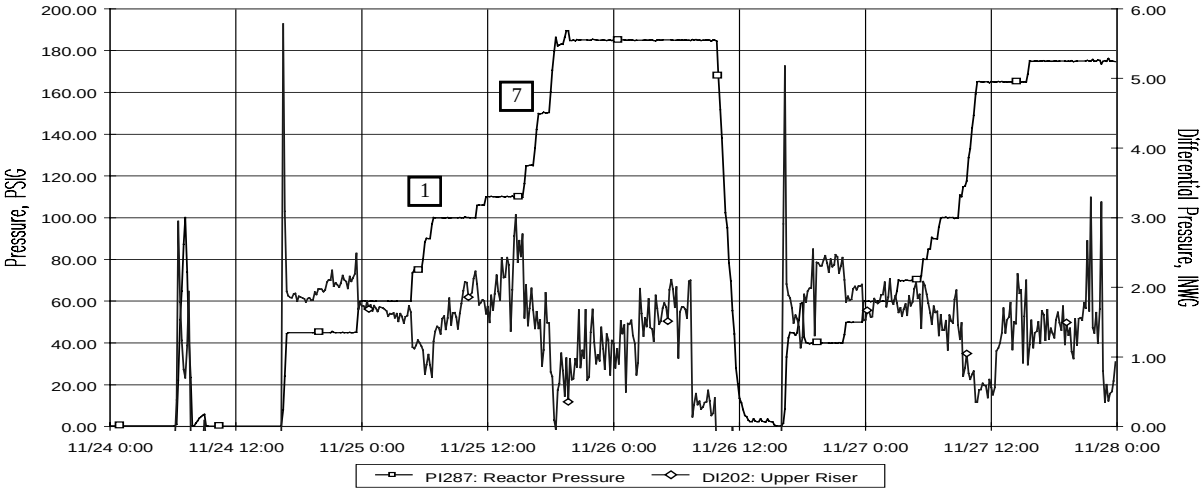

Figure 4.1.4.9-12 Reactor Pressure/Riser Differential Pressure Profiles

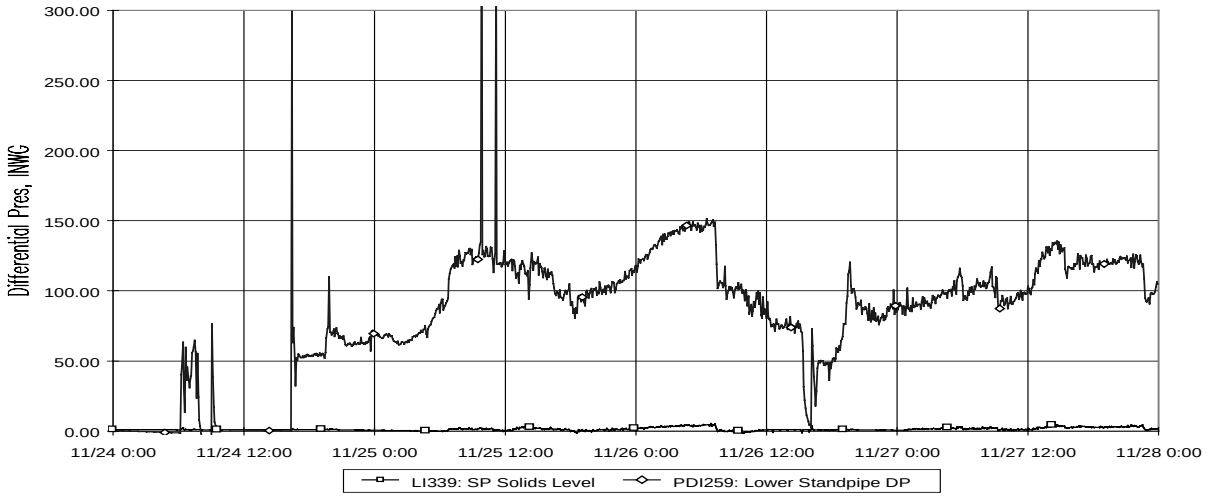

Figure 4.1.4.9-13 Standpipe Differential Pressure Profiles

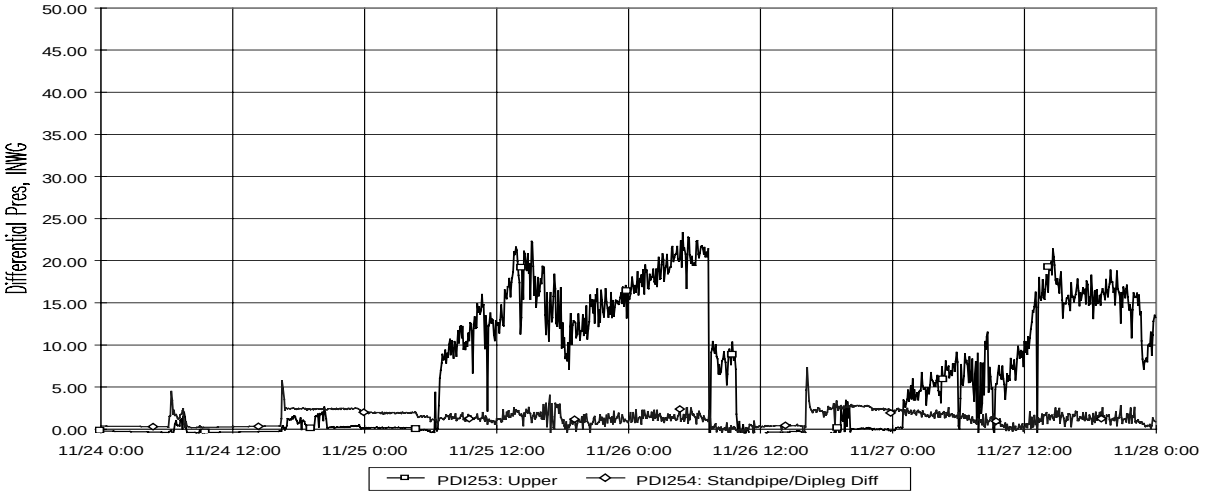

Figure 4.1.4.9-14 Cyclone Dipleg Differential Pressure Profiles

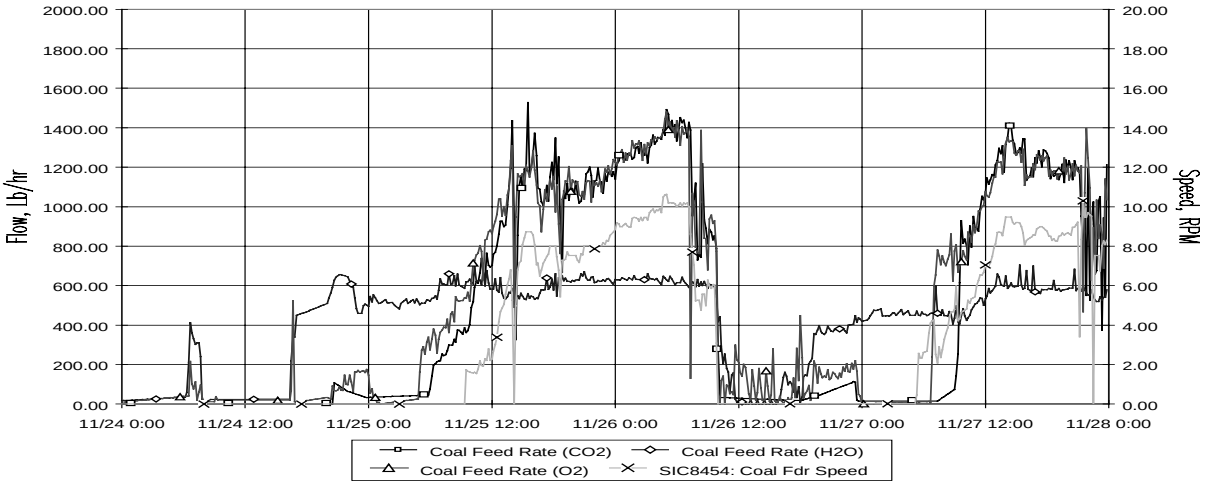

Figure 4.1.4.9-15 Coal Feed Rate Based on Gas Analysis

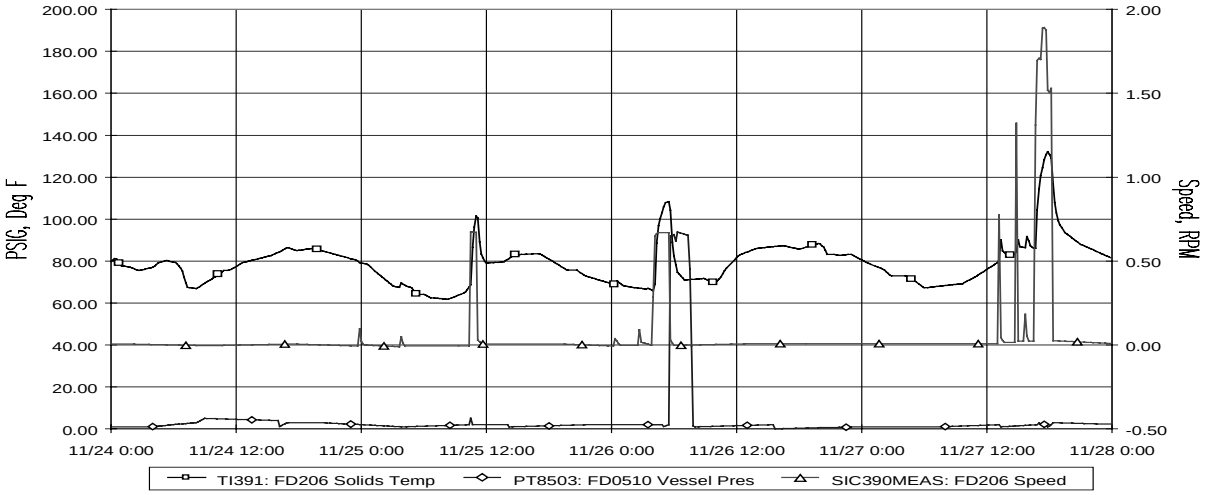

Figure 4.1.4.9-16 FD0206 Profiles

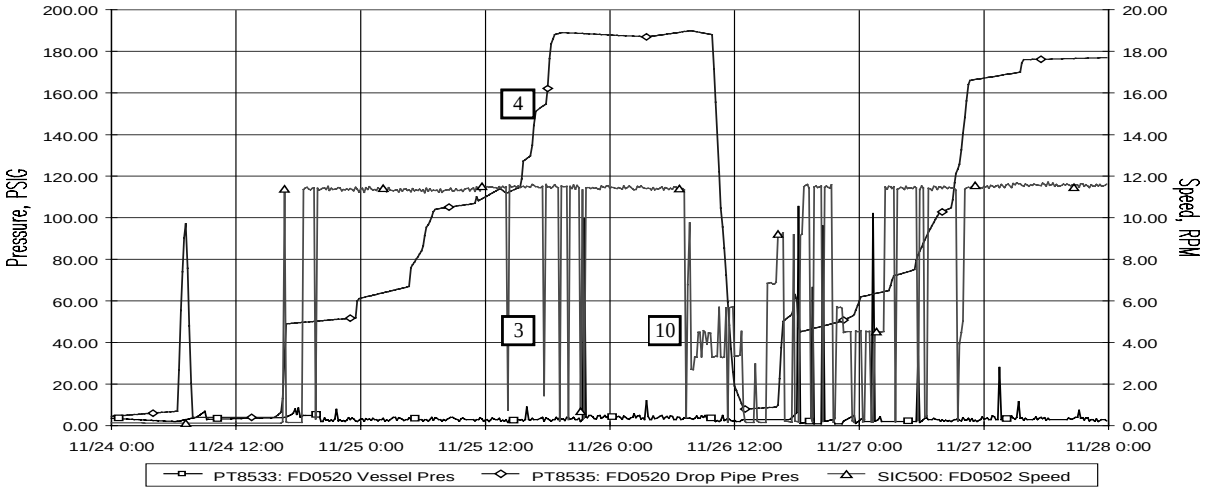

Figure 4.1.4.9-17 FD0520 Pressure Profiles

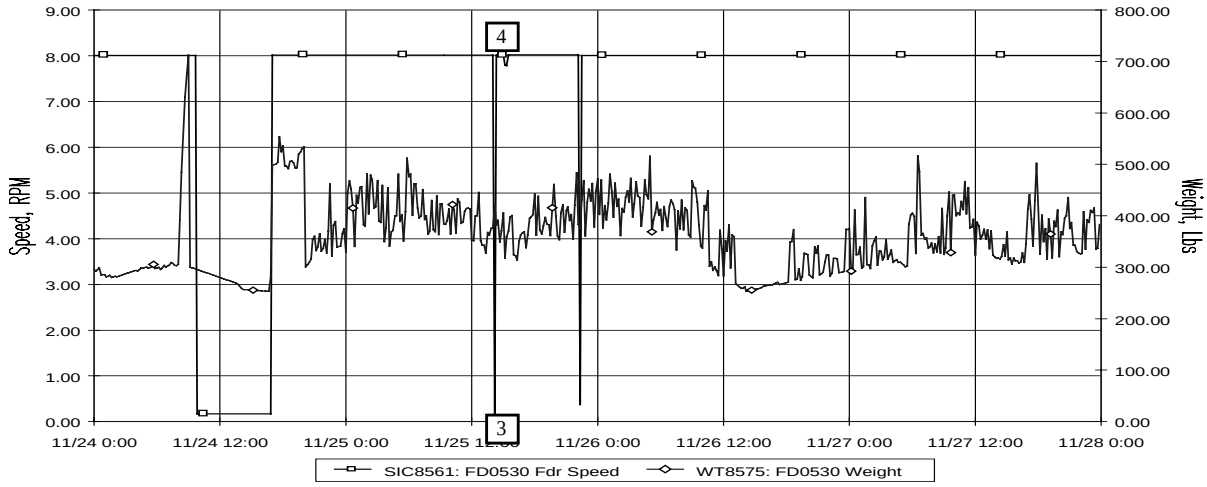

Figure 4.1.4.9-18 FD0530 Feeder Profile

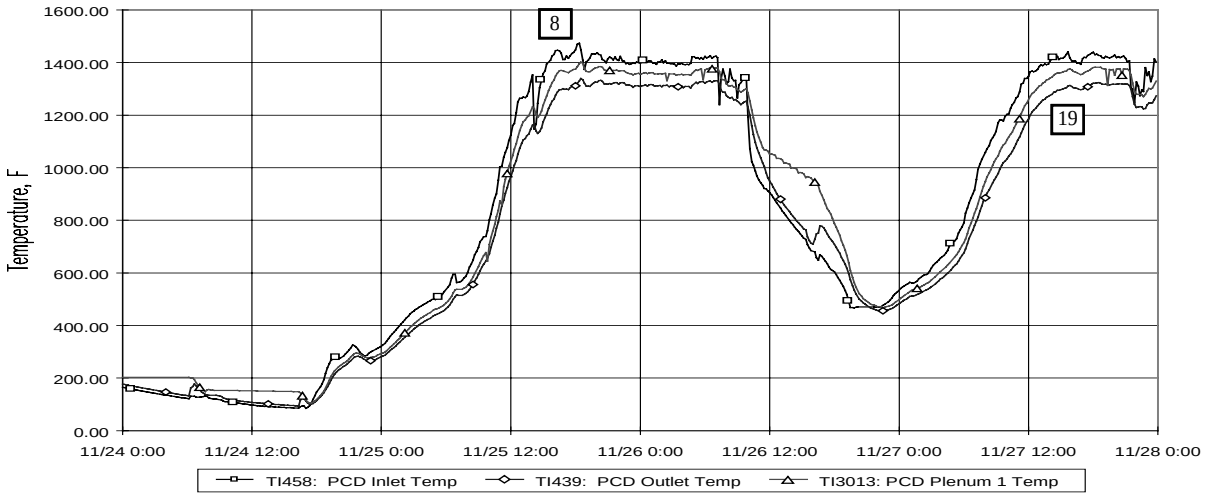

Figure 4.1.4.9-19 PCD Temperatures

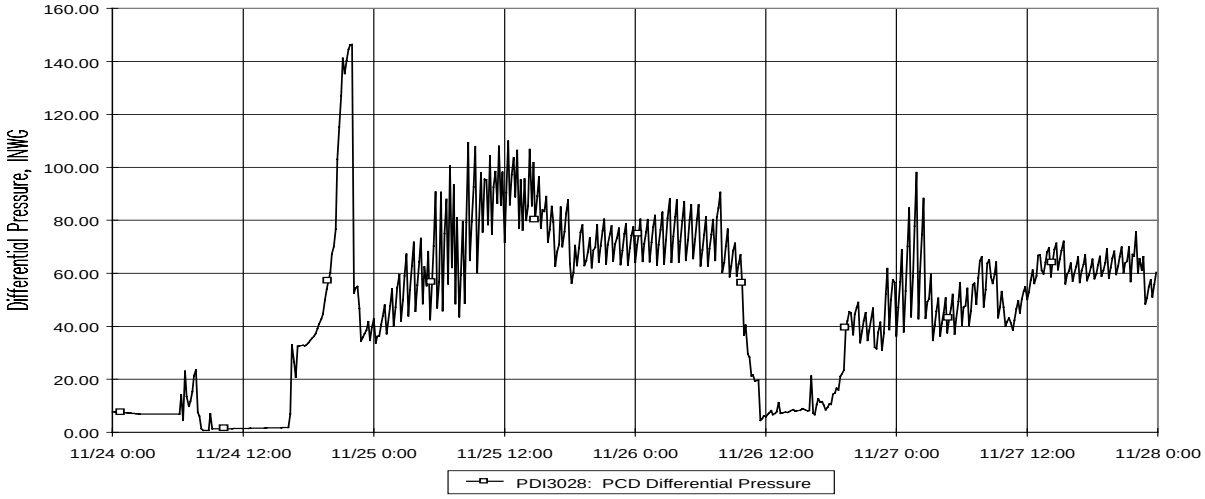

Figure 4.1.4.9-20 PCD Differential Pressure Profile

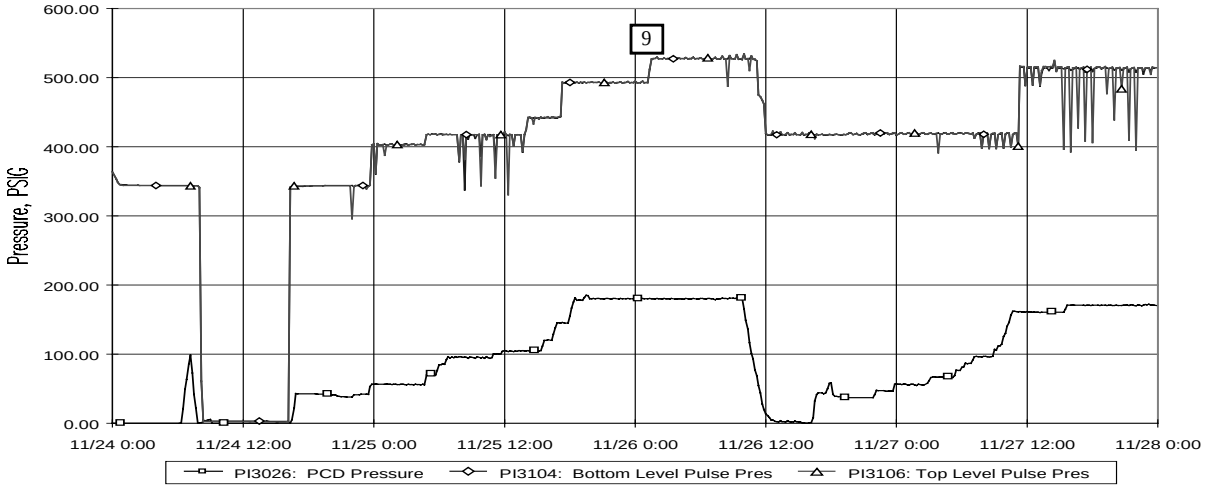

Figure 4.1.4.9-21 PCD Pressure and Pulse Pressure

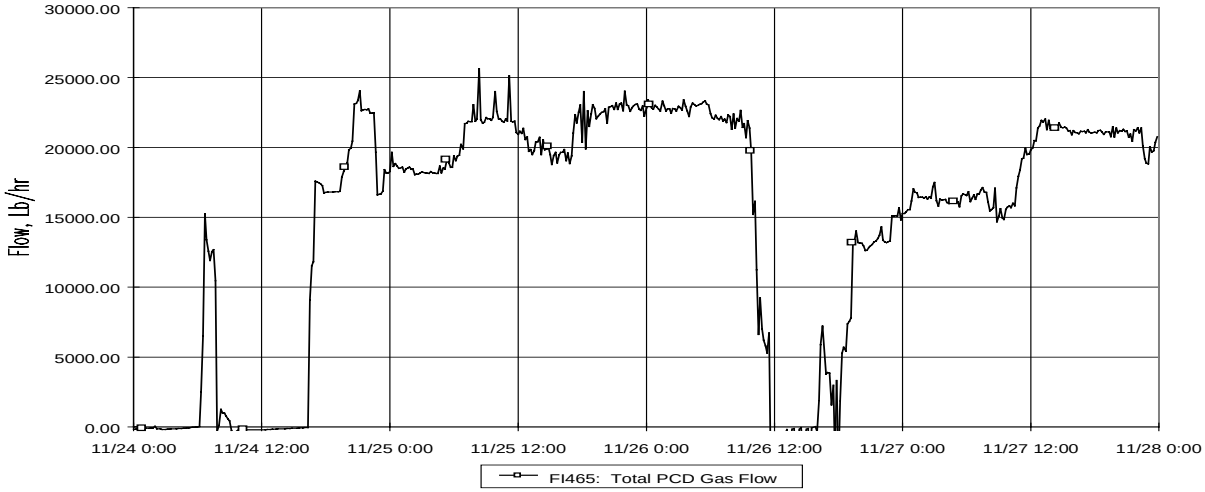

Figure 4.1.4.9-22 Gas Flow Through PCD

Section 4.1.4.9

Graphs 23 through 41

Test Run TC01I

November 28 through December 1, 1997

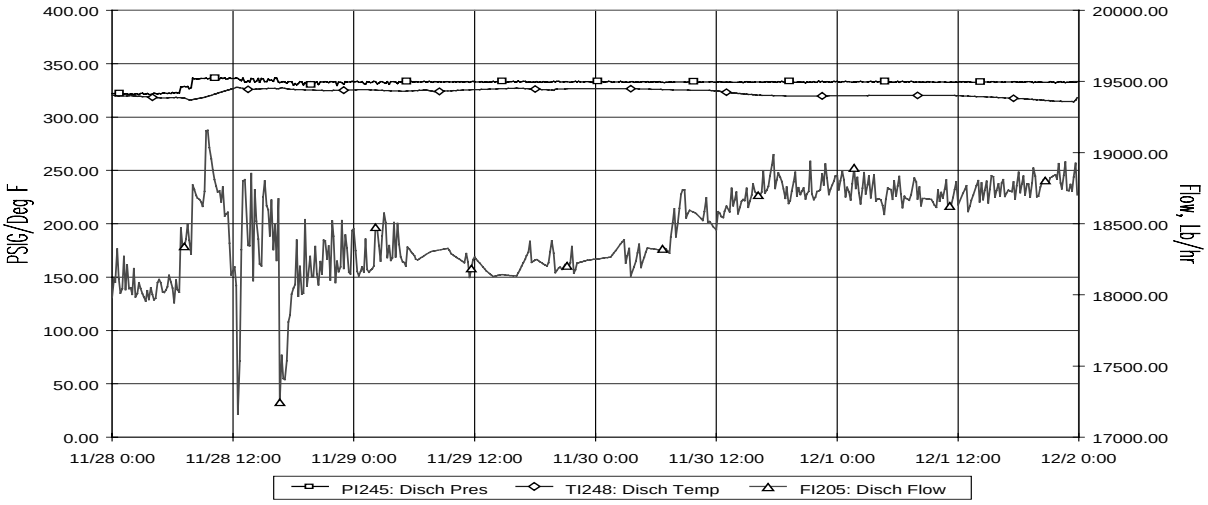

Figure 4.1.4.9-23 CO0201 System Profile

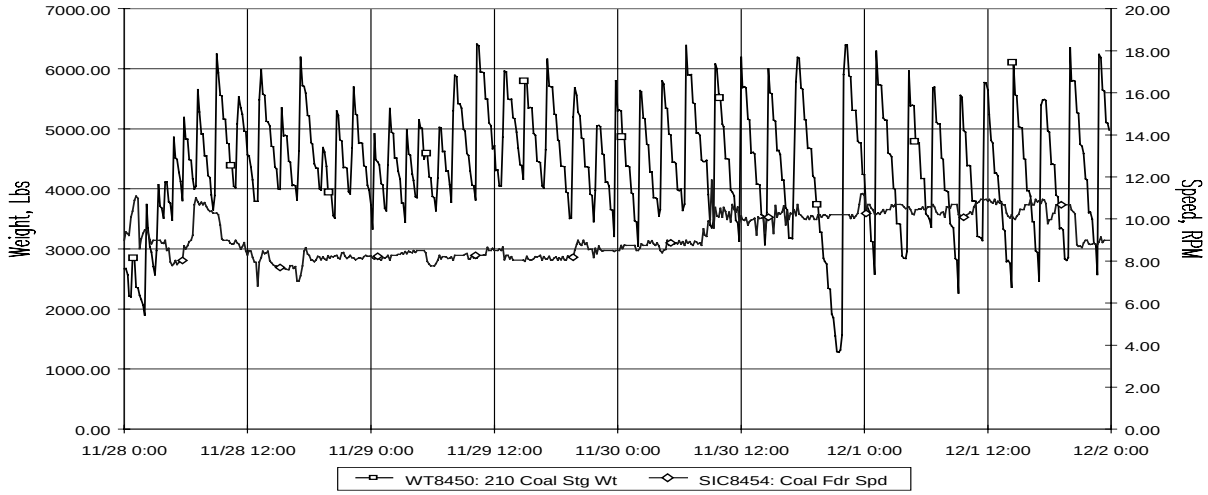

Figure 4.1.4.9-24 Coal Feed System Profile

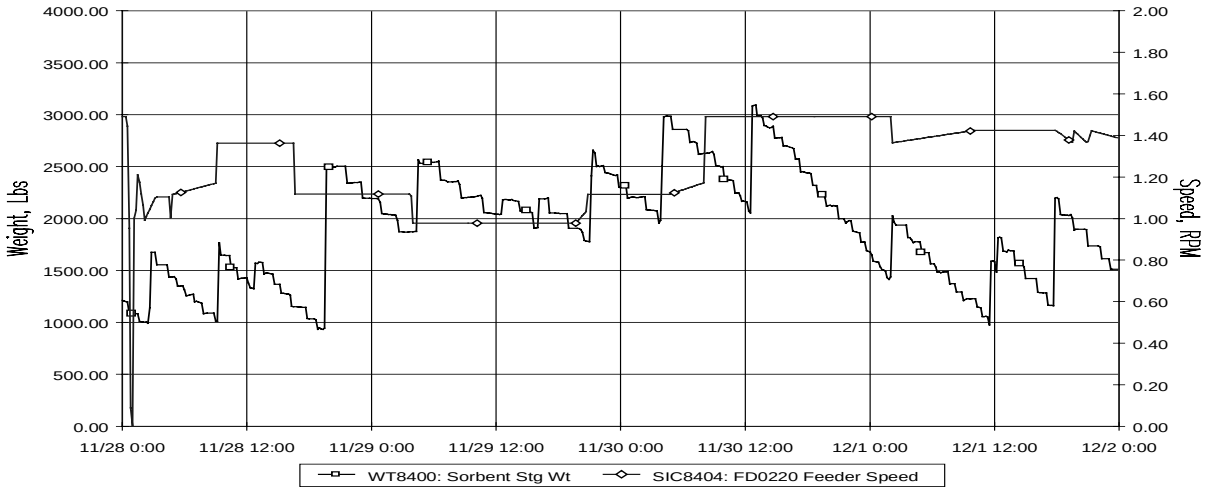

Figure 4.1.4.9-25 Sorbent Feed System Profile

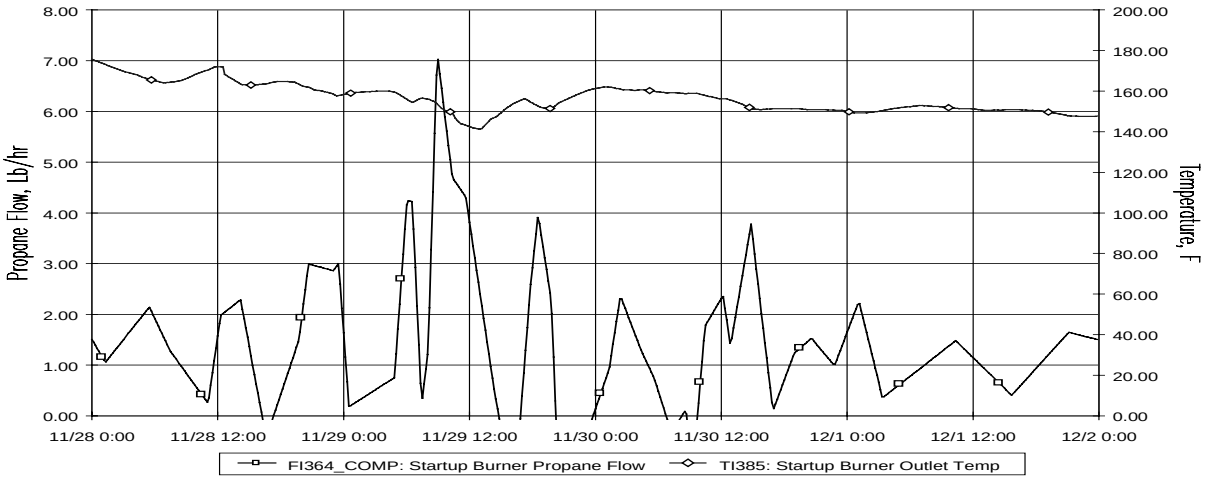

Figure 4.1.4.9-26 Start-Up Burner Flow/Temperature

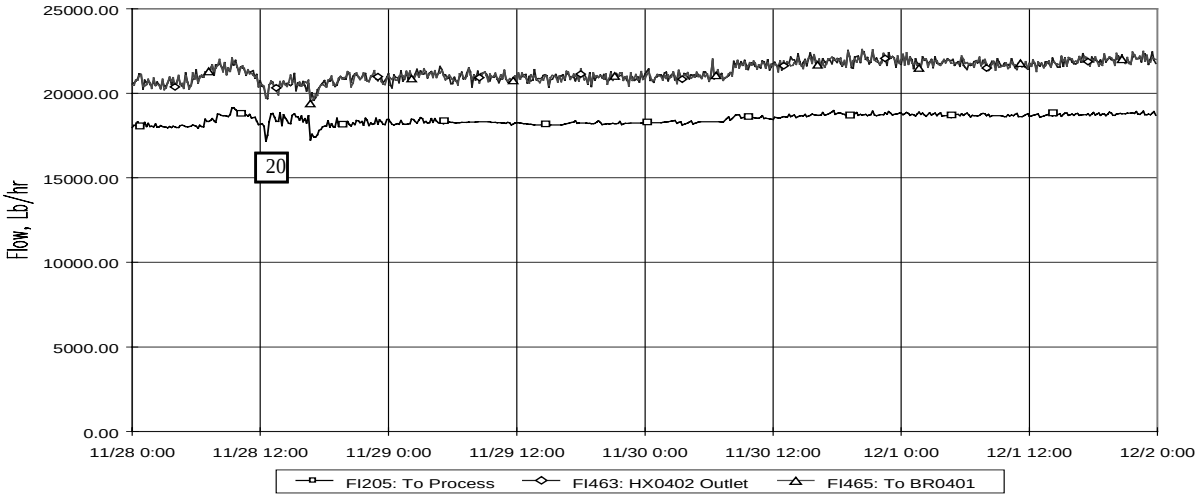

Figure 4.1.4.9-27 Total Gas In/Out Flow Rates

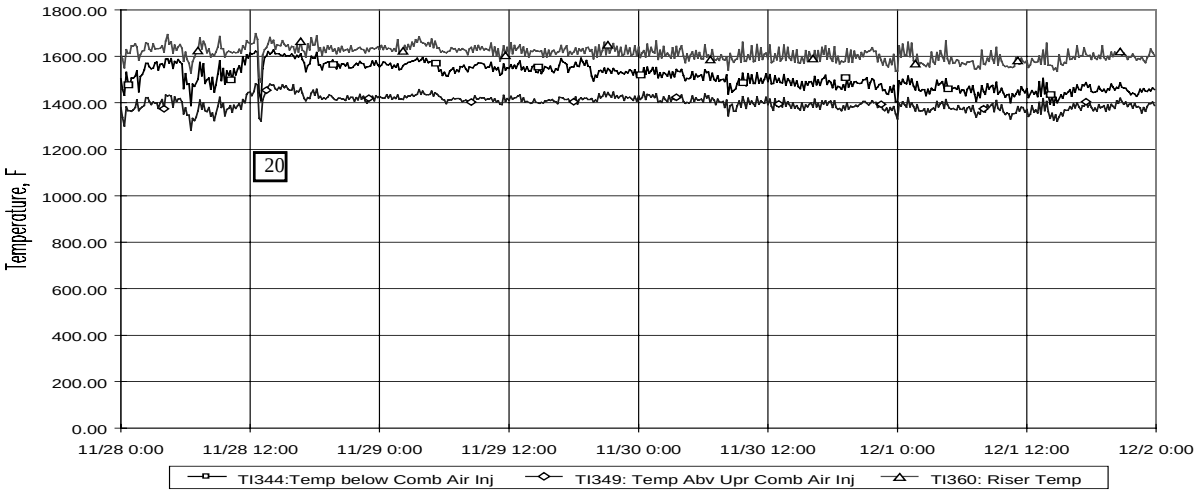

Figure 4.1.4.9-28 Reactor Mixing Zone and Riser Temperatures

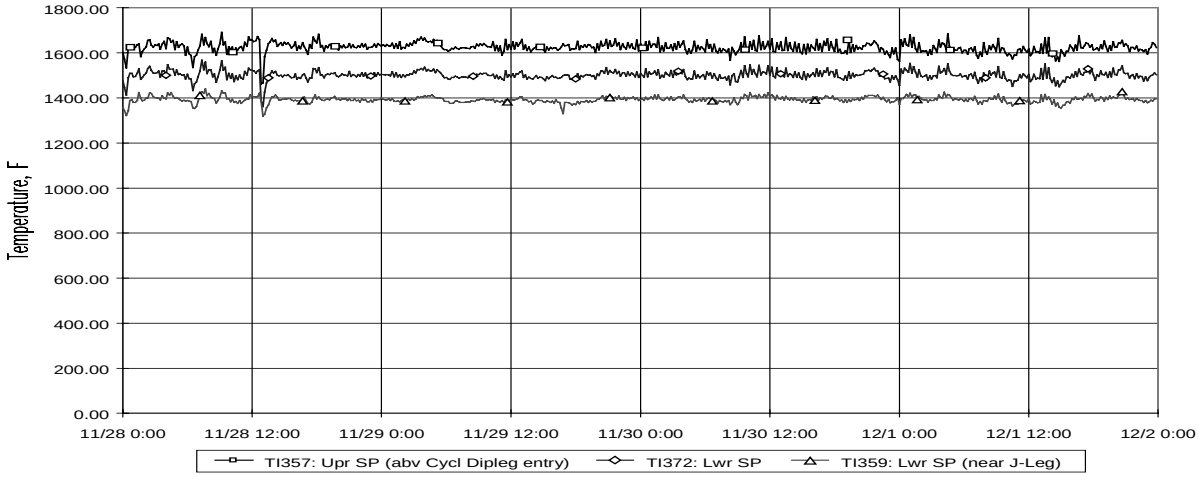

Figure 4.1.4.9-29 Standpipe Temperatures

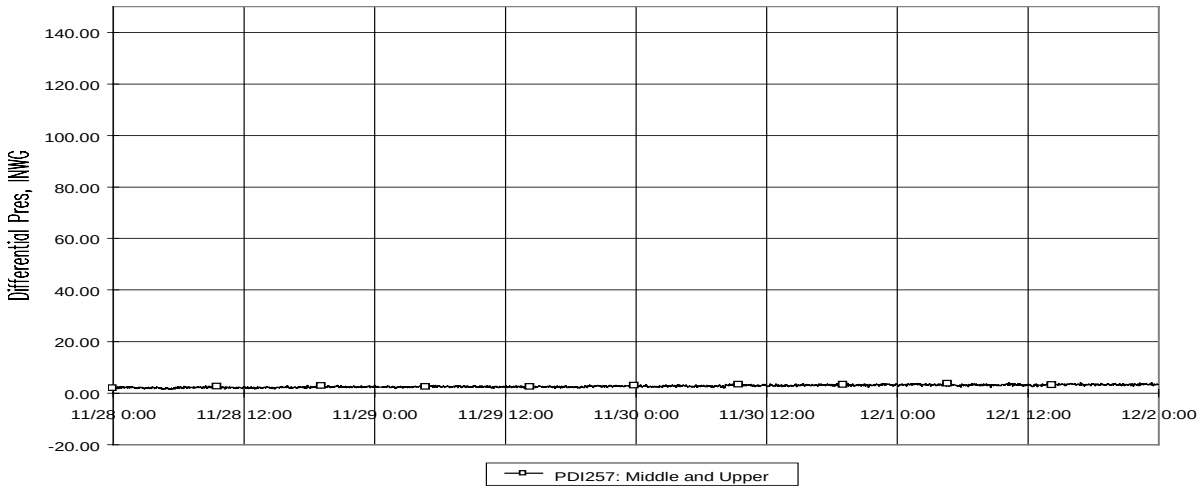

Figure 4.1.4.9-30 Cyclone Dipleg Temperatures

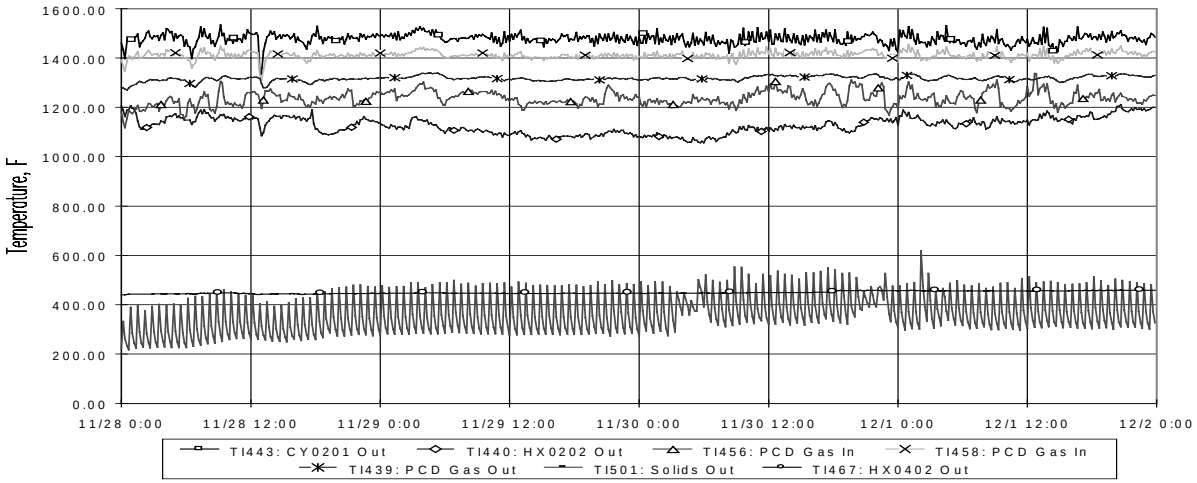

Figure 4.1.4.9-31 Temperature Profile Downstream of Reactor

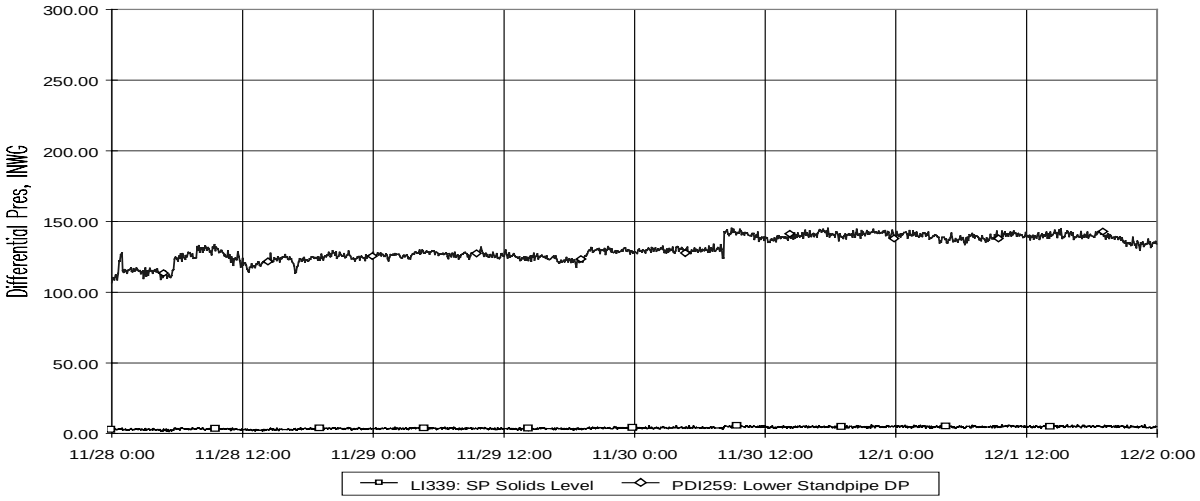

Figure 4.1.4.9-32 System Temperatures Downstream of PCD

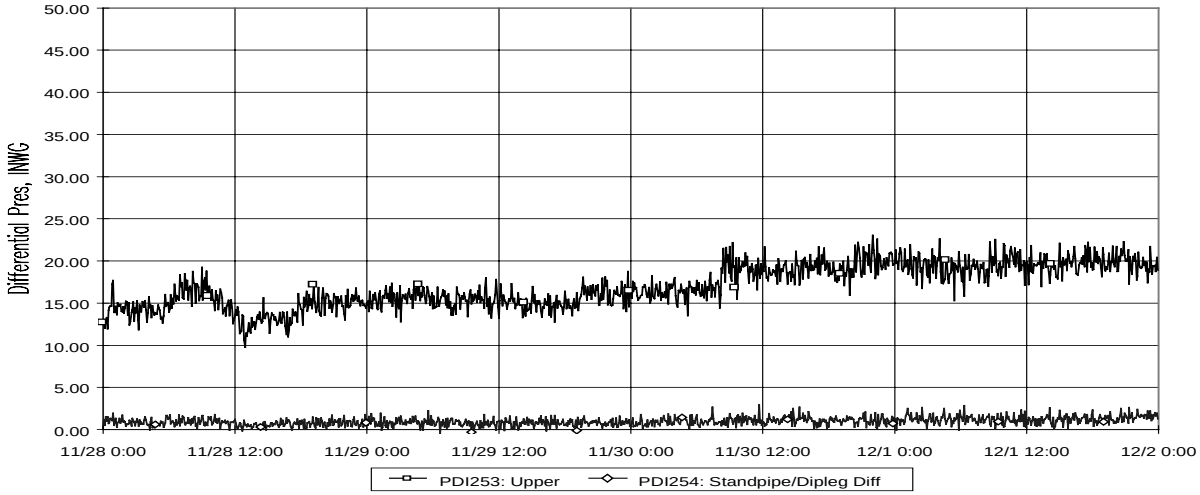

Figure 4.1.4.9-33 Mixing Zone Differential Pressure Profile

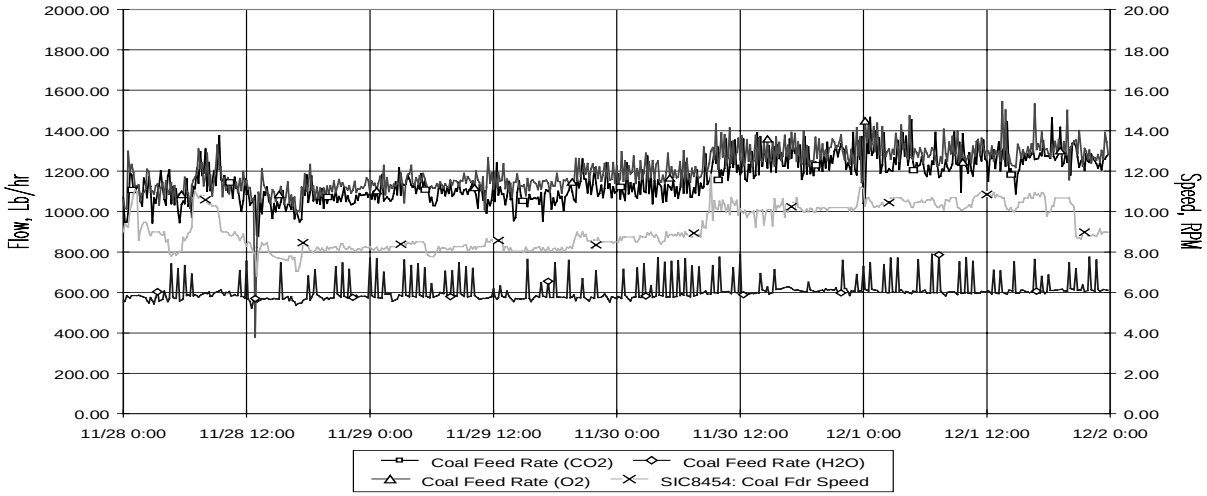

Figure 4.1.4.9-34 Reactor Pressure/Riser Differential Pressure Profiles

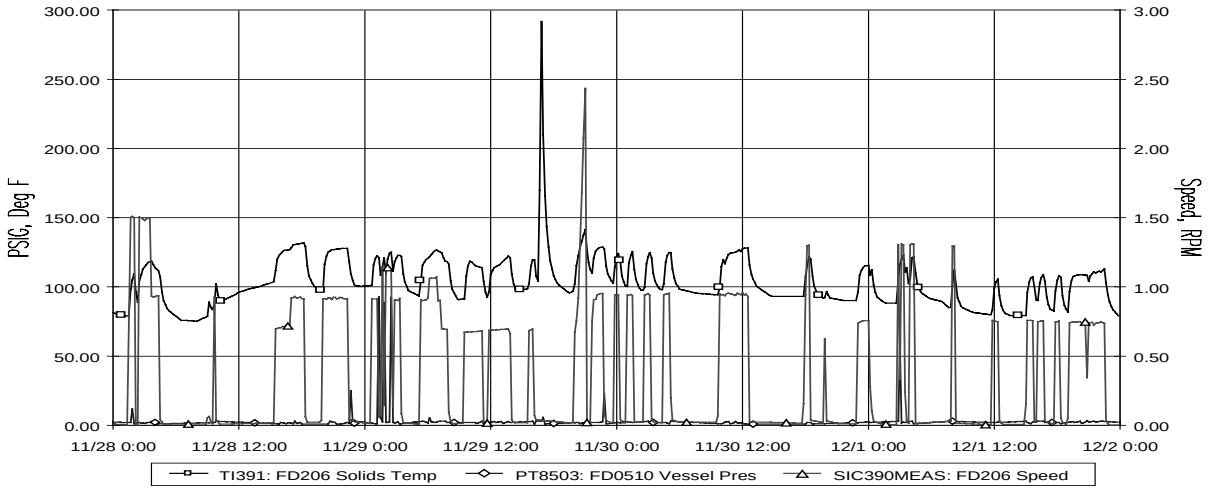

Figure 4.1.4.9-35 Standpipe Differential Pressure Profiles

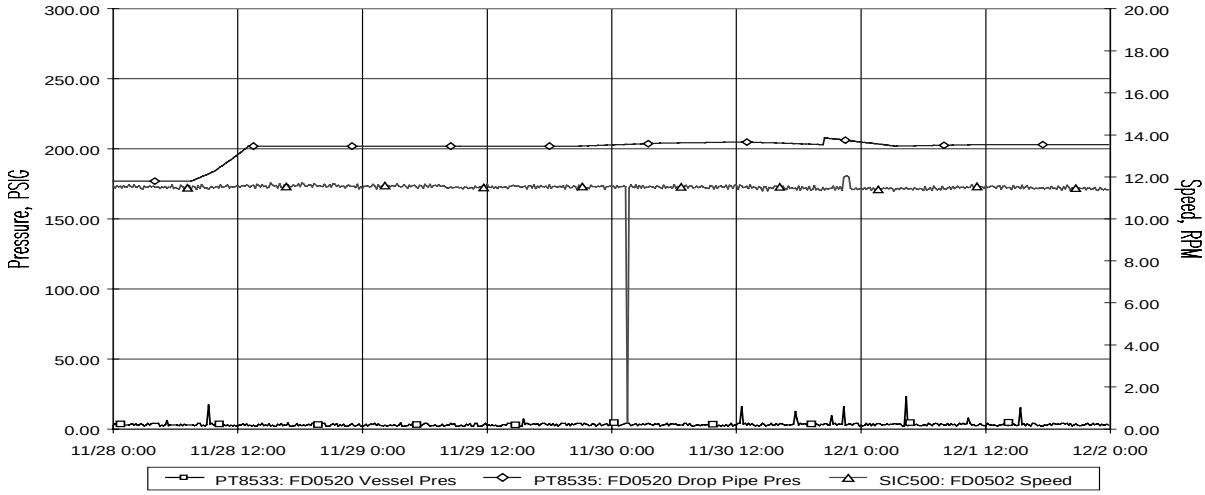

Figure 4.1.4.9-36 Cyclone Dipleg Differential Pressure Profiles

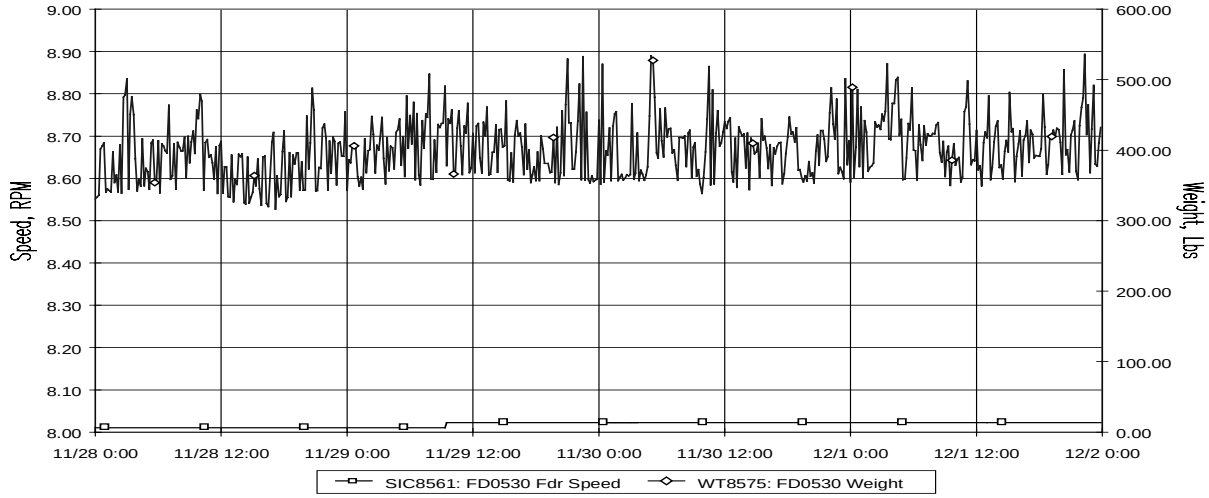

Figure 4.1.4.9-37 Coal Feed Rate Based on Gas Analysis

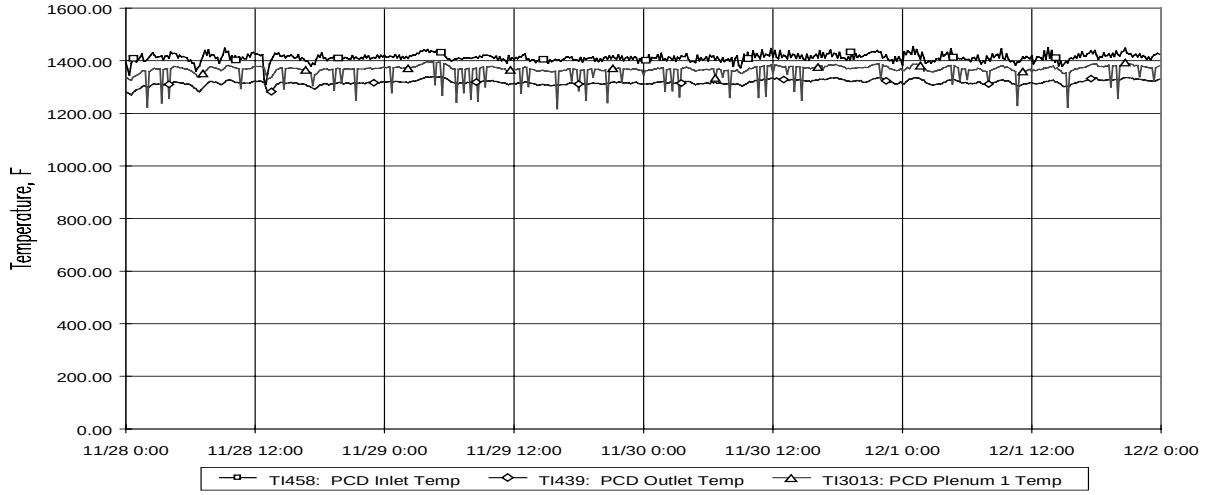

Figure 4.1.4.9-38 PCD Temperatures

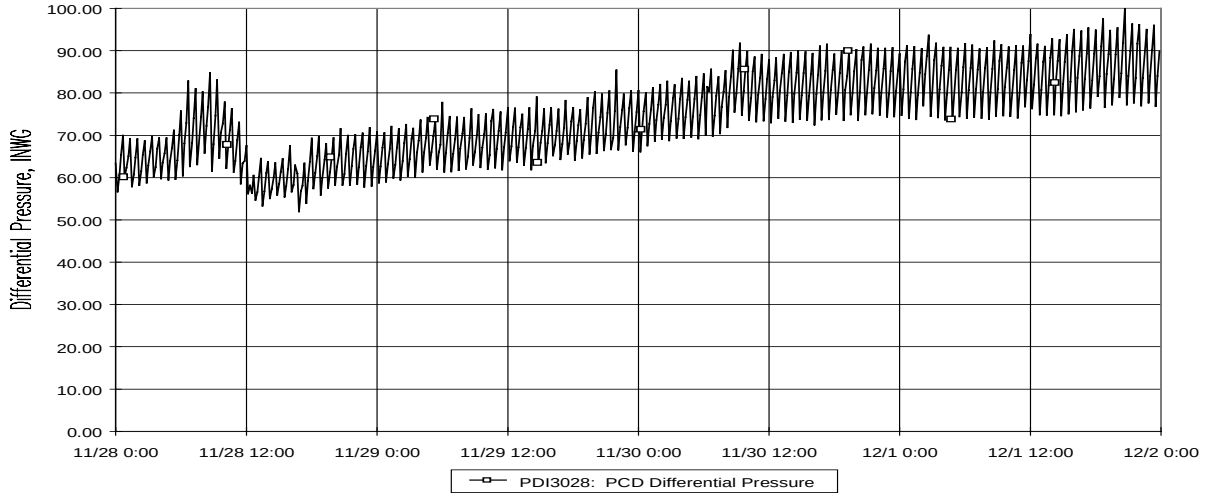

Figure 4.1.4.9-39 PCD Differential Pressure Profile

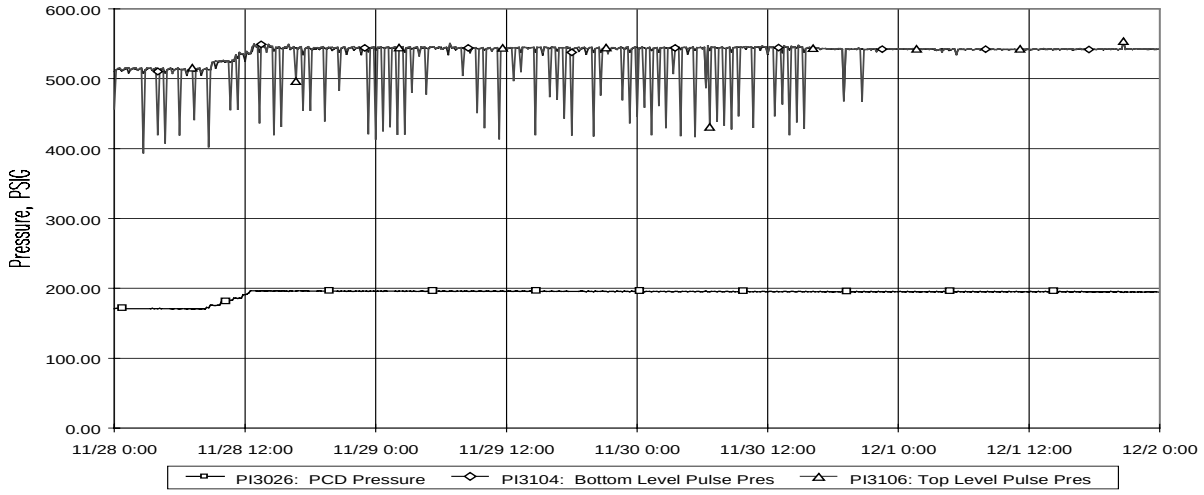

Figure 4.1.4.9-40 PCD Pressure and Pulse Pressure

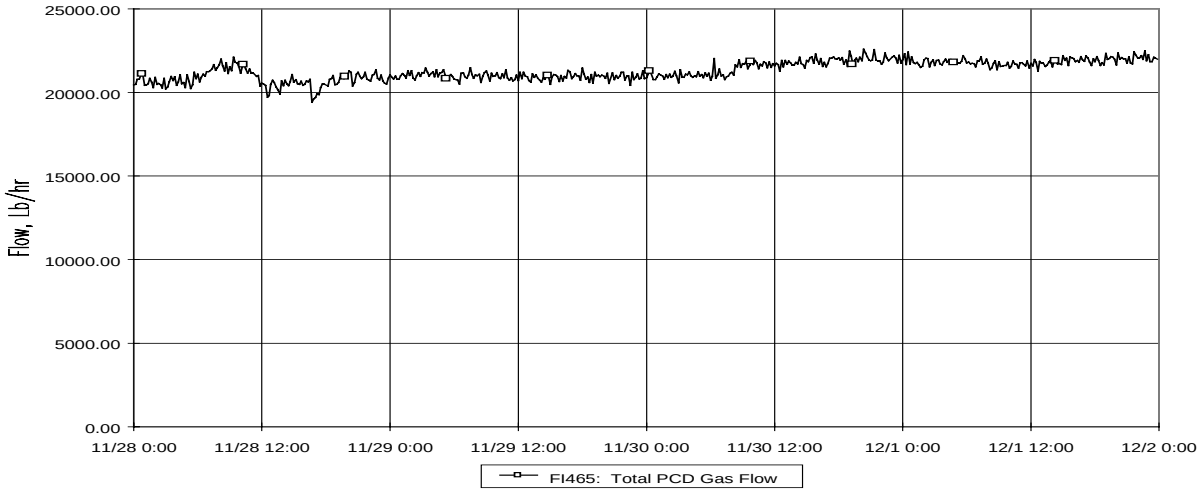

Figure 4.1.4.9-41 Gas Flow Through PCD

Section 4.1.4.9

Graphs 45 through 66

Test Run TC01I

December 2 through 5, 1997

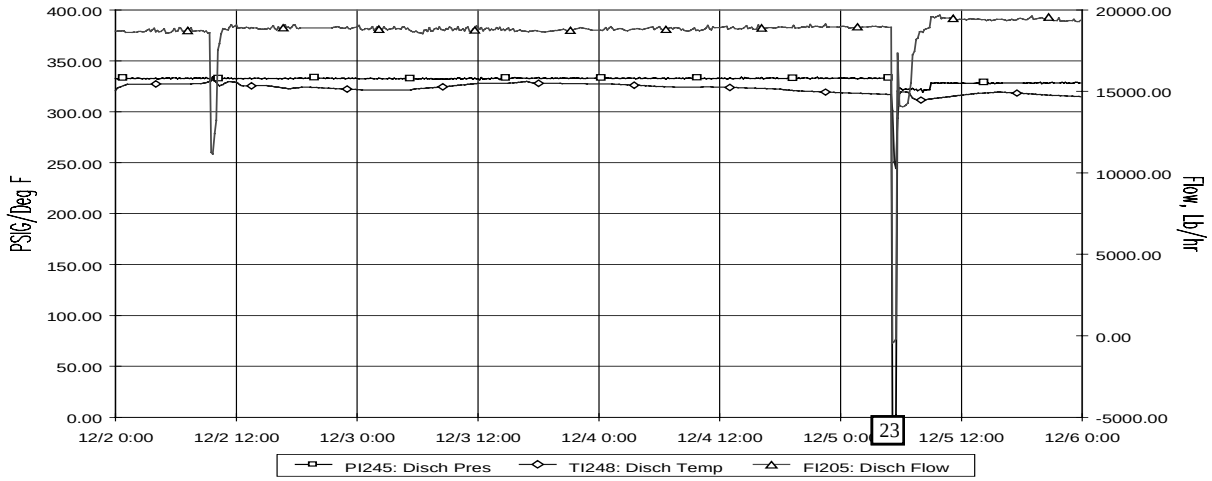

Figure 4.1.4.9-45 CO0201 System Profile

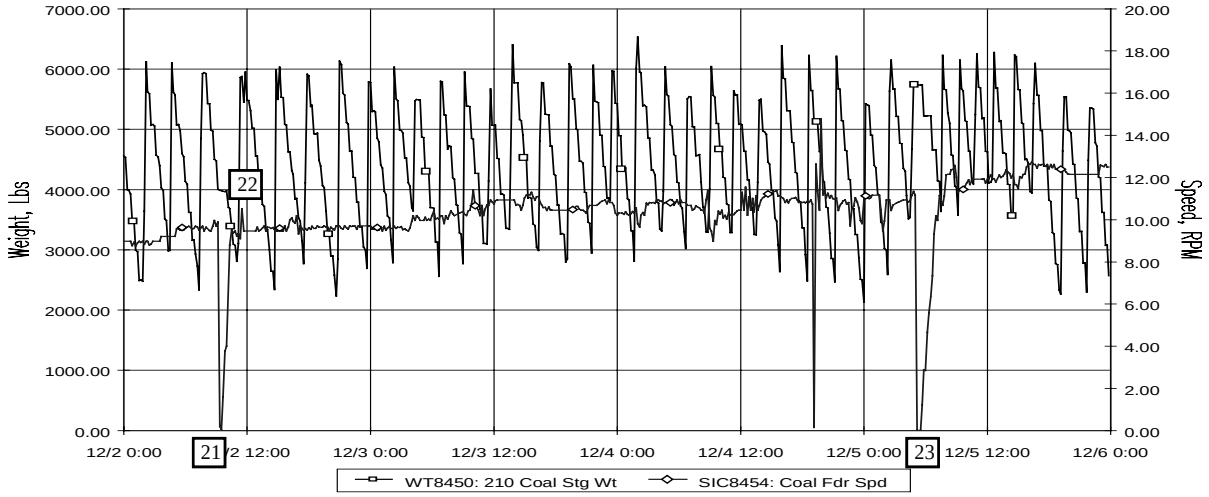

Figure 4.1.4.9-46 Coal Feed System Profile

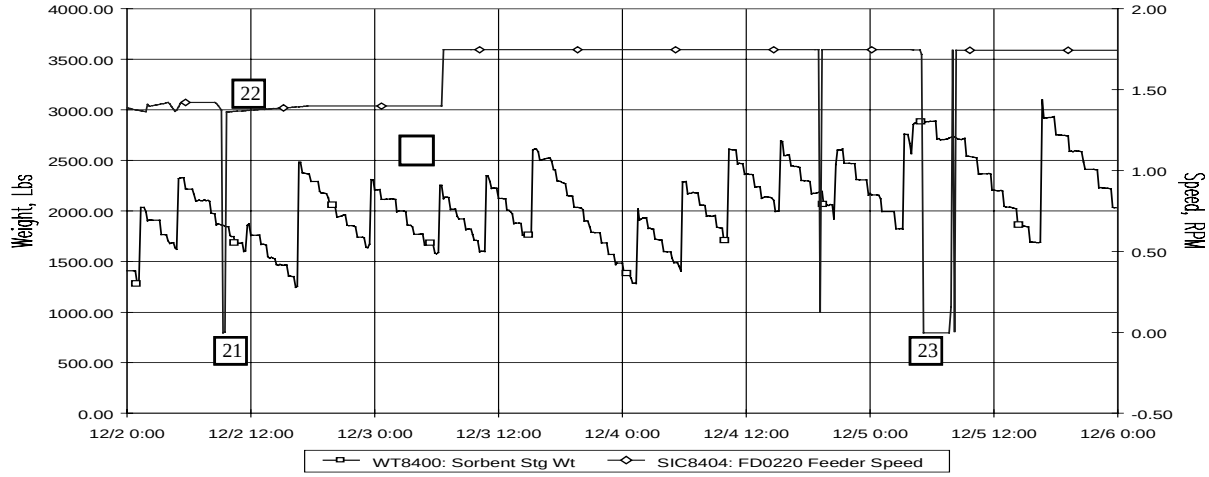

Figure 4.1.4.9-47 Sorbent Feed System Profile

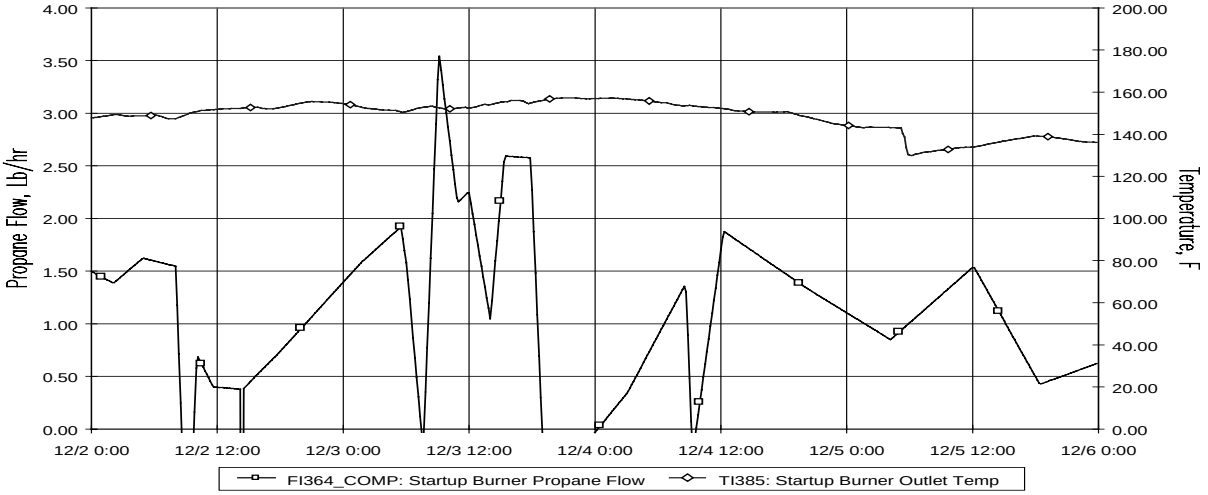

Figure 4.1.4.9-48 Start-Up Burner Flow/Temperature

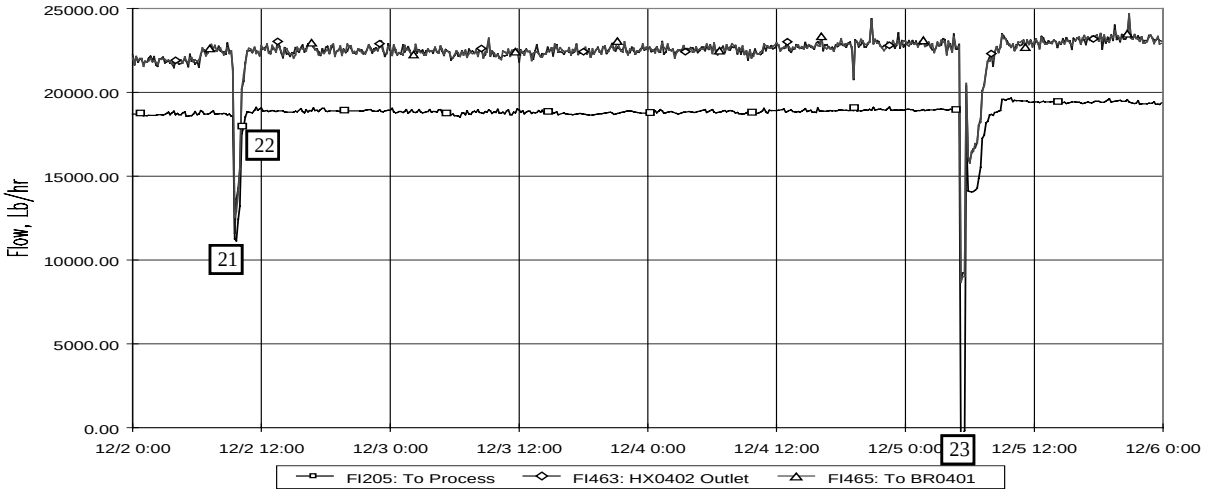

Figure 4.1.4.9-49 Total Gas In/Out Flow Rates

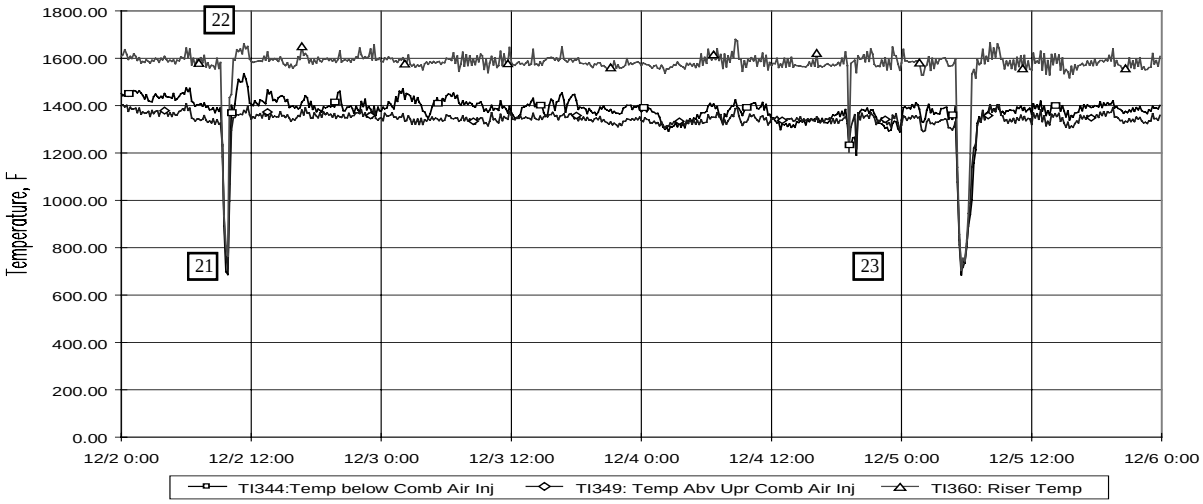

Figure 4.1.4.9-50 Reactor Mixing Zone and Riser Temperatures

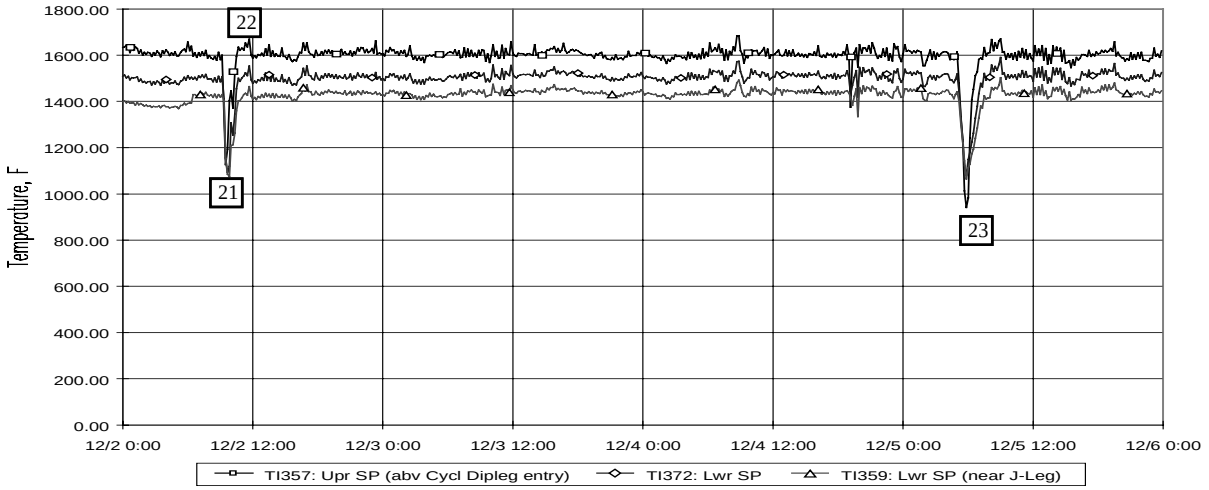

Figure 4.1.4.9-51 Standpipe Temperatures

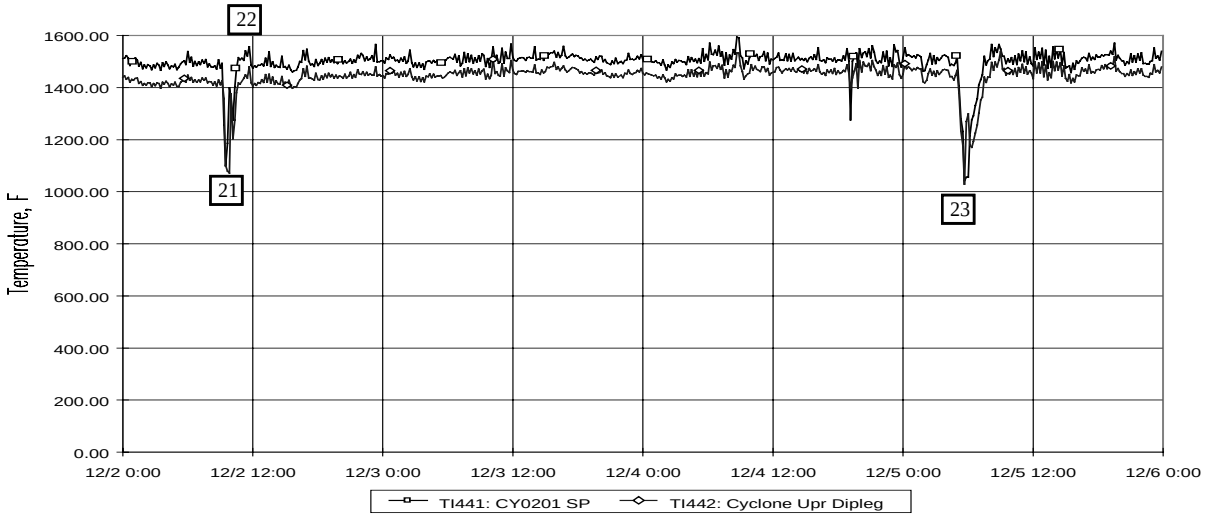

Figure 4.1.4.9-52 Cyclone Dipleg Temperatures

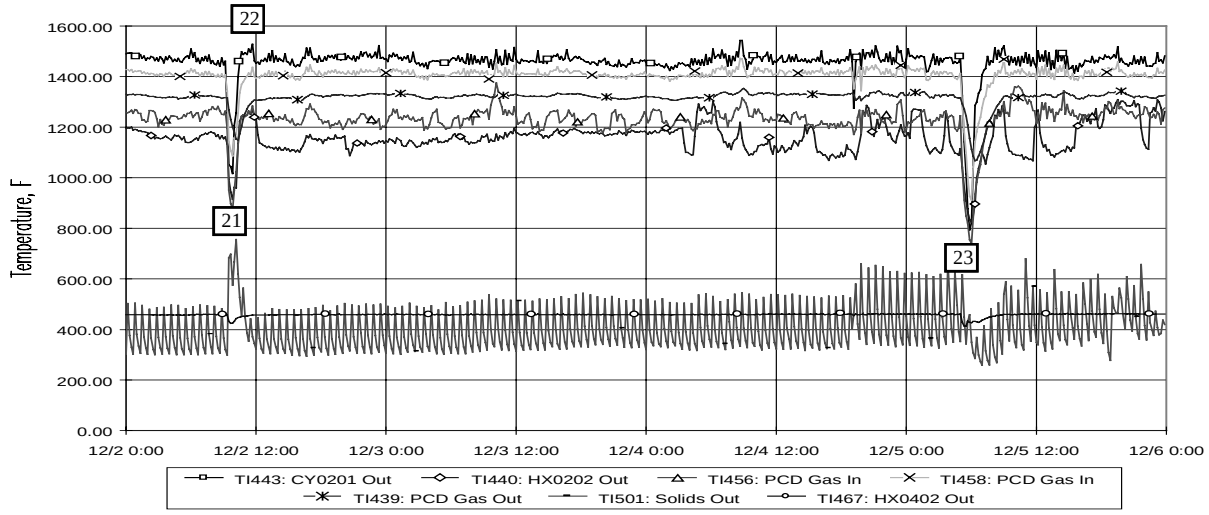

Figure 4.1.4.9-53 Temperature Profile Downstream of Reactor

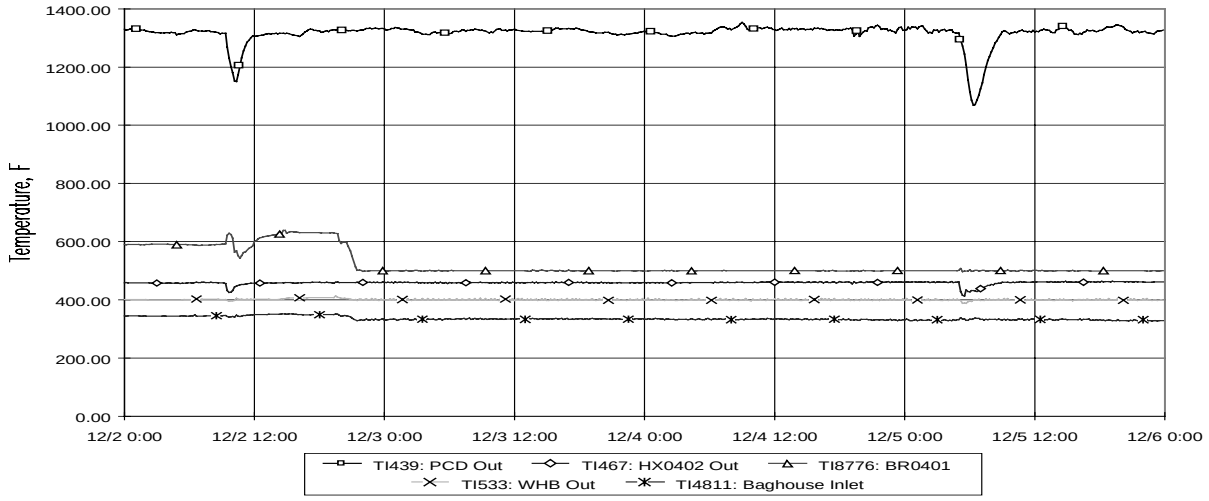

Figure 4.1.4.9-54 System Temperatures Downstream of PCD

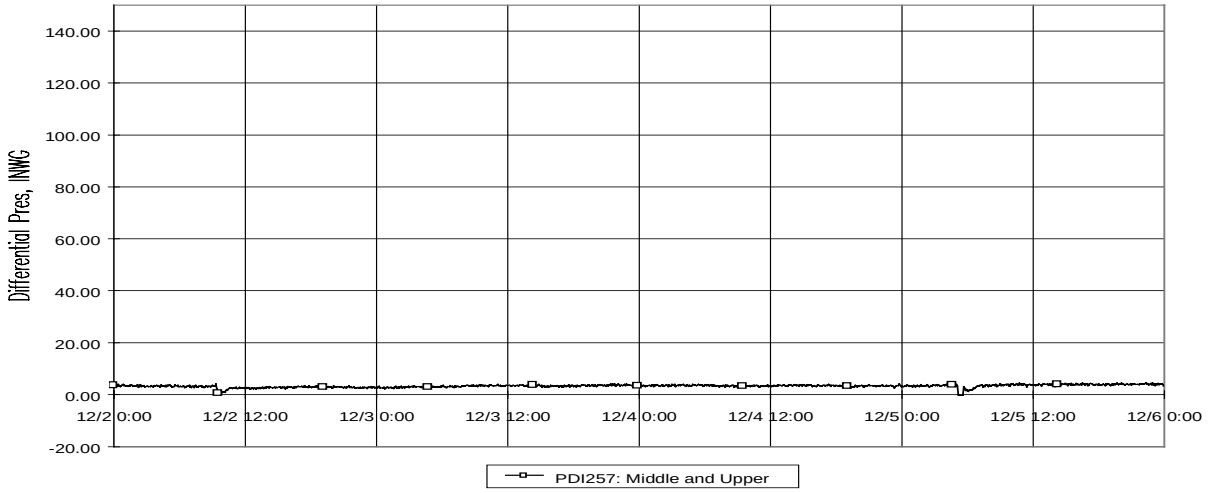

Figure 4.1.4.9-55 Mixing Zone Differential Pressure Profile

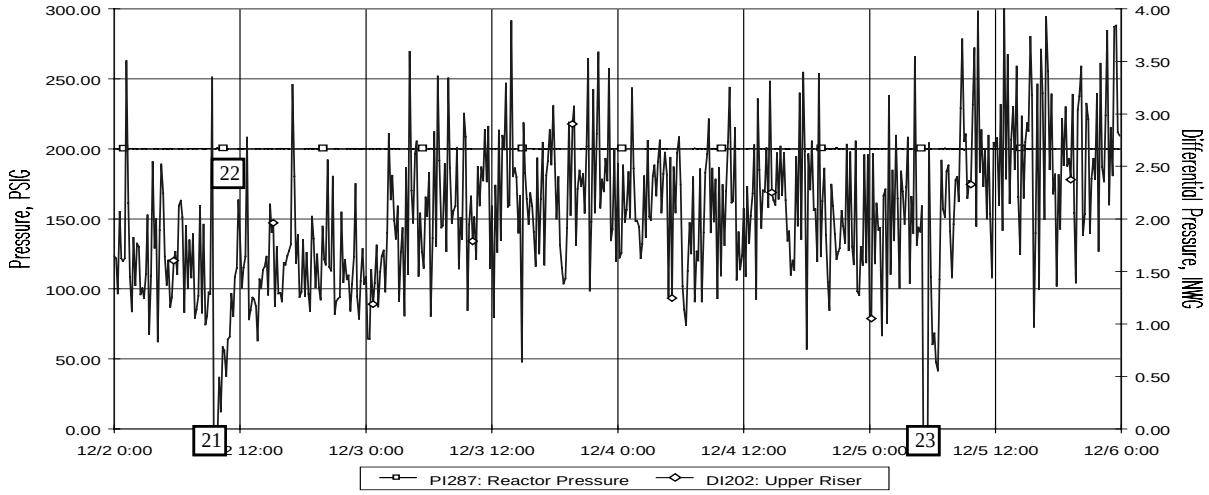

Figure 4.1.4.9-56 Reactor Pressure/Riser Differential Pressure Profiles

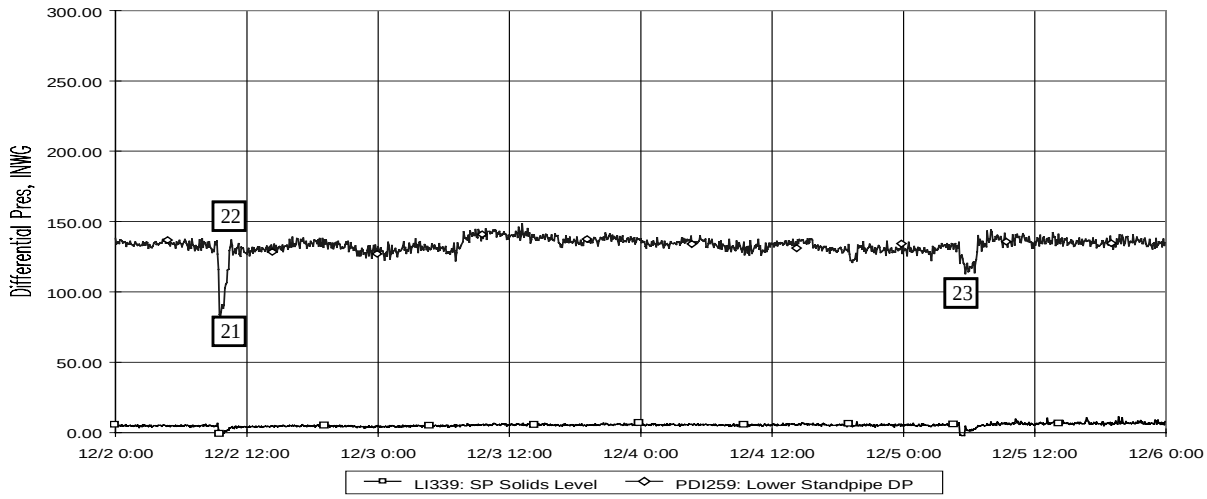

Figure 4.1.4.9-57 Standpipe Differential Pressure Profiles

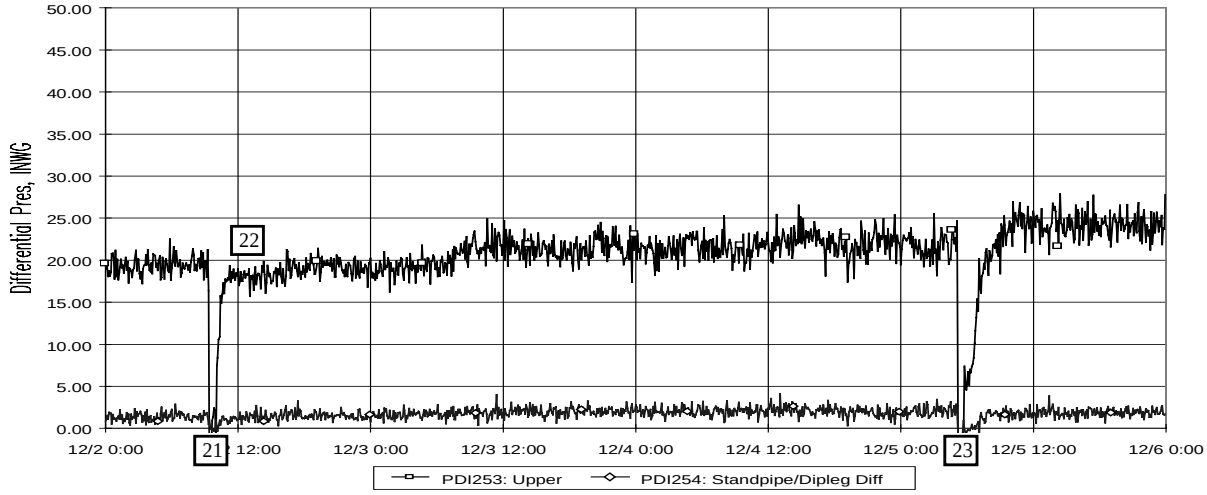

Figure 4.1.4.9-58 Cyclone Dipleg Differential Pressure Profiles

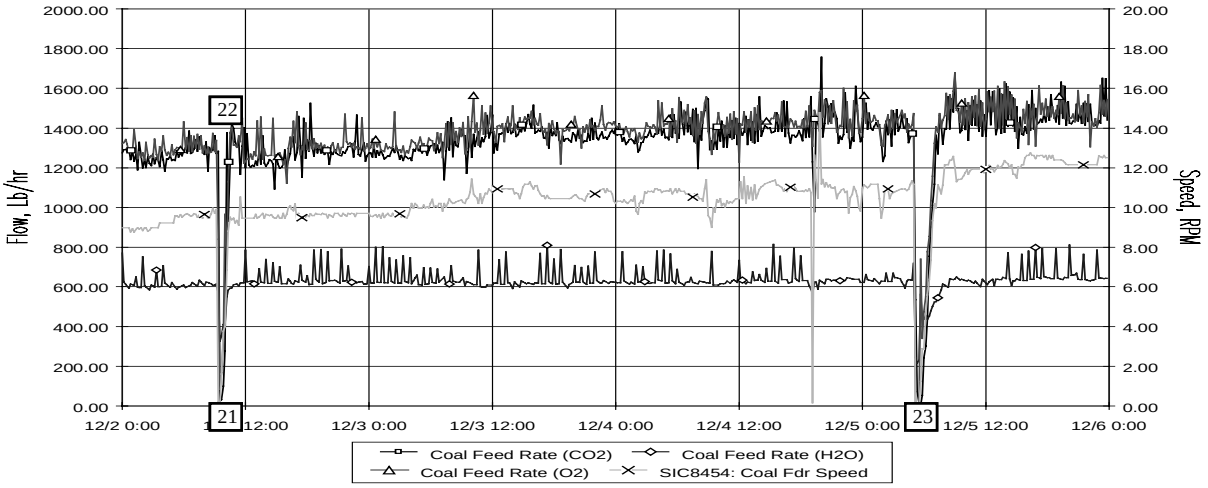

Figure 4.1.4.9-59 Coal Feed Rate Based on Gas Analysis

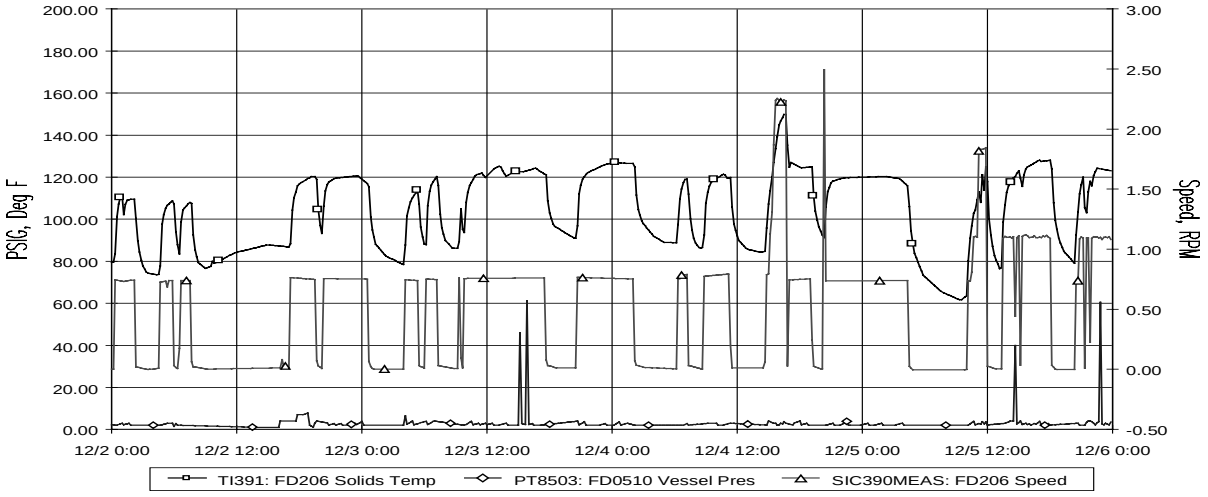

Figure 4.1.4.9-60 FD0206 Profiles

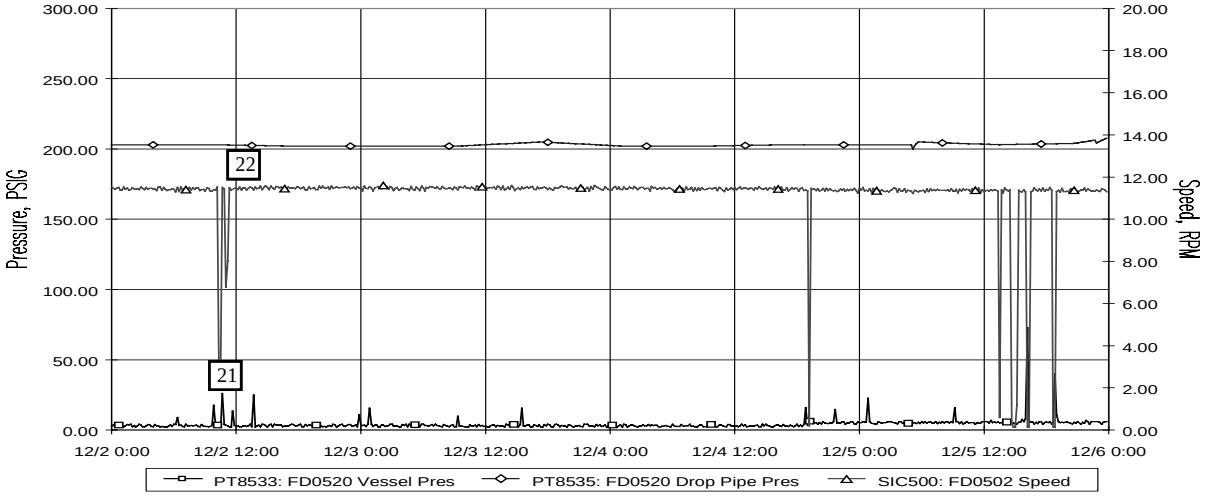

Figure 4.1.4.9-61 FD0520 Pressure Profiles

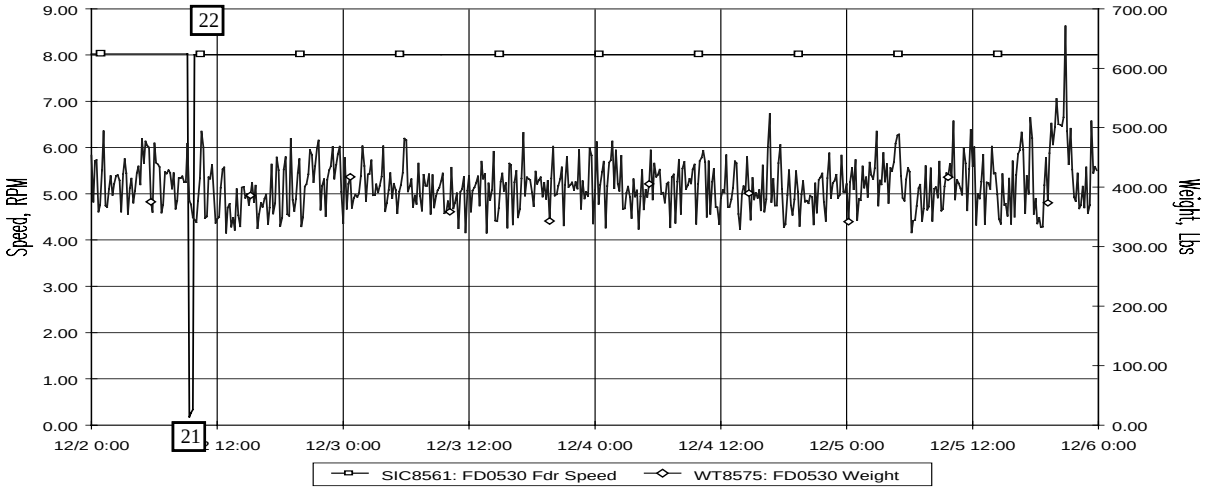

Figure 4.1.4.9-62 FD0530 Feeder Profile

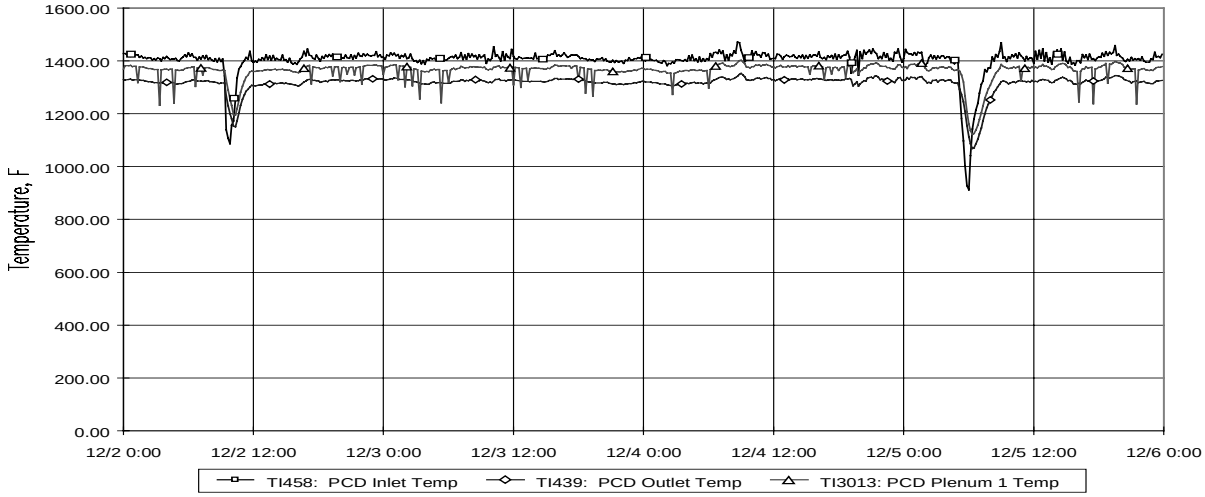

Figure 4.1.4.9-63 PCD Temperatures

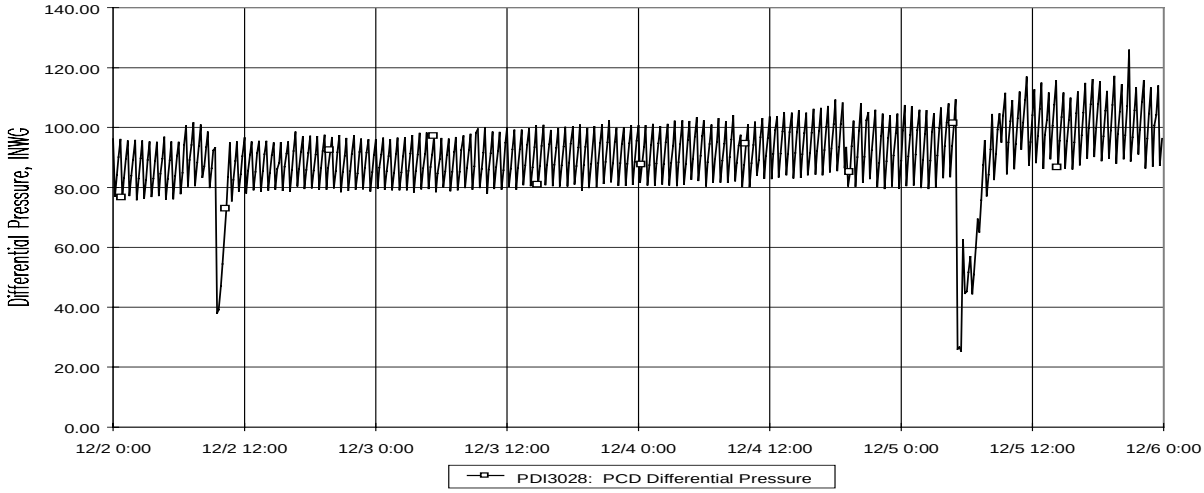

Figure 4.1.4.9-64 PCD Differential Pressure Profile

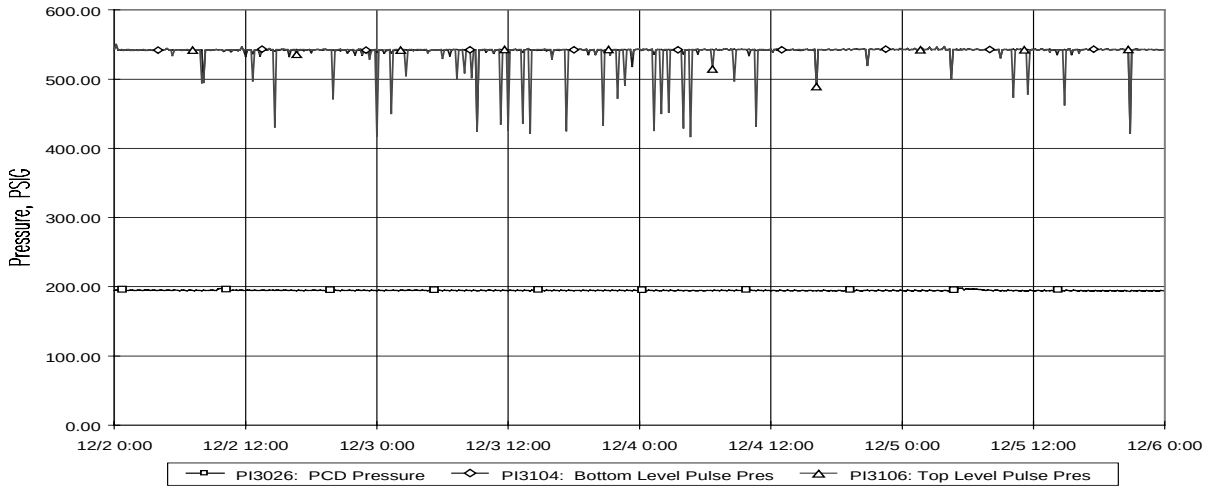

Figure 4.1.4.9-65 PCD Pressure and Pulse Pressure

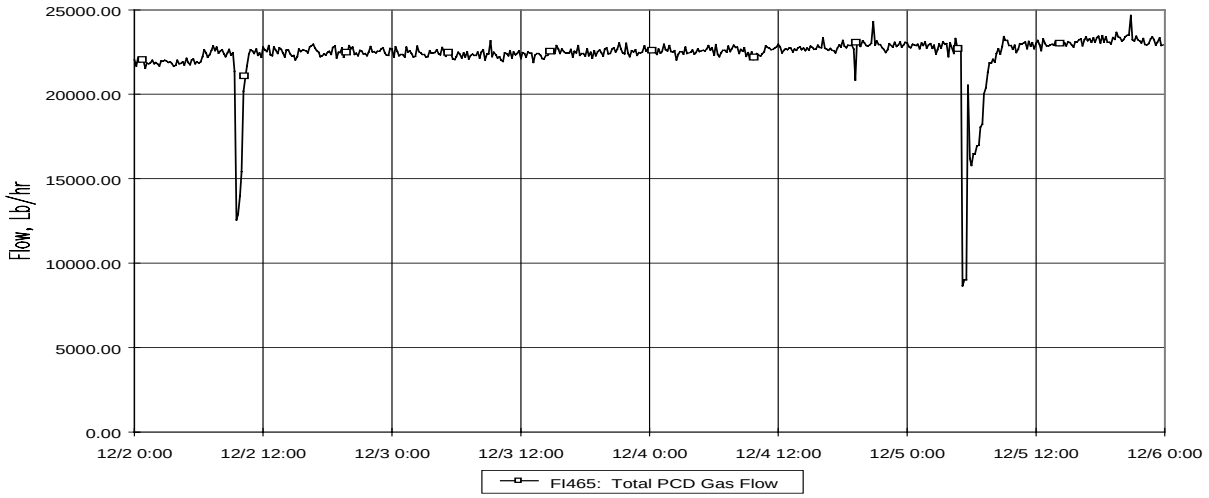

Figure 4.1.4.9-66 Gas Flow Through PCD

Section 4.1.4.9

Graphs 67 through 88

Test Run TC01I

December 6 through 9, 1997

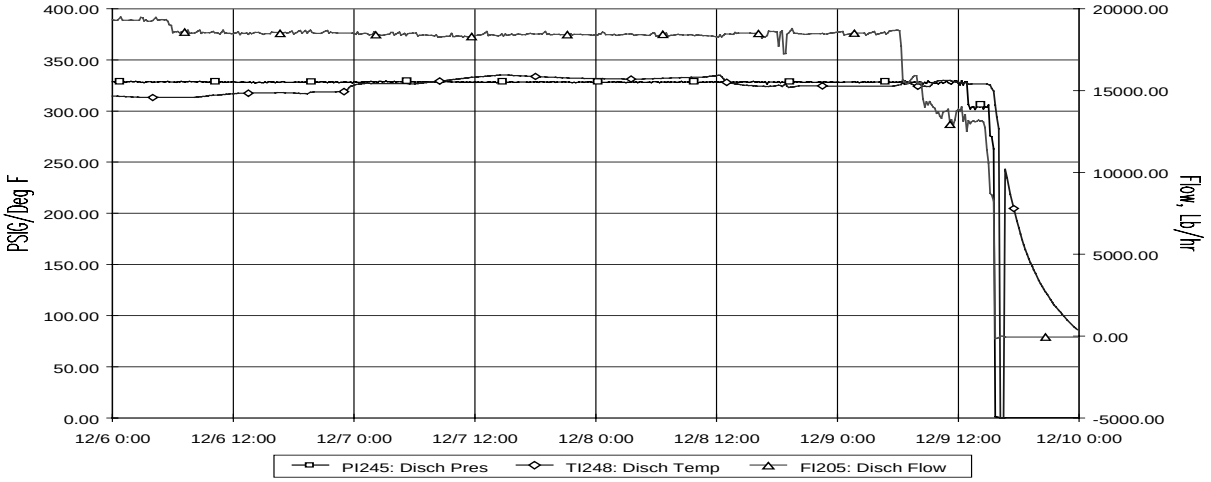

Figure 4.1.4.9-67 CO0201 System Profile

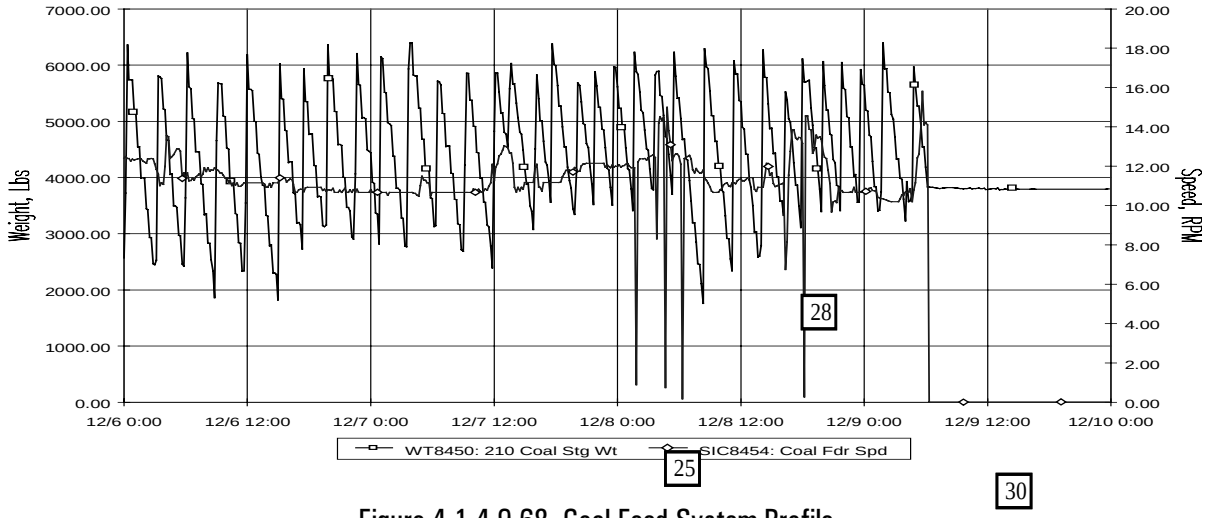

Figure 4.1.4.9-68 Coal Feed System Profile

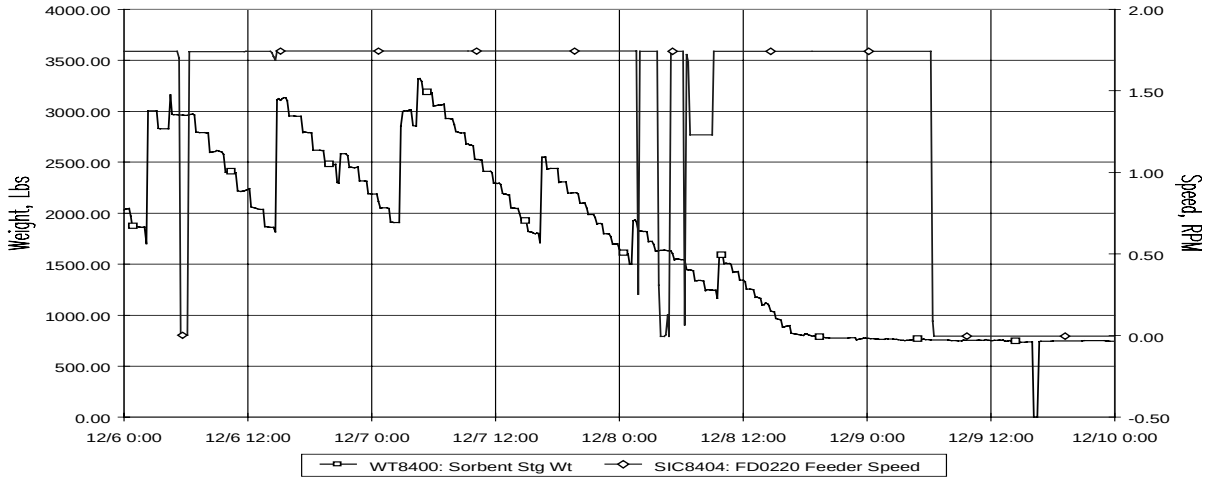

Figure 4.1.4.9-69 Sorbent Feed System Profile

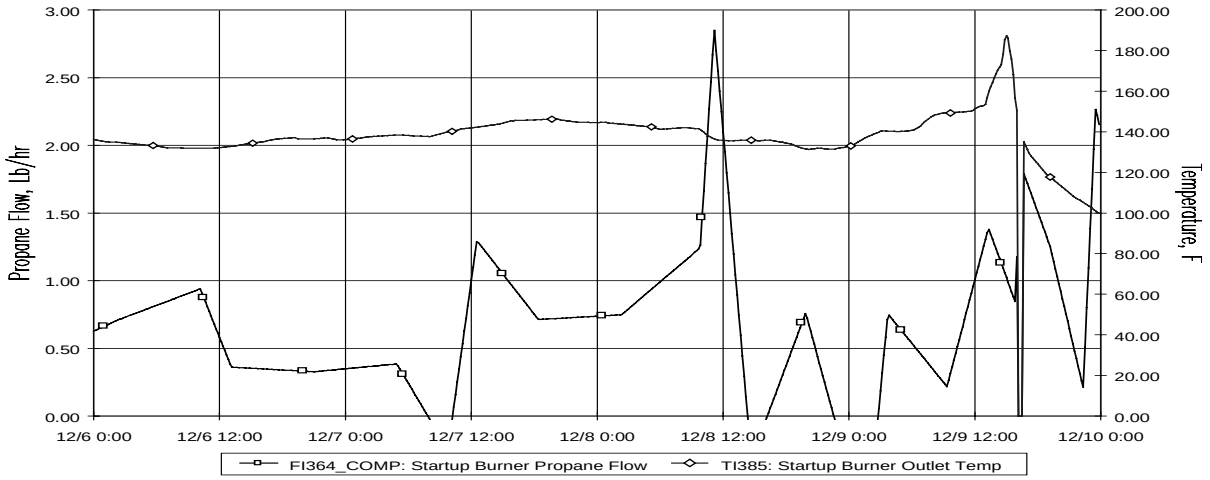

Figure 4.1.4.9-70 Start-Up Burner Flow/Temperature

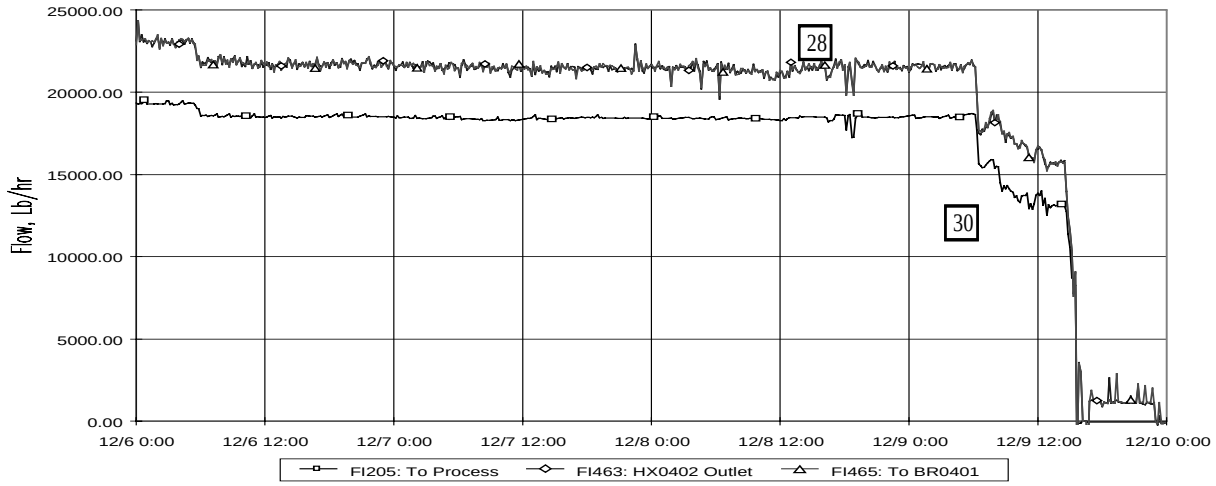

Figure 4.1.4.9-71 Total Gas In/Out Flow Rates

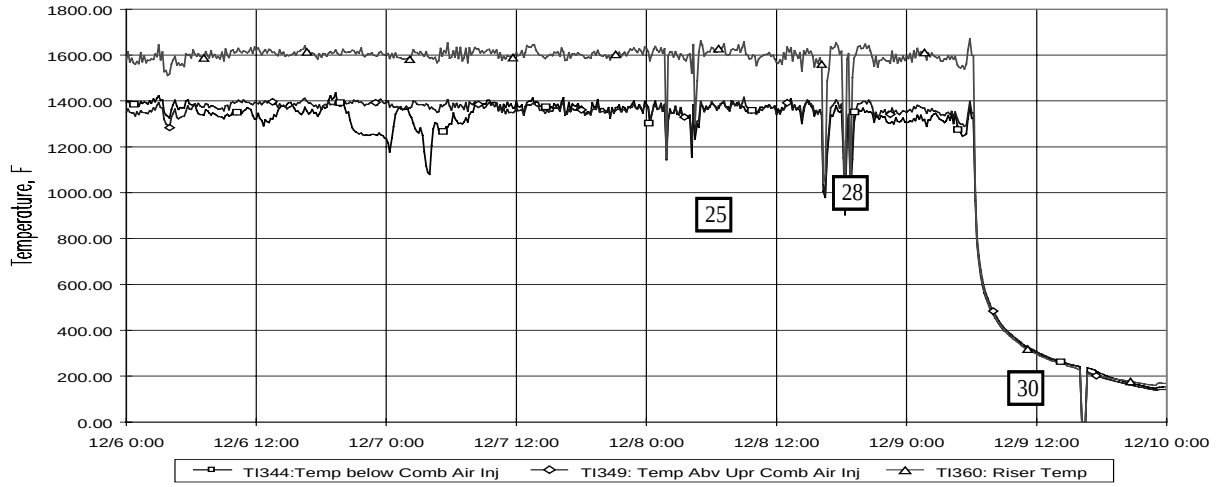

Figure 4.1.4.9-72 Reactor Mixing Zone and Riser Temperatures

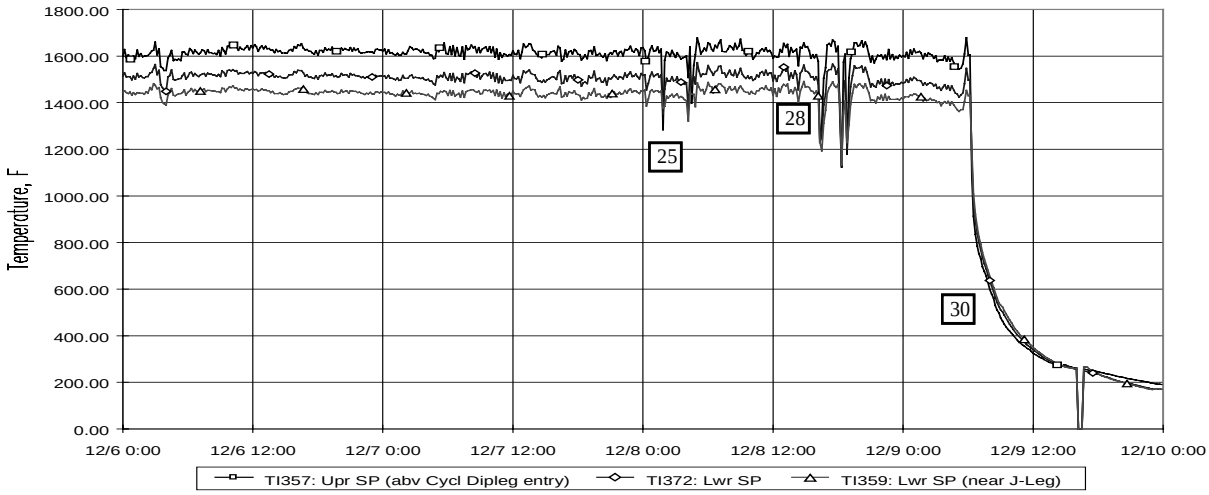

Figure 4.1.4.9-73 Standpipe Temperatures

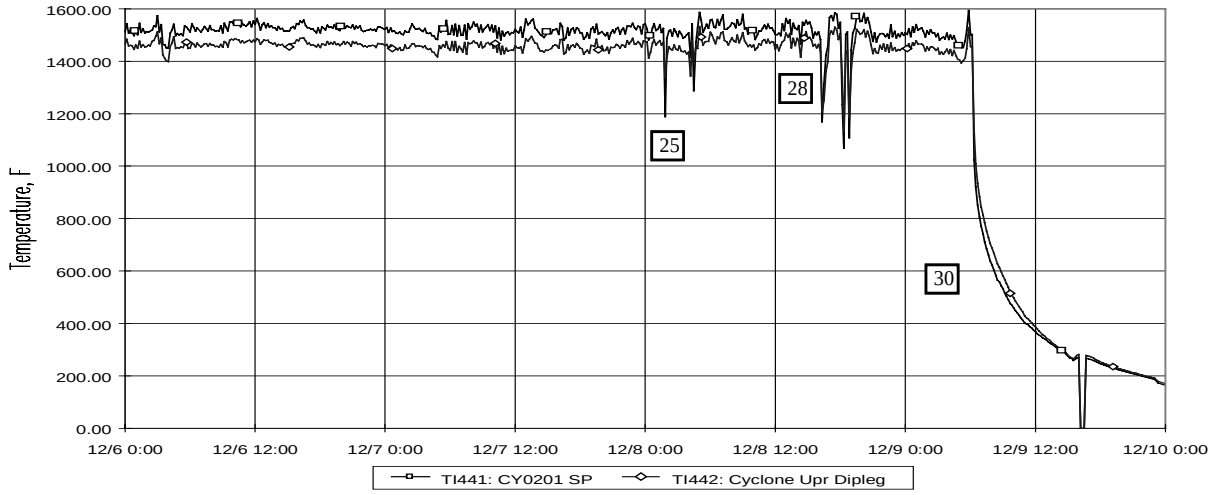

Figure 4.1.4.9-74 Cyclone Dipleg Temperatures

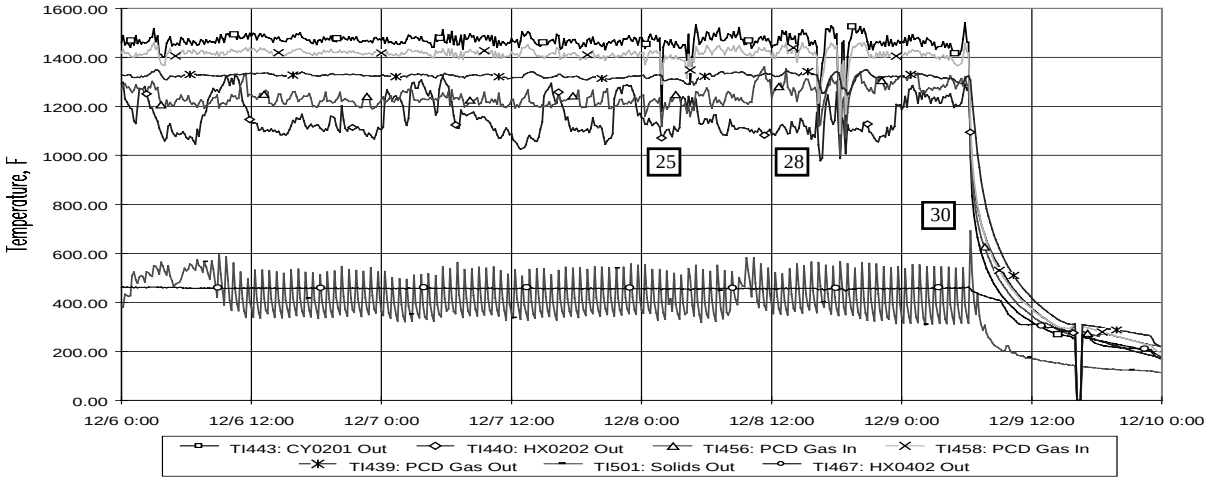

Figure 4.1.4.9-75 Temperature Profile Downstream of Reactor

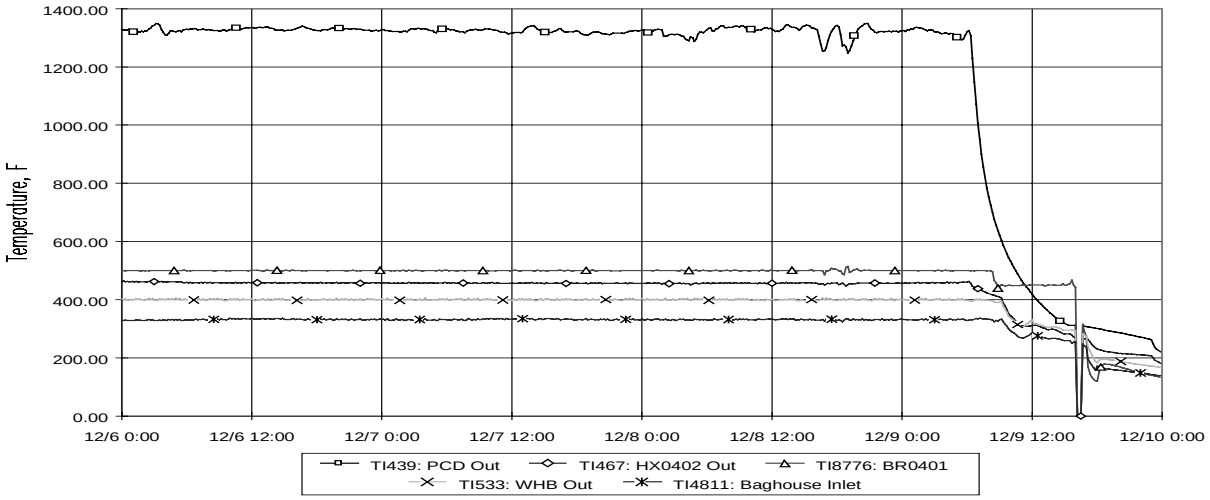

Figure 4.1.4.9-76 System Temperatures Downstream of PCD

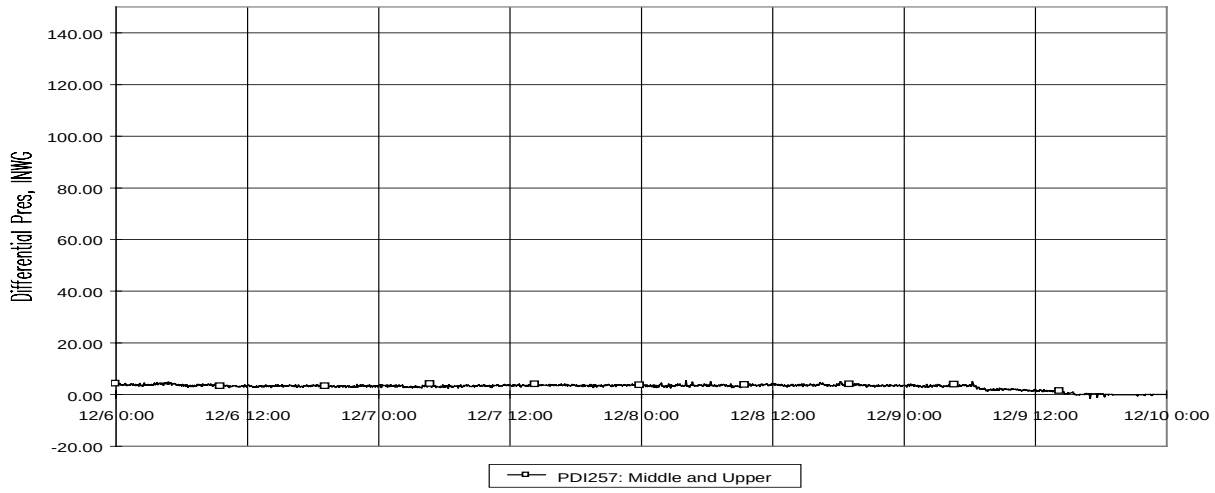

Figure 4.1.4.9-77 Mixing Zone Differential Pressure Profile

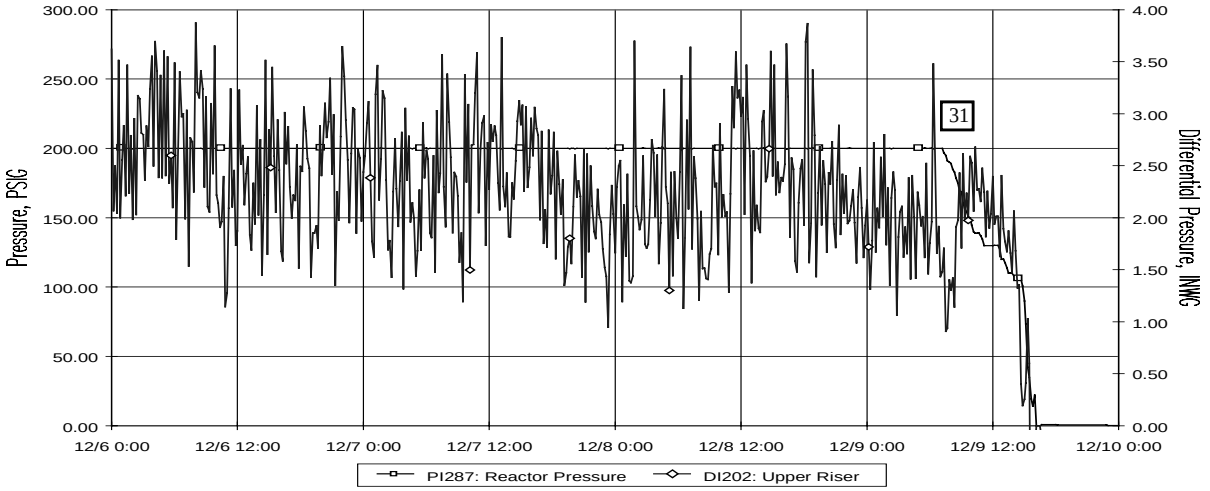

Figure 4.1.4.9-78 Reactor Pressure/Riser Differential Pressure Profiles

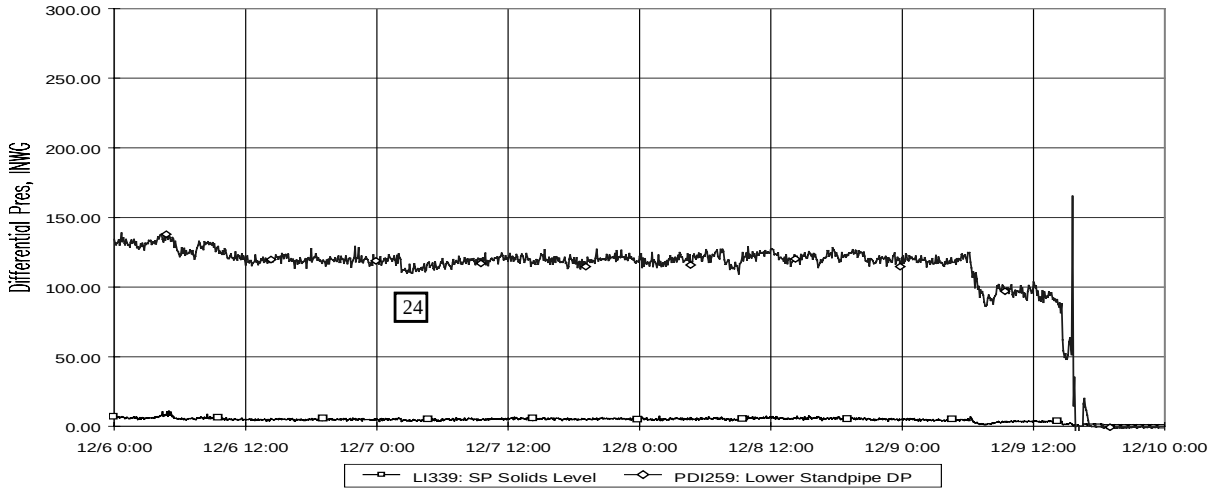

Figure 4.1.4.9-79 Standpipe Differential Pressure Profiles

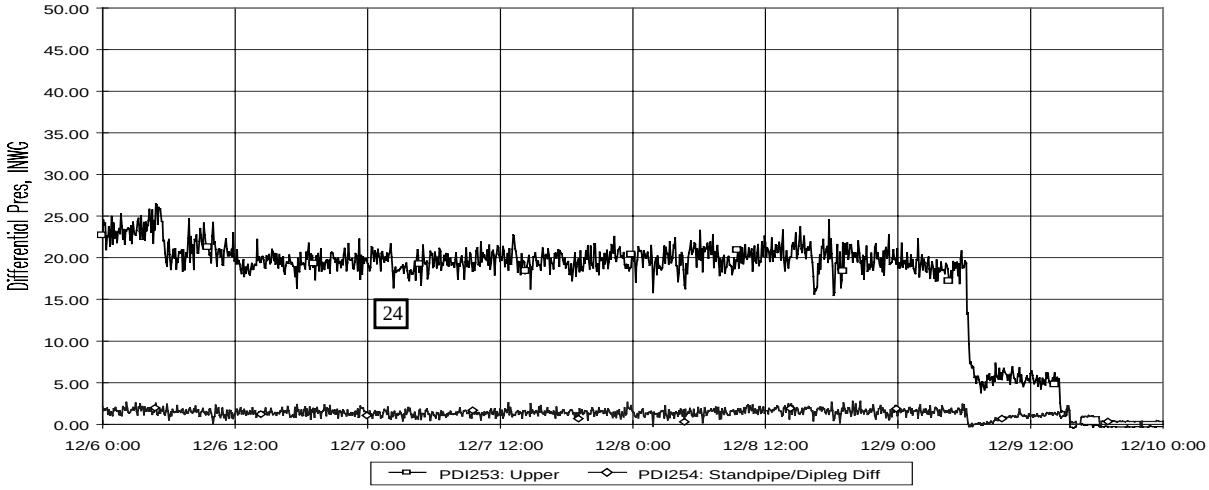

Figure 4.1.4.9-80 Cyclone Dipleg Differential Pressure Profiles

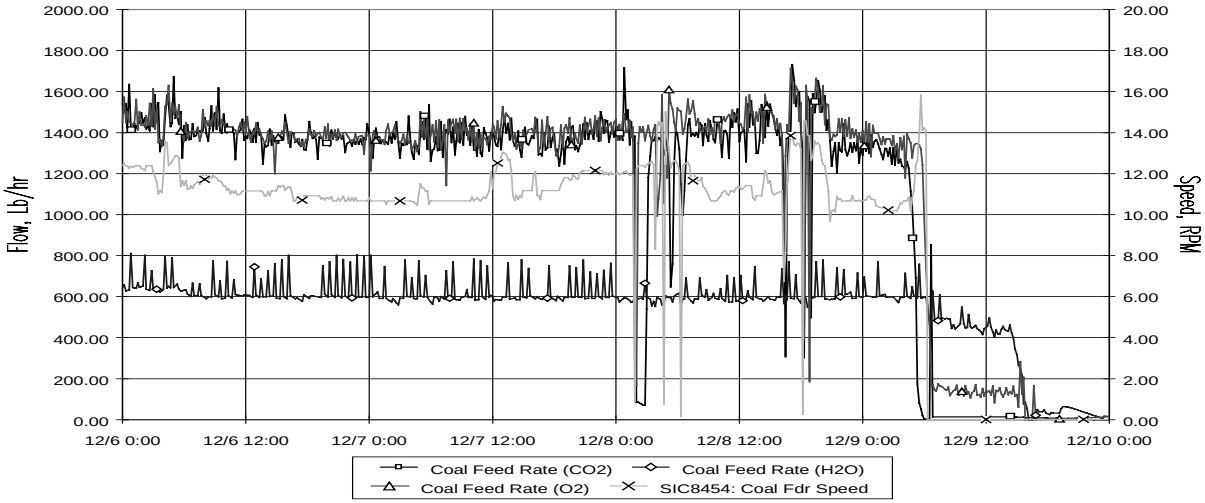

Figure 4.1.4.9-81 Coal Feed Rate Based on Gas Analysis

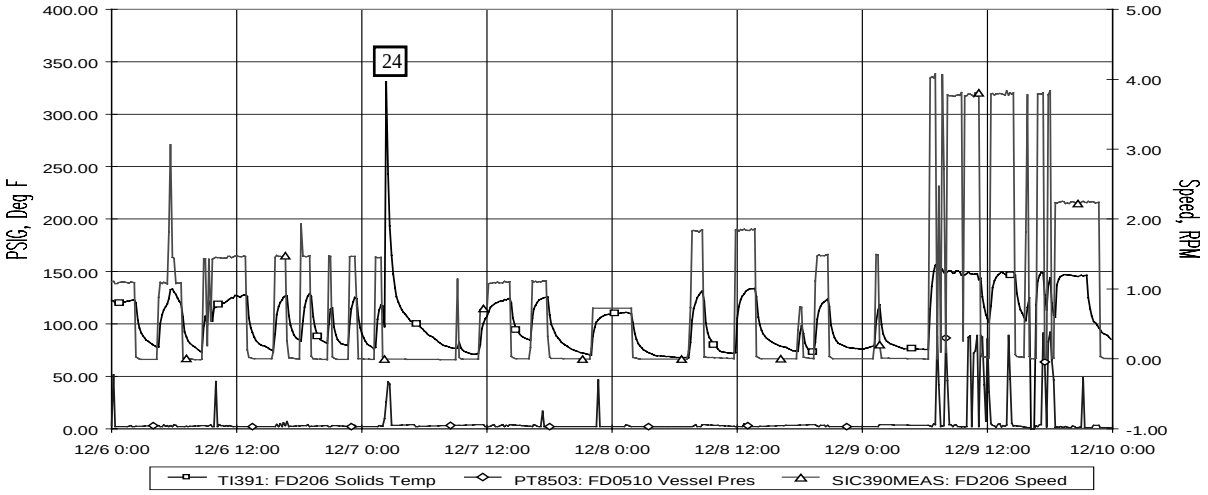

Figure 4.1.4.9-82 FD0206 Profiles

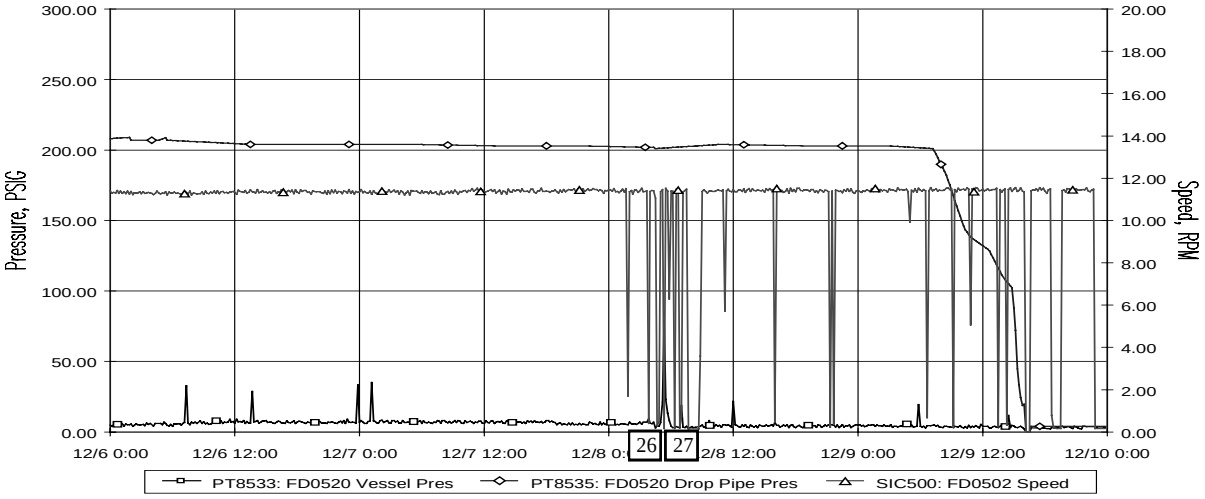

Figure 4.1.4.9-83 FD0520 Pressure Profiles

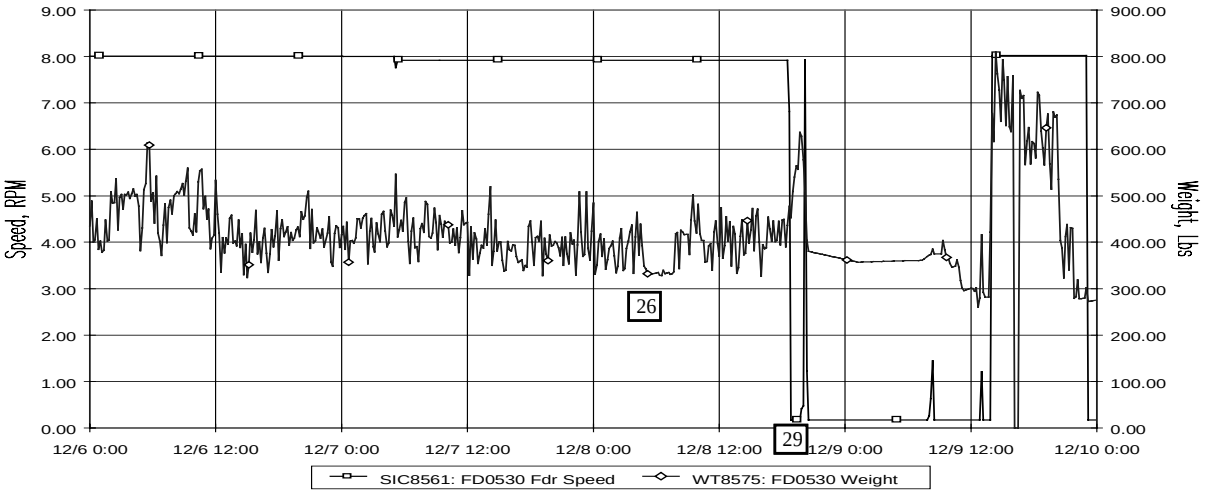

Figure 4.1.4.9-84 FD0530 Feeder Profile

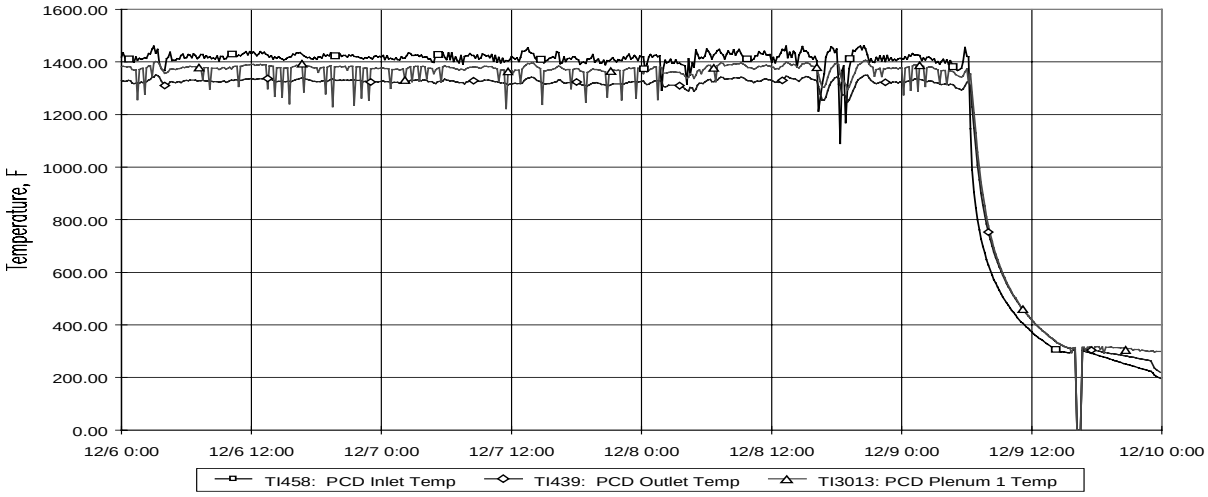

Figure 4.1.4.9-85 PCD Temperatures

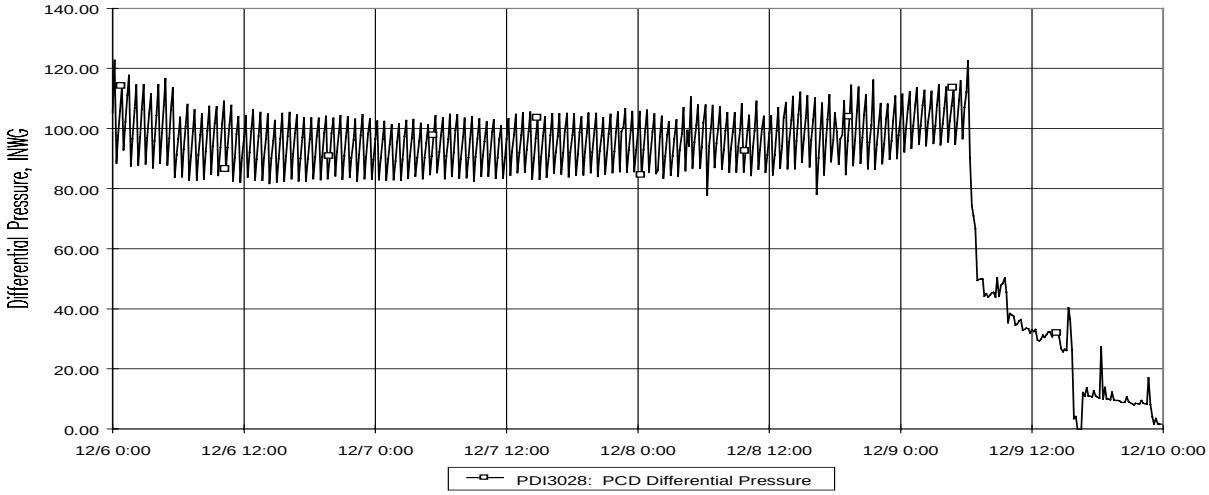

Figure 4.1.4.9-86 PCD Differential Pressure Profile

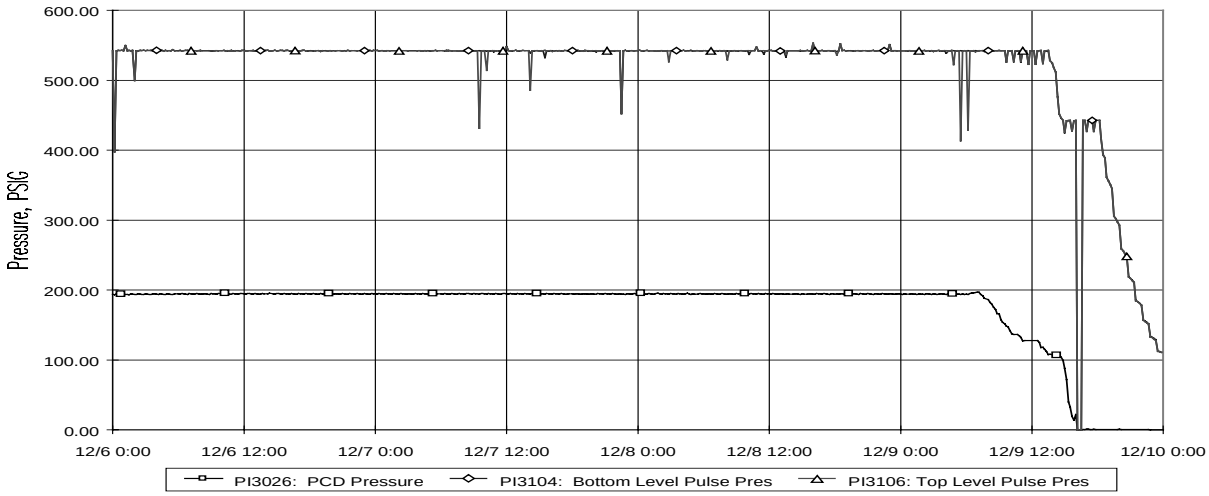

Figure 4.1.4.9-87 PCD Pressure and Pulse Pressure

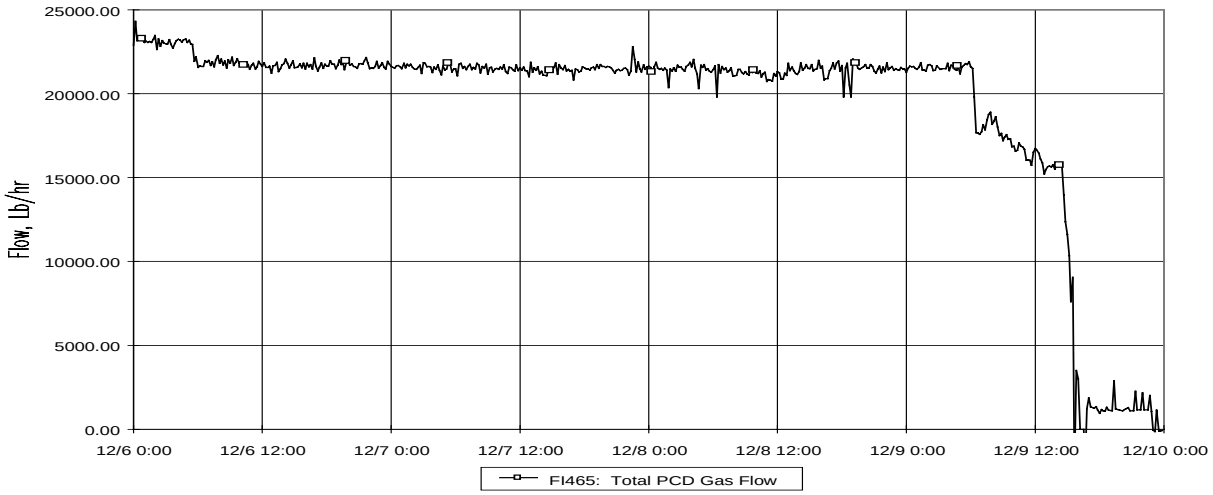

Figure 4.1.4.9-88 Gas Flow Through PCD

4.2 PERFORMANCE ANALYSIS

The data collected in 1997 was analyzed largely over steady-state periods to evaluate different areas of reactor operation and performance. The specific areas investigated are presented in the following sections:

4.2.1 Material Balances.
4.2.2 Disengager Efficiency.
4.2.3 Particulate Loading to PCD.
4.2.4 SO_2 Emissions.
4.2.5 Solids Analysis.
4.2.6 NO_x Emissions.
4.2.7 Circulation Rates.
4.2.8 Pressure Balances.
4.2.9 Temperature Profiles.
4.2.10 Skin Temperature Profiles.
4.2.11 Reactor Feed System Issues.

4.2.1 Material Balance

The greatest impediment to successfully calculating a material balance on the transport reactor system is measuring the solids flows into and out of the system. Weigh cells are provided on the coal and sorbent surge bins and the spent solids receiver. However, it is often difficult to turn a series of weigh cell readings into an accurate estimate of solids flow rates. It is possible to calculate the coal feed rate using the flue gas flow, the flue gas composition, and the coal composition. This gives another set of data from which to calculate the coal feed rate, but does not help determine the sorbent feed rate or the ash removal rate. With this in mind, this section will look at a typical material balance over 2 days at steady-state operation in TC01I, at 12:00 on December 2 through 12:00 on December 4, 1997.

The average coal feed rate during the period was 1,313 lb/hr and a total of 31.5 tons of coal was fed. The sorbent rate was 124 lb/hr, giving a Ca/S ratio of 1.9. The other flows are summarized in table 4.2.1-1.

This gives a ratio of inputs to accumulation and outputs of 1.05, which is acceptable considering the limitations in measuring solids flow rates.

The material balance also gives good closure when looking at the air and nitrogen in the system. For the period, the total air feed was 18,237 lb/hr to the reactor as calculated by adding together the various flow meters. The flow meter at the compressor discharge averaged 18,830 lb/hr, a ratio of 0.97. The nitrogen balance shows that 17,808 lb/hr of nitrogen were fed to the reactor through a combination of air, nitrogen, and coal. There were 17,094 lb/hr of nitrogen in the flue gas, giving a ratio of 1.04. A total of 4,541 lb/hr of oxygen were fed to the reactor. A total of 4,532 lb/hr of oxygen can be accounted for leaving the reactor giving a closure of nearly 1.0. The oxygen balance also shows that 13 percent excess air was fed to the mixing zone and riser.

An elemental balance on carbon shows 880 lb/hr of carbon was fed to the reactor with the coal and sorbent. Flue gas analysis shows 905 lb/hr of carbon and preliminary spent solids analysis shows about 2 lb/hr of carbon. Here the ratio input to output is 0.97. For sulfur, the coal provided 11 lb/hr while preliminary solids analysis shows about 6 lb/hr of sulfur in the solids removed from the reactor. The SO_2 level in the flue gas was below detectable limits for the gas sampling system. This gives an in/out ratio of 1.83.

A heat and material balance around the steam drum was used to find the steam flow from the combustion heat exchanger. This was also used to estimate the solids flow through the combustion heat exchanger. The calculated and measured flows around the steam drum are summarized in table 4.2.1-2.

Using the steam production in the combustion heat exchanger and the temperature change of the solids passing through the combustion heat exchanger, the solids flow through the exchanger was estimated to be 46,184 lb/hr.

By knowing the heat removed by the heat exchanger and using the flows, temperatures, and compositions of the materials entering and leaving the transport reactor, the heat loss to the environment from the transport reactor was calculated. The heat loss was 1.8 MBtu/hr.

Table 4.2.1-1

Bulk Material Balance Information

Inputs :		
Coal	1,313 lb/hr	
Sorbent	124 lb/hr	
Air	18,830 lb/hr	
Nitrogen	3,603 lb/hr	
TOTAL		23,870 lb/hr
Outputs :		
Flue Gas	22,513 lb/hr	
Coarse Ash	48 lb/hr	
Fine Ash	194 lb/hr	
TOTAL		22,755 lb/hr
Accumulation		16 lb/hr

Table 4.2.1-2

Steam Drum Balance

Inputs :	
Boiler Feed Water	10,970 lb/hr
Steam From Secondary Gas Cooler	5,787 lb/hr
Steam From Thermal Oxidizer	1,507 lb/hr
Steam From Combustion Heat Exchanger	7,208 lb/hr
Outputs :	
Steam to BOP	10,049 lb/hr

4.2.2 Disengager Efficiency

The collection efficiency of the disengager and cyclone has received a great deal of attention due to the issue of dipleg instability and the resulting large carryover of solids to the PCD. In this section the efficiency of the disengager and the factors that influence the collection efficiency will be investigated.

Several factors influence the performance of the disengager. By design the disengager is not a very efficient solids separation device. The gas and entrained solids enter through the top and the gas exits through the side. Testing has shown the disengager to be 60- to 80-percent efficient under normal operating conditions. Figure 4.2.2-1 shows the changes in the disengager efficiency during a period of more than 5 days of steady operation during TC01I. The circulation rate was mostly steady for much of the period. The disengager efficiency rather steadily declined during the run. This can be attributed to a change in the density of the solids in the reactor. The density of the reactor solids as measured by the differential pressure in the bottom of the combustion heat exchanger decreased during the period. Figure 4.2.2-2 shows the relationship between the solids density and the disengager efficiency. The disengager efficiency steadily increased with increasing solid density. The decrease in solids density as a run progresses occurred because of the replacement of sand, the start-up bed material, with ash and dolomite.

Another observation on disengager efficiency came from looking at the change in efficiency at different riser velocities. Previous disengager testing at the PSDF in 1996 revealed that the disengager performs better with a lower inlet velocity. Figure 4.2.2-3 shows the relationship between the riser velocity and the disengager efficiency. There is a clear reduction in the efficiency of the disengager as the inlet velocity increases over the range shown in the graph.

The inlet solids loading to the disengager also has an effect on disengager efficiency, although the effect is not as strong as particle density and inlet velocity. Figure 4.2.2-4 is a plot showing how the disengager efficiency changes as the circulation rate increases. The relationship between circulation rate and disengager efficiency seems to show a slight increase in efficiency with an increase in solids loading, but the data shows a large degree of scatter. The disengager testing in 1996 also showed an increase in disengager efficiency with increasing solids loading.

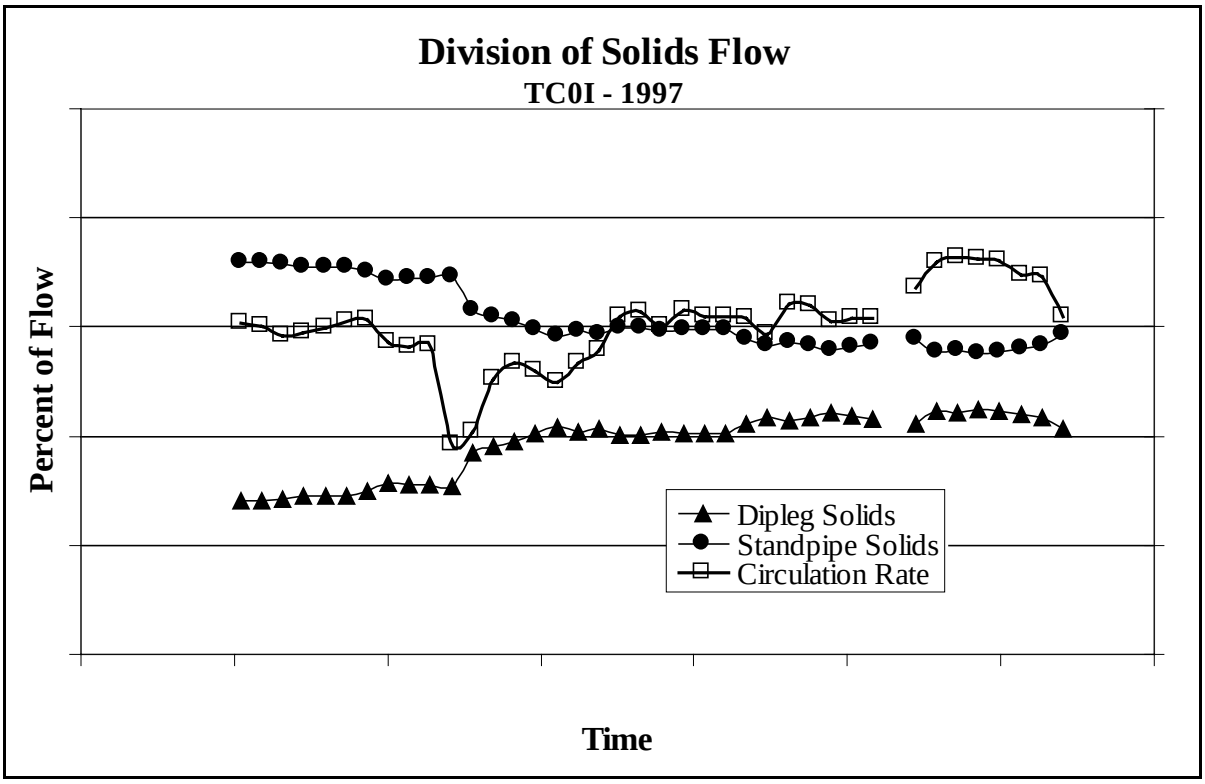

Figure 4.2.2-1 Change in Disengager Efficiency and Circulation Rate Over Several Days

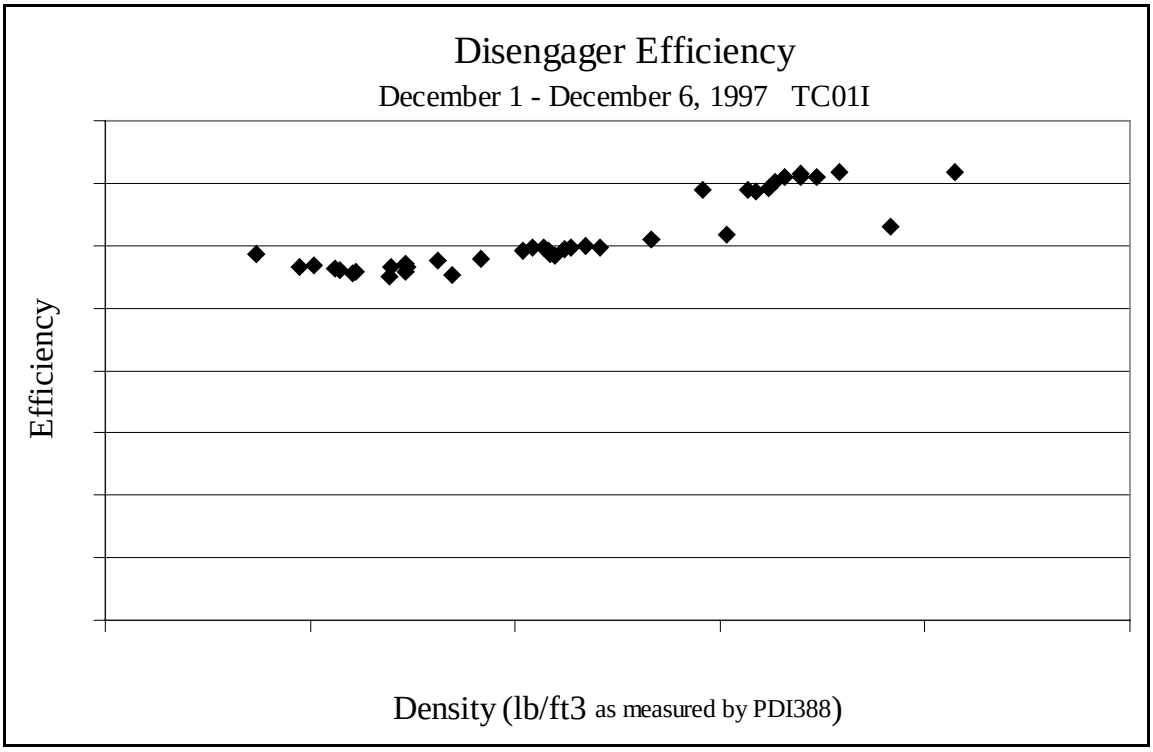

Figure 4.2.2-2 Effect of Density on Disengager Efficiency

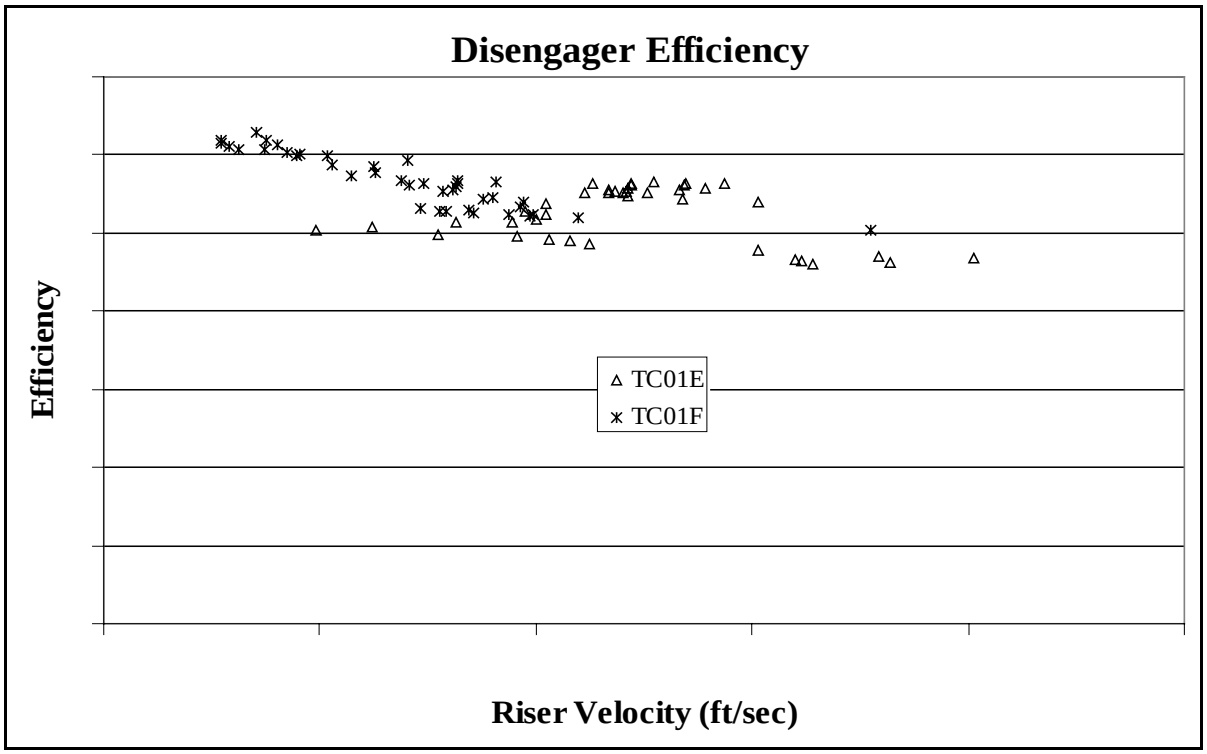

Figure 4.2.2-3 Effect of Inlet Velocity on Disengager Efficiency (October 10, 1997, During TC01E and October 20, 1997, During TC01F; Chart 1 of 2)

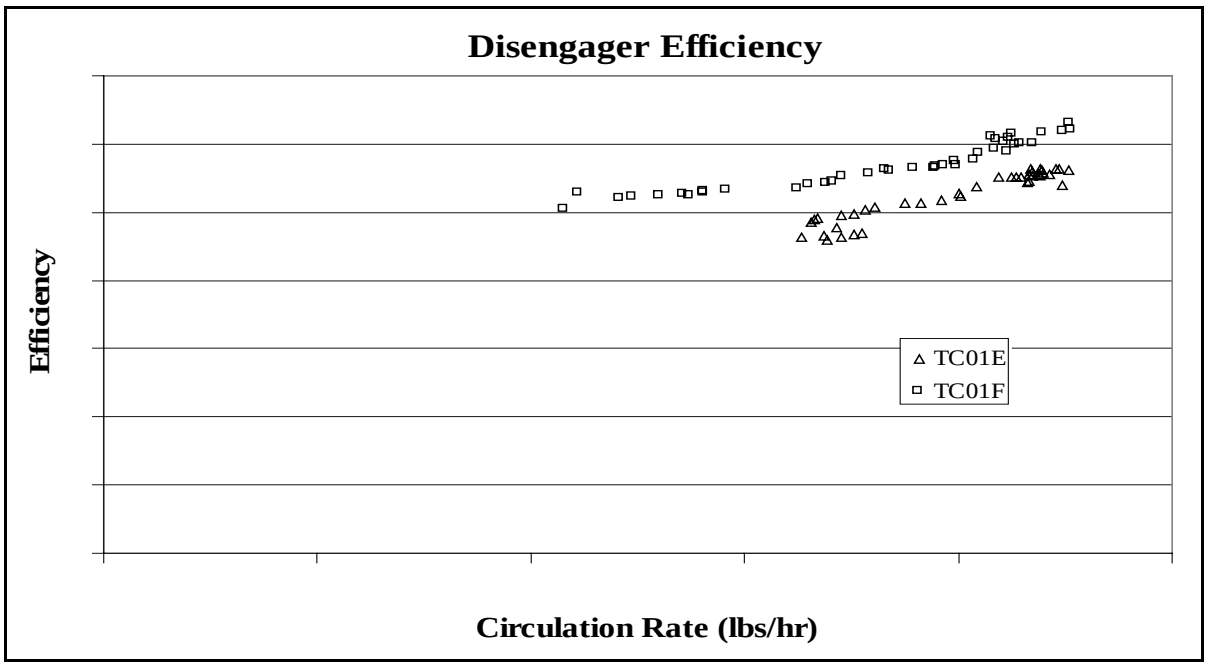

Figure 4.2.2-4 Effect of Circulation Rate on Disengager Efficiency (October 10, 1997, During TC01E, and October 20, 1997, During TC01F; Chart 2 of 2)

4.2.3 Particulate Loading to PCD

The PCD inlet particulate mass loading data for MWK tests CCT4, CCT5, CCT6, and TC01 were measured and reported by Southern Research Institute (SRI). The values for these tests are given in tables 4.2.3-1 and -2. Each particulate concentration was taken over a 25- to 40-minute period. The sampling periods for both when the PCD was pulsed and when there was no PCD pulse are noted for MWK test TC01.

The PCD inlet particulate mass loading is the particulate emissions from the transport reactor cyclone CY0201. Particulate emissions from the cyclone are a function of the cyclone efficiency, cyclone pressure drop, cyclone inlet velocity, and the solids loading to the cyclone. The 1997 PCD inlet particulate mass loadings are plotted against cyclone pressure drop in figure 4.2.3-1.

The PCD inlet concentrations decreased as the year progressed because additional experience was gained in operating the transport reactor in a more stable manner. CCT4 was performed in March, April, and May; CCT5 in May; CCT6 in June; and CCT01 in September to December 1997. CCT4 was characterized by low solids circulation, high-particulate emissions, and unstable cyclone dipleg pressure drop. CCT6 was designed to study the cyclone dipleg operation, and dipleg operation was often 'on the edge' of dipleg stability, producing high-cyclone particulate emissions.

As more experience was gained with operating the reactor, the cyclone pressure drop increased, cyclone dipleg operation became more stable, and the particulate concentrations decreased. The final test of the year, TC01, was characterized by high-cyclone pressure drops and low-PCD particulate emissions. MWK test TC01 was the only 1997 test in which the transport reactor was operated for long periods of time at steady conditions, so the PCD inlet particulate concentration for these tests is more characteristic of typical transport reactor operation. TCO1 runs were all made at reactor pressures of 180 to 215 psig.

Cyclone pressure drop is a function of inlet gas velocity and solids loading. The cyclone pressure drop data is plotted against inlet cyclone velocity in figure 4.2.3-2.

There is a strong dependence of cyclone pressure drop on inlet cyclone velocity for test TC01, while the other tests did not show as strong a trend.

To determine the cyclone efficiency, the cyclone inlet solids loading had to be calculated from the data. The solids rate to the cyclone was determined from two methods of calculating the riser solids circulation rate. The two methods of calculating the solids circulation rate were:

- Assume a slip of 2.0 slip velocity (ratio of the gas velocity to the solids velocity) and use the riser pressure drop value (PDT258) from the PI data acquisition and storage system. The PI value was corrected for the zero differential pressure value.

- The value calculated from the Konno and Saito (KS) Correlation (PSRI Desktop Design manual, Edition 1, June, 1994, 5-2), which calculates the solids velocity. The KS correlation calculates the relative solids velocity to the gas velocity from the terminal

velocity of the particles. For the conditions studied, the slip velocity was typically about 1.1 and the voidage above 0.98. The DP values used in the calculation were corrected for zero pressure values.

The solids circulation rate is the riser solids flow rate. The disengager acts as a cyclone and does a size separation on the circulated solids. The finer solids go to the cyclone and the coarser solids go to the standpipe. The cyclone solids flow rate was determined by calculating the cyclone dipleg and standpipe solids flow rates. The solids flow rates were determined by a heat balance around the cyclone dipleg entrance to the standpipe, using temperature readings near the dipleg entrance to the standpipe. The flows were corrected for aeration air. Once the solids loading to the cyclone was calculated, the cyclone efficiency could be determined.

The cyclone pressure drop data is plotted against the cyclone solids loading in figure 4.2.3-3 for the slip = 2 solids circulation rate calculation. The cyclone solids inlet loading is expressed in weight percent solids (50 percent = 500,000 ppmw).

There is a trend of increasing cyclone pressure drop with increasing inlet loading for all the data except for CCT6.

The cyclone efficiency is plotted against cyclone inlet loading in figure 4.2.3-4, assuming a slip of 2.

Note the increase in cyclone collection efficiency when the inlet loading is above XX wt%, for the later test runs, CCT6 and TC01. Since all of the TC01 collection efficiencies are above 98 percent, the TC01 data is plotted using an expanded efficiency scale, as shown in figure 4.2.3-5.

The general trend within the range of cyclone inlet solids loadings tested is an increase in cyclone efficiency with inlet loading. Figure 4.2.3-5 also shows which PCD inlet particulate data were obtained during a PCD pulse (pulse) and which were obtained between PCD pulses (no pulse). There were four tests (TC01IMT-4, -12, -13, and -17) where the sampling was done between two PCD pulses. However these no-pulse tests were started less than 5 minutes after a PCD pulse that caused a major loss of the cyclone dipleg seal. These tests are considered pulse tests due to the likelihood that the particulate emissions were effected by the pulse and resulting dipleg upset. The dipleg probably did not recover sufficiently to prevent some additional particulate emissions. The plot shows the general trend of lower cyclone efficiency during a PCD pulse.

Figure 4.2.3-6 plots the cyclone efficiency against cyclone pressure drop for all the 1997 data and figure 4.2.3-7 plots the cyclone efficiency in expanded scale against the cyclone pressure drop.

Note the drop off in cyclone efficiency below XX inches water cyclone pressure drop in figure 4.2.3-6. Figure 4.2.3-7 indicates a slight decrease in efficiency as cyclone pressure drop increases from 16 to 23 inches water. Again there is a general trend of lower cyclone efficiency during a PCD back-pulse.

Figure 4.2.3-8 plots the cyclone efficiency against cyclone inlet velocity for all the 1997 data and figure 4.2.3-9 plots the cyclone efficiency in expanded scale against the cyclone inlet velocity.

Figure 4.2.3-9 shows a slight decrease in cyclone efficiency with increased velocity.

Figure 4.2.3-10 is the plot of the slip = 2 riser solids rate verses KS riser solids circulation rate for the 1997 data.

This plot gives a straight line because the two solids circulation calculations inherently have the same basis and use the same data. Note that the slope is near 1.76, while the ratio of the slip velocities is 1.82 (2.0/1.1). Both calculations have voidages above 0.98. There are fewer CCT4 and CCT5 data points than given in table 4.2.3-1 because the KS equation gave negative solids flow rates at the low riser-pressure drops measured during CCT4 and CCT5.

Since the KS equation usually calculated a higher circulation rate than the slip = 2, the cyclone inlet loading and cyclone efficiencies were usually higher using the KS equation for solids circulation rates. This is shown in figure 4.2.3-11 for the cyclone inlet loadings.

Table 4.2.3-1

PCD Inlet Particulate Mass Loading Data MWK Test Programs CCT4, CCT5, and CCT6

SRI Run No	Date	Run Time Start	Run Time End	Loading ppm	Comments
CCT4IMT-2	3/15/97	13:53	14:08	18800	Coal
CCT4IMT-3	3/22/97	11:03	11:34	95700	Drum test, Coal
CCT4IMT-4	4/22/97	14:13	14:28	53500	Hot Circ., No Coal
CCT4IMT-5	4/23/97	10:59	11:14	39900	Coal
CCT4IMT-6	4/24/97	11:15	11:30	28300	Coal
CCT4IMT-7	5/1/97	10:30	10:57	19800	Drum test, Coal
CCT4IMT-8	5/2/97	10:30	11:01	18400	Drum test, Coal
CCT5IMT-1	5/13/97	9:08	9:38	9800	Coal Only - Acid Plume
CCT5IMT-2	5/14/97	9:03	9:33	14200	Coal + Dolomite
CCT5IMT-3	5/15/97	10:00	10:30	10700	Coal + Dolomite
CCT5IMT-4	5/16/97	8:50	9:20	25500	High Carryover
CCT5IMT-5	5/16/97	13:32	13:52	23000	No PCD Pulse - High Carryover
CCT5IMT-6	5/19/97	10:23	10:43	4200	No PCD Pulse - Low Carryover
CCT6IMT-1	6/24/97	10:39	11:09	25500	No PCD Pulse
CCT6IMT-2	6/24/97	15:10	15:24	41100	No PCD Pulse

Table 4.2.3-2

PCD Inlet Particulate Mass Loading Data MWK Test Program TC01

SRI Run No	Date Sampled	Run Time** Start	Run Time** End	Run Time** Duration	Particle Loading ppmw	Particle Loading gr/acf	Particle Loading mg/scm	PCD Pulse
TC01IMT-1	9/10/97	8:20	8:50	30.0	6100	12.6	7400	No
TC01IMT-2	9/11/97	9:20	9:50	30.0	10500	20.7	12700	Yes
TC01IMT-3	9/12/97	8:05	8:35	30.0	15200	30.3	18500	Yes
TC01IMT-4	9/16/97	8:30	9:00	30.0	15600	32.1	19000	Yes
TC01IMT-5	9/19/97	12:40	13:10	30.0	9600	20.0	11600	Yes
TC01IMT-6	9/25/97	11:50	12:20	30.0	12300	26.9	15000	No
TC01IMT-7	10/3/97	7:50	8:15	25.0	11200	24.3	13500	No
TC01IMT-8	10/15/97	8:58	9:28	30.0	10500	23.5	12700	No
TC01IMT-9	10/21/97	8:45	9:15	30.0	10400	21.7	12700	No
TC01IMT-10	10/23/97	9:15	9:45	30.0	10900	23.7	13200	No
TC01IMT-11	10/28/97	9:38	10:03	25.0	10800	23.2	13100	No
TC01IMT-12	10/29/97	10:15	10:45	30.0	13500	29.5	16400	Yes
TC01IMT-13	10/30/97	10:13	10:43	30.0	12700	28.3	15400	Yes
TC01IMT-14	10/31/97	12:12	12:42	30.0	11100	25.0	13500	No
TC01IMT-15	12/3/97	9:55	10:25	30.0	12200	26.6	14900	Yes
TC01IMT-16	12/5/97	9:50	10:35	45.0	8200	17.9	10000	Yes
TC01IMT-17	12/8/97	10:55	11:25	30.0	12400	27.0	15200	Yes

** All times are central standard time. Times prior to 10/26/97 have been reduced by one hour.

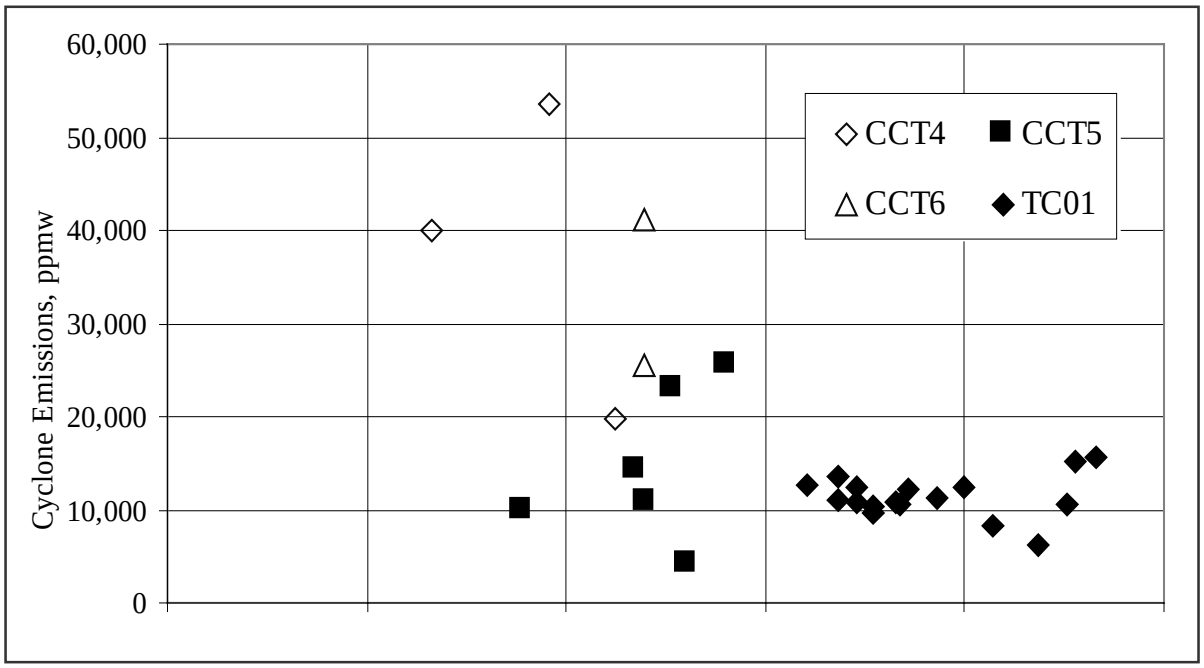

Figure 4.2.3-1 Cyclone Emissions – Pressure Drop (Cyclone Pressure Drop, In H_2O)

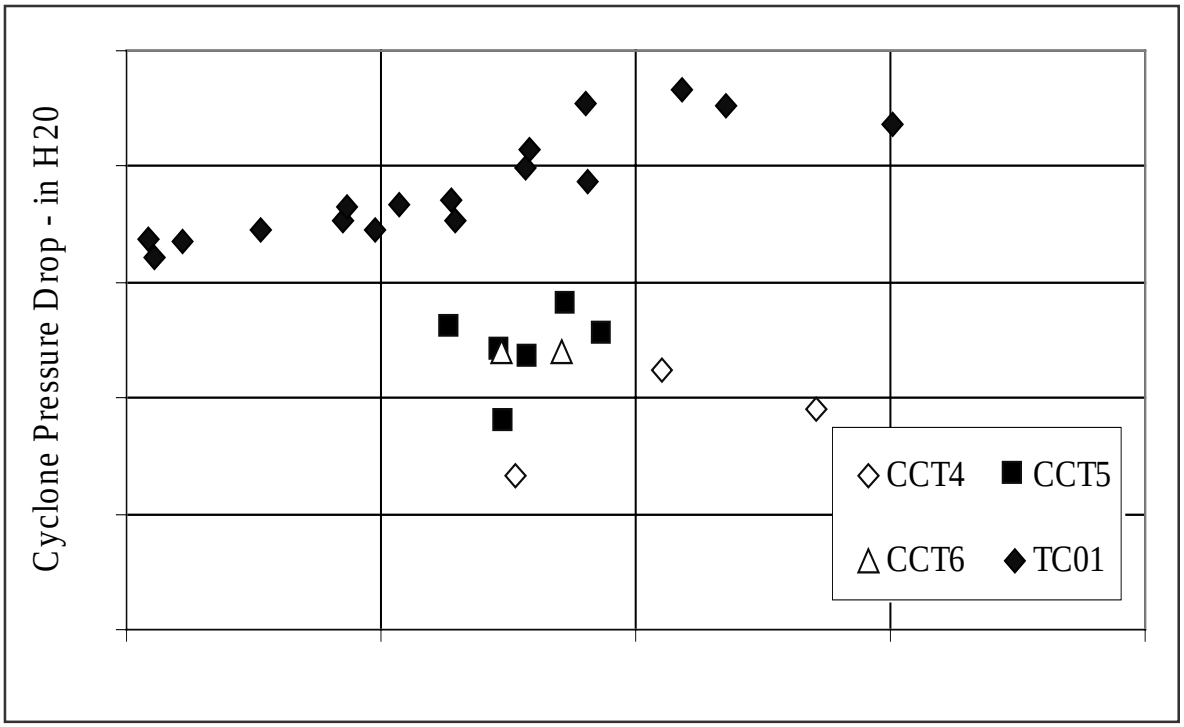

Figure 4.2.3-2 Cyclone Pressure – Flow (Cyclone Inlet Velocity, FPS)

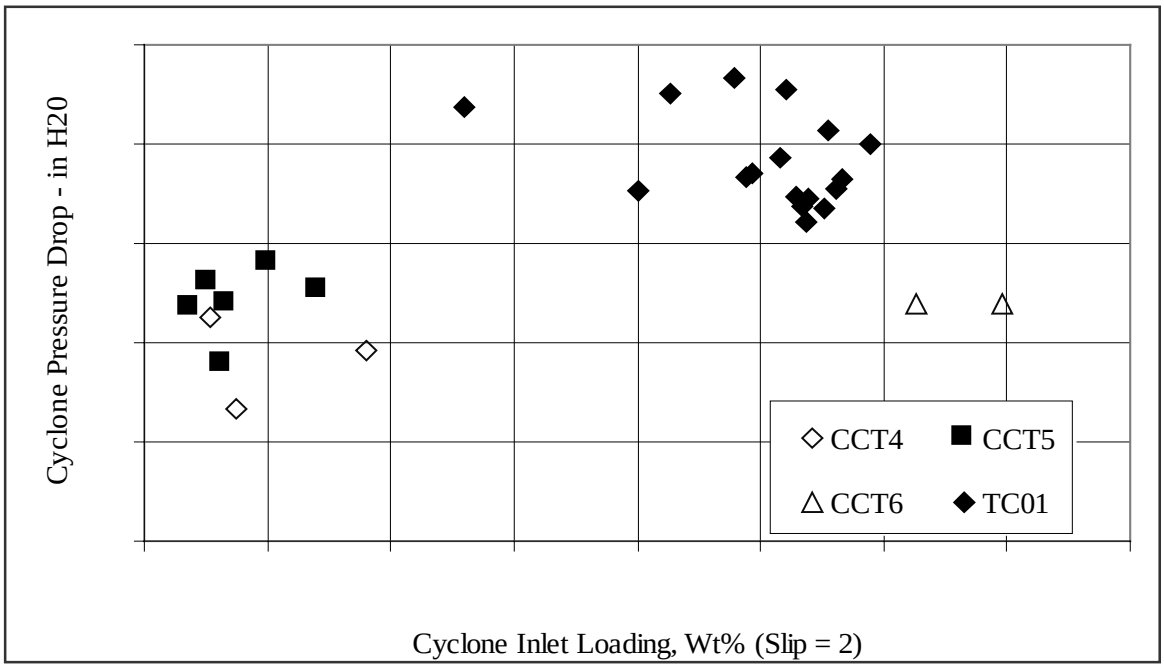

Figure 4.2.3-3 Cyclone Pressure – Inlet Loading

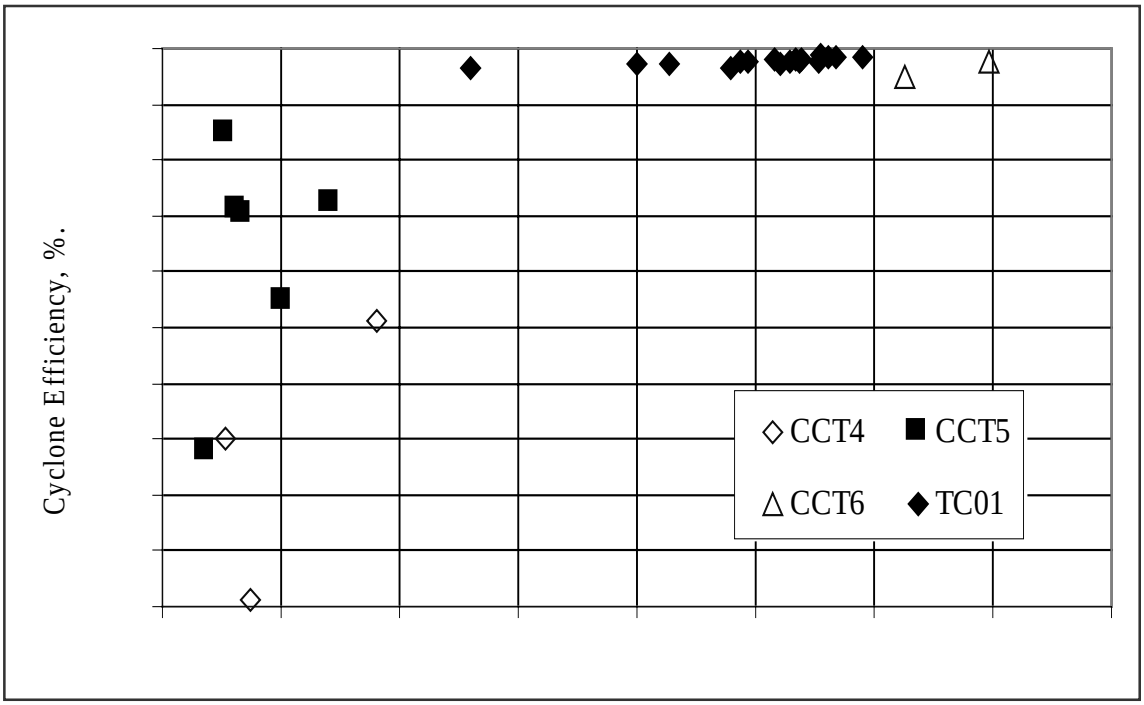

Figure 4.2.3-4 Cyclone Efficiency – Inlet Loading (Slip Velocity = 2) (Cyclone Inlet Loading Wt%)

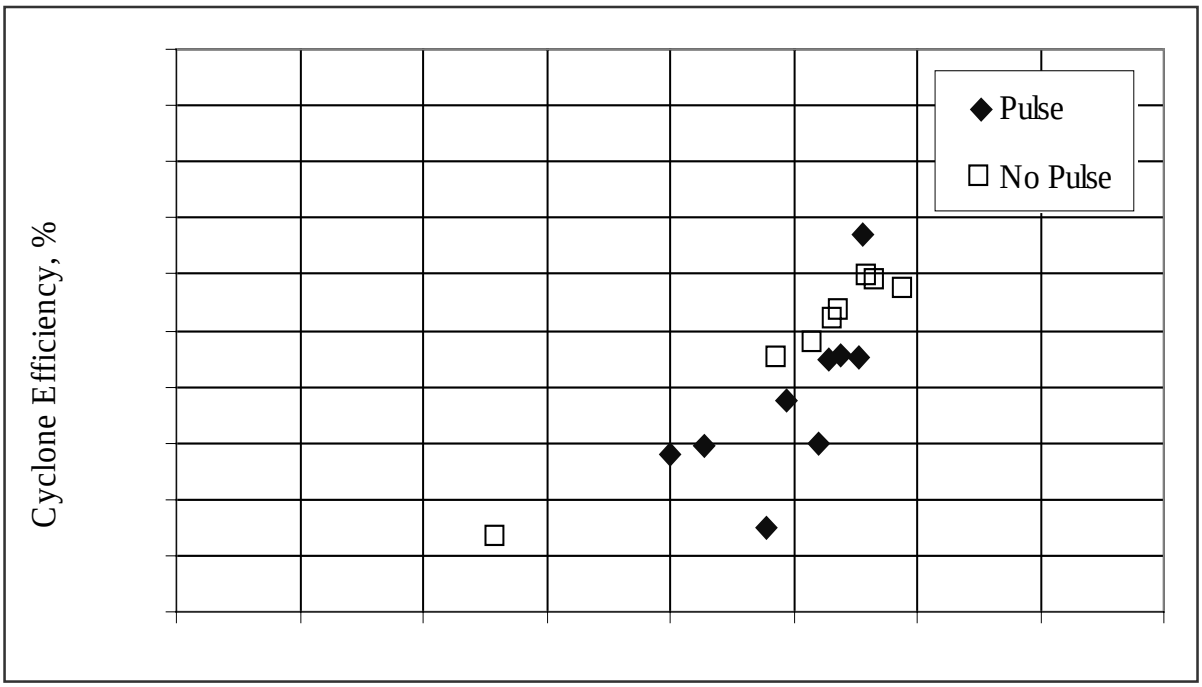

Figure 4.2.3-5 TC01 Cyclone Efficiency – Inlet Loading (Slip Velocity = 2) (Cyclone Inlet Loading, Wt%)

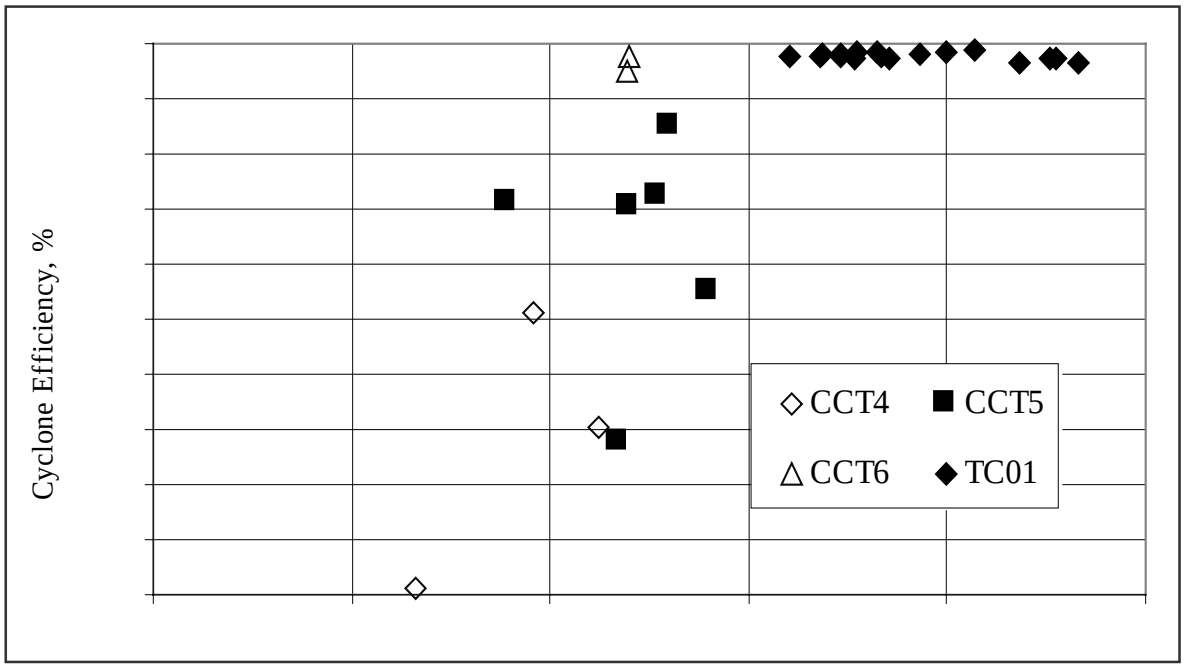

Figure 4.2.3-6 Cyclone Efficiency – Pressure Drop (Slip Velocity = 2) (Cyclone Pressure Drop, InH_2O)

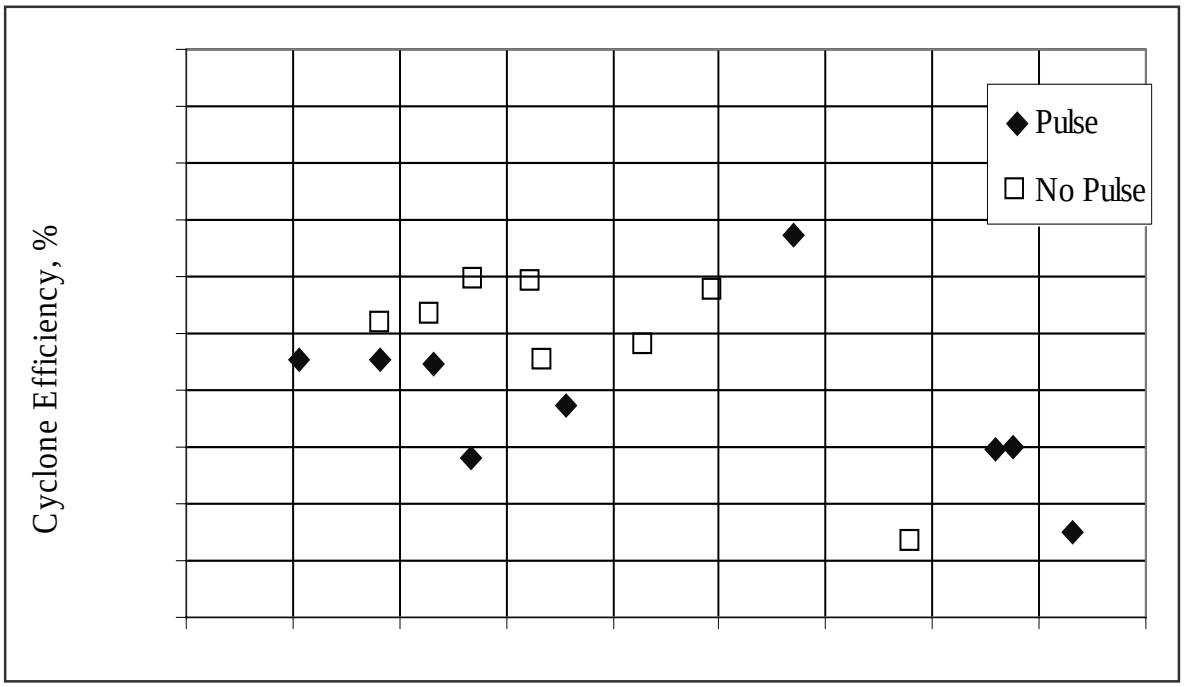

Figure 4.2.3-7 TC01 Cyclone Efficiency – Pressure Drop (Slip Velocity = 2) (Cyclone Pressure Drop, InH_2O

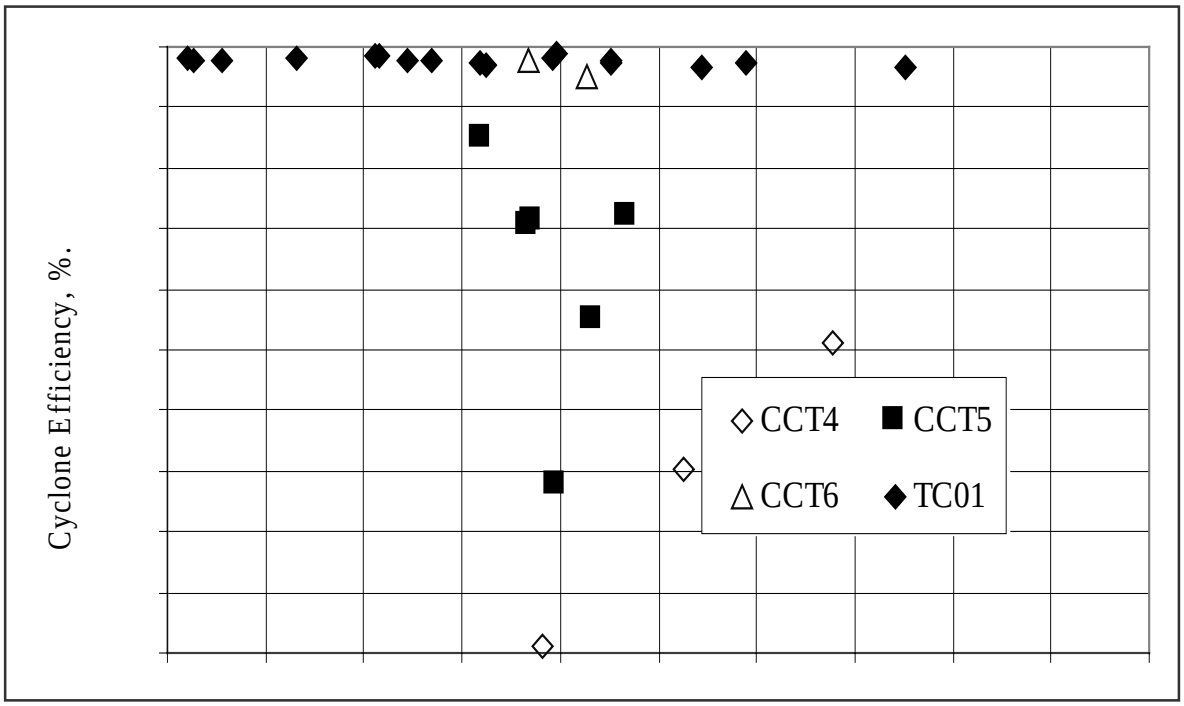

Figure 4.2.3-8 Cyclone Efficiency – Inlet Loading (Slip Velocity = 2) (Cyclone Inlet Velocity, FPS)

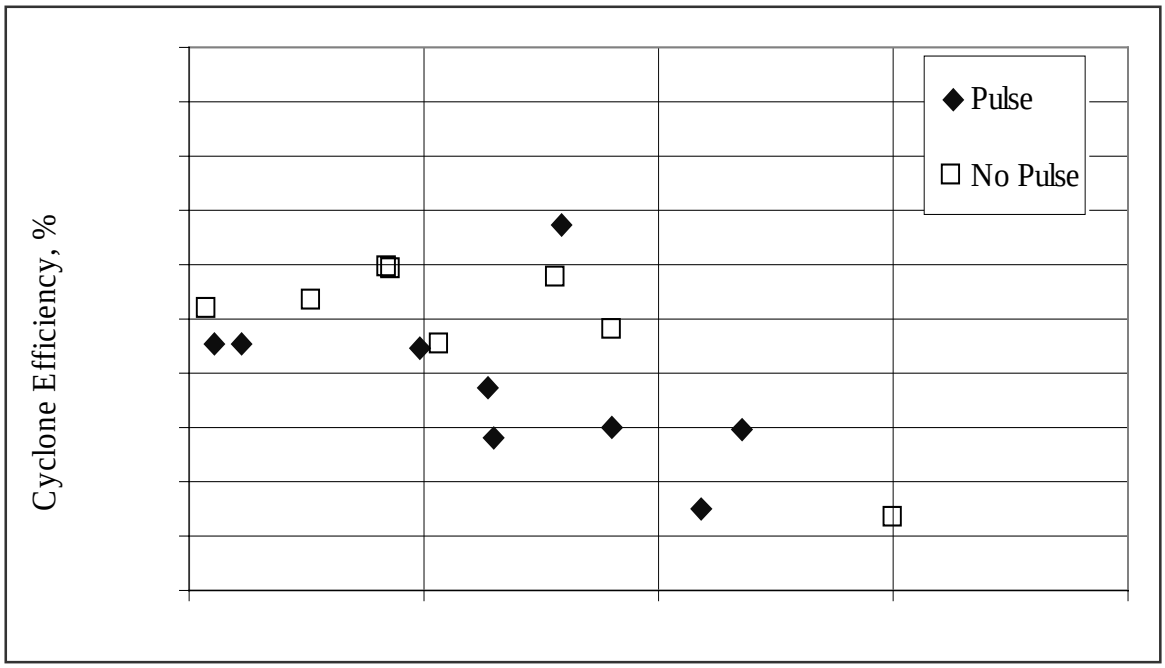

Figure 4.2.3-9 TC01 Cyclone Efficiency – Inlet Velocity (Slip Velocity = 2) (Cyclone Inlet Velocity, FPS)

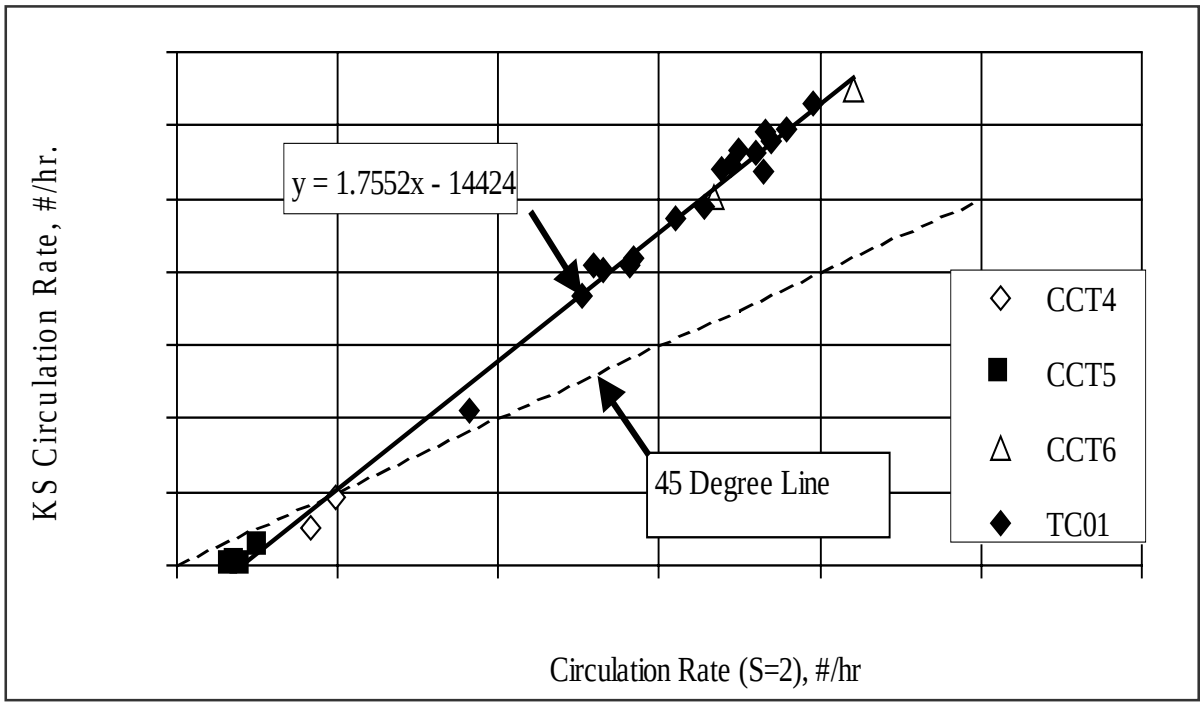

Figure 4.2.3-10 S = 2 Vs KS Circulation Rates

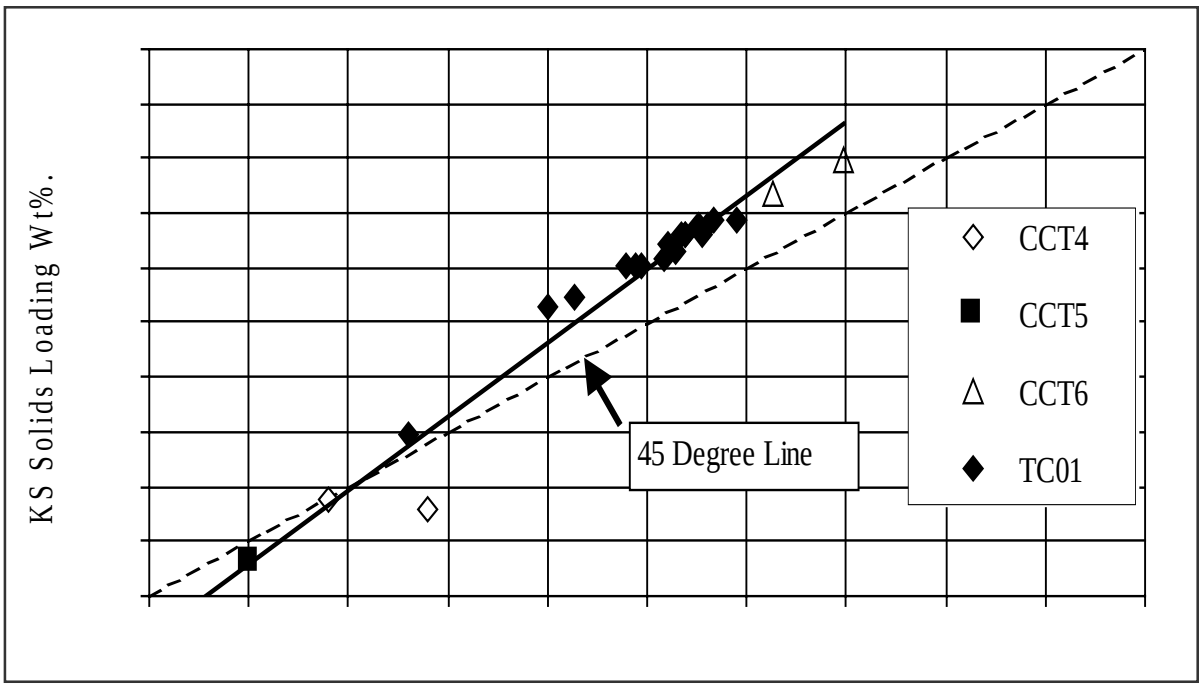

Figure 4.2.3-11 S = 2 Vs KS Solids Loading (Slip = 2) (Solids Loading, Wt%)

4.2.4 SO_2 Emissions

During the 1997 MWK transport reactor tests, SO_2 emissions were measured at the outlet of the PCD. When dolomite was used as the bed material, the SO_2 analyzer read essentially zero, but there were measurable readings when sand was used as bed material. Solids analyses of spent bed material for the 1997 test runs indicate that sulfur was always present in the bed material (see section 4.2.5 for details) when either dolomite or sand was fed to the reactor.

CCT4 was operated primarily with sand, and the resulting SO_2 emissions were between 100 and 160 ppm SO_2, with an average value of 125 ppm. Since sand was not expected to absorb SO_2, all coal sulfur was expected to exit with the flue gas. Based on the coal rate, fuel gas rate, and coal percent sulfur, the expected SO_2 emissions from the transport reactor should have been about 350 ppm. Figure 4.2.4-1 gives the analyzer readings and calculated SO_2 concentrations. Solids analyses of the CCT4D spent bed material indicate an average of 2.2 percent calcium sulfate ($CaSO_4$) in the solids and a calcium to sulfur molar ratio (Ca/S) of 0.95. This indicates that there was enough alkalinity in the bed to remove some of the inlet sulfur. Figure 4.2.4-2 plots the sulfur removal for CCT4D against the Ca/S ratio of the PCD solids.

Whenever dolmite replaced sand as the bed sorbent, the SO_2 emissions immediately dropped to essentially zero. This can be clearly seen on figure 4.2.4-3. The SO_2 emissions were from 100 to 120 ppm SO_2 during sand addition. A small amount of dolomite was added at 12:30 and the SO_2 emissions dropped to 10 ppm and then recovered to 100 ppm. Dolomite was then added continuously starting at 15:15, with another rapid decrease in SO_2 concentration from above 100 ppm to nearly zero, where it remained while dolomite was added.

The first two steady periods of CCT5 had average SO_2 readings of 57 and 22 ppm SO_2. This was during operation with sand in the reactor. When the sand was replaced by dolomite during the second steady period, the SO_2 emissions quickly went to zero where they remained for the rest of CCT5 as dolomite was fed to the reactor.

The only time that the SO_2 analyzer read above 100 ppm in CCT6 was when coal was burned and sand was added to the reactor. When dolomite was added to the reactor, the readings went to 20 ppm SO_2 or below.

The SO_2 readings for the entire TC01 test were below 20 ppm SO_2. Since there were no significant SO_2 concentrations measured during TC01, it was suspected that the analyzer was malfunctioning. Several 500cc bomb samples of the transport reactor gas were collected at the PCD inlet and outlet to confirm the unexpectedly low-SO_2 concentrations. The contents of each sample bomb were slowly bubbled through 50 ml of 3 percent hydrogen peroxide (H_2O_2) solution over a period of about 1 hour and the resulting solution was analyzed for sulfate, using an ion chromatograph at the APC lab. The SO_2 concentration of the bomb was calculated assuming a pressure of 200 psig for the sample bomb, 70°F for the PCD inlet sample (collected at the SRI particulate sampling site), and 300°F for the PCD outlet sample. The results are given in table 4.2.4-1 and compared with the SO_2 concentrations measured by the analyzer. The SO_2 analyzer span is zero to 1,000 ppm SO_2 and is calibrated with 750 ppm SO_2 calibration gas, so it cannot be expected to discriminate SO_2 concentrations of less than 25 ppm SO_2. All of the SO_2 analyzer measurements in table 4.2.4-1 should be considered to be nondetectable SO_2.

Table 4.2.4-1

Bomb Samples Data

Date & Time	Test	Sample Number	Sample Location	Bomb Sulfate mg/L	Bomb SO_2 Concentration ppm	Analyzer SO_2 Concentration ppm
10/13/97 9:35	TC01E	AB01955	PCD Inlet	1.00	2.0	1.7
10/14/97 9:30	TC01E	AB01956	PCD Outlet	1.55	3.8	1.9
10/28/97 13:08	TC01G	AB02101	PCD Inlet	ND	0.0	1.4
10/29/97 14:00	TC01G	AB02116	PCD Outlet	ND	0.0	1.4
12/5/97 14:30	TC01I	AB02444	PCD Inlet	1.29	2.6	8.6
12/8/97 13:15	TC01I	AB02471	PCD Outlet	0.25	0.6	8.6

Notes: Bomb is 500cc, 50 ml of H_2O_2 solution is analyzed for sulfate.

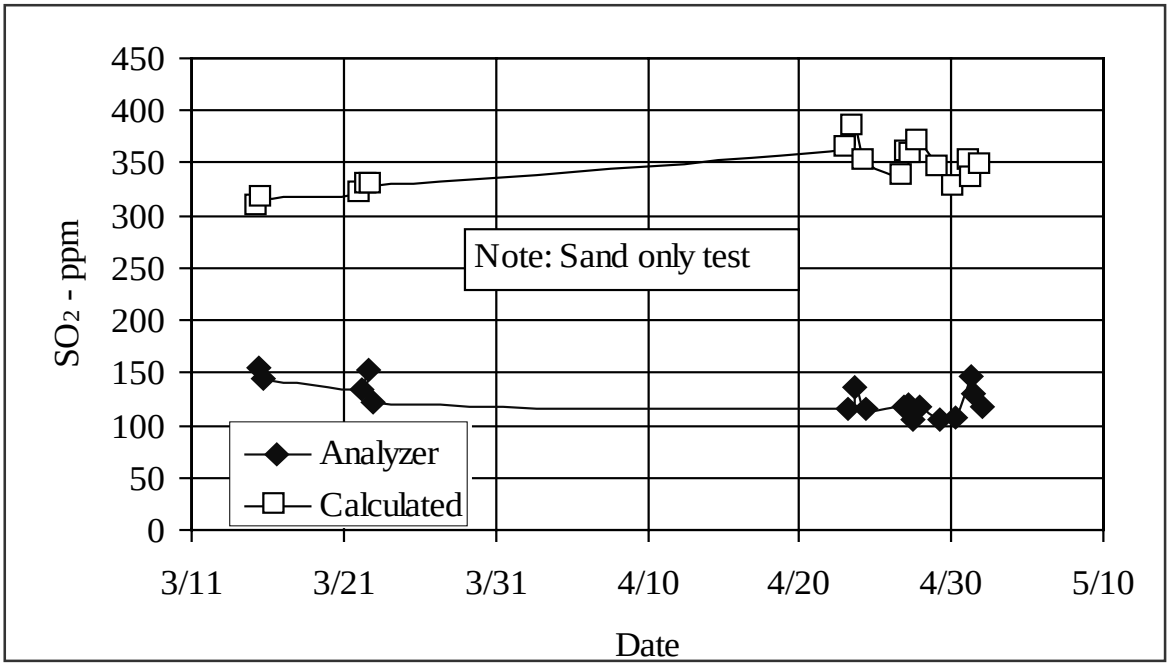

Figure 4.2.4-1 CCT4 SO_2 Concentrations

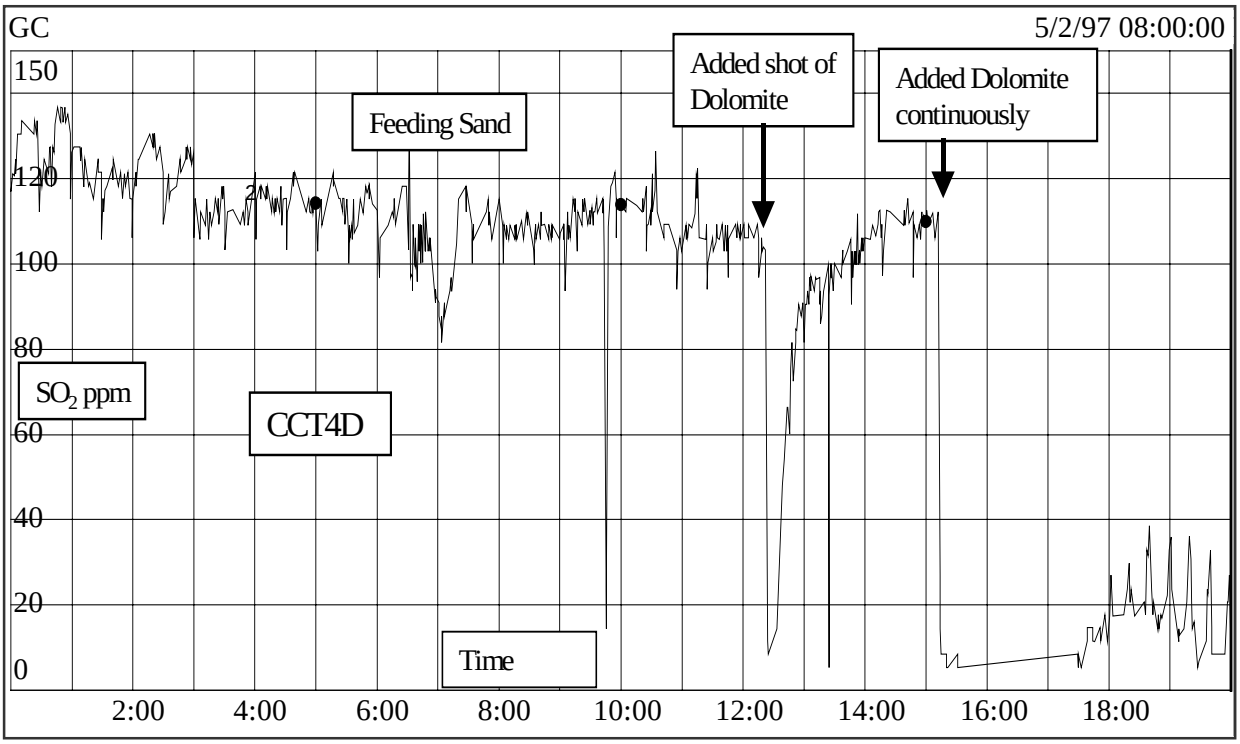

4.2.4-2 CCT4D PCD Solids Analysis, SO_2 Removal

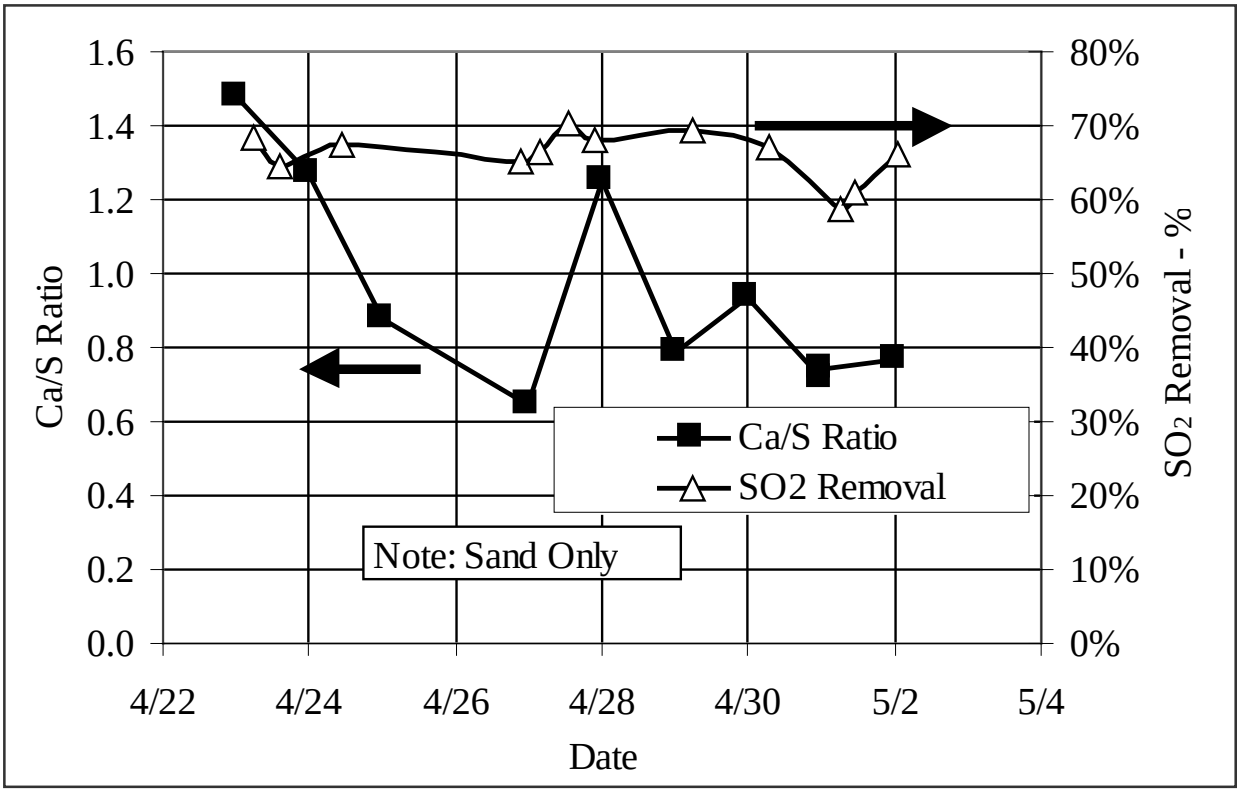

Figure 4.2.4-3 Effect of Dolomite Addition on SO_2 Concentrations

4.2.5 Solids Analyses

Solids were collected on a regular basis from the standpipe (FD0510) and PCD (FD0520) and sent to the Alabama Power Company (APC) laboratory for analyses. The solids were analyzed for:

- Calcium (reported as CaO).
- Magnesium (reported as MgO).
- Sulfur (reported as S).
- Silicon (reported as SiO_2).
- Aluminum (reported as Al_2O_3).
- Titanium (reported as TiO_2).
- Iron (reported as Fe_2O_3).
- Potassium (reported as K_2O).
- Sodium (reported as Na_2O).
- Phosphorus (reported as P_2O_5).
- Carbon dioxide (reported as CO_2).
- Carbon (reported as carbon).

The ash minerals, silicon, aluminum, titanium, iron, potassium, phosphorus, and sodium are reported in the oxide form, at which they are probably present after combustion. These compounds are from the coal ash, dolomite inerts, and sand. The raw data from the APC laboratory for two typical samples are given in table 4.2.5-1. These two samples are from FD0520 (PCD solids) taken during tests CCT5A and TC01B. The CCT5A sample is the composite of several individual samples taken during a 1- or 2- day period. The TC01B sample is an individual sample taken at the date and time indicated.

Calcium, magnesium, and sulfur are not present as the compounds reported in the raw data. Free energy minimization calculations done by Dr. Shadle at FETC give guidance as to the calcium and magnesium compounds at transport reactor conditions. Calculations at pressures from 150 to 200 psig and from 1,350 to 1,600°F indicate that the permissible sulfur-magnesium-calcium compounds are:

- $CaCO_3$ (limestone).
- CaO•MgO (dolomitic lime).
- $CaSO_4$.
- MgO (magnesia).

Lime (CaO) and magnesium sulfate ($MgSO_4$) are not thermodynamically stable compounds at these conditions.

The laboratory data reports carbon in two forms: elemental carbon and carbon dioxide (CO_2). The measured elemental carbon is the total carbon in the sample and includes the carbon dioxide carbon. The actual elemental carbon in the solids is the difference between the measured elemental carbon and the measured carbon dioxide. The actual carbon in the solids is

a measure of combustion efficiency. Zero carbon in the solids would indicate 100 percent combustion efficiency.

The solid compounds produced by the reactor were determined using the following assumptions:

1. All carbon dioxide measured came from $CaCO_3$, hence moles CO_2 = moles $CaCO_3$.
2. All sulfur measured came from $CaSO_4$, hence moles sulfur = moles $CaSO_4$.
3. All remaining calcium not taken by $CaSO_4$ and $CaCO_3$ came from CaO•MgO.
4. All remaining magnesium not taken by CaO•MgO came from MgO.
5. All carbon dioxide measured was also measured as carbon, hence unburned carbon in the solids is moles measured carbon minus moles measured CO_2.

Results of two typical calculations are given on table 4.2.5-1 under "Analysis." The analysis is given with the breakdown into the individual calcium, magnesium, and sulfur compounds. The compounds SiO_2, Al_2O_3, TiO_2, Fe_2O_3, K_2O, Na_2O, and P_2O_5 are lumped into 'inerts'. These inerts would come from the coal ash, sand, and dolomite impurities and are not expected to react with sulfur or carbon dioxide. The total of the compounds should be 100 percent if the analytical results and the component assumptions are correct. In analyses of this type, 95 to 105 percent solids total indicates good solids composition results. During the 1997 testing, this criterion was usually satisfied.

An assumption made in determining the compound species included that there would be no free lime (CaO) present. To confirm this assumption, four 1997 PCD samples were analyzed for free lime content using the APC laboratory procedure 3498, which uses sucrose. The results are given in table 4.2.5-2 and show minimal free lime content for all samples analyzed. If there were a significant amount of free lime in the solids, it would be noticed when the bed material was handled, since any moisture added would release heat as the free lime is hydrated. This has never been noticed during PSDF transport reactor solids handling. Dolomitic lime (CaO•MgO) will not hydrate at atmospheric conditions. Free lime should be present in the bed solids when limestone rather than dolomite is used as the sorbent.

The carbon content of the solids is calculated as the difference of two small numbers, which are typically close to each other in value. Hence, there is a lot of relative variation in the carbon content of the solids. Often the CO_2 content of solids is larger than the total carbon. Whenever the measured CO_2 is larger than the measured carbon, the carbon in the solids was assumed to be zero. In table 4.2.5-1, both examples had more moles of measured CO_2 than moles of measured carbon and hence the carbon in the solids was assumed to be zero (100 percent combustion efficiency).

The relative sources of bed material were calculated using the compositions of pure sand, coal ash, and dolomite and the measured solids analysis. The results of this calculation are given in table 4.2.5-1 under Relative Feeds Based on Feed Composition. The bed material is a mixture of dolomite, sand, and coal ash, and this calculation determines the relative percent of each feed material. This calculation uses the silicon and aluminum concentrations in dolomite, coal ash, and sand, with the assumption that silicon, aluminum, and the total solids are in mass balance.

The sum of the sand and coal ash should be about equal to the inerts since the major source of inerts is the sand and coal ash. The calculation is useful in determining how much of the original sand start-up material is remaining in the bed.

Two molar ratios were calculated for each solid sample:

- Calcium to magnesium (Ca/Mg).
- Calcium to sulfur (Ca/S).

The Ca/Mg ratio is calculated as a consistency check. The Ca/Mg ratio is 1.0 in the raw dolomite, which is the major source of calcium and magnesium for the system during dolomite sorbent feed. For the analytical results to be consistent, the Ca/Mg ratio of the spent bed material should also be close to 1.0, unless sand is being fed as the bed material.

The Ca/S ratio is the measure of excess sorbent required for sulfur removal, according to the equation:

$$SO_2 + CaCO_3 \bullet MgCO_3 + (1/2)O_2 \rightarrow CaSO_4 + 2CO_2 + MgO$$

To react, SO_2 requires an equal molar amount of dolomite and SO_2, which would result in the same molar amount of calcium in the solids as sulfur (Ca/S = 1.0). Solids with the minimum amount of dolomite required would then have calcium present only as $CaSO_4$ and there would be neither $CaCO_3$ nor CaO•MgO present. (It has been assumed that $MgSO_4$ does not form at the conditions at which the transport reactor has been operated.) The higher the Ca/S ratio, the more excess dolomite is used than required for 100-percent SO_2 capture. Since SO_2 emissions were zero during periods of dolomite addition, the 1997 tests never determined the minimum dolomite feed required to obtain 90-percent SO_2 removal.

Table 4.2.5-3 gives the FD0520 average solid analyses for each 1997 test. FD0520 samples are not representative of the bed material, but are representative of the solids collected by the PCD. This material should be finer than the bed material removed by FD0510 from the standpipe. Note that the compound totals are between 95 and 105 percent, very good considering the assumptions that went into the compounds calculations and analytical variations in solids analyses.

The solids carbon in all runs except CCT5A, TC01D, and TC01H averaged zero carbon in the bed material. For runs CCT5A and TC01H the carbon was less than the standard deviation of the sample average, indicating that statistically the carbon was zero. Run CCT5A only had two samples out of eight that had nonzero carbon in the ash. Run TC01D had an average carbon of 0.5 with a standard deviation of 0.4, indicating that there was some carbon in the solids.

The PCD solids relative feed analysis for CCT4D indicates very little dolomite feed to the reactor. This is consistent with the run logs. The Ca/Mg ratio is near 1.0 for all the runs except CCT4D, which was run using sand as the bed material. Run CCT4D (FD0520) solids are characterized by a higher amount of inerts and a lower Ca/S ratio when compared with the other 1997 tests.

PCD feeds analyses for run CCT5A indicated nearly equal amounts of sand and dolomite fed to the reactor, again consistent with the run logs, whereas CCT5B feed analyses indicated dolomite used as the bed material and sand was not fed into the reactor. Tests CCT5A and CCT5B were characterized by high Ca/S ratios because the dolomite feed rate was much higher than required for 100-percent SO_2 removal.

The FDO520 analyses for test TC01 were all fairly consistent during the entire 1,000-hour test. There was minimal sand in the PCD solids based on feeds analyses, which was consistent with the sorbent run logs showing mainly dolomite feed. The Ca/S ratio varied between 2.14 and 2.82, neglecting the single sample of TC01C. Feeds analyses were not calculated for TC01C through TC01H. The SO_2 emissions were essentially zero during TC01.

Table 4.2.5-4 gives the FD0510 average solids analyses of several 1997 tests in same format as table 4.2.5-3. These solids are the bed material during a run, and they remain in the transport reactor much longer than do the PCD solids. They represent several days of feeds and operation because of the large volume of solids in the transport reactor and low FD0510 discharge rate. TC01I was split into two periods. The Ca/Mg values were nearly 1.0 for all of the dolomite runs.

Three of the test runs indicated carbon in the reactor bed solids. Test CCT4D was based on only one sample. Test TC01B had only one of four samples with nonzero carbon in the solids and the standard deviation was larger than the average value, indicating that statistically there was zero carbon. Test TC01H1 had only one of twelve samples with a nonzero carbon in the solids and the standard deviation was larger than the average value.

Figure 4.2.5-1 compares the inerts based on solids analysis in standpipe (FD0510) and PCD (FD0520) samples. The standpipe samples generally had less inerts than the PCD samples, indicating that the coal ash was finer than the average bed material and tended to leave the bed before other solids.

Figure 4.2.5-2 compares the sand based on feeds in the standpipe and the PCD. As expected, the coarser sand tended to accumulate in the reactor. Sand is usually used as start-up bed material, which then gradually leaves the bed through the standpipe during a run.

Figure 4.2.5-3 compares the Ca/S ratio for the standpipe and the PCD solids. The standpipe always has a higher Ca/S ratio than the PCD solids. For TC01G and TC01IA, there is a slight difference, while for TC01H and TC01IB there is a tremendous difference. The $CaSO_4$ content on table 4.2.5-4 indicates that the higher Ca/S ratios are due to a decrease in sulfur content, not an increase in calcium. Comparison with the PCD solids indicates that the increased Ca/S are not caused by an increase in dolomite, which would be indicated immediately by the PCD Ca/S. The decrease in sulfur may be related to the final purging of the start-up sand and a build up of inactive sorbent in the bed.

During CCT4D, sand only was fed to the reactor, and minimal SO_2 removal and low-sulfur content of the recovered solids was expected. However, an average of 0.5 percent sulfur was found in the PCD solids for 13 samples. The SO_2 removal averaged 60 to 70 percent for the test, assuming that the feed coal contained 0.9 percent sulfur. The Ca/S ratio of the PCD solids

averaged 0.95. The Ca/S ratio and SO_2 removal are plotted against time in figure 4.2.4-2 (see section 4.2.4). Note that the Ca/S ratio decreased during the run. Dolomite was fed into the reactor twice during CCT4D, but the rest of the time sand was fed into the reactor. The PCD solids Ca/S ratio should control the SO_2 emissions because the final sorbent that the gas sees is the dust layer on the PCD candles, which should increase the SO_2 removal. The CCT4D solids are characterized as having a large percentage of ash and low values of carbon dioxide. Since there was a calcium to sulfur ratio of nearly 1.0 there was minimal $CaCO_3$ and CaO•MgO.

Test CCT5A was started up on sand and then switched to dolomite after the run started. During the run numerous shots of sand were added to the reactor. The first solids sample analyzed was from a composite of several samples taken before coal feed was started and had sulfur at a nondetectable level. The next eight PCD solid samples during CCT5A averaged Ca/S of 28.12. The Ca/S values ranged from 8.8 to 75.9 indicating that a large excess of dolomite was added during the run. The calculated relative feeds are plotted in figure 4.2.5-4. All solid samples were daily composites of two or three grab samples, so it is difficult to locate exact additions of either sand or dolomite. Figure 4.2.5-4 indicates that the unit was started with a mixture of sand and dolomite in the reactor, and during the run mostly dolomite was added, up to May 17. During May 17 and 18, sand was added, alternating with dolomite, thus increasing the sand content of the reactor. During CCT5, there was minimal solids removed from the standpipe and none were analyzed.

The solid samples from CCT5B were similar to CCT5A, with the initial samples containing no sulfur and later samples having a high-Ca/S ratio. Dolomite was fed exclusively to the reactor from May 24 to 27. The SO_2 emissions were also zero during this time, confirming that a large excess of dolomite was fed to the reactor. The solids analysis indicated that there was very little sand in the feed, based on the FD0520 solids.

The TC01 PCD solids analyses were characterized by fairly consistent results during a test, while the standpipe solids show some variation during a test.

Figure 4.2.5-5 plots the Ca/S ratio for the PCD solids of TC01B. The Ca/S ratio begins at around 2.0 on September 11, then increases to a high value when the coal feed is stopped. Once the coal comes on September 16, the Ca/S ratio again decreases to around 2.0. The PCD and standpipe inerts were consistent with each other and tracked well during the cool-off period.

Runs TC01C through TC01F did not last long enough at steady conditions to analyze solids trends with time. Generally they were fairly consistent. Typical of these runs was TC01G. Figure 4.2.5-6 plots the PCD Ca/S ratio and percent inerts against time and figure 4.2.5-7 plots the percent of the PCD compounds against time. The TC01H plots are about the same as TC01G, except that the Ca/S ratio increased just at the end of the run. All values were fairly consistent during a run.

Figure 4.2.5-8 compares the Ca/S ratio for TC01H for the standpipe and PCD solids. Note that the standpipe solids Ca/S are significantly higher than the PCD solids.

A system mass balance was done for several periods of the TC01I. This mass balance reported the coal and dolomite feed rates based on the feeder weight cells for 6-hour periods. Using coal

and dolomite analyses and the feed rates, a Ca/S ratio and amount of inerts in the reactor, based on the mass balance, could be calculated. (About 5 percent of the calcium is from coal ash.) These mass balance results are compared with the lab results in figure 4.2.5-9 for TC01I. Note that the Ca/S and inerts values are consistent. This is a good self-consistency check for the APC laboratory analyses and the FDO210 and FD0220 weight cells.

The standpipe solids analyses for TC01I are plotted in figure 4.2.4-10 and -11. Note the sudden increase in Ca/S and the sudden decrease inwt% $CaSO_4$ on December 5. There was a decrease in sulfur in the bed, not a sudden increase in calcium. Figure 4.2.4-12 gives the solids analyses based on the relative feeds. Note the steady decrease of sand in the bed, but nothing dramatic on December 5. The decrease of the sulfur in the bed might be linked to the slow purging of start-up sand from the bed. During this test, neither the dolomite nor the coal feed changed. FDO510 was averaging 75 lb/hr and FD0520 was averaging about 200 lb/hr. There were a few 6-hour periods when FD0510 cycled only once. There is also a significant time lag in FD0510, in that the solids cooler (FD0206) volume is about 1,000 pounds, so that there is a time lag of 13 hours between when the solids are in the bed and when they are actually sampled.

The standpipe and PCD solids are compared for TC01I in figures 4.2.5-13 and -14. Figure 4.2.5-13 compares the Ca/S and inerts for the standpipe and PCD solids. Note that the PCD Ca/S ratio, PCD inerts, and standpipe inerts were constant duringTC01I, but the Ca/S ratio for the standpipe increased during the run. Figure 4.2.5-14 compares the sand in the PCD and standpipe solids. The PCD sand percent stayed the same during the run, while the standpipe percent sand decreased during the run, finally approaching the PCD values on December 7, 1997. This is probably when the bed finally reached steady state, indicating that under steady state, very little $CaSO_4$ will be circulating in the bed, but that most $CaSO_4$ formed will immediately exit from the reactor.

The standpipe solids exhibited a similar phenomenon if tests TC01G and TC01H are combined into one run, in that the standpipe Ca/S increased from TC01G to TC01H. Test TC01G ended the day before TC01H and the bed material at the end of TC01G was the same as the bed material at the start of TC01H.

Table 4.2.5-1

Solids Analysis

Sample No.	AB01275	AB01707
Date	5/18/97	9/11/97
Time	Composite	16:00
Run	CCT5A	TC01B
Sample	FD0520	FD0520
Data		
Compound	**Wt%**	**Wt%**
SiO_2	44.6	39.5
Al_2O_3	17.7	17.6
TiO_2	0.8	0.9
Fe_2O_3	4.2	3.9
CaO	16.5	12.3
MgO	11.6	8.6
K_2O	1.1	1.3
Na_2O	1.5	1.7
P_2O_5	0.2	0.4
CO_2	4.0	0.9
S	0.6	3.2
C	1.0	0.2
Analysis		
Inerts	70.2	65.3
$CaCO_3$	9.0	2.1
$CaSO_4$	2.7	13.4
CaO*MgO	17.7	9.7
MgO	4.2	4.6
Carbon	0.0	0.0
Total	103.8	95.0
Realtive Feeds based on Feed Compostions		
Ash %	63.1	58.2
Sand %	6.1	1.4
Dolomite %	30.8	40.4
Ratios	**Ratio**	**Ratio**
Ca/Mg	1.02	1.02
Ca/S	14.74	2.23

Table 4.2.5-2

Free Lime Analyses

Test	Date	Time	Sample #	Free Lime % CaO
TC01B	9/18/97	0800	AB01773	0.08
TC01E	10/13/97	0830	AB01963	0.23
TC01F	10/23/97	1600	AB02064	0.06
TC01G	11/1/97	1600	AB01773	0.08

Note: APCO Lab free lime method 3498 (sucrose)

Table 4.2.5-3

FDO520 Solids Analyses

FDO 520 Averages Test	CCT4D	CCT5A	CCT5B	TC01B	TC01C	TC01D	TC01E	TC01F	TC01G	TC01H	TC01I
Samples Averaged	13	8	5	17	2	7	5	5	14	9	20
Samples Excluded	3	0	2	6	1	2	1	0	2	3	1
Weight %											
Inerts	92.5	74.3	77.0	72.9	76.6	80.4	68.0	80.6	73.2	72.5	72.5
CaCO3	0.2	9.7	4.0	4.2	0.8	0.4	5.9	0.5	0.9	2.2	1.2
CaSO4	2.2	1.4	2.9	11.8	14.9	10.8	11.7	10.5	13.7	12.3	11.1
CaO*MgO	0.0	12.8	16.9	9.8	5.6	7.1	6.2	9.3	10.2	9.9	7.3
MgO	0.9	4.2	2.1	5.1	4.9	3.6	6.7	3.5	4.4	4.7	4.0
Carbon	(1)	0.2	0.0	0.0	0.0	0.1	0.0	0.0	0.0	0.5	0.0
Total	95.9	102.6	102.9	103.7	102.9	102.4	98.6	104.4	102.4	101.9	96.1
Relative Feeds by Feeds Composition (4)											
Ash %	46.5	52.2	75.0	66.0							61.3
Sand %	45.2	21.4	1.4	1.2							4.2
Dolomite %	8.2	26.5	23.5	32.8							34.5
Ratios											
Ca/Mg Ratio	0.64	1.01	1.04	1.01	0.97	0.97	0.91	0.98	1.00	0.98	0.97
Ca/S Ratio	0.95	28.42	11.23	2.82	1.60	2.18	2.43	2.61	2.14	2.39	2.08

Notes:

1. CO_2 not reported for CCT4D, $CaCO_3$ calculated from Carbon - 100% carbon conversion assumed
2. Two analyses deleted from TC01B CO2/C Ratio
3. Only one carbon reported for TC01C
4. Calculations not performed for all samples

Table 4.2.5-4

FDO510 Solids Analyses

FDO 510 Averages						(4)	(4)
Test	CCT4D	TC01B	TC01F	TC01G	TC01H	TC01IA	TC0IB
Samples Averaged	1	4	2	3	7	12	7
Samples Excluded	0	0	0	0	0	2	0
Weight %							
Inerts	87.1	69.0	63.8	63.3	69.9	61.9	58.3
CaCO3	0.1	6.2	6.8	5.4	4.4	4.0	6.1
CaSO4	0.3	0.0	0.0	18.1	3.6	12.8	4.9
CaO*MgO	0.0	17.5	25.1	13.4	15.3	14.8	20.2
MgO	0.1	2.3	2.8	7.7	2.9	5.4	3.8
Carbon	3.6	0.3	0.0	0.0	0.0	0.1	0.0
Total	91.1	95.3	98.4	107.9	96.2	99.0	93.2
Relative Feeds based on Feed Composition							
Ash %	2.6	22.3	41.0	50.3	38.5	36.8	43.9
Sand %	83.9	44.8	25.5	16.6	25.3	20.9	10.2
Dolomite %	13.5	32.9	33.5	33.1	36.3	42.3	46.0
Ratios							
Ca/Mg Ratio	1.44	1.01	1.00	0.95	1.00	1.01	1.01
Ca/S Ratio	1.33	(2)	(3)	2.38	9.99	3.15	8.95

Notes:

1. CO_2 not reported for CCT4D, $CaCO_3$ calculated from Carbon. 3.6% carbon left over
2. Sulfur reported as 0.0 for all TC01B samples
3. Sulfur reported as 0.0 for all TC01F samples
4. FDO510 samples changed during run TC01I

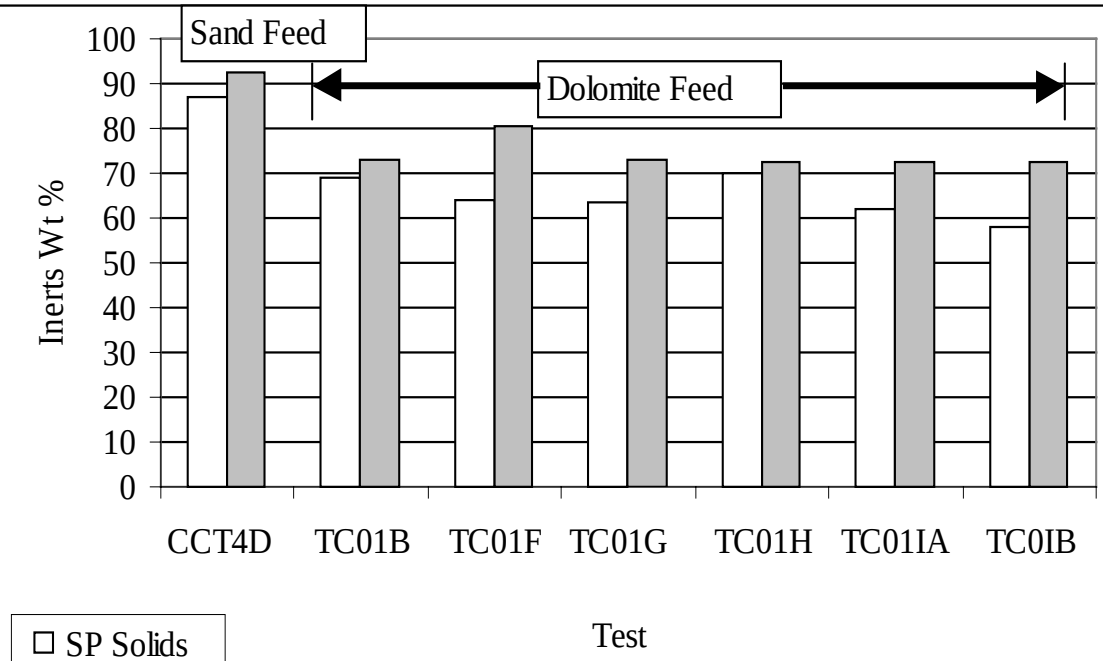

Figure 4.2.5-1 Standpipe and PCD Inerts

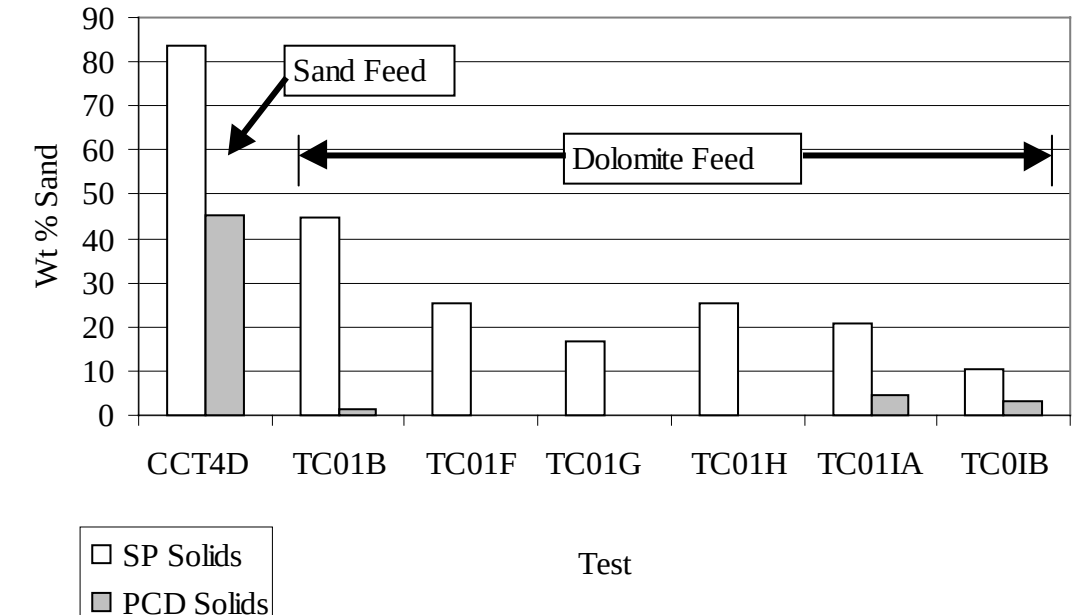

Figure 4.2.5-2 Standpipe and PCD Feed Sand %

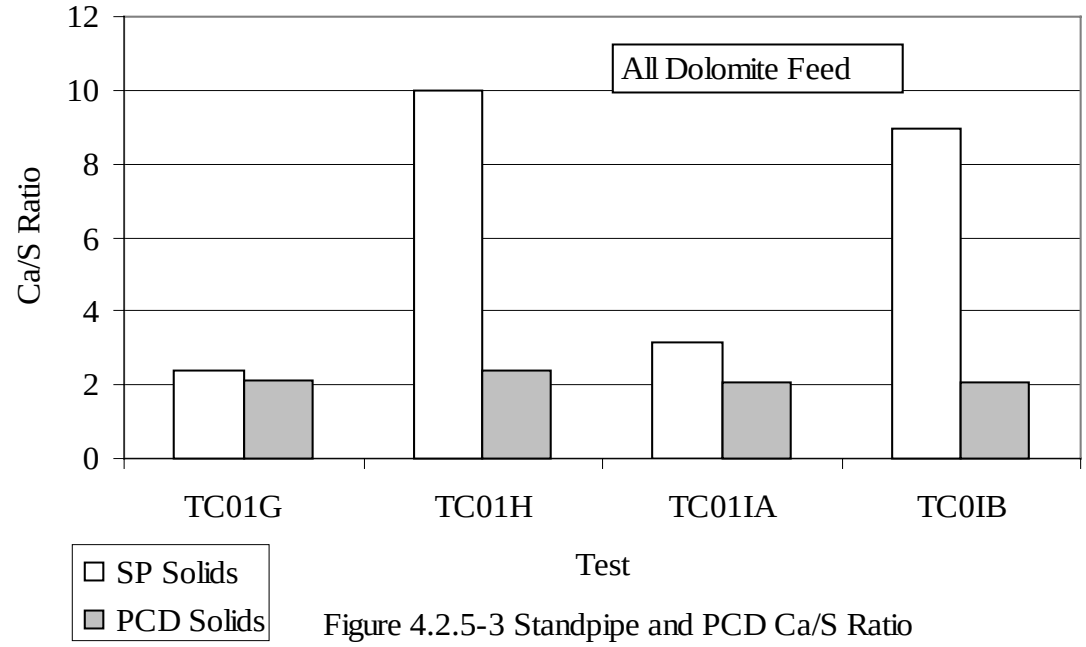

Figure 4.2.5-3 Standpipe and PCD Ca/S Ratio

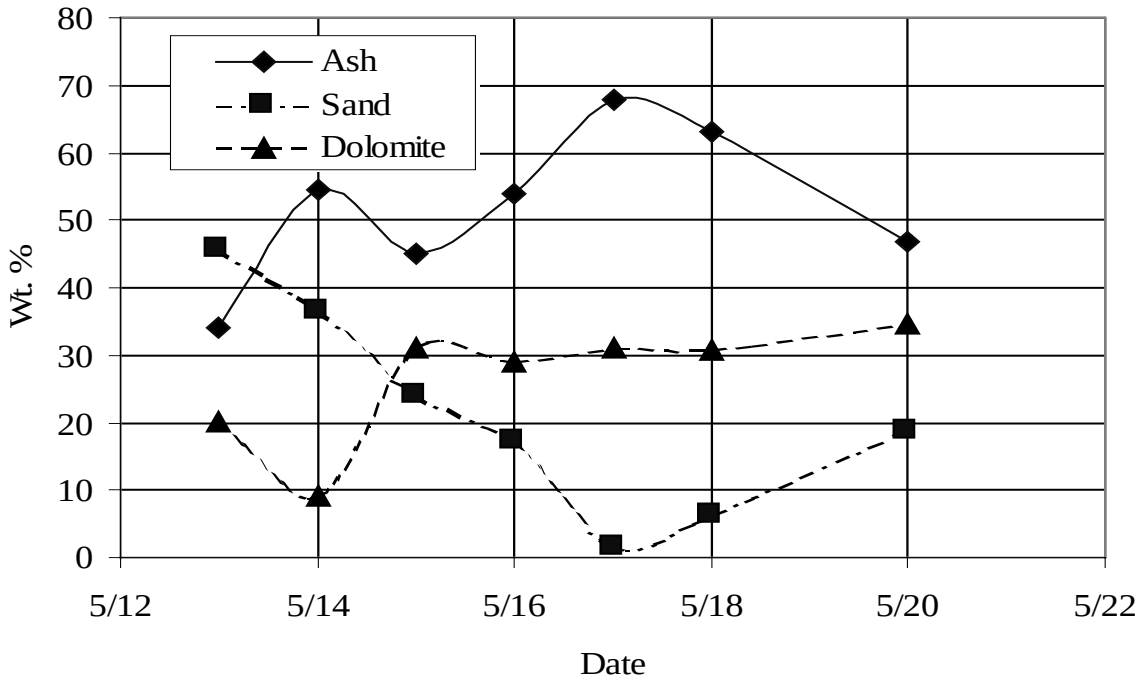

4.2.5-4 CCT5A PCD Solids Feeds

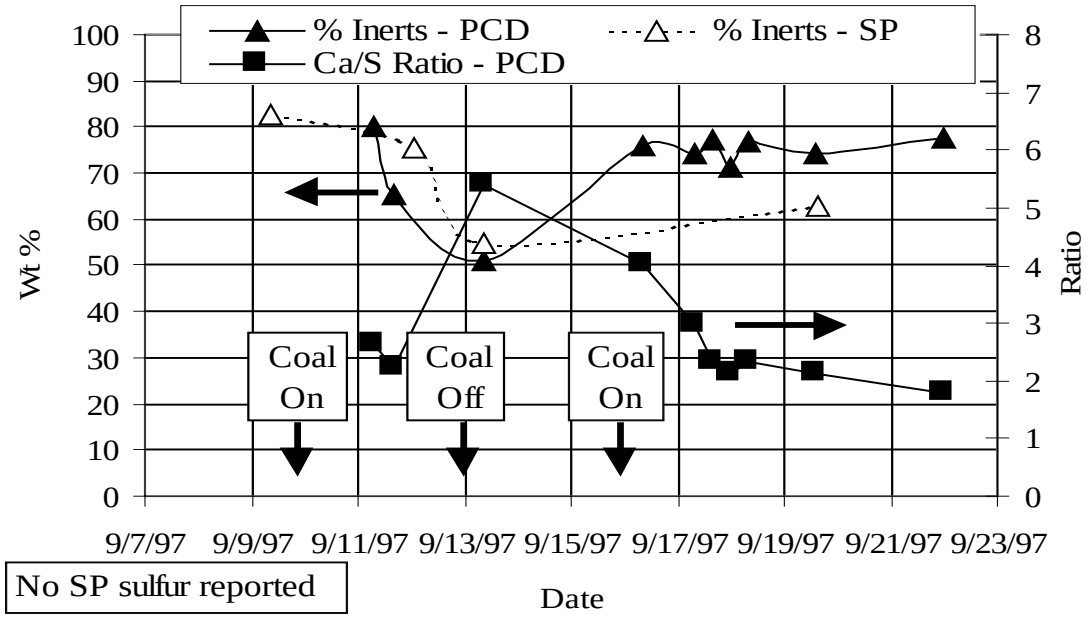

Figure 4.2.5-5 TC01B Solids Analysis

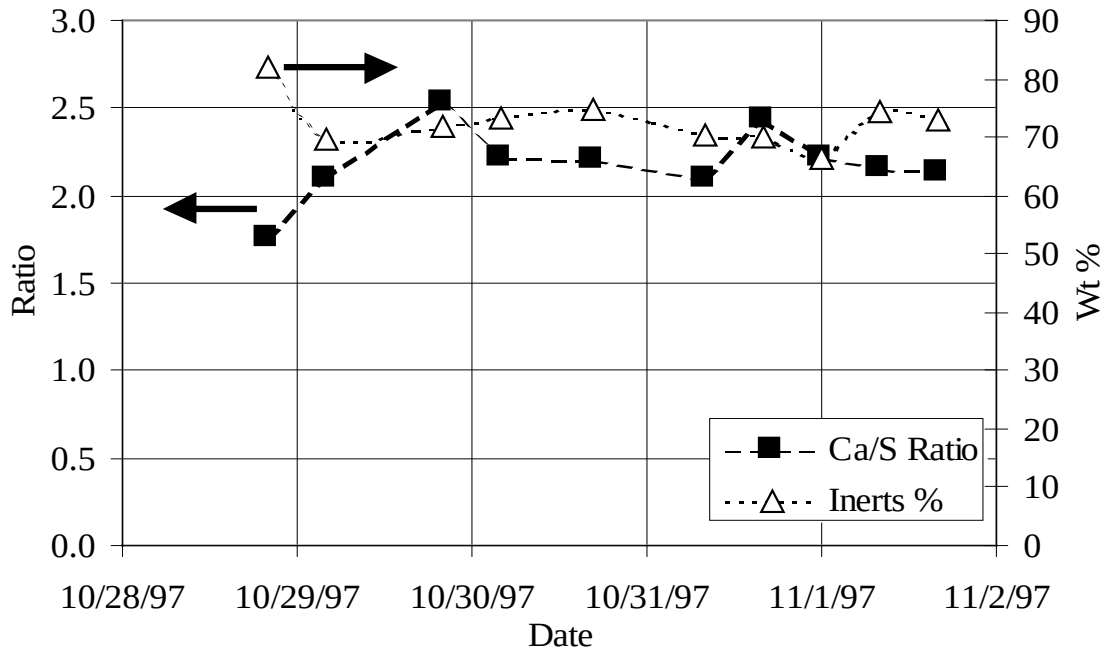

Figure 4.2.5-6 TC01G PCD Solids Analysis

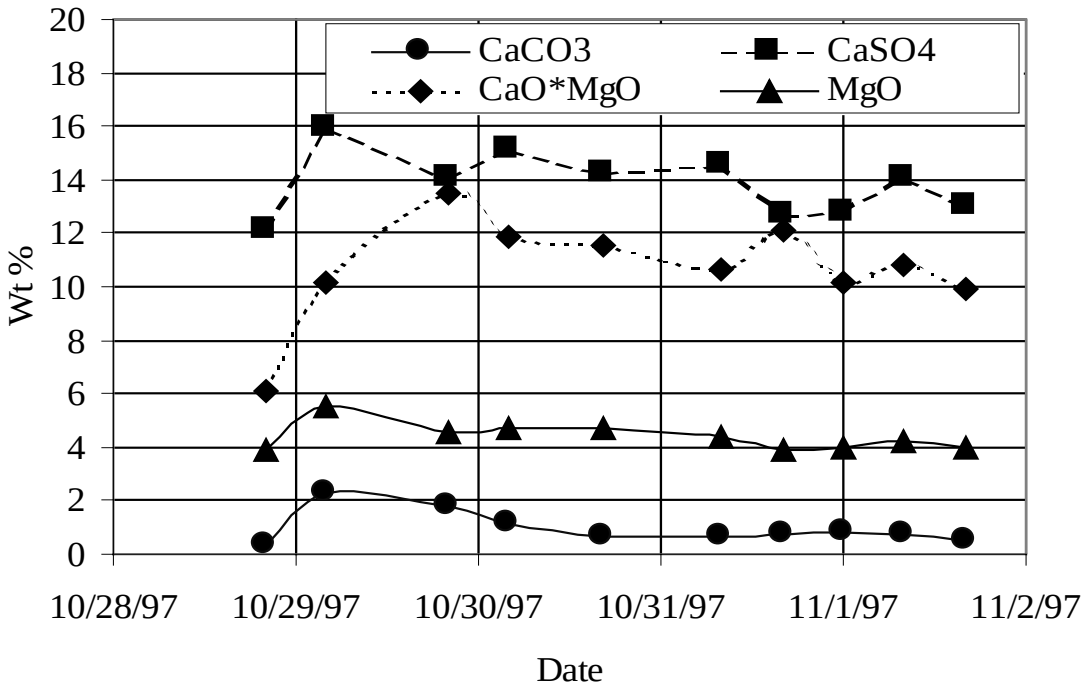

Figure 4.2.5-7 TC01G PCD Solids Analysis

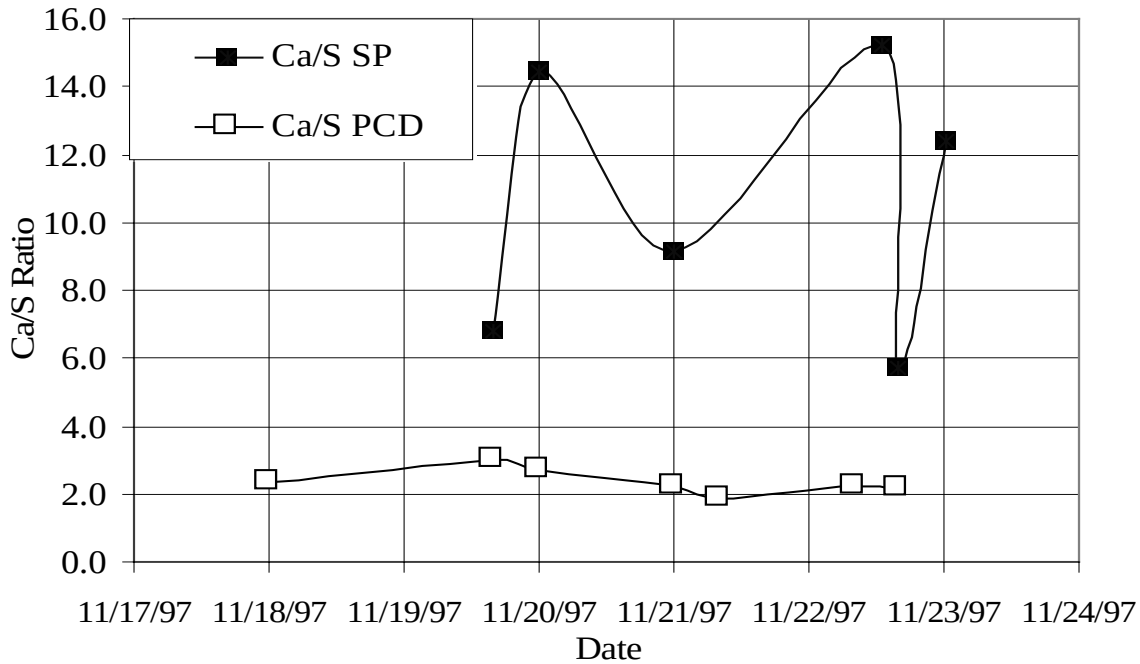

Figure 4.2.5-8 TC01H Ca/S Ratios

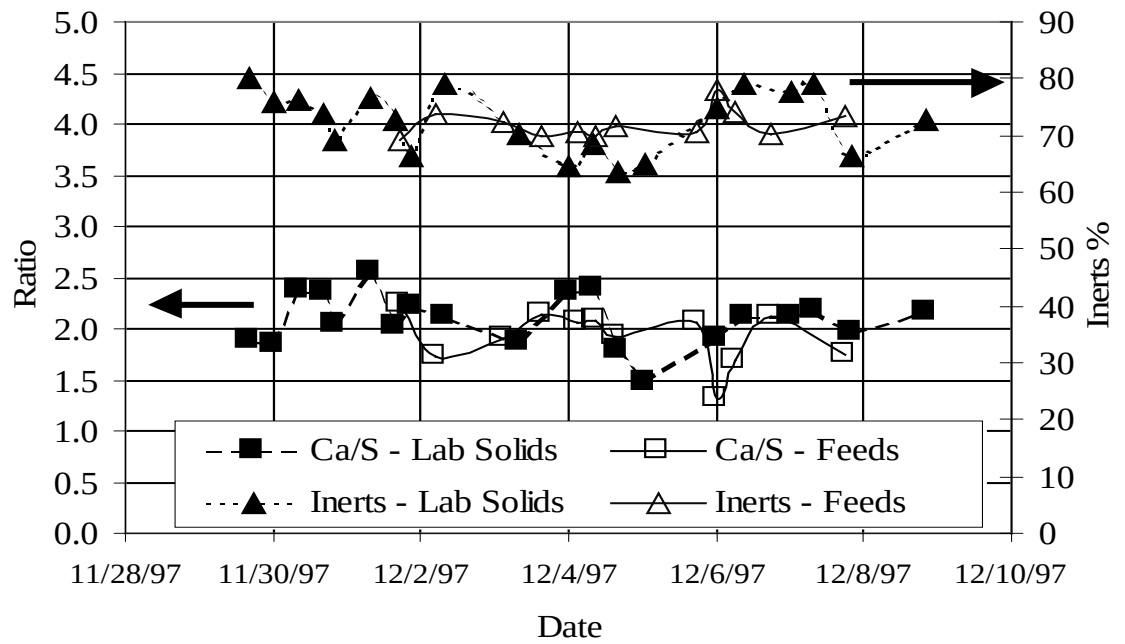

Figure 4.2.5-9 TC01I PCD Solids

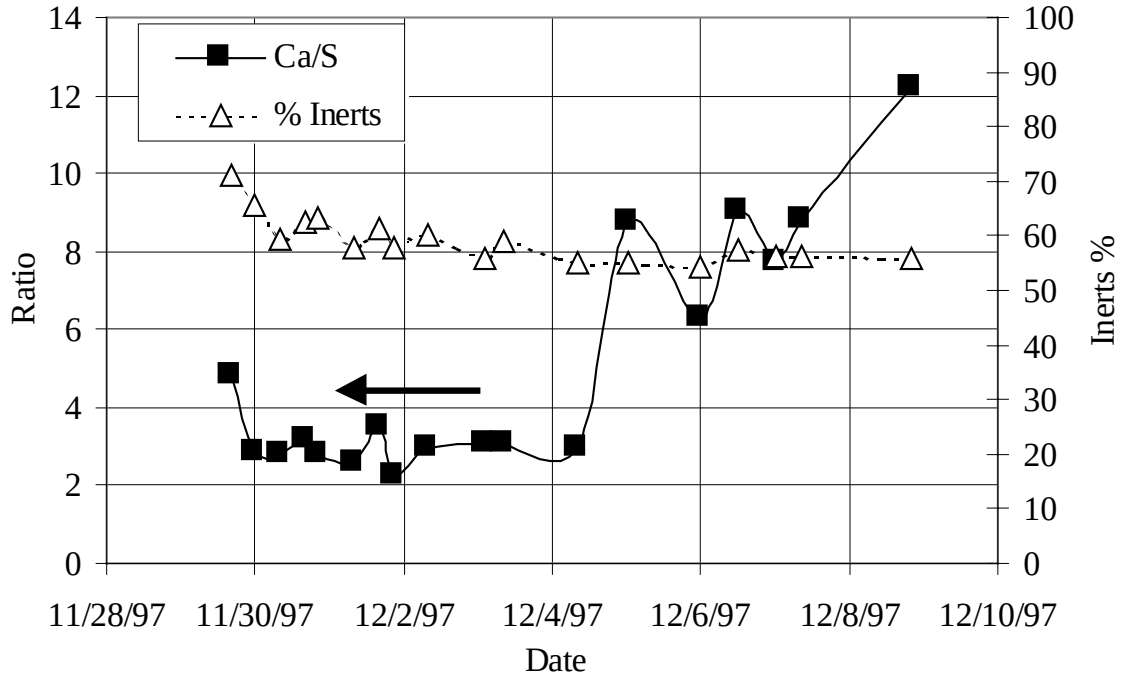

Figure 4.2.5-10 TC01I Standpipe Solids

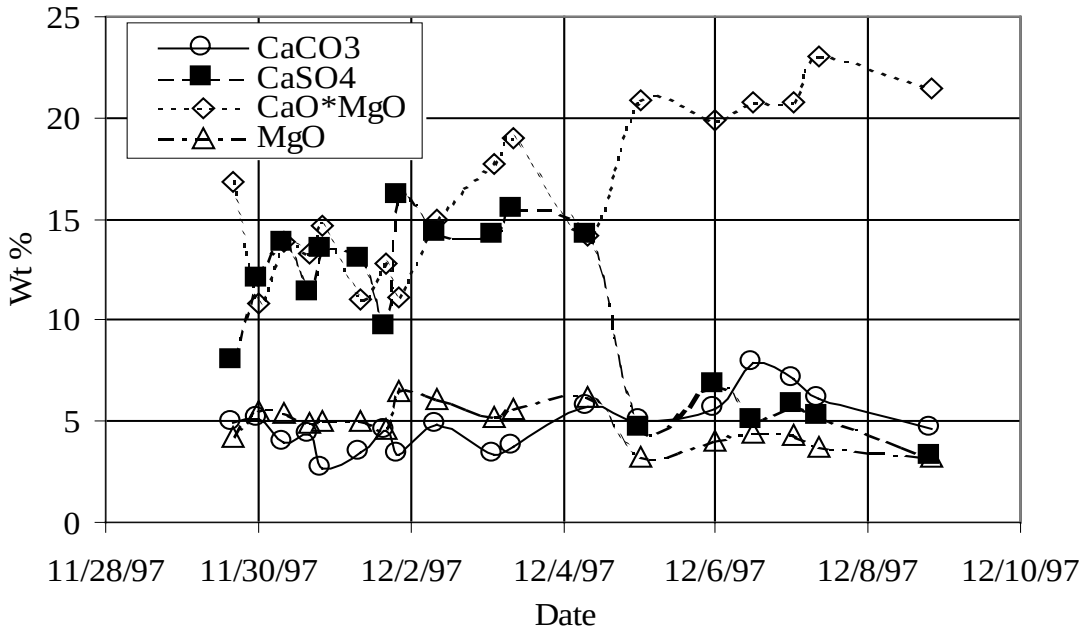

Figure 4.2.5-11 TC01I SP Solids

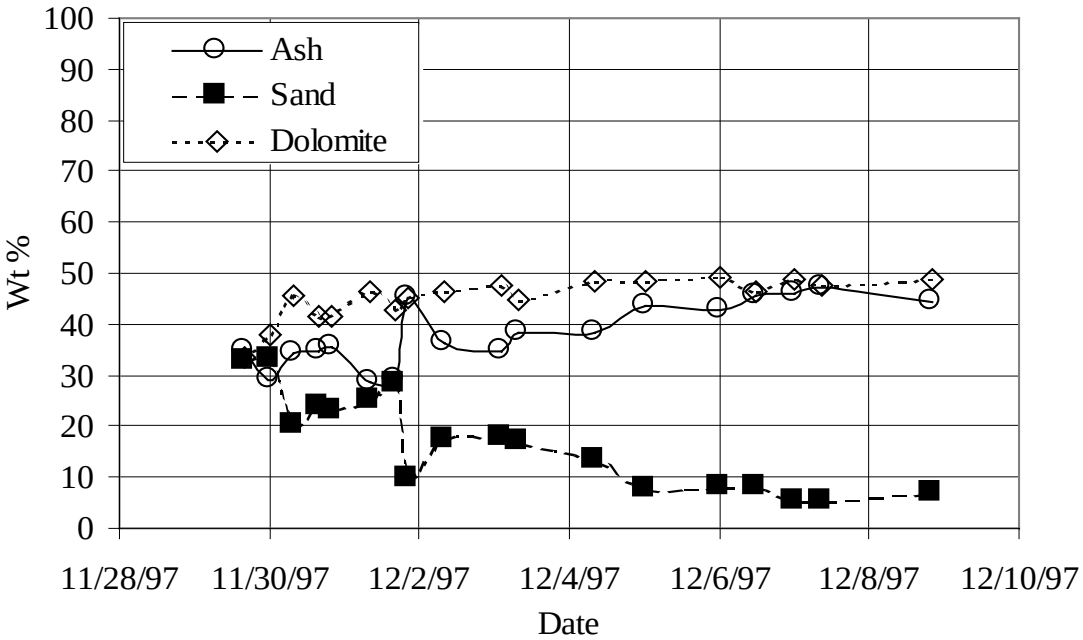

Figure 4.2.5-12 TC01I SP Solids Analysis

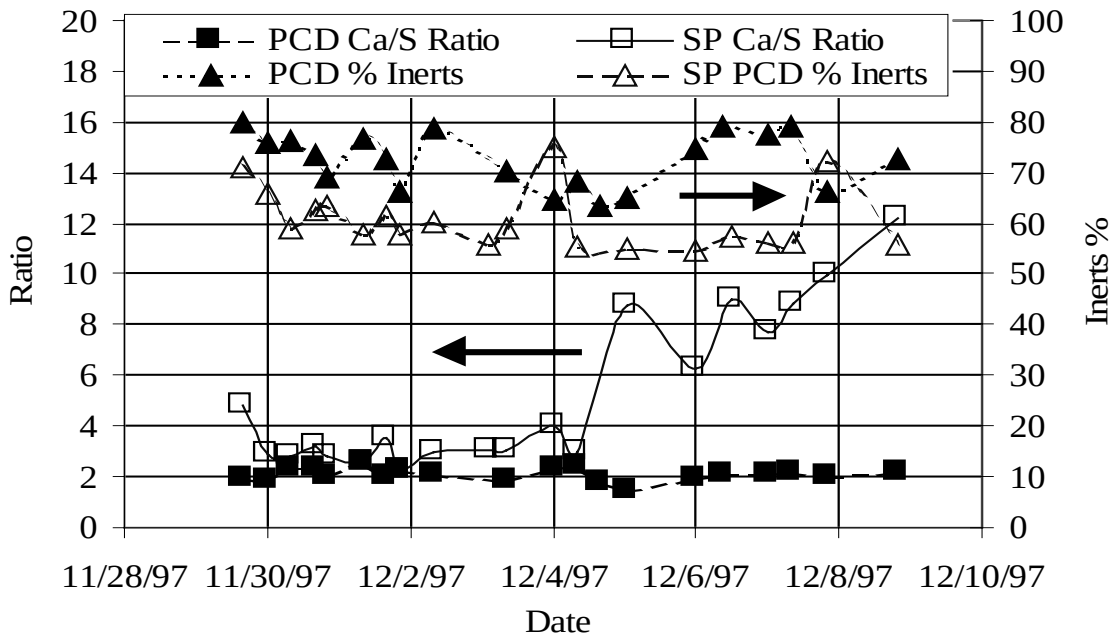

Figure 4.2.5-13 TC01I Solids Analysis

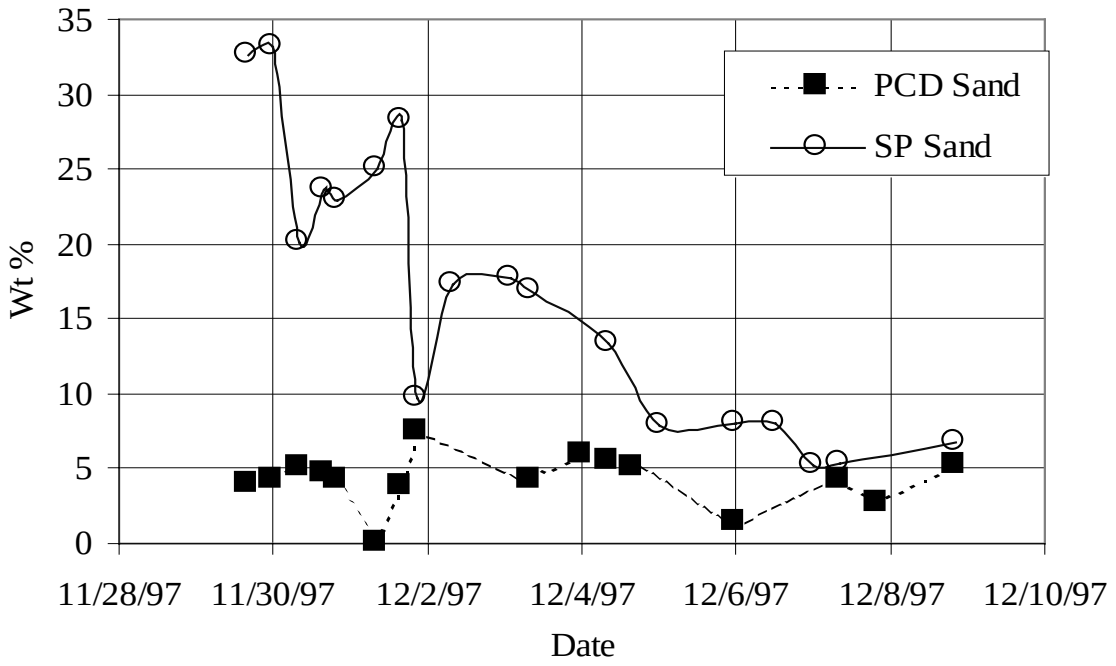

Figure 4.2.5-14 TC01I Solids Analysis

4.2.6 NO_X Emissions

A chemiluminescent analyzer was used to measure NO_X emissions for the 1997 MWK transport reactor tests at the outlet of the PCD. The NO_X concentrations are shown in figures 4.2.6-1 for CCT5 and in 4.2.6-2 for TC01. The NO_X emissions are given in both ppm NO_X and pounds of NO_X per MBtu of fuel fired (# NO_X/MBtu).

The NO_X data plotted is for 6-hour periods of constant operation, except for two periods at the end of CCT5 where the various combustion air rates changed during the 6-hour steady-state period. These two periods were changed to 1.5-hour periods when the combustion air rates were constant. There were no periods of constant operation for CCT4. The NO_X data for CCT6 is not representative of coal-fired transport reactor conditions because the unit was 25 percent cofired with propane. The propane was fired at high-excess air to prevent start-up burner refractory damage. As a result, the CCT6 NO_X data was not plotted and will not be analyzed.

There were limited NO_X analyzer data secured in 1997 due to problems with operability and off-site repair time requirements. The analyzer is ready for the 1998 runs and there are multiple back-up analyzer options ready, if needed.

The NO_X concentration should be a function of the amount of air staging, excess air, and the riser temperature. The purpose of 1997 testing was not to optimize or study NO_X emissions, and as a result the expected trends in operating conditions for the NO_X emissions were not always observed. This occurred mainly because the transport reactor was operated at essentially the same excess air, riser temperature, and amount of air staging for each test. Hence, there was not enough variability in the independent variables to change the NO_X concentration and clearly determine trends in NO_X concentration. The first combustion test of 1998 will be devoted to obtaining some parametric data on the effect of operating conditions on NO_X emissions, as well as determining the minimum NO_X emissions for a given coal feed rate.

The NO_X emissions should decrease with increased staged air. Figure 4.2.6-3 plots the percent staged air against NO_X emissions. There is no dependence of NO_X emissions on percent staged air since there was insufficient variation in percent staged air within each test. Essentially each test produced one data point. However, TC01 had slightly lower NO_X emissions than CCT5 at higher percent staged air, as expected. Further tests at different percent staging should increase confidence in this trend.

The NO_X concentrations for CCT5 and TC01 are plotted against oxygen content of the flue gas on figure 4.2.6-4. The NO_X and O_2 were measured at the PCD outlet. The NO_X emissions slightly increased with increasing percent O_2 concentration, as found when examining all the data. Within each test there does not appear to be any dependence of NO_X on percent O_2. A comparison of figure 4.2.6-3 and -4 indicates that percent staging has a larger effect on NO_X than percent excess air. This conclusion will be tested in 1998 with more extensive NO_X testing.

The NO_X emissions should increase with increasing riser temperature. The riser temperature is plotted against NO_X emissions in figure 4.2.6-5. There does not appear to be any effect of riser

temperature on NO_X emissions, because either there was not enough variation in the riser temperature or the effect of percent staging and excess air overwhelmed the effect of riser temperature. The increased NO_X concentrations in CCT5B probably occurred because CCT5B had higher excess O_2 and less staged air than TC01.

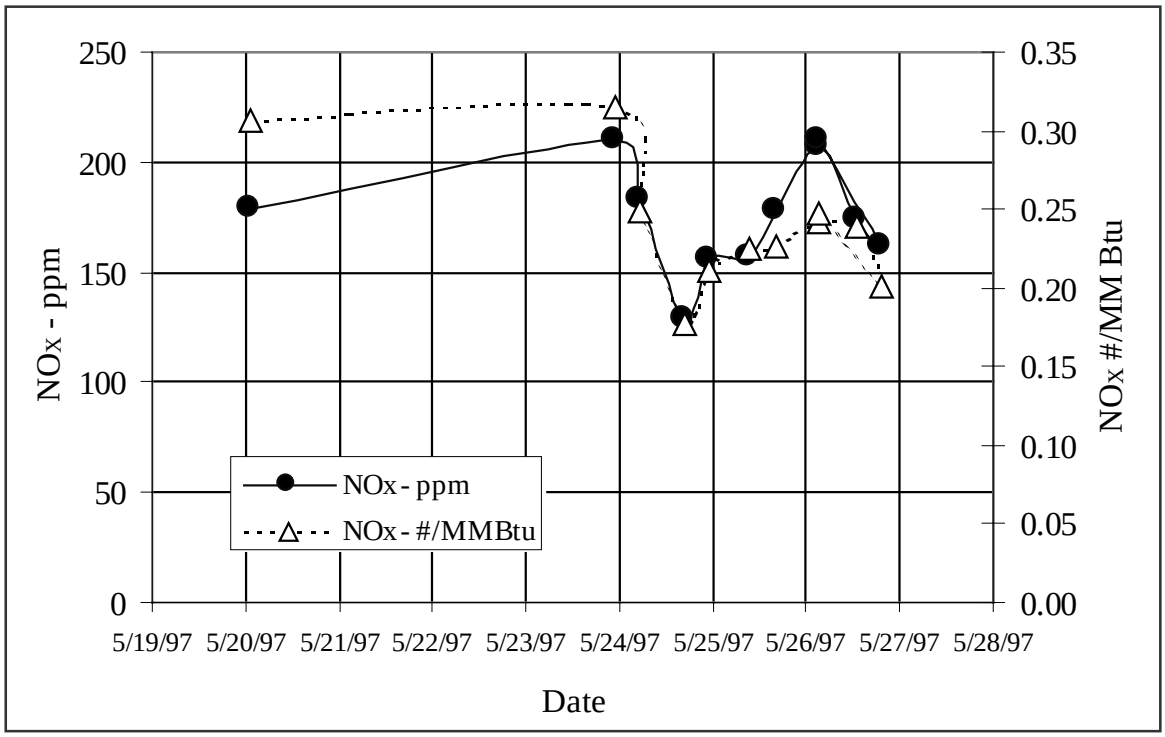

Figure 4.2.6-1 CCT5B NO_x Emissions

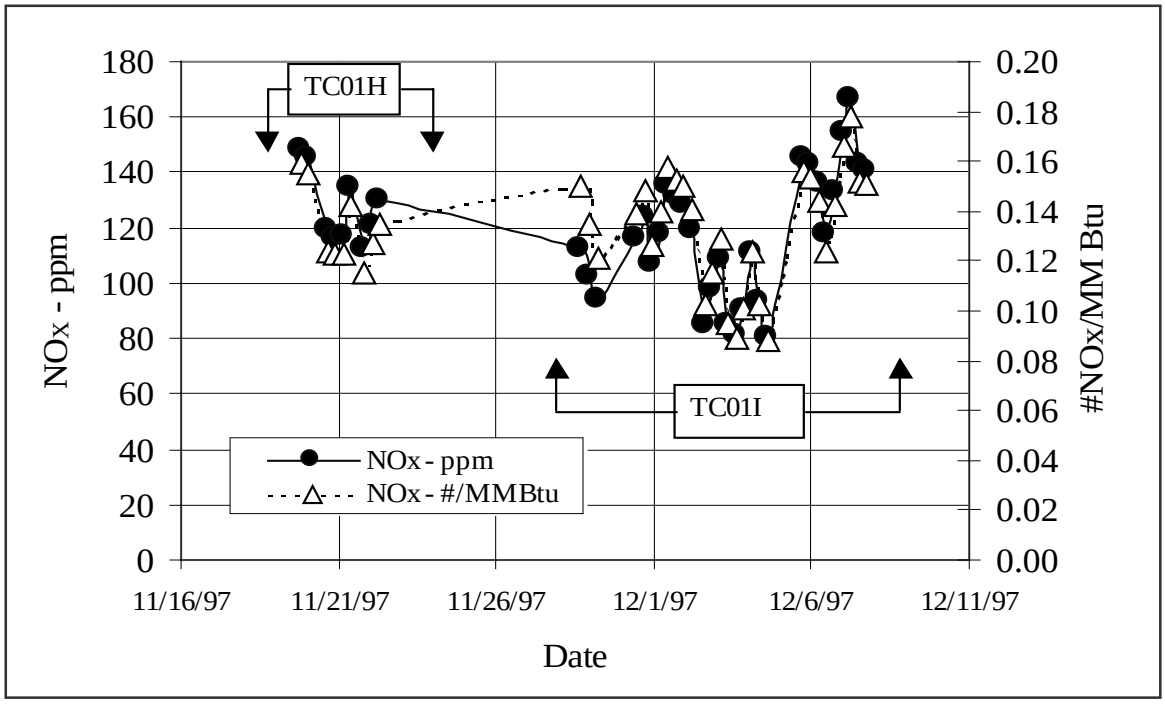

Figure 4.2.6-2 TC01 NO_x Emissions

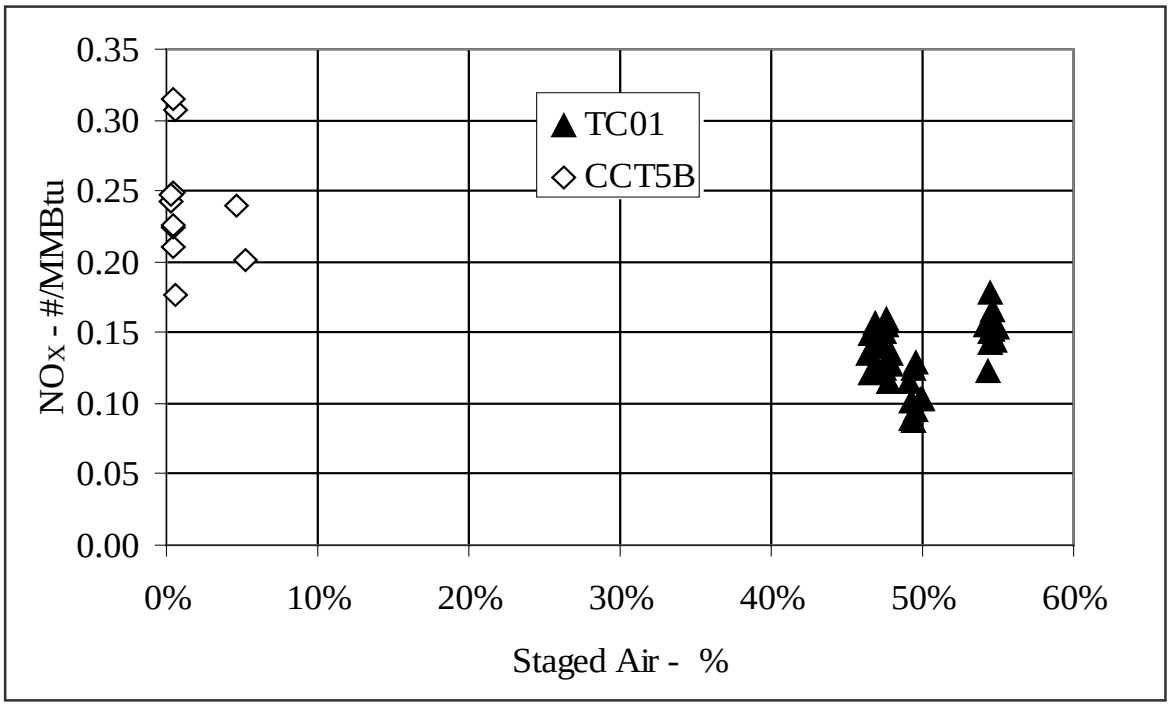

Figure 4.2.6-3 1997 NO_x Emissions and Staged Air

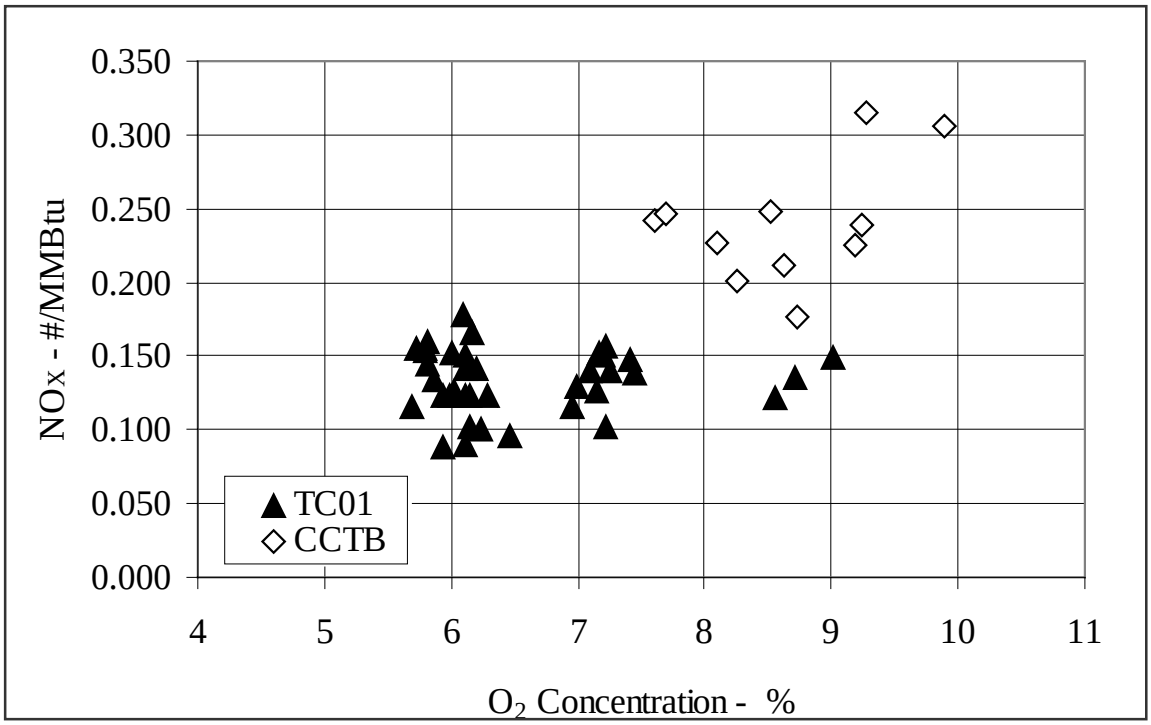

Figure 4.2.6-4 1997 NO_x Emissions and O_2

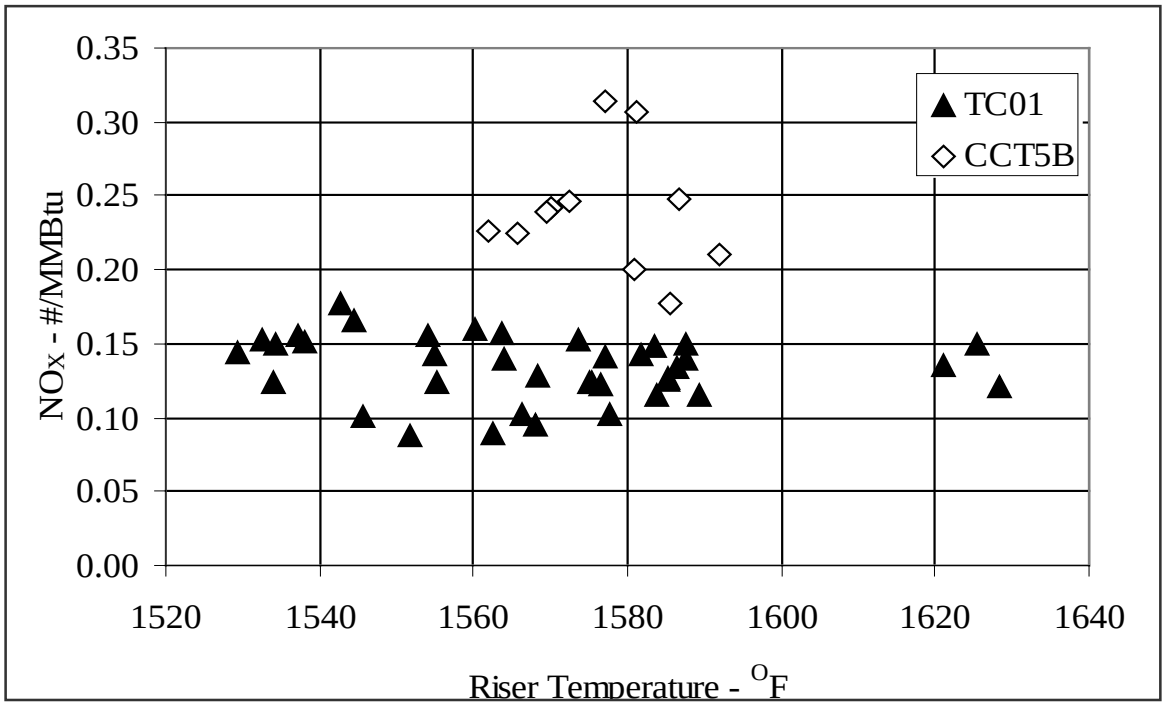

Figure 4.2.6-5 1997 NO_x Emissions and Riser Temperature

4.2.7 Circulation Rate

During 1997, the transport reactor was operated with a wide range of circulation rates. In early 1997, operational problems with the dipleg forced the circulation rate to be held low to avoid excessive carryover of solids to the PCD. As the causes of the instability of the dipleg became better understood, reactor operation became possible at higher circulation rates and without the need to periodically add sand to replace bed material lost due to carryover.

The circulation rate is estimated from the pressure drop in the riser as measured by PDI258 using a modified version of the Konno-Saito (KS) correlation. The acceleration/deceleration terms are ignored and the pressure drop is broken into head losses and friction losses. The simplifying assumptions are that all of the gas enters through the bottom of the riser, there is no internal recirculation of solids, and the slip velocity of the particles is equal to the particles terminal velocity. Under the highest circulation rates calculated, the voidages were calculated to be no less 0.983 with voidages greater than .99 at lower circulation rates. Because of the variability in the measurement of PDI258, the calculation is not considered valid at very low circulation rates.

During CCT4, the circulation rate was very low. In CCT5A, the circulation rates were low, but not as low as in CCT4 (using 1.0 as relative value for the upper range of circulation for CCT4, the upper range of circulation of CCT5A was 1.2 times this period). In CCT5B, the circulation rate was slightly higher (with a relative value of 1.8 for the upper range). In CCT6, the circulation rates varied considerably because of the dipleg testing. The circulation rates in CCT6 were considerably higher on average than CCT5B with some of the circulation rates being the highest measured so far in testing (relative value of 2.8 for the upper range). Immediately after a dipleg upset, however, the rates were extremely low. In TC01, the circulation rate (relative value of 4.0) was higher than in CCT6. Near the end of TC01, the rates were closer to the highest rates in CCT5B because of plugged aeration nozzles.

Many different factors influence the circulation rate in the reactor. The four most important factors are the level of solids in the standpipe, the level of solids in the combustion heat exchanger, the flow of aeration gas to the reactor J-leg, and the flow of aeration gas to the heat exchanger J-leg. Figure 4.2.7-1 from TC01C shows the effect on circulation rate of varying FI680, aeration gas to the heat exchanger J-leg, while holding FI681, aeration to the reactor J-leg, steady. PDI259, a measure of solids level in the standpipe, varied in a narrow range and PDI389, a measure of the solids level in the combustion heat exchanger, also varied in a narrow range. The graph clearly shows the overall circulation rate increasing as the amount of aeration to the heat exchanger J-leg increases. Changing the reactor J-leg aeration has a similar effect on overall circulation rate.

Changing the level of solids in the reactor has a similar predictable effect. Raising the solids level in the standpipe or the heat exchanger increases the overall circulation rate. Figure 4.2.7-2 shows the effect of increasing PDI259, the lower standpipe differential pressure, on the circulation rate. In this case, the solids level in both the standpipe and the heat exchanger were changing while FI681 and FI680 were held steady. Because the circulation rate is a function of both the solids level in the standpipe and the heat exchanger, a better example is figure 4.2.7-3 from CCT6 when the heat exchanger was not in service. In this case, the change in circulation

rate is due solely to the change in the static head of solids in the standpipe since the fluidization to the reactor J-leg was held constant. This graph shows the relationship between PDI255, the middle standpipe DP, and the circulation rate.

It is also interesting to note the relationship between the standpipe level and the heat exchanger level when the aeration to each is constant. Figure 4.2.7-4 from TC01D shows PDI259 plotted against PDI389, the middle DP of the heat exchanger. FI681 and FI680 were both steady. As the level in one of the legs increased, the level in the other leg also increased. This is what one would expect in order to maintain a proper pressure balance as the reactor inventory increases.

Figure 4.2.7-5 shows the variation of the solids circulation rate with the solids level in the heat exchanger. In this case, the level is being measured by PDI388, the overall pressure drop in the heat exchanger. Both FI680 and FI681 were steady. However, increasing heat exchanger level does not always mean an increase in the overall circulation rate. As the solids level in the combustion heat exchanger is raised, a level is reached above which a further increase in the heat exchanger level alone does not increase the circulation rate appreciably. This can best be demonstrated by showing the solids level in the upper heat exchanger plotted against the overall circulation rate. Figure 4.2.7-6 shows PDI236, the level in the upper combustion heat exchanger plotted against the circulation rate. Notice that the plot is essentially flat suggesting that there is no relationship between the two. Plotting the next lower heat exchanger DP, PDI389, and the circulation rate also shows that there is no increase in solids circulation rate once the heat exchanger level reaches a certain level. In figure 4.2.7-7, the circulation rate is shown to increase with PDI389 until PDI389 reaches a certain pressure drop. It should be noted that fluidization through the distribution grid within the heat exchanger, FI230, and fluidization just below the distributor was not varied to determine its effect on solids circulation through the heat exchanger.

Another way to demonstrate this limit is to plot the overall circulation rate and the circulation rate through the heat exchanger with time. Figure 4.2.7-8 shows overall circulation rate and the circulation rate through the combustion heat exchanger in each of the steady operating periods in TC01 from October 23, 1997, through December 8, 1997. At overall circulation rates below a certain value, about 50 percent of the solids circulate through the heat exchanger at the operating conditions present. There is little increase in the amount of solids circulating through the heat exchanger at higher overall circulation rates. The circulation rate through the heat exchanger is limited to a maximum. The balance of the solids circulates through the standpipe alone. Figure 4.2.7-9 shows the same data from TC01 plotted as overall circulation rate versus heat exchanger circulation rate. A trend line has been added showing where the 50-percent split would be located for comparison. The plot follows this line and then shows a sharp change in slope for higher circulation rates. Once a maximum flow rate through the combustion heat exchanger has been reached, the coal feed cannot be increased due to the inability to remove additional heat via the combustion heat exchanger for temperature control.

An explanation for this limiting effect is found by looking at the temperatures in the boot and the J-leg of the heat exchanger at different solids flow rates. TI379 is located at the bottom of the heat exchanger J-leg where the solids enter the J-leg from the heat exchanger boot. TI378 is at the top of the heat exchanger J-leg. When the heat exchanger level is high, TI378 and TI379 read roughly the same temperatures. However, TI378 is higher than TI379 at lower circulation

rates. Figure 4.2.7-10 shows TI378 and TI379 plotted against the overall circulation rate during TC01E. The graph shows a difference of 300°F at low circulation rates and a difference of only a few degrees a circulation rate of 60,000 lb/hr. This difference can be as much as 500°F at very low heat exchanger levels. Because the aeration gas to the J-leg is relatively cold, the best explanation for the elevated temperatures is that solids from the mixing zone are back mixing into the heat exchanger J-leg. For this to occur, the J-leg could not be full of solids. When the circulation rate through the heat exchanger becomes great enough, the J-leg becomes full of fluidized solids and no back mixing from the mixing zone can occur. It is at this point that additional solids level in the heat exchanger can no longer provide an increase in the rate of solids circulating through the heat exchanger. The rate can only be increased through additional aeration.

This limit on the circulation rate has an important effect on the coal-feed rate to the reactor. Because the combustion heat exchanger is used for temperature control in the reactor, a limit on the rate of solids circulation through the heat exchanger limits the coal-feed rate. It has been shown that increasing the heat exchanger solids level does not increase the circulation through the heat exchanger once PDI389 reaches a certain level. In TC01, the heat exchanger level was filled to the solids inlet on December 3 and 4, 1997, without increasing the circulation rate. FI680 was also operated at 80- to 90-percent open during most of TC01, leaving little room for additional circulation through increasing aeration in the J-leg. It may be possible to increase the solids circulation through the heat exchanger by changing the aeration rate in the boot of the heat exchanger or in the heat exchanger itself.

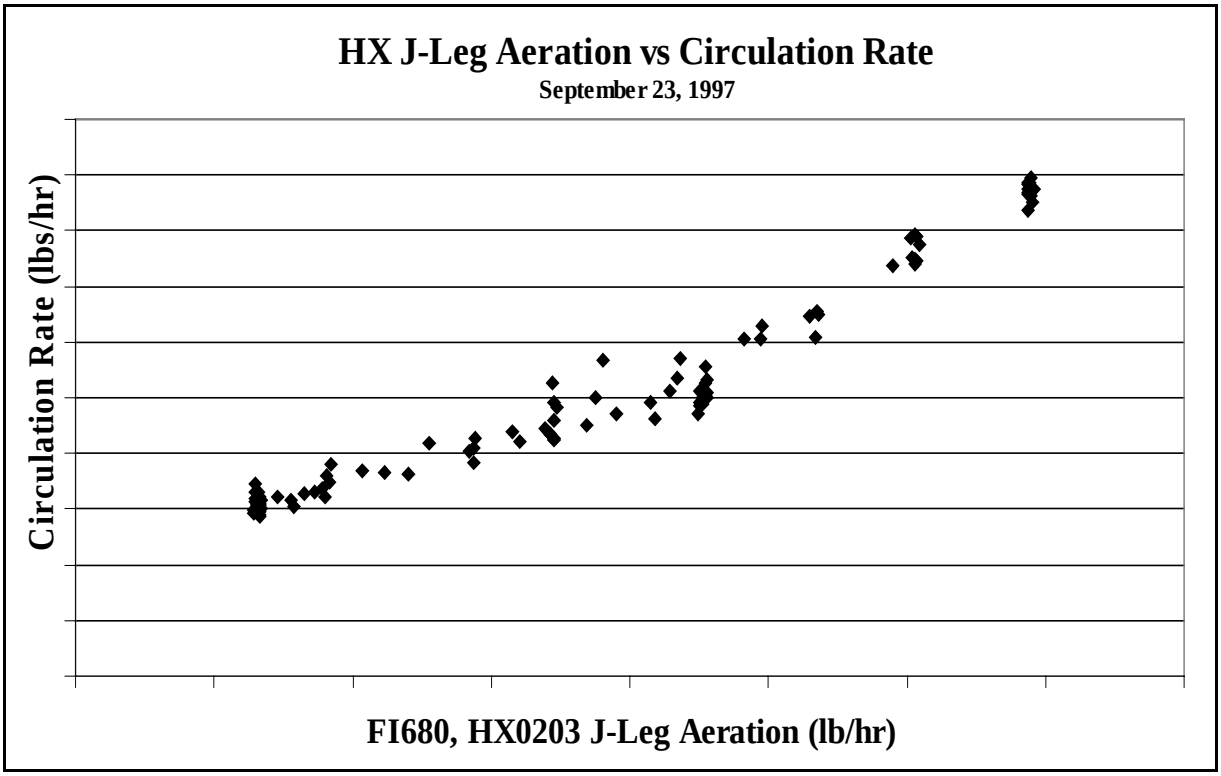

Figure 4.2.7- 1 Effect on Overall Circulation Rate by Changing Heat Exchanger J-leg Aeration

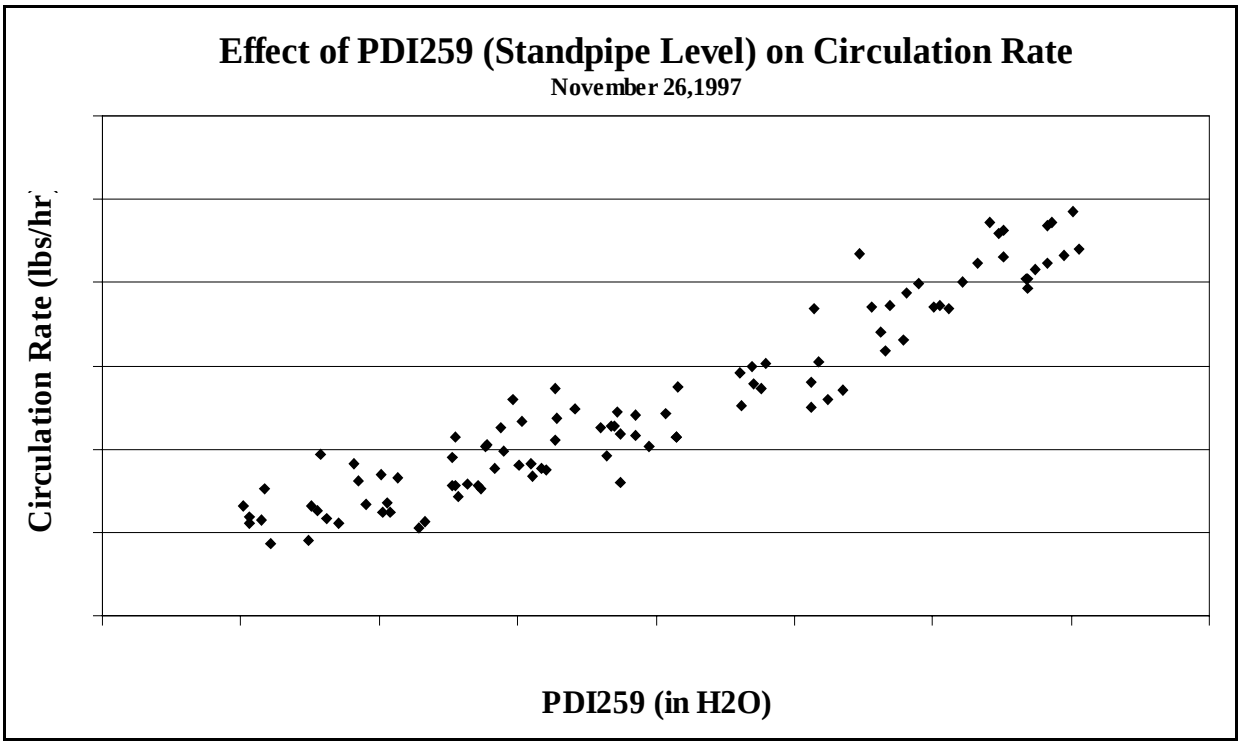

Figure 4.2.7- 2 Change in Circulation Rate With Increasing Standpipe Solids Level

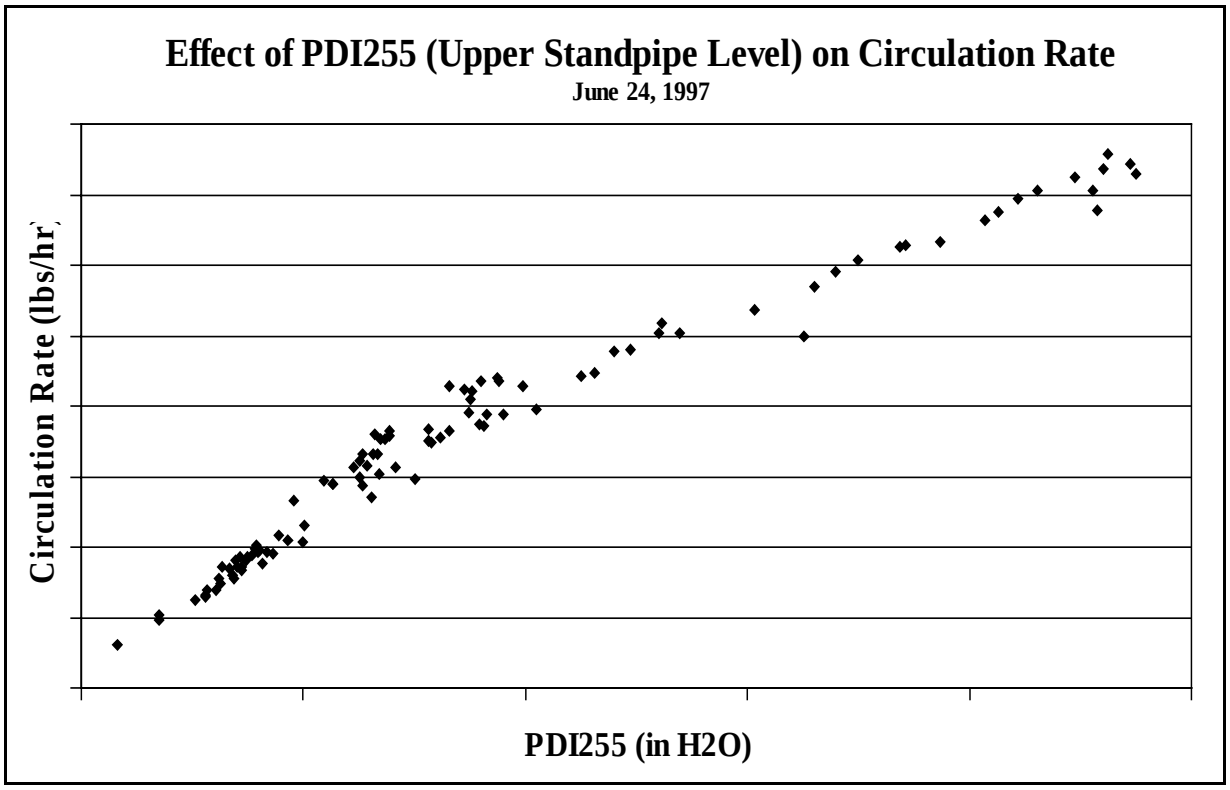

Figure 4.2.7- 3 Change in Circulation Rate With Increasing Standpipe Solids Level

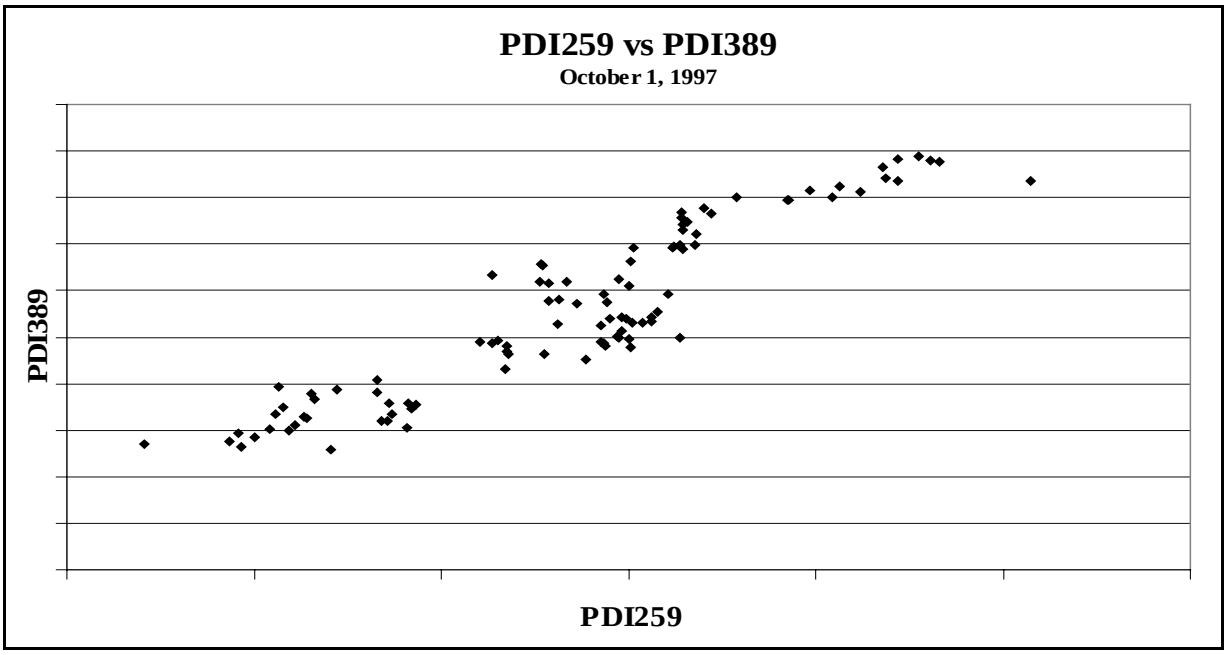

Figure 4.2.7- 4 Relationship Between the Standpipe and Heat Exchanger Solids Level

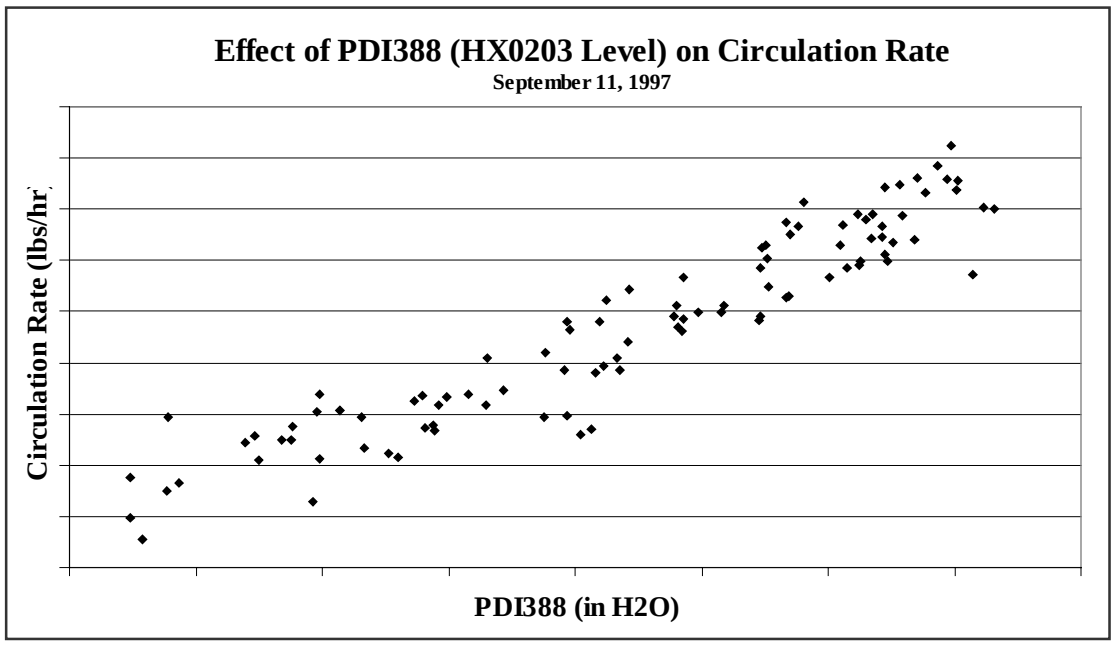

Figure 4.2.7- 5 Change in Circulation Rate With Increasing Heat Exchanger Solids Level

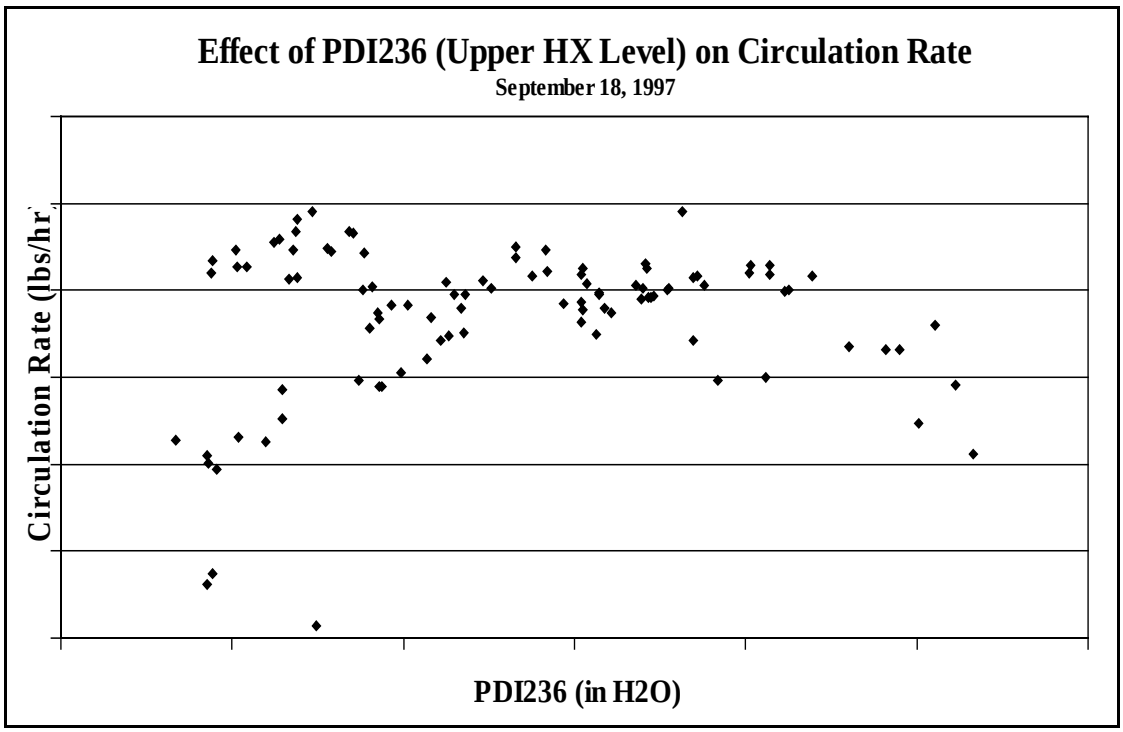

Figure 4.2.7- 6 Lack of Change in the Circulation Rate as Solids Level Increases In Upper HX

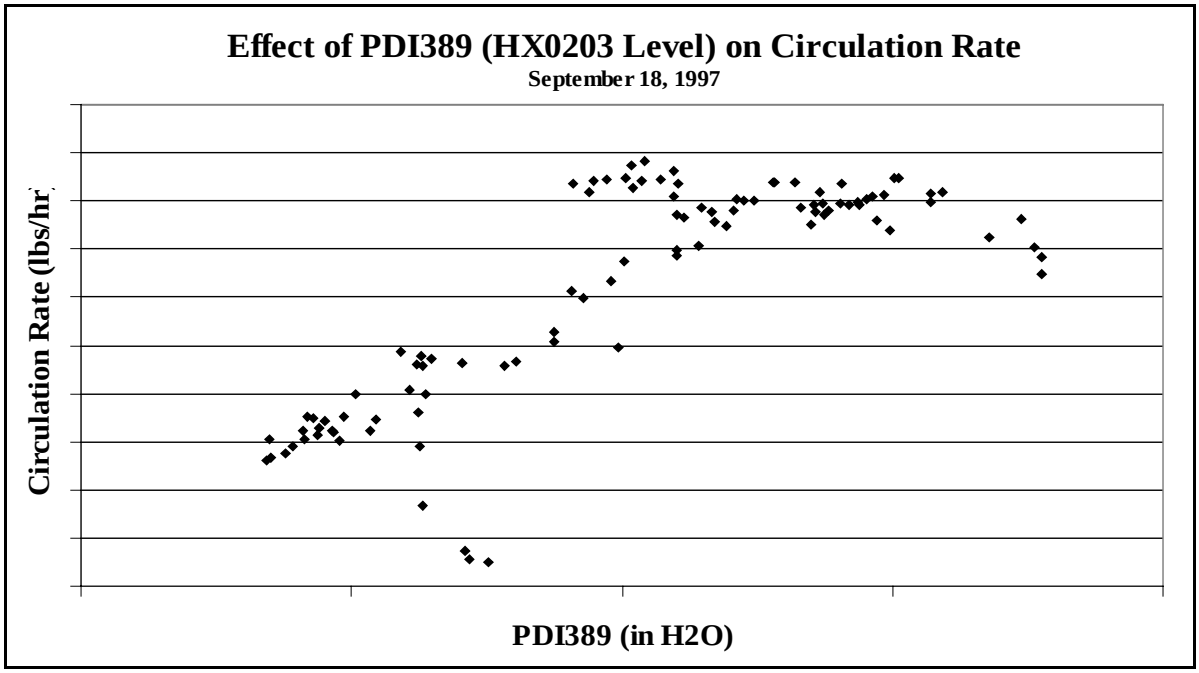

Figure 4.2.7- 7 Circulation Rate Fails to Increase Once PDI389 Reaches Certain Value

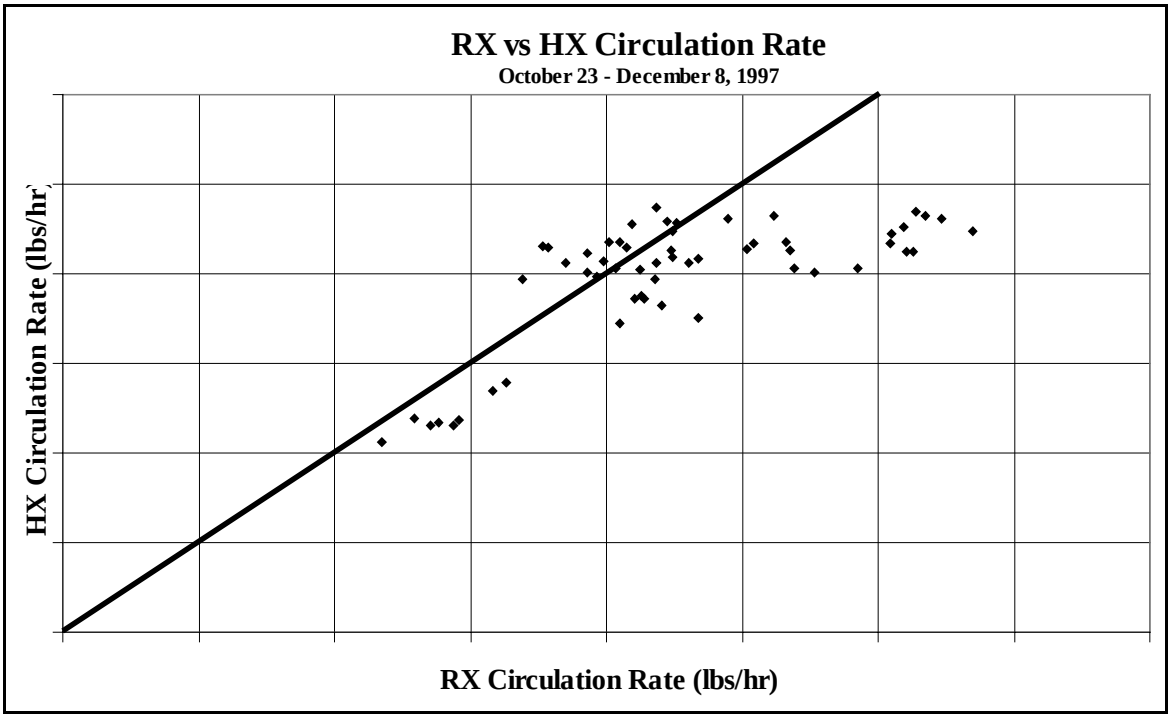

Figure 4.2.7- 8 Overall Circulation Rate and Heat Exchanger Circulation Rate

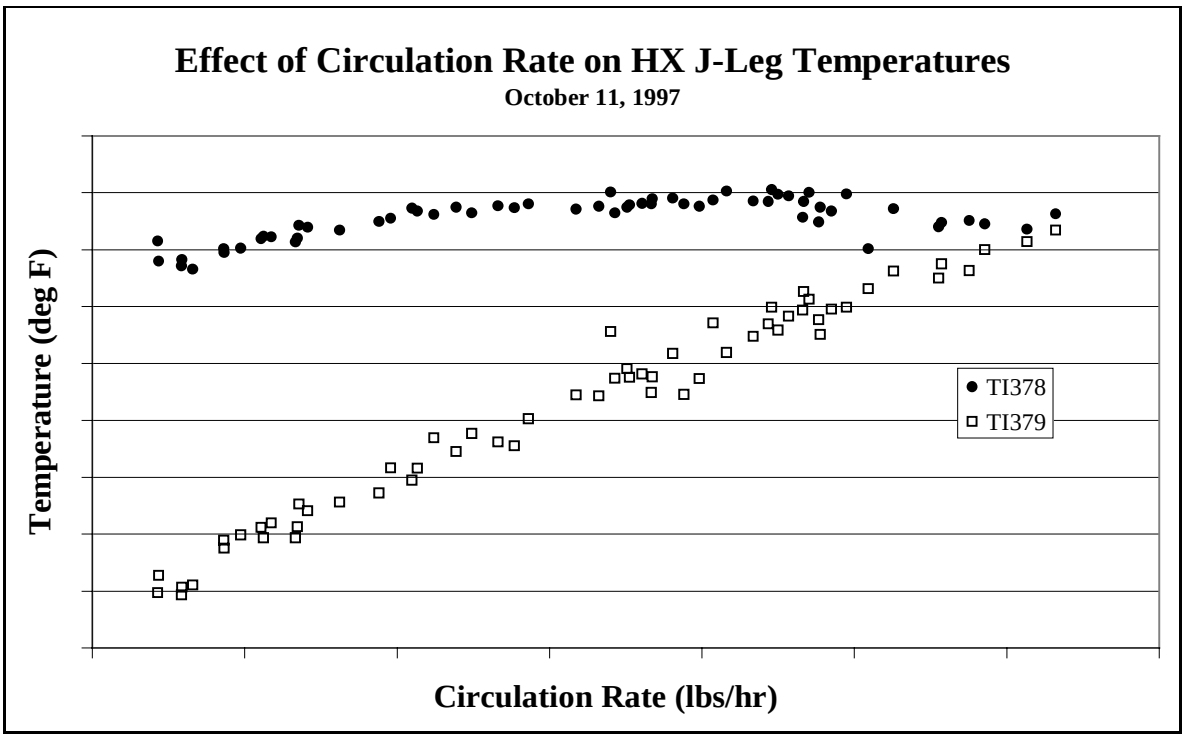

Figure 4.2.7- 9 Overall Circulation Rate and Heat Exchanger Circulation Rate

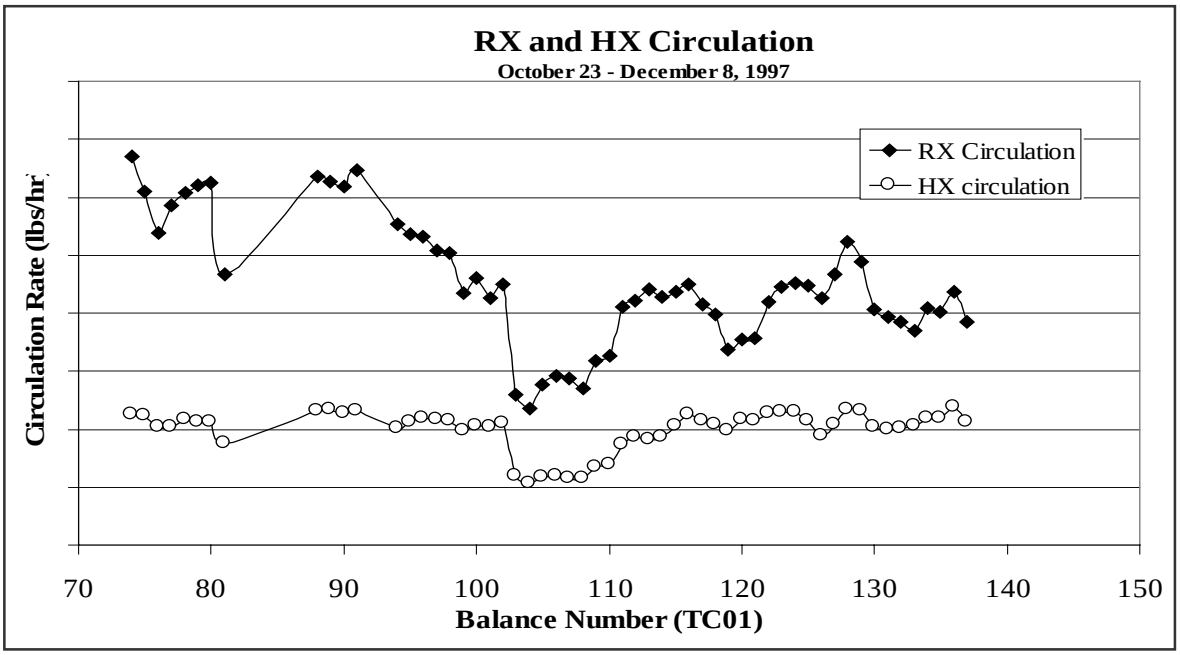

Figure 4.2.7-10 Effect of Overall Circulation Rate on Heat Exchanger J-leg Temperatures (TI378 at Top of J-leg, TI379 at Bottom of J-leg)

4.2.8 Pressure Profile

The relationship between circulation rate and pressure drop can be divided into three basic categories: 1) areas in which the entire flow is in the dilute phase; 2) areas where an interface exists between the dilute phase and the dense phase; and 3) areas where the entire flow is in the dense phase.

Figure 4.2.8-1 shows a typical pressure profile for the transport reactor. The pressure is plotted at various heights in the reactor. The solid line shows the profile through the main reactor components. At the top left of the figure is the riser crossover. Moving down in the figure is the standpipe. Up the right side of the chart are the J-leg, the mixing zone, and the riser. The dashed lines show the pressure drop in the dipleg, the primary cyclone, and the combustion heat exchanger. The two ends do not meet because of areas in the reactor where the pressure drop is not measured. The chart shows a typical pressure profile for the reactor. Pressure is lost in the J-legs, mixing zone, riser, disengager, and cyclone due to friction losses and losses associated with lifting the solids. In the standpipe, the dipleg, and the combustion heat exchanger the pressure is recovered as the solids flow by gravity back to the J-legs.

In the areas of the reactor in which high voidages occur, the circulation rate has a strong influence on the pressure drop. These areas are the mixing zone, the riser, the disengager, and the top of the standpipe, with voidages in excess of 90 percent. The pressure drop measured in these areas tends to be much lower than the pressure drop in areas of higher density. Figure 4.2.8-2 plots four differential pressure cell readings from dilute-phase regions of the reactor against circulation rate. These readings show very strong linear relationships between pressure drop and circulation rate. The circulation rate for this example was calculated based on PDI258 (the riser differential pressure).

In the standpipe and heat exchanger are interfaces between dilute- and dense-phase solids flow. Differential pressure measurements across this boundary are measuring the level of solids in the reactor. Section 4.2.7 of this report contains a discussion of the strong correlation between solids level and circulation rate. A higher solids level increases the driving force available to propel the circulation rate.

The pressure drop in regions of the reactor that are continually filled with solids, such as the lower levels of the standpipe and heat exchanger and the J-legs, shows little variation with changing circulation rates. Pressure drop variations in these areas are mainly a function of changes in bed density. The bed density changes as a function of solids density and aeration rates. Figure 4.2.8-3 shows the pressure drop measured in the J-legs and in the heat exchanger standpipe during a period in TC01E when the circulation rate was reduced due to a plug in the fine ash conveying line. All three measurements show very little change in pressure drop during the changes in circulation rate. In contrast, figure 4.2.8-4 shows the decrease in pressure drop with time for these same instruments at the beginning of TC01D as sand is replaced in the bed. As the sand in the bed is replaced with ash and dolomite the bed density decreases, which lowers the differential pressure across these regions.

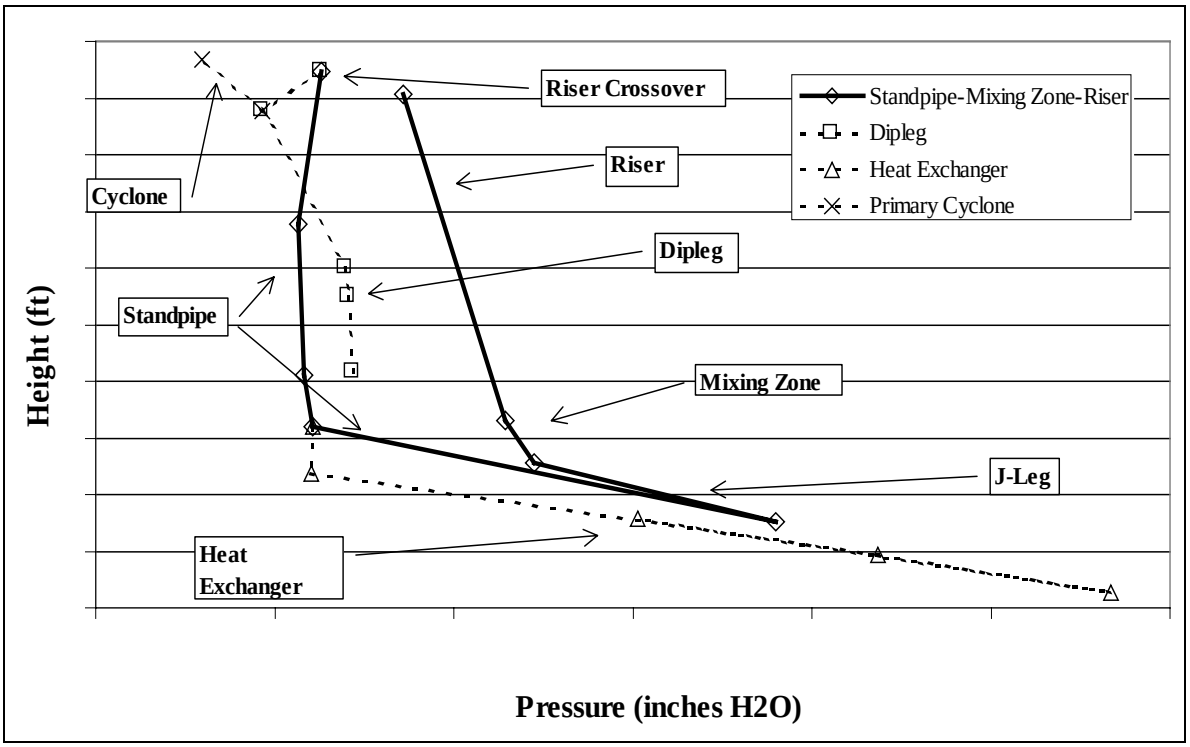

Figure 4.2.8-1 Typical Pressure Profile in Transport Reactor From 12:00 on October 23, 1997, in TC01F

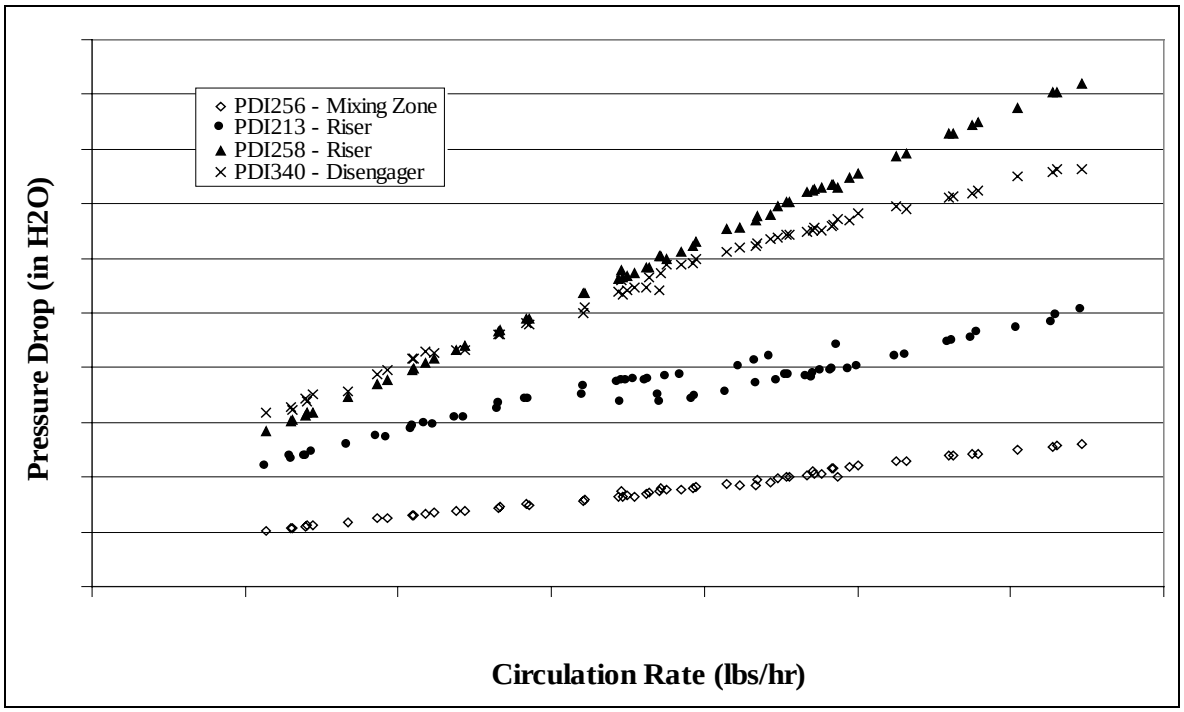

Figure 4.2.8-2 Effect of Circulation Rate on Pressure Drop in Areas of Transport Reactor With High Voidages From October 12, 1997, During TC01E

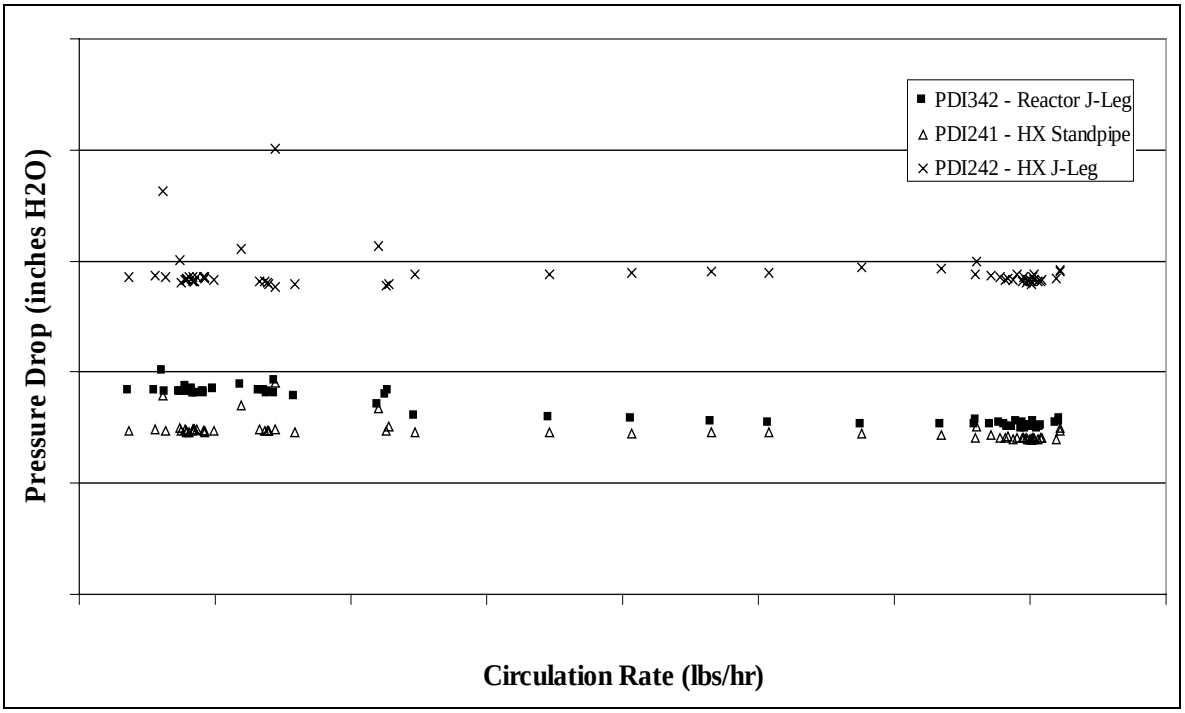

Figure 4.2.8-3 Effect of Circulation Rate on Pressure Drop in Areas of Transport Reactor Filled With Solids From October 14, 1997, During TC01E

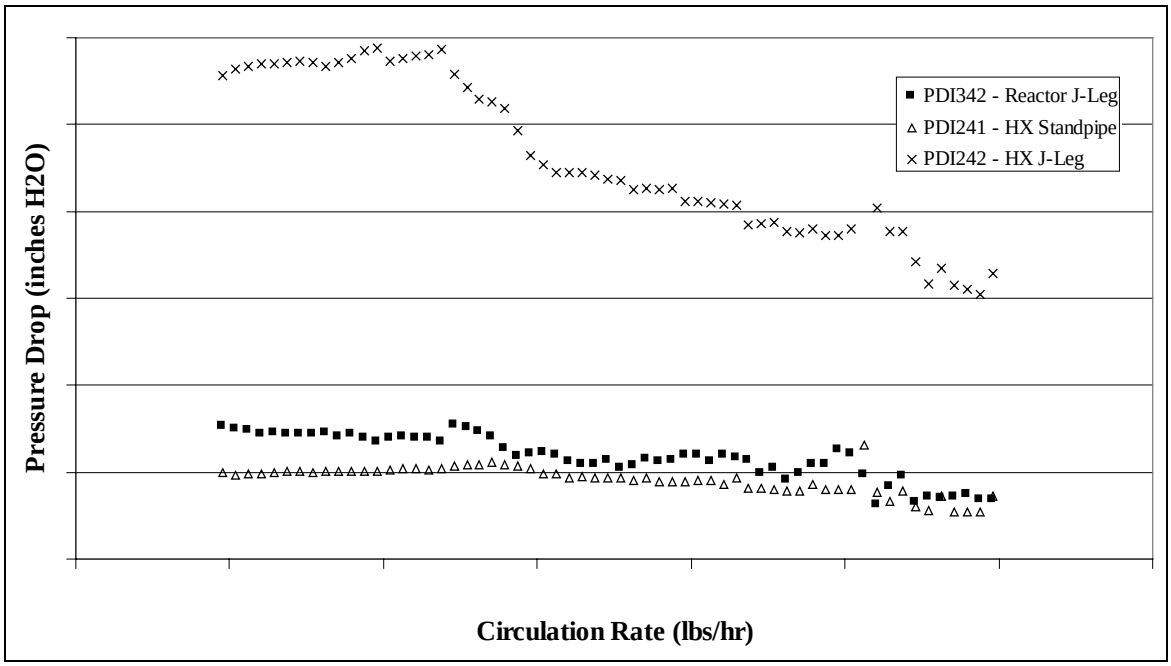

Figure 4.2.8-4 Change in Pressure Drop in Dense-Phase Areas as Ash and Dolomite Replace Sand as the Bed Material From the Start of TC01D on October 2, 1997

4.2.9 Temperature Profile

More than 40 thermocouples are distributed throughout the transport reactor. Temperature profiles of the various parts of the reactor can be developed by using different combinations of these thermocouples. Figure 4.2.9-1 shows typical temperature profiles from both a period of low-solids circulation and a period of high-solids circulation. The period of low-solids circulation rate is from October 11 and 12, 1997, during TC01E. The average circulation rate during this time was about 30,000 lb/hr. The high-circulation rate data is from September 12, 1997, during TC01B and features an average circulation rate of about 110,000 lb/hr. Included on figure 4.2.9-1 are the temperatures in the reactor and heat exchanger J-legs.

Regarding the relationship between the temperatures in the J-legs and the temperature in the bottom of the mixing zone, as would be expected, the solids from the heat exchanger J-leg are cooler than the solids in the mixing zone and the solids from the standpipe are much hotter than the solids in the mixing zone. The introduction of the hot standpipe solids produces a noticeable change in the temperature of the mixing zone. The heat exchanger solids are warmed as they are lifted in the J-leg, while standpipe solids are cooled as they pass through the reactor J-leg. An explanation for this observation is provided in section 4.2.9. The solids increase in temperature as they travel up the mixing zone due to coal combustion. The temperature at the top of the mixing zone is higher in the low-circulation case because there are fewer solids available to absorb the heat released by the coal. The solids in the low circulation case are cooler as they return from the standpipe and the heat exchanger because the longer residence times in the standpipe and heat exchanger allow more heat loss from the solids to the surroundings.

Figure 4.2.9-2 shows the riser temperature profile from the same two periods as shown in figure 4.2.9-1. However, this figure shows the profile from the top measurement in the mixing zone through the riser to the top of the standpipe. The temperature profile through primary cyclone is included on this figure. The temperatures in the standpipe are higher than the riser temperatures and the high temperature at the cyclone entrance at low-circulation rates. The conclusion is that with the conditions present during these tests, solids continued to burn in the riser crossover, the disengager, and the upper standpipe. This temperature pattern is normal with the exception of the temperature at the entrance to the primary cyclone. The elevated temperatures at the cyclone entrance are generally seen only during the early parts of a test run when the reactor pressures are lower and the velocities higher. The other characteristics of this profile are normal. The temperature of the material in the reactor increases due to combustion as the materials flow through the riser. The material exiting the primary cyclone is noticeably cooler due to the effect of the cool gas in the vent line from the combustion heat exchanger entering the cyclone crossover.

The standpipe, dipleg, and combustion heat exchanger temperature profiles for the same period are shown in figure 4.2.9-3. In the standpipe and the dipleg, the solids cool as they flow downward, but the solids at low circulation are much cooler at the bottom of the standpipe than the solids at high-circulation rate, despite starting at a slightly higher temperature. The effect on temperature from mixing the hot solids in the standpipe with the

cooler solids from the dipleg can also be noticed. The solids level in the combustion heat exchanger can easily be discerned from the temperature profile.

More can be learned by looking at the variation in temperature profiles with changing circulation rates. As the circulation rate increases, the differences in temperature from place to place become less evident. Figure 4.2.9-4 shows the highest and lowest temperature in the riser for the steady state periods in CCT5, CCT6, and TC01. Figure 4.2.9-5 shows the highest and lowest temperature in the dipleg for the same period. For all of the regions of the reactor there were noteworthy differences in the range of the temperature when looking at low-circulation rates and high-circulation rates. In this example 20,000 lb/hr was used as the value for a low-circulation rate and 100,000 lb/hr was used as the value for a high-circulation rate. Table 4.2.9-1 summarizes the differences.

Increasing circulation rates leveled the temperature profile in the reactor by decreasing the higher temperatures and raising the lower temperatures. The increased flow of solids decreased the residence time of the solids in the standpipe, dipleg, and combustion heat exchanger. The solids did not lose as much heat to the surroundings and were returned to the mixing zone at a higher temperature because of this. The increased solids in the mixing zone and the riser absorbed more heat, which was released by the burning coal, and lowered the rise in temperature. Under the normal operating conditions during 1997, the highest temperature in the reactor was found in the top of the standpipe. At very low-circulation and coal-feed rates, the highest temperature was found at some point in the riser. There were even isolated instances where the highest temperature was measured at the boundary between the mixing zone and the riser.

As discussed in section 4.2.9, at overall circulation rates of less than about 80,000 lb/hr there was evidence of hot solids back-mixing into the heat exchanger J-leg. Figure 4.2.9-6 shows the change in temperatures with increasing circulation rate for TI377, TI378, and TI379 (the bottom of the mixing zone, the top of the J-leg, and the bottom of the J-leg, respectively). The steady state values from CCT5, CCT6, and TC01 are included. The graph shows TI378 and TI379 becoming roughly equal in temperature above a certain circulation rate. Below this circulation rate the temperature in the top of the J-leg is higher than the temperature in the bottom of the J-leg, therefore providing evidence of hot solids back-mixing from the mixing zone. Above this rate the two temperatures are approximately equal. In contrast, the solids from the standpipe do not show any evidence of back-mixing in the reactor J-leg. Figure 4.2.9-7 shows the estimated temperature at the top of the reactor J-leg, when the cooling effect of the aeration gas is taken into account, and the actual temperature at the top of the J-leg measured by TI376. If solids from the mixing zone were being back-mixed into the J-leg, the temperatures measured by TI376 would be lower.

Table 4.2.9-1

Temperature Profile of the Standpipe

Region	Temperature Difference at Low-Circulation Rate	Temperature Difference at High-Circulation Rate
Mixing Zone	500	300
Riser	150	100
Standpipe	125	100
Dipleg	175	50

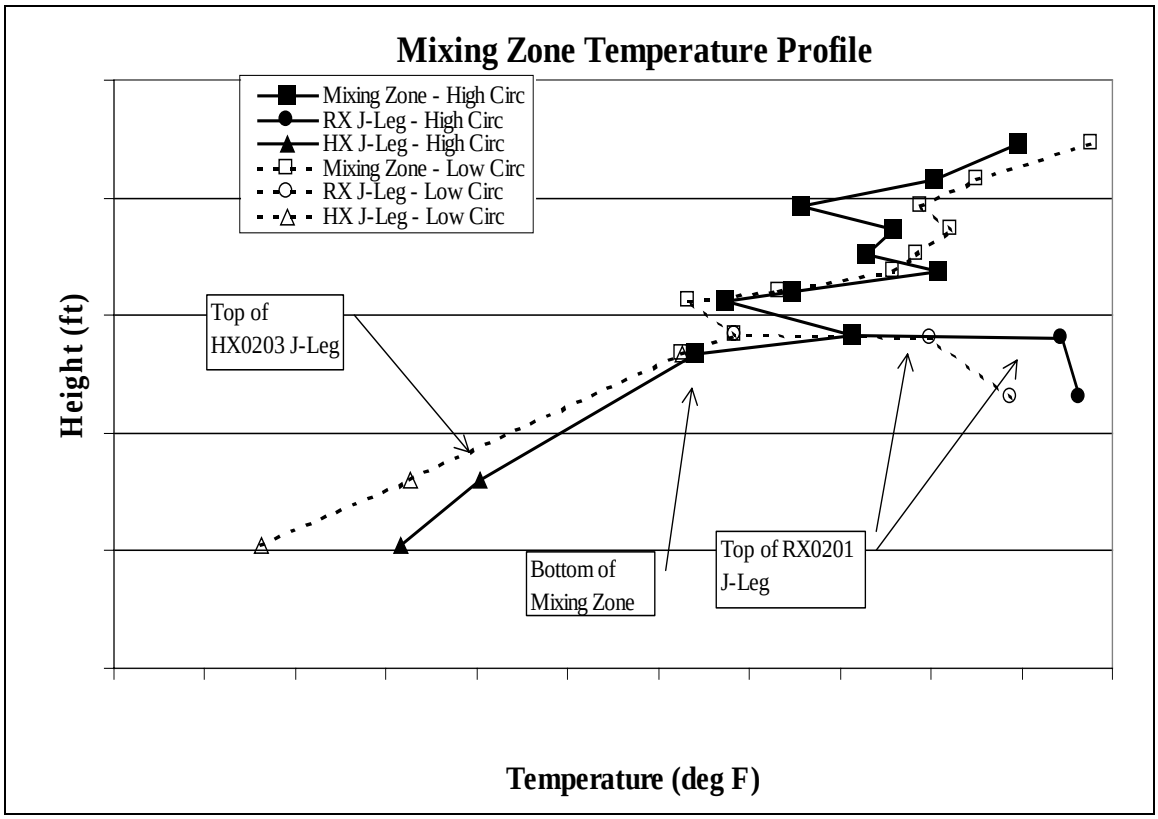

Figure 4.2.9-1 Temperature Profile of the Reactor Mixing Zone

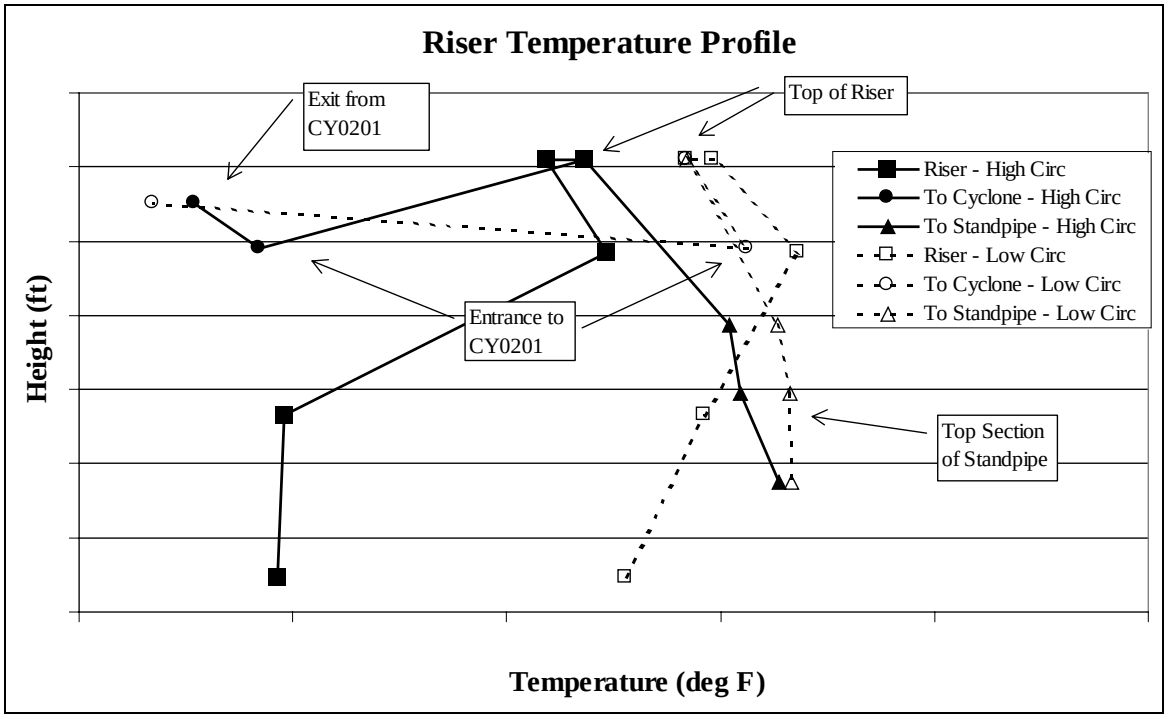

Figure 4.2.9-2 Temperature Profile of the Riser

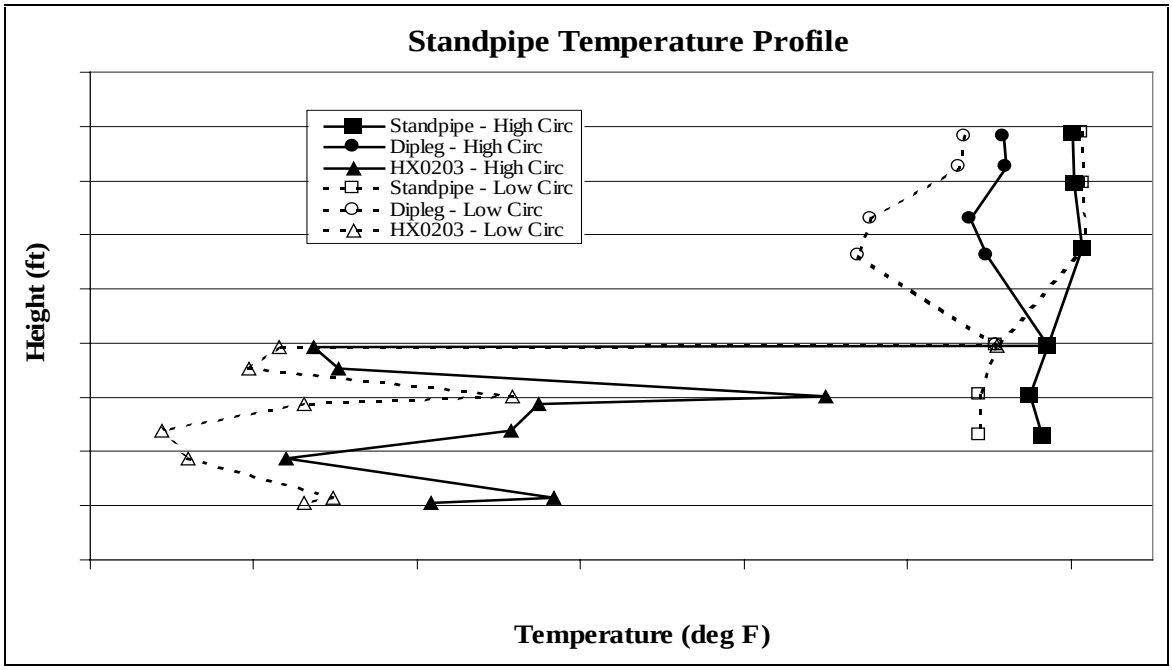

Figure 4.2.9-3 Temperature Profile of the Standpipe

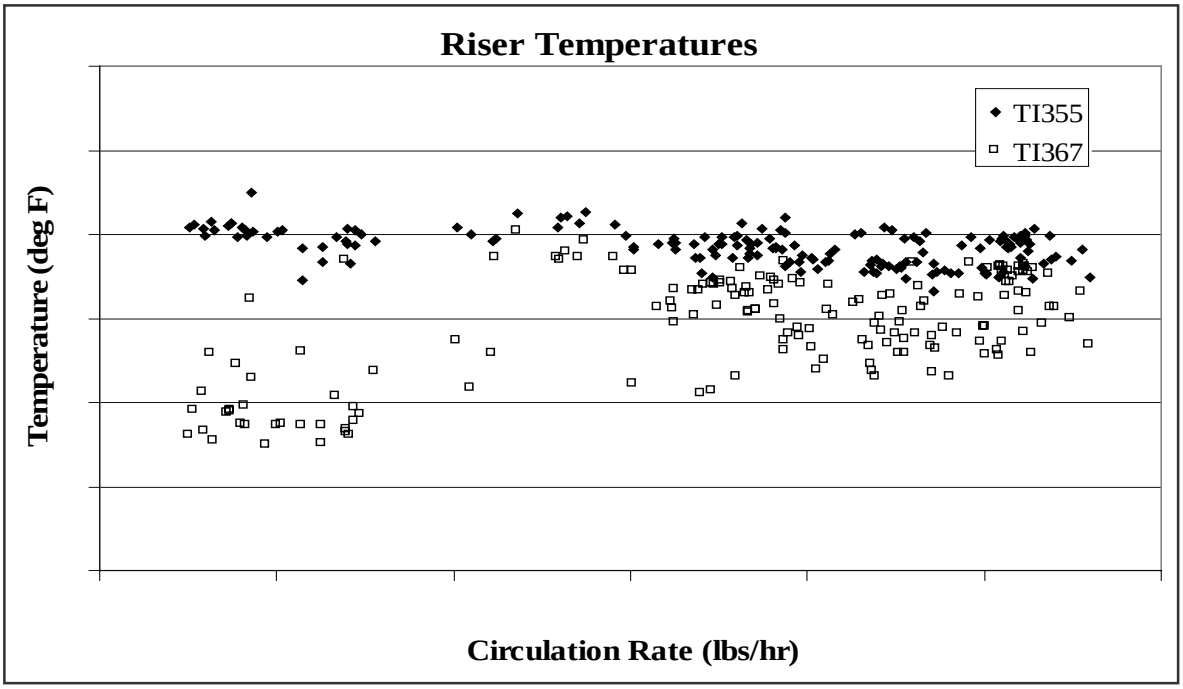

Figure 4.2.9-4 Highest and Lowest Temperatures in the Riser

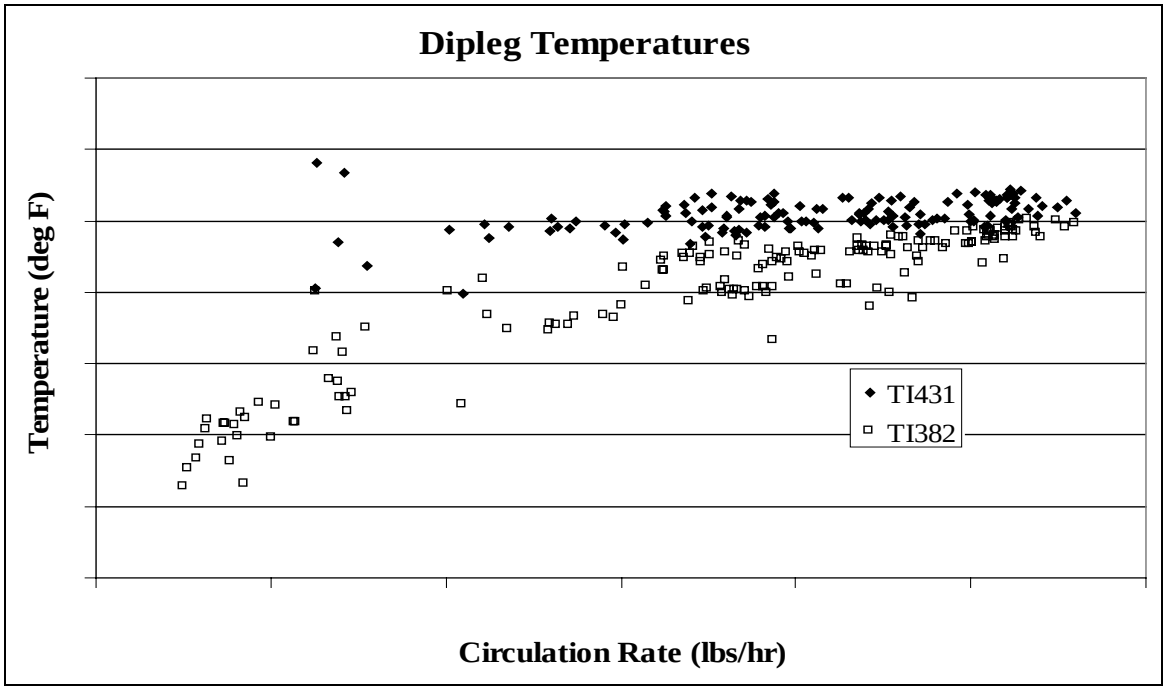

Figure 4.2.9-5 Highest and Lowest Temperature in the Dipleg

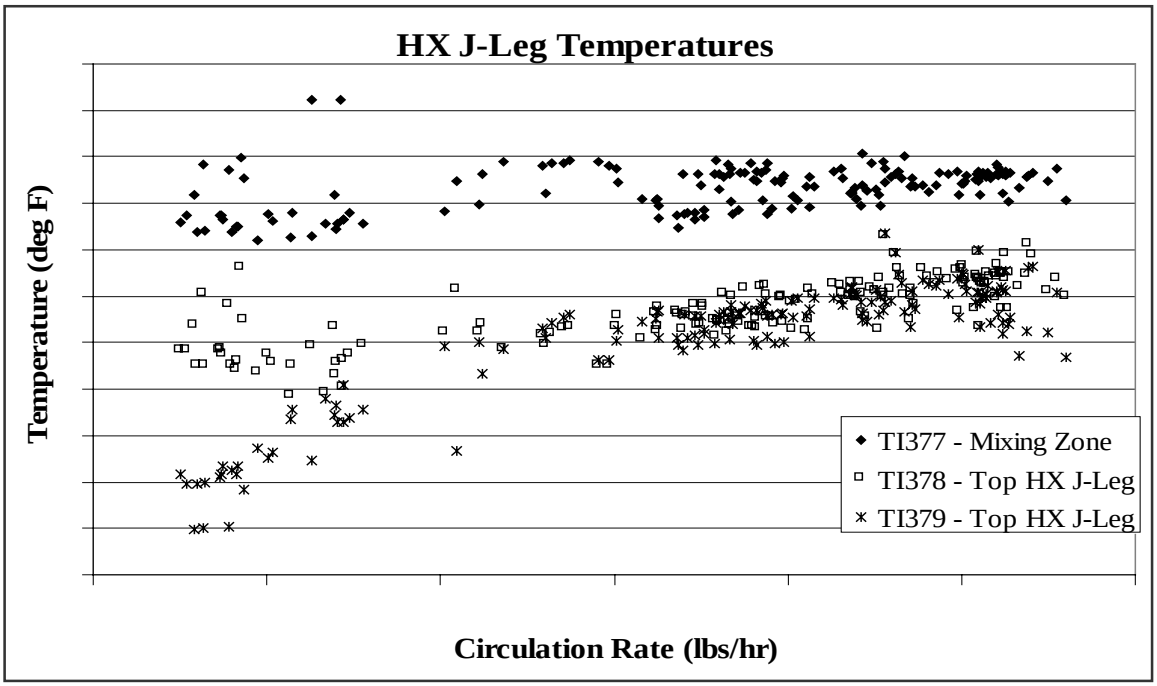

Figure 4.2.9-6 Temperatures in the Heat Exchanger J-leg and the Mixing Zone

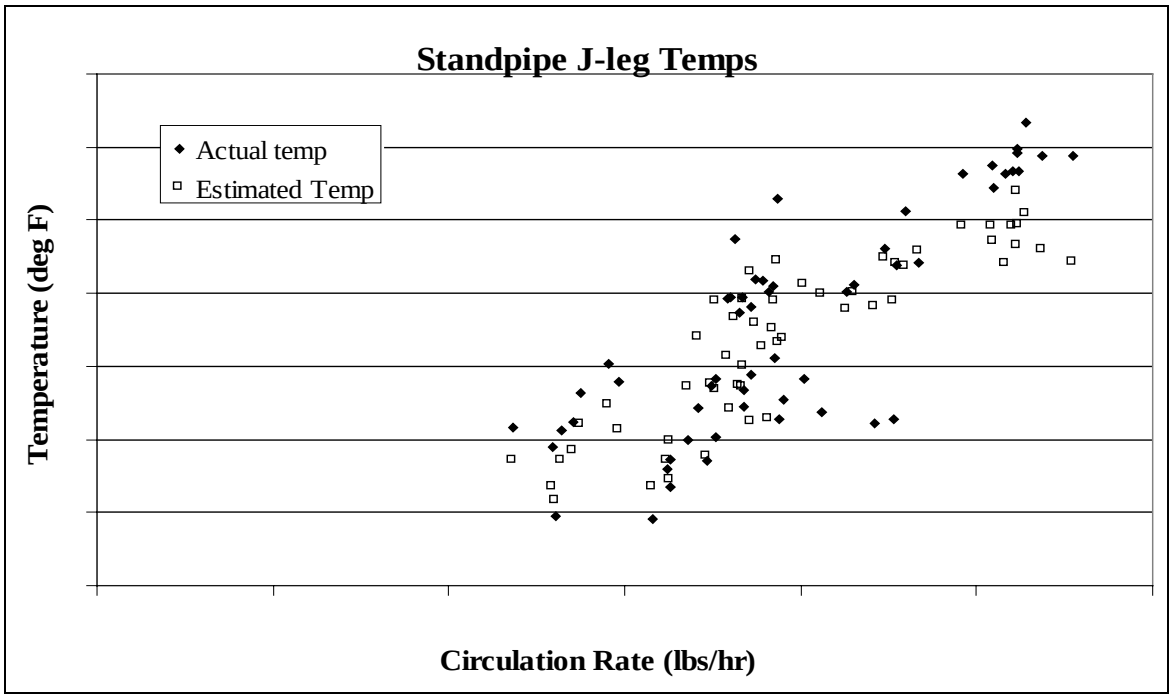

Figure 4.2.9-7 Estimated and Actual Reactor J-leg Temperatures at Top of J-leg

4.2.10 Skin Temperature Profile

Skin temperature measurements of the transport reactor loop were taken at various times during test run TC01. The results did not reveal any hot spots. The highest temperatures encountered were around 300°F. A discussion of the major observations is presented below.

The objectives of the skin temperature monitoring were:

- To monitor the differential growth between the various pipe loops.
- To monitor the performance of the refractory lining, as degradation of the lining would be reflected as "hot spots" in the piping and equipment.
- To periodically document and identify trends in the temperature signatures of the various piping and equipment in the reactor loop. Monitoring these trends assures that the integrity of the refractory is maintained.

During test run TC01 skin temperature measurements were taken on the following days:

Test Run	Date	Riser Exit Temperature
TC01B	September 9, 1997	1,600°F
TC01B	September 11, 1997	1,559°F
TC01B	September 12, 1997	1,554°F
TC01B	September 17, 1997	1,570°F
TC01B	September 18, 1997	1,559°F
TC01I	November 29, 1997	1,601°F
TC01I	December 8, 1997	1,597°F

The temperatures were measured with a surface probe digital thermometer and an infrared thermometer. Temperature readings were taken under steady-reactor operating conditions.

Figure 4.2.10-1 shows a plot of the differential temperature between different portions of the reactor loop. As can be seen from the profiles the maximum temperature difference between the riser and standpipe was 34°F and between the standpipe and cyclone dipleg was 32°F. Both these differentials were below the allowable limit of 75°F. Similarly, the maximum temperature difference between the combustion heat exchanger (HX0203) and the standpipe, and between HX0203 and the riser/mixing zone was 77 and 72°F, respectively. The maximum allowable value was 135°F.

The average skin temperatures at various locations in the loop for the entire test run are given in figure 4.2.10-2. As would be expected, the reactor skin temperature increased along the length of the riser, an indication that combustion occurred throughout the riser to the riser crossover. The temperature of solids in the reactor ranged from 1,140°F in the mixing zone to about

1,600°F at the riser exit. At the top of the riser, and along the riser crossover, the skin temperature dropped due to higher heat losses. Along the riser crossover, cyclone crossover, and the cyclone outlet the skin temperature decreased with increasing distance from the reactor due to heat losses and gas/solid disengagement.

The temperature of solids in the upper standpipe was about 1,615°F and decreased to about 1,544°F at the bottom. The average skin temperature on the standpipe decreased along the length of the standpipe (from 270 to 260°F) but has a higher value below the heat exchanger draw-off. This higher temperature at the bottom of the standpipe was also the highest in the reactor loop. The skin temperature at the bottom of the standpipe was highest in the loop, even though the solids temperature in that location was lower than the maximum in the reactor. This was due to a slow-moving bed of hot solids.

The average skin temperature in the midsection of HX0203 was 222°F as compared to about 260°F above the solids entry port into HX0203. The skin temperature reduced to 218°F at the HX0203 standpipe and decreased through the J-leg. This trend revealed effective heat removal in the HX0203.

Considering the HX0203 vent gas line (VGL), the average skin temperature at the exit of HX0203 was 168°F (with a standard deviation of 7°F). This temperature increased to 198°F along the refractory-lined pipe and then decreased to 187°F. Finally, the average skin temperature at the junction between the VGL and the cyclone crossover was 220°F. The expectation was that as a result of the hot gases leaving HX0203 into the VGL the average skin temperature would decrease steadily along the VGL, with the highest value at the exit of HX0203.

Another interesting phenomenon was the skin temperature reading on the cyclone dipleg. The temperature on the upper half of the dipleg was 262°F. Contrary to expectations, the skin temperature took a dip along the dipleg before rising again to 273°F.

In order to have an idea about the solids level in the cyclone dipleg, skin temperature measurements were taken of the dipleg. Figures 4.2.10-3a and -3b show plots of skin temperature against distance for the upper and lower dipleg respectively. Data for the plots were taken during test run TC01I between December 4 and December 6, 1997. The locations of aeration ports on the upper dipleg are indicated on the plot.

As shown by figure 4.2.10-3a there is a steady drop in skin temperature along the upper dipleg up to a minimum value, about XX ft below the cyclone flange. This minimum value could have been due to effective heat removal by the mechanical support for the cyclone, which effectively acted as cooling fins at that portion of the dipleg. Below the support the skin temperature increased steadily up to about XX ft below the cyclone flange. This increase in temperature is an indication of the presence of hot solids in this section of the cyclone. One could infer from this plot that the level of solids in the cyclone was between points B and C, as shown in figure 4.2.10-3a.

After attaining a maximum at point C (see figure 4.2.10-3a), the skin temperature drops primarily as a result of cooling of solids by aeration gas at point D. The drop in skin temperature at this

point was due to localized cooling of the dipleg by aeration gas. After point D the skin temperature increases again as a result of increased heat release by the solids. A maximum is attained at point E, after which the temperature drops again due to cooling of aeration gas at point F. Below point F the skin temperature increased again, but because the solids at this point had been cooled sufficiently the heat release and, hence, the skin temperature, was not as high as at points C and E.

Figure 4.2.10-3b shows the profiles of skin temperature along the lower dipleg. As can be seen from these profiles there was a steady decrease in skin temperature, which was the result of lower heat release from the solids.

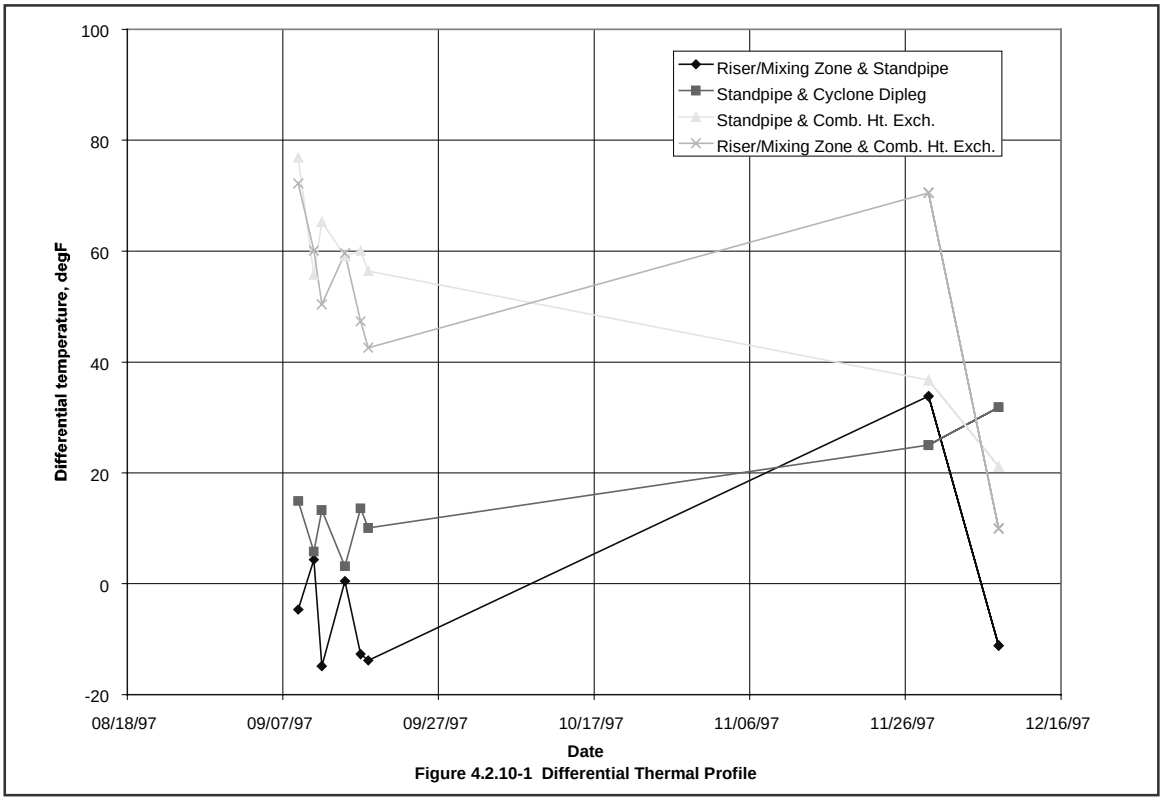

Figure 4.2.10-1 Differential Thermal Profile

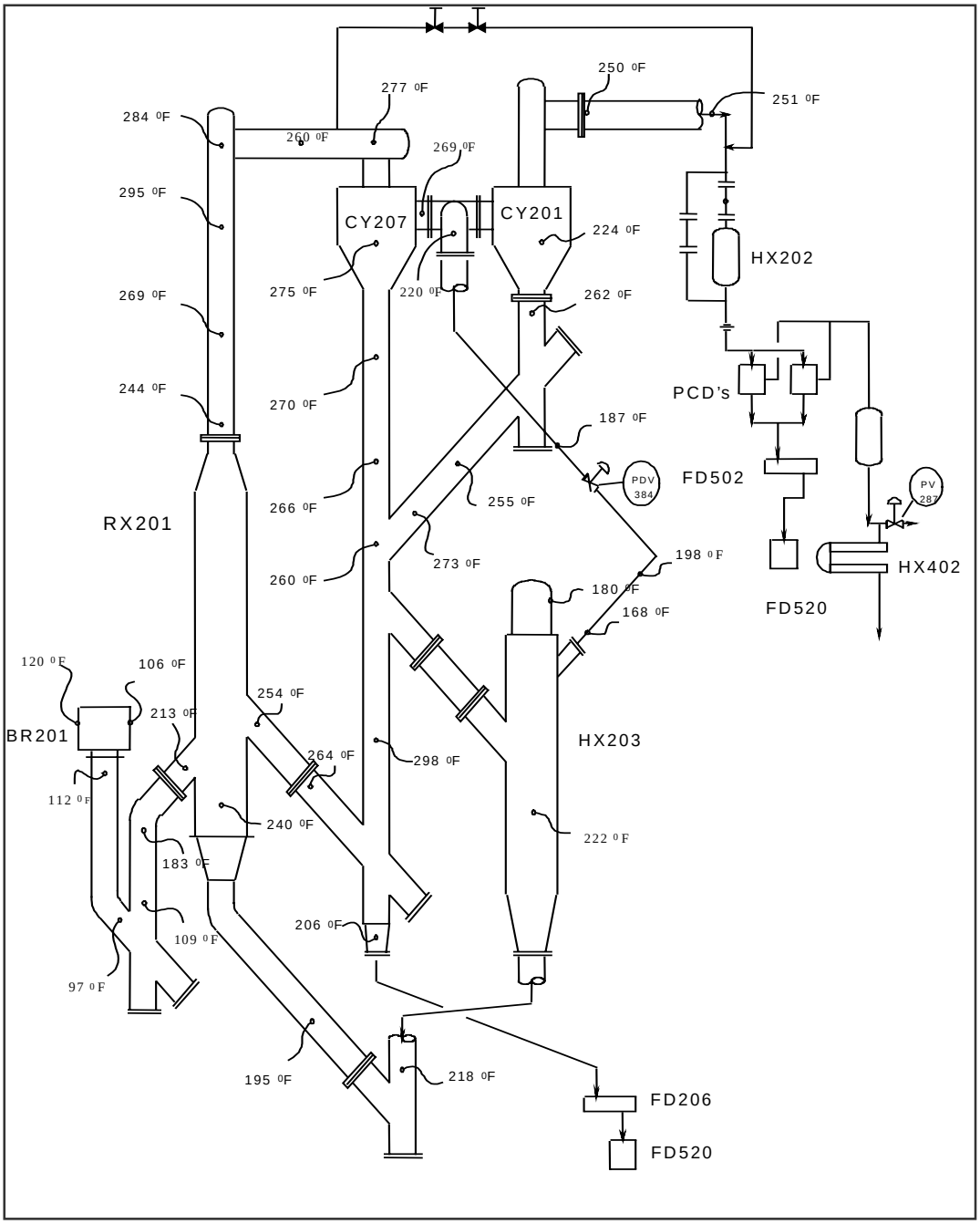

Figure 4.2.10-2 Average Skin Temperature in Reactor Loop

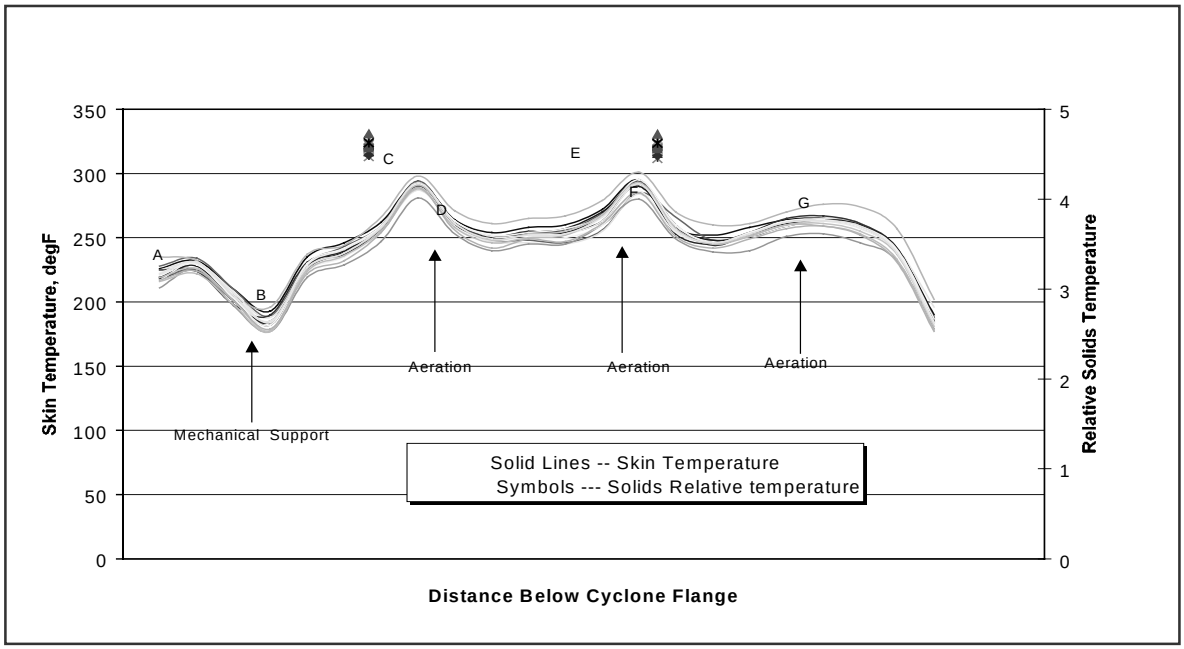

Figure 4.2.10-3A Dipleg Skin Temperature Profiles (December 4 to 6, 1997)

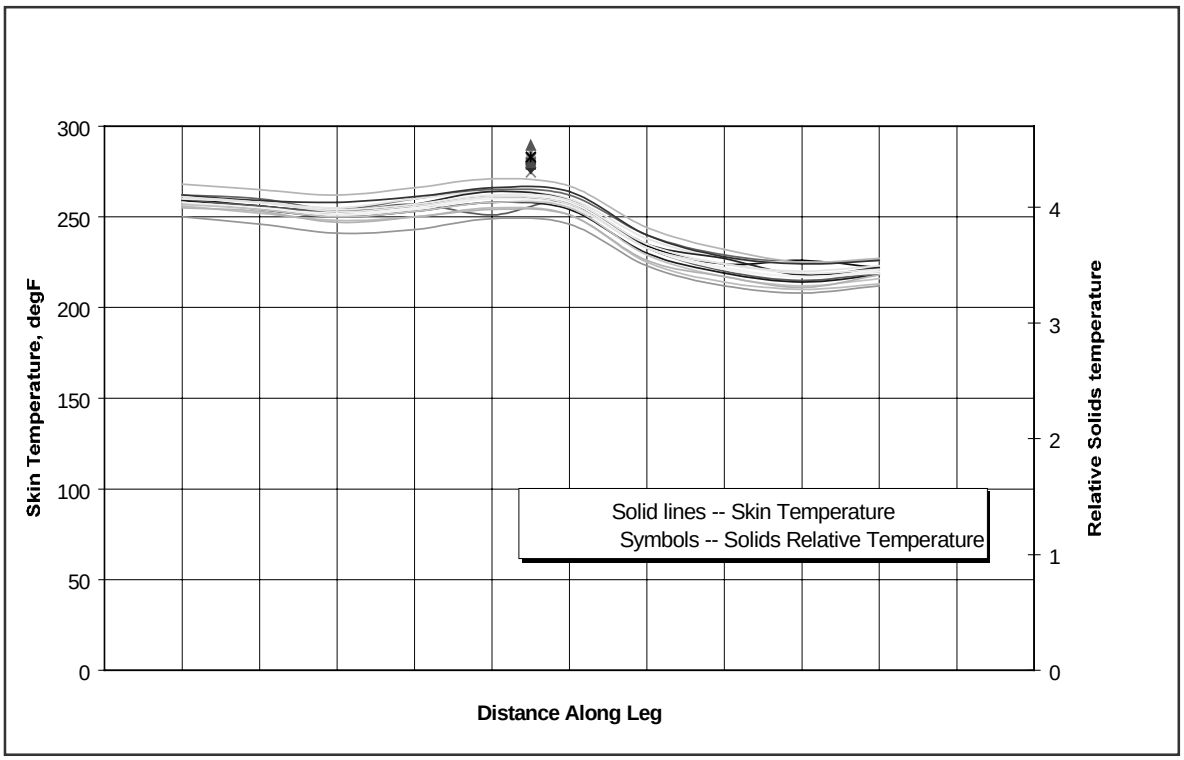

Figure 4.2.10-3b Dipleg Skin Temperature Profiles (December 4 to 6, 1997)

4.2.11 Reactor Feed System Issues

During the 1997 transport reactor operations there continued to be problems with both the coal and dolomite feed systems (FD0210 and FD0220). First, after 4 to 6 days of satisfactory operation, suddenly coal would not fall from the lock vessel to the dispense vessel. This is shown on figures 4.2.11-1 and -2 for FD0210 during runs CCT4D and CCT5A/B. During run CCT6A, the coal feed was from the smaller dolomite feeder, FD0220, and the same problems were present (see figures 4.2.11-3 and -4). Analysis suggested that the solids remaining in the lock vessel were finer than those in the silo, indicating an accumulation of fines in the lock vessel. Nozzles were installed into the side of the lock vessel to blow the coal away from the sides so that the coal did not pack. The lock vessel was also "fluffed" every 4 hours to keep the coal from packing. There is also a tendency for the coal to overfill the lock vessel when the spheri valves are opened. The knife gate valve under the coal surge bin was throttled to slow down the flow.

Figures 4.2.11-5, -6, and -7 show the interruptions in coal flow during TC01. Clyde Pneumatic Conveying was consulted and recommended that a vent on the lock vessel be added so that the fluidizing nitrogen would pass through the dispense vessel. This vent would also prevent the dispense vessel from over pressurizing. In November, the proposed vent system was installed; however, the venting system (after November 6, 1997, as shown in figures 4.2.11-5, -6, and -7) by itself did not really improve the performance. The large scatter on figure 4.2.11-7 is due to the calculation method when the part cycles are calculated. During the last 2 weeks of operation, a small purge of nitrogen was maintained under the fluidizing pad of the lock vessel. This purge substantially increased the reliability but had a tendency to make the coal rate vary when the dispense vessel was being filled.

Since the coal feeder is still not reliable, additional modifications will be made. A nozzle on the elbow in the coal feed line will be added with a small nitrogen purge to keep the tube below the rotofeeder from plugging. Also, coal feeding can be stopped when the equalizing line between the dispenser vessel and lock vessel plugs. A large, 2-in., equalizing line is being fabricated for installation. In addition, the pressure control on the dispense vessel needs improvement. As supplied, the dispense vessel scheme of pressure control is through the use of orifices and solenoid valves that open and close depending on the differential pressure difference between the dispense vessel and the coal feed line.

The dolomite feeder FD0220 has the same reliability issues as FD0210; however, temporary loss of dolomite feed does not significantly impact the reactor operation. If the fluidizing nitrogen flow is too high, an additional problem may result from the air flow carrying large amounts of dolomite through the rotofeeder feed plate into the reactor.

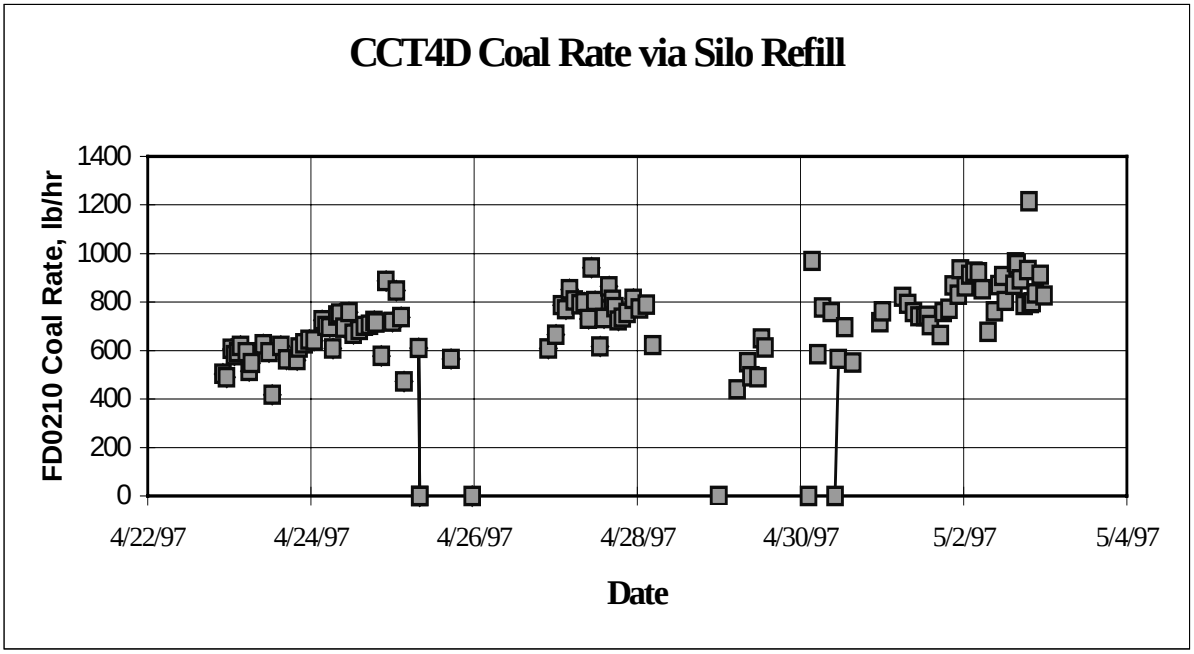

Figure 4.2.11-1 CCT4D Coal Feed Rate (lb/hr) Via Silo Refill Vs Time (Date: May 4, 1997)

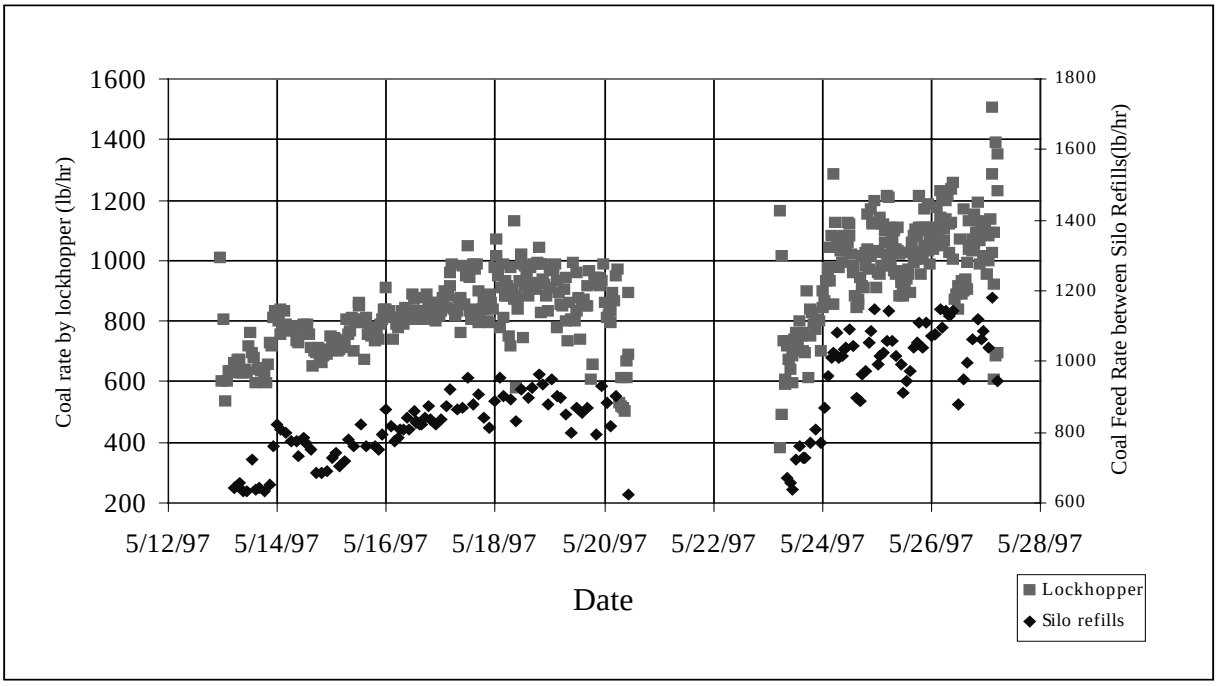

Figure 4.2.11-2 CCT5A and CCT5B Coal Feed Rates (lb/hr) Vs Time

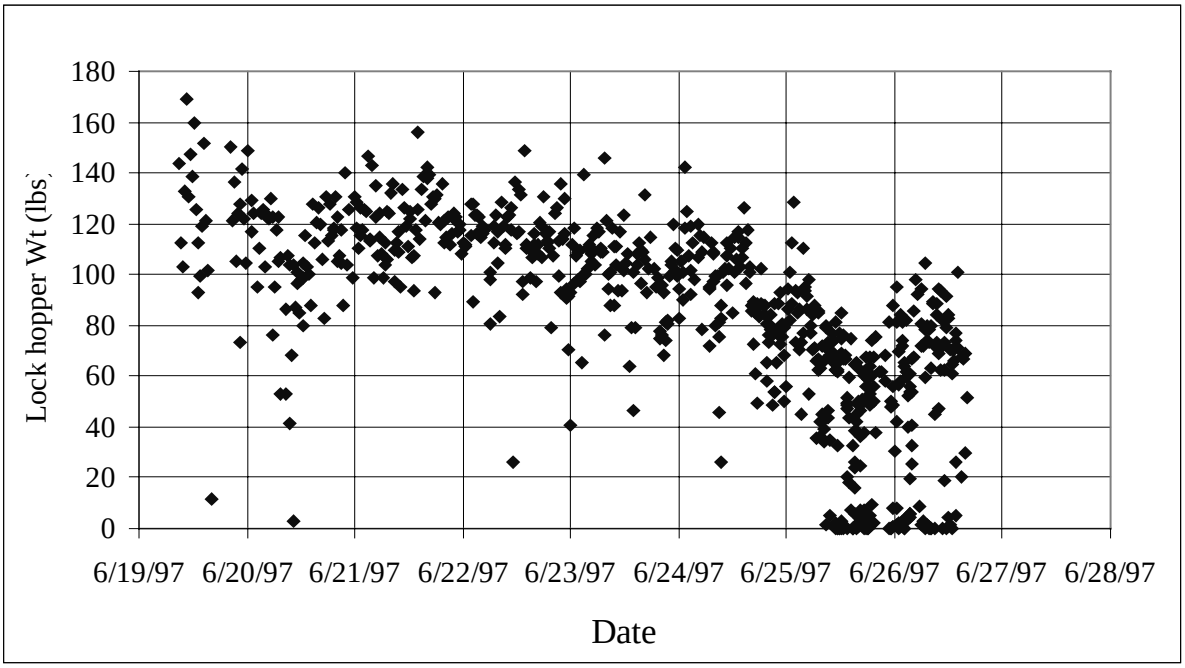

Figure 4.2.11-3 CCT6A Coal Feed Rates (lb/hr) and FD0220 Feeder Speed (RPM) Vs Time

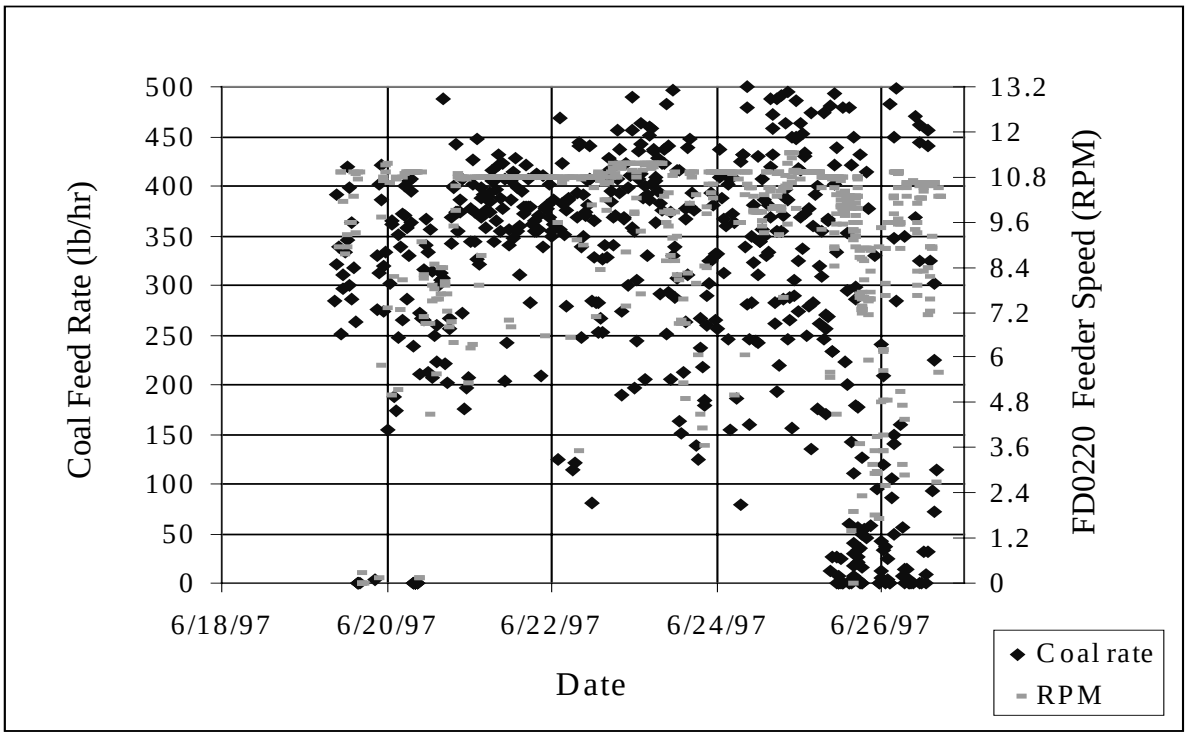

Figure 4.2.11-4 CCT6a Lock Hopper Refill Weight Vs Time

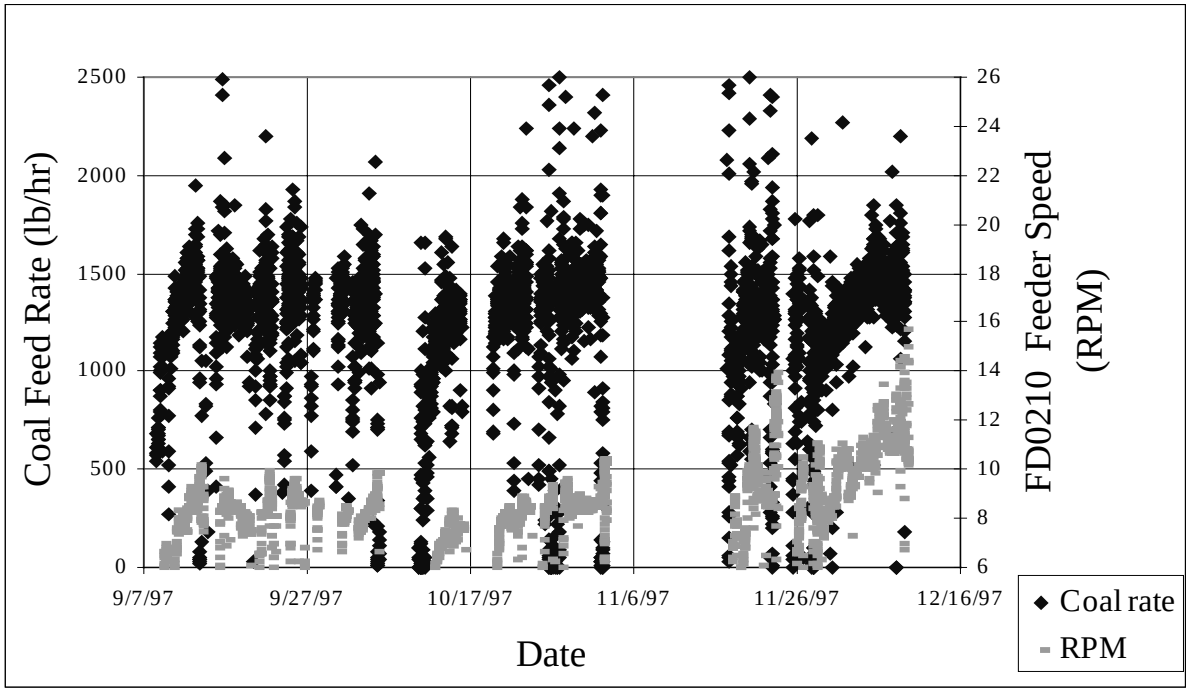

Figure 4.2.11-5 TC01Coal Feed Rates (lb/hr) and FD0210 Feeder Speed (RPM) Vs Time

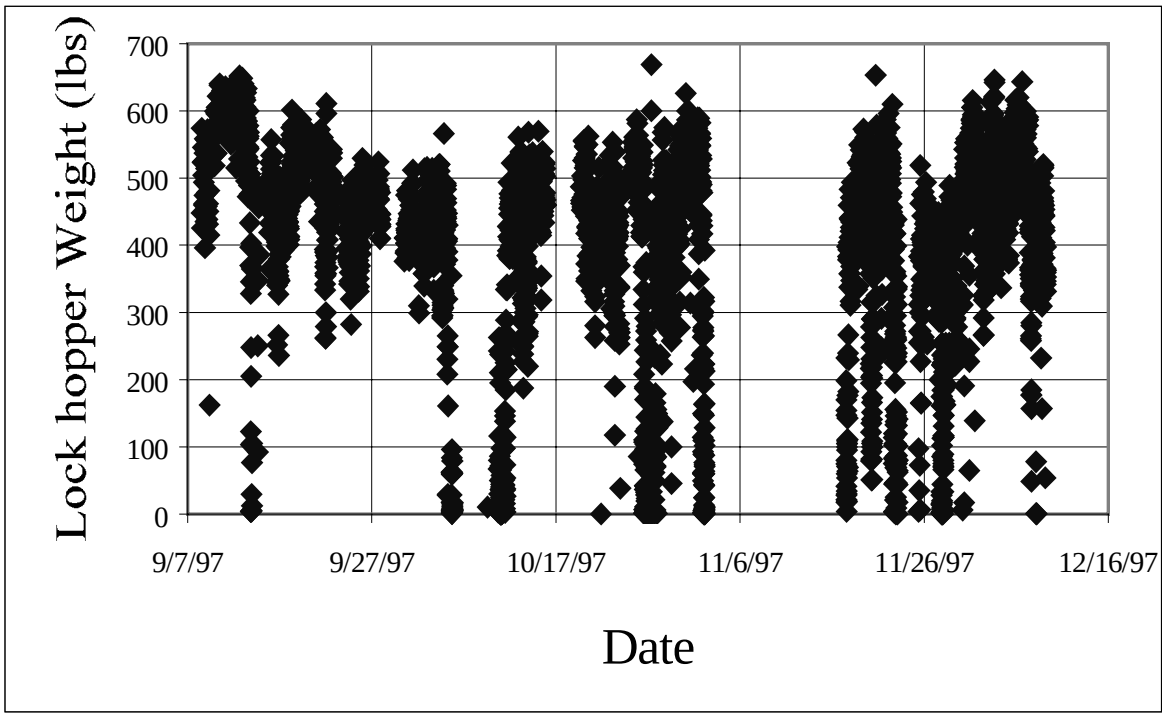

Figure 4.2.11-6 TC01 FD0210 Lock Hopper Refill Weight Vs Time

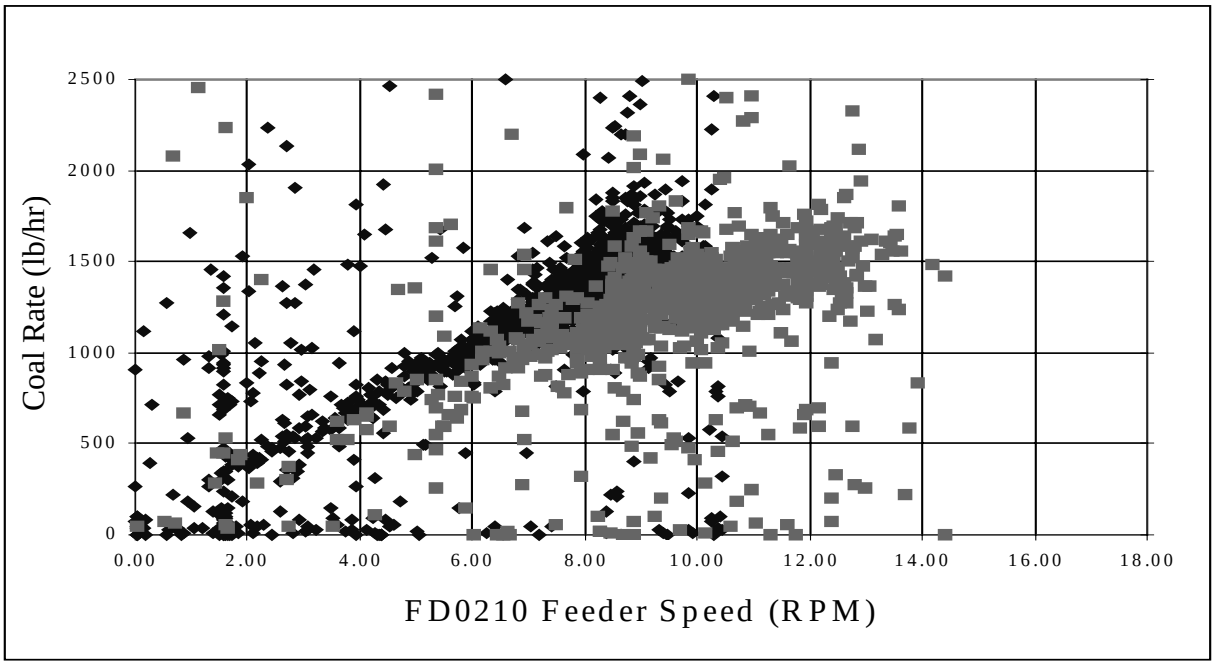

Figure 4.2.11-7 TC01 Coal Feed Rate (lb/hr) Vs FD020 Feeder Speed (RPM)

4.3 CYCLONE DIPLEG OPERATION AND DATA ANALYSIS

A brief history and the troubleshooting processes related to dipleg operation problems are described in this section. Also, applications of the drift flux model and the continuity wave theory to the dipleg operations are discussed. The successful application of these theoretical models may provide some new and useful concepts in the dipleg operation and design. The discussions and explanations provided are contrary to conventional thought of cyclone dipleg design and operation, and should be research carefully for any particular application.

4.3.1 Brief History of the Dipleg Problems and Troubleshooting Processes

Excessive solids carryover was a major operational problem for the transport reactor in early test runs. Due to the high-solids carryover rate from the reactor to the particulate control device (PCD) the solids inventory in the reactor could not be kept constant without periodically adding inert bed materials.

The high-solids carryover rate also influences the reactor heat capacity, which is closely related to the solids circulation rate. Because an increase in the solids circulation rate could result in higher solids carryover rate the solids circulation rate had to be tailored to keep the solids carryover rate at a reasonable level. As the result of this compromise the coal feed rate was relatively low before the problem of the solids carryover rate was solved.

This high-solids carryover rate also influences the PCD operation. At a very high-solids carryover rate particle size distribution in the PCD samples is quite different from that at a lower solids carryover rate. Generally, the mean particle size is larger at a higher solids carryover rate. The data collected under the conditions with the high-solids carryover rate were not representative of the normal operational particle size distribution. Flow resistance of a dust-collecting element might also be different for the different particle size distribution in the dust samples. Furthermore, since a commercial transport reactor will operate at a much lower solids carryover rate the data collected from the PCD operation with a high-solids carryover rate does not provide insightful information for evaluation and future reactor design.

Many different causes of the excessive solids carryover were proposed. The first thought was that the disengager (CY0207) efficiency was too low. This speculation was evaluated by a cold-flow model test at General Electric Environmental Services, Inc. (GEESI) and found not to be completely true. The cold-flow test result showed that the experimental disengager efficiency was greater than 90 percent for the particle size used in the reactor operations. Although lower than the design value of 96 percent, the 90 percent collection efficiency does not explain the extreme carryover rates. Due to dynamics of the system, the collection efficiency of a disengager in a process will be different from that in a stand above a cold-flow test.

Another speculation was that the cyclone (CY0201) efficiency was low. The cyclone inlet cross-sectional area was reduced to increase the cyclone inlet velocity and, thereby, increases the cyclone efficiency. This modification slightly lowered the solids carryover rate because of a change in the pressure balance in a loop consisting of the cyclone, dipleg, standpipe, disengager, and the secondary crossover between the cyclone and the disengager. The pressure balance

change affected the gas-solids flow in the dipleg. Notwithstanding the improvement, the solids carryover rate was still too high to maintain a constant reactor inventory.

Overloading the cyclone with solids was also speculated as a cause of the excessive solids loss problem. This speculation was too vague to give a definite direction in finding the true cause of the excessive solids carryover. The concept of cyclone overloading can mean that the momentum of the gas is too low, or the solids concentration is too high at the inlet of the cyclone, so that the vortex in the cyclone is too weak to remove all solids from the gas stream. The concept of cyclone overloading can also mean that the cyclone dipleg is incapable of moving the solids from the cyclone to the standpipe. Apparently, the latter reason was partially true. The high-solids carryover rate was due to poor solids movement from the dipleg to the standpipe. However, it was because of flooding, not overloading; dipleg flooding will be addressed in detail later.

The cyclone dipleg malfunction was first diagnosed near the end of CCT4D test run in April 1997. Whenever the pressure differences in the dipleg became negative for more than 1 minute the solids carryover rate would increase dramatically. A typical example is given in figure 4.3.1-1 in which the isolated peaks are the conveying line pressure downstream of the PCD and the continuous fluctuating curve is the measured pressure difference in the vertical section of the cyclone dipleg. Each PT8533 peak in figure 4.3.1-1 corresponds to one batch of solids conveyed out of the PCD. Each batch of solids weighs about 100 lb. Under normal operating conditions, with the pressure difference in the dipleg varying between zero and 8 inH_2O, 100 lb of solids leaving the PCD occurred every few hours, as shown in figure 4.3.1-1. It can be seen that between 02:00 and 03:00 the pressure difference (PDI253) stayed near-zero values for a period of more than 20 minutes. During this period, the total amount of solids carried to the PCD is about 1,000 lb. Depending upon the solids circulation rate and the time period that the PDI253 stays in near-zero values, the amount of solids carried to the PCD varies from 100 to 2,000 lb each time the PDI253 is negative for a substantial time period (more than 1 minute). The event of pressure difference staying near zero in value for a substantial time period was referred to as a "dipleg upset" condition. Note in figure 4.3.1-1 that if the pressure difference in the dipleg is fluctuating around 4 inH_2O (the mean value for this operation period) the solids carryover rate is less than 30 lb/hr.

Many operating conditions may cause the dipleg upset. Also, sudden changes in the coal feed rate, reactor pressure (e.g., due to a PCD back-pulse), particle size distribution of feed materials, or solids circulation rate (e.g., uneven combustor heat exchanger circulation) have the potential to upset the dipleg.

Figure 4.3.1-2 gives an example of the dipleg upset induced by a coal feeder failure in CCT5A test run. The apparent reason is the sudden change in the coal feed rate. At around 05:19 on May 20, 1997, the coal feeder failed. Because of the coal feeder failure, no coal was fed to the reactor at that moment. Immediately after the coal feeder failure the dipleg upset occurred. In this case the dipleg upset could have been induced by changes in process conditions associated with loss of coal feed, such as sudden changes in the reactor temperatures and gas velocities, pressure balances, and solids loading to the dipleg.

Figure 4.3.1-3 illustrates the dipleg upset due to a PCD back-pulse. In figure 4.3.1-3, the pressure differential, PDI3027B, is essentially the pressure difference across the PCD. Whenever the PCD back-pulses, the PDI3027B has a peak, as shown in figure 4.3.1-3. Figure 4.3.1-3 clearly shows that immediately after the PCD back-pulse, the dipleg upset occurred. One of the apparent reasons is that the reactor pressure suddenly changed at the PCD back-pulse. As shown in figure 4.3.1-3, the pressure in the reactor increased by 3 psi for a period of a few seconds at the PCD back-pulse.

Another example of the dipleg upset is given in figure 4.3.1-4. For this case, the major cause of the dipleg upset is the sudden change in the particle size distribution of solids to the dipleg. Before the time period shown in the figure, the reactor was running for more than 12-hours without a dipleg upset. During this time period, the reactor supplemental materials had been dolomite for the purpose of sulfur removal and to change the solids circulation rate. Since the combustion heat exchanger had been taken out of the reactor loop for the test (CCT6), the reactor inventory was relatively low (about 3,000 to 4,000 lb). After the 12 hour run almost all the bed solids left in the reactor were dolomite (fresh and calcined) and coal ash. When sand addition to the reactor was initiated the dipleg was immediately upset. The added sand had a much larger particle size than what was left in the reactor. Since the disengager efficiency is higher with a larger particle size the amount of solids was suddenly reduced to the dipleg. All these changes are apparent reasons for the dipleg upset.

A solids circulation rate increase caused the dipleg upset shown in figure 4.3.1-5. In this case the solids circulation rate was increased by increasing the solids inventory in the reactor. During test runs CCT4D through CCT6 many dipleg upsets occurred from increases in the solids circulation rate. The increase in the solids circulation rate will cause an increase in solids loading to the dipleg.

Although the length of a dipleg upset varies for different upsets, in general, the length of the dipleg upset condition increased with increasing solids circulation rate. A typical example is given figure 4.3.1-6. There are two dipleg upsets in figure 4.3.1-6. As shown in figure 4.3.1-6, the first upset occurred at about 15:45 on May 17, 1997, as the PDI253 pressure differential remained near zero for about 7 minutes. Before the upset, the pressure differentials were about 16 inH_2O in the vertical section of the dipleg. After this upset, because of loss of solids from the transport reactor to the PCD and the consequent reduction in the solids inventory in the reactor, the solids circulation rate in the reactor decreased. The pressure differentials were about 11 inH_2O in the vertical section of the dipleg after recovering from the dipleg upset. A second dipleg upset occurred 30 minutes after the first upset. Because both the solids circulation rate and solids inventory were low in the reactor, the time period for the second upset was about 3 minutes, which is much shorter than the first upset. One may also notice that the behavior of the PDI253 pressure differential in the vertical section of the dipleg is different between these two upsets. During the first upset the pressure differential in the dipleg was negative for most of the time. For the second upset, the PDI253 pressure differential oscillated between positive and negative values.

Knowing that the dipleg upsets cause increased amounts of solids carried over to the PCD and that many factors may cause a dipleg upset is not a complete answer to operational problems. Further questions include the following: What is the exact cause for dipleg malfunction? What causes the pressure differential in the dipleg to stay around zero? More importantly, how can a stable reactor operation be achieved without dipleg upsets? In the following sections of this report some theoretical analyses are conducted to answer some of the questions.

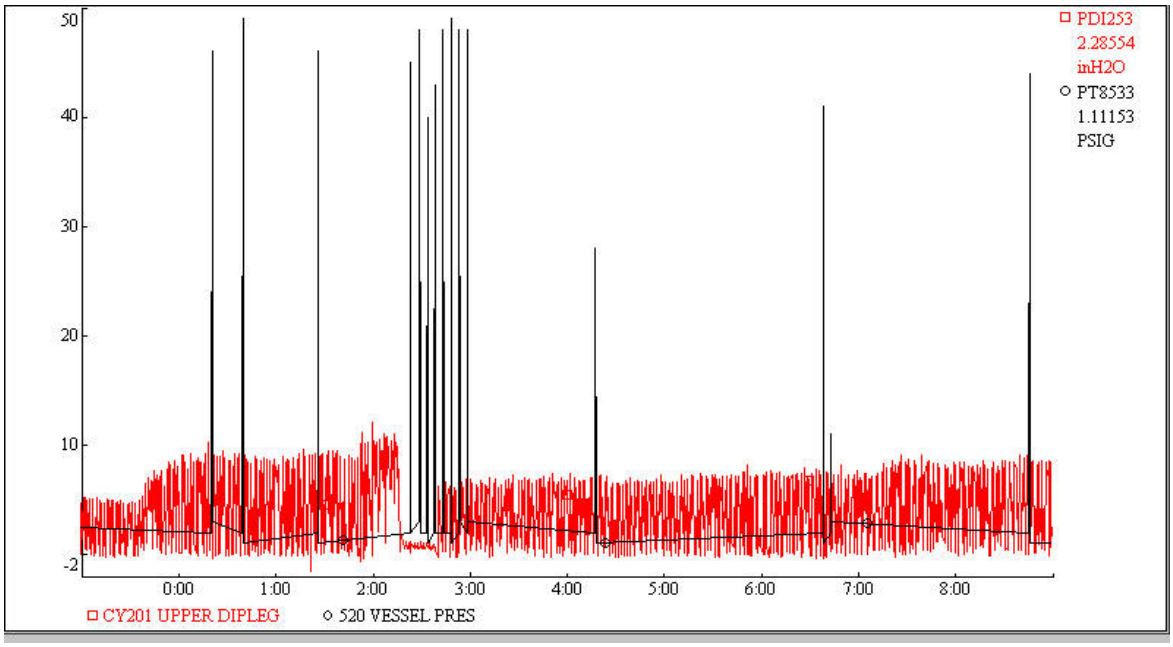

Figure 4.3.1-1 Typical Example of High-Solids Carryover Rate When the Dipleg DP Stays in Negative Values (April 22, 1997)

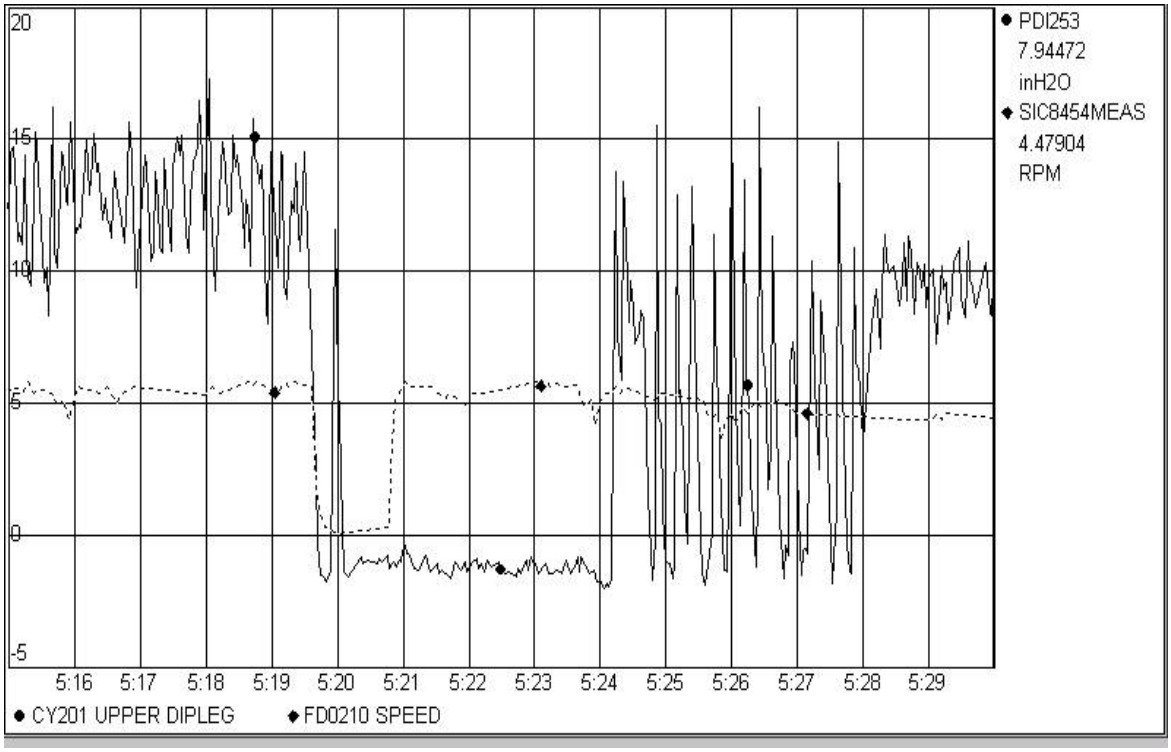

Figure 4.3.1-2 Example of Coal Feeder Failure-Induced Dipleg Upset (May 20, 1997)

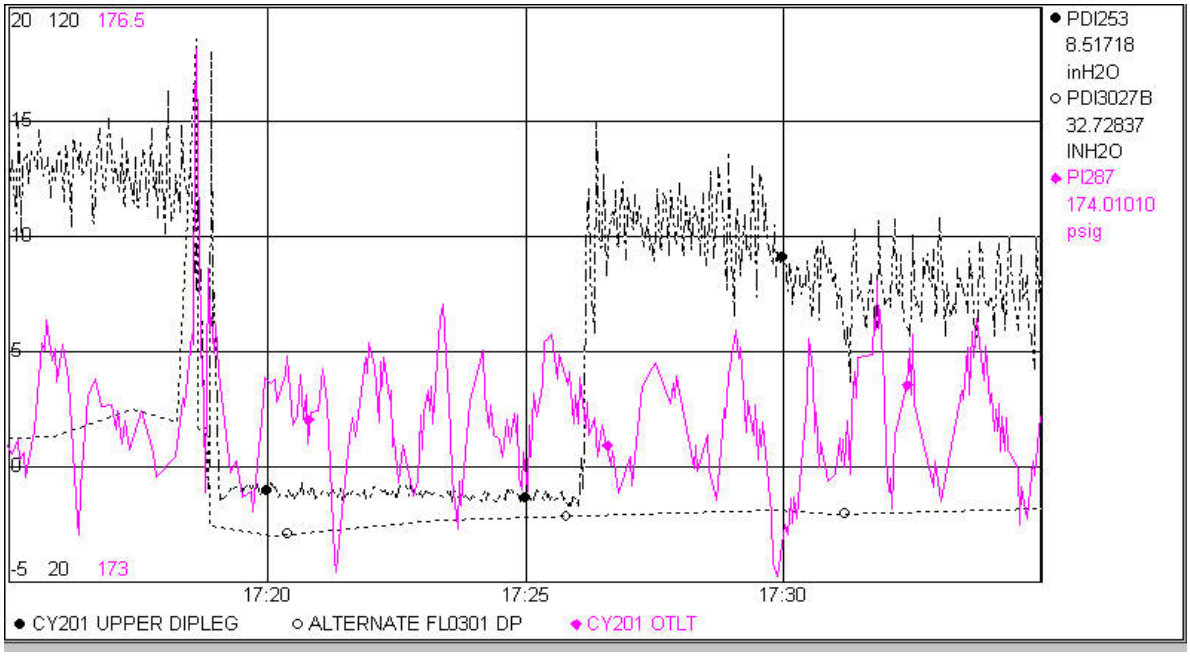

Figure 4.3.1-3 Example of PCD Back Pulse–Induced Dipleg Upset in CCT5A (May 19, 1997)

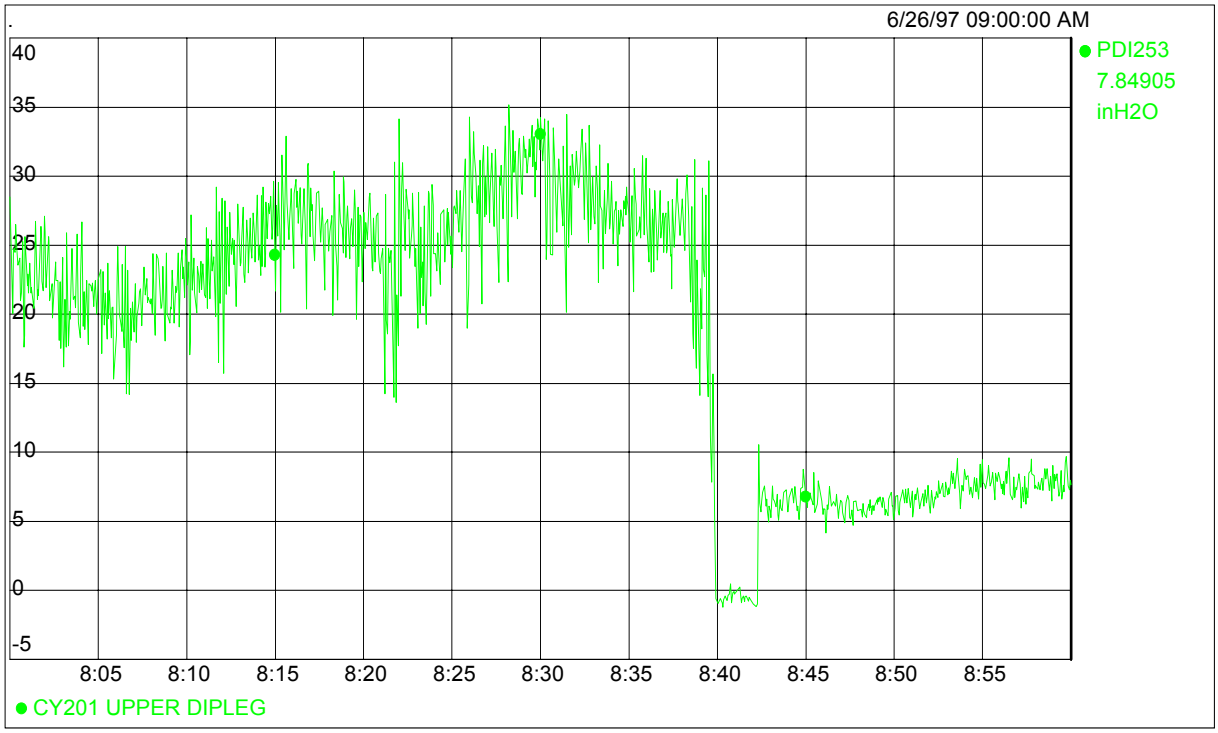

Figure 4.3.1-4 Example of Dipleg Upset Due to Changes of Bed Materials (June 26, 1997)

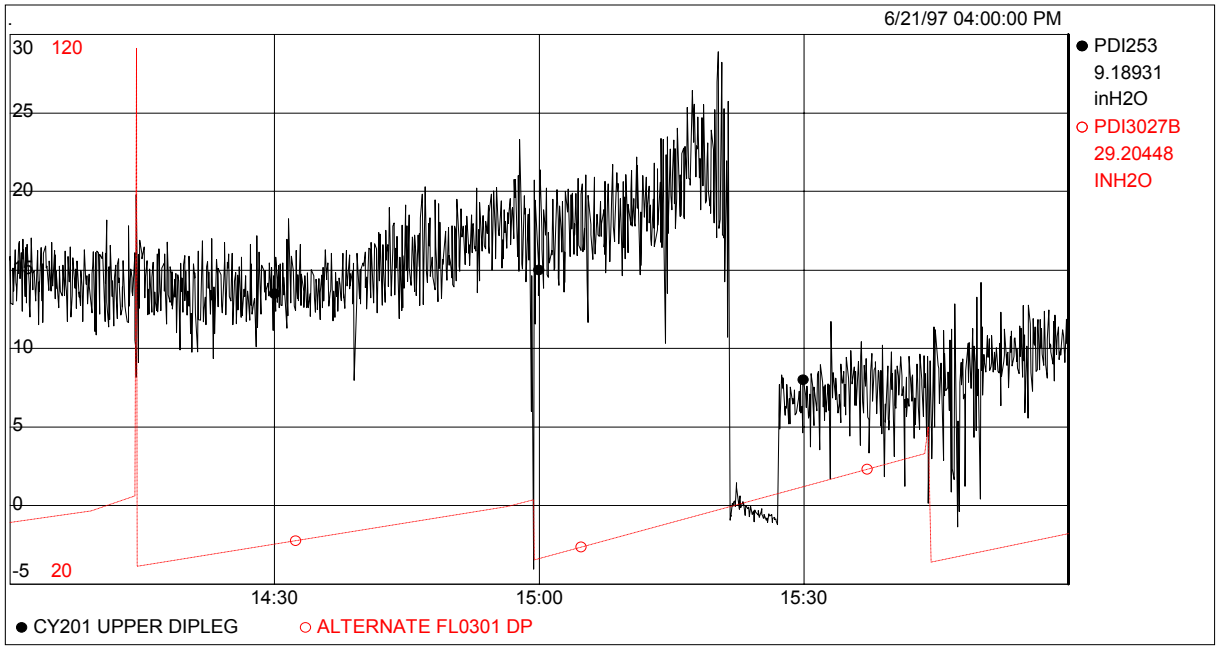

Figure 4.3.1-5 Example of Dipleg Upset Due to Change in Solids Circulation Rate (June 21, 1997)

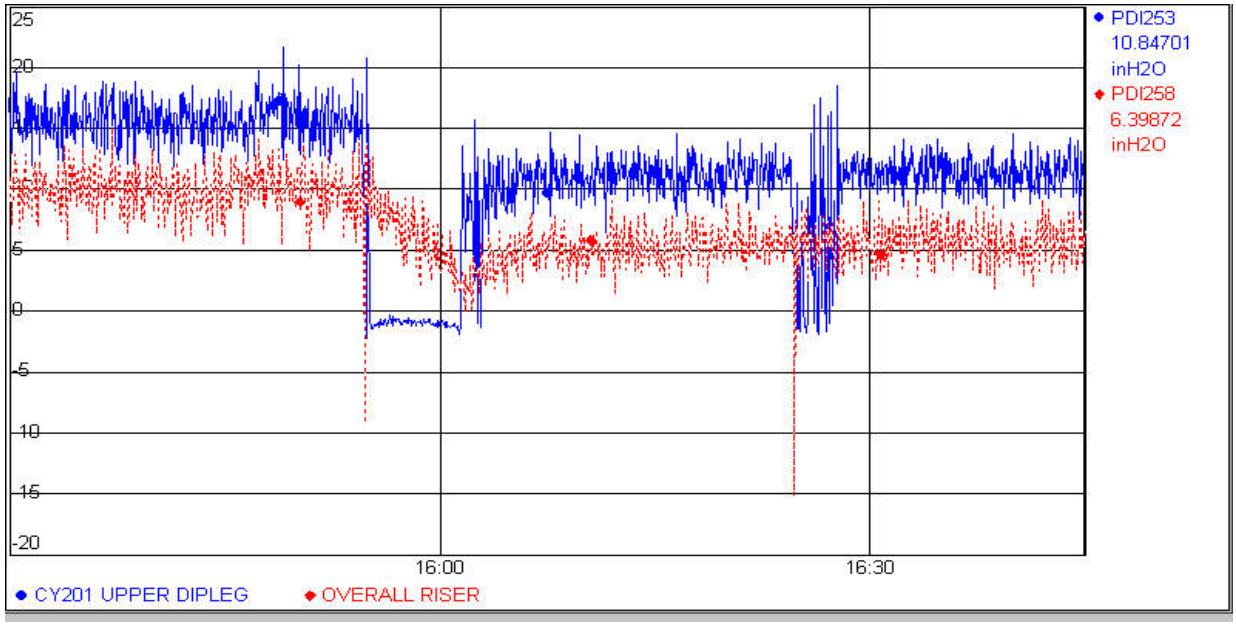

Figure 4.3.1-6 Example of Solids Circulation Rate – Time Period of Dipleg Upset May 17, 1997

4.3.2 Analyses of Dipleg Upsets

The logic at the onset of the theoretical analyses is based on the near-zero pressure difference in the dipleg being an indication of the dipleg upset condition and finding the reasons for such pressure difference behavior. Then, ways to improve dipleg operations can be researched.

There are a few possible reasons for the pressure difference in the dipleg being near zero. Under certain solid flow conditions, zero or negative pressure differences can be observed in the dipleg. However, the most straightforward speculation is that the dipleg is empty. This explanation is based on the assumption that as long as solids are in the dipleg the pressure differential indicator should be able to detect the weight of the solids per unit cross-section of the dipleg. This speculation can be proven to be impractical due to the very short time period of the recovery process after a dipleg upset. In the first upset shown in figure 4.3.1-6, as an example, the system recovered to a new stable (or quasi-stable) state in about 2 seconds after the pressure differential stayed near-zero values for about 7 minutes. For a reasonable assumption that the dipleg needs at least 30 lb of solids to have a positive pressure difference reading in the vertical section, the solids flow rate to the cyclone dipleg would have to be 54,000 lb/hr. It is unlikely to have that high a solids flow rate to the dipleg because the total solids circulation rate is about 40,000 to 50,000 lb/hr at that time. The disengager collection efficiency is at least 60 percent. The maximum solids flow rate to the cyclone dipleg cannot be more than 20,000 lb/hr. If one considers that the dipleg requires more than 30 lb of solids to recover from the upset it is highly unlikely for the dipleg to be empty during an upset time.

If solids exist in the dipleg at the time of upsets the solids in the dipleg cannot be in a fluidized condition no matter what is the cause of the negative pressure difference readings in the dipleg. If the dipleg is in fluidized condition the pressure difference should be equal to the weight of the solids between the pressure difference measurement per unit cross-section area. The pressure difference must be positive for a fluidized-bed dipleg. This means that in the period of a dipleg upset the solids in the vertical section of the dipleg must be in a packed-bed condition. Furthermore, the excessive solids carryover indicates that the solids in the dipleg are not flowing downwards at the time of an upset. If the flux is high in a fluidized downward flow the pressure difference can become negative. However, in this case there should not be any excessive solids carryover to the PCD.

From this reasoning it can be concluded that a flow stoppage in the dipleg caused the dipleg upset. The flow stoppage may result from the dipleg being either bridged or flooded at the time of the dipleg upset. The dipleg flooding or bridging phenomena can be observed by a cold-flow model. The phenomena can also be analyzed with the help of some theoretical modeling. The theoretical analysis provides an opportunity to gain a better understanding of the phenomena.

In the information below some detailed analyses are presented to understand the gas-solids flow in the dipleg. It should be noted that at the onset of these analyses the study of gas-solids flow systems in industry and academia is still in a rudimentary stage. The essentials of the complexity of the flow system are still not mastered, and for reasons that are understandable there is a dearth of literature in fundamental understanding of this subject area. The models presented below are oversimplified for the real system. Hopefully, such models will give some qualitative understanding of the flow system. Based on such an enhanced understanding some

improvement in the operation of the dipleg can be made so that stable operation can be achieved.

The first part of these analyses uses the drift flux model to study the possible flow regimes in the dipleg. The flow regime study or classification may make a study of the complex flow system easier. In the ideal world, or with future improvement to the system, understanding the essential factors that influence the different flow regimes can be pinpointed. The effort here is to explore the different flow regimes in terms of improvement to the operating stability of the dipleg.

The second part of the analysis involves the use of continuity wave theory to search for the right direction to go in order to improve the dipleg stability. The continuity wave theory will give more insight on the dynamics of the gas-solids flow system. A way to improve the stability of the system may be found through study of the dynamics of the system.

4.3.2.1 Analysis Using Drift Flux Model

The drift flux model developed by Wallis (1969) is one of the tools that can be used to analyze the gas-solids flow in the dipleg. Although quite a few applications of the drift flux model have appeared in the literature (Hewitt, 1982; Teo and Leung, 1986; Gidaspow, 1994), using the drift flux model in the dipleg flow is still quite a challenge. In the most fundamental level various parameters that are vital to the prediction of the gas-solids flow in the dipleg are very difficult to measure experimentally and predict from first principles. One of these parameters, for example, is the relationship between the drift flux and the void fraction. Notwithstanding the challenge in the application of the drift flux model to the dipleg flow, a qualitative analysis is still beneficial to the dipleg design and operation.

In a gas-solids downward flow system the drift flux defined by Wallis (1969) can be expressed as:

$$j_{sg} = (1-\varepsilon)(V - U_0) \tag{1}$$

Here j_{sg} denotes the drift flux; V is the linear phase velocity of the solids; ε is the void fraction; and U_0 is the total flux. The total flux is given by

$$U_0 = U_g + U_s \tag{2}$$

Here U_g and U_s are the superficial velocities of the gas and solids phases, respectively.

In the original development of the drift flux model, Wallis (1969) explicitly stated that the total flux is the scalar component in the direction of the motion along the pipe. This means that the total flux is always positive. More specifically, if the gas phase is flowing upward and the solids phase is flowing downward, the velocity of the solids phase must be greater than that of the gas phase to make the definition of the total flux in conformity with the original development of the drift flux model. Furthermore, the total flux is a constant and does not depend on the position of the flow field. This assertion becomes clear from the consideration of the continuity equations for both gas and solids phases.

For gas phase, under one-dimensional flow assumption, the continuity equation is:

$$\frac{\partial \varepsilon}{\partial t} + \frac{\partial (U\varepsilon)}{\partial x} = 0 \tag{3}$$

Here, U is the gas-phase linear velocity, x is the coordinate, and t is time. For the solids phase the continuity equation is:

$$\frac{\partial (1-\varepsilon)}{\partial t} + \frac{\partial [V(1-\varepsilon)]}{\partial x} = 0 \tag{4}$$

Combination of equations (3) and (4) and integration of the resultant equation give:

$$U\varepsilon + V(1-\varepsilon) = U_0 \tag{5}$$

The following equations result by the definition of the phase and superficial velocities:

$$U = \frac{U_g}{\varepsilon} \tag{6}$$

and

$$V = \frac{U_s}{1-\varepsilon} \tag{7}$$

Substitution of equations (6) and (7) into equation (5) will give equation (2). This means that the total flux will be a constant, and independent of the position of the flow field. The phase velocities and the void fraction are noted to be a function of the position of the flow field. Their combination in the form of equation (2) will be a constant.

Having clarified the fundamental meanings about the total flux in the drift flux model, the application of the drift flux model to dipleg flows can be further explored. Combining equations (1), (2), and (7) yields the following:

$$j_{sg} = U_s\varepsilon - U_g(1-\varepsilon) = U_0\varepsilon - U_g \tag{8}$$

Equation (8) is generally called the operation line in the plot of drift flux versus void fraction. Notice that for the given gas-and solids-flow rates the plot of the drift flux, j_{sg}, against the void fraction will be a straight line. The slope of the straight lines will change with the gas- and solids-flow rates. Therefore, the operation line will change with process conditions.

An intrinsic relationship between the drift flux and the void fraction is needed to describe the gas-solids flows in the dipleg. This is a relationship that depends on only the flow system properties (e.g., the particle size distribution, particle true density, the angle of repose, the carrying gas viscosity, density, the diameter of dipleg, etc.).

The most widely used relationship between the void fraction and the drift flux has been an empirical correlation by Richardson and Zaki (1954):

$$j_{gs} = U_t(1-\varepsilon)\varepsilon^n \tag{9}$$

Here U_t is the particle terminal velocity. By the convention introduced in the drift flux model, U_t is always positive. The exponent n is a constant. The commonly cited values for n are 2.4 and 4.8 for the turbulent (the particle Reynolds number greater than 500) and laminar (the particle Reynolds number less than 0.2) flow, respectively. In the intermediate flow region (the particle Reynolds number between laminar and turbulent flow region), the exponent n is a function of the particle Reynolds number.

Combination of equations (8) and (9) gives the steady operation conditions for a system as has been done by Wallis (1969) and Jones and Leung (1985). It is easier to explain from a qualitative drift-flux analysis plot as given in figure 4.3.2-1, in which the dimensionless drift flux (j_{sg}/U_t) is plotted against the void fraction. This drift-flux plot gives a lot of information for operation of the standpipe and the dipleg. In the following, this plot is examined in detail.

In figure 4.3.2-1 the curve HFG is an illustrative plot of equation (9) and all the straight lines are plots of equation (8) at a given solids-phase superficial velocity with different gas velocities. There is a short straight-line section in the curve HFG at the low-void fraction. This is because of the assumption that the relationship between the drift flux and the void fraction is linear for a packed-bed flow. The point A in figure 4.3.2.1 is the value of dimensionless solids velocity (U_s/U_t). Points N, B, C, D, and E are the values of the dimensionless gas velocities (U_g/U_t). The intersections of the straight lines with the curve HFG are the possible equilibrium (stable) operation points. In the following, those straight lines are referred to as operation lines and the curve HFG as the phase line.

The operation line AB, as shown in figure 4.3.2-1, represents an operation condition in which both the gas and solids flow downwards and the gas-phase velocity is larger than the solids-phase velocity. This operation line has a single intersection point with the phase line. Thus, only one stable operation condition is possible. If the system is subjected to a local disturbance (keeping overall flow constant), the system will return to the stable operation point since no other equilibrium point can be reached. Therefore, the system is absolutely stable under the given operation conditions delineated by the operation line AB. This is a highly desirable operation condition.

If the downward flow gas-phase speed is decreased, the operation line can have two intersection points with the phase line, as shown by the operation line AC. At the lower intersection point H, the void fraction in the bed is too low to have a fluidized bed. The flow system is in a packed-bed mode. At the higher intersection point, L, the bed is fluidized. Between these two equilibrium points, according to Teo and Leung (1986), the higher void fraction point is more stable. As has been pointed out by Leung and Jones (1978), different flow regime may coexist in a standpipe.

Special attention needs to be given to the operation line AC. For illustration purposes, the lower intersection point H is intentionally shown as zero-drift flux. From the definition of the drift flux (equation (1)) and equation (5), the following relation is equivalent to equation (1):

$$j_{sg} = \varepsilon(1-\varepsilon)(V-U) \tag{1a}$$

Since the void fraction can be neither zero (the minimum void fraction is the closed-pack void fraction) nor 1 (which is pure gas and is not the flow concerned about here), the zero-drift flux means that the velocity difference is zero between the solids and gas phase. According to Kunii and Levenspiel (1991), the pressure drop for the packed-bed flow is proportional to the difference in phase velocities, V-U. Then, the pressure difference in the dipleg will be zero when the system is running at conditions corresponding to point H. Because the system that operates at the condition depicted by the operation line AC has two stable operation points, it is possible that the flow periodically "switches" between these two operation points. The experimental data from the transport reactor operation indicates that it is possible that the dipleg might be operating at this condition.

A flow system that has multiple stable operation points may switch between stable operation points. Maron and Dukler (1984) have elaborated this viewpoint in great detail for a gas-liquid upward film-flow system. The similarity exists between the falling film flow and the gas-solids flow in the dipleg in terms of the mechanism that underlines the operation mode switching. For the gas-liquid film flow system the flooding or switching to the unstable flow is caused by countercurrent gas flow (interfacial shear) and liquid entrainment. Essentially, the liquid film deceleration on the wave crest causes the film flooding. For the gas-solids flow system, when the flow switches from the fluidized bed to the packed bed, the solids flow rate decelerates. This is the most plausible mechanism for the dipleg flooding or upset. Teo and Leung (1986) have also speculated that the transition from the fluidized bed flow to the packed-bed flow in the bottom of the standpipe can cause the system to become unstable. The unstable operations experienced by one of the Chevron FCC units (King, 1989) may be a very good manifestation of this flow mechanism. A leak in the fixed grid seal caused a section of the standpipe to lose fluidization. This, in turn, caused severe catalyst flow problems in the standpipe. In the dipleg (or standpipe operation), the switch between the stable operation points should be avoided.

Similar to the operation line AC, the operation line AD also has two stable operation points. Furthermore, the operation line AD illustrates that for the given solids flow rate the gas velocity can be zero. This phenomenon only occurs in the gas-solids downward flow system. When the upward flow of gas driven by the pressure difference is balanced by just the downward flow of gas entrained by the solids flow the overall gas-flow rate is zero.

In practice, the operation conditions delineated by the operation line AD should be avoided. The system has the potential to switch between the stable operation points and cause flow instability. An additional feature for a system with the operation line AD is that the flow direction of the gas phase may oscillate. In an ideal flow situation the gas-phase velocity can be zero under the conditions delineated by the operation line AD. In real operation both the gas- and solids-phase velocities will fluctuate. Since the mean gas velocity is zero any fluctuation may

result in a reversal in the flow direction of the gas phase. This may cause the system to become more unstable.

The operation line AE is tangent to the phase line. Under this condition the dipleg will be flooded. At flooding, the upward flow of gas holds the solids from flowing downward. Therefore, it is impossible to operate the dipleg under the flooding condition. Ideally, if the phase line (or an expression for the phase line) and the operating conditions are known, dipleg flooding can be predicted. Once the flooding condition is predictable the dipleg may be operated away from the flooding. Practically, it is very difficult if not impossible to do so. One of the reasons is that the phase line is very difficult to measure or to predict, as has been pointed out previously. Equation (9) based on Richardson and Zaki correlation may not apply to the dipleg operation.

He and Rudolph (1996) have questioned the applicability of the Richardson and Zaki equation if the system has net solids flow. They further argued that because the net solids velocity is an additional variable, the void fraction must be a function of both the gas- and solids-phase velocities. This argument is valid from the continuity point of view, as shown in equation (5). The experimental data by Avidan and Yerushalmi (1982) support this viewpoint. Avidan and Yerushalmi suggested that although the Richardson and Zaki equation is still applicable for the system with net solids flow, the characteristic velocity should be an "effective" terminal velocity instead of the single particle terminal velocity, as used in the Richardson and Zaki correlation. According to Avidan and Yerushalmi, the effective terminal velocity can be almost two orders of magnitude higher than that of a single particle.

The inference drawn from these findings is that the solids settling velocity or the dipleg capacity is much larger than those predicted from the Richardson and Zaki equation. This assertion can be directly inferred from the experimental results of Avidan and Yerushalmi (1982) because for a given void fraction using the same exponent with a larger terminal velocity (called cluster falling velocity) means a higher solids settling velocity. Although at present no reasonable correlation has been developed to predict the cluster size and falling velocity, the idea of using different characteristic velocities may be very fruitful in the future research and design of gas-solids downward flow devices. The cluster velocity may be too simplistic because the cluster size and the falling velocity is also a function of the void fraction.

Notwithstanding these uncertainties in the phase line correlations, the drift flux model is still a useful tool in predicting the gas-solids flow in the dipleg. Some other qualitative properties of the gas-solids flow in the dipleg can also be explored through a similar drift-flux plot.
For example, the influence of the solids loading to the dipleg on dipleg operation can be examined. In the transport reactor operation, an increase in solids loading to the dipleg accompanies an increase in the solids circulation rate, if the particle size distribution remains unchanged. The pressure balance in the loop around the cyclone, dipleg, standpipe, and disengager will change with the increase in the solids circulation rate. All these changes generally result in an increased pressure difference in the dipleg. The amount of gas percolated through the dipleg has the potential to increase. However, the amount of gas entrained by the solids will also increase with the increased solids loading to the dipleg. This reasoning indicates that under equilibrium condition a constant gas-phase velocity can be achieved with the increased solids velocity.

For example, imagine that the dipleg is operating at the condition delineated by the operation line AB (figure 4.3.2-1). Due to an increase in the solids velocity while keeping the gas velocity constant, the new operation line becomes the line MB. This new operation line has two stable operation points and the system becomes unstable. This illustrates that the increase in the solids loading to dipleg can cause instability in the dipleg operation. This may also partially explain the dipleg upset shown in figure 4.3.1.-5.

The influence of a change in gas velocity at a given solids velocity is another revealing application of the drift-flux plot to the dipleg operation. This case is very special to the current design of the dipleg and standpipe. Because no mechanical valves exist in the dipleg standpipe flow loop, the pressure in the loop will balance itself according to the flow rate and the system properties. An increase in the solids level in the standpipe by increasing the solids inventory in the reactor will increase the solids loading to the dipleg and also increase the pressure difference in the dipleg due to the change in pressure balance in the loop. If the solids level in the standpipe is not too high above the dipleg inlet to the standpipe, the solids velocity in the dipleg will increase owing to the increased driving force by the increased solids column height and the gas velocity is essentially constant. This situation has been discussed in great detail above. If the solids level in the standpipe is further increased, the back-pressure created by the solids column in the standpipe above the dipleg inlet will cause the solids flow rate through the dipleg to decrease. The solids inventory in the reactor or the solids level in the standpipe can be adjusted so that a change in solids circulation rate will not change the solids flow rate in the dipleg. This will effectively increase the amount of gas flowing upward. In terms of the drift-flux plot, this operation change will vary the slope of the operation line with the point A unchanged. For example, a change in the solids inventory causes the operation line to change from AB to AC. The nature of the stability of the operation system has changed due to the operation line changes caused by the change of the solids inventory. As has been discussed before, the system under the conditions delineated by the operation line AB has only one stable operation point, with the system "absolutely" stable. However, the system under the conditions delineated by the operation line AC has two equilibrium points with the phase line: and the system is unstable.

Under most circumstances an increase in the solids circulation rate is highly desirable to increase the reactor throughput. To avoid the change in the system operation stability due to the change in solids circulation rate, the drift-flux plot can be used to guide the operation. Based on the above argument it is desirable to have an increase in solids circulation rate resulting in an increase in the solids flow rate in the dipleg and the downward gas-phase flow rate. For example, if the system has been operating at the conditions described by the operation line AB, the new operation line should be MN after the increase in solids circulation rate in the reactor and the solids loading to the dipleg. The increasing solids flow rate will move the point A to M. To move the point B to point N, the gas-downward-flow rate must be increased. For the given pressure balance in the dipleg and standpipe loop, increasing the aeration rate at the inlet of the dipleg to the standpipe will induce more gas flow to the standpipe from the dipleg. This will increase the gas-downward-flow rate so that an increase in the solids flow rate will not change the operation stability of the dipleg.

The other factors that influence the dipleg operations can be explored by a similar drift-flux plot. For example, the change in the particle size distribution of the solids can change the phase line. Another example is introduction of aeration gas to the dipleg. The introduction of the aeration

gas to the dipleg will change the slope of the operation line and the solids and gas-flow rates in a complex pattern. In all these applications of the drift-flux plot and drift-flux model the key is to find the phase line for a given operating system. At present, the phase line can only be obtained by experiment and cannot be predicted based on first principles.

Figure 4.3.2-2 is a drift-flux plot based on the experimental data of November 27 to December 1, 1997. The solid line is the operation line and the phase line can be obtained by connecting the scattered data points. The solids flow rate is calculated based on the total solids circulation rate and energy balance around the dipleg inlet to the standpipe. The gas velocity is calculated based on the assumption that all gas is flowing downwards. Figure 4.3.2-2 indicates that the dipleg was operated in a dilute flow regime. The void fraction is 0.93 at the known operation point. At this void fraction, the bulk density of the dipleg is about 10 lb/ft^3.

The drift-flux model is also useful in studying the flow regions and the operation conditions. For example, if an operation system gets upset and the gas- and solids-flow rates and particles properties are known, then we probably can analyze the causes of upsets. However, the drift-flux model generally does not reveal much to prevent the dipleg upset. In this regard, the continuity wave theory provides a better tool.

4.3.2.2 Analysis Using Continuity Wave Theory

The continuity wave (also called kinematic wave) theory states that there are continuity waves whenever there is a relationship between flow rate and concentration (Wallis, 1969). The gas-solids flow in the dipleg obviously fits into this general category because flow rates change with the void fraction (the gas-phase concentration). In the following, the continuity wave theory is used to analyze flows in the dipleg so that some insight into the dipleg operation and design can be gained. It is interesting to repeat here the comments made by Shingles and Dry (1986) about standpipe and dipleg design and operations:

> "Though standpipes have been employed industrially for more than thirty years, their design and operation is still regarded as something of a black art: past experience and rules of thumb are relied on heavily."

These comments still apply today.

The emphasis of this analysis is to achieve a better understanding of the flow phenomena in the dipleg. A deeper understanding of the gravity driven gas-solids flows can be very beneficial to the design and operation of the dipleg or standpipe. At the current stage of understanding of the flow system it is too complex to completely describe the flow system. A very simple model system is explained below to explore the fundamental nature of the flow system.

The continuity wave velocity can be directly derived from the gas-solids continuity equations. Under the assumption of one-dimensional flow, combination of equations (3) and (4), after some algebraic manipulations, gives:

$$\frac{\partial \varepsilon}{\partial t} + \hat{U}\frac{\partial \varepsilon}{\partial x} = \varepsilon(1-\varepsilon)\frac{\partial (V-U)}{\partial x} \tag{10}$$

where,

$$\hat{U} = U(1-\varepsilon) + V\varepsilon \tag{11}$$

Equations (10) and (11) are the same as those derived by Gadaspow (1994). However, equation (11) was misinterpreted as continuity wave velocity. Since there is some functional dependence between the phase velocity difference, V-U, and the void fraction, equation (11) does not describe the continuity wave velocity.

For the sake of definiteness the following relationship is assumed to exist for the gas-solids flow in the dipleg:

$$V - U = U_c f(\varepsilon) \tag{12}$$

In equation (12), U_c is a characteristic velocity similar to the particle terminal velocity used in Richardson and Zaki equation and its exact value is not very important for the qualitative study performed here. Further, the characteristic velocity is assumed to be independent of void fractions. The term f(ε) denotes an unknown function of the void fraction.

Substitution of equation (12) into (10) gives:

$$\frac{\partial \varepsilon}{\partial t} + C(\varepsilon)\frac{\partial \varepsilon}{\partial x} = 0 \tag{13}$$

Here C(ε) is the propagation velocity of the continuity waves and expressed as:

$$C(\varepsilon) = U(1-\varepsilon) + V\varepsilon - U_c\varepsilon(1-\varepsilon)f'(\varepsilon) \tag{14}$$

In equation (14), f'(ε) stands for the derivative of the void function f(ε) with respect to the void fraction, ε.

In terms of gas- and solids-phase superficial velocities, the continuity wave velocity can be expressed as:

$$C(\varepsilon) = \frac{U_g(1-\varepsilon)}{\varepsilon} + \frac{U_s\varepsilon}{1-\varepsilon} - U_c\varepsilon(1-\varepsilon)f'(\varepsilon) \tag{15}$$

Equation (14) or (15) can be applied to the flow in the dipleg. The first application is to study the flooding phenomena. As has been pointed out earlier, the dipleg cannot be operated under the flooding conditions. There is a known connection between flooding and the continuity

wave velocity. If the propagation velocity of a continuity wave becomes zero, the system is in a flooding condition (Moron and Dukler, 1984).

Under the zero propagation velocity of the continuity wave, equation (15) can be rewritten as:

$$U_g = -\varepsilon^2 \left[\frac{U_s}{(1-\varepsilon)^2} - U_c f'(\varepsilon) \right] \tag{16}$$

Equation (16) will give a flooding diagram when the superficial gas velocity is plotted against the solids velocity for a given void fraction function, f(ε), void fractions, and the characteristic velocity.

The flooding conditions can also be studied from the individual-phase flow velocity. Eliminating the solids velocity, V, from equation (14) by application of equation (12), produces the following:

$$C(\varepsilon) = \frac{U_g}{\varepsilon} + U_c \varepsilon \left[f(\varepsilon) - (1-\varepsilon) f'(\varepsilon) \right] \tag{17}$$

Setting the propagation velocity at zero yields the superficial gas velocity at flooding:

$$U_g = -U_c \varepsilon^2 [f(\varepsilon) - (1-\varepsilon) f'(\varepsilon)] \tag{18}$$

Similarly, we can obtain the solids-phase superficial velocity at flooding:

$$C(\varepsilon) = \frac{U_s}{1-\varepsilon} - U_c (1-\varepsilon)[f(\varepsilon) + \varepsilon f'(\varepsilon)] \tag{19}$$

Setting the propagation velocity to be zero, we have the superficial solids velocity at flooding:

$$U_s = U_c (1-\varepsilon)^2 [f(\varepsilon) + \varepsilon f'(\varepsilon)] \tag{20}$$

Equations (18) and (20) can be used to calculate the solids and gas-flow rate at flooding. To avoid flooding the dipleg, the operation gas and solids velocity should be away from the flooding conditions.

It is interesting to notice that combination of equations (18) and (20) will give an equation:

$$\frac{U_g}{U_s} = -\frac{\varepsilon^2 \left[f(\varepsilon) - (1-\varepsilon) f'(\varepsilon) \right]}{(1-\varepsilon)^2 \left[f(\varepsilon) + \varepsilon f'(\varepsilon) \right]} \tag{21}$$

The characteristic velocity does not appear in this equation. One application of this equation is to derive an expression for the void fraction function for a gas-solids flow system. Equation (21) can be used to solve for f(ε):

$$f(\varepsilon) = f_0 \exp\left(- \int \frac{K+1}{(K+1)\varepsilon - 1} d\varepsilon \right) \tag{22}$$

in which:

$$K = \frac{(1-\varepsilon)^2 U_g}{\varepsilon^2 U_s} \tag{23}$$

and f_0 is an integration constant. Although the exact form of the functional relationship between the void fraction and f(ε) cannot be solved from equation (22) because the ratio of U_g /U_S is also a function of the void fraction, equation (22) indeed indicates that the functional relationship is quite complex. It is difficult to have a simple form as the Richardson and Zaki type of correlation.

For the purpose of illustration and comparison with the literature, the Richardson and Zaki type correlation is assumed applicable, notwithstanding the complexities mentioned above. According to Richardson and Zaki correlation, the void function f(ε) can be expressed per the following:

$$f(\varepsilon) = \varepsilon^{n-1} \tag{24}$$

The exponent n is a constant depending on the particle Reynolds number.

Inserting equation (24) into equation (18), gives the following results:

$$U_g = U_c \varepsilon^n [n(1-\varepsilon) - 1] \tag{25}$$

Equation (25) gives the same result as that derived by Kwauk (1963) although the path of derivation is quite different.

Similarly, inserting equation (24) into (20), we have:

$$U_s = U_c (1-\varepsilon)^2 n \varepsilon^{n-1} \tag{26}$$

Again, this result is also identical to that obtained by Kwauk (1963) and indicates a valid approach.

Eliminating the characteristic velocity U_c from equations (25) and (26), yields equation (27).

$$\frac{U_g}{U_s} = \frac{[n(1-\varepsilon)-1]\varepsilon}{n(1-\varepsilon)^2} \tag{27}$$

This equation can be used to calculate the flooding conditions at different gas and solids velocity for given void fractions.

Figure 4.3.2-3 is a plot of equation (27) at different void fractions. Also shown in figure 4.3.2-3 are the two points of the test data from CCT5A and CCT6.

It is interesting to note that although equation (27) is derived from the oversimplified void function (i.e., the Richardson and Zaki type of correlation), the two points of the test data indeed fall on the flooding curve of the void fraction of 0.95. The void fraction at the time of the dipleg upset is not known. The estimation is that the void fraction ranged from 0.93 to 0.98 depending on the position of the solids in the dipleg. In the calculation of the solids superficial velocity in the dipleg, the solids circulation rate and the energy balance around the dipleg inlet to the standpipe are used. The gas-phase superficial velocity is estimated based on the assumption that at the time of the flooding all aeration gas is flowing upwards.

A more important application of the continuity wave theory is to infer possible guidelines to operation to improve the stability of the dipleg. This application can be inferred by reexamining equation (13). It is noted that equation (13) is a total derivative of ε. That is:

$$\frac{d\varepsilon}{dt} = \frac{\partial\varepsilon}{\partial t} + \frac{\partial\varepsilon}{\partial x}\frac{dx}{dt} \tag{28}$$

Comparing of equation (28) with (13) shows the following:

$$\frac{d\varepsilon}{dt} = 0, \qquad \frac{\mathrm{dx}}{\mathrm{dt}} = C(\varepsilon) \tag{29}$$

Special attention needs to be paid to the process in which the wave velocity "becomes" zero when flooding occurs. It is important to realize the process dynamics. Any disturbance in the dipleg will generate a continuity wave in a gas-solids flow system. The zero wave velocity means that the disturbance cannot be propagated.

Whenever a disturbance is referred to, it is easier to think of it in terms of strong disturbances. In the process, there are some strong disturbances affecting dipleg operation such as the PCD back-pulse and coal feeder failure. To keep the dipleg flow stable when such strong disturbances occur, the flow itself needs to be able to propagate the continuity waves properly without causing flooding. However, less obvious disturbances always exist in the gas-solids flow system. The pressure fluctuations in the riser, for example, can cause disturbances to flow in the dipleg. Another example is that the fluctuations in the solids level in the standpipe can introduce disturbances in the dipleg.

All kinds of disturbances will generate continuity waves with different initial velocities. Under one-dimensional assumption, the continuity wave can propagate in either of two directions. No matter which direction that the continuity wave will propagate, the wave velocity has to decay to reach zero velocity so that flooding occurs. Mathematically speaking, the flooding condition is:

$$C(\varepsilon) = \frac{dx}{dt} < 0 \qquad \text{and} \qquad \frac{\mathrm{dC}(\varepsilon)}{d\varepsilon} > 0 \tag{30}$$

or

$$C(\varepsilon) = \frac{dx}{dt} > 0 \qquad \text{and} \qquad \frac{\mathrm{dC}(\varepsilon)}{\mathrm{d}\varepsilon} < 0 \tag{31}$$

Equations (30) and (31) state the simple fact that if the wave velocity is less than zero, it must increase to reach zero velocity.

Next, the conditions prescribed by equations (30) and (31) effect on the dipleg operations are examined. To be more specific, the coordinate is set as follows: the origin is at the inlet of the dipleg to the standpipe and the positive direction is upward. It is noted that it does not matter how the coordinate is setup.

In examining equation (30) first, the continuity wave velocity, C(ε), at less than zero means that the wave will propagate towards the origin. If the wave velocity becomes zero, the velocity gradient of continuity wave shall be negative, i.e., $dC(\varepsilon)/dx$ <0, for flooding to occur before the waves leave the dipleg. To satisfy that:

$$\frac{dC(\varepsilon)}{d\varepsilon} = \frac{dC(\varepsilon)/dx}{d\varepsilon/dx} > 0 \tag{32}$$

So $d\varepsilon/dx$ must be less than zero. On the other hand, if flooding is to be avoided, $dC(\varepsilon)/dx > 0$ is required (the wave will propagate along the flow direction) and $d\varepsilon/dx$ <0 . This means that in order to avoid flooding, when the wave propagates in the same direction as mean flow, the wave velocity is growing in the flow direction. Furthermore, this also means that the void fraction is increasing along the mean flow direction. It is emphasized that the positive direction of coordinate is upward and the mean flow direction is downward.

For the flooding condition expressed in equation (31), a slightly different line of reasoning needs to be applied but the same conclusion as from equation (30) can be reached. For the continuity waves propagating in the positive direction (C(ε) >0), the wave velocity decay is unavoidable because the wave is propagating against the mean flow and the gravity forces. It is also desirable, from the operation view point, that the waves propagating against mean flow have a decayed velocity because the waves are disturbances to the flow. From this reasoning, the wave

velocity decay ($dC(\varepsilon)/dx < 0$) is concluded to be system in nature. For the given $dC(\varepsilon)/dx < 0$, and to satisfy the flooding conditions given by equation (31), it is required that $d\varepsilon/dx > 0$. On the other hand, in order to avoid flooding in the dipleg, the condition that $d\varepsilon/dx < 0$ must be satisfied. It is the same conclusion that has been obtained from equation (30). Therefore, from the dipleg operation and design viewpoint, the void fraction should increase in the flow direction to avoid flooding in the dipleg.

This is valuable information for the dipleg operation and design, and to the author's knowledge it is the first time that the dipleg flow has been put into the theoretical perspective in this way. This is contrary to the current conventional thought that for a stable flow the bed density should increase in the downward flow direction because of compression. This conforms with other most observed gravity flow systems, such as sedimentation. From the above theoretical analysis the stable flow mode is to increase the void fraction in the flow direction.

From above theoretical analysis, under certain flow conditions the gravity flow system can be flooded. The cause of the flooding is the unfavorable void fraction profile. This theoretical analysis indicates that the substantial amount of aeration required in the bottom of the standpipe or dipleg is to increase the void fraction in the flow direction to have a stable operation. This is contrary to conventional thought, in which the static head in the dipleg governs the solids flow. The analysis also explains that the transition to the packed bed in the flow direction can cause flooding because the void fraction in the flow direction is decreasing.

In practice, it will be very difficult for the void fraction to keep increasing in the flow direction. If the flow in the dipleg is in the direction of increasing void fraction, the entire dipleg flow must be in a dilute flow regime because the void fraction is already very low in the bottom of the cyclone. It is very difficult to design the cyclone loop to have a good pressure balance with very low pressure drop in the dipleg because the purpose of the dipleg is to transfer solids from a low-pressure region to a high-pressure region. If the entire dipleg is in a dilute flow region, this purpose cannot be served and the operation will be difficult. Fortunately, the transition from the very dilute-phase flow below the cyclone to the dense-phase flow is short. This short transition can have some influence on the dipleg operations. However, if the flow in the rest of the dipleg is stable, the short transition is manageable. From this reasoning, a section of the dipleg can be in a dense-phase mode. Once the dense phase is formed the bed density should decrease along the flow direction or the void fraction should increase in the flow direction.

To gain some quantitative information, let us consider a specific problem. Suppose that before the disturbance starts, the void fraction profile in the dipleg is a known function and can be described by:

$$\varepsilon = g(x), \qquad @t = 0, \quad 0 < x < \infty \tag{33}$$

Equation (33) is an initial condition for equation (29). First, observe that since the total derivative $d\varepsilon/dt = 0$, the void fraction remains constant on a curve (say, $\Re$). It is then further

reasoned that C(ε) remains constant along the same curve. Therefore, the curve $\Re$ must be a straight line in (x,t) plane with a slope of C(ε). Thus, the general solution of equation (29) depends on the construction of a family of straight lines in (x,t) plane, each line with a slope of C(ε) corresponding to the value of the void fraction, ε, on it. Figure 4.3.2-4 is an example of the plot of the family of curves.

From the initial condition given by equation (33), if one of the curves intersects t = 0 at x =ξ, then ε = g(ξ) on that curve, as shown in figure 4.3.2-4. The corresponding slope of the curve is C(g(ξ)), denoted by F(ξ). Then the equation for the curve is:

$$x = \xi + F(\xi)t \tag{34}$$

This determines one typical curve and the value of ε on it is g(ξ). Allowing ξ to vary, the whole family of curves is obtained:

$$\varepsilon = g(\xi), \qquad C(\varepsilon) = C(g(\xi)) = F(\xi) \tag{35}$$

from the curve defined by equation (34).

Since equation (35), defined from equation (34), is a characteristic solution, the circumstances under which the dipleg will be in upset condition can be explored from these equations. Therefore, the following is obtained from equation (35):

$$\frac{\partial \varepsilon}{\partial t} = g'(\xi)\frac{\partial \xi}{\partial t} \qquad \frac{\partial \varepsilon}{\partial \mathrm{x}} = g'(\xi)\frac{\partial \xi}{\partial x} \tag{36}$$

From t and x derivatives of equation (34):

$$0 = F(\xi) + [1 + F'(\xi)t]\frac{\partial \xi}{\partial t} \tag{37}$$

and

$$1 = [1 + F'(\xi)t]\frac{\partial \xi}{\partial x} \tag{38}$$

Inserting equation (37) and (38) into (36):

$$\frac{\partial \varepsilon}{\partial t} = -\frac{F(\xi)g'(\xi)}{1 + F'(\xi)t} \tag{39}$$

and

$$\frac{\partial \varepsilon}{\partial x} = \frac{g'(\xi)}{1 + F'(\xi)t} \tag{40}$$

It can be immediately seen that equations (39) and (40) are indeed the solution of equation (29) since C(ε) = F(ξ). More importantly, both the space and time derivatives "break" when:

$$t = t_b = -\frac{1}{F'(\xi)} \tag{41}$$

Sine $t_b > 0$, then $F'(\xi) < 0$ when the void fraction loses the continuity in both time and space. Since $F'(\xi) < 0$ implies that $C'(\varepsilon) < 0$, the most possible flooding condition may be concluded to be the condition given by equation (31). As has been discussed above, to avoid flooding from occurring the dipleg should operate under the condition that the void fraction increases along the flow direction once the dense phase has been formed below the cyclone.

The position inside the dipleg where flooding may start can also be predicted from equation (34) and (41). Substitution of equation (41) into equation (34) gives the flooding position as:

$$X_B = \xi_B - F(\xi)/F'(\xi) \tag{42}$$

Here X_B is the final location of flooding and ξ_B is the initial location of the disturbance. If the initial distribution of the void fraction in the dipleg is known and the flooding condition such as equation (30) or (31) is also satisfied, the location of the dipleg flooding is predictable. However, at the current stage, the initial distribution of the void fraction and wave velocity is not known. Therefore, the prediction of flooding position has to be qualitative.

It should be pointed out that although using continuity wave theory to describe the flow in the dipleg is qualitative in nature, this theory can explain many dipleg upset phenomena given in section 4.3.1. Detailed discussion will be reserved for the future.

In summary, dipleg flooding can be predicted qualitatively. A set of conditions given in equation (30) or (31) must be satisfied for flooding to occur. To avoid the dipleg flooding, the void fraction in the dipleg should increase along the flow direction once the dense phase has been reached in the dipleg. In practice, adjusting the aeration rate in the dipleg can make the void fraction higher in the flow direction.

In order to better understand, quantitatively predict, and confidently design the flow in the dipleg, the most fundamental aspect that needs a careful study is the relationship between the solids downward flow rate and the void fraction. In this analysis, the Richardson and Zaki type correlation has been shown to oversimplify the problem.

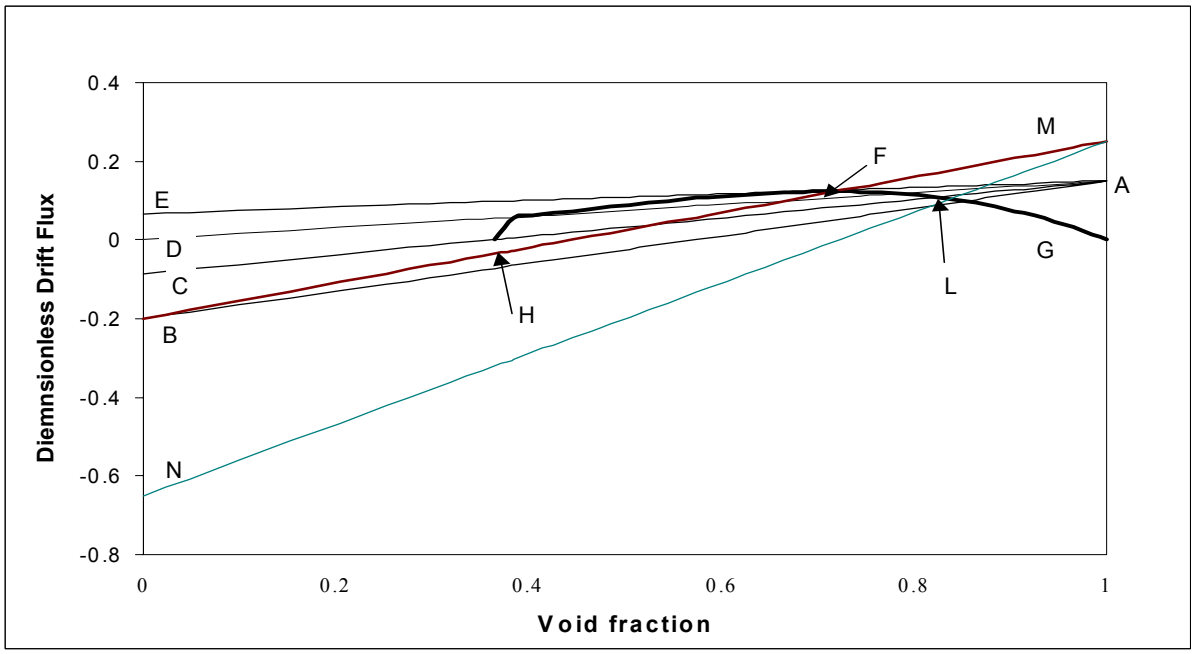

Figure 4.3.2-1 Illustration of Drift-Flux Plot

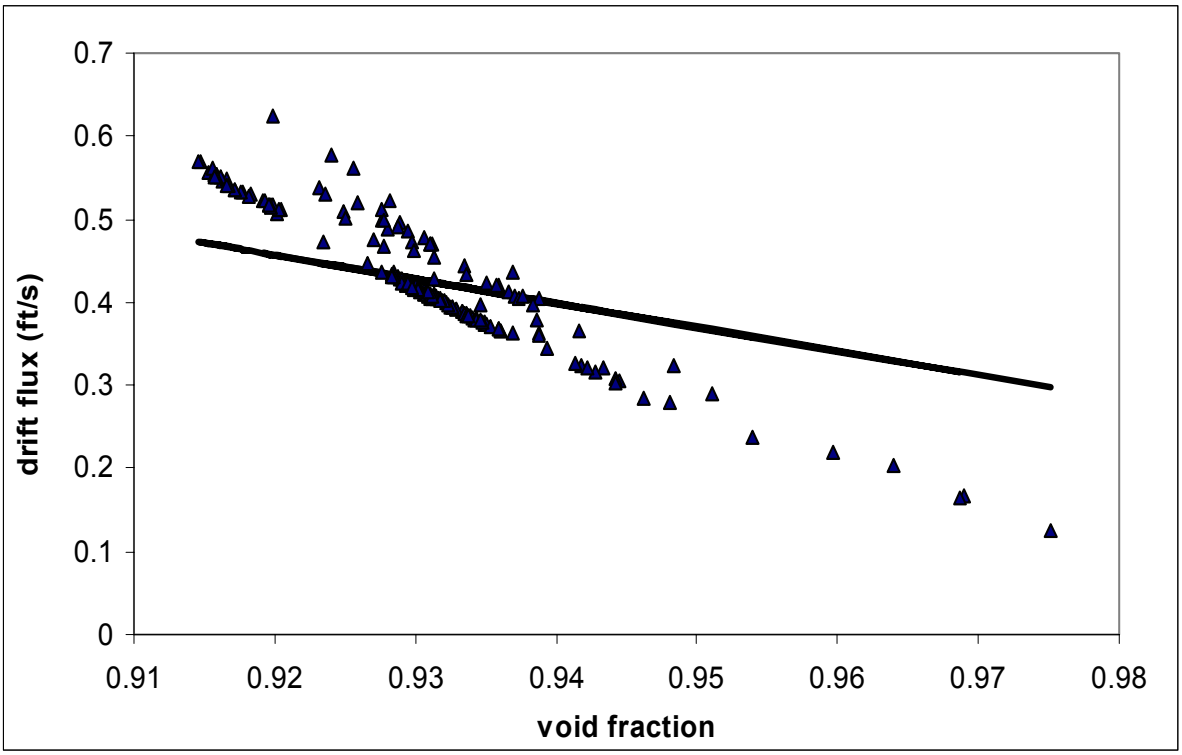

Figure 4.3.2-2 Illustration of the Experimental Drift-Flux Plot

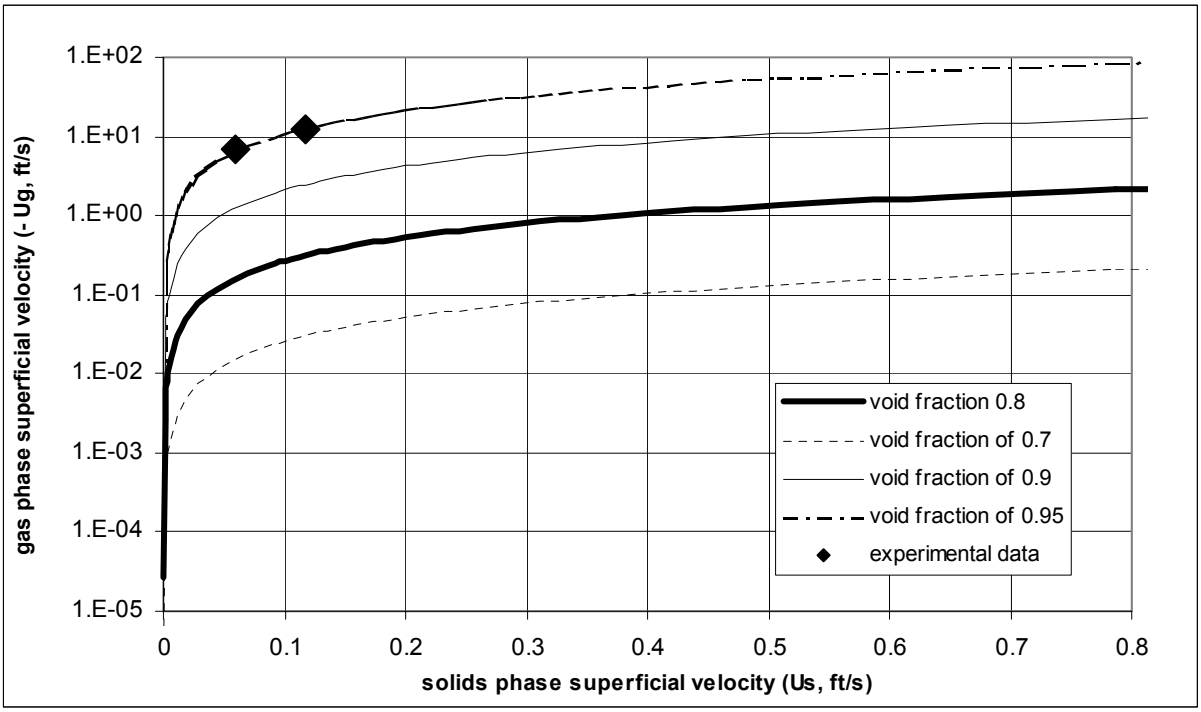

Figure 4.3.2-3 Plot of Flooding Lines at Different Void Fractions

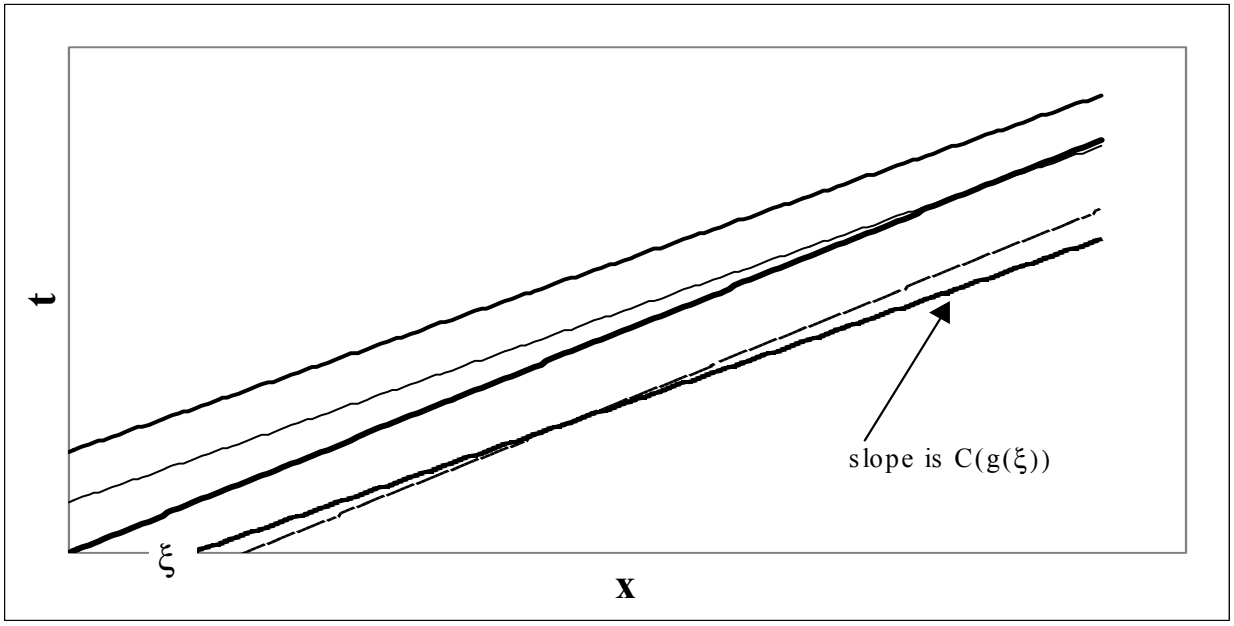

Figure 4.3.2-4 Wave Lines for Different Initial Time and Locations

4.3.3 The Stable Operation of the Dipleg and Related Design Issues

As has been discussed above, the stable operation of the dipleg can be achieved by increasing the void fraction in the solids flow direction. In terms of practical operation, the only means at PSDF's disposal is to adjust the aeration rate and the solids circulation rate. The major adjustable parameter to increase the solids circulation rate is the solids inventory and the aeration rate in the entire reactor loop.

An increase in aeration rate at the bottom of the dipleg will serve the purpose of increasing the void fraction in the flow direction. This makes sense both intuitively and theoretically. Consider the gas-flow path when it is injected from the aeration nozzle at the bottom of the dipleg. Since flows in both dipleg and standpipe are gravity driven flow, the pressure at the inlet of the dipleg to the standpipe is higher than that at the cyclone and the disengager. The natural flow path of gas is toward the cyclone and disengager. The solids flow, however, provides a force (momentum) that can at least slow down the gas upward flow. Furthermore, the downward flow solids also entrain a certain amount of gas with them. The amount of gas entrained by the solids depends on the void fraction in the dipleg. The higher the void fraction, the more the gas is entrained. At the aeration nozzle the void fraction will suddenly increase and the amount of gas entrained by the solids will increase. Therefore, the solids will be the carrier for the gas flow against the pressure gradient in the downward direction. This is one reason that aeration can increase the void fraction in the flow direction.

Another factor that favors gas flow in the flow direction is the solids velocity. As can be seen from the Richardson and Zaki correlation, the solids flow velocity will increase with the increased void fraction. The solids particles will accelerate at the aeration nozzle because of higher void fraction in the region. Incidentally, this is the major contribution of aeration to increasing the solids flow rate. The accelerated solids particles will entrain more gas with them so that the amount of gas flow in the downward direction will increase. The void fraction in the flow direction will increase.

A further theoretical consideration will reveal that the gas injected into the dipleg through the aeration nozzle will not be "exactly" trapped in the nozzle region. The first factor that favors the gas upward flow is the pressure difference as has been mentioned above. The amount of gas percolated through the solids phase is proportional to the square root of the pressure difference if no other force is acting against the gas flowing upward. Any reasonable pressure difference (to compensate loop pressure balance) in the dipleg will render most of the aeration gas flow upward. This will make it difficult to increase the void fraction in the mean flow direction. Fortunately, as pointed out previously, the solids flow will entrain gas flow with them and at higher void fraction the solids will entrain more gas with them. This effect will compensate the pressure difference and the addition of aeration will be beneficial to the flow stability.

It becomes clear that in order to make the dipleg operation stable the addition of aeration to the bottom of the dipleg is necessary. Figure 4.3.3-1 gives the pressure difference in the vertical section of the dipleg for a stable operation period. As can be seen from the figure, within this time period the pressure difference in the dipleg remains positive. The disturbances caused by the PCD back-pulse can be clearly seen from this plot. The rapid recovery of the pressure

difference in the dipleg indicates that the dipleg operation is indeed very stable. This stable operation was achieved through adjusting the aeration in the dipleg so that the void fraction in the flow direction will be higher.

The desired void fraction profile has been achieved in the dipleg as seen in figure 4.3.3-2, in which the relative bulk density of the dipleg is plotted against the relative height of the dipleg. The relative bulk density is calculated by dividing every measured point density by the bulk density at the top of dipleg, which is 6 ft below the cyclone outlet. The bulk density of the dipleg was measured by gamma ray transmission scans by specifying the density in the top of the standpipe as zero. Therefore, the bulk density measured by gamma transmission scans is also a relative density. Figure 4.3.3-2 shows that the bulk density at the top of the dipleg is about 20 times higher than that at the bottom, which is located in the standpipe at the dipleg inlet. It should be noted that during this operation period the solids level in the standpipe is above the dipleg inlet shown by the same measurement. The low-density region created by aeration around the dipleg inlet is beneficial to the stable operation of the dipleg.

The key design issue that can be inferred from theoretical analysis of the dipleg flow is that the pressure difference and balance in the loop is a result of flow. Controlling the flow rate is the key, not pressure balance. From this viewpoint the flow rate in the dipleg, and neither the solids level nor the bulk density, is critical to prevent gas-reverse flow. This does not mean that the solids level and the bulk density are not important in the design of the dipleg. Rather, these variables are not related to the reverse-gas flow (flowing upwards). In other words, the pressure difference, pressure drops, and sometimes even the bulk density will set itself to a certain equilibrium values once the flow rate and the diameter of the dipleg are fixed.

In the application of the concepts presented here to the dipleg design, it should be realized that uniformly aerated dipleg will not be stable. The aeration flow rate should increase in the flow direction because of the requirement of the increasing void fraction in the flow direction. Incidentally, PSDF operation has repeatedly proved that the uniform flow rate through all aeration nozzles in the dipleg will cause the dipleg upset. The reason for this is that some sections downstream of some aeration nozzles in the mean flow direction have a lower void fraction than that around aeration nozzles. As has been pointed out, this will cause flooding.

All these concepts are important to enhance understanding dipleg and standpipe design and operation. These concepts, and what was attempted at PSDF to achieve stable operations, are contrary to conventional thought and practice.

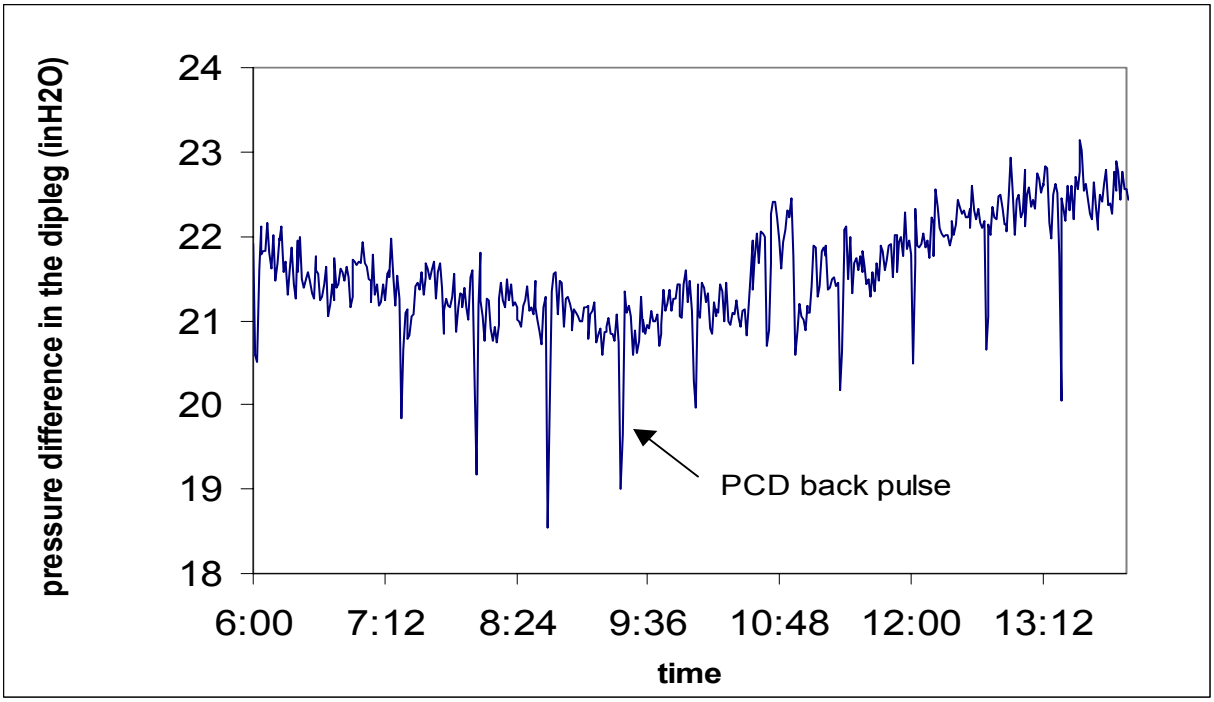

Note: The pressure difference never goes to negative in this time period. The PCD back-pulse is still "seen" by the pressure difference in the dipleg.

Figure 4.3.3-1 Example of Stable Operation of Dipleg

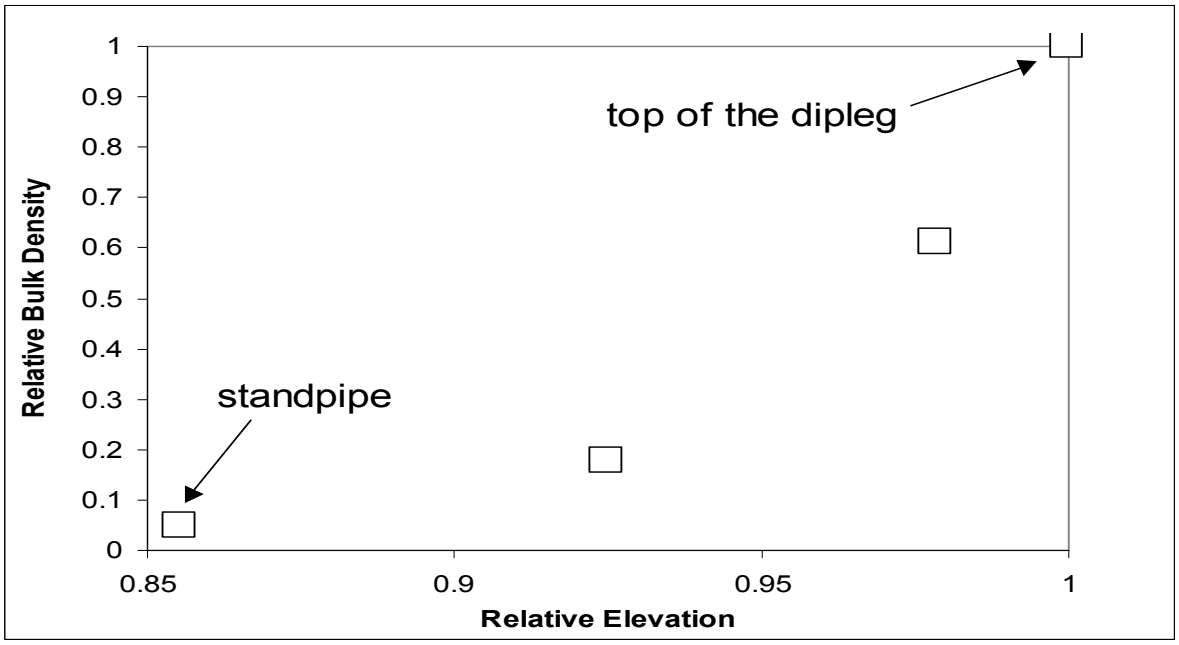

Figure 4.3.3-2 Variation of the Bulk Density With Height in the Dipleg to Show Density is Decreasing Along the Flow Direction Measured by Gamma Transmission Scans

4.3.4 Summary

In this section the brief history of the operation and troubleshooting process of the dipleg problem is reviewed. Although many operational parameters and disturbances can cause dipleg upsets and excessive solids carryover to the PCD the key cause of these dipleg upsets is flooding. The analysis from the drift flux model can qualitatively indicate possible flooding condition and the flow regime in the dipleg. The continuity wave theory gives direction to improve the stability of the dipleg. The continuity wave theory analysis concludes that an increase in void fraction in the solids flow direction, regardless of which direction the continuity wave propagates, will always prevent dipleg flooding from occurring.

It is also reasoned that the flow rate is more important in the dipleg design. The pressure difference is a secondary variable. In other words, the mixture velocity is the critical parameter to be controlled. The pressure difference and pressure balance in a flow loop sets itself once the flow velocity has been set up. The position of aeration nozzles and flow rate at each nozzle are also important in improving the stability of the dipleg operations.

REFERENCES

Avidan, A. A. and Yerushalmi, J., 1982, "Bed expansion in high velocity fluidization," *Powder Technology*, 32, 223-242.

Gidaspow, D., 1994, *Multiphase Flow and Fluidization: Continuum and Kinetic Theory Descriptions*, Academic Press, New York.

He, Y. and Rudolph, V., 1996, "The volume-average voidage in the riser of a circulating fluidized bed," Powder Technology, 89, 79-82.

Hewitt, G. F., 1982, "Void Fraction," Ch. 2.3 in *Handbook of Multiphase Systems* (Hetsroni, G. Ed.), McGraw-Hill, New York.

Jones, P. J. and Leung, L. S., 1985, "Downflow of solids through pipes and valves," in *Fluidization, 2nd edition* (Davidson, J. F., Clift, R. and Harrison, D. ed.), Academic Press, New York.

King, D. F., Forde, R. M., Leaney, P. W., MaKar, E. M., and Zenz, F. A., 1989, "FCC cold modeling helps solve FCC standpipe flow problems," in *Fluidization VI* (Grace, J. R. Shemilt, L. W., and Bergougnou, M. A. eds.), Engineering Foundation, New York.

Kunii, D. and Levenspiel, O., 1991, *Fluidization Engineering, Second Edition*, Butterworht-Heinemann, Boston, 375.

Kwauk, M. (1963), Scientia Sinica 12(4), 587.

Leung, L. S. and Jones, P. J., 1978, "Flow of Gas-Solid Mixtures in Standpipes. A Review," Powder Technology, 20, 145-160.

Maron, M. D. and Dukler, A. E., 1984, "Flooding and Upward Film Flow in Vertical Tubes—II, Speculations on Film Flow Mechanisms," *Int. J. Multiphase Flow*, 10, 599-621.

Richardson, J. F. and Zaki, W. N., 1954, "Sedimentation and Fluidization Part I," Trans. Instn. Chem. Engrs. 32, 35-53.

Shingles, T. and Dry, R. J., 1986, "Circulating Fluidized Beds," Ch. 33 in *Encyclopedia of Fluid Mechanics, Vol. 4, Solids and Gas-Solids Flows* (Cheremisinoff, N. P., Ed.), Gulf Publishing Com., Houston, Texas.

Teo, C. S. and Leung, L. S., "Vertical Flow of Particulate Solids in Standpipes and Risers," Ch. 20 in *Encyclopedia of Fluid Mechanics, Vol. 4, Solids and Gas-Solids Flows* (Cheremisinoff, N. P., Ed.), Gulf Publishing Com., Houston, Texas.

Wallis, G. B., 1969, *One-dimensional Two-phase Flow,* McGraw-Hill, New York.

5.0 AUXILIARIES AND BALANCE-OF-PLANT

There are a number of auxiliaries and balance-of-plant systems to support the operation of the transport reactor train, most of which are of conventional design and commercially available. Deviations from conventional design were mainly due to either the sizing of the facility or process requirements. Design revisions were addressed during the course of construction, start-up, commissioning, and operation of the balance-of-plant equipment. Several of these were due to assumptions that changed significantly during the final design phase from those made during the early design phases. Other design changes were made to more adequately cover the requirements of operating at less than design conditions, i.e., during start-ups and low load operations. Some equipment designs were optimized towards one operating point (for example, solids handling system and pressure letdown valve), while others were designed for excessively wide ranges (propane vaporizer and condensate coolers). At least two modifications were due to the advancement of technology for this application.

5.1 FEEDSTOCK PREPARATION

5.1.1 Description

The PSDF feedstock (coal and sorbent) preparation area consists of the feedstock reclaim system and the coal and sorbent mill systems. The feedstock is loaded into a reclaim hopper from the feedstock shed by use of a front-end loader. The feedstock travels from the reclaim hopper via conveyor through a magnetic separator to a crusher. After being reduced to ¾ in. or smaller at the crusher, the feedstock is conveyed to the respective crushed silo (coal or sorbent). In the separate coal/sorbent mill systems, feedstock is fed to a roller mill and pulverized. A certain amount of oversize particles are returned to the mill while heated air transports the bulk of the pulverized material to a cyclone collector where the material is separated from the transport air. The solids collected at the baghouse are deposited into the pulverized coal (or sorbent) silo. The pulverized material is fed to a vibrating screen where oversize particles are returned to the crushed coal (sorbent) silo while the correct size material flows to the pulverized coal (sorbent) silo. The coal mill is sealed with nitrogen and the sorbent mill is sealed with air.

The sorbent mill system performed well in 1997 and no modifications were made. During the first half of 1997 there was too great a variability in the coal particle size that was produced as feed to the transport reactor system. The investigation into the cause and resulting changes to improve the particle size variation in the latter half of 1997 are described below.

5.1.2 MWK Coal Pulverizer System Modifications to Improve Grind Consistency

Figure 5.1.2-1 shows the mean coal particle size of samples taken during runs of the coal pulverizer system while processing coal for the transport reactor before run TC01. The mean particle sizes range from 250 to 619 μm. The target mean particle size for this time period was 300 μm. Obviously, variations from the target of ±319 and -50 μm are not ideal.

Tests to ascertain the sources contributing to overall particle size variation were performed that focused on the pulverizer control system, the reclaim system (hammer mill) operation, and the feedstock size variation. It quickly became evident that variation introduced by the pulverizer control system or the reclaim system was not the source of the large variation in output size. The pulverizer inlet feedstock size, however, did prove to be one large (or major) source of the variation.

As the system was originally designed there were two sources for coal fed to the crushed material storage hopper (pulverizer feed hopper). The first source was the reclaim system, with ¾ x 0 in. coal coming from the pile through the hammer mill, and the second was the 1,000- to 4,000-μm oversize particles (with respect to the target mean particle size of 300 μm) coming from the scalping screen in the pulverizer system itself. During pulverizer system operation oversize particles were continuously introduced into the pulverizer feed hopper. Coal from the coal pile is fed into the hopper in 10- to 20-ton batches. This combination of coal feed sources resulted in layers within the pulverizer feed hopper of alternately large (¾ x 0 in.) and smaller (1,000 to 4,000 μm) coal.

Since the pulverizer system was tuned for the ¾ x 0 in. coal, the output mean particle size was achieved with relatively less variation as compared to the above when this large coal was fed to the pulverizer. However, as the smaller coal began feeding into the pulverizer the output mean particle size doubled.

This doubling of particle size is explained as follows. Since the small particle size coal has already passed through the pulverizer once, the particles are small enough to be entrained in the transport gas stream and are transported out of the pulverizer. Therefore the particles have minimal work done on them, meaning the particle sizes are reduced very little, and there are no fines, because this coal has been through the pulverizer once, so the mean particle size actually increases. Consequently, it was shown that the pulverizer coal feed size variation was the major contributor to the overall variation in the mean particle size at the output of the pulverizer system. To correct this, consistent mixing of the smaller-size coal stream with the larger-size coal stream is required.

Mixing these two coal streams could occur in any of the following three places:

1. The pulverizer feed hopper.

2. The pulverizer.

3. The feed stream between the storage hopper and the pulverizer.

Mixing in the storage hopper would require either a stirring mechanism in the hopper or a modification to the raw coal feed process. Both of these solutions would require major modifications and were not considered practical. Mixing in the mill would mean cutting the mill wall and adding an additional feed chute. Concerns about inducing additional stress to the mill wall and therefore shortening its life eliminated adding a second feed chute as a possible solution. The third possible solution, which posed the least problems and allowed adequate mixing, was to mix the coal streams somewhere between the storage hopper and the pulverizer.

Implementation of this mixing solution was achieved by disconnecting the existing oversize coal duct that was originally routed to the pulverizer feed hopper from the pulverizer system scalping screen and rerouting it to the pulverizer feed chute. In the feed chute large coal from the pulverizer storage hopper is gravity fed from a feed screw into the mill. In the top of the feed chute the scalped coal particles are introduced directly into the large coal and are mixed by the gravity feed as the coal falls into the mill.

Figure 5.1.2-2 shows the mean particle size achieved after the modification. The mean coal particle sizes range from 251 to 301 μm. During this time period the target mean particle size was 275 μm. Also, some of the variation seen after the change was due to the pulverizer retuning needed because of the more consistent feed size. Over time, the variation is expected to be less than the ±25 μm shown in figure 5.1.2-2 because of the ability to more precisely tune the pulverizer system.

This pulverizer modification resulted in the additional benefit of increased throughput, which is almost as important as the improved control over output particle size. As a result of the modification the pulverizer throughput has increased from 3,600 to 6,000 lb/hr, or for a 67-percent improvement.

The increase is realized because the system no longer encounters batches of scalped coal particles. During periods when only scalped particles were in the pulverizer, these particles had little work performed on them in the mill and would tend to recirculate, reducing the overall system throughput to a few hundred pounds per hour.

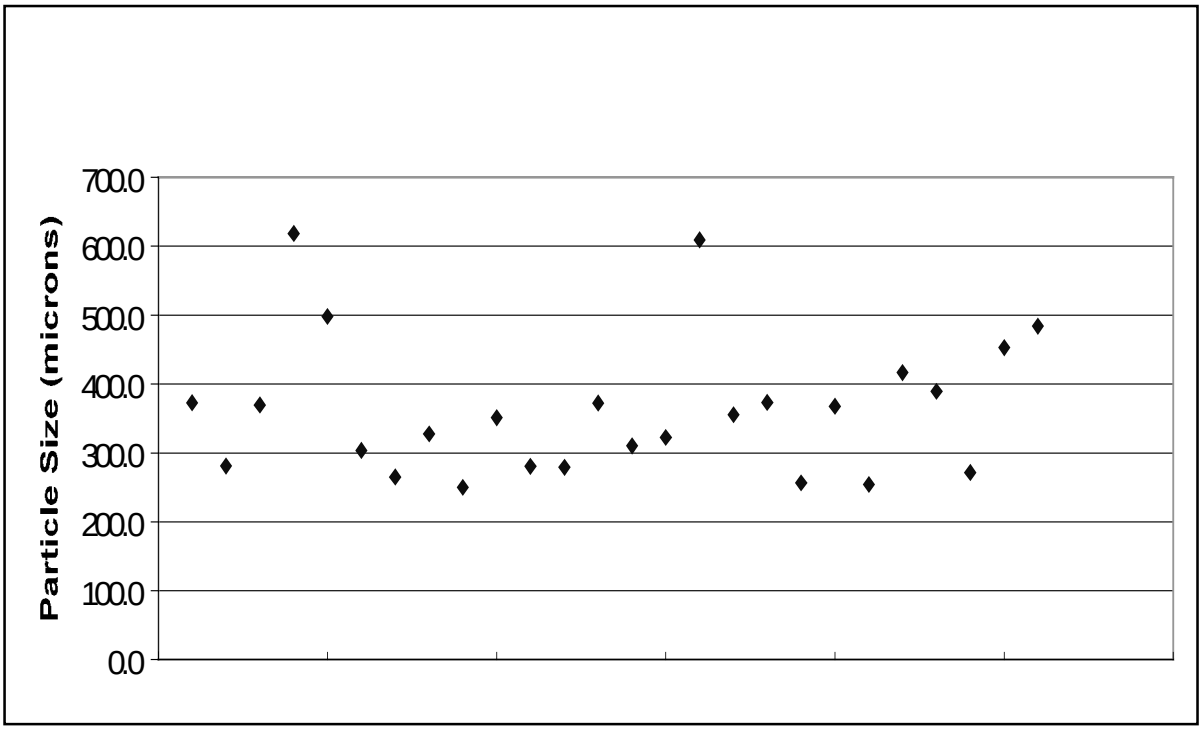

Figure 5.1.2-1 Mean Coal Particle Size Before Process Change

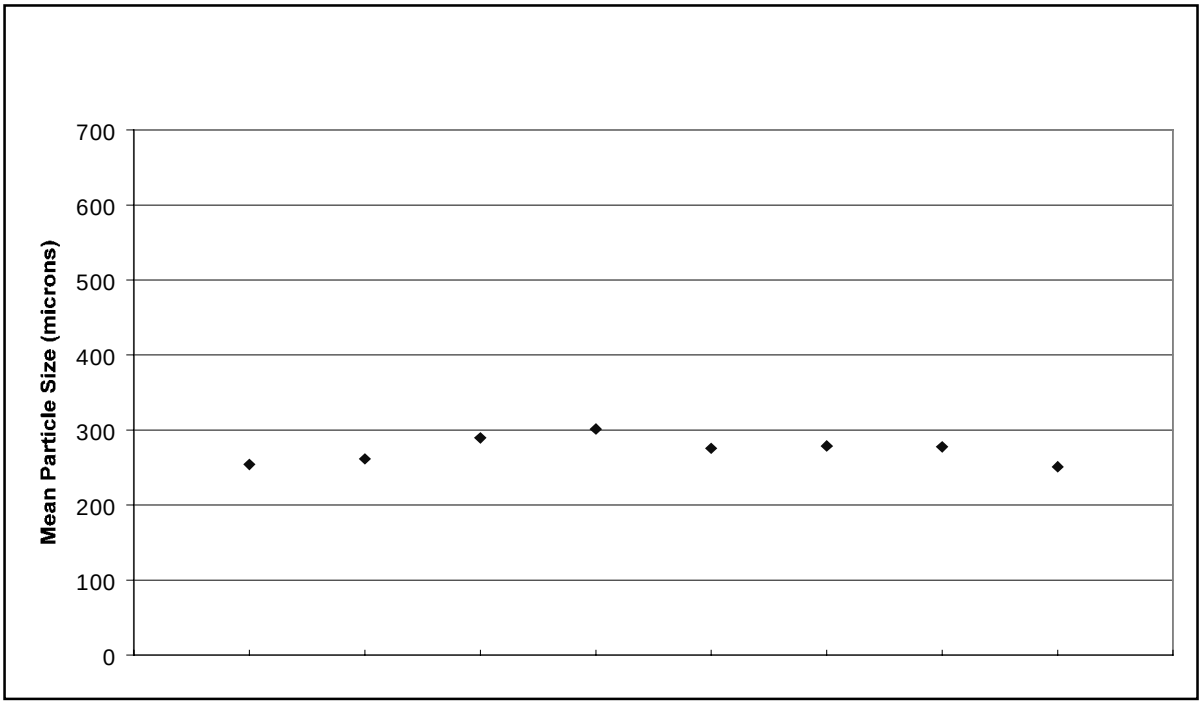

Figure 5.1.2-2 Mean Coal Particle Size After Process Change

5.2 REACTOR FEEDSTOCK INJECTION AND ASH REMOVAL SYSTEMS

Probably the single biggest challenge to the reliable transport reactor operation has been failures of the feedstock injection and the ash removal systems supplied by Clyde Pneumatic Company. These systems have to pressurize and depressurize the material while moving it into and out of the process. Failures in these systems account for over 75 percent of the transport reactor's forced outages since commissioning. However, in the past 2 years of operation, there have been only minor problems with the atmospheric dense-phase transport systems. Only the rotofeed-equipped spent solids feeder system (FD0530) presented problems other than plugged transport lines, and most of those were solved during commissioning. During the same period while working to commission (and later improve) the operation of the transport reactor, the mean time between failure of the high-pressure dense-phase systems was substantially increased from hours to weeks.

The failures of the Clyde systems can be characterized into three classes: 1) spheri valve failures; 2) level probe failures and vessel bridging; and 3) starfeeder failures.

The biggest problem involves the spheri valve operation, primarily the operation of the high-pressure (nitrogen-assisted) seals.

All of the Clyde systems rely on pneumatic interlocks for timing the spheri valve operations. These are:

1. Seal deflation.

2. Valve opening and closing.

3. Seal inflation.

This pneumatic timing is accomplished by the use of several shuttle (or pilot) valves used as pneumatic relays and the use of poppet valves as a pneumatic position switch. This design looks like a standard pneumatic application designed in the 1950's and used reliably for years. It has the additional advantage of requiring only one electrically actuated solenoid to operate the entire process, thereby saving on PLC I/O count and cabinet size. The atmospheric seal spheri valves do not have as complex an arrangement of pneumatic relays to control the seal inflation; this simplicity has been rewarding in the reliable service of these valves and seals. While the pneumatic signal to pressurize the seals originates from the cylinder-closing air routed through the "valve-closed" limit poppet valve on both the atmospheric and the high-pressure spheri valves, the high-pressure valves have an additional pilot-operated valve that controls the seal nitrogen to the seals. The signal to this pilot valve has another relay (sensing the "open" signal to the cylinder) included in the pneumatic circuit to assure early venting of the signal air to the seal pilot valve; but there is not a positive, interlock style feedback to prevent operation of the spheri valve cylinder while the seal is pressurized.

The atmospheric seal spheri valves use 100-psi instrument air to pressurize their seals, but the high-pressure seal spheri valves use 365-psi nitrogen to pressurize their seals. The loss of a spheri valve seal also causes catastrophic header pressure loss on the nitrogen seal header.

Normally, the flow/pressure control valve on this header operates at 3 to 5 percent open because this header has a very small loss rate. When a seal fails, the header pressure drops to less than 100 psi before the control valve can respond, tripping all other feeders with high-pressure seals. In the worst case, the seal pressure can fall so far that the seals themselves will deflate, allowing either the hot gases or material to escape. Several such failures (with pressure loss on the seal header) seemed to be the root cause of some failures of the FD0520 spheri valve, possibly due to ash and sand getting trapped between the seal and the dome on the lower valve. Erosion on the seal was visible, indicative of the seal not pressurizing and allowing a flow path to exist long enough for channels to start eroding in the seals and/or the dome itself.

Level probe failures result in system operating difficulties, since the level probes are the prime trigger to initiate a pressurization/depressurization cycle. These failures can cause short cycling, preventing any real movement of solids, or they can cause overfilling of the vessels, plugging, or bridging the vessels, all of which prevent any real movement of solids. The sensitivity of the probe's electronics has been the usual problem, one caused by calibration in "clean" settings yet with exposure of the probe to dusty conditions that allow a layer to collect on the probe itself and changing the probe's calibration. There have also been several electronic failures of the probes. In some cases a malfunction of the level probe causes caking and bridging (especially in coal) in the vessels due to overfilling of the vessels. In other cases, malfunction of the systems that was attributed to level probe failure was actually a result of large masses of material not moving out of the vessels.

The rotary metering feeders (starfeeders) caused several failures, usually due to plugging or binding. These are present on both coal and sorbent feeder systems (FD0210 and FD0220, respectively) as well as on FD0530. The starfeeders were equipped with inductive motors and variable frequency motor drives to adjust the injection rate of the feedstock. While such a design is very efficient and controllable in the upper half of the speed range, the motors do not generate much torque (force) in the lowest quarter of the speed range. Because the lower half of the speed range is the most critical for accurate control during start-ups and low-load operation, the choice of a DC motor or hydraulic motor would have been better for this application. Because the starfeeder relies on close clearances for sealing the star's pockets, it is susceptible to binding by material in the clearances and to oversized material wedged into the pockets. Epoxy lining was discovered in 1997 to have flaked off the feeder vessels and was getting caught in the starfeeder, both binding the star and sometimes blinding the discharge port.

As a result of the last year's work and modifications to all of the high-pressure dense-phase and feed systems, the reliability of the systems has improved significantly. These modifications include:

1. Rerouting the feeder dispense vessel vent piping.

2. Increasing the clearances in the starfeeder.

3. Rebuilding the reactor injection piping.

4. Removing the epoxy lining (that was specifically excluded in the original specification.

5. Adding differential pressure control on the dispense vessel fluidizing nitrogen.

6. Replacing every Wade tubing fitting.

7. Adding additional fluidization ports on the FD0210 lockvessel to break up cake bridges.

8. Adding the high-pressure seal dump valves (providing 3 to 4 times the flow capacity of the pilot valve vent).

9. Adding check valves and reservoirs in the feeders' seal supply lines.

10. Adjusting numerous timing and differential pressure setpoints in the PLC configuration.

The FD0210 starfeeder motor was also rewound from a 4- to a 10-pole design, which cut the speed by 60 percent and increased the motor torque by a similar amount at the same motor speed. Because this motor is powered by a variable frequency drive (VFD) to provide speed control, the functionality of the system is not compromised by such a modification since the parameters of the VFD were also adjusted to compensate for the modified speed of the rewound motor.

The system's vendor recommended scrapping the pneumatic controls on the spheri valves for a completely programmable logic controller (PLC)-based control system with additional features that were not included in the original control system design. After further review of the functionality of proposed changes, the only feature in the proposed modification that was not already in place as a result of previous PSDF modifications was a time delay in dome opening after the seal is depressurized. Other features not included in the Clyde proposal that were previously installed as a result of the PSDF experience include:

- Increasing the venting capacity of the seal pressurizing solenoid. A dump valve was installed in the spring of 1997 in parallel with the shuttle valve that controls seal pressure. This dump valve had 4 times the flow capacity of the shuttle valve vent, and ever since the installation, seal failures on all of the high-pressure Clyde systems were reduced measurably.

- Adding a low-pressure switch on the seal line. A pressure switch was installed in the fall of 1997 in parallel with the seal pressurized switch. This low-pressure switch (directly) operates a solenoid valve that prevents air from moving the dome-positioning cylinder.

It was agreed to incorporate the time delay feature proposed by Clyde into the existing control system by adding a time delay relay between the low-pressure switch and the cylinder blocking solenoid. The rationale for the decision was an elastic delay (set) in the seals returning to their original shape, causing the dome to drag across the seals if the dome was moved immediately after the seal is depressurized. Additionally, concerns about the reliability of position switches (a well-known, high-maintenance item) and the probability of severely damaging components

when solenoids are over-ridden were both arguments against making the change from pneumatic sequencing to PLC sequencing.

During a site visit in the fall the vendor participated in extrusion testing, which showed that the originally supplied silicone seals were closing the gap between the dome and the seal after the first pressurization cycle. This is caused by either the material being pull-extruded by the pressure on the seal or by the seal creeping out of the clamp mechanism. Regardless, this seal growth is a major contributor to the seal failures, for as the clearances are reduced the dome (which is roughcast) eventually rubs the seal and causes the damage. These tests were performed at ambient temperature and 200 psig seal pressure. On one test the seal was pressurized overnight (~18 hours); when depressurized there was no clearance found. When neoprene seals were tested no such tightening of the seal clearances was found.

Two suggestions were made to deal with the silicone seal extruding/creeping and taking up the clearance between the dome and the seal when depressurized. The first suggestion was to replace as many seals as possible with the neoprene seal inserts. The neoprene inserts exhibited no creep, thereby avoiding the clearance reduction mechanism of potential seal failure. The second idea was to round off the dome's leading edge to prevent the dome from cutting into the seal material. By rounding the leading edge, the seal insert would be pushed out of the way, rather than being caught and cut by the leading edge. After discussion as to applicability of the neoprene seal for use in the FD0520 system, it was decided to reconfigure the temperature trip point to protect the neoprene, because the neoprene represents a higher probability for longer time between failure.

As spheri valve seals fail they will be changed to neoprene seal inserts until Clyde supplies new material seal inserts suitable for high-pressure and high-temperature applications. The dome leading edge reshaping will be addressed as failures occur and time allows. Clyde has taken the results of the extrusion tests and begun a search for either a different material that will meet the higher temperature requirement without extruding or for a different design that would allow for the use of the existing silicone material.

In summary, while the Clyde systems have been the leading cause of forced outages of the transport reactor there has been substantial progress in the development of those systems for this application. While most of the work to date has been focused on critical issues that brought about process shutdown, there are additional operational issues to address in the future.

Issues to be addressed in the future include: lockvessel caking, bridging and other plugging on FD0210 and FD0220; level probe reliability; discharge line plugging on FD0510, FD0520, and FD0530, especially the reduction in pipe internal diameter on the first lined elbow on FD0520 discharge line from the reducing elbow under the transport vessel; erosion of the lockvessel vent and equalization valves, possibly due to solids carryover into the vent lines; and the repeated plugging of the FD0520 vent line orifice.

The mean time between failure has improved to a point that all equipment in the transport reactor train operated without an outage for 2 weeks at the end of the 1997 fall test campaign.

5.3 MWK PROCESS AIR COMPRESSOR

The transport reactor process air compressor is an Atlas-Copco 1,700 hp multistage high-speed turbo-compressor with interstage cooling and inlet vane control, and a pressure blow-off valve for surge protection. This compressor is required to vary flow at a constant discharge pressure from 0 to 18,000 pounds per hour, holding discharge pressure constant (+/- 2 psi) while being subject to varying load conditions. The requirement to maintain pressure under rapidly varying conditions (of almost 20 percent full load) forces the control system to be dynamic and not overly damped and stable. Typical process air compressor applications are tuned for single point operation, with the controls in place for three reasons: 1) to maximize the compressor efficiency; 2) to protect the machine from compressor stall (surges) that would quickly and severely damage the compressor internals; and 3) to prevent overloading the compressor motor. The last two points must be maintained for the transport reactor's process air compressor; however, stability in the face of extreme changes in process flow should be the ultimate goal of the compressor control system.

The process air compressor experienced unstable operation in both 1996 and early in 1997. Atlas-Copco added programming in 1996 for more stable operation by keeping the blow-off valve open until the inlet vanes were more than a certain percentage open. Although not the most economical method of operation this modification allowed the stable operation needed during load changes. However, these modifications failed to completely solve the problem with stability. These changes were made in midsummer and the compressor was tuned at that time; the compressor became unstable at night in cooler weather as winter approached and "diverged" to the point that the compressor had to be manually operated to finish the test run. The Copco service personnel agreed that the 17 percent difference in inlet air density between the summer and winter conditions was affecting the compressor stability and recommended inlet temperature compensation to cure the surging problems. This compensation package was installed early in 1997 and after several iterations of the control configuration the compressor was tuned to allow the required stability and protection from surge.

With the exception of some electro-static discharge damage to some control components during the summer the process air compressor ran flawlessly during the 1997 fall test campaign.

5.4 TRANSPORT AIR SYSTEM

The transport air system, which supplies the dried transport air for FD0210 and FD0220 for both operating regimes, continued to be challenged by condensate problems throughout the year. The moisture separator was replaced early in 1997 with centrifugal separator/trap system, but the condensate carry-over continued. Both the original and the replacement separator have a minimum velocity requirement, which at times during low-pressure operation was not being met. Other work included supplying instrument air and/or nitrogen to control the dryer operation rather than relying on the transport air for dryer control due to the condensate problem and attendant trash in the transport air fouling the pneumatic control solenoids. Work continues on more effective precooling of the transport air and more reliable condensate separation at lower velocities.

5.5 RECYCLE GAS SYSTEM

The recycle gas system is designed to minimize the transport reactor's requirements for process air or nitrogen, especially in high-pressure, high-throughput combustion operation or for gasification operation. The recycle gas system was commissioned and demonstrated in 1996 but was not operated extensively. The system was exercised during 1997 test runs with limited success. The supply gas is drawn off of the process downstream of the secondary gas cooler, further cooled before being filtered, and compressed for use.

The compressor showed signs of overheating during a test run in the spring. The compressor valves were found damaged by particulate, vibration, and over-temperature. The gas filtration and conditioning systems were found to be badly fouled by condensate and particulate and were cleaned at this time. The system was successfully exercised when the compressor maintenance was completed.

During another system test in the fall 1997 test campaign the gas cooler was found to have several casing leaks caused by corrosive condensates. The system isolation valve did not adequately prevent gas infiltration and the gas cooler was continuously supplied with cooling water providing a condensation sink for the flue gases. These gases have been sampled by SRI in response to some corrosive attack of their equipment and were found to contain chlorine and fluorine. Measures will need to be taken to bring the recycle gas system on-line during combustion, and thereby keep the system hot, or to provide a purging system to prevent the condensation of the flue gases in the recycle gas cooler and piping.

5.6 PROCESS GAS SAMPLING

The gas sampling and analysis system supplied by Cegelec has been challenging to maintain in 1997. Cegelec closed their gas analysis system business in 1996 and did not provide any support in troubleshooting their system. The recurrent problem from 1996 was sample conditioning; the sample cooler/dryer system never operated reliably and was completely replaced in the spring. The drawbacks of using a system optimized for synfuel analysis to analyze combustion flue gas were apparent when all the analyzers were on-line. The NO_x analyzer failed several times in 1997, finally requiring nearly a complete rebuild and replacement before the end of the year. The SO_2 analyzer continued to give low readings during every test run, however the problem seems to be more in the process with probably more than expected sulfur capture than in the analyzer itself. The CO monitor's functional range was high, making combustion calculations and evaluations difficult to complete. The gas sample line and conditioning equipment were failing by the end of the year due to corrosive attack from the condensates in the sample gas line. The corrosion and other problems are being addressed.

5.7 MWK STEAM GENERATION SYSTEM

During the initial commissioning trials in 1996, the MWK steam generation system was operated with the combustion heat exchanger, both primary and secondary heat exchangers, and the thermal oxidizer's heat recovery steam generator (HRSG) in service. The steam generated by the thermal oxidizer's HRSG was used to preheat the PCD to prevent condensation on the filter elements by firing the thermal oxidizer before establishing a propane fire in the transport reactor. Hot air was sent to the PCD by using the primary heat exchanger as a condensing heater. The only operational concern emerging from the 1996 test runs was a water hammer on the condensate drum fill line. This was corrected during the 1996-1997 winter outage by installing a low-range condensate drum fill valve to handle the relatively small amounts of steam generation while the transport reactor is operated as a combustor.

Several heat exchangers were taken out of operation in 1997 during different test runs. First the flow through the primary heat exchanger was partially bypassed, then the combustion heat exchanger was taken out of service for a test run, and then the primary heat exchanger was completely removed from service for the fall PCD high-temperature test campaign. The removal of the primary heat exchanger required the use of the sulfator start-up burner to prewarm the PCD prior to firing the transport reactor.

The biggest issue in 1997 was water hammer in steam risers from the secondary heat exchanger and the combustion heat exchanger. These water hammers were due to two-phase flow in these lines caused by the higher operating temperatures in these heat exchangers and flash cooling in piping elbows. Piping snubbers were installed to minimize the damage to these lines and additional insulation will be installed to these lines in the future.

5.8 SULFATOR

The sulfator was not operated in 1997, however the vessel's refractory was dried out using the start-up heater package and the sulfator air compressor. Piping was completed to allow the start-up material transport system (FD0140) to directly inject feedstock into the combustion vessel. This will allow the direct injection of start-up bed material as well as carbon bearing material into the combustor to establish combustion prior to the injection of char from the transport reactor operating as a gasifier. Another modification includes the addition of a bed material extraction system to prevent hydration of the calcium carbonate bearing bed materials in the vessel after the AFBC is shut down. This system was designed and procurement was started, but the system has not yet been installed.

5.9 BAGHOUSE

The baghouse did not experience significant particulate loadings in 1997 although the loadings increased slightly during the fall test run. The baghouse was operated near the maximum operating temperature most of the year with no problems noted. The only issue noted with the baghouse was water infiltration while the transport reactor was off-line. Some minor corrosion was noted so the use of cover tarps was begun when the reactor is off-line.

5.10 BAGHOUSE ASH REMOVAL

The only issue of concern in 1997 was that of an audible rub of the screw feeder that collects any particulate and feeds it to the dense-phase transport pot. Uneven heating of the screw probably caused this rub. This is more of a nuisance than a real equipment concern; the operating procedure has been changed to leave the screw turning whenever the baghouse is hot. The level probes that trigger transport system operation were not as reliable as desired; the transport system was placed on operation by timer.

5.11 HEAT TRANSFER FLUID SYSTEM

There were no significant issues to report with the heat transfer fluid system. There were several incidents due to a full PCD cone when the system was operated at the edges of its envelope; however, there were no problems resulting from such operation.

5.12 NITROGEN SUPPLY

Other than some minor failures on the nitrogen vendor equipment there were no significant issues to report on the nitrogen supply system.

5.13 PROPANE SUPPLY

After the modifications to the MWK start-up burner were completed the required supply pressure for the propane was increased from 180 psi to 250 psi. A pressure resonance was found at system header pressures above 220 psi regardless of the flow on the header. The current operating parameters for the propane system are 250 psi, 180°F rather than at the design conditions of 235 psi, 150°F. The higher temperature is due to the unexpected heavy hydrocarbons (butanes) in commercial propane that tends to carbonize in burner tips at high metal temperatures. All of the mechanical piping and components are individually rated for 300 psi and the vaporizer pressure relief valve (on the propane side) is set for 295 psi.

This resonance is partially caused by the changing liquid level and temperature in the vaporizer. As the level in the vaporizer rises there is more liquid in contact with the heat exchanger surface resulting in greater amounts of liquid being vaporized. The higher level reduces the heat transfer surface to the gas, which decreases the gas temperature and causes more condensation, reduces the saturation pressure in the vaporizer, and allows more liquid into the vaporizer. Once the propane level reaches the point that the heat transfer to the liquid (vaporizing more gas) and the heat transfer to the gas balance (maintaining saturation temperature in the gas), the pressure swing in the vaporizer stabilizes. At the present time all of the propane pressure regulators are simple zero-order feedback controlled regulators; the pressure rises and then the regulator closes off until the pressure reaches the setpoint. If the pressure swings from high to low the regulator will continue to open and close in response to the pressure, with no way to trim regulator response due to the rate of change or to average error.

In summary, the propane supply system will not be able to maintain a stable pressure or temperature at the design conditions, as it was designed or as it is presently configured. The use of smart controllers in lieu of simple pressure regulators, the addition of flow based control to the burner fuel valves, and if necessary, the addition of a separate propane superheater should work together to minimize any pressure, temperature, and flow swings experienced by any of the high-pressure propane burners. The various design alternatives are being evaluated.

5.14 INSTRUMENT AIR SYSTEM

During the course of the Foster Wheeler (FW) system commissioning the instrument air headers on the FW side of the process structure were blown down to clean out any debris left from construction. This blow down served to loosen some debris in the supply headers that was introduced into the MWK instrument air headers. This debris caused some minor equipment upsets in November.

5.15 WATER SYSTEMS (CLOSED LOOP, COOLING TOWER, CONDENSATE, SERVICE, FIRE, POTABLE)

There were only two issues in 1997 dealing with the water systems. These were:

1. Tube erosion in a condensate heat exchanger from flow-induced vibration.

2. Marginally sized couplings on the cooling tower fans.

Both issues required replacement of the failed components. In the case of the heat exchanger the replacement design was improved to prevent such wear from reoccurring.

5.16 WASTEWATER TREATMENT

There were no significant wastewater treatment issues to be reported.

5.17 CONDENSATE TREATMENT

Additional preventive maintenance inspections were started on the instrument air dryers and on the baghouse. The pressure relief valves were reinstalled after they were removed for testing in July. The inspections of the condensate heat exchangers are being completed; one heat exchanger was subjected to heavy vibrational wear during operations and will have to be replaced. This wear was due to tubing bundles vibrating and wearing against the support plates.

5.18 STATION SERVICE AND UPS (INCLUDING DIESEL GENERATOR)

The diesel generator was operated during a planned power outage in the last half of January 1997. The power outage was required by Alabama Power Company to upgrade their transmission line and was coordinated with the project in order to minimize the impact to the project. Other than this occurrence the diesel generator has been tested on a biweekly basis, as is all project emergency equipment including the fire pumps. The station service (electrical supply) system has received minor upgrades to meet the increased demands of the project.

5.19 MWK START-UP BURNER

The reactor start-up burner was modified early in 1997 to include ultraviolet (UV) flame detection (Honeywell's Purple Peepers), a separately regulated pilot air supply, and an additional baffle on the pilot gun assembly to force air into the fuel mixer/eductor. This was in addition to previous modifications made to the start-up burner (cooling air purges on the flame rod and the sparker, the redesigned main gun tip, and a nonretracting pilot sparker). These modifications allow better reliability due to the UV detection and reduced burning of the pilot gun components because of air lean conditions experienced by the pilot relying on eductors to draw enough air into the pilot tube.

Additional benefits include:

1. Better air and temperature control because the high air flow is no longer required to avoid the burning of the pilot by empirical operation.

2. Reduced riser velocity by reaching desired outlet temperatures at lower gas flows.

3. Reduced burner can metal temperatures by using the quench air on the burner.

UV flame detection on the main burner gun will allow the pilot gun to be shut down while the main gun is lit, thereby improving turndown of the burner. Also, using the quench air to control the burner metal temperatures will allow more flow at the high end of the scale, shortening the time to initiate combustion in the transport reactor. During subsequent test runs the start-up burner never failed to start once all required conditions were met, except for one instance when the purge air was not applied to the burner package. The burner was repeatedly restarted at 100 psig reactor pressure and once an initial partial plug of solid carbon (coke) was formed, reducing the total flow capacity, there were no further degradations in performance experienced.

After the extensive modifications installed on the Zink start-up burner (SUB) were tested the only continuing problem being experienced with the SUB operation sometimes is the buildup of solid carbon (coke) and subsequent plugging of the main burner gun fuel tip. This plugging reduces the throughput of the burner and impacts the heat input to the reactor. The plugging normally occurs 4 to 8 hours after the burner reaches maximum exit temperature of 2,000°F, and represents about a 30-percent drop in flow (at a consistent pressure drop). The propane supplied to the burner is pressurized to up to 225 psi and heated to between 150 and 170°F. Typically, liquids and solids carbonize and gases tend to combust; therefore, the impurities in the supplied propane are coking up the burner gun. PSDF is purchasing the highest commercial grade of propane available (HD-5). The specification for this propane allows a maximum of 2.5 percent (by liquid volume) of butanes and heavier, of which all but an indistinguishable amount is C_5 isomers.

Isobutane's saturation temperature at 225 psi is 188°F, n-butane's is 212°F. Thus, it is suspected that liquid butane is present at the end of the fuel gun, where it is partially (flash) carbonized, building the small amount (< 2 oz) of coke required to partially plug the nozzle ports that are .062 and .091 inches in diameter. This will be addressed with the propane supply modifications.

5.20 TRANSPORT REACTOR PRESSURE CONTROL VALVE PV-287

Outages and upsets have occurred several times during the past year due to excessive vibration in the reactor's backpressure regulating valve (PV-287). The internals of this valve have been changed and modified since the original commissioning of the transport reactor to meet the flow, controllability, and noise requirements.

The trim was originally supplied as a "whisper-trim" equal-percentage design but was unable to flow enough mass at low reactor pressures. This was temporarily replaced with a standard equal-percentage trim that tended to concentrate abrasive solids into three areas of the valve's body, quickly eroding the body to failure. The whisper-trim cage was modified to handle the extra flow requirements and used for most of the year. This trim set experienced several vibration events during the year that caused the valve operator to vibrate loose twice and further damage the pneumatic operator internals another time.

When the valve was inspected after the second-quarter test runs, the plug's graphite seal ring was found broken in several places; similar damage was found during the outage in October 1997. The valve internals (trim) were changed to an equal-percentage trim when additional damage in the existing trim was found that could not be easily repaired. A larger valve was ordered to replace this valve to better position the typical operating point further from the choke flow conditions of the existing valve design. The results of a feed-forward control loop triggered on the PCD back-pulse were found to be successful to the limits of the PV-287, but the control valve/operator cannot move fast enough to completely compensate for the back-pulse volume. This will also be corrected by the installation of the new larger size PV-287 valve.

.

TERMS

Listing of Abbreviations

AAS	Automated Analytical Solutions
ADEM	Alabama Department of Environmental Management
APC	Alabama Power Company
APFBC	Advance Pressurized Fluidized-Bed Combustion
ASME	American Society of Mechanical Engineers
AW	Application Workstation
BFI	Browning-Ferris Industries
BFW	Boiler Feed Water
BMS	Burner Management System
BOC	BOC Gases
BOP	Balance-of-Plant
BPIR	Ball Pass Inner Race, Frequencies
BPOR	Ball Pass Outer Race, Frequencies
BSF	Ball Spin Frequency
CAD	Computer-Aided Design
CEM	Continuous Emissions Monitor
CFB	Circulating Fluidized Bed
CFR	Code of Federal Regulations
CHE	Combustor Heat Exchanger
CPC	Combustion Power Company
CPR	Cardiopulmonary Resuscitation
DC	Direct Current
DCS	Distributed Control System
DOE	U.S. Department of Energy
E & I	Electrical and Instrumentation
EERC	Energy and Environmental Research Center
EPRI	Electric Power Research Institute
FCC	Fluidized Catalytic Cracker
FETC	Federal Energy Technology Center
FFG	Flame Front Generator
FI	Flow Indicator
FIC	Flow Indicator Controller
FOAK	First-of-a-Kind
FTF	Fundamental Train Frequency
FW	Foster Wheeler
GBF	Granular Bed Filter
GC	Gas Chromatograph
GEESI	General Electric Environmental Services, Inc.
HP	High Pressure
HRSG	Heat Recovery Steam Generator
HTF	Heat Transfer Fluid
HTHP	High-Temperature, High-Pressure

I/O	Inputs/Outputs
ID	Inside Diameter
IF&P	Industrial Filter & Pump
IGV	Inlet Guide Vanes
IR	Infrared
LAN	Local Area Network
LIMS	Laboratory Information Management System
LOC	Limiting Oxygen Concentration
LOI	Loss on Ignition
LPG	Liquefied Propane Gas
LSLL	Level Switch, Low Level
MAC	Main Air Compressor
MCC	Motor Control Center
MS	Microsoft Corporation
MWK	The M. W. Kellogg Company
NDIR	Nondestructive Infrared
NFPA	National Fire Protection Association
NOx	Nitrogen Oxides
NPDES	National Pollutant Discharge Elimination System
NPS	Nominal Pipe Size
OD	Outside Diameter
OSHA	Occupational Safety Health Administration
OSI	OSI Software, Inc.
P&IDs	Piping and Instrumentation Diagrams
PC	Pulverized Coal
PCD	Particulate Control Device
PDI	Pressure Differential Indicator
PDT	Pressure Differential Transmitter
PFBC	Pressurized Fluidized-Bed Combustion
PI	Plant Information
PLC	Programmable Logic Controller
PPE	Personal Protection Equipment
PRB	Powder River Basin
PSD	Particle Size Distribution
PSDF	Power Systems Development Facility
ΔP	Pressure Drop
PT	Pressure Transmitter
RFQ	Request for Quotation
RO	Restriction Orifice
RSSE	Reactor Solid Separation Efficiency
SCS	Southern Company Services, Inc
SRI	Southern Research Institute
SUB	Start-up Burner
TCLP	Toxicity Characteristic Leaching Procedure
TR	Transport Reactor
TRDU	Transport Reactor Demonstration Unit
TSS	Total Suspended Solids

UND	University of North Dakota
UPS	Uninterruptible Power Supply
UV	Ultraviolet
VFD	Variable Frequency Drive
VOCs	Volatile Organic Compounds
WPC	William's Patent Crusher
XXS	Extra, Extra Strong

Listing of Units

acfm	Actual Cubic Feet Per Minute
Btu	British Thermal Units
°F	Degrees Fahrenheit
ft	Feet
FPS	Feet Per Second
gpm	Gallons Per Minute
hp	Horsepower
hr	Hour
inWg	Inches, Water Gauge
MB	Megabytes
MW	Megawatts
m/s	Meters per second
μ or μm	Microns or Micrometers
dp_{50}	Particle Size Distribution at 50 Percentile
ppm	Parts Per Million
lb	Pounds
pph	Pounds per hour
psia	Pounds Per Square Inch Gauge
psig	Pounds Per Square Inch Gauge
ΔP	Pressure Drop
rpm	Revolutions Per Minute
s or sec	Seconds
scf	Standard Cubic Feet
scfm	Standard Cubic Feet Per Minute
V	Volts
W/PPPM	weight/parts per million